THE EFFECTS SURCHARGING HAS ON THE RATE OF SECONDARY SETTLEMENT ON CLAYS ALONG THE WASATCH FRONT

by

Zach Montgomery Gibbs

A thesis submitted to the faculty of
The University of Utah
in partial fulfillment of the requirements for the degree of

Master of Science

Department of Civil and Environmental Engineering

The University of Utah

December 2015

The University of Utah Graduate School

STATEMENT OF THESIS APPROVAL

The thesis of **Zach Montgomery Gibbs**

has been approved by the following supervisory committee members:

Steven Bartlett	, Chair	**12/10/2014** Date Approved
Evert Lawton	, Member	**12/10/2014** Date Approved
Richard Porter	, Member	**12/10/2014** Date Approved

and by **Michael Barber** , Chair/Dean of

the Department/College/School of **Civil and Environmental Engineering**

and by David B. Kieda, Dean of The Graduate School.

ABSTRACT

Secondary compression of foundation soils can cause long-term settlement damage to bridges, their foundations and approach embankments, overlying pavements, and other nearby constructed works. Because this type of settlement is long-term and manifests itself many months to years following embankment construction, it sometime goes unnoticed until it damages overlying or nearby infrastructure.

Surcharging or preloading of the earthen embankments and underlying compressible soils is the most commonly deployed strategy to reduce the magnitude of secondary compression. Surcharging or overconsolidating of the foundation soils can be used to reduce the postconstruction secondary settlement. In the course of this research, twenty-two consolidation tests and eighty-eight time rate tests were performed on Pleistocene and recent fine-grained, cohesive, lacustrine deposits comprised of Lake Bonneville and more recent clays, most likely of Utah Lake origin located along the Wasatch Front. Prior to analyzing the data, the test results were screened using the sample quality designation (SQD).

Plots of the adjusted amount of surcharge (AAOS) were plotted versus the normalized rate of secondary settlement (C_α'/C_α) and compared with the research performed by Ng. The data from this thesis plot higher than those reported by

Ng. This higher trend agrees better with the long-term settlement performance monitoring data obtained from the I-15 Reconstruction Project. Data from the time rate tests were used to determine the C_α/CR ratio, giving a mean value of $C_\alpha/CR = 0.0442$. This value was also compared with the research performed by Ng, which had a value of $C_\alpha/CR = 0.0433$. This correlates well. A plot of moisture content vs. CR was developed and compared with research done by Bartlett and Lee. The data from this thesis trendline are slightly lower than that reported by Bartlett and Lee, but still correlate well. The correlation of moisture content versus the C_α/CR ratio was explored which shows promise, but more observations are needed to improve the statistical support for this relation.

TABLE OF CONTENTS

LIST OF TABLES

ACKNOWLEDGEMENTS

I would like to thank Dr. Steven Bartlett for approaching me and giving me this great opportunity. I have gained a lot of knowledge and experience while performing the research for this thesis. I would also like to thank him for the help and guidance he has provided.

I would like to thank Ramesh Neupane and Shun Li for the help they both provided with gathering lab readings and the support they offered.

I would like to thank my wife, Stacie, for her unwavering support and patience through the course of this thesis and for always reminding me to be diligent.

1 INTRODUCTION

1.1 Overview

Secondary compression or secondary settlement or creep settlement is a continuation of the volume change of a compressible soil under a constant (i.e., nonchanging) loading without the associated changes in the effective stress of the soil fabric. This behavior begins to be manifested near the end of primary consolidation and continues indefinitely, but at a nonlinear diminishing rate. In contrast to primary consolidation which is associated with compression due to pore water pressure dissipation, secondary compression begins when the specimen achieves a constant effective stress after essentially all excess pore water pressure has dissipated that was induced by the initial loading event (Holtz et al., 2011). Secondary compression of foundation soils at deep, compressible, soil sites can cause long-term settlement damage to bridges, their foundations and approach embankments, overlying pavements, and other nearby constructed works. Because this type of settlement is long-term and manifests itself many months to years following embankment construction, it sometime goes unnoticed until it damages overlying or nearby infrastructure. For example, the collective secondary compression is often significantly large enough to produce a severe “bump” at pile-supported bridges where the approach embankment has settled differentially relative to the bridge and bridge abutments.

The magnitude and potential deleterious effects of secondary compression on the future performance of the interstate system were important geotechnical design and performance considerations during the reconstruction of I-15 in the northern part of Salt Lake Valley, Utah during 1998 to 2001. Surcharging or preloading of the earthen embankments and underlying compressible soils was the most commonly deployed strategy to reduce the magnitude of secondary compression; however, soil improvement and light-weight embankment materials were also used as settlement mitigative measures. An important part of embankment design for the I-15 project was a systematic evaluation of the required amount (i.e., height) of surcharge to reduce the secondary compression to acceptable, postconstruction, performance goals. Associated with this issue is also the required time that such surcharge is to remain in place to achieve the desired long-term settlement performance goal. For the I-15 project, the performance goal was to surcharge the foundation soils enough that the embankment in the bridge approach area did not settle more than 3 inches in a 10-year, postconstruction period. Whatever the desired outcome, the settlement performance goals should be clearly defined by the project team in consultation with the owner. For fast-paced construction, the corresponding settlement calculations and design, construction settlement monitoring, and project communication are vital if these goals are to be realized. In addition to the amount of surcharging employed, the time or duration that the surcharge is to remain in place (i.e., surcharge duration) strongly impacts the postconstruction settlement performance and the construction schedule.

Because the surcharge duration can be long for deep soil sites, this can significantly impact the construction schedule; hence, there is an inherent tendency by the contractor and the project team to try to shorten the surcharge duration in order to expedite the construction. Therefore, construction settlement monitoring to assess the progression of primary consolidation settlement and a decision framework for selecting when to remove the surcharge are essential in achieving the settlement performance goals and delivering a timely project.

1.2 Scope and Purpose of Research

The primary purpose of this research is: (1) to quantify the effects that surcharging (i.e., preloading) has on secondary compression settlement for fine-grained soils located along the Wasatch Front, Utah area using one-dimensional (1D) consolidation tests performed on conventional table top oedometers and (2) to develop the information, relations, equations, charts, etc. required to develop and implement a surcharge design for these sediments using the framework developed by Ladd (1989) and Ng (1998), (3) to confirm or recommend changes, if any, to the relations required for surcharge design as presented by Ladd (1989) and Ng (1998), and (4) to make other recommendations about the implementation of the results of this research in regard to surcharge calculations and design.

These purposes and objectives will be explored via: (1) reviewing the geotechnical literature that supports the approaches of Mesri et al. (Mesri and Castro, 1987; Mesri et al., 1994) and of Ladd (Ladd, 1989 and, Ng 1998), (2) undisturbed sampling of cohesive soils from four soft soil sites located along the

urban Wasatch Front, Utah, (3) laboratory testing of these specimens in conventional oedometers to determine the rate of secondary compression as a function of preloading (i.e., overconsolidation ratio), (4) evaluating and presenting the results of the laboratory test program in the analysis framework developed by (Ladd, 1989 and Ng 1998), and (5) making recommendations, if any, about modifications to the relationships or methods developed by Ladd (1989) and Ng (1998).

2 BACKGROUND

2.1 General Discussion

Consolidation settlement of soil occurs from three general mechanisms: (1) quasi elastic compression of the soil fabric upon reloading that occurs below the preconsolidation stress, (2) primary consolidation settlement resulting from significant compression of the soil fabric from an applied stress that exceeds the preconsolidation stress, and (3) secondary consolidation or secondary compression of the soil fabric which is a complex combination of processes that initiates near the end of primary consolidation and continues as a long-term process under a constant load or unchanging effective stress (Holtz et al., 2011). Secondary compression is generally thought of as void ratio change in the soil fabric occurring at a relatively slow rate after primary consolidation is essentially completed. However, some researchers have noted that secondary compression occurs in conjunction with primary consolidation settlement, but at a slower rate; hence, its effects are in a large part masked by the significantly greater magnitude and faster rate of primary consolidation settlement realized during the initial part of the consolidation process. Therefore, it is difficult to distinguish secondary compression from experimental data when the sample is undergoing large void ratio changes associated with primary consolidation (Takeda et al., 2013). Although such distinctions are important for the advancement of

consolidation theory, this research will adopt the classical construction shown in Figure 2.1 to define the time corresponding to the end of primary consolidation, t_p, which also marks the beginning of secondary compression (Raymond and Wahls, 1976). In this definition, t_p is calculated as the intersection of the straight lines that define primary consolidation and secondary compression on a void ratio, e, versus log of time plot.

As the rate of primary consolidation diminishes, secondary compression becomes the dominate process. At this point, almost all of the excess porewater pressure (i.e., porewater pressure above hydrostatic) has dissipated from the soil fabric that was caused by the initial loading event. Hence, secondary compression is also defined as void ratio change or settlement occurring when the effective stress in the soil fabric is no longer significantly changing (Holtz et al., 2011). The continued settlement at a diminishing rate is a result of creep, viscous behavior of the soil fabric, compression of organic matter, and other processes.

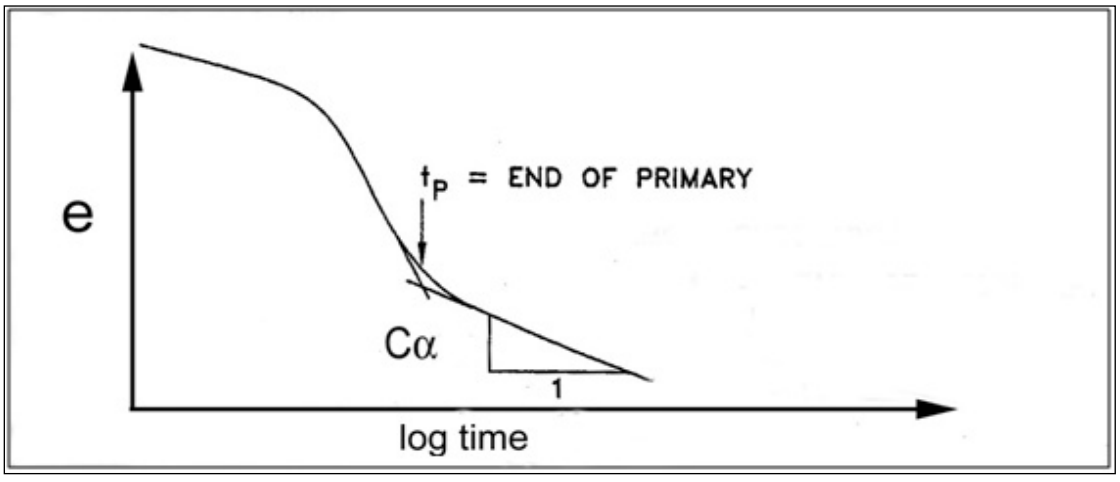

Figure 2.1 Definition of C_α from 1D time rate of consolidation test (after Raymond and Wahls, 1976; Ng 1998).

Holtz et al. (2011) suggest that the following assumptions must be adopted to provide a working hypothesis about the behavior of fine-grained sediments undergoing secondary compression based on work by Ladd (1971) and Raymond and Wahls (1976). They discuss the relative merits and practical consequences associated with these assumptions which have been briefly summarized below:

1. The rate of secondary compression is independent of time, at least during the time span of engineering interest. (This assumption is discussed later in this report.)
2. The rate of secondary compression is independent of the soil layer.
3. The rate of secondary compression is independent of the load increment ratio (LIR), as long as some primary consolidation occurs.
4. The ratio of the rate of secondary compression to the compression index is approximately constant for many geo-materials over the range of engineering stresses (also discussed later in this report).

The amount of volume change during secondary compression is calculated from the secondary compression index, C_α, which represents the rate of secondary compression defined by:

$$C_\alpha = \Delta e / \Delta \log t \qquad (2\text{-}1)$$

where: Δe is the change in void ratio, $\Delta \log t$ is $\log t - \log t_p$. The value of C_α represents the change in void ratio, e, divided by the change in log of time for the portion of the time rate of consolidation curve extending beyond the end-of-

primary (EOP) consolidation (Figure 2.1) (Holtz et al., 2011). When plotted on a semi-log plot, C_α represents the slope of this semi-log linear portion of secondary compression that occurs beyond EOP consolidation (Figure 2.1).

The magnitude of secondary compression or settlement for a specimen or layer is typically calculated by the following formula for 1D consolidation:

$$S = [C_\alpha / (1+ e_o)] H_o \log t / t_p \quad (2\text{-}2)$$

where: H_o is the height of the specimen or layer, e_o is the initial void ratio, C_α is the rate of secondary compression, t is the elapsed time after the end of primary consolidation and t_p is the time required to reach the end of primary consolidation (Figure 2.1) (Holtz et al., 2011; Terzaghi et al., 1996).

2.2 Mesri et al. Concept of Secondary Compression

Mesri et al. have shown that the secondary compression index for a normally consolidated soil, C_α NC, is correlated with and can be estimated from the virgin compression index, C_c, or the compression ratio CR of that soil (Mesri and Castro, 1987; Ladd 1989; Mesri and Feng, 1991; Mesri et al., 1994; Terzaghi et al. 1996; Ng, 1998; Saye and Ladd, 2000) where the compression ratio is defined as:

$$CR = C_c / (1 + e_o). \quad (2\text{-}3)$$

Because of this correlation, the method proposed by Mesri et al. (Mesri and Castro, 1987; Mesri et al., 1994) is often used to estimate the rate of secondary compression for a given geologic unit. In the approach proposed by Mesri et al.,

the ratio of C_α/C_c or C_α/CR has been found to be considered relatively constant for sediments of the same geologic origin. Therefore, this ratio can be used to estimate C_α NC if C_c or CR has been determined for the soil of interest. It should be noted that the C_α/CR ratio used in this research is the same as C_α/C_c ratio of Mesri and Castro (1987) and Mesri et al. (1994) because for C_α/CR, the unit of strain in $C_\alpha = d\varepsilon_v$ / dlog t and that found in CR = $d\varepsilon_v$ / dlog σ'_{vc} cancel each other; and for C_α/C_c, the unit of change in void ratio C_α = de / dlogt and that found in C_c = de / dlog σ'_{vc} cancel each other (Ng, 1998), thus C_α/CR or C_α/C_c can be used interchangeably.

To implement the Mesri et al. method (Mesri and Castro, 1987; Mesri et al., 1994), values of C_α/C_c or C_α/CR are typically determined from a laboratory consolidation testing program from each geologic unit of interest. Once this ratio is established, additional estimates of C_α can be made for a given deposit using laboratory or field estimates of C_c or CR and the corresponding values of C_α/C_c or C_α/CR ratio for that deposit.

2.3 Surcharging to Reduce Secondary Compression

Terzaghi et al. (1996) recognized the fact that if the final in situ state of stress resulting from a loading event imparted to a foundation soil is higher than the original preconsolidation stress of the soil and if the time for primary consolidation, t_p, is small perhaps due to the installation of prefabricated vertical drains (PVD), then the amount of secondary compression settlement can be relatively large. However, this can be reduced to acceptable levels by using surcharging of the foundation soil during the last stage of embankment

construction. Surcharging has the effect of preloading the soil (i.e., overconsolidating) and reducing the rate of secondary compression when compared to the rate of secondary compression for a normally consolidated soil (i.e., a soil that has not been surcharged).

Surcharge methodologies developed by Ladd (1989) and by Mesri (1986) have been used in engineering practice to develop a surcharge approach to reduce the effects of secondary compression associated with embankment construction atop on relatively soft, compressible, foundation soils. The next two sections of this report describe Mesri's and Ladd's methodologies. The final section of this report discusses how Ladd (1989) methodology was applied to the I-15 Reconstruction Project to reduce the effects of secondary compression. The data developed from this roadway project in conjunction with additional field and laboratory testing and evaluations performed as part of this research become, in part, the basis for the surcharge design guidance developed herein.

2.4 Surcharge Design Using Methodology Developed by Mesri

Mesri (1991) has shown the behavior of a soil subjected to surcharging (Figure 2.2). The removal of the surcharge leads to rebound of the specimen, including primary rebound up to the time t_{pr} and secondary rebound that levels off at time t_l and is followed by secondary compression occurring at a nonlinear rate on a log of time plot. In this figure, t_{pr}, t_l, and t are measured from the time when the surcharge load was removed (i.e., t'_s). The postsurcharge secondary compression behavior, C'_α, shown in Figure 2.2 is initially small and subsequently gradually increases with time. Mesri has shown that at large values of t, the

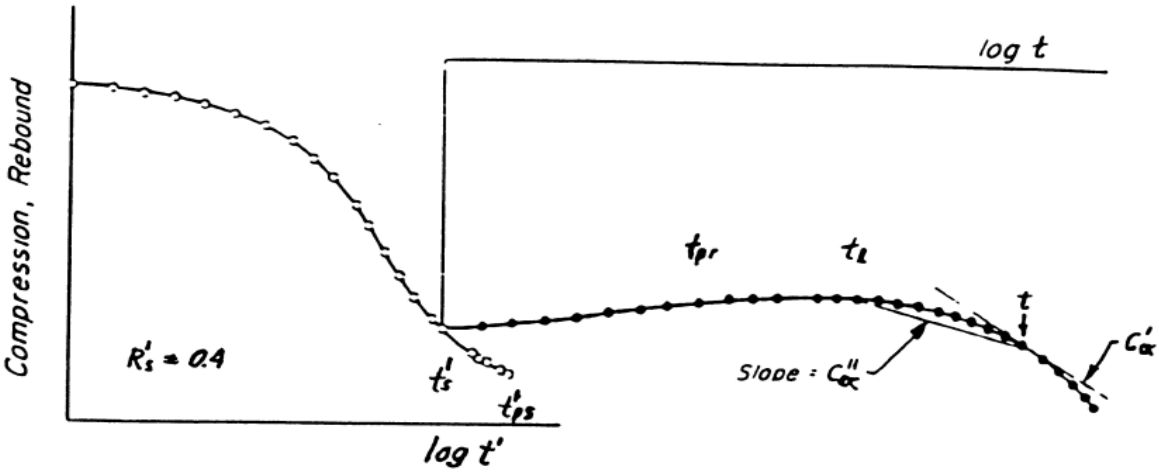

Figure 2.2 Mesri's basic concepts of the effects of surcharge on secondary compression (Mesri 1991 from GEO-COAST 91, unpublished proceedings).

behavior of the secondary compression depends on the initial shape of the EOP e vs log σ'_v curve at the state of stress with the surcharged load applied. Hence, because C'_α is not constant with time, a secant value C''_α is used in evaluations where the slope of C''_α is defined by the line connecting t_l with t.

In Mesri's approach, the surcharging effort is expressed as the total surcharge ratio:

$$R_s = (\sigma_{vs} / \sigma'_{vf}) - 1 \qquad (2\text{-}4)$$

where: σ_{vs} is equal to $\sigma'_{vf} + \Delta\sigma_{vs}$ and σ'_{vf} is the final effective vertical stress after removal of surcharge and $\Delta\sigma_{vs}$ is the total stress applied by the surcharge load. The surcharging time ratio, t'_s / t'_{ps}, affects the behavior of the curve where t'_s is the duration of the surcharge, and t'_{ps} is the time to EOP compression under the surcharge load. For cases where the surcharge load is removed before EOP compression, the above equation is rewritten as:

$$R'_s = (\sigma'_{vs} / \sigma'_{vf}) - 1 \quad (2\text{-}5)$$

where: σ'_{vs} is the maximum effective vertical stress reached before the removal or surcharge. Hence, when $t'_s / t'_{ps} = 1$, then $R_s = R'_s$.

If t'_s exceeds the time to the EOP compression, then the value of R'_s is adjusted to reflect the aging and the effective surcharge ratio, R'_s, is equal to:

$$R'_s = (\sigma_p' - \sigma_{vf}') / \sigma_{vf}' \quad (2\text{-}6)$$

where: σ_p' is the apparent preconsolidation stress due to aging of the soil under the surcharge load.

2.5 Surcharge Design Using Methodology Developed by Ladd

The methodology of Ladd (1989) has many aspects that are similar to that of Mesri, but the part of the curve that defines secondary compression has been simplified (Figure 2.3). The most important difference is that Ladd's method assumes that the rate of secondary compression is linear when plotted on a semi-log plot. The linear portion begins after the start of secondary compression, t_s, and continues thereafter (Figure 2.3). Hence, C_α' is calculated from the slope of a line fitted through the linear most part of the vertical strain measurements that follow t_s. This construction makes Ladd's method easier to apply than that of Mesri.

In Ladd's method, if the soil is surcharged (i.e., overconsolidated) and subsequently aged under this surcharge load, it undergoes secondary compression at a reduced rate, C_α', when compared with the, unsurcharged, unaged rate of secondary compression C_α (Figure 2.3). The aging time of the soil

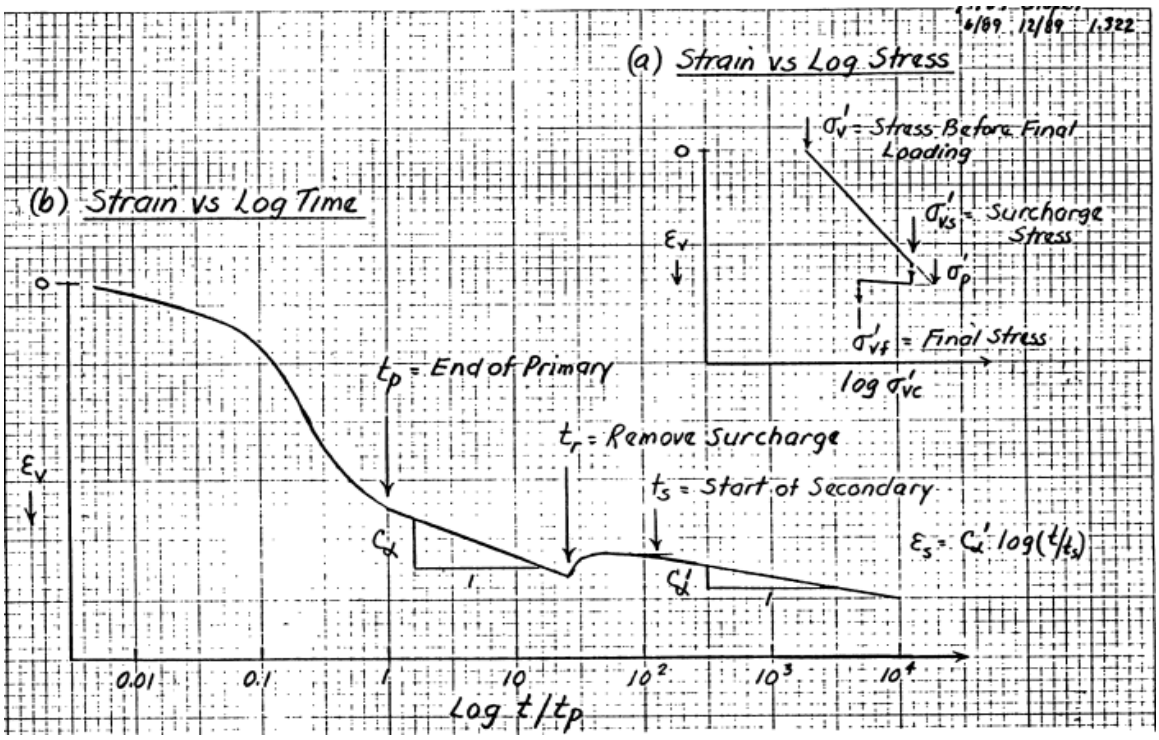

Figure 2.3 The effects of surcharging (i.e., preloading) on the rate of secondary compression (after Ladd, unpublished notes).

under the surcharge stress (i.e., elapsed time between t_p and t_r) reduces the rate of secondary compression from C_α, the normally consolidated value, to a lesser, overconsolidated value, C_α', which has a reduced slope (Figure 2.3). Hence, if a soil can be surcharged and aged, the amount of postconstruction creep settlement is reduced when compared with the unsurcharged, normally consolidated value. Therefore, in applying this concept to developing the surcharge design for an embankment and its foundation soil, an evaluation is made to provide sufficient surcharging of the foundation soil so as to reduce C_α' to a value that will reduce the amount of secondary compression. The value of C_α' required is a function of the thickness of the foundation soil layer undergoing secondary compression and the postconstruction settlement goal selected by the

project team. The amount of secondary compression settlement for normally consolidated sediments (i.e., unsurcharged soils) is calculated from:

$$S_s = H_1 C_\alpha \log (t / t_p) \quad (2\text{-}7)$$

where: S_s is the amount of secondary compression settlement, H_1 is the thickness of the layer undergoing secondary compression, C_α is the normally consolidated rate of secondary compression, t_p is time to end of primary consolidation and t is the time beyond t_p. If the soil has been surcharged (i.e., overconsolidated) and then unloaded, then a reduced rate of secondary compression, C_α', is used in lieu of C_α:

$$S_s = H_1 C_\alpha' \log (t / t_p) \quad (2\text{-}8)$$

When using Ladd's methodology for a surcharge design, the soil is loaded from (σ'_v) to the surcharge stress (σ'_{vs}) and then is unloaded to the final stress (σ'_{vf}). The difference between these values is defined as the amount of surcharge (AOS) which is determined from the following:

$$AOS = (\sigma'_{vs} - \sigma'_{vf}) / \sigma'_{vf} \quad (2\text{-}9)$$

For staged embankment construction, σ'_{vs} should be calculated using the full embankment height plus the height of surcharge and σ'_{vf} should be calculated using the final embankment height after surcharge removal, but including the weight of the overlying pavement system, if present.

If the surcharge stress σ'_{vs} exceeds the preconsolidation stress of the soil (i.e., primary consolidation is initiated) and primary consolidation is allowed to go to completion, but significant secondary compression is not allowed under the

surcharge load (i.e., soil is not allowed to age by removing the surcharge, t_r, at the same time as t_p is achieve), then Equation 2-9 is appropriate and Equation 2-8 should be used to calculate the secondary compression of the soil using C_α' appropriate for the AOS achieved by the surcharge load. The AOS and the overconsolidation ratio, OCR, are related by:

$$AOS = OCR - 1 \qquad (2\text{-}10)$$

If the soil is aged by allowing the surcharge to remain in place for some time after the end of primary consolidation (i.e., $t_r > t_p$), then the AOS is adjusted to account for the apparent increase of σ'_p above σ'_{vs}, due to the aging. The adjusted amount of surcharge (AAOS) is determined using the following:

$$AAOS = (\sigma'_p - \sigma'_{vf})/ \sigma'_{vf} \qquad (2\text{-}11)$$

where: $\sigma'_p = \sigma'_{vs}(t_r/t_p)^{C\alpha/CR}$.

Figure 2.3 also shows a time delay between the removal of the surcharge, t_r, and the initiation of the reduced rate of secondary compression, t_s. Initially, there is a brief heave event, followed by the initiation of secondary compression at a reduce rate represented by C_α'. The length of this time delay is a function of AAOS (Ladd, 1989 and Ng, 1998). The time delay is longer for higher AOS values, as discussed in the next section using data from the I-15 Reconstruction Project (Ng, 1998). This delay is also beneficial in reducing the amount of secondary compression occurring in the postconstruction period. For evaluation purposes, the value of t_s represents the point in time when the soil has reached its maximum heave value (Figure 2.3).

2.6 Application of Ladd's Method to the I-15 Reconstruction Project

The I-15 Project was a fast-paced reconstruction project that began during the spring of 1998 and ended in the fall of 2001, just prior to the 2002 Winter Olympic Games in Salt Lake City, Utah. At that time, it was the largest public highway construction project to be accomplished using a design-build project delivery system. During this 3.5-year period, the design-build consortium demolished and rebuilt 26 km (16.2 miles) of urban interstate, widening the roadway from 6 to up to 12 lanes at a total cost of about $1.4 billion. A large part of this cost was spent erecting 144 overpass bridge structures, constructing 160 mechanically stabilized earth (MSE) retaining walls and placing 3.8 million m^3 (134 million ft^3) of new embankment. The design-build contract featured a 50-year design life and an optional 10-year corrective maintenance agreement (Farnsworth et al., 2008).

The strict project completion date presented unique challenges to the design-build team. Perhaps the most demanding was developing strategies to address the impacts of consolidation settlement in the northern segment of the project near the downtown area. Here, compressible, fine-grained lacustrine sediments deposited by Pleistocene-age Lake Bonneville underlie about 5 m (16.4 ft) of Holocene alluvium (Figure 2.4). The lacustrine sediments are approximately 15 m (49.2 ft) thick, consisting of inter-bedded silty clay and clayey silt (CL, ML), plastic clays and silts (CH, MH), and fine clayey and silty sands (SC, SM) and are lightly overconsolidated (OCR $\approx$ 1.5). Interbedded, subaqueous silts, fine sands and low plasticity clays are found in the middle of

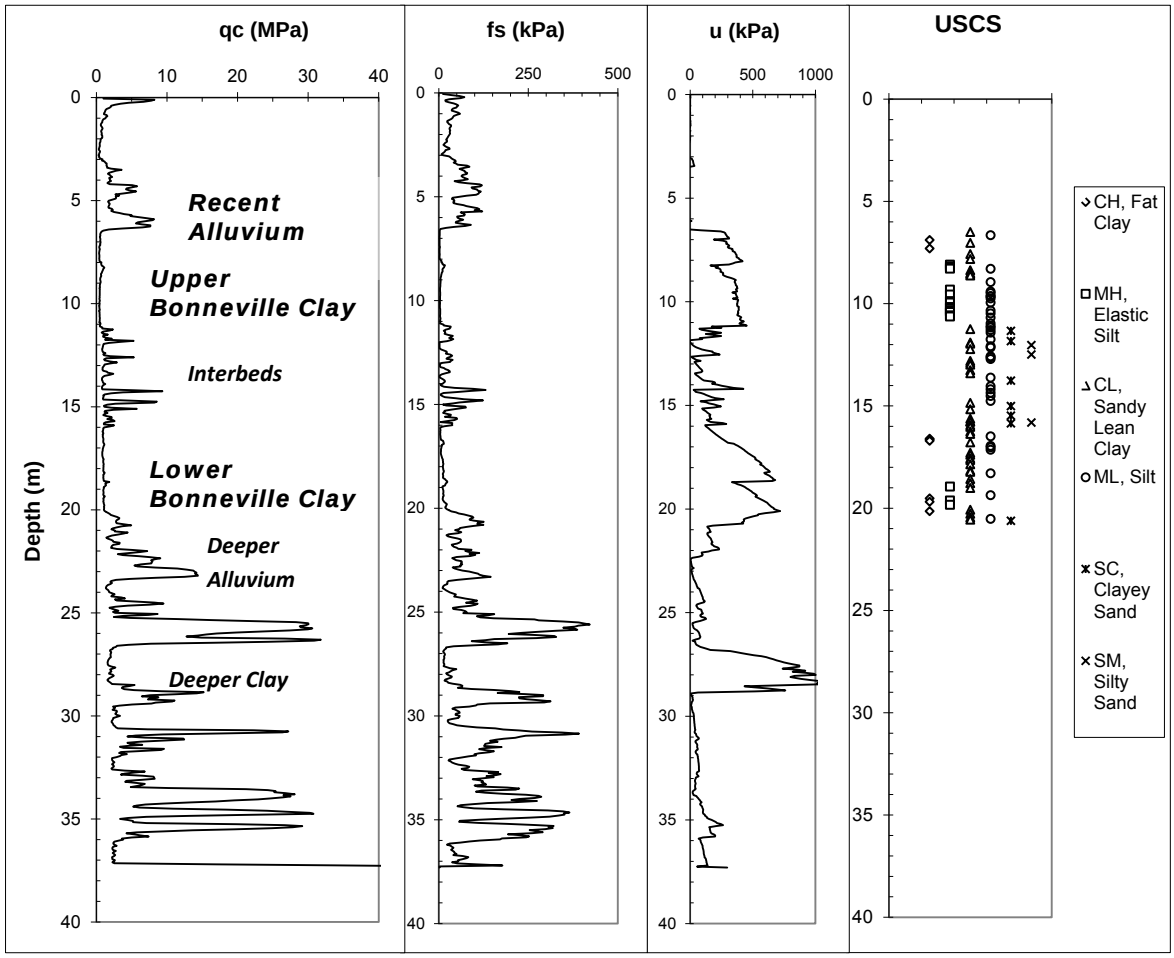

Figure 2.4 Typical cone penetrometer (CPT) log and soil descriptions for downtown segment of I-15 Reconstruction Project, Salt Lake City, Utah (Unpublished I-15 data).

the Lake Bonneville sediments and separate the upper and lower Lake Bonneville clays. These upper and lower clay units are compressible (CR values ranging from 0.1 to 0.35), have relatively low undrained shear strength (25 to 50 kPa) and require substantial time to complete primary consolidation. In this regard, settlement records from the mid-1960s construction of I-15 show that a consolidation settlement over a period of 2 to 3 years. For example, Figure 2-5 shows a settlement record from the mid-1960s construction, for an embankment constructed over the typical soil conditions represented in Figure 2-4. The record

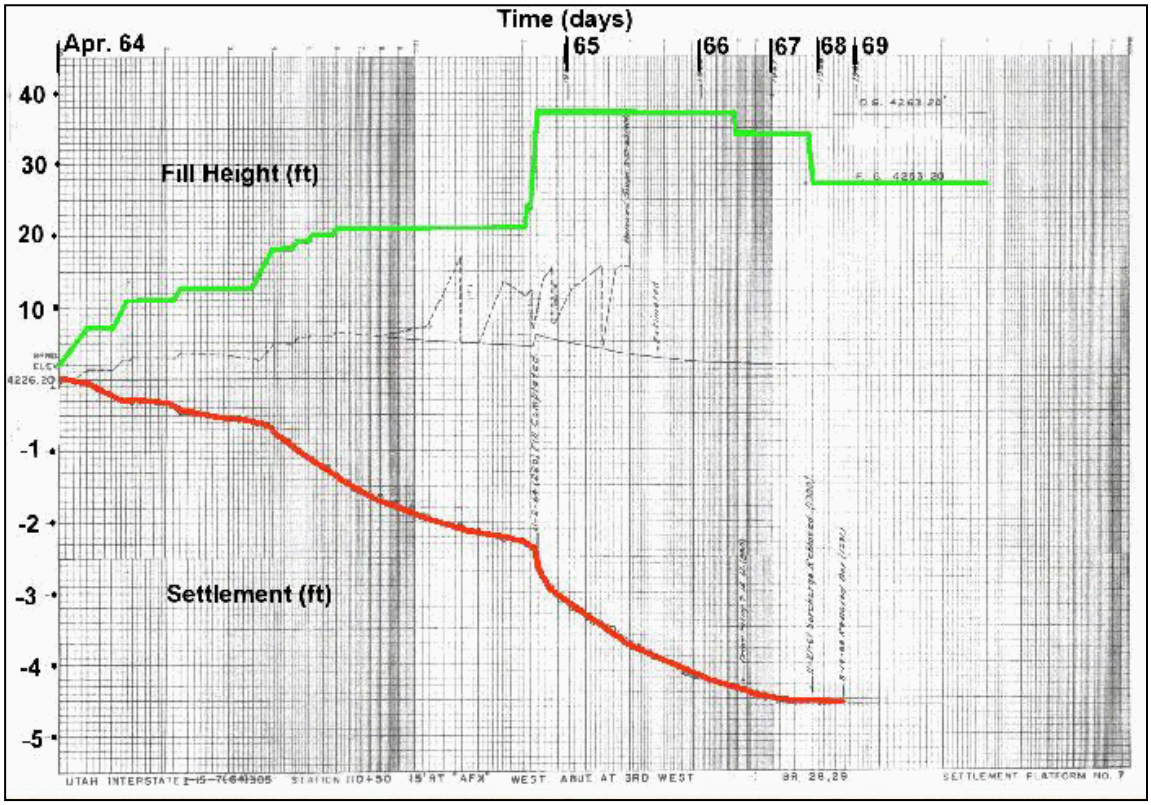

Figure 2-5 Typical settlement record for the mid-1960s construction of I1-5 in downtown Salt Lake City, Utah.

typical 8 to 10 m high embankment underwent 1 to 1.5 m of primary shown in Figure 2-5 is typical of those recorded during the mid-1960s construction for this type of soil condition. This figure shows that fill placement was performed in multiple stages to reach the peak loading condition and then the primary settlement was allowed to take place prior to removal of the surcharge. These large magnitudes of settlement (1.4 m or 4.5 ft) and long consolidation settlement durations (approximately 2 years) can be attributed directly to the soft, thick, compressible Lake Bonneville clay layers. In the mid-1960s, the bridge foundations, bridge, approaches and pavement were not placed until such settlement was essentially finished (Farnsworth et al., 2008).

The I-15 Reconstruction Project team established a long-term performance goal to limit the amount of postconstruction settlement (i.e., secondary compression settlement) of the foundation soils to 3 inches, or less, in a 10-year postconstruction period. The design surcharge height and surcharge duration were calculated to meet this performance goal (Saye and Ladd, 2000).

The I-15 Reconstruction Project utilized three geotechnologies to address the large and potentially damaging effects of primary and secondary consolidation originating from compression of the soft foundation soils prevalent beneath much of the northern part of the project. The first and most widely utilized approach was to apply surcharging in conjunction with the construction of drain (PVDS) were installed in the foundation soils prior to wall or embankment construction. Once the surcharged embankments had reached their design height, primary consolidation settlement of the foundation soil was allowed to take place, followed by surcharge removal.

The second approach was to essentially eliminate most of the potential foundation settlement by using light-weight fill (e.g., scoria and EPS geofoam), thus greatly minimizing the loading condition imposed on the foundation soils.

The third approach involved strengthening the foundation soils by installing lime cement columns prior to placing an MSE wall, thus reducing the magnitude of settlement within the stiffened foundation soils (Farnsworth et al., 2008).

Ladd's (1989) method was used to develop the surcharge design for the MSE walls and earthen embankment construction. For this, it was important to

determine the thickness of the compressible layer(s) and to estimate the reduced rate of secondary compression for the underlying sediments as a function of the amount of surcharge and the surcharge duration. The former was determined from field investigations (i.e., soil boring and CPT soundings) at various locations along the project, and the latter soil properties were evaluated from a laboratory test program using "undisturbed" samples obtained from the field investigation program (Ng, 1998). The laboratory testing was done in a relatively rigorous manner for the project because C. C. Ladd was retained by Woodward-Clyde Consultants as a senior consultant and reviewer for the project. The consolidation and shear strength testing to support the design were done at Massachusetts Institute of Technology (MIT) soil mechanics laboratory under the supervision of C. C. Ladd and the results were reported in Ng (1998).

While the evaluations of Ng (1998) were being performed and finalized, the project team used interim values of C_α /CR equal to 0.0425 from preliminary laboratory testing for the Lake Bonneville deposits performed by Woodward-Clyde Consultants (Saye and Ladd, 2000). Estimates of CR values were back-calculated using soil models developed in M.S. Excel spreadsheets for the Lake Bonneville deposits. To calibrate the CR values used in these models, foundation settlement versus time data were used as obtained by the Utah Department of Transportation (UDOT) from the original I-15 embankment construction records from the northern part of Salt Lake Valley. To constrain the layer thickness used in these models, soil layering was developed from borehole logs at the corresponding locales as obtained from baseline geotechnical investigations

performed just prior to the I-15 Reconstruction Project by various geotechnical consulting firms. As the MIT report (Ng, 1998) became available, the average C_α/CR of 0.0433 was adopted based on laboratory testing by Woodward-Clyde Consultants (WCC) and MIT for the Lake Bonneville deposits, see Figure 2.6. In addition to this design chart, the effects of AAOS on C_α' and the time of initiation of secondary compression, t_s, were needed to complete the design. For the AAOS versus C_α'/C_α relation (Figure 2.7 top), the maximum reduction line (i.e., bottom solid line surrounded by black dots) was used. This was selected because it was based on site-specific samples obtained from the I-15 Project as tested by Ng (1998). Figure 2.7 (bottom) quantifies this the time delay between surcharge removal, t_r, and start of secondary compression, t_s, as a function of

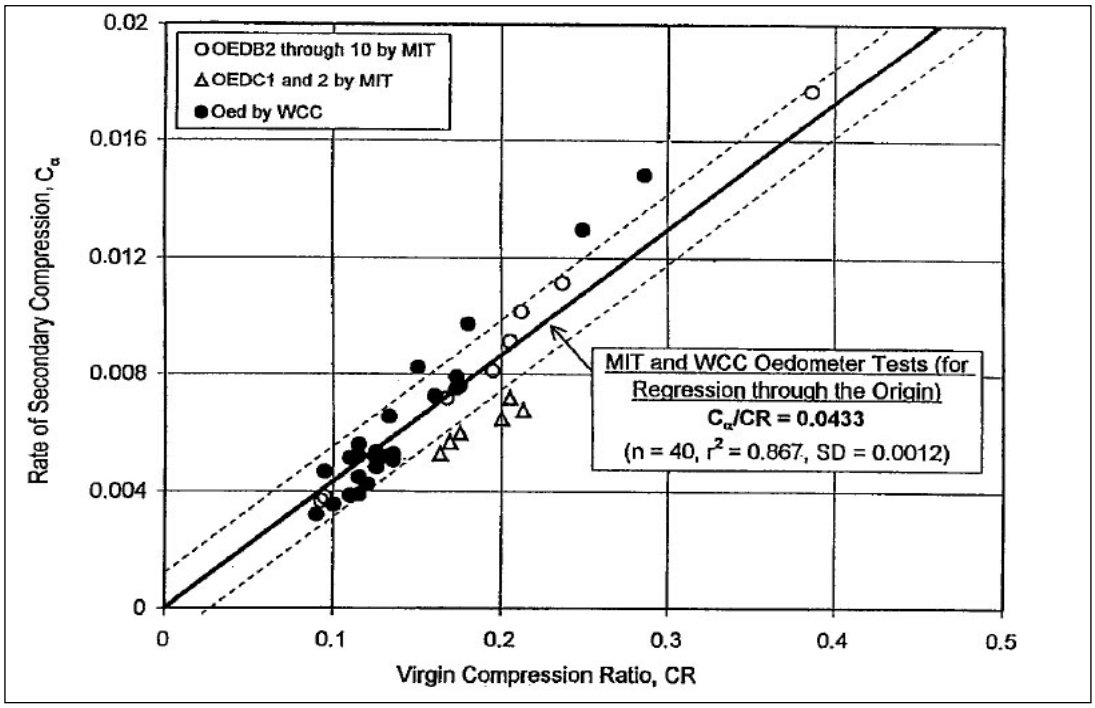

Figure 2.6 Relationship between rate of secondary compression and compression ratio for Lake Bonneville clays. MIT data are labeled by MIT and Woodward-Clyde Consultants are labeled WCC (Saye and Ladd, 2000, unpublished).

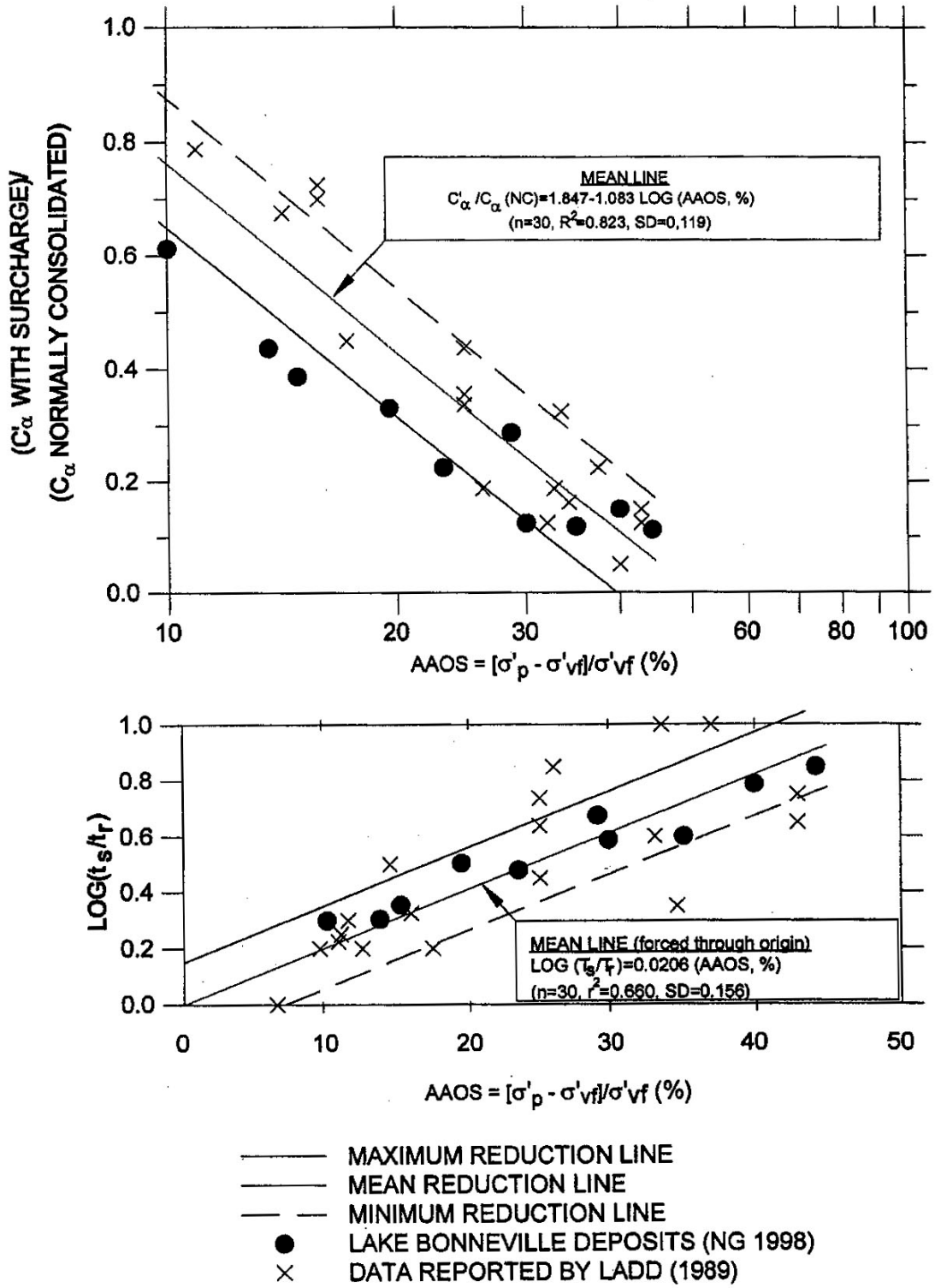

Figure 2.7 Plots showing the relationship of AAOS on C_{α}' and the time of initiation of secondary compression, t_s. (Top) C_{α}'/ C_{α} as a function of AAOS (Bottom) Log(t_s/t_r) ratios as a function of AAOS (Saye and Ladd, 2000, unpublished).

AAOS based on testing done by Ladd (1989) and Ng (1998). This figure shows that the start of secondary compression has greater delay for higher amounts of surcharge. Such delay is beneficial in reducing the amount of secondary compression over a given postconstruction period. In regards to t_s/t_r versus AAOS, the average line was selected for design purposes for the I-15 Reconstruction Project (Saye and Ladd, 2000).

3 RESEARCH OBJECTIVES AND TASKS

3.1 Research Objectives

The primary objectives addressed in this research are as follows: 1) corroborate Mesri's concept of secondary compression (i.e., C_α/CR is relatively constant) for the Lake Bonneville deposits along the Wasatch Front in Utah, 2) supplement and/or revise, as necessary, the design relationships developed by Ng (1998) for the I-15 surcharge design using a larger set of field and laboratory test data, (3) recommend an appropriate laboratory testing and evaluation program to support project-specific surcharge design for future highway embankment projects sponsored by the Utah Department of Transportation (UDOT) in the Wasatch Front Area.

3.2 Research Plan

To accomplish these research objectives, a field investigation and collection of undisturbed samples of soils in the Wasatch Front area will be performed. The specimens acquired during the field investigation will be tested to develop design charts consistent with the design parameters required to implement Ladd's (1989) method. In addition, the data acquired from this research will be evaluated and compared with existing data and relations developed by Ng (1998).

3.3 Tasks

The major tasks needed to achieve the above research objective are:

1) Review of the existing literature regarding secondary compression and how a surcharging program can be implemented to reduce secondary settlement. This will include a description of Ladd's and Mesri's methodologies. This has been completed and is summarized in Chapter 2.
2) Obtain undisturbed samples from 4 locations located along the Wasatch Front, Utah including: (1) 400 South Street in Salt Lake City, (2) Provo South Interchange, (3) Springville 400 South Overpass Structure, and (4) Layton Interchange. The undisturbed samples will be obtained using mud rotary drilling and piston sampling at sites where long-term monitoring of settlement has been ongoing as part of instrument arrays sponsored by the UDOT. Soil samples from the area near these arrays will be used in the laboratory test program.
3) Develop and implement a laboratory test program to acquire secondary compression consolidation data and the design parameters associated with Ladd's (1989) method. The undisturbed samples and the associated laboratory tests will be performed on fine-grained, cohesive soils to determine design parameters such as σ_p, CR, RR, C_α, and C_α'.
4) Evaluate the design parameters obtained from the laboratory testing program and compare them with those published by Ng (1998). Specifically, the parameters compared will be the C_α/CR ratio of Ng (1998) and the normalized C_α'/C_α and $\log(t_s/t_r)$ versus AAOS.

5) Make recommendations regarding the implementation of laboratory testing program and the steps and procedures required to implement a site-specific surcharge design for future UDOT embankment projects founded on soft soil sites.

4 FIELD INVESTIGATIONS

4.1 Introduction

A field investigation was performed for the purpose of collecting samples of fine-grained soils along the Wasatch Front at sites where long-term settlement data were available. These sites were selected because long-term instrumentation and settlement monitoring had been performed at these sites over the past 10 years. These undisturbed soil samples were tested in the U of U Civil and Environmental Engineering Soil Mechanics laboratory to determine soil properties and design parameters required for engineering evaluations such as σ_p, CR, RR, C_α, and C_α'.

4.2 Field Investigations

The four drilling sites were: (1) 400 South at 400 South and 800 West just east of I-15 in Salt Lake City Utah (see Figure 4.1) (2) South Layton at Layton Parkway and Main Street in South Layton Utah. This site is in an empty lot northeast of the Layton Parkway and Main Street intersection west of I-15 (see Figure 4.2). (3) Springville at 400 South and just south of 750 East in Springville Utah. This site is west of the railroad tracks and on the south side of the railroad tracks overpasses (see Figure 4.3). (4) Provo at the University Avenue I-15 southbound on ramp in Provo Utah. This site is at the point where the

Figure 4.1 400 South site (400 South 800 West). (Top) Vicinity map for drilling site (Bottom) Close up of drilling site.

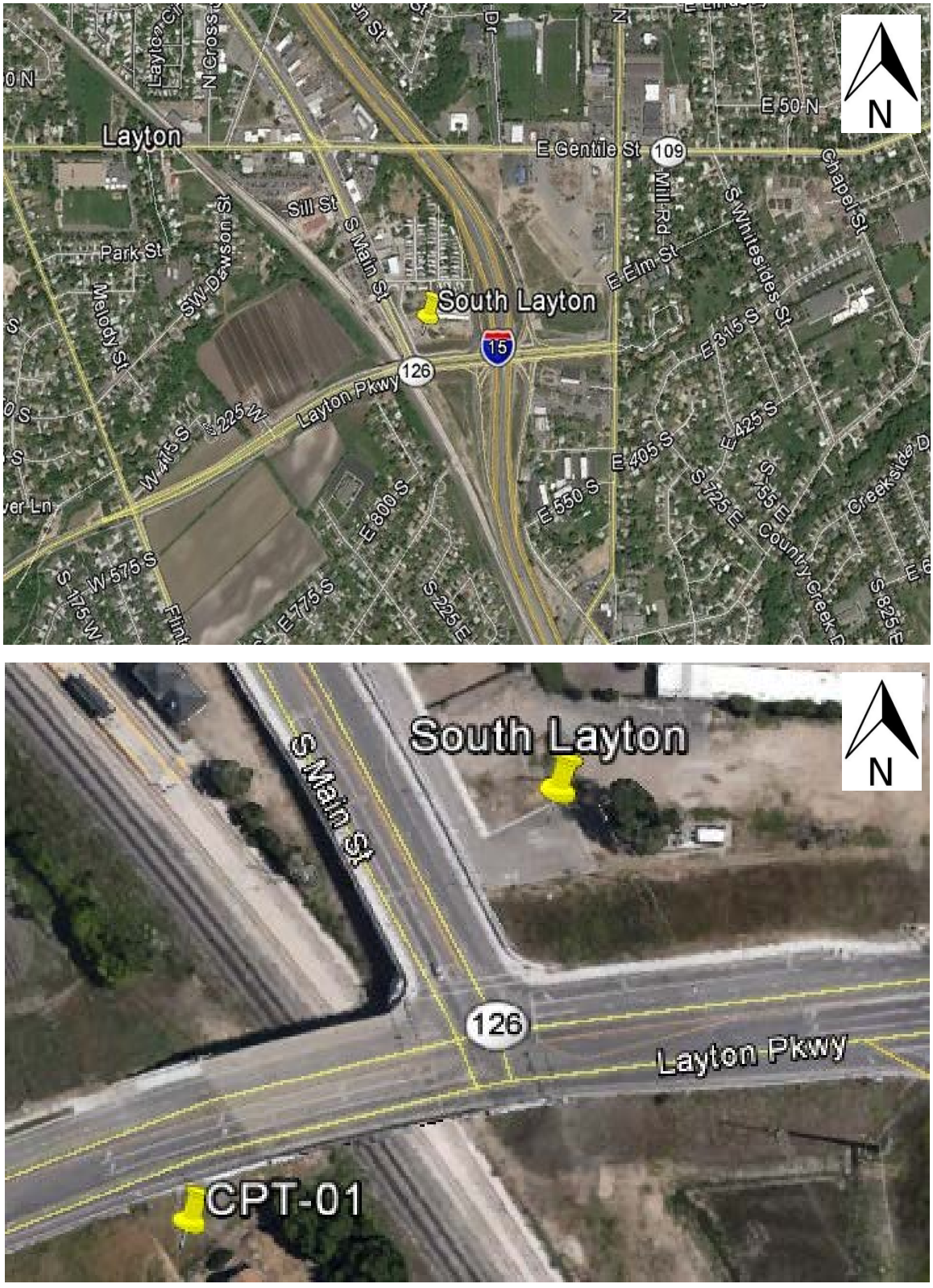

Figure 4.2 South Layton site (Layton Parkway and Main Street). (Top) Vicinity map for drilling site (Bottom) Close up of drilling site.

Figure 4.3 Springville site (400 South and 1500 West). (Top) Vicinity map for drilling site (Bottom) Close up of drilling site.

southbound on ramp for University Avenue and the on and off ramp for southbound traffic for 1860 South meet see Figure 4.4. For longitude and latitude, depths, and drilling dates, see Table 4.1

The drilling was performed with the use of a truck-mounted CME 75 drill rig using mud rotary drilling in a 4-inch casing. The primary purpose of the drilling was to obtain piston samples from the cohesive, fine-grained soils of Lake Bonneville and recent lacustrine deposits. The piston sampling used standard galvanized-steel Shelby tubes with a 2.8 inch inner diameter and a 3.0 inch outer diameter, with an overall length of 30 inches.

The depths selected for soil sampling were determined using CPT logs that were performed by others at or near the locations of the boreholes. The locations of the CPT soundings are shown in Table 4.2. For the CPT logs, see Figures 4.5 to 4.9.

The samples were immediately logged and labeled by location and depth. The logs for the boreholes are given in Figures 4.10 to 4.14. Samples were sealed with plastic Shelby caps and wrapped with duct tape to maintain their in situ moisture content. They were carefully transported and stored in a humidified room in the University of Utah Concrete Laboratory until the consolidation testing could be performed.

Figure 4.4 Provo site (Southbound I-15 on ramp for University Avenue). (Top) Vicinity map for drilling site (Bottom) Close up of drilling site and CPT location.

Table 4.1 Boring locations, depths, and drilling dates

#	Site	Latitude	Longitude	BH Depth (ft.)	Drilling Date
1	400 South	40°45'40.02"N	111°54'45.61"W	92	12/5/2012
2	S. Layton	41° 3'23.25"N	111°57'47.63"W	142	2/5/2013
3	Springville	40° 9'39.78"N	111°38'18.43"W	129	4/1/2013
4	Provo	40°12'26.41"N	111°39'39.43"W	127	4/5/2013

Table 4.2 CPT Locations

Site	CPT	Latitude	Longitude
400 South	06-SC-159	40° 45’ 39.06”N	111° 54’ 49.02”W
S. Layton	CPT-01	41° 3' 16.42"N	111° 57' 47.63"W
Springville	CPT-01	40° 9' 39.89"N	111° 38' 20.03"W
Springville	CPT-07	40° 9' 39.90"N	111° 38' 17.75"W
Provo	CPT-07	40°12' 25.08"N	111° 39' 39.30"W

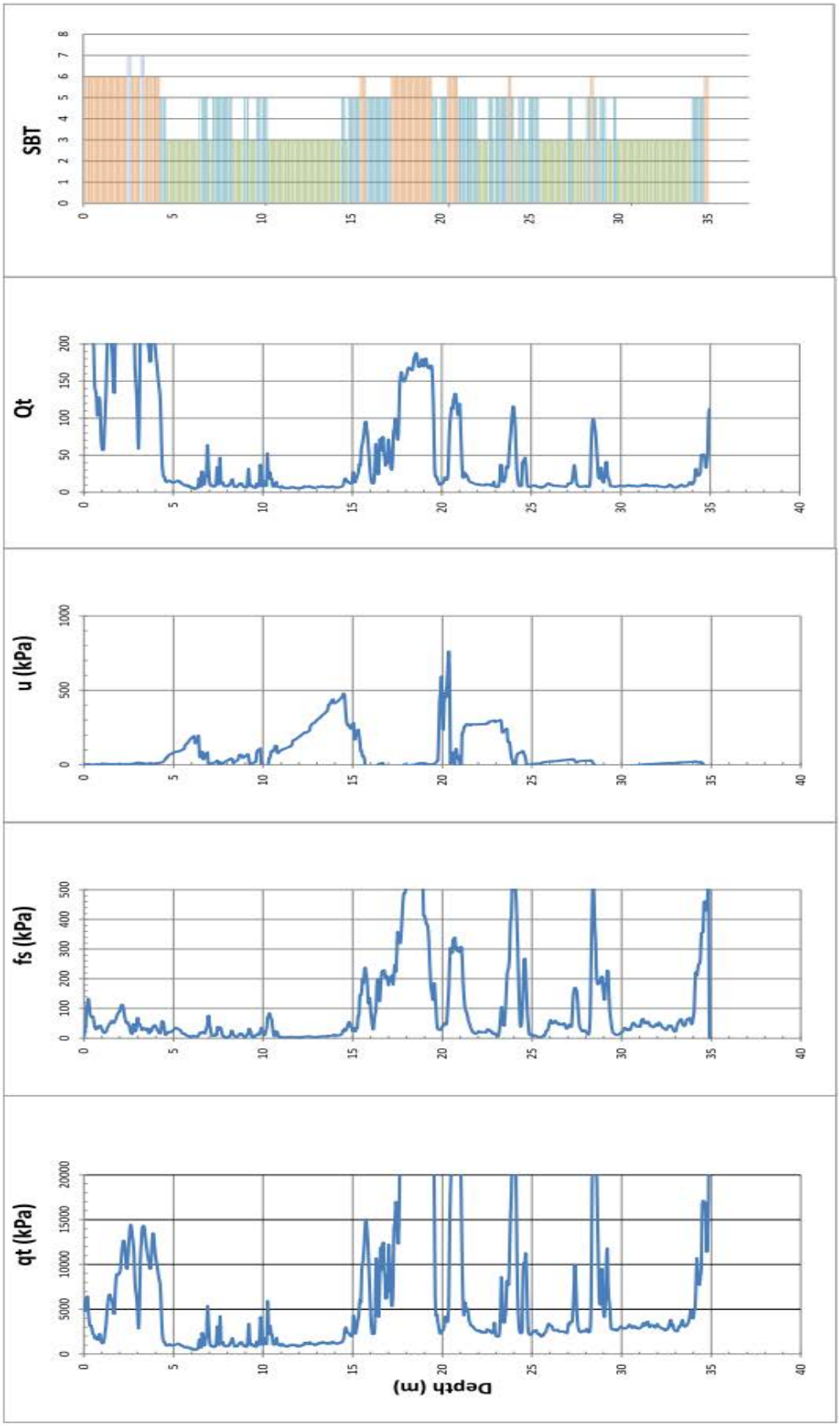

Figure 4.5 CPT for 400 South 06-SC-159.

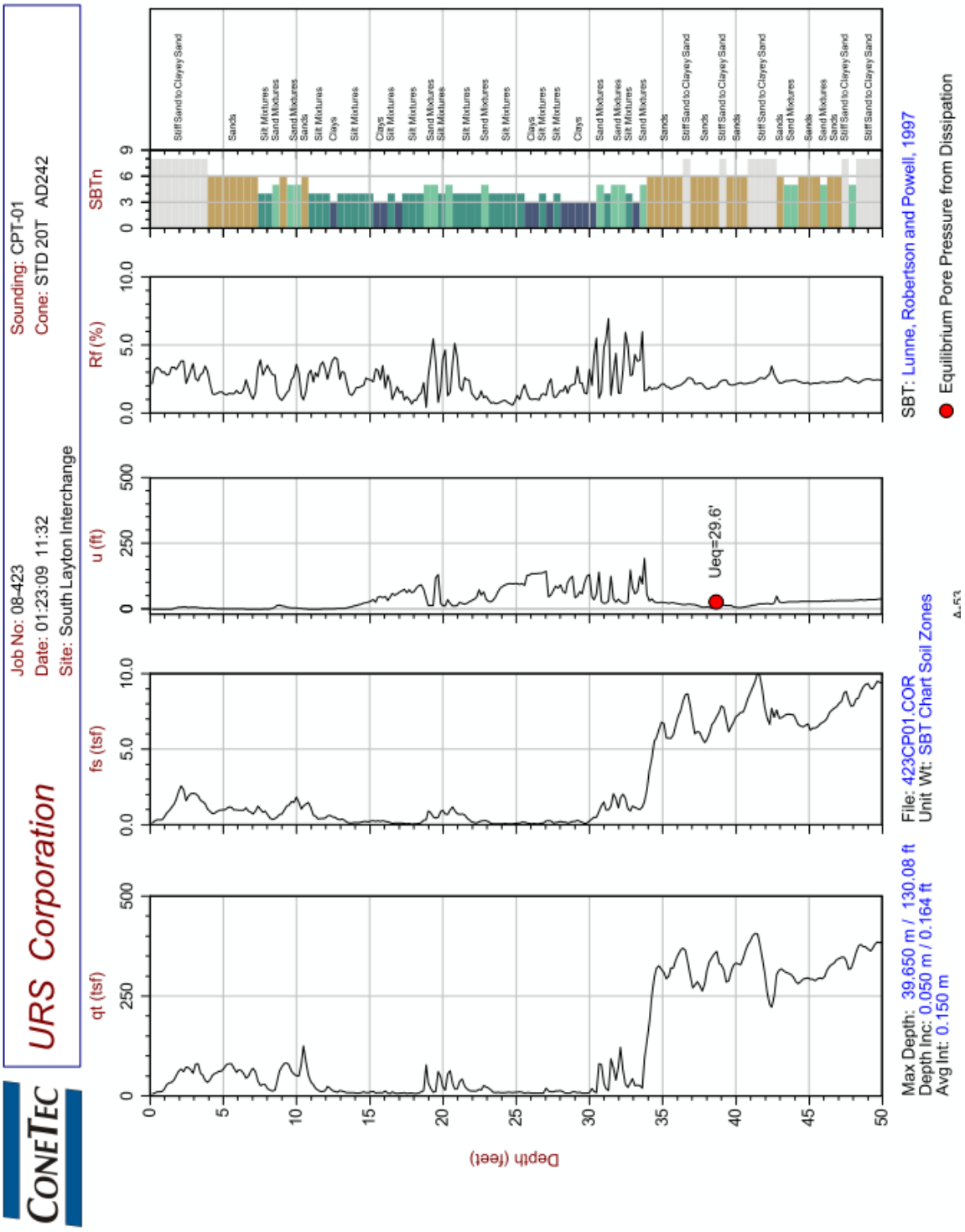

Figure 4.6 CPT for South Layton CPT-01.

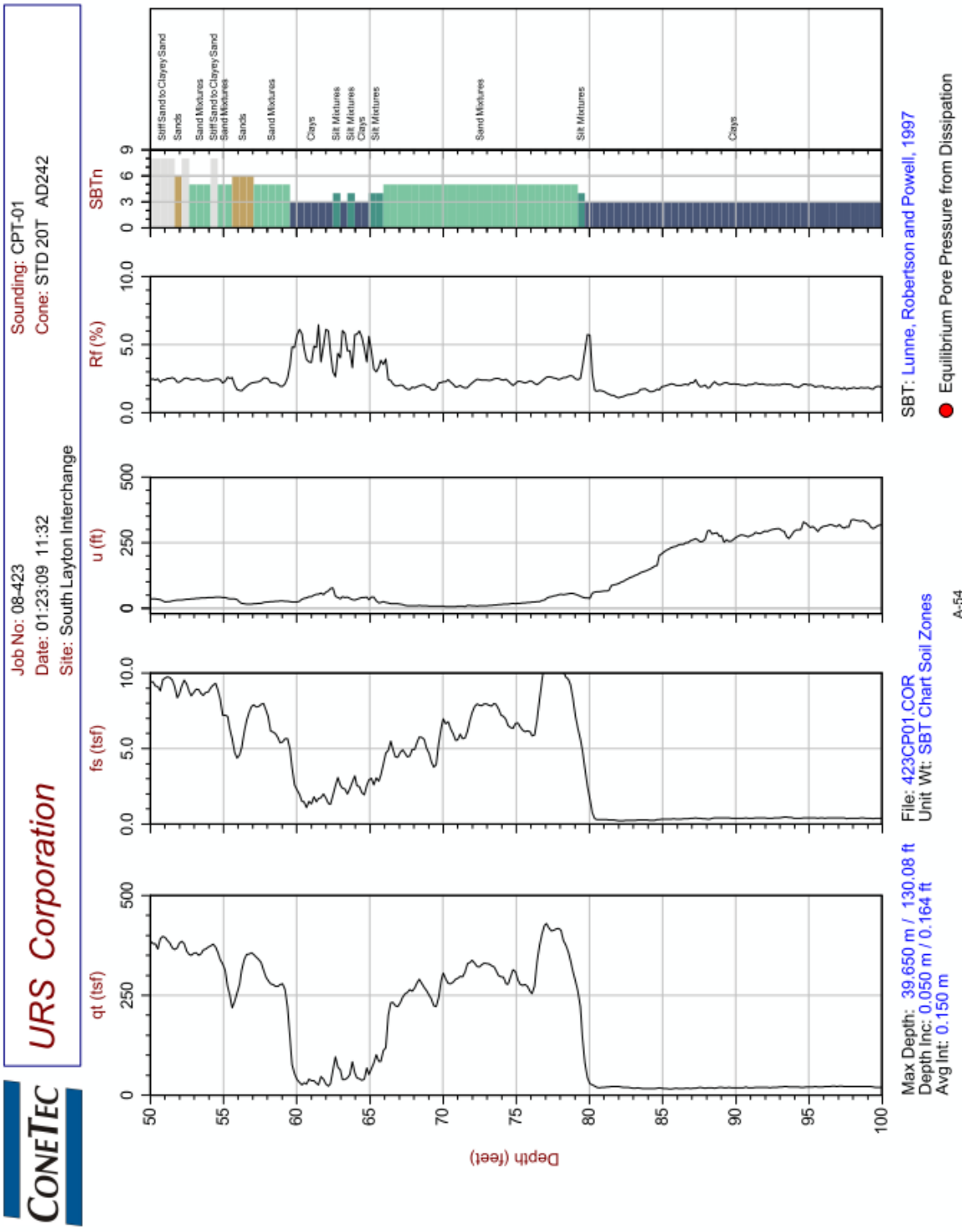

Figure 4.6 Continued.

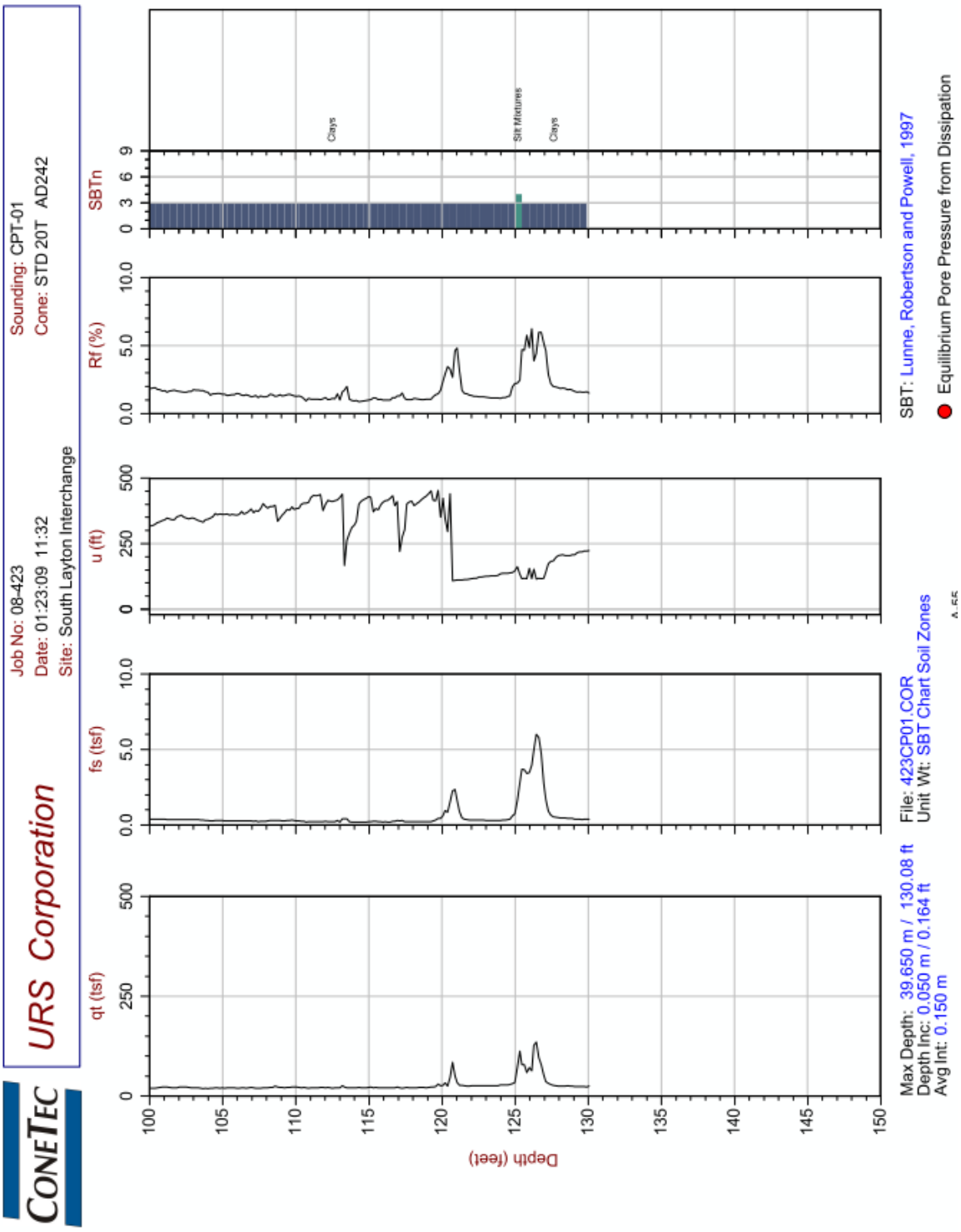

Figure 4.6 Continued.

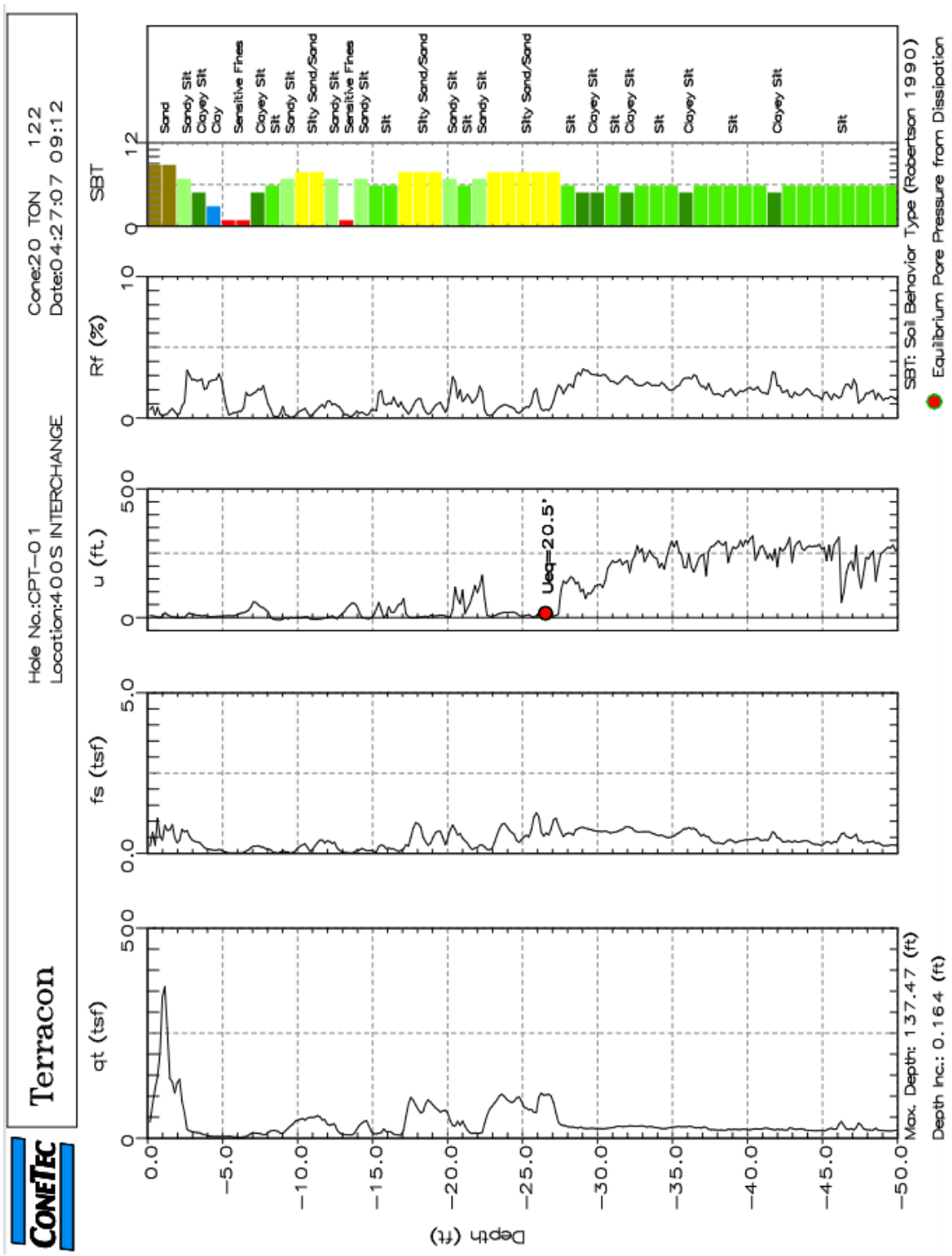

Figure 4.7 CPT for Springville CPT-01.

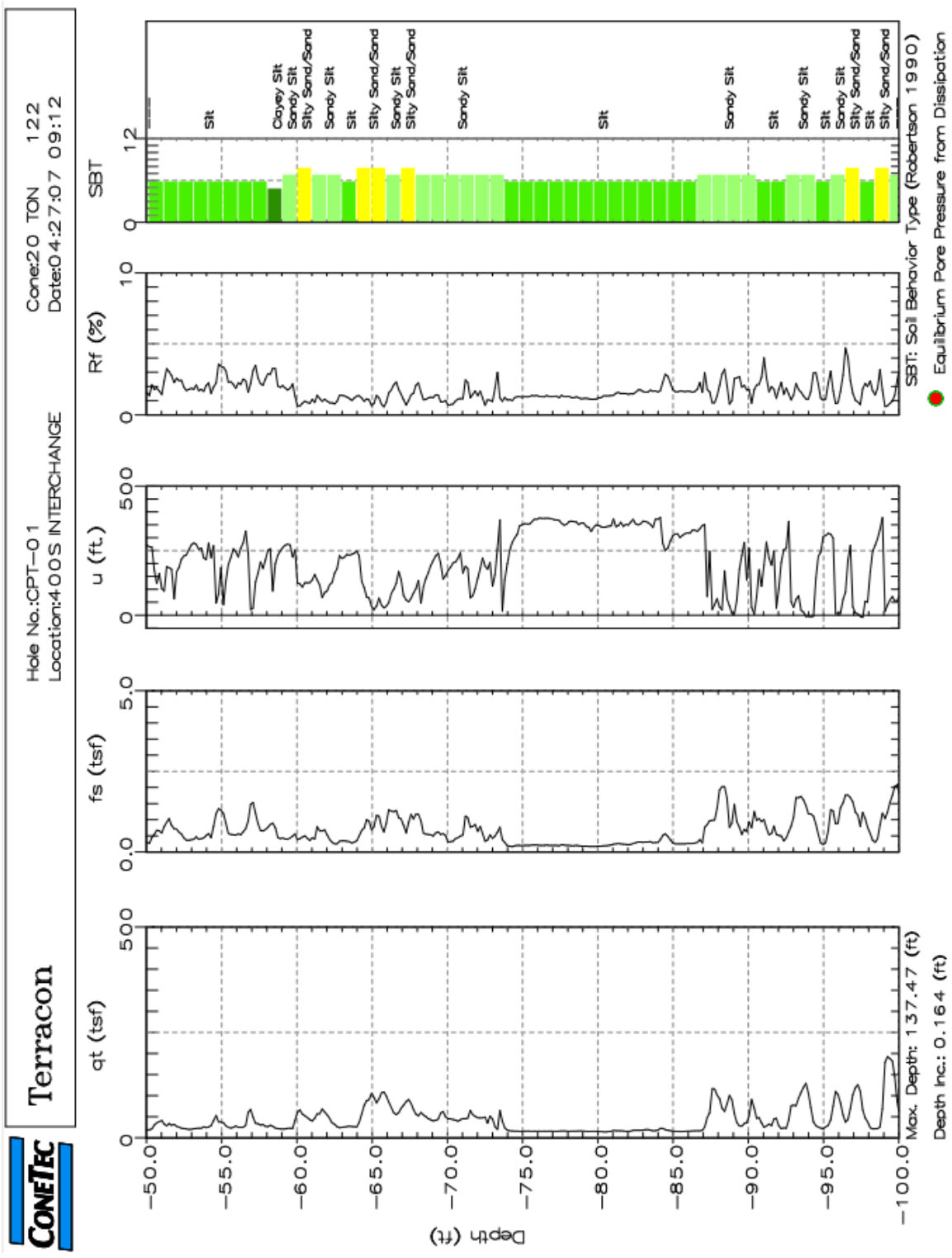

Figure 4.7 Continued.

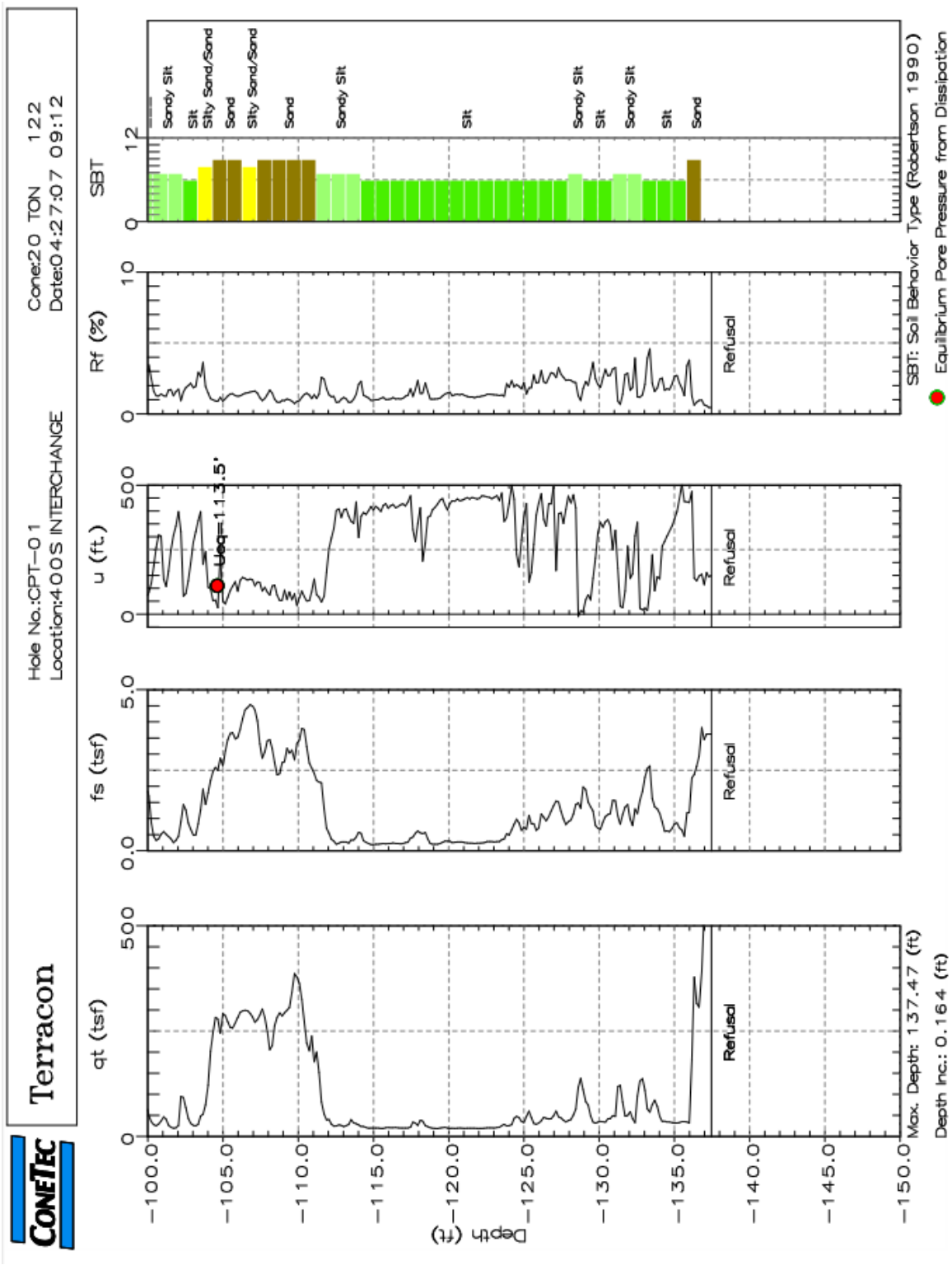

Figure 4.7 Continued.

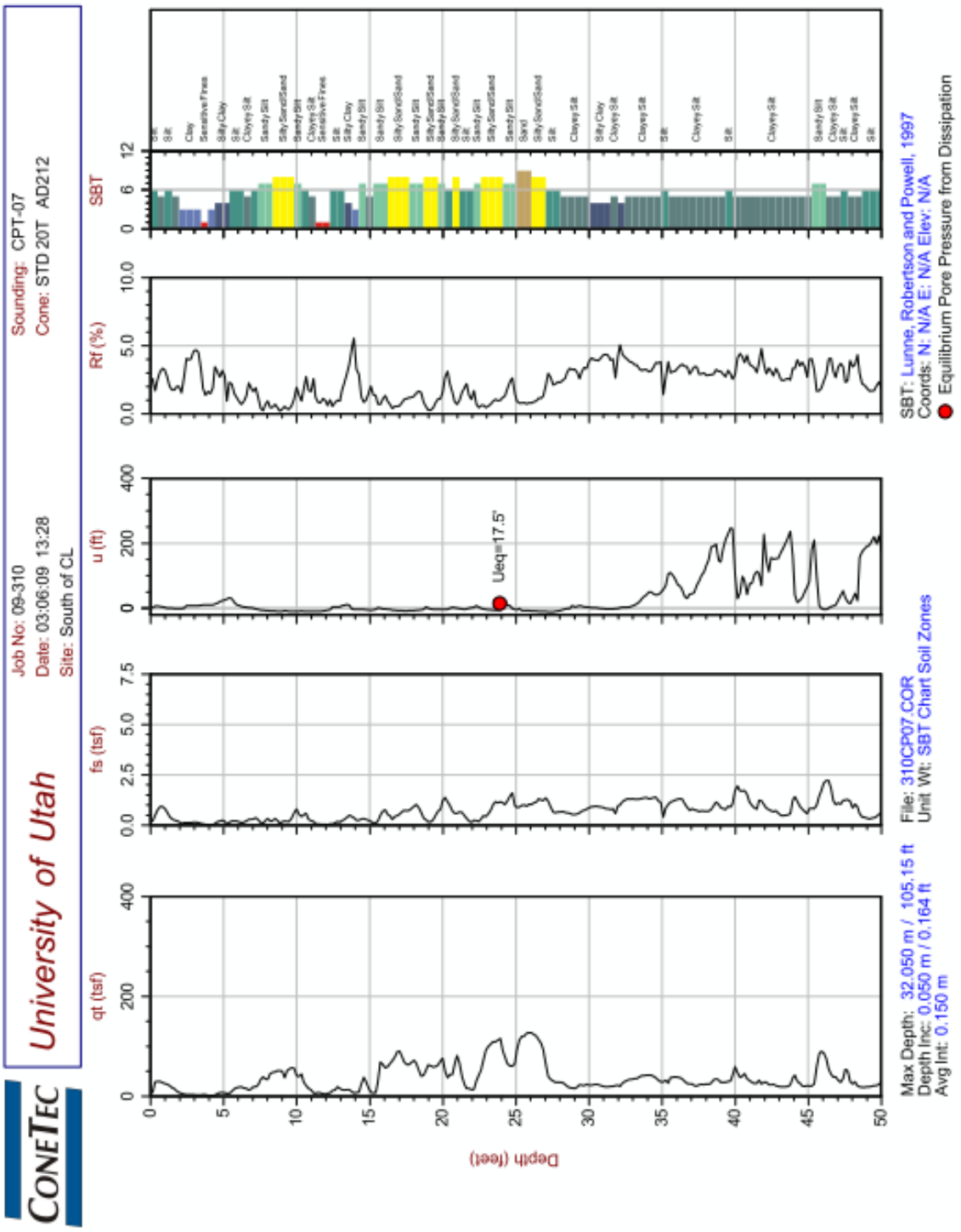

Figure 4.8 CPT for Springville CPT-07.

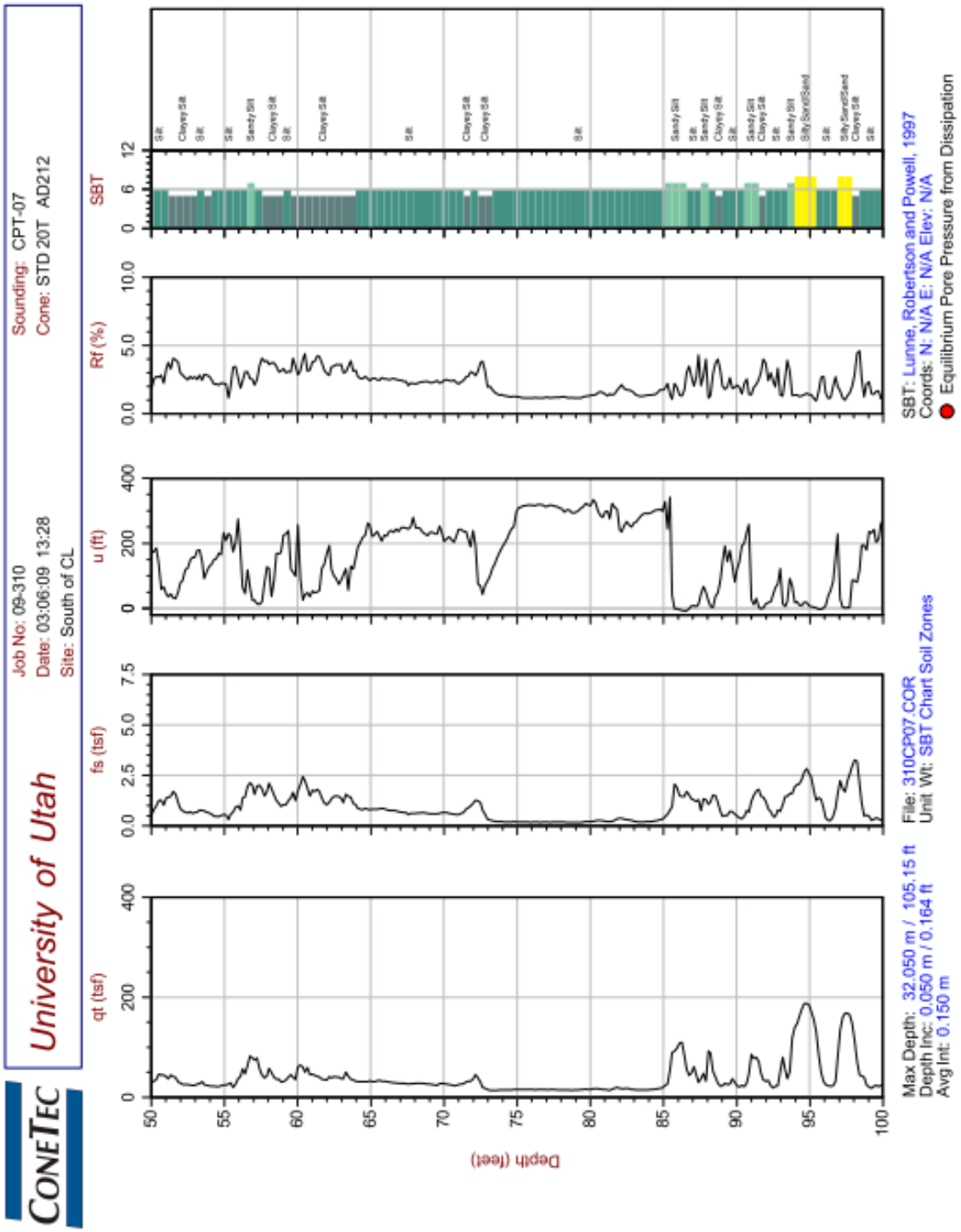

Figure 4.8 Continued.

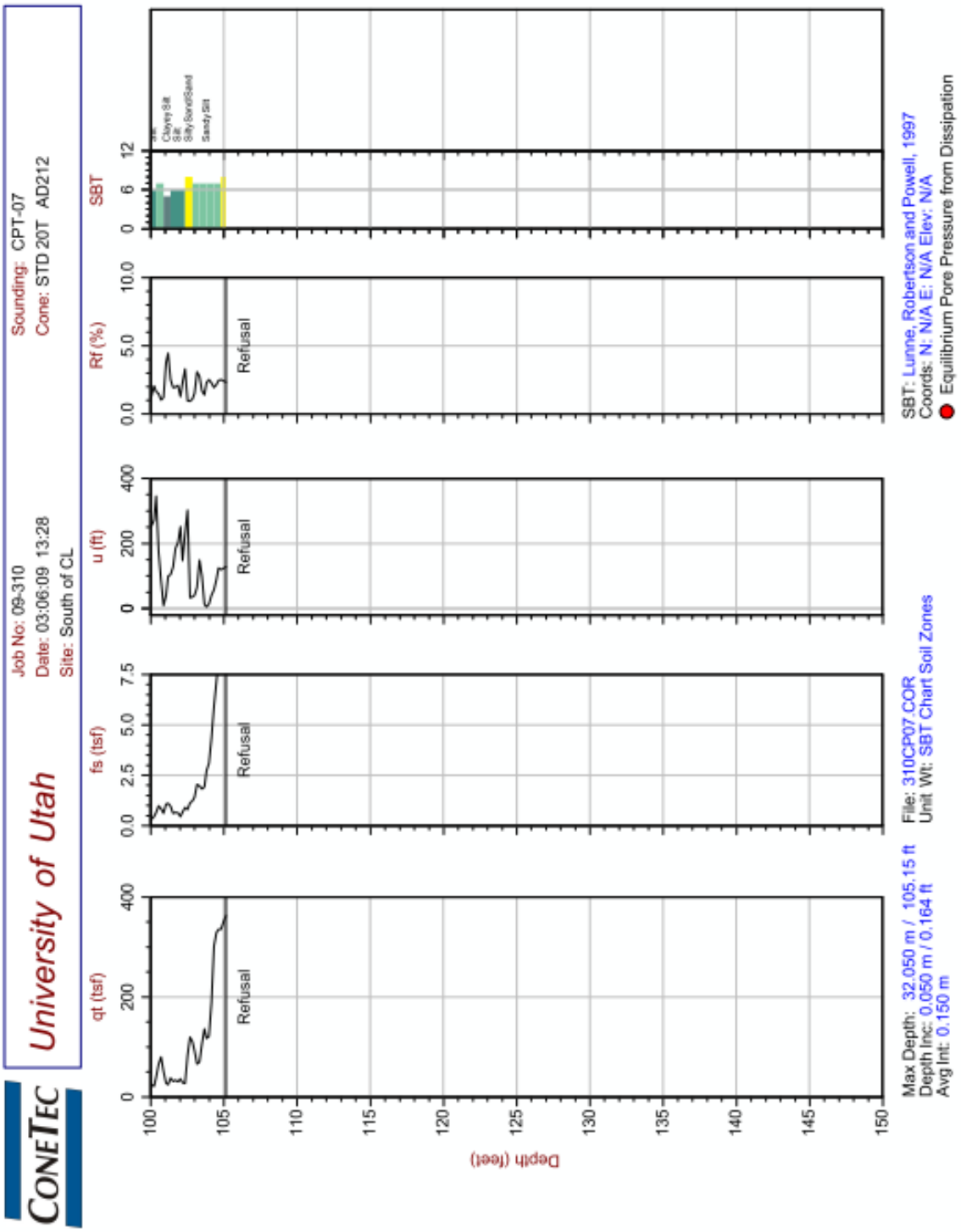

Figure 4.8 Continued.

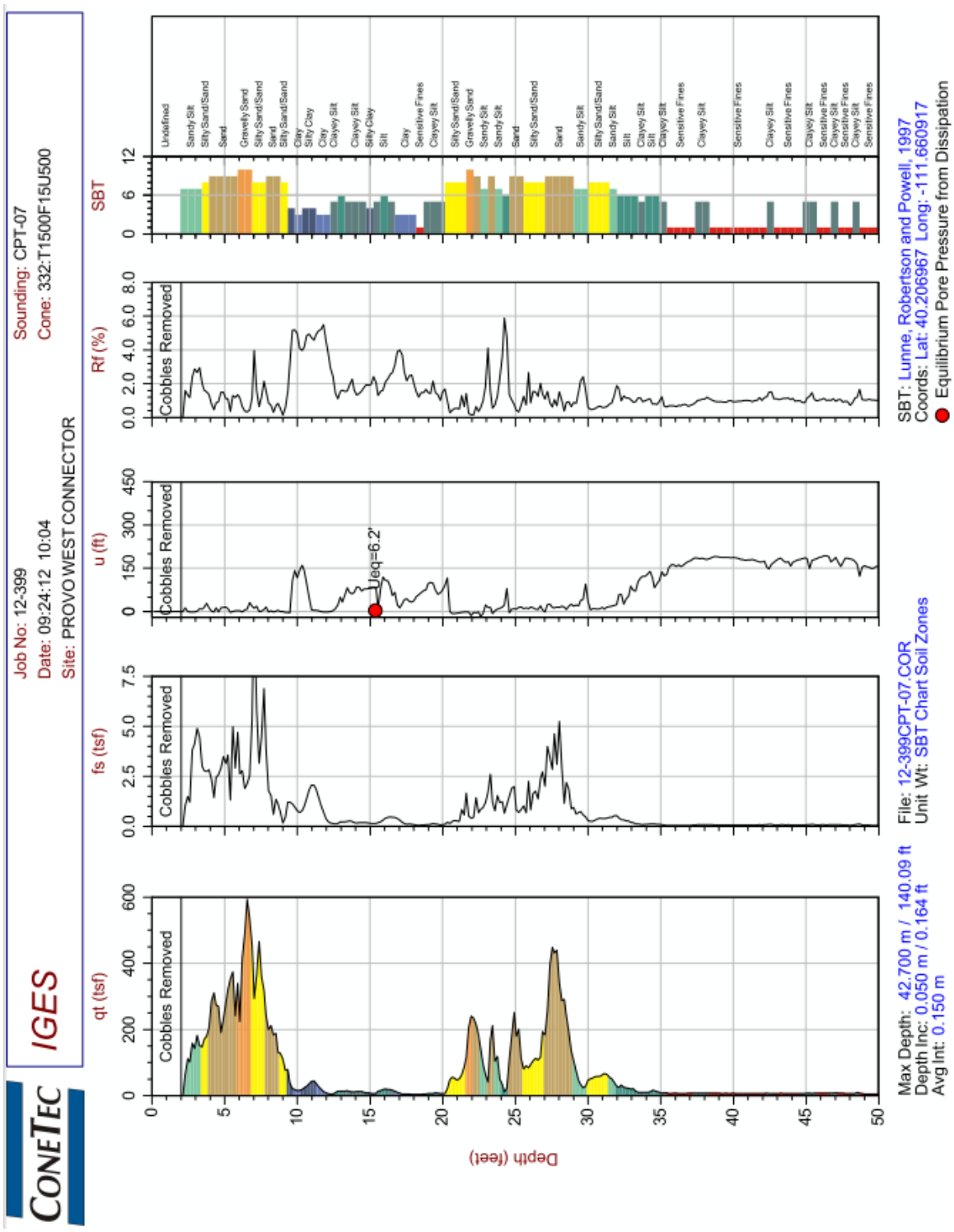

Figure 4.9 CPT for Provo CPT-07.

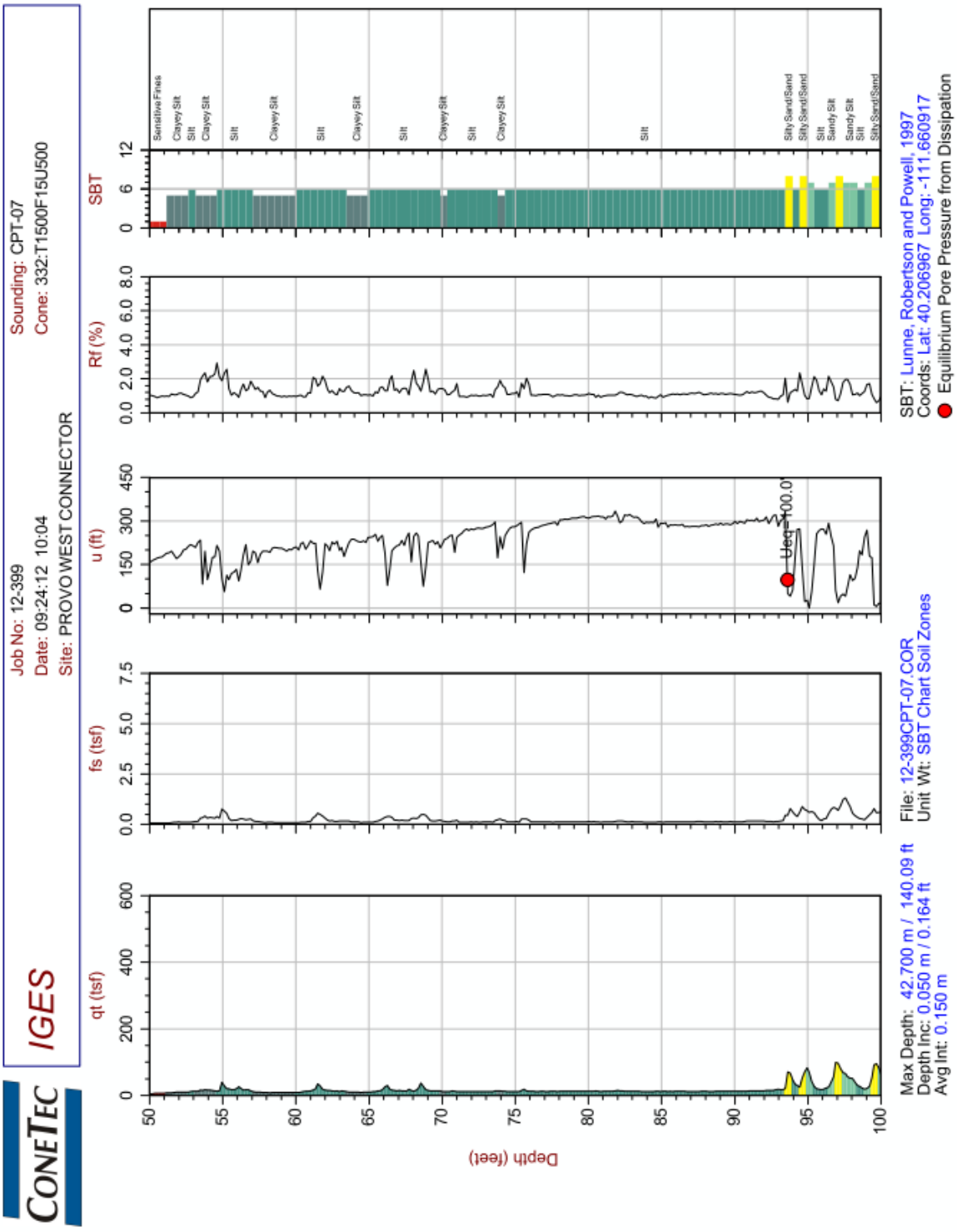

Figure 4.9 Continued.

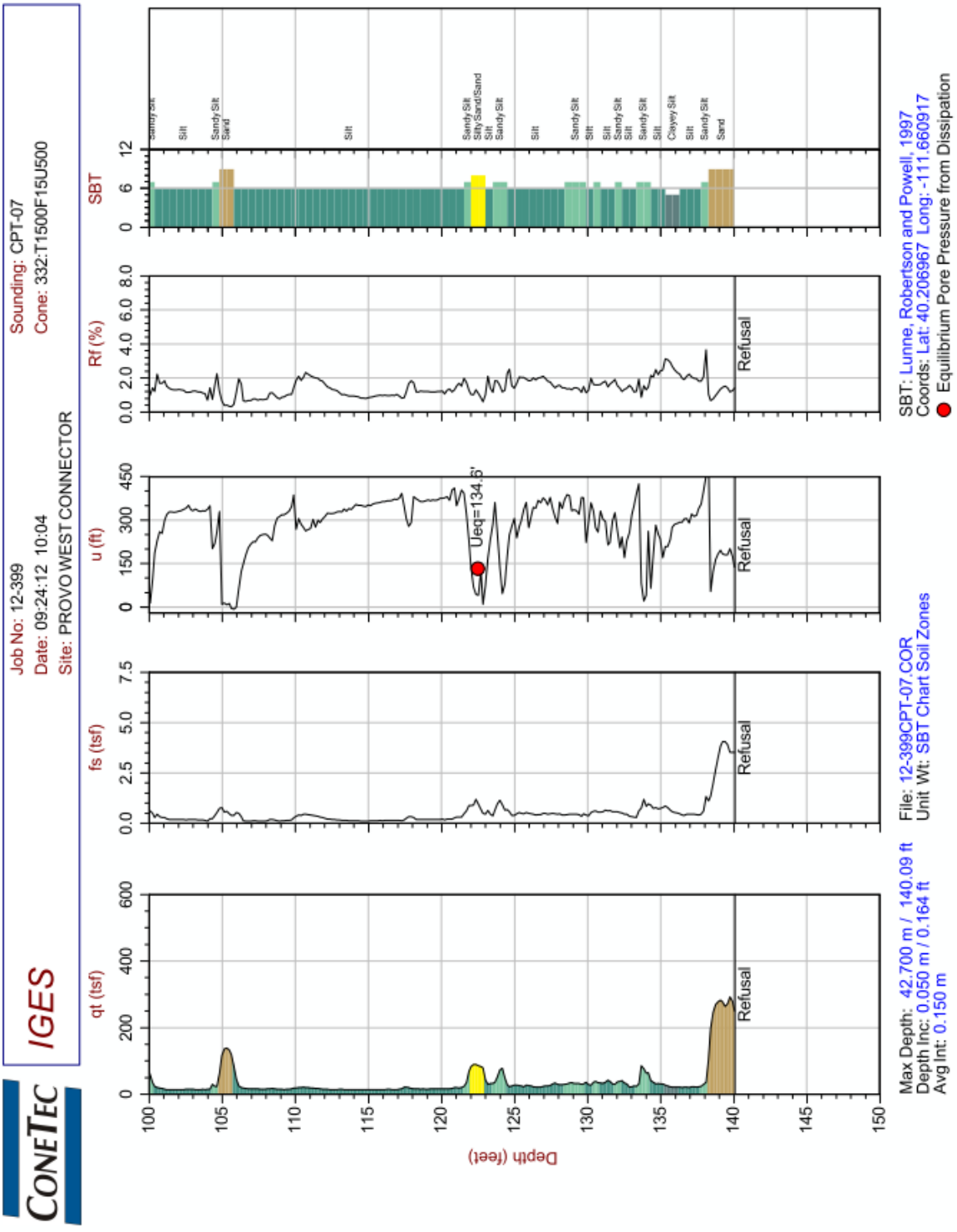

Figure 4.9 Continued.

400 South

By Zach Gibbs — Test Hole I

Elevation (ft)	Sample Depth (ft)	Visual Soil Description	Sample Recovery (in)	Soil Symbols	Penetration N (blows/ft)	Remarks and raw SPT data
4196						- No samples taken
4185	10-12	SAND, medium grained, gray to green gray (SP)	24		20	- 5 9 9 11
	12.5-14.5	CLAY, silty, gray (CL)	24		0	- 0 weight of hammer
	15-17	SILT, soft, gray (MH)	24		ST	
	17.5-19.5	SILT, soft, gray (MH)	24		ST	
4175	20-22	SILT, soft, gray (MH)	24		ST	- sluff sand had to clean out the hole
	22.5-24.5	CLAY, silty, gray (CL)	24		ST	
	25-27	CLAY, silty, gray (CL)	24		ST	- Inter beds
	27.5-29.5	CLAY, silty, gray (CL)	24		ST	
4165	30-32	CLAY, silty, gray (CL)	24		ST	
	32.5-34.5	SILT, soft, gray (ML)	24		ST	
	35-37	No recovery	0		ST	- probably sands
	37.5-39.5	CLAY, silty, gray (CH)	24		ST	
4155	40-42	CLAY, silty, gray (CH)	24		ST	
	42.5-44.5	CLAY, silty, gray (CL)	24		ST	
	45-47	CLAY, silty, gray (CL)	24		ST	
	47.5-49.5	CLAY, silty, gray (CL)	24		ST	
4145	50-52	CLAY, silty, with sand, gray (CL)	24		ST	
	52.5-54.5	CLAY, silty, with sand, gray (CL)	24		ST	
	55-57	No recovery	0		14	- put a spt after no recovery 5 4 5 9
4135	60-62	CLAY, silty, with sand, gray (CL)	24		ST	
	65-67	CLAY, silty, gray (CL)	24		ST	
4125	70-72	SAND, silty (SM)	24		ST	
4115	80-82	SAND, clayey, fine grained (SC)	24		ST	
4105	90-92	CLAY, gray (CL)	24		ST	

Soil Symbols

Sand:
Silt:
Clay:

Other Symbols

Notes :

Driller :	Bedke
Boring Number :	400 South
Date Drilled :	12/5/2012
Job Number :	1
Site Location :	Salt Lake City, Ut.
	400 South
Test Method :	ASTM D 1586
Hammer Type :	Automatic Trip Hammer
	140 lb
Sampler :	Shelby tube
	24 in. Sampler
Drilling Method :	Mud Rodery
	4" casing
Make of Drilling Rig :	CME 75
	(Truck Mounted)

Figure 4.10 Test Hole Log for 400 South.

South Layton

By Zach Gibbs — Test Hole I

Elevation (ft)	Sample Depth (ft)	Visual Soil Description	Sample Recovery (in)	Soil Symbols	Penetration N (blows/ft)	Remarks and raw SPT data
4341						
4337.5	2.5-4.5	SAND, silty (SM)	24		ST	
4335	5-7	SAND, silty (SM)	24		ST	
4332.5	7.5-9.5	SAND, silty (SM)	24		ST	
4330	10-12	SAND, silty (SM)	24		ST	
4327.5	12.5-14.5	CLAY (CL)	24		ST	
4325	15-17	CLAY (CL)	24		ST	
4322.5	17.5-19.5	CLAY (CL)	24		ST	
4320	20-22	CLAY, sandy (CL)	24		ST	

Soil Symbols

Sand:
Silt:
Clay:

Other Symbols

Notes :

Driller :	Bedke
Boring Number :	South Layton
Date Drilled :	2/5/2013
Job Number :	2
Site Location :	South Layton Ut.
	Layton Parkway and Main street
Test Method :	ASTM D 1586
Hammer Type :	Automatic Trip Hammer
	140 lb
Sampler :	Shelby tube
	24 in. Sampler
Drilling Method :	Mud Rodery
	4" casing
Make of Drilling Rig :	CME 75
	(Truck Mounted)

Figure 4.11 Test Hole Log for South Layton Test Hole I.

South Layton

By Zach Gibbs — Test Hole II

Elevation (ft)	Sample Depth (ft)	Visual Soil Description	Sample Recovery (in)	Soil Symbols	Penetration N (blows/ft)	Remarks and raw SPT data
4341						
4337.5	2.5-4.5	SAND, silty (SM)	24		ST	
4335	5-7	SAND, silty (SM)	24		ST	
4332.5	7.5-9.5	SAND, silty (SM)	24		ST	
4330	10-12	SAND, silty (SM)	24		ST	
4327.5	12.5-14.5	CLAY (CL)	24		ST	
4325	15-17	CLAY (CL)	24		ST	
4322.5	17.5-19.5	CLAY (CL)	24		ST	
4320	20-22	CLAY, sandy (CL)	24		ST	
4290	50-52	SAND, clayey (SC)	24		ST	
4285	55-57	SAND, clayey (SC)	24		ST	
4260	80-82	CLAY (CL)	24		ST	
4255	85-87	CLAY (CL)	24		ST	
4250	90-92	CLAY (CL)	24		ST	
4245	95-97	CLAY (CL)	24		ST	
4240	100-102	CLAY (CL)	24		ST	
4235	105-107	CLAY (CL)	24		ST	
4230	110-112	CLAY (CL)	24		ST	
4225	115-117	CLAY (CL)	24		ST	
4220	120-122	CLAY (CL)	24		ST	
4215	125-127	CLAY (CL)	24		ST	
4210	130-132	CLAY (CL)	24		ST	
4205	135-137	CLAY (CL)	24		ST	
4200	140-142	CLAY (CL)	24		ST	

Soil Symbols

Sand:
Silt:
Clay:

Other Symbols

Notes : BH II is located 5 ft. north of BH I

Driller :	Bedke
Boring Number :	South Layton
Date Drilled :	2/5/2013 - 2/6/2013
Job Number :	2
Site Location :	South Layton Ut. Layton Parkway and Main street
Test Method :	ASTM D 1586
Hammer Type :	Automatic Trip Hammer 140 lb
Sampler :	Shelby tube 24 in. Sampler
Drilling Method :	Mud Rodery 4" casing
Make of Drilling Rig :	CME 75 (Truck Mounted)

Figure 4.12 Test Hole Log for South Layton Test Hole II.

Springville

By Zach Gibbs — Test Hole I

Elevation (ft)	Sample Depth (ft)	Visual Soil Description	Sample Recovery (in)	Soil Symbols	Penetration N (blows/ft)	Remarks and raw SPT data
4520						- No samples taken
4504	15-17	SILT, sandy (ML)	24		ST	- little sandy
4499	20-22	No recovery	0		ST	
4489	30-32	CLAY, silty (CL)	24		ST	
4484	35-37	CLAY, silty (CL)	24		ST	
4479	40-42	CLAY, silty (CL)	24		ST	
4469	50-52	CLAY, silty (CL)	24		ST	
4464	55-57	CLAY, silty (CL)	24		ST	
4459	60-62	CLAY, silty (CL)	24		ST	
4454	65-67	CLAY, silty (CL)	24		ST	
4449	70-72	CLAY (CL)	24		ST	
4439	80-82	CLAY (CL)	24		ST	
4435	84-86	CLAY, silty (CH)	24			
4429	90-92	SILT (ML)	24			
4418	101-103	SILT, sandy (ML)	12			- little recovery, less than half
4402	117-119	SILT (ML)	24			
4397	122-124	SILT (ML)	24			
4392	127-129	SILT (ML)	24			

Soil Symbols

Sand:
Silt:
Clay:

Other Symbols

Notes :

Driller :	Bedke
Boring Number :	Springville
Date Drilled :	4/1/2013
Job Number :	3
Site Location :	Springville Ut.
	400 South 1500 West
Test Method :	ASTM D 1586
Hammer Type :	Automatic Trip Hammer
	140 lb
Sampler :	Shelby tube
	24 in. Sampler
Drilling Method :	Mud Rodery
	4" casing
Make of Drilling Rig :	CME 75
	(Truck Mounted)

Figure 4.13 Test Hole Log for Springville.

Provo

By Zach Gibbs — **Test Hole I**

Elevation (ft)	Sample Depth (ft)	Visual Soil Description	Sample Recovery (in)	Soil Symbols	Penetration N (blows/ft)	Remarks and raw SPT data
4498						- No samples taken
						- drove casing to 10 ft (very dense)
4485	12-14	SILT, clayey (ML)	24		ST	
4480	17-19	SILT, clayey (ML)	24		ST	
						- gravels
						- drove casing to 40 ft
						- casing broke/came apart
4457	40-42	No Recovery	0		ST	- fine sands and silts
4447	50-52	CLAY, gray (CH)	24		ST	
4437	60-62	CLAY, silty, gray (CL)	24		ST	
4427	70-72	CLAY, gray (CL)	24		ST	
4417	80-82	CLAY, gray (CL)	24		ST	
4407	90-92	CLAY, gray (CL)	24		ST	- had artesian conditions at 90 ft.
4387	110-112	CLAY, gray (CH)	24		ST	
4382	115-117	CLAY, gray (CH)	24		ST	
4372	125-127	CLAY, silty, gray (CL)	24		ST	

Soil Symbols

Sand:
Silt:
Clay:

Other Symbols

Notes :

Driller :	Bedke
Boring Number :	Provo
Date Drilled :	4/5/2013
Job Number :	4
Site Location :	Provo Ut. University Ave.
	University Ave./ I-15 onramp
Test Method :	ASTM D 1586
Hammer Type :	Automatic Trip Hammer
	140 lb
Sampler :	Shelby tube
	24 in. Sampler
Drilling Method :	Mud Rodery
	4" casing
Make of Drilling Rig :	CME 75
	(Truck Mounted)

Figure 4.14 Test Hole Log for Provo.

5 LABORATORY TESTING

5.1 Test Procedures

5.1.1 Introduction

One of the outcomes of this research is to produce a recommended laboratory testing program that can be routinely executed by geotechnical consulting firms to develop surcharge evaluations and design for support of highway transportation projects. Recent research by the University of Utah (Ozer et al., 2012; Bartlett and Ozer 2005) and that of Ng (1998) has shown that the controlled rate of strain consolidation (CRS) test (D4186M-12e1) is generally preferable to standard incremental loading oedometer tests (ASTM D2435M-11) for producing high-quality laboratory data for consolidation evaluations. CRS testing better defines the shape of the consolidation curve due to the higher density of data points produced by this test, especially as the specimen transitions from recompression to virgin compression behavior.

Notwithstanding, conventional incremental load oedometer tests were selected instead of CRS consolidation tests for this research. This was done in discussions with the UDOT technical advisory committee, and the reasons for this selection were: (1) incremental load tests are the standard of practice, (2) multiple secondary compression tests needed to be performed simultaneously for this research and there was not sufficient CRS devices at the University for such

testing, (3) it is unclear if the CRS test offers any advantage over incremental load oedometer tests when secondary compression is the primary topic of the research.

Therefore, it is hoped that careful sample preparation and incremental load testing in conventional tabletop oedometers would produce data that are of sufficient quality to be incorporated in the research plan. In addition, it is hoped that if consulting engineers and technicians review and follow, as applicable, the procedures and recommendations developed herein, sufficient data quality and quantity can be obtained to support future surcharge design and evaluation strategies for UDOT projects.

The following sections describe the test procedures that were used to perform the laboratory testing that supports this research.

5.1.2 Testing equipment

The equipment used for the laboratory test program were tabletop oedometers (Figure 5.1) located in the University of Utah Soil Mechanics Laboratory. These devices consisted of a 1.0-inch high and 2.5-inch diameter stainless steel consolidation ring, a standard consolidation cell with base plate having an O-ring, two 2.5-inch porous stones, a top reservoir, a top cap to provide evenly dispersed pressure on the sample, and three bolts to hold the cell together (Figure 5.2). Filter paper was used between the porous stones and the soil sample to prevent plugging of the stones. Suspended weights, which produced a reaction on the sample equivalent to 0.25, 0.5, 1.0, and 2.0 tsf, were

Figure 5.1 Tabletop oedometer.

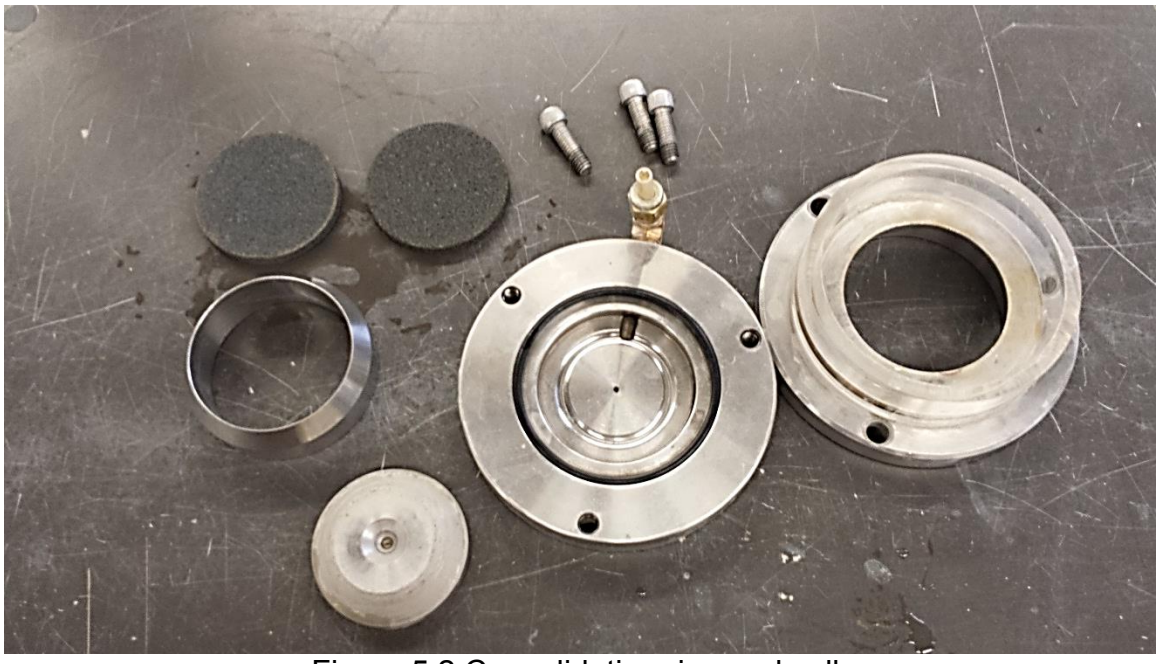

Figure 5.2 Consolidation ring and cell.

used to load the specimens. These weights were used in various combinations to produce the loading increments discussed in Section 5.2. The dial gages used for the vertical settlement readings had a precision of 0.0001 inch.

5.1.3 Sample Setup

All Shelby tubes collected from the sites remained sealed and were stored in a humidified room in the University of Utah Concrete Laboratory to preserve their initial water content. The Shelby tubes were cut with a commercial ban saw (Figure 5.3). The sample was cut approximately 1 inch above and below the test specimen to provide sufficient soil for trimming and moisture content testing without producing a lot of waste.

Ng (1998), Ladd (1999), and Bartlett and Ozer (2005) have found that radiography can serve as an aid to detecting variations in the soil fabric (e.g., heterogeneity, layer, anomalies, disturbance), if desired, but radiography was not

Figure 5.3 Horizontal ban saw used to cut samples for testing.

performed on specimens used for this research. In addition, prior to extrusion of soft samples, it is recommended that a piano wire be inserted between the outer edge of the specimen and the cut Shelby tube and carefully used to cut or break the perimeter adhesion bond between the tube and the specimen to reduce sample disturbance (Ladd et al., 1998).

The samples were carefully extruded from the tubes using the sample extruder shown in Figure 5.4. Immediately following extruding, they were trimmed to fit the consolidation ring using a turntable (Figure 5.5), a fine-gauge wire saw, and reference straight edge. Soil trimmings were immediately weighed to prevent change in mass due to drying and were subsequently placed in the drying oven for moisture content determinations. It is important to obtain accurate moisture content measurements of the specimens for determination of the initial void ratio, which is required in the consolidation calculation, and also as an index of compressibility.

Regarding this latter point, Bartlett and Lee (2004) have shown that the compression index of the soil, C_c, can be reasonable estimated from the in situ moisture content of the soil, because moisture content is highly correlated with void ratio, which is in turn correlated with soil compressibility. Because of this, it is recommended that moisture content and other index properties be obtained for the specimens for further correlation with laboratory-determined consolidation properties.

The height, weight, and diameter of the consolidation ring were recorded using precision scales and a micrometer. The consolidation rings used had

Figure 5.4 Extruding sample from Shelby tube.

Figure 5.5 Sample in turntable.

heights of 1 inch and diameters of 2.5 inches. To reduce the friction between the soil and the consolidometer rings, the inner circumference of the rings were lubricated with a low-friction, silicone-based lubricant.

The samples were then carefully placed into the consolidation ring and trimmed flush with the top and bottom of the ring (Figure 5.6). If there were any small voids present on the top or bottom of the specimens from the trimming process, these imperfections were carefully filled with trimmed soil.

After the trimming and preparation were completed, the weights of the rings with the soil present were then recorded. Porous stones were boiled in demonized water and soaked in de-aired water prior to assembly. Standard 0.15-mm thick filter paper was used between the sample and the porous stones on both top and bottom of the specimens to prevent clogging of the stones and the loss of the solids during the tests.

The samples in the consolidation ring were then assembled in the cell with porous stones and filter paper, and the top caps were placed on the top reservoir and secured with bolts to prevent leakage (Figure 5.7). The cell were then placed in tabletop oedometers and deionized, de-aired water was used to fill the reservoir to saturate the specimen (Figure 5.8). Testing was then performed using the interpretive methodologies described in the following section.

5.2 Laboratory Test Program

The specimens selected for testing were determined by evaluating nearby CPT soundings and selecting the sampling depth having the most clay-like behavior. This was usually manifest on the adjacent CPT sounding as low tip

Figure 5.6 Sample in consolidation ring.

Figure 5.7 Sample fully assembled in cell.

Figure 5.8 A fully assembled cell in table top oedometer.

resistance and relatively high excess pore water pressure relative to hydrostatic conditions. The CPT sounding used in the evaluations are found in Chapter 4. At the 400 South site, a CPT sounding was not available; hence, the sampling depths started at 15 feet (i.e., below the alluvium) and sampling was done every 5 feet until a depth of 50 feet was reached. All of these samples from 400 South appeared to be very similar to each other and were cohesive sediments.

For each sampling interval, the specimens were used to determine the following consolidation properties: (1) preconsolidation stress (σ_p), (2) rate of secondary compression for normally consolidated specimen, C_α, (3) rates of secondary compression for overconsolidated specimens, C'_α, for OCR values of

1.25, 1.5, and 2.0. The preconsolidation stress was determined using 1-D incremental loading tests with time rate of consolidation measurements taken for each loading increment. The following describes the procedures used to determine these properties.

5.2.1 Determination of the Preconsolidation Stress

The preconsolidation stress of the specimens was evaluated using a 1-D incremental loading consolidation test with the sample preparation described in section 5.1. The following loading schedule was implemented: 0.25, 0.5, 1.0, 2.0, 4.0, 8.0, and 16.0 tsf (500, 1000, 2000, 4000, 8000, 16000, and 32000 psf, respectively), and the unloading schedule was 16.0, 4.0, 1.0, and 0.25 tsf (8000, 2000, and 500 psf, respectively). This is equivalent to applying a load increment ratio, $\Delta P/P$, of unity (1.0), which is most commonly used in practice. However, Jamiolkowski et al. (1985) recommend that the $\Delta P/P$ ratio be reduced to about 0.5 to obtain better defined consolidation curves in the vicinity of the preconsolidation stress as used by Canadian practice for sensitive clays in eastern Canada.

In standard geotechnical practice, each load increment is usually maintained for one day (24 hours) to define the consolidation curve and estimate the preconsolidation stress. However, because the end of primary consolidation usually occurs in less than 1 hour after the newly applied load, the virgin portion of consolidation curves based on 24-hour waiting periods is displaced downward by one or more cycle of secondary compression (Jamiolkowski et al., 1985). This is not desirable for two obvious reasons: (1) it makes interpretation of the

preconsolidation stress more variable, especially for soft soils, (2) data needed for interpretation of the rate of secondary compression at the applied stress are not obtained.

Thus, contrary to standard practice and in order to produce as little as possible secondary compression between each incremental loading, time rate of consolidation tests were done for every loading increment. These data were used to decide when end of primary consolidation was essentially completed so that the next load increment could be applied. To this end, Taylor's square root of time method (as found in Holtz and Kovacs 2011) was performed on the time rate of consolidation data to determine when 90% of primary consolidation had occurred. To accelerate the consolidation process 90% of primary consolidation was selected; when consolidating soft clays, it can take substantially more time to reach 95 or 100% of consolidation. When this value was reached, the next load increment was then applied. This accomplished three things: (1) it allowed for the incremental loading test to be completed in a more expeditious manner similar to that of CRS testing, (2) it allowed for a more consistent interpretation of the preconsolidation stress, and (3) it produced more repeatable results for the rate of secondary compression.

The incremental loading results were then plotted and the pre-consolidation stress (σ'_p) was determined using the work/strain method (Becker et al. 1987) and Casagrande's method (Casagrande 1936). The compression ratio (CR) and recompression ratio (RR) were also determined from plots of log of applied stress versus vertical strain.

5.2.2 Determination of the Rate of Secondary Compression C_α

The rate of secondary compression varies with the preconsolidation stress and amount of aging (Jamiolkowski et al., 1985; Ng 1998). For this research, it is important to determine rate of secondary compression for the normally consolidated condition, i.e., C_α. This was done by first determining the preconsolidation stress from the incremental load tests described in the previous section. After this, specimens from the same depth interval and borehole were loaded to a new stress state that was 1.5 to 2.0 times the in situ σ'_p value. This ensured that specimens had reached a new normally consolidated state and any effects of aging or past preconsolidation had been removed.

The method of Ladd (1989) was used to interpret the time rate of consolidation data for secondary compression (Figure 2.3).

When using Ladd's methodology, the value of secondary settlement C_α is the slope of the line through the linear most portion of the data, after primary consolidation has occurred, on the strain vs. log of time plot.

The reading schedule used for this part of the test was, 4 min, 8 min, 15 min, 30 min, 1 hour, 2 hour, and 4 hours. Then readings were taken about once a day for the remainder of the test, usually about once every 24 hours. The first few readings were removed because they have very little effect on the value of C_α, it was decided to take the first reading at 4 minutes to increase the number of tests that could be ran at one time. This test ran for 1 to 2 weeks to be sure that a good value of C_α is achieved.

5.2.3 Determining C'_{α}

The process for determining C'_{α} was done using the same procedure to determine C_{α} but with a few variations. The specimen is loaded to a state of stress that is 1.5 to 2.0 times the in situ σ'_{p} value as was done in the section stated above.

After the 1 or 2 hour reading was taken, the load was then reduced to a known OCR of ether 1.25, 1.5, or 2.0.These values were selected because this range is likely to bracket the values used for surcharge design. The reading schedule for this part of the test is the same as stated above and will run for 1 to 2 weeks.

The method of Ladd (1989) was also used to interpret the time rate of consolidation data for secondary compression. Additional detail was provided in Chapter 2.

6 RESULTS AND INTERPRETATIONS

6.1 Lab Tests and Data Screening

In the course of this research, a total of five 1-D consolidation tests were performed at each sampling depth from the individual boreholes completed during the field investigations. For each depth, one test was performed to determine the preconsolidation stress, and the remaining four tests consisted of time rate of consolidation tests to determine the rate of secondary compression at OCR values of 1.0, 1.25, 1.5, and 2.0. These OCR values were selected to represent a reasonable range of overconsolidation states that could be effectively achieved in the foundation soils during embankment construction.

At the 400 South Street site in Salt Lake City, Utah, specimens from eight sample depths were tested. At the South Layton, Utah, site located just off of Layton Parkway and Main Street a total of four sample depths were tested. At the Springville, Utah, 400 South Street site, specimens from seven sample depths were tested. Similarly at the Provo, Utah, interchange, specimens from seven sample depths were tested. Thus, in total twenty-six consolidation tests and one hundred and four time rate tests were performed on Pleistocene and recent fine-grained, cohesive, lacustrine deposits comprised of Lake Bonneville and more recent clays, most likely of Utah Lake origin. A list of the locations, sample depths and results of these tests are presented in Table 6.1.

Table 6.1 Listing the sites, depths, moisture content, pre consolidation stress, compression and recompression ratio, and the rate of secondary settlement at different OCR's

Site	Avg. depth (ft)	ω (%)	Casagrande σ'_p (psf)	Work σ'_p (psf)	CR	RR	C_α	C_α' OCR 1.25	C_α' OCR 1.50	C_α' OCR 2.00
400 South	16[b]	53.0	2671	2780	0.21	0.021	0.0164	0.0230	0.0017	0.0009
	21	52.0	6338	6420	0.20	0.026	0.0127	0.0089	0.0044	0.0020
	26	49.2	2989	3040	0.18	0.021	0.0095	0.0072	0.0028	0.0007
	31	47.2	5473	5280	0.15	0.018	0.0066	0.0022	0.0012	0.0003
	39	40.3	5423	5520	0.15	0.024	0.0105	0.0058	0.0015	0.0010
	41[a]	46.7	1610	1660	0.13	0.016	0.0103	0.0103	0.0029	0.0010
	46[a]	40.3	4262	4240	0.12	0.018	0.0036	0.0047	0.0026	0.0010
	51[a]	48.5	2350	2120	0.17	0.016	0.0049	0.0047	0.0041	0.0018
S. Layton	16	32.8	5067	5120	0.13	0.012	0.0030	0.0017	0.0007	0.0004
	91	34.7	6510	6580	0.07	0.013	0.0026	0.0015	0.0006	0.0005
	106	28.4	6408	7140	0.04	0.008	0.0023	0.0018	0.0011	0.0005
	131	25.5	5974	6320	0.11	0.017	0.0048	0.0033	0.0012	0.0006
Springville	31	26.7	7101	7060	0.09	0.023	0.0018	0.0012	0.0006	0.0003
	41	26.8	6682	6780	0.09	0.014	0.0021	0.0011	0.0003	0.0002
	66	23.6	5810	6040	0.05	0.008	0.0024	0.0022	0.0014	0.0010
	71	27.7	12125	12420	0.12	0.018	0.0040	0.0026	0.0012	0.0012
	76	32.8	6274	6280	0.15	0.022	0.0051	0.0050	0.0019	0.0007
	81[a]	41.9	6643	6880	0.19	0.023	0.0074	0.0060	0.0016	0.0007
	85[a]	40.6	5503	5503	0.17	0.023	0.0047	0.0025	0.0006	0.0001
Provo	13	45.5	7358	7820	0.11	0.017	0.0046	0.0023	0.0007	0.0004
	18	35.2	2969	3120	0.14	0.013	0.0036	0.0021	0.0008	0.0016
	51[a]	51.1	3803	4000	0.12	0.020	0.0037	0.0014	0.0010	0.0004
	61[a]	32.6	4740	4800	0.10	0.017	0.0032	0.0026	0.0015	0.0009
	81	47.8	6331	6340	0.18	0.023	0.0075	0.0027	0.0018	0.0018
	91	34.1	7014	7300	0.13	0.015	0.0045	0.0040	0.0007	0.0005
	111[a]	41.3	5512	5520	0.14	0.021	0.0037	0.0030	0.0008	0.0005

a. Data that has been removed from analysis due to a high SQD value.
b. Data was removed from analysis due to poor result for C_α by not running long enough.

Prior to developing the consolidation parameters from the specimens, the consolidation test results were screened using the sample quality designation (SQD) developed by Andresen and Kolstad (1979) of the Norwegian Geotechnical Institute (NGI). This method uses the recompression vertical strain during the initial reloading loading of the specimen back to the in situ effective vertical stress. For example, in this method, a SQD value of 4 indicates that the specimen underwent 4 % vertical strain during the reloading. Andresen and Kolstad (1979) developed a SQD nomenclature that corresponds with the vertical strain values given in Table 6.2. For example, a SQD value between 2 to 4 receives a "fair" designation. Saye and Ladd (2000) used SQD values of 4, or greater, to screen out (i.e., omit) consolidation data from their evaluations. The 1D consolidation data used by these authors were obtained by the various geotechnical firms during the baseline investigations for the I-15 Reconstruction project and had varying levels of quality. Therefore, in general, based on Andersen and Kolstad (1979) and Saye and Ladd (2000), it is recommended that a SQD criterion of 4, or higher, be used as a screening criterion for future project evaluations.

Table 6.2 Values of strain at σ'_{vo} and the corresponding rating of SQD

Strain on Reloading to σ'_{vo} (%)	Sample Quality Designation (SQD)
<1	A, Very good to excellent
1-2	B, Good
2-4	C, Fair
4-8	D, Poor
>8	E, Very poor

However, some of the specimens obtained for this research exceeded this recommended screening threshold (Table 6.3). In order to improve the sample size for the statistical analysis herein, it was decided to slightly relax this criterion. Thus, consolidation tests results having SQD greater than 6 were excluded from the subsequent analysis herein. The footnotes in Table 6.1 give information on which specimens were screened from the statistical analyses due to poor SQD, or other testing or data reduction issues.

Some of the specimens sampled from the 400 South Street site in Salt Lake City, Utah and from the Provo, Utah South Interchange site had relatively high SQD values indicating higher amounts of sample disturbance. The reasons for this are unclear, but may be partly attributable to the softer soil deposits found at these locations. Such soils may be more susceptible to disturbance effects associated with sampling, handling, and preparation processes.

The consequences of sample disturbance appear to have had a larger impact on specimens tested at or slightly above the normally-consolidated state of stress (i.e., OCR ≈ 1). For example, when the screened tests results for C_α and C_α' from this research are plotted versus OCR values (Figure 6.1), the variance (i.e., scatter) of the data is higher for results obtained at lower OCR values when compared with that obtained at higher OCR values. This holds true for both the total variance (scatter of data from all sites) and for the sample variance (scatter of data obtained from a particular site). Some of this variation is due to natural variability of the layered sediments at a given site, because not all specimens at each site were obtained from the same layer. However, it is also likely that some

Table 6.3 Site, Depth, Effective Vertical Stress, and SQD

Site	Avg. Depth (ft)	σ'_v (psf)	SQD
400 S	16	1198	2.7
	21	1436	2.7
	26	1674	5.5
	31	1912	4.7
	38.5	2269	5.6
	41	2388	11.2
	46	2626	8.2
	51	2864	11.8
S. Layton	16	1483	3.0
	91	5803	5.0
	106	6667	3.3
	131	8107	7.0
Springville	31	2067	2.8
	41	2593	4.3
	66	3908	3.0
	71	4171	2.4
	76	4434	5.2
	81	4697	8.9
	85	4908	6.5
Provo	13	1245	1.4
	18	1508	3.2
	51	3244	17.5
	61	3770	8.1
	81	4822	7
	91	5348	6.4
	111	6400	13.5

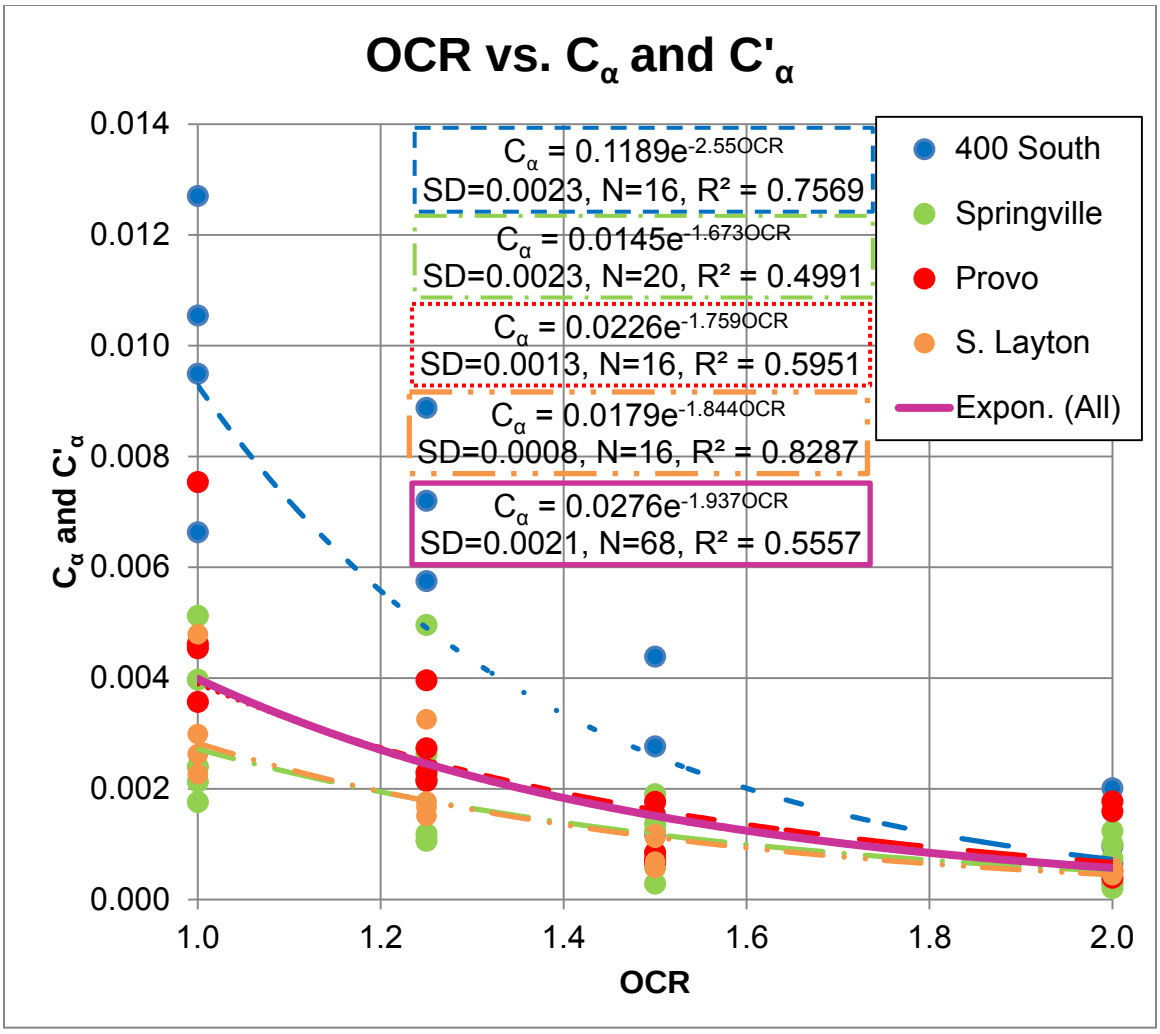

Figure 6.1 Plot of C_α and C_α' vs. OCR for 400 South, South Layton, Springville, and Provo Sites

of the variation can be attributed to the effects of sample disturbance. Therefore, it is reasonable to conclude that the apparent decrease in variance with increasing OCR values is, in part, due to the ameliorating effect of overconsolidation of the soil specimens prior to performing the time rate of consolidation tests to determine C_α'. A similar beneficial effect of overconsolidating soils prior to performing undrained shear strength tests have been discussed by Ladd and Foott (1974) in developing the SHANSEP (Stress

History and Normalized Soil Engineering Properties) method.

A plot of preconsolidation stress versus depth for the higher quality samples shows that the soils at the various test sites are overconsolidated at all depths (Figure 6.2). This is a typical finding which has been documented by many geotechnical investigations for the surficial alluvium and underlying lacustrine sediments in the Wasatch Front Area. The apparent overconsolidation originates from aging, void ratio change due to repeated drying and wetting

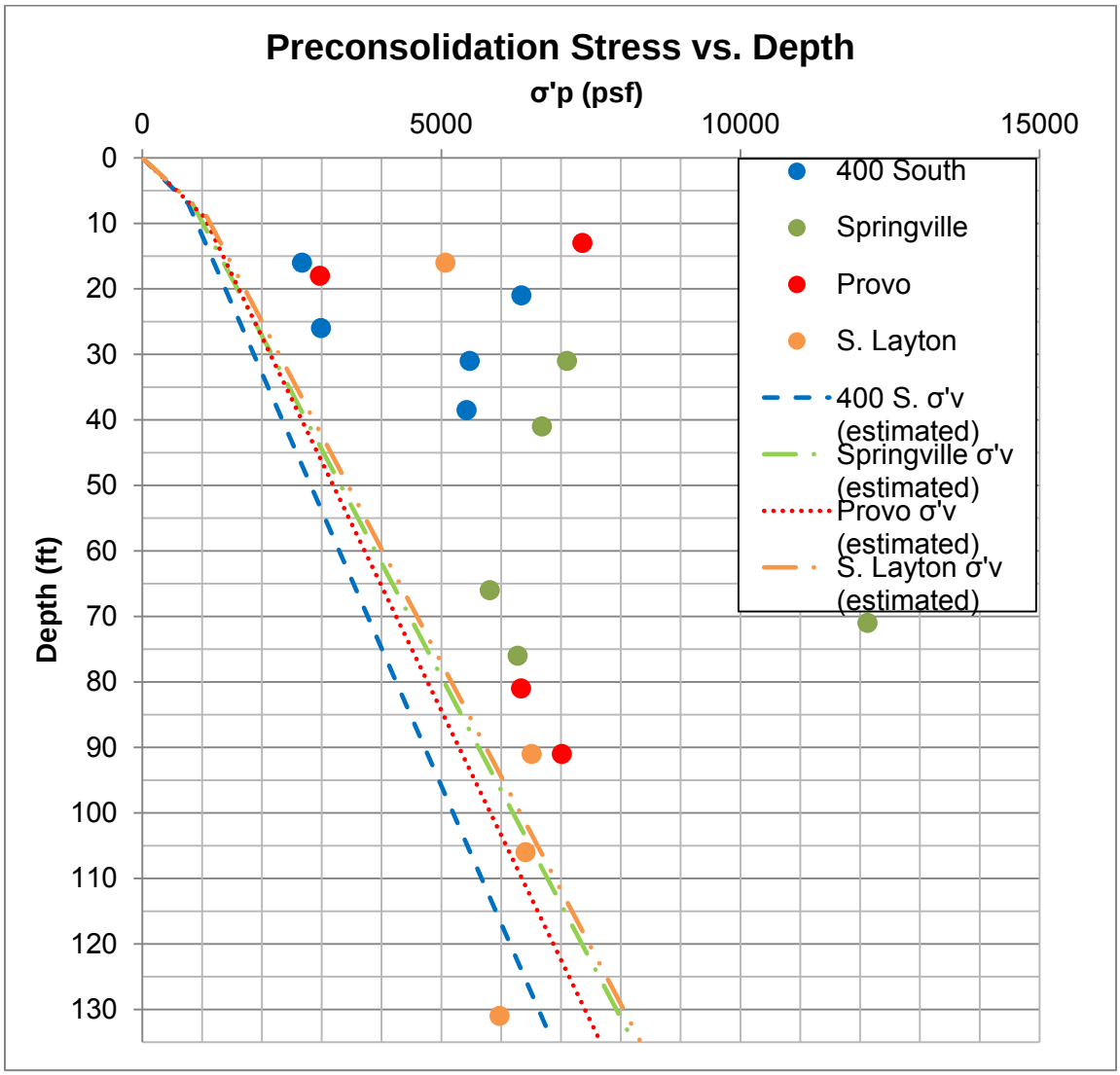

Figure 6.2 Plot of preconsolidation stress vs. depth for 400 South, South Layton, Springville, and Provo.

cycles resulting from ground fluctuations and in some cases, minor cementation from calcium carbonate.

The effective vertical stress profile is also shown on Figure 6.2 using an estimation of the water table level determined from piezometer readings for CPT soundings performed nearby. The CPT soundings were used to infer the equilibrium water table condition instead of the boreholes because the drilling operations required that the boreholes be “abandoned” (filled with grout) soon after the drilling had ceased. The in situ OCR values range from 1.3 to 5.8, where the higher values of OCR tend to be at shallow depths and then decreases with depth.

6.2 Relationships for C_α, C_α', and C_α'/C_α

The plot C_α and C_α' versus OCR shows that there is a non linear trend that exists between the dependent and independent variables. This trend is best fit using the exponential trendline feature in MS Excel. This plot and its corresponding nonlinear relationships indicate a relatively small change in C_α' for OCR values greater than about 1.5. At higher OCR values, the C_α' values appear to converge to a value slightly less than 0.001 (Figure 6.1). From an application standpoint, this behavior suggests that there is a point of diminishing return when surcharging soils beyond an OCR value of about 1.5 for the sediments tested in this study.

While the C_α' values for the various sites tend to converge at an OCR value of 2.0, it is also apparent that the fitted relationship for the 400 South Site in Salt Lake City is higher than the average fitted trendline; whereas the fitted

trendlines for Springville and South Layton tend to be lower than the average trendline. A possible reason for this difference in behavior may be attributed to nature of the lacustrine sediments. In the Salt Lake Valley, the lacustrine sediments sampled are solely from Lake Bonneville deposits, whereas at the Provo and Springville sites, in Utah Valley, the sampled sediments consisted of recent Lake Utah and earlier Lake Bonneville sediments. In general, it appears that the Utah Lake sediments are siltier than those obtained from Lake Bonneville, and this may be causing the difference in the C_{α}' values.

Because of these relatively large differences in the trendlines for the various sites, a better interpretation and graphical representation of the data are required. This can be done by normalizing C_{α}' using C_{α} (i.e., forming C_{α}'/C_{α} ratios) and plotting the normalized values versus OCR (Figure 6.3). This method produces a normalized average trendline for C_{α}'/C_{α} that fits all data reasonably well which can be used as a good representation of the average of all data.

Ladd (1989) introduced the concepts of amount of surcharge (AOS) and adjusted amount of surcharge (AAOS) instead of OCR to represent the data trends. These factors are more useful for applied surcharge purposes (see Chapter 2). A plot of C_{α}'/C_{α} versus AAOS is shown in Figure 6.4

Ng (1998) plotted C'_{α}/C_{α} versus AAOS values from testing developed for the I-15 Reconstruction Project on a semi-log plot. The data from this study have been superimposed on the Ng (1998) relationship for comparative purposes in Figure 6.5. The average trendline for this research plots significantly higher than that developed by Ng (1998). There are several possible explanations for this, as

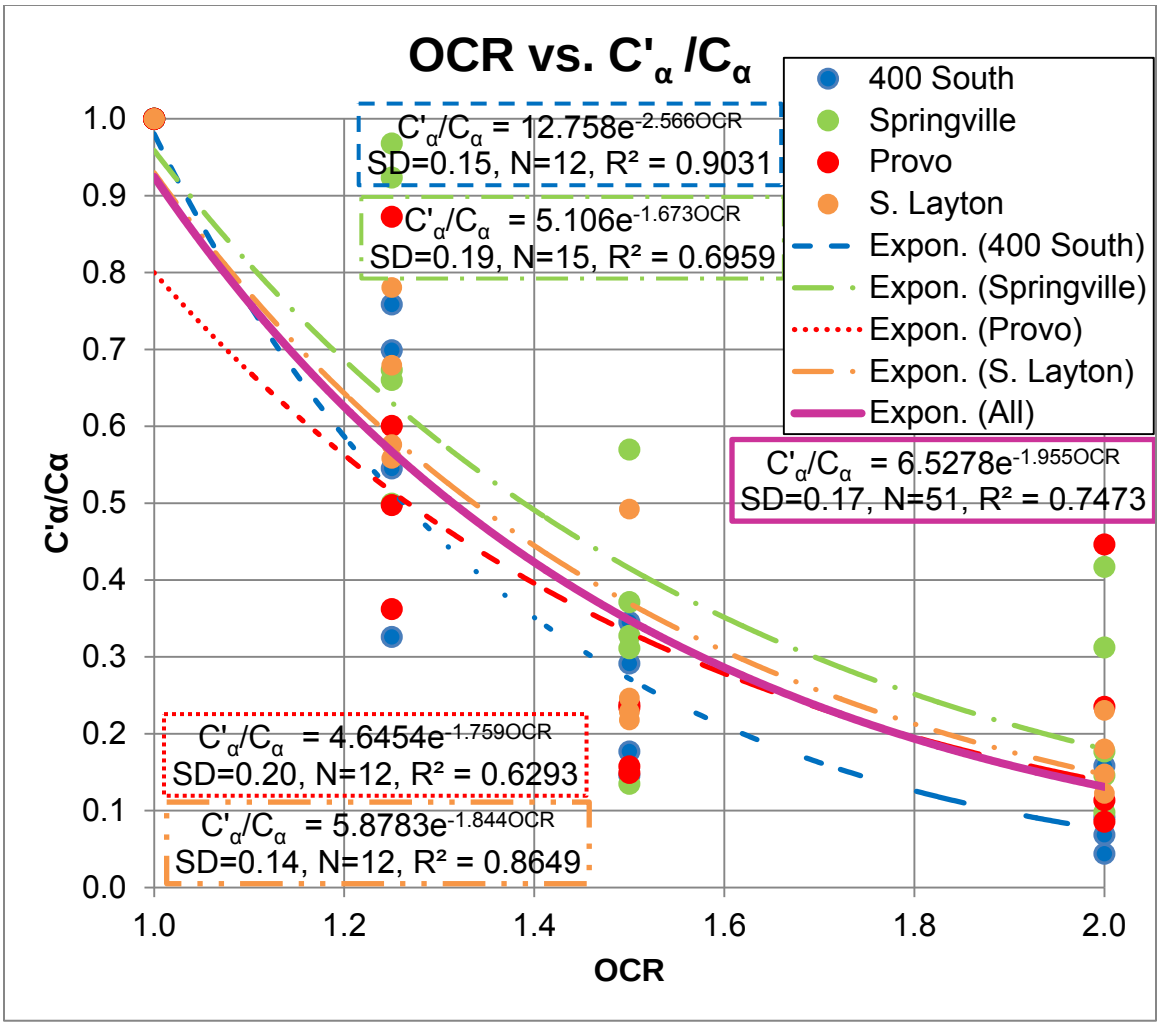

Figure 6.3 Plot of C_α'/C_α vs. OCR for 400 South, South Layton, Springville, and Provo Sites

discussed in the next few paragraphs.

First, the soil specimens from this research may be significantly different from those tested by of Ng (1998). The Springville and Provo sites are located several tens of miles to the south of Salt Lake City in an adjacent valley and appear to be siltier in nature due to the presence of near shore sediments deposited in the Utah Lake. Only one test site (400 S. Street in Salt Lake City)

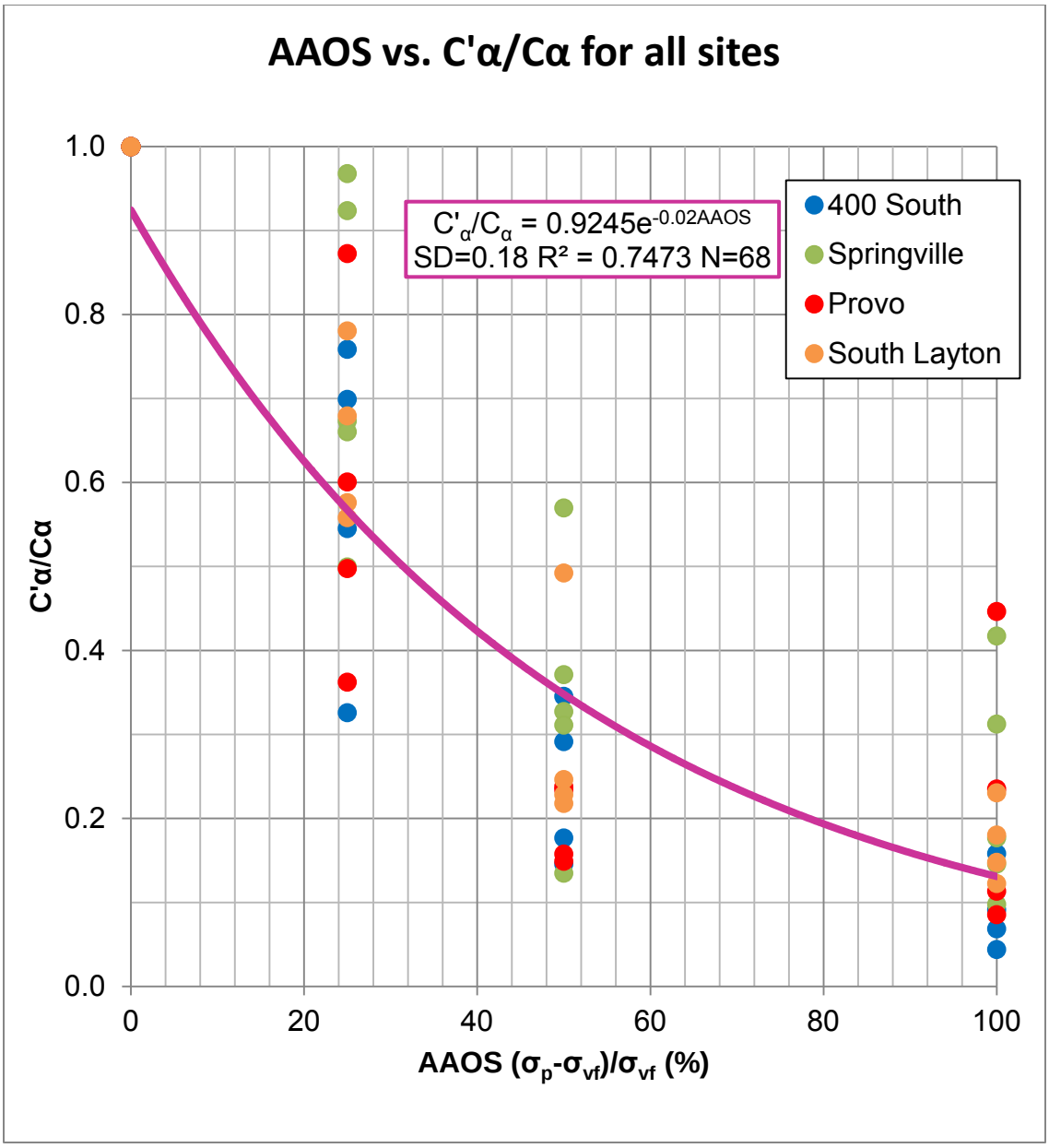

Figure 6.4 Plot of AAOS vs. C_α'/C_α using an average exponential trend line

was geographically near the drill hole locations where Ng (1998) and Woodward-Clyde Consultants obtained soil samples for the I-15 project. When the results for the 400 South Street site (blue line in Figure 6.5) are compared with those of Ng (1998), significant differences still remain. However, the lower bound data points from the 400 South Site plot within the upper range of the Ng (1998) data.

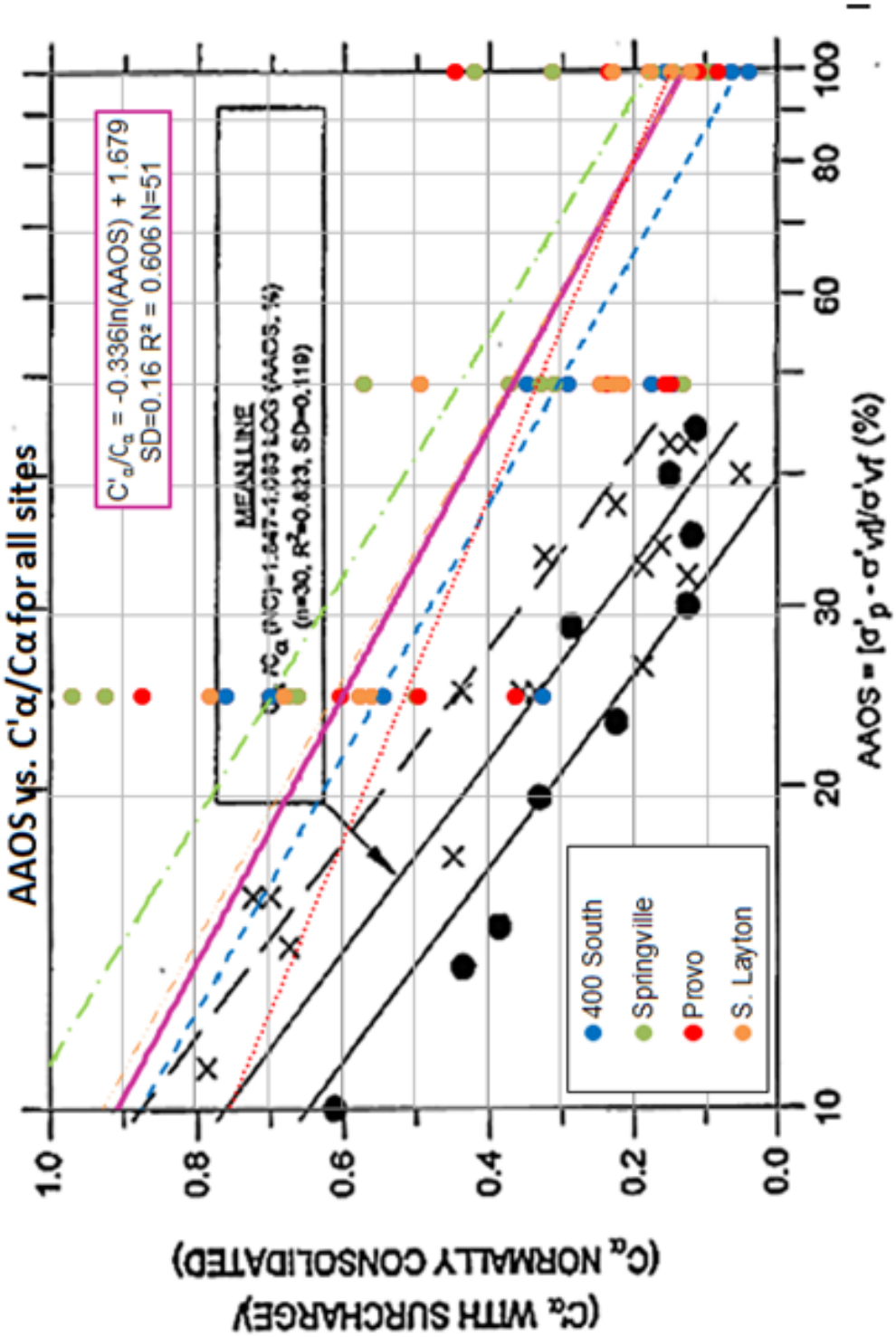

Figure 6.5 Comparison plot of AAOS vs. C_α'/C_α on a semi-log plot with data acquired by MIT.

Second, the trend of the Ng (1998) relationship appears to overstate the reduction in C_{α}'/C_{α} as a function of AAOS. For example, if extrapolated to an AAOS value of 50 % (i.e., OCR = 1.5), the average trendline of Ng (1998) would predict a C_{α}'/C_{α} ratio of near zero, which appears to be unlikely, especially when considering that this research shows a minimum value of C_{α}'/C_{α} of about 0.1 at an OCR value of 2.0. This latter result appears to be more realistic and intuitive based on the data presented in this report.

Third, long-term settlement performance monitoring data obtained from the I-15 Reconstruction Project for the surcharged earthen embankments and MSE walls show that the measured creep settlement is somewhat larger than desired performance goal (Figure 6.6) (Farnsworth et al., 2008). The settlement performance goal adopted by the project was to limit the creep settlement to 75 mm, or less, in a 10-year postconstruction period. Large earthen embankments located at 400 S. and 2400 S. Streets were constructed with surcharged embankments designed to meet this performance goal. However, the 10-year post construction settlement at these sites is projected to exceed this settlement goal by a factor of about 1.5 to 2 (Figure 6.6). This suggests that the rate of secondary compression in the subsurface soils at these locales is greater than that anticipated in the surcharge design. One possible reason for the underestimation of the actual settlement could rest in the value of C_{α}' selected for the design calculations. Because the amount of secondary settlement is directly proportional to C_{α}' based on Equation 2-8, the additional settlement incurred at these sites may have resulted from an underestimation of the actual C_{α}' for the

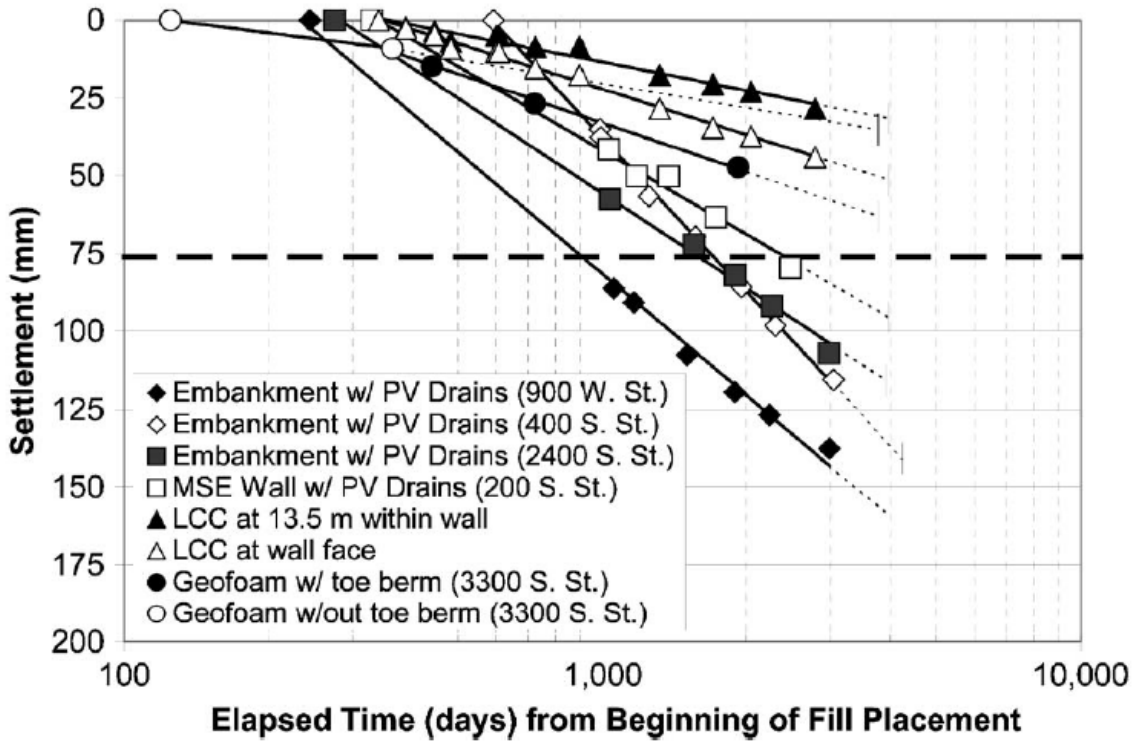

Figure 6.6 Rate of foundation creep extrapolated to 10 years of postconstruction (from Farnsworth et al., 2008).

foundation settlement for these locales. For example, if the design C_α' values were approximately 1.5 to 2.0 times higher than those reported by Ng (1998), then such a change would produce a more reasonable result that is in better agreement with the average C_α'/C_α trendline developed for the 400 South street site in Salt Lake City from this research.

Nonetheless, despite the various interpretations of the existing laboratory and field data that could be offered, it is clear that site-specific field and laboratory evaluations are needed for future sites to avoid pitfalls associated with applying data and relationships developed from other sites that may have significantly differing soil conditions than the site of interest.

6.3 C_α/CR Ratio

Mesri has shown that the C_α/CR ratio is relatively constant for a given soil type. Knowledge of this ratio has proven to be very helpful in performing secondary settlement calculations because C_α can be estimated if values of CR and the C_α/CR ratio are known for a particular soil or can be reasonably estimated. Values of CR easily attainable from standard consolidation testing and C_α/CR ratios can be estimated from this research and that of Ng (1998), as shown in Figures 6.7 and 6.8, respectively.

The ratios developed by this research (Figure 6.7) were calculated using a linear trendline function and by forcing the trendline through the origin; hence, the slopes of these lines also represent the C_α/CR ratio. These results show that each individual research site has a slightly different C_α/CR relationship when compared with the average trendline. In short, the 400 South street site in Salt Lake City has a somewhat steeper slope (higher ratio) than the South Layton, Springville, and Provo sites. However, when the average slope of all the data from the four research sites is calculated, the corresponding value is C_α/CR = 0.0442. This average ratio correlates reasonably well with that of Ng (1998) of C_α/CR = 0.0433. The Ng (1998) average relation included consolidation tests performed at MIT and by Woodward-Clyde Consultants for the Lake Bonneville deposits (Figure 6.8). Although this research supports a similar average C_α/CR ratio when compared with Ng (1998), the results for the 400 South street site in Salt Lake City plot somewhat above the average trendline of Ng (1998).

In addition to this, the time delay for when secondary compression

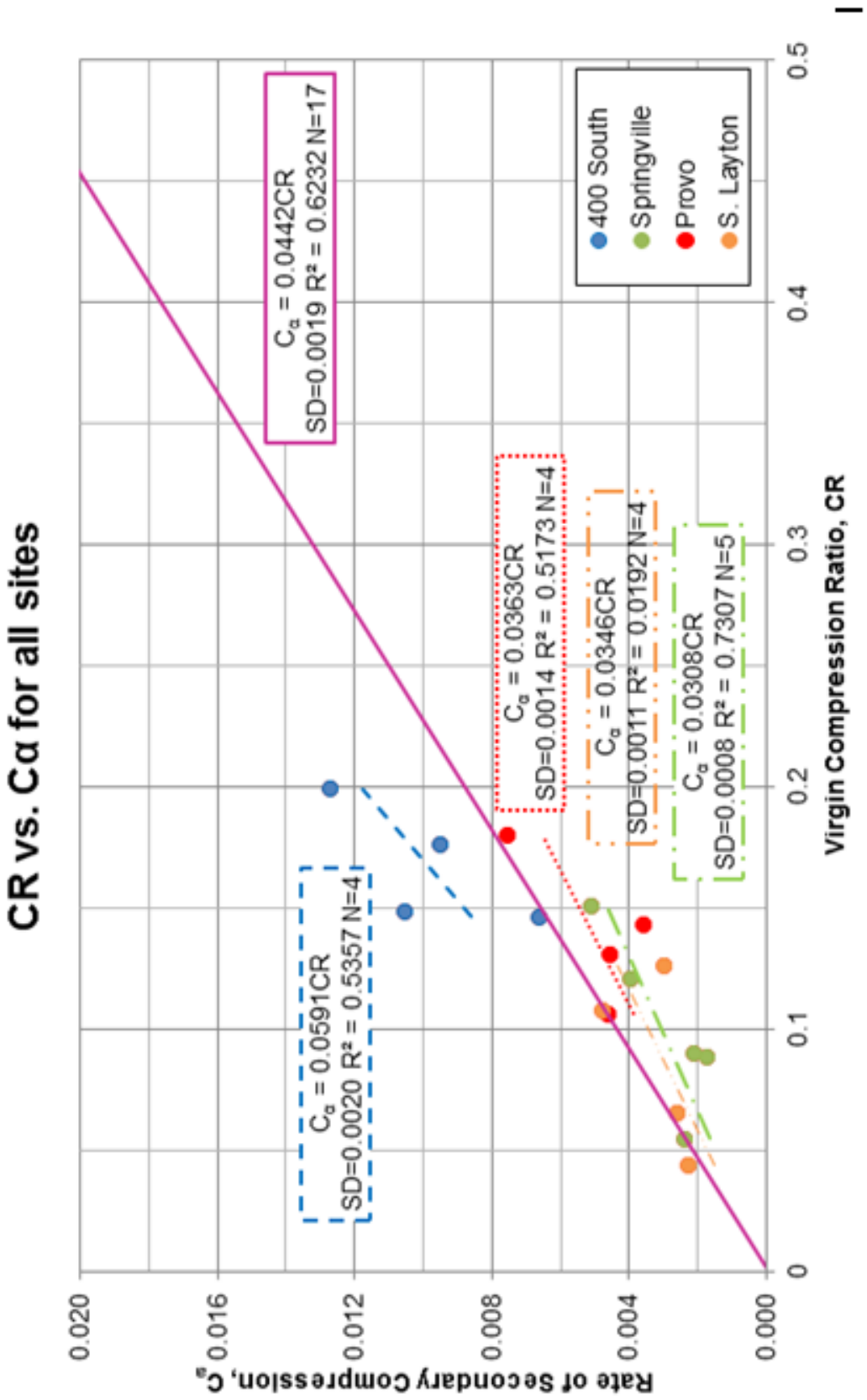

Figure 6.7 Plot of CR vs. Cα for all sites

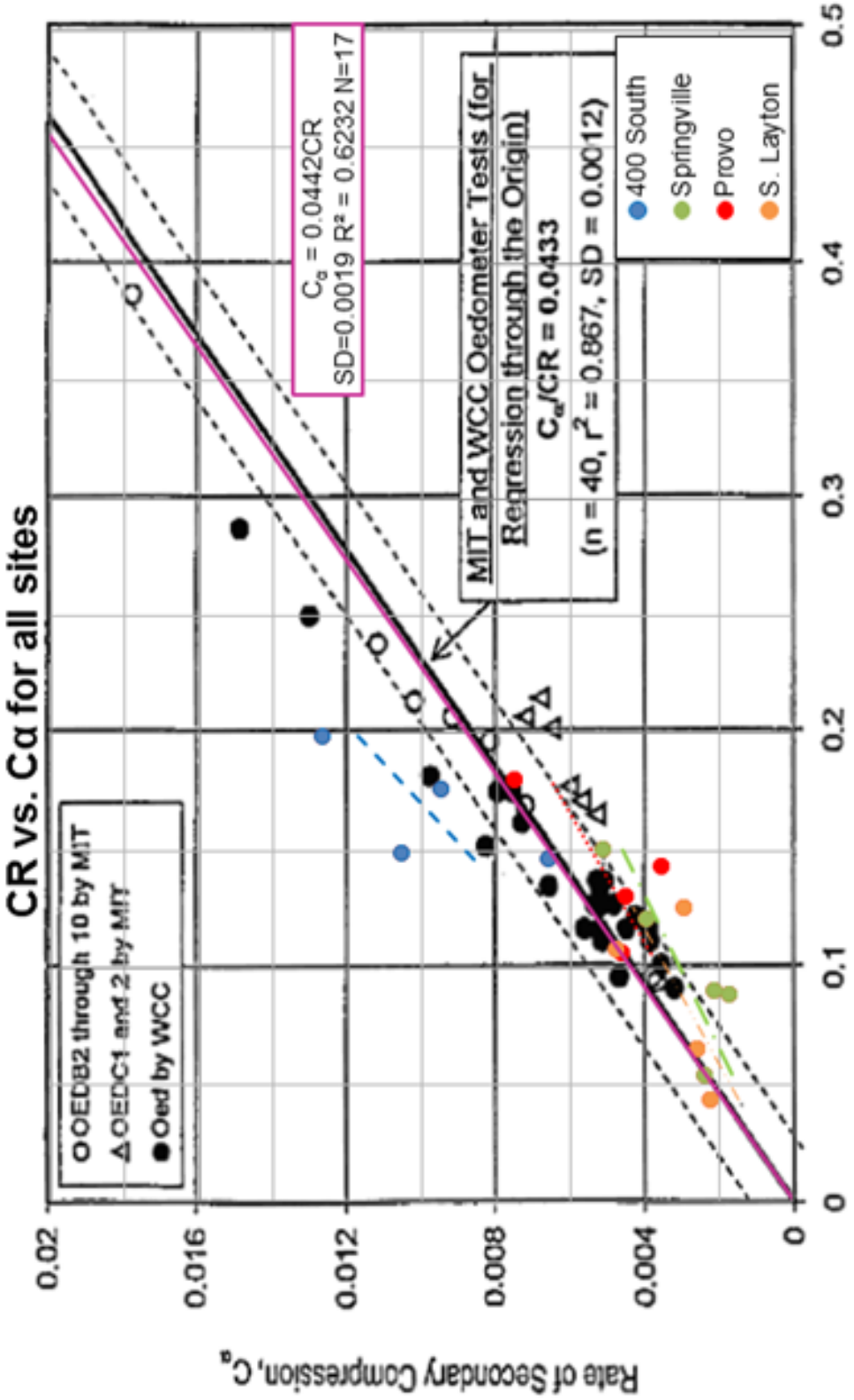

Figure 6.8 Comparison plot of CR vs. C_α with data collected from MIT and WCC

resumes is shown in Figure 6.9 as a plot of AAOS vs. LOG (t_s/t_r). When comparing the data from this research and the data from MIT and WWC (Ng, 1998), the trendline is slightly lower but compares well with previous work.

6.4 Moisture Content Correlations

Many researchers have shown that the moisture content, ω, of soil is highly correlated with soil compressibility (i.e., C_c and CR) for saturated soils. This is because when the soil fabric is saturated, the in situ moisture content is directly correlated with the in situ void ratio for soils with a given specific gravity. For many cohesive soils, there is a relatively minor variation in the specific gravity of the soil solids; hence, moisture content is an excellent predictor of void ratio. In addition, void ratio in turn is highly correlated C_c and CR because soils with high voids have more opportunity for compression (i.e., void ratio reduction) upon loading.

Figure 6.10 shows a ω versus CR relation using the test results from this research. The data indicate a relatively good correlation between these properties. In addition to this, Bartlett and Lee (2004) developed moisture content and compressibility correlations for the Lake Bonneville deposits. These correlations were made from laboratory data obtained from various geotechnical reports associated with the I-15 Reconstruction Project. Test results with a SQD value greater than 4 were screened (excluded) from their evaluations (Figure 6.11). The data from this research have been superimposed on the Bartlett and Lee (2004) plot for comparative purposes. The trendline developed from this research plots somewhat lower than that of Bartlett and Lee (2004). However,

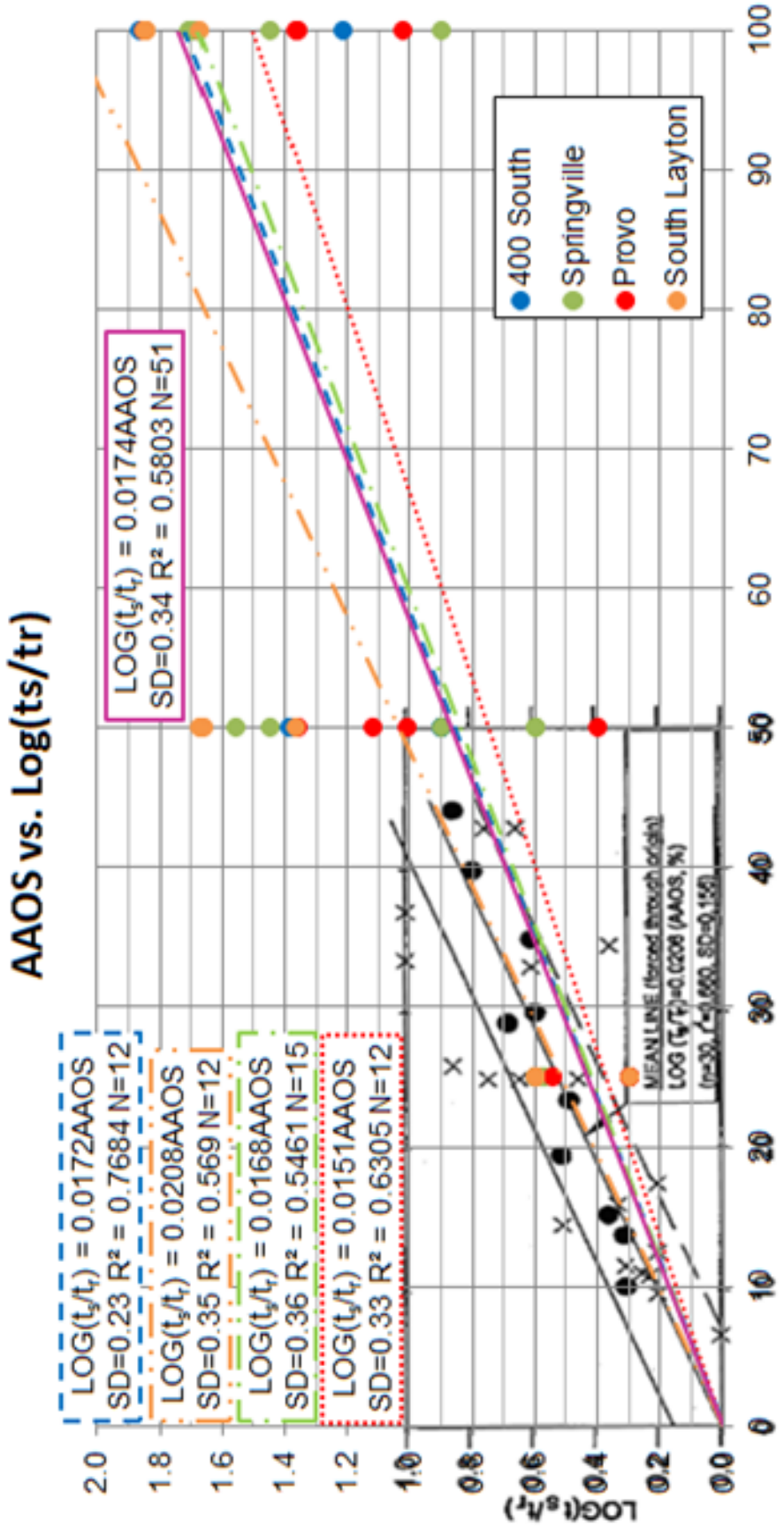

Figure 6.9 Comparison plot of AAOS vs. LOG(ts/tr) with data collected from MIT and WCC

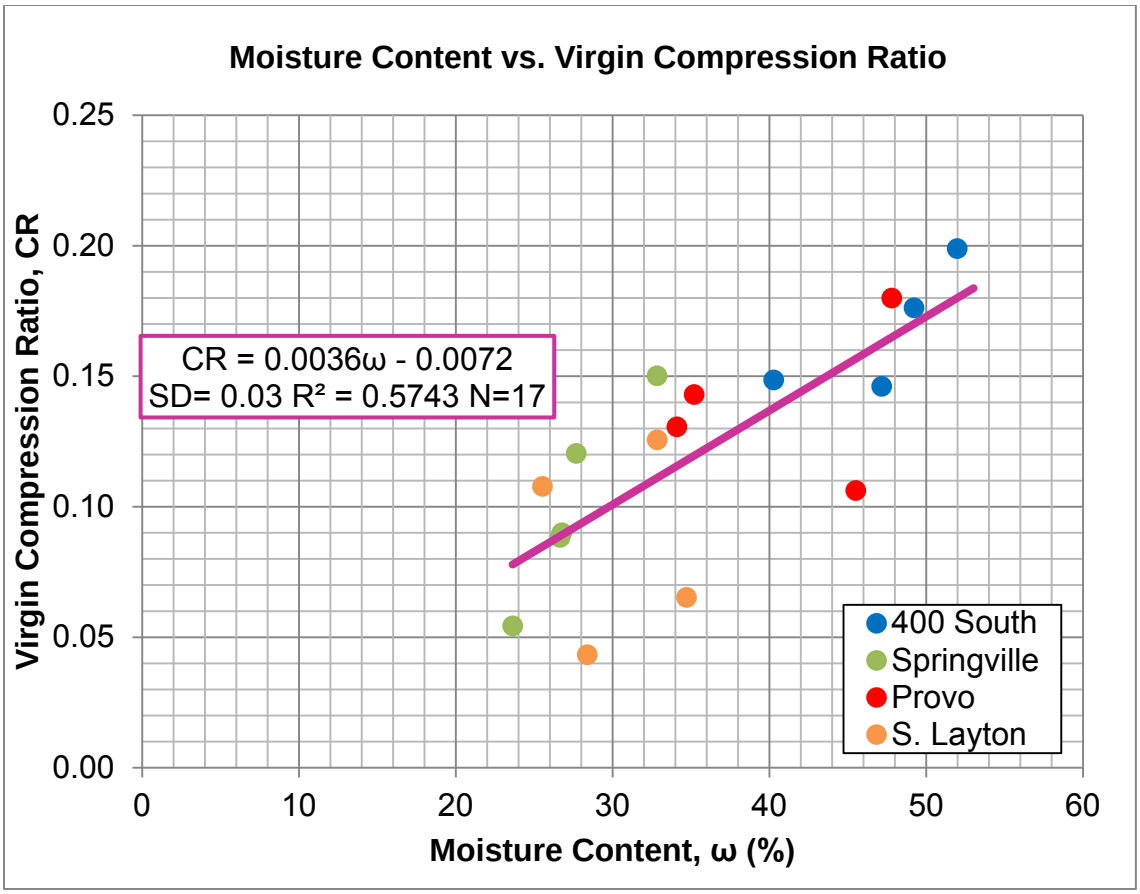

Figure 6.10 Plot of moisture content vs. virgin compression ratio

this does not imply that the two equations are inconsistent for the following reasons: (1) The soils from this research appear to be somewhat siltier, on average, than those used by Bartlett and Lee (2004), (2) The Bartlett and Lee (2004) relation has more statistical support because of the larger sample size, (3) The data from this research do not plot outside the data range of the Bartlett and Lee (2004) relation, suggesting the two data sets are not entirely inconsistent. For application purposes, it is recommended the Bartlett and Lee relation be used because of its greater statistical support.

In addition to the correlations just discussed, correlations that included rate of secondary compression properties and moisture content were explored.

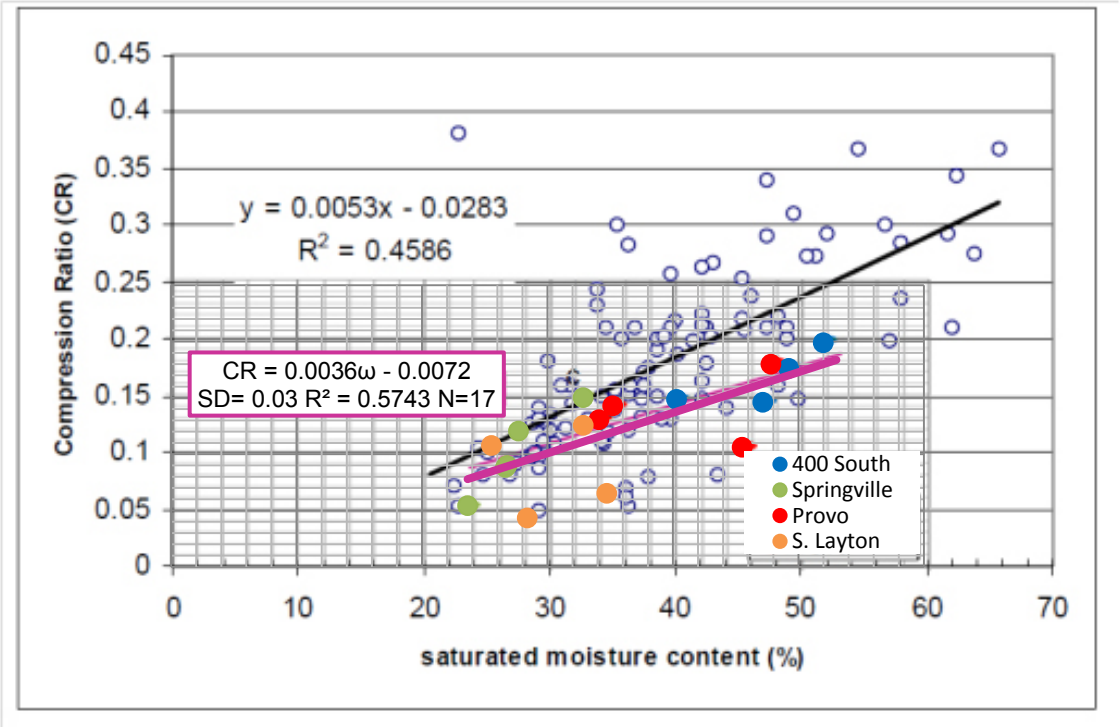

Figure 6.11 Plot of moisture content vs. virgin compression ratio (Bartlett and Lee, (2004)

The correlations as attempted included: C_α, C_α'/CR, C_α'/C_α as shown in Figures 6.12, 6.13, and 6.14. Based on these plots, there is poor to very poor correlation between C_α and C_α'/C_α and ω (Figures 6.12 and 6.14, respectively). However, the correlation between C_α/CR and ω has some promise for future development and application (Figure 6.13). However, more observations are needed to improve the statistical support for this relation.

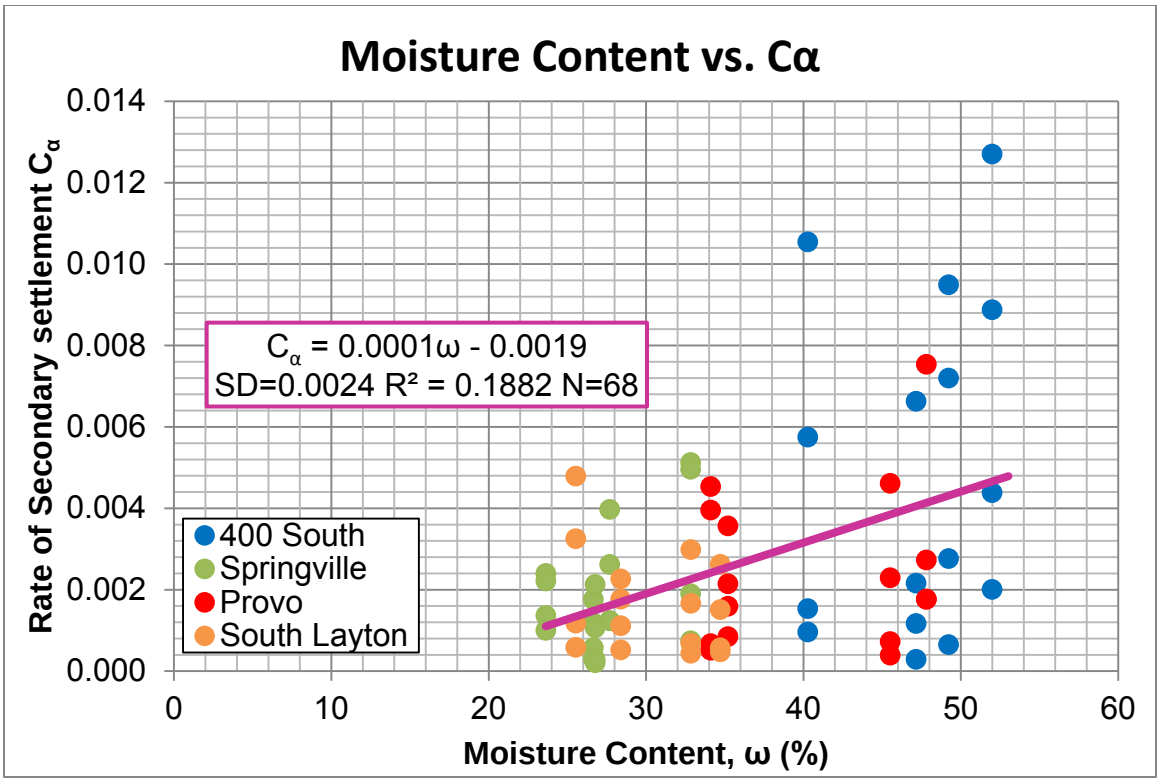

Figure 6.12 Plot of moisture content vs. rate of secondary settlement

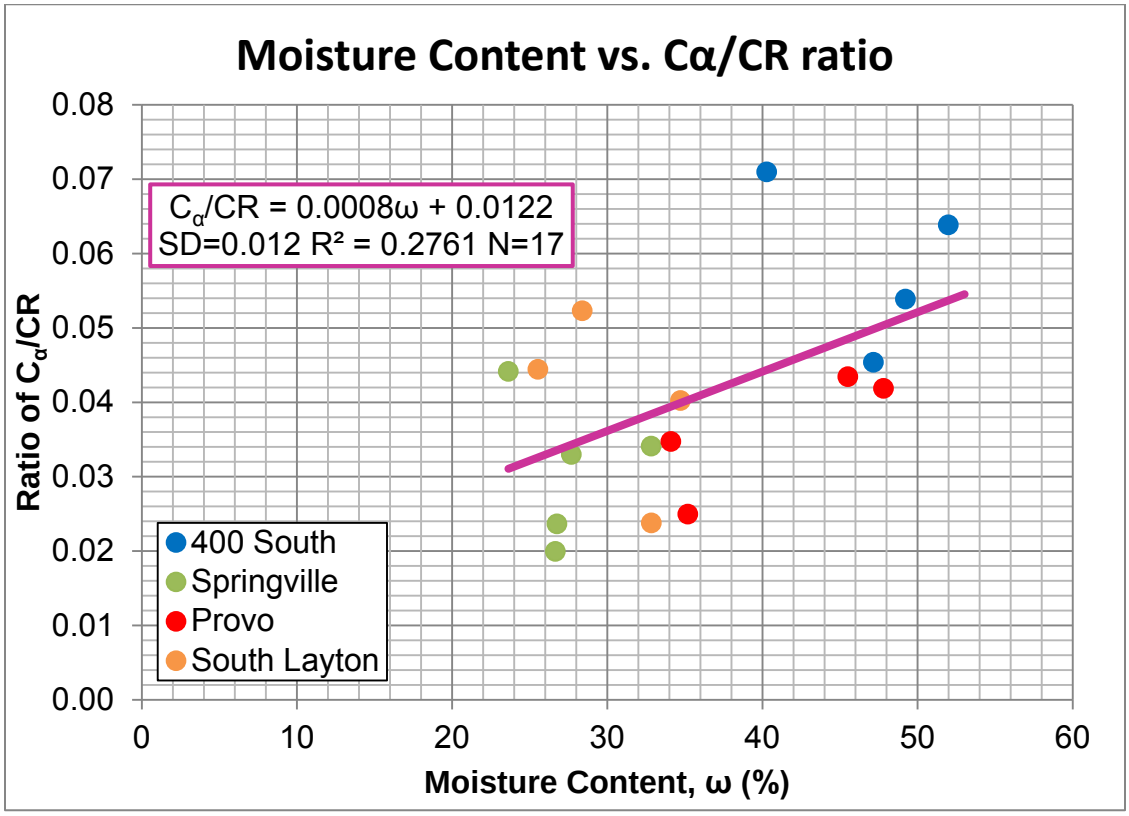

Figure 6.13 Plot of moisture content vs. C_α/CR ratio

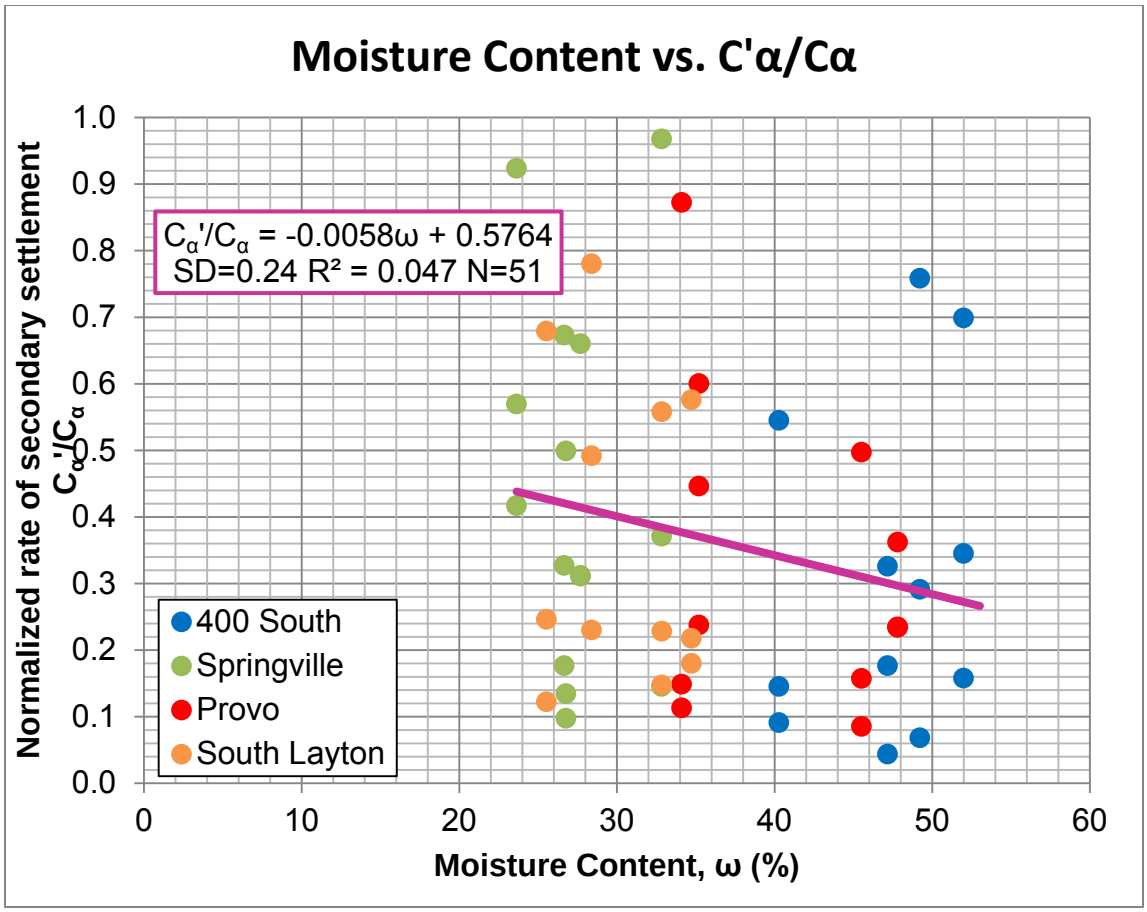

Figure 6.14 Plot of moisture content vs. normalized rate of secondary settlement

7 CONCLUSION

7.1 Summary of Thesis Objectives

The main objectives in this research are 1) corroborate Mesri's concept of secondary compression (i.e., C_α/CR is relatively constant) for the Lake Bonneville deposits along the Wasatch Front in Utah, 2) supplement and/or revise, as necessary, the design relationships developed by Ng (1998) for the I-15 surcharge design using a larger set of field and laboratory test data, 3) recommend an appropriate laboratory testing and evaluation program to support project-specific surcharge design for future highway embankment projects sponsored by the Utah Department of Transportation (UDOT) in the Wasatch Front Area, and 4) develop additional design guidance and/or recommendations for developing and evaluating the surcharge design.

7.2 Mesri's Concept of Secondary Compression

Based on the results of the oedometer tests run at MIT and WCC they have recommended values of the following creep properties: 1) C_α/CR 2) creep behavior as a function of AAOS 3) the delay to the amount of time before creep resumes after the removal of a surcharge as a function of AAOS. The data acquired during testing from this research are being compared with that produced by MIT and WCC.

7.2.1 C_α/CR

An analysis from this research, the C_α/CR ratio with the regression line passing through the origin (Figure 6.8) gives an average value of C_α/CR = 0.0442. The site of 400 South C_α/CR = 0.0598, South Layton C_α/CR = 0.0346, Springville C_α/CR = 0.0308, and Provo C_α/CR = 0.0359 (Figure 6.7). The trend at the 400 S. Street site in Salt Lake City has a somewhat steeper slope (higher ratio) than the South Layton, Springville and Provo sites.

The average ratio obtained though this research of C_α/CR = 0.0442 correlates reasonably well with that obtained by the results from Ng's (1998) of C_α/CR = 0.0433, thus confirming that Mesri's concept of secondary compression is constant along the Wasatch Front (i.e., the C_α/CR ratio).

7.2.2 Creep Behavior as a Function of AAOS

Using the methodology developed by Ladd (1989), when plotting AAOS vs. C'_α/C_α on a semi-log plot and comparing this with research done by Ng (1998), these data show that the trend seems to be higher than that estimated by Ng (1998) (Figure 6.5). In fact the trend seems to be closer to the upper bound of the data from Ng (1998). During the I-15 reconstruction project, the lower bound was used for the calculations of long-term settlement. The 10-year post-construction settlement at these sites is projected to be almost 1.5 to 2 times that of what was calculated (Figure 6.6). This suggests that the rate of secondary compression in the subsurface soils at these locales is greater than that anticipated in the surcharge design.

In Figure 6.5, it can be seen that with AAOS above 50% (OCR = 1.5) the average trendline of Ng (1998) would predict a C_{α}'/C_{α} ratio of near zero. The data from this research show a minimum value of C_{α}'/C_{α} of about 0.1 at an AAOS of 100 percent (OCR = 2.0) (Figure 6.5). However, the data seem to fit better with the use of an exponential trend line (Figure 6.4).

Therefore, it is recommended that when estimating the value of C'_{α}/C_{α} from AAOS to use the exponential equation $C'_{\alpha}/C_{\alpha} = 0.9245e^{-0.02(AAOS)}$, or if using the plot produced by MIT and an AAOS below 50% to use the upper bound trend line.

7.2.3 The Time Before Creep Resumes After the Removal of a Surcharge

When comparing the data from this research with that done by MIT and WWC (Ng 1998) for the plot of AAOS vs. $Log(t_s/t_r)$ (Figure 6.9), it can be seen that the average trend line through the origin is lower than that produced by MIT. Where Ng (1998) has the equation of $Log(t_s/t_r) = 0.0206$ (AAOS) and the equation for the average trend from this research is $Log(t_s/t_r) = 0.0174$ (AAOS). This trendline is slightly lower but compares well with previous work.

7.3 Recommendation for a Laboratory Testing Program

When performing laboratory testing to determine the Mesri's C_{α}/CR ratio, the procedure is as follows: (1) perform a 1-D consolidation test on the sample; this is done to determine the consolidation properties such as σ_p, CR, and RR, (2) determine the rate of secondary compression for normally consolidated specimen, C_{α} by loading the soil sample to 1.5 to 2.0 times that of σ_p (to remove

any disturbance from the soil sample and to be sure that the soil is normally consolidated, (3) determine the rates of secondary compression for overconsolidated specimens, C'_{α}. Refer to Appendix C for the detailed procedure used in this research.

It is recommended that when determining the preconsolidation stress, each loading step should be moved to the next step with as little as possible secondary settlement occurring. If a large amount of secondary settlement occurs, the soil then becomes aged and it can have an impact on the results of the consolidation data. It is also advantageous to move to the next loading step with as little secondary compression occurring because the tests can be run in a shorter amount of time as opposed to the traditional 24-hour loading steps.

7.4 Additional Design Guidance

The moisture content can be used for the estimating of C_c and CR of a saturated soil (Figures 6.10 and 6.11). For application purposes, it is recommended the Bartlett and Lee (2004) equation CR = 0.0053(ω) - 0.0283 be used because of its greater statistical support.

Correlations for C_{α}, C_{α}'/CR, and C_{α}'/C_{α} with ω were explored in this research (Figures 6.12 to 6.14). Based on these plots, there is poor to very poor correlation between C_{α} and C_{α}'/C_{α} with ω (Figures 6.12 and 6.14, respectively). The correlation between C_{α}/CR and ω has some promise for future development and application (Figure 6.13). However, more observations are needed to improve the statistical support for this relation.

7.5 Recommendation for Further Testing

It is recommended that when future testing is being performed, Atterburg limits and fines wash to be performed on every test specimen for a better classification of the soil being tested. This will also lead to a better understanding of how each type of soil behaves during long-term settlement.

It is also recommended that in the future, a more advanced testing with pore water pressures mesurements be performed, so as to know when primary settlement is complete and to have very little secondary settlement occur.

APPENDIX A

PLOTS FOR PRECONSOLIDATION STRESS

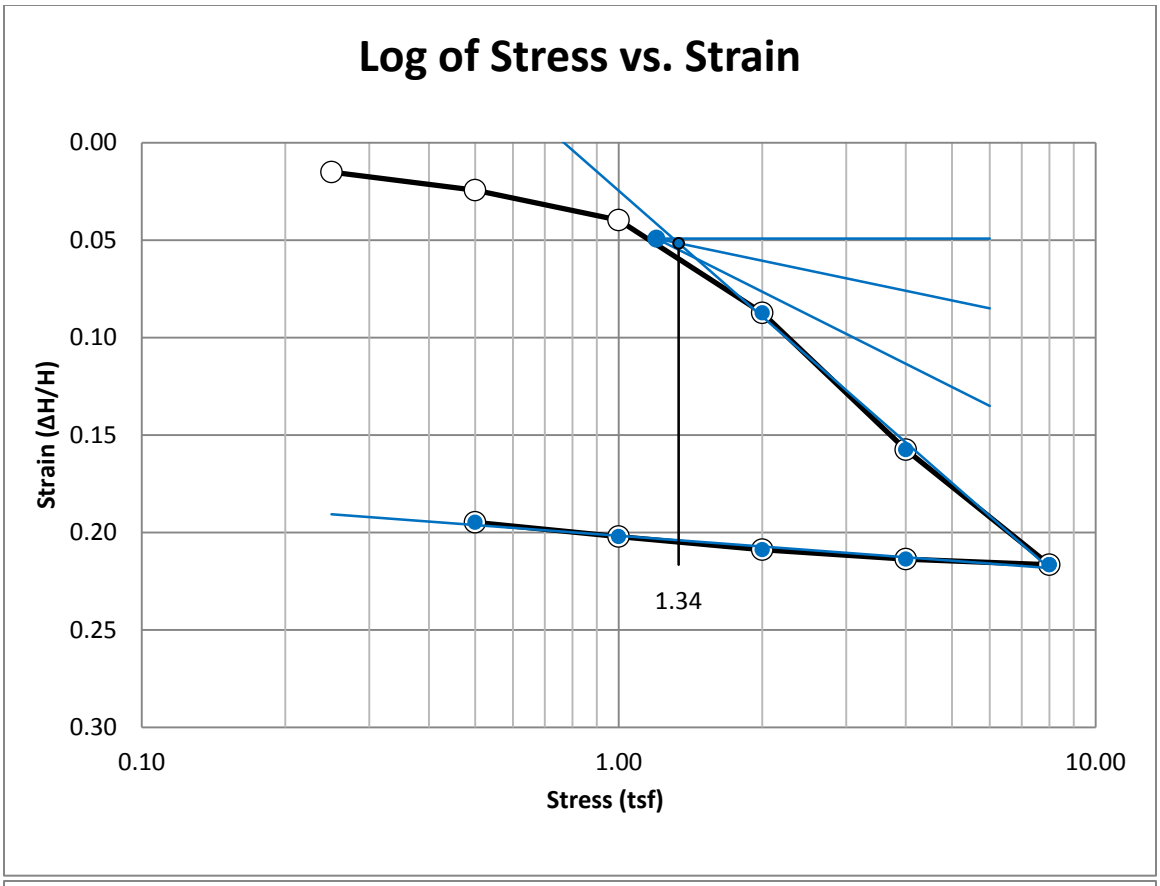

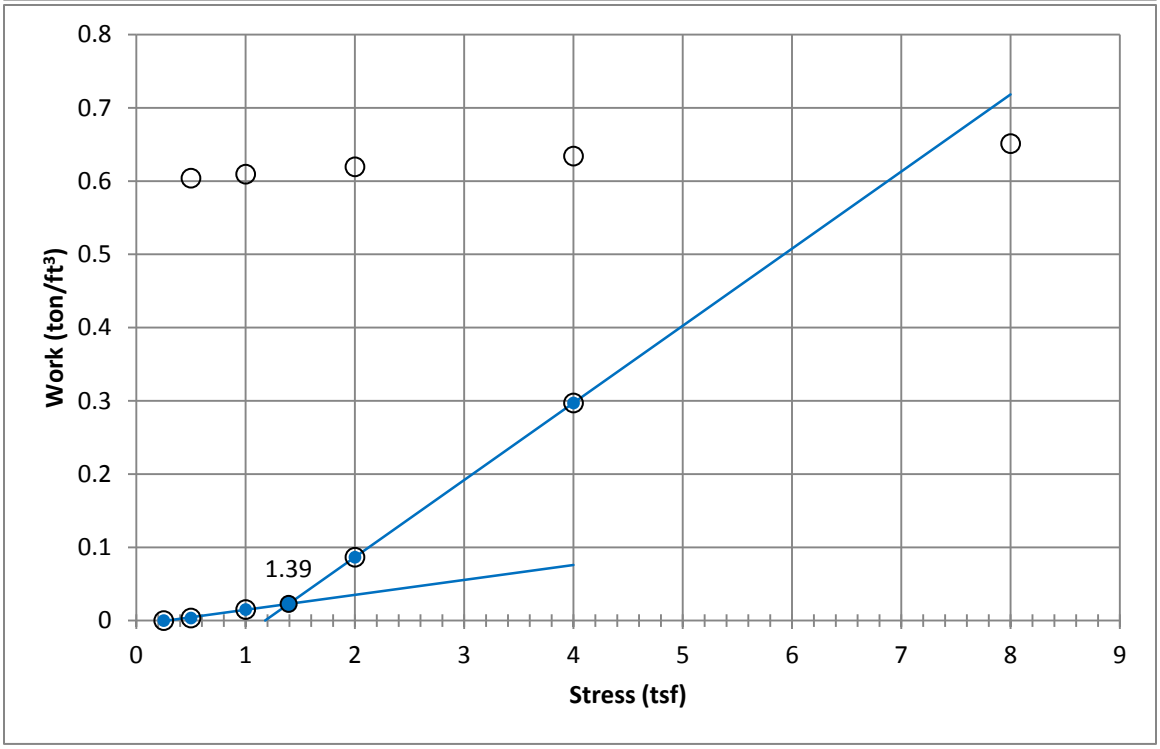

A1 400 South at 15-17 feet

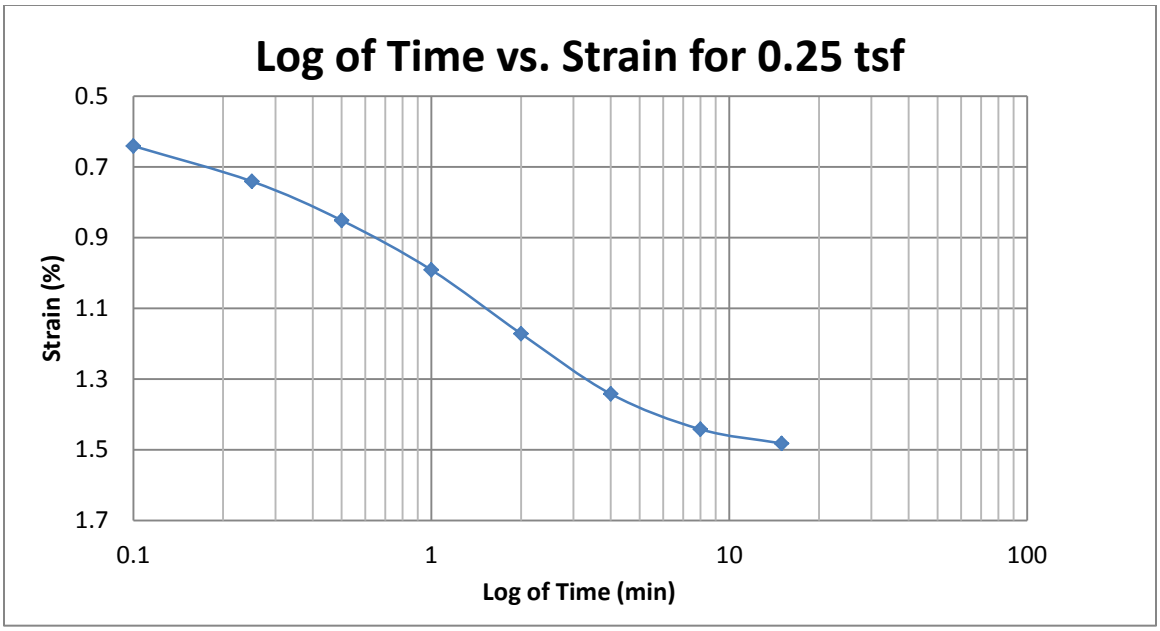

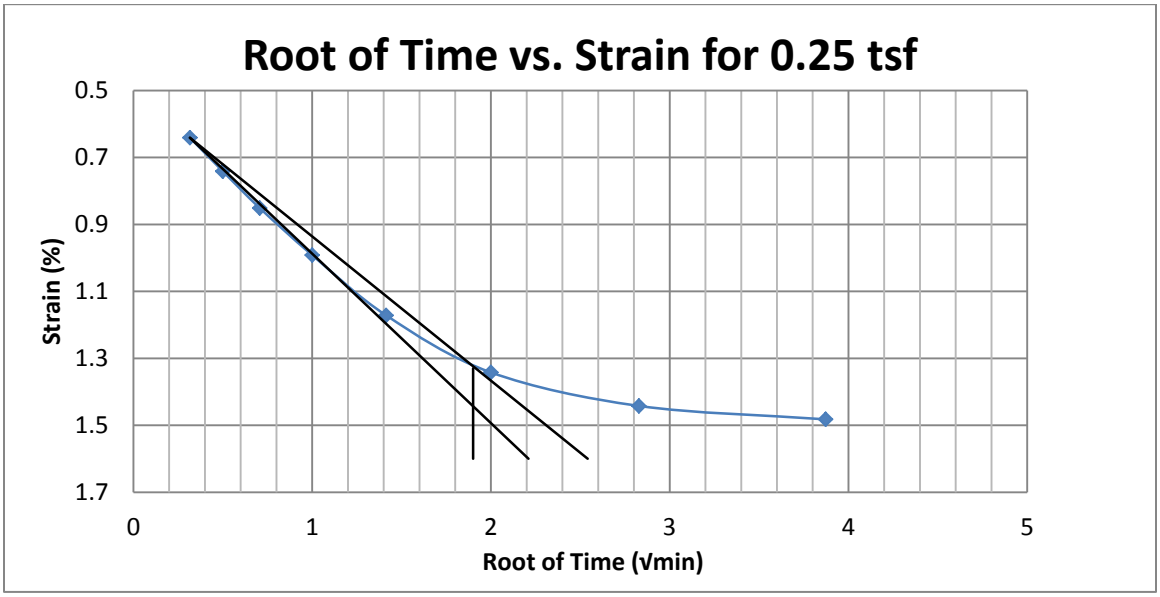

A2 400 South at 15-17 feet

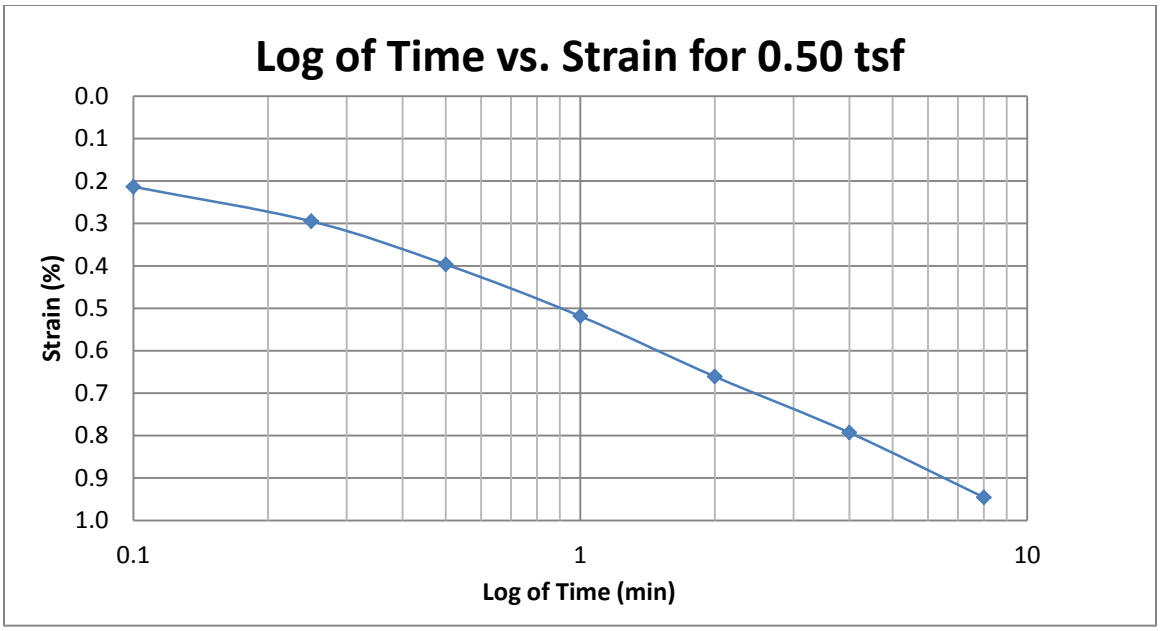

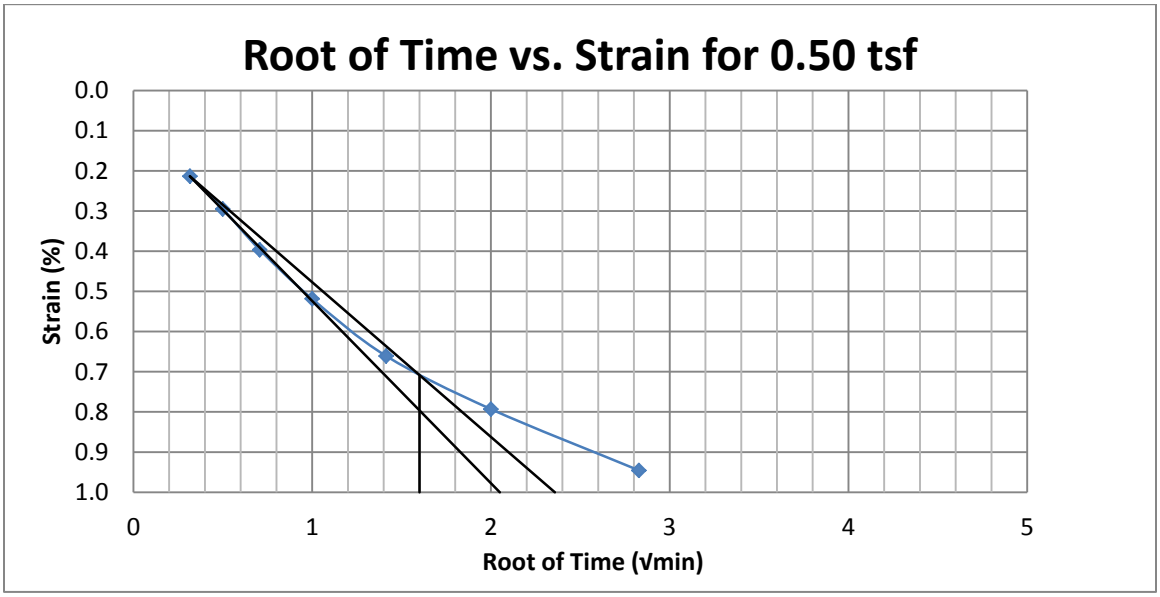

A3 400 South at 15-17 feet

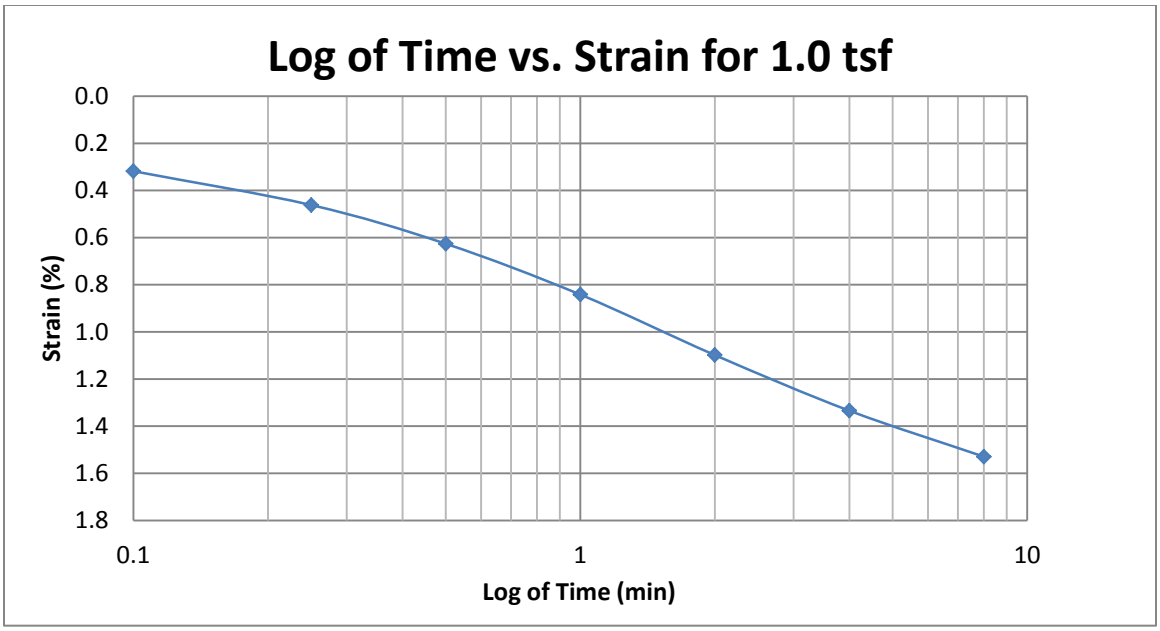

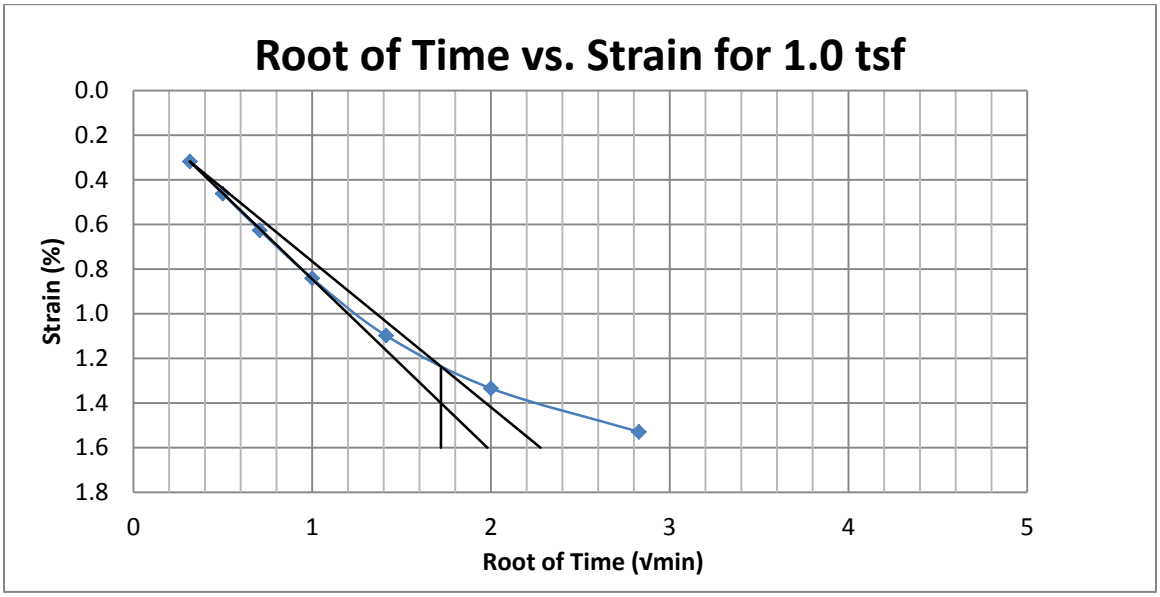

A4 400 South at 15-17 feet

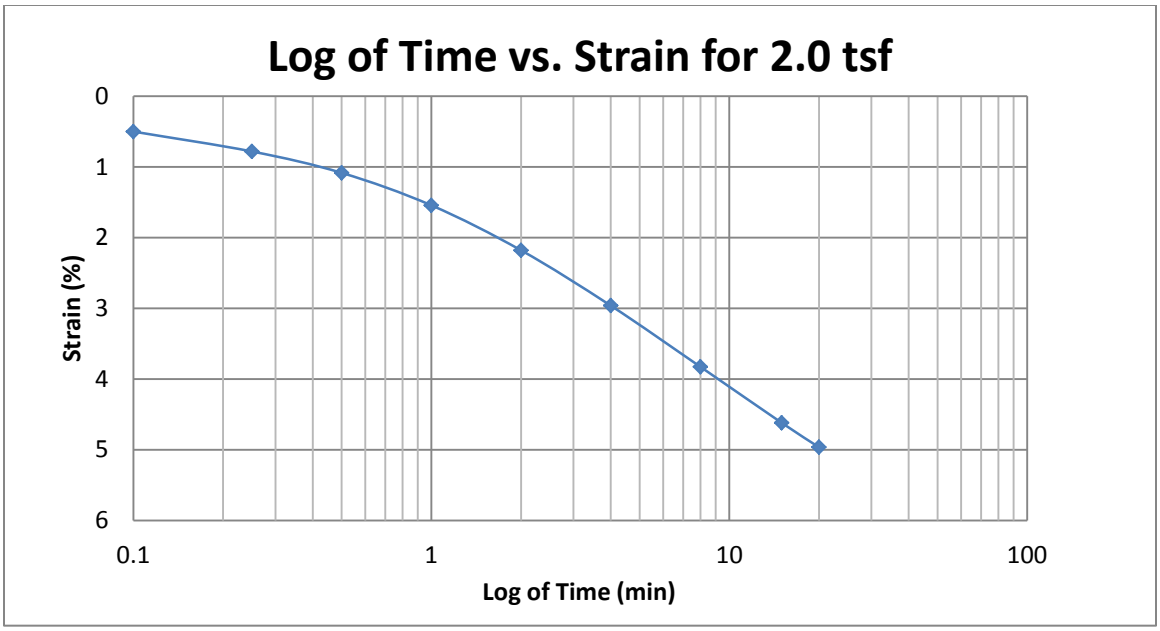

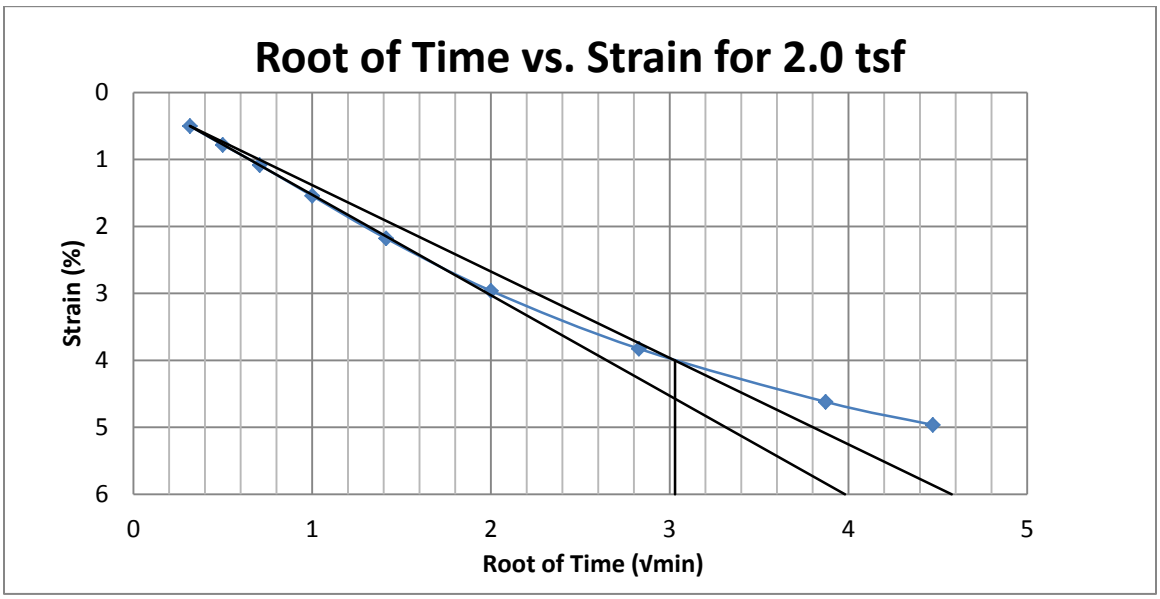

A 5 400 South at 15-17 feet

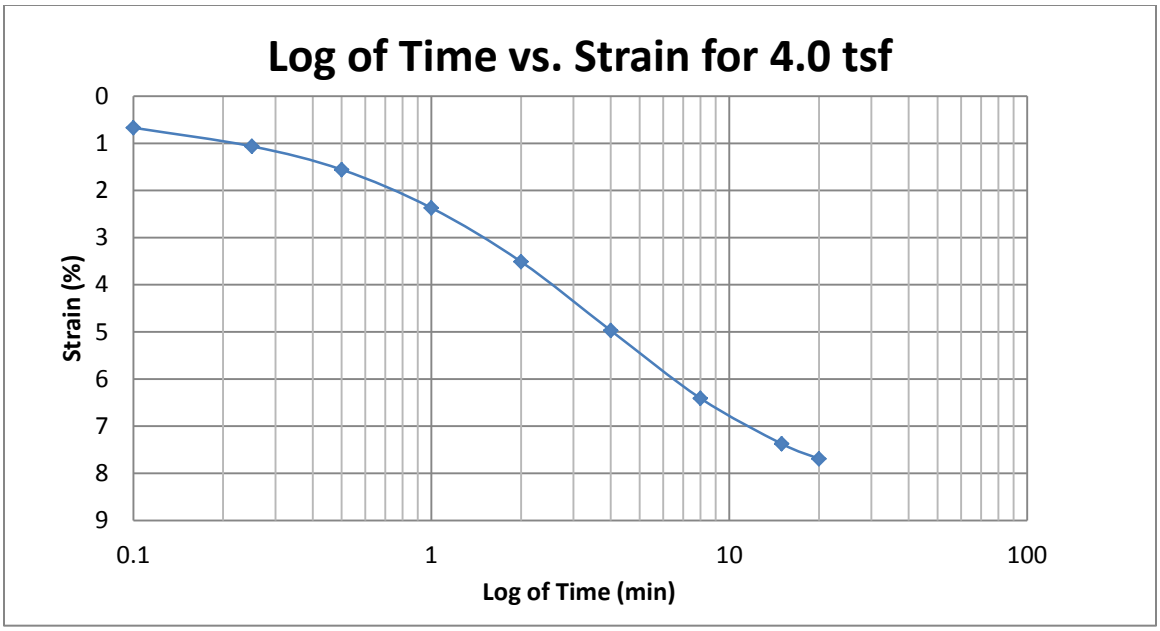

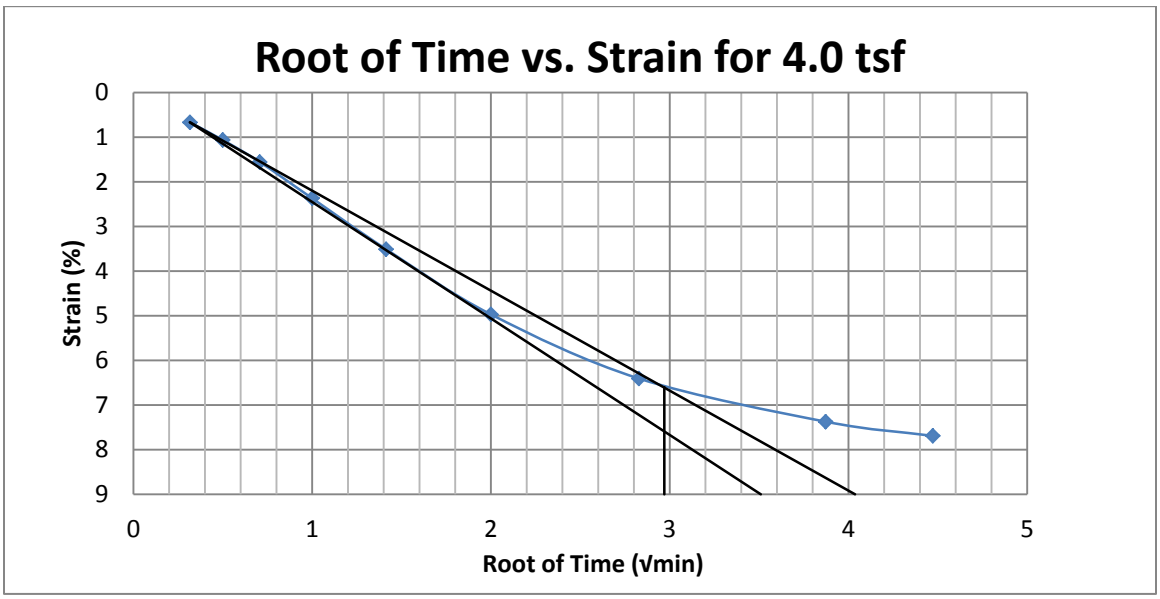

A6 400 South at 15-17 feet

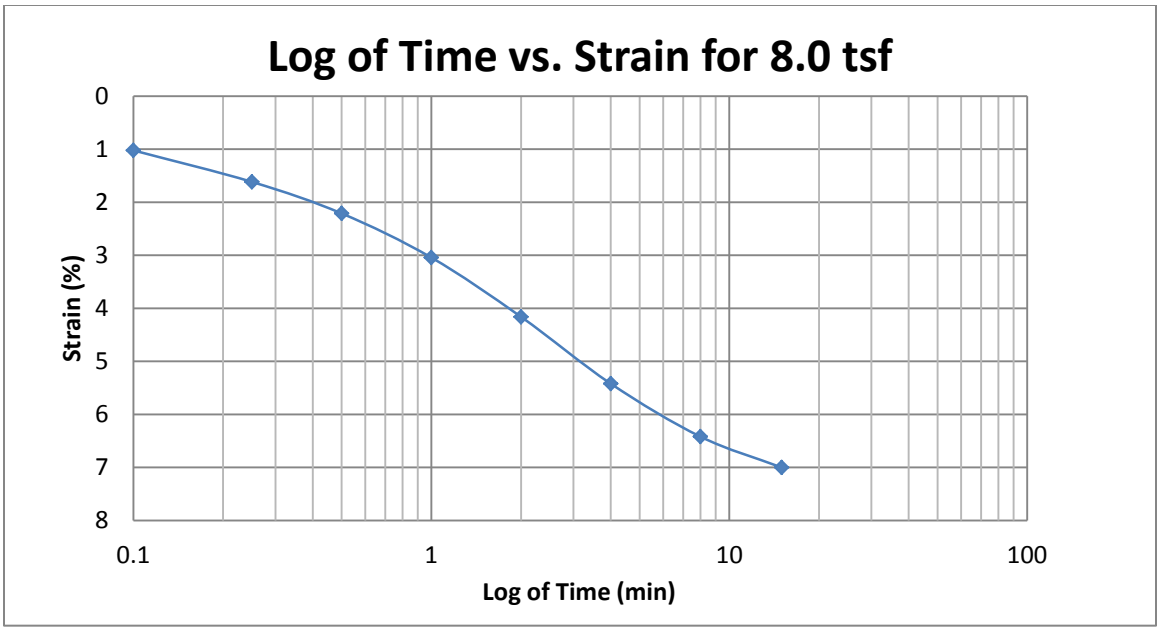

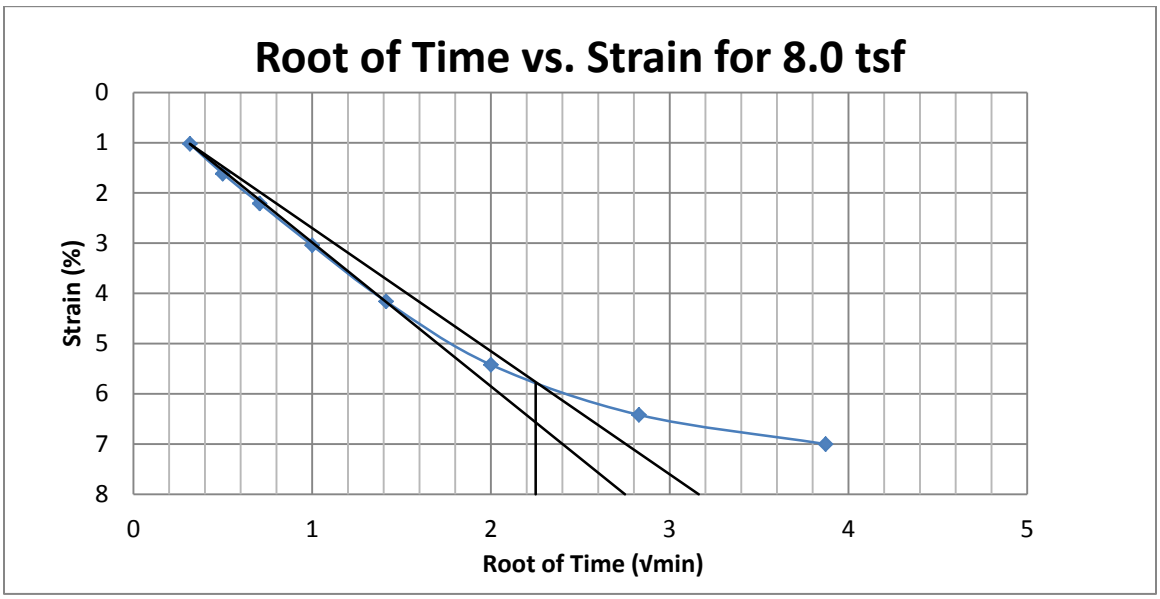

A7 400 South at 15-17 feet

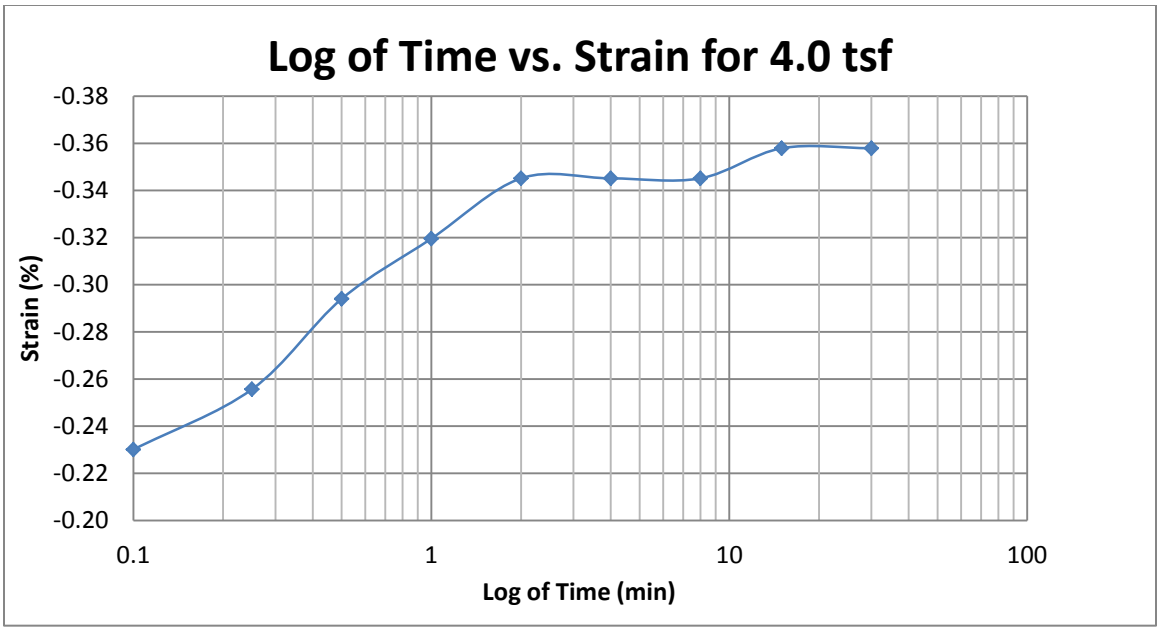

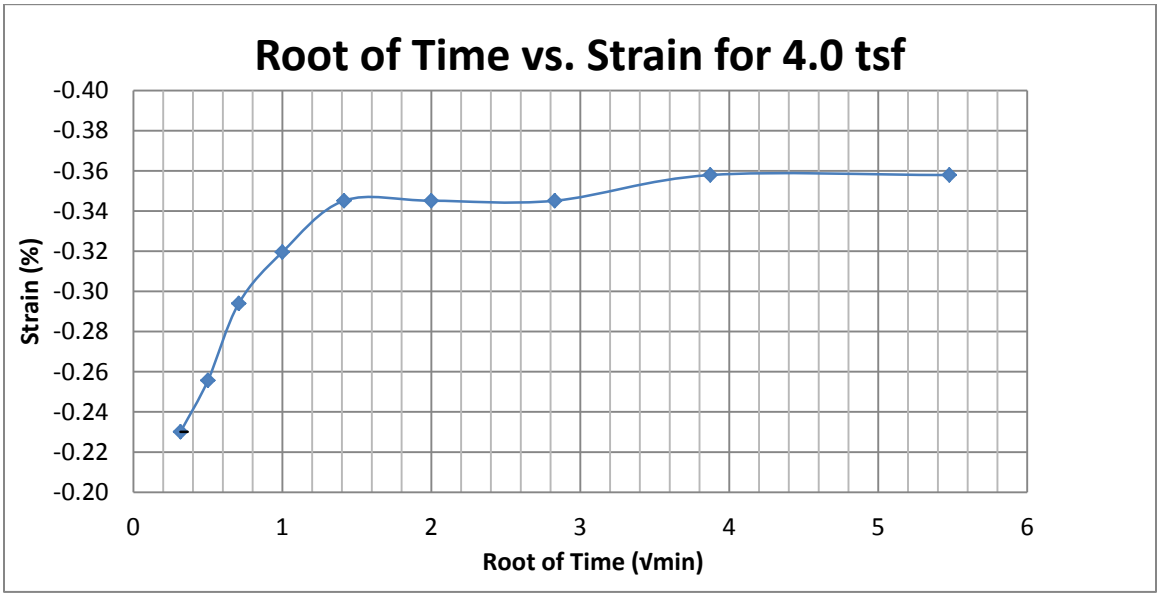

A8 400 South at 15-17 feet

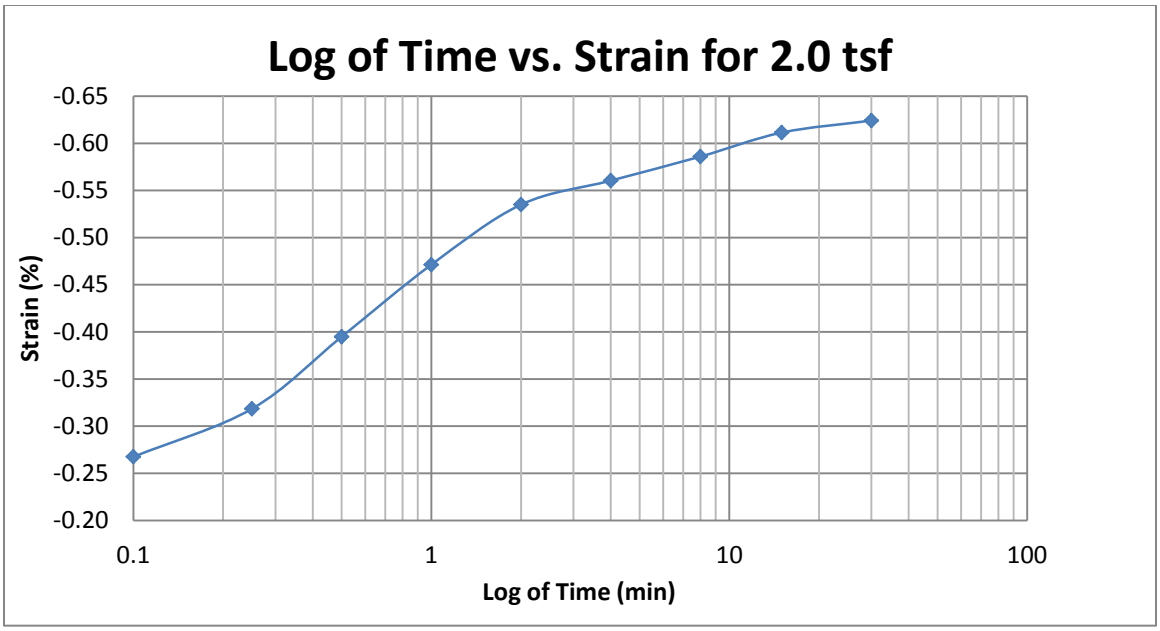

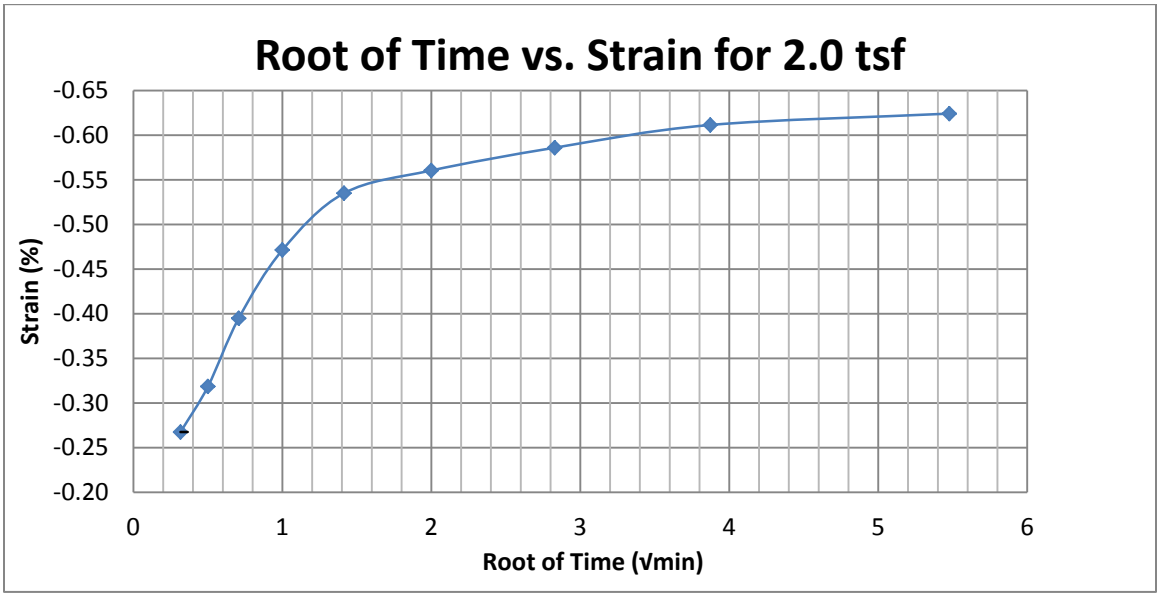

A9 400 South at 15-17 feet

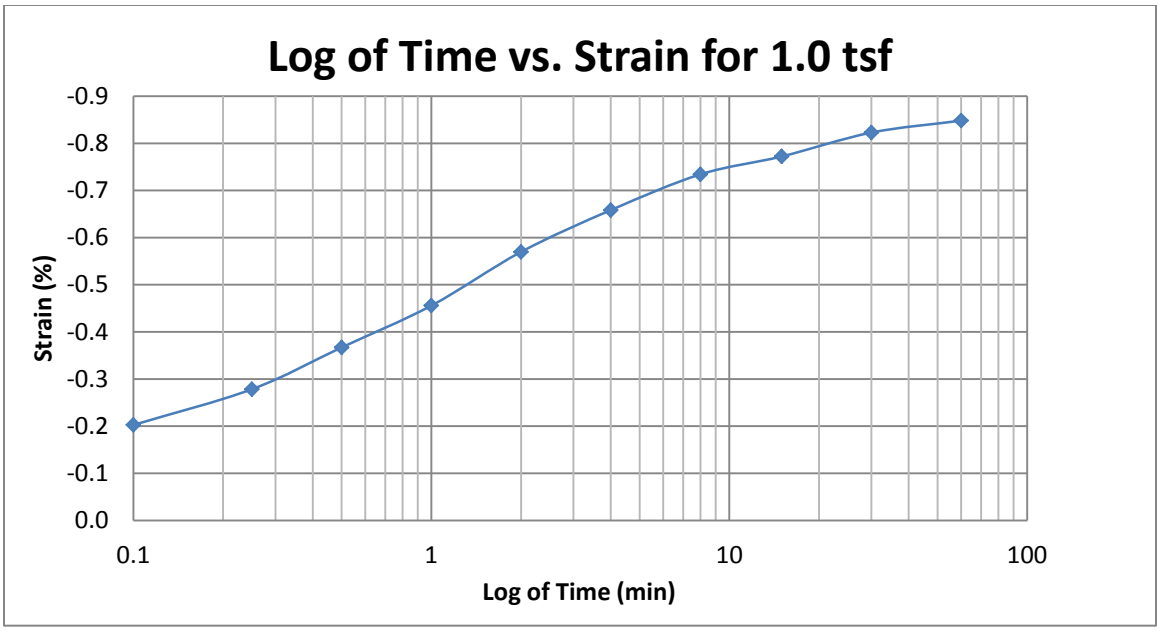

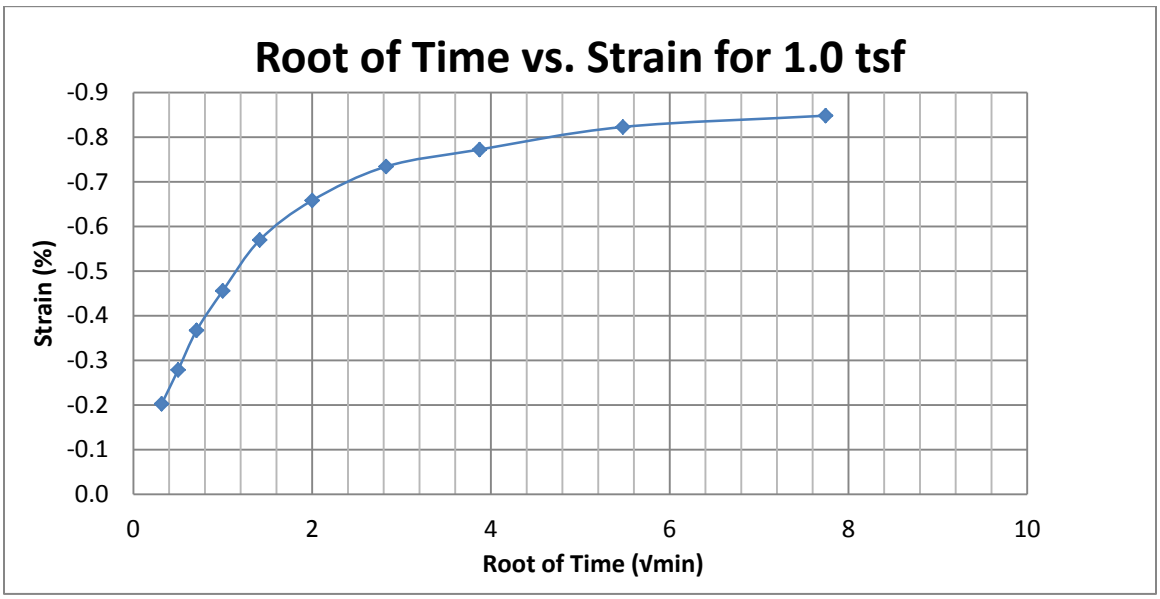

A10 400 South at 15-17 feet

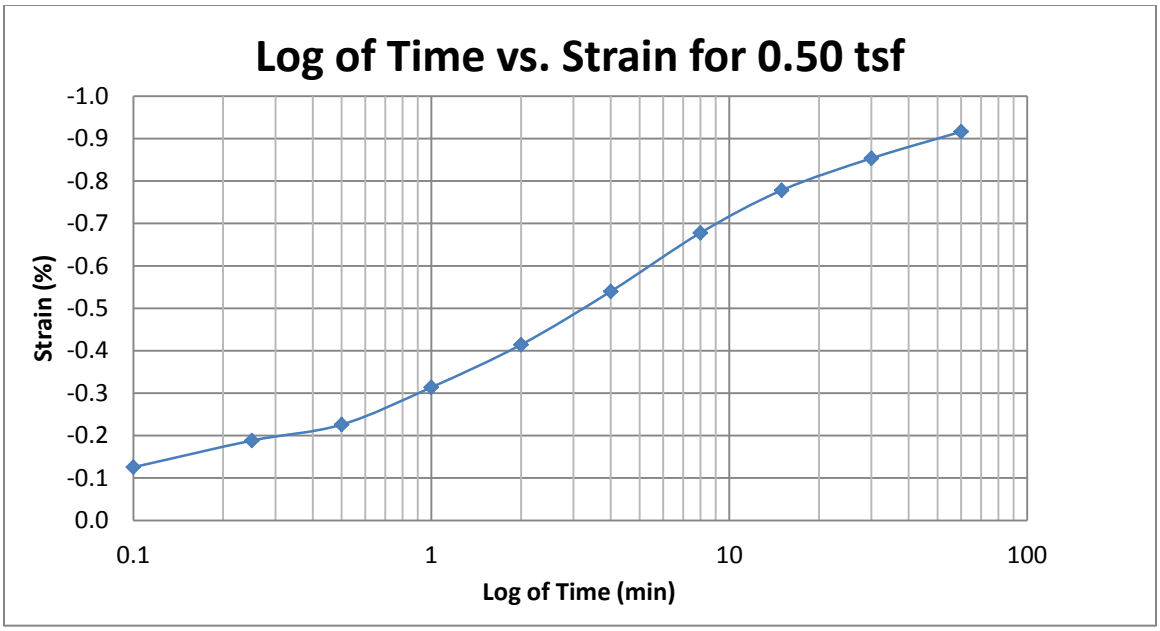

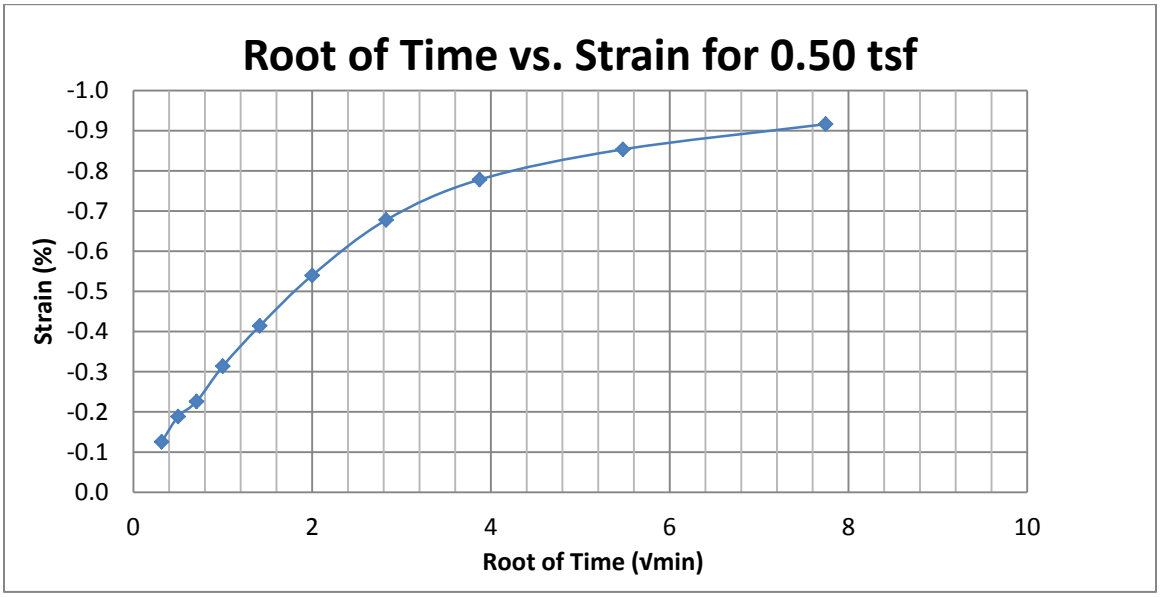

A11 400 South at 15-17 feet

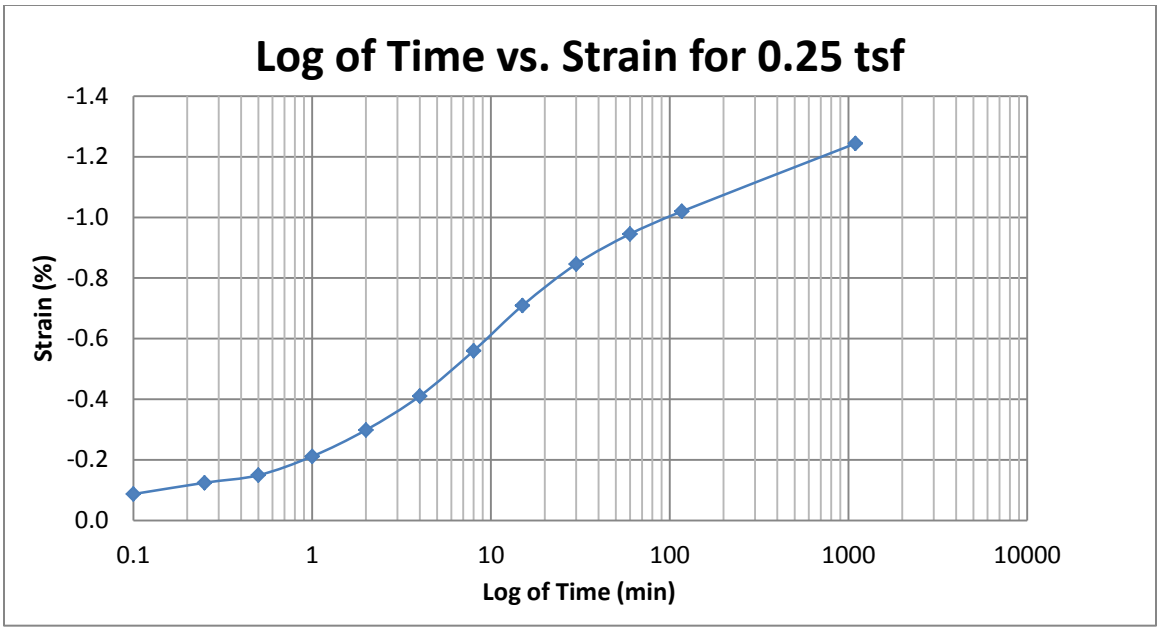

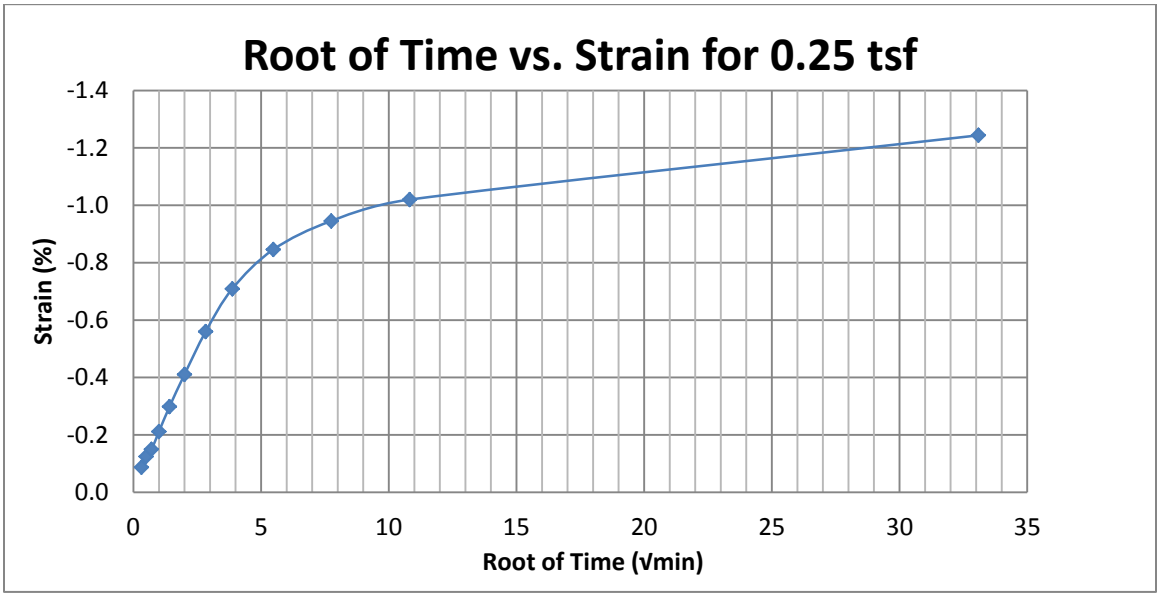

A12 400 South at 15-17 feet

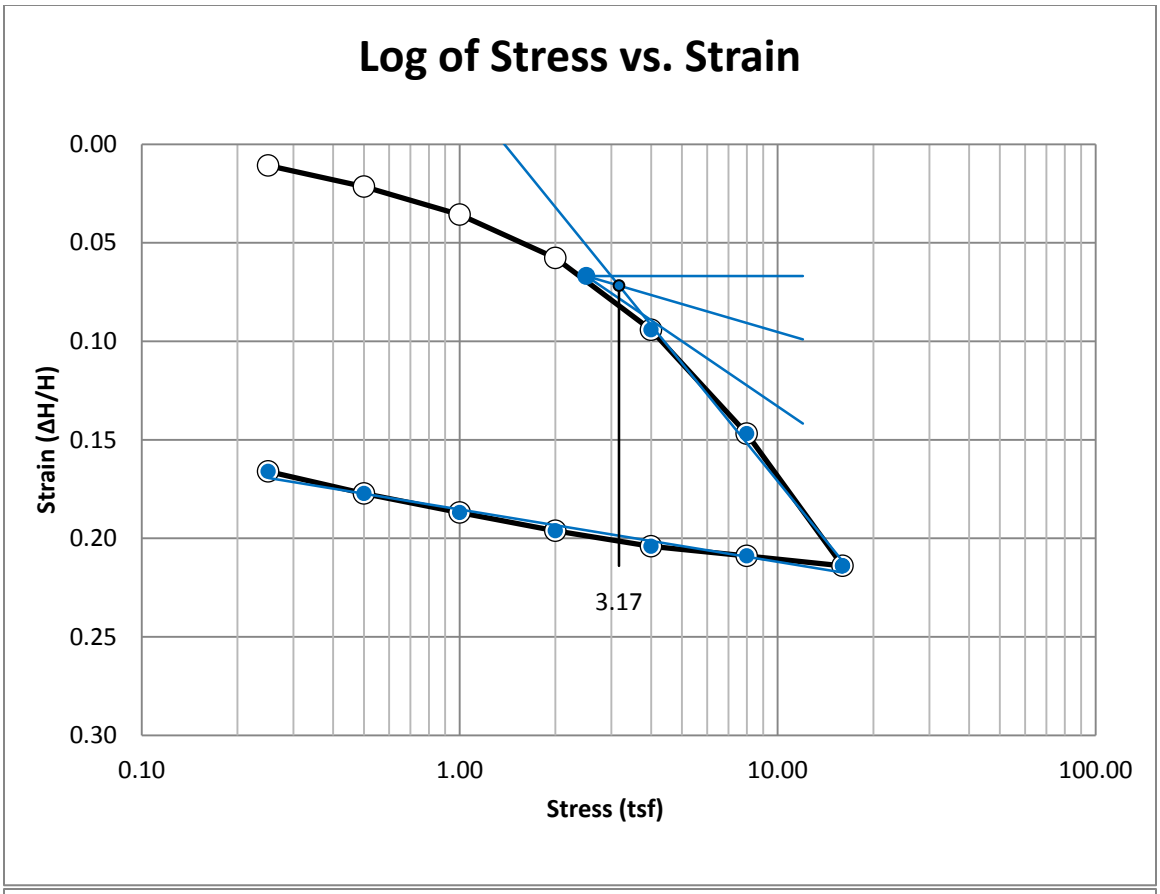

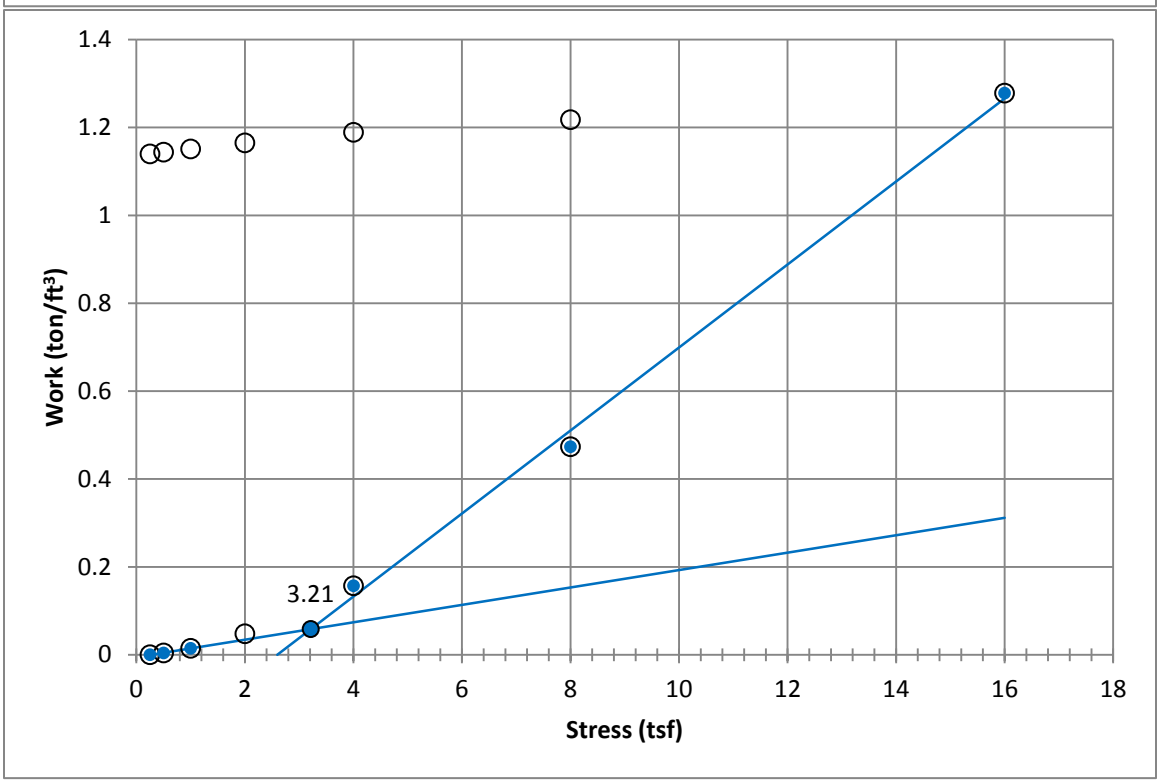

A13 400 South at 20-22 feet

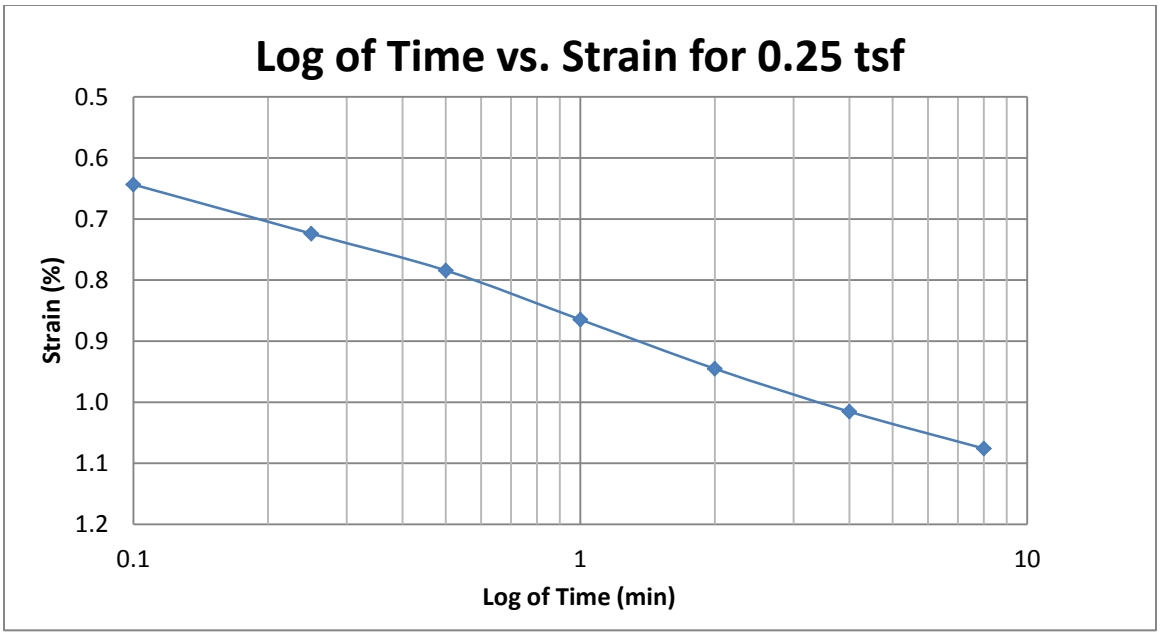

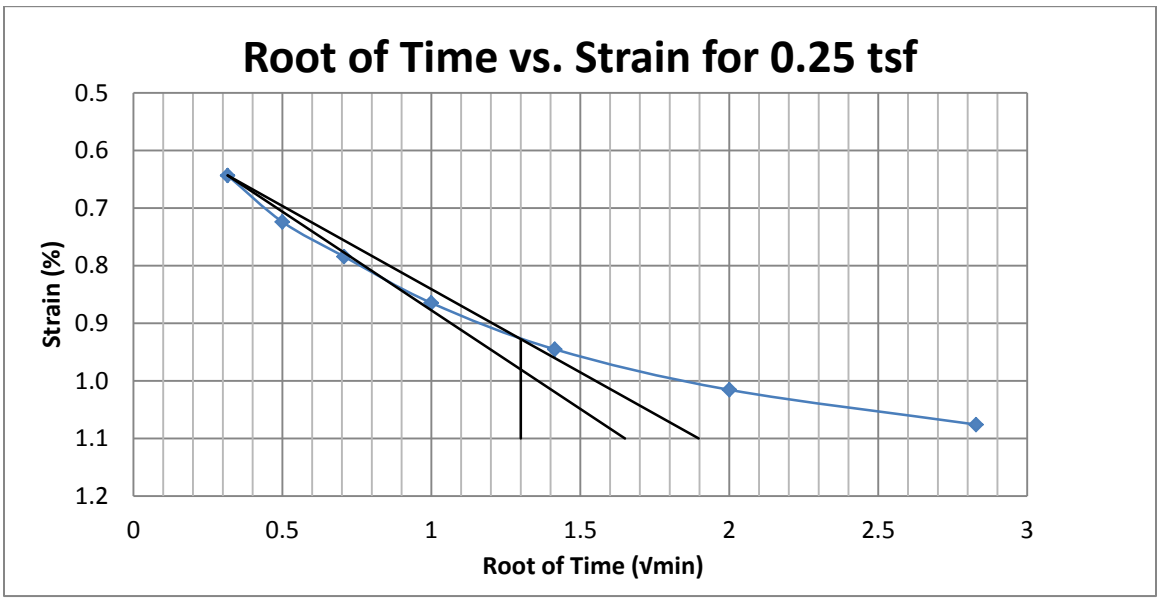

A14 400 South at 20-22 feet

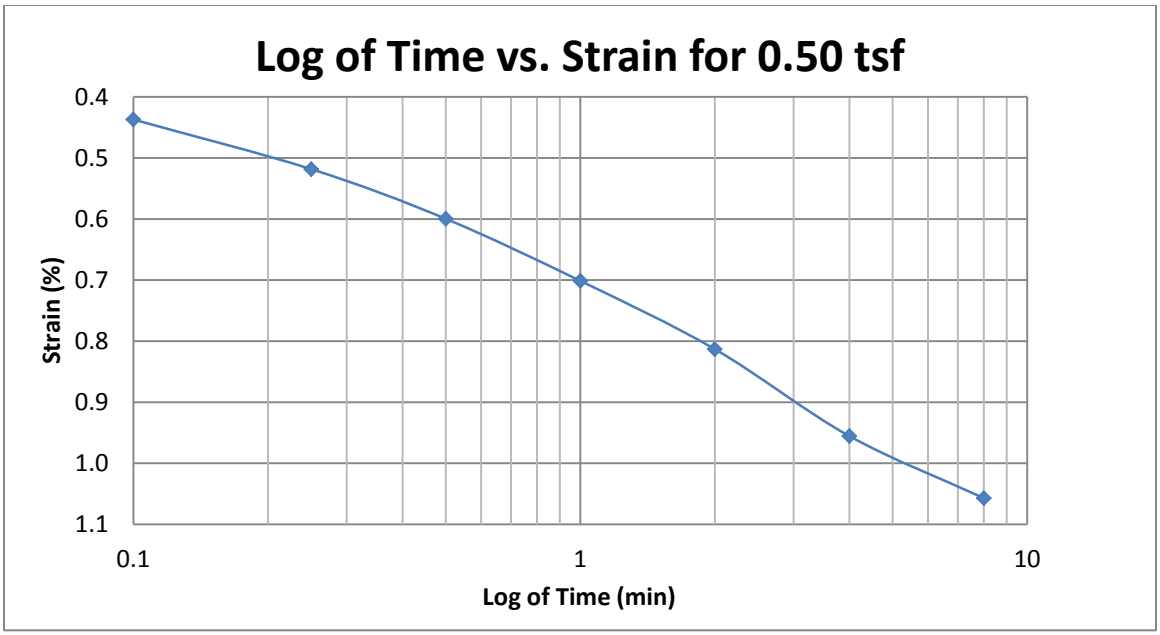

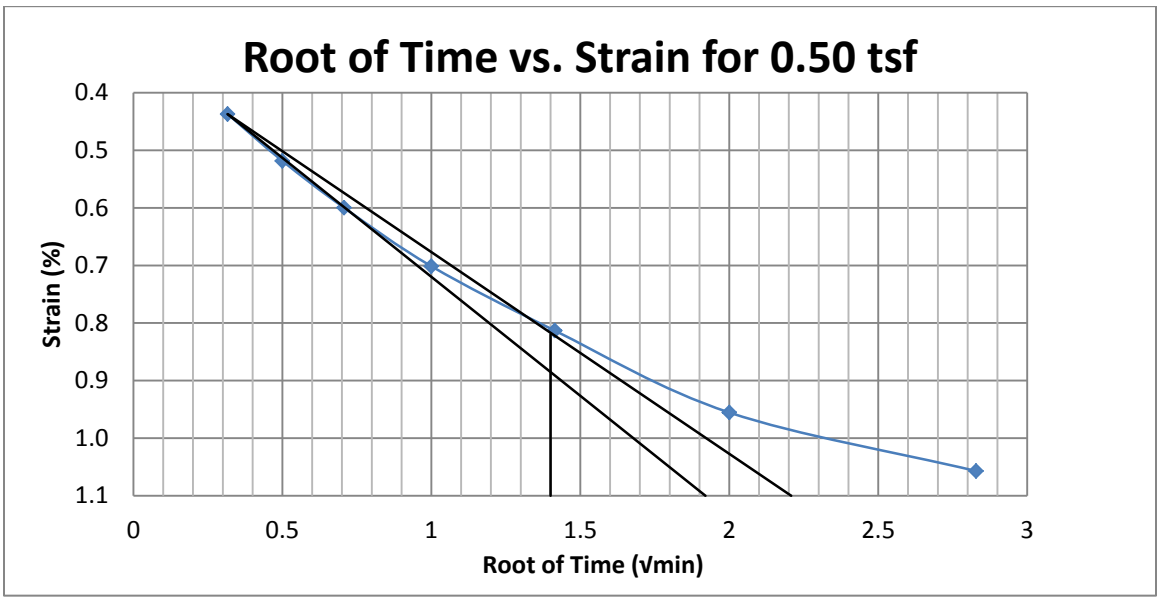

A15 400 South at 20-25 feet

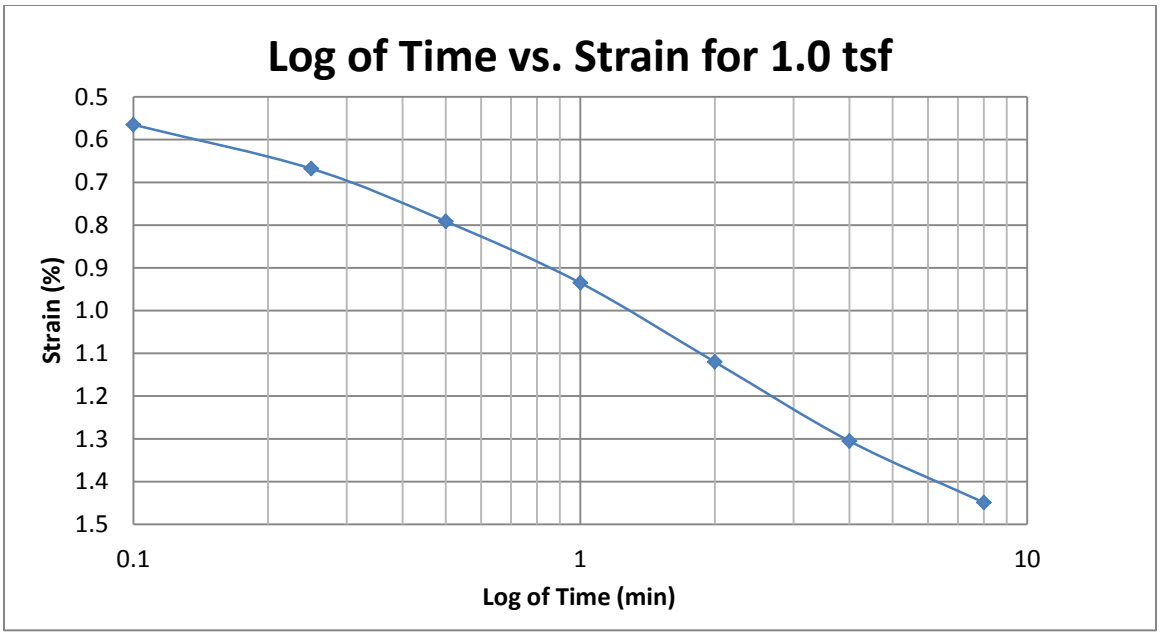

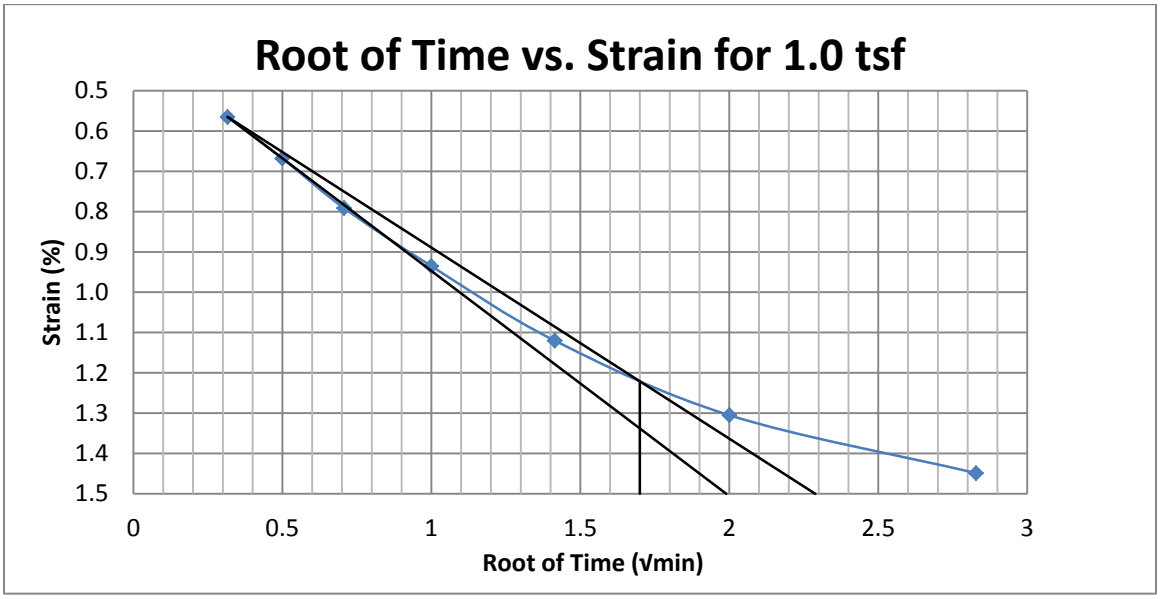

A16 400 South at 20-25 feet

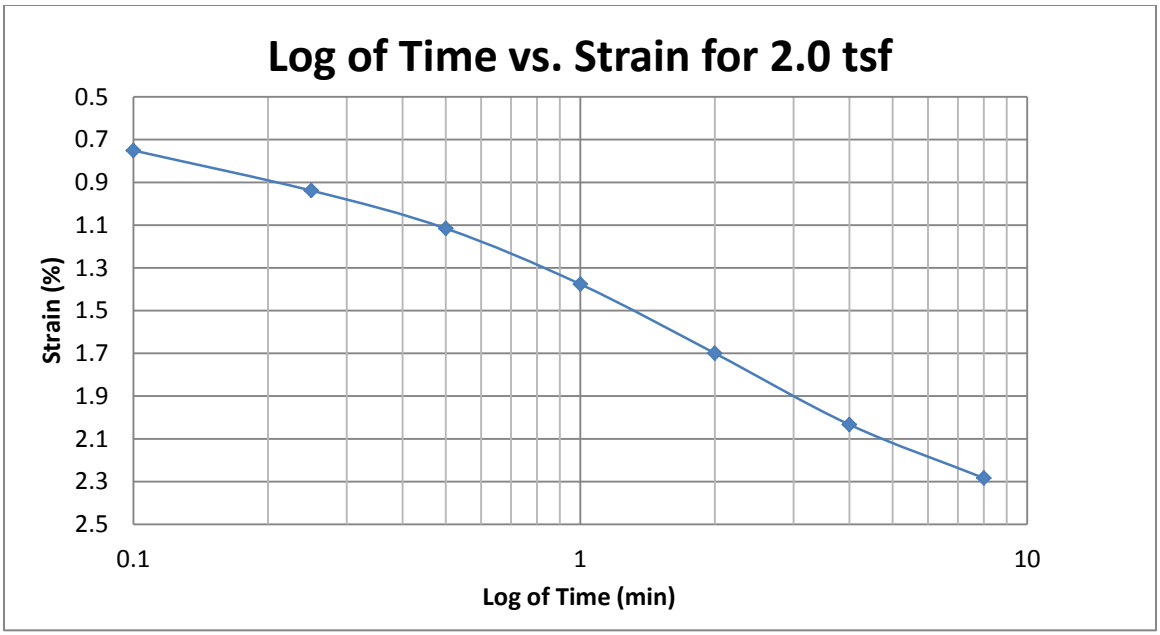

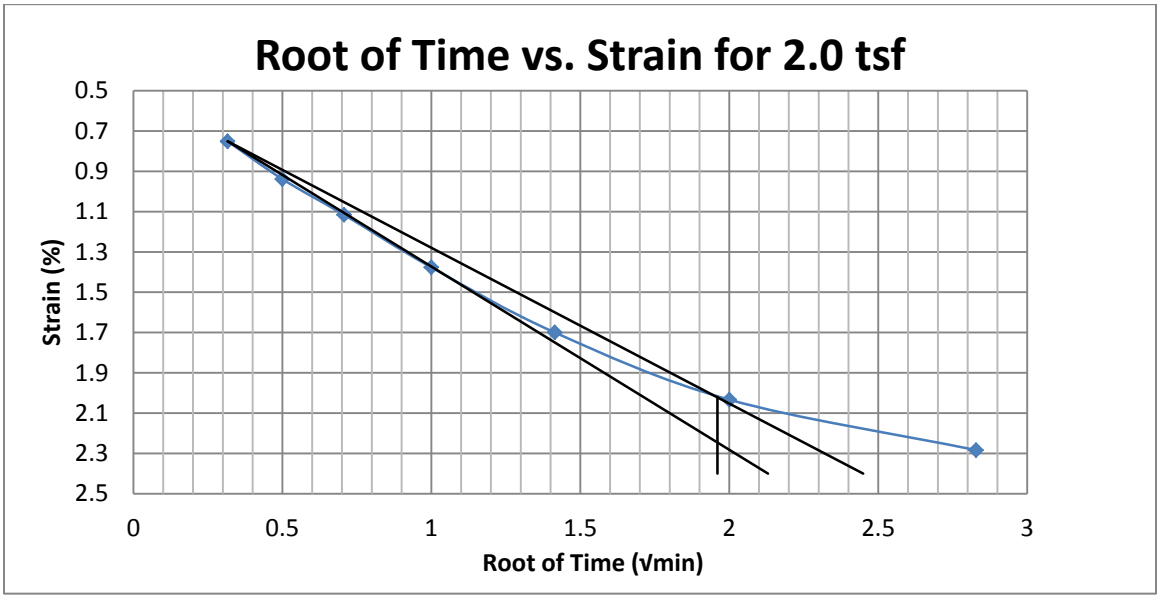

A17 400 South at 20-22 feet

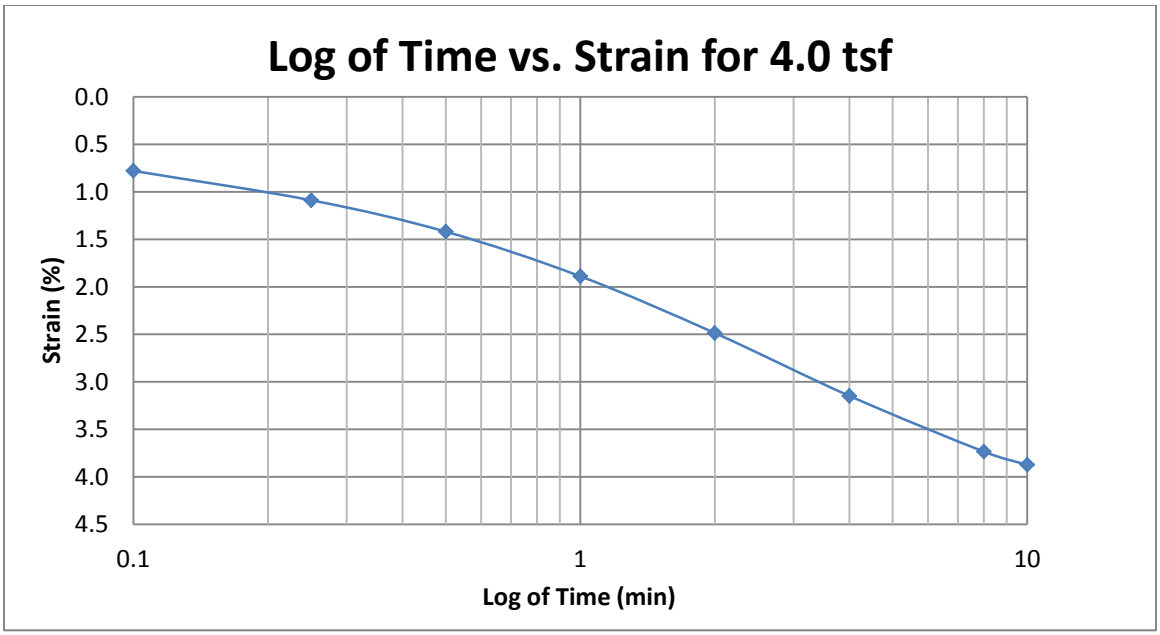

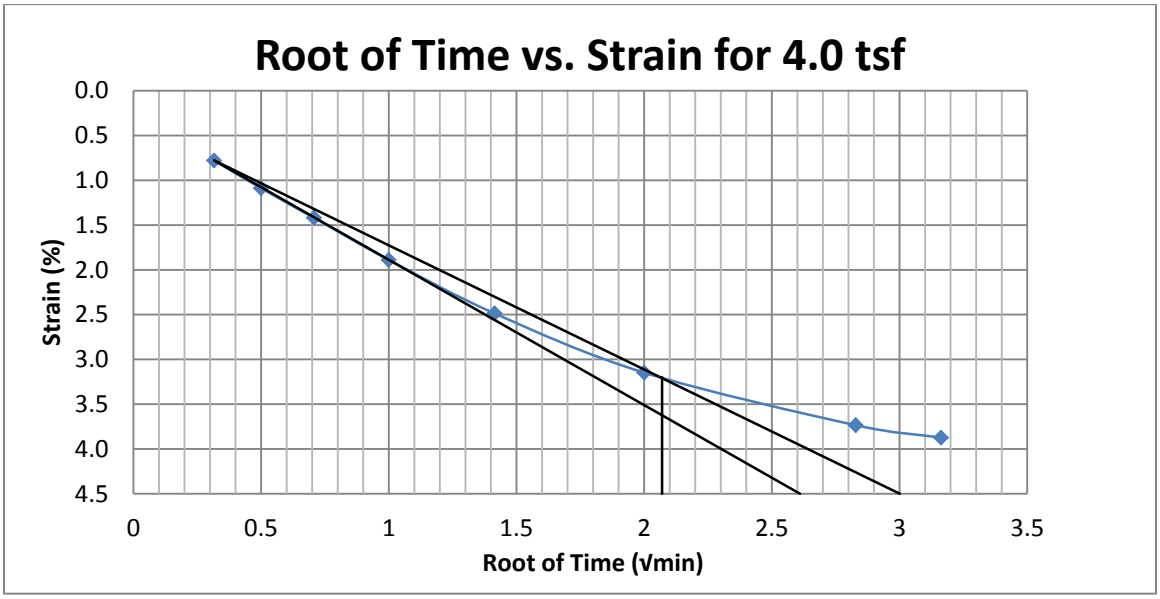

A18 400 South at 20-22 feet

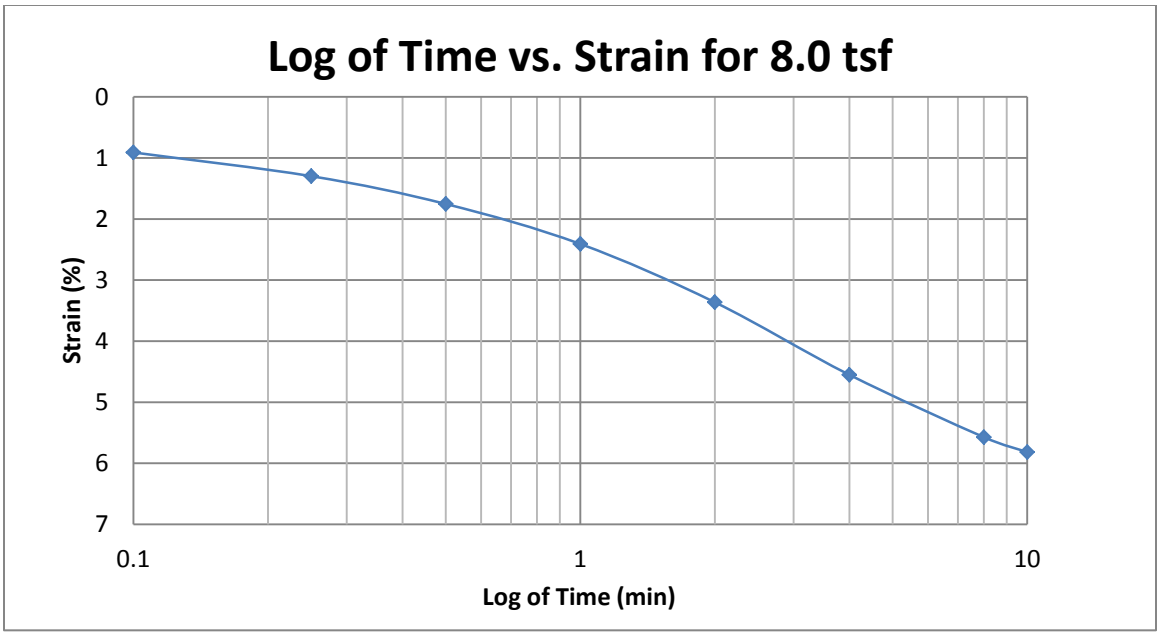

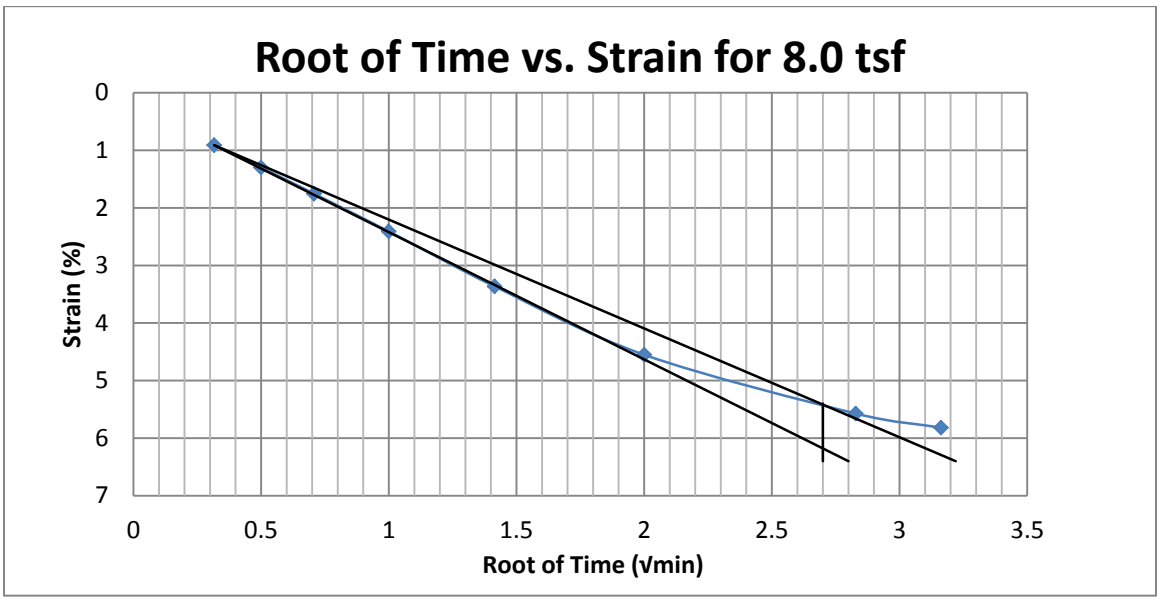

A19 400 South at 20-22 feet

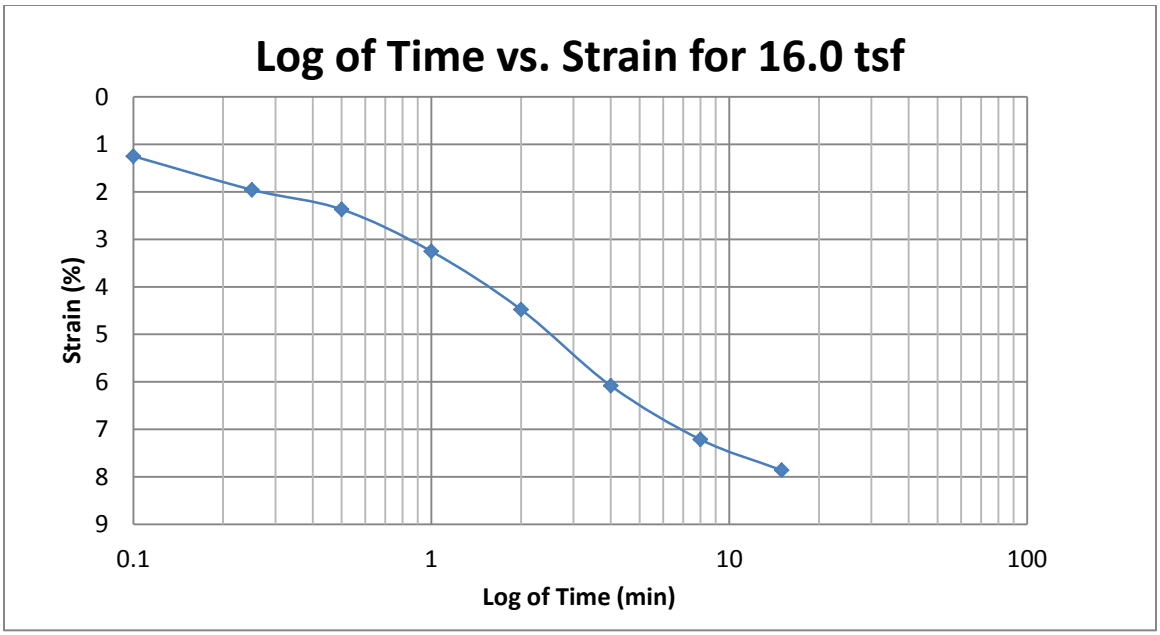

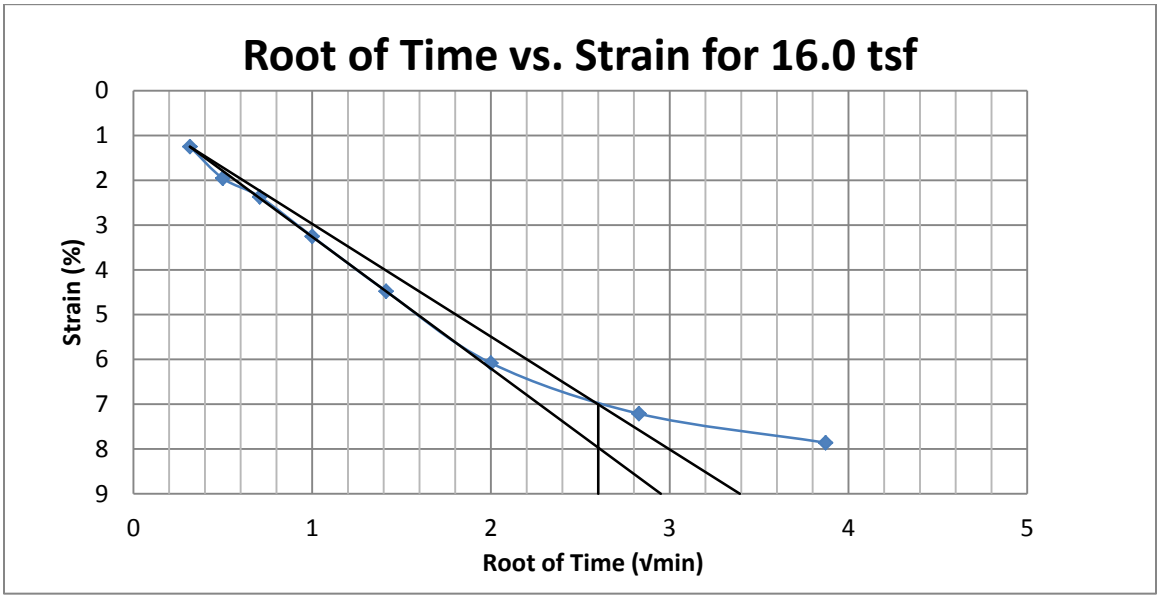

A20 400 South at 20-22 feet

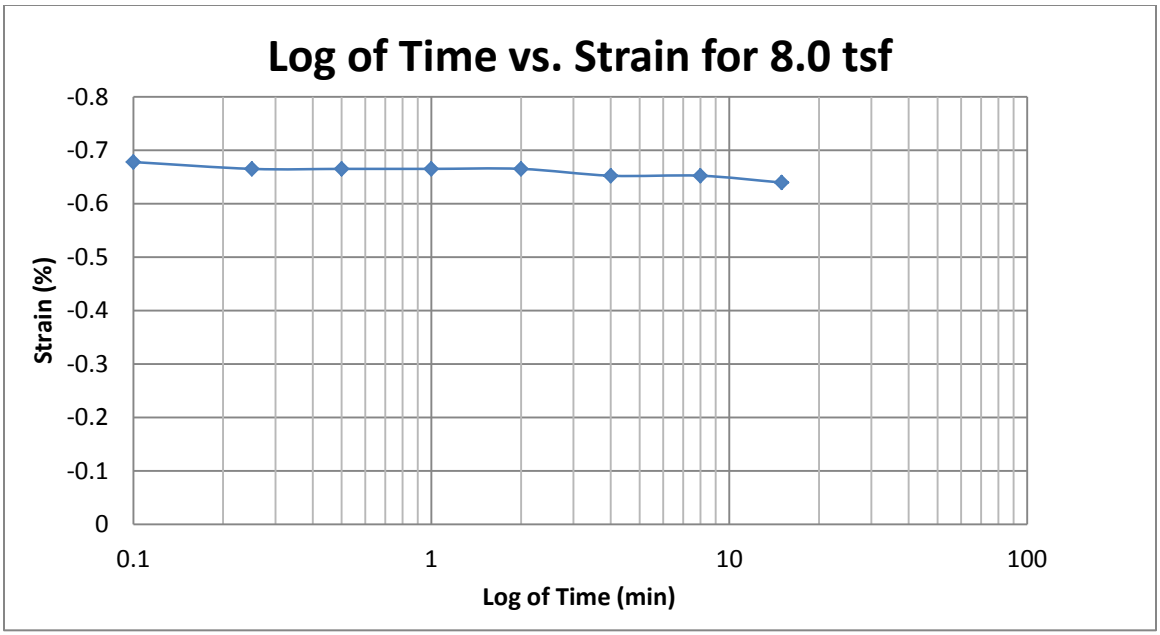

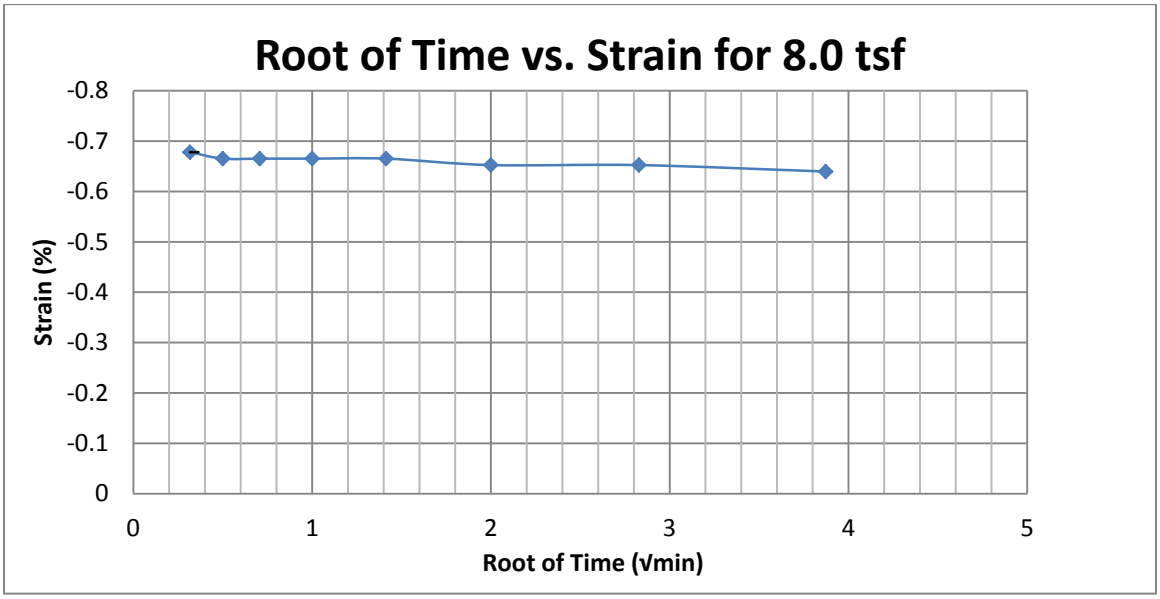

A21 400 South at 20-22 feet

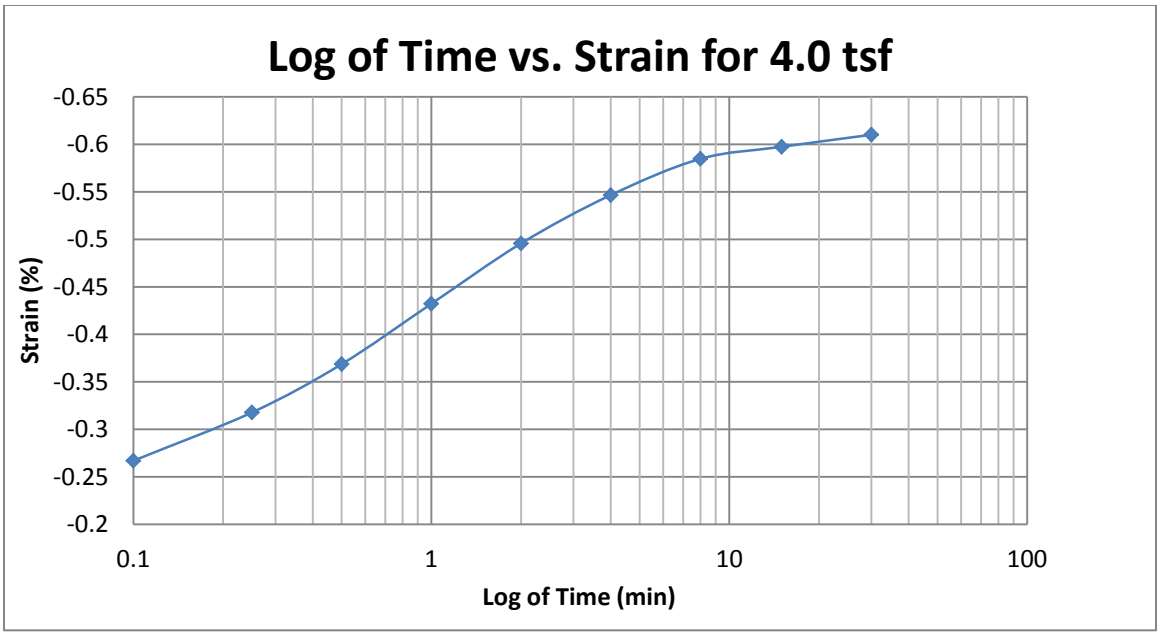

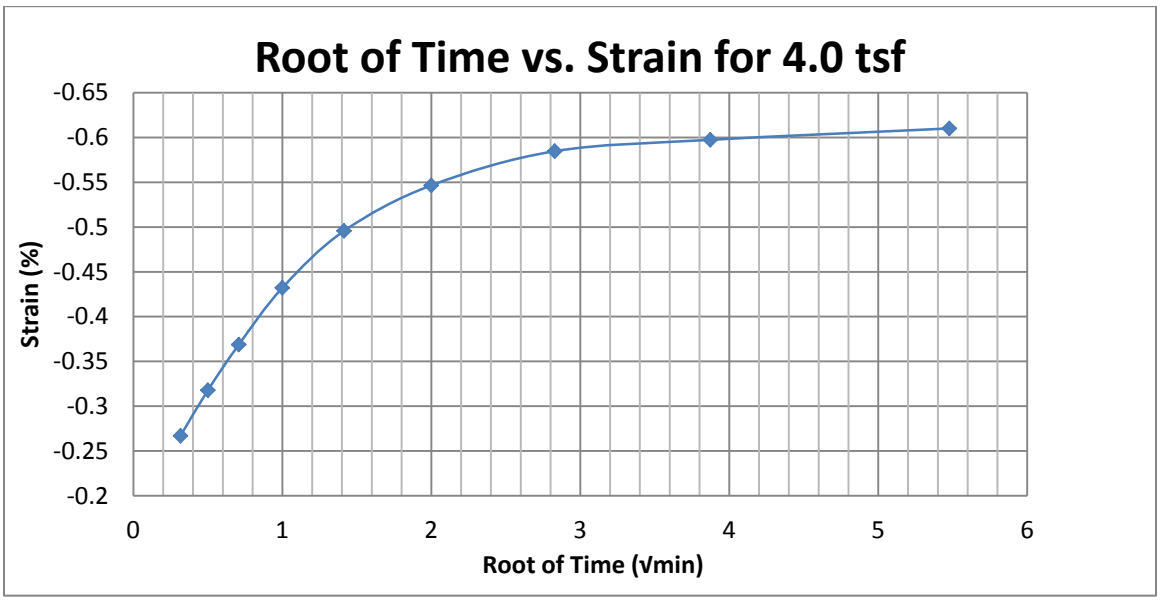

A22 400 South at 20-22 feet

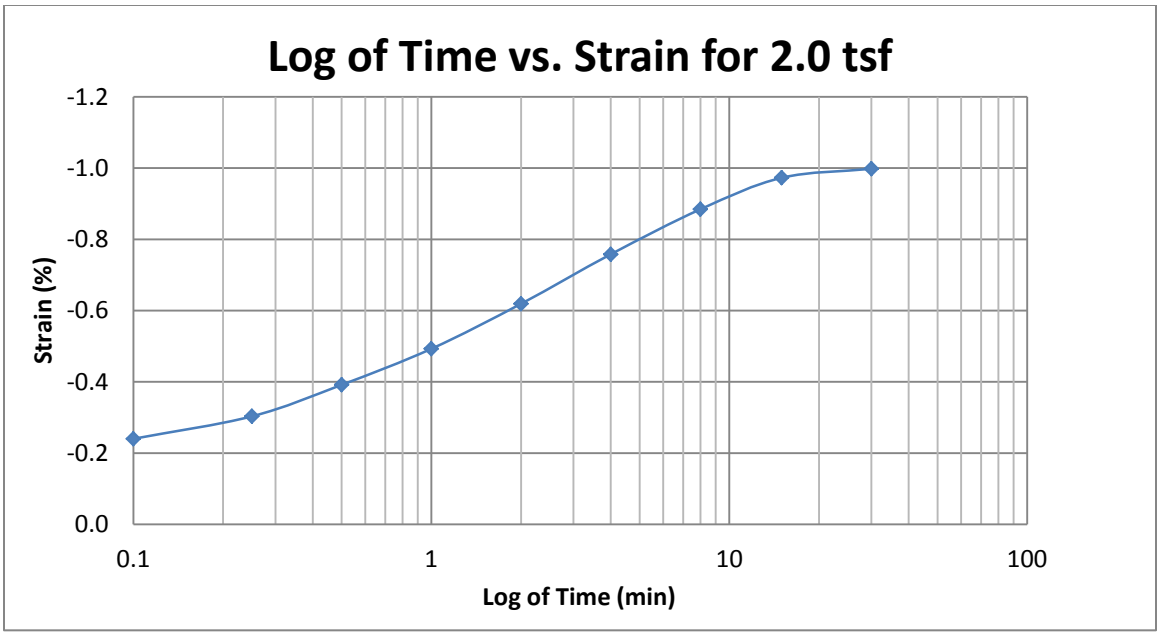

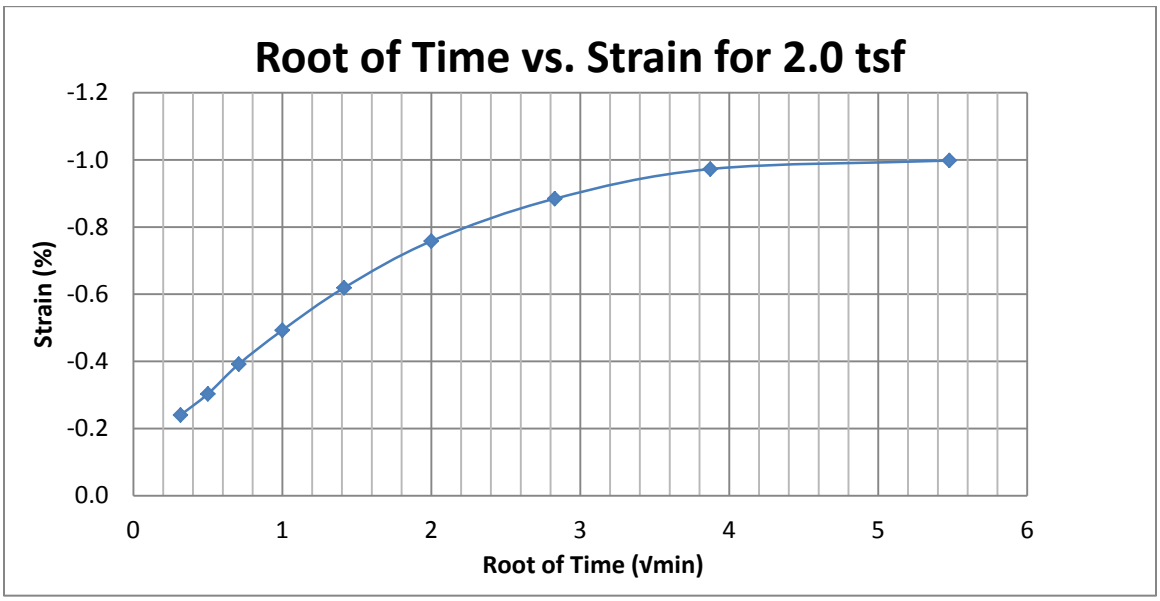

A23 400 South at 20-22 feet

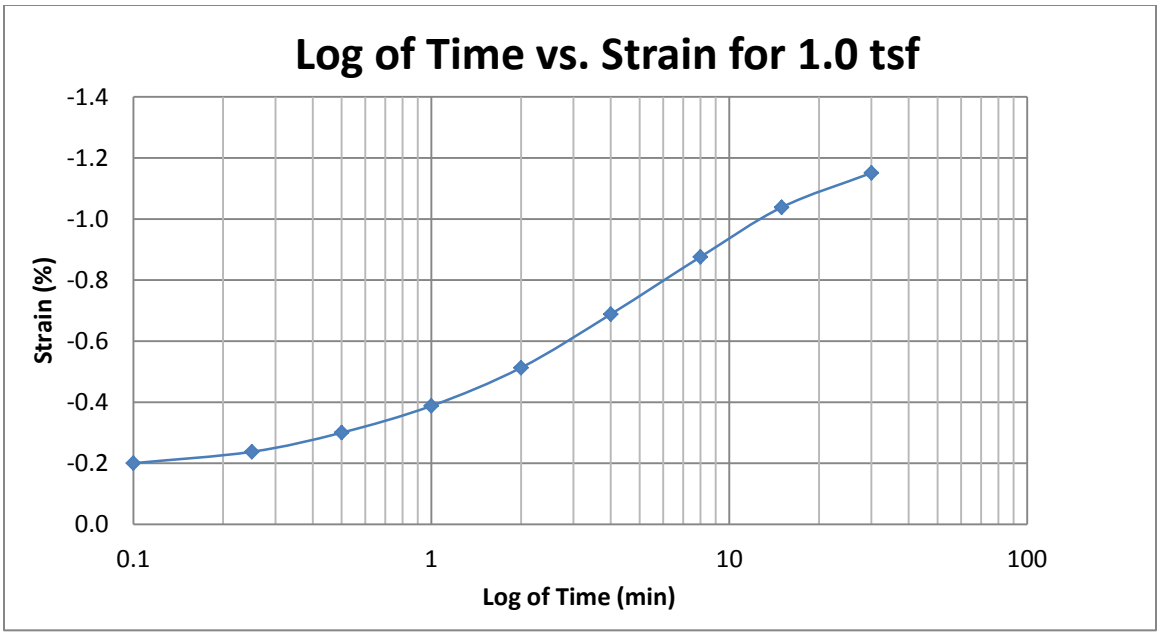

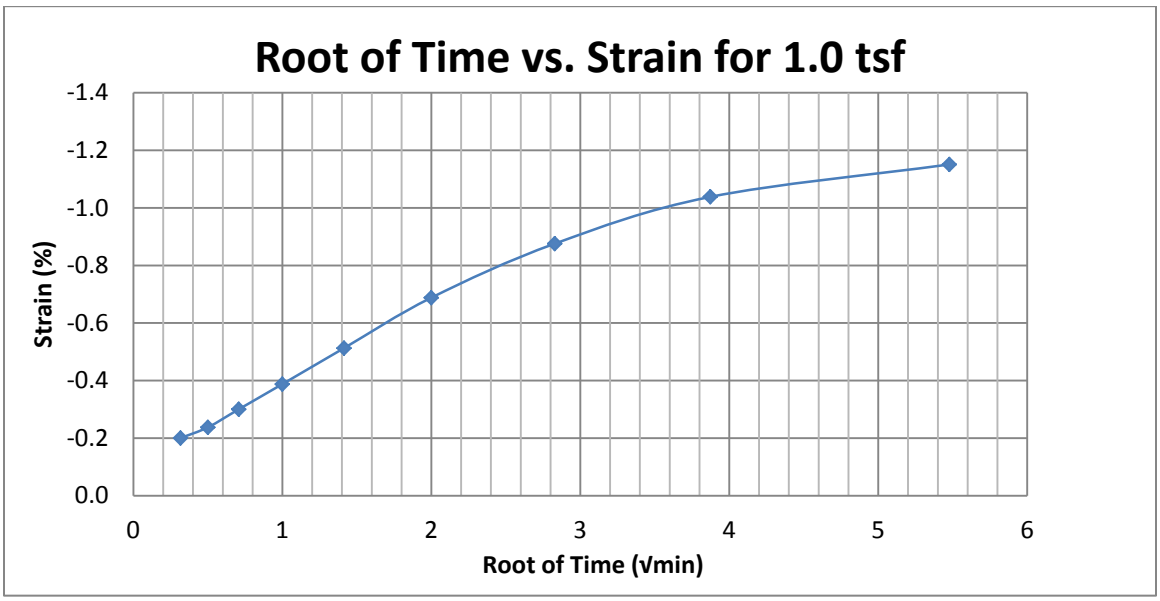

A24 400 South at 20-22 feet

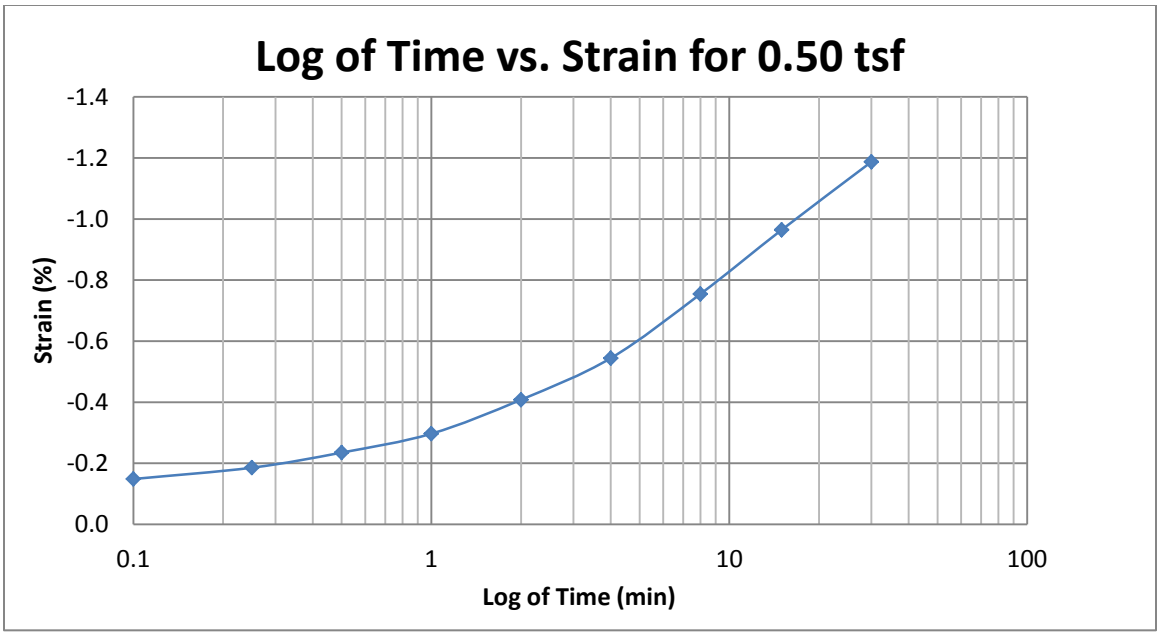

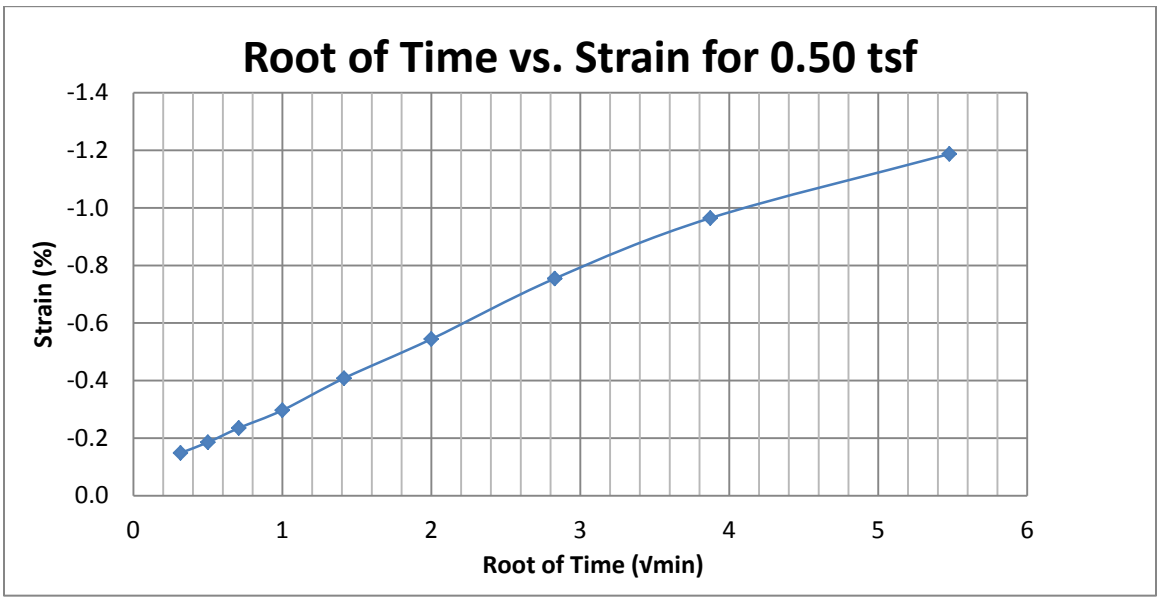

A25 400 South at 20-22 feet

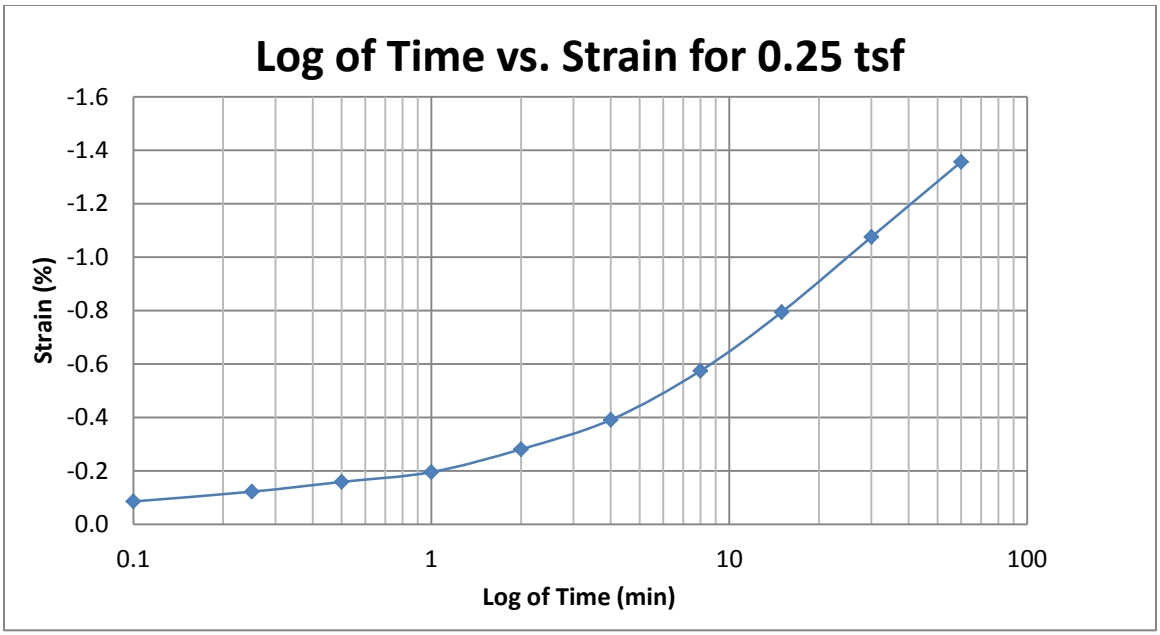

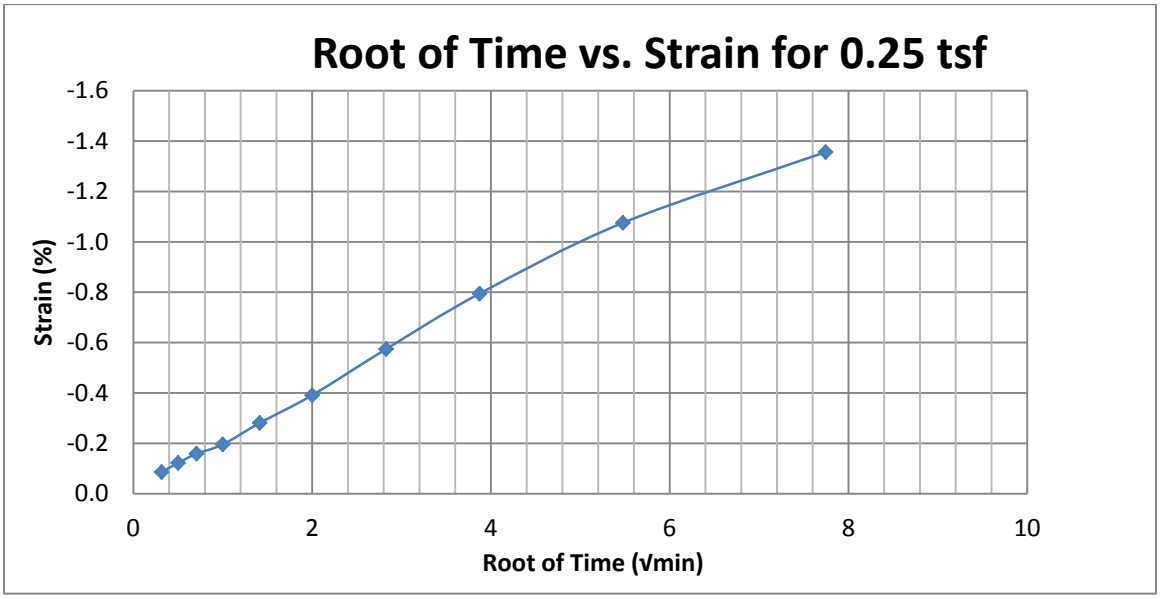

A 26 400 South at 20-22 feet

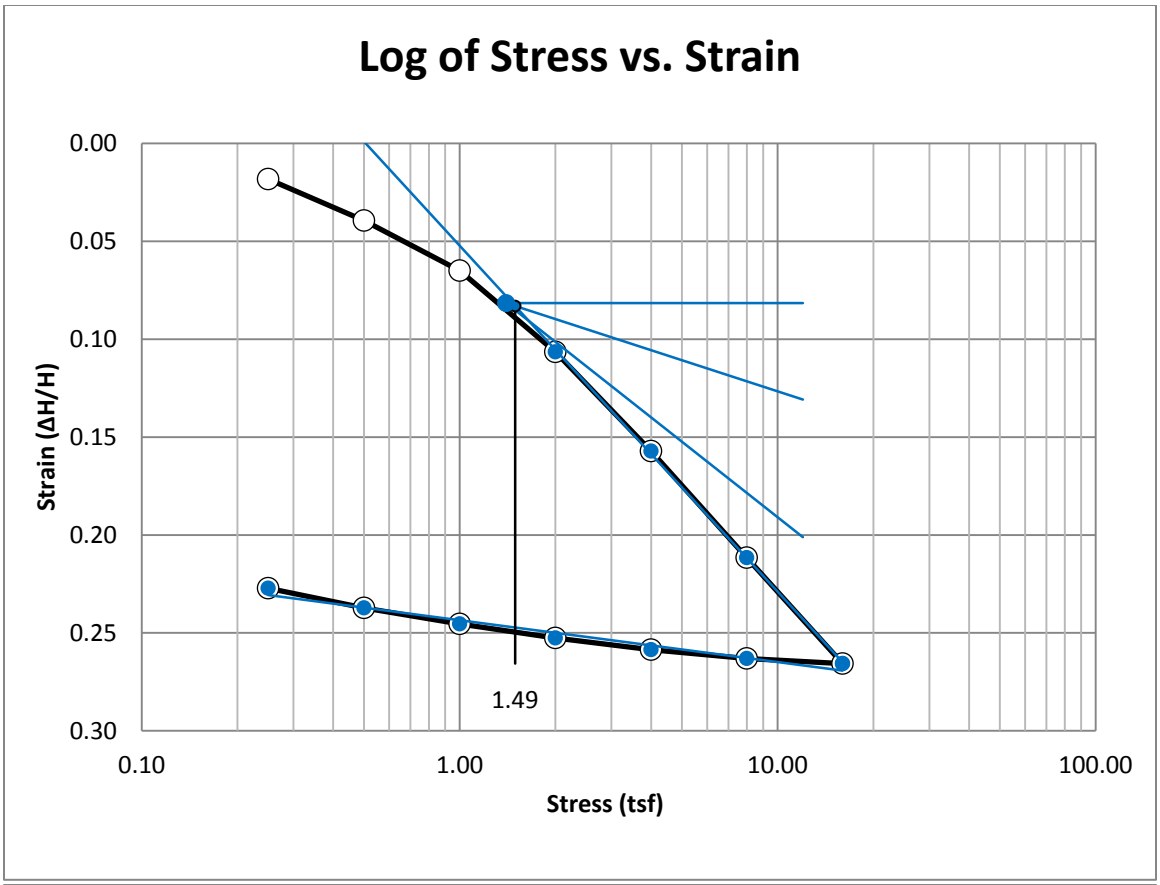

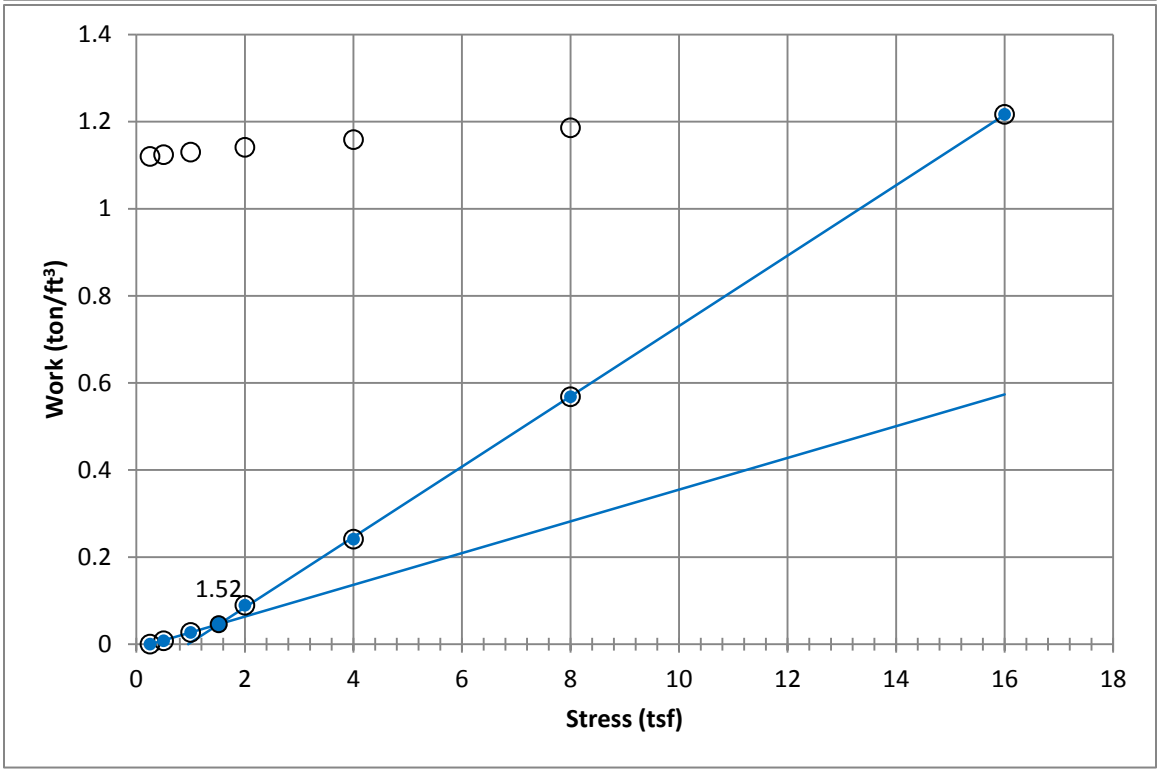

A27 400 South at 25-27 feet

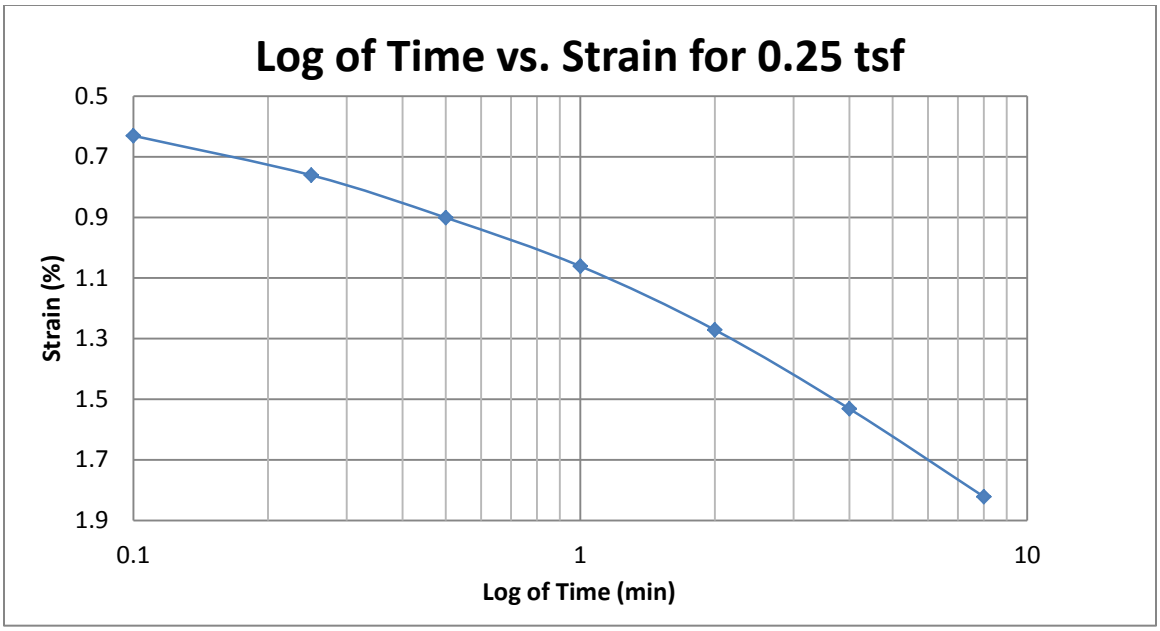

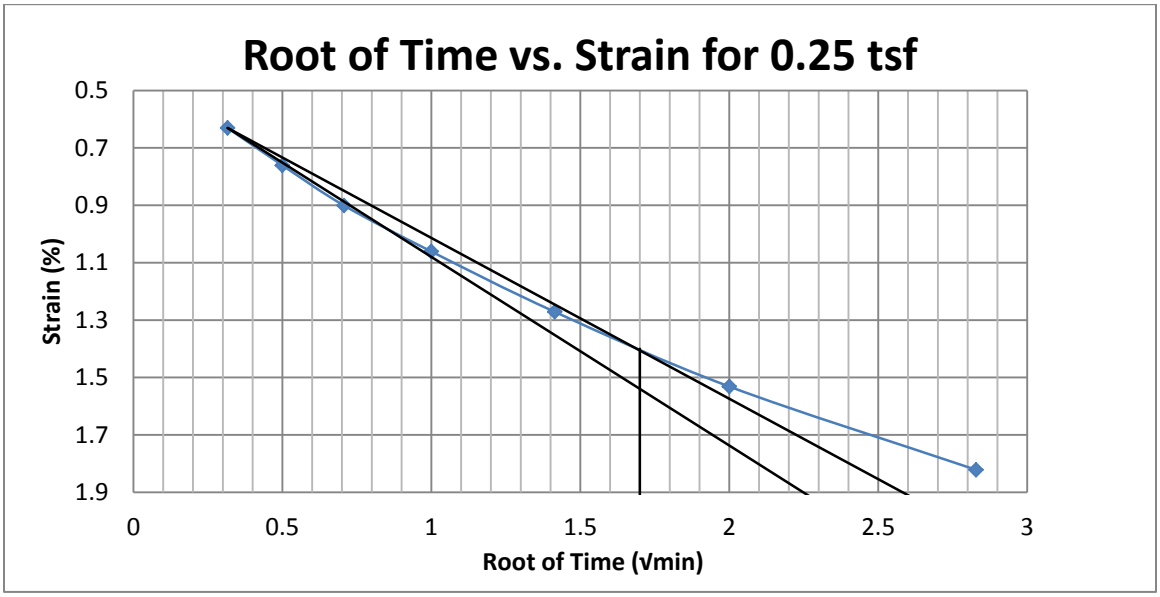

A28 400 South at 25-27 feet

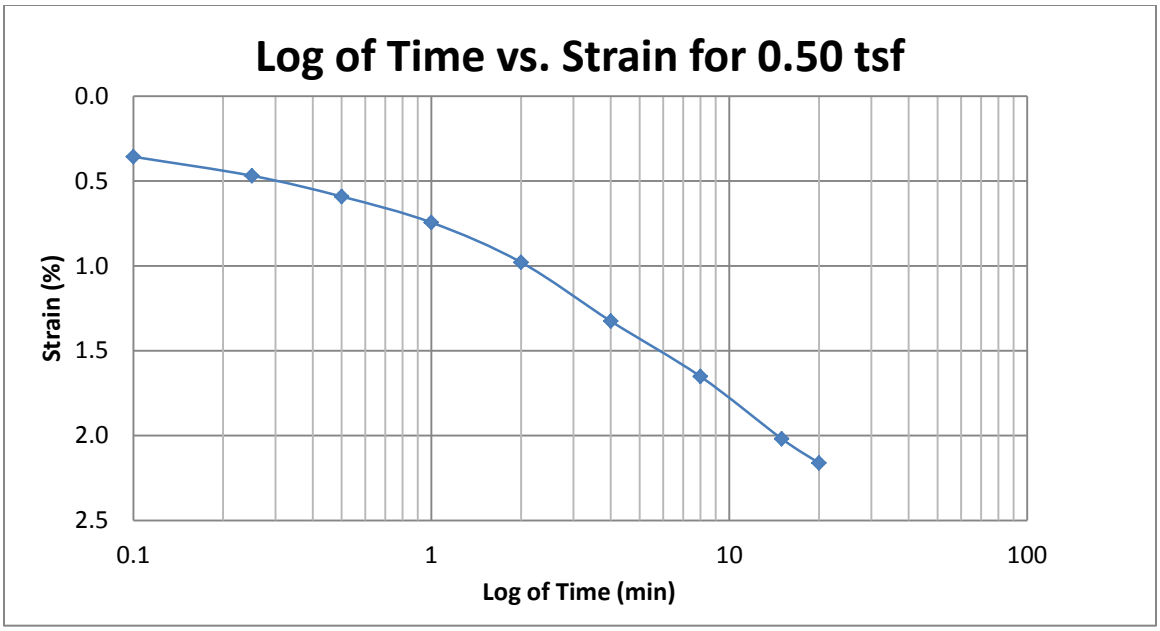

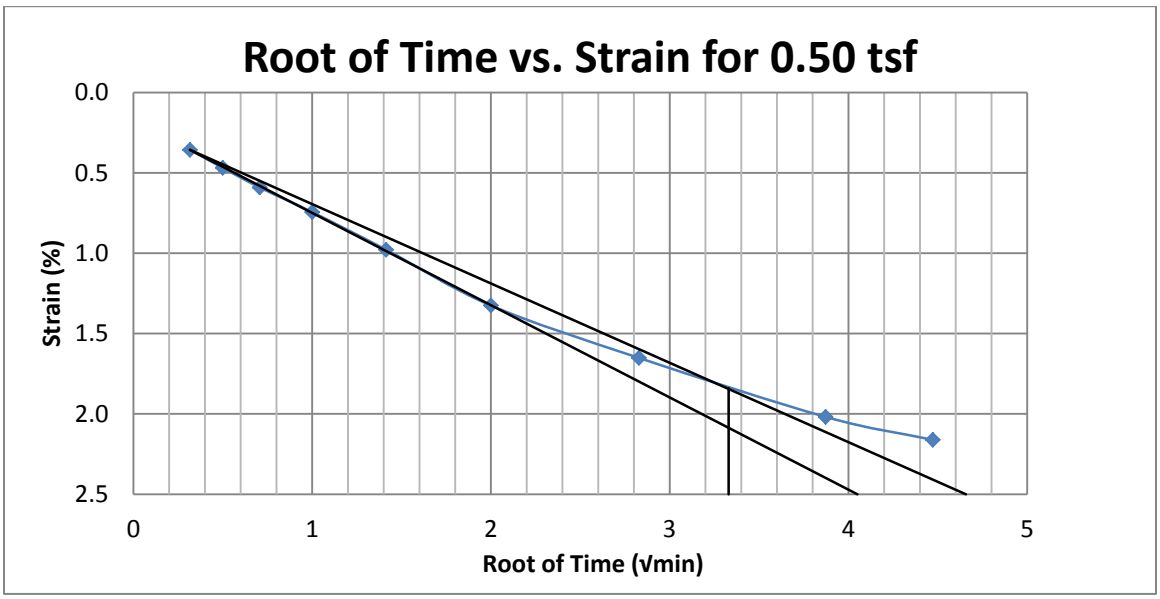

A29 400 South at 25-27 feet

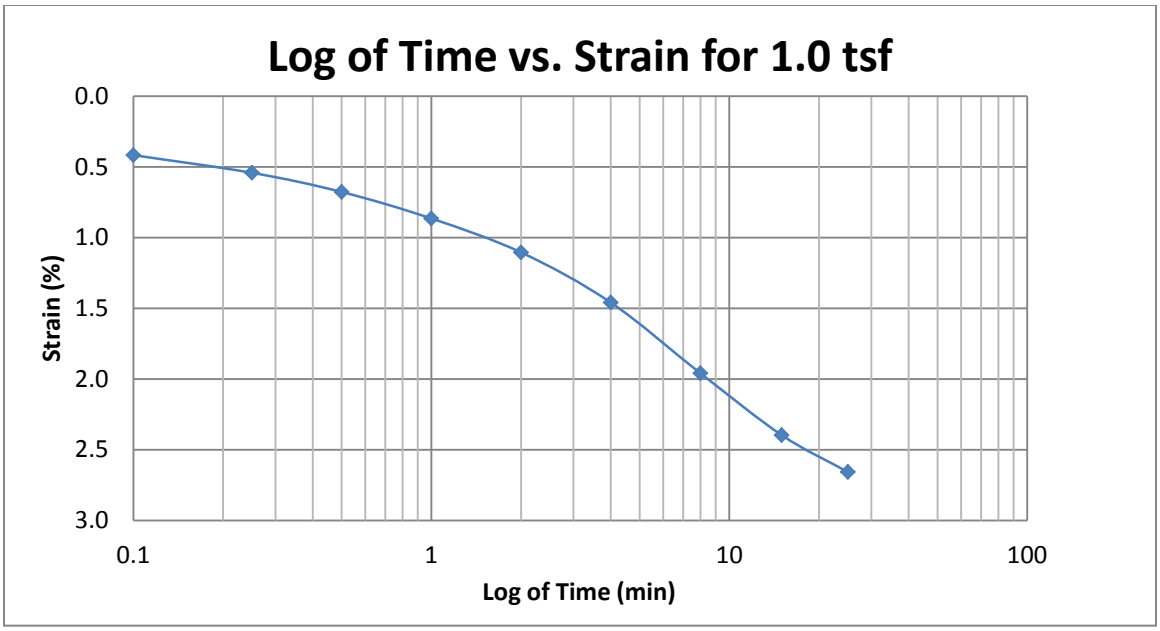

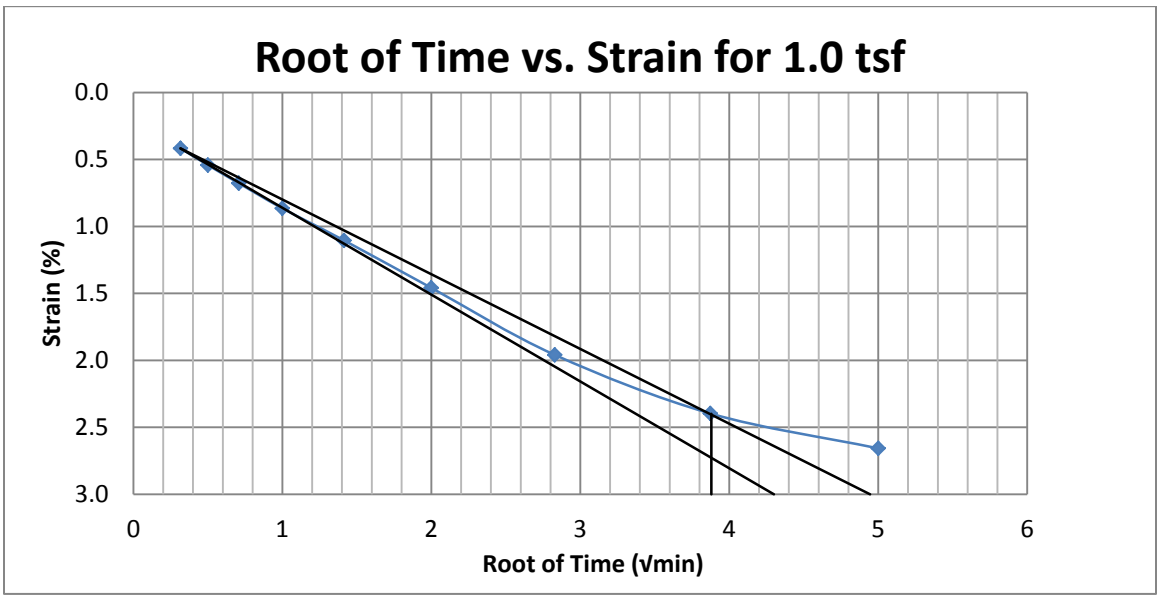

A30 400 South at 25-27 feet

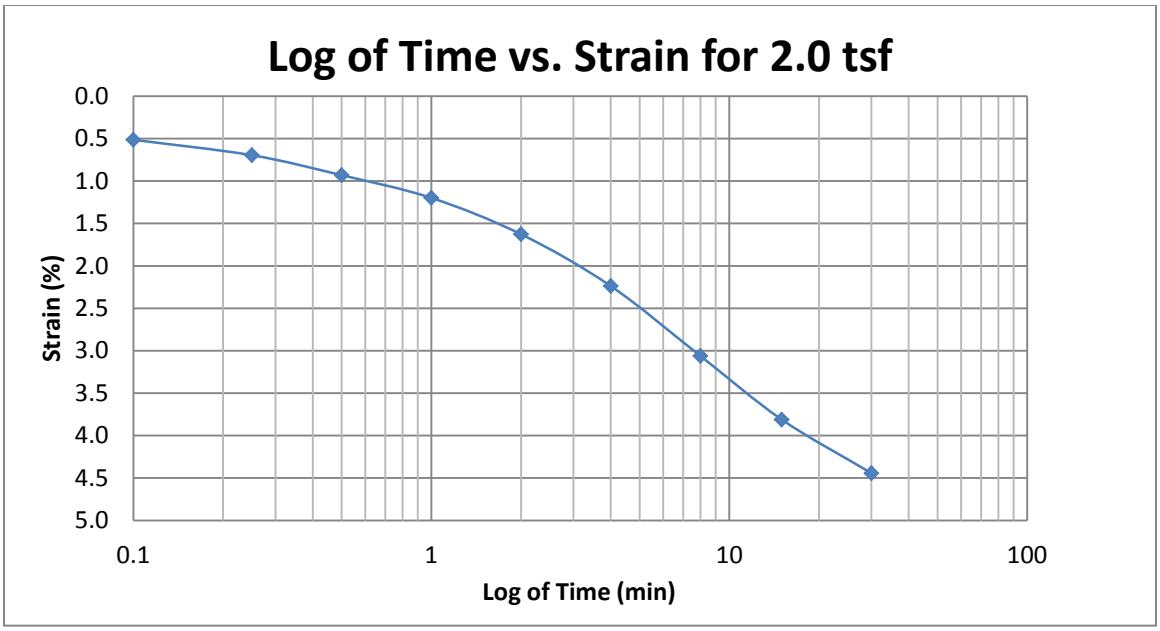

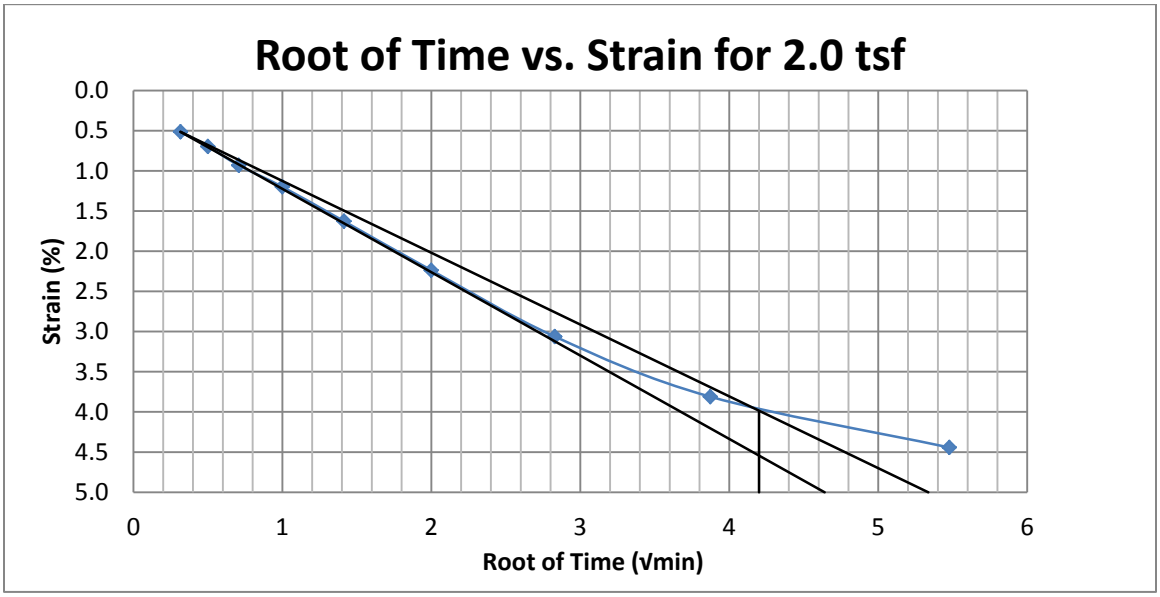

A31 400 South at 25-27 feet

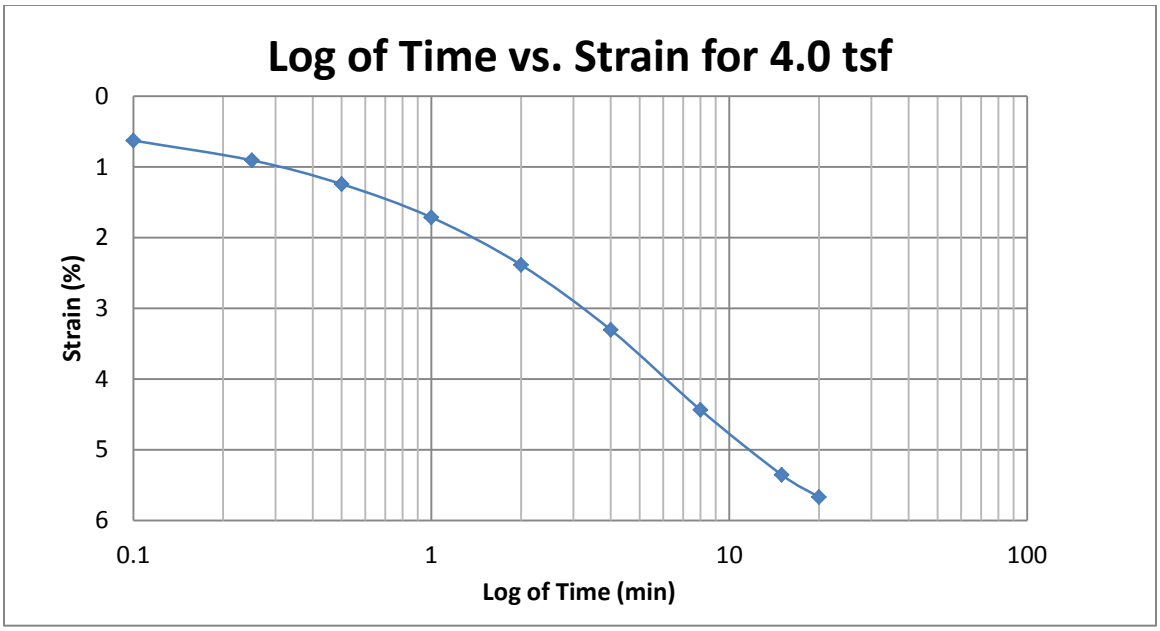

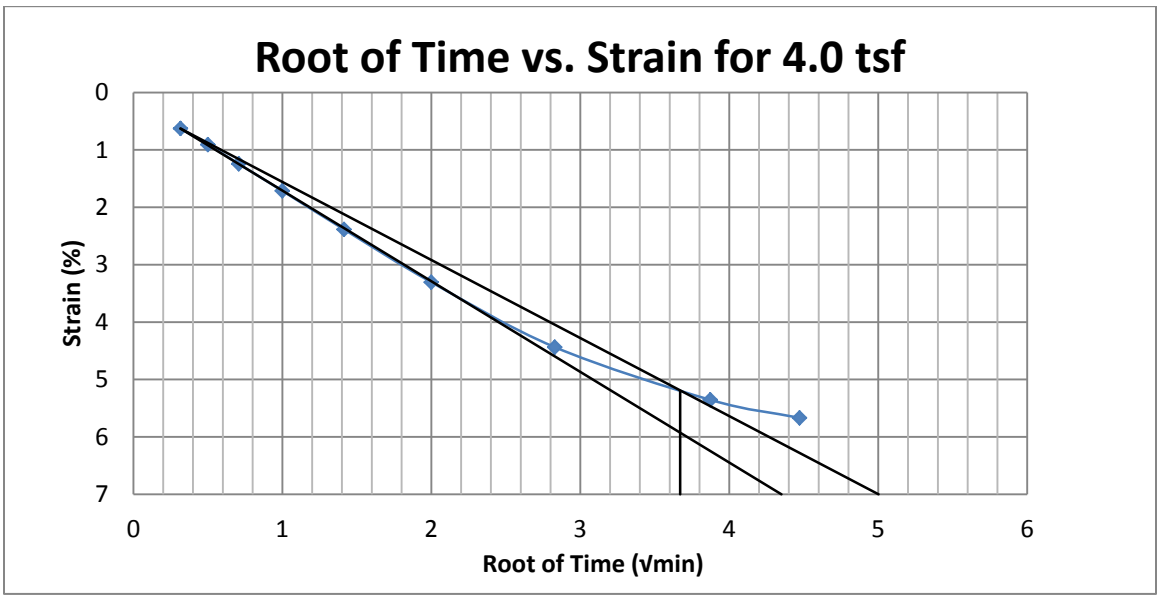

A32 400 South at 25-27 feet

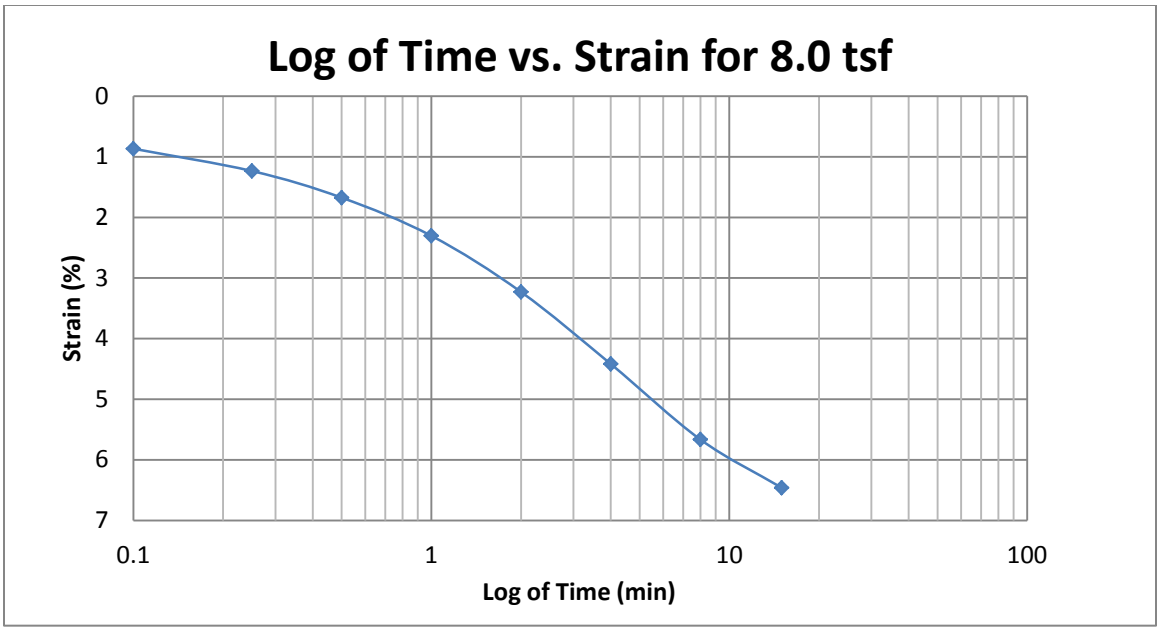

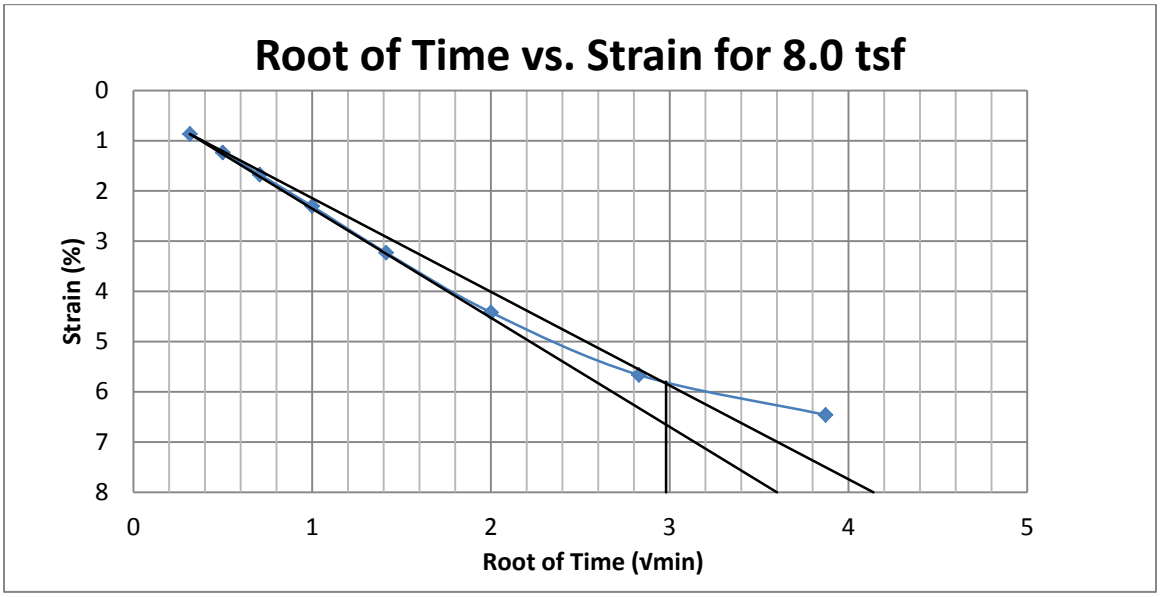

A33 400 South at 25-27 feet

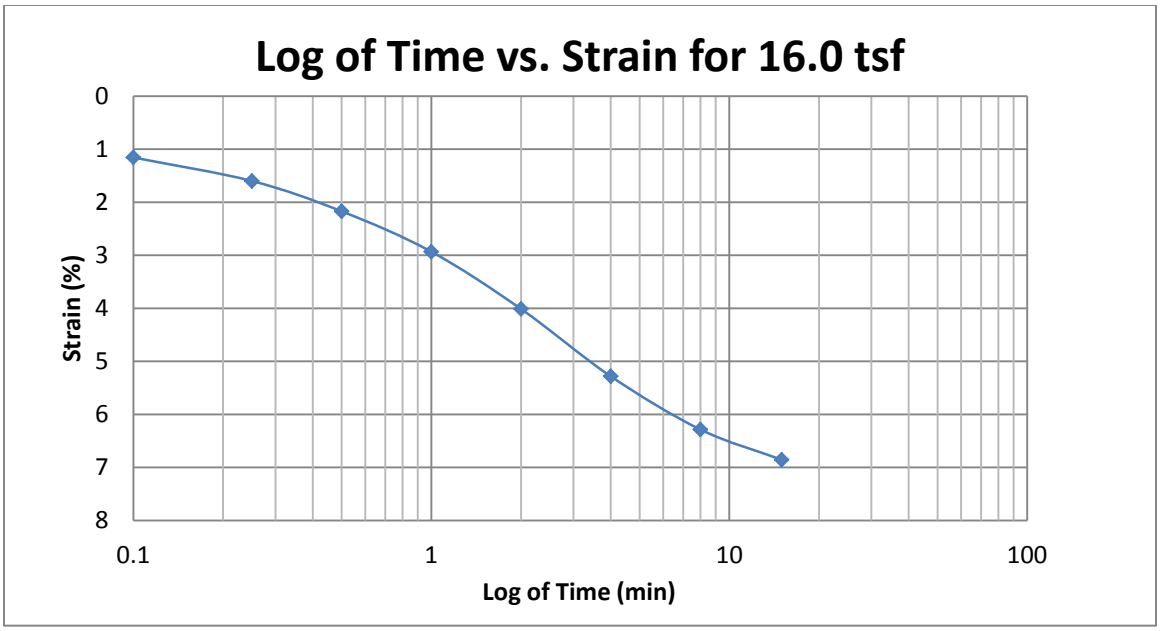

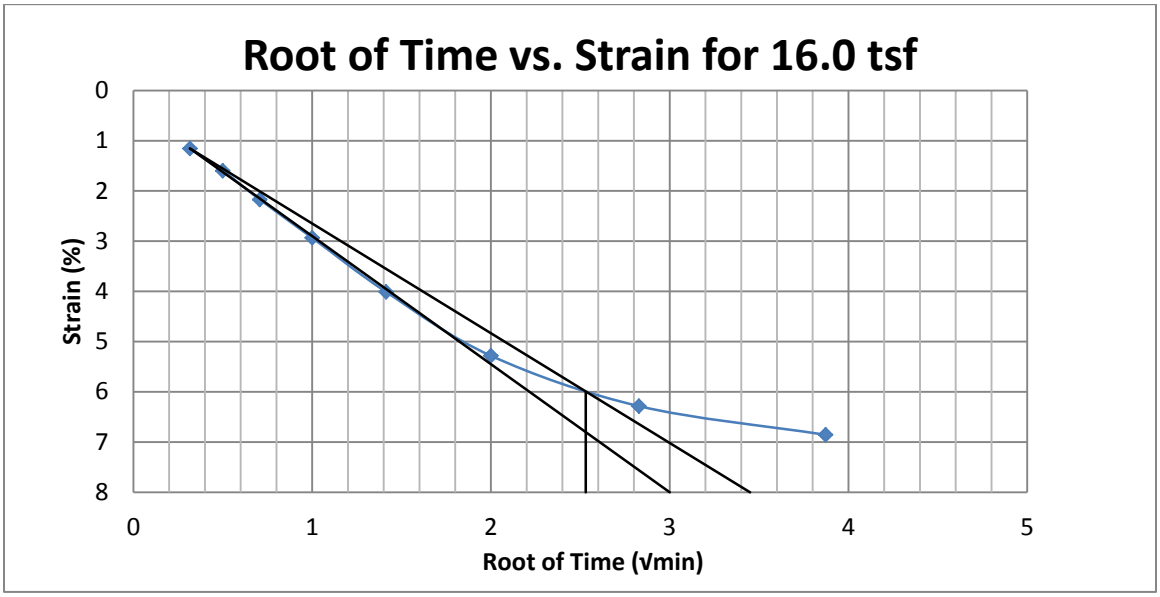

A34 400 South at 25-27 feet

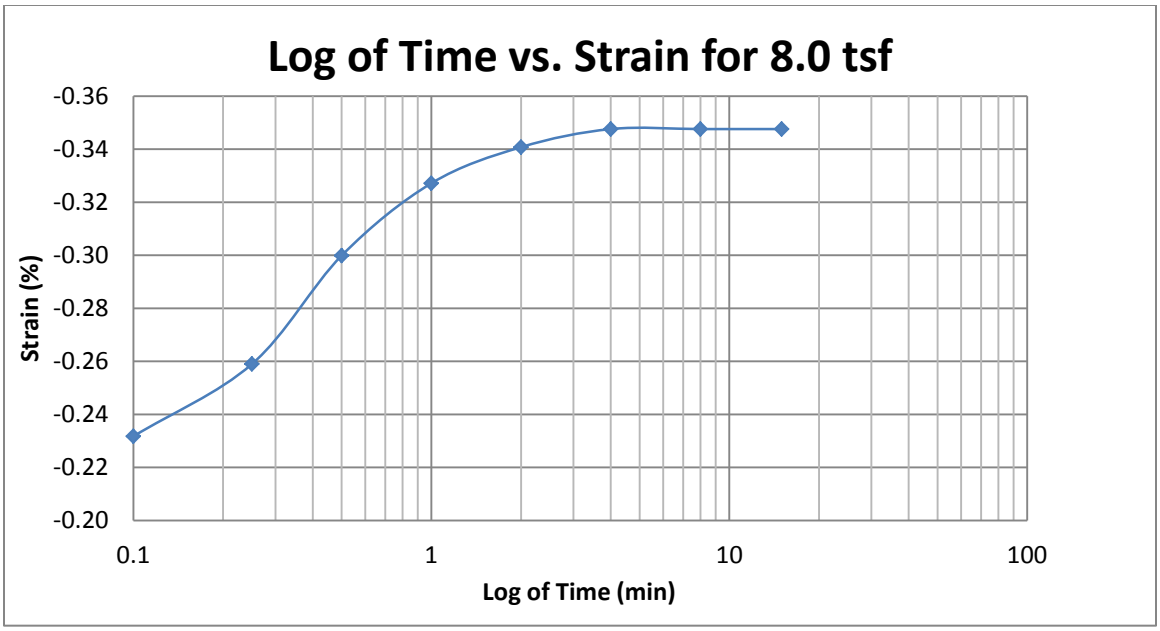

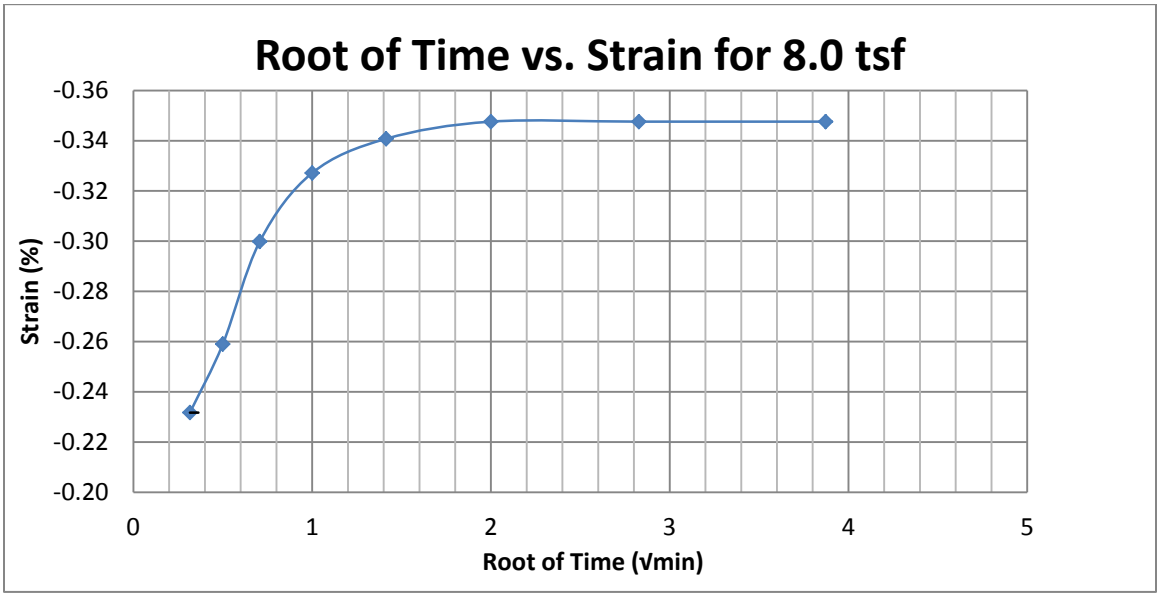

A35 400 South at 25-27 feet

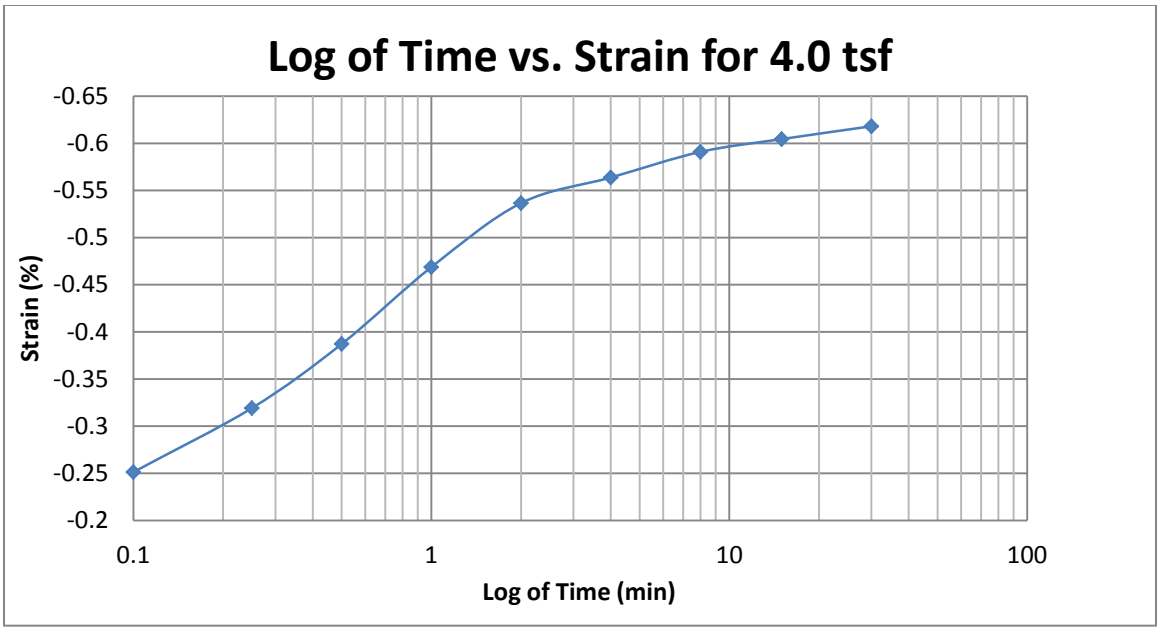

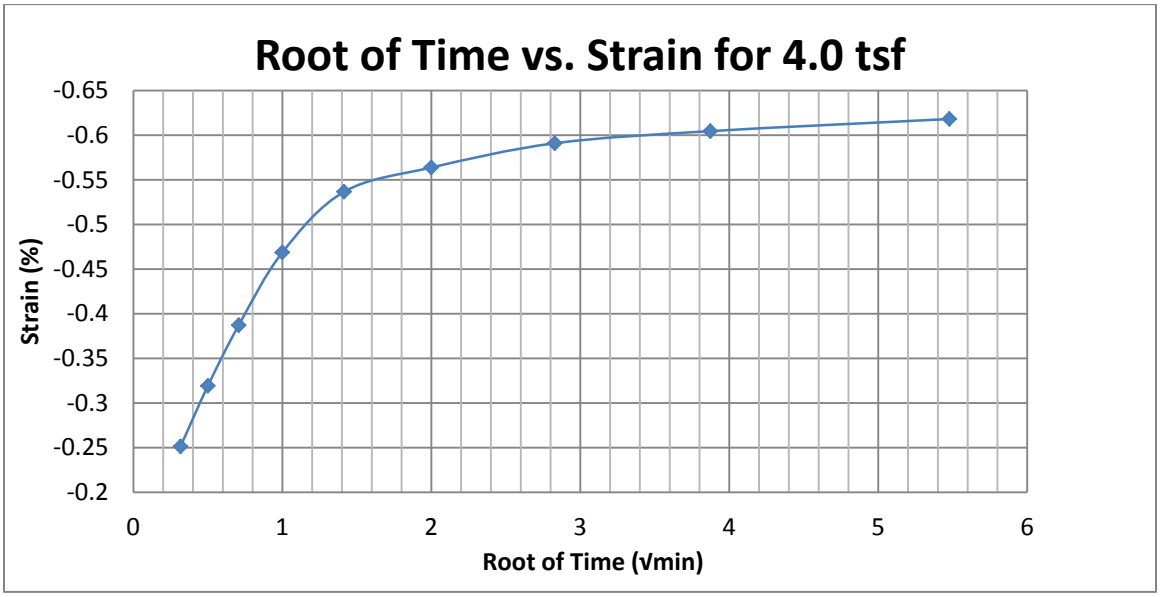

A36 400 South at 25-27 feet

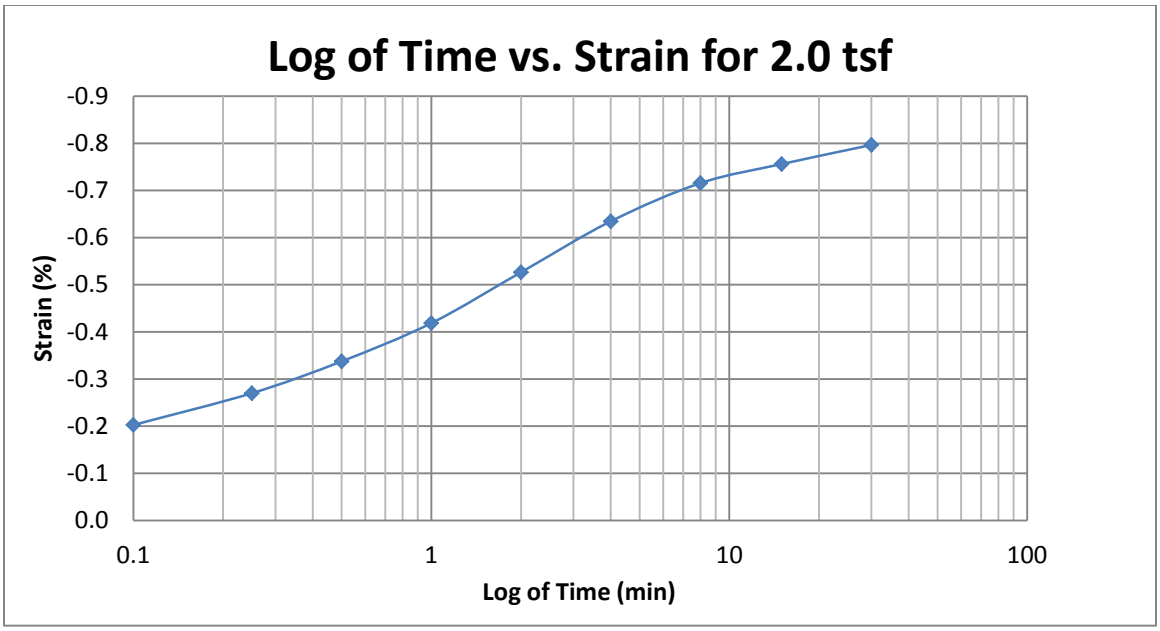

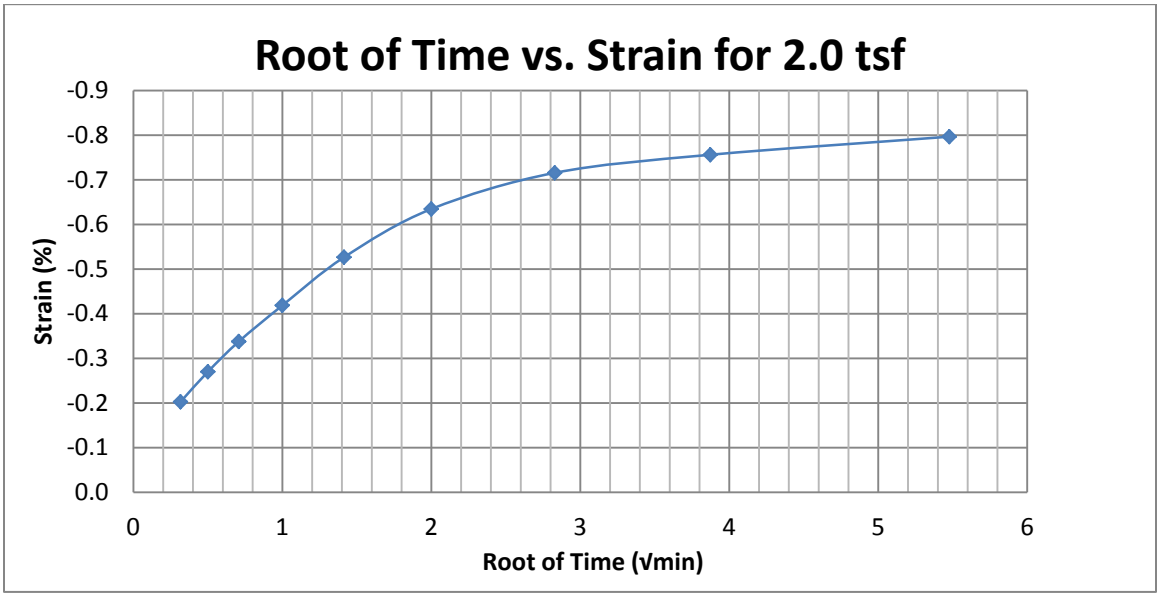

A37 400 South at 25-27 feet

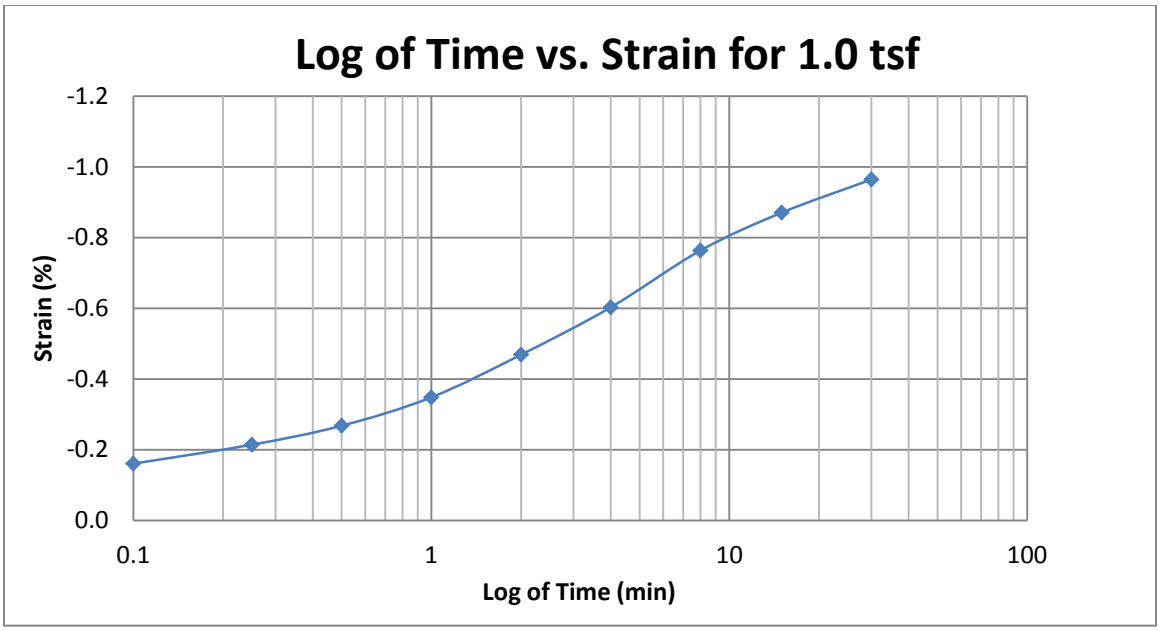

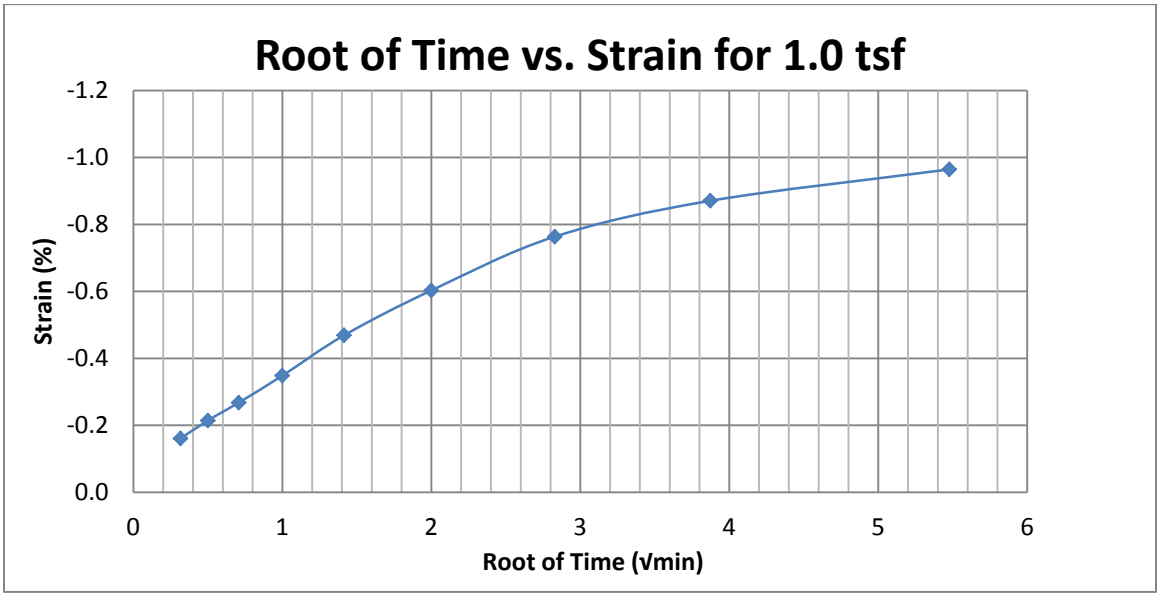

A38 400 South at 25-27 feet

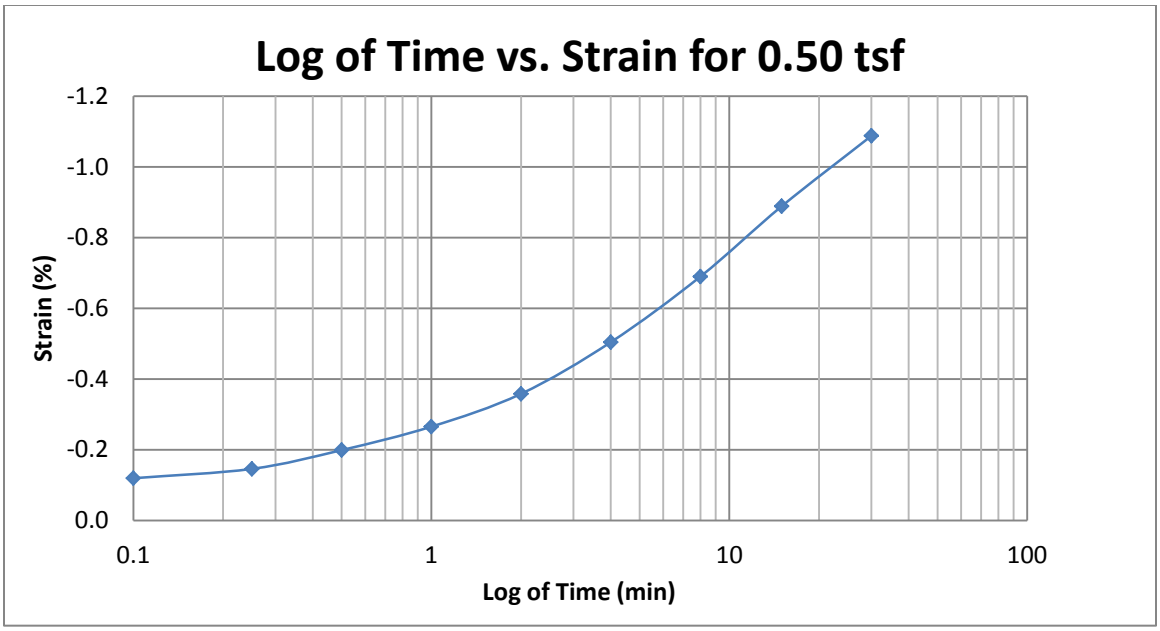

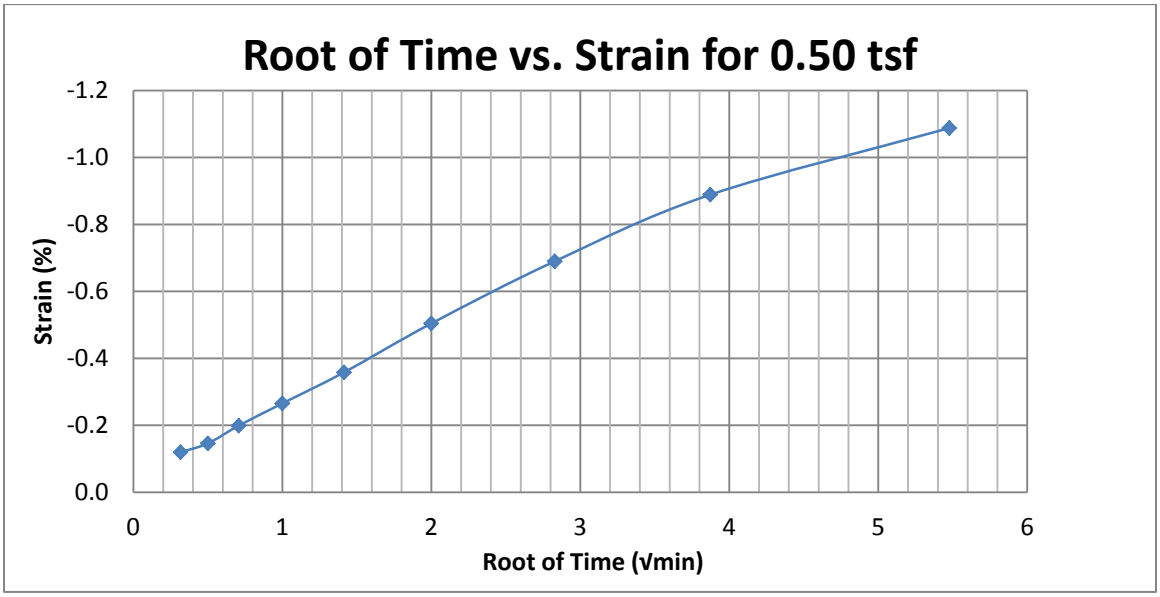

A39 400 South at 25-27 feet

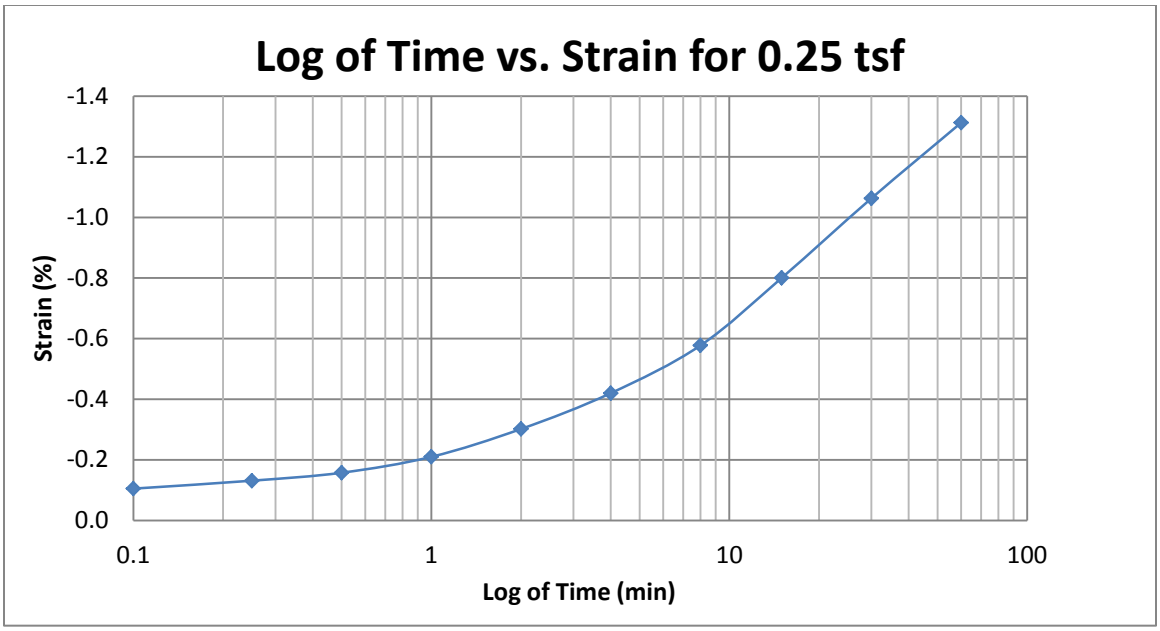

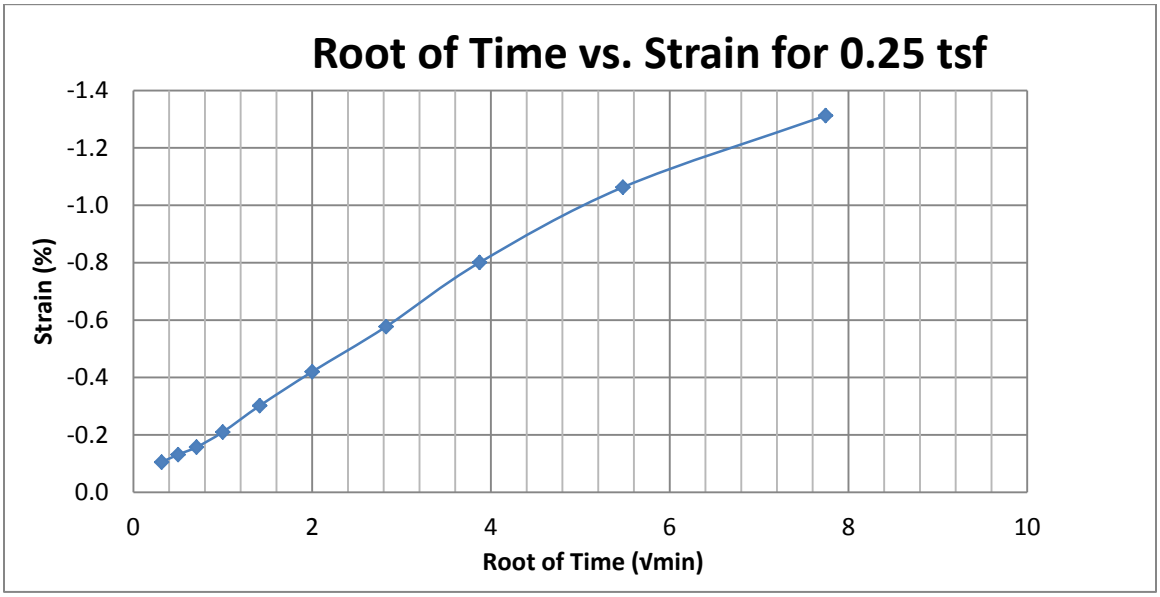

A40 400 South at 25-27 feet

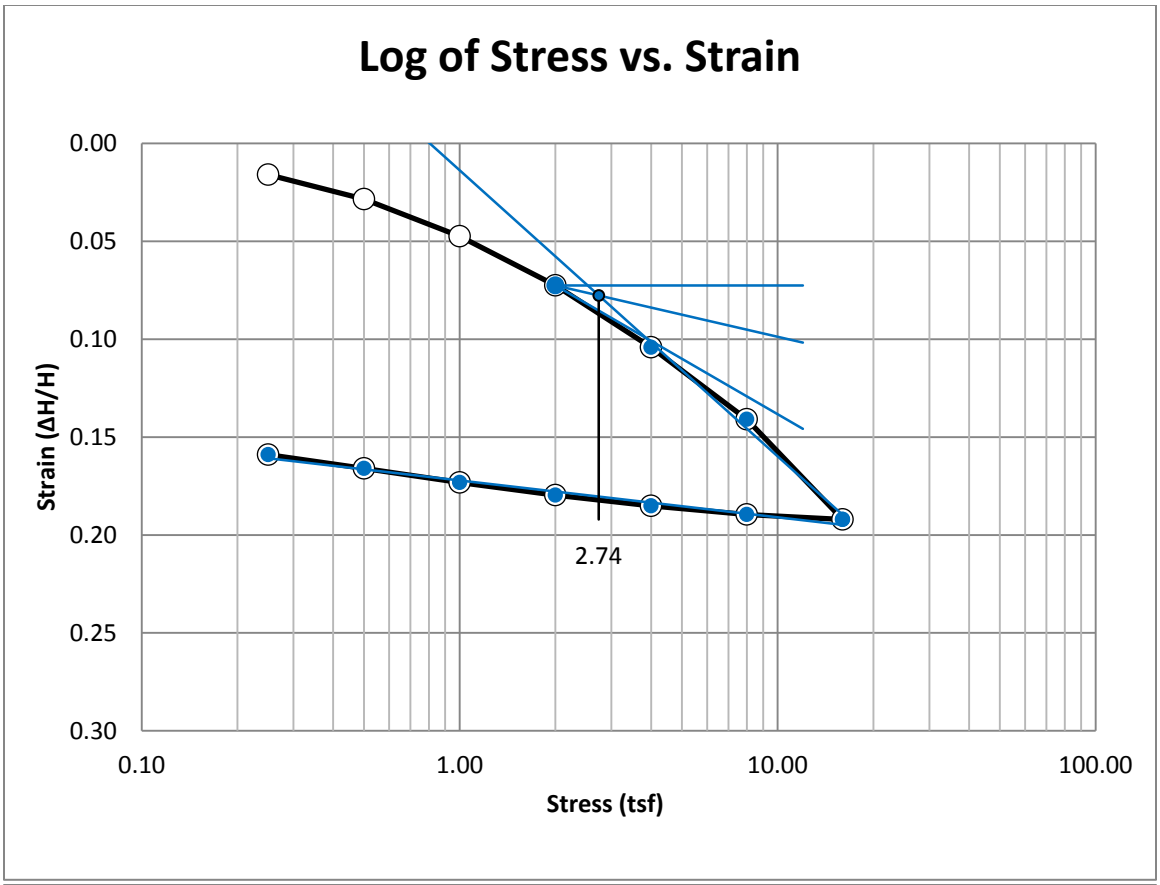

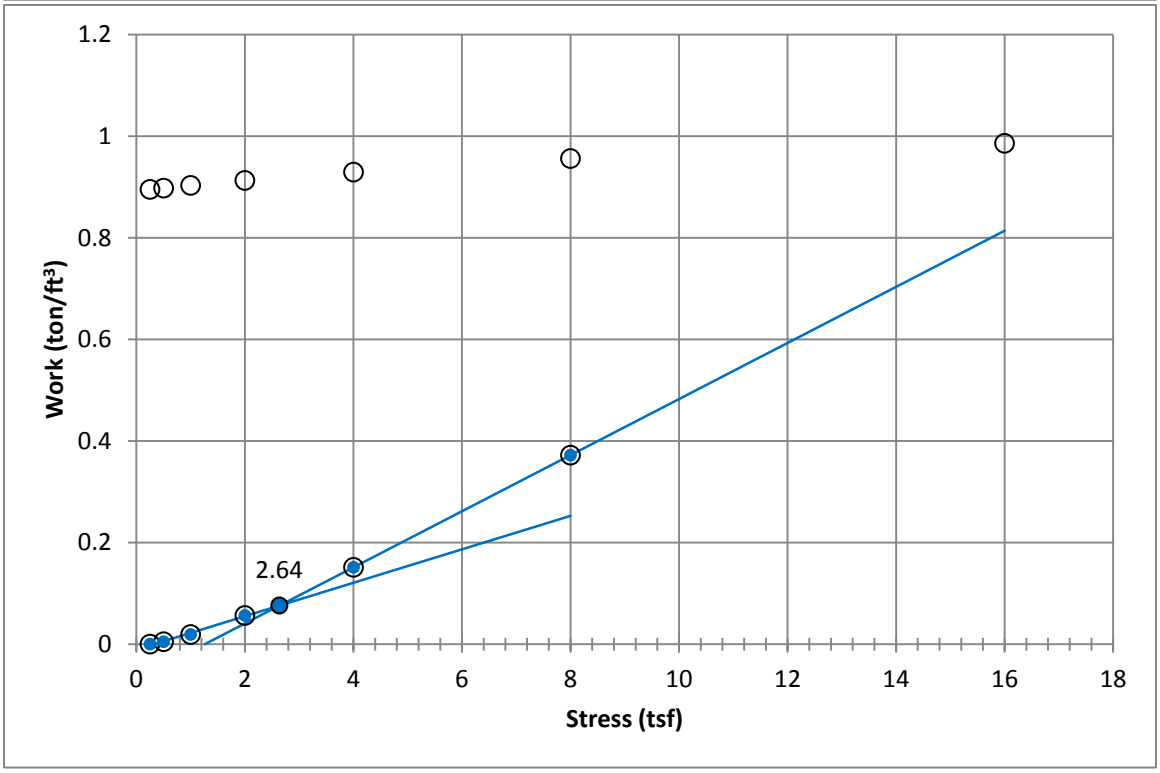

A41 400 South at 30-32 feet

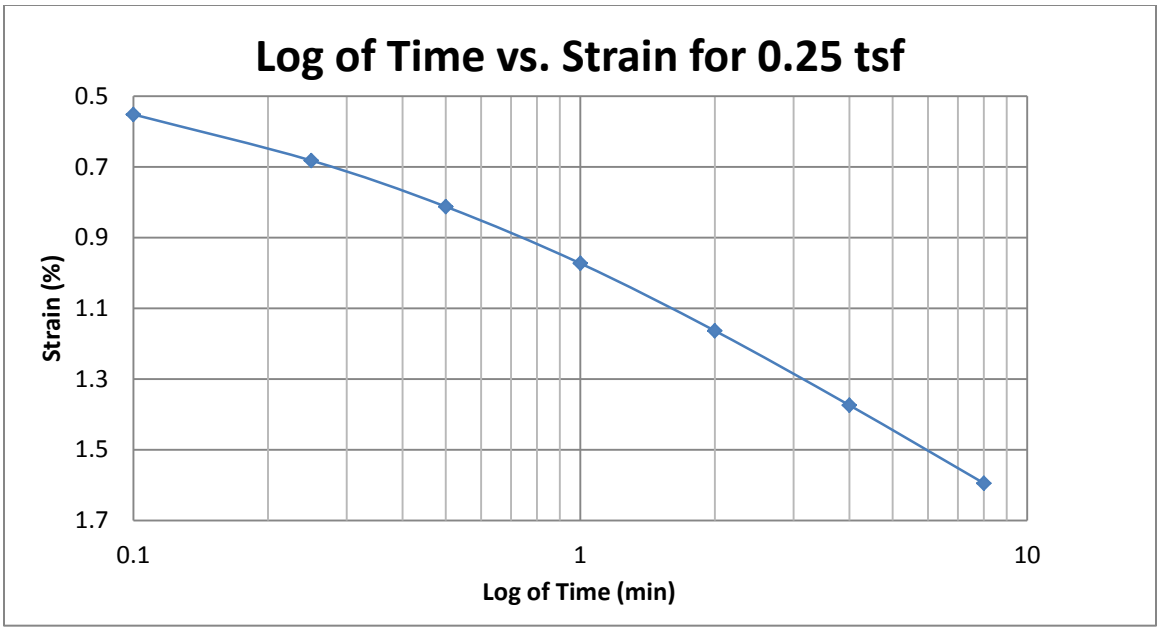

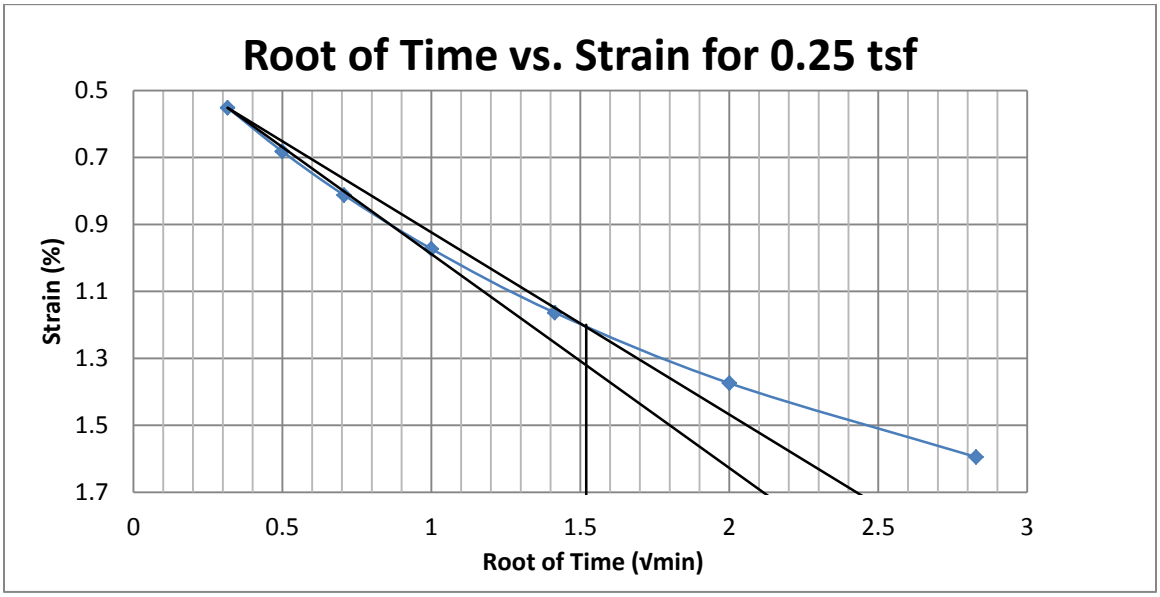

A42 400 South at 30-32 feet

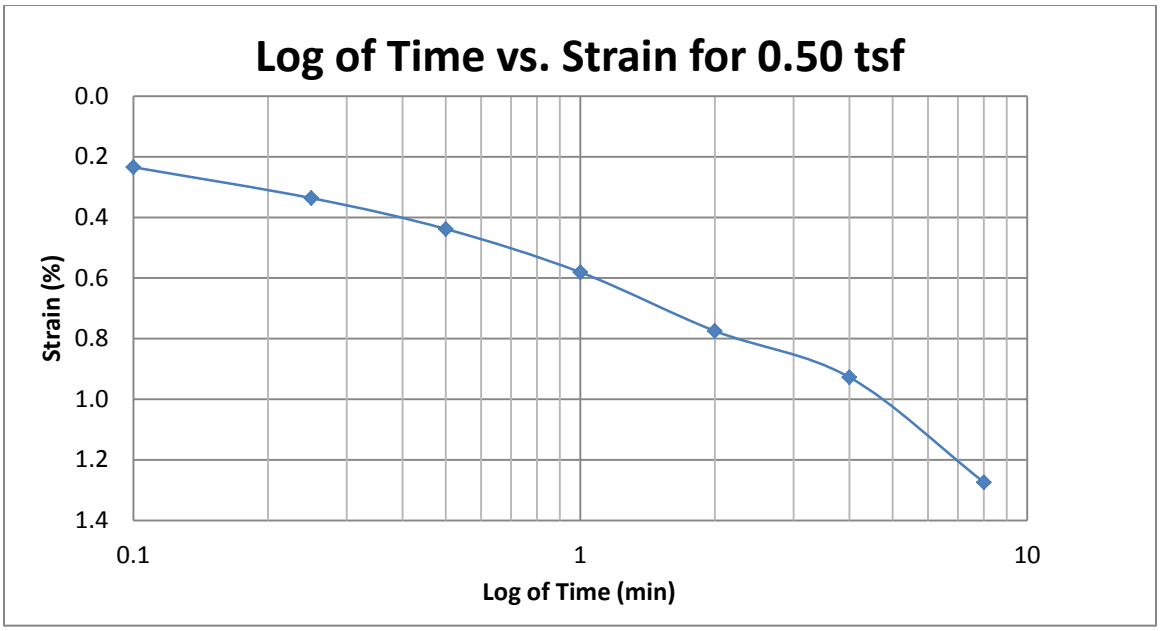

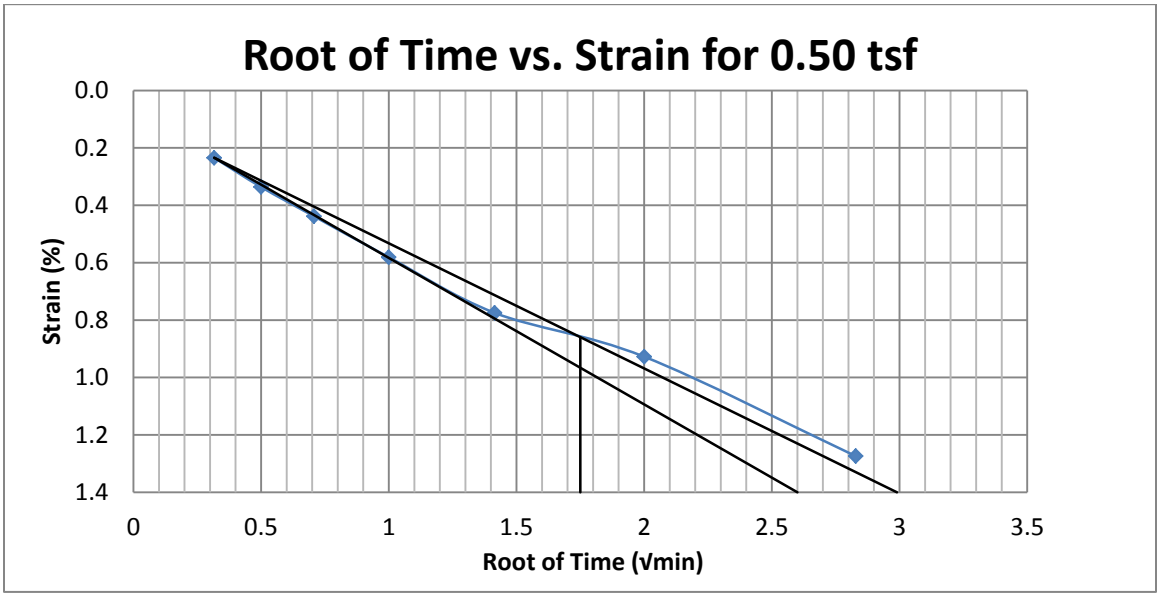

A43 400 South at 30-32 feet

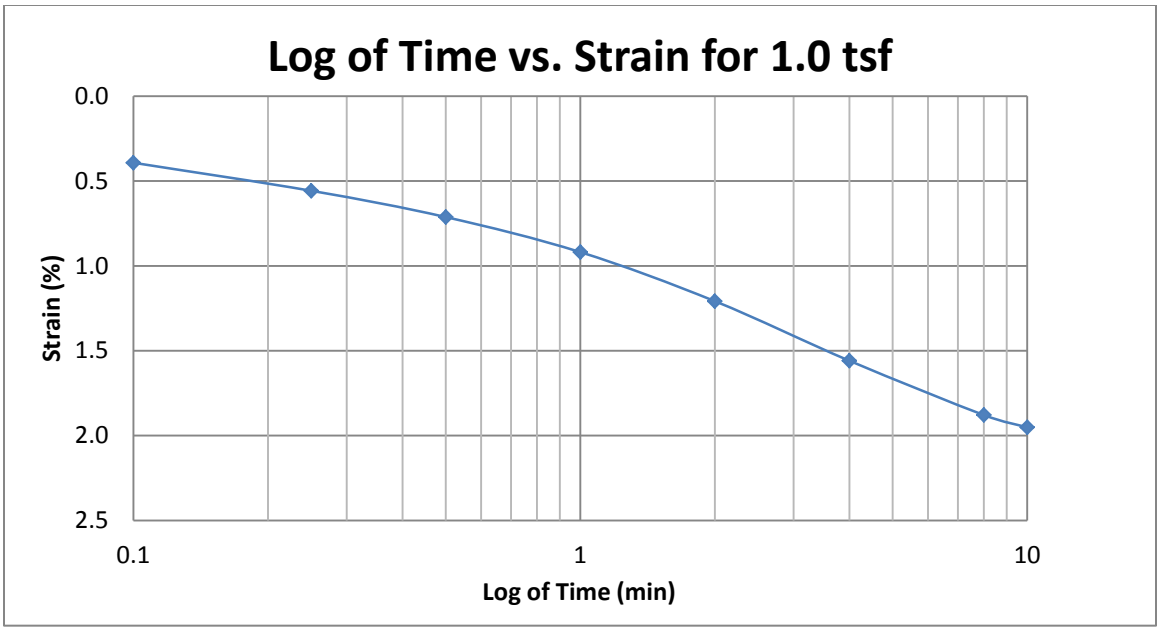

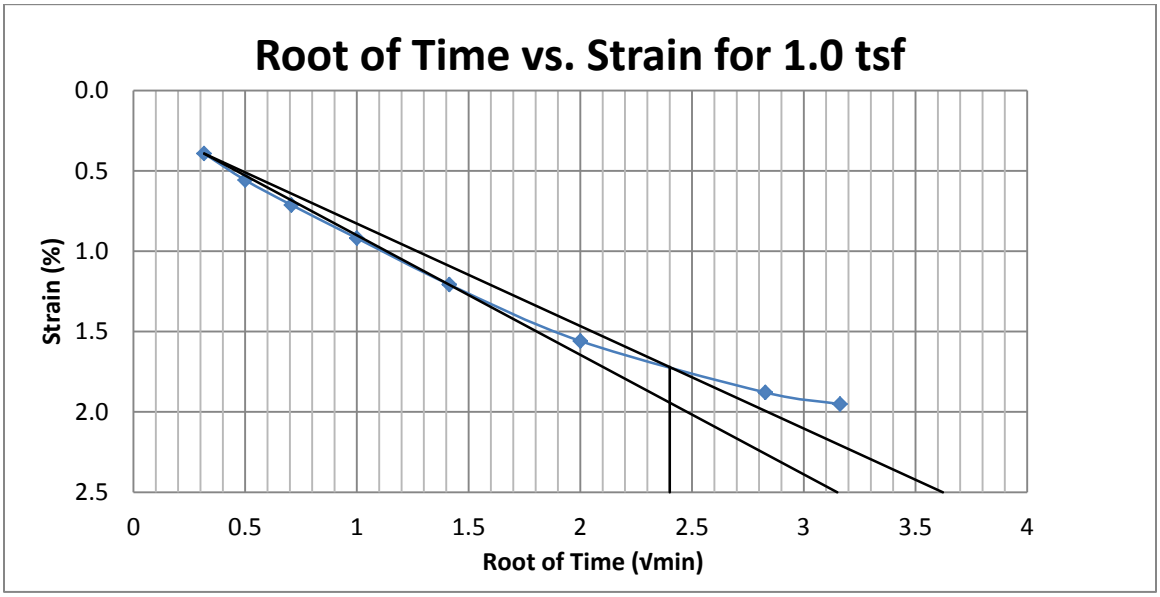

A44 400 South at 30-32 feet

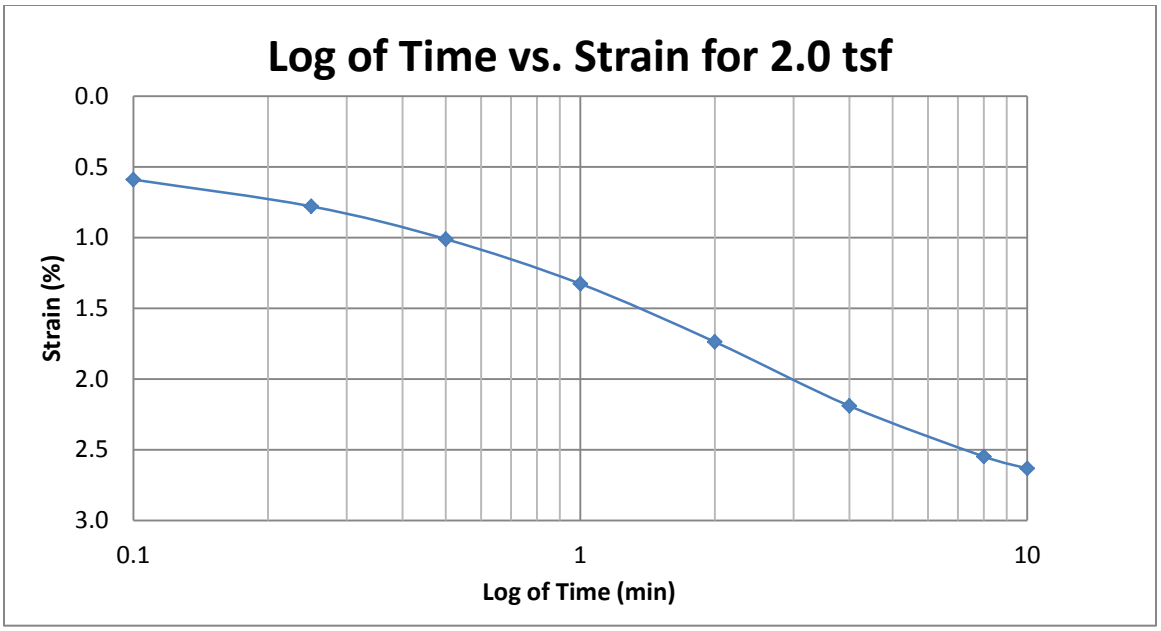

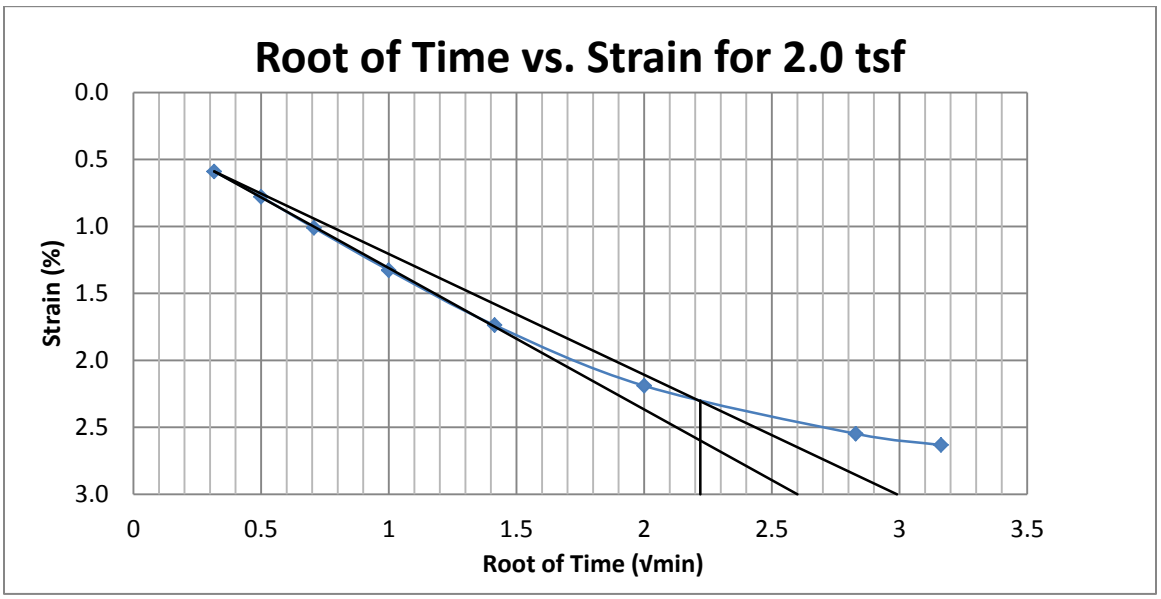

A45 400 South at 30-32 feet

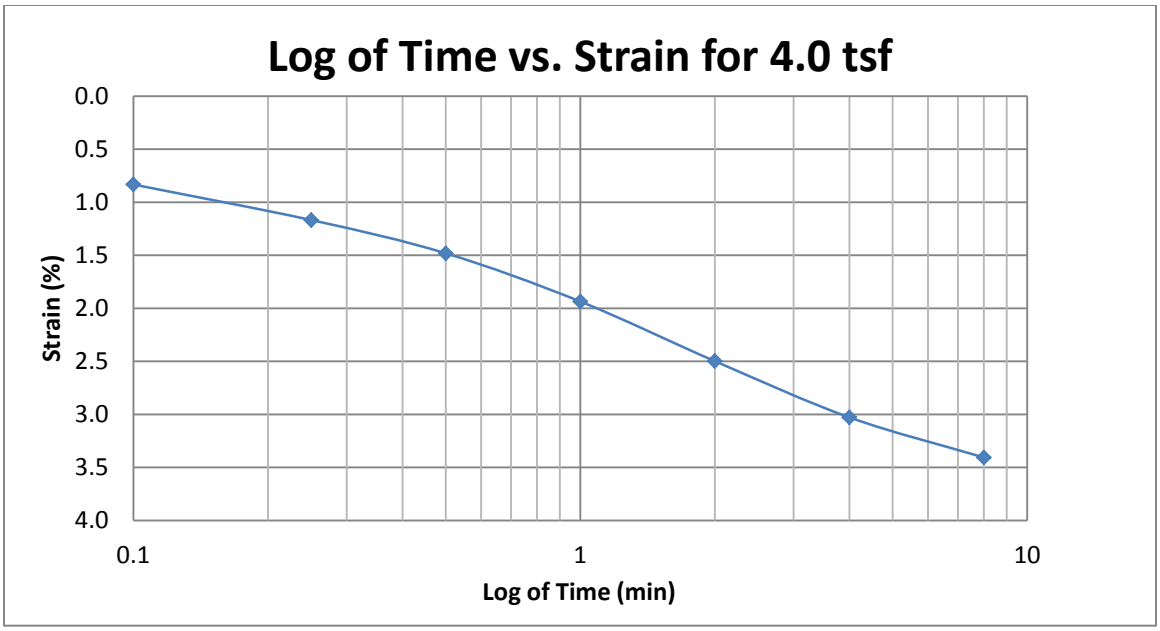

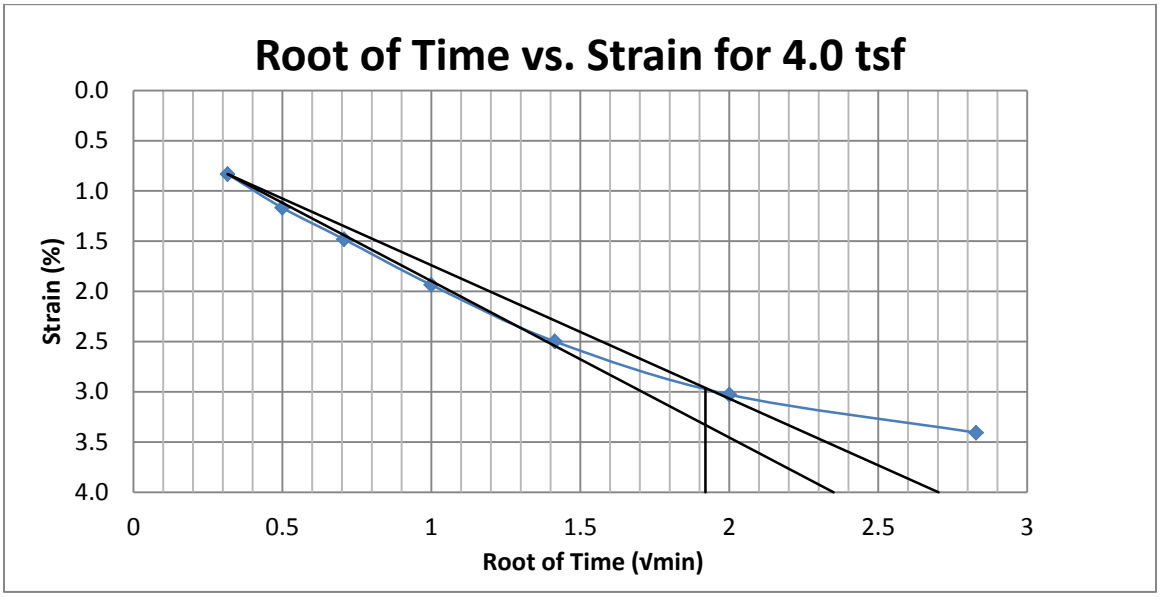

A46 400 South at 30-32 feet

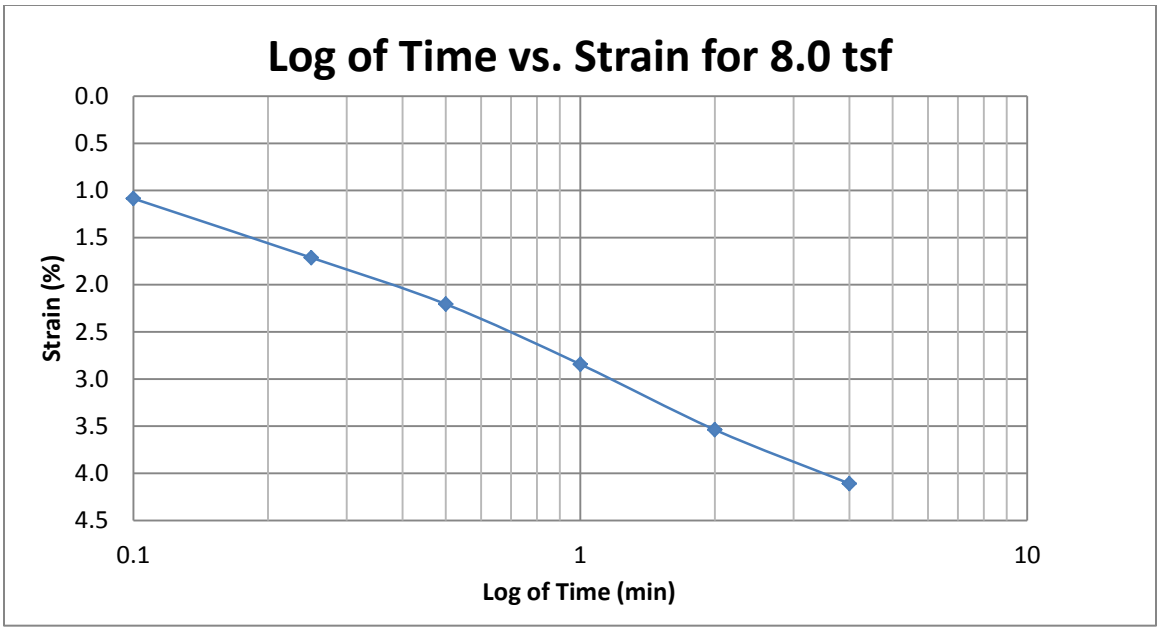

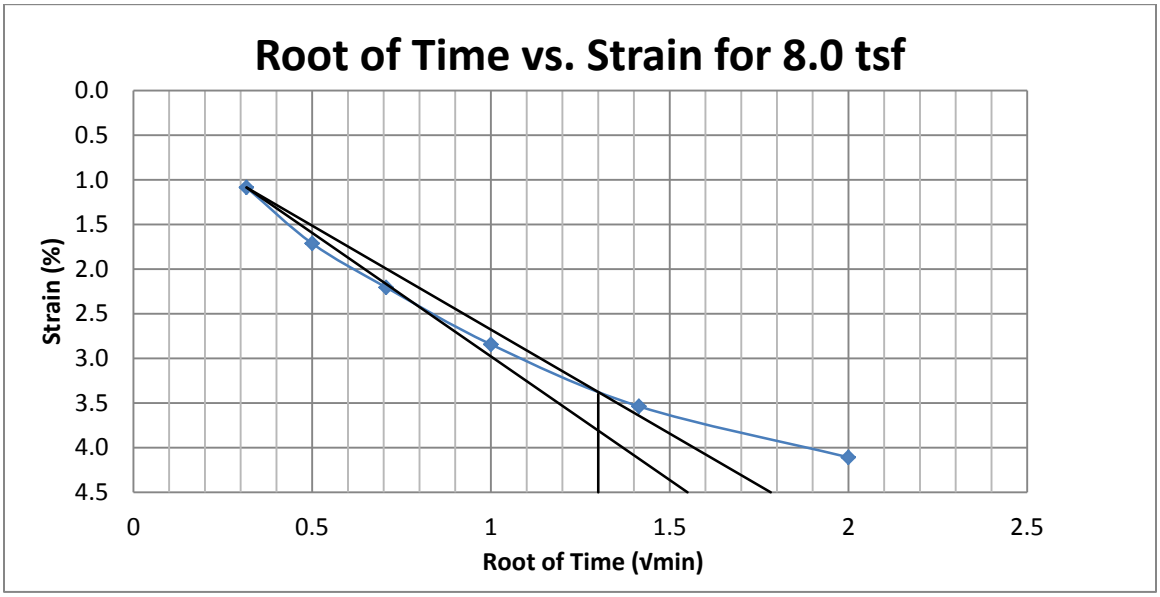

A47 400 South at 30-32 feet

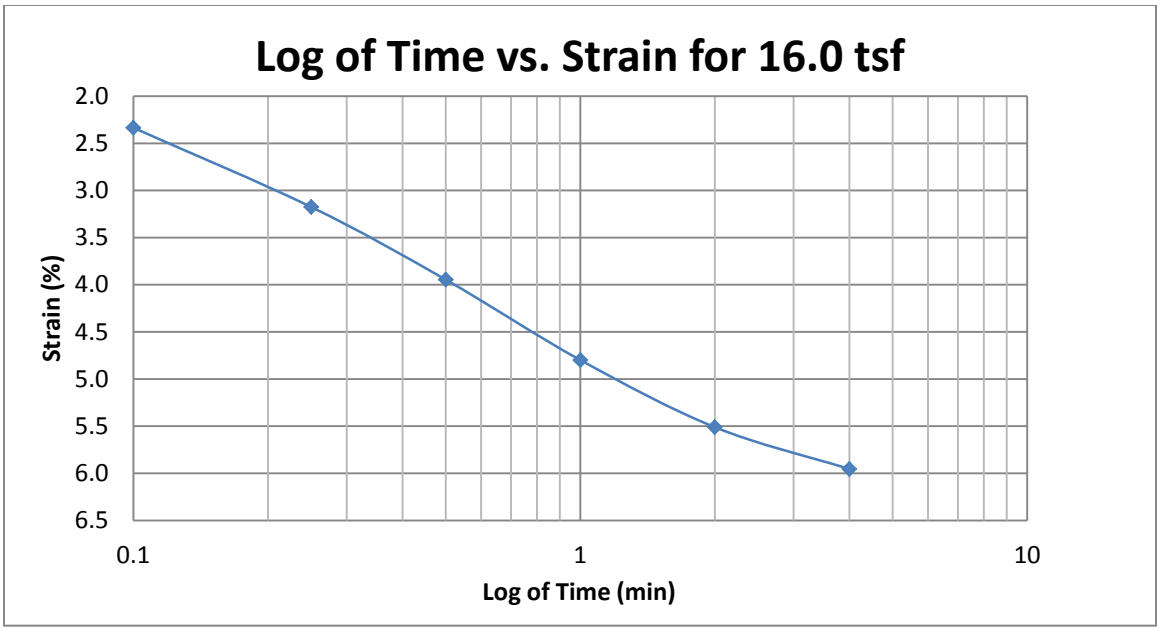

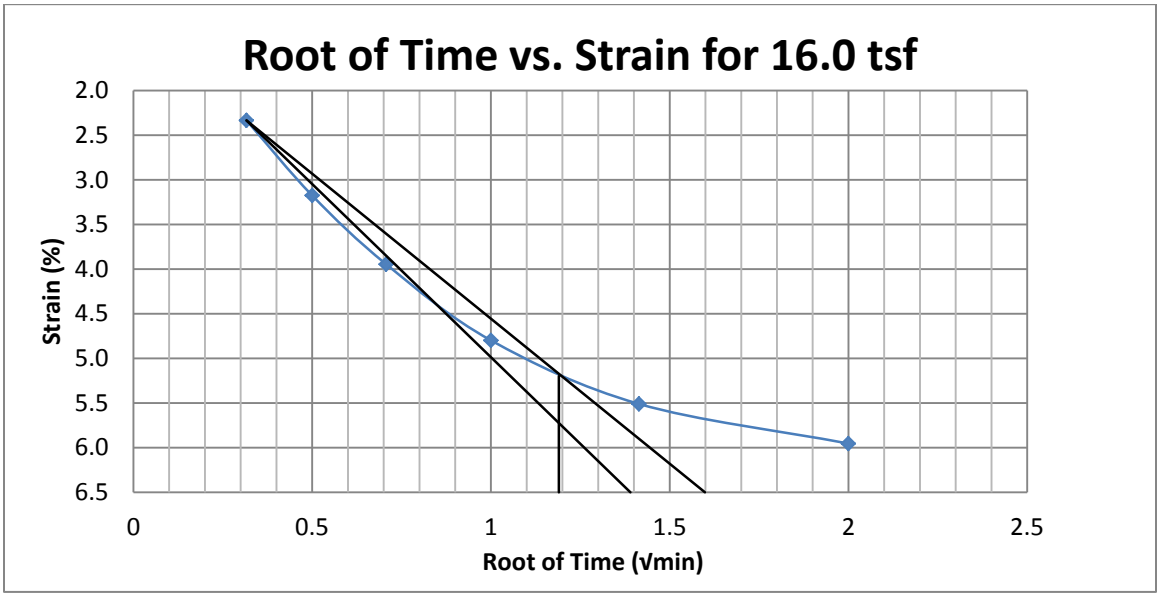

A48 400 South at 30-32 feet

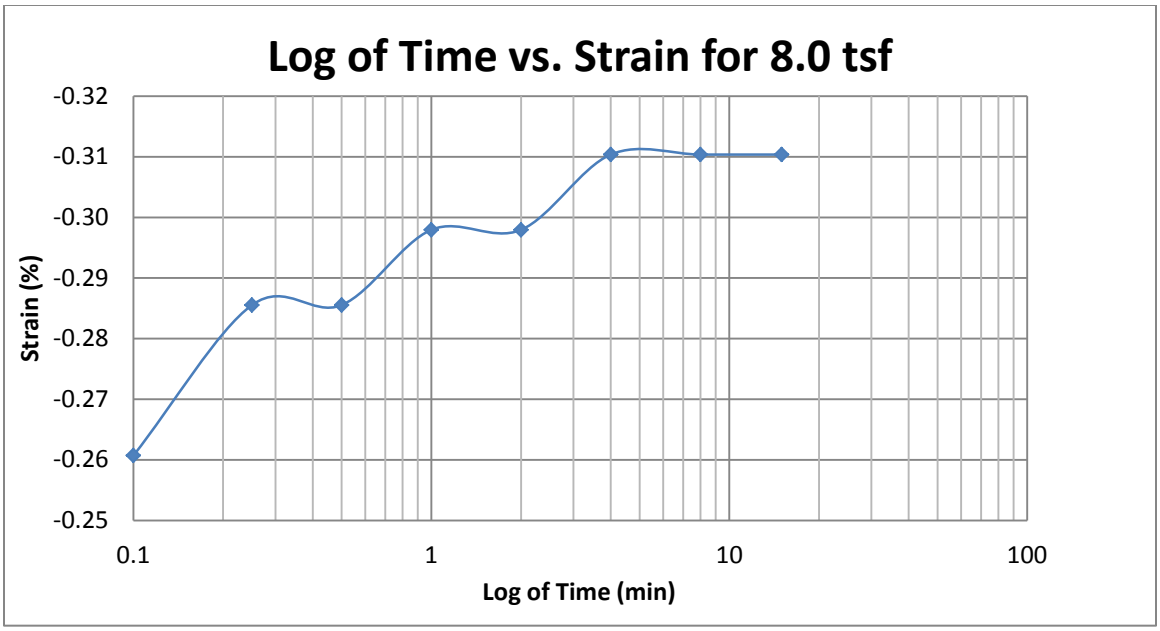

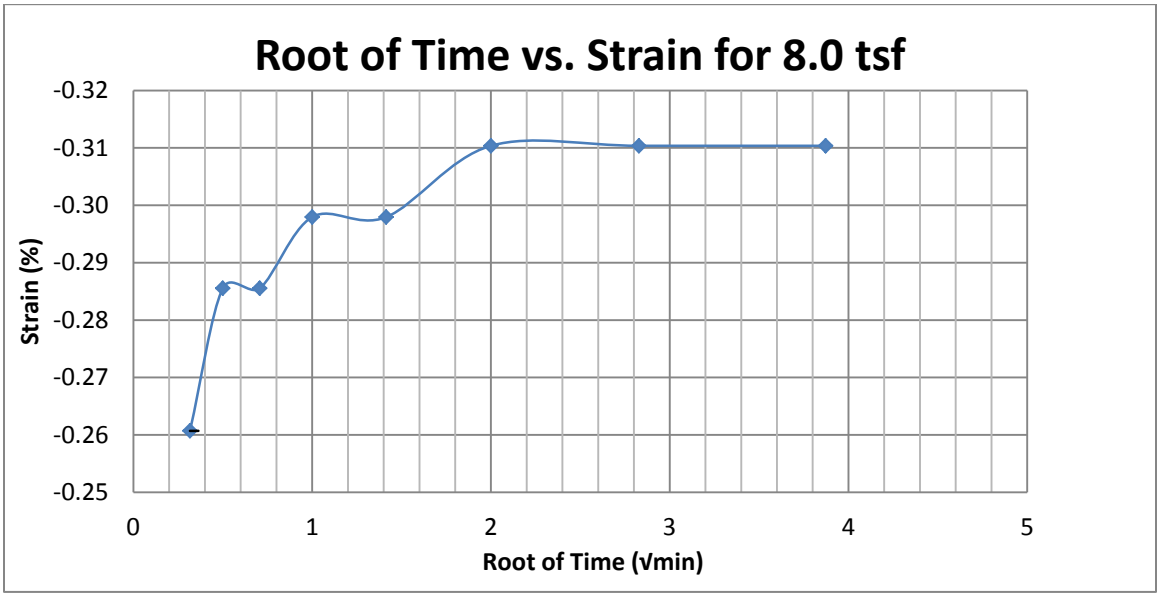

A49 400 South at 30-32 feet

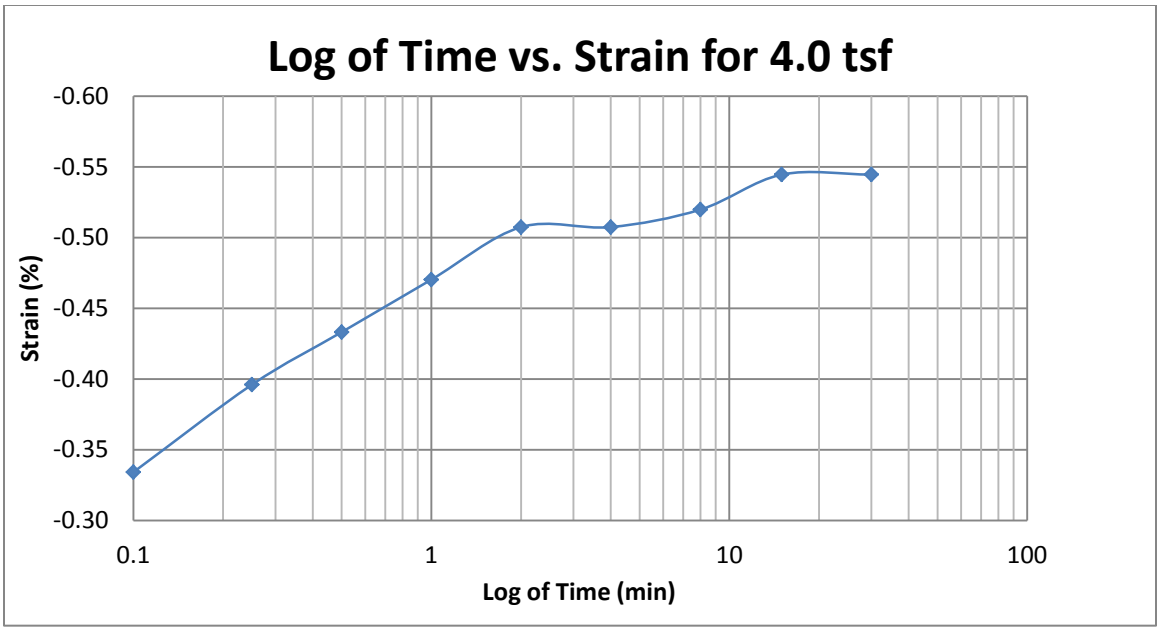

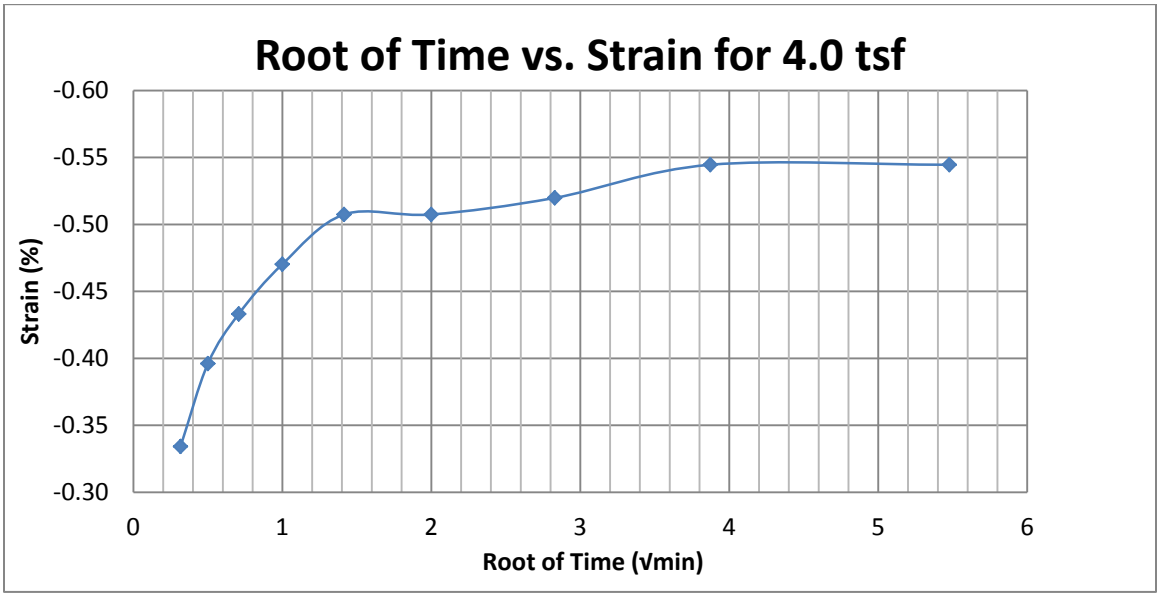

A50 400 South at 30-32 feet

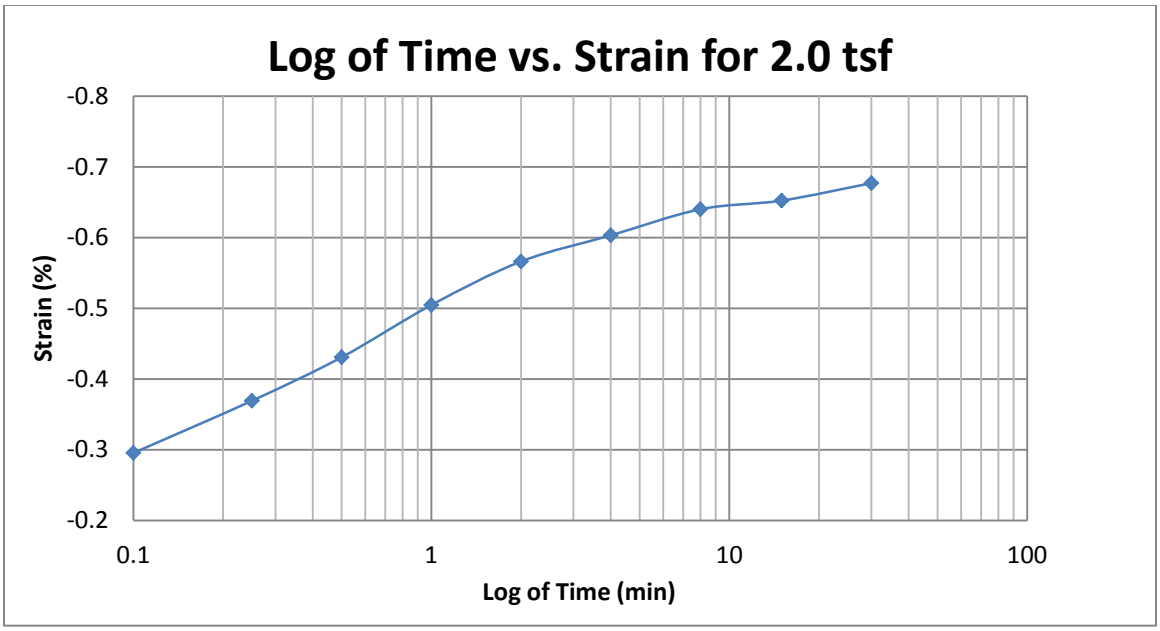

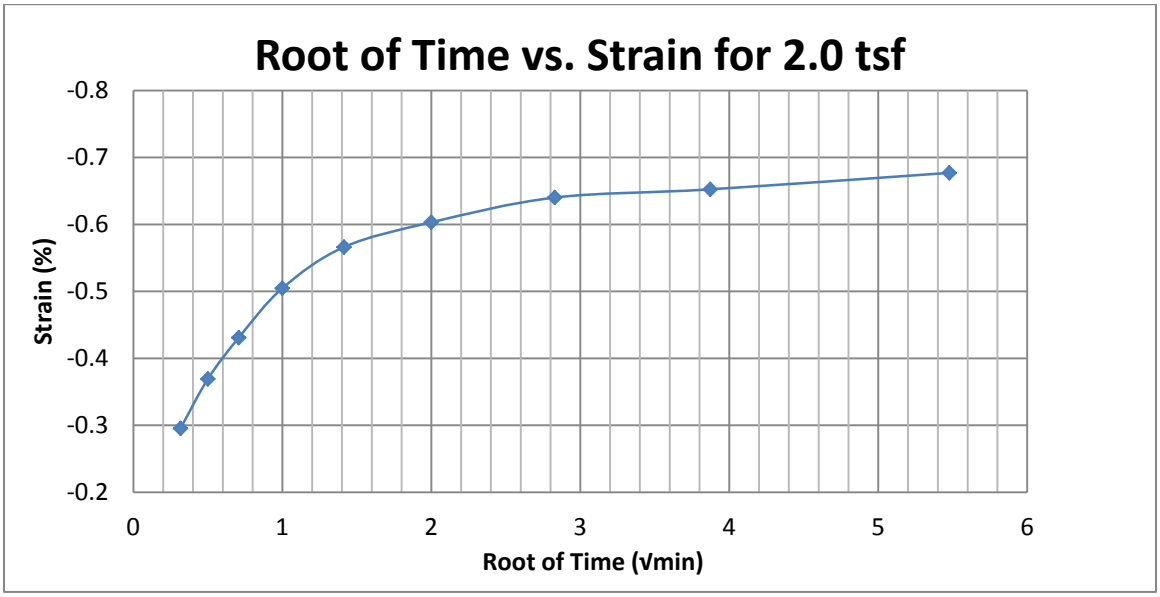

A51 400 South at 30-32 feet

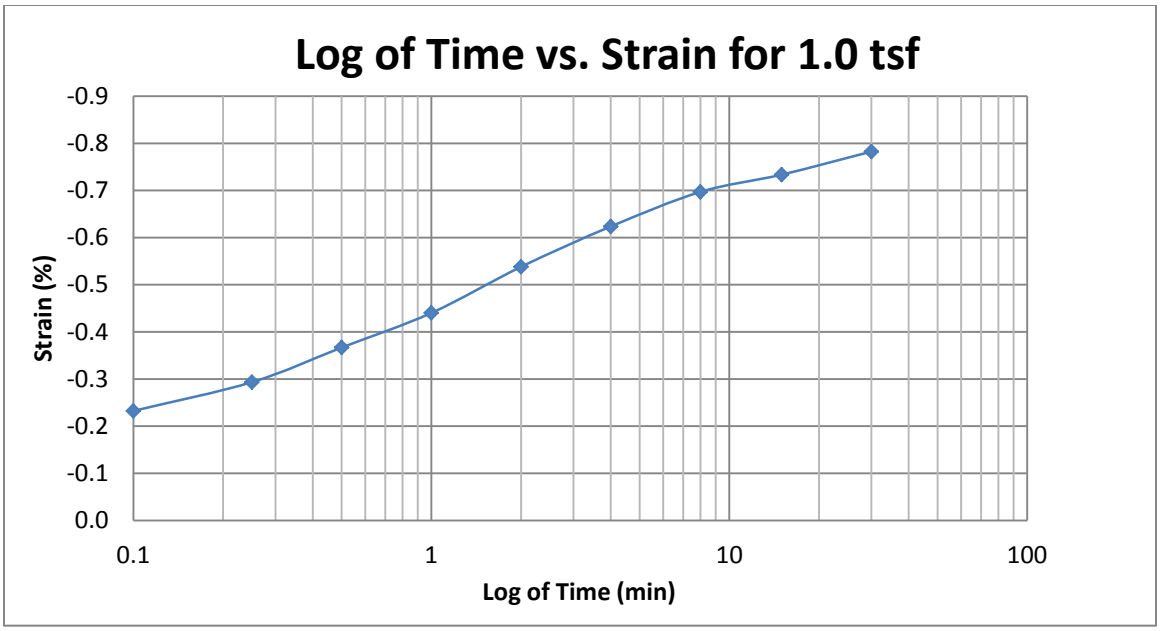

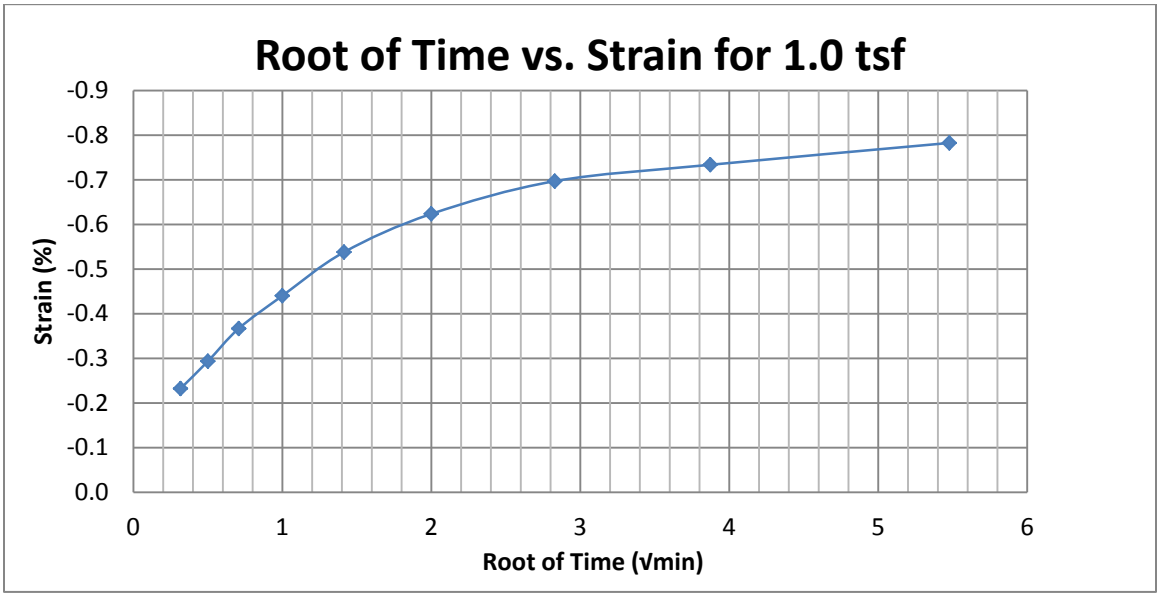

A52 400 South at 30-32 feet

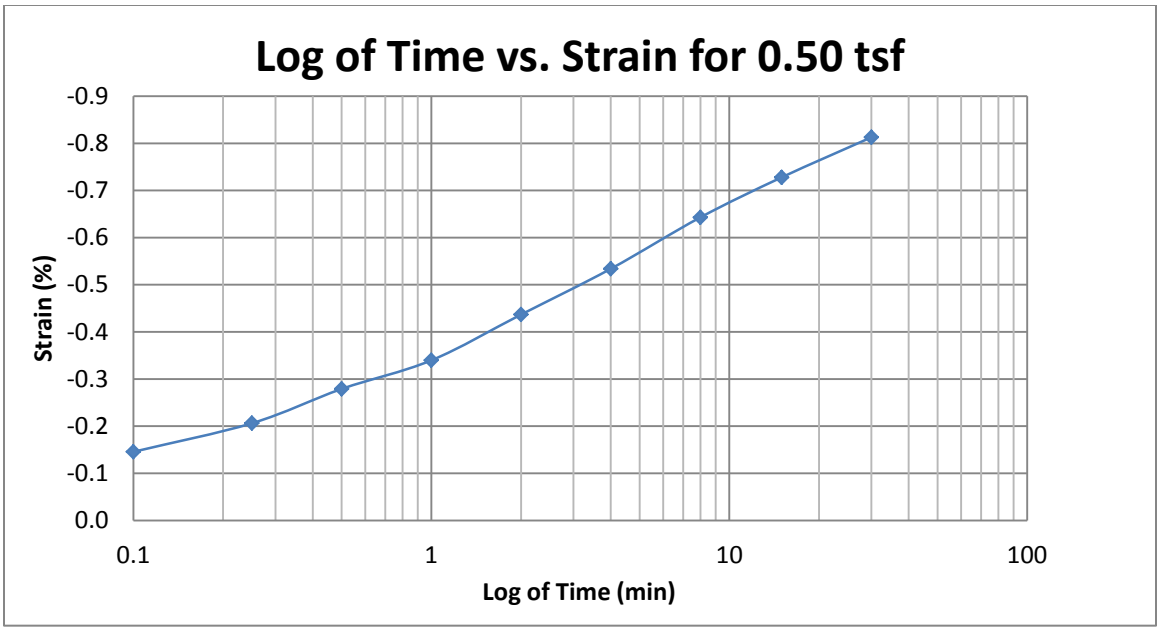

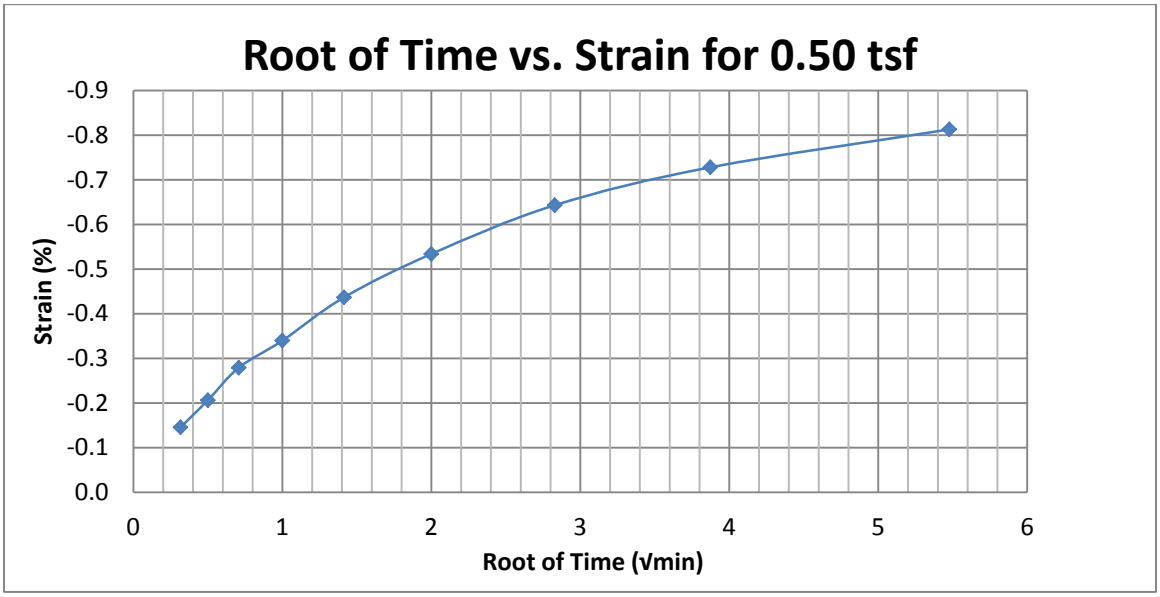

A53 400 South at 30-32 feet

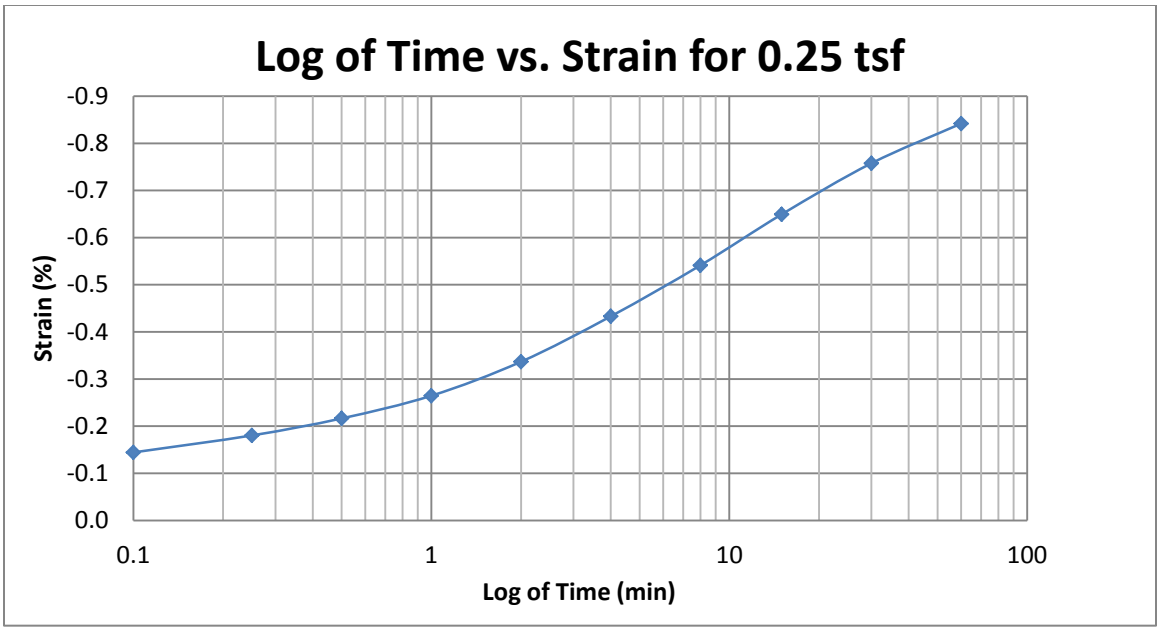

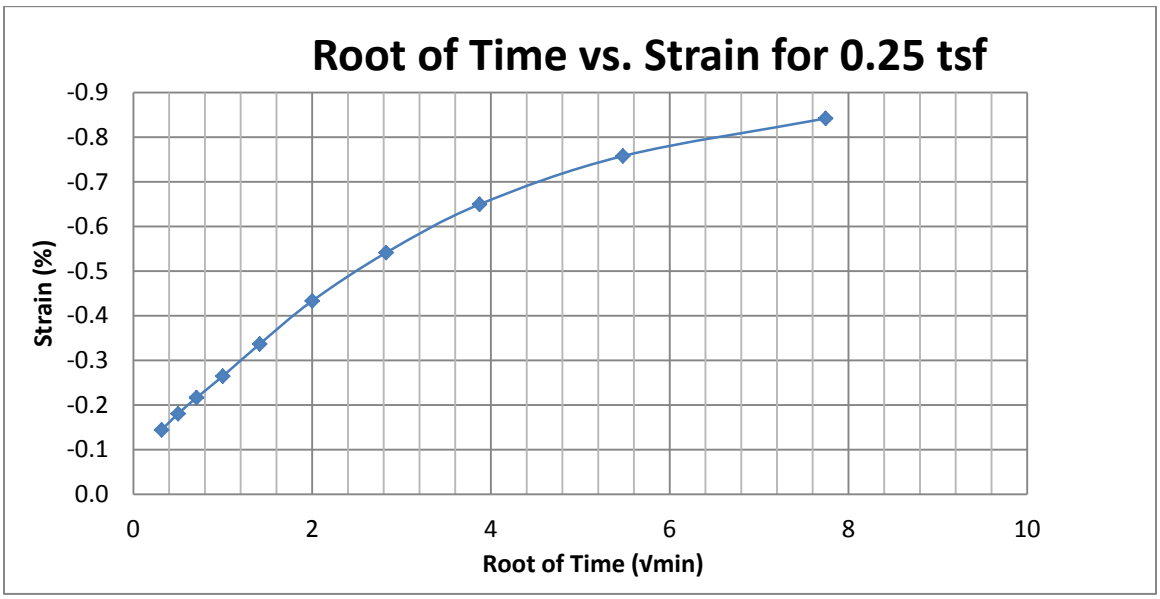

A54 400 South at 30-32 feet

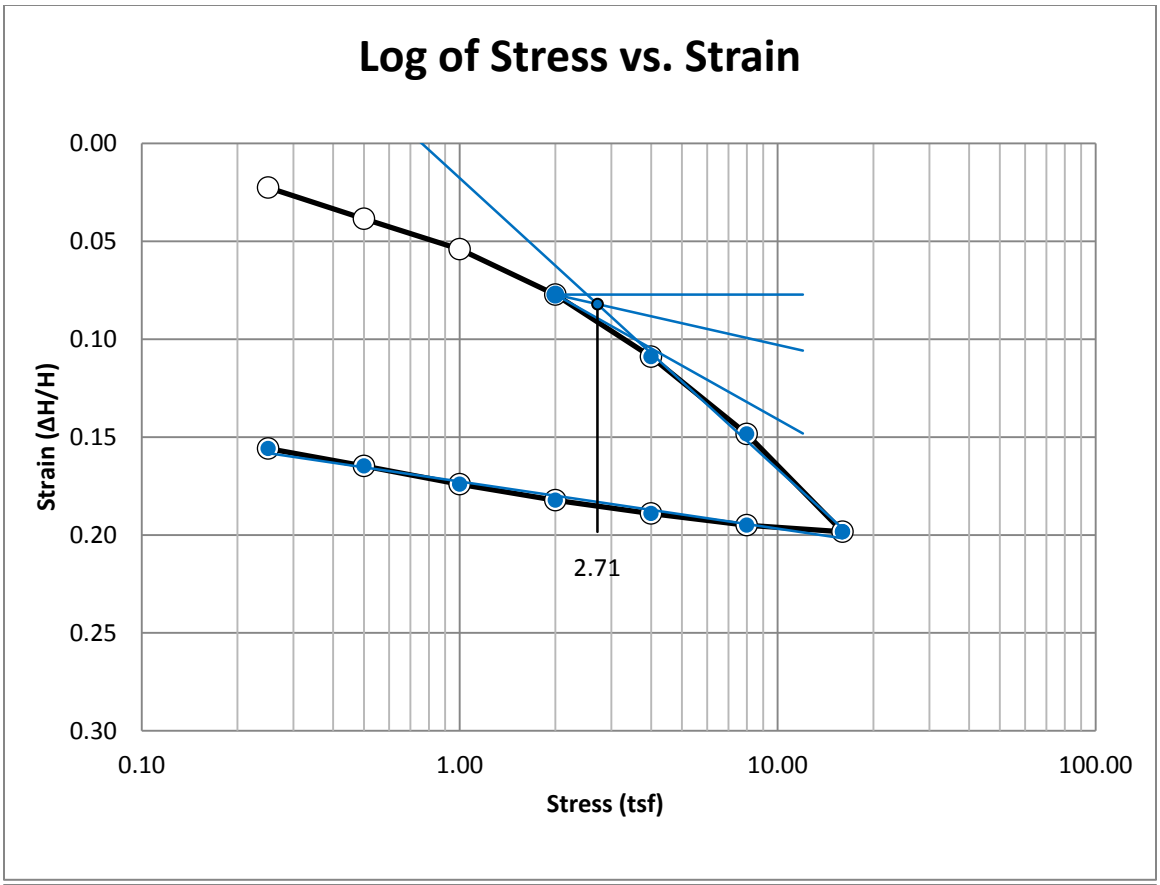

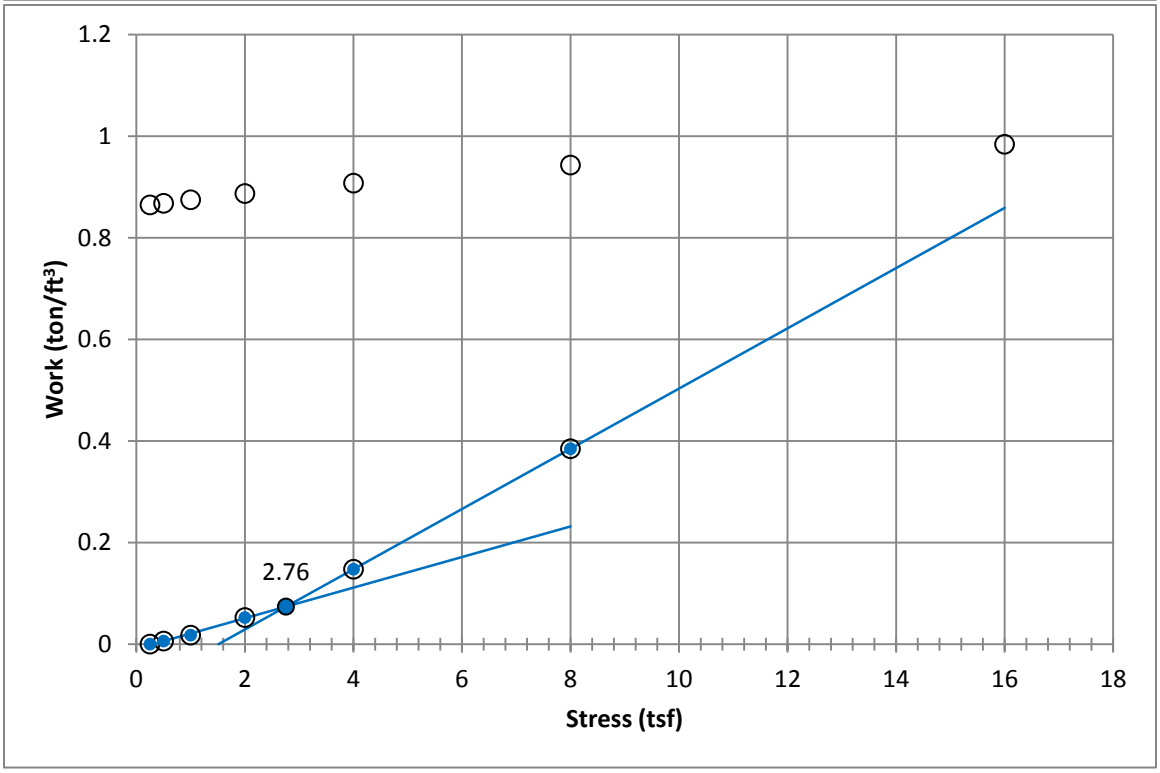

A55 400 South at 37.5-39.5 feet

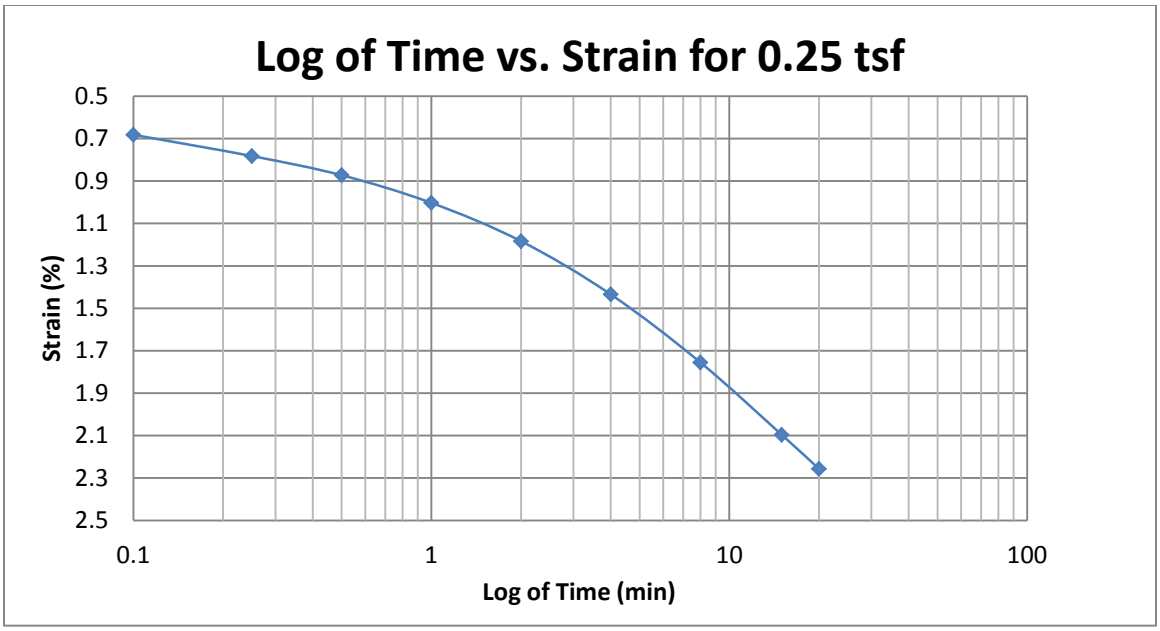

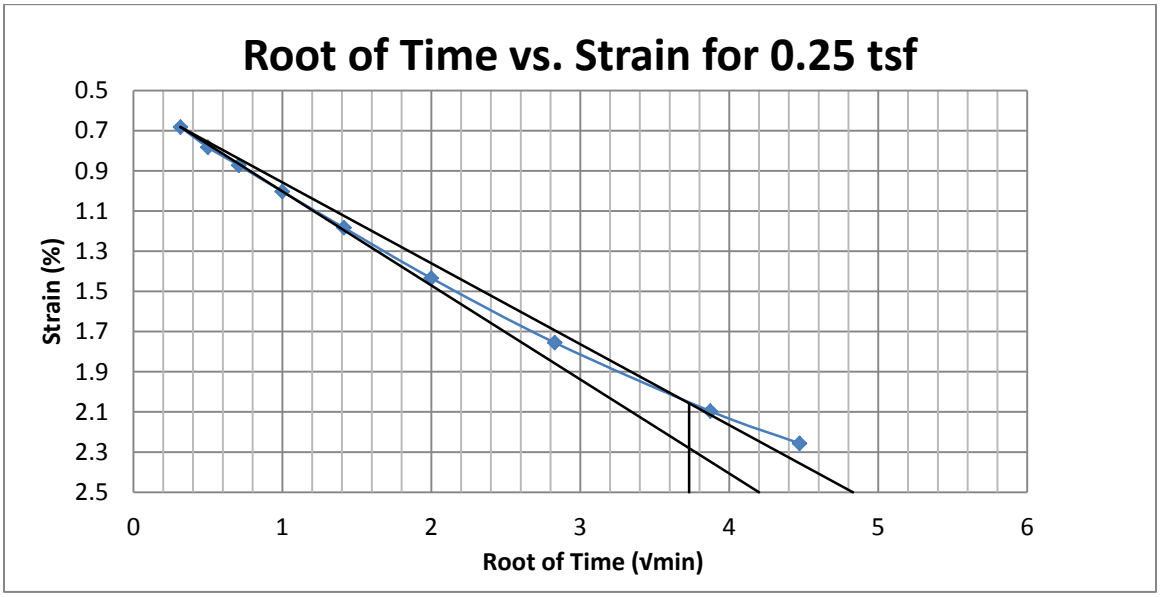

A56 400 South at 37.5-39.5 feet

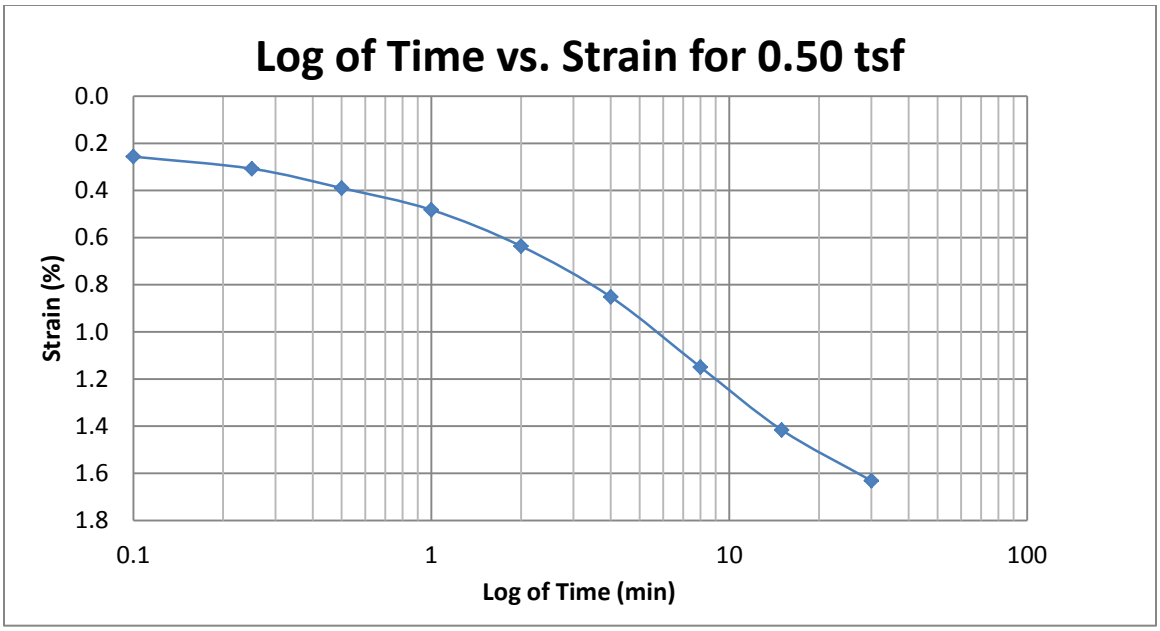

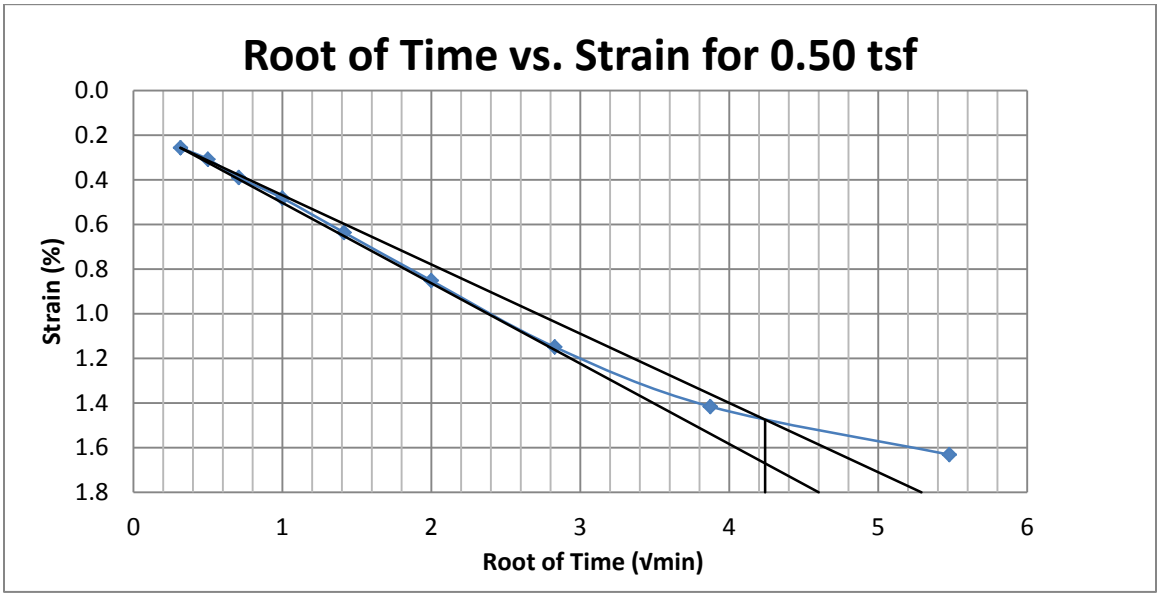

A57 400 South at 37.5-39.5 feet

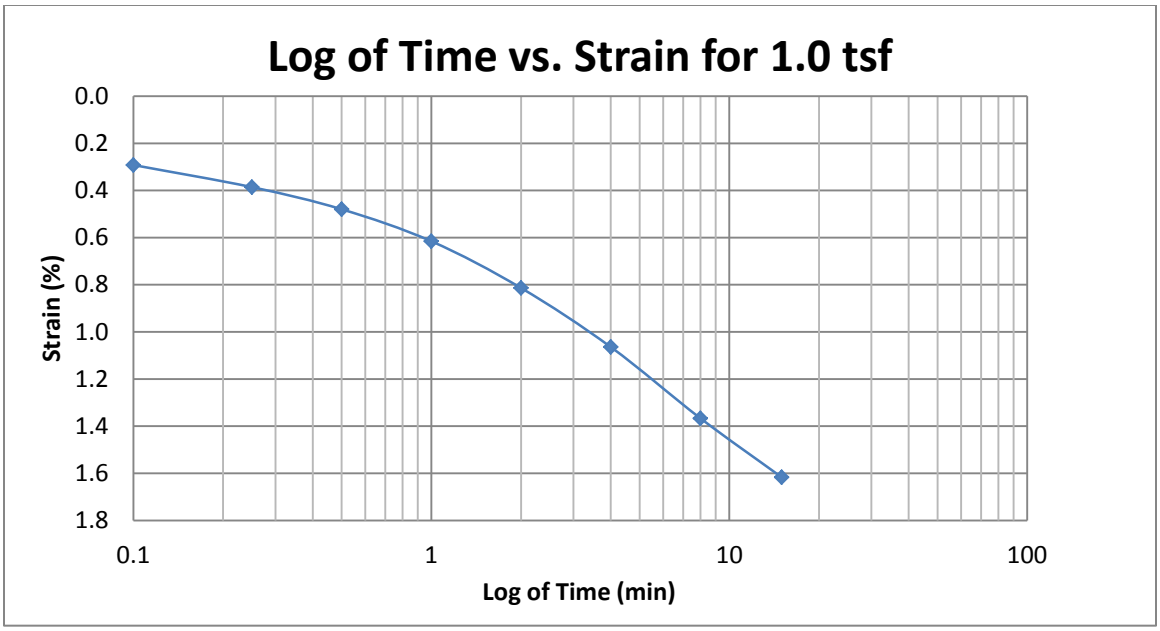

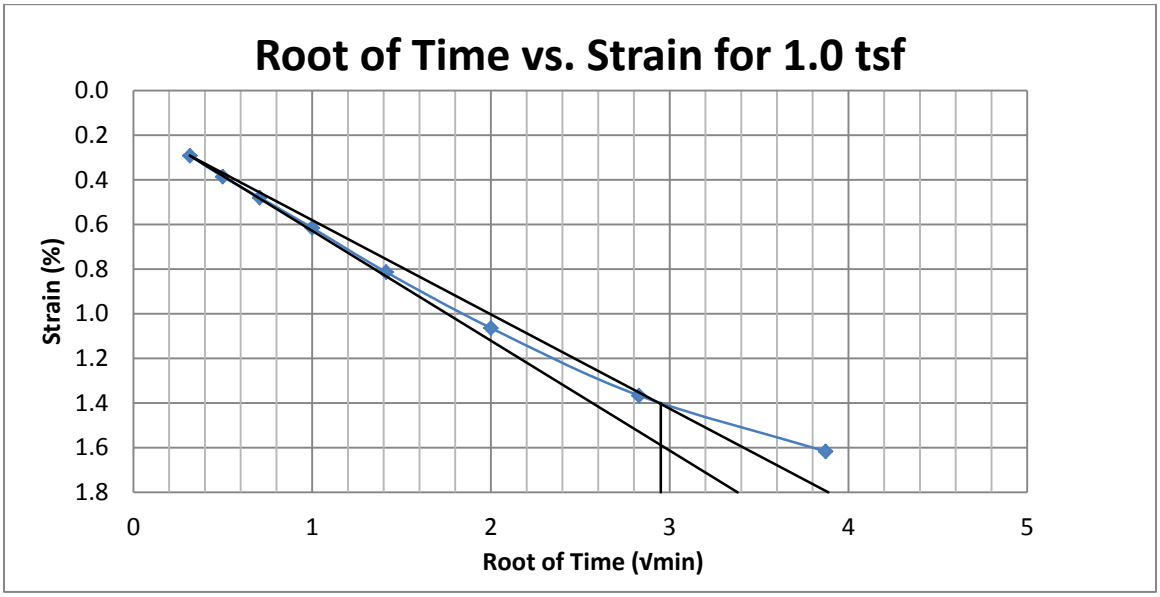

A58 400 South at 37.5-39.5 feet

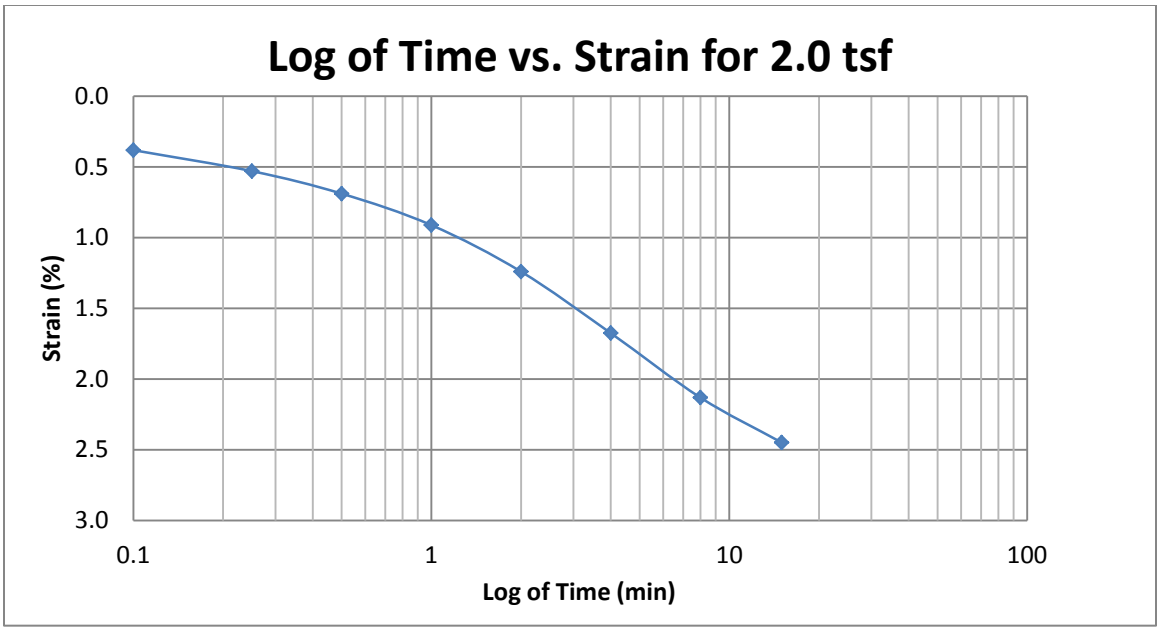

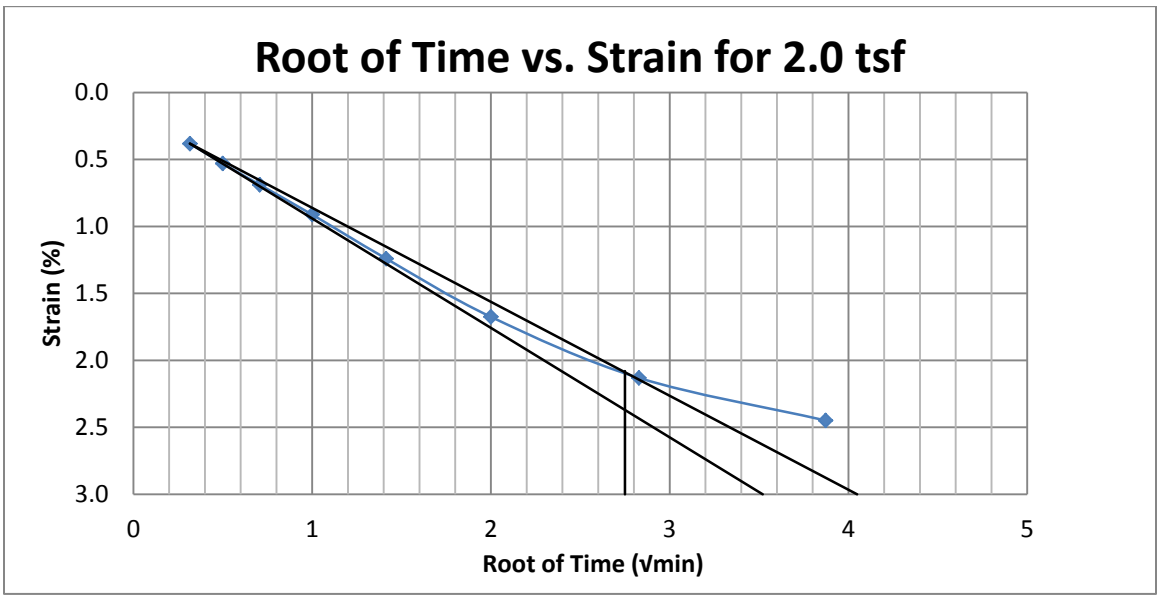

A59 400 South at 37.5-39.5 feet

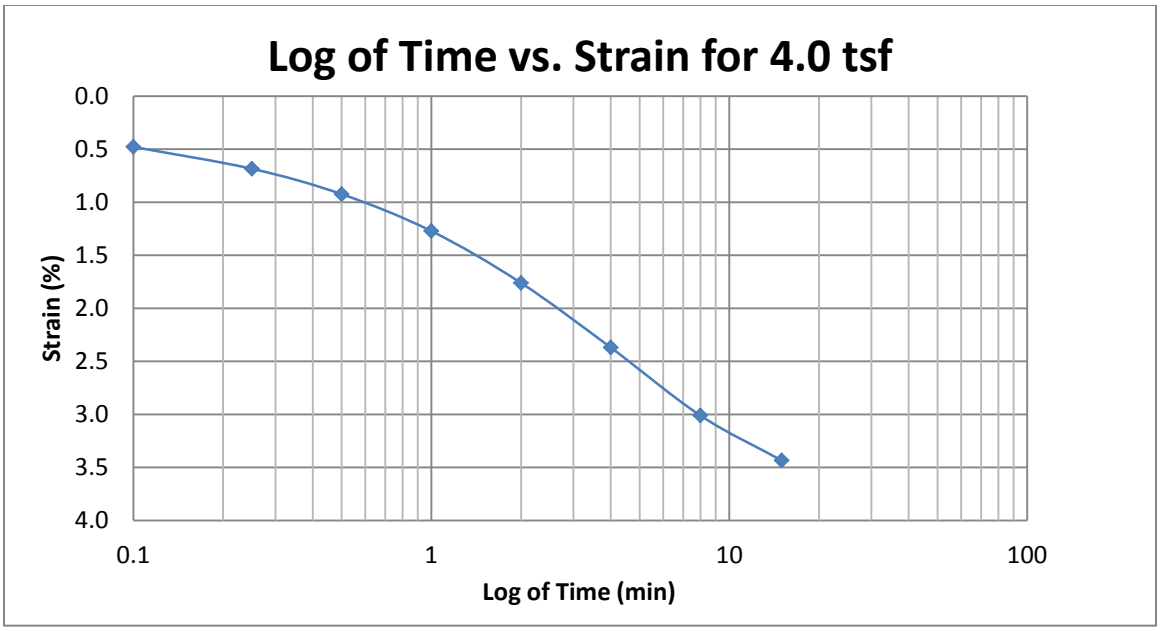

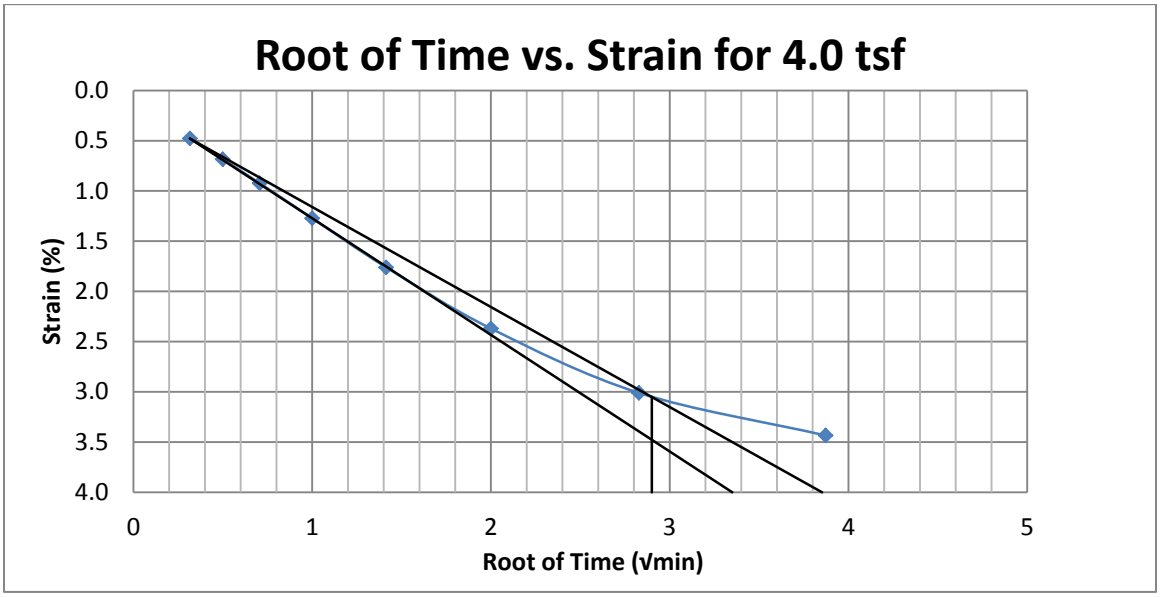

A60 400 South at 37.5-39.5 feet

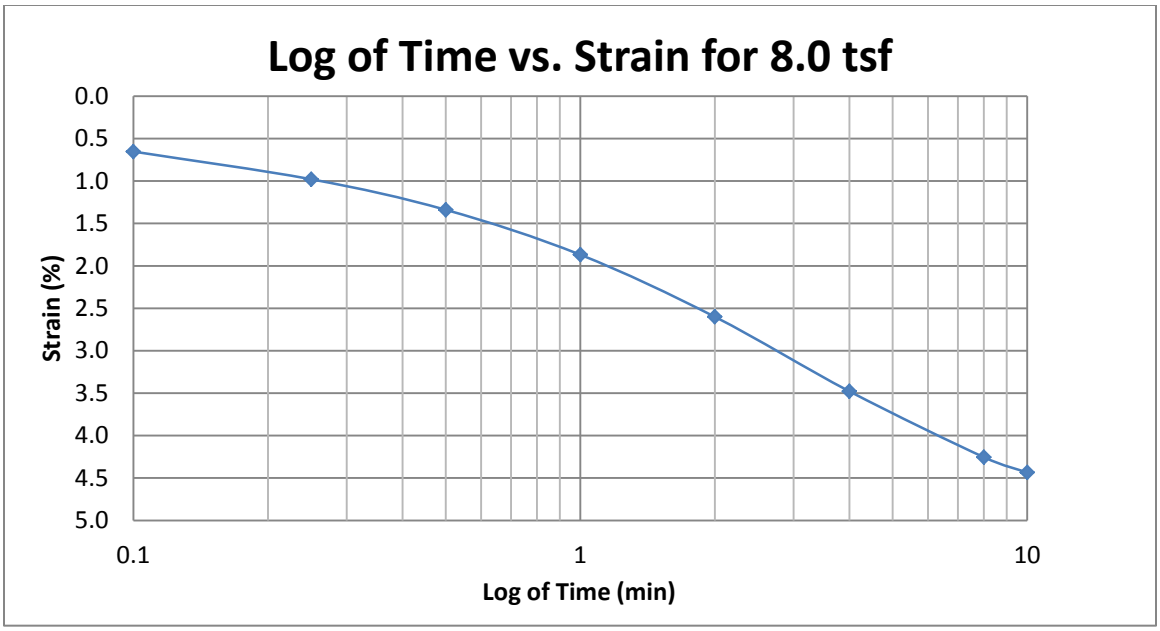

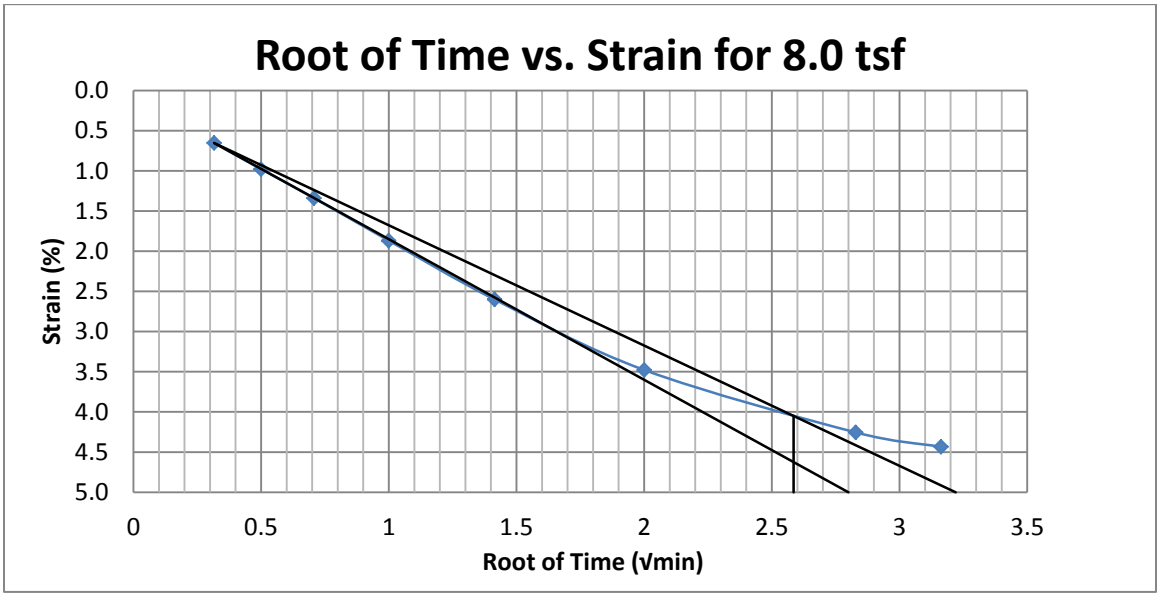

A61 400 South at 37.5-39.5 feet

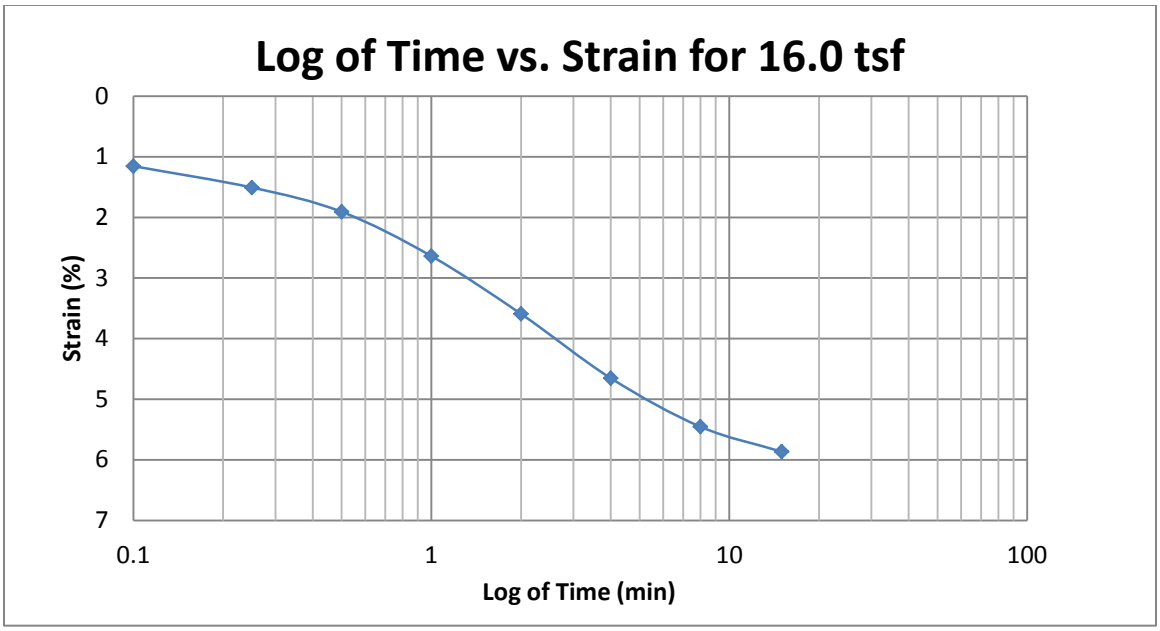

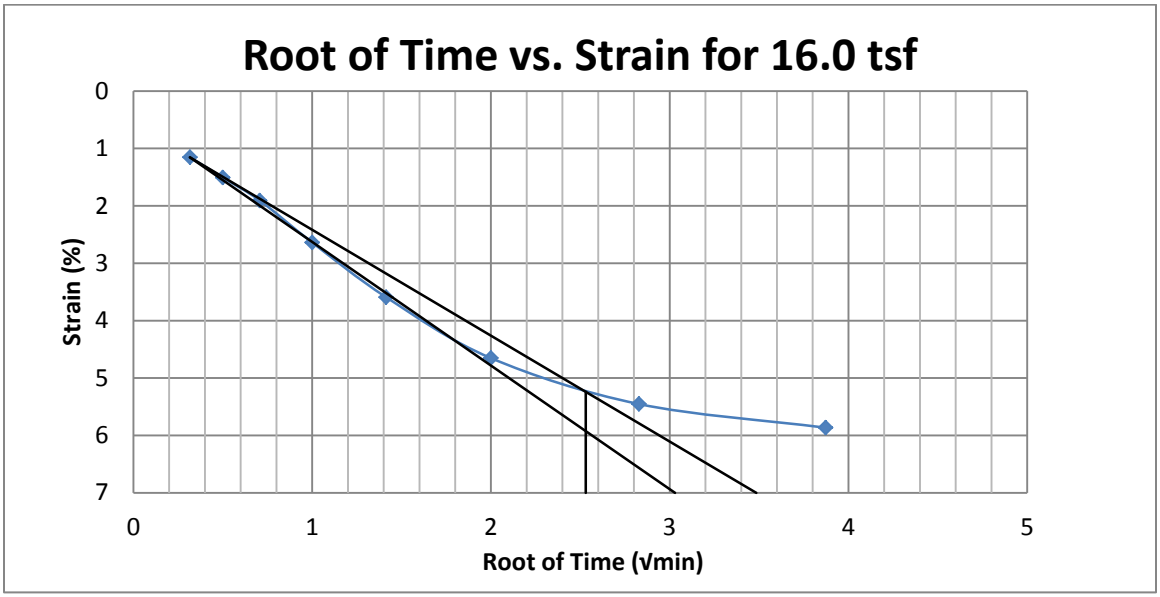

A62 400 South at 37.5-39.5 feet

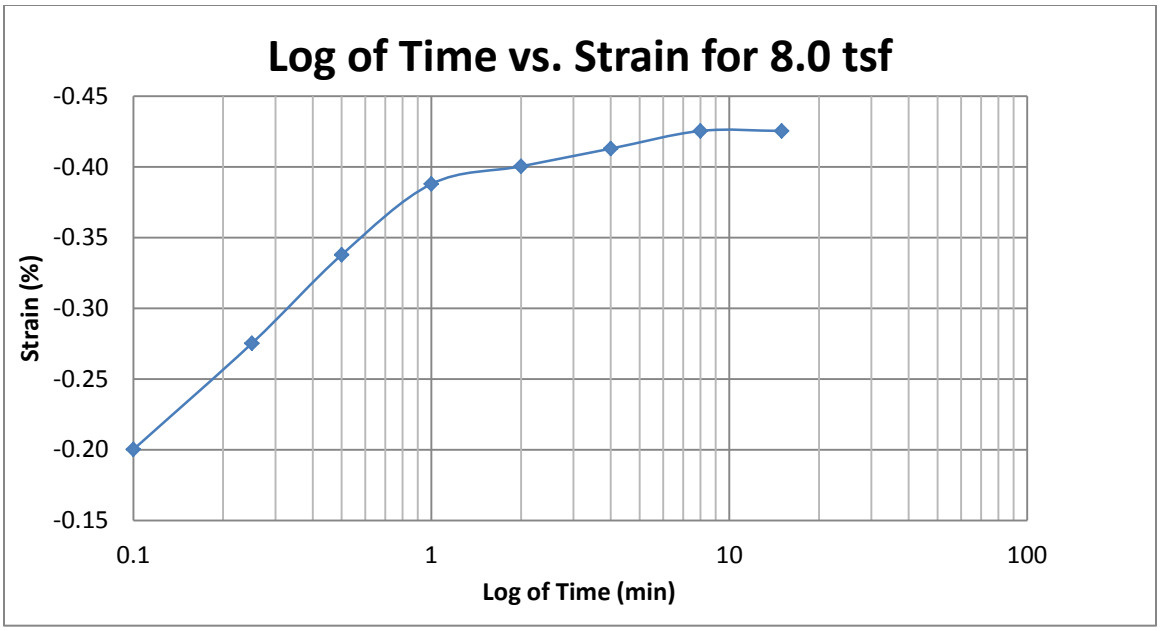

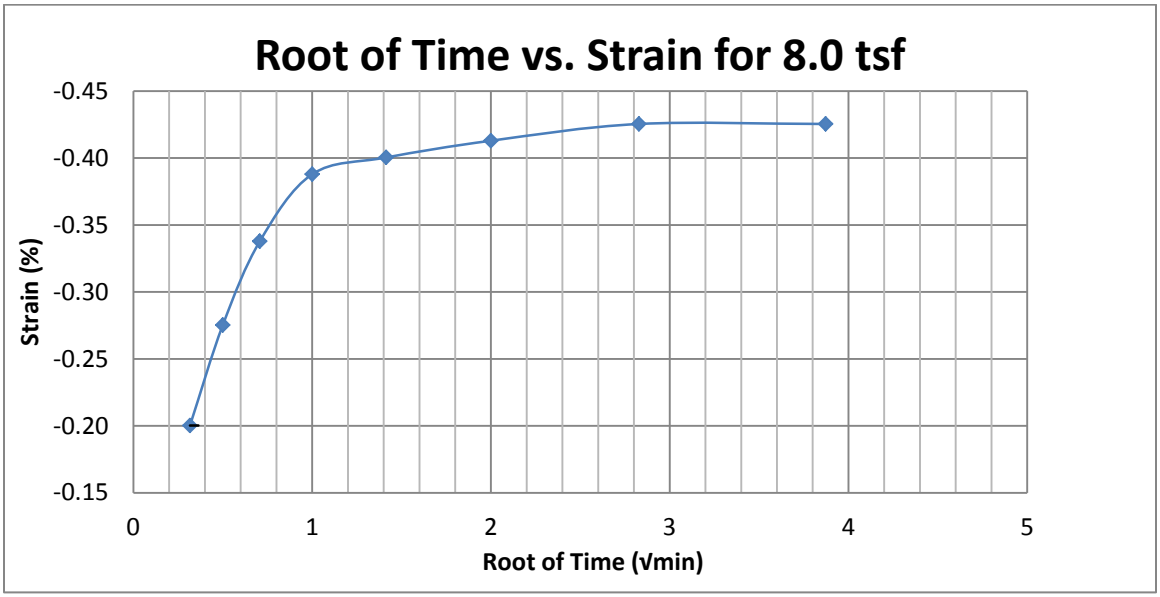

A63 400 South at 37.5-39.5 feet

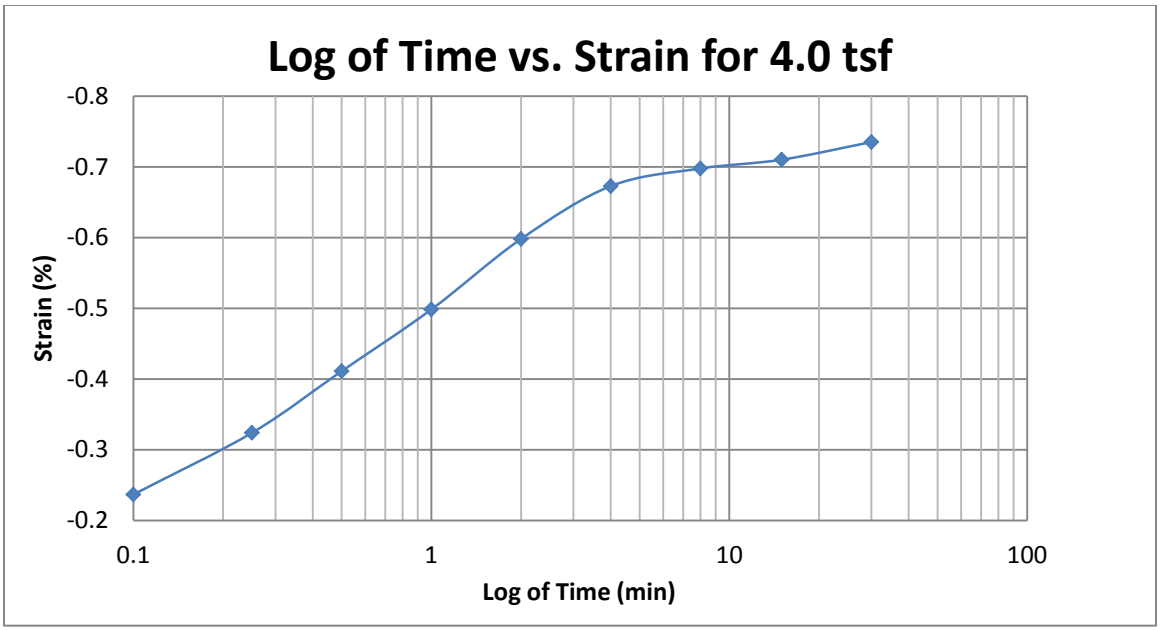

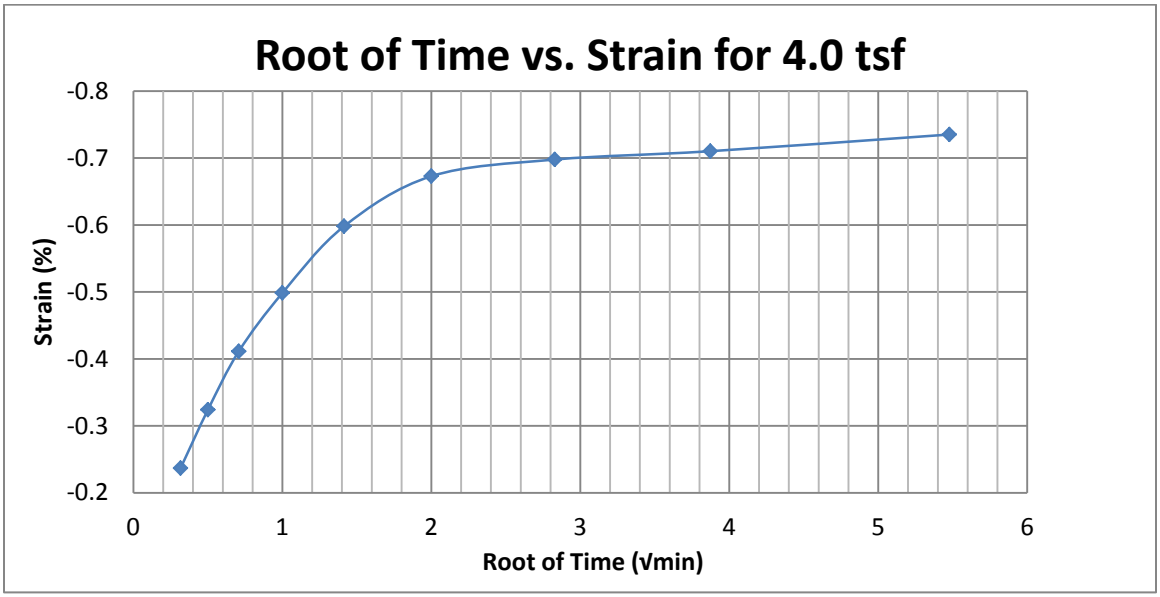

A64 400 South at 37.5-39.5 feet

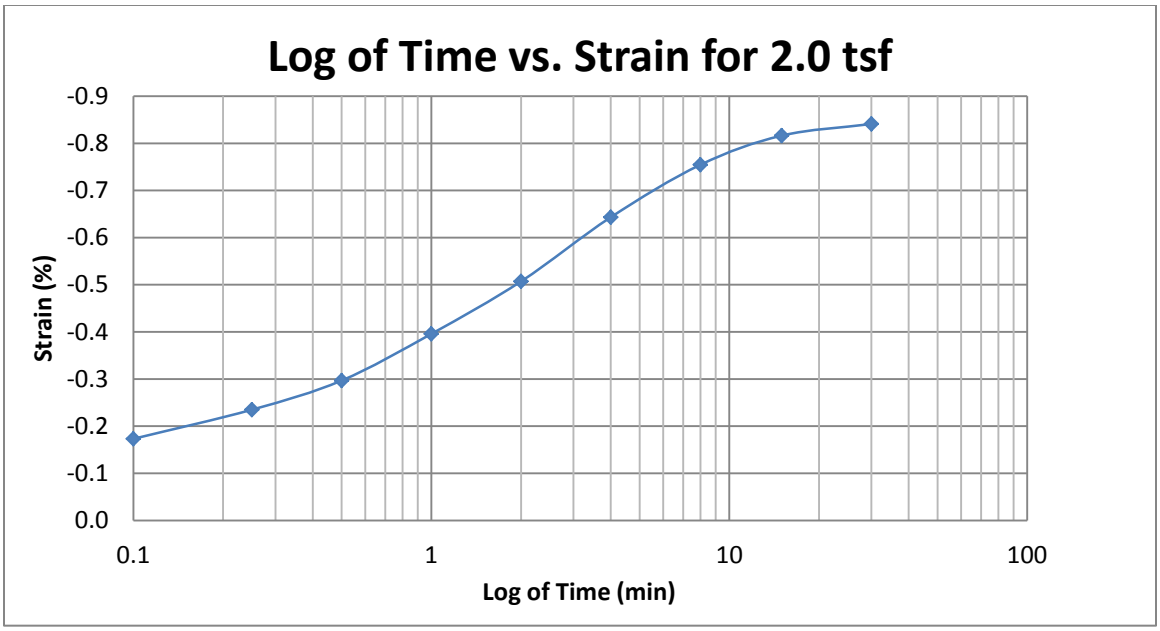

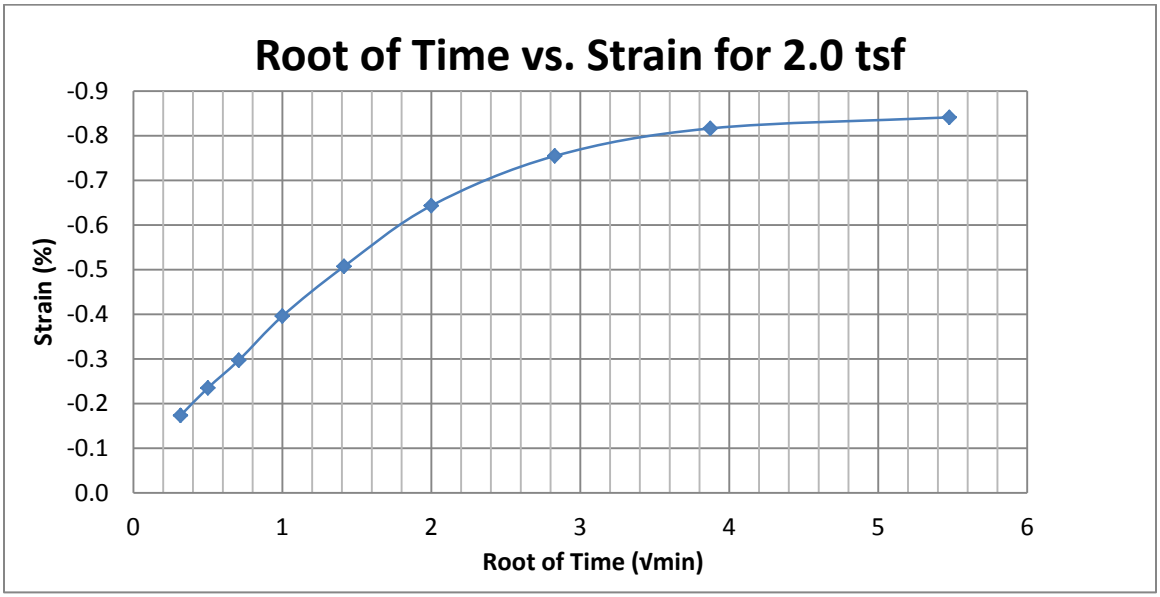

A65 400 South at 37.5-39.5 feet

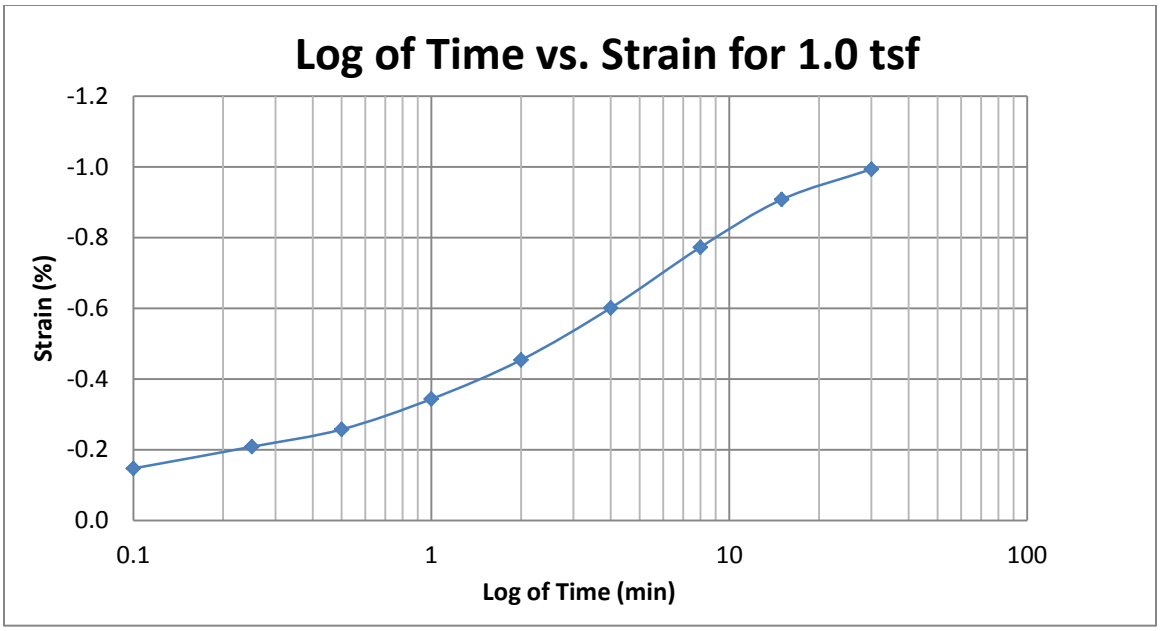

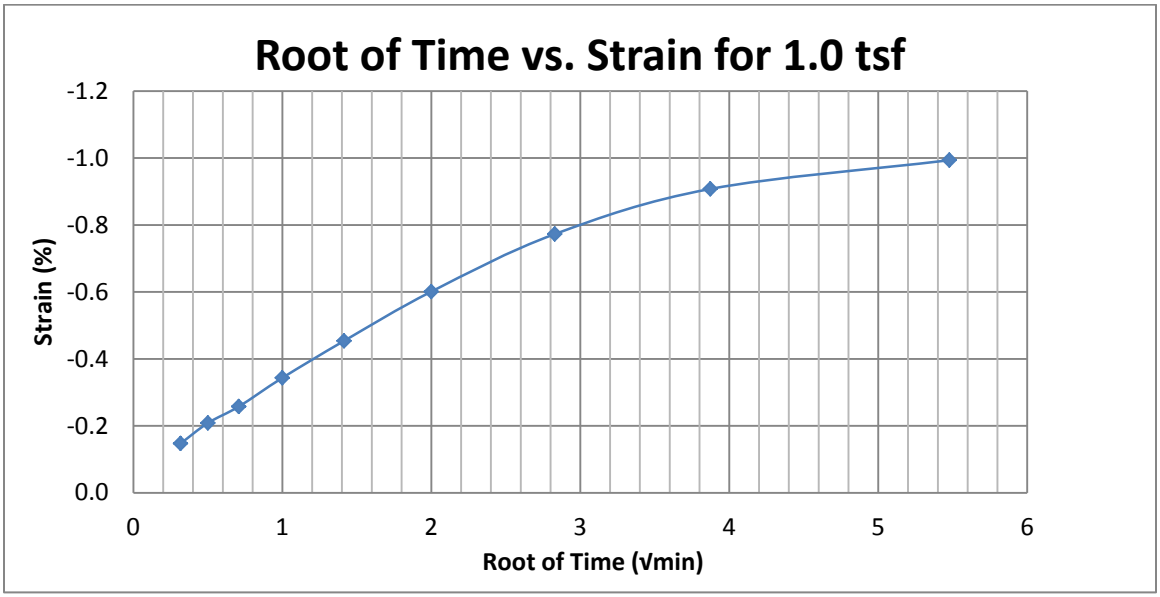

A66 400 South at 37.5-39.5 feet

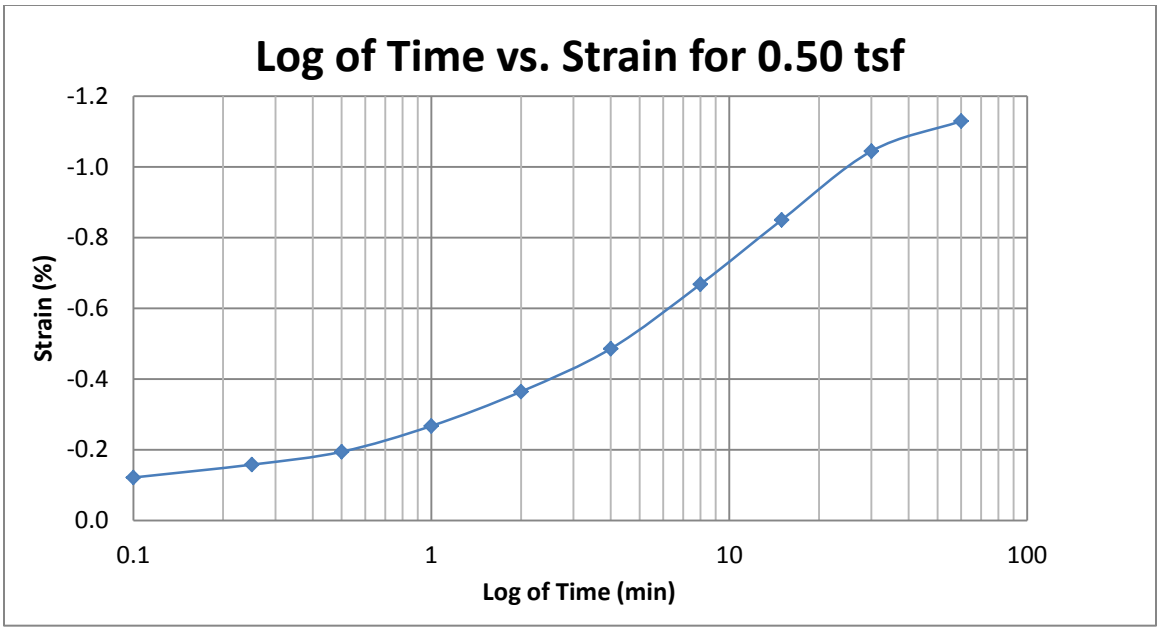

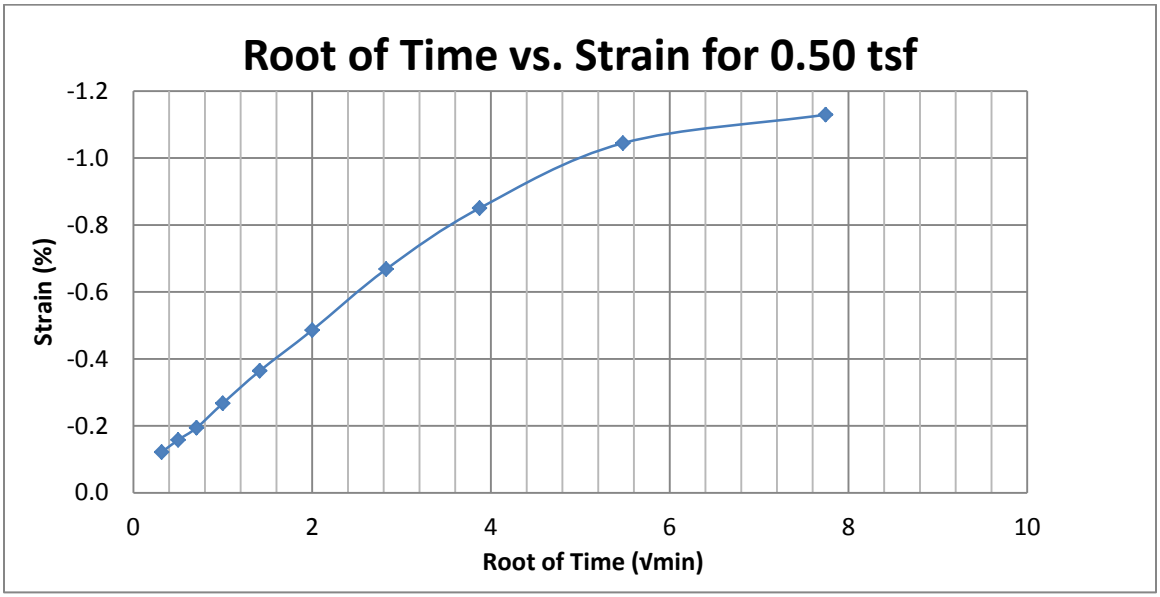

A67 400 South at 37.5-39.5 feet

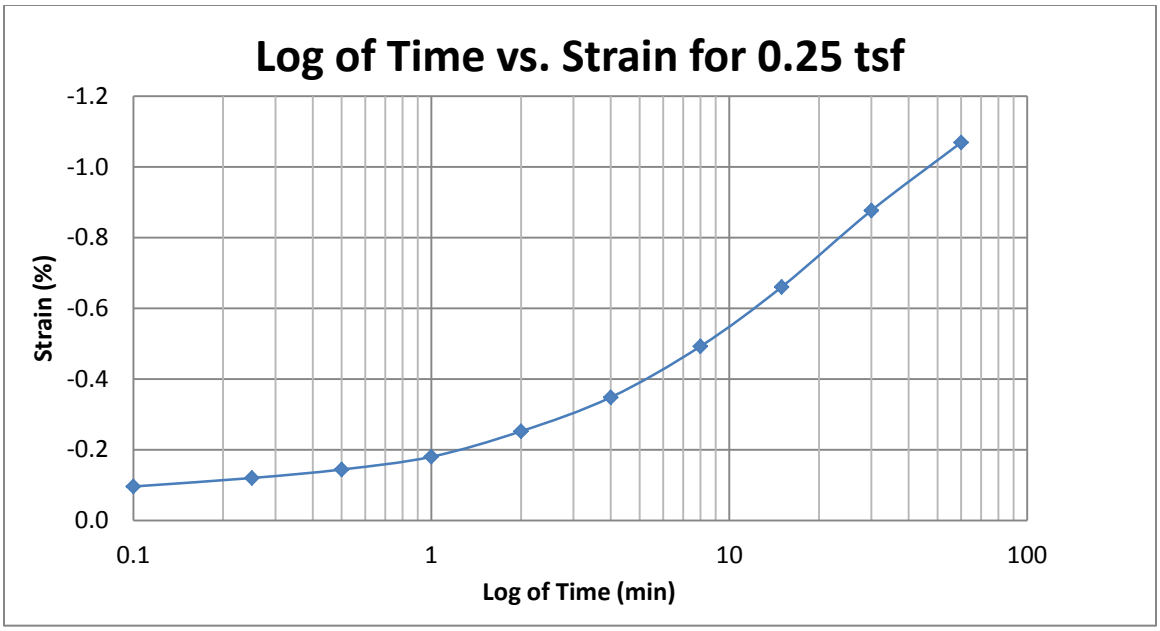

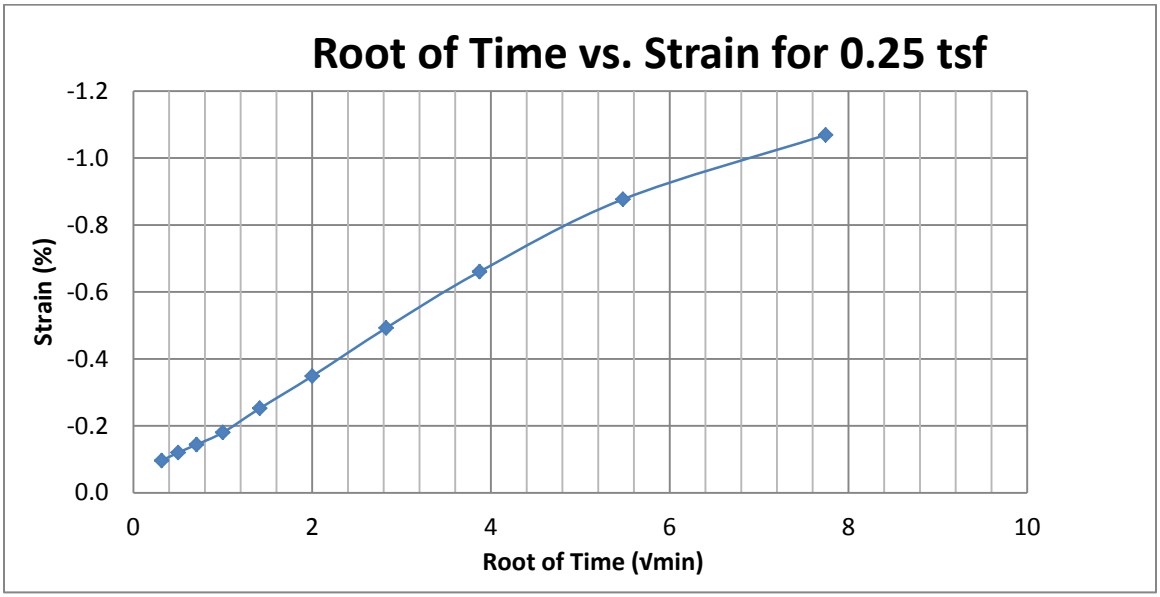

A68 400 South at 37.5-39.5 feet

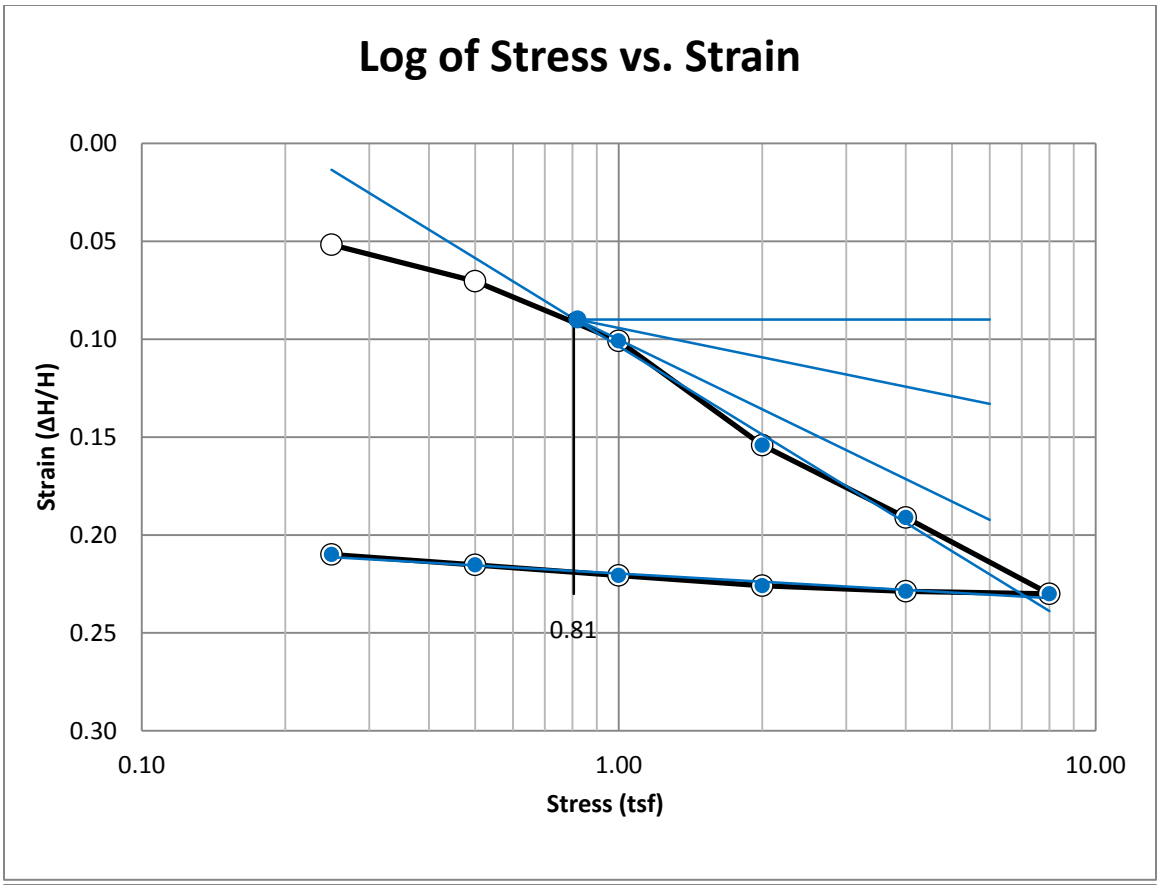

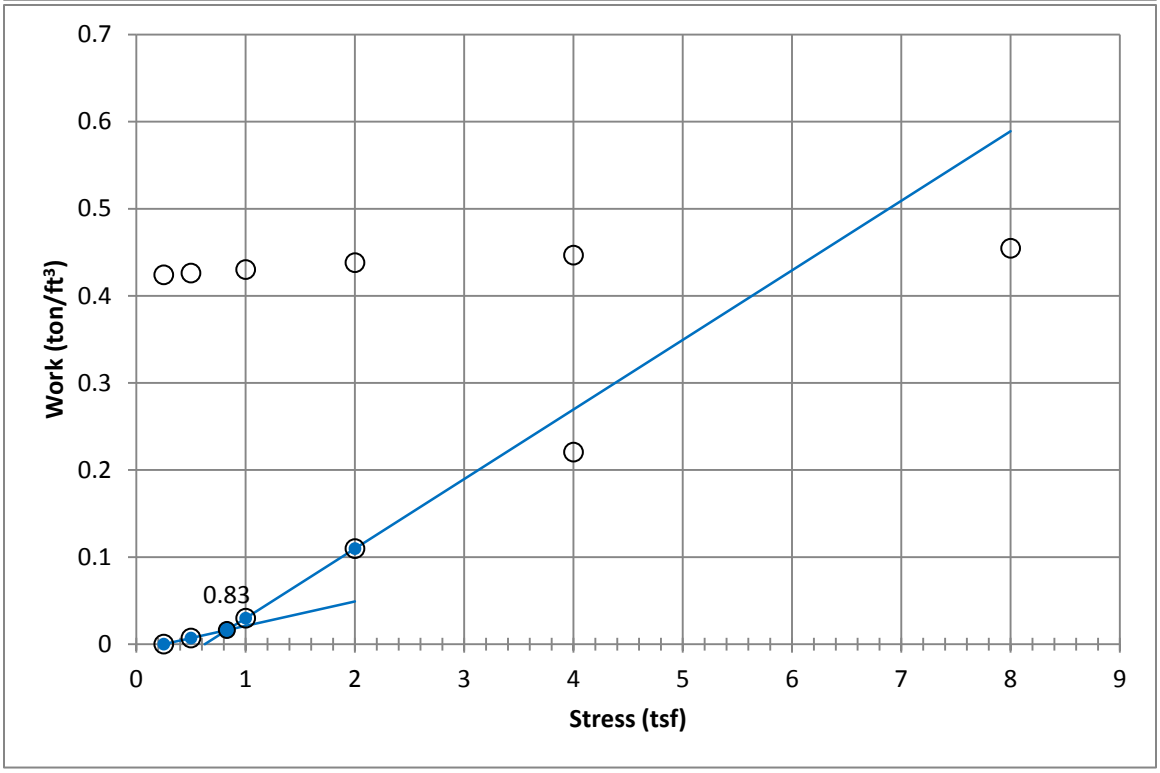

A69 400 South at 40-42 feet

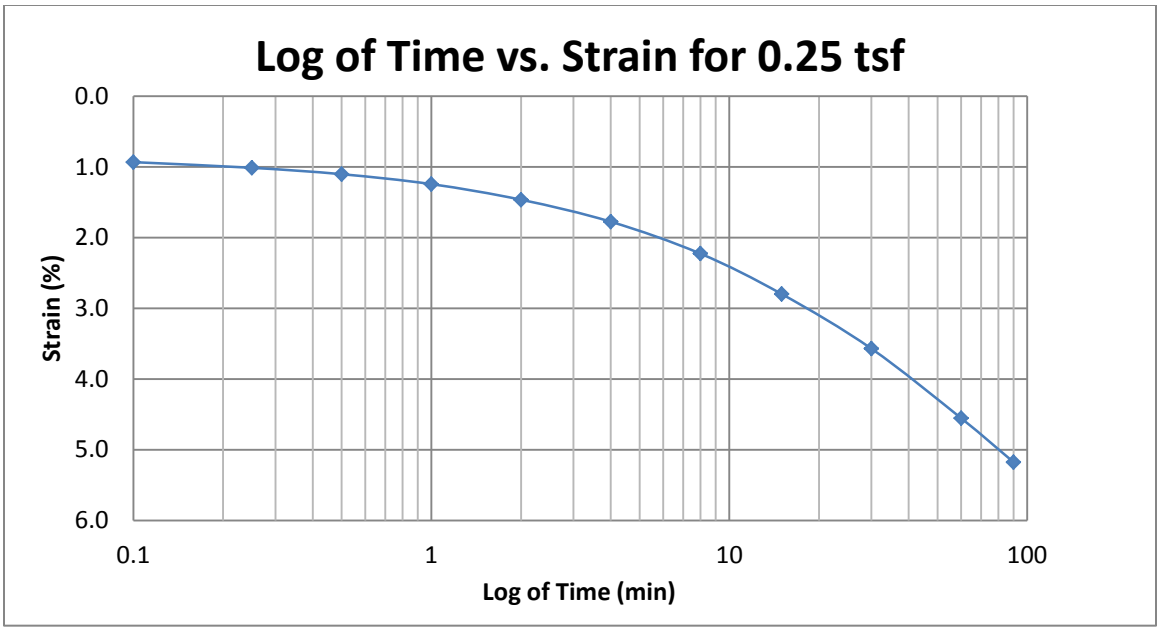

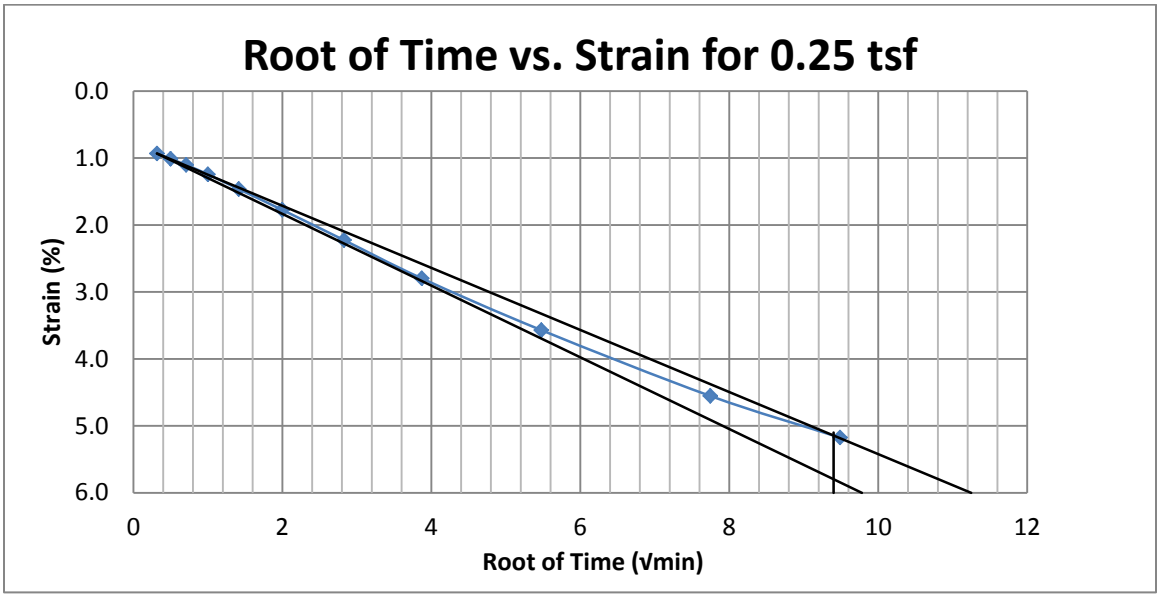

A70 400 South at 40-42 feet

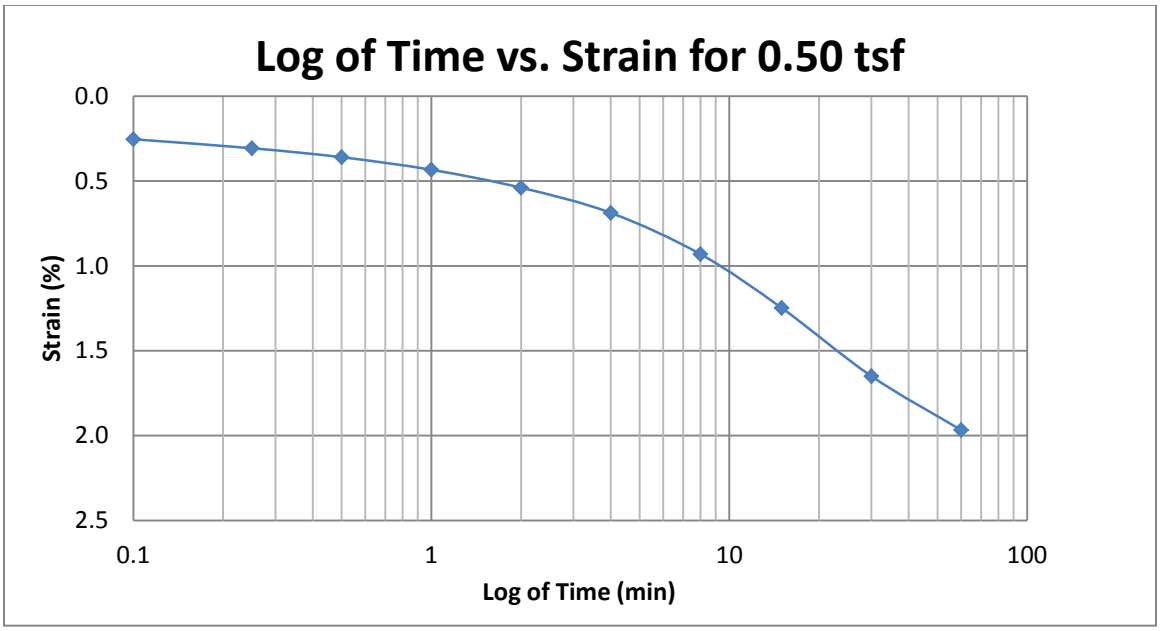

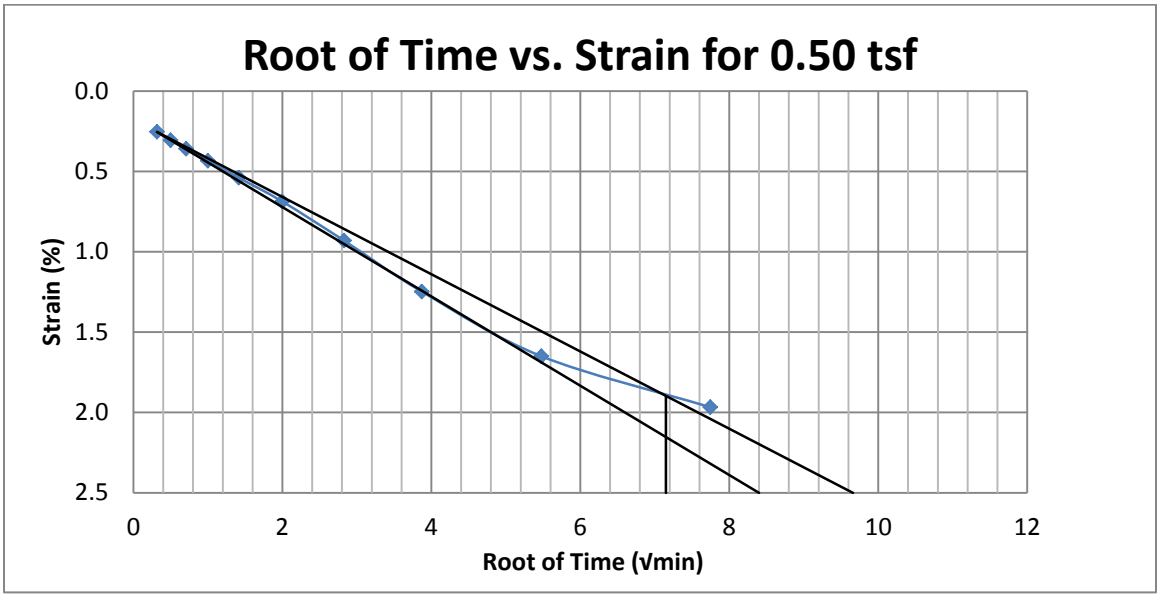

A71 400 South at 40-42 feet

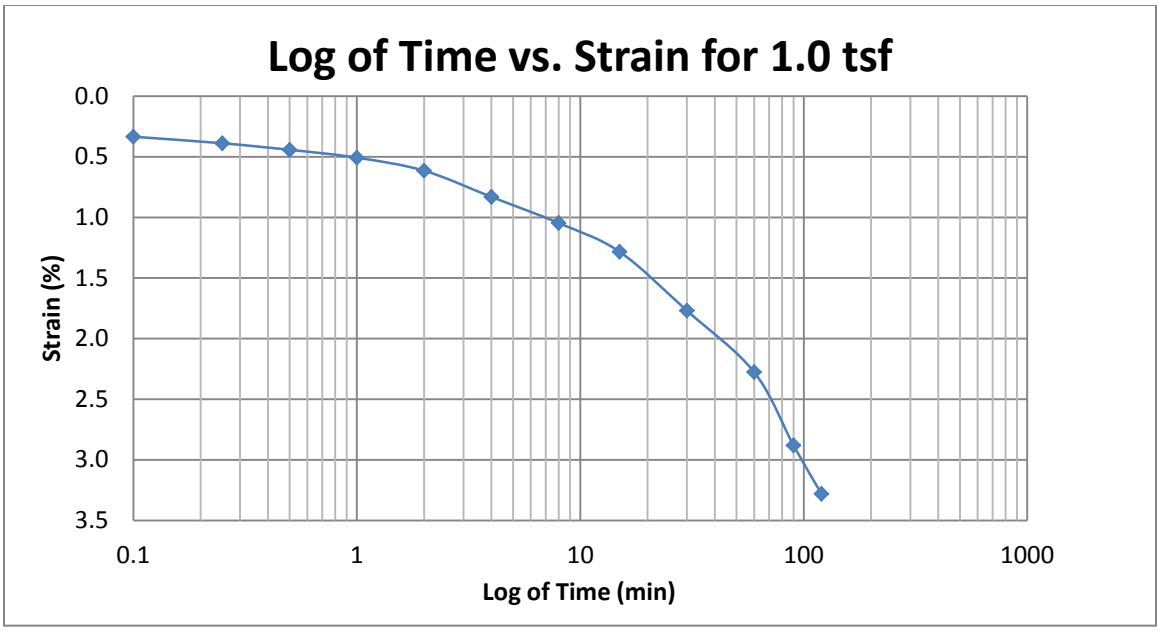

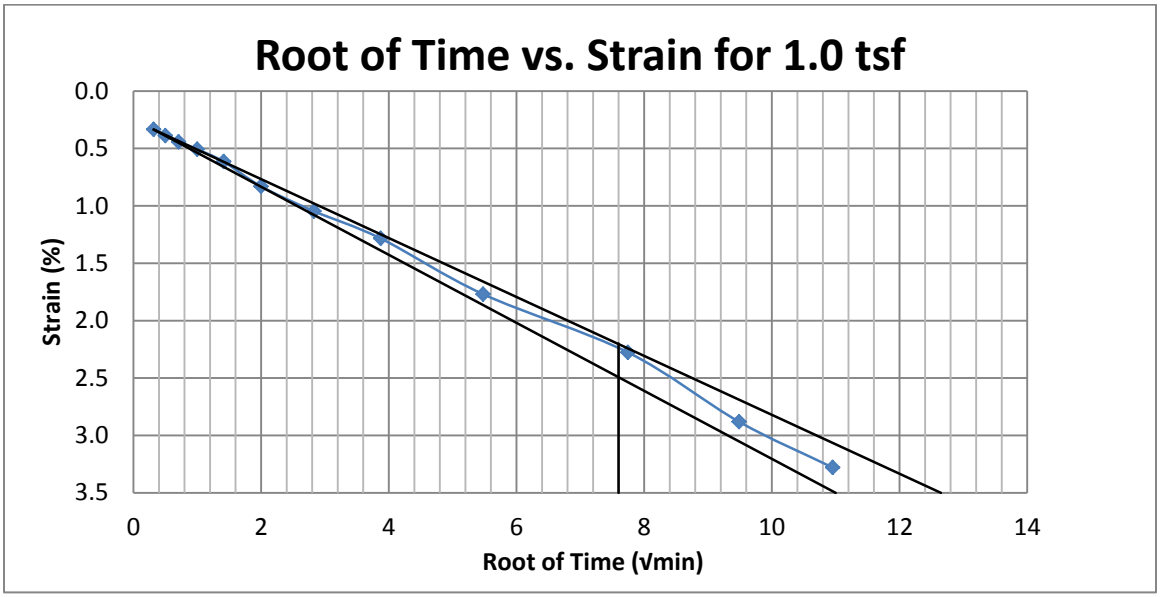

A72 400 South at 40-42 feet

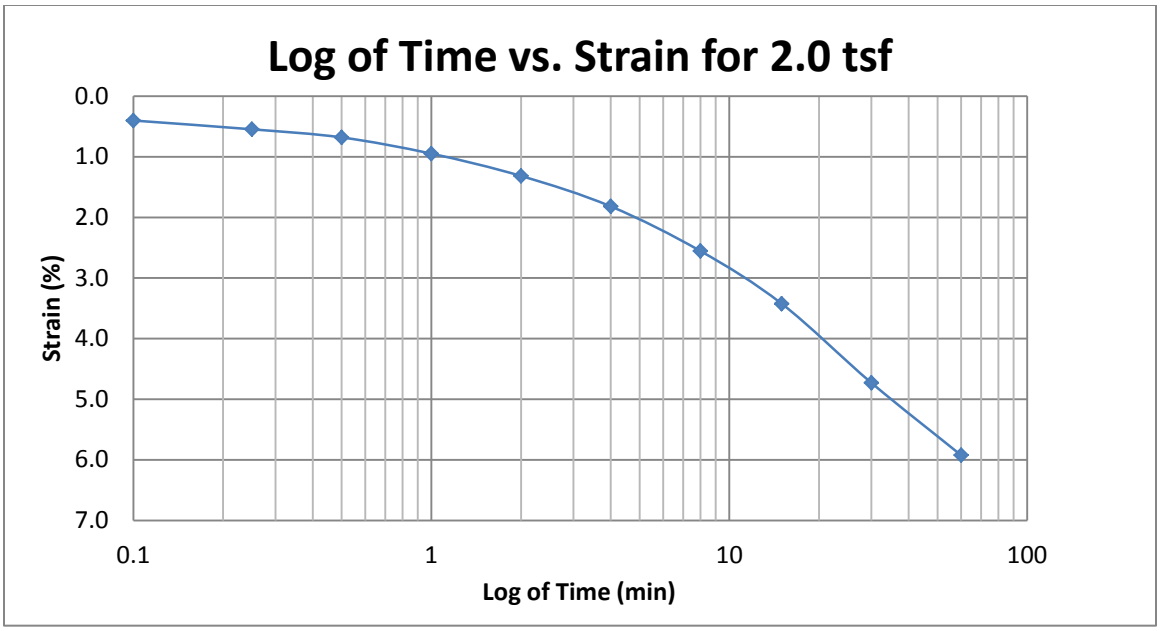

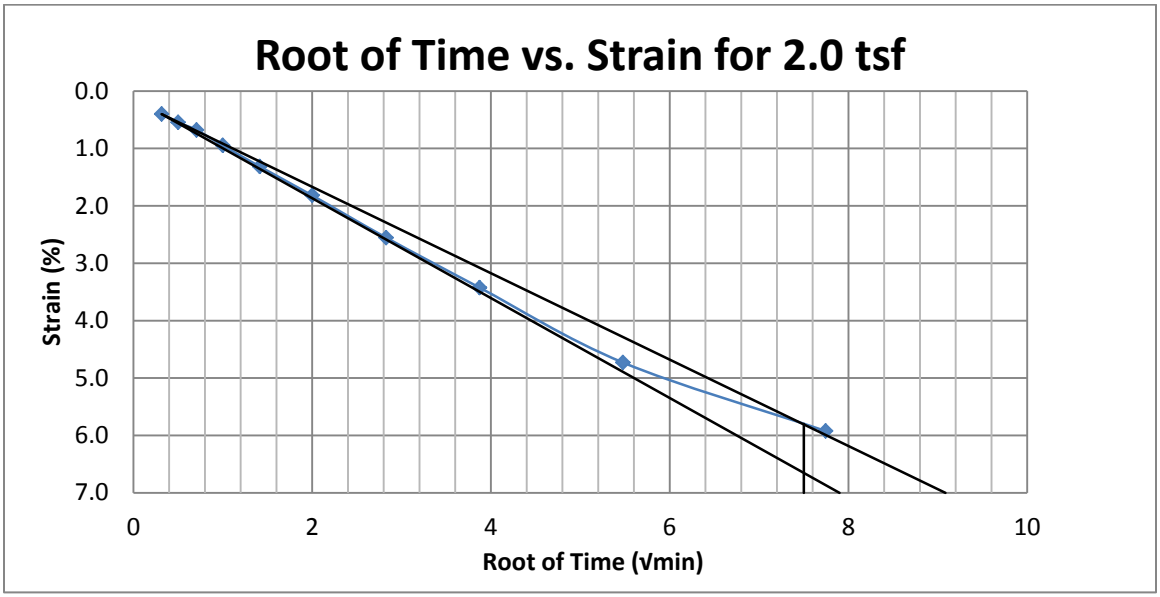

A73 400 South at 40-42 feet

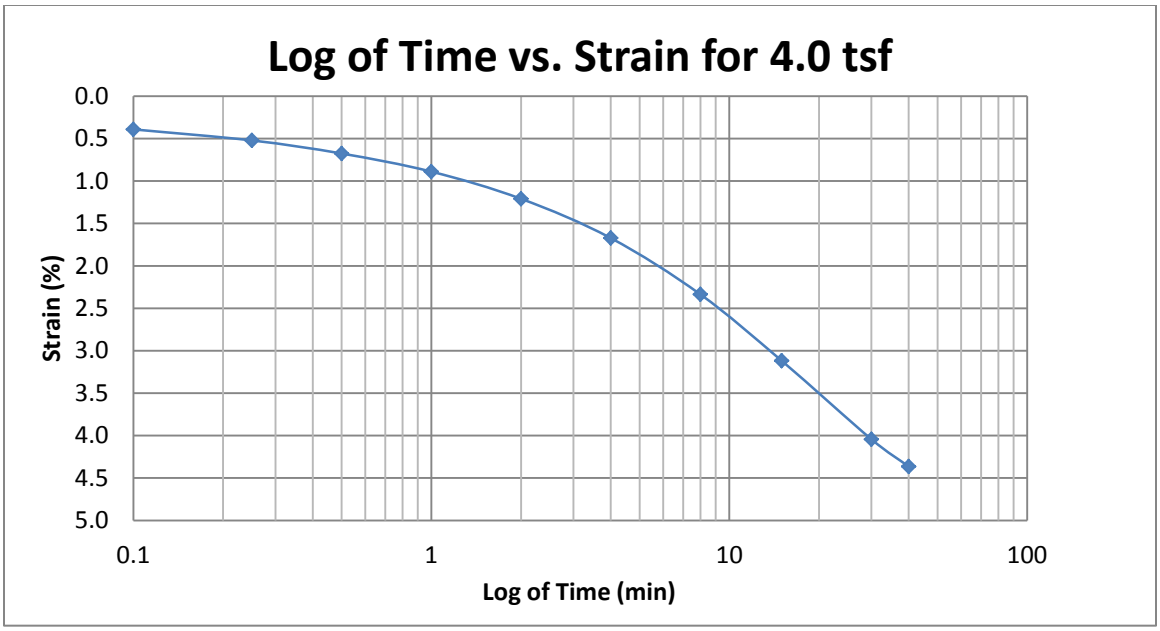

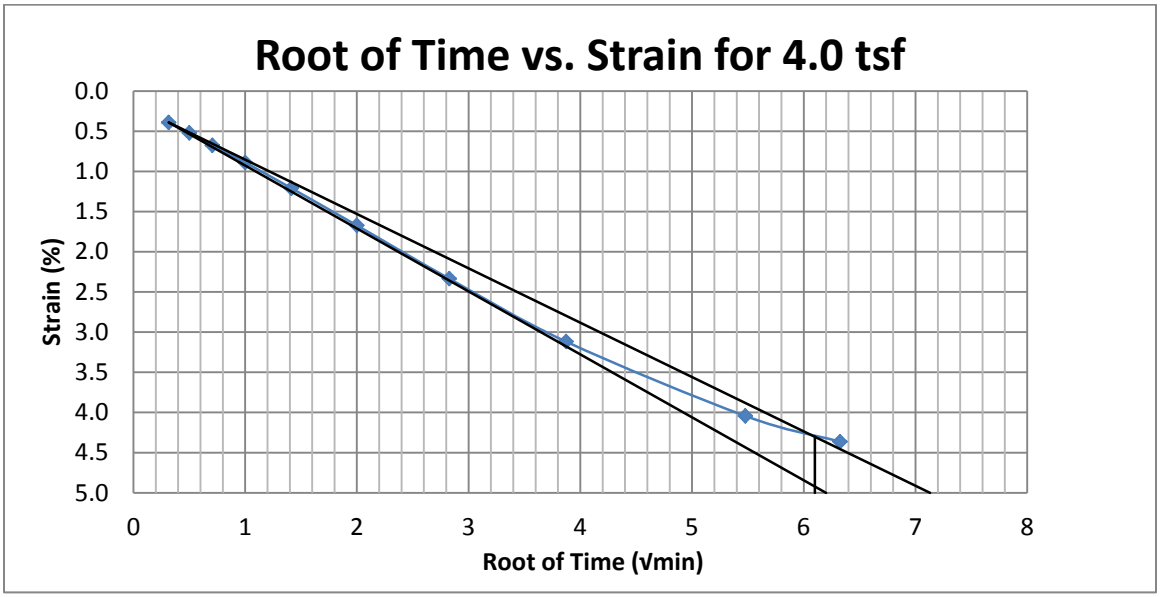

A 74 400 South at 40-42 feet

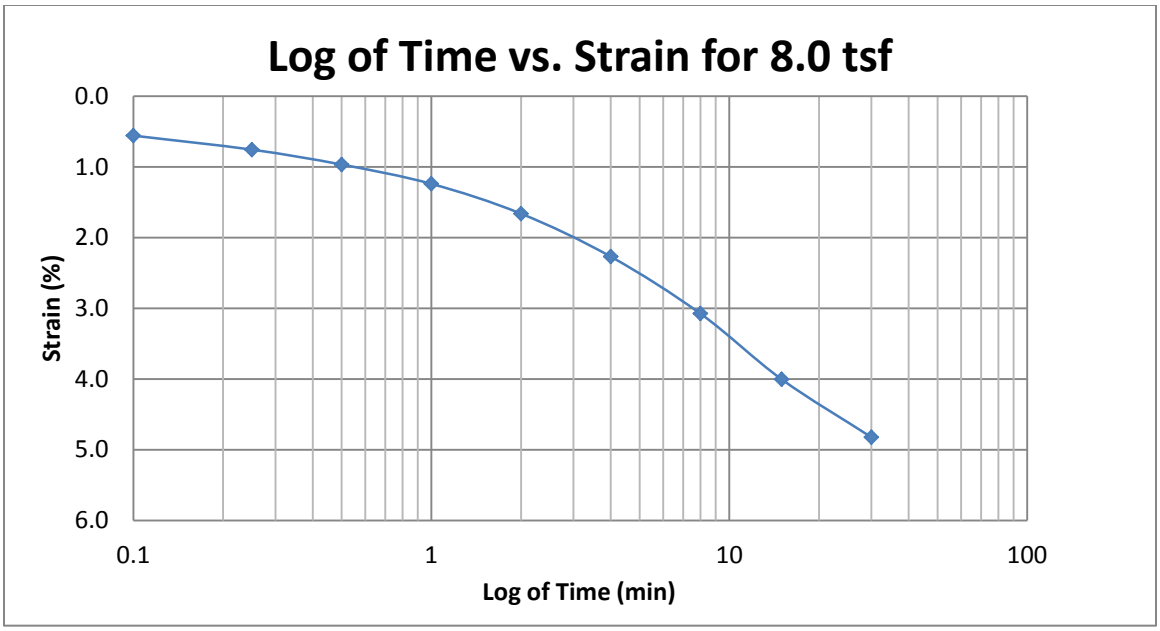

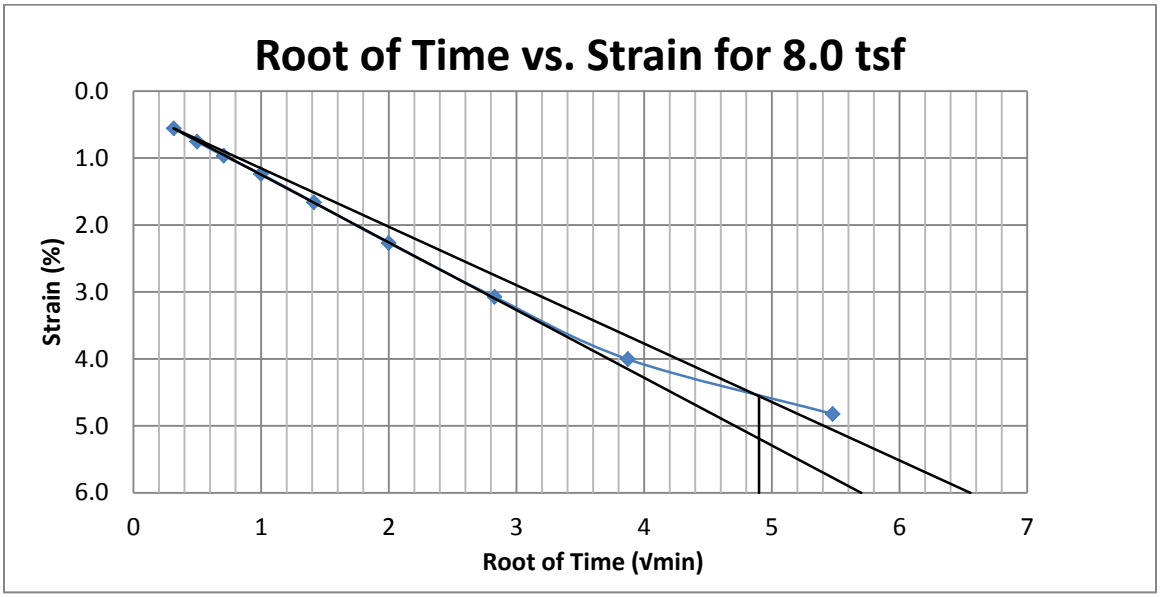

A 75 400 South at 40-42 feet

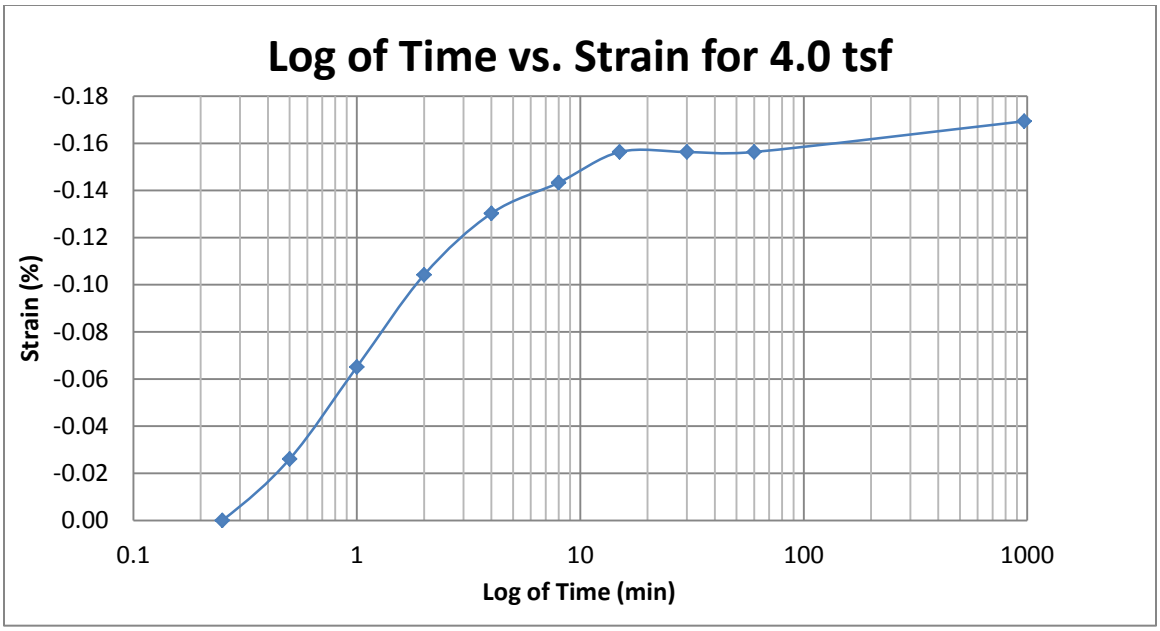

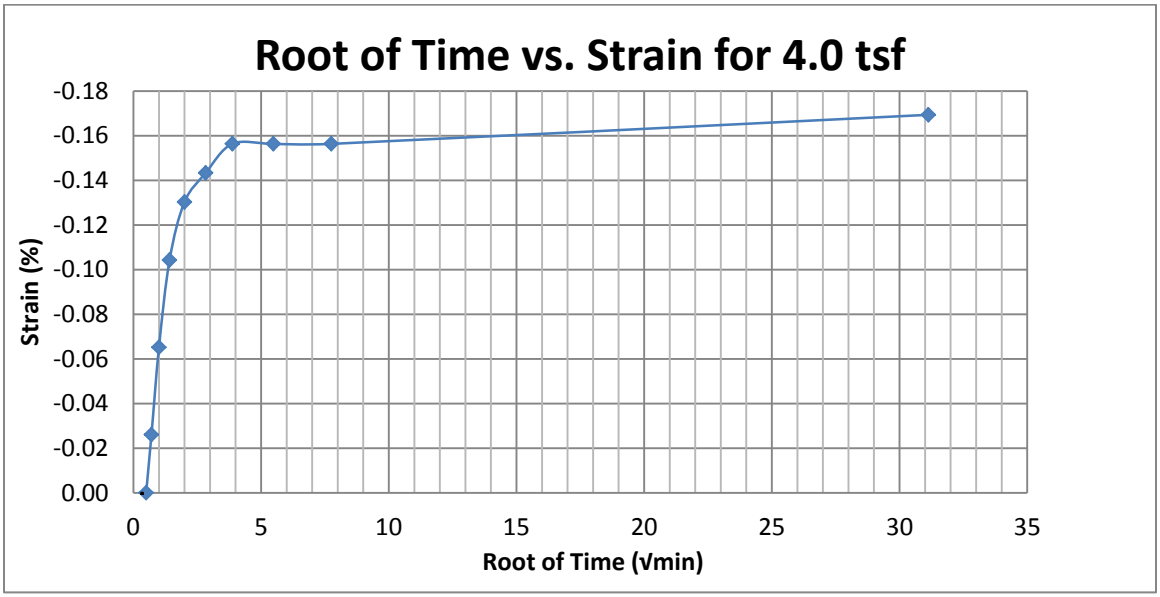

A 76 400 South at 40-42 feet

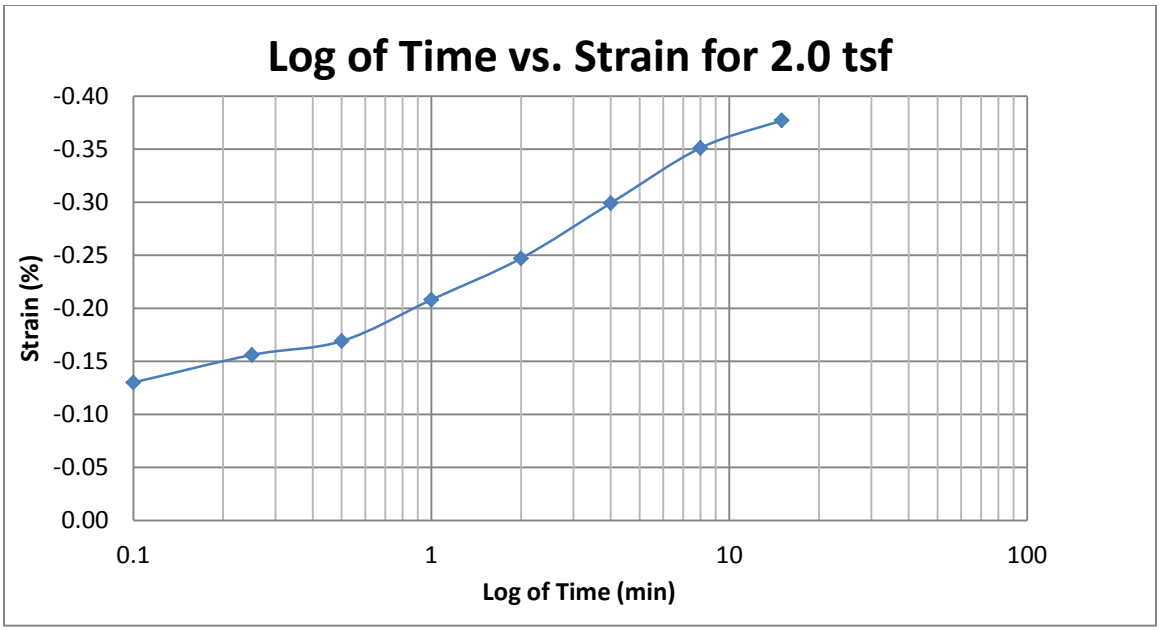

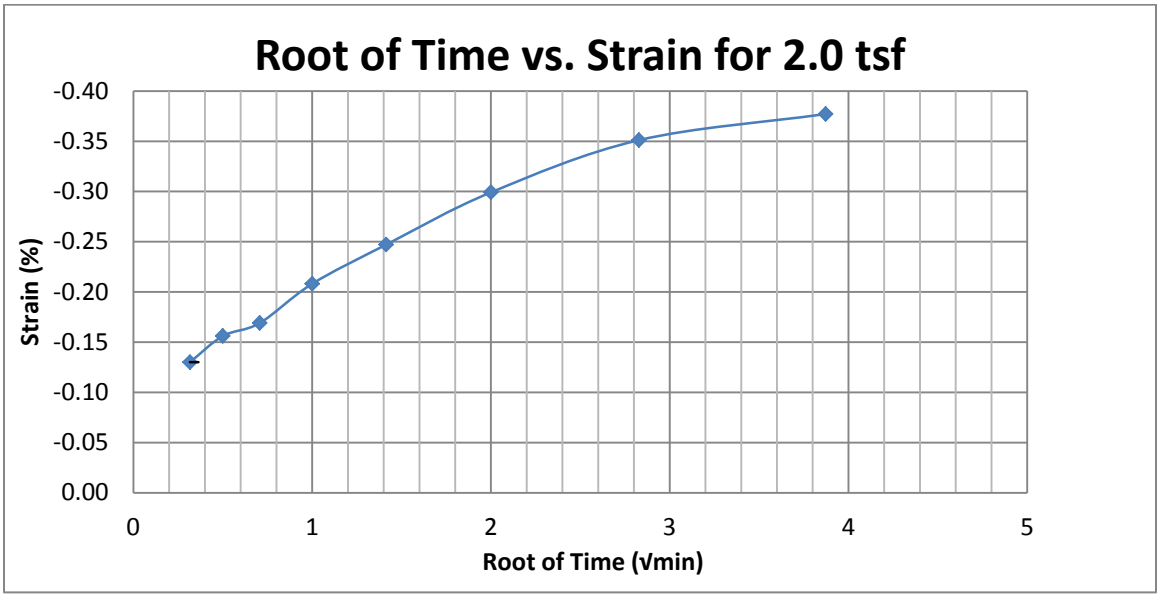

A 77 400 South at 40-42 feet

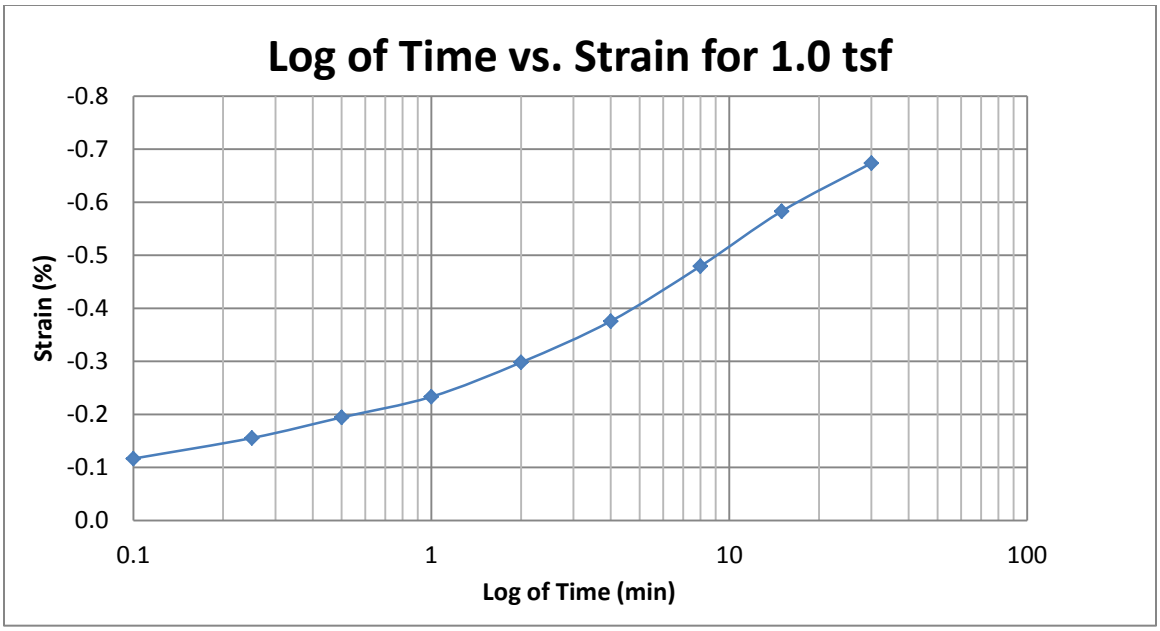

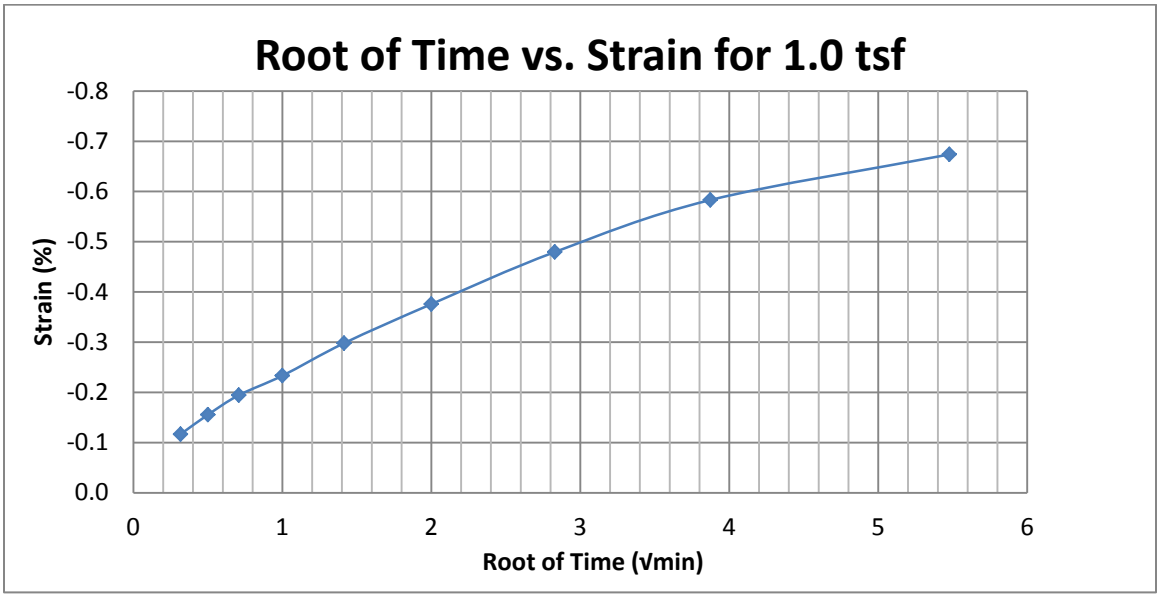

A 78 400 South at 40-42 feet

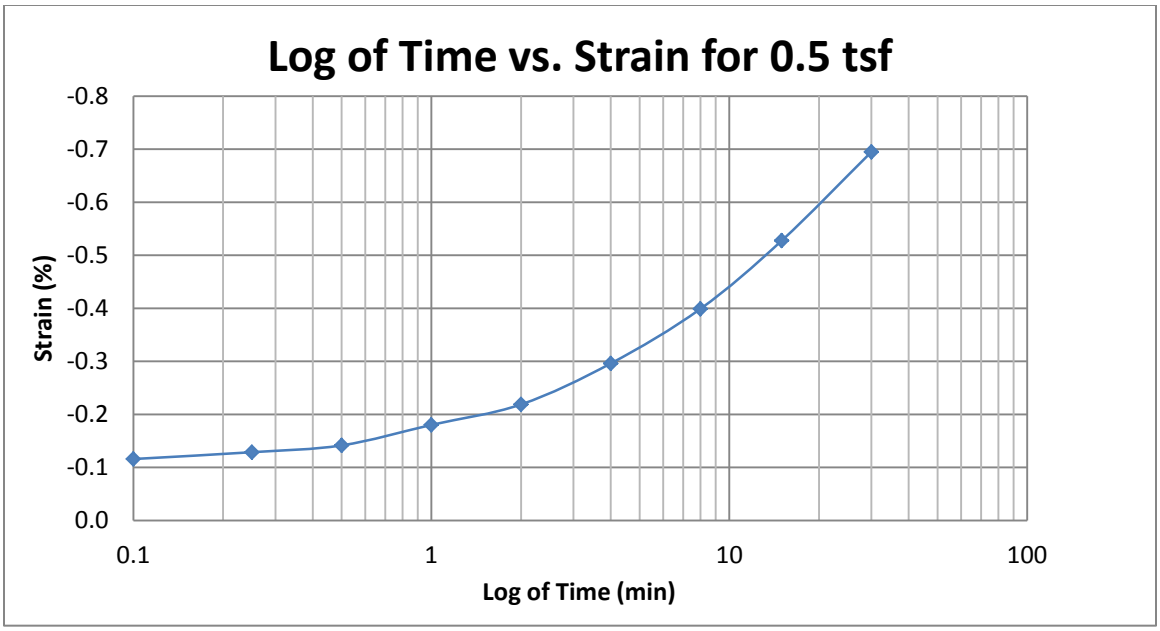

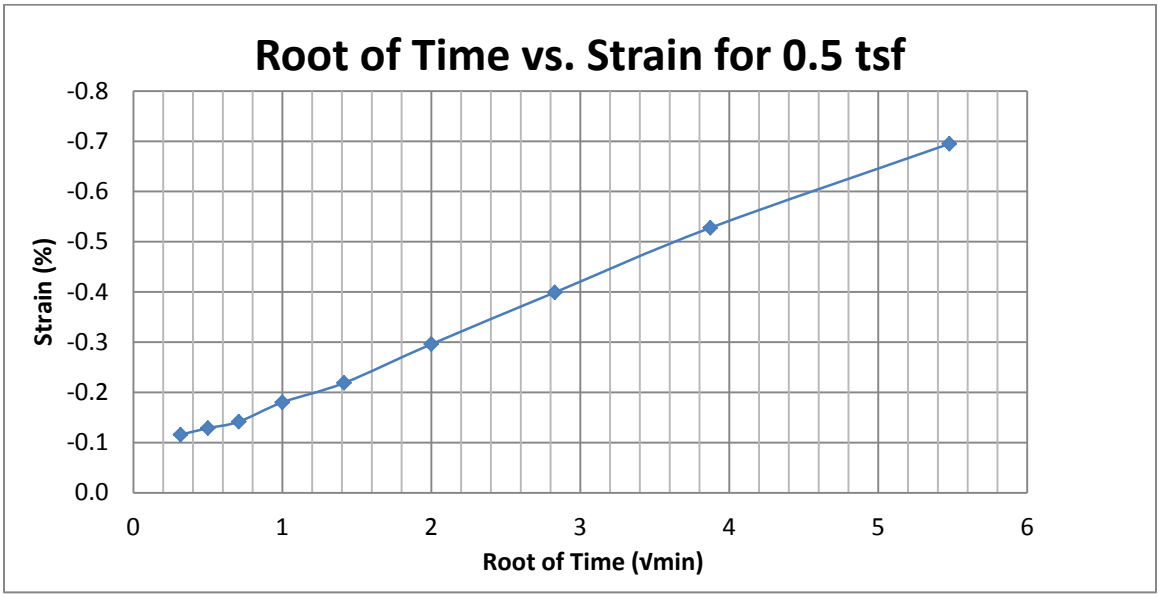

A 79 400 South at 40-42 feet

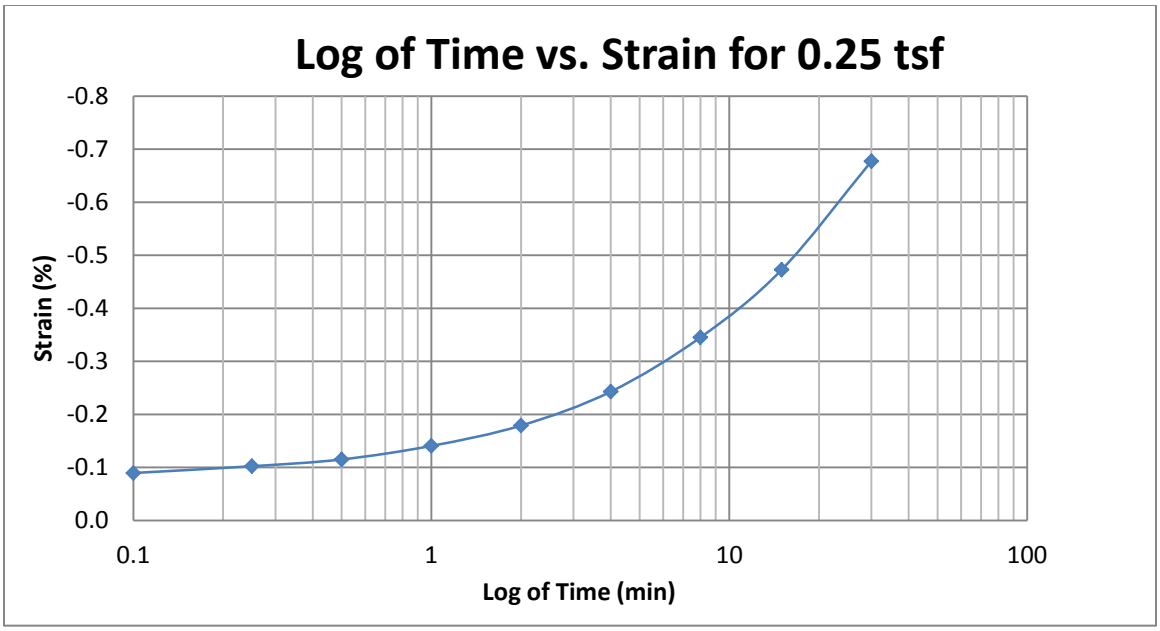

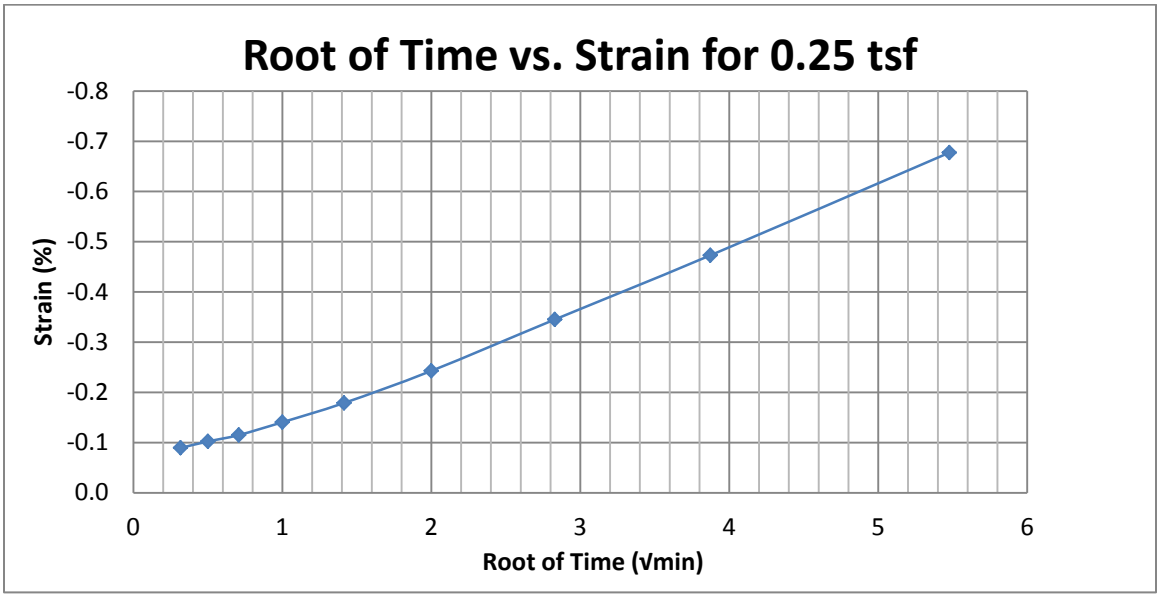

A 80 400 South at 40-42 feet

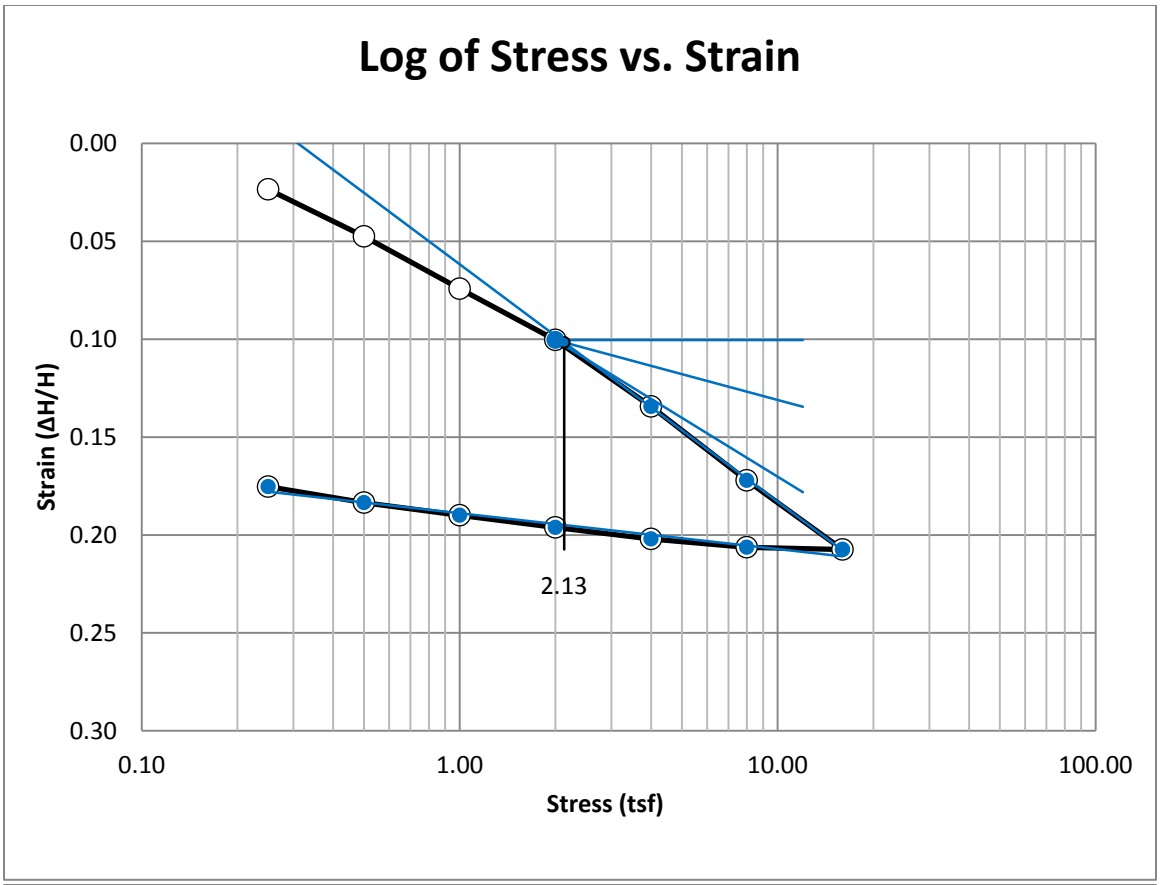

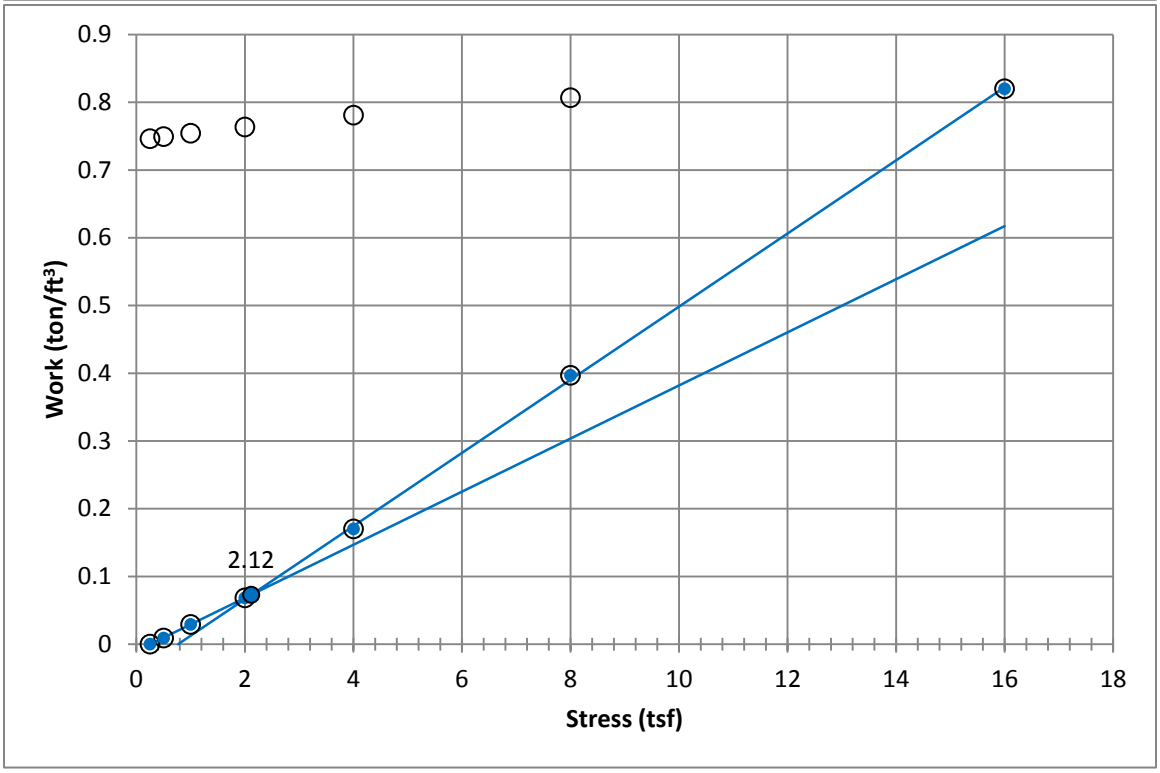

A81 400 South at 45-47 feet

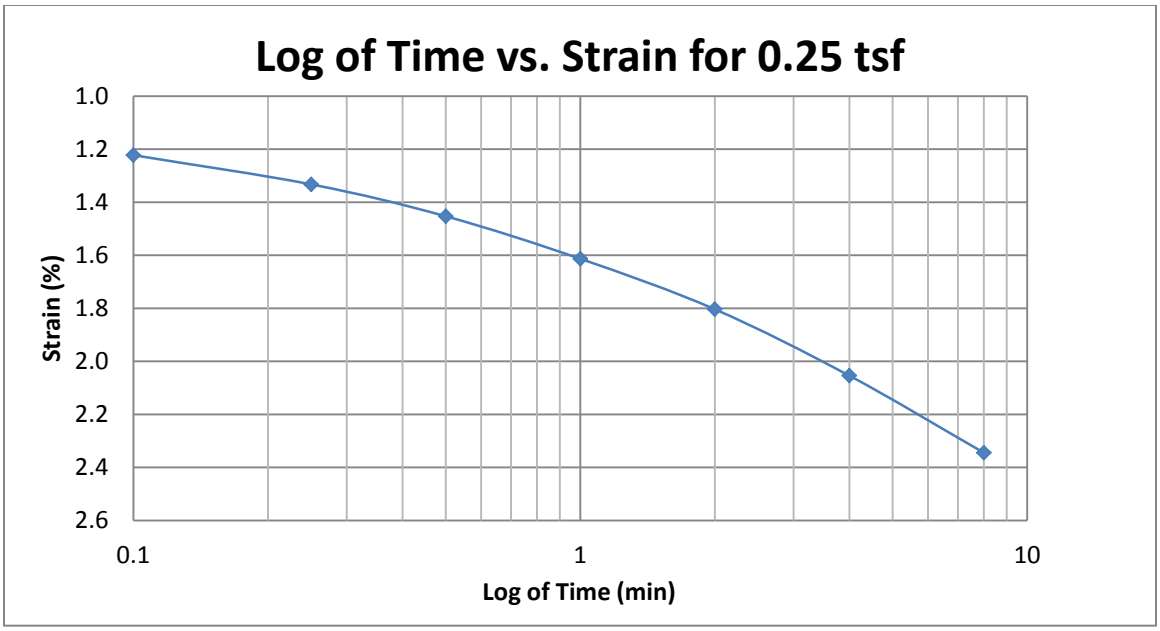

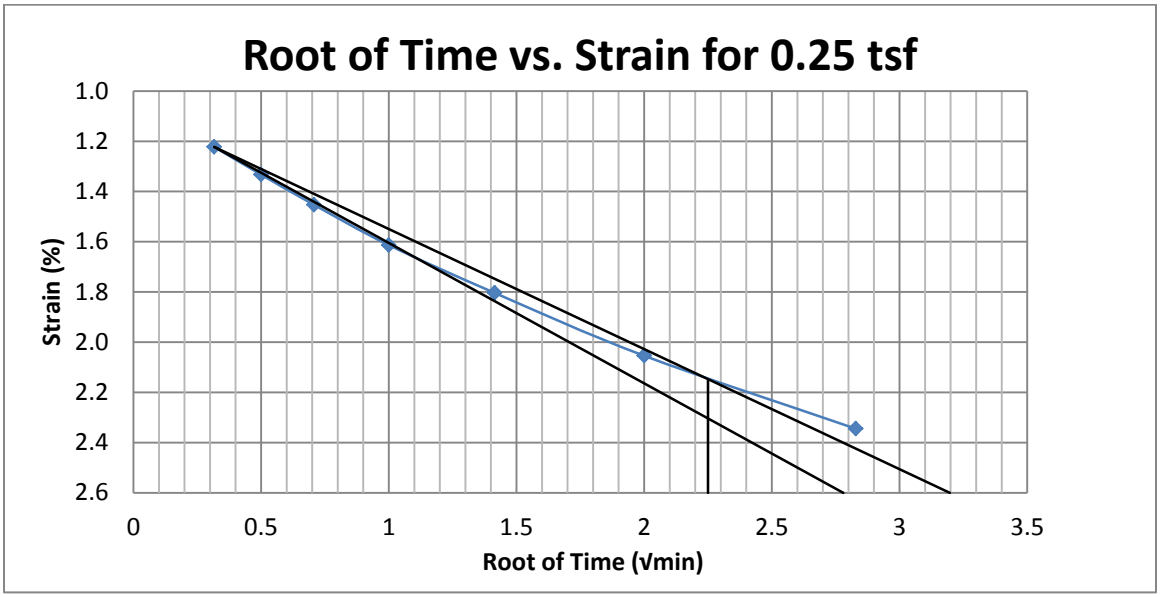

A 82 400 South at 45-47 feet

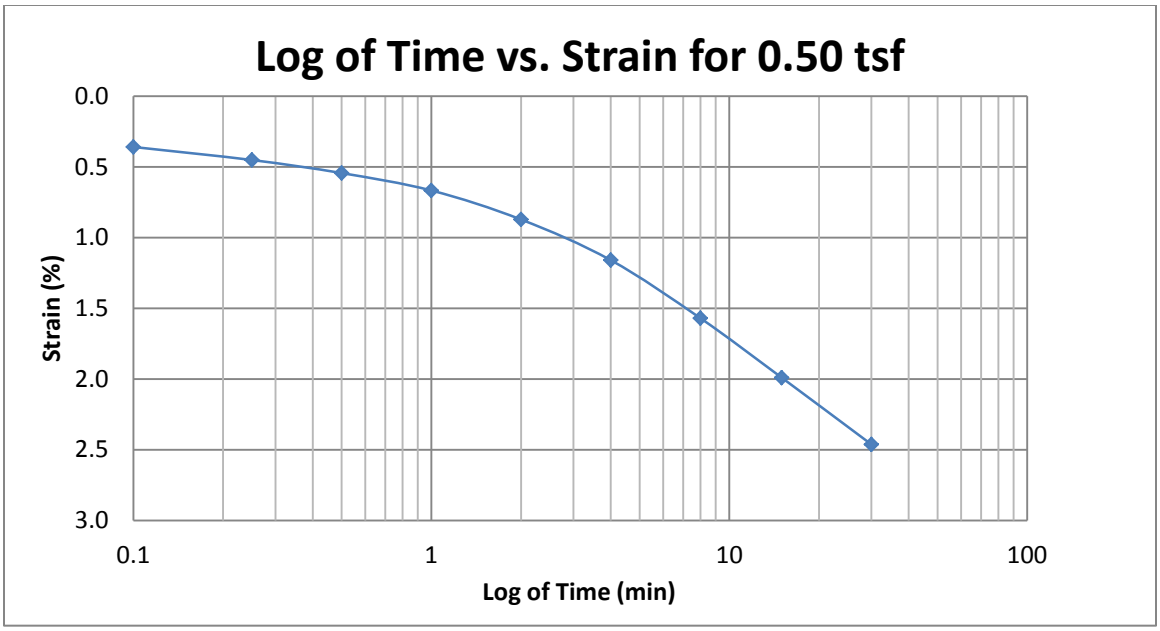

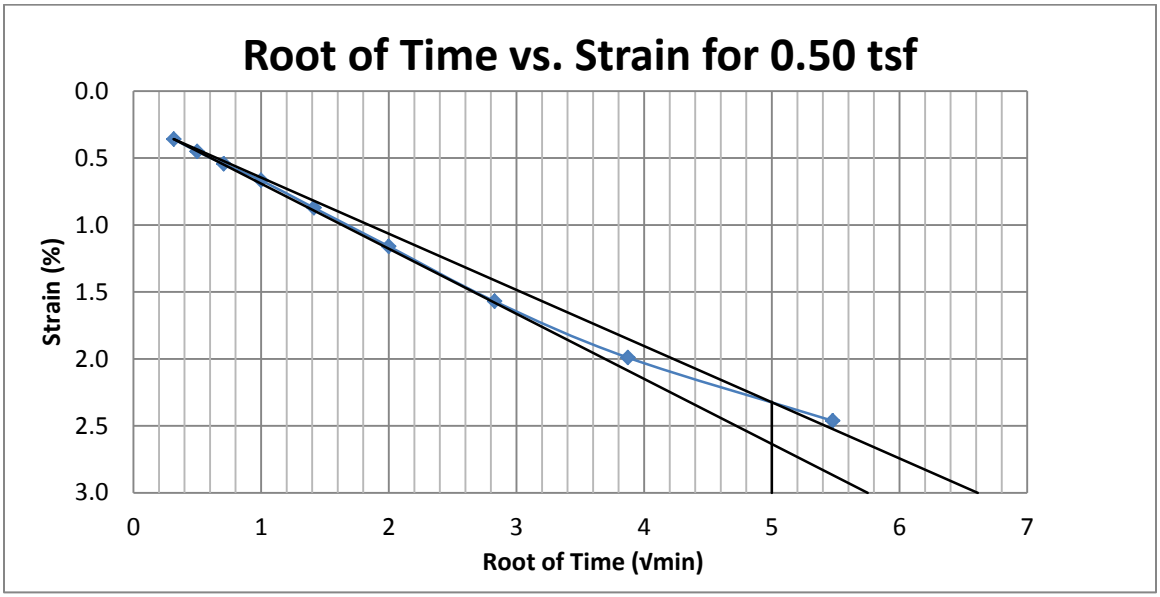

A 83 400 South at 45-47 feet

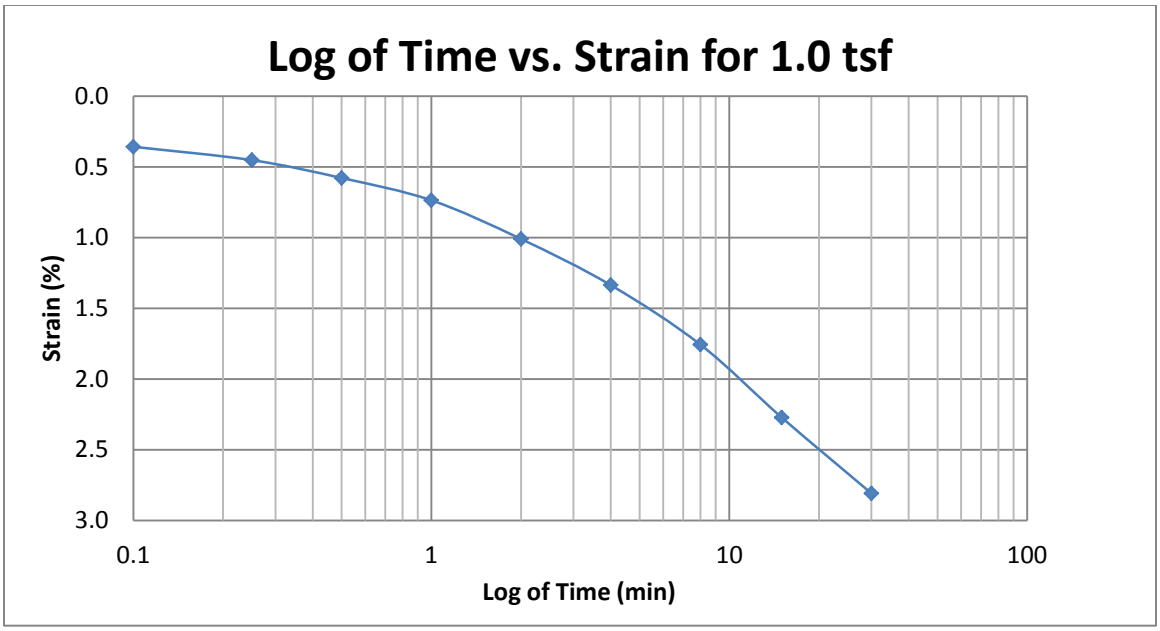

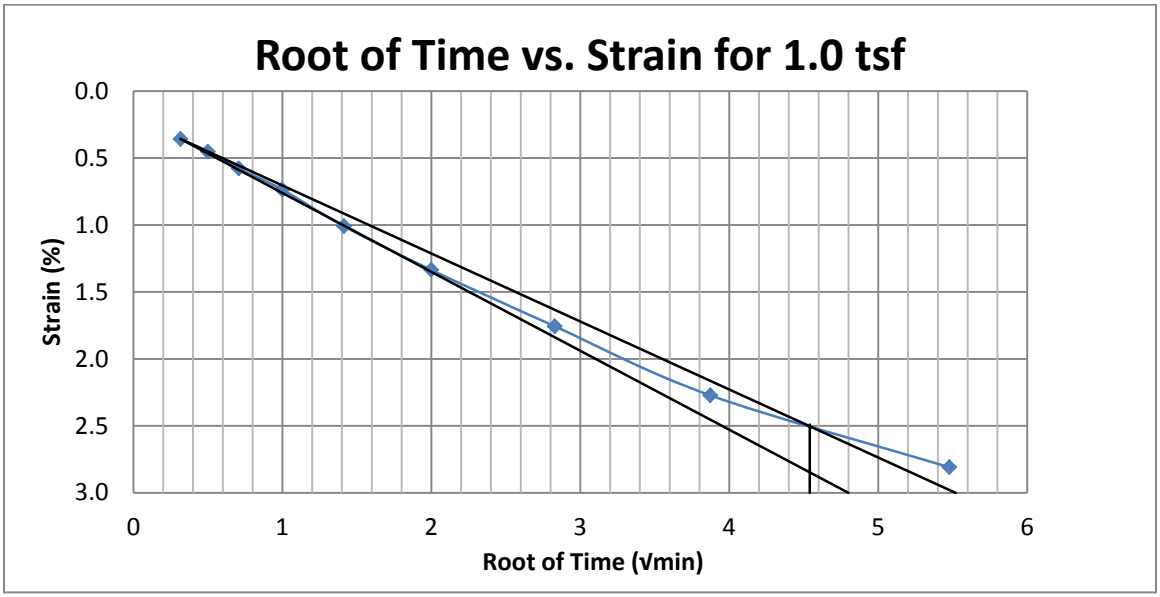

A 84 400 South at 45-47 feet

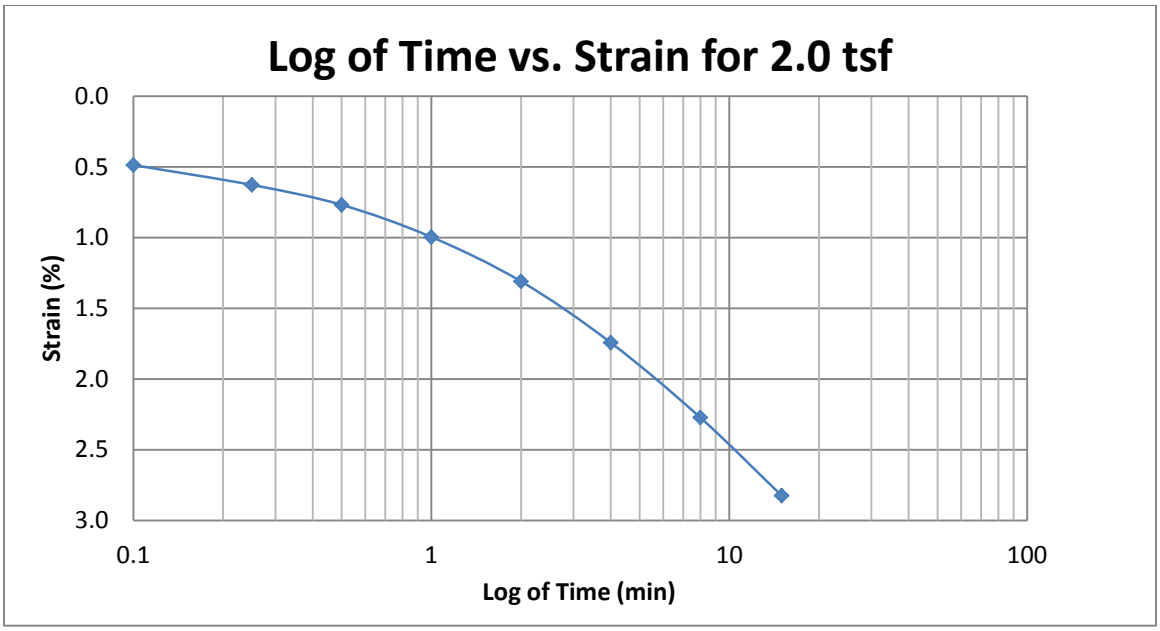

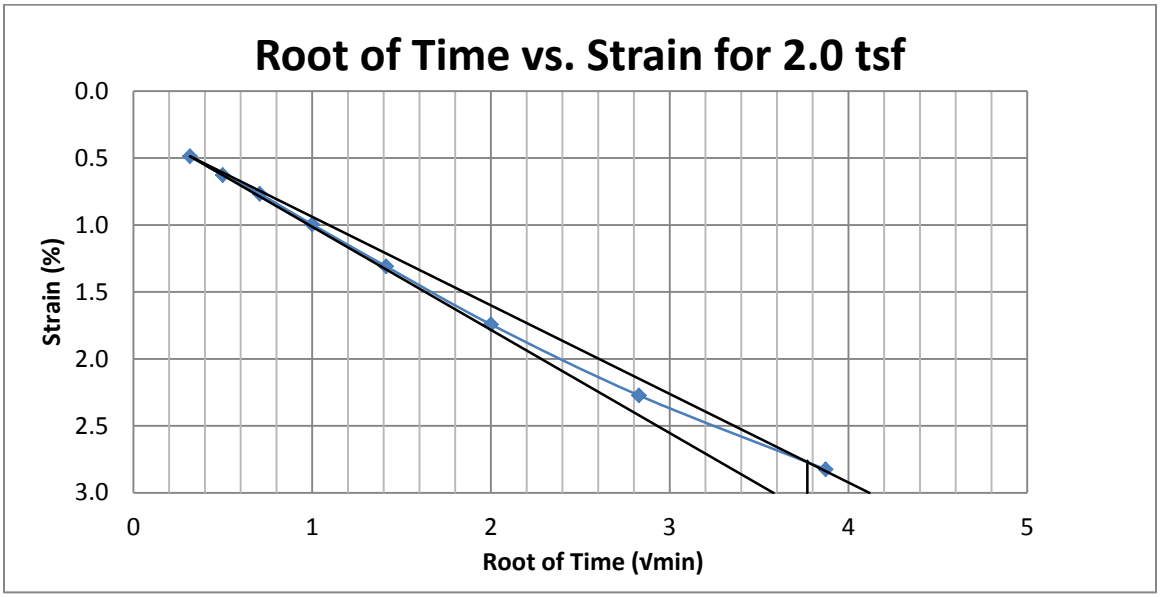

A 85 400 South at 45-47 feet

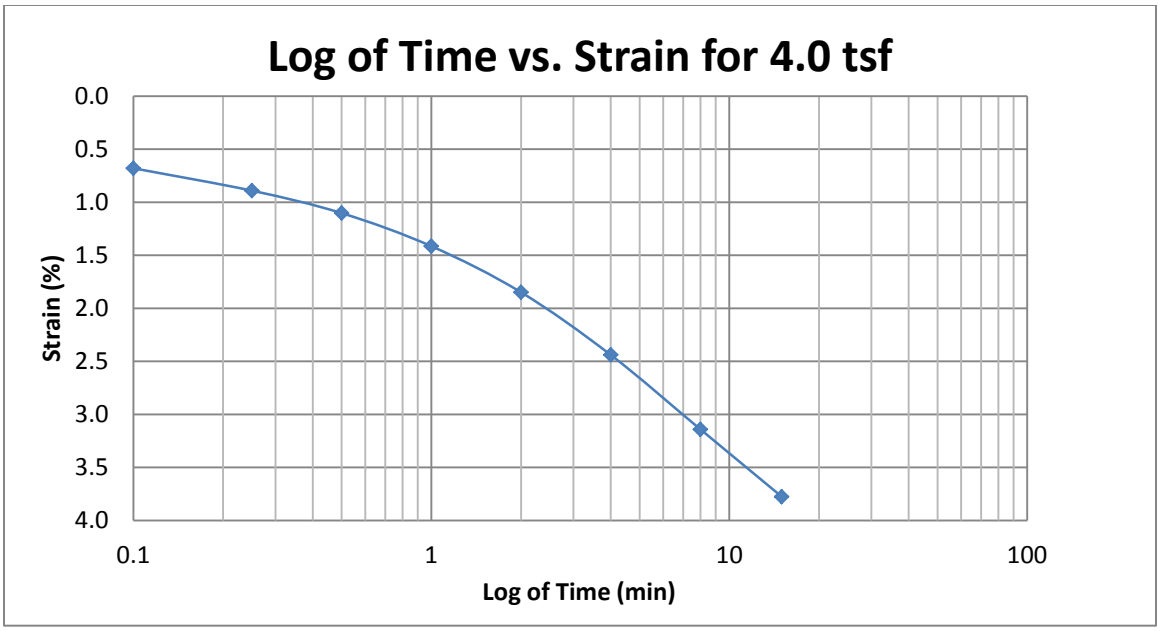

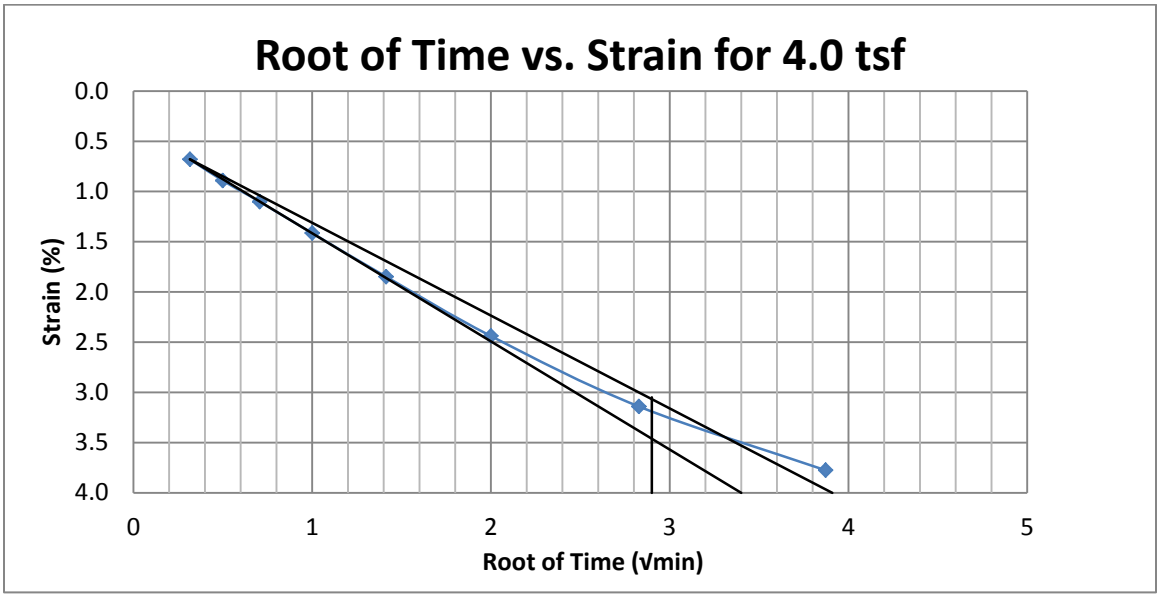

A 86 400 South at 45-47 feet

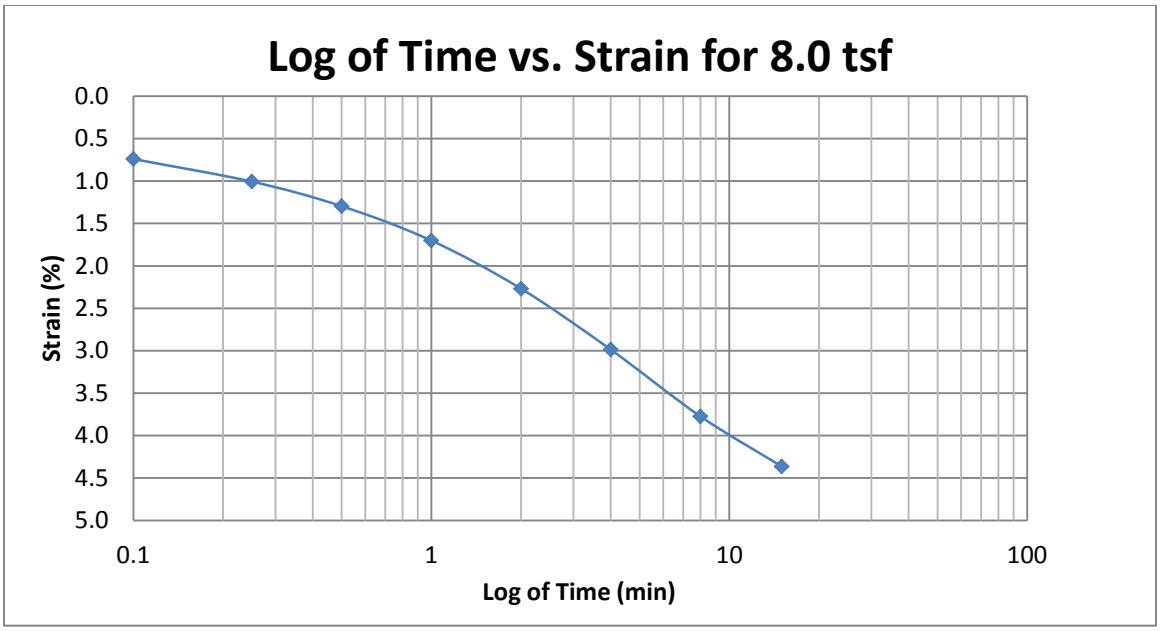

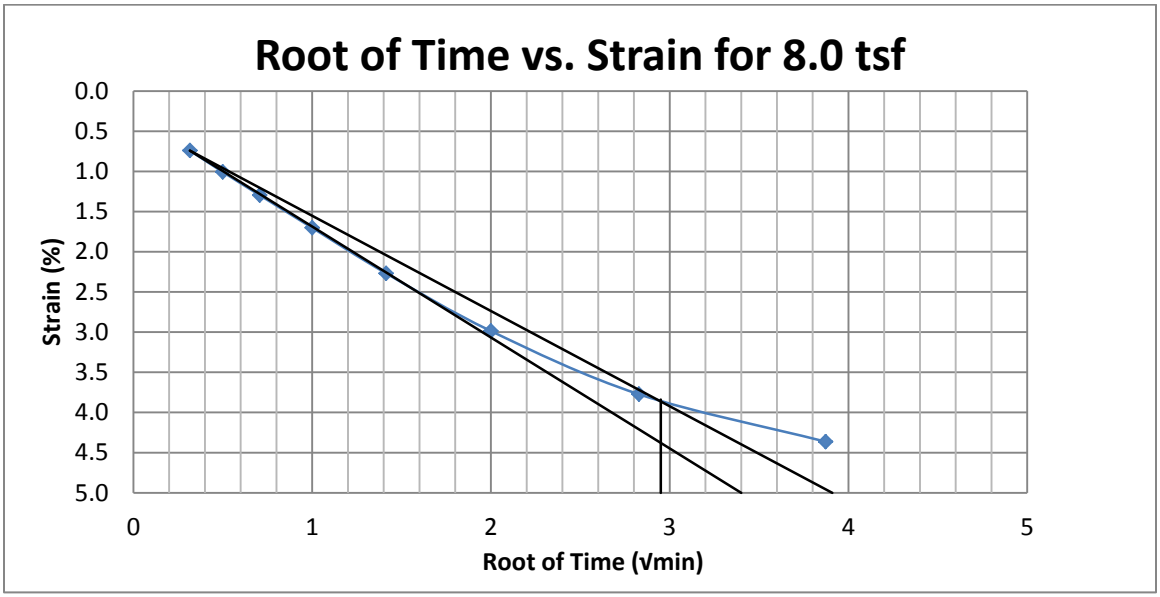

A 87 400 South at 45-47 feet

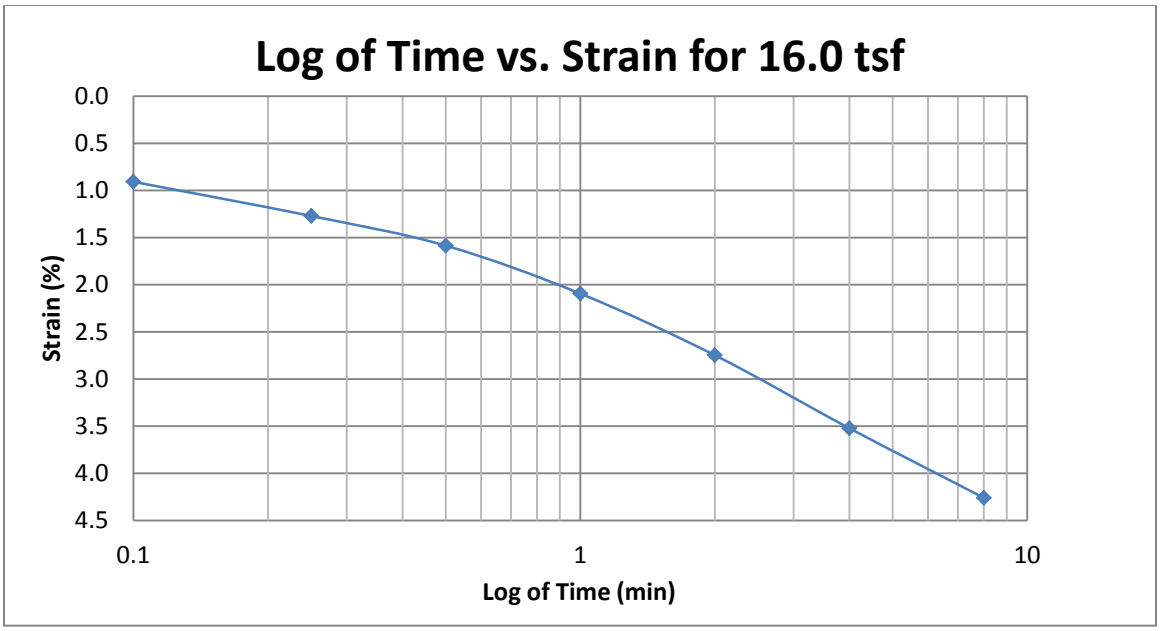

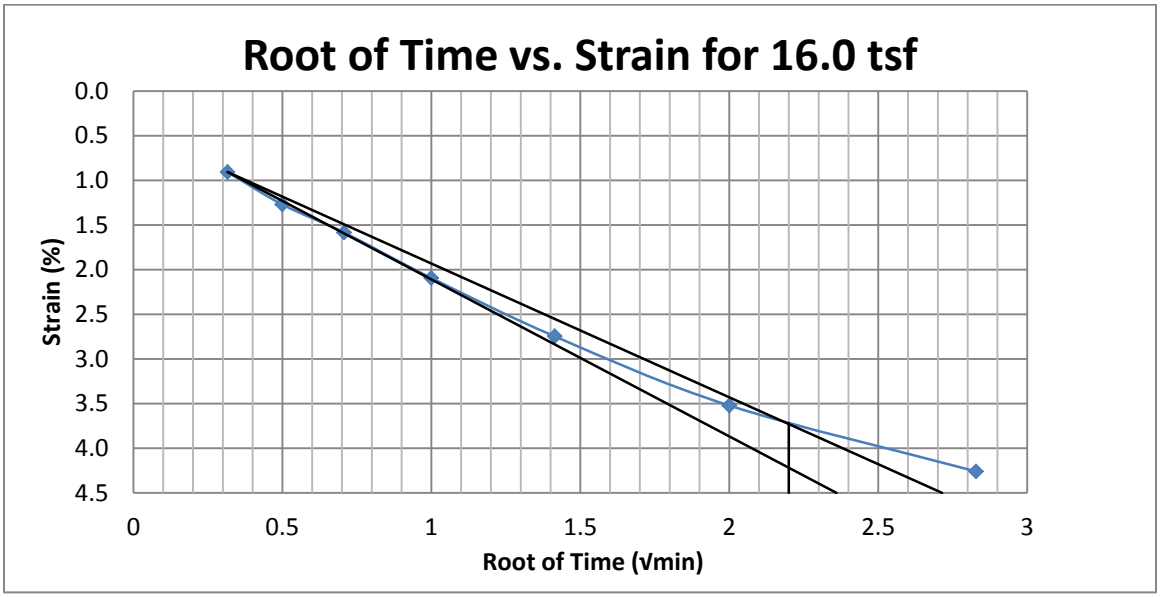

A 88 400 South at 45-47 feet

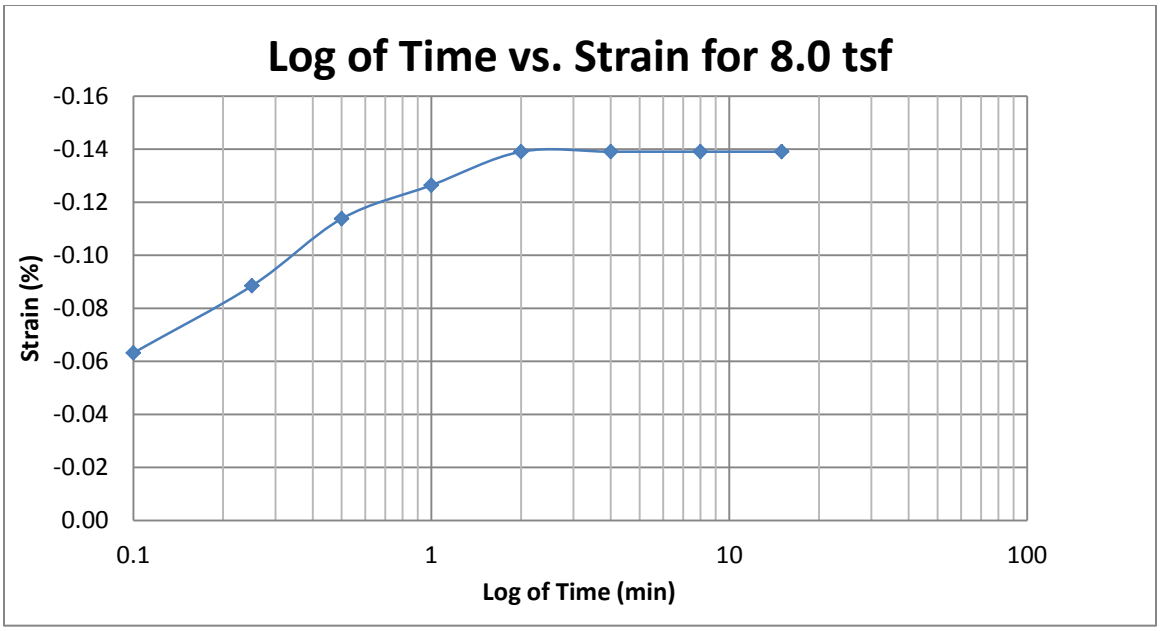

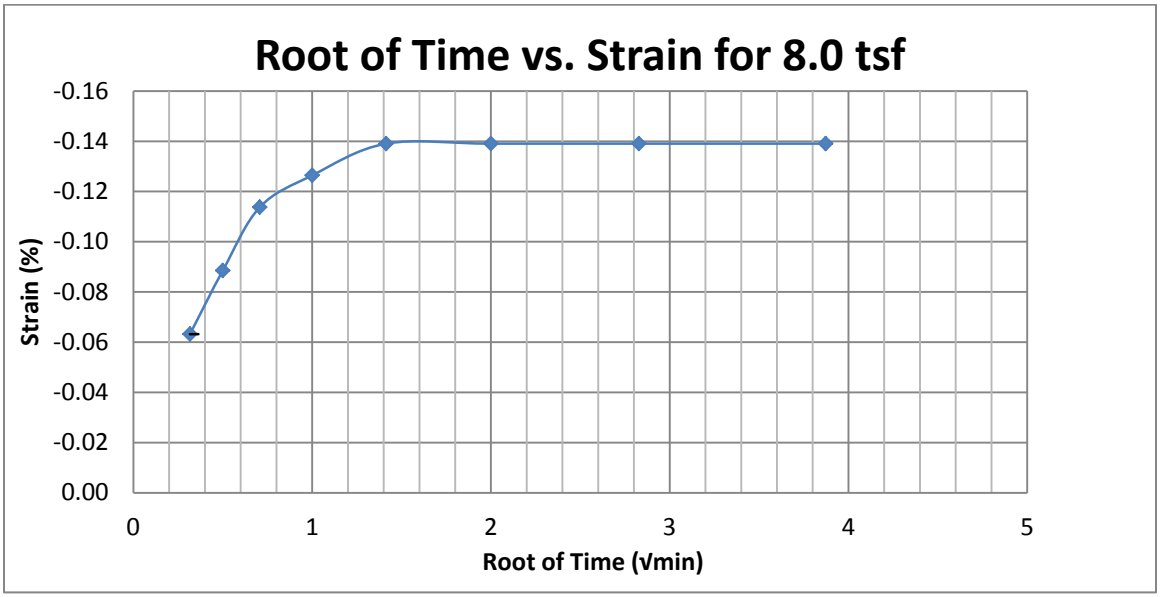

A 89 400 South at 45-47 feet

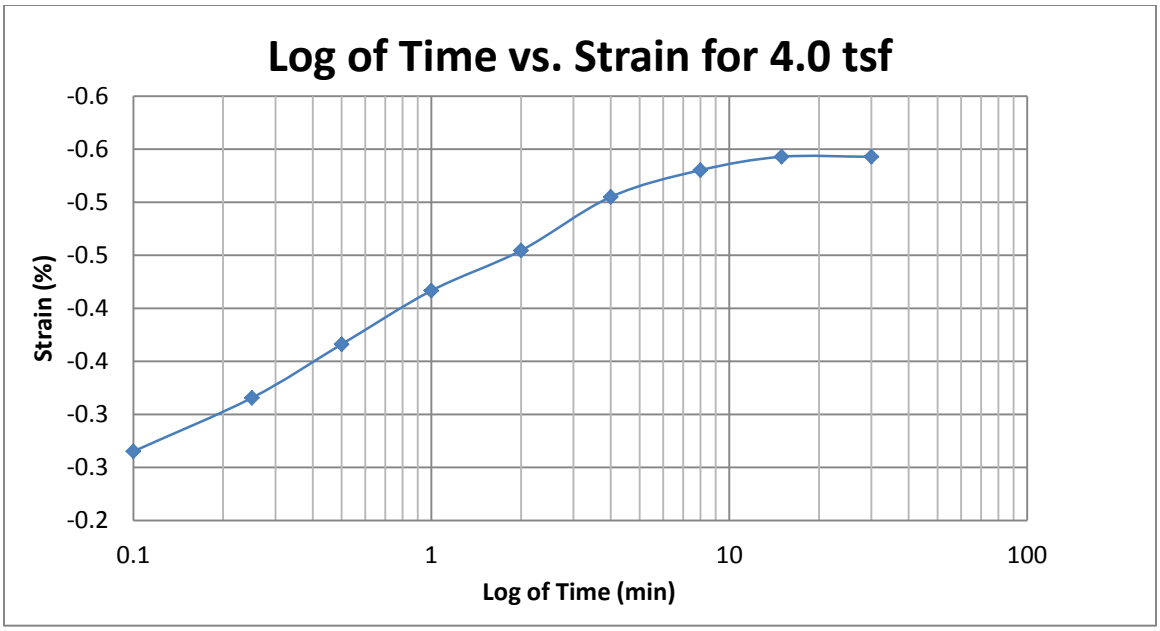

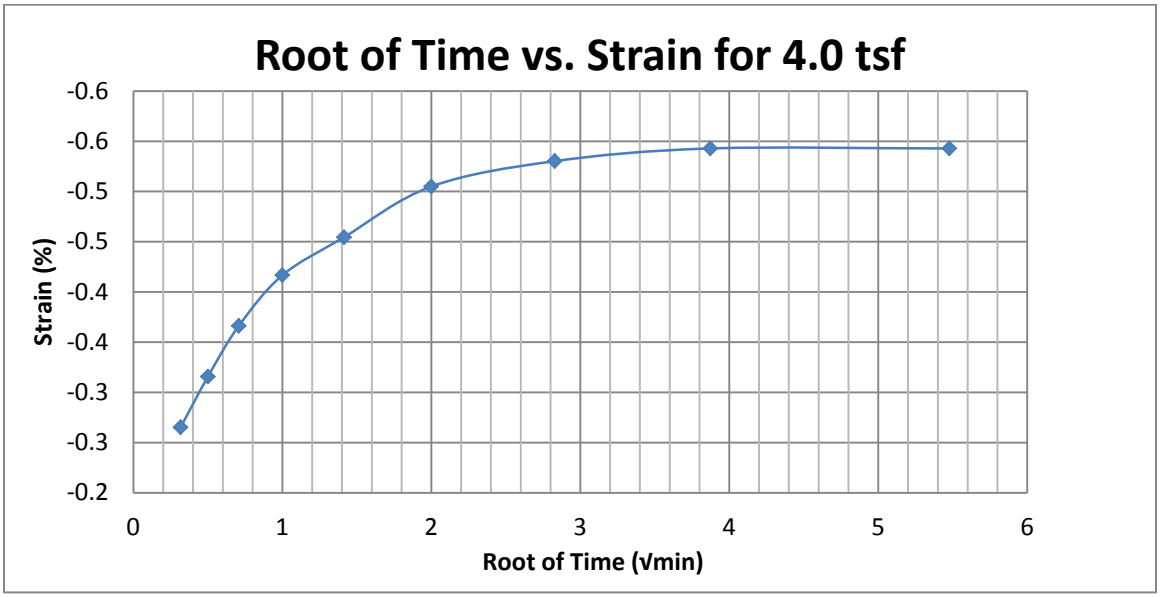

A 90 400 South at 45-47 feet

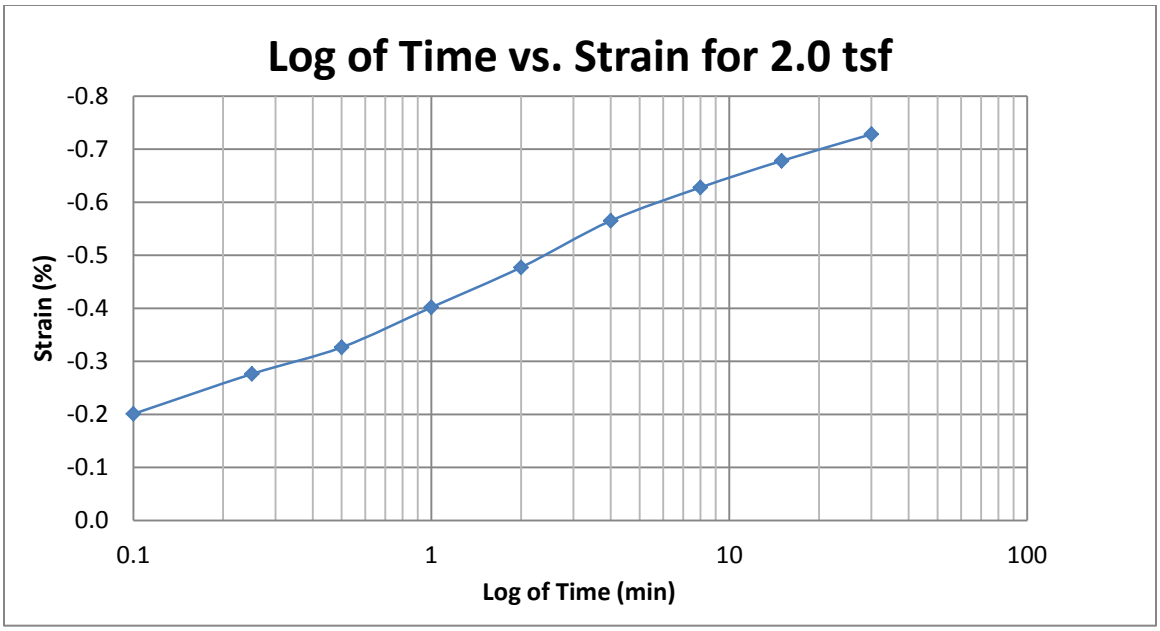

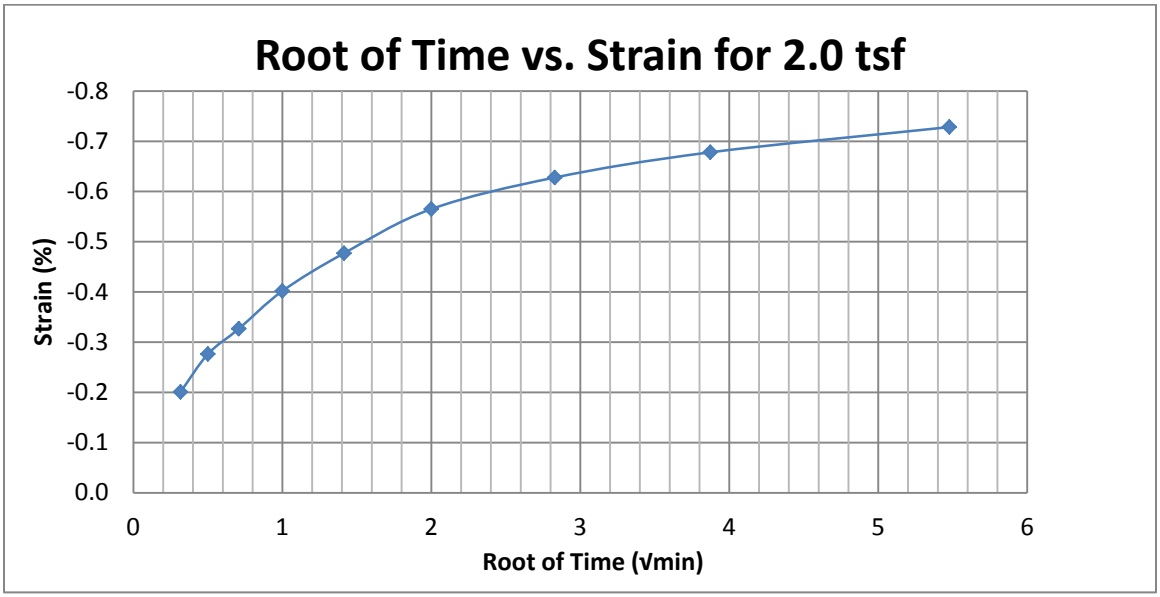

A 91 400 South at 45-47 feet

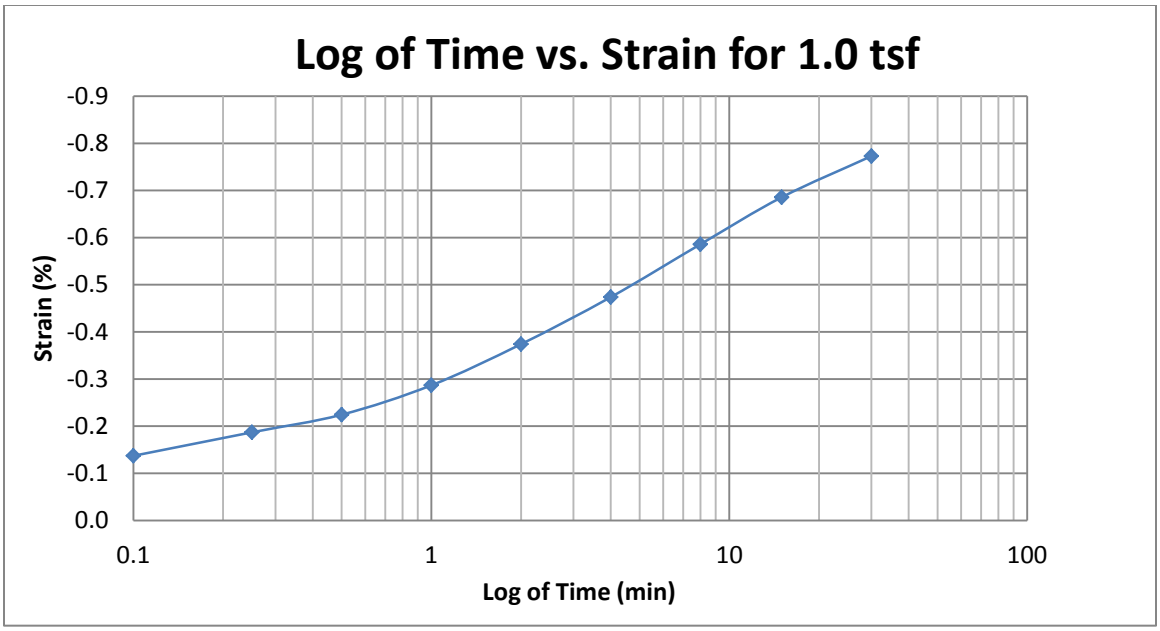

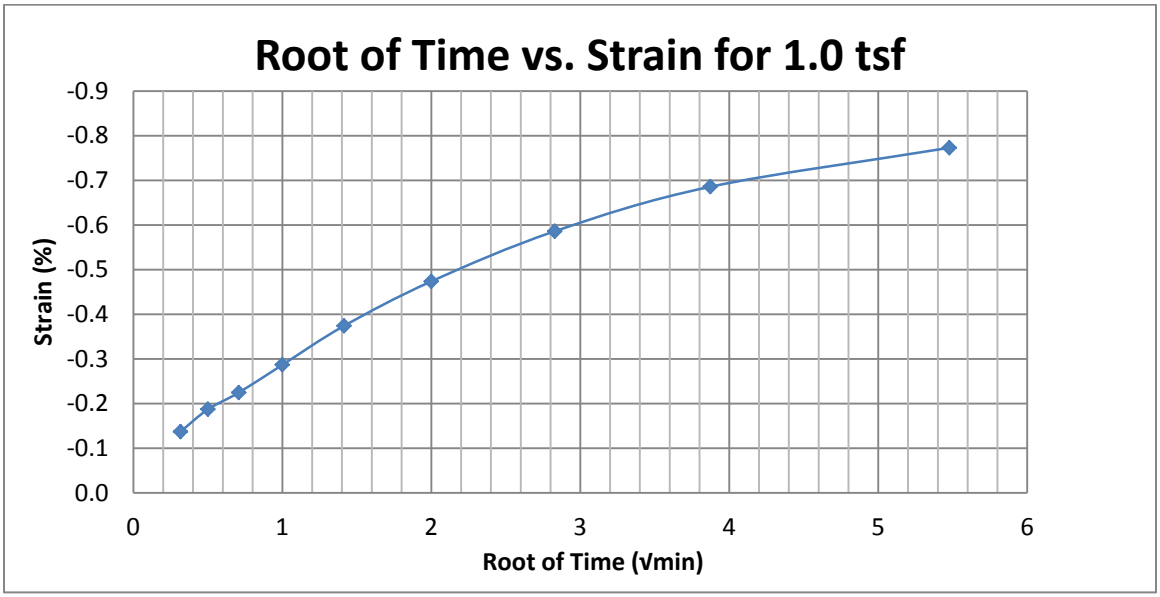

A 92 400 South at 45-47 feet

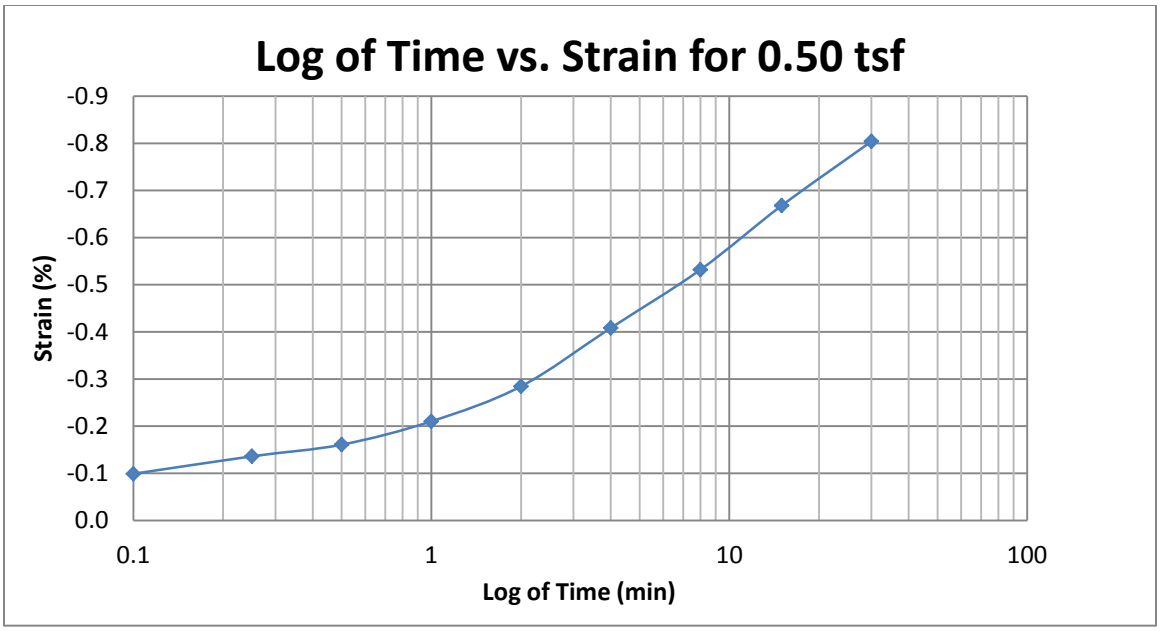

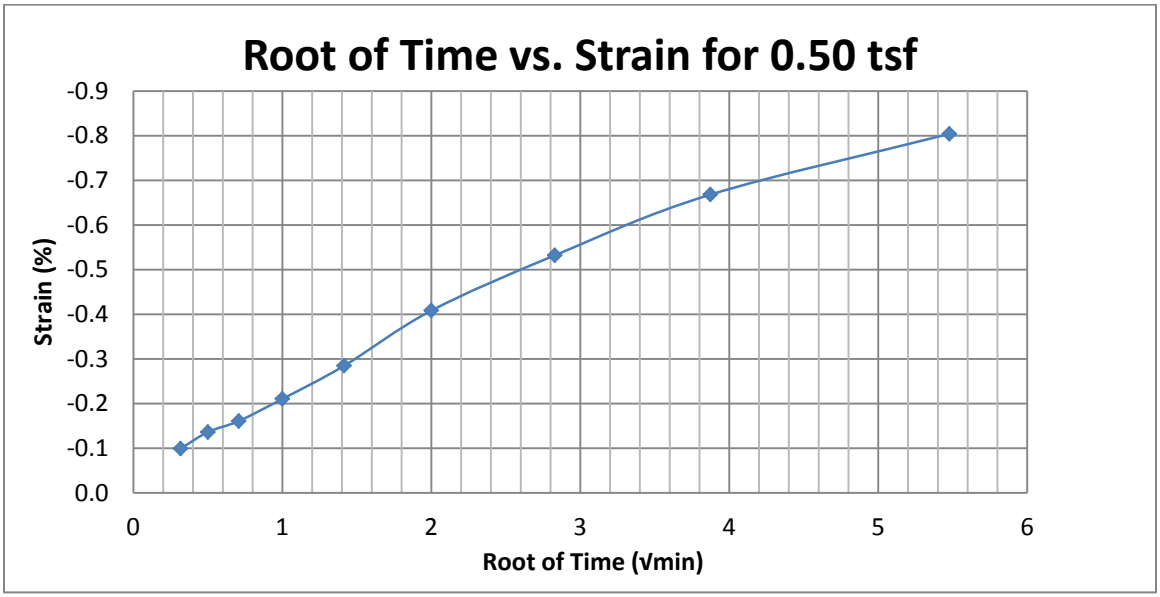

A 93 400 South at 45-47 feet

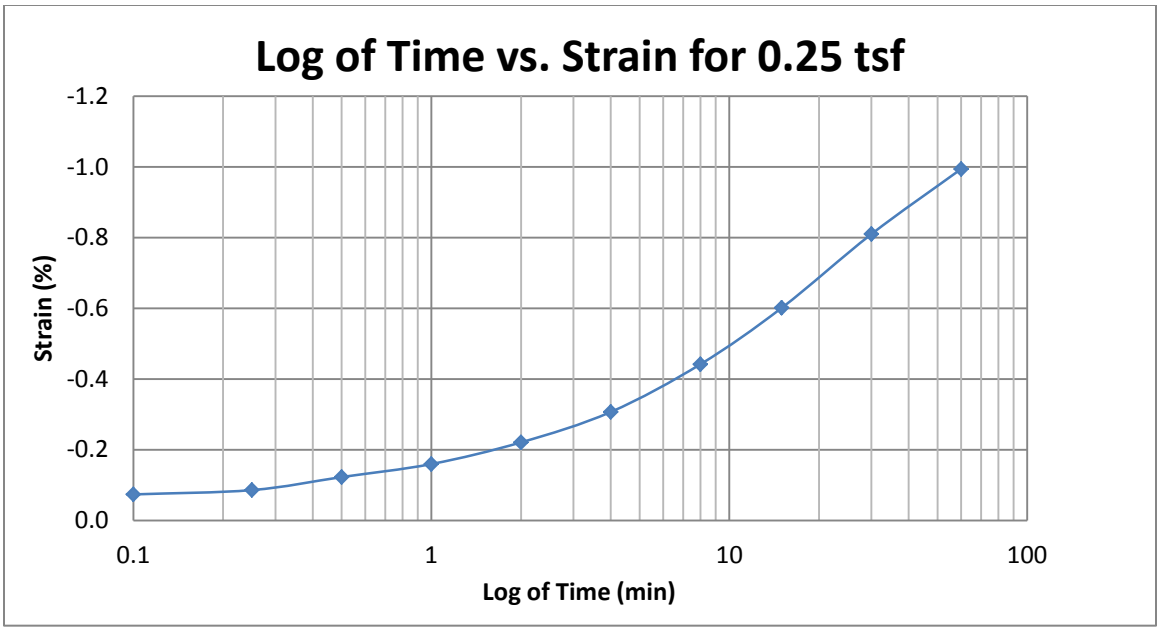

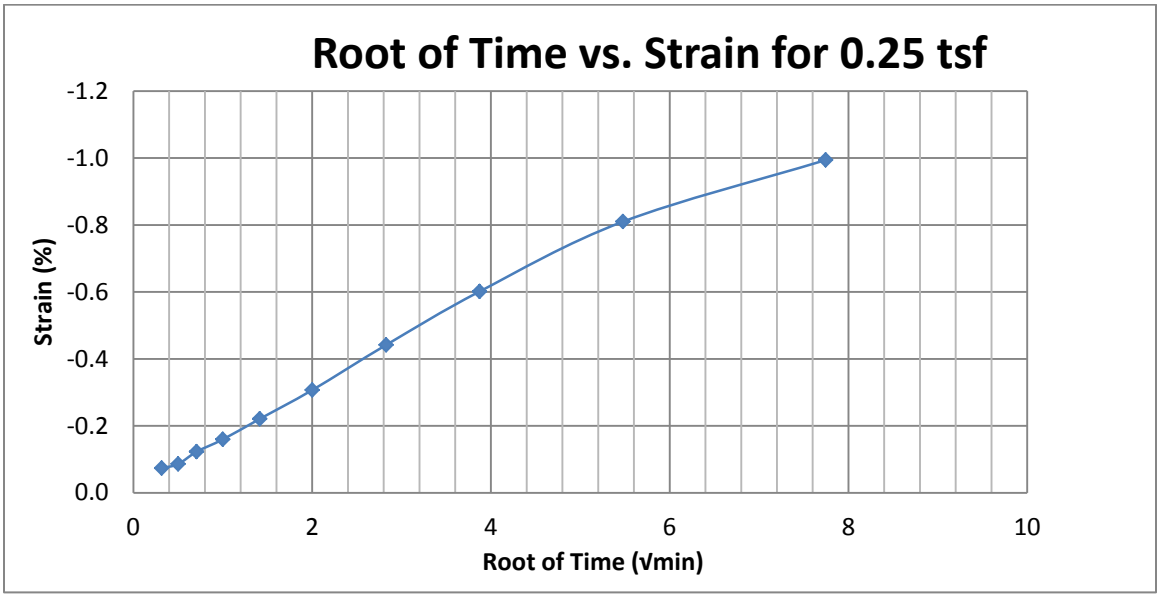

A 94 400 South at 45-47 feet

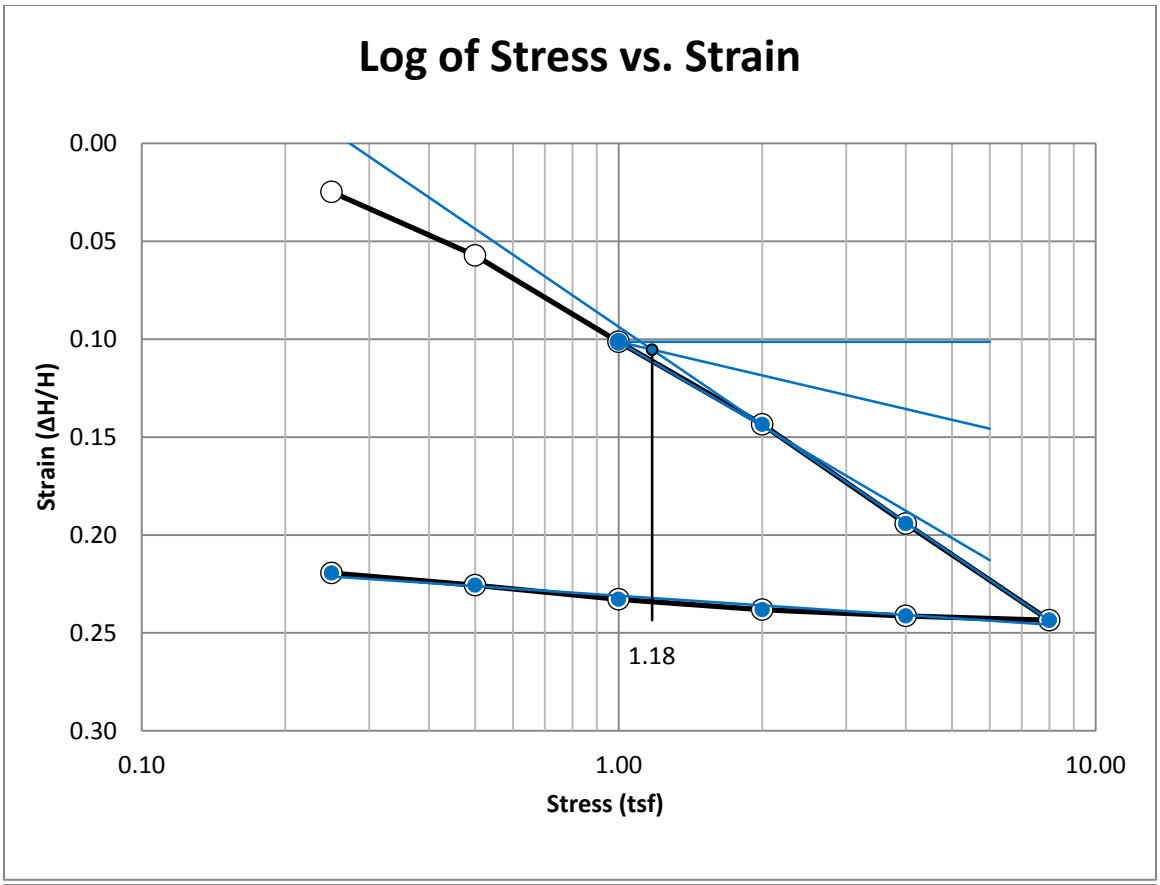

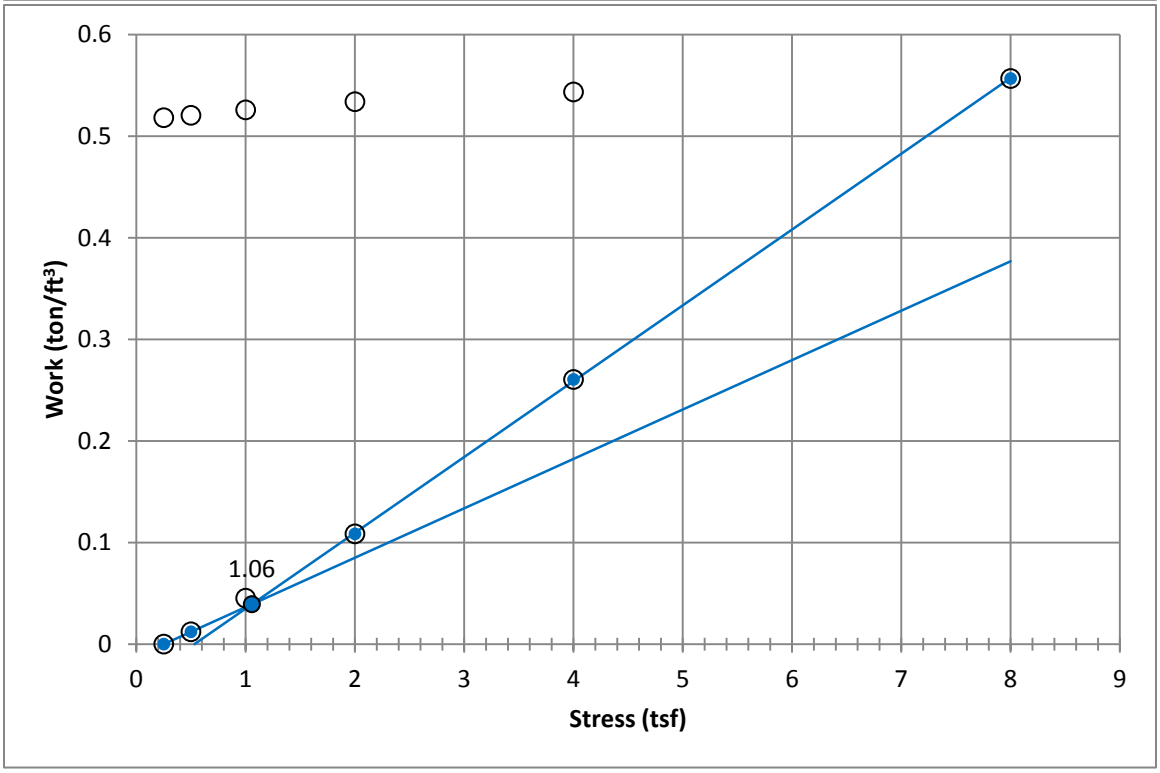

A95 400 South at 50-52 feet

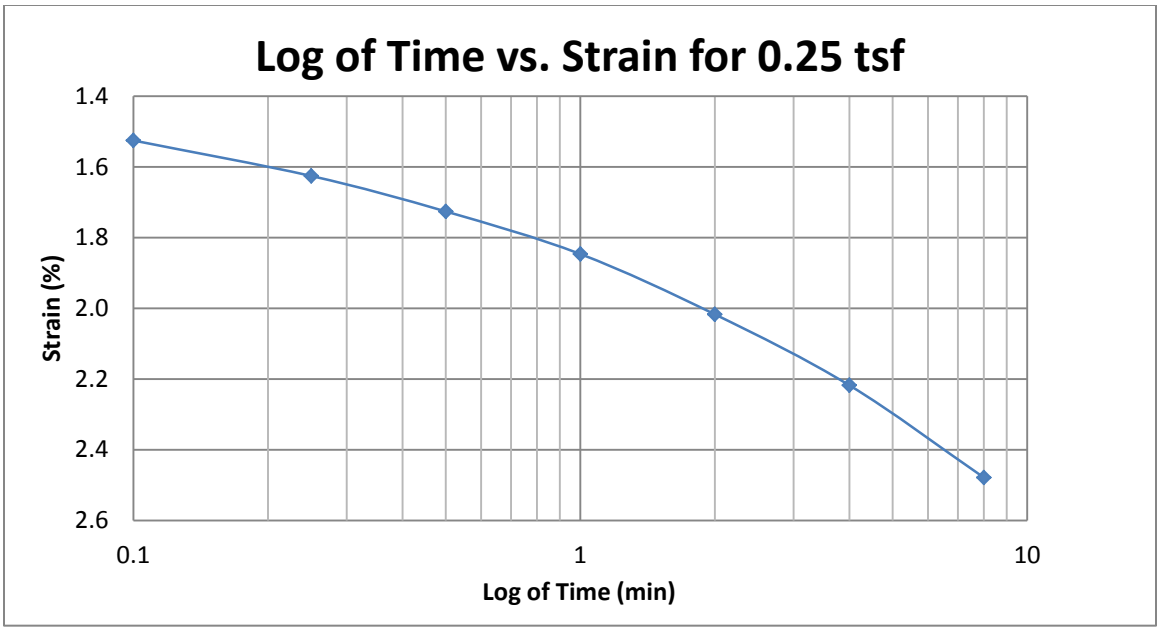

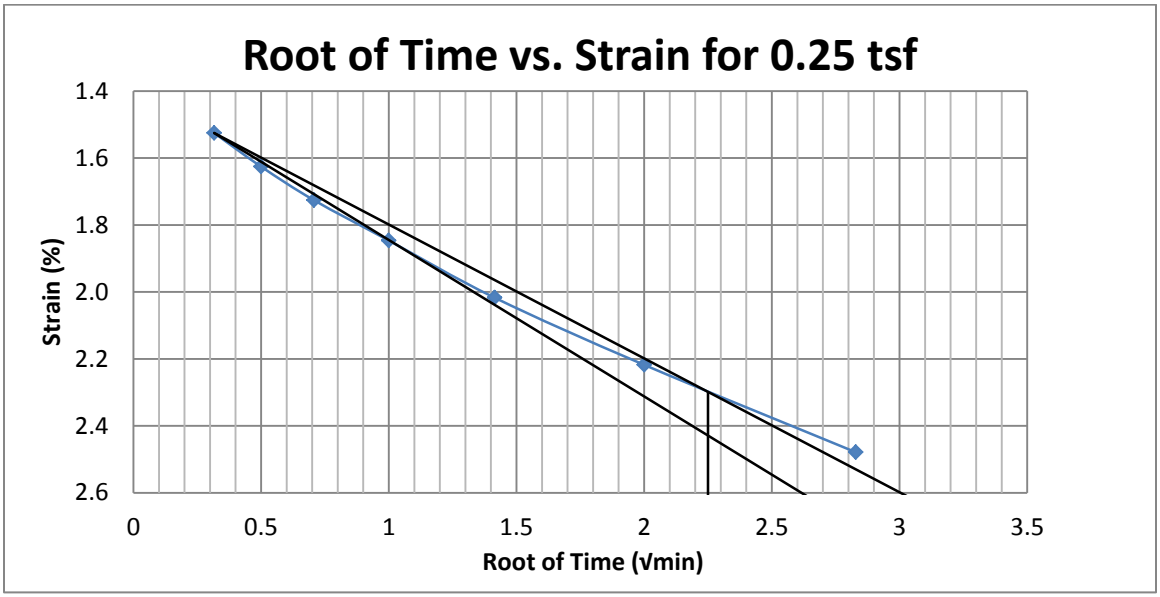

A96 400 South at 50-52 feet

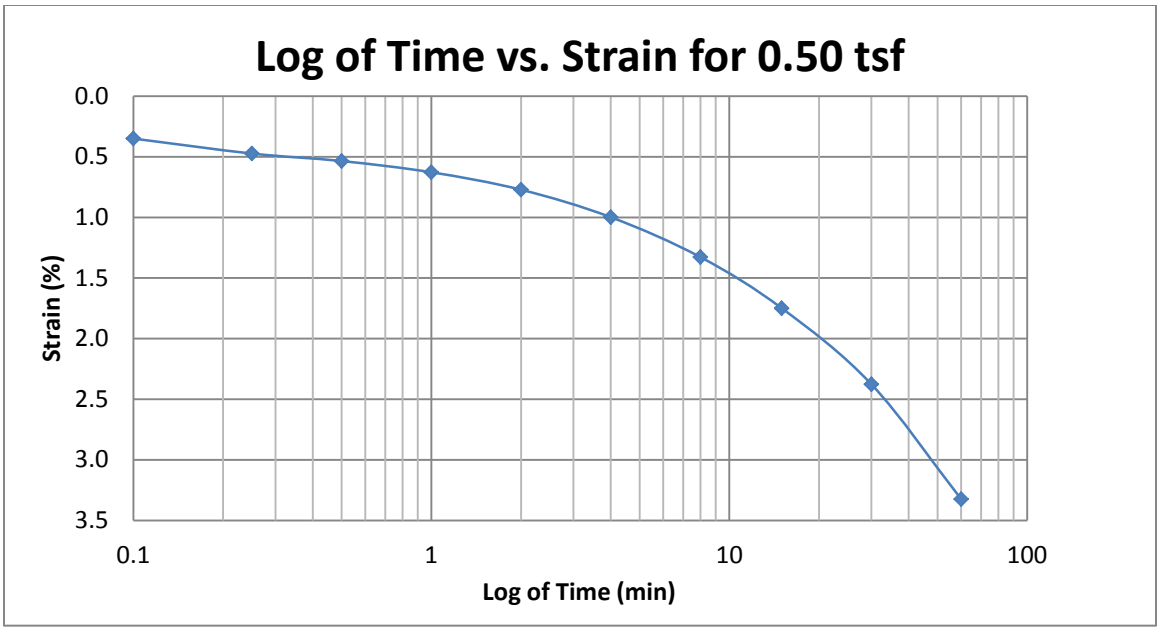

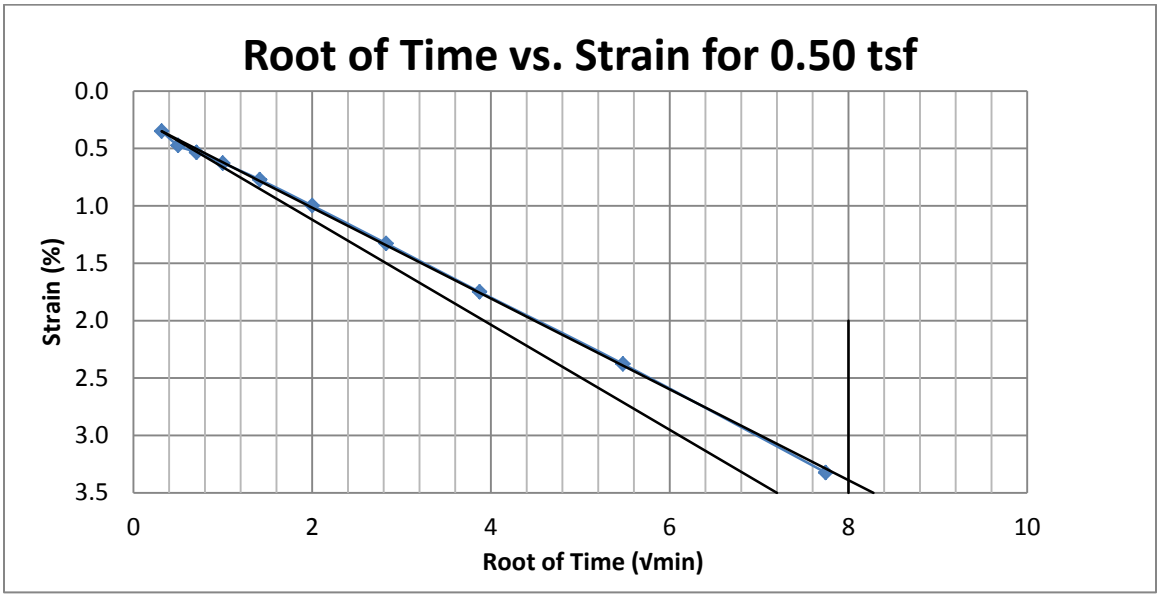

A97 400 South at 50-52 feet

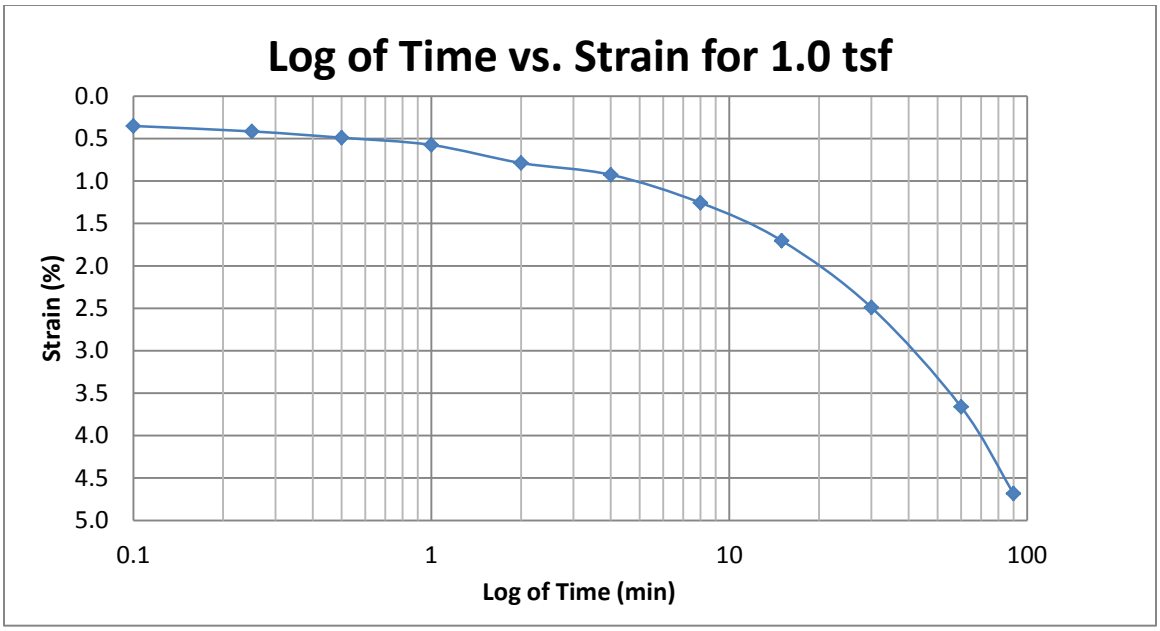

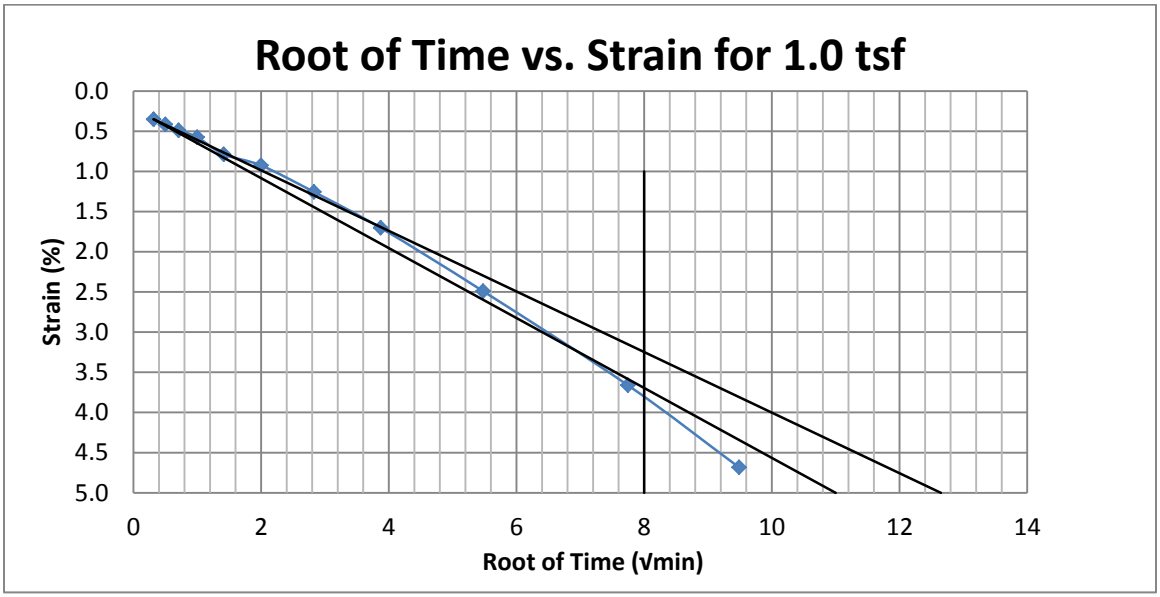

A98 400 South at 50-52 feet

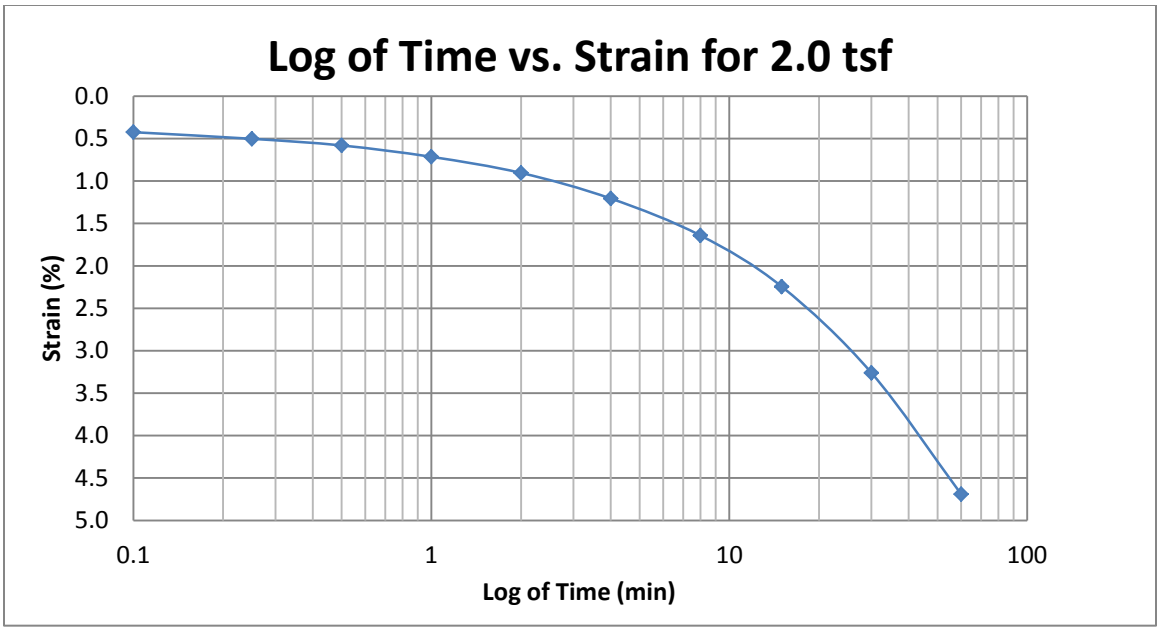

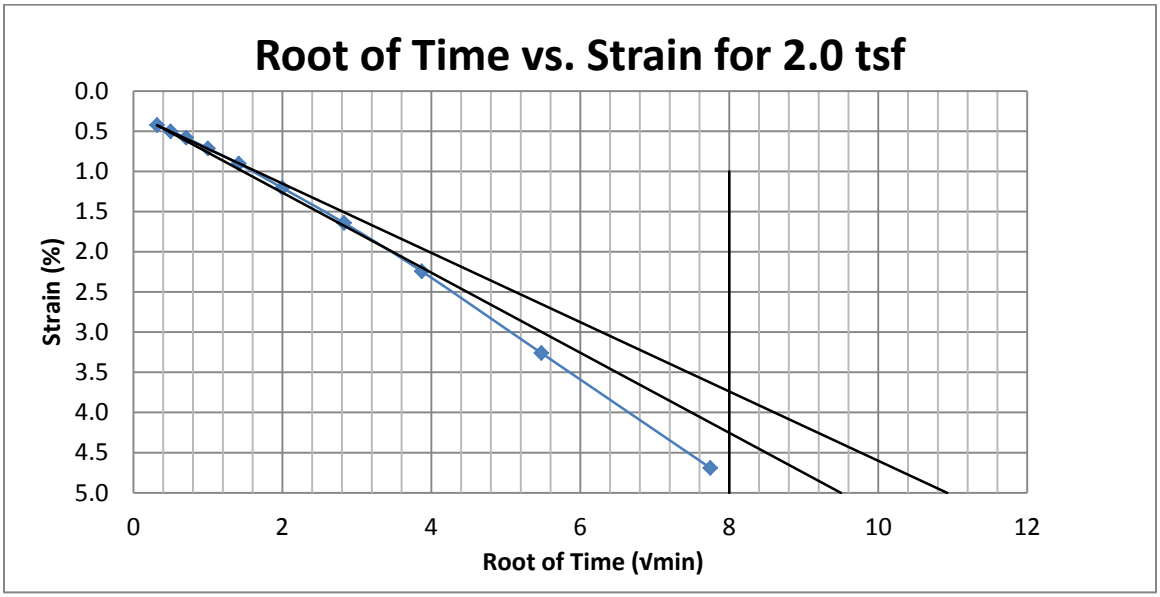

A99 400 South at 50-52 feet

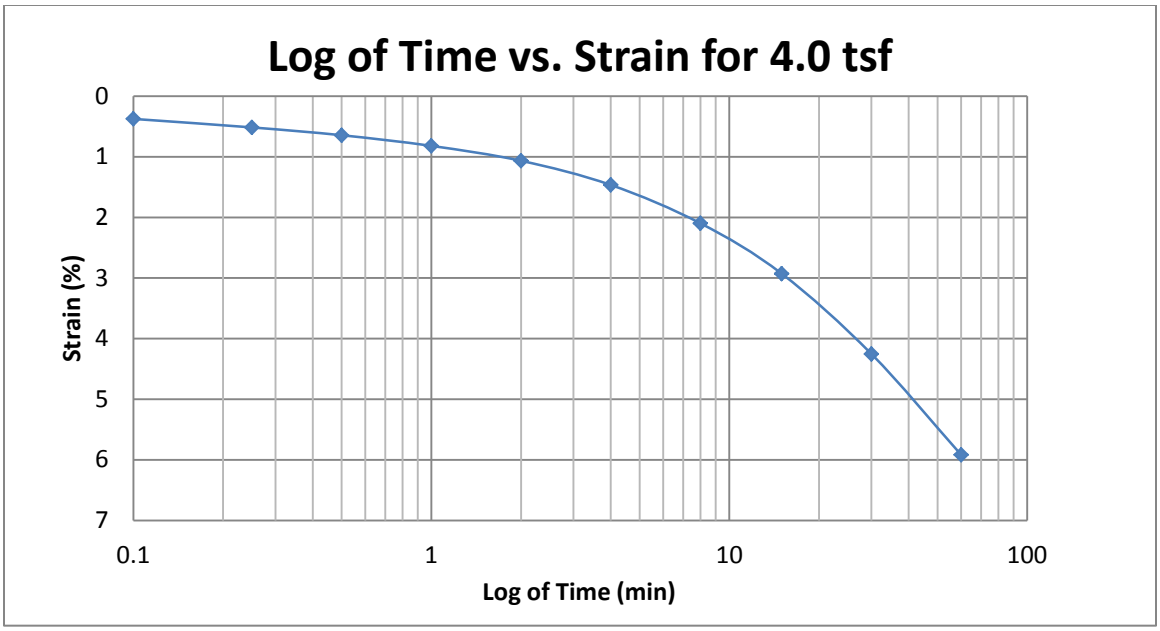

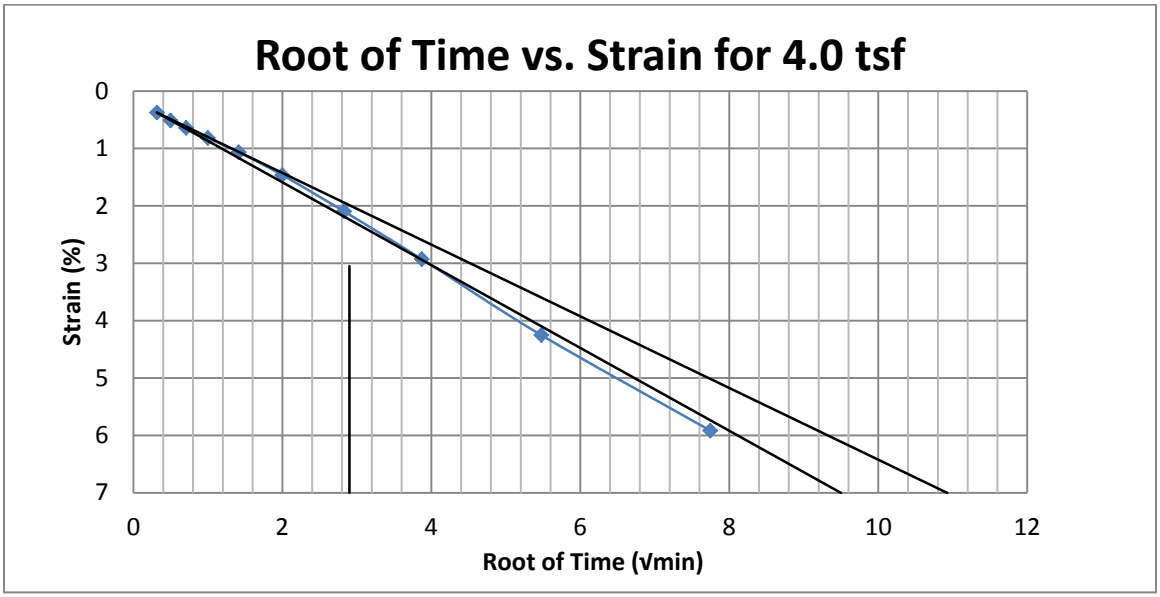

A100 400 South at 50-52 feet

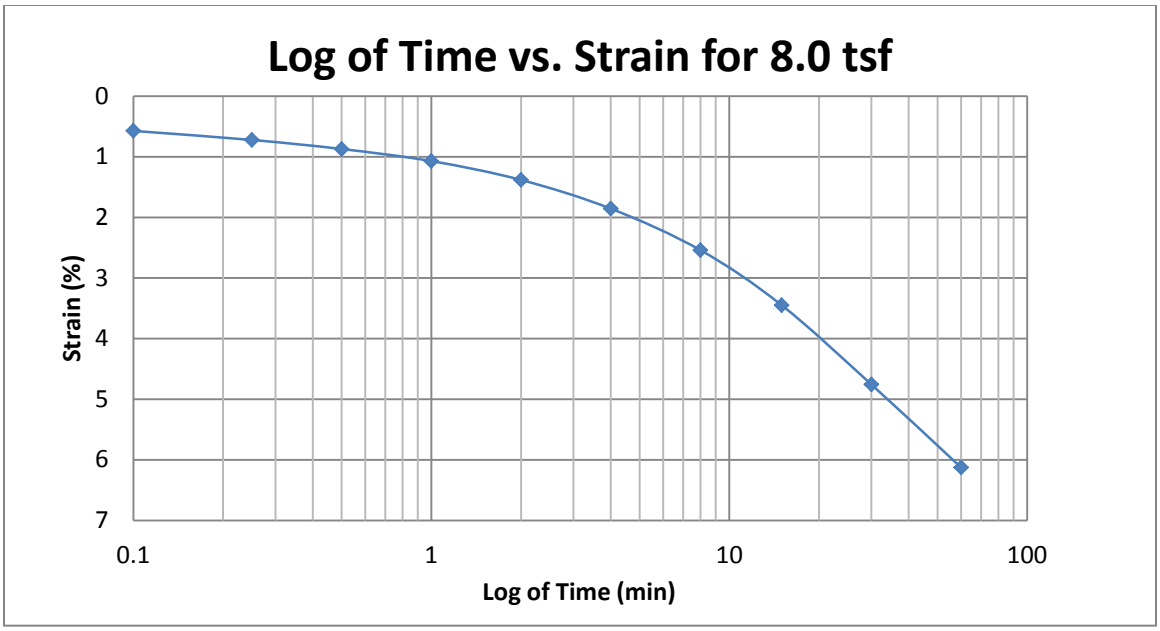

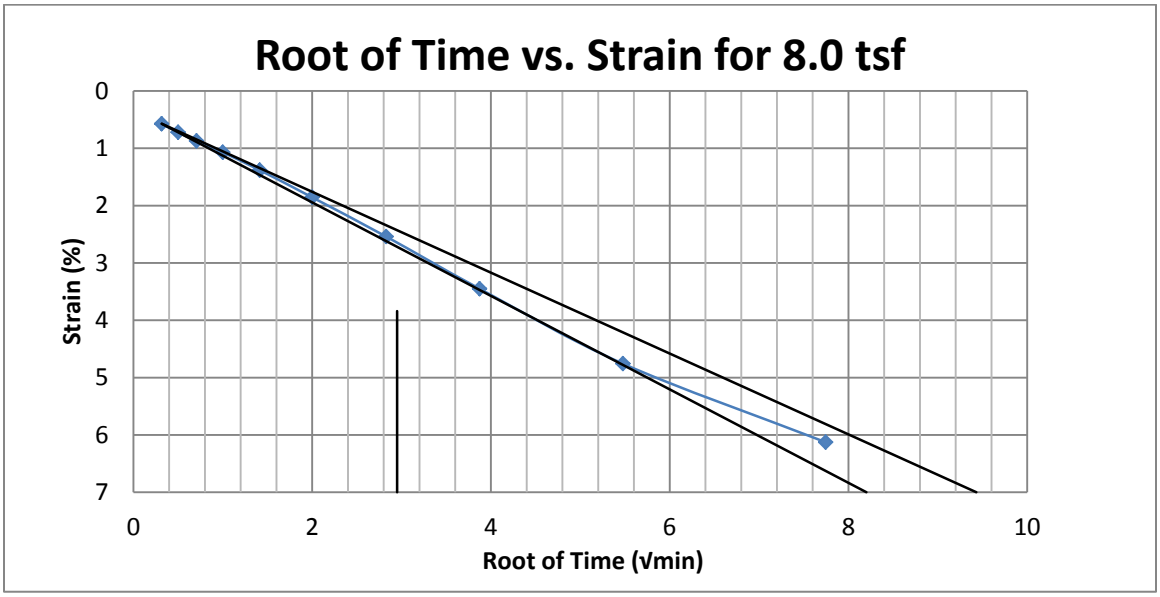

A101 400 South at 50-52 feet

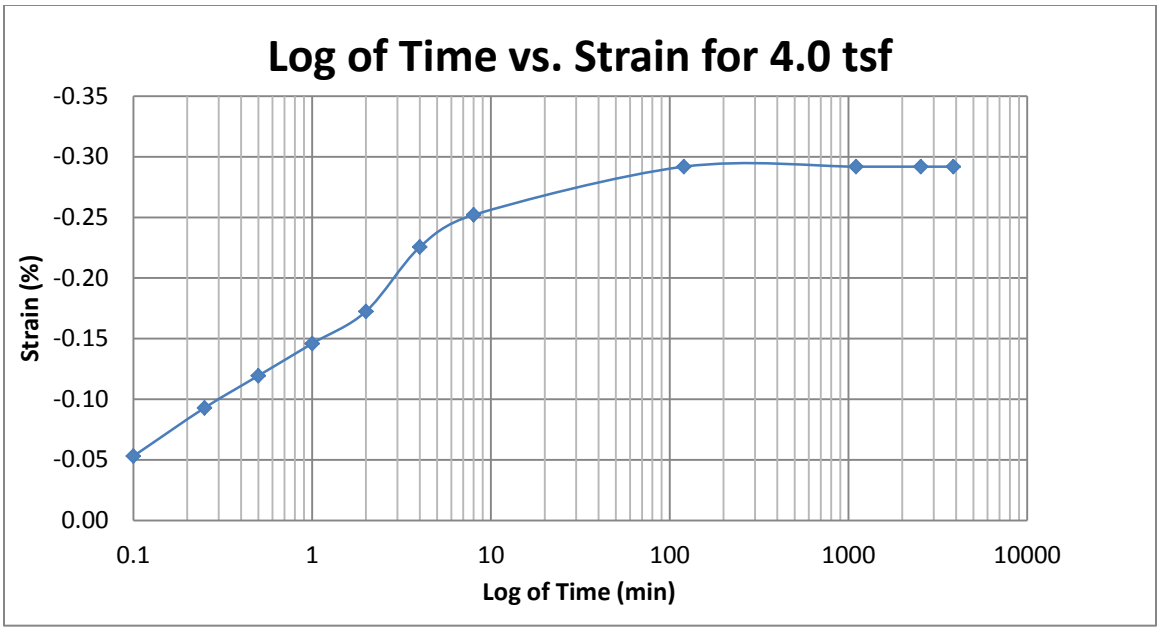

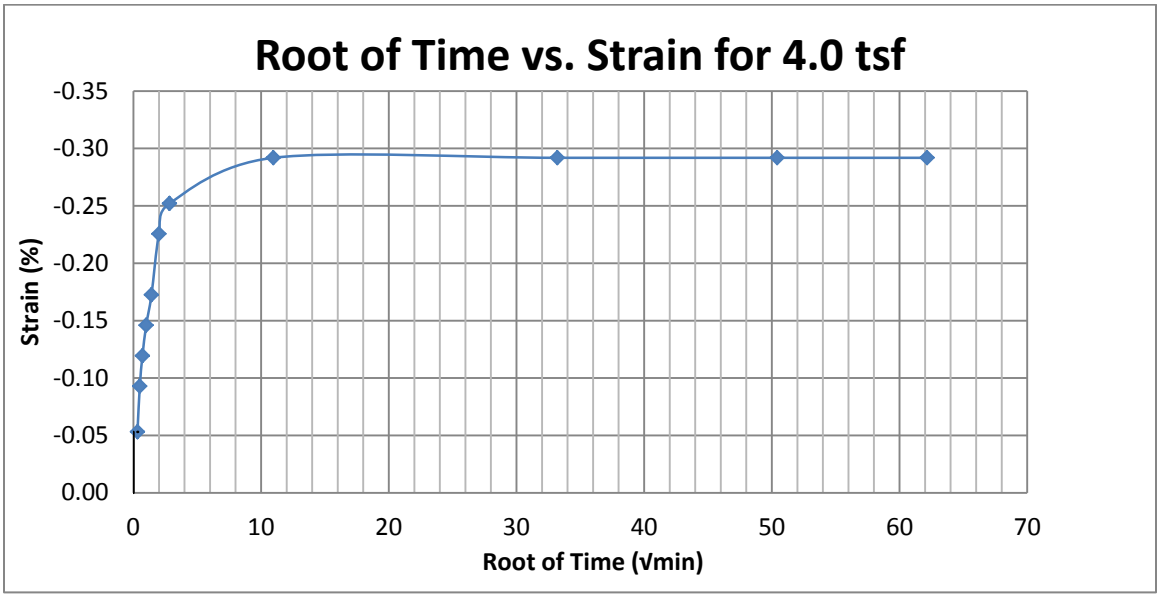

A102 400 South at 50-52 feet

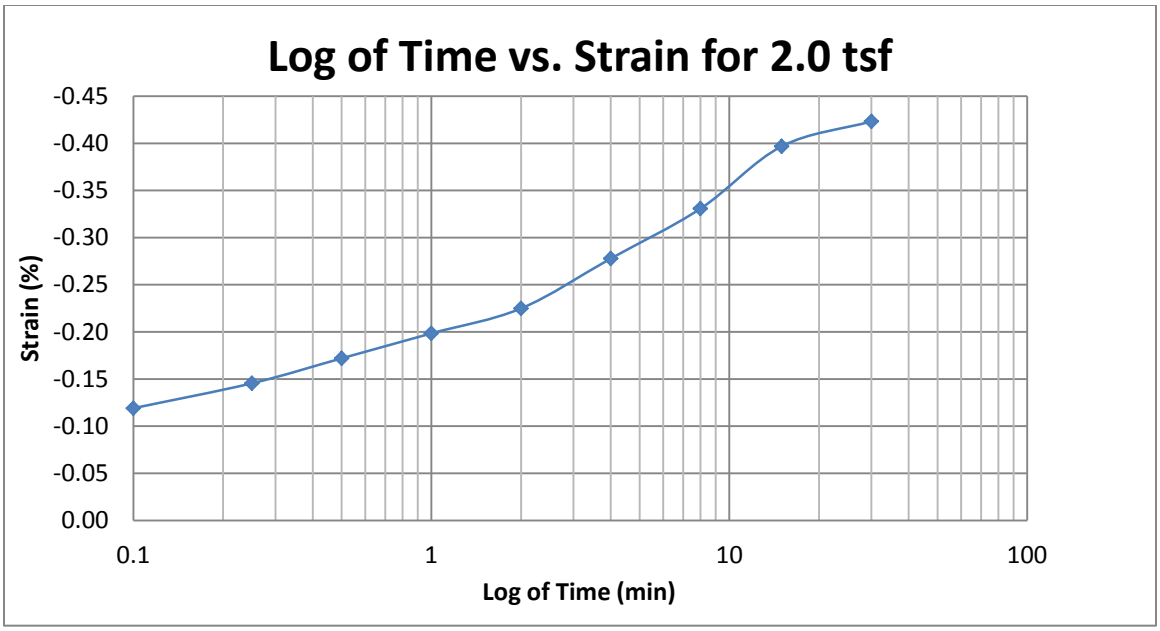

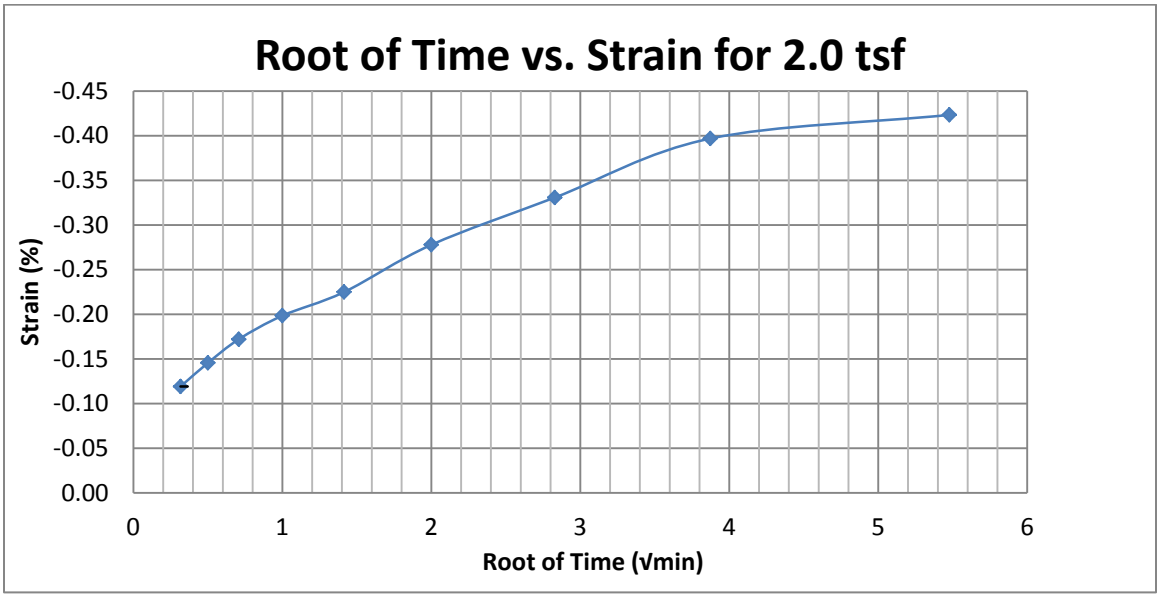

A103 400 South at 50-52 feet

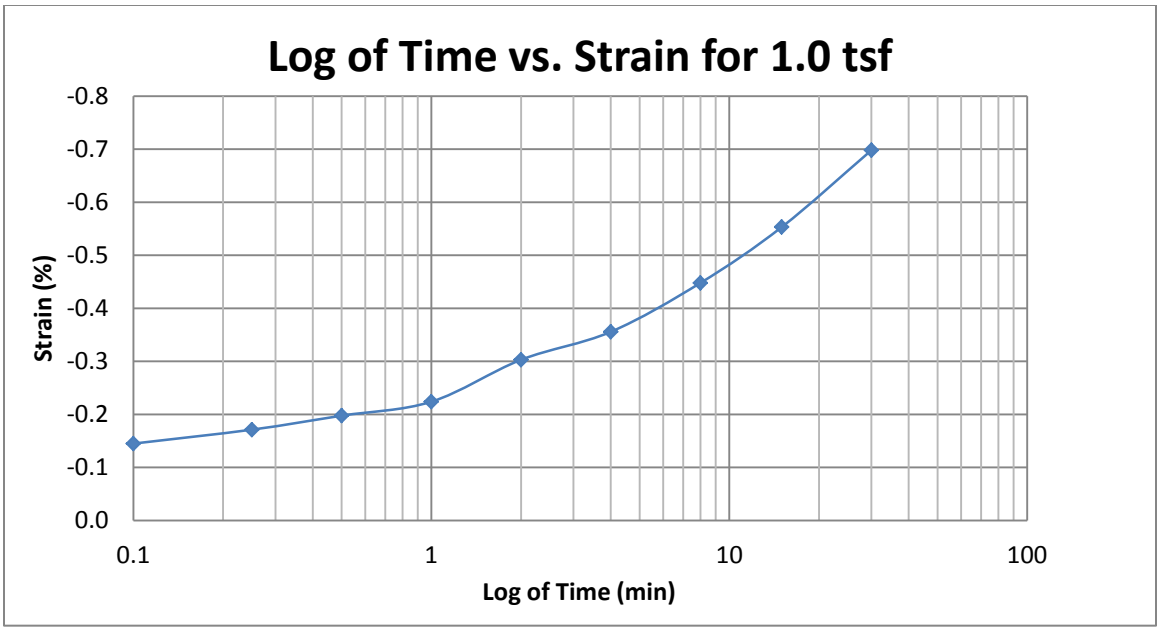

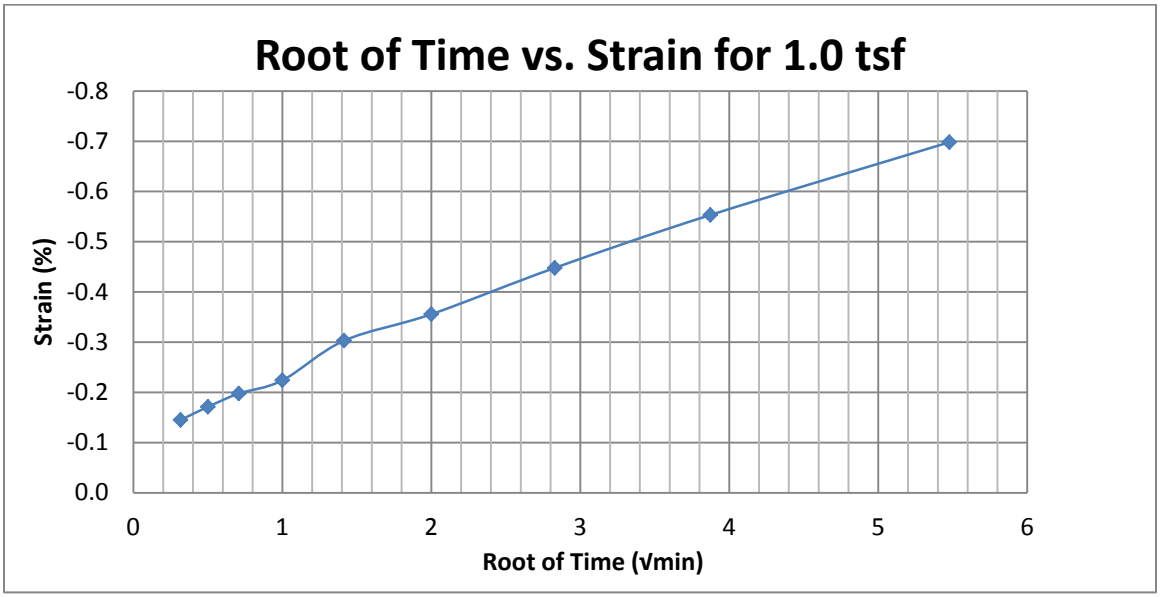

A104 400 South at 50-52 feet

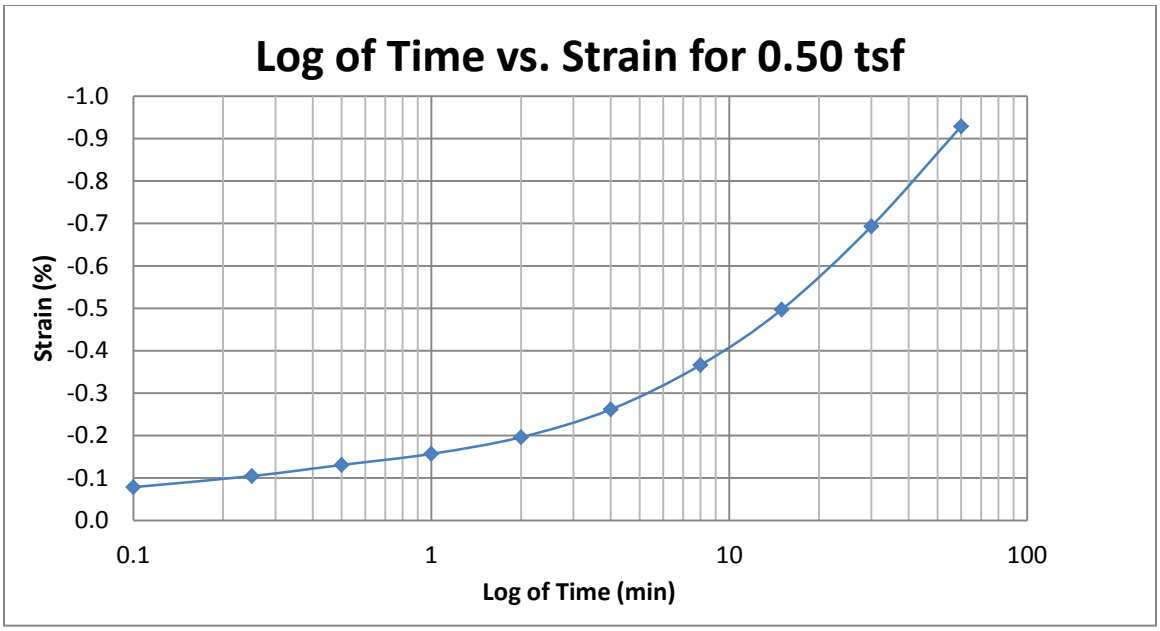

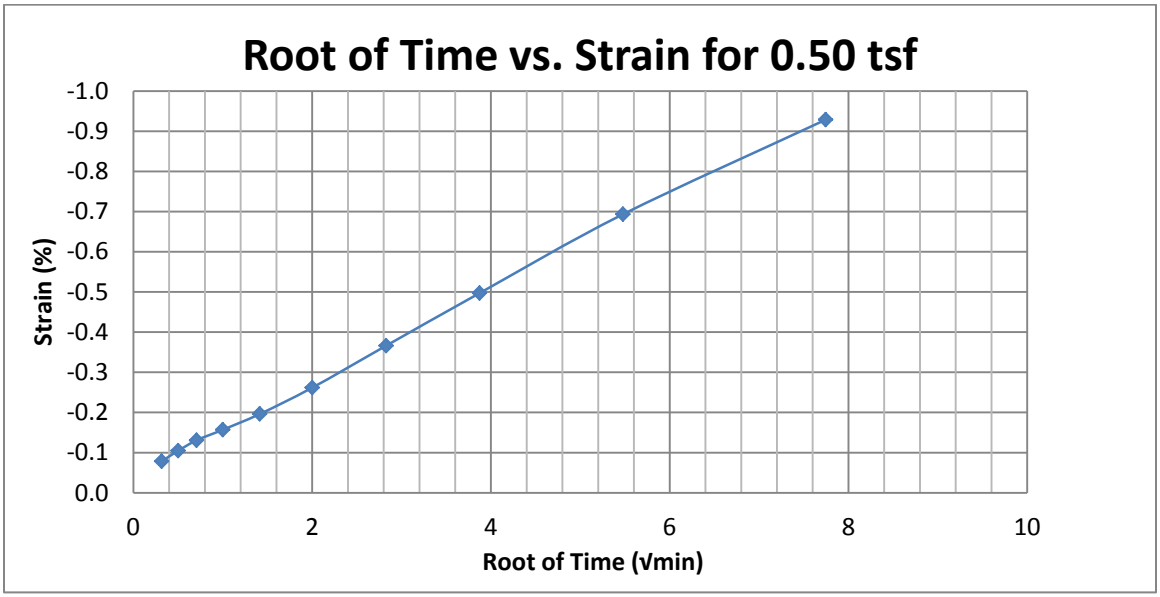

A105 400 South at 50-52 feet

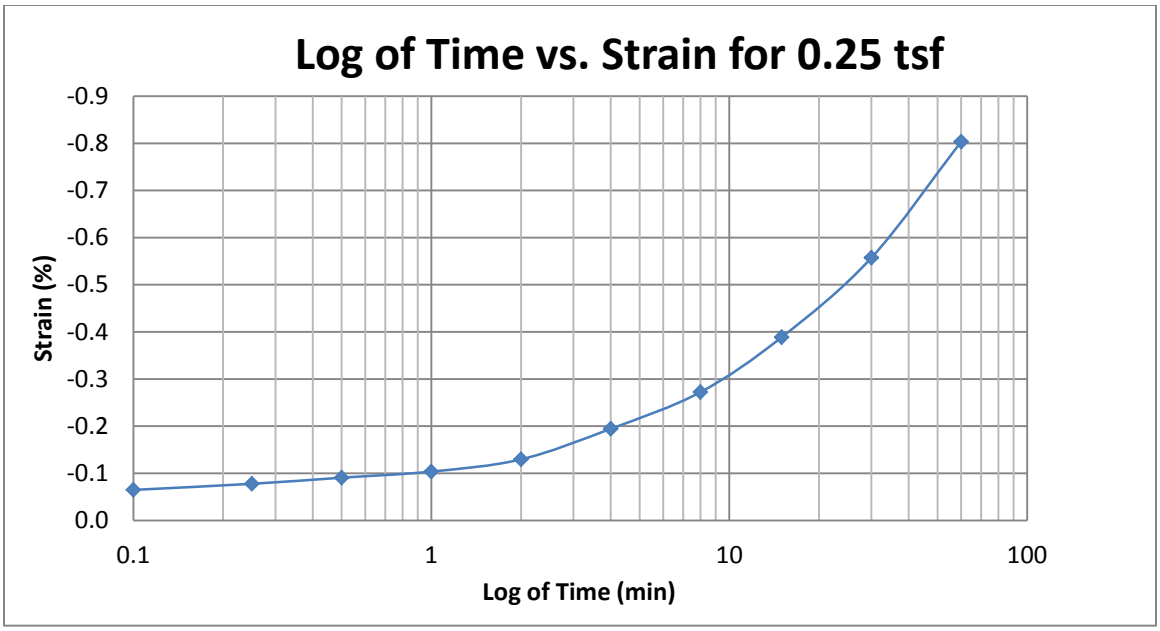

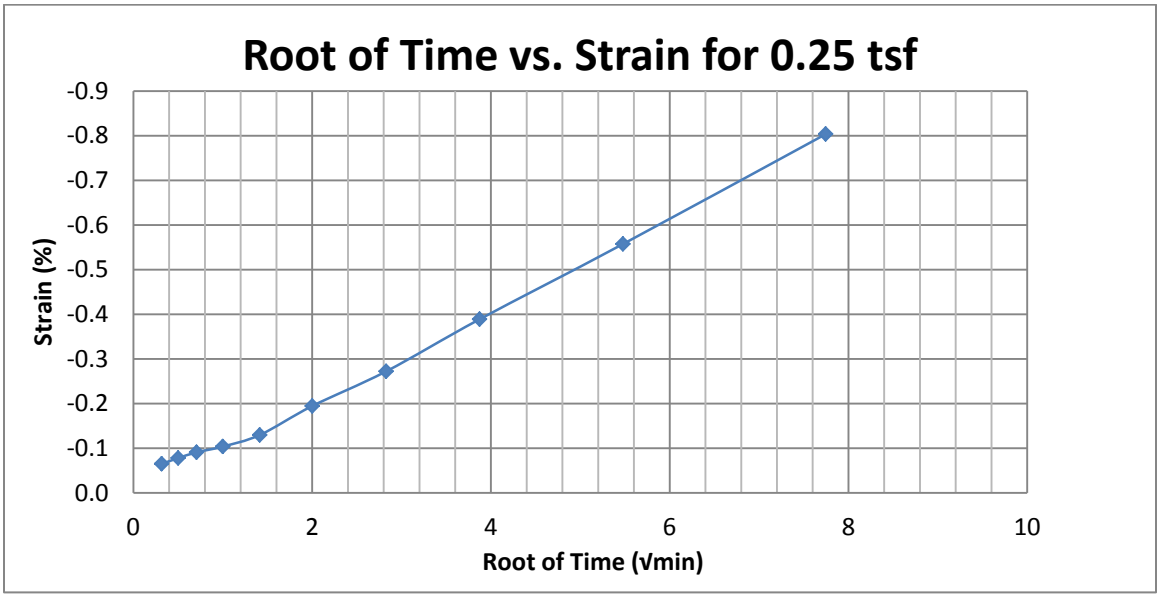

A106 400 South at 50-52 feet

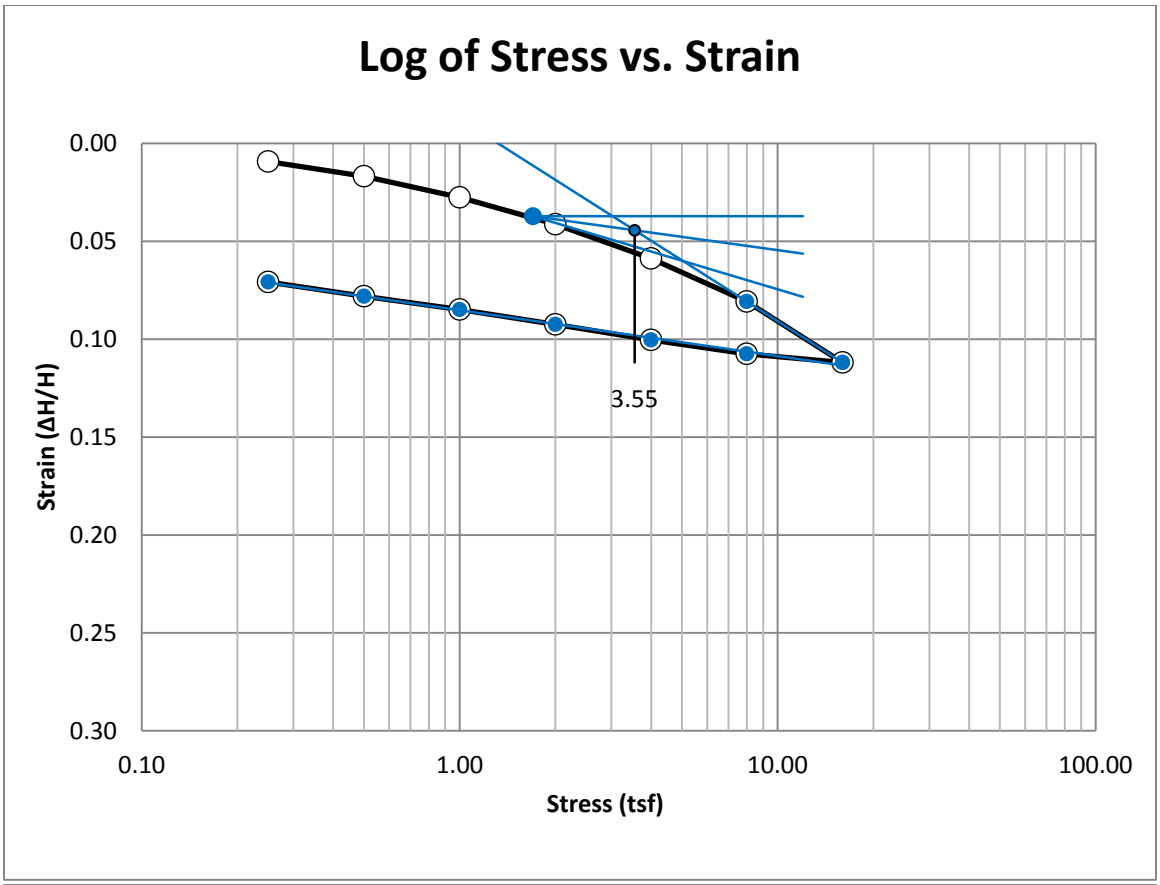

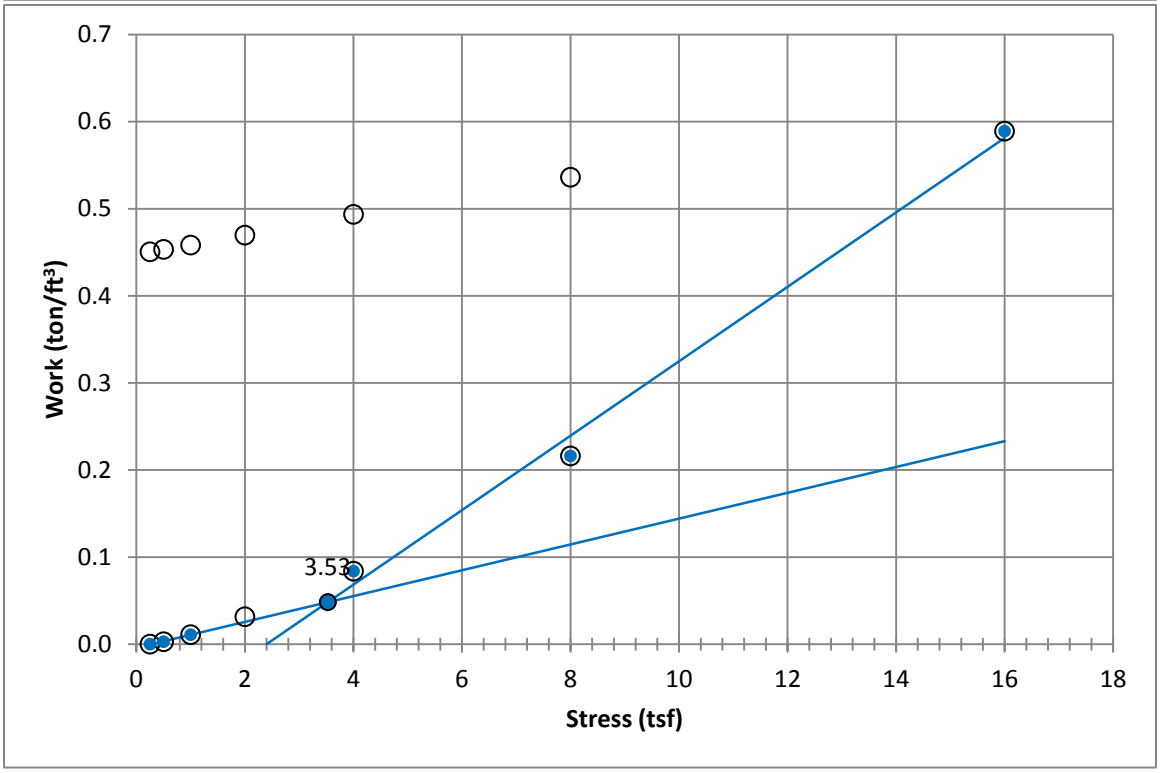

A107 Springville at 30-32 feet

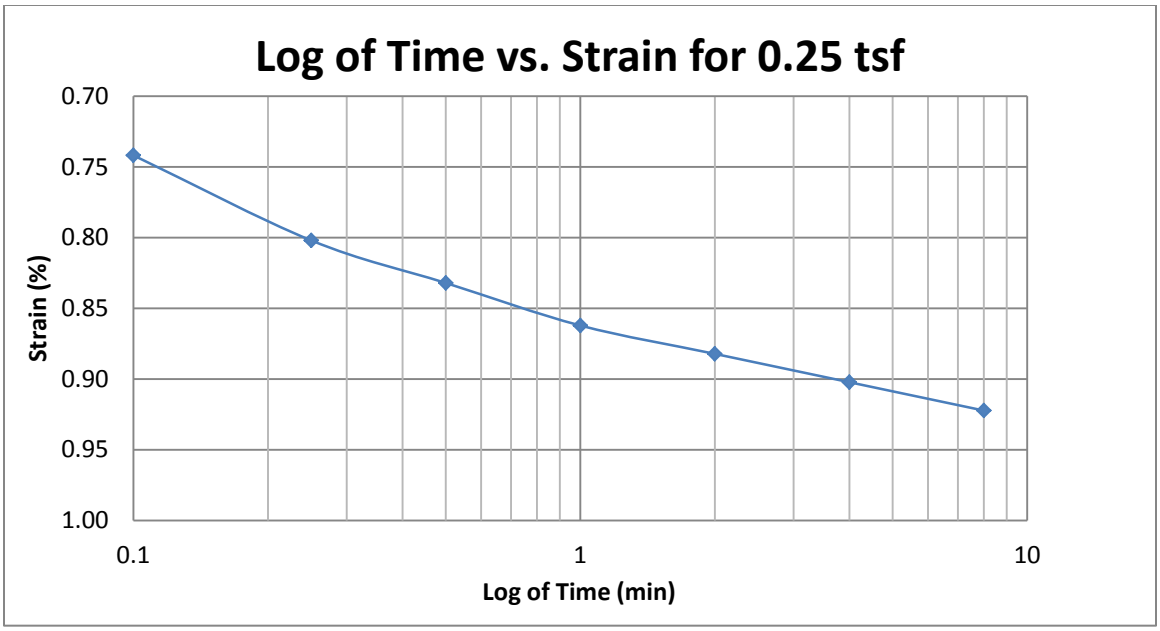

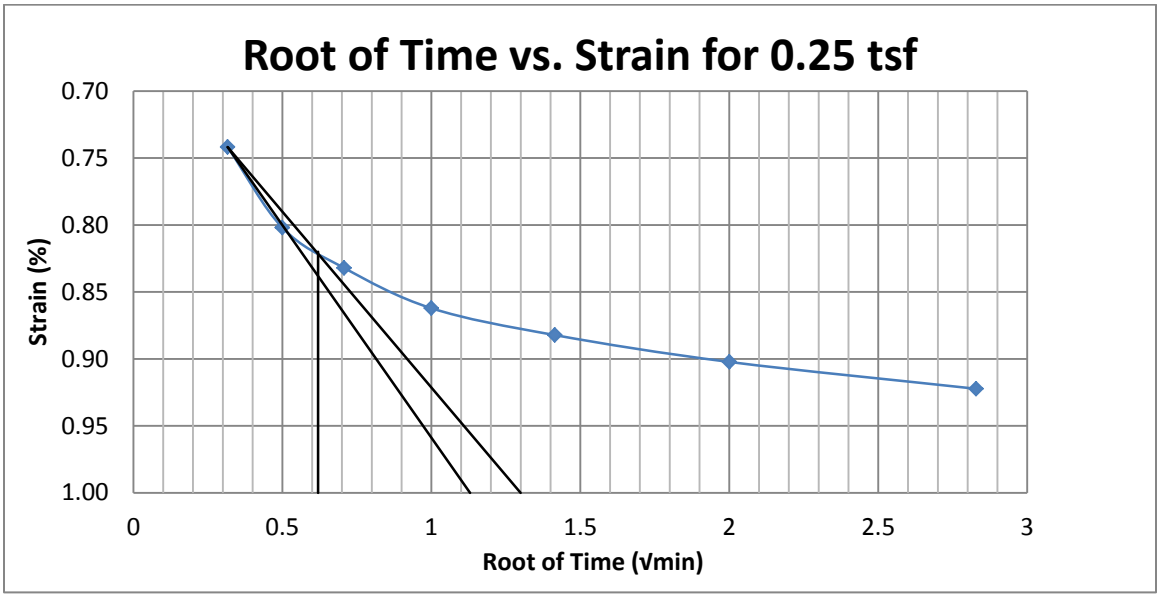

A108 Springville at 30-32 feet

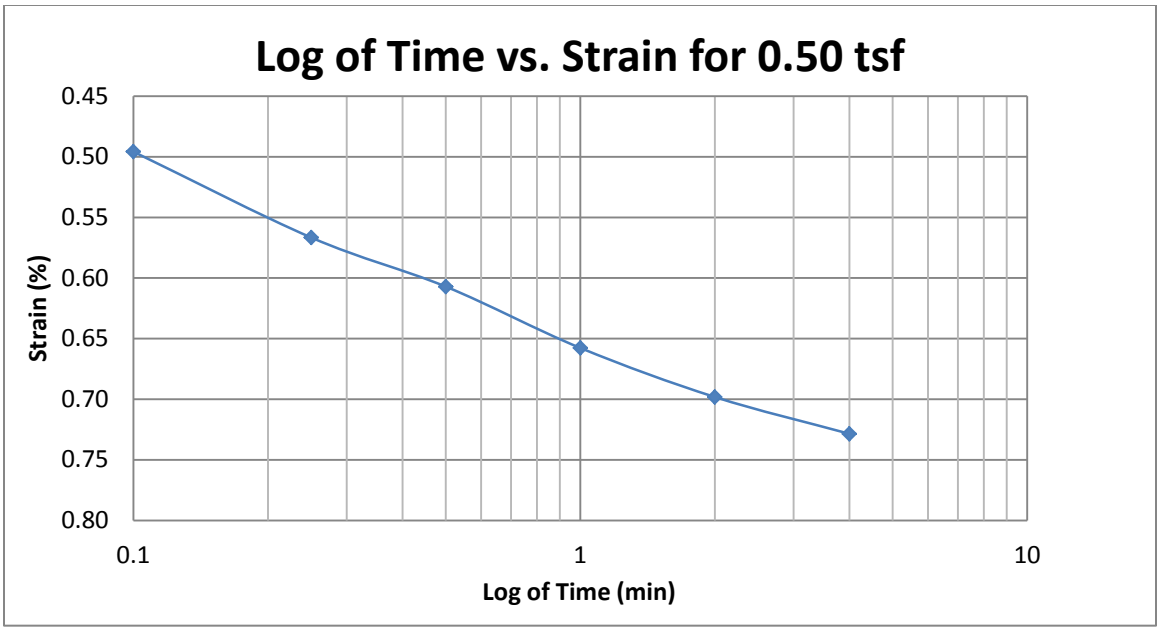

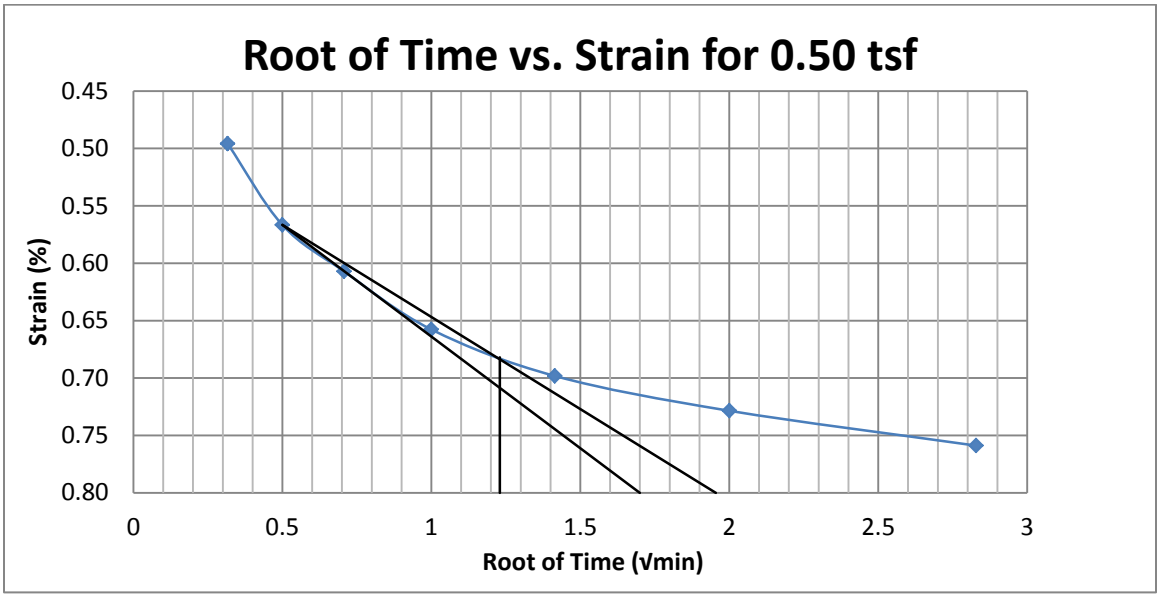

A109 Springville at 30-32 feet

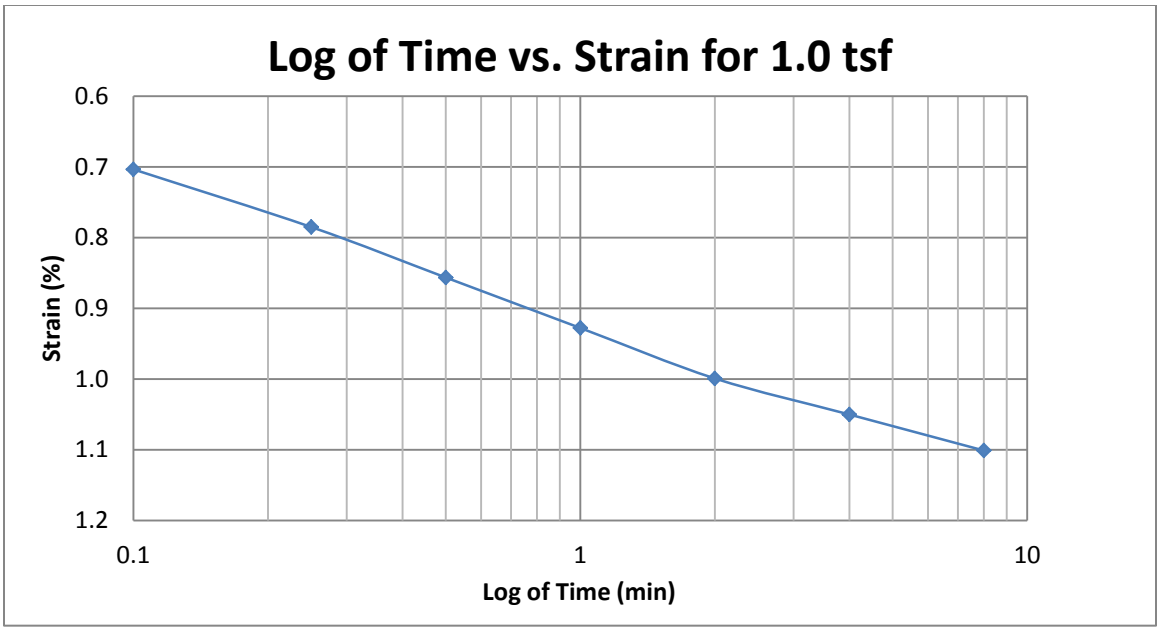

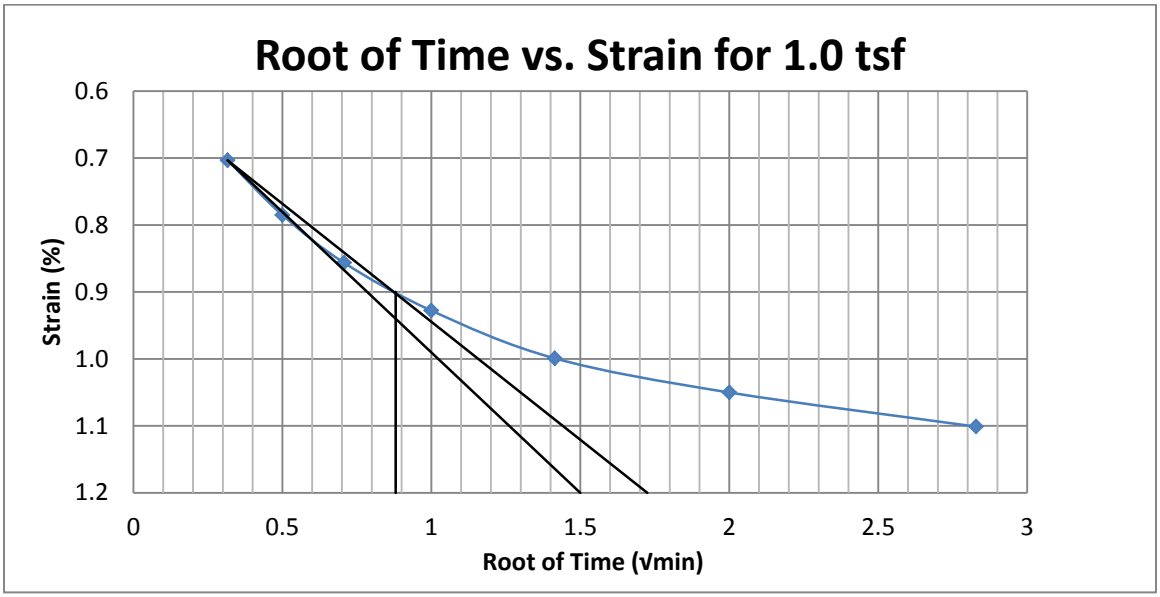

A110 Springville at 30-32 feet

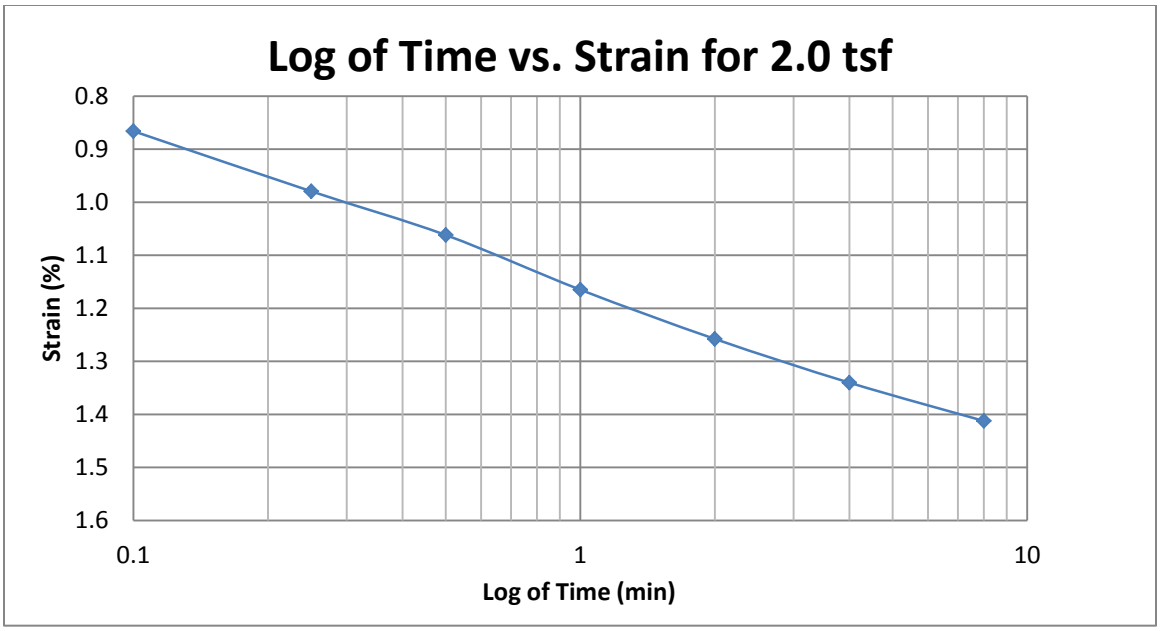

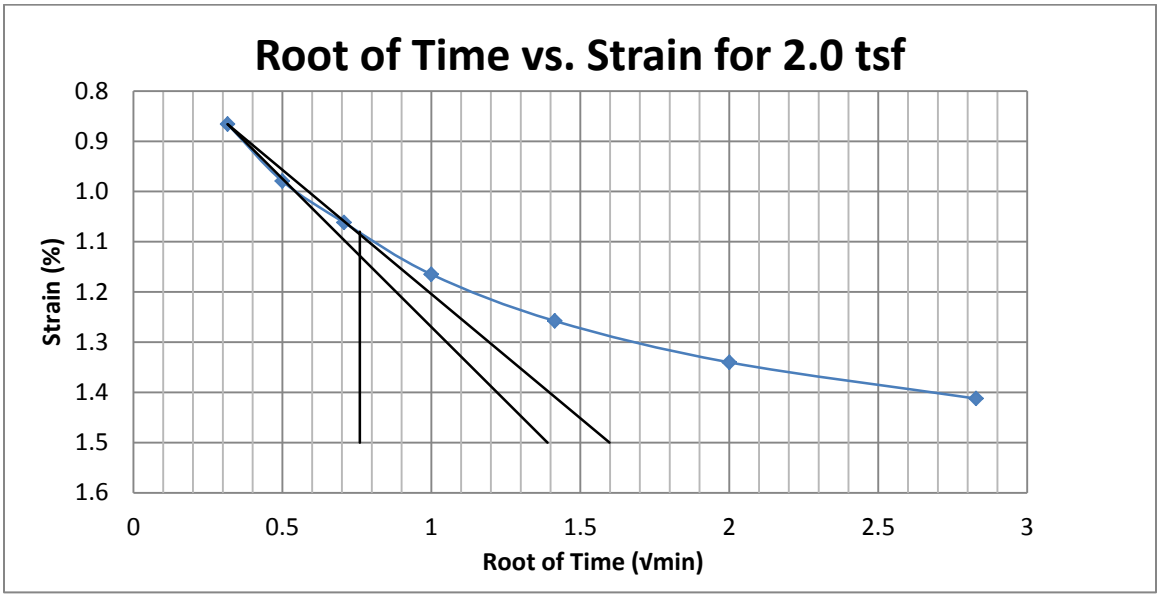

A111 Springville at 30-32 feet

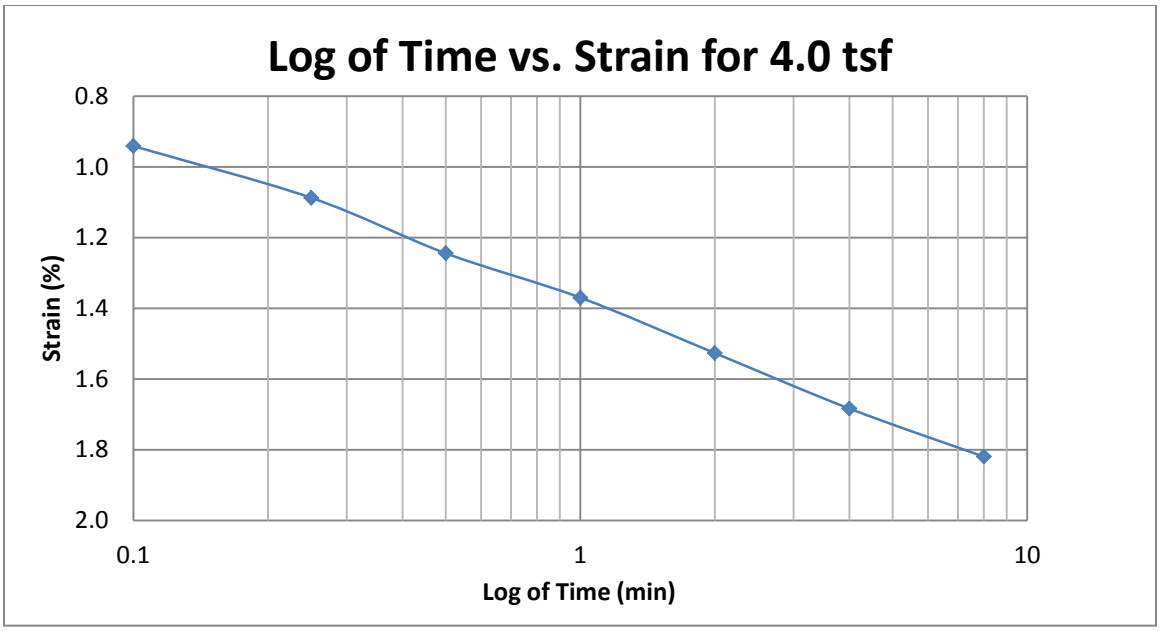

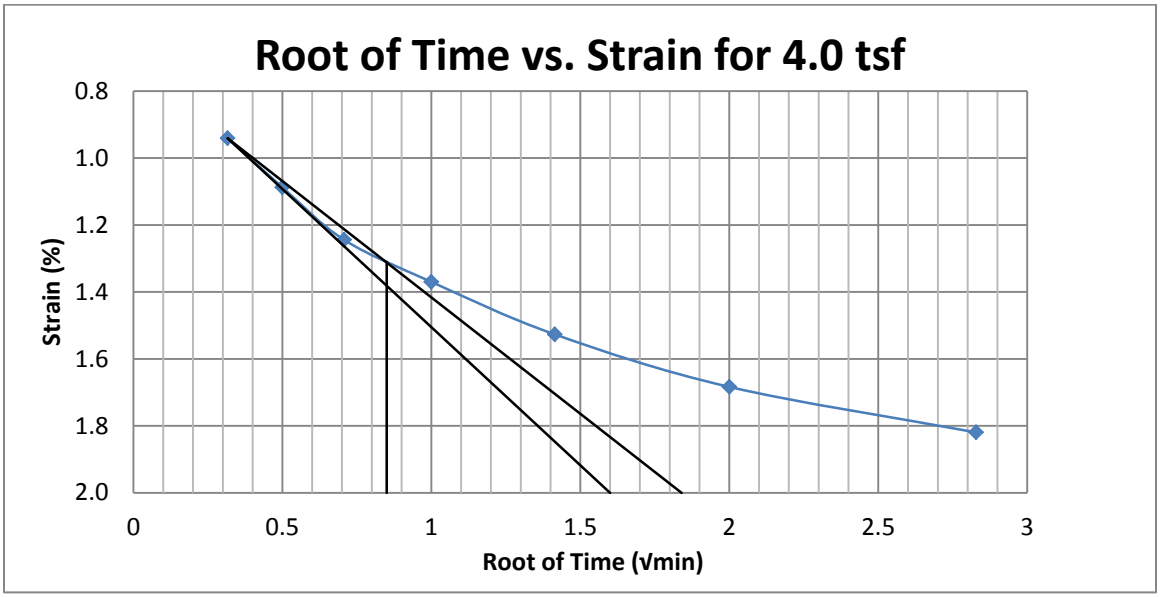

A112 Springville at 30-32 feet

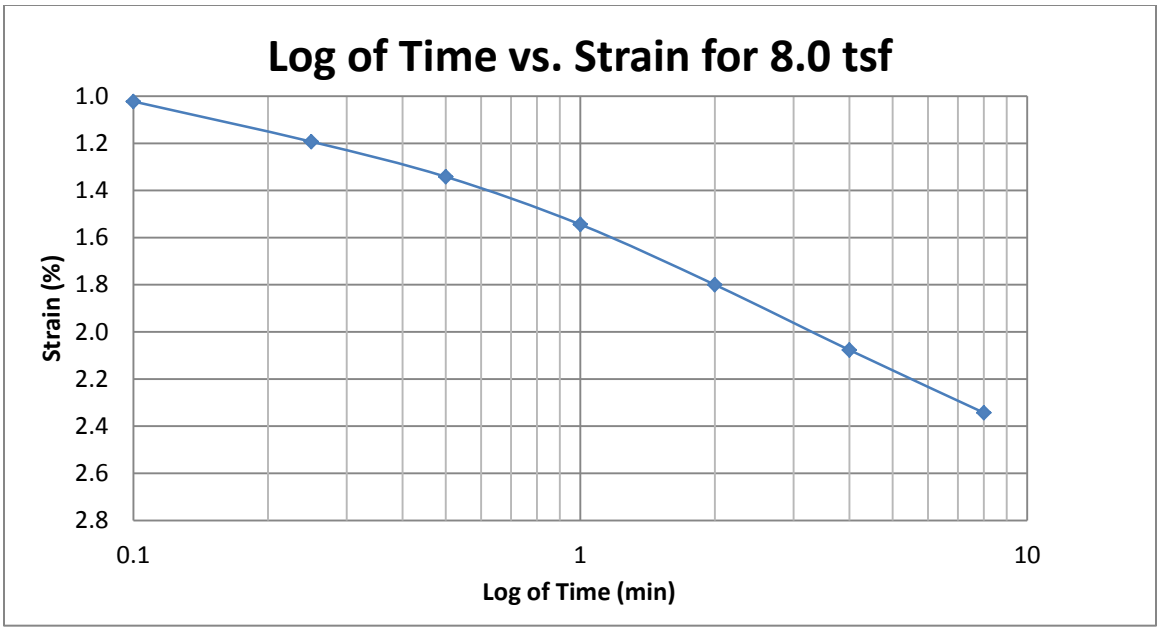

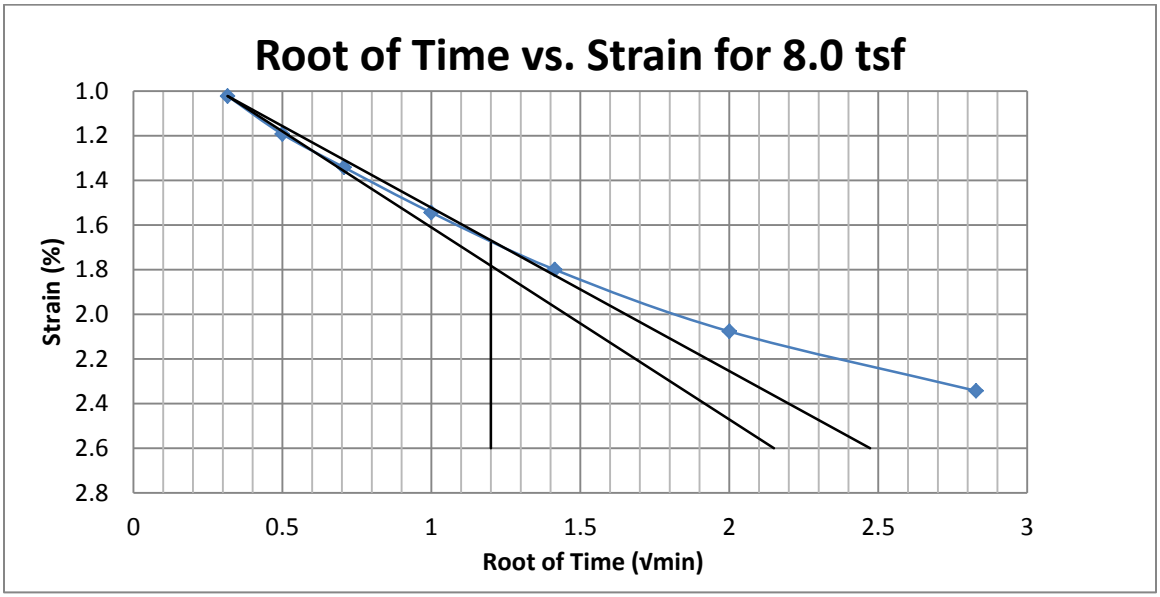

A113 Springville at 30-32 feet

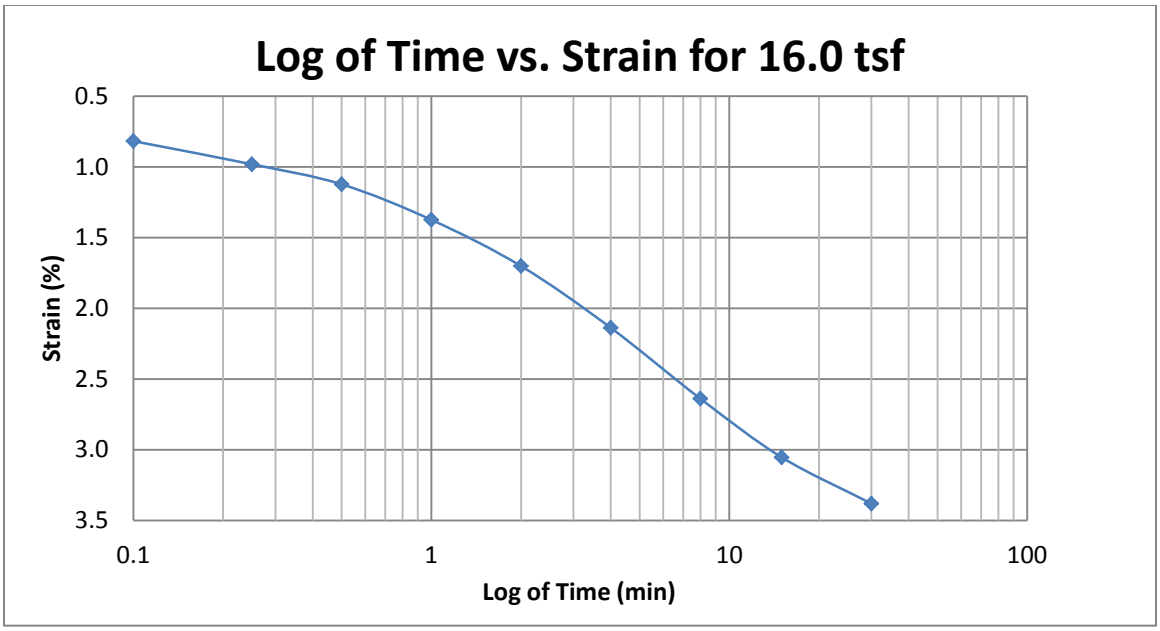

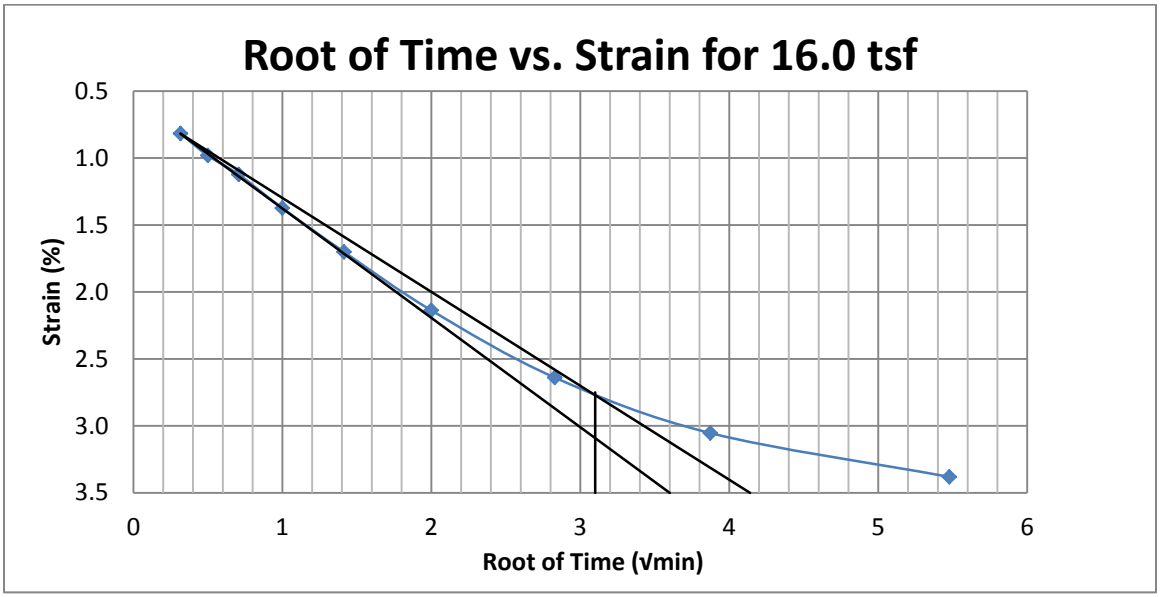

A114 Springville at 30-32 feet

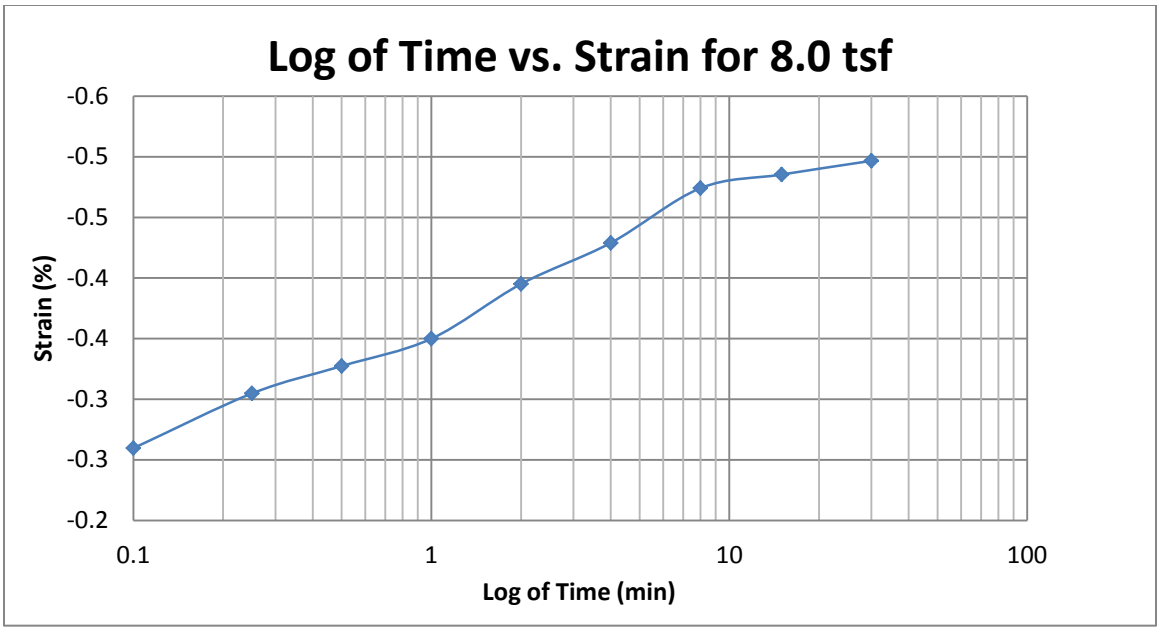

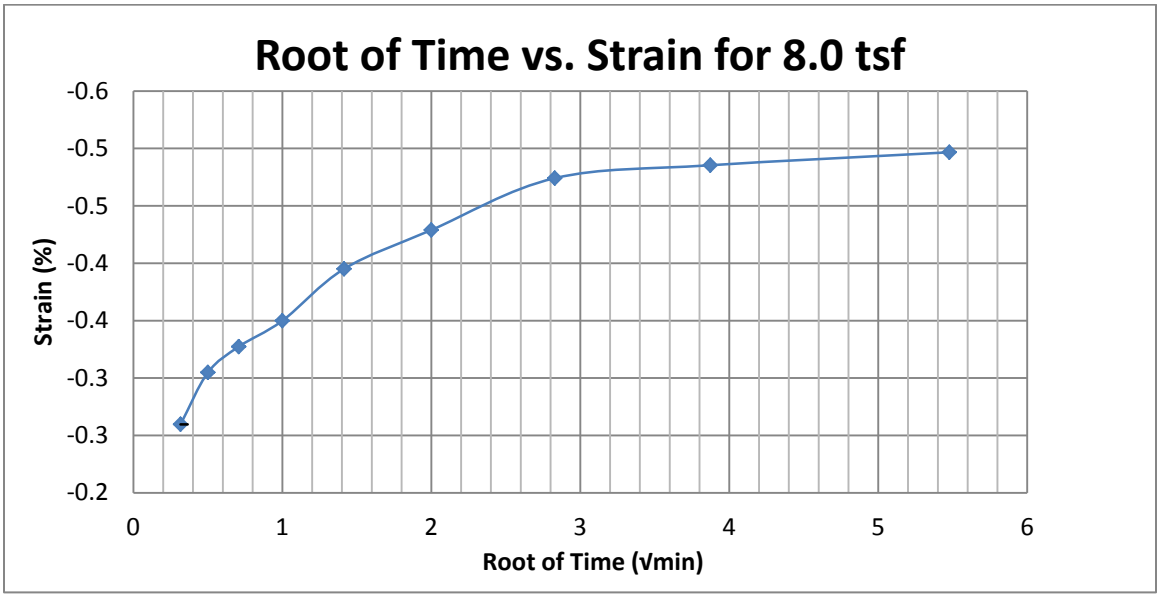

A115 Springville at 30-32 feet

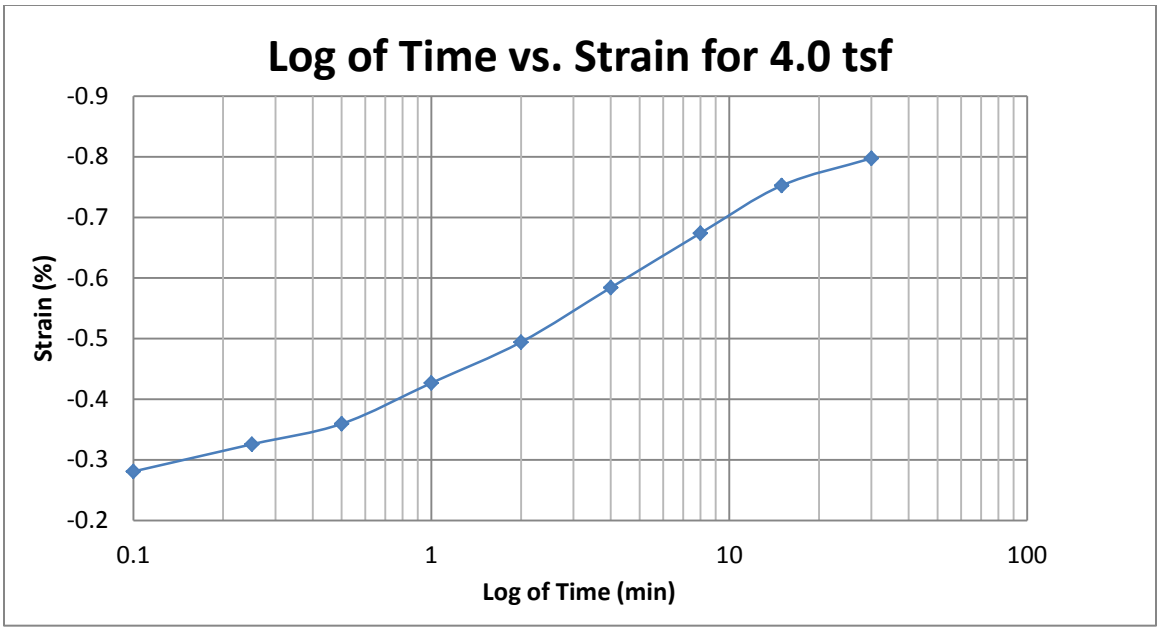

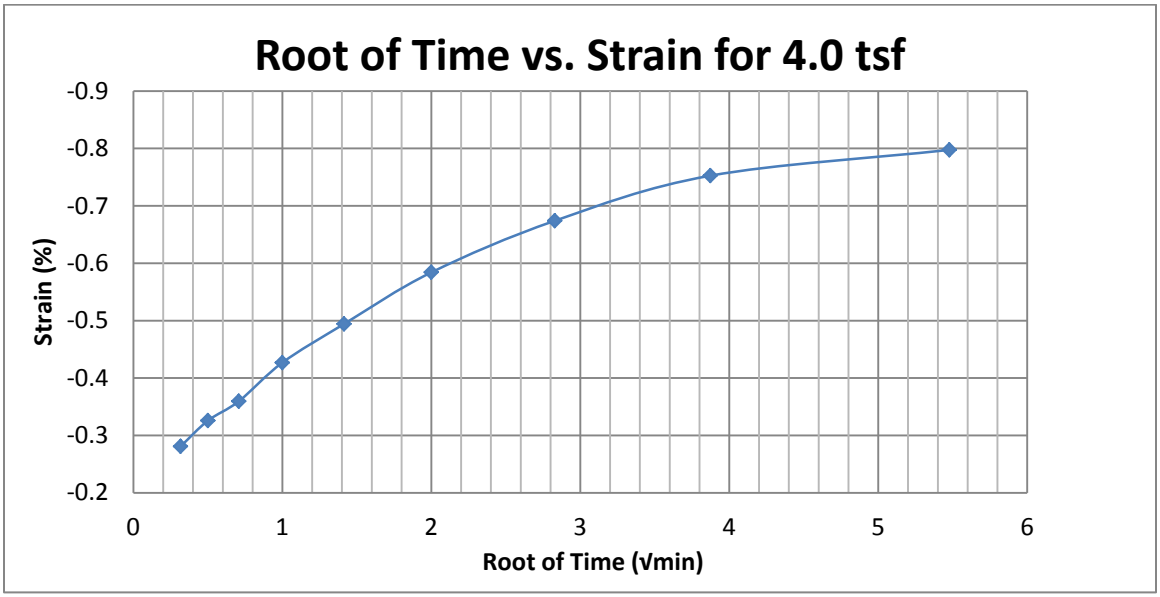

A116 Springville at 30-32 feet

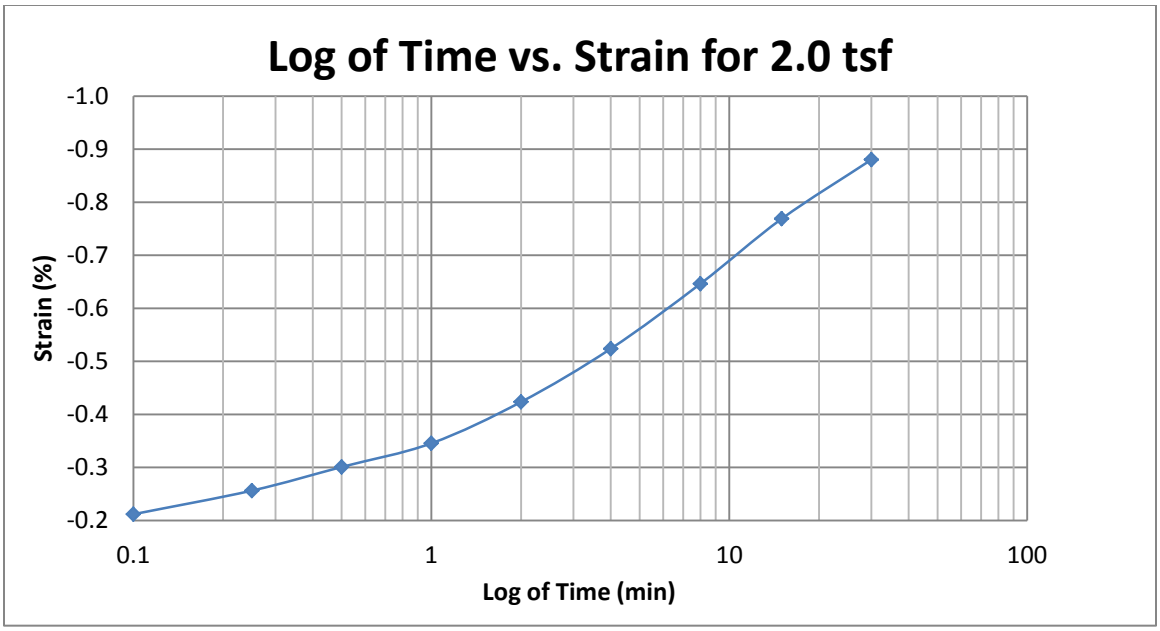

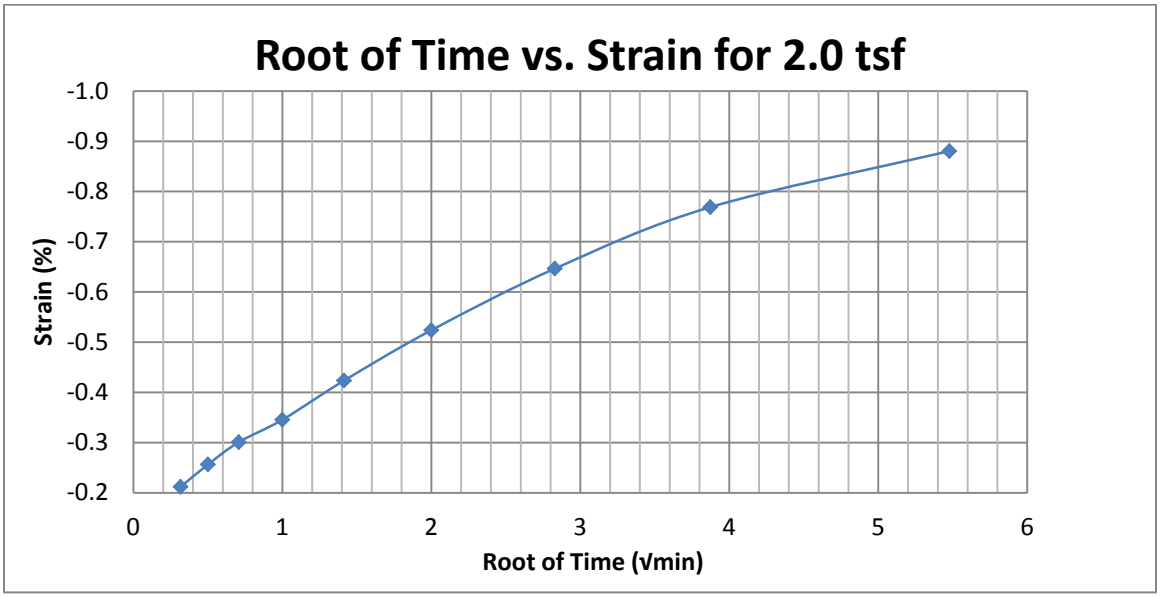

A117 Springville at 30-32 feet

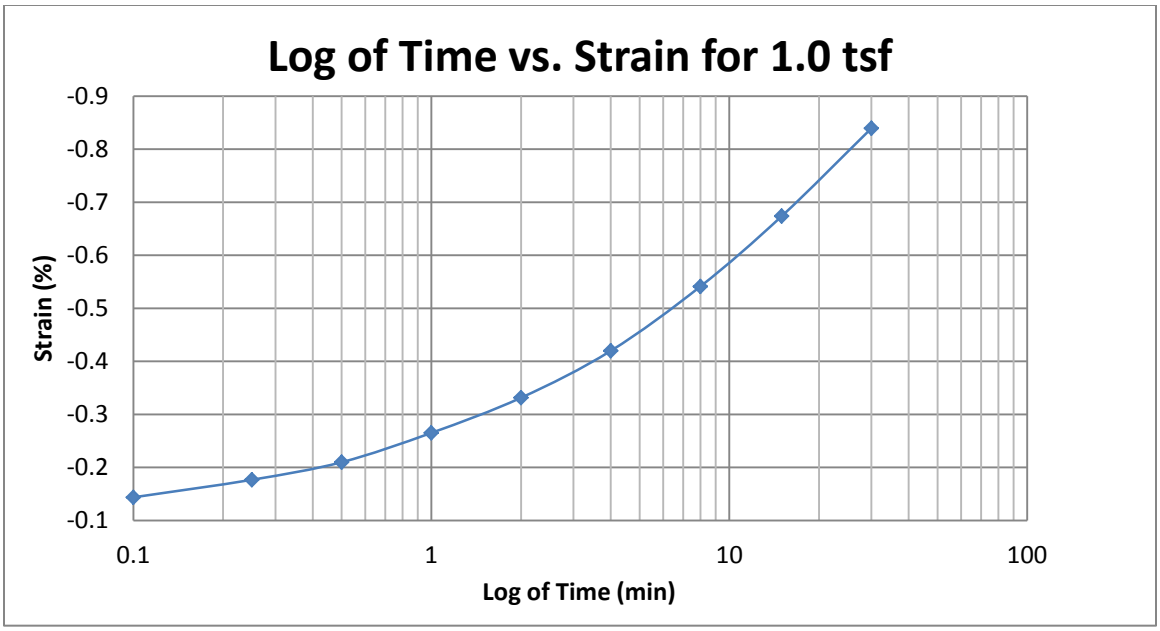

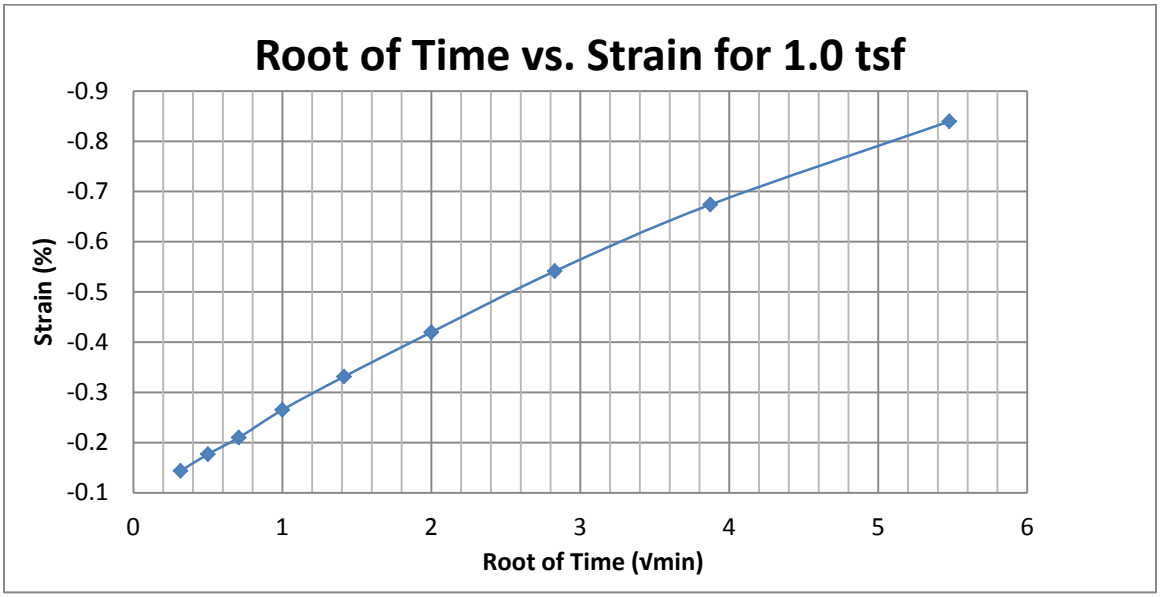

A118 Springville at 30-32 feet

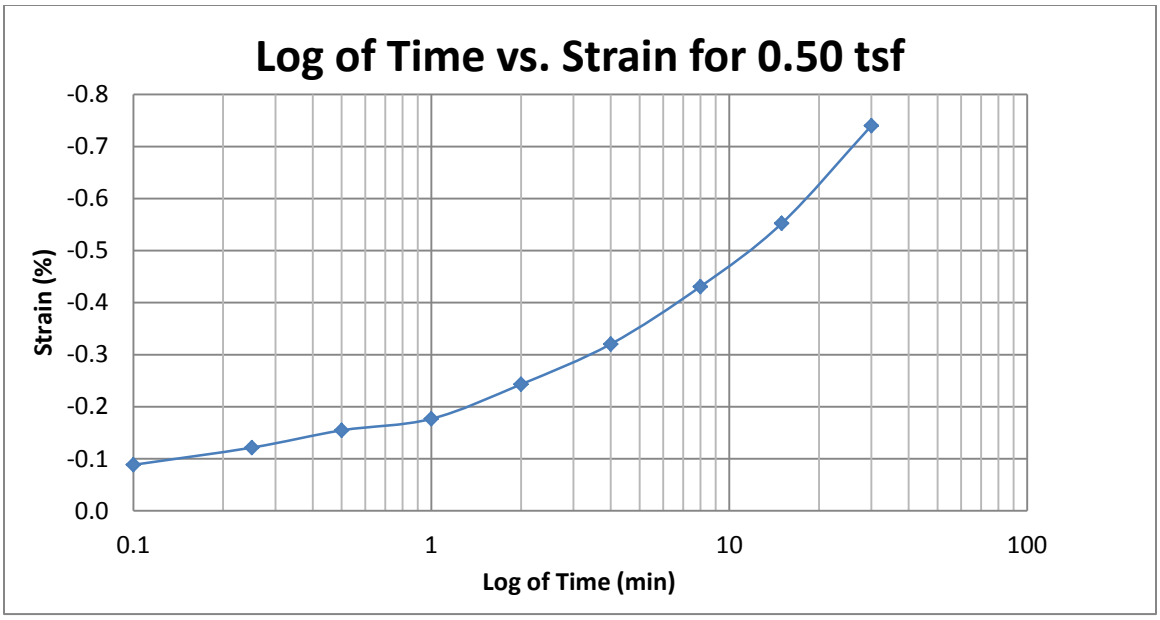

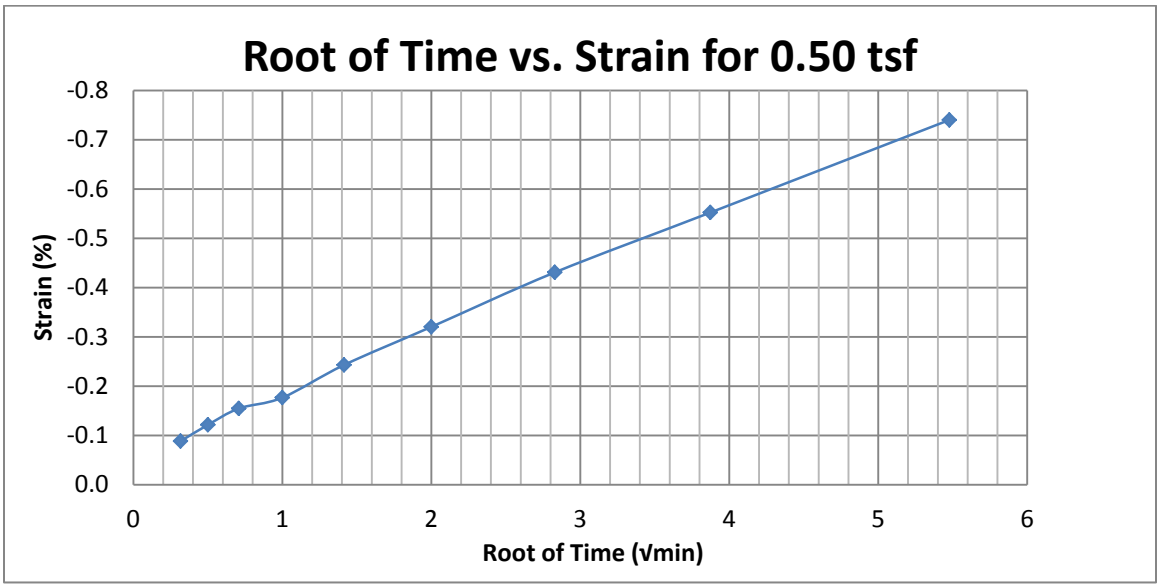

A119 Springville at 30-32 feet

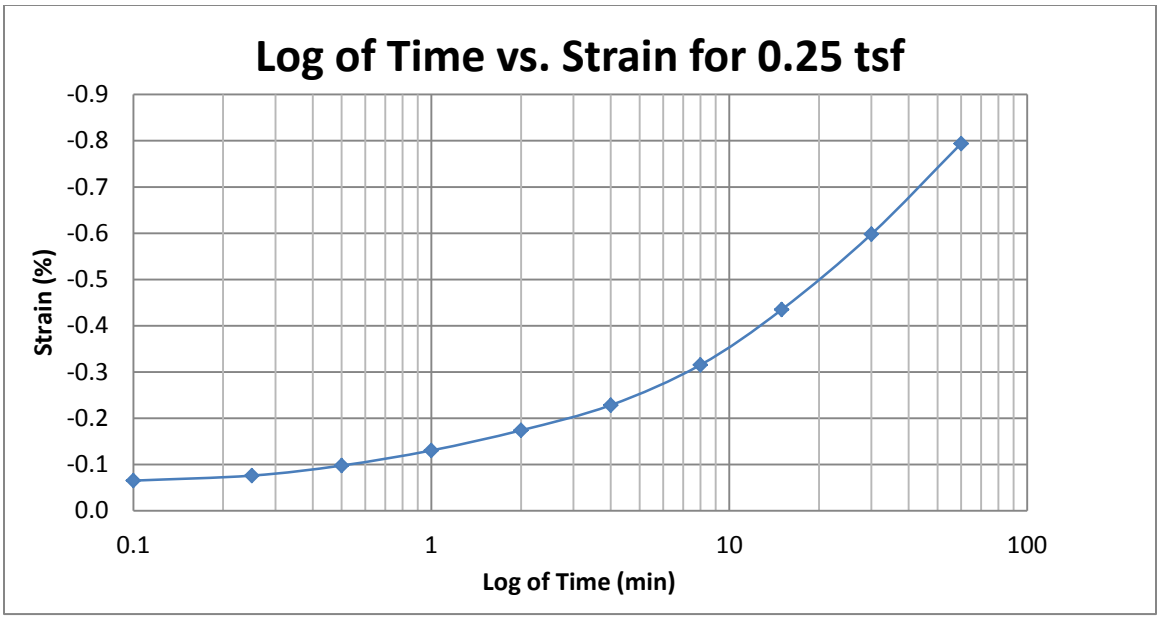

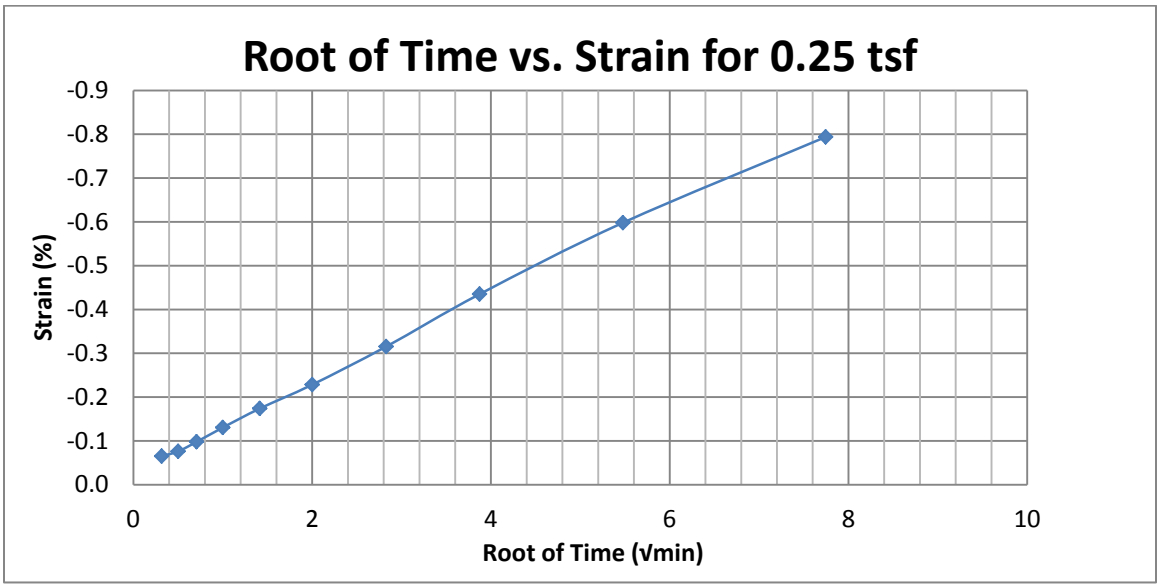

A120 Springville at 30-32 feet

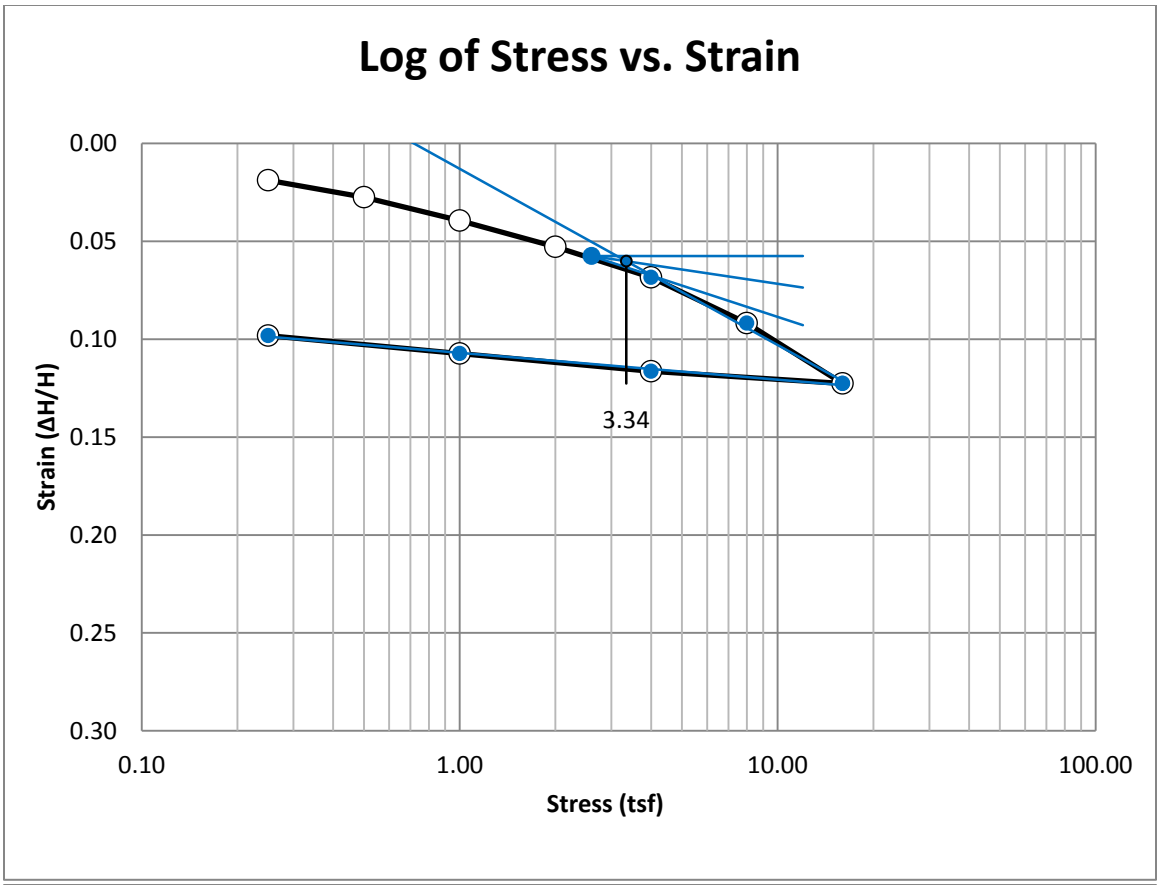

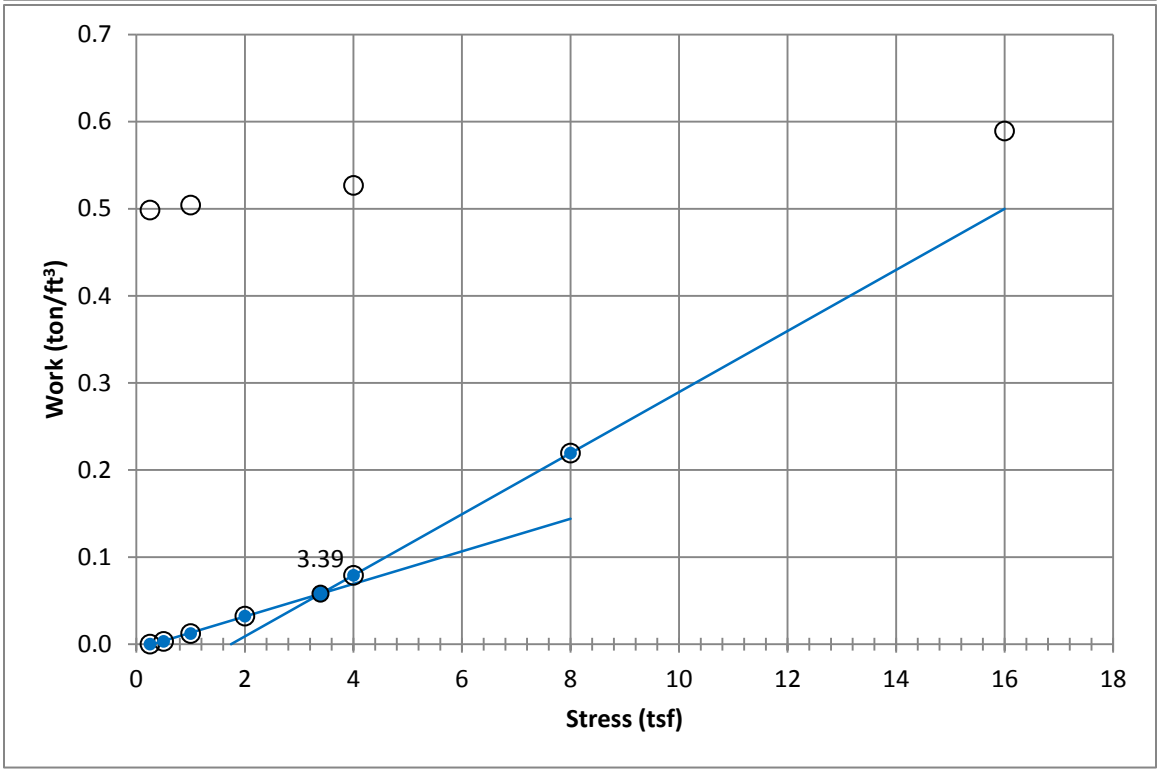

A121 Springville at 40-42 feet

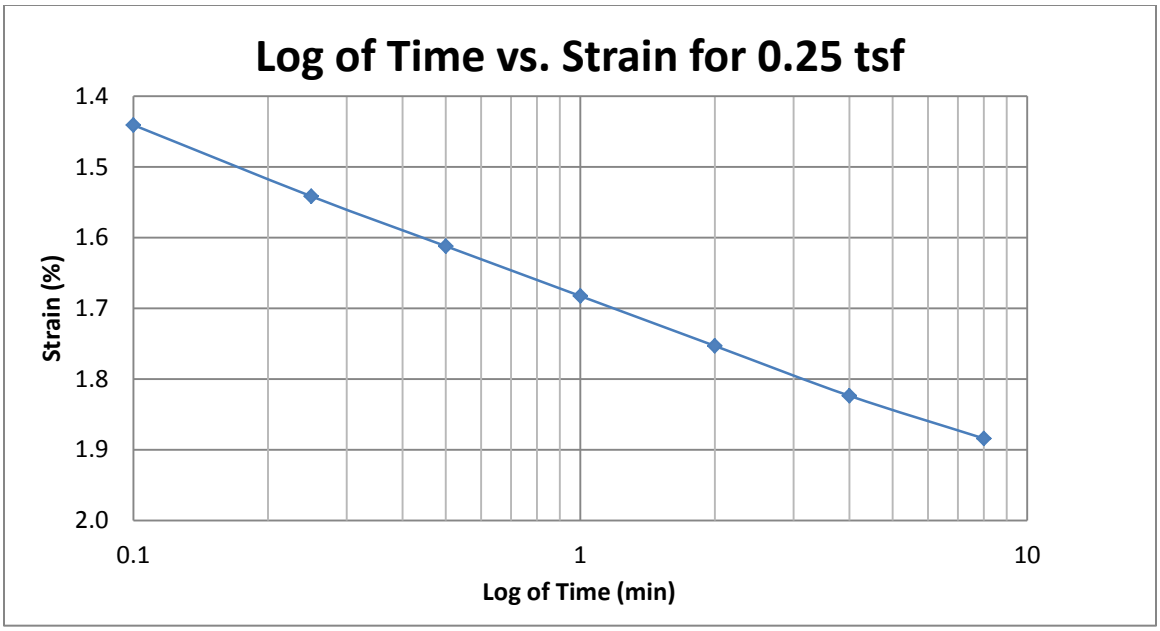

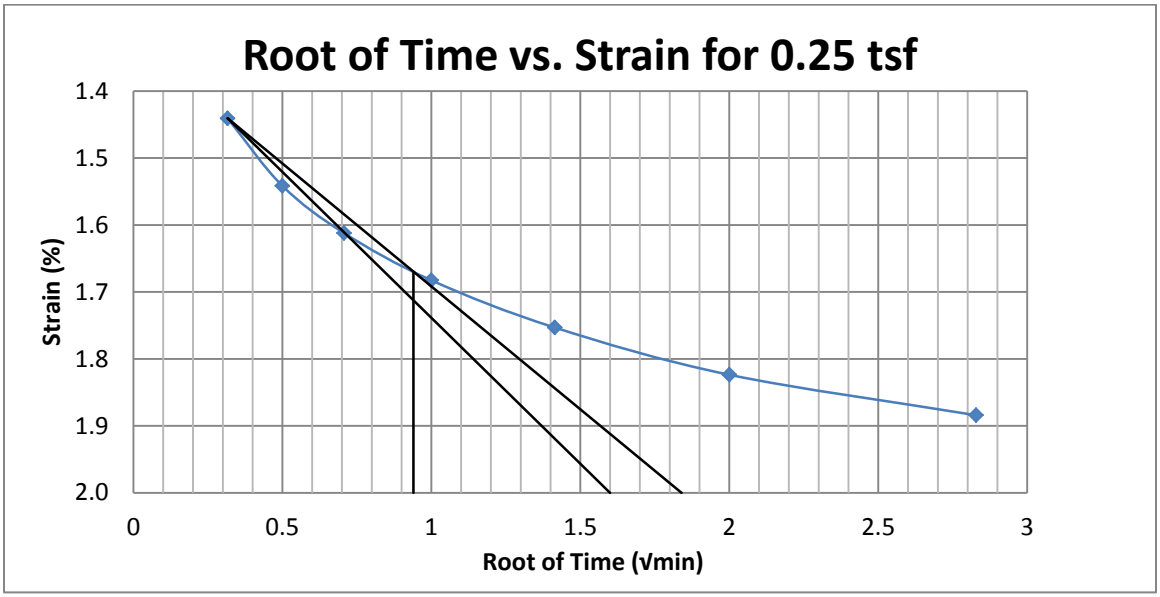

A122 Springville at 40-42 feet

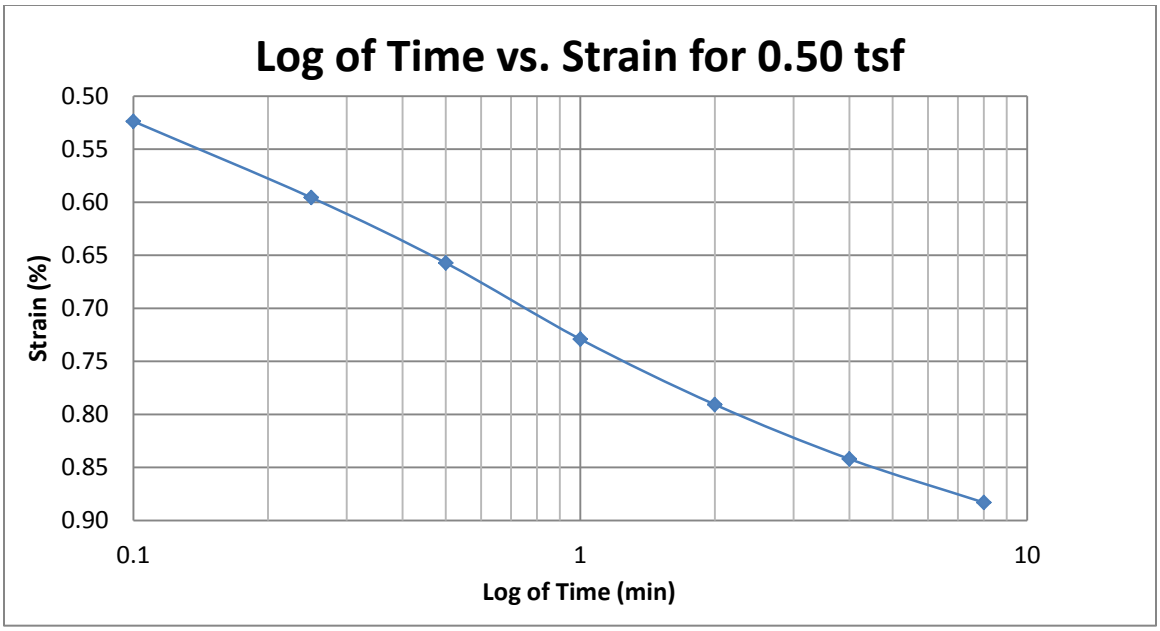

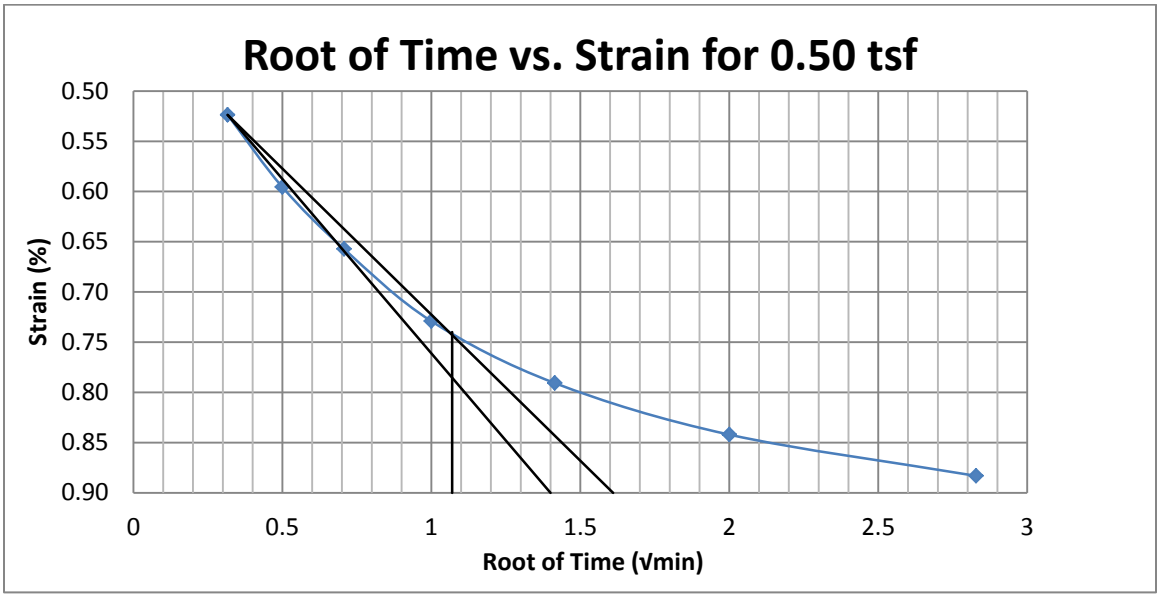

A123 Springville at 40-42 feet

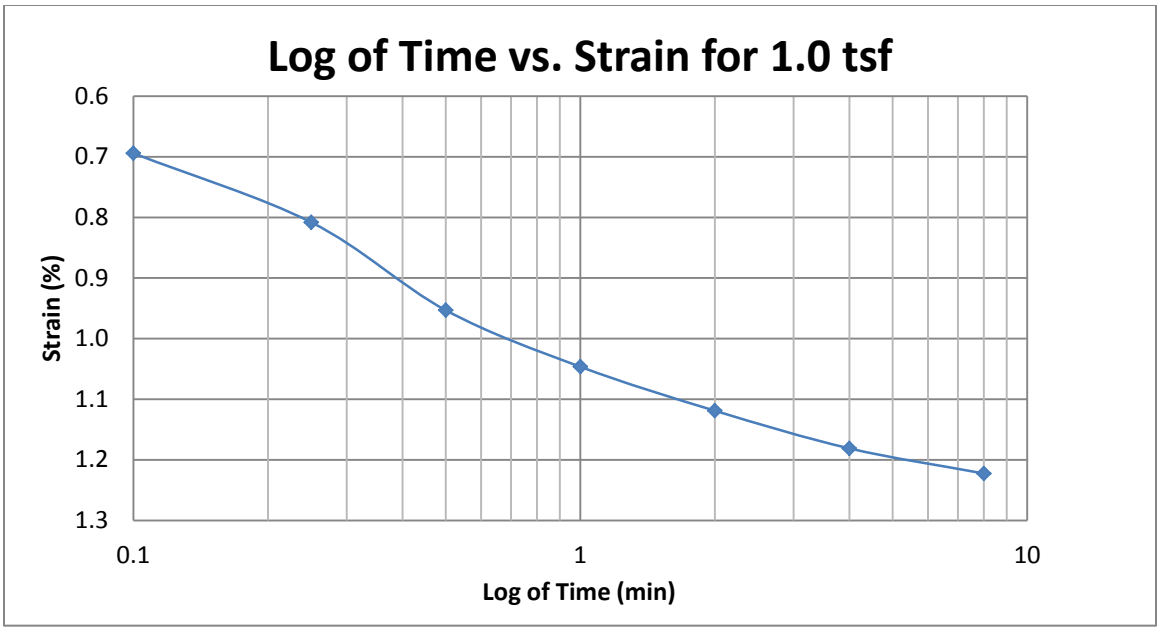

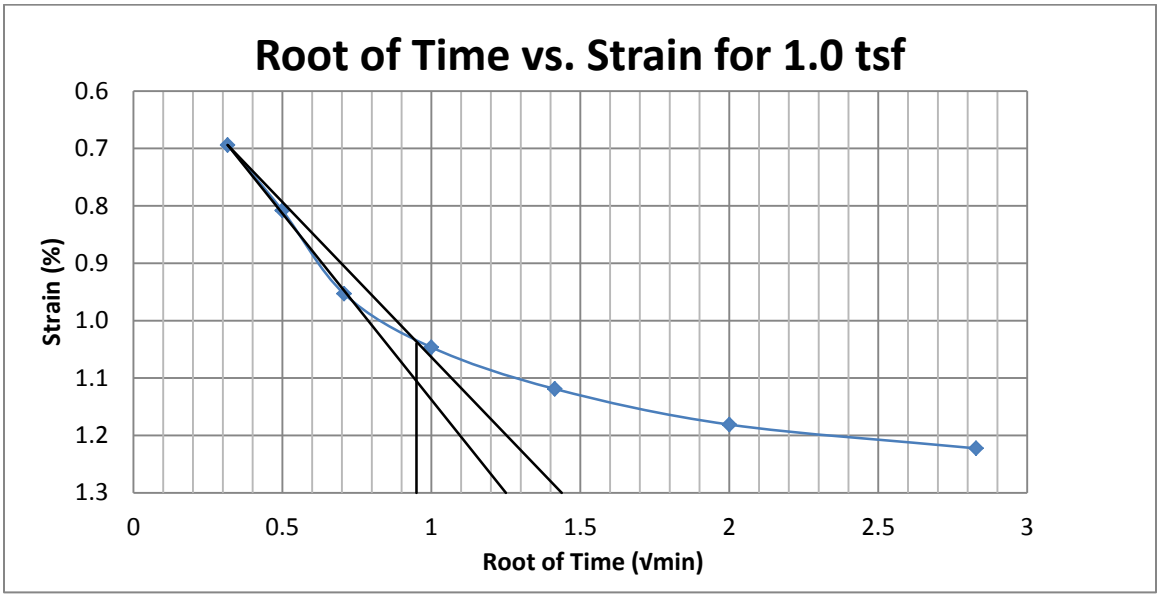

A124 Springville at 40-42 feet

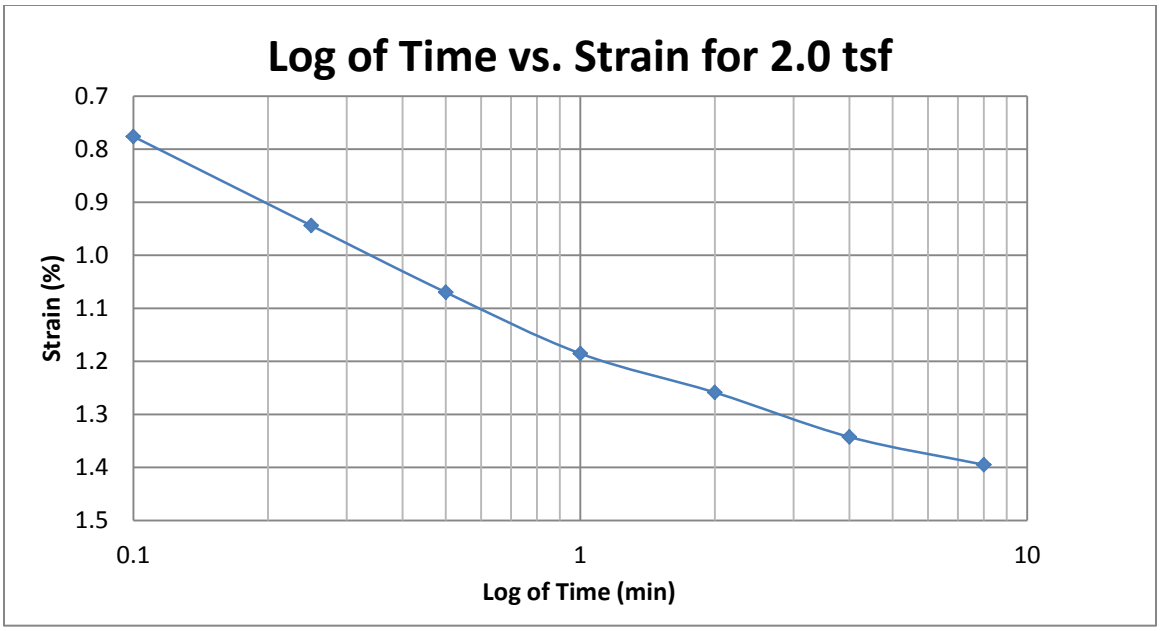

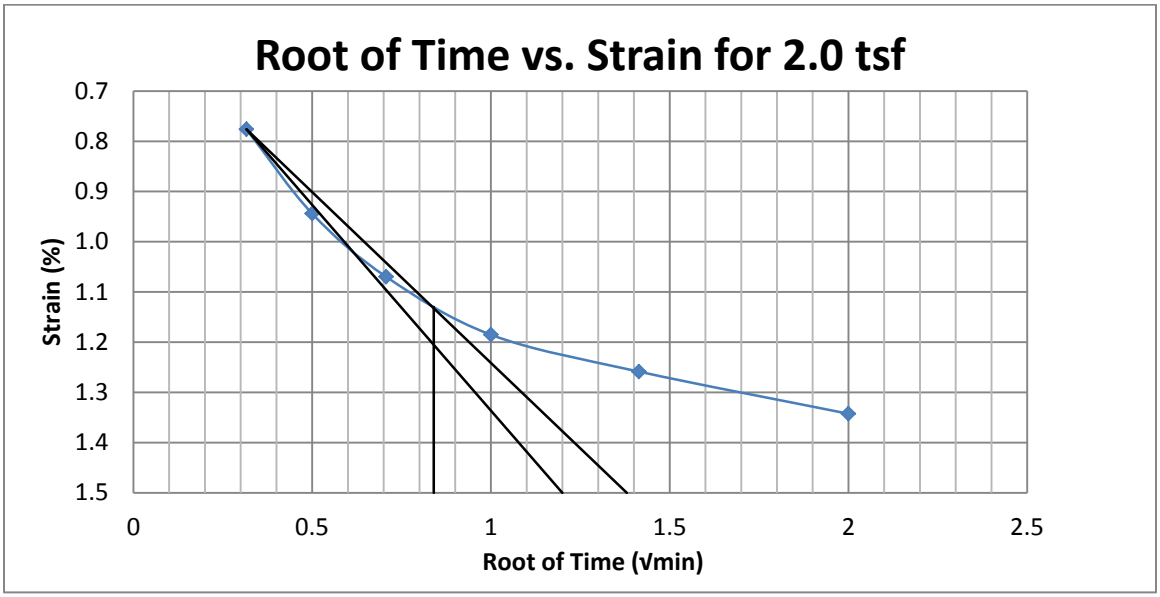

A125 Springville at 40-42 feet

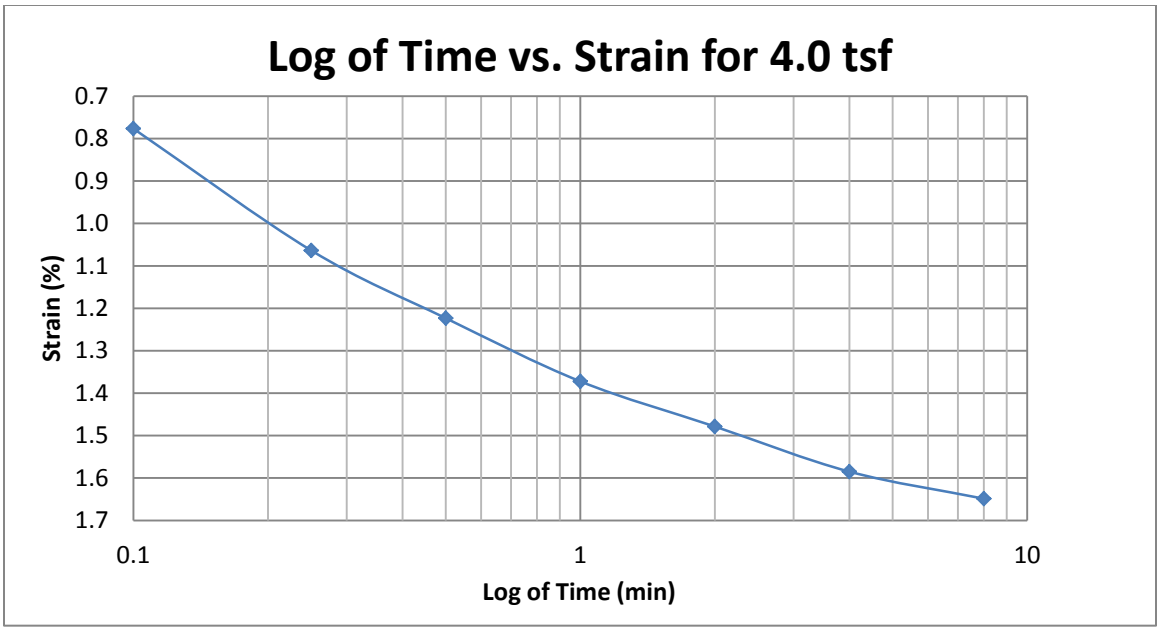

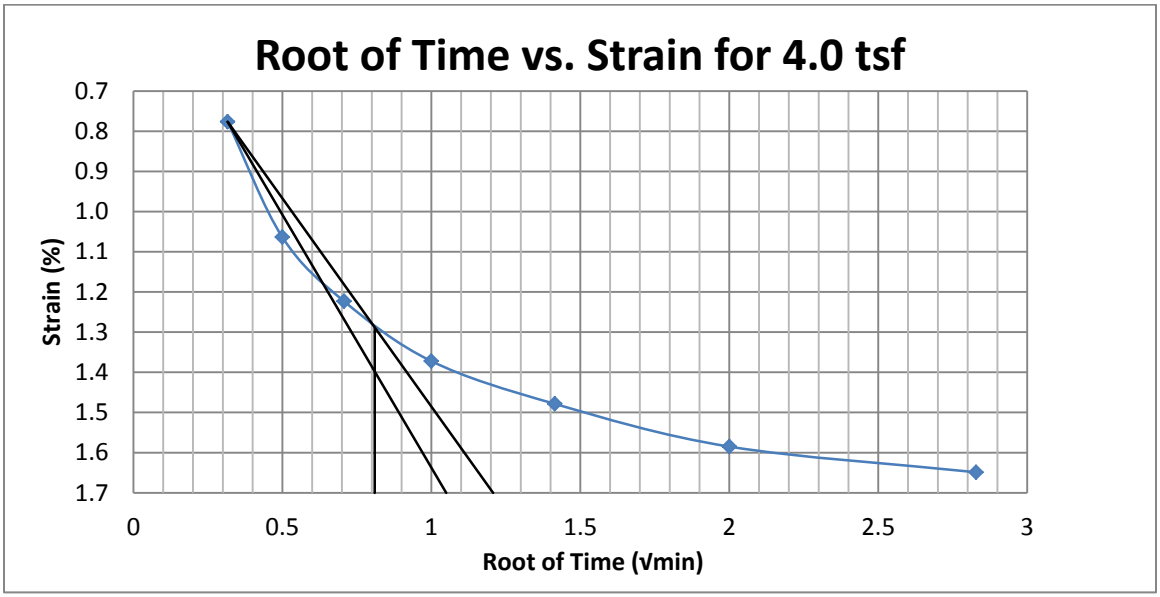

A126 Springville at 40-42 feet

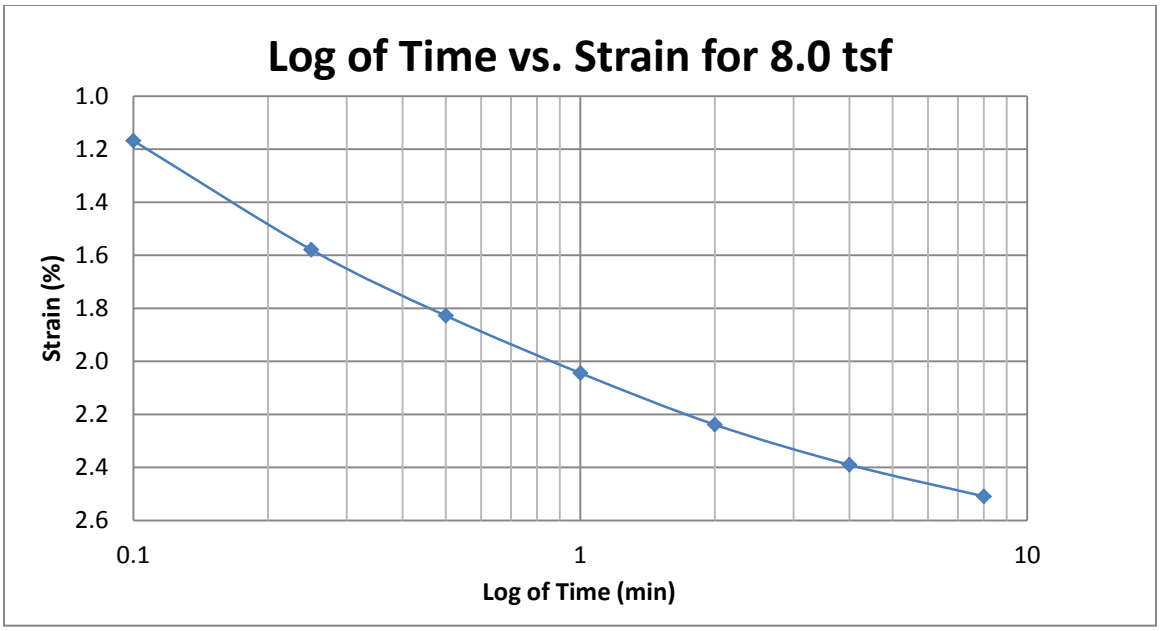

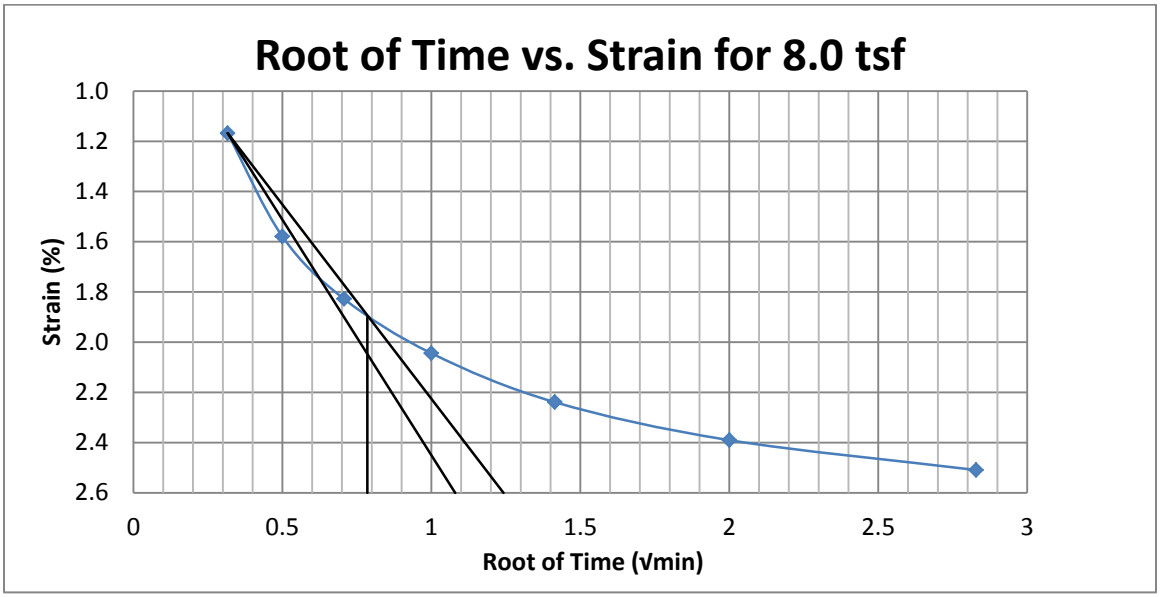

A127 Springville at 40-42 feet

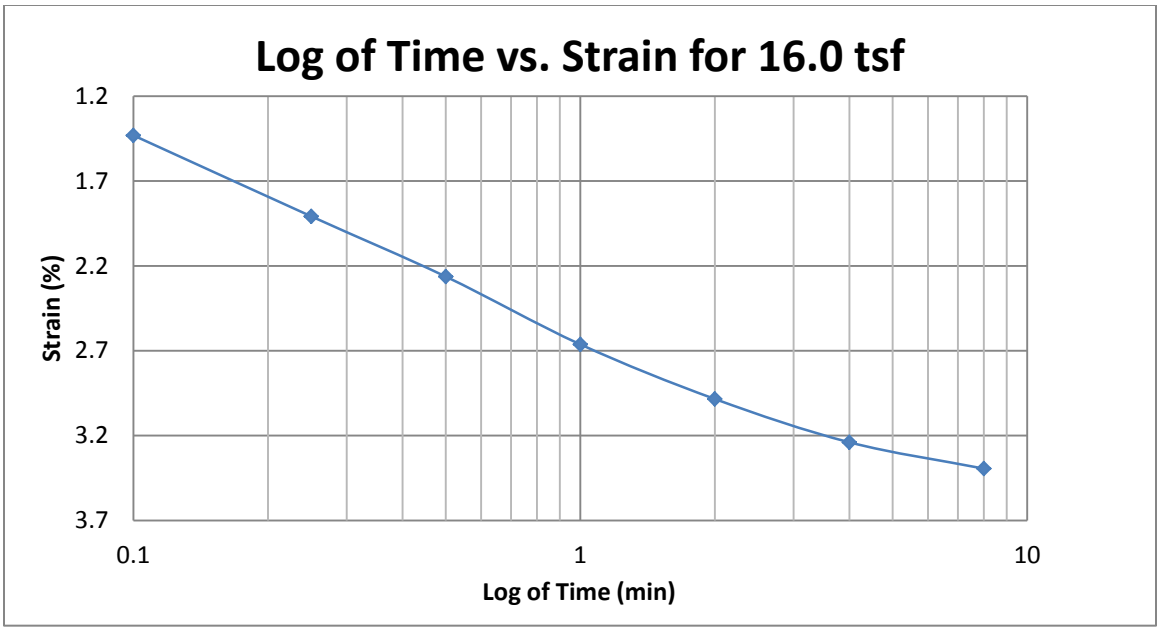

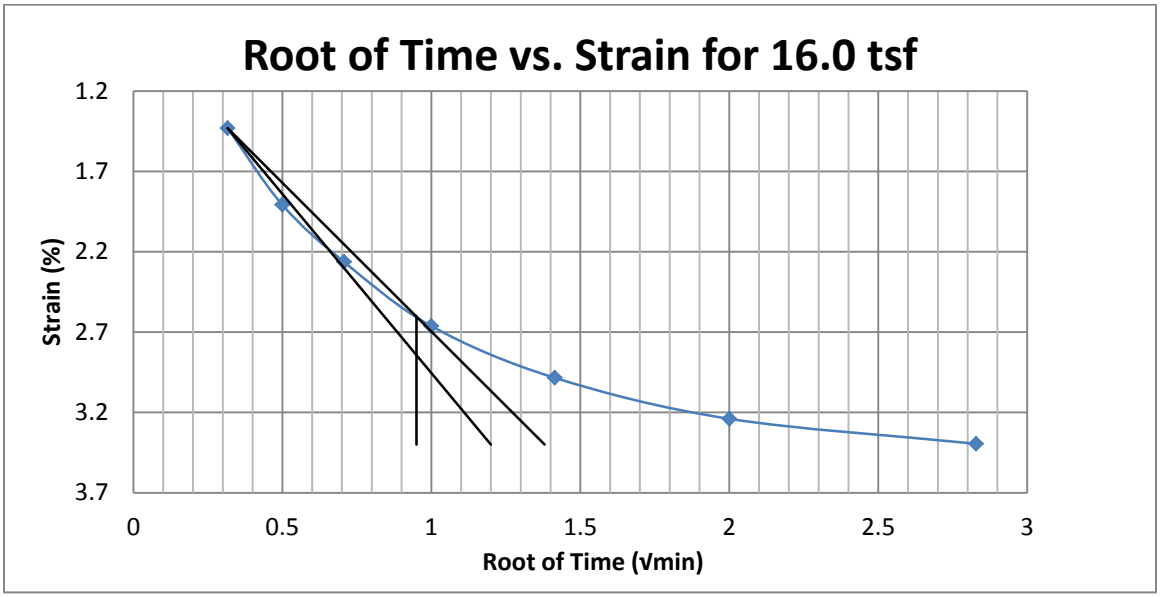

A128 Springville at 40-42 feet

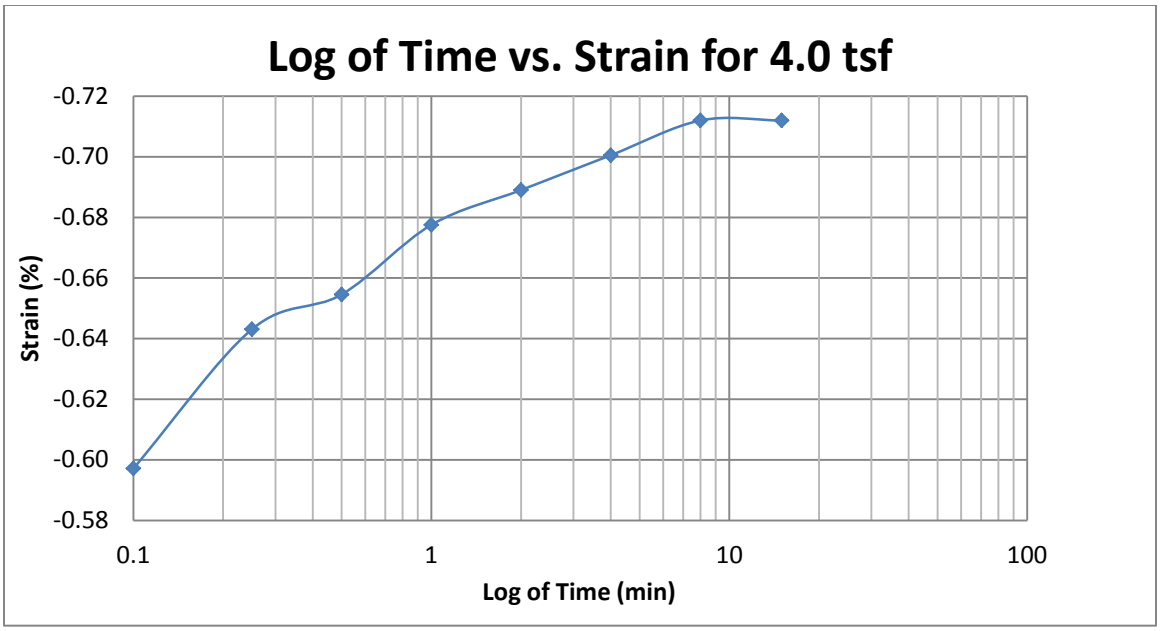

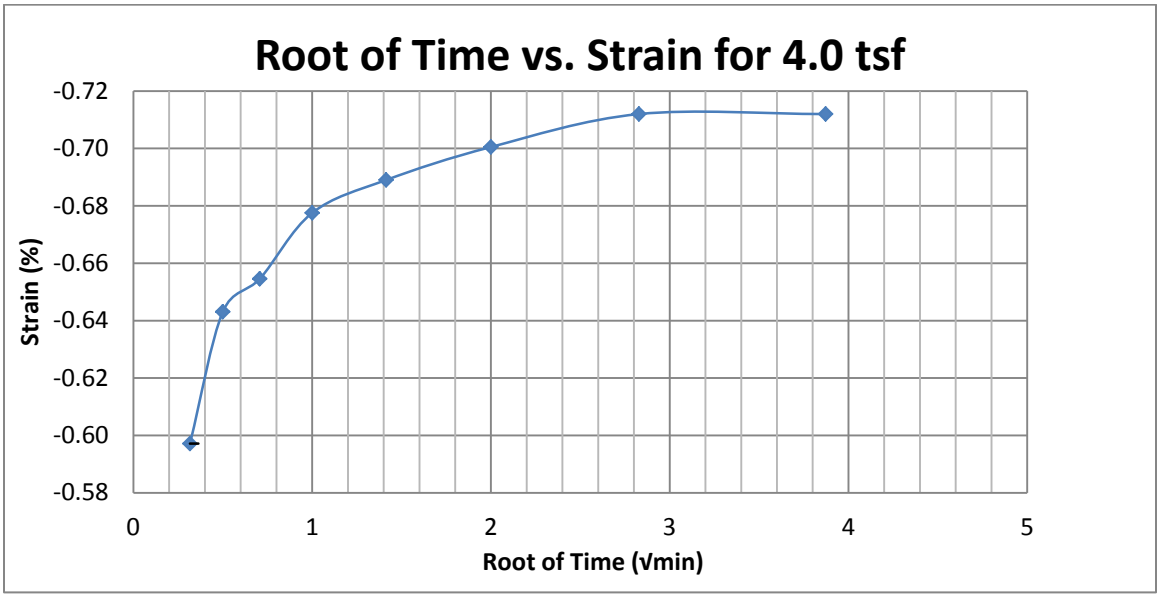

A129 Springville at 40-42 feet

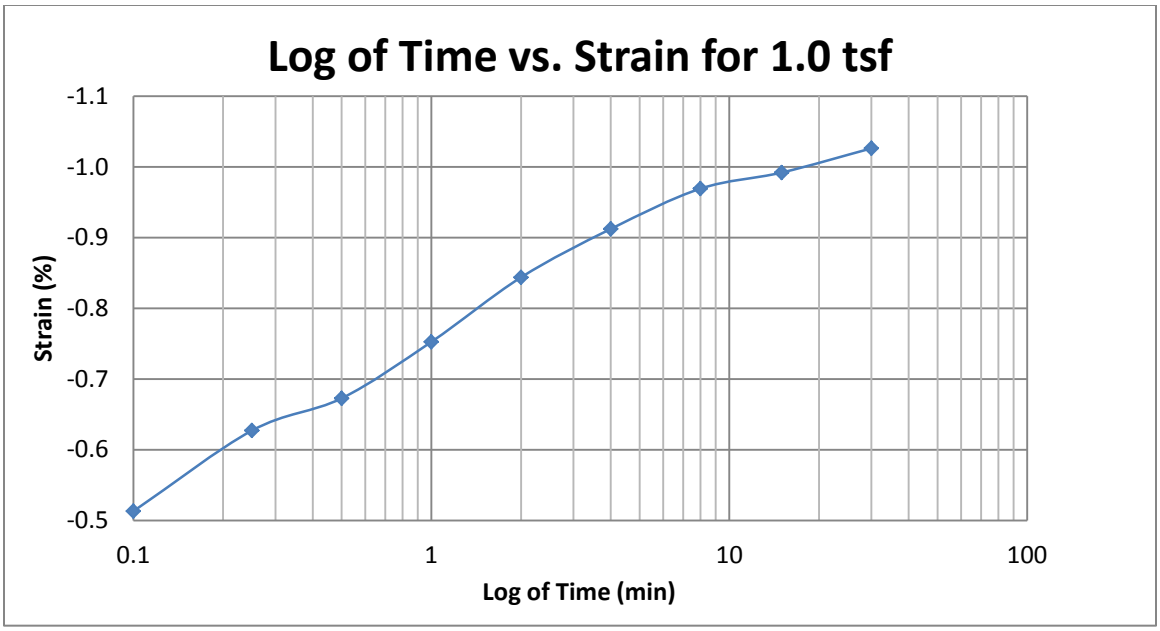

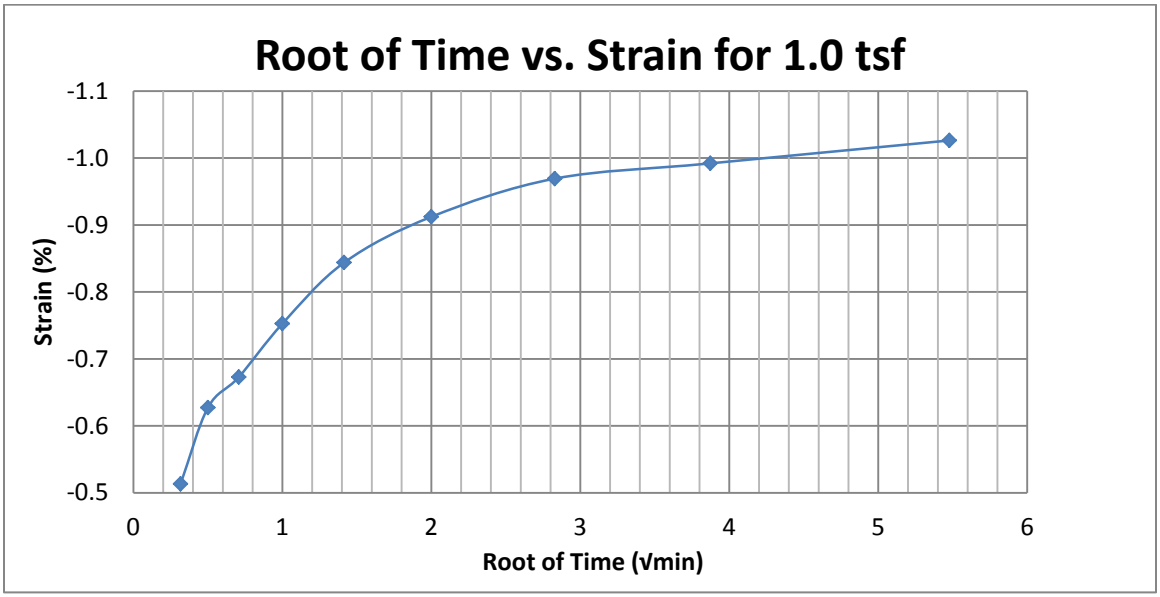

A130 Springville at 40-42 feet

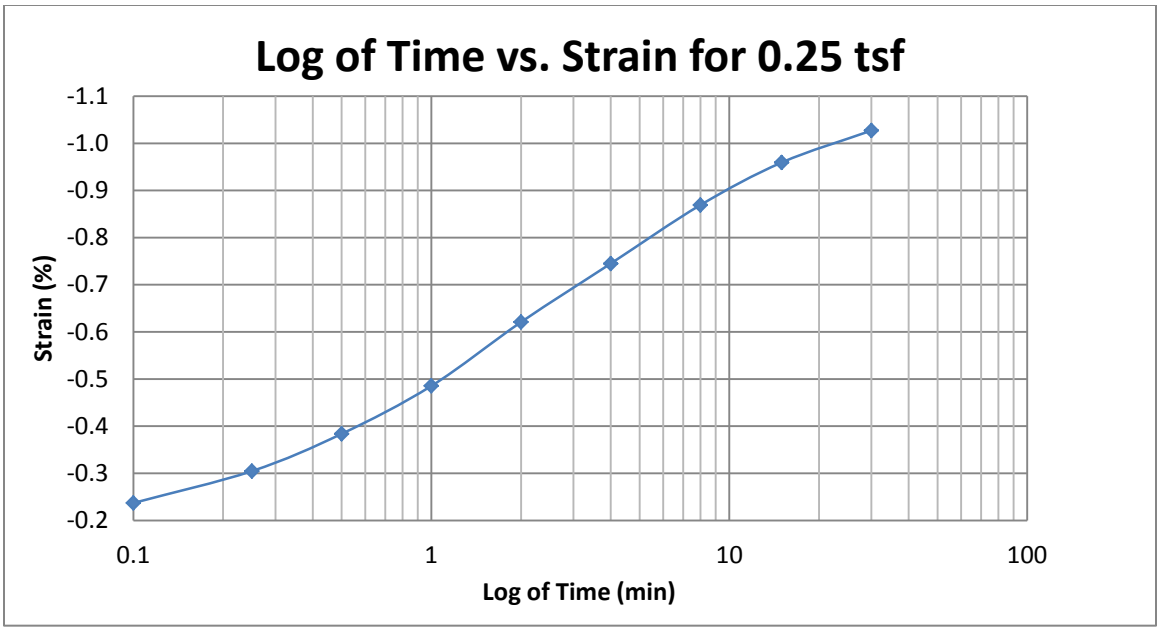

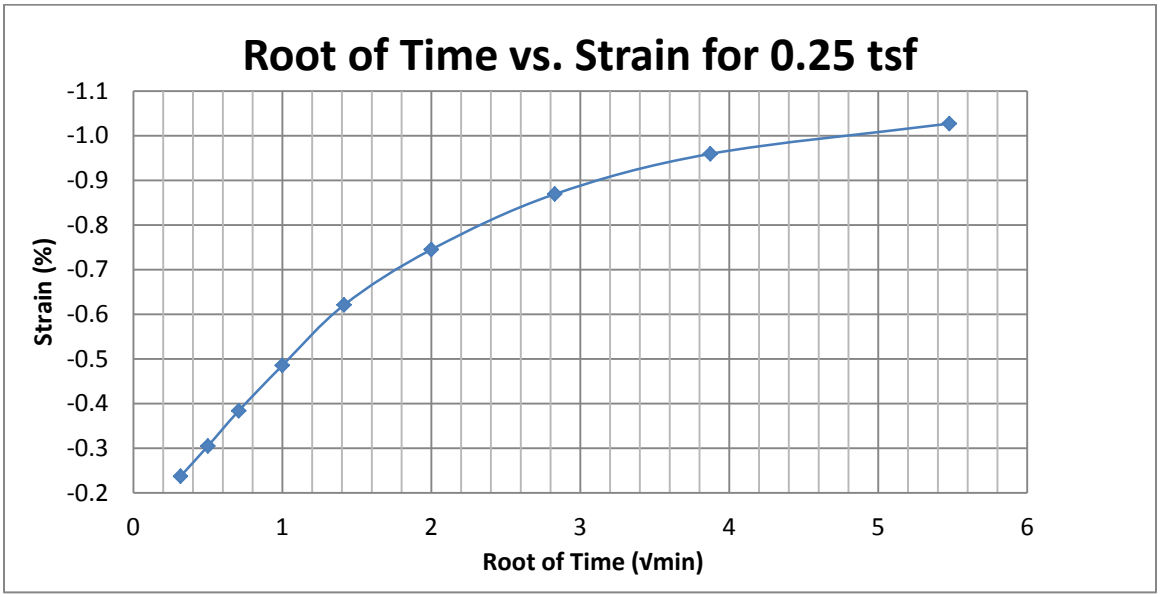

A131 Springville at 40-42 feet

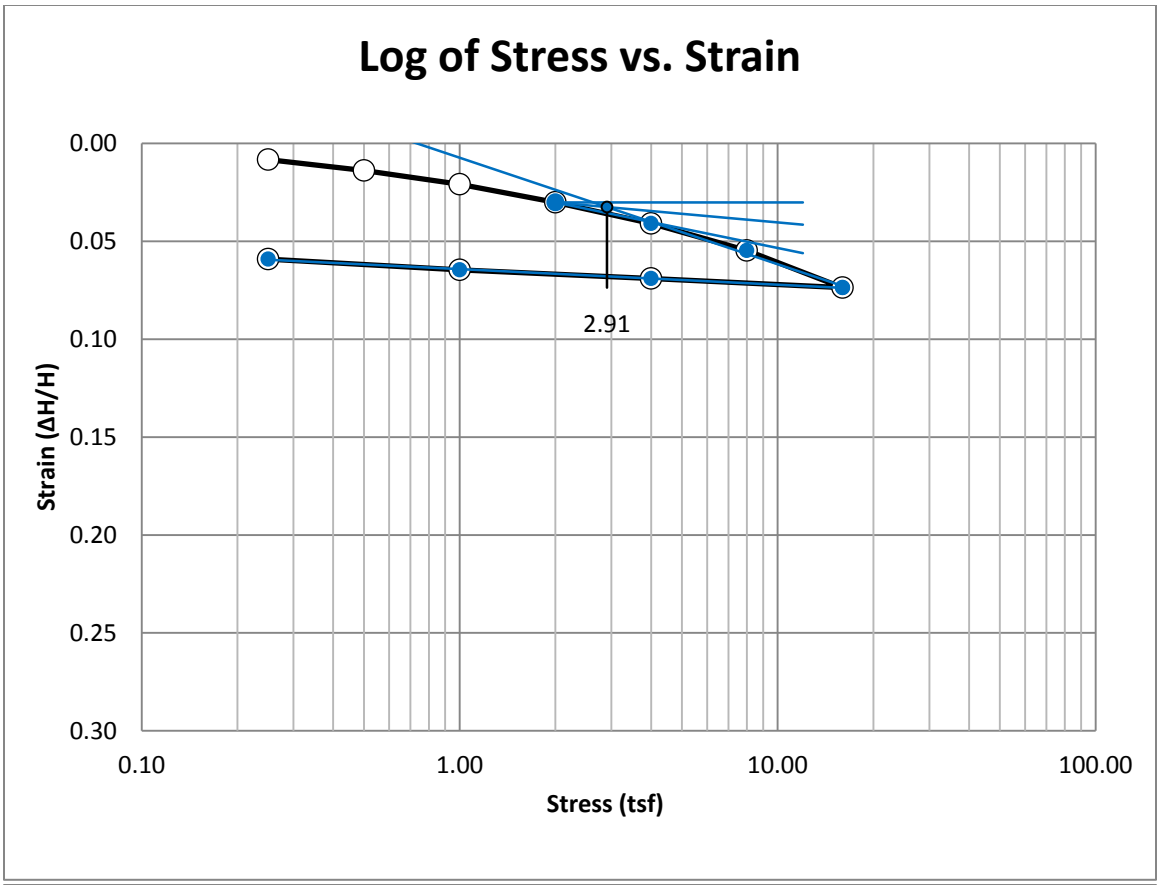

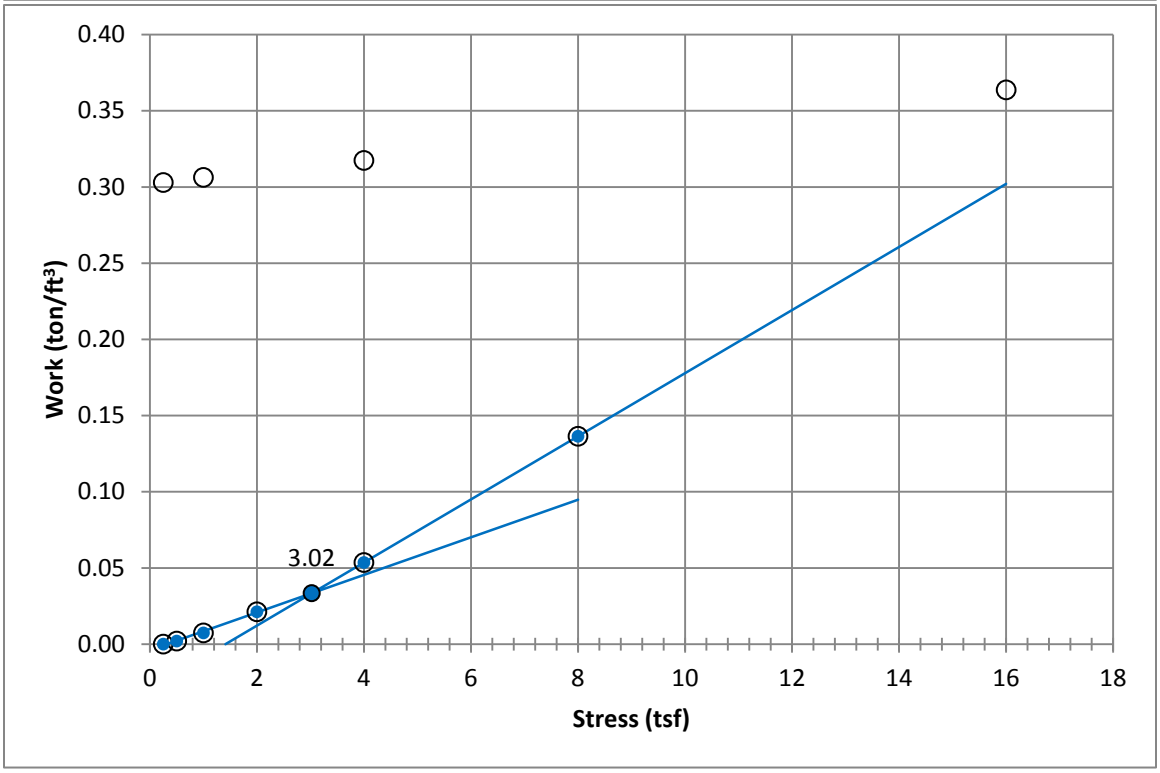

A132 Springville at 65-67 feet

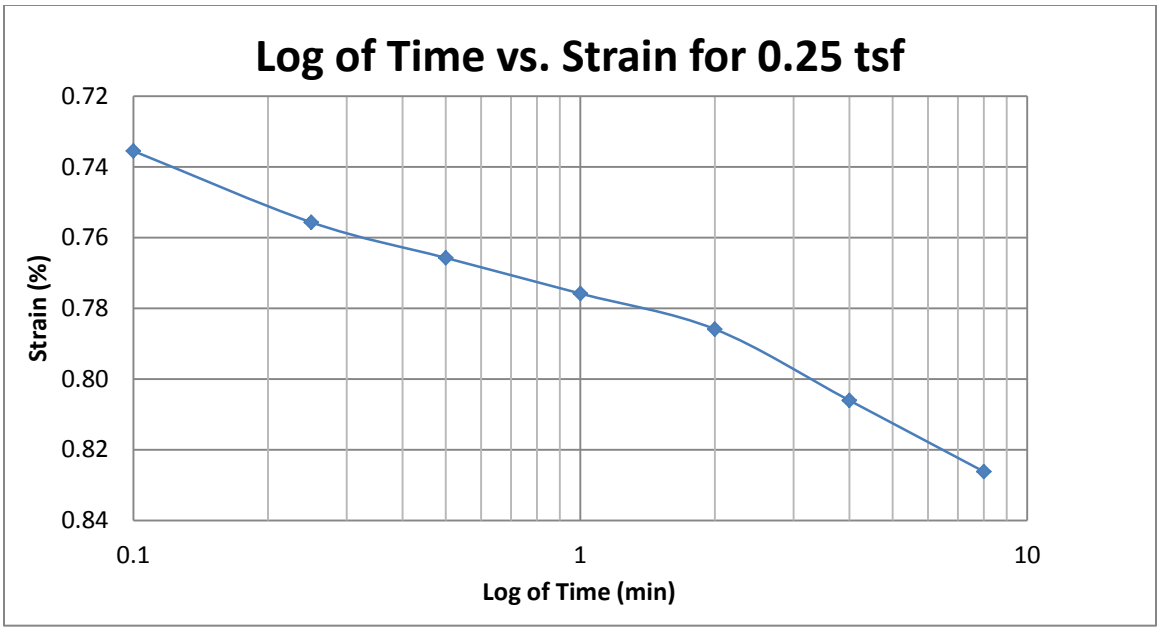

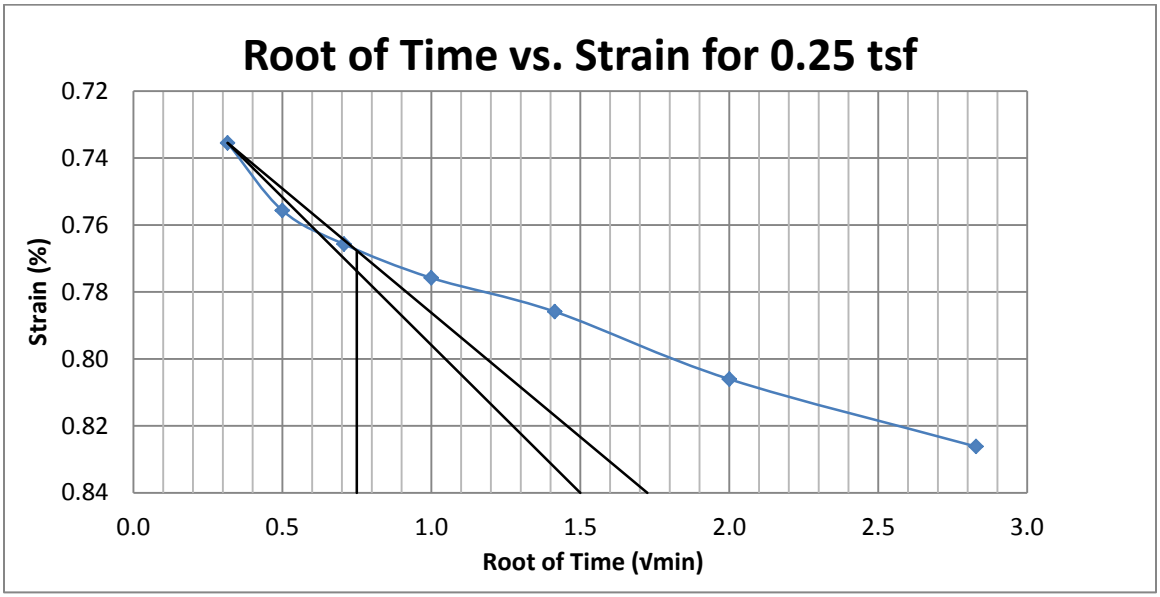

A133 Springville at 65-67 feet

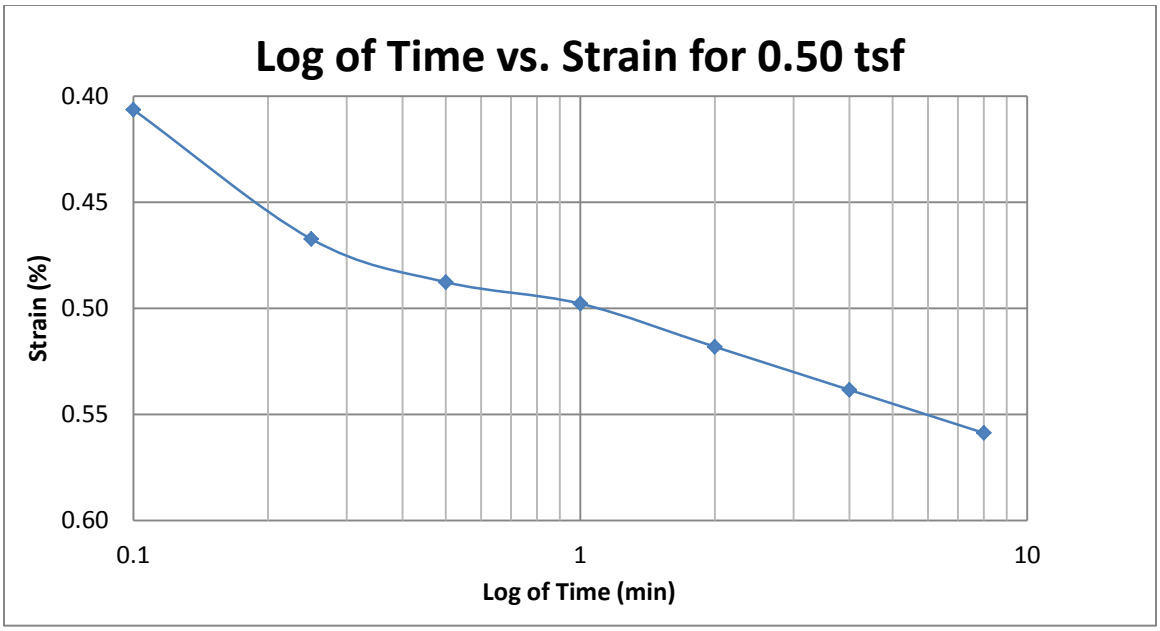

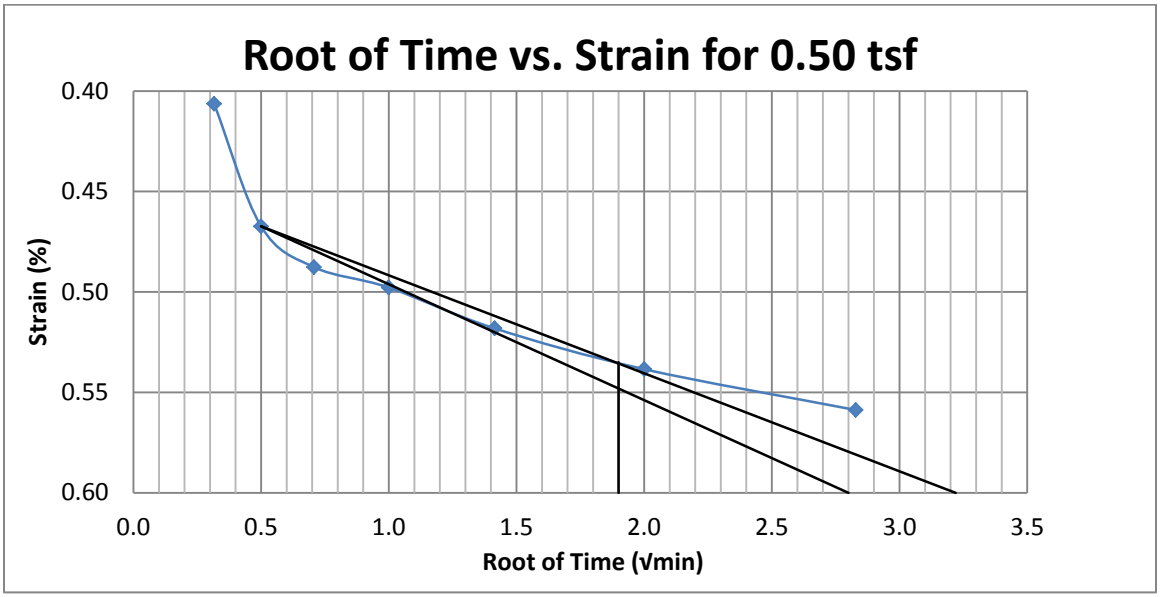

A134 Springville at 65-67 feet

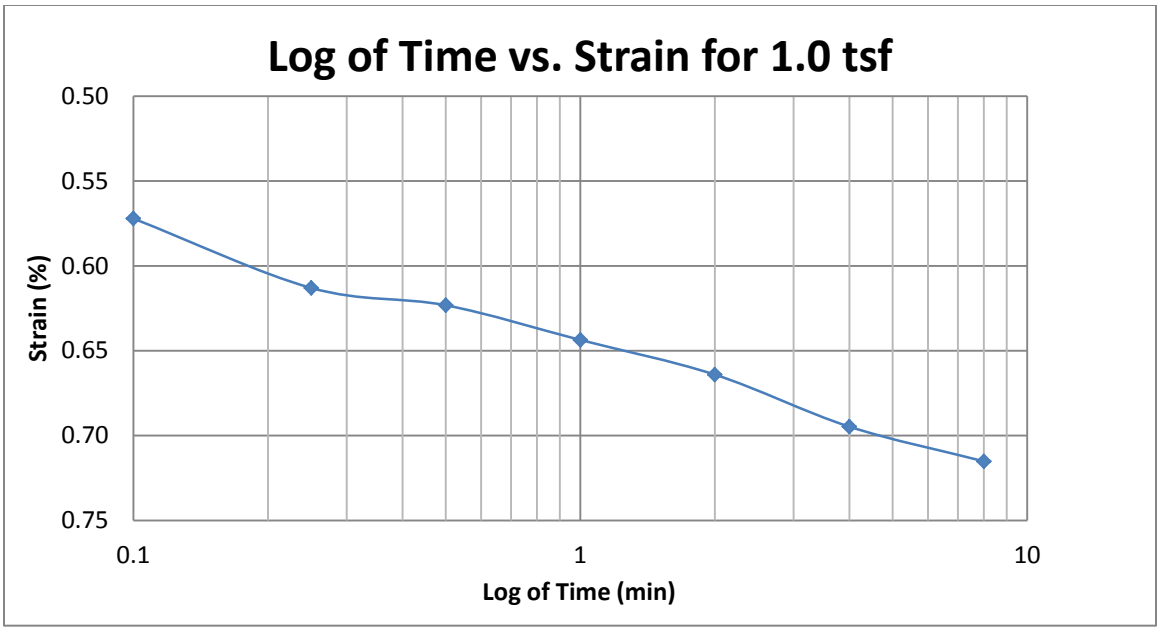

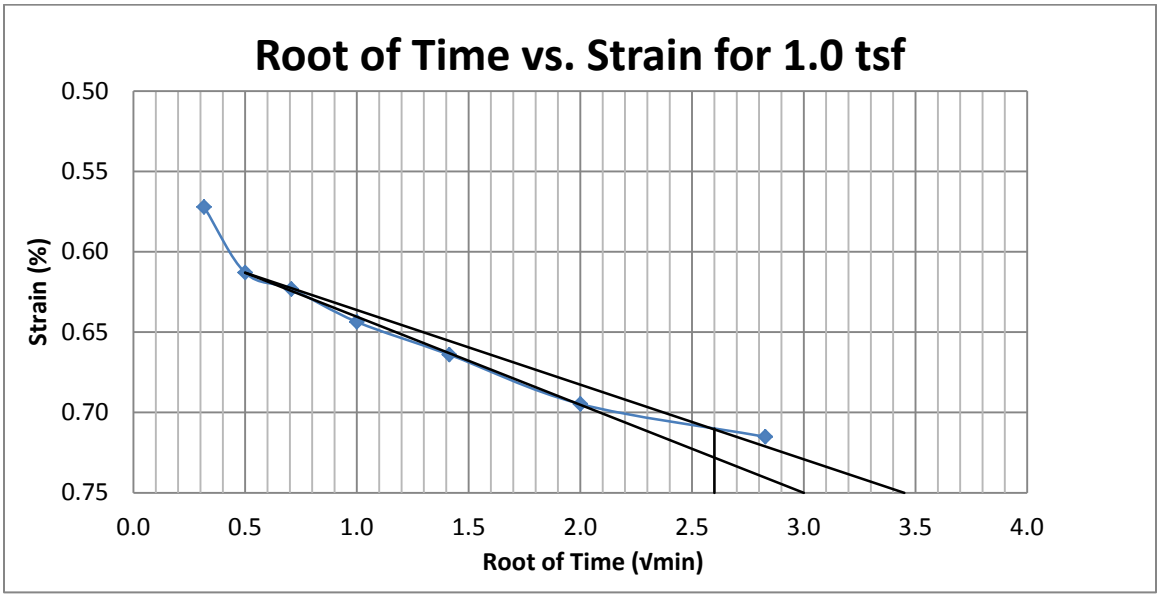

A135 Springville at 65-67 feet

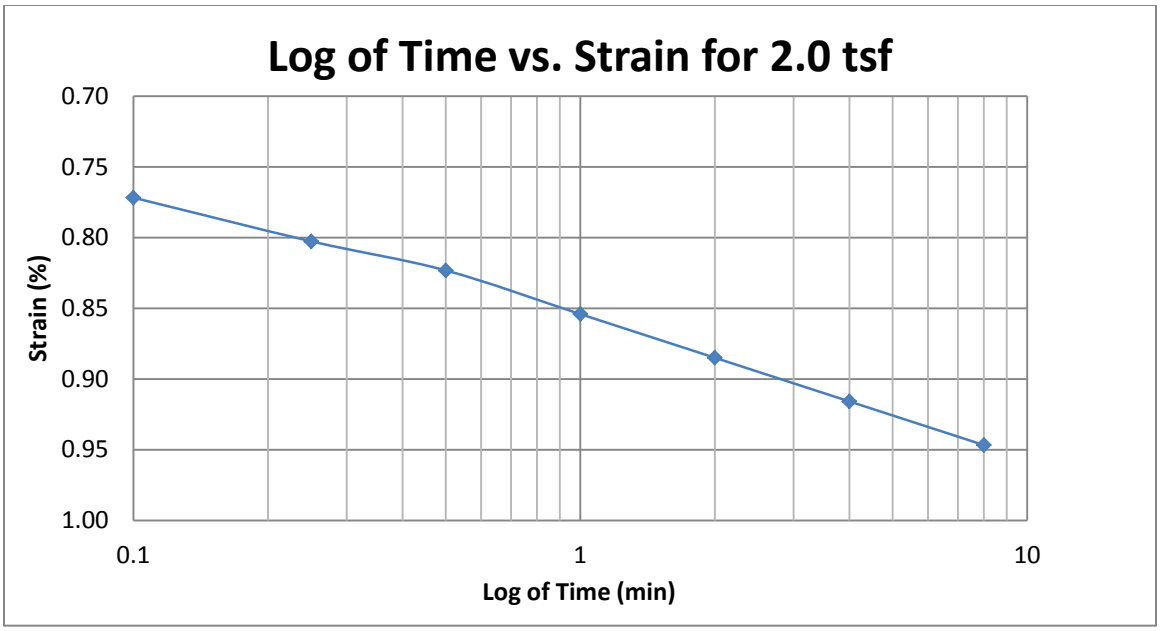

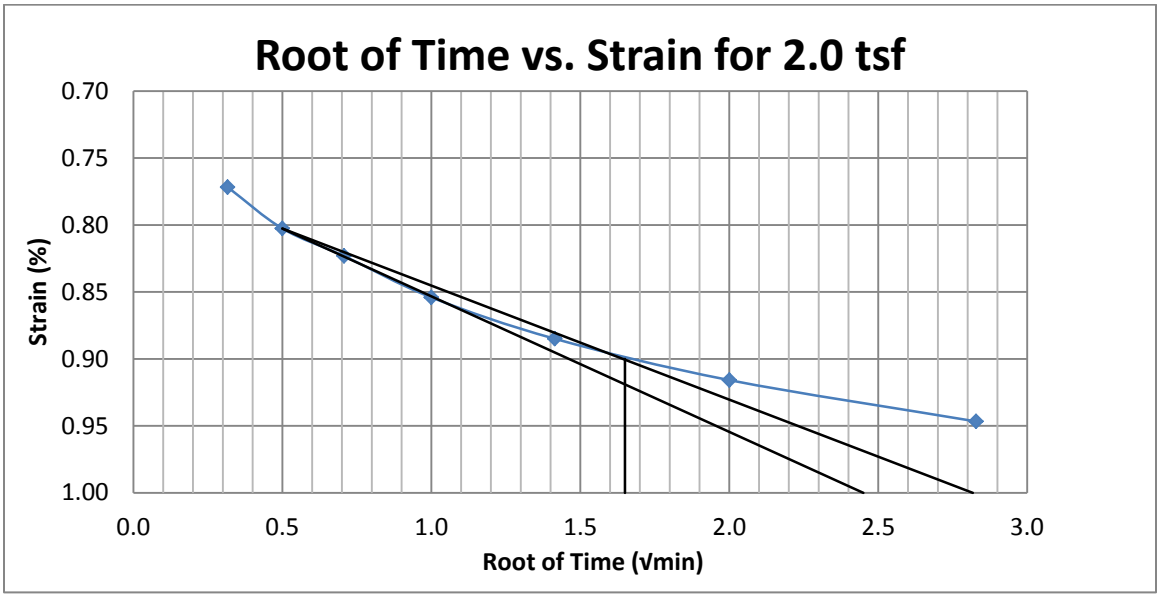

A136 Springville at 65-67 feet

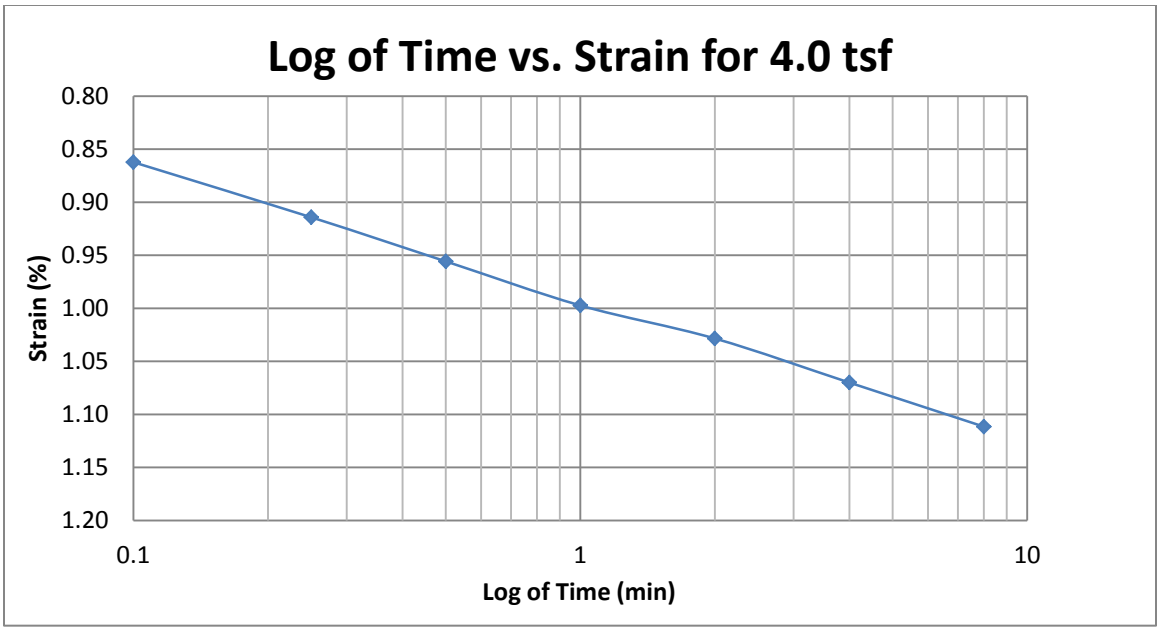

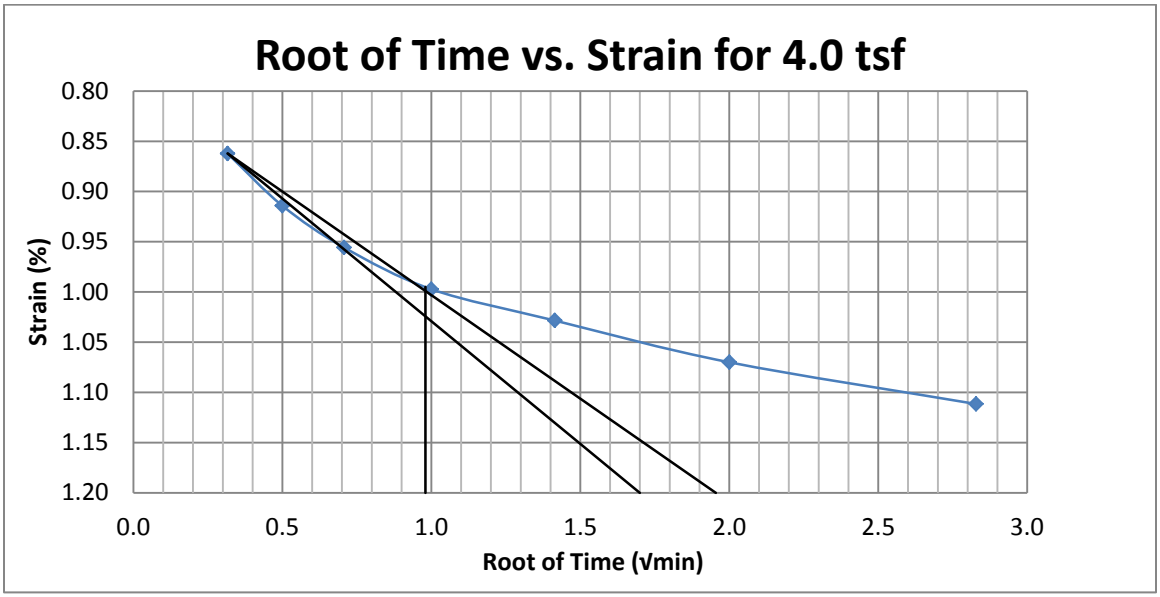

A137 Springville at 65-67 feet

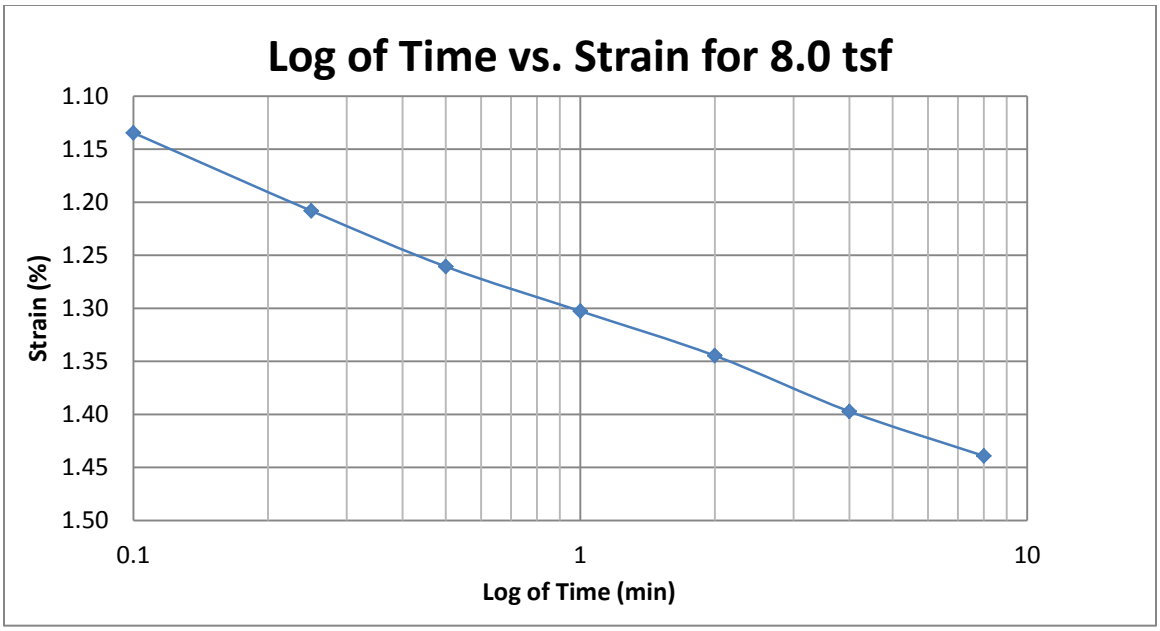

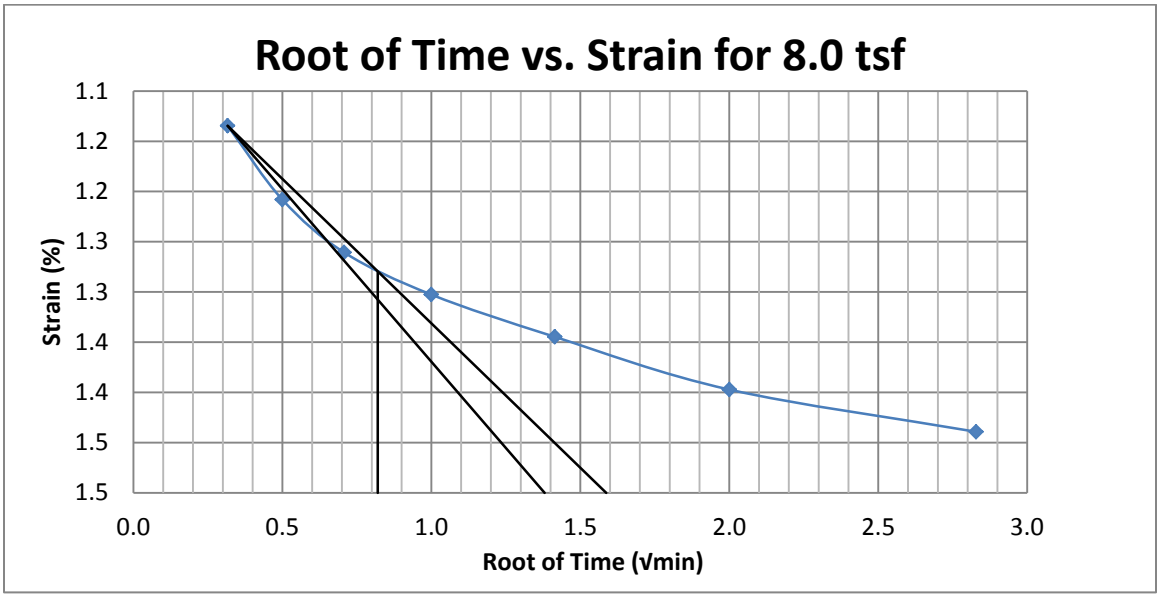

A138 Springville at 65-67 feet

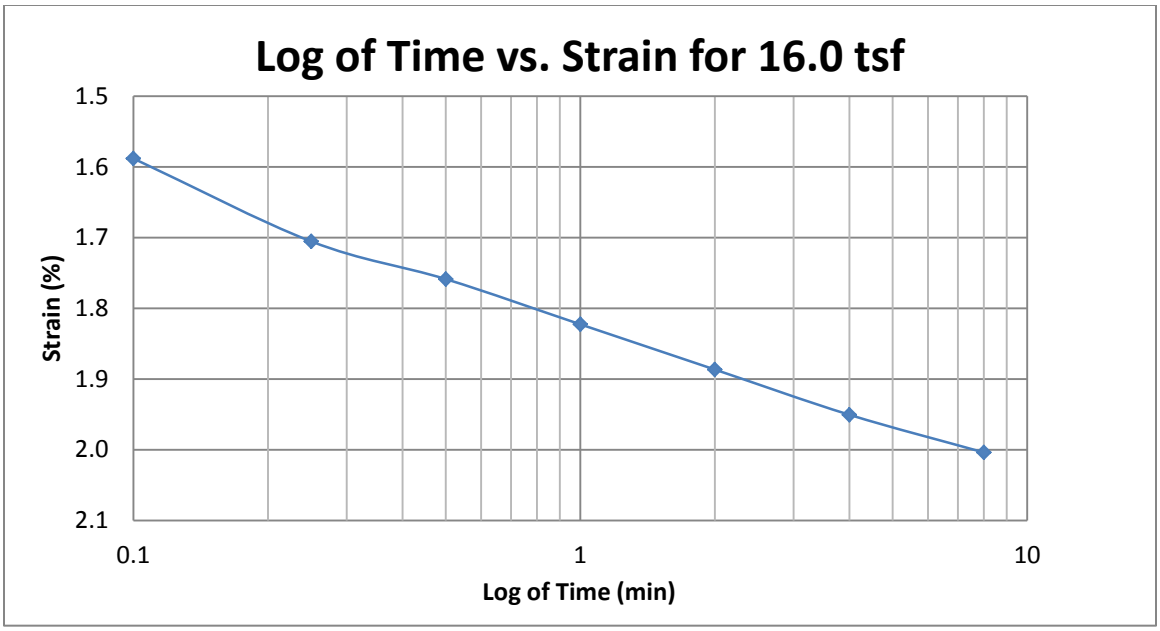

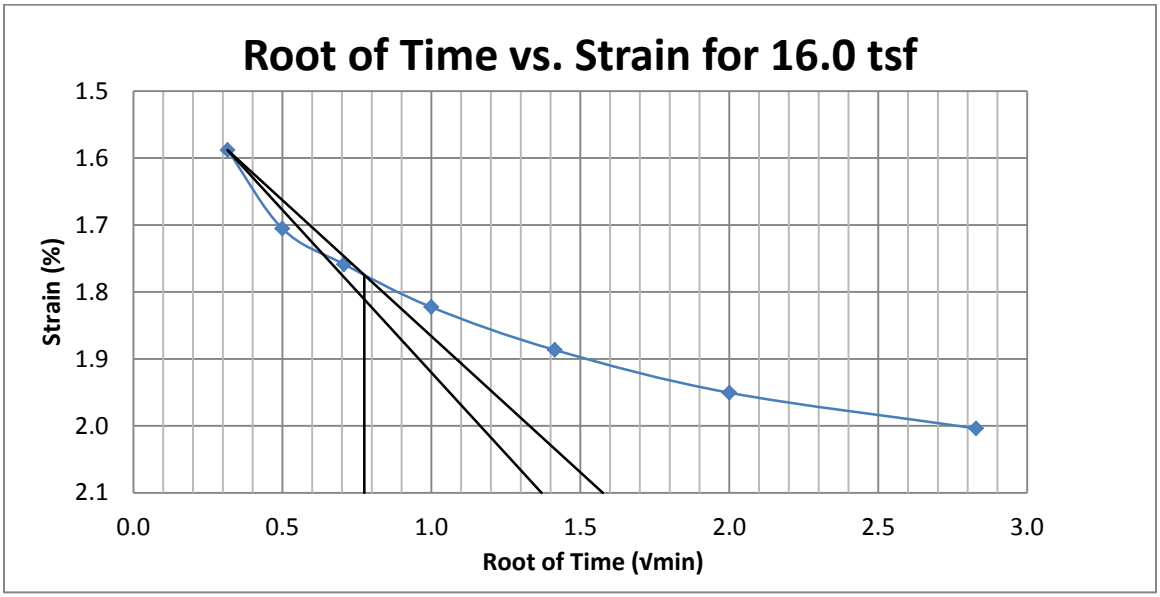

A139 Springville at 65-67 feet

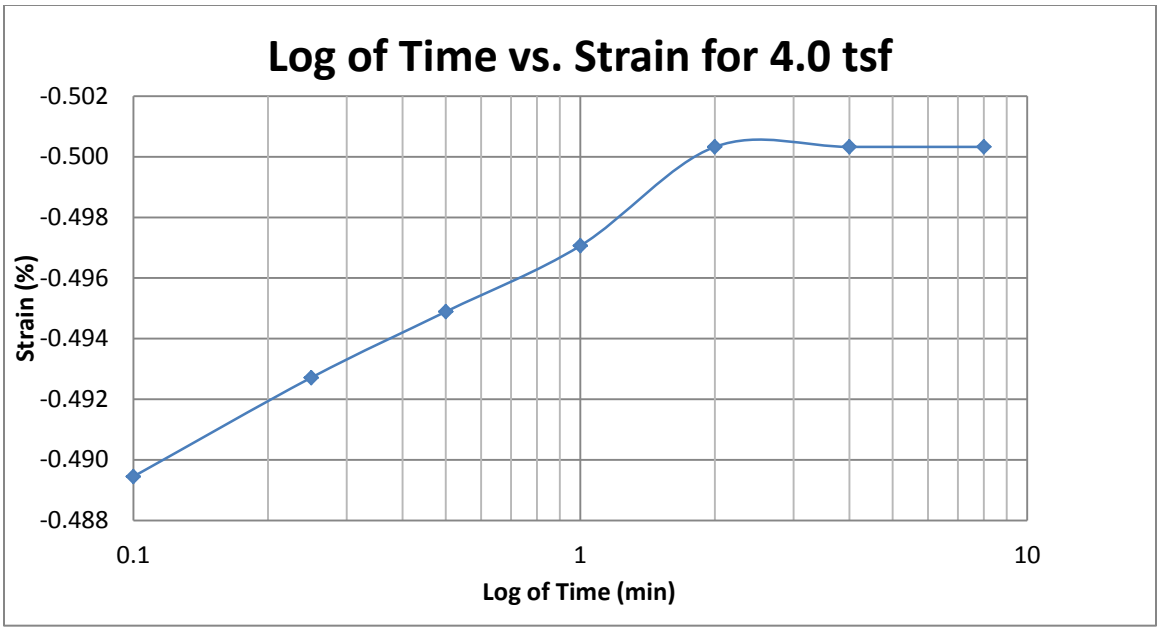

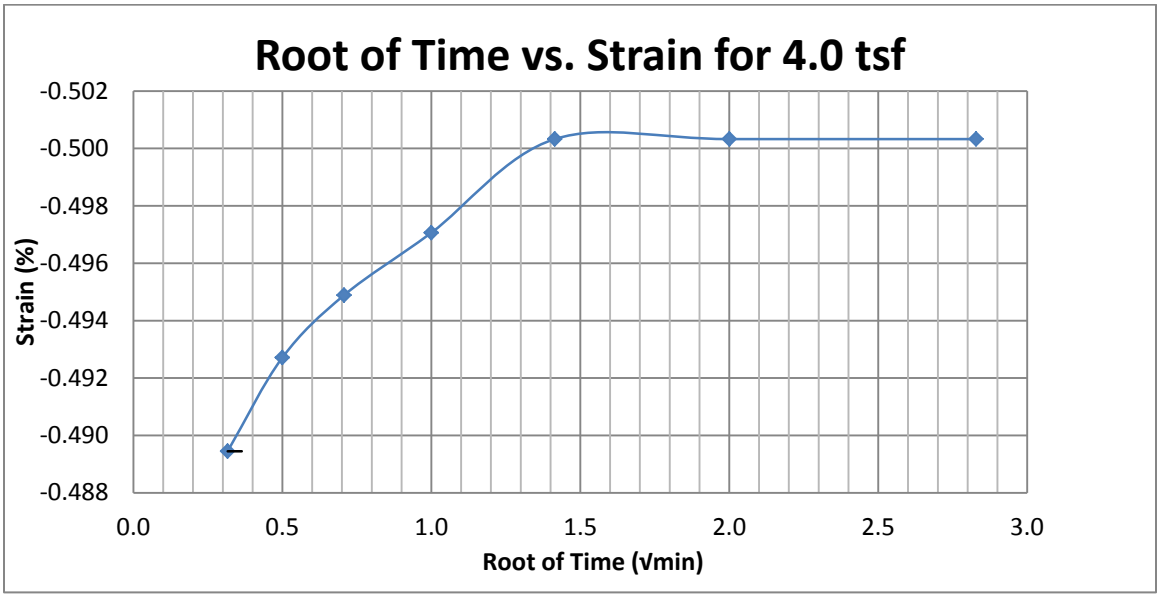

A140 Springville at 65-67 feet

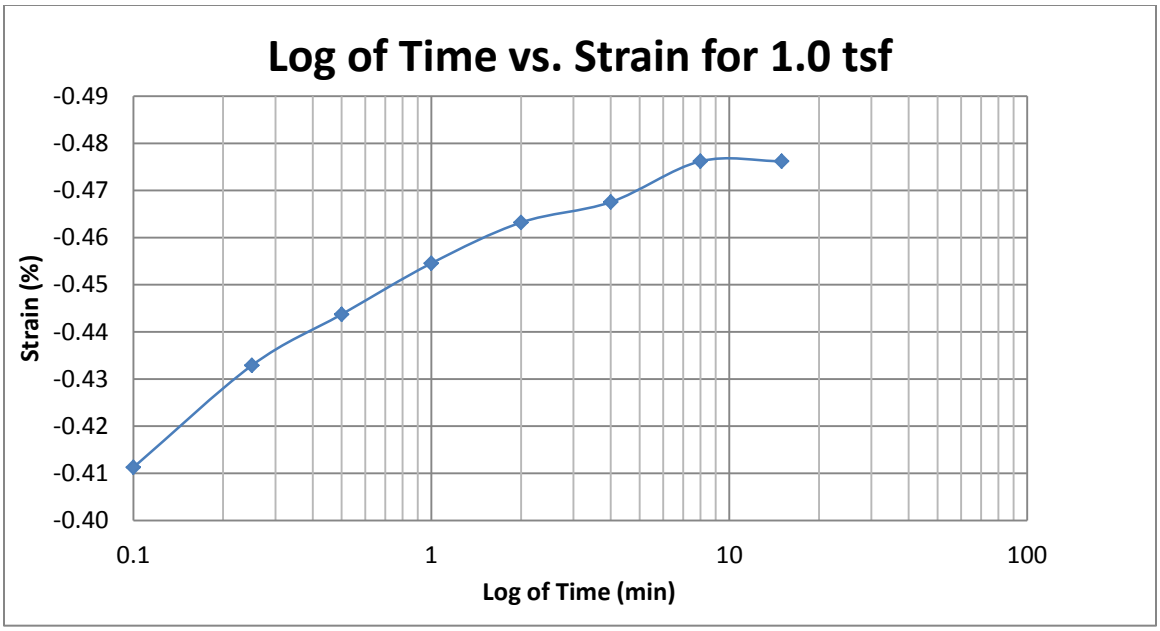

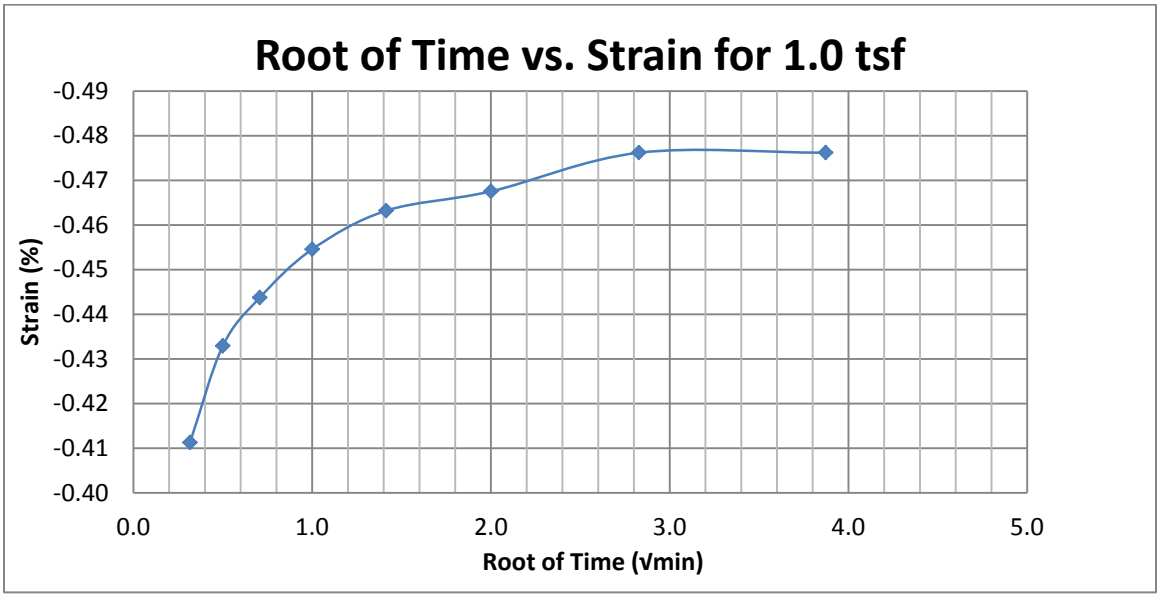

A141 Springville at 65-67 feet

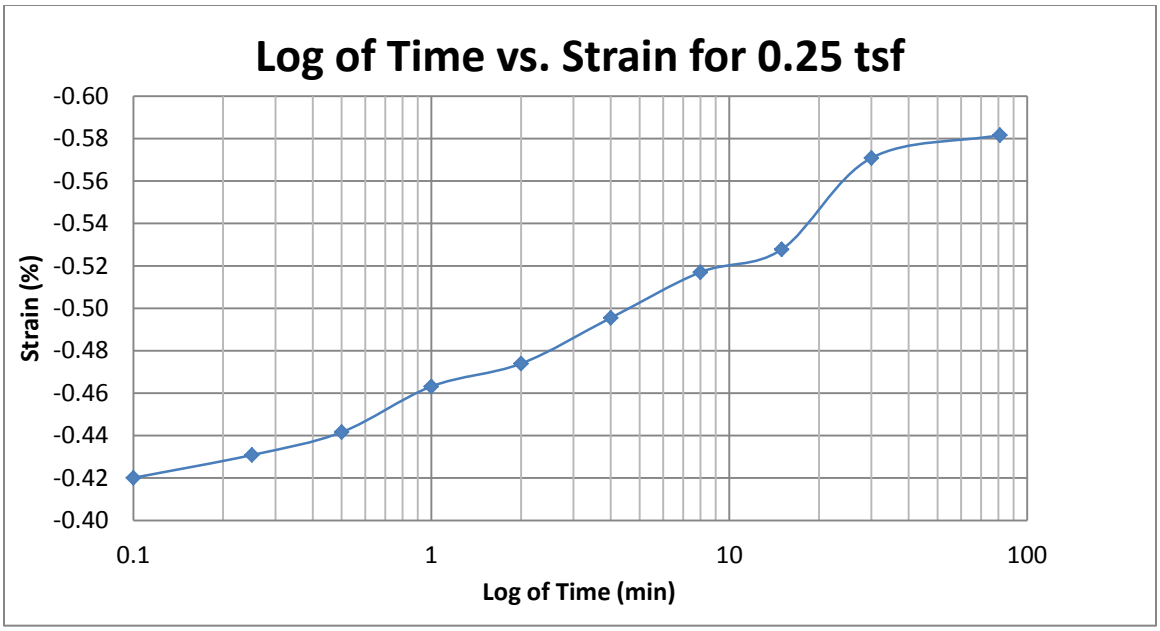

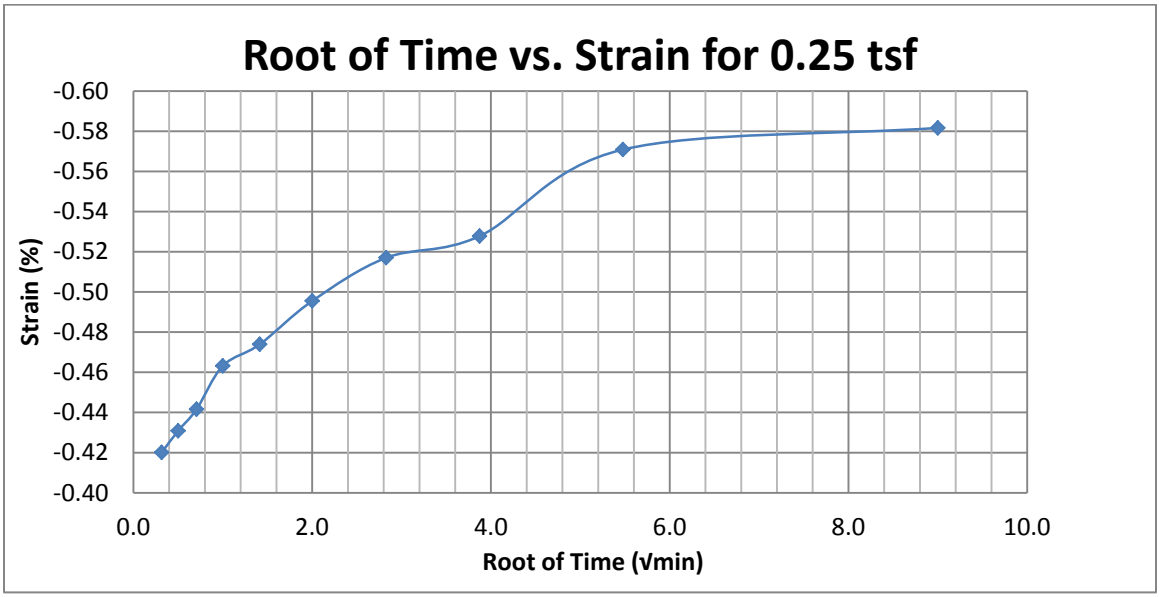

A142 Springville at 65-67 feet

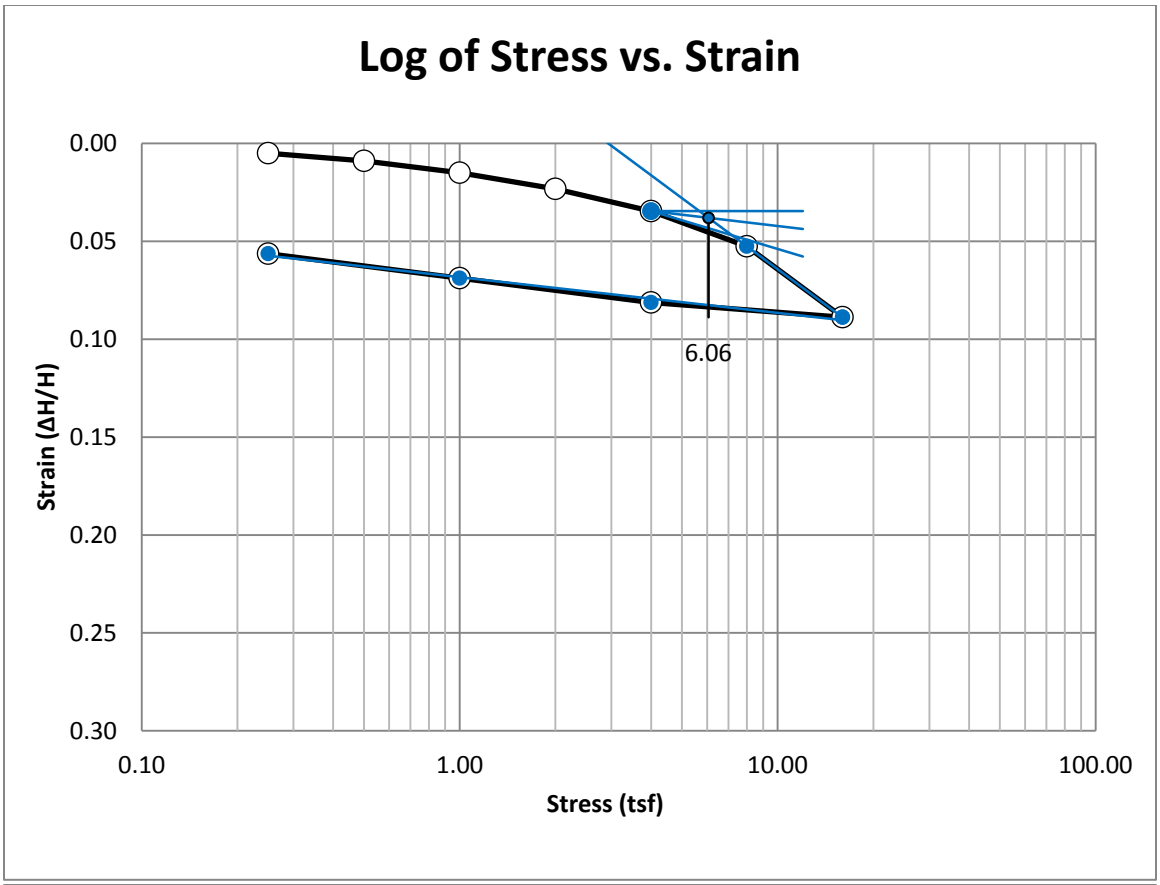

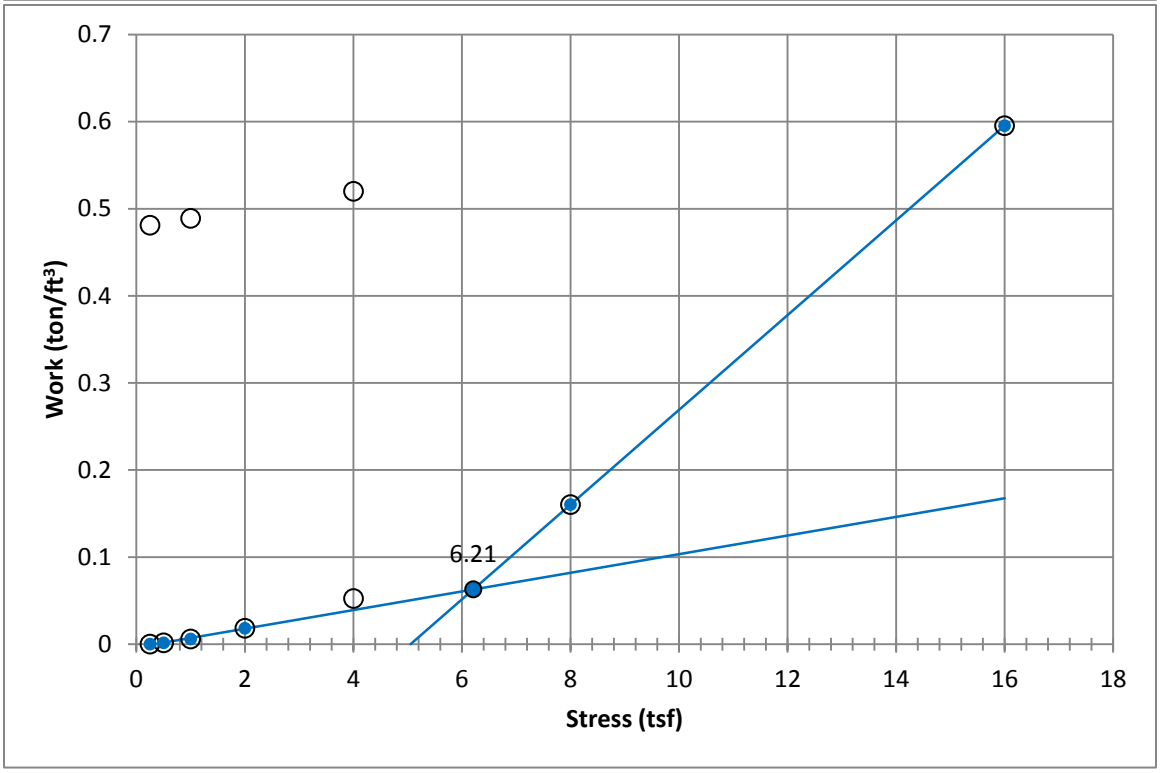

A143 Springville at 70-72 feet

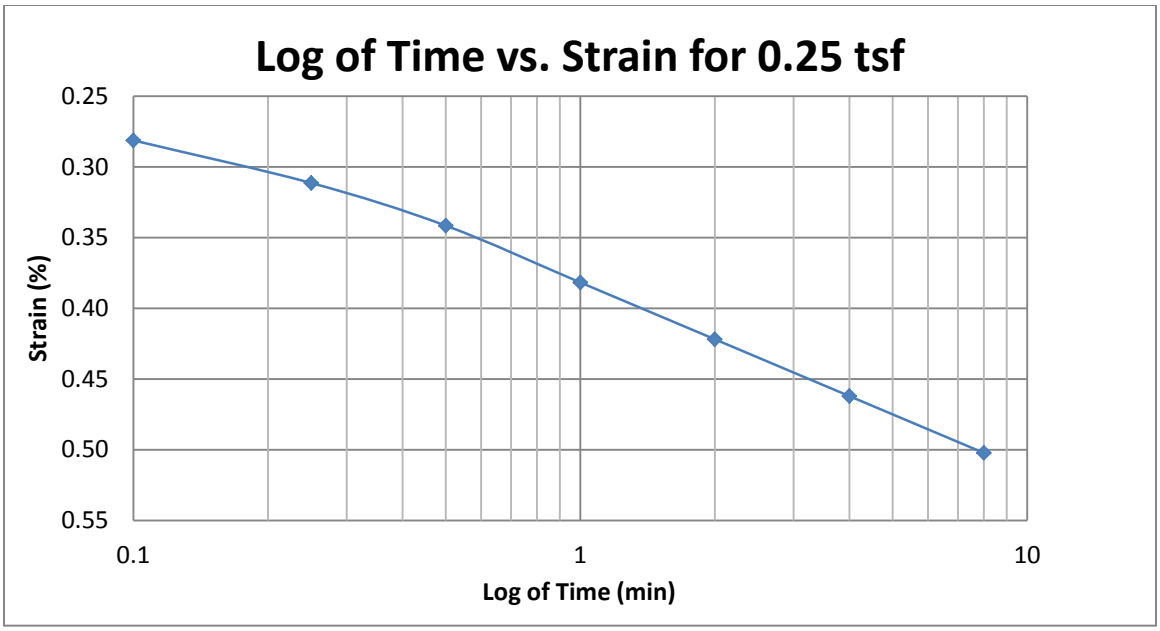

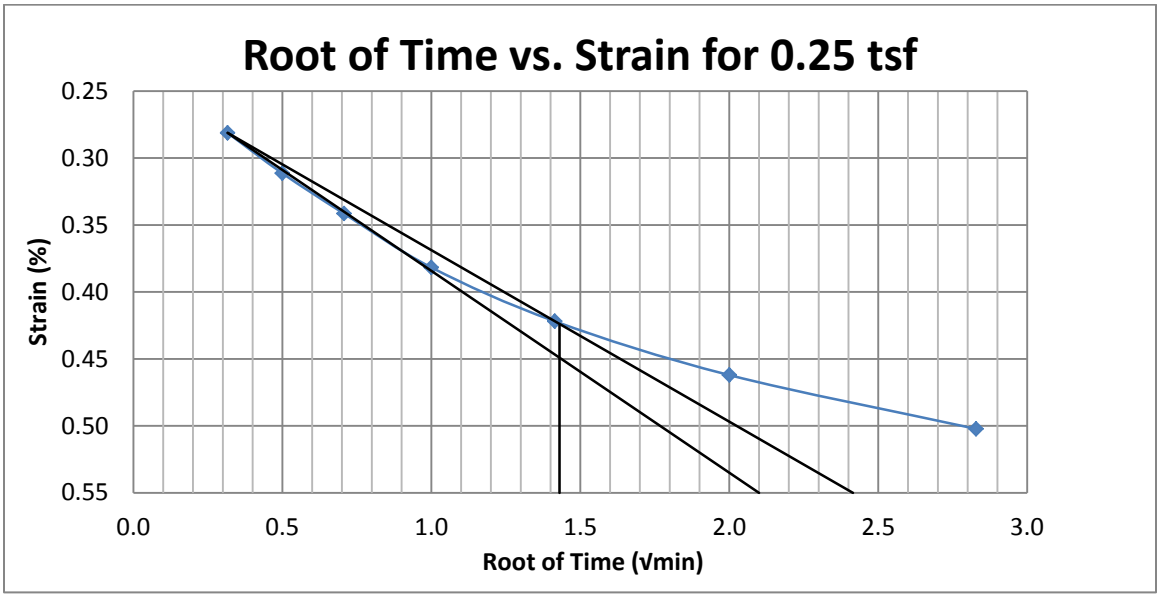

A144 Springville at 70-72 feet

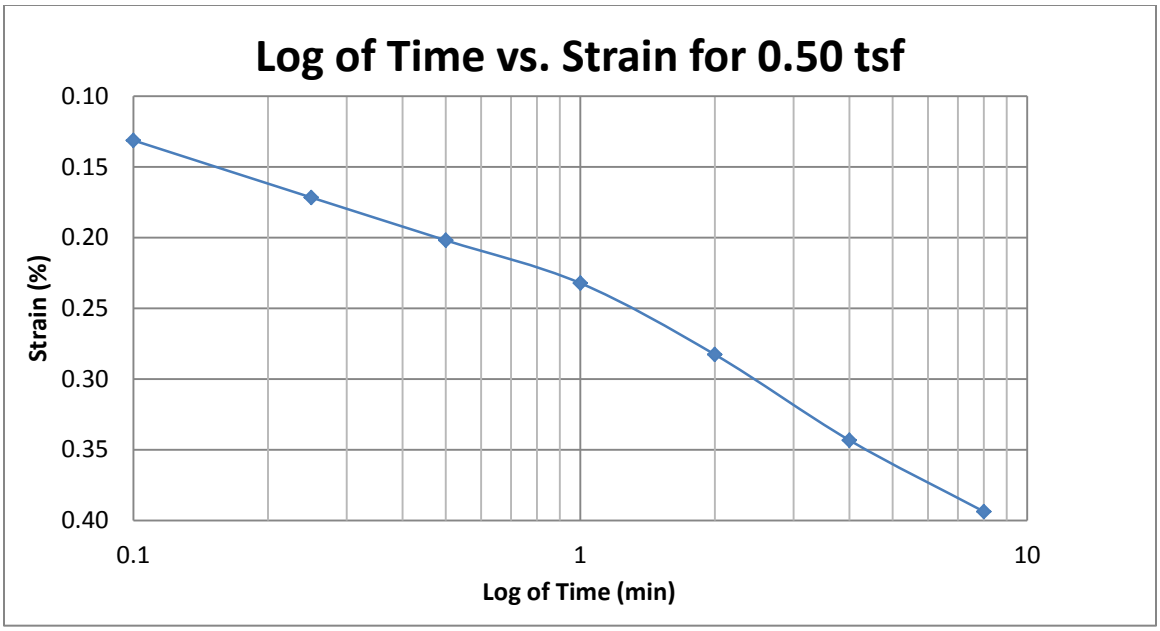

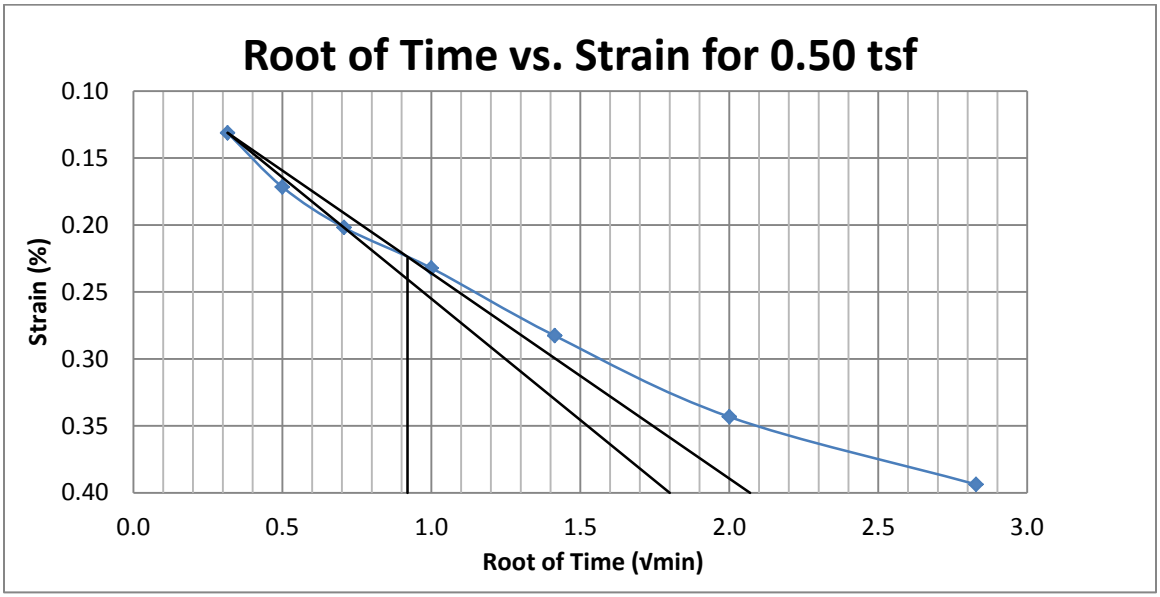

A145 Springville at 70-72 feet

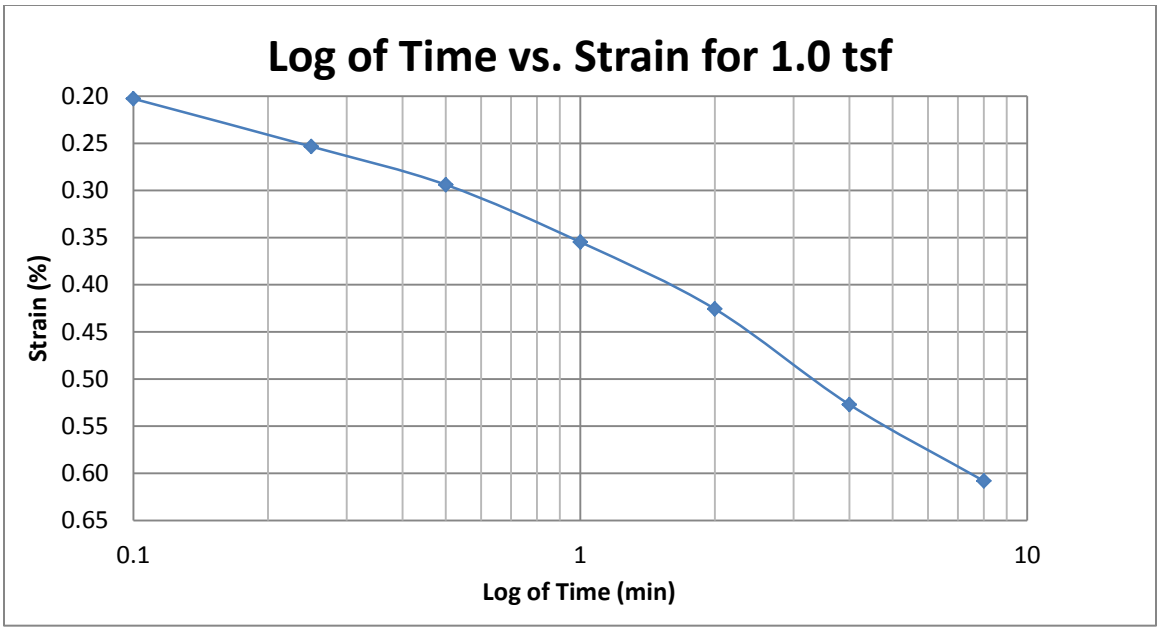

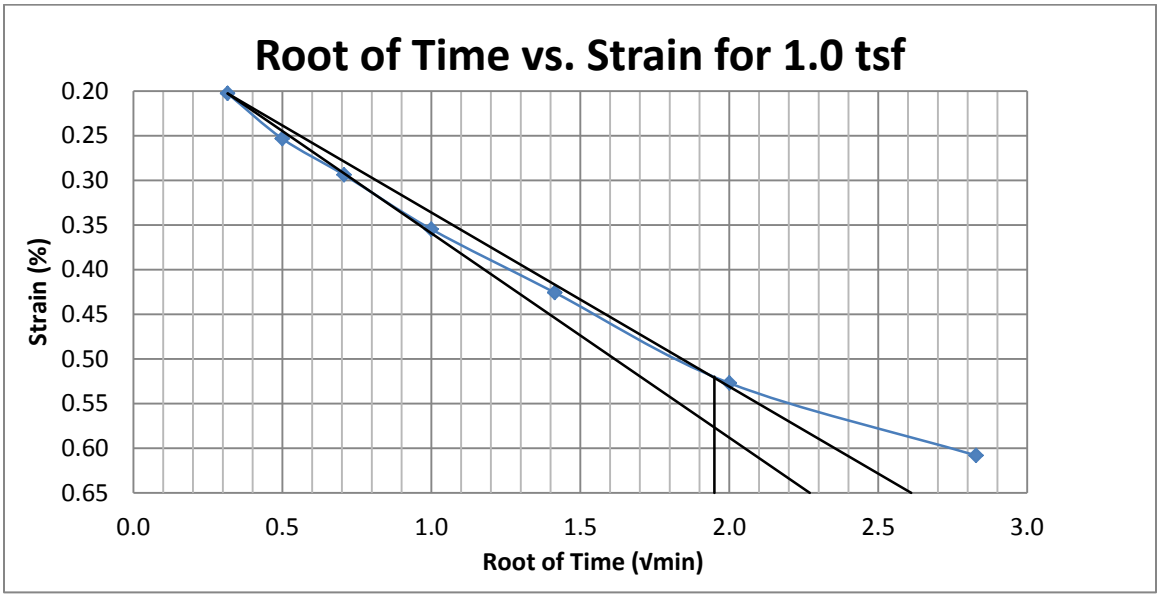

A146 Springville at 70-72 feet

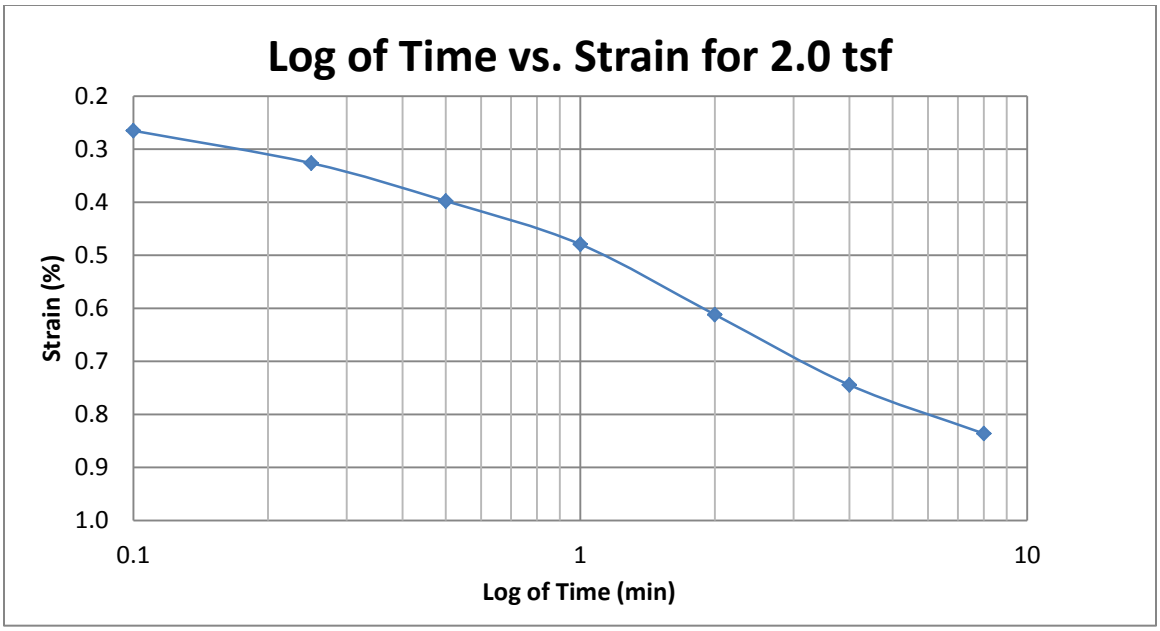

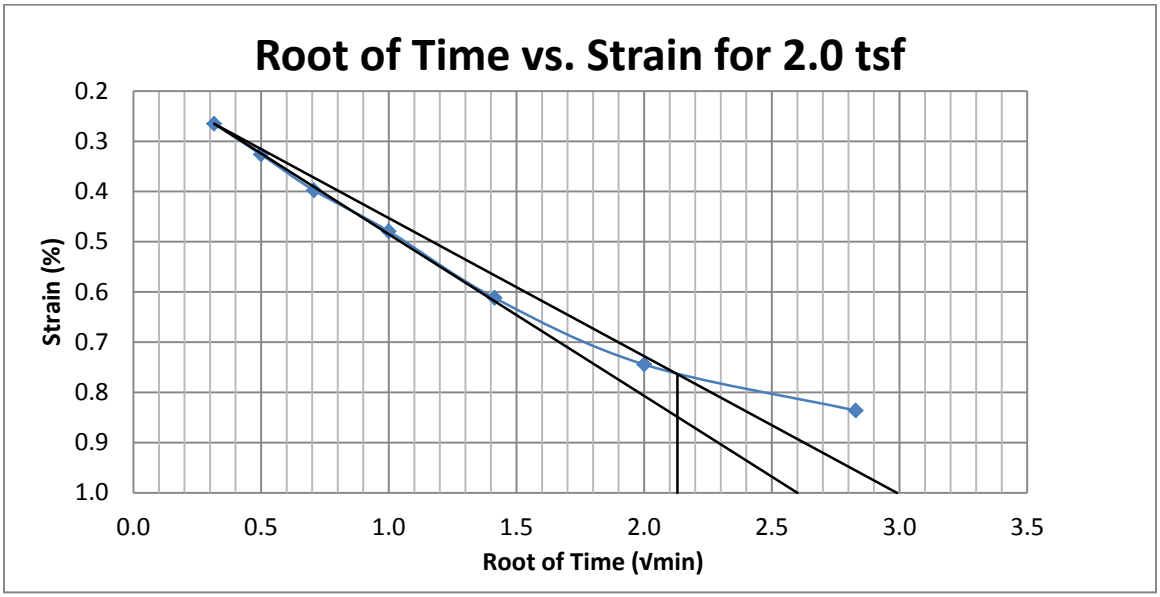

A147 Springville at 70-72 feet

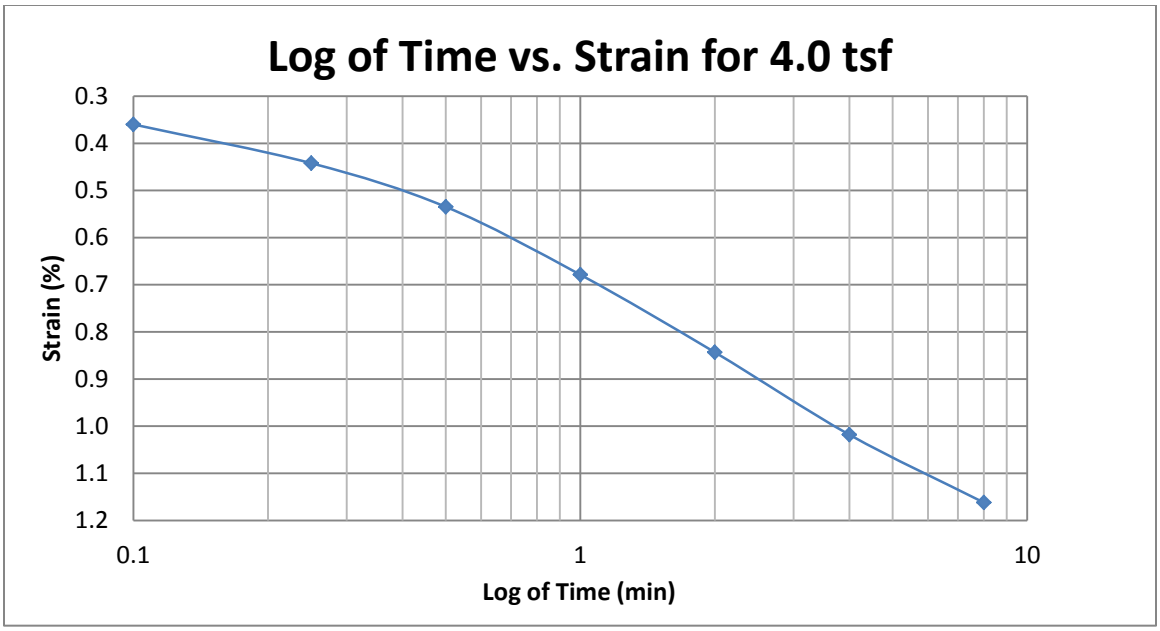

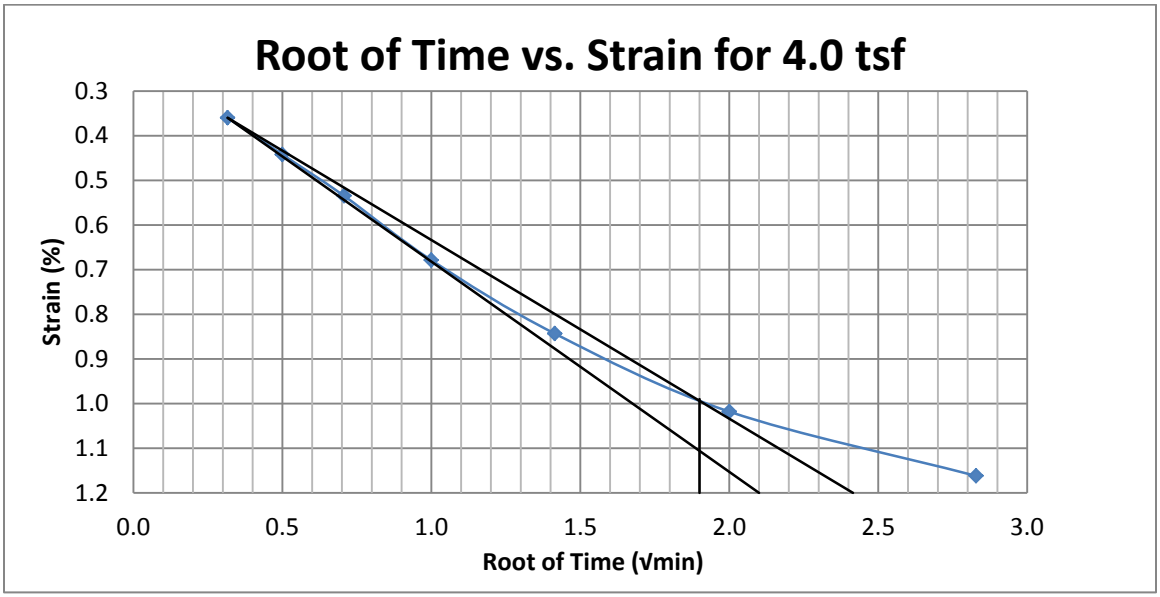

A148 Springville at 70-72 feet

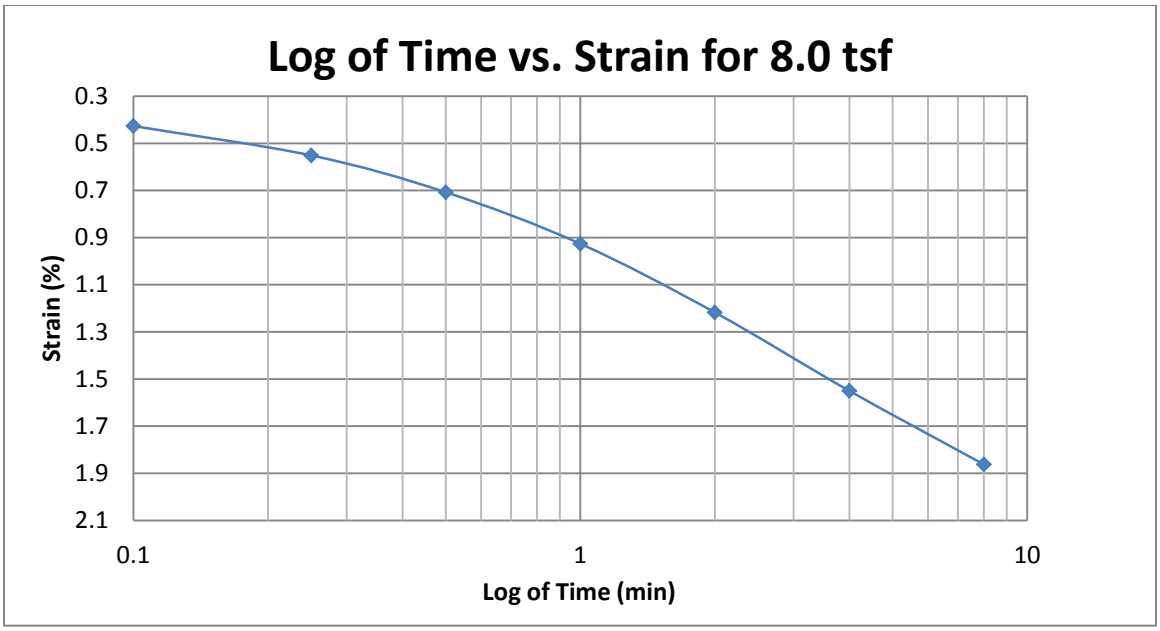

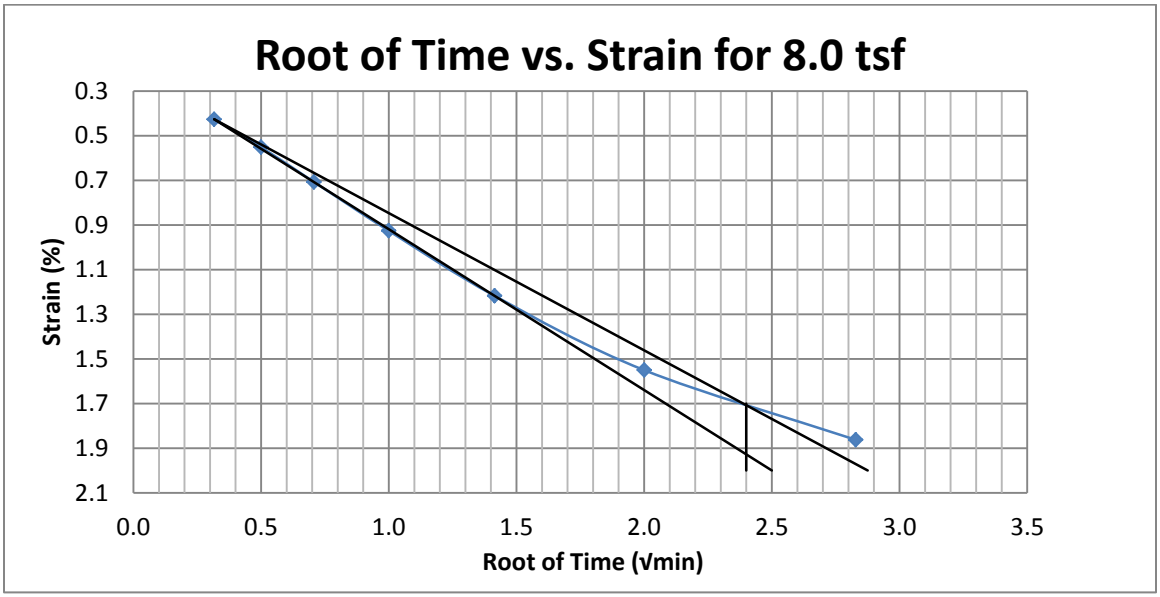

A149 Springville at 70-72 feet

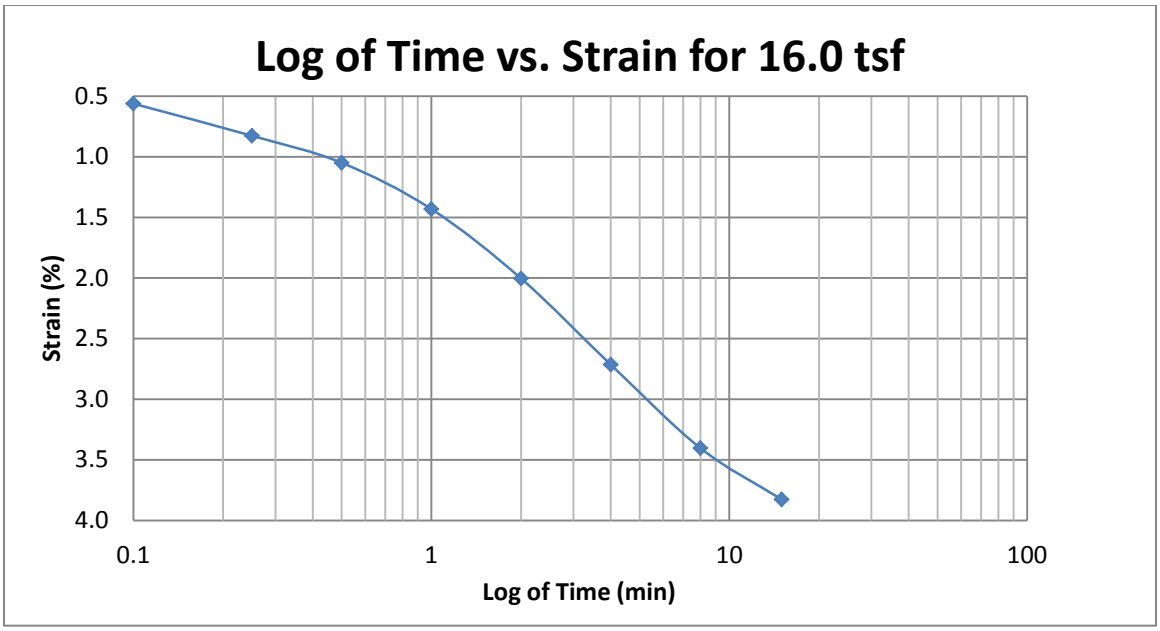

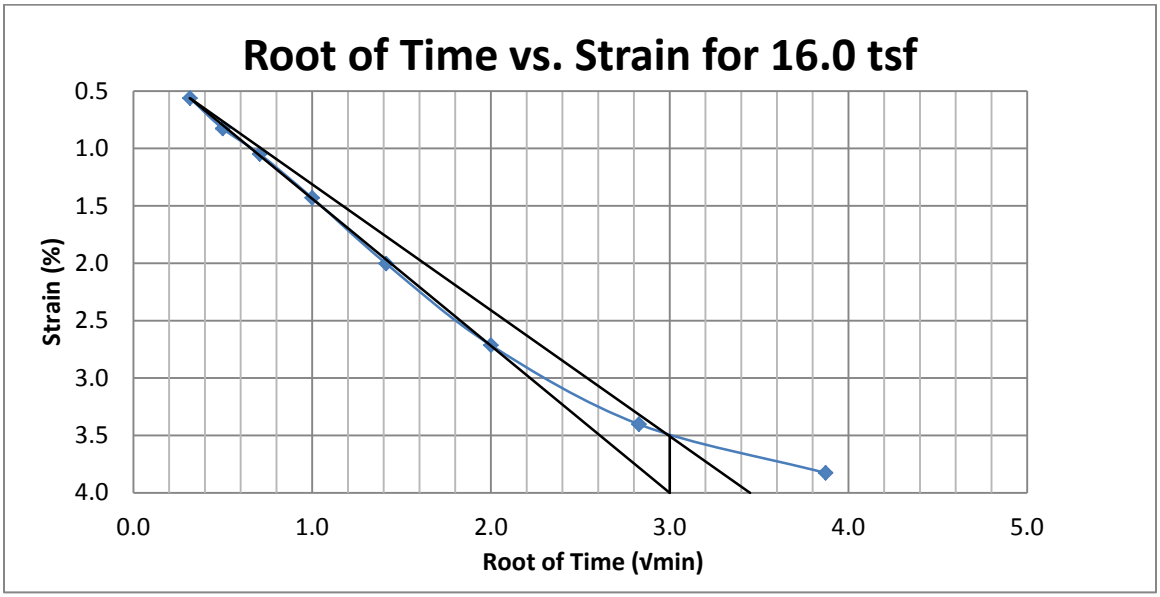

A150 Springville at 70-72 feet

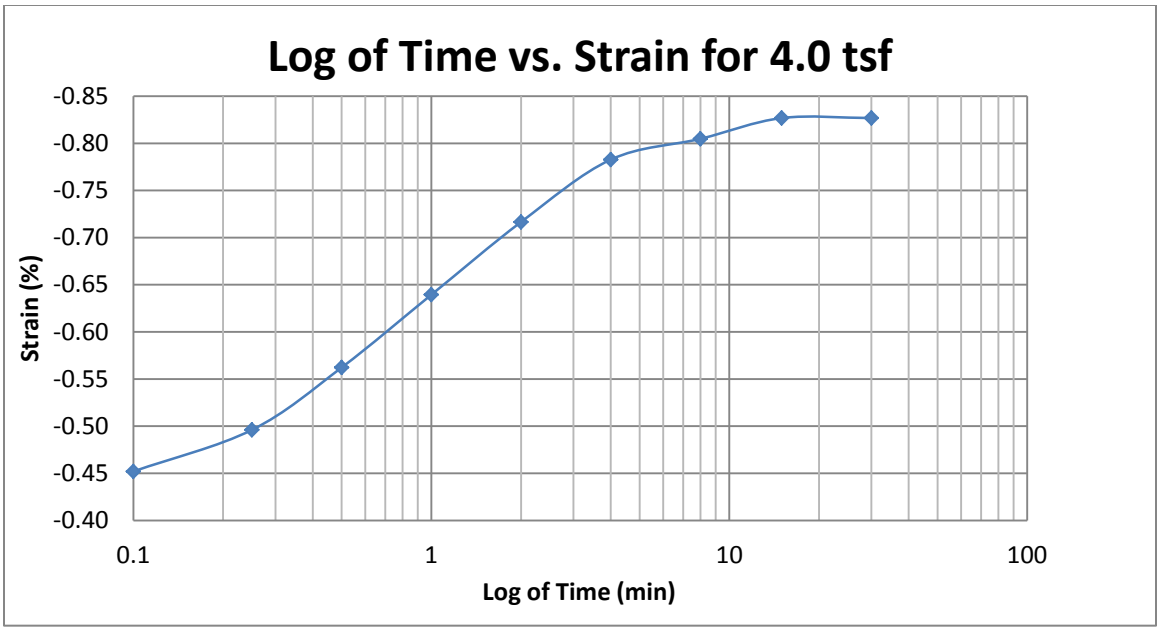

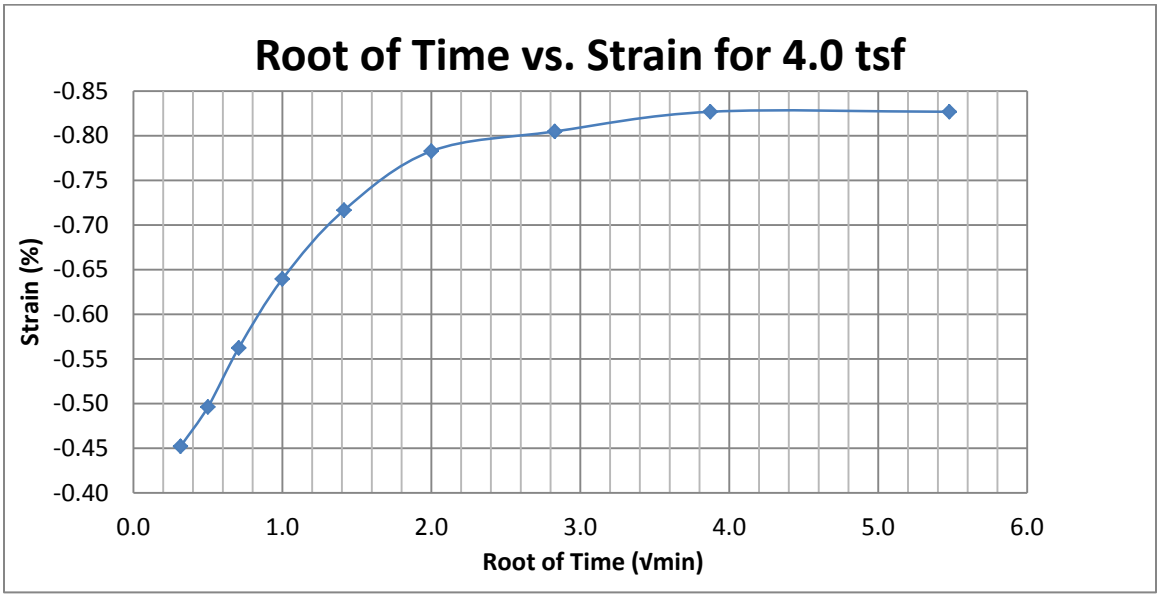

A151 Springville at 70-72 feet

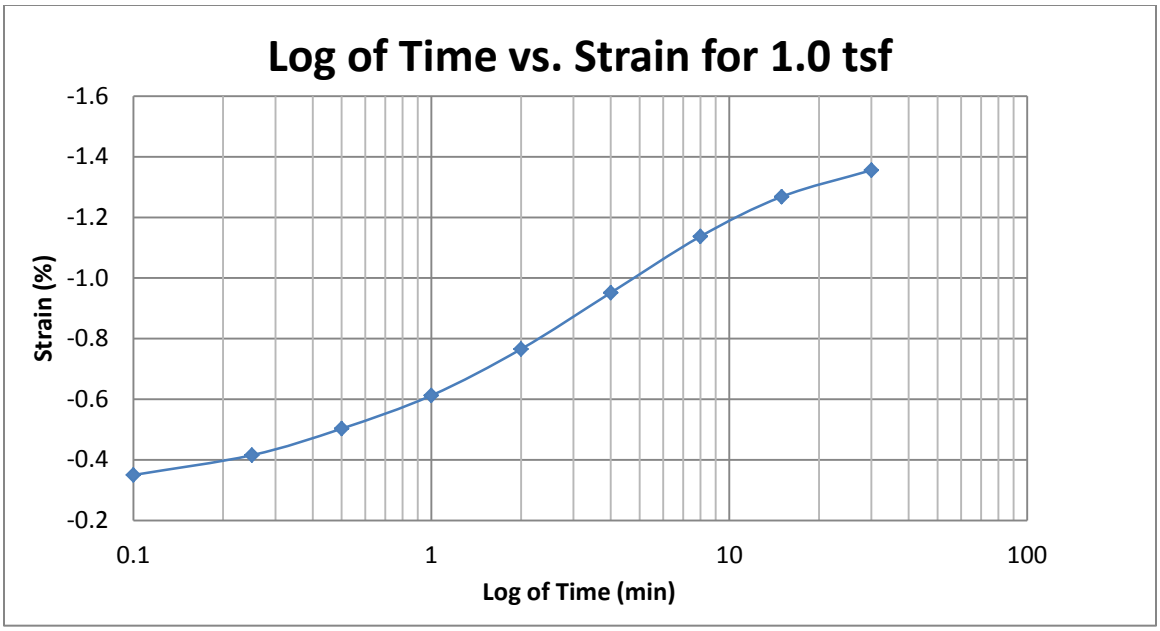

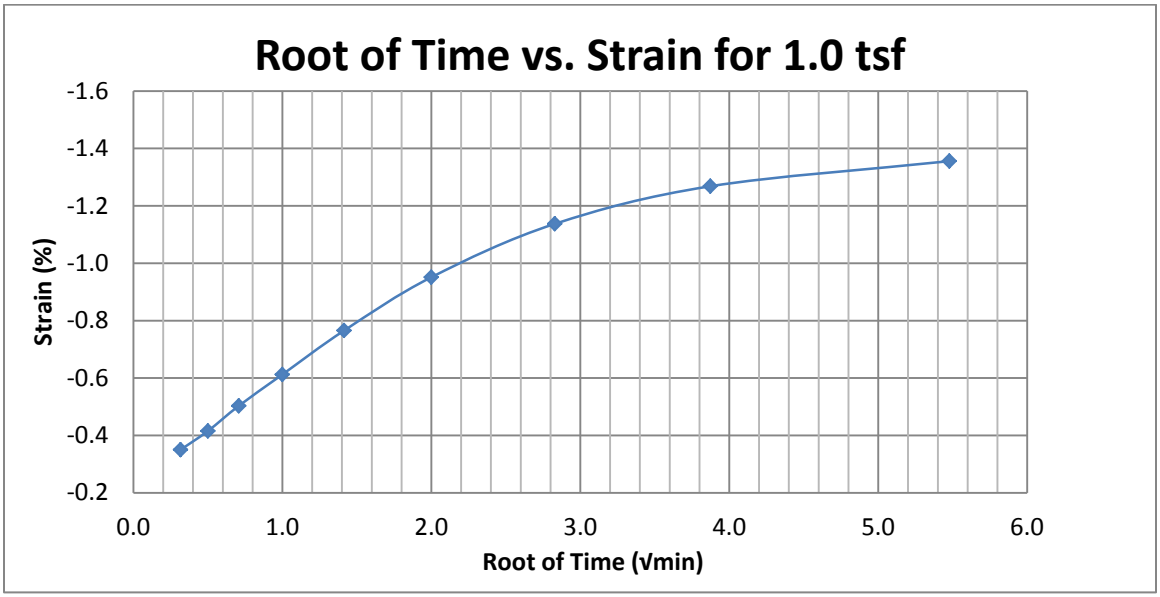

A152 Springville at 70-72 feet

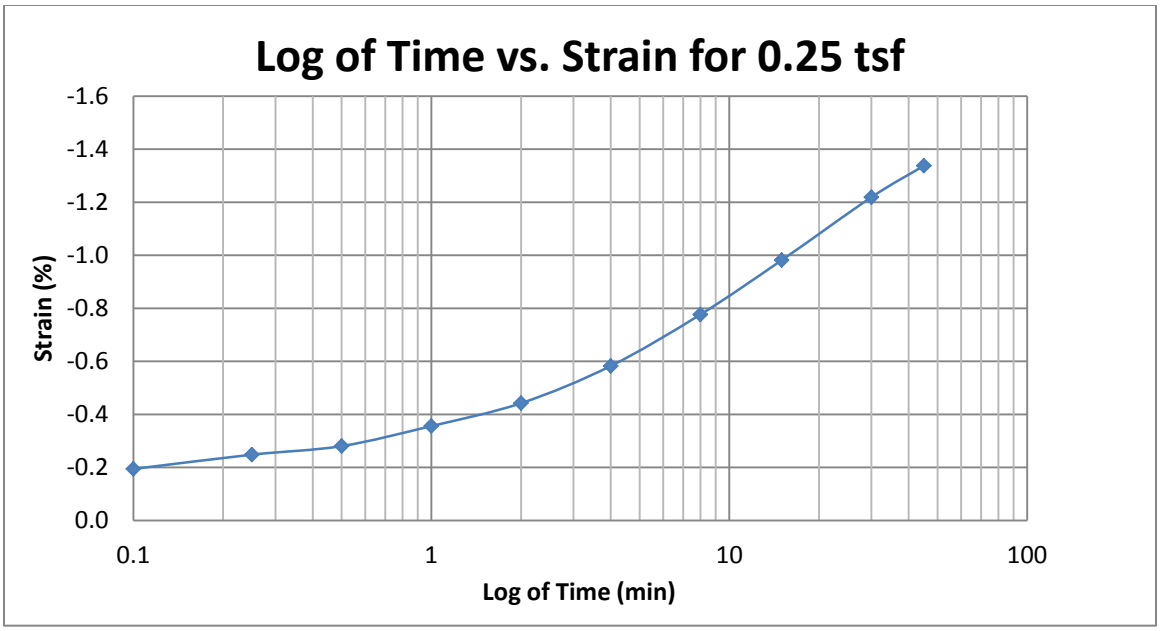

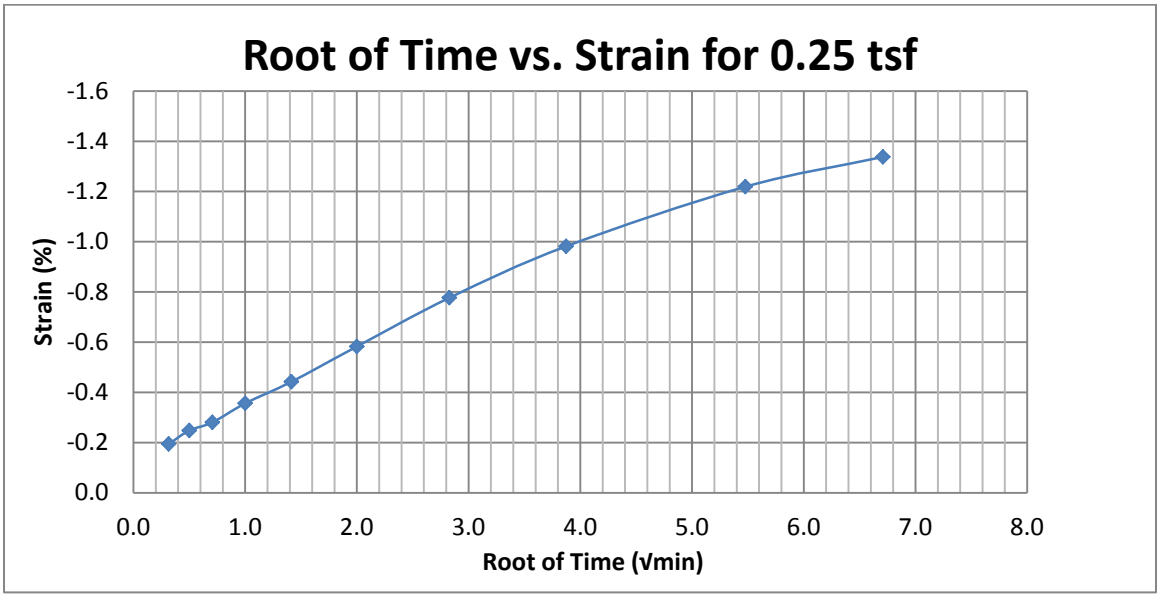

A153 Springville at 70-72 feet

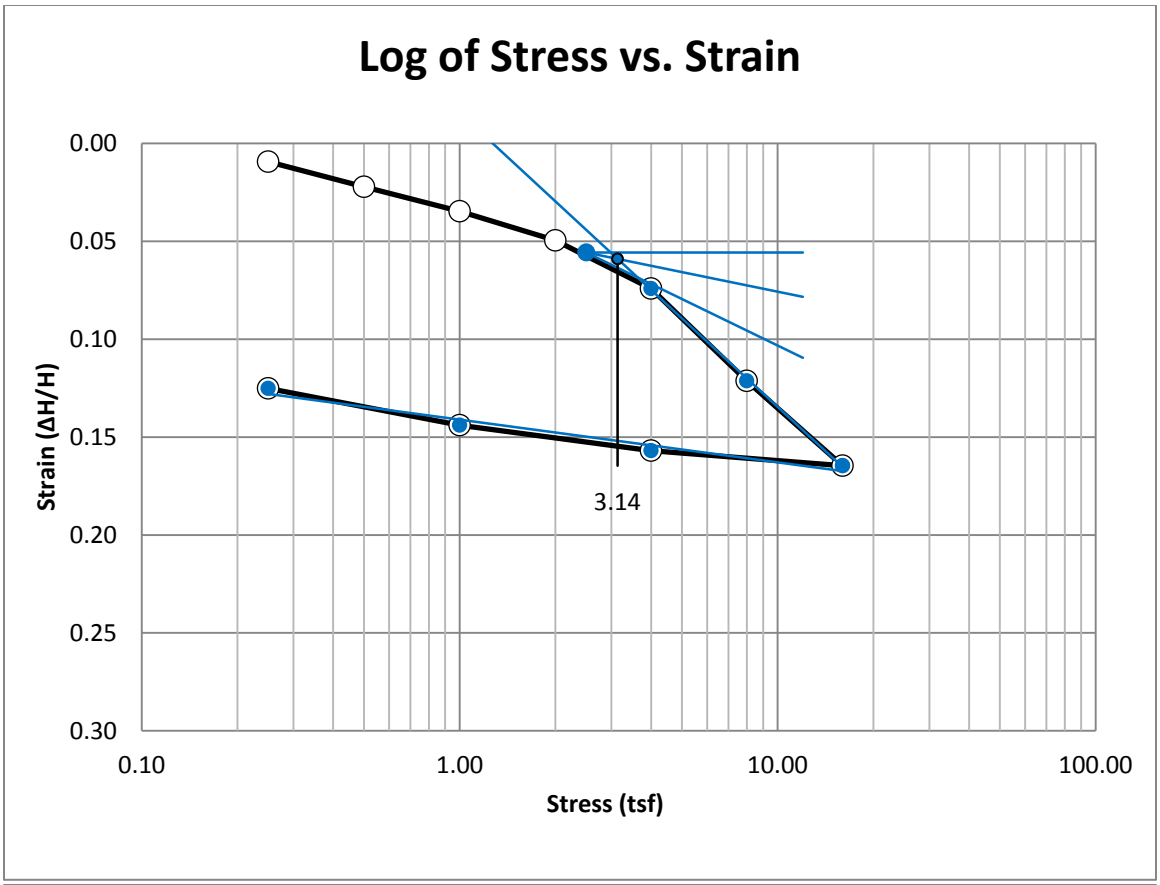

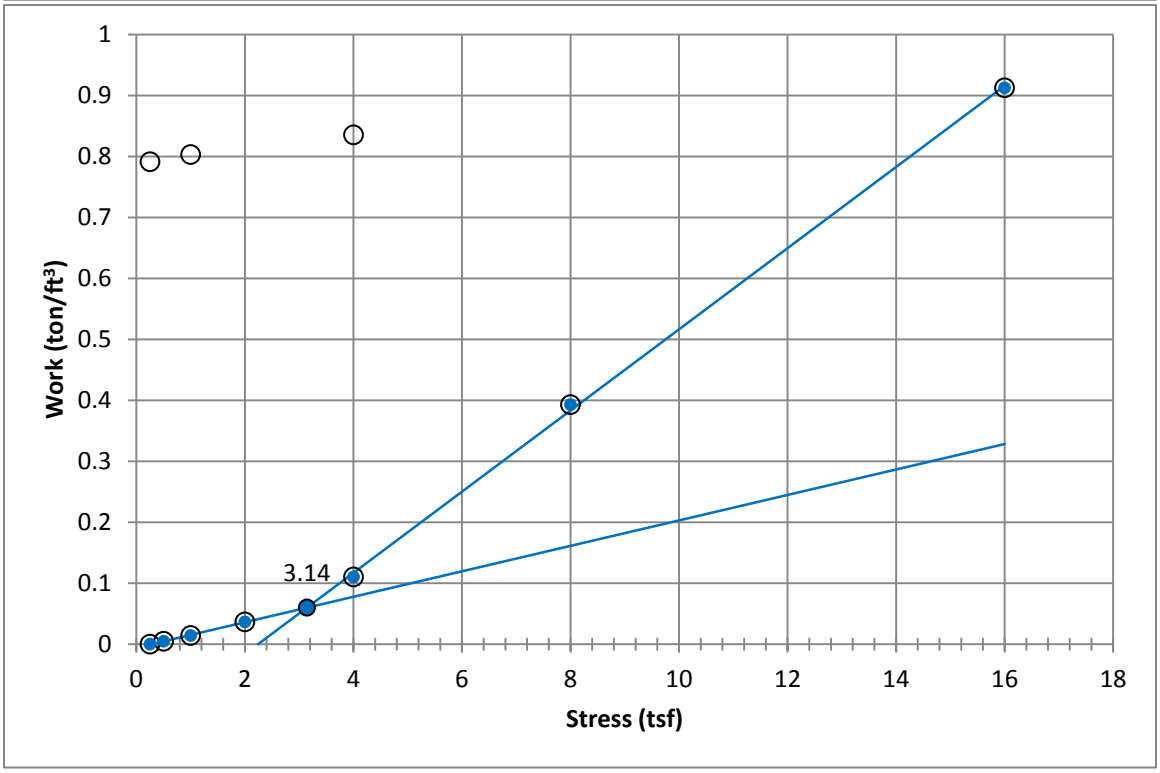

A154 Springville at 75-77 feet

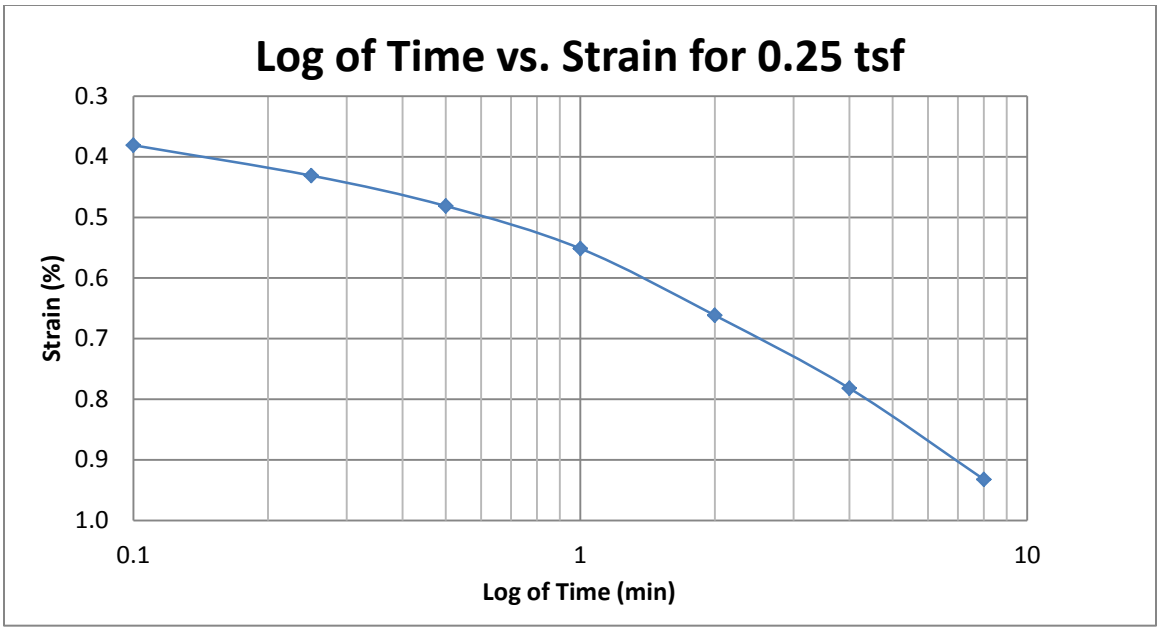

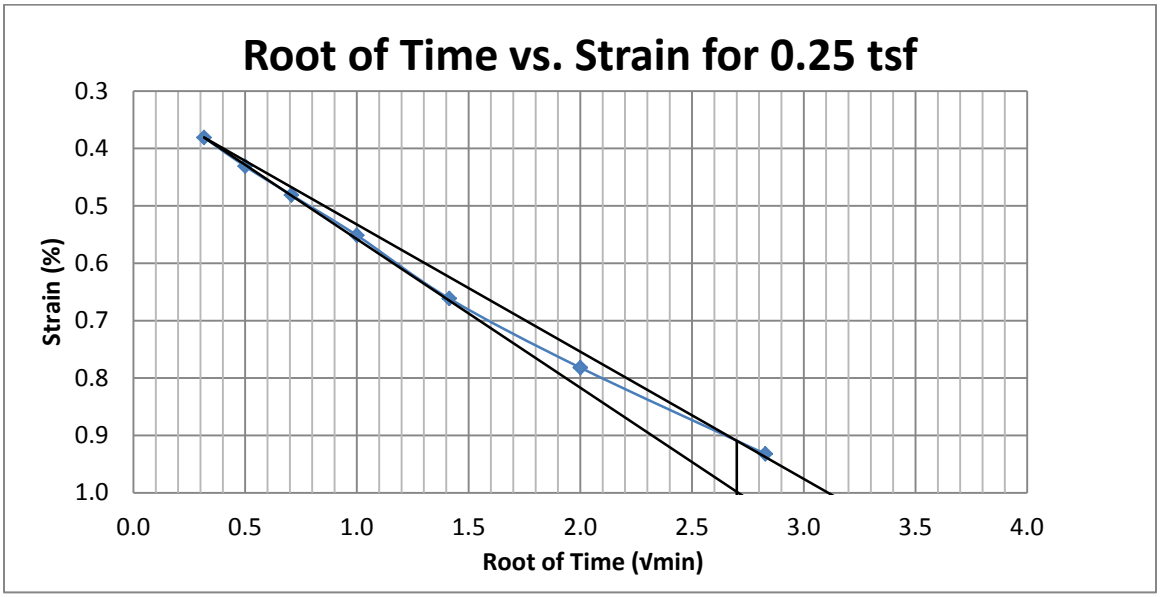

A155 Springville at 75-77 feet

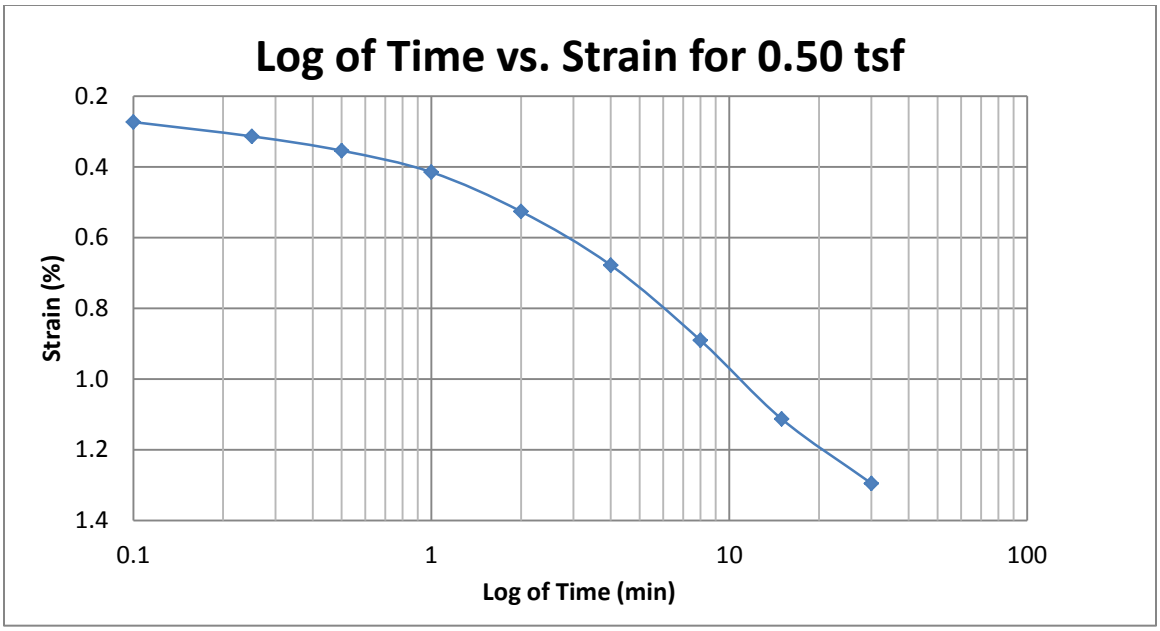

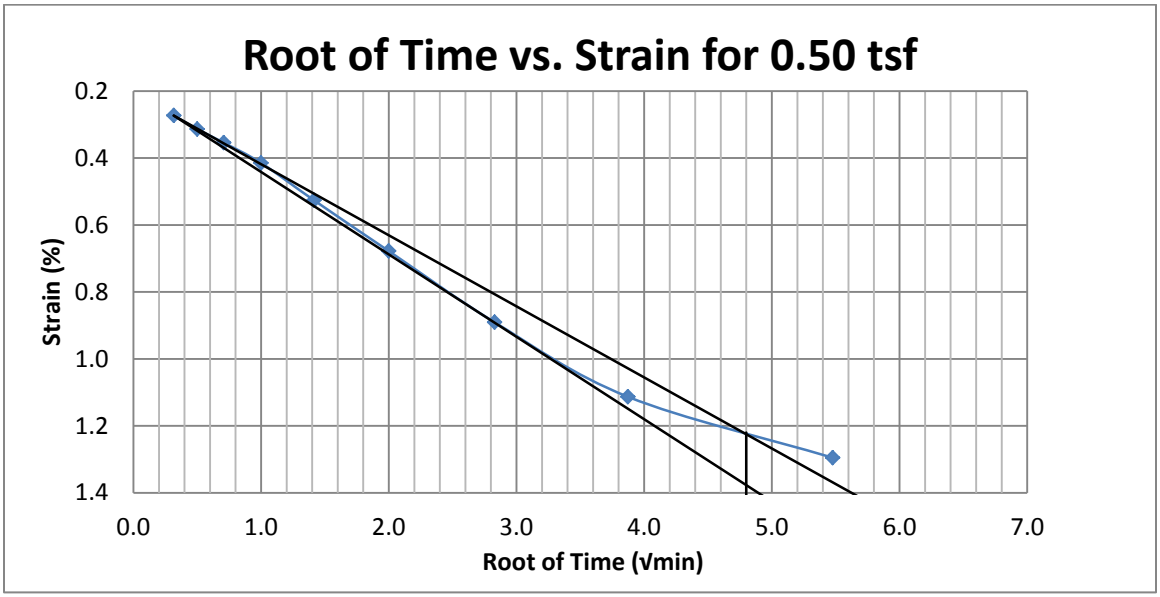

A156 Springville at 75-77 feet

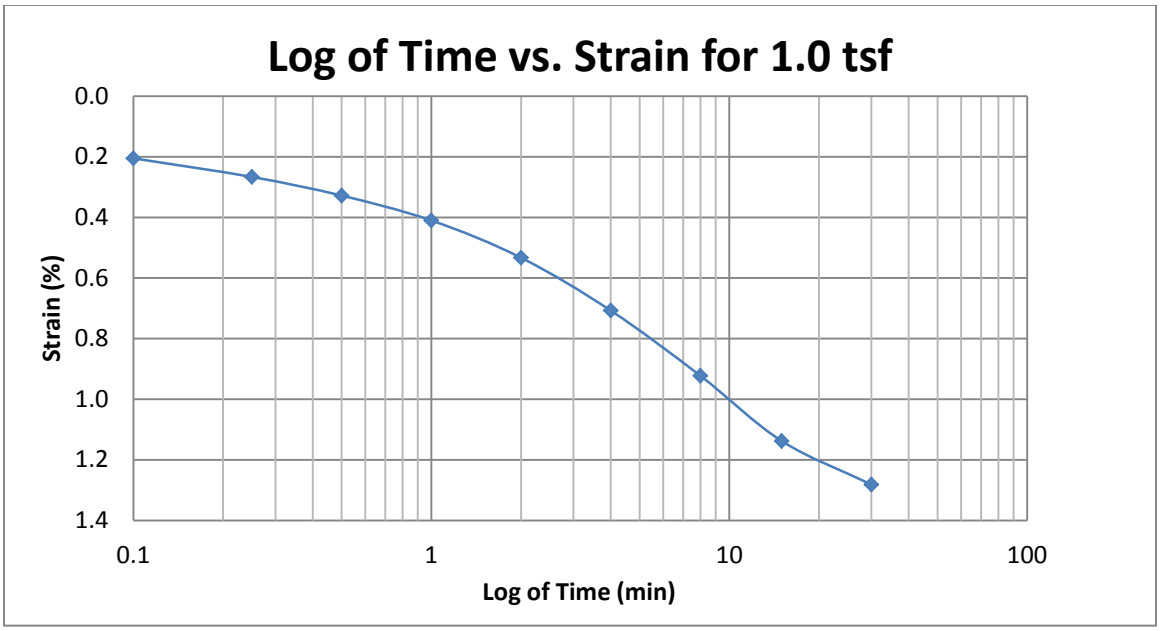

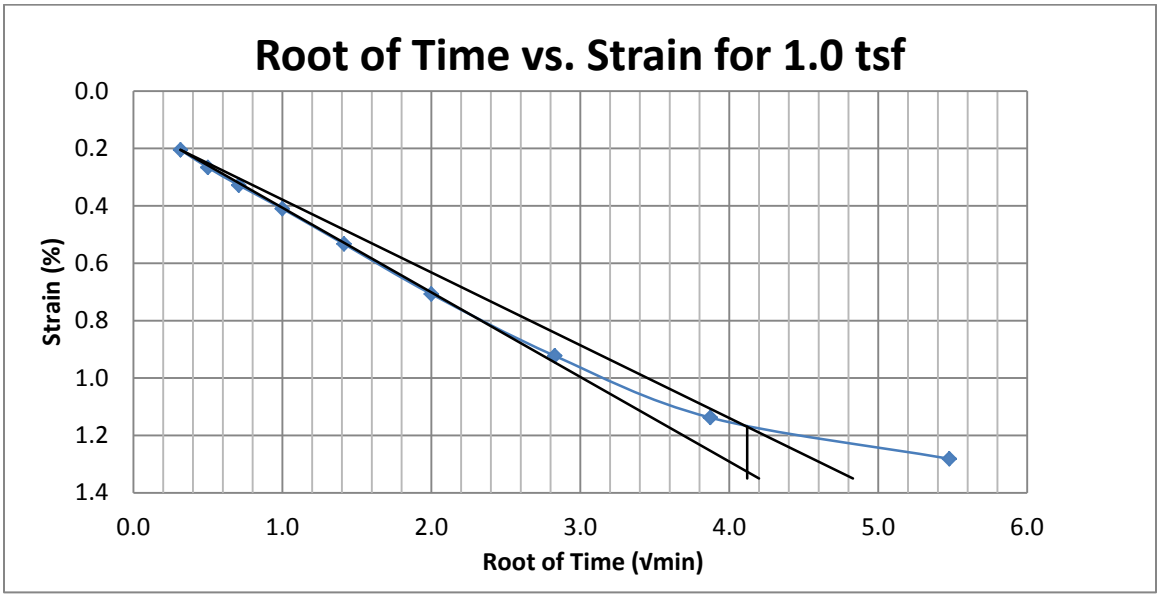

A157 Springville at 75-77 feet

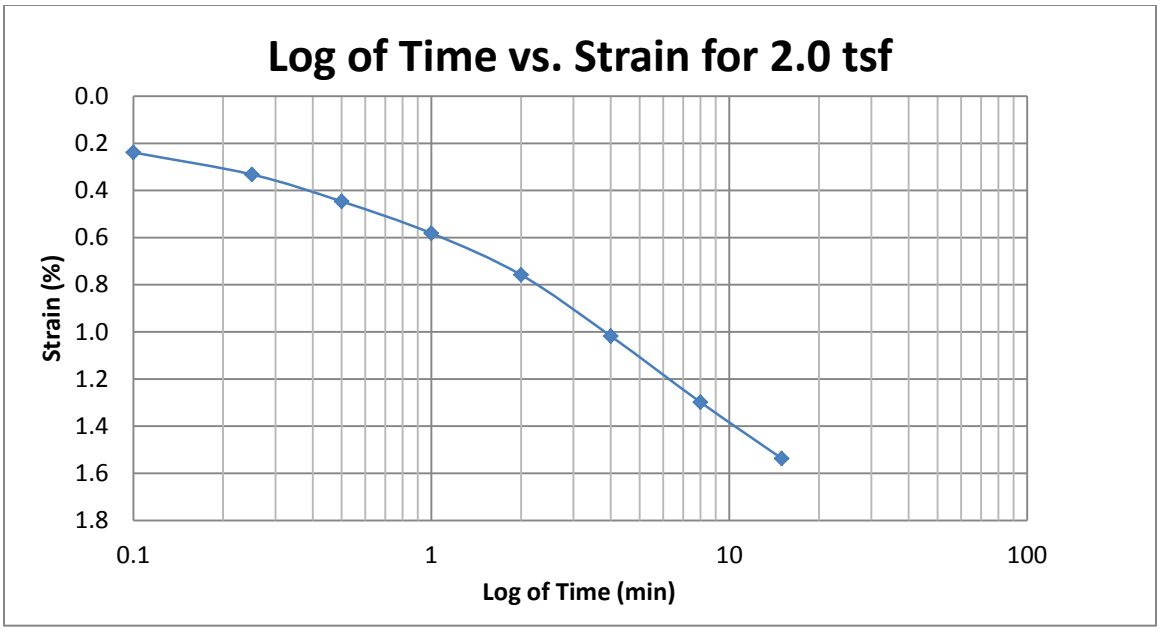

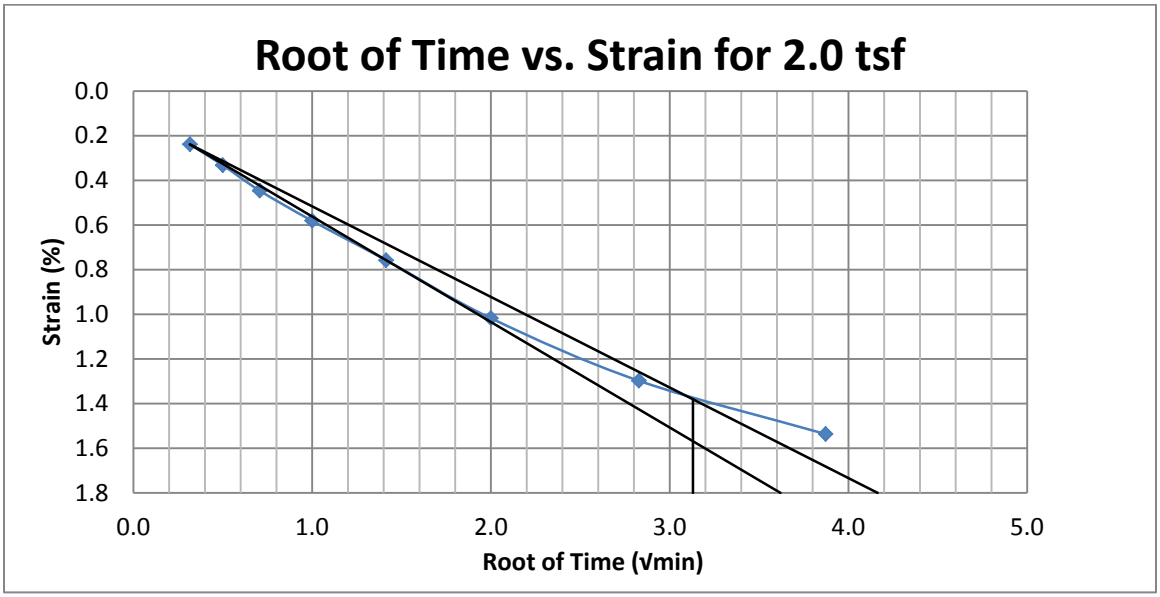

A158 Springville at 75-77 feet

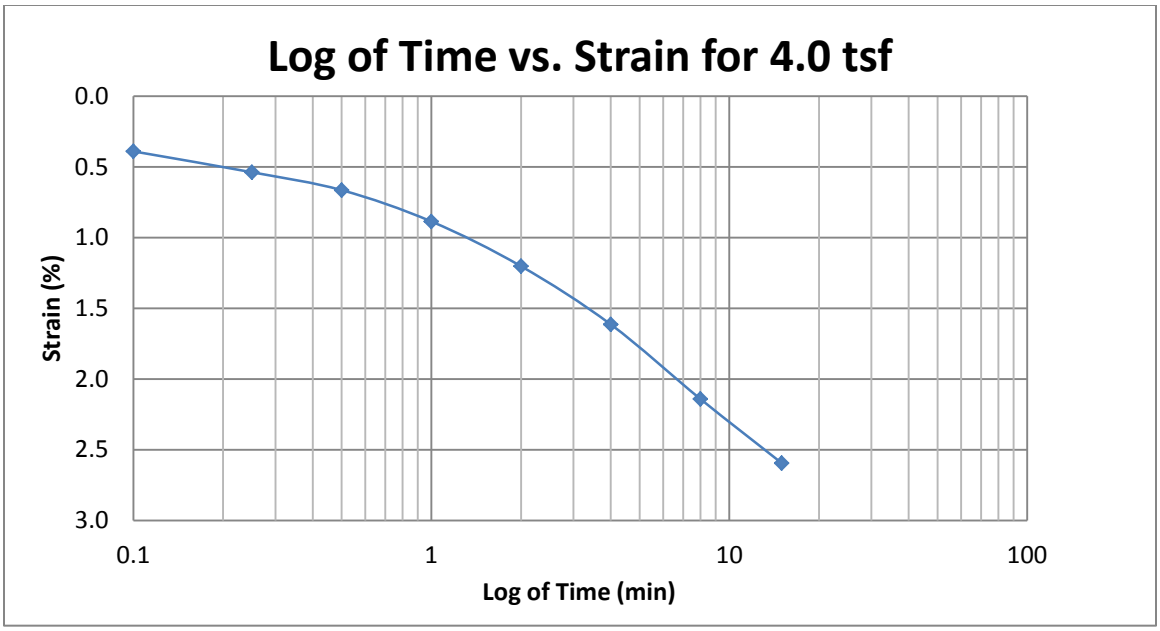

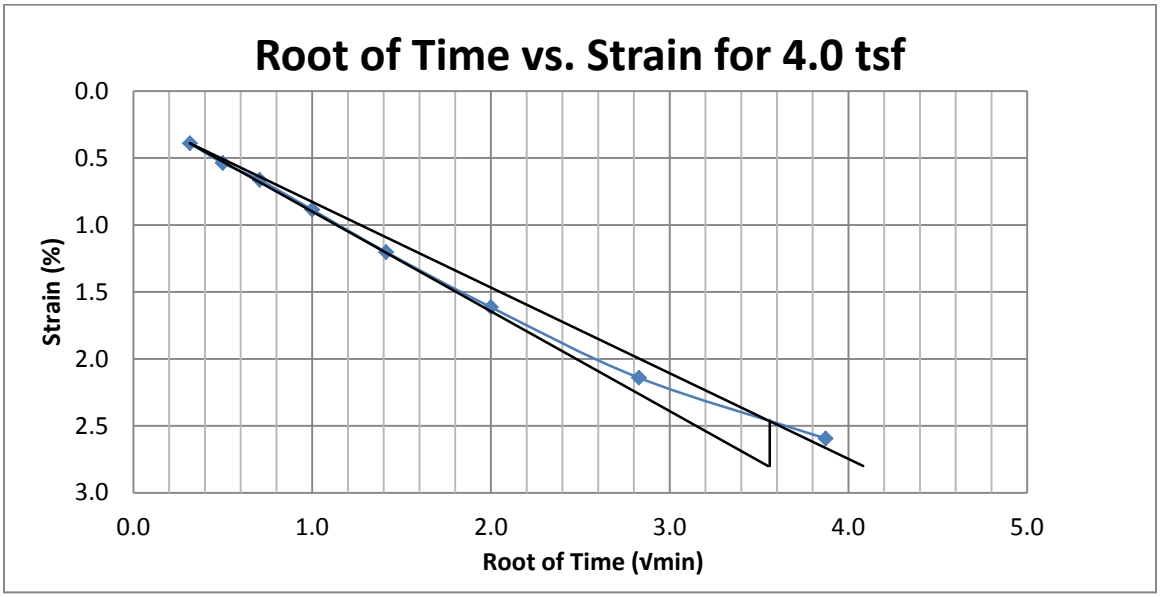

A159 Springville at 75-77 feet

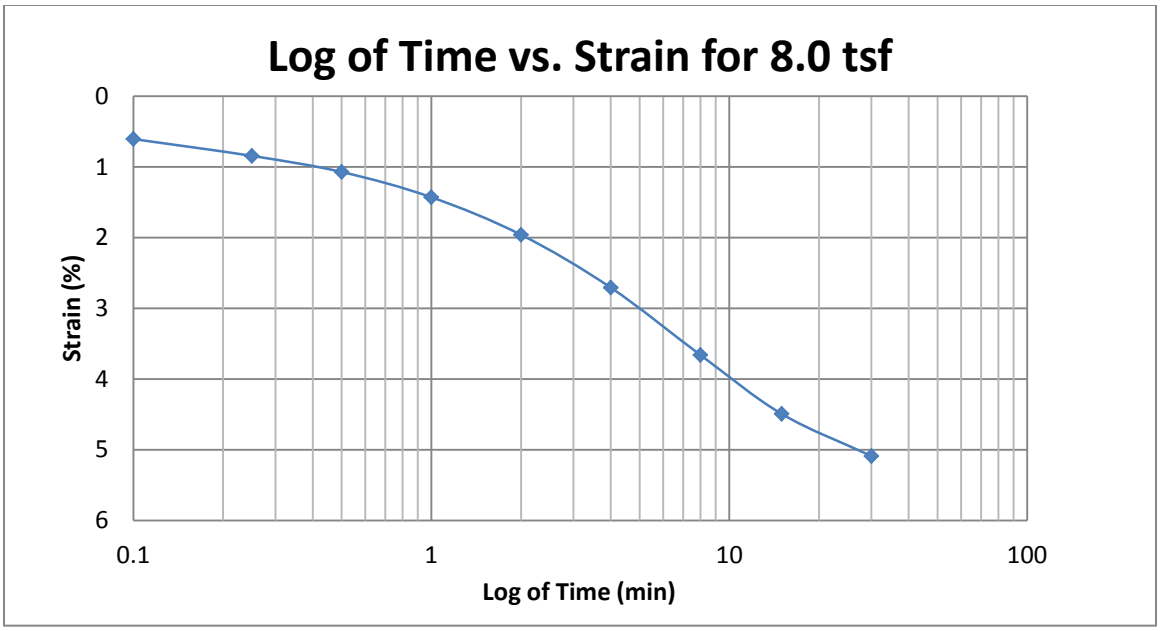

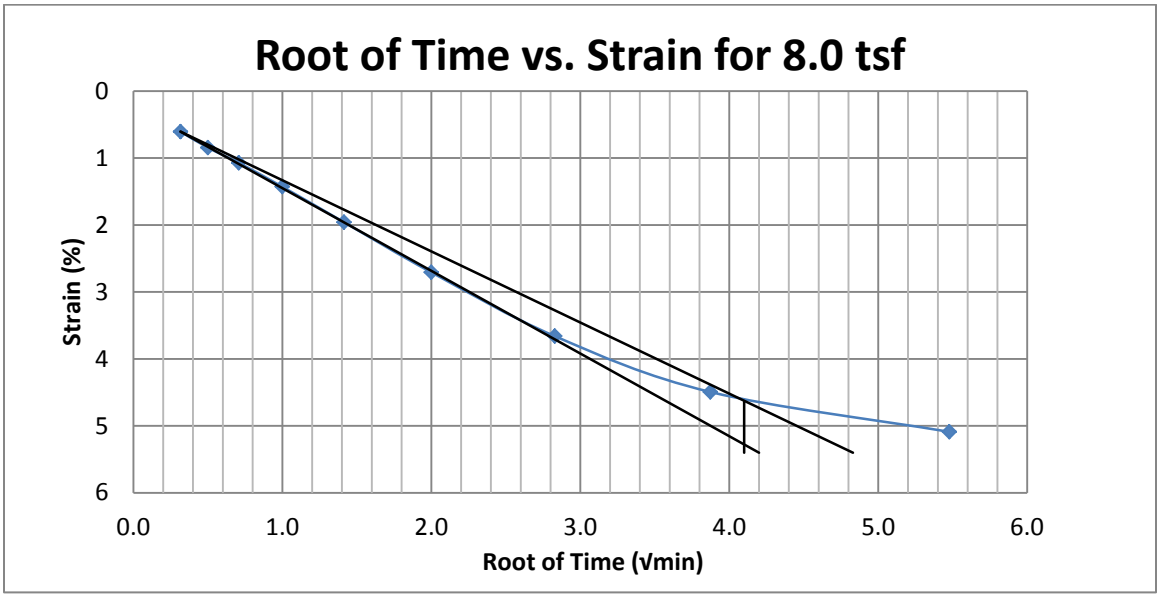

A160 Springville at 75-77 feet

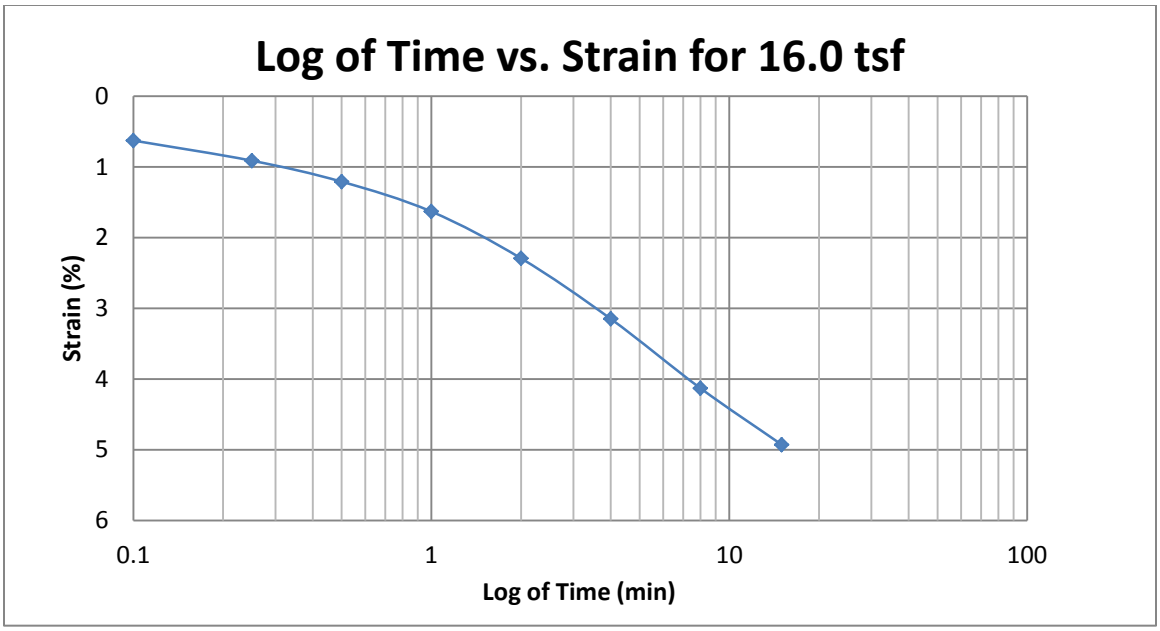

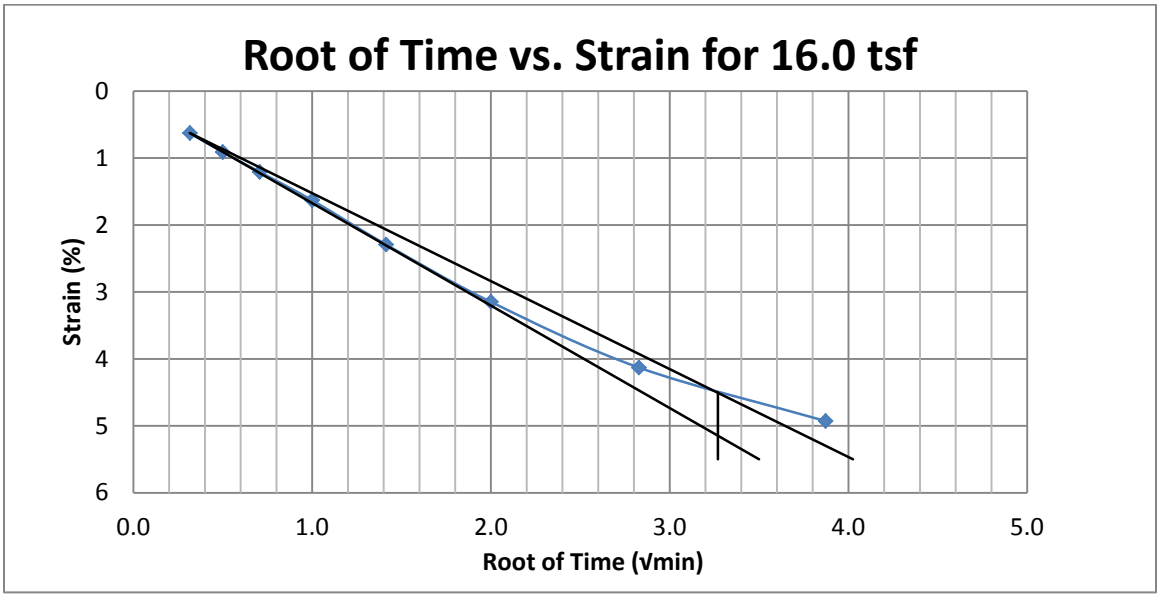

A161 Springville at 75-77 feet

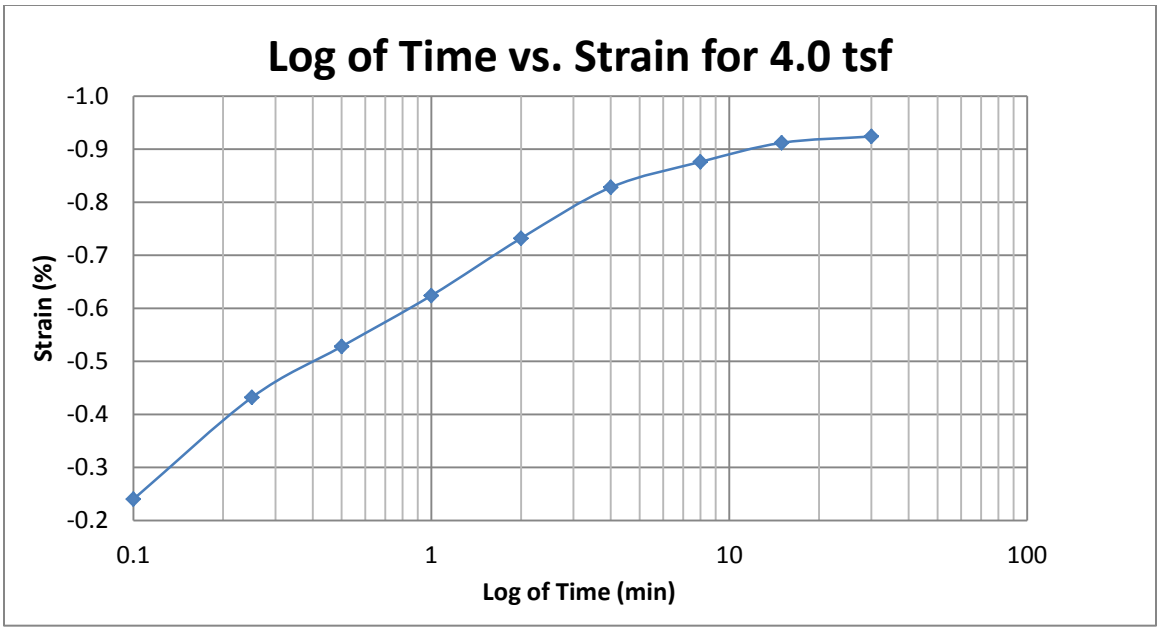

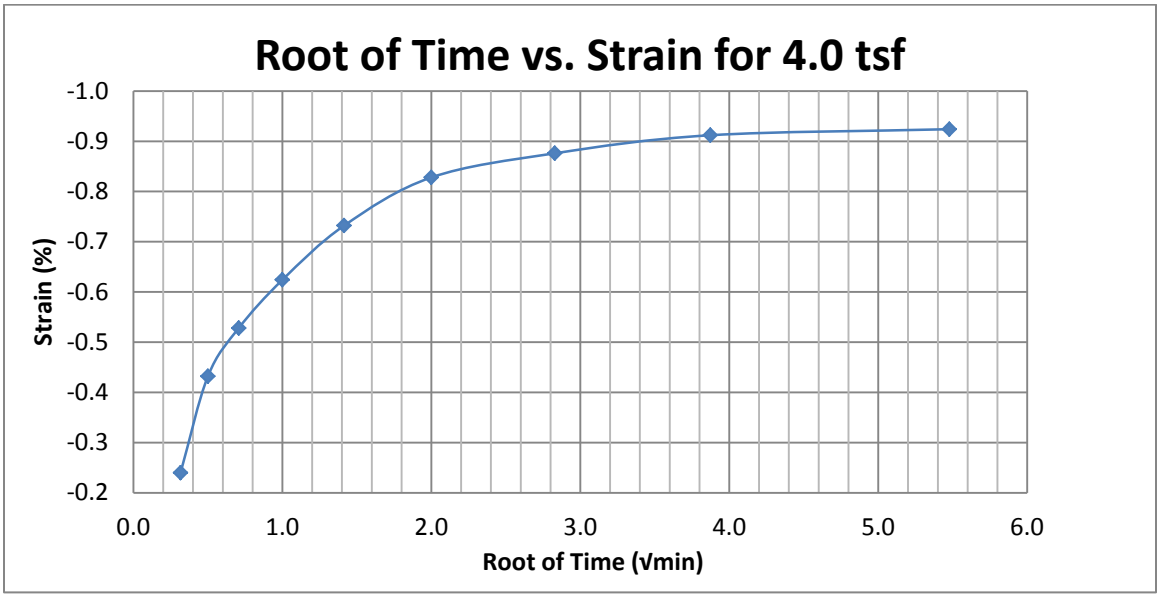

A162 Springville at 75-77 feet

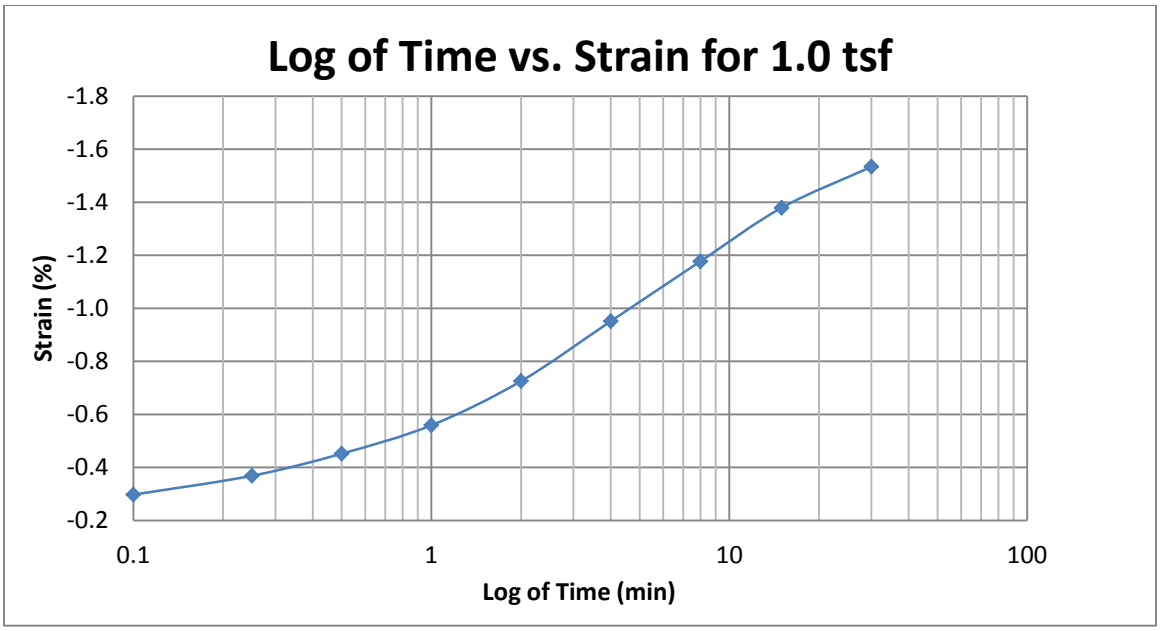

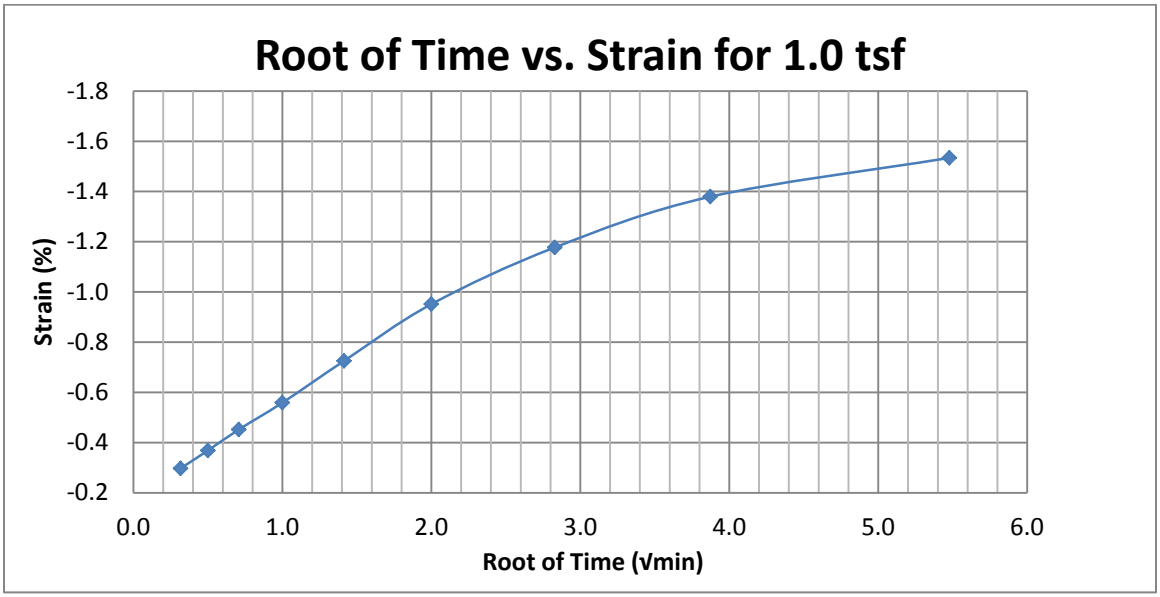

A163 Springville at 75-77 feet

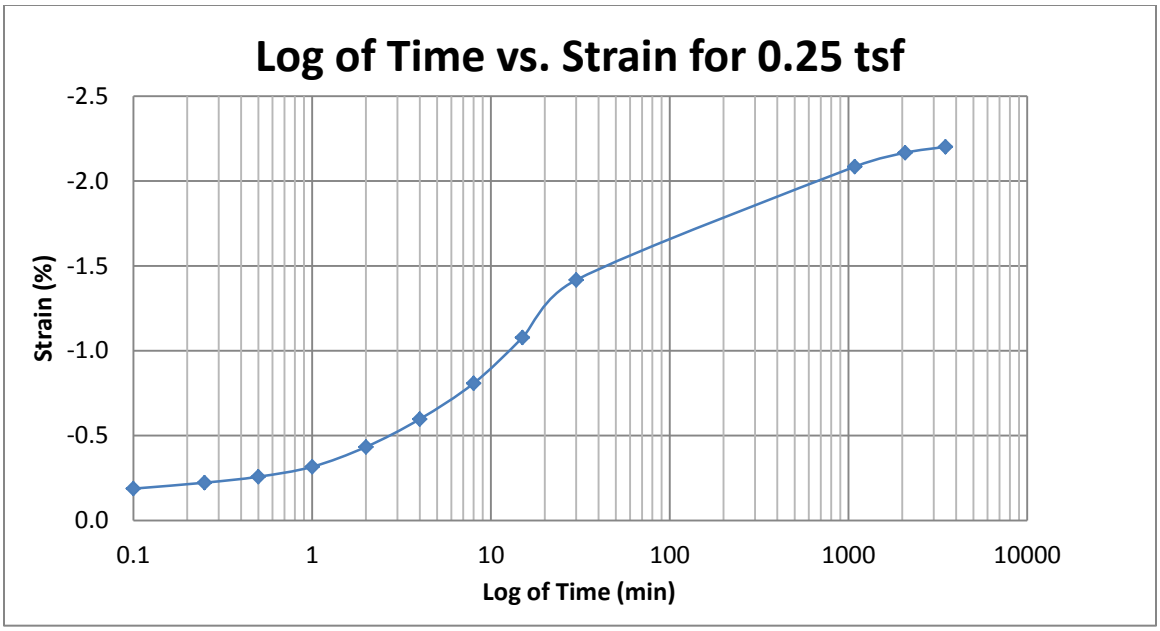

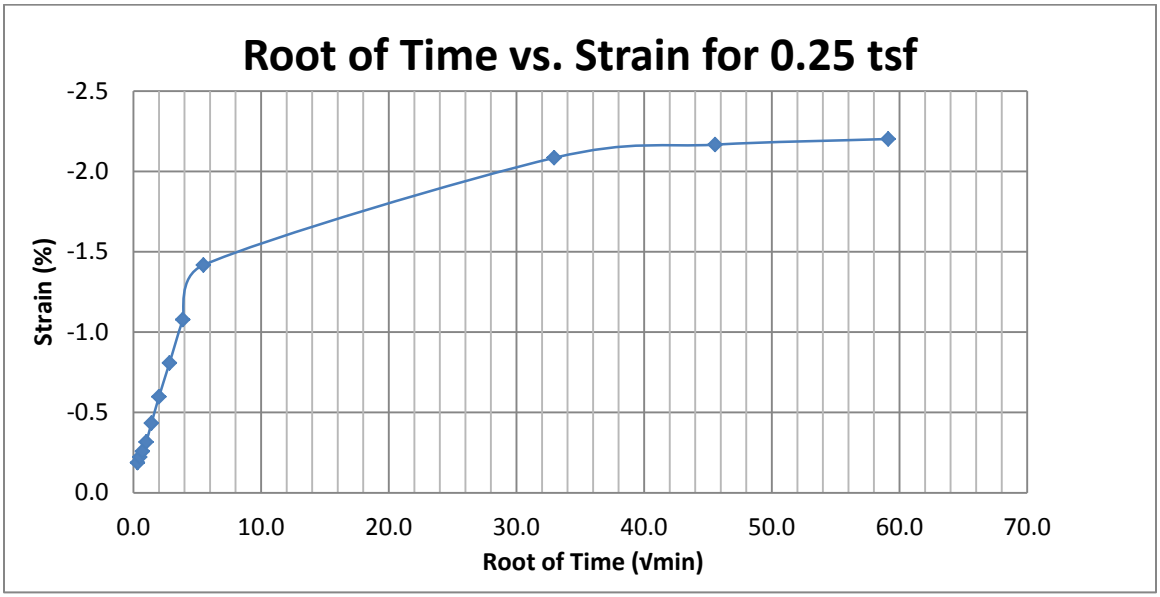

A164 Springville at 75-77 feet

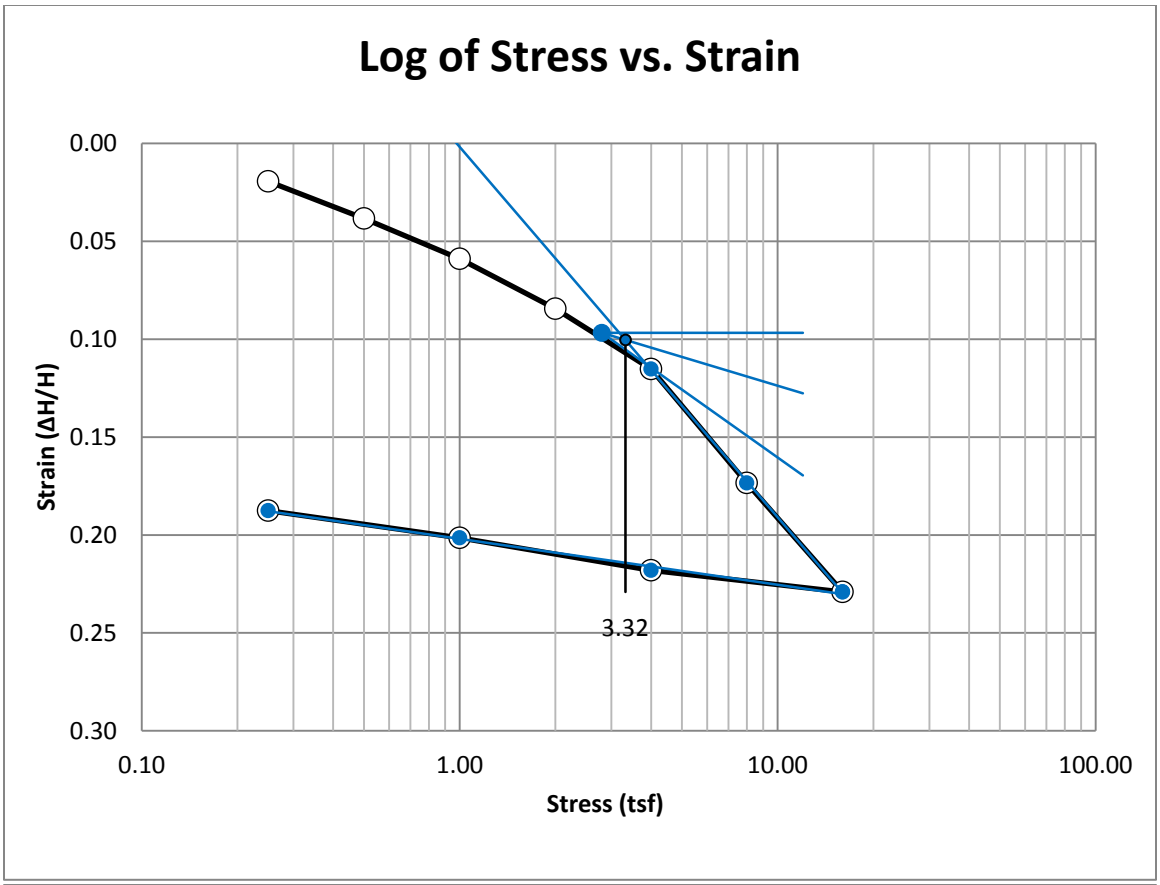

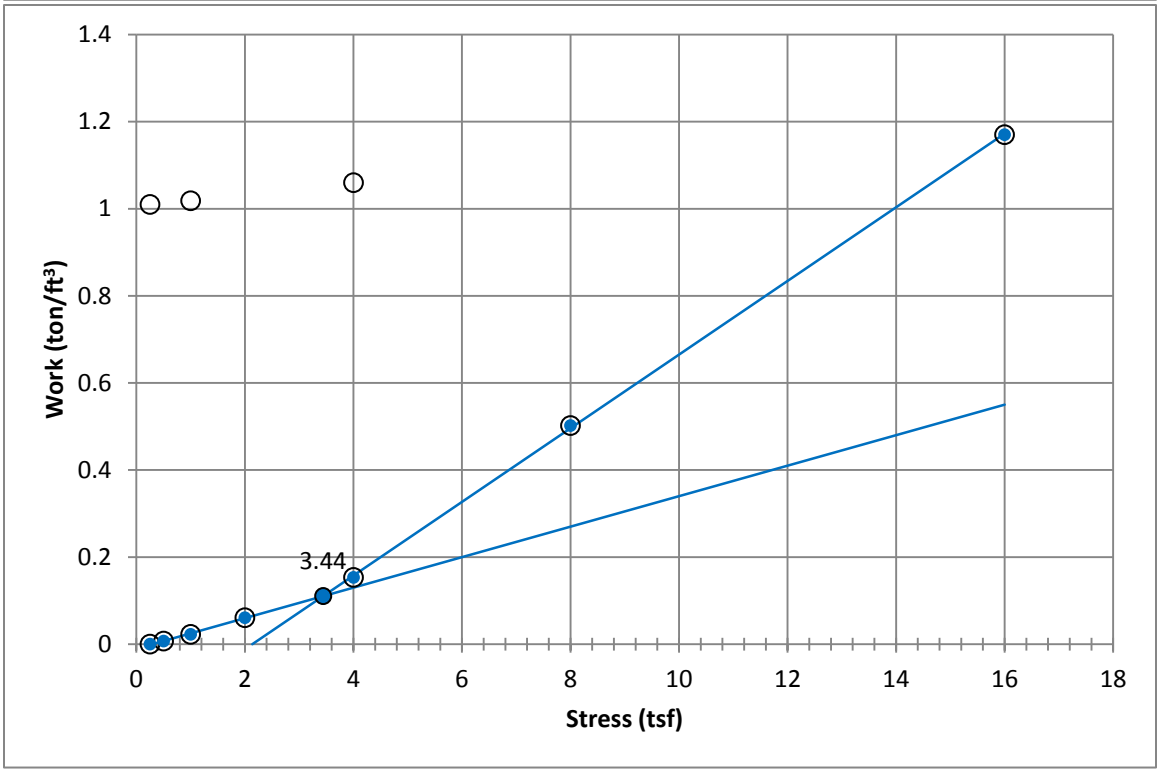

A165 Springville at 80-82 feet

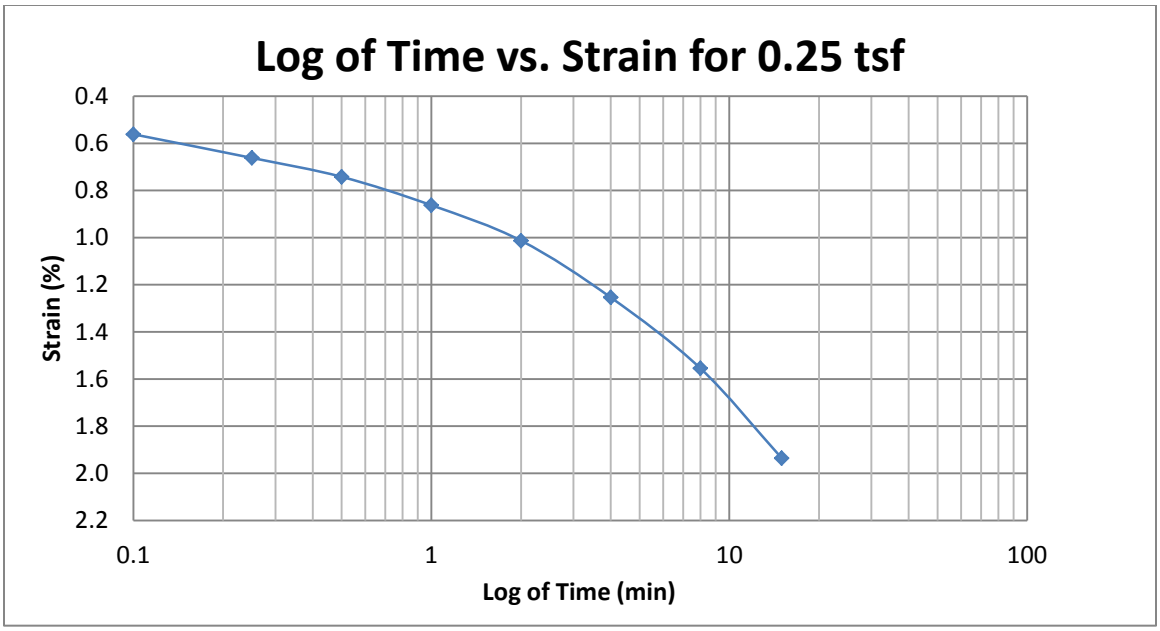

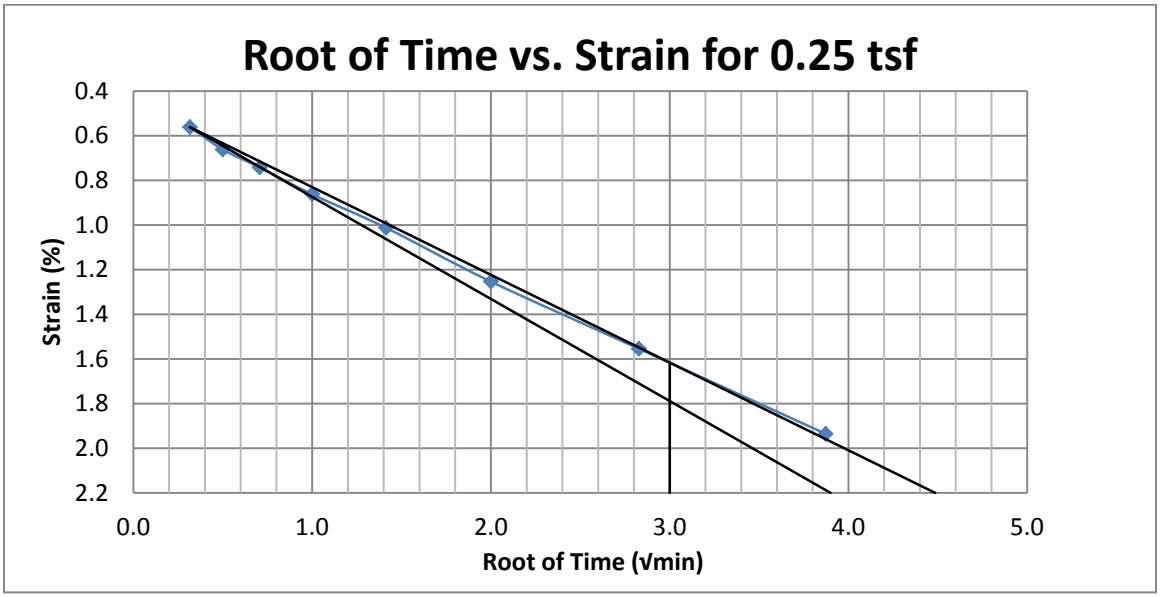

A166 Springville at 80-82 feet

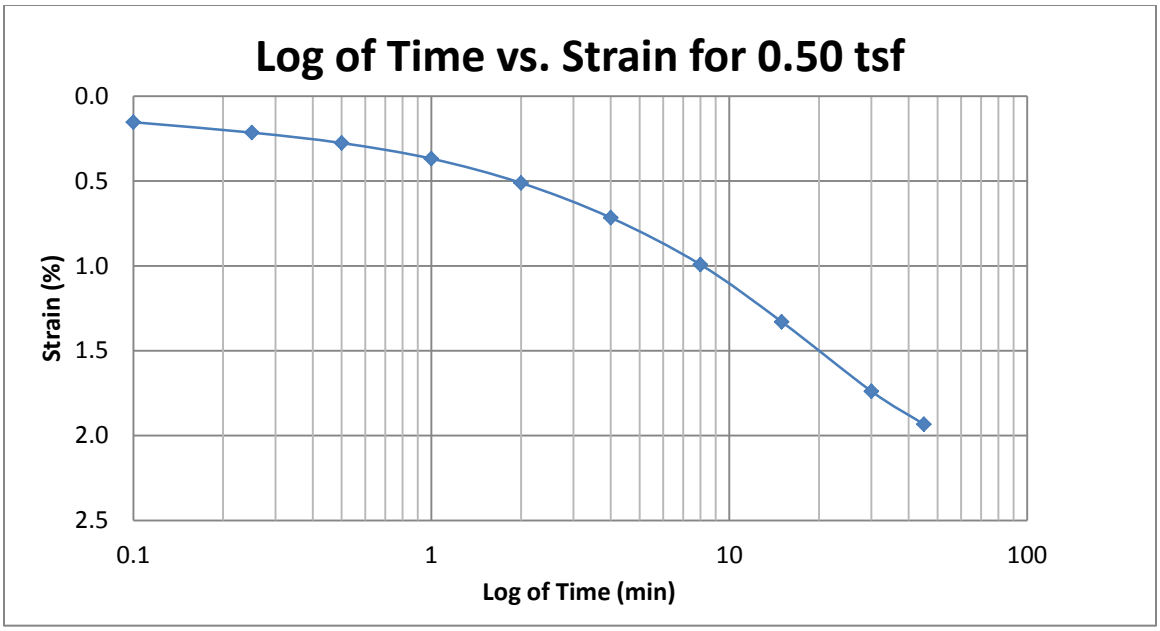

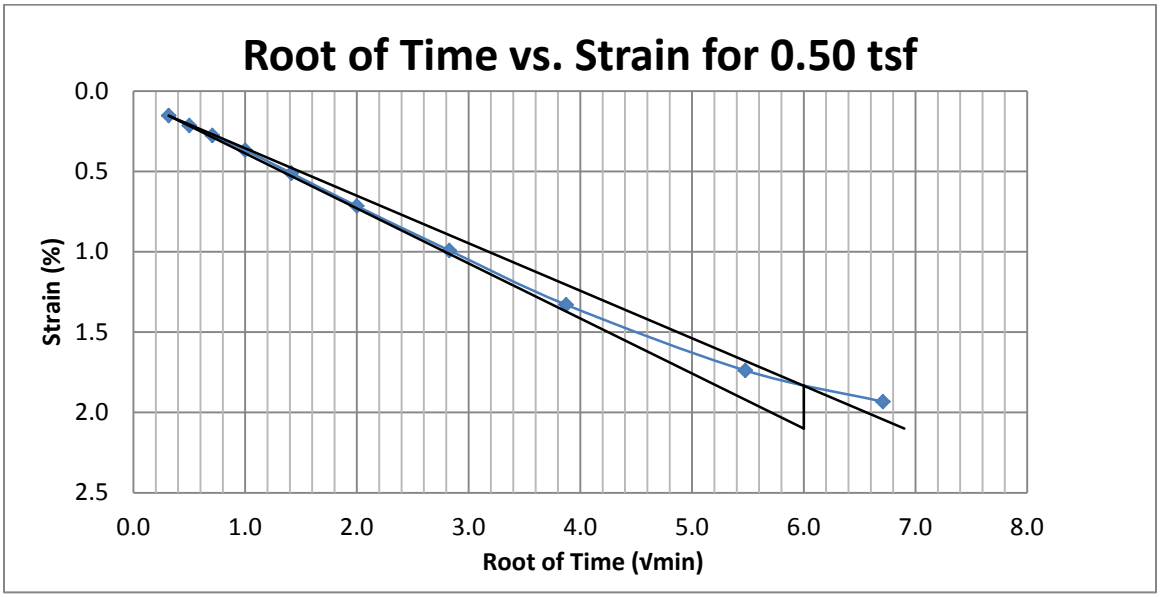

A167 Springville at 80-82 feet

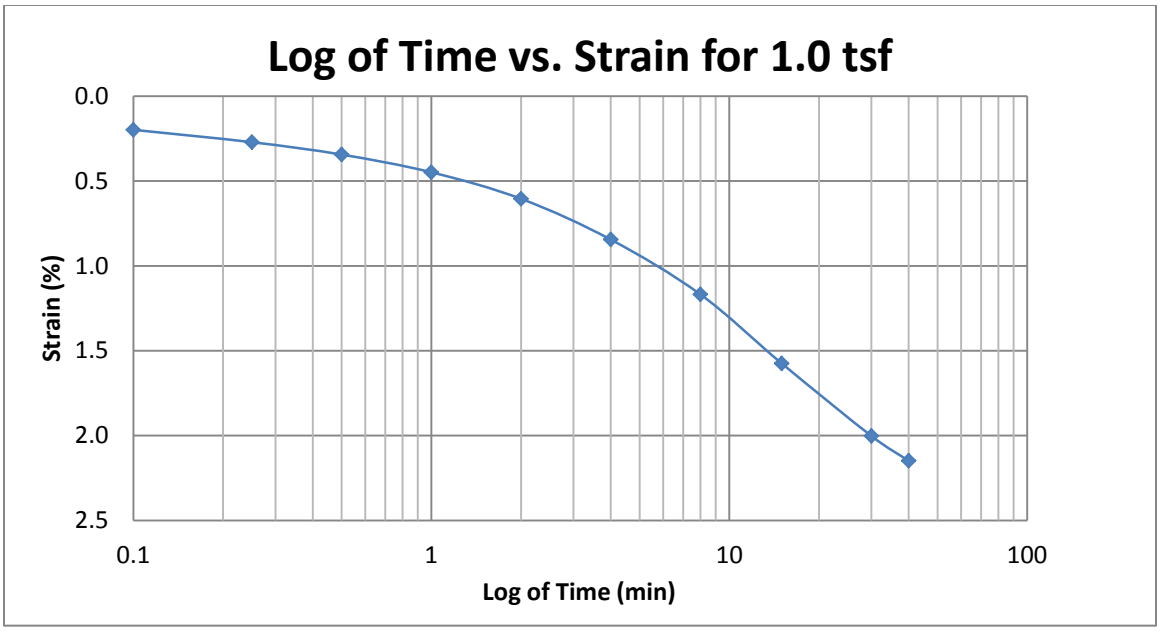

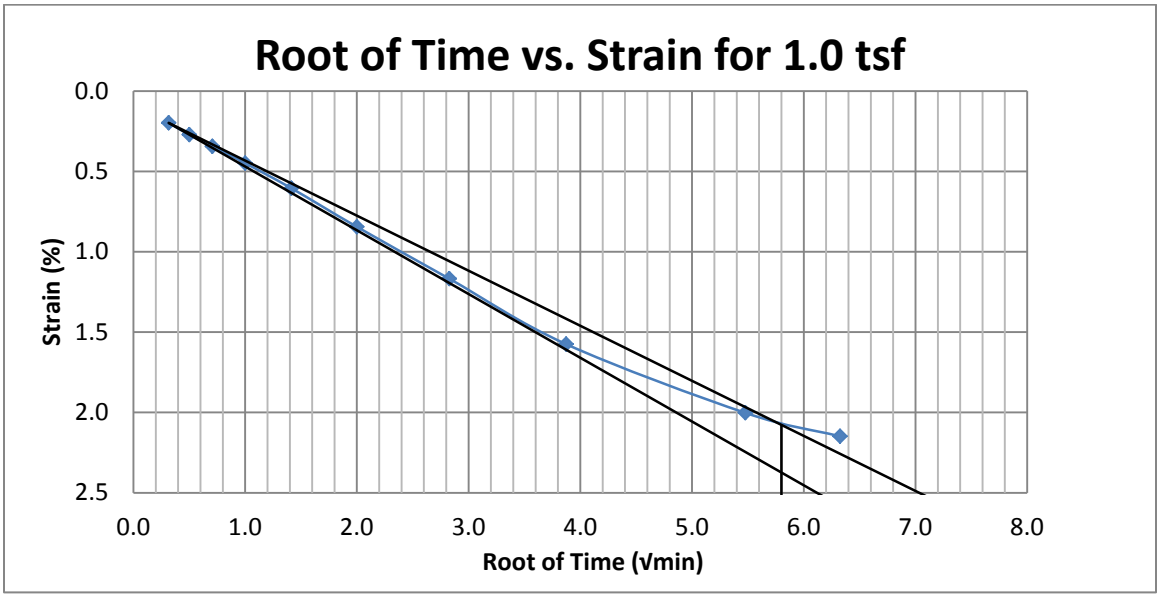

A168 Springville at 80-82 feet

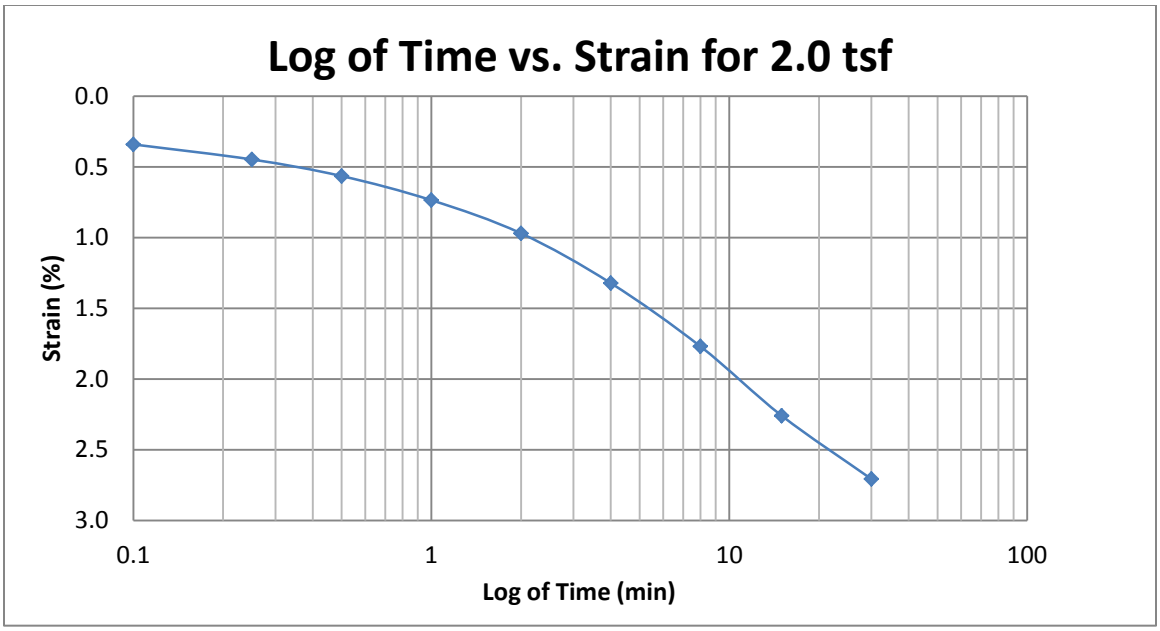

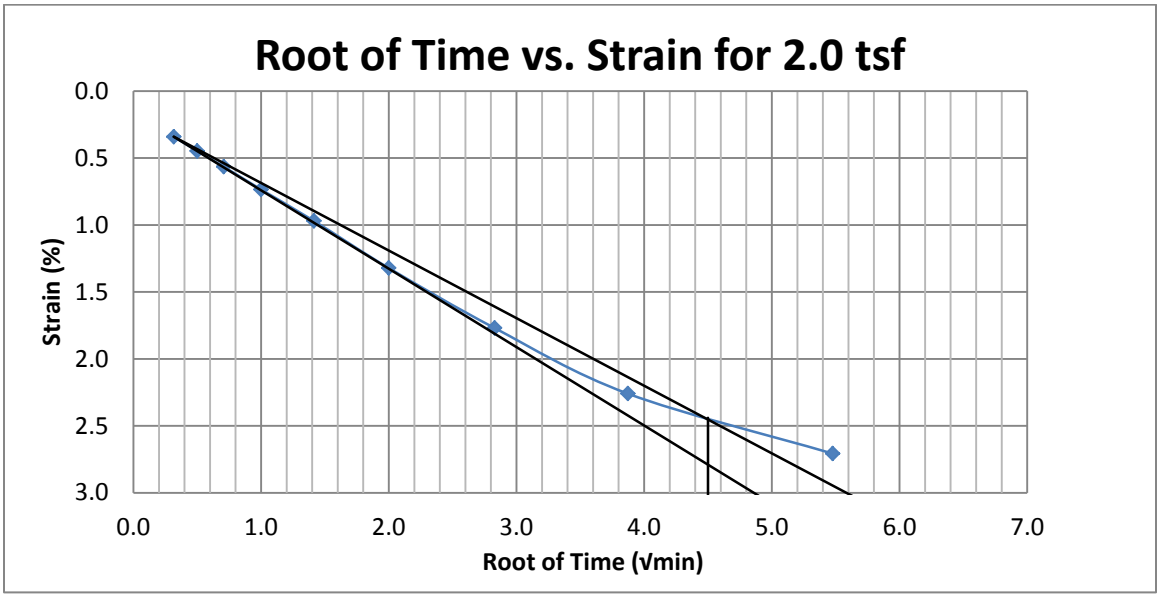

A169 Springville at 80-82 feet

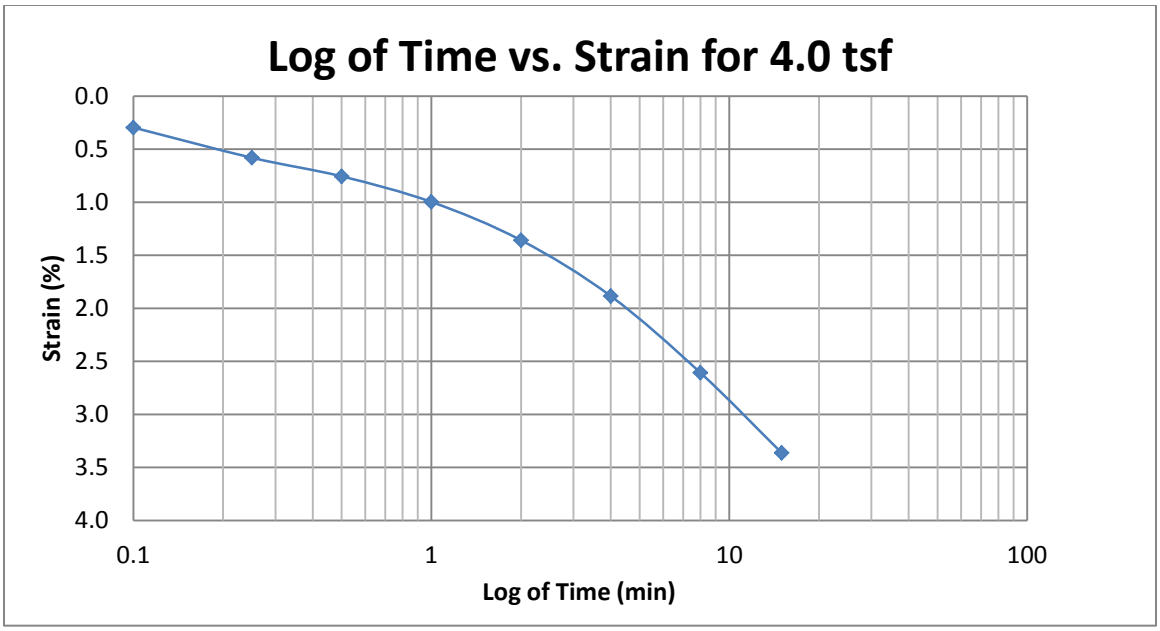

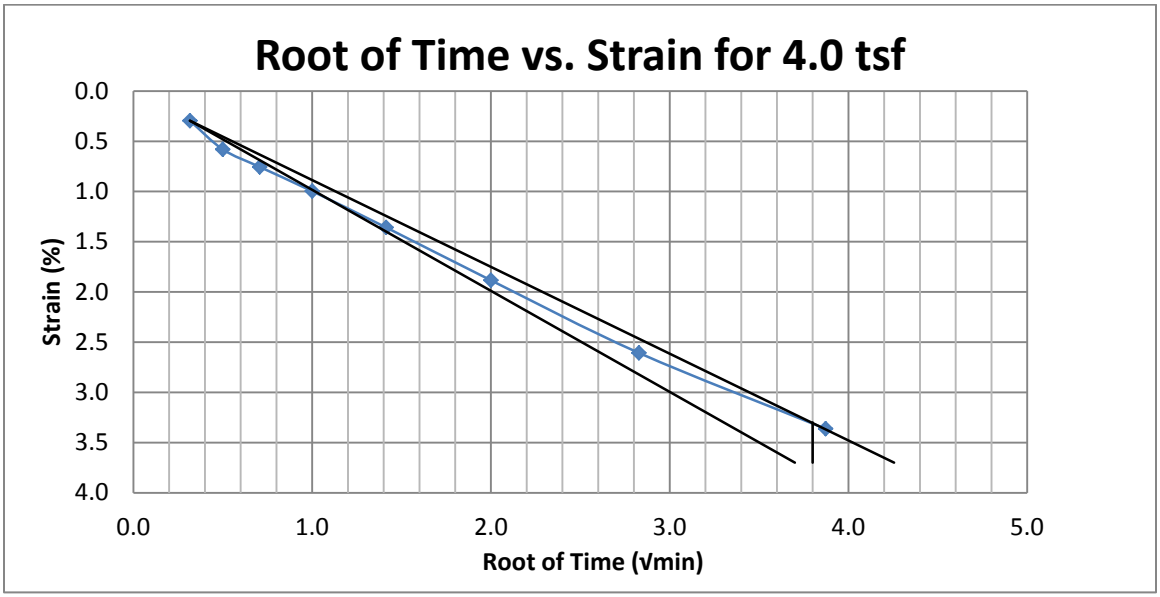

A170 Springville at 80-82 feet

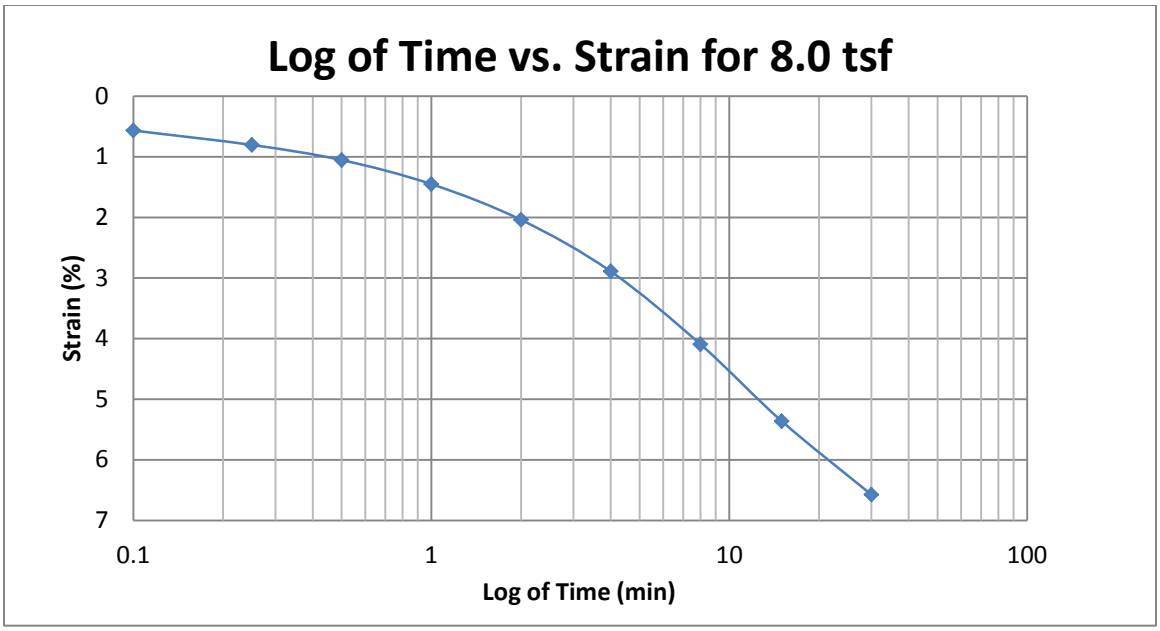

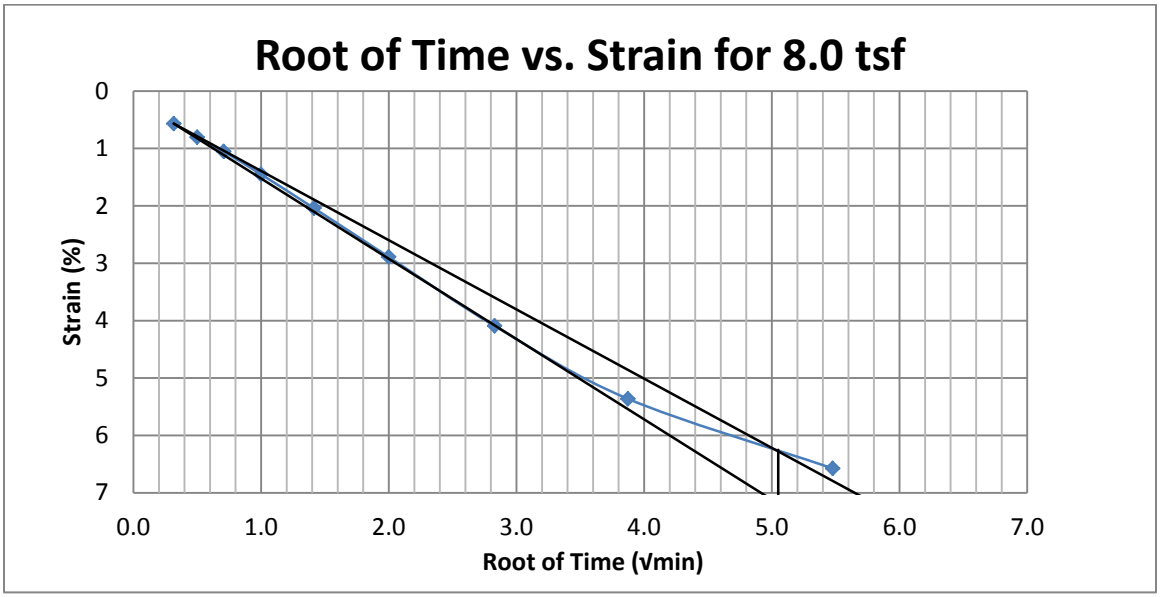

A171 Springville at 80-82 feet

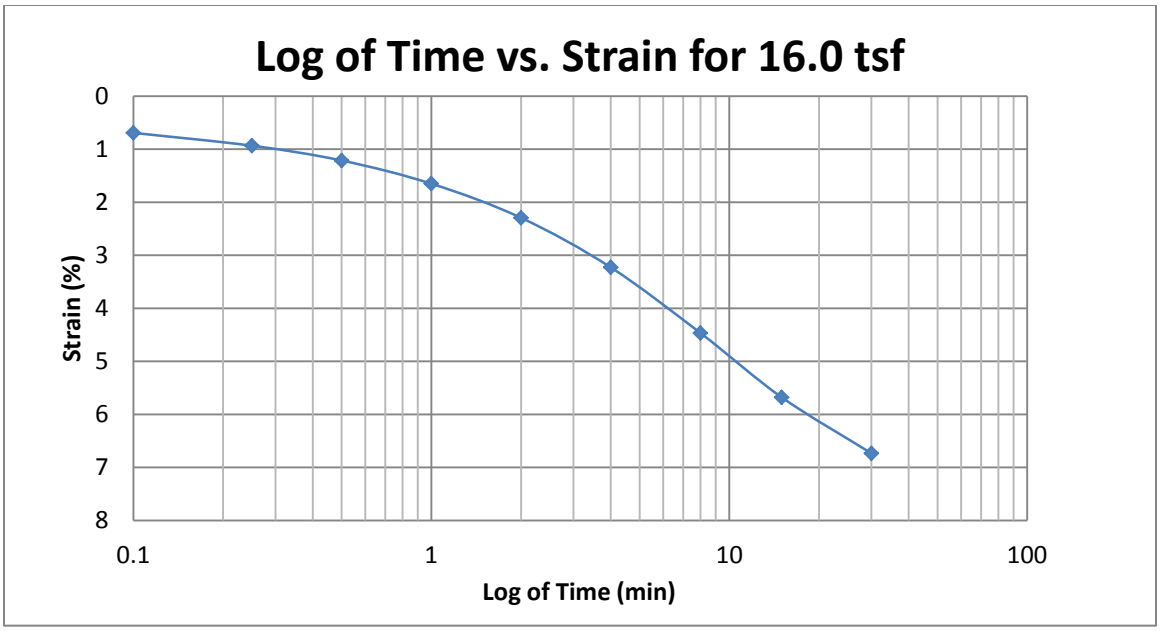

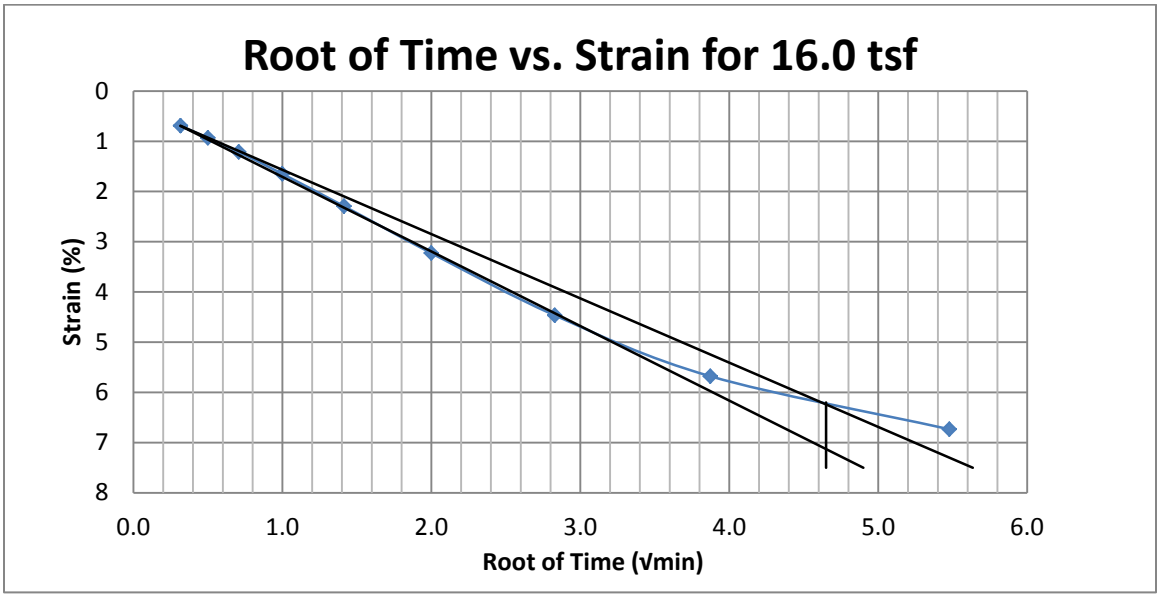

A172 Springville at 80-82 feet

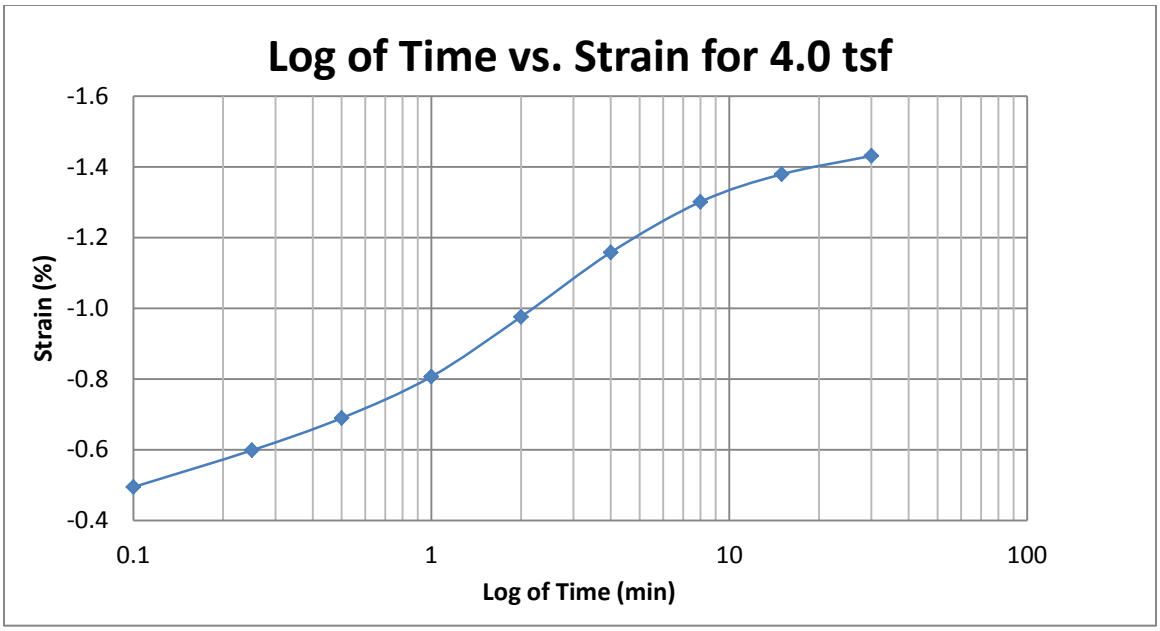

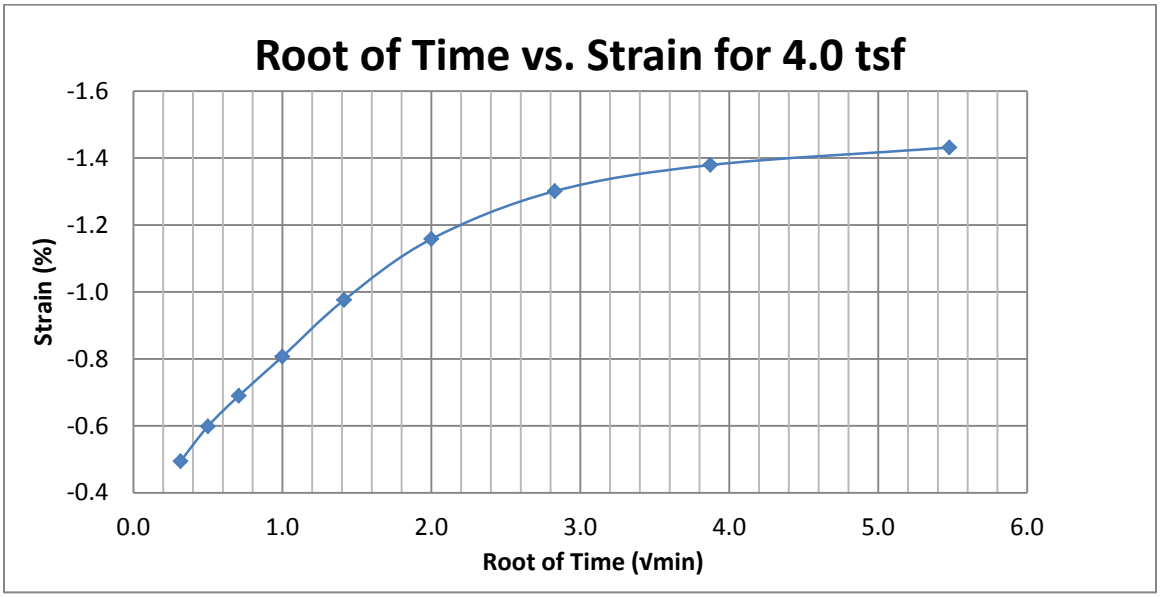

A173 Springville at 80-82 feet

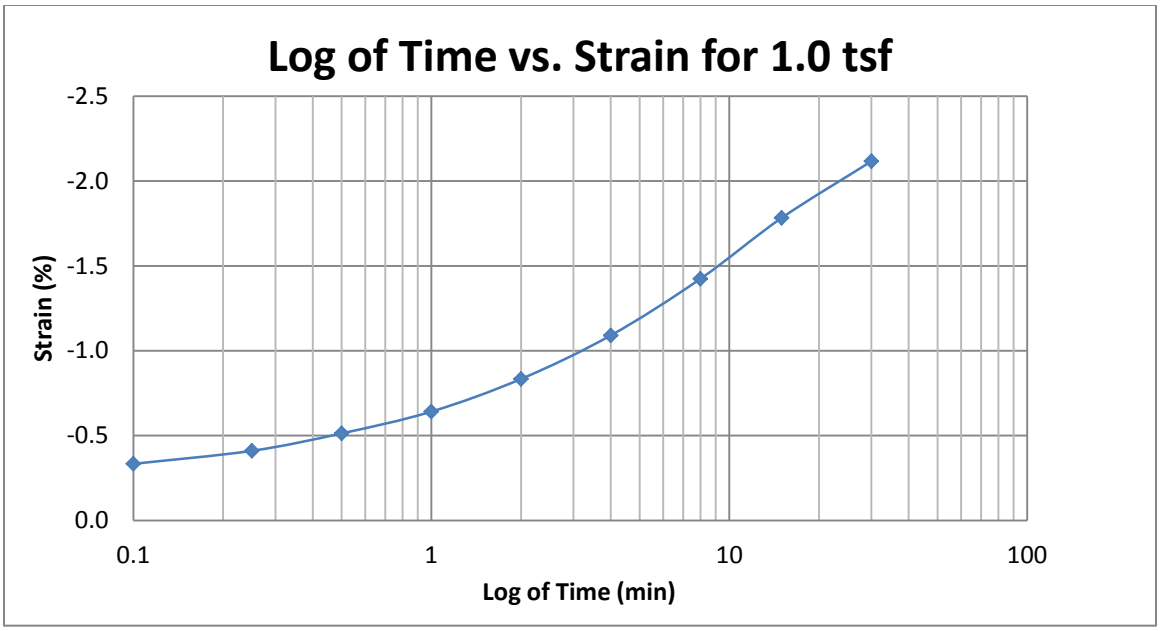

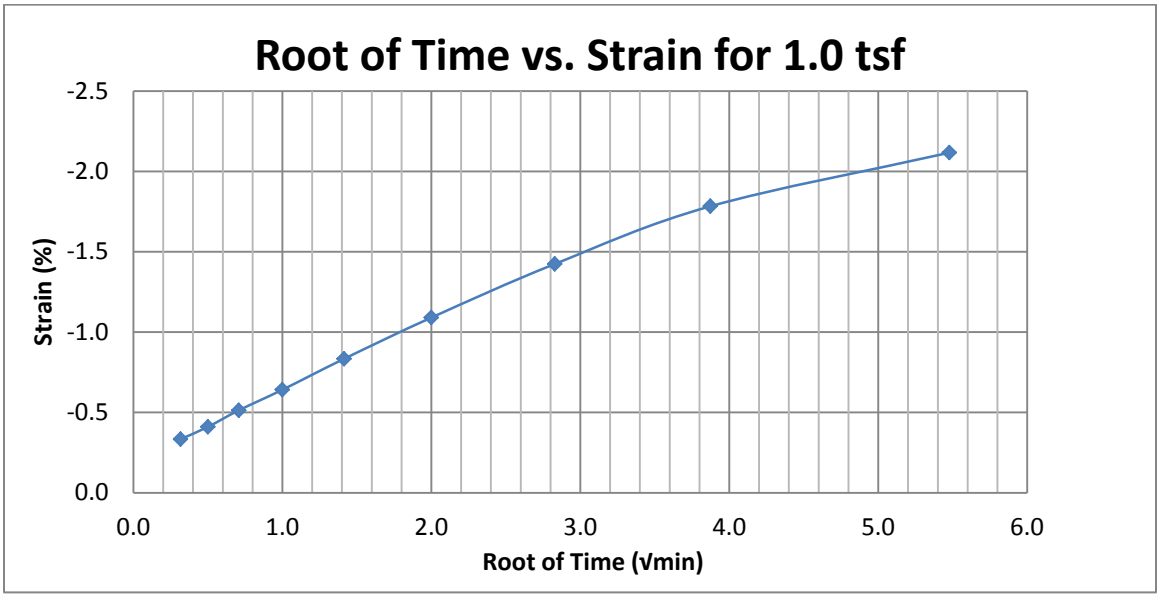

A174 Springville at 80-82 feet

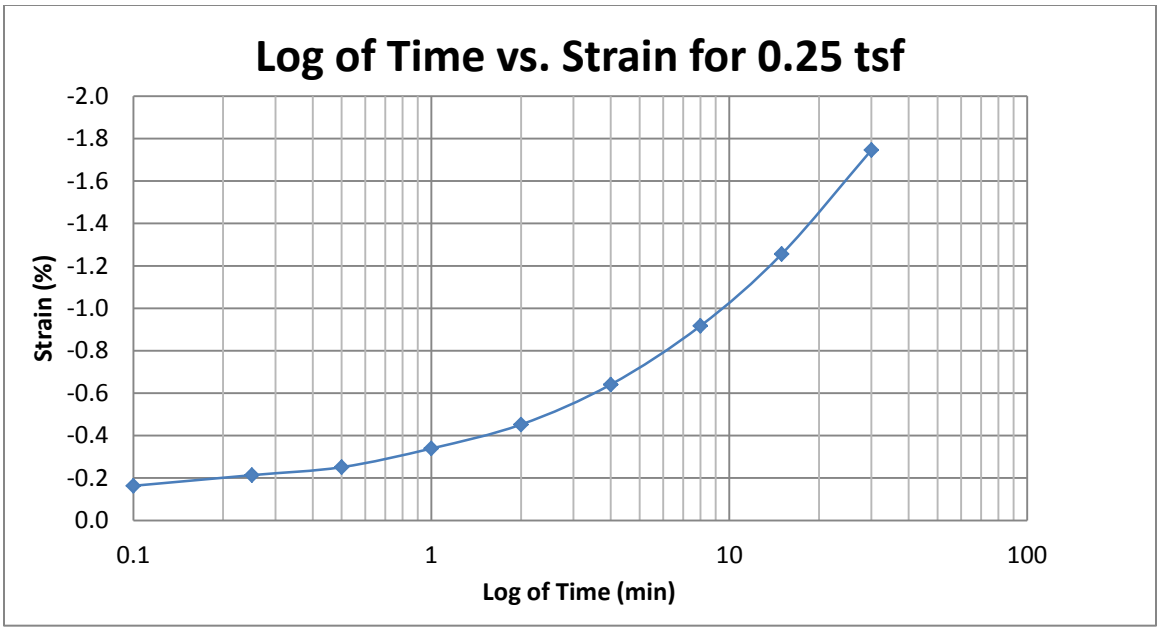

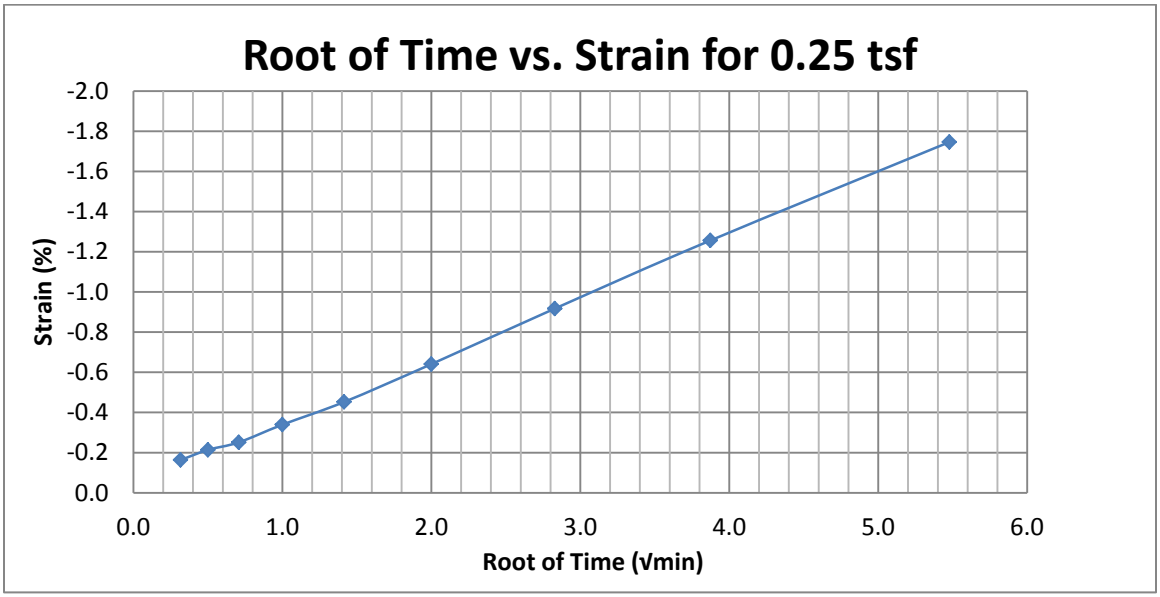

A175 Springville at 80-82 feet

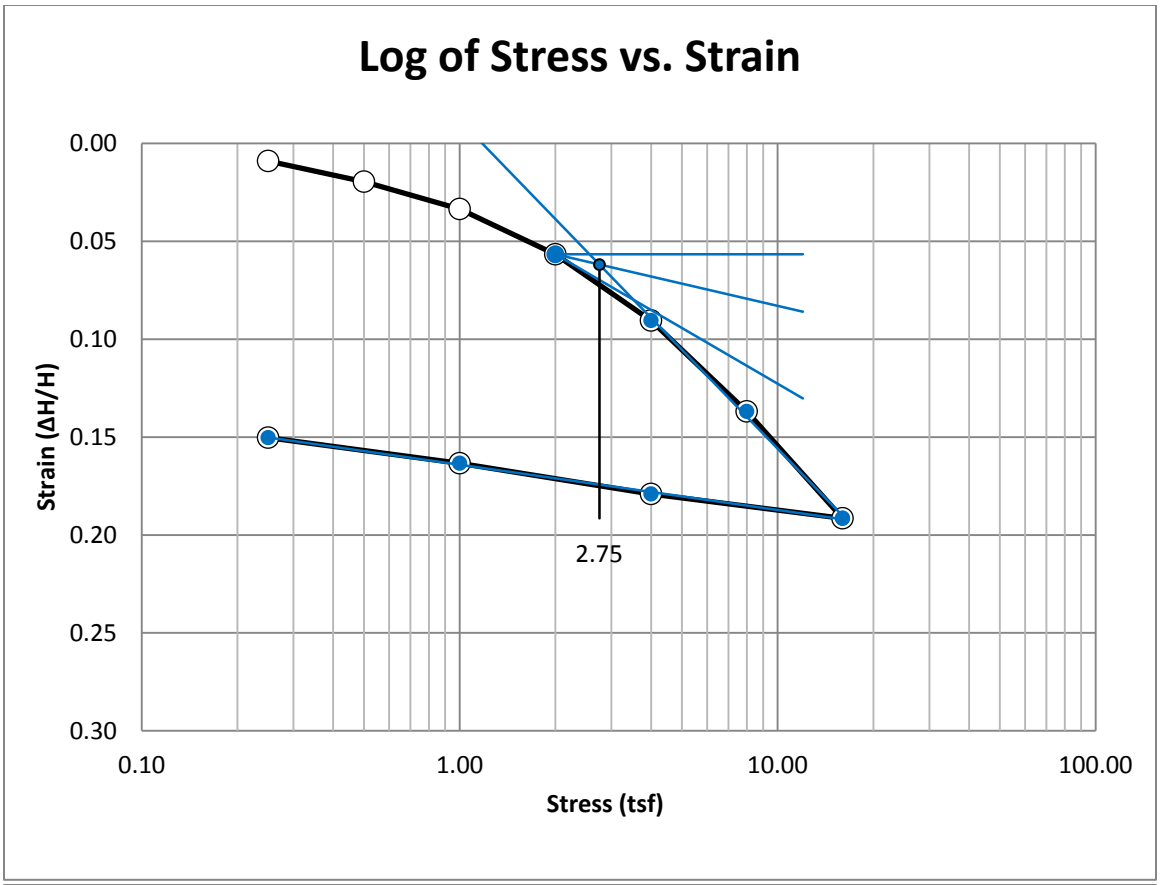

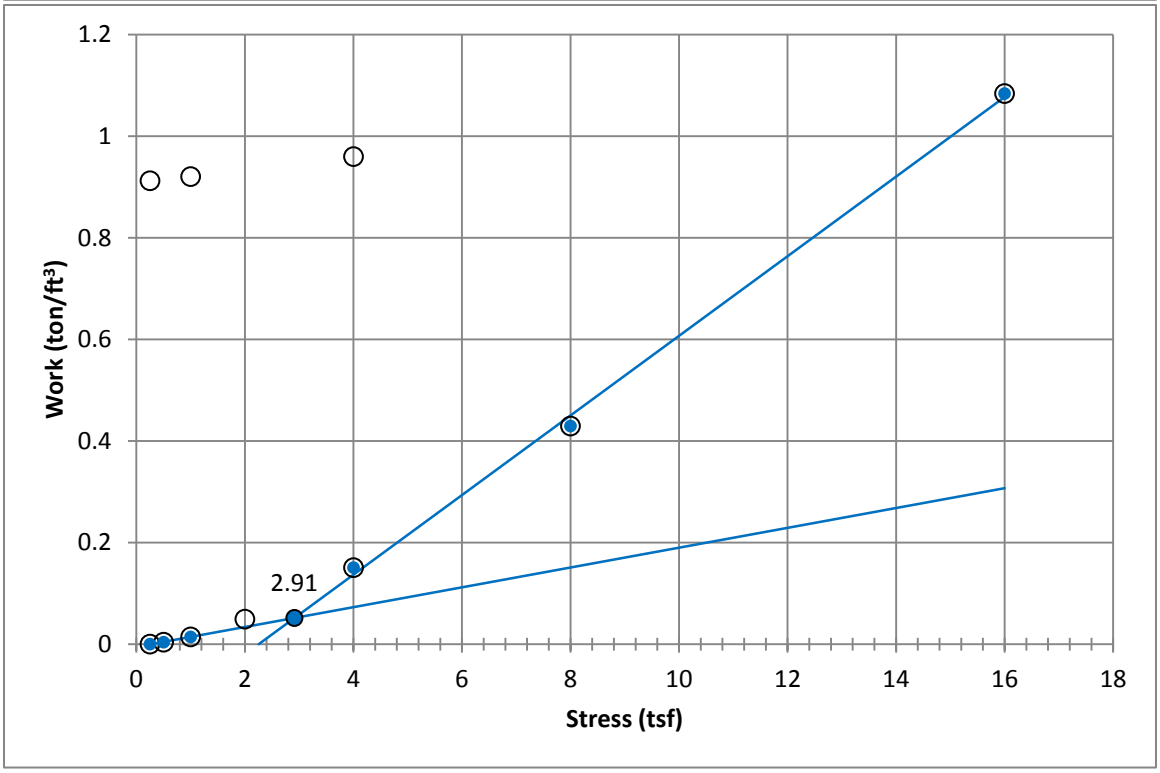

A176 Springville at 84-86 feet

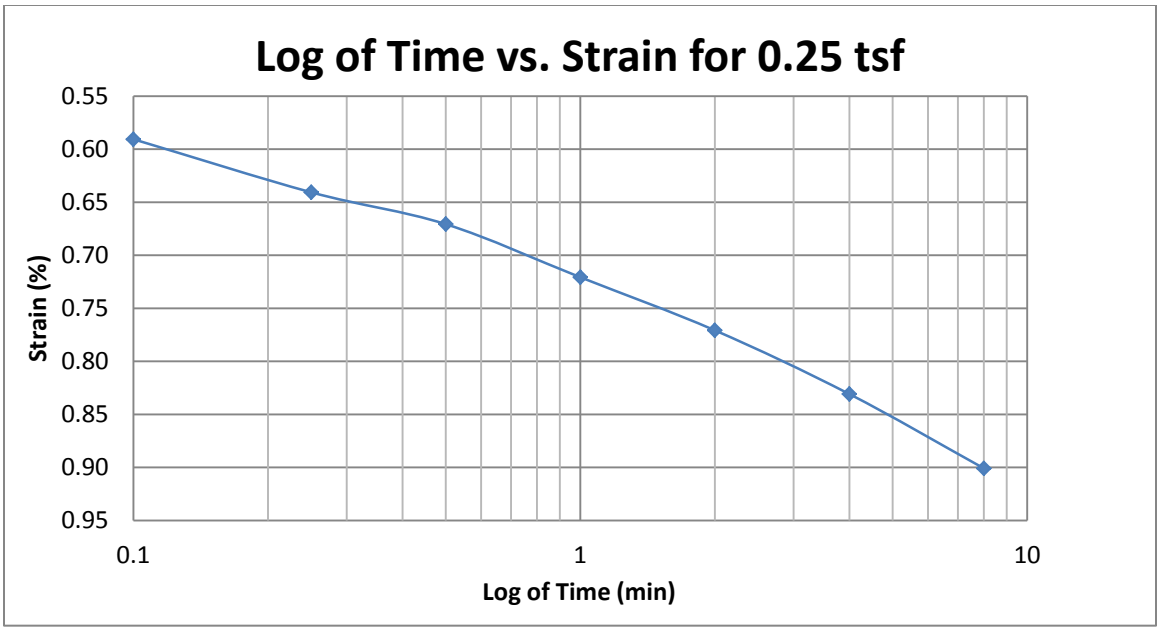

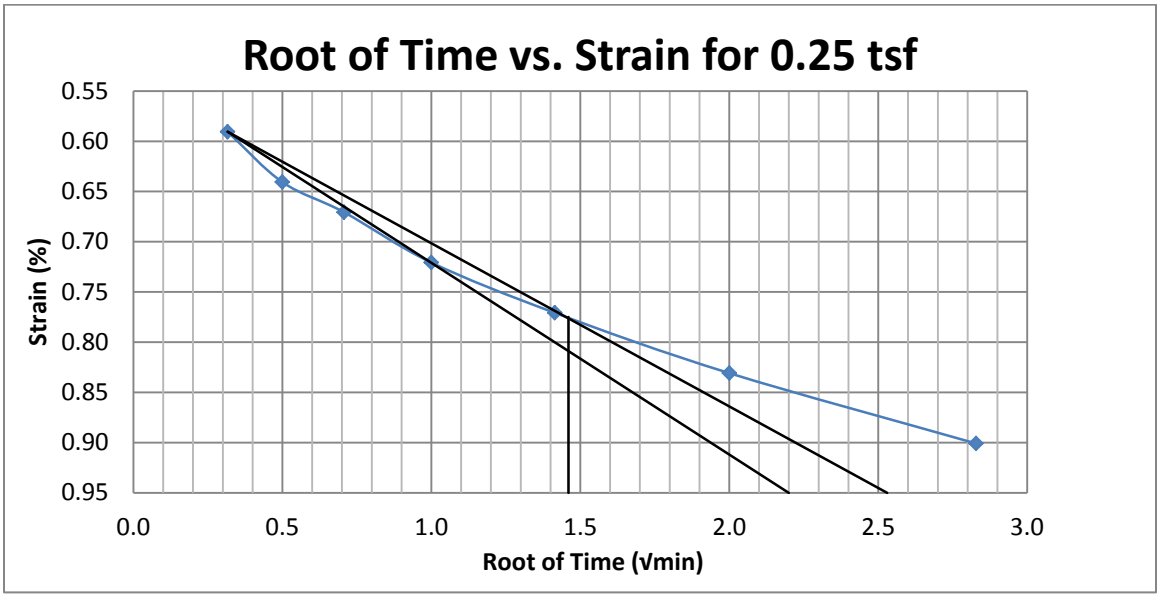

A177 Springville at 84-86 feet

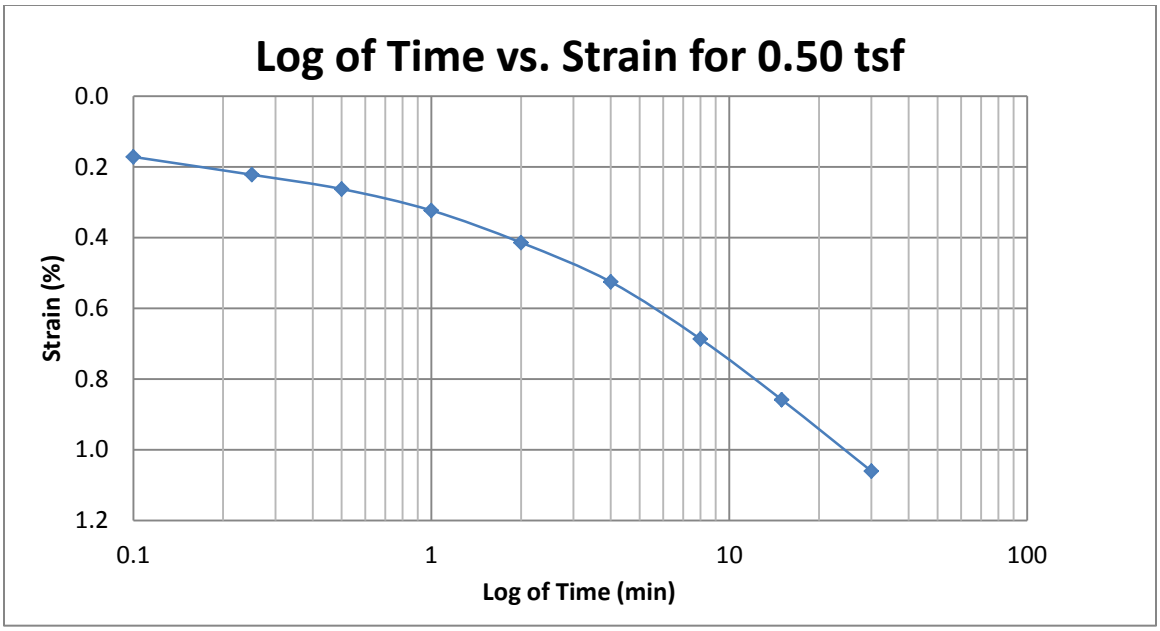

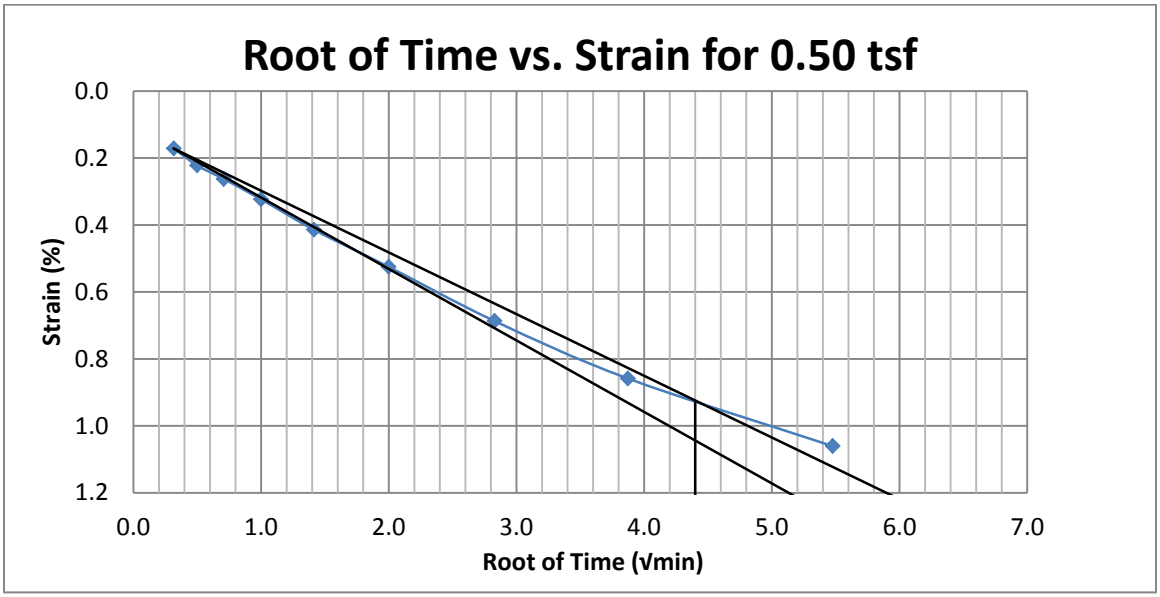

A178 Springville at 84-86 feet

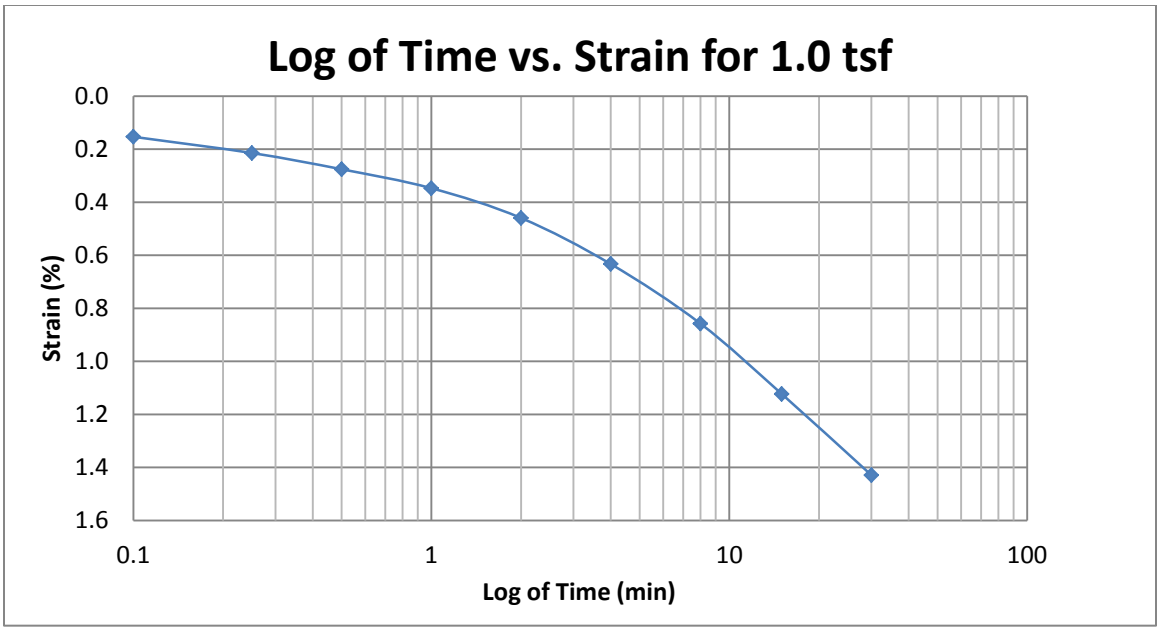

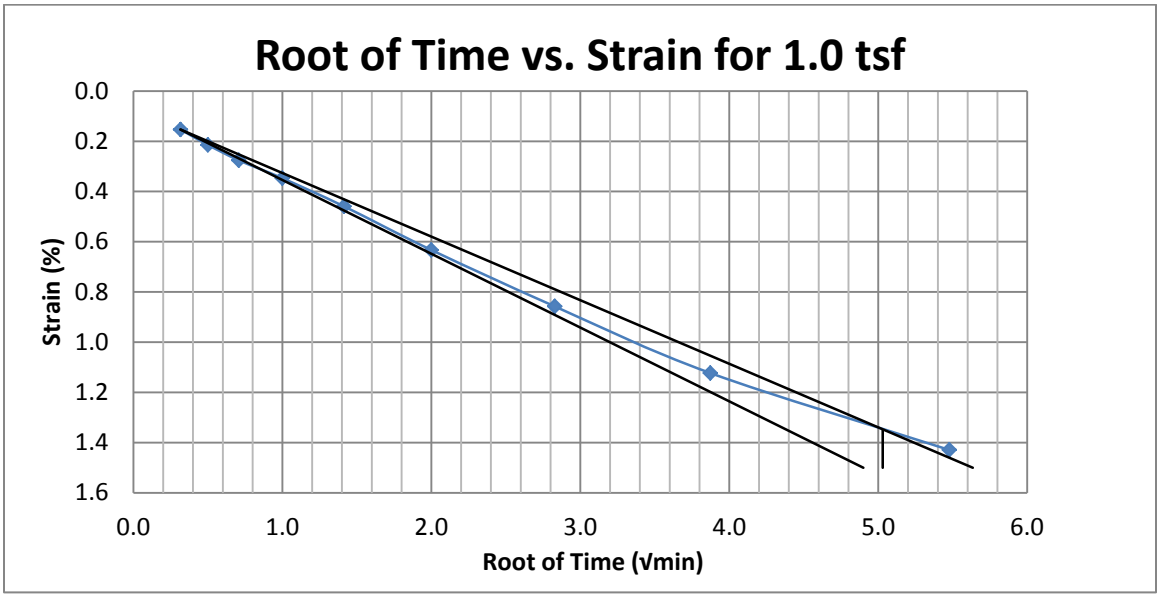

A179 Springville at 84-86 feet

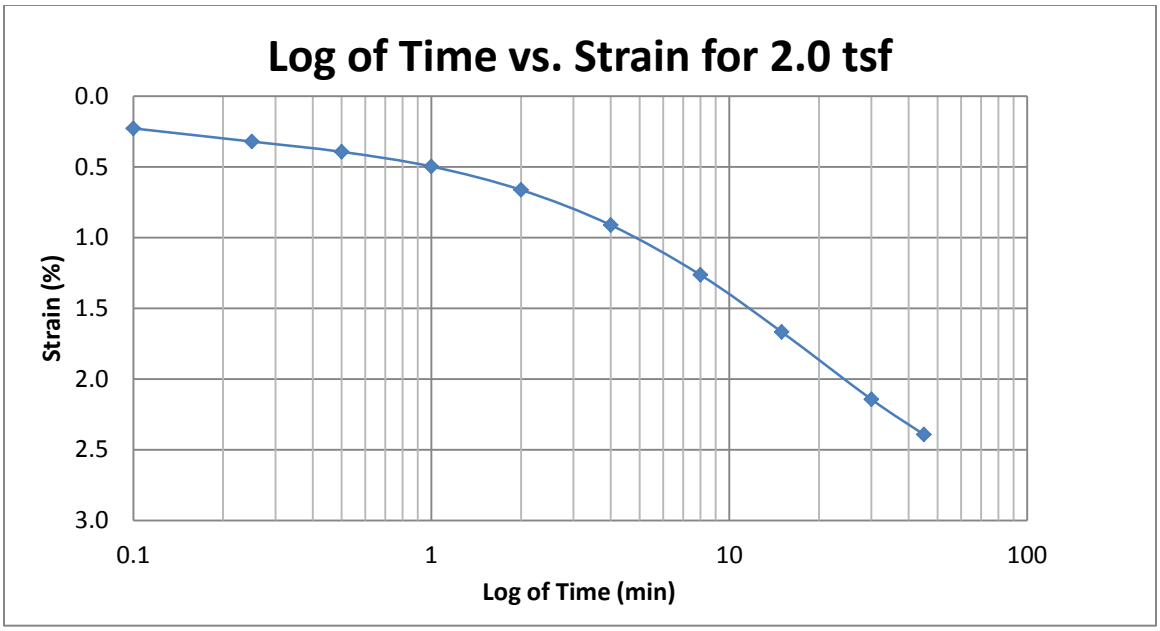

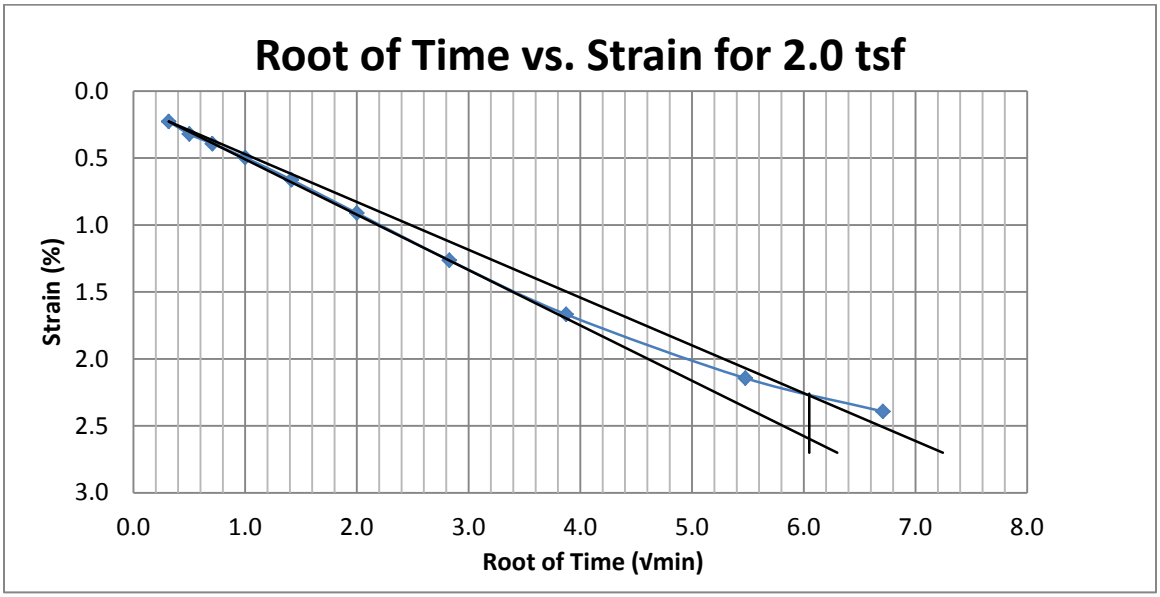

A180 Springville at 84-86 feet

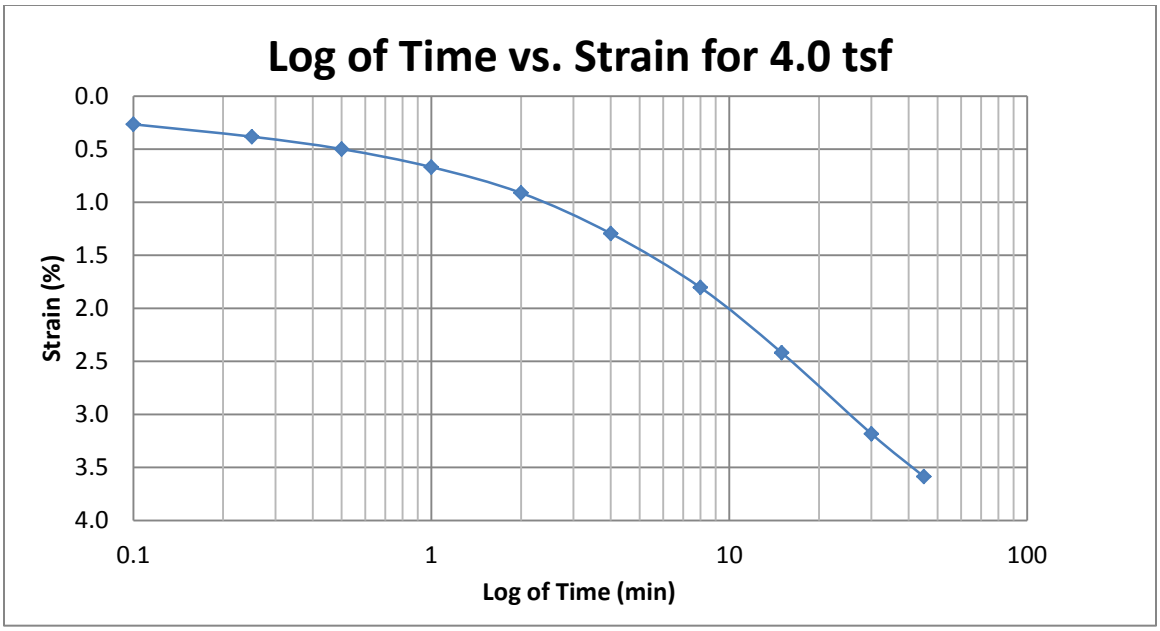

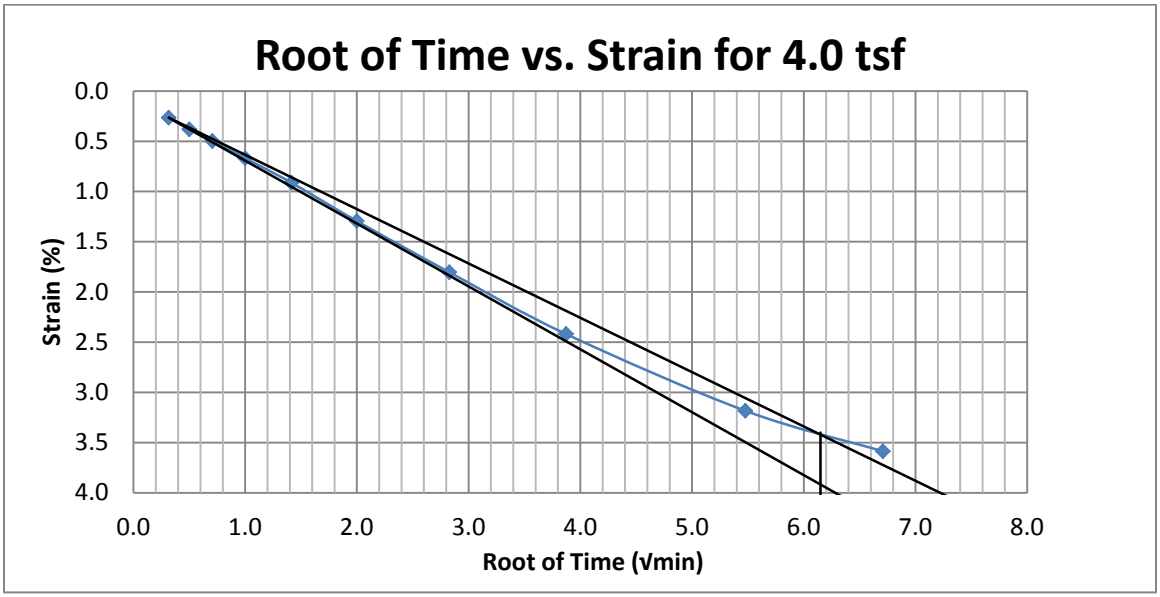

A181 Springville at 84-86 feet

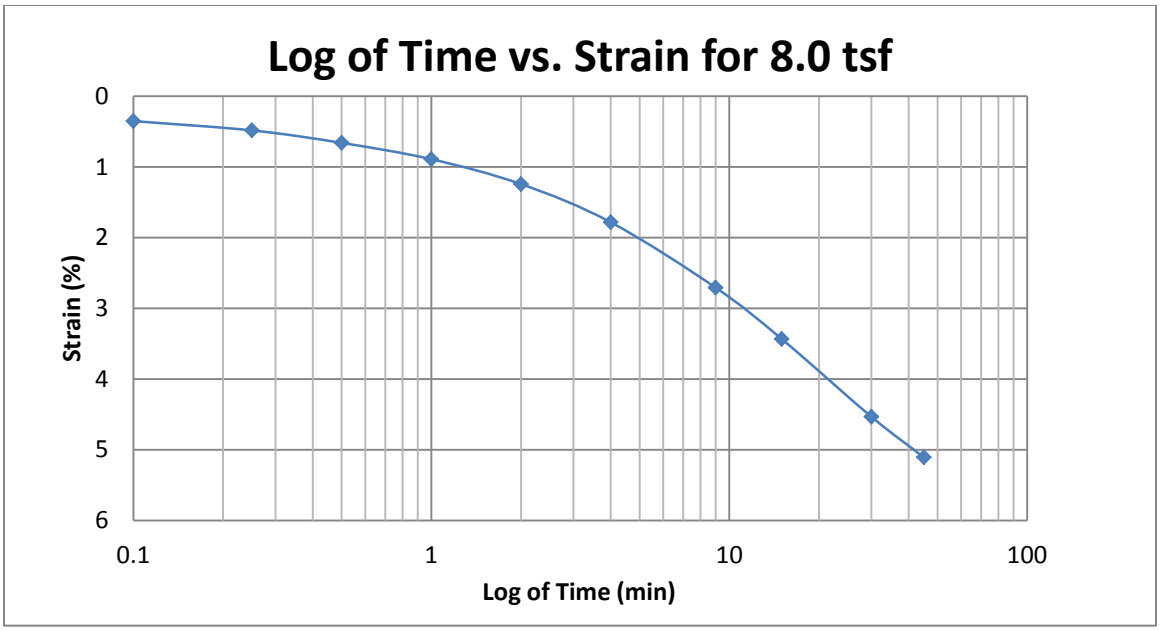

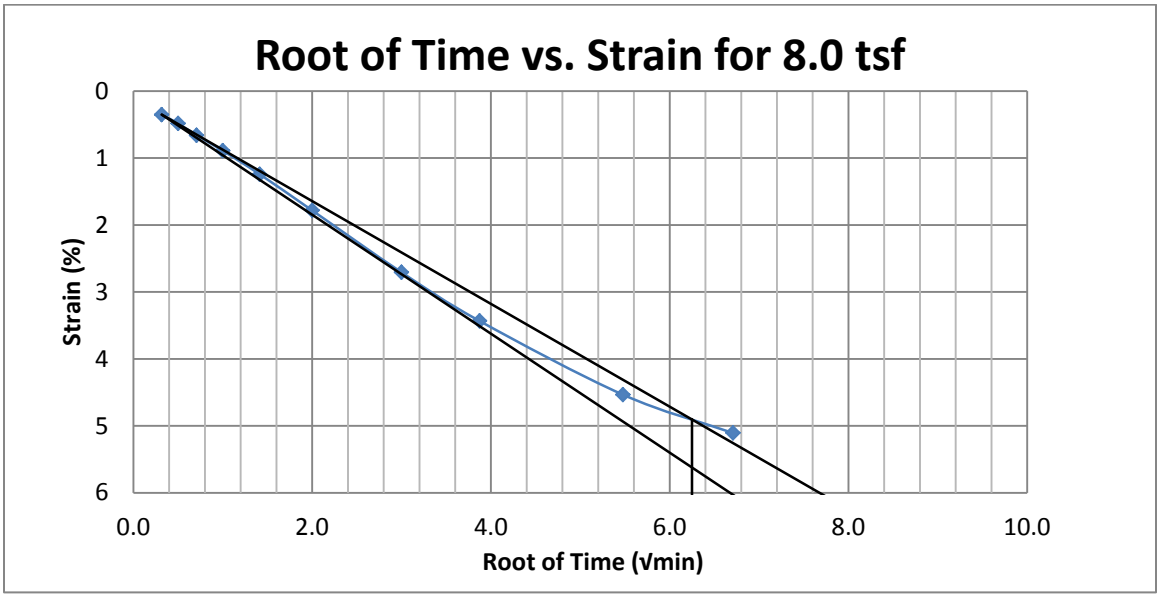

A182 Springville at 84-86 feet

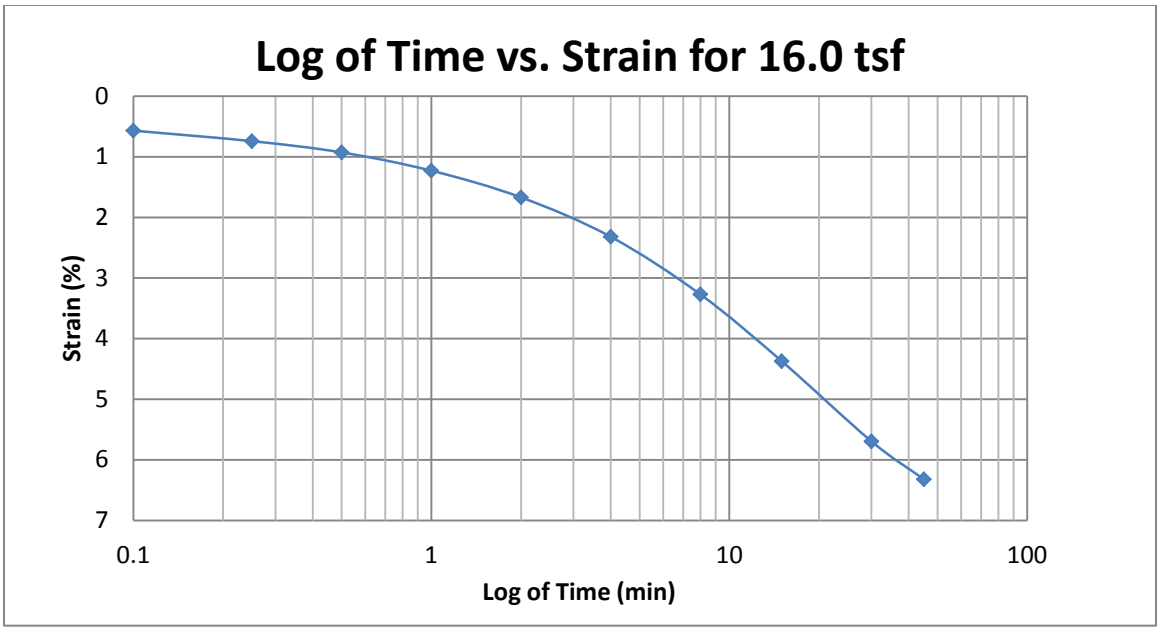

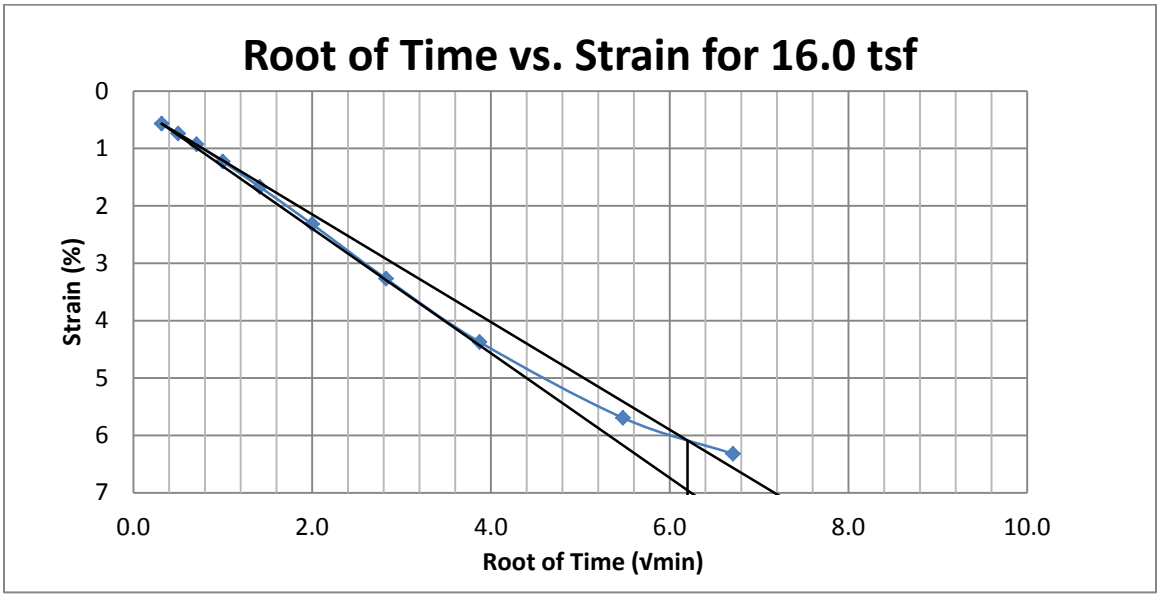

A183 Springville at 84-86 feet

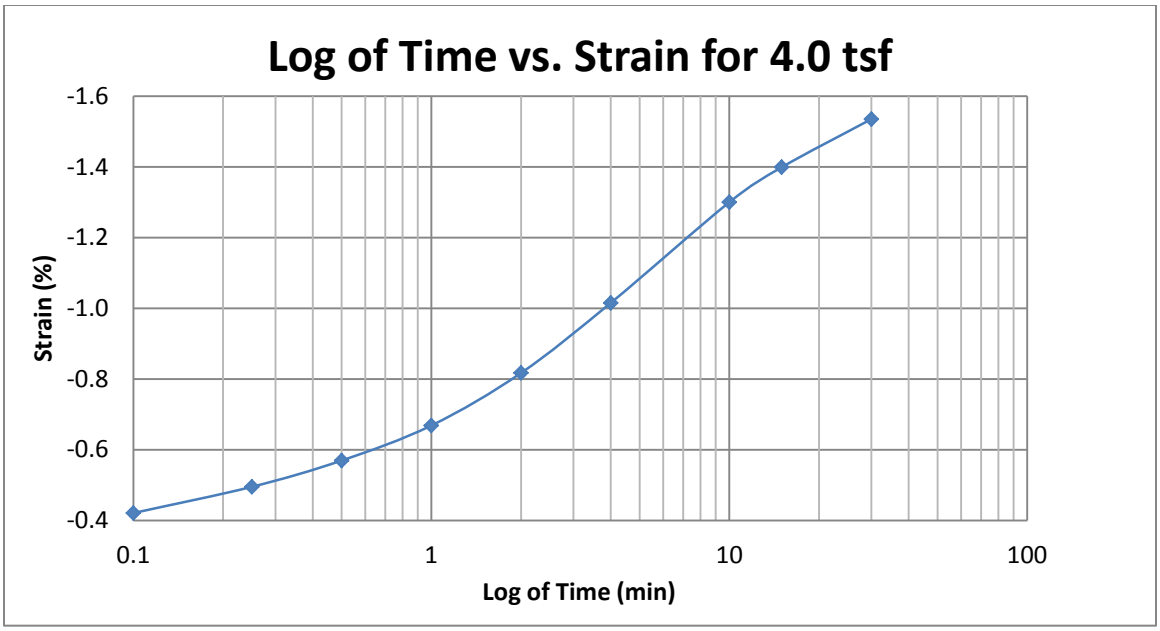

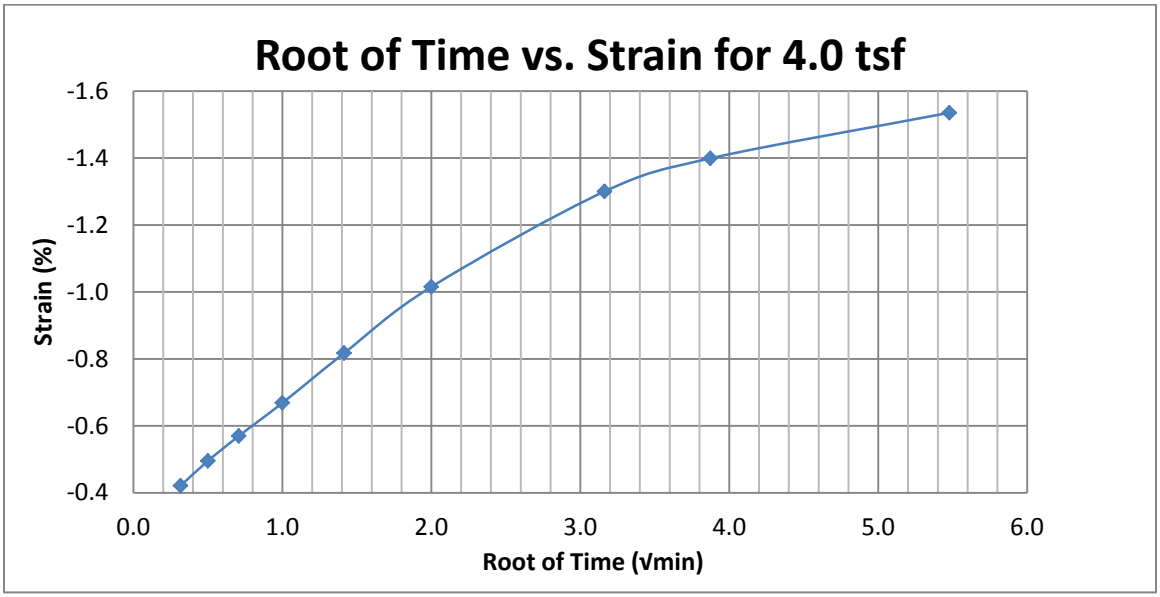

A184 Springville at 84-86 feet

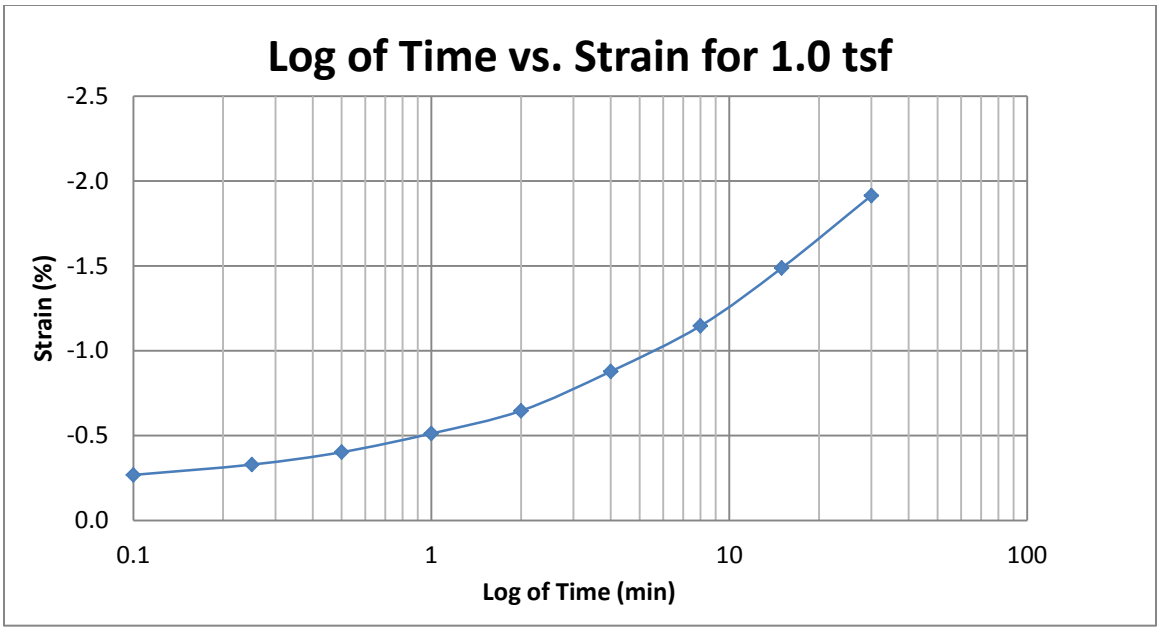

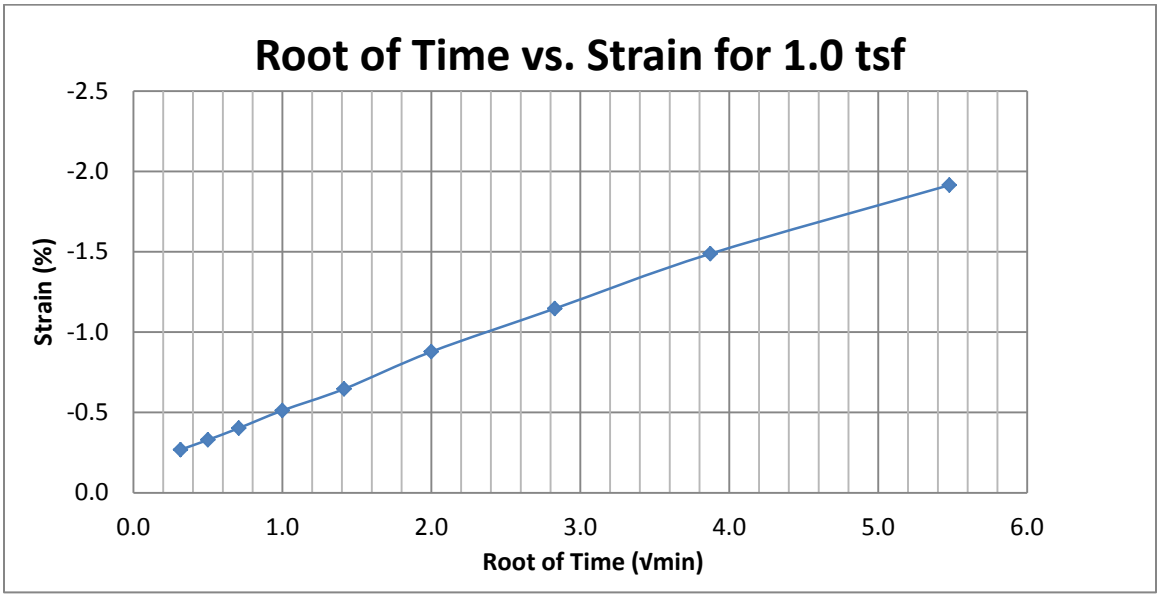

A185 Springville at 84-86 feet

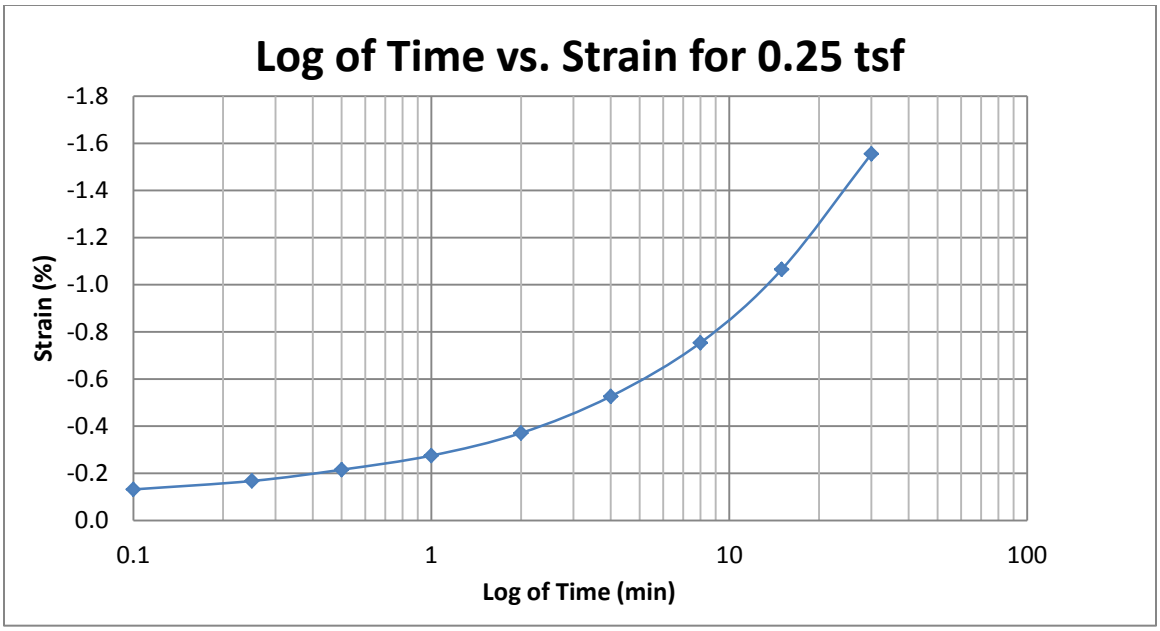

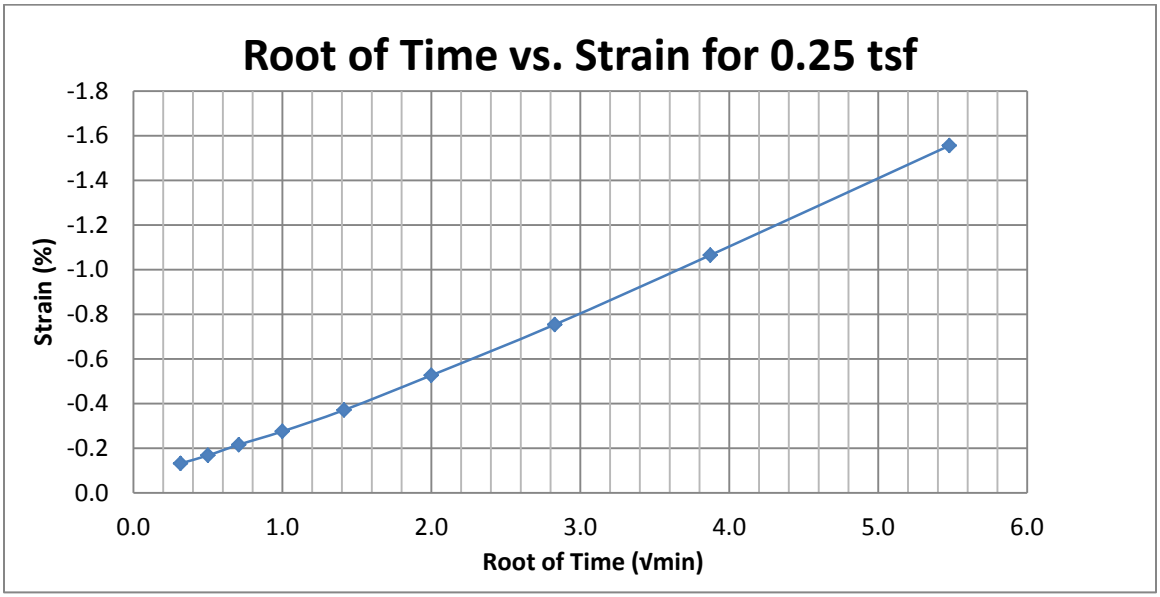

A186 Springville at 84-86 feet

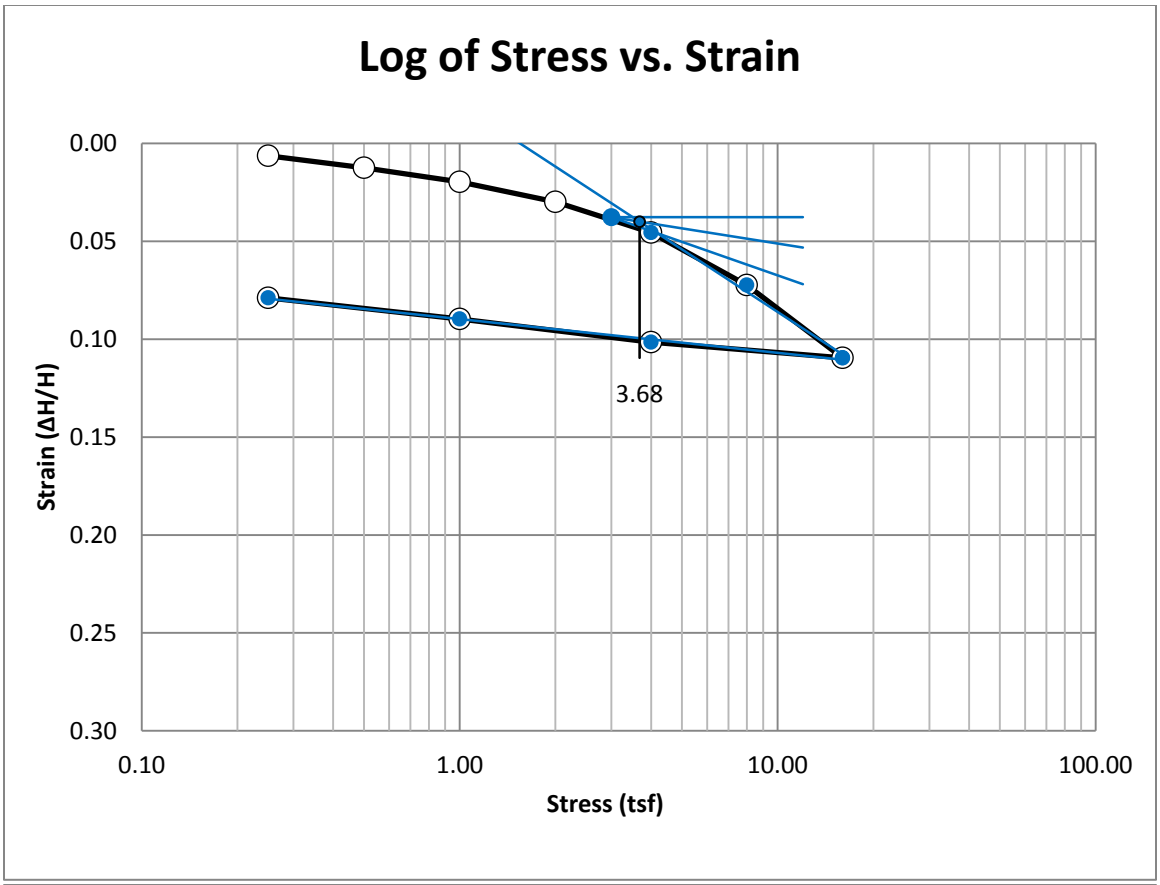

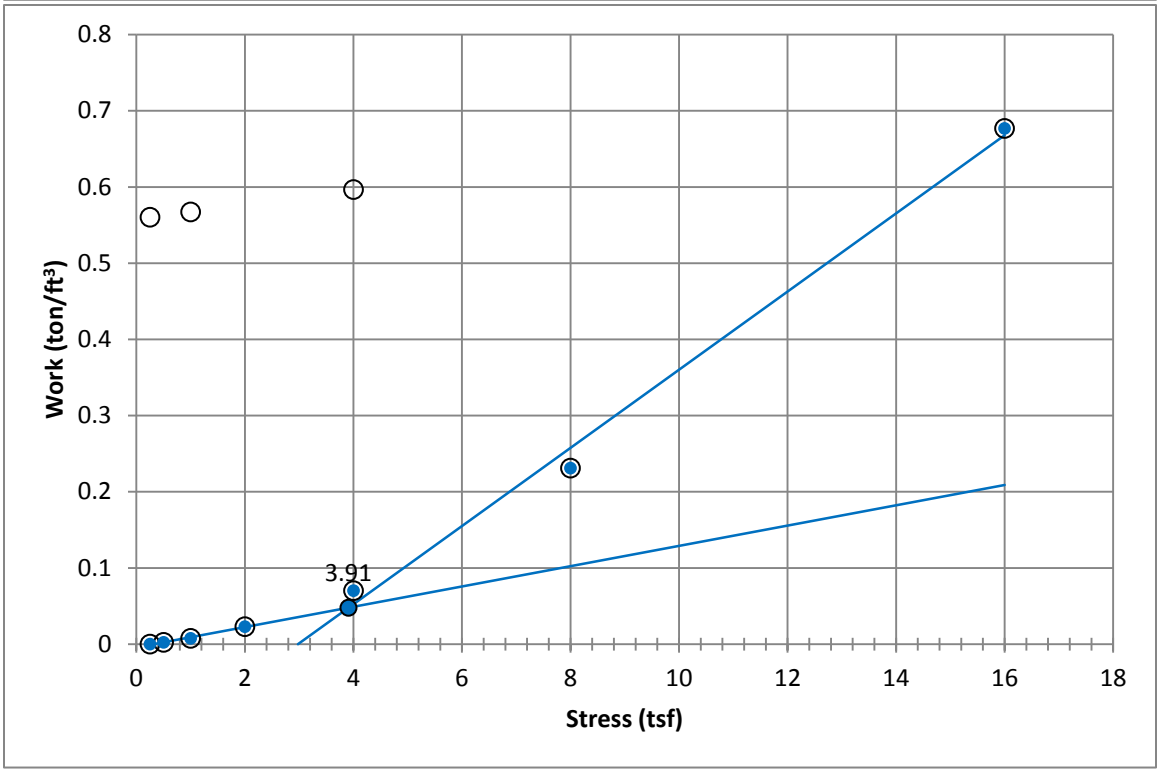

A187 Provo at 12-14 feet

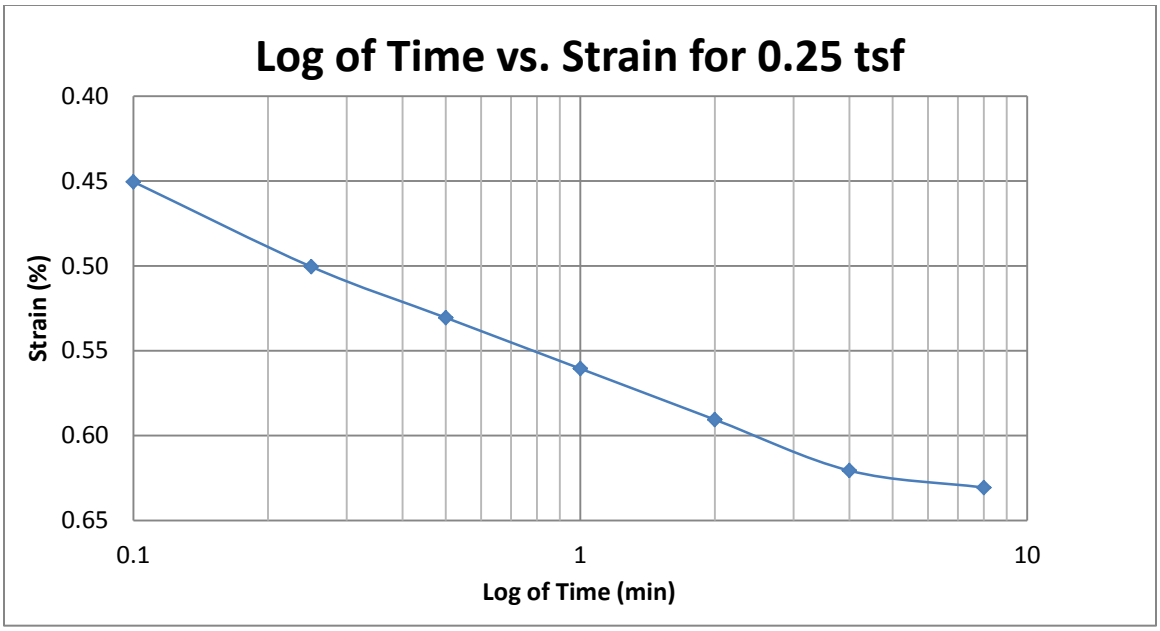

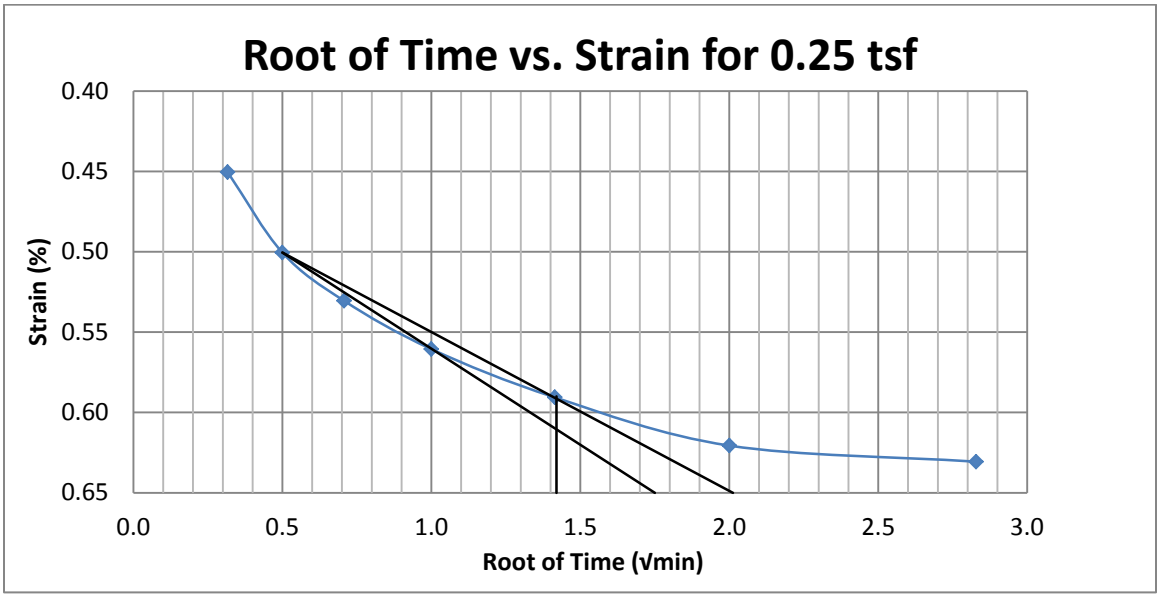

A188 Provo at 12-14 feet

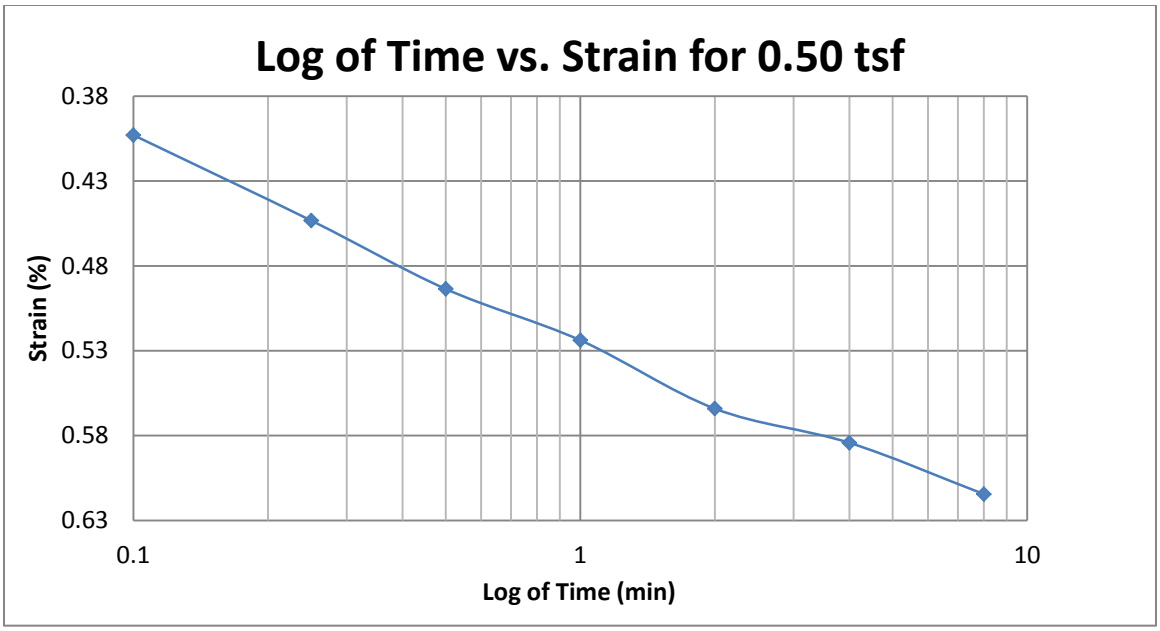

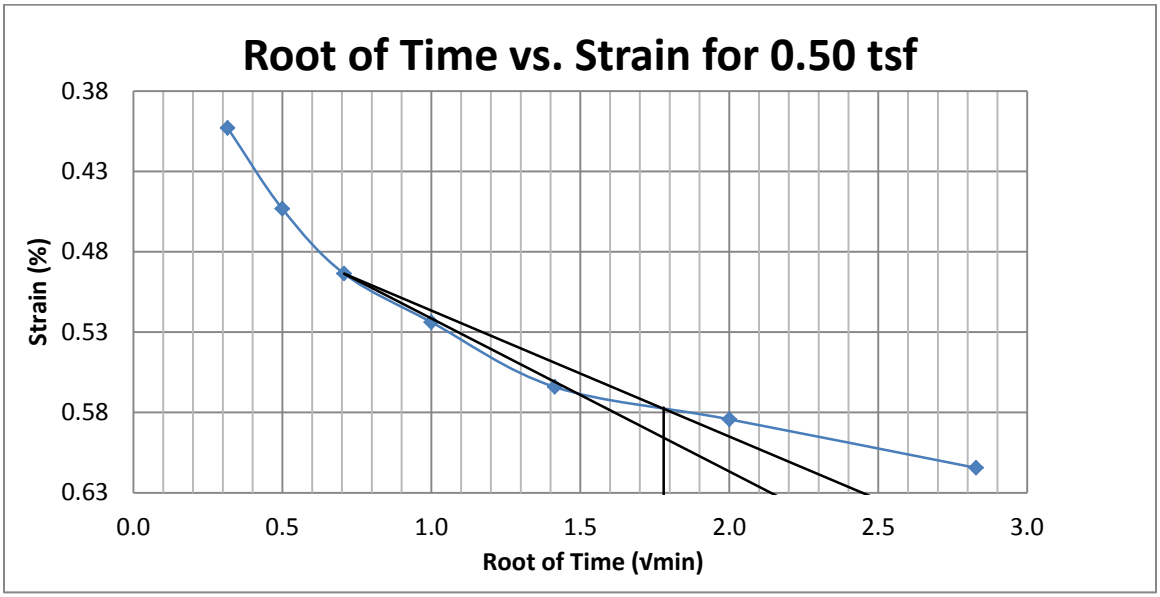

A189 Provo at 12-14 feet

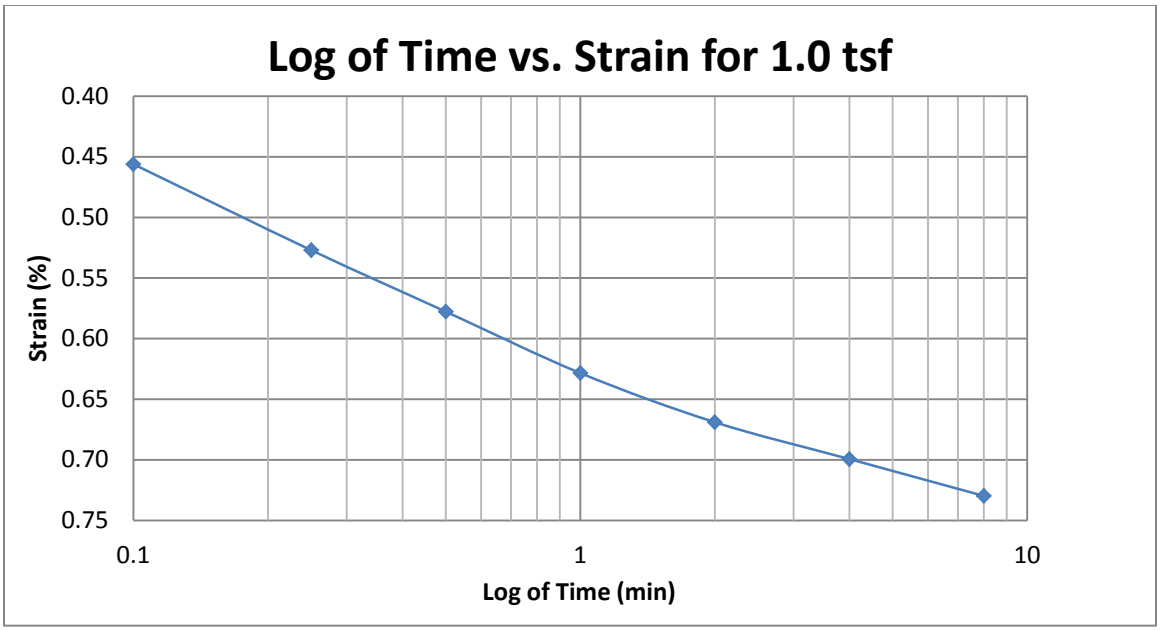

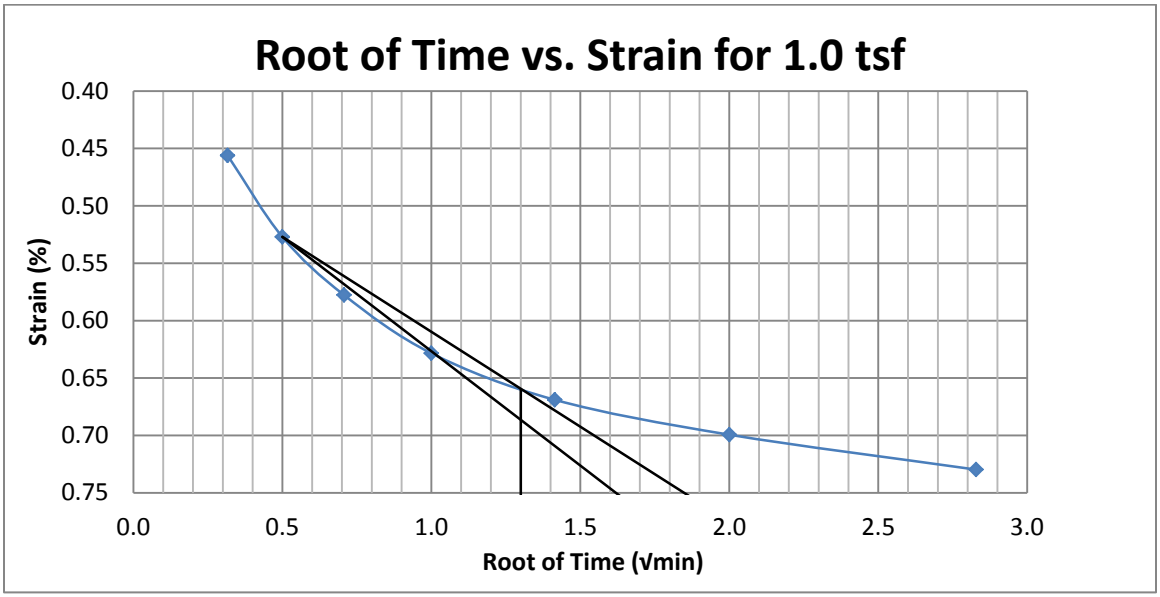

A190 Provo at 12-14 feet

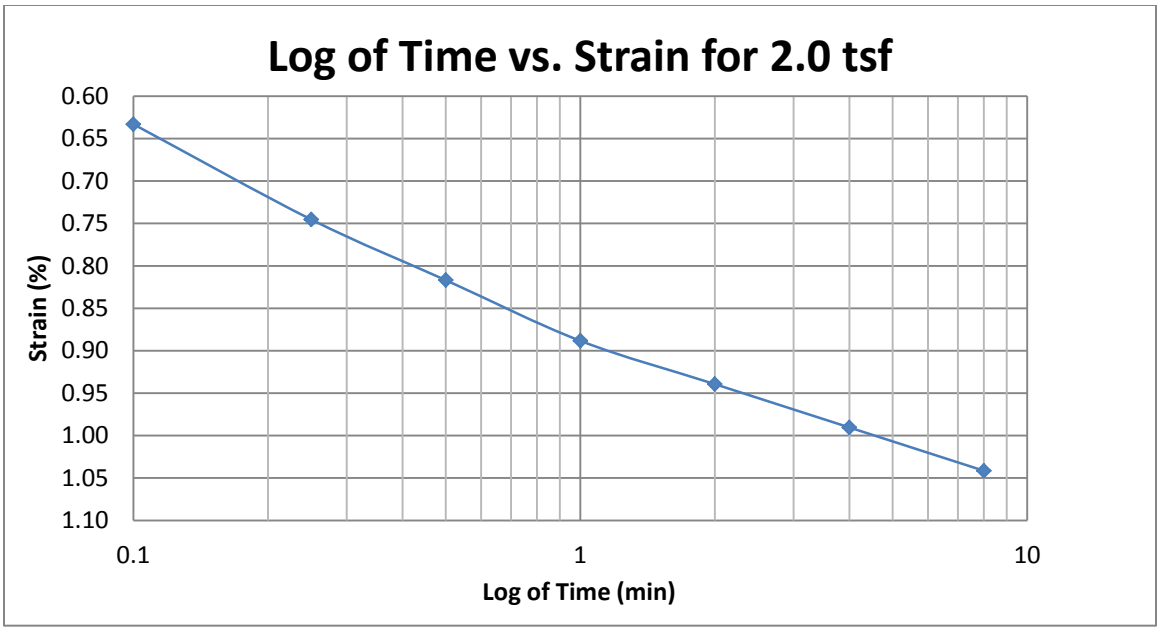

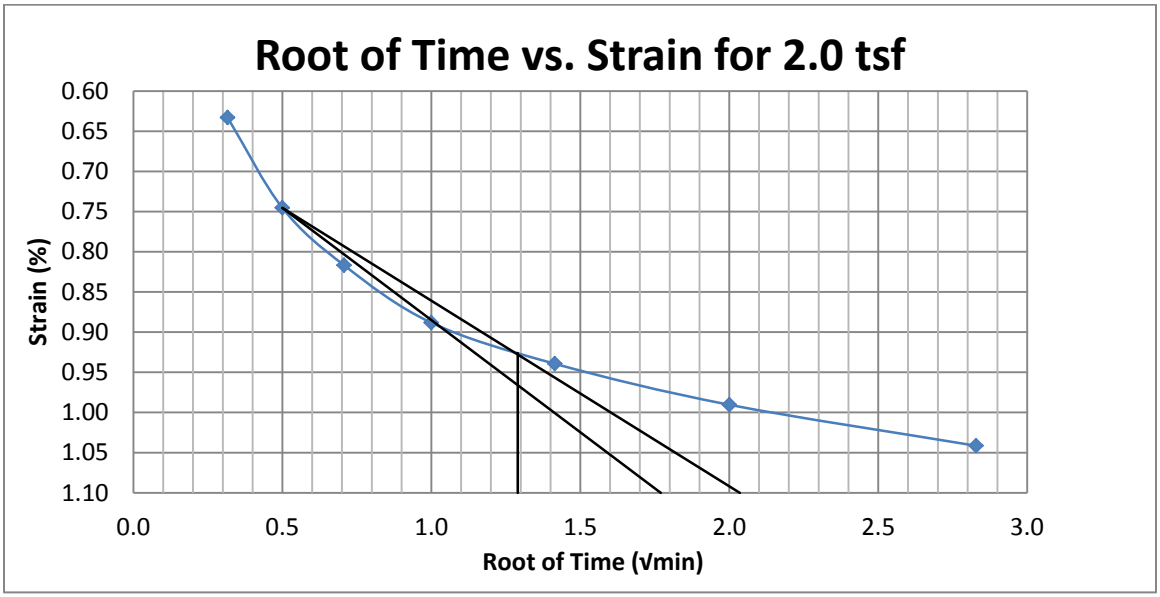

A191 Provo at 12-14 feet

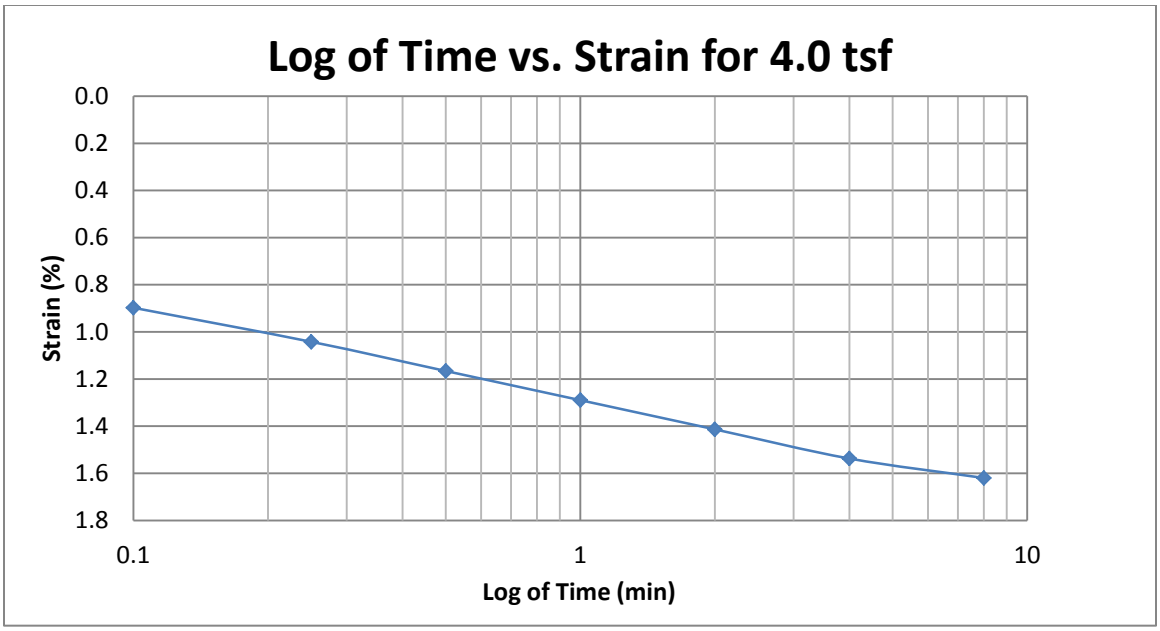

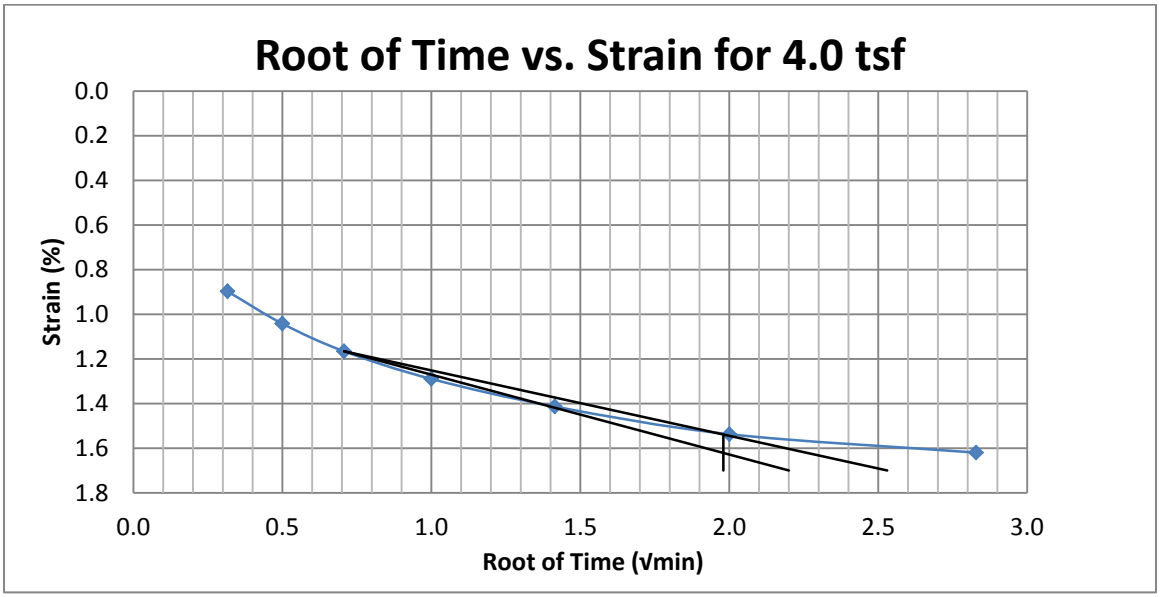

A192 Provo at 12-14 feet

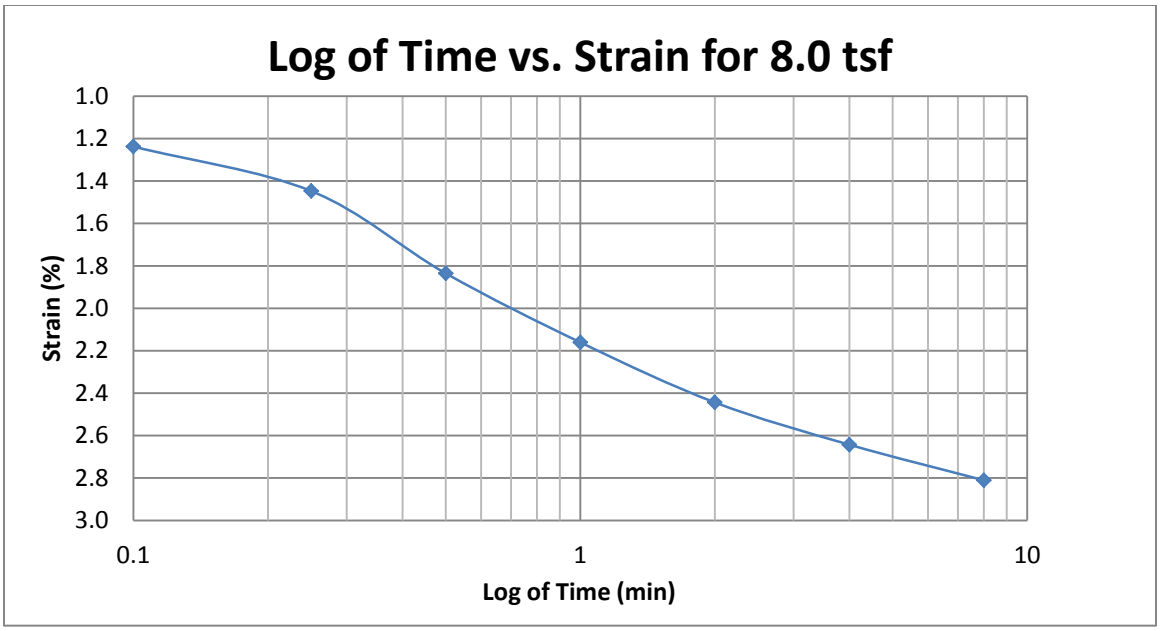

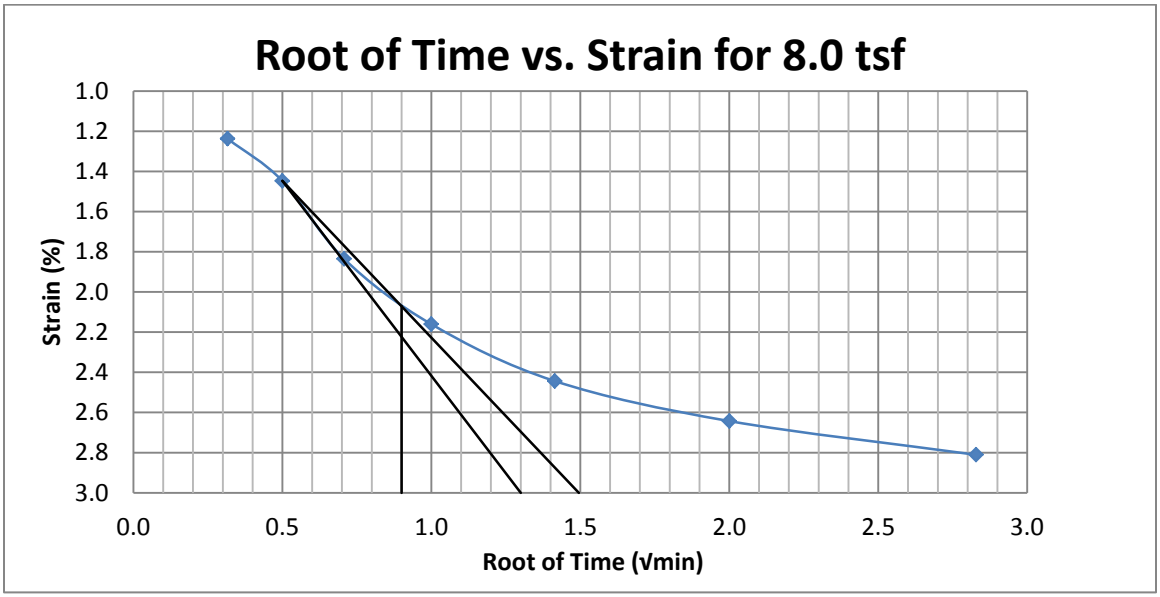

A193 Provo at 12-14 feet

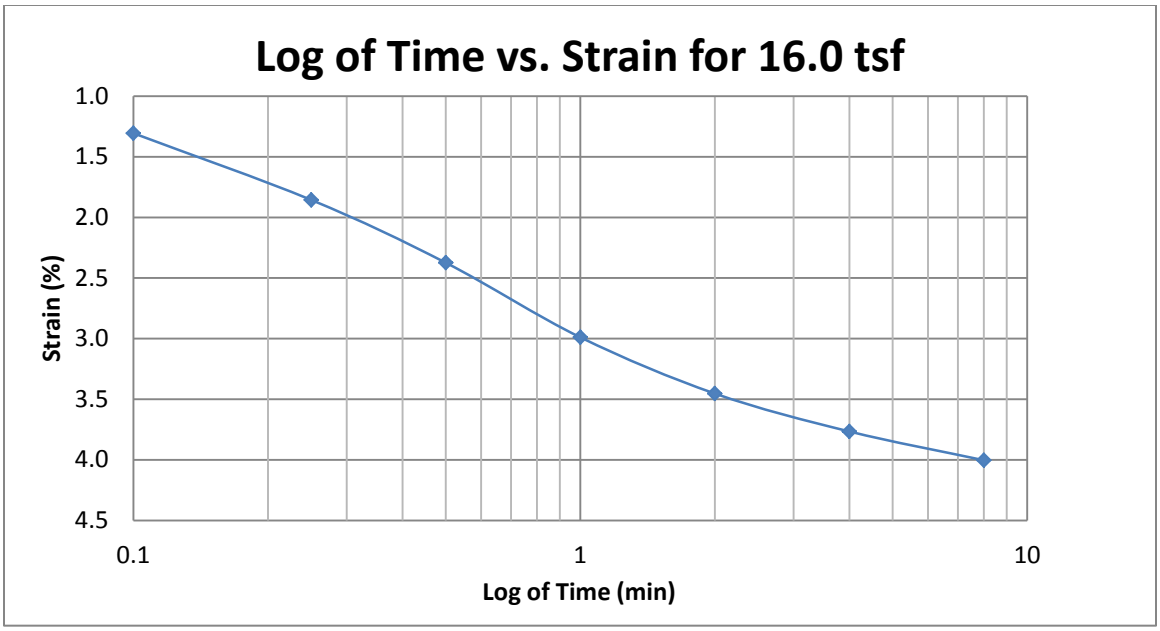

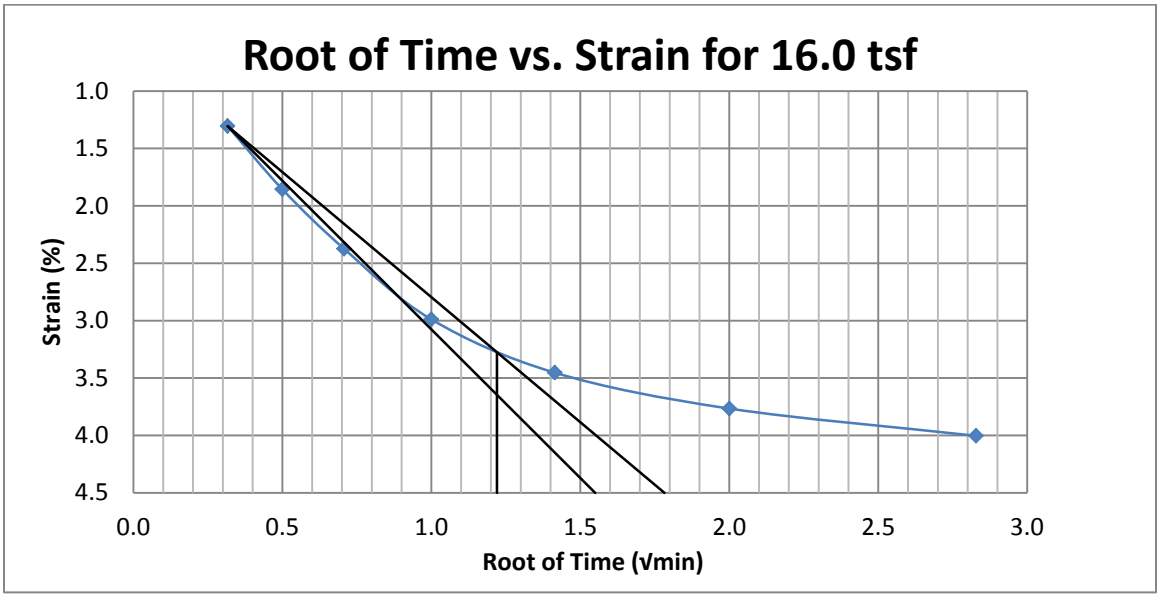

A194 Provo at 12-14 feet

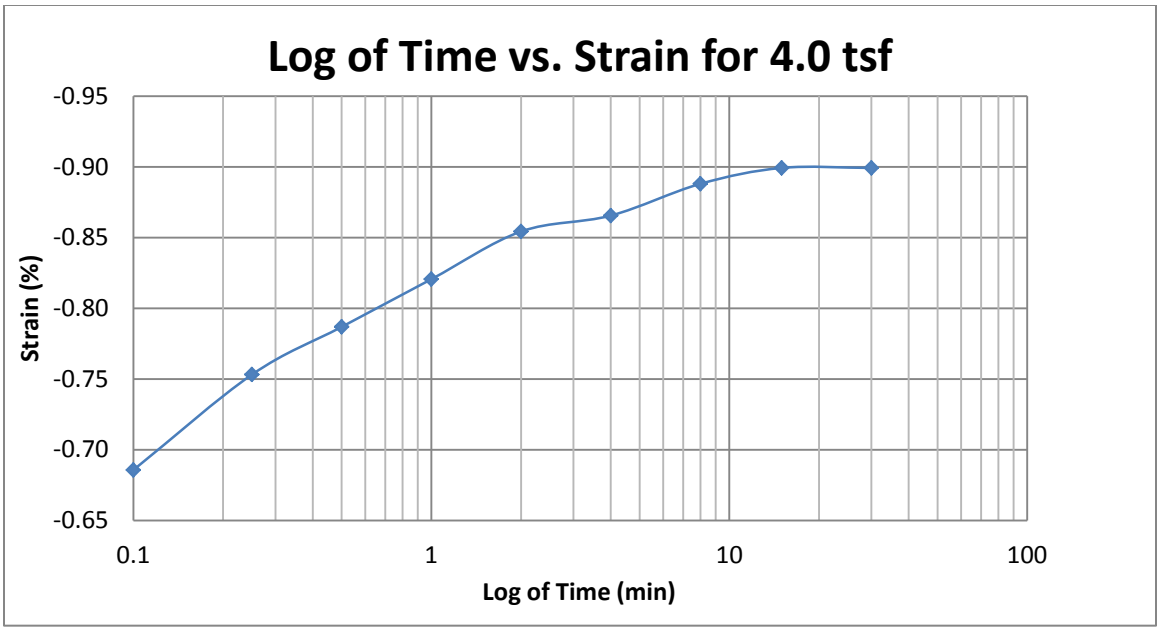

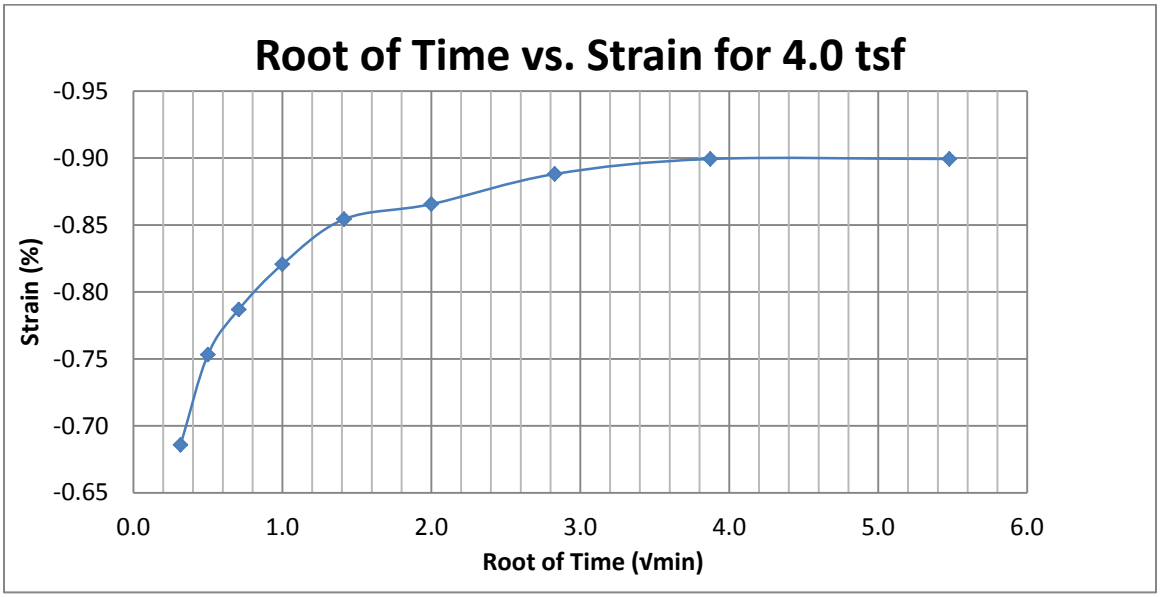

A195 Provo at 12-14 feet

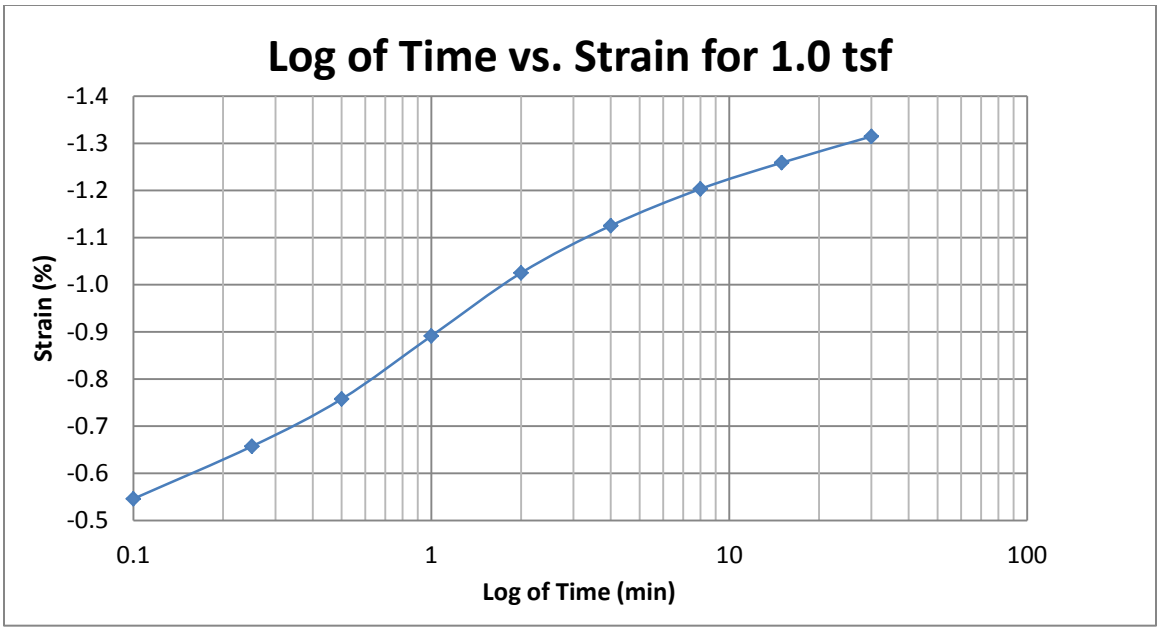

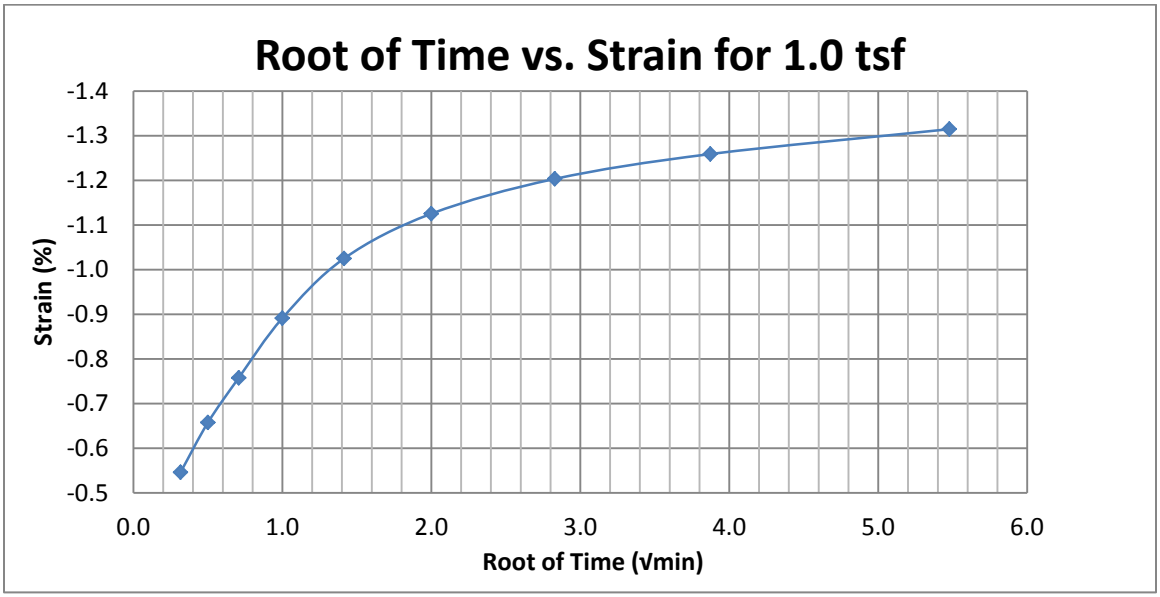

A196 Provo at 12-14 feet

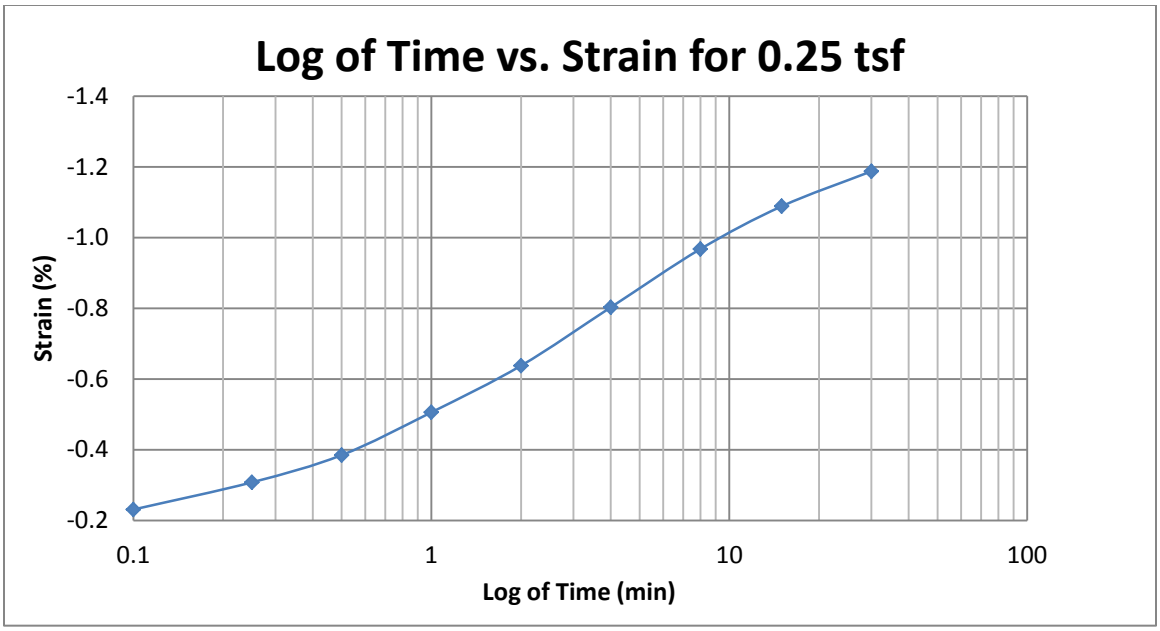

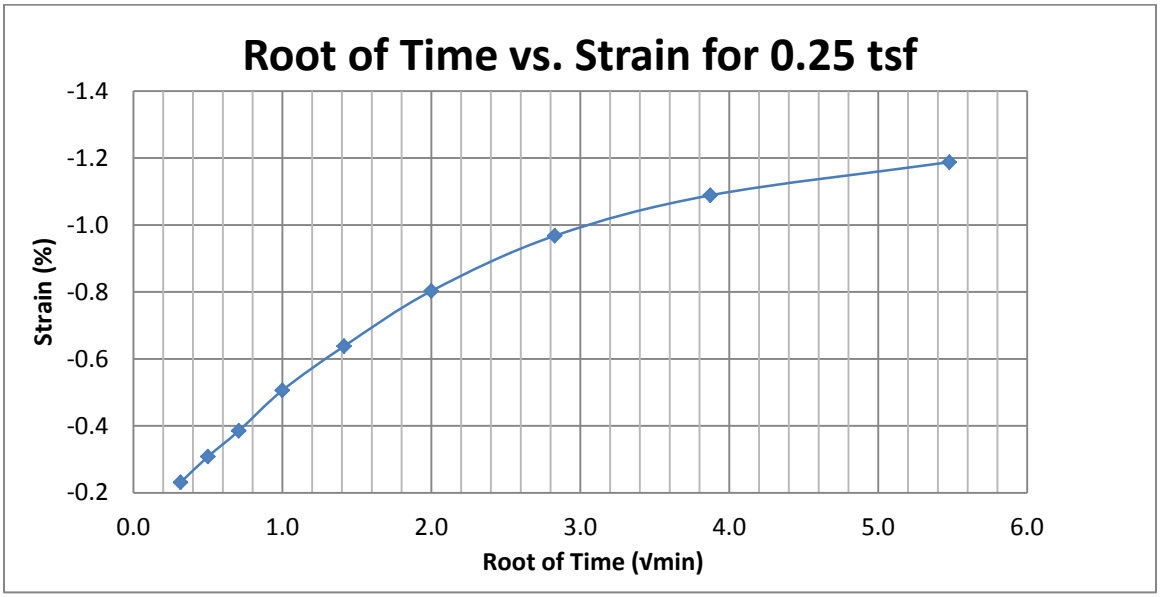

A197 Provo at 12-14 feet

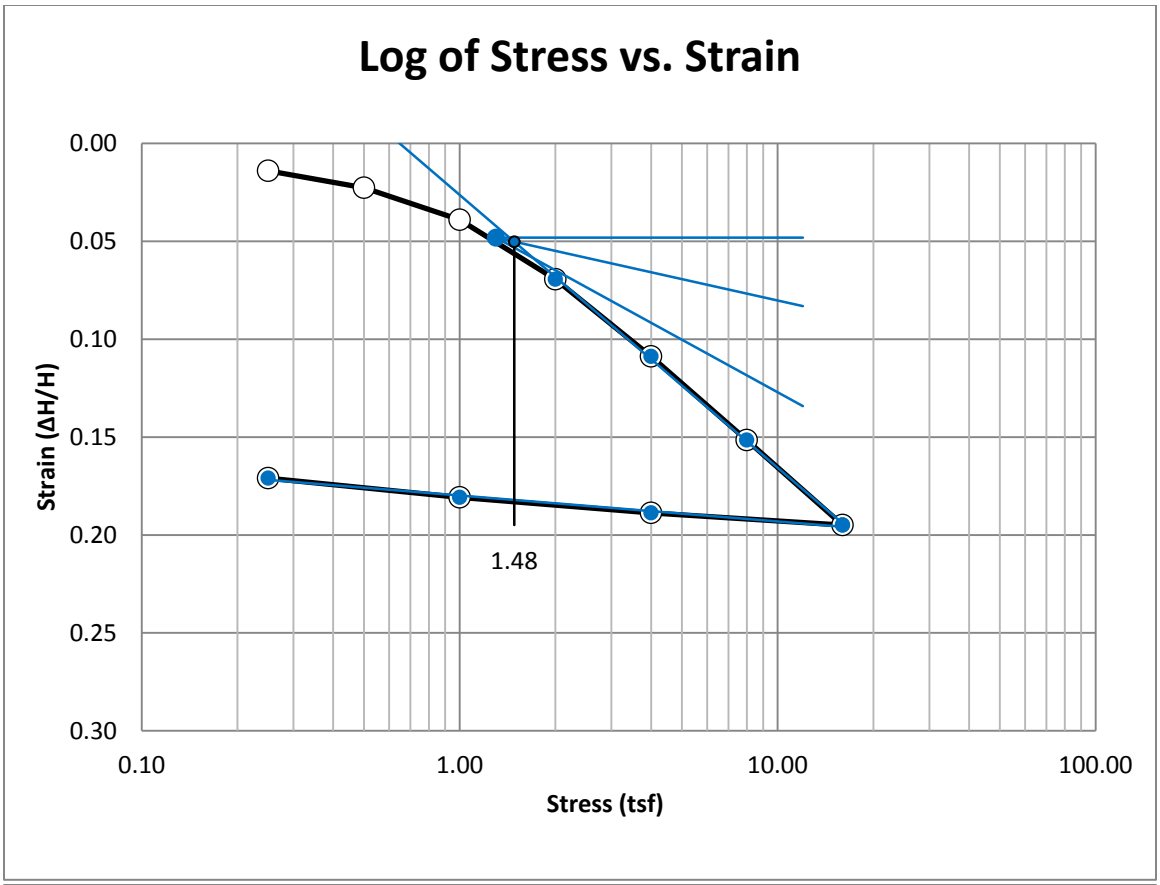

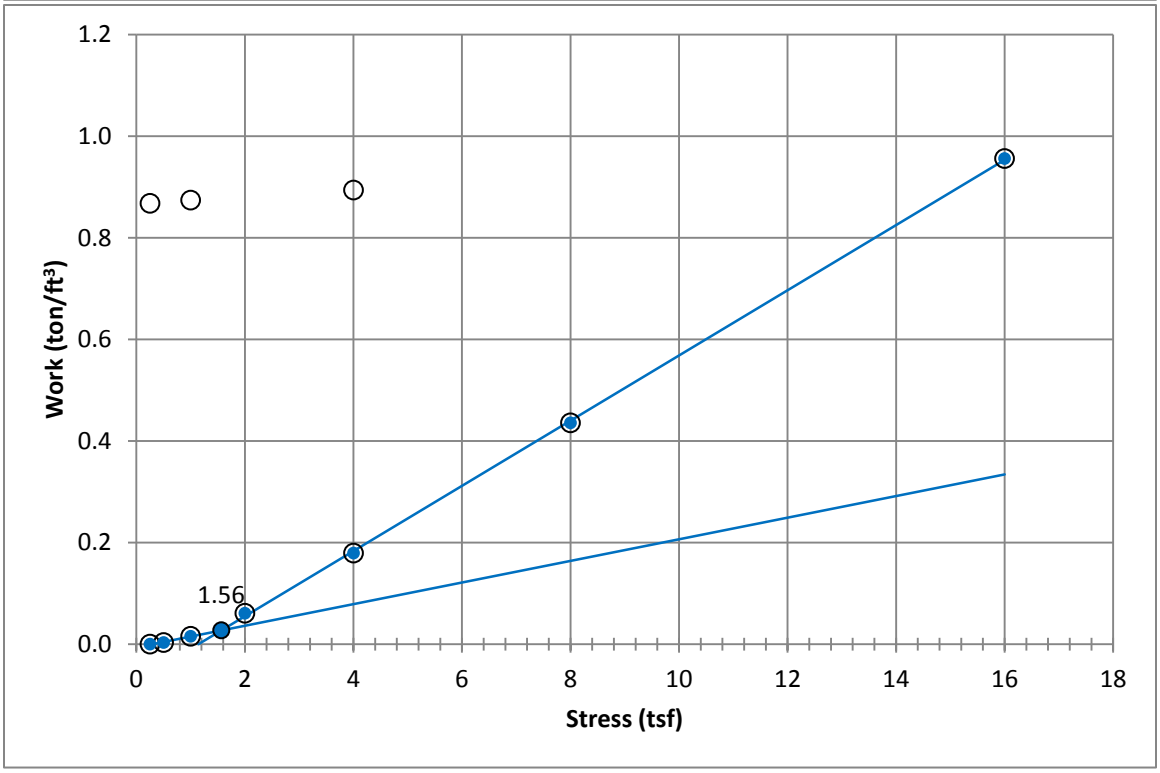

A198 Provo at 17-19 feet

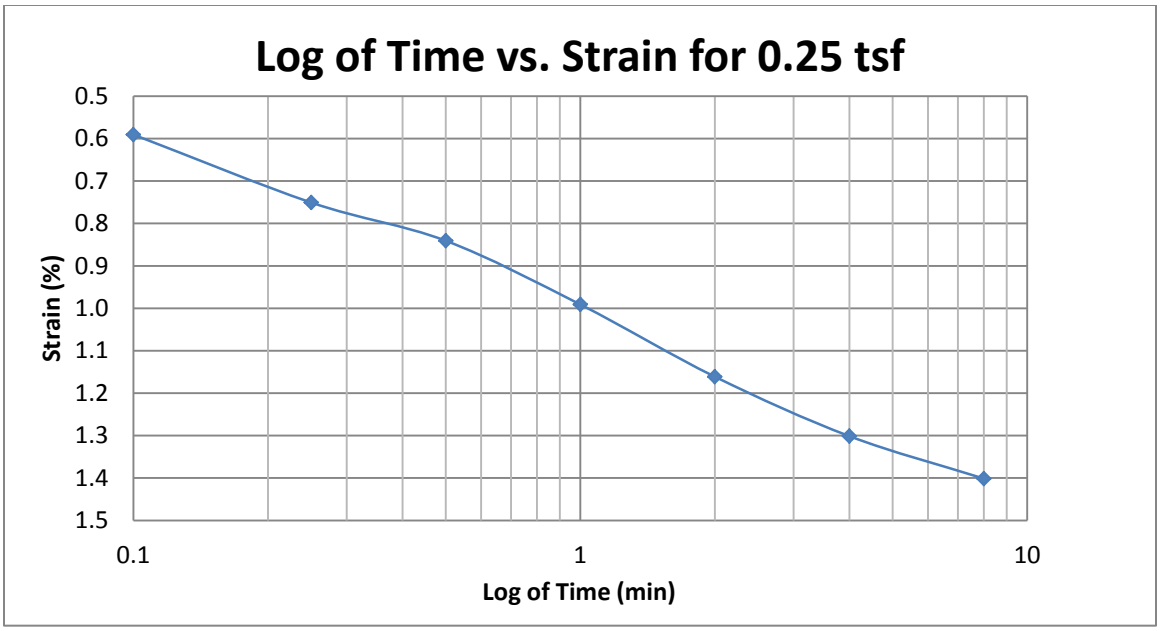

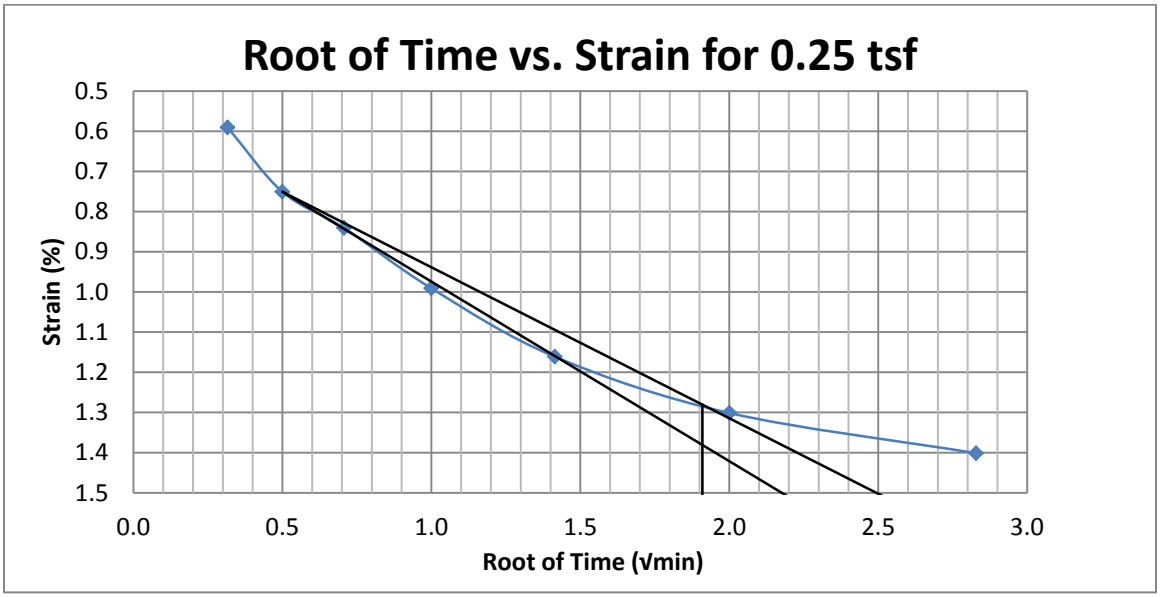

A199 Provo at 17-19 feet

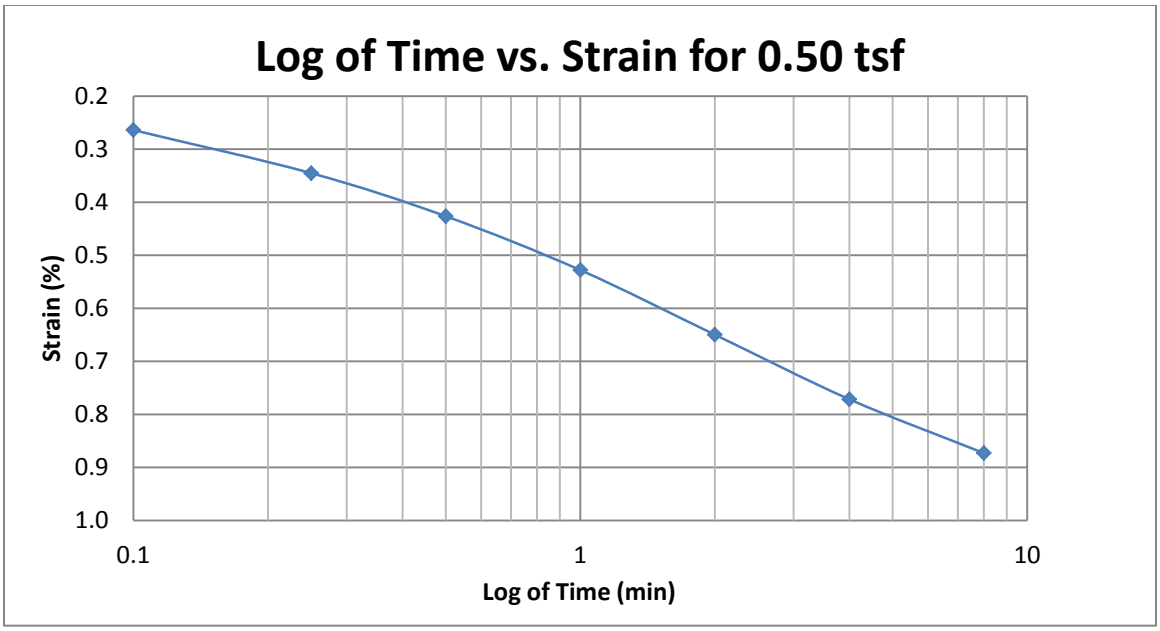

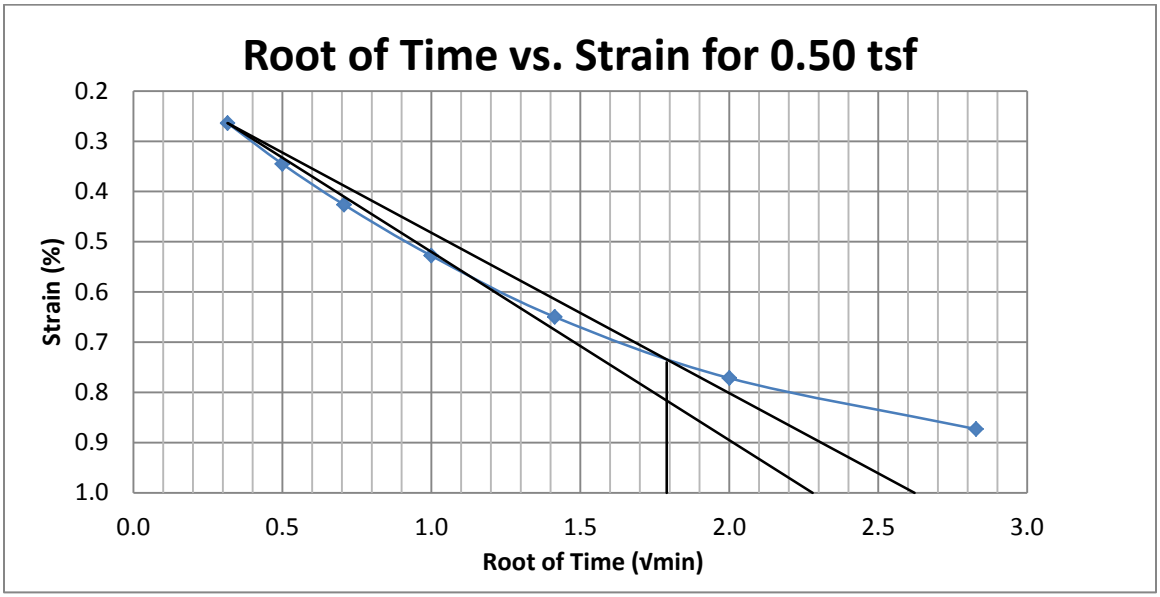

A200 Provo at 17-19 feet

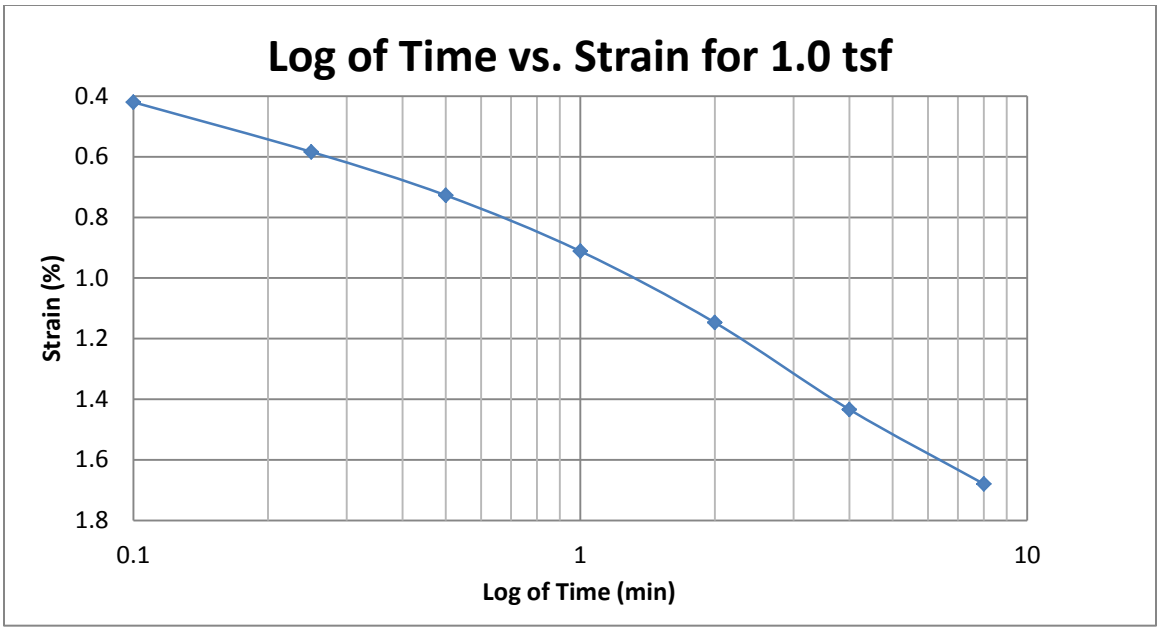

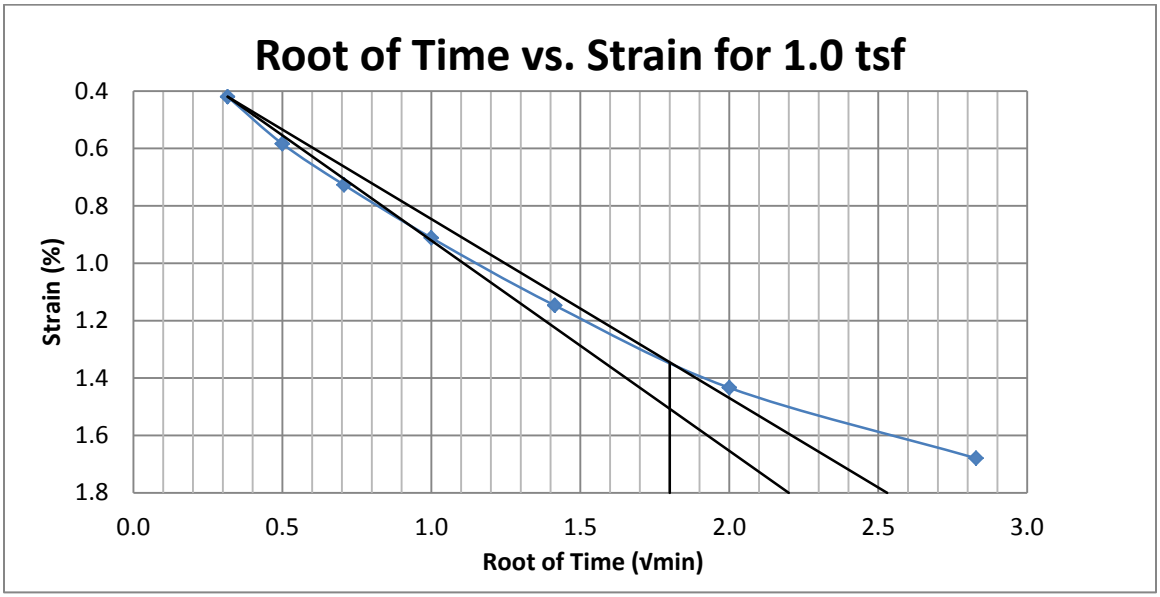

A201 Provo at 17-19 feet

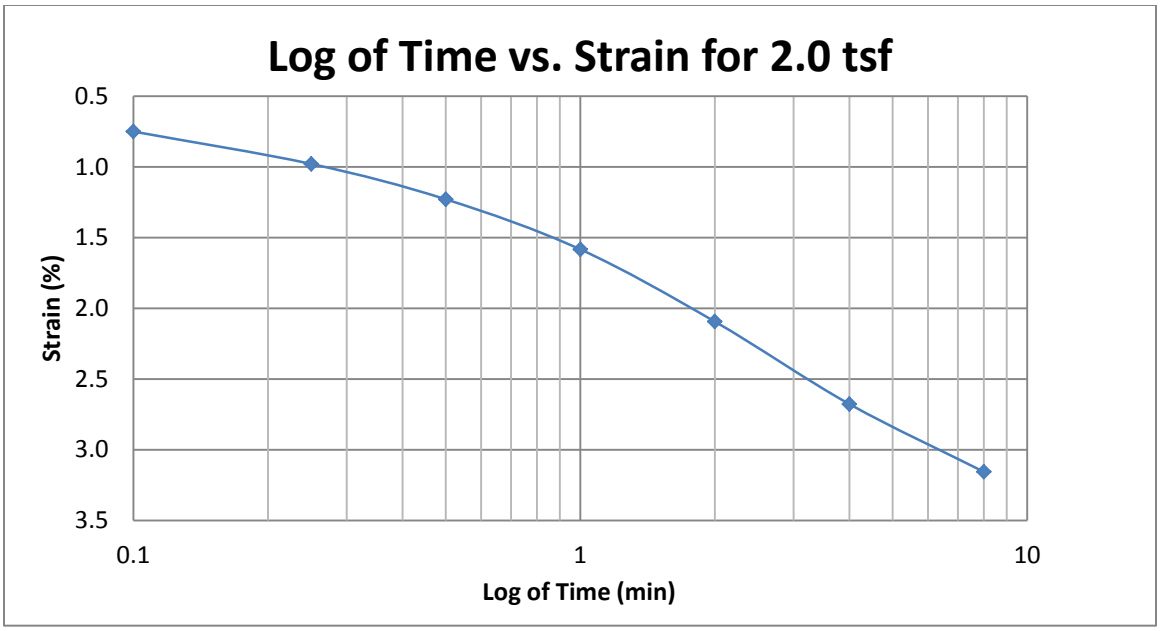

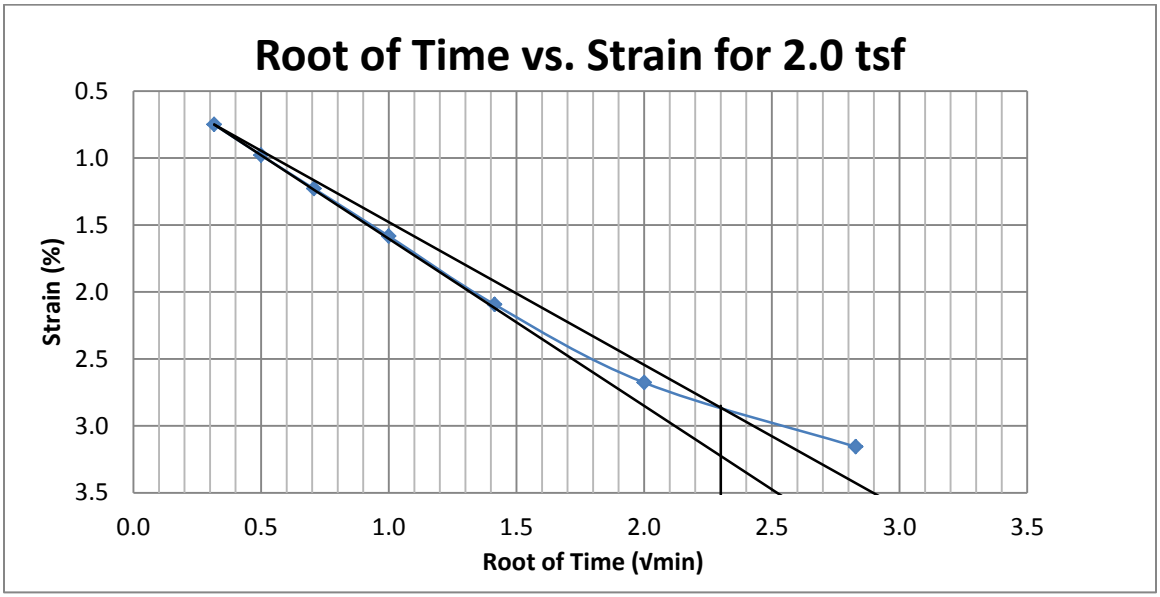

A202 Provo at 17-19 feet

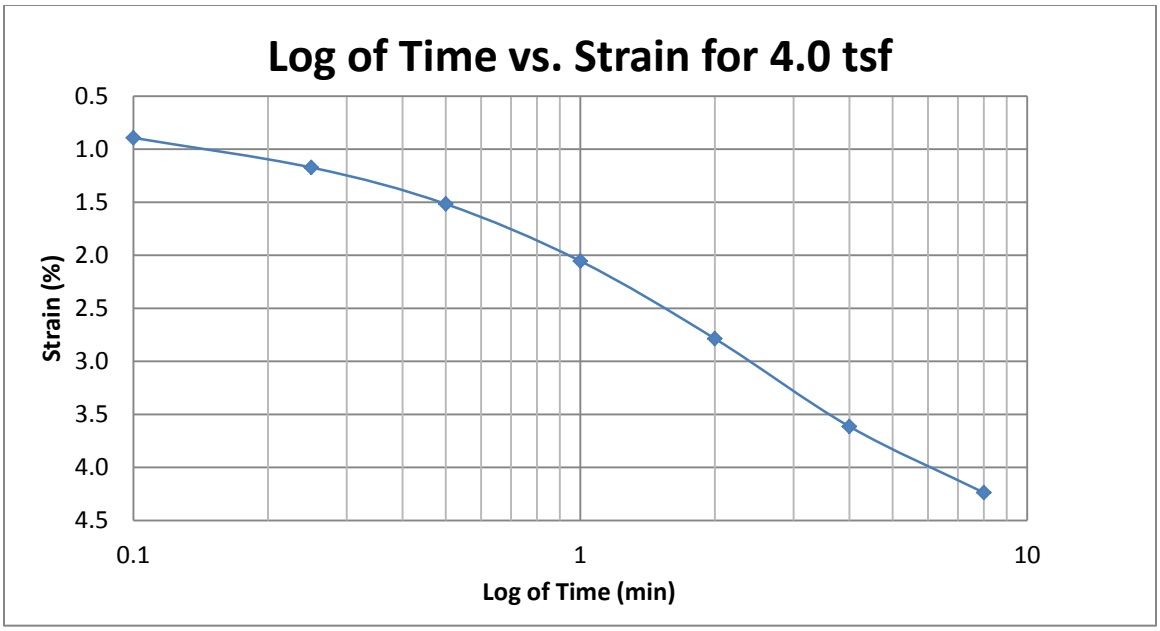

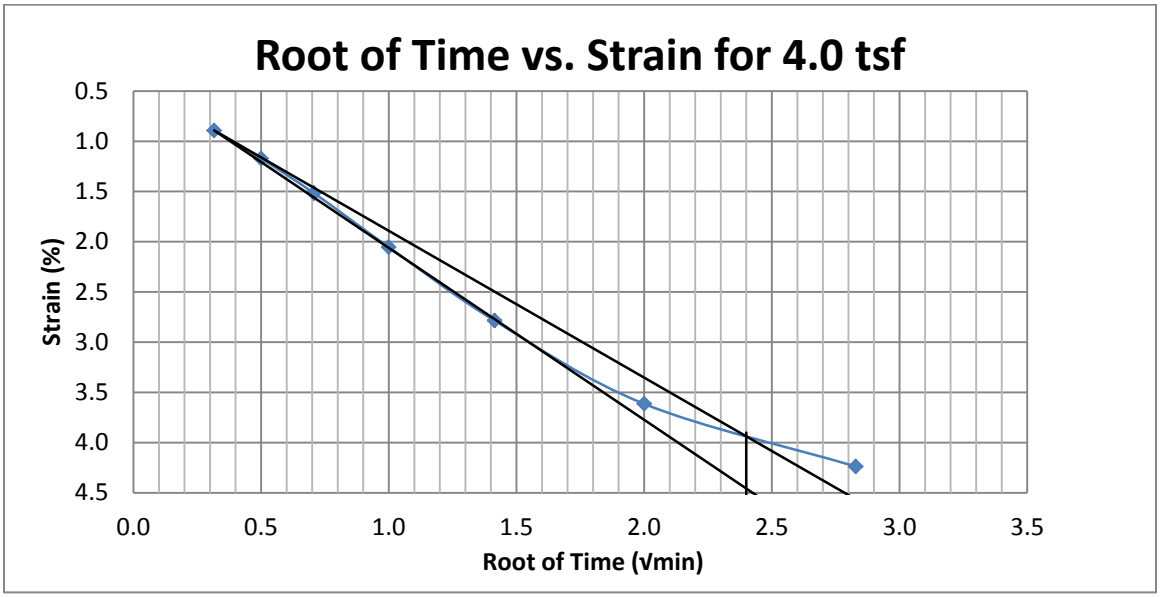

A203 Provo at 17-19 feet

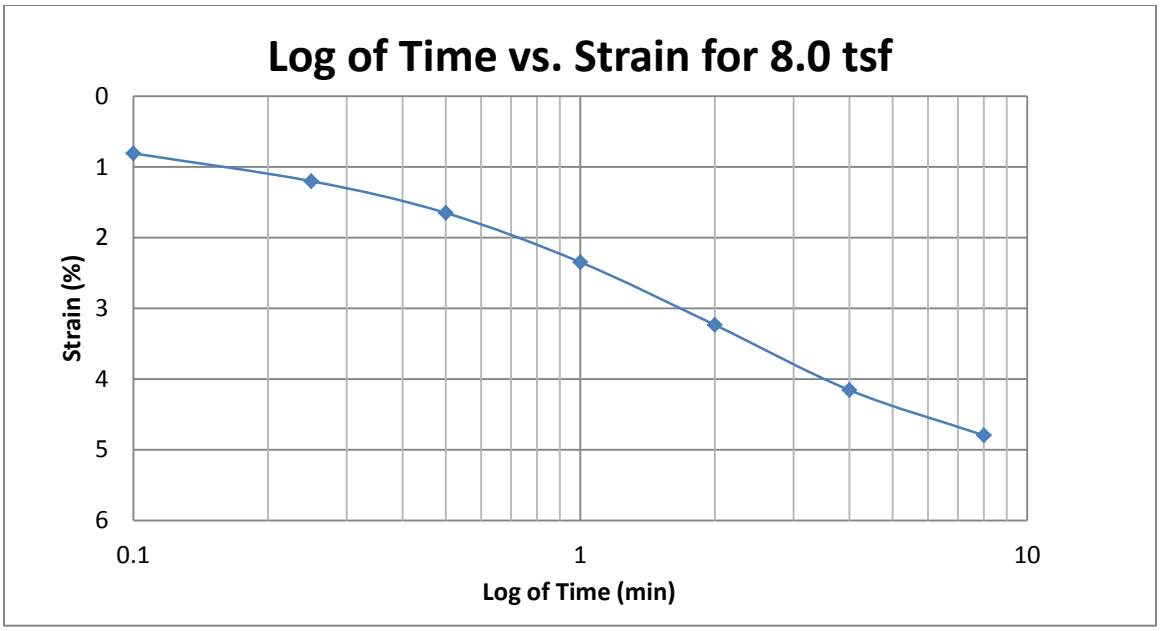

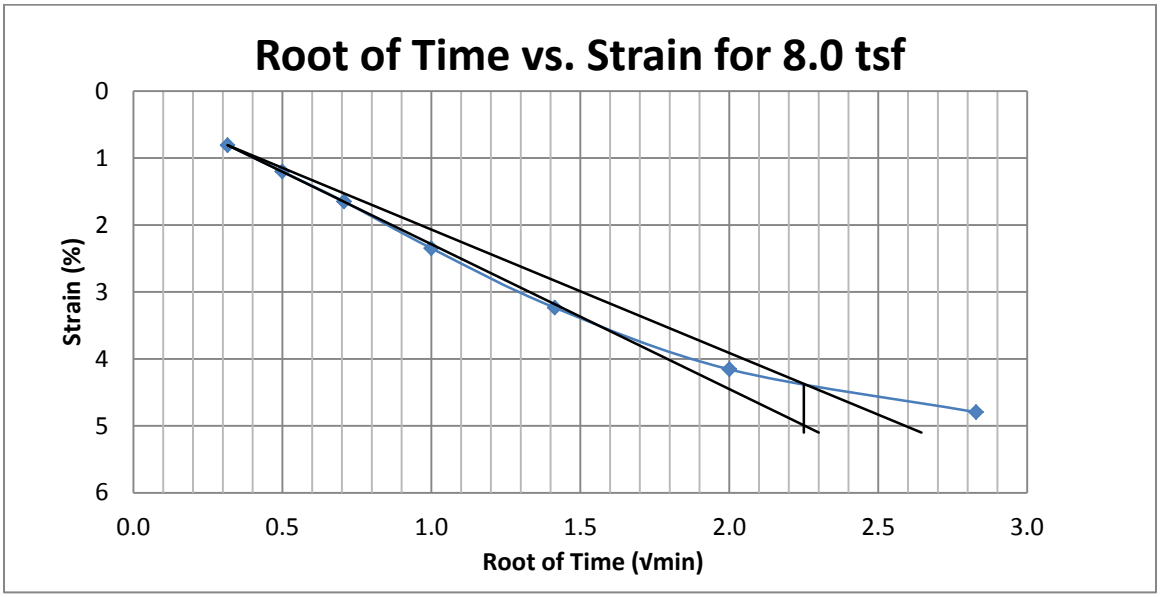

A204 Provo at 17-19 feet

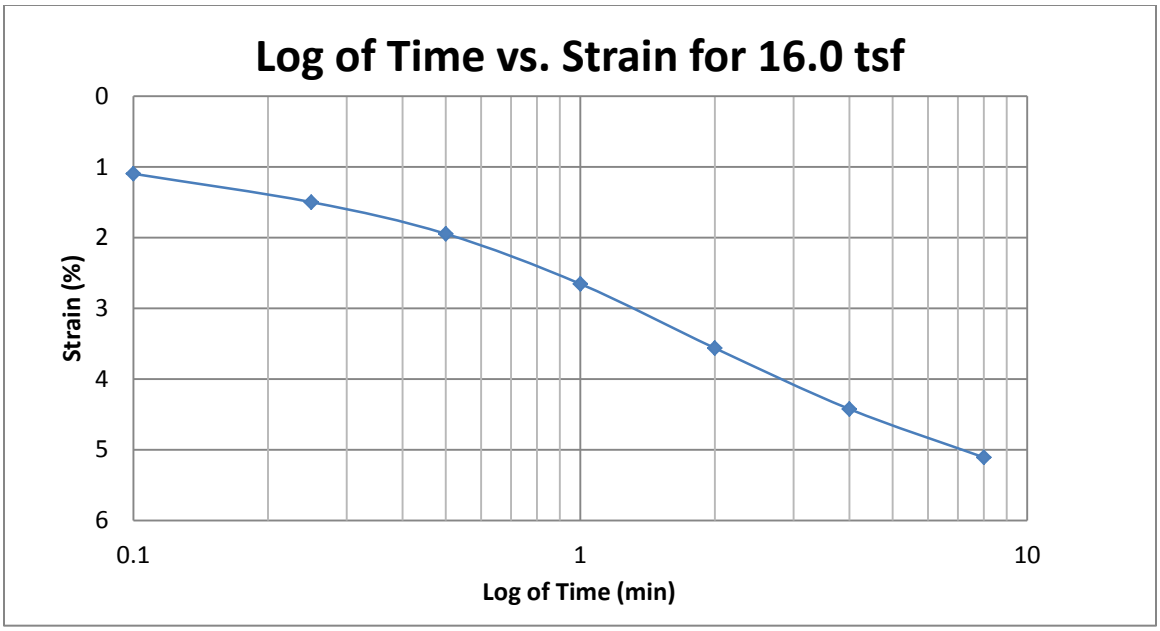

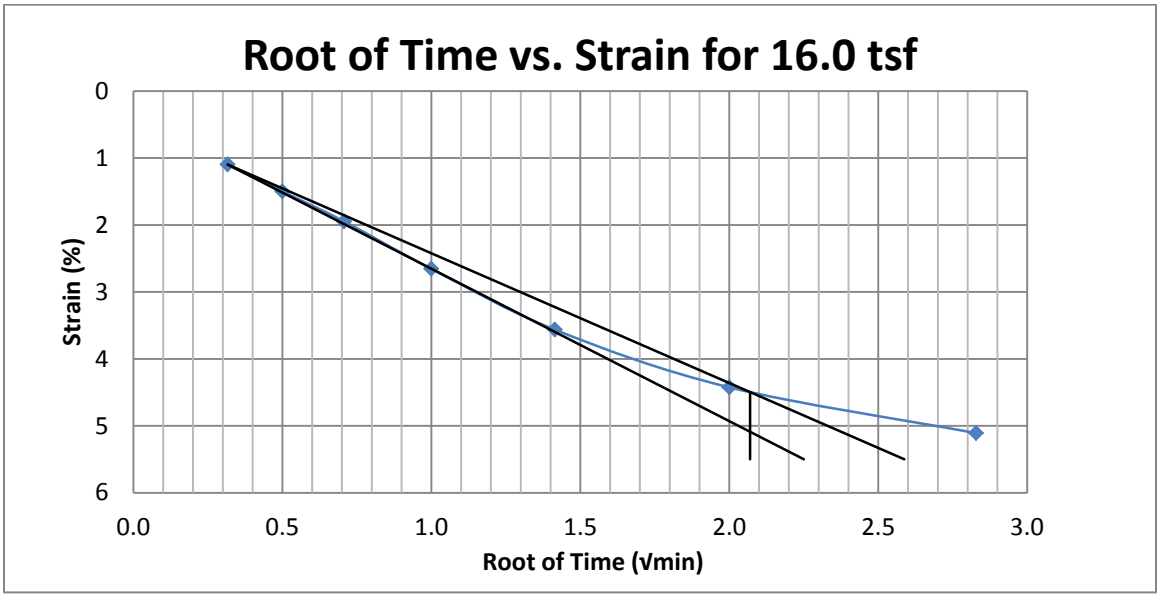

A205 Provo at 17-19 feet

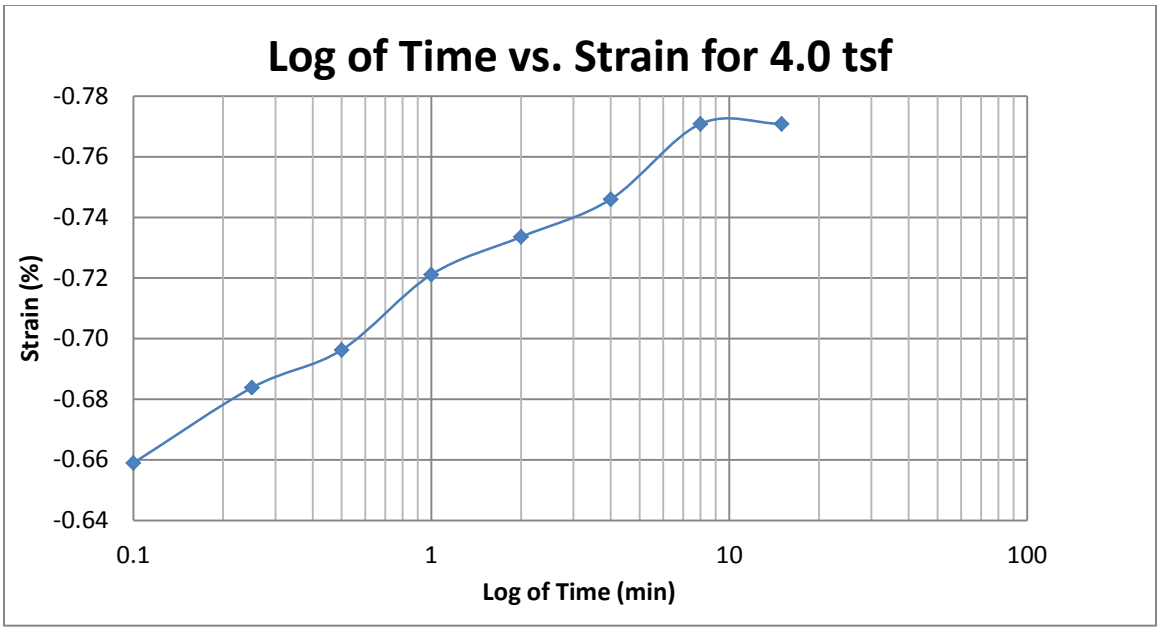

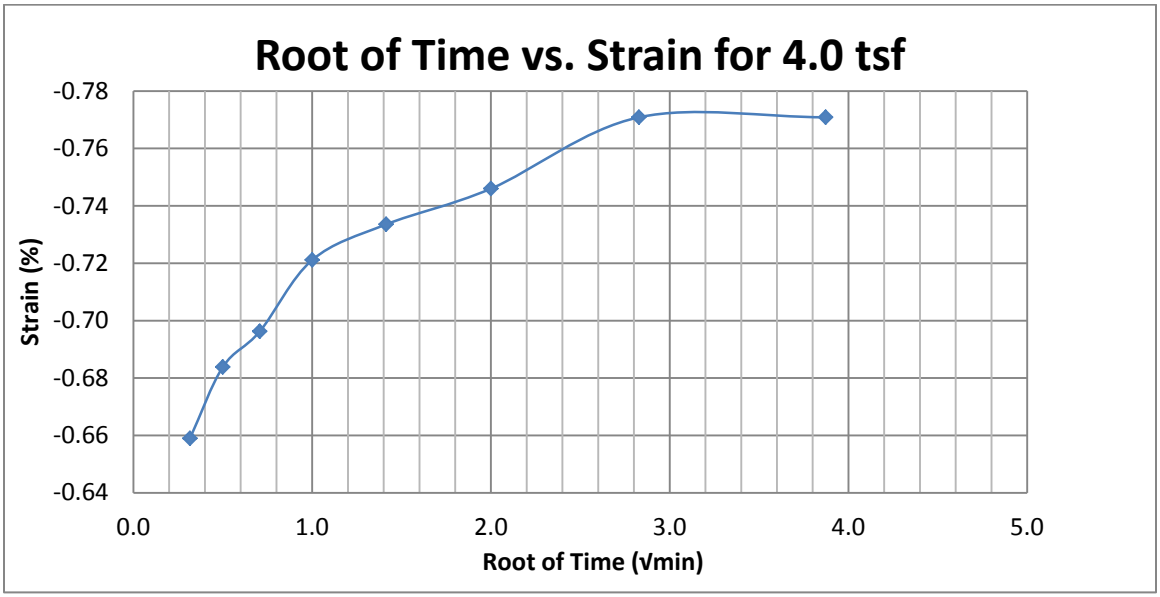

A206 Provo at 17-19 feet

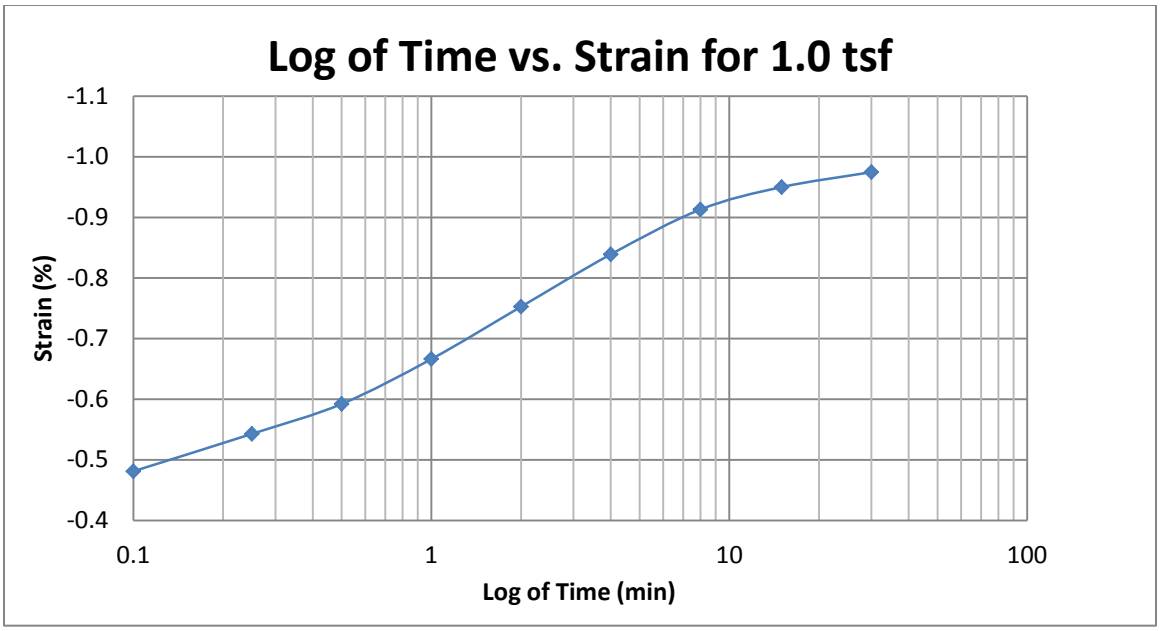

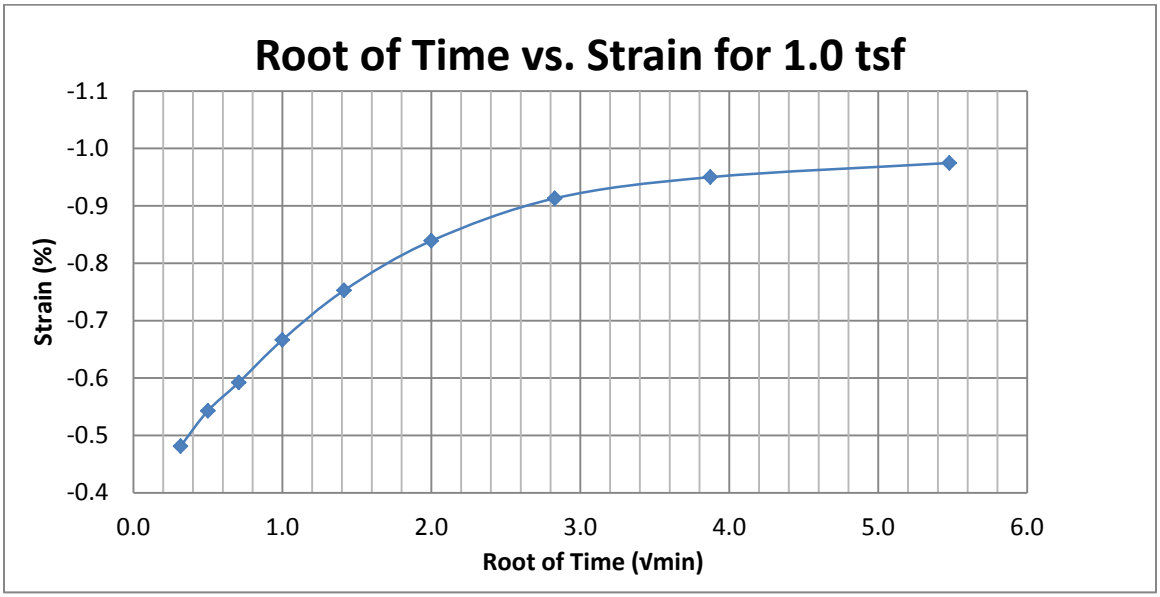

A207 Provo at 17-19 feet

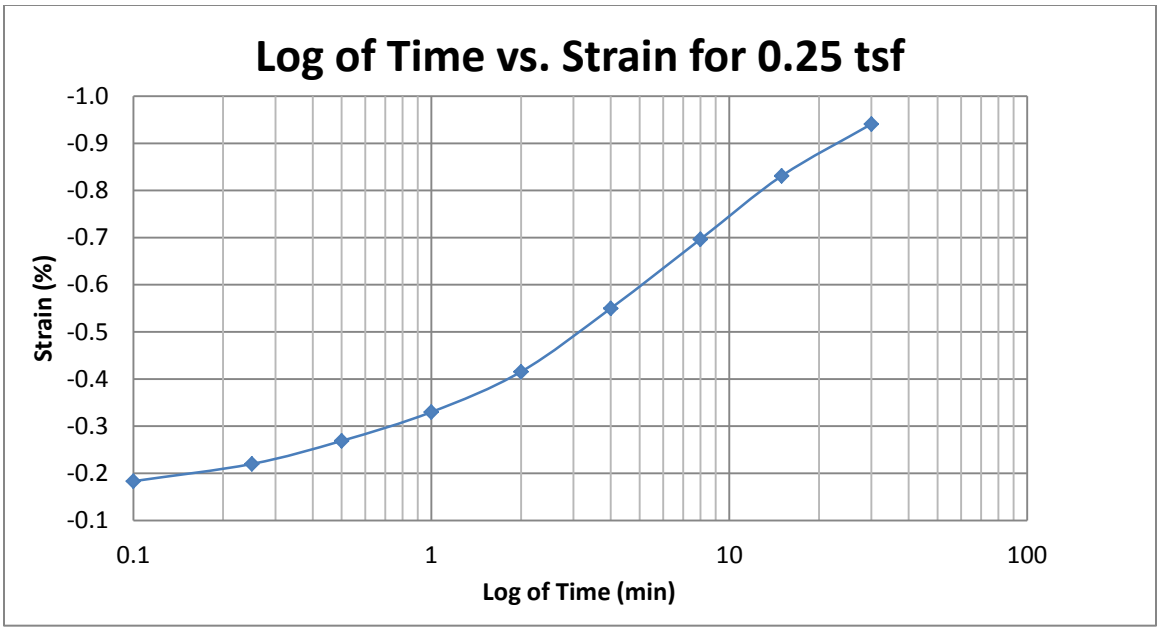

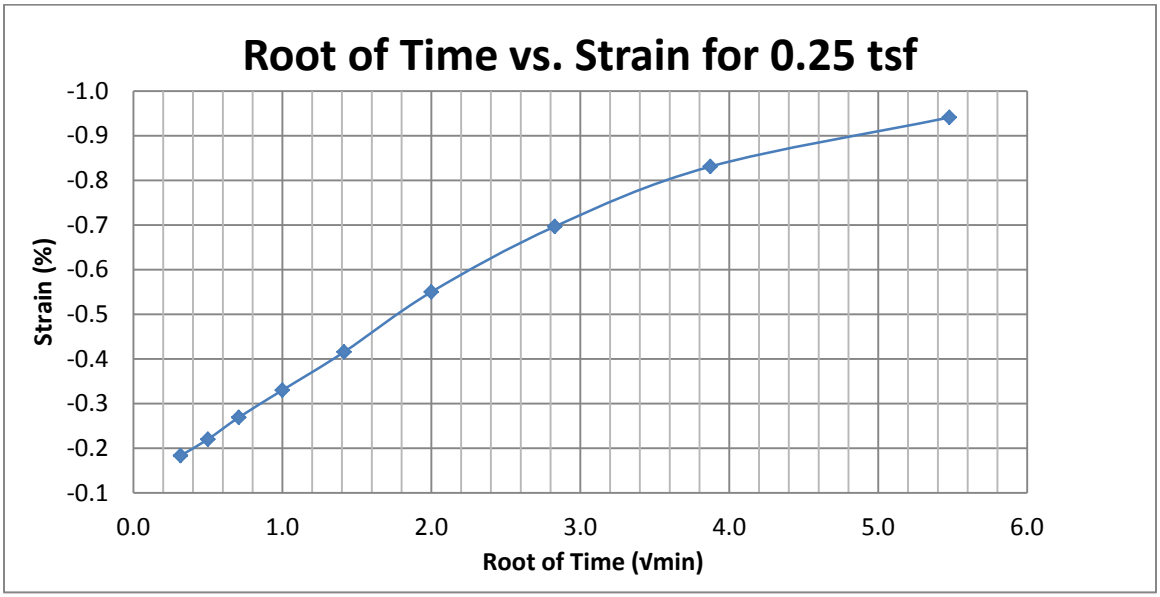

A208 Provo at 17-19 feet

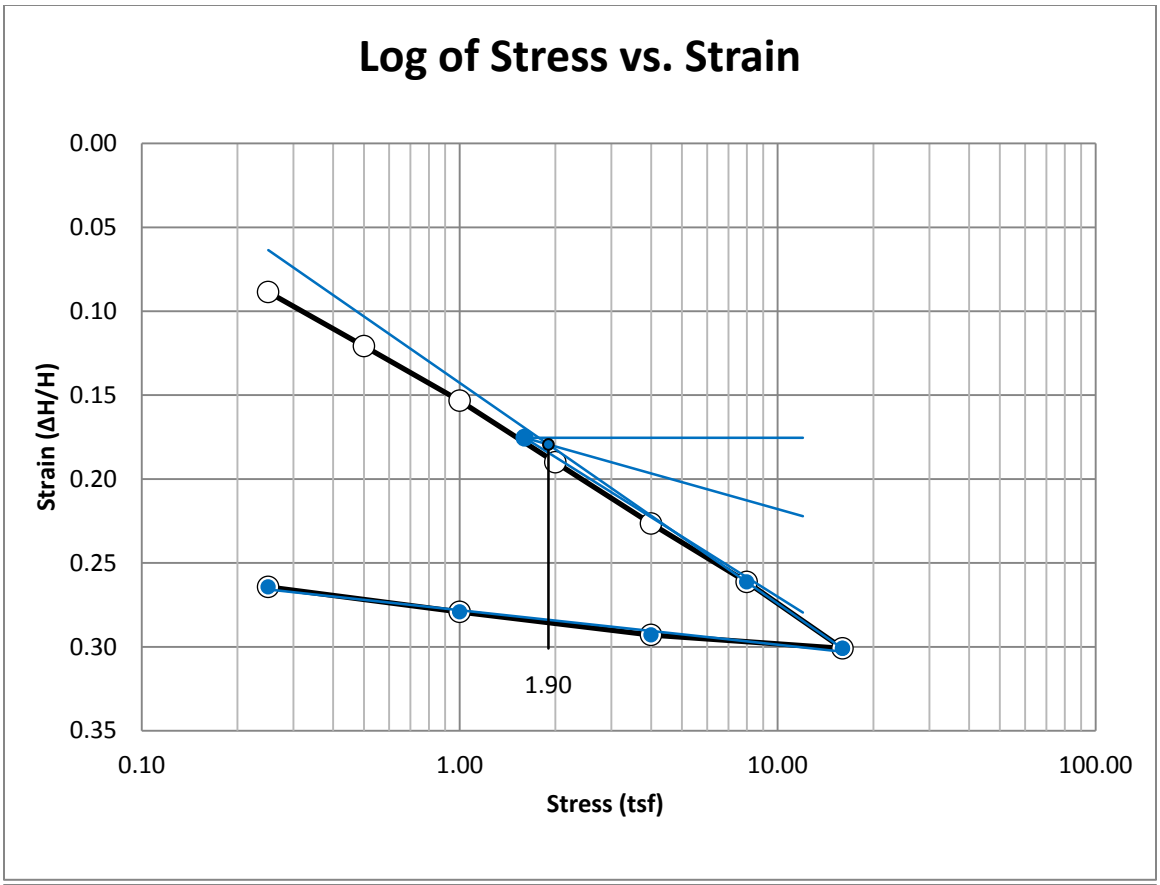

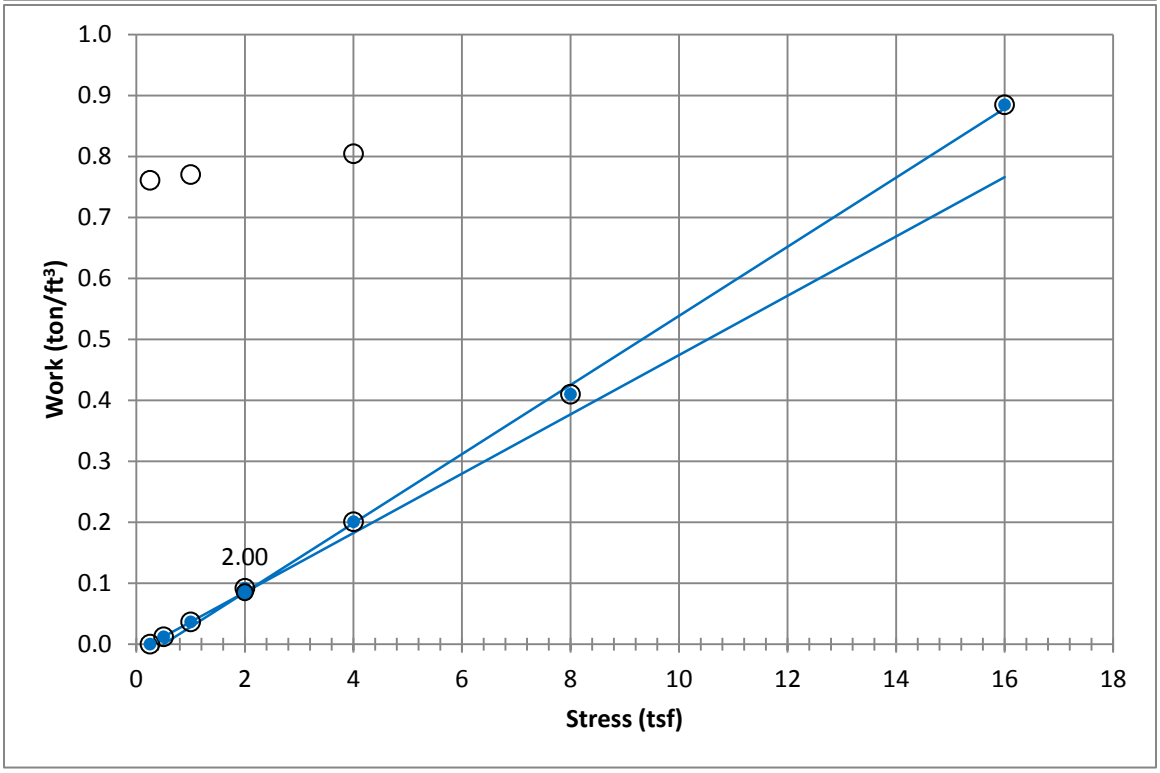

A209 Provo at 50-52 feet

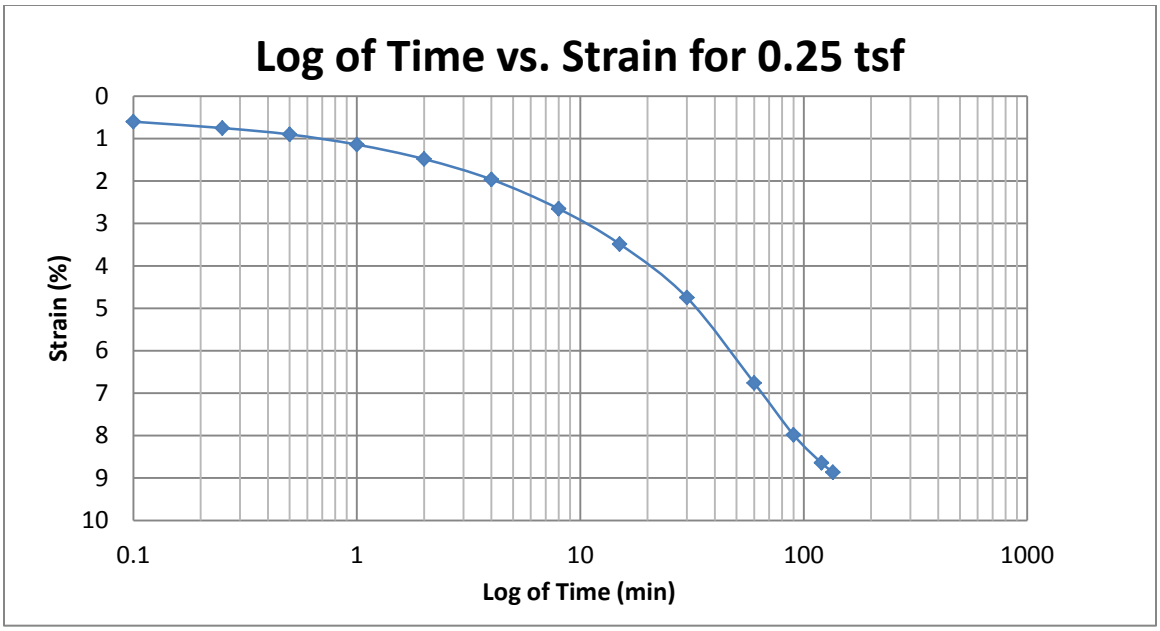

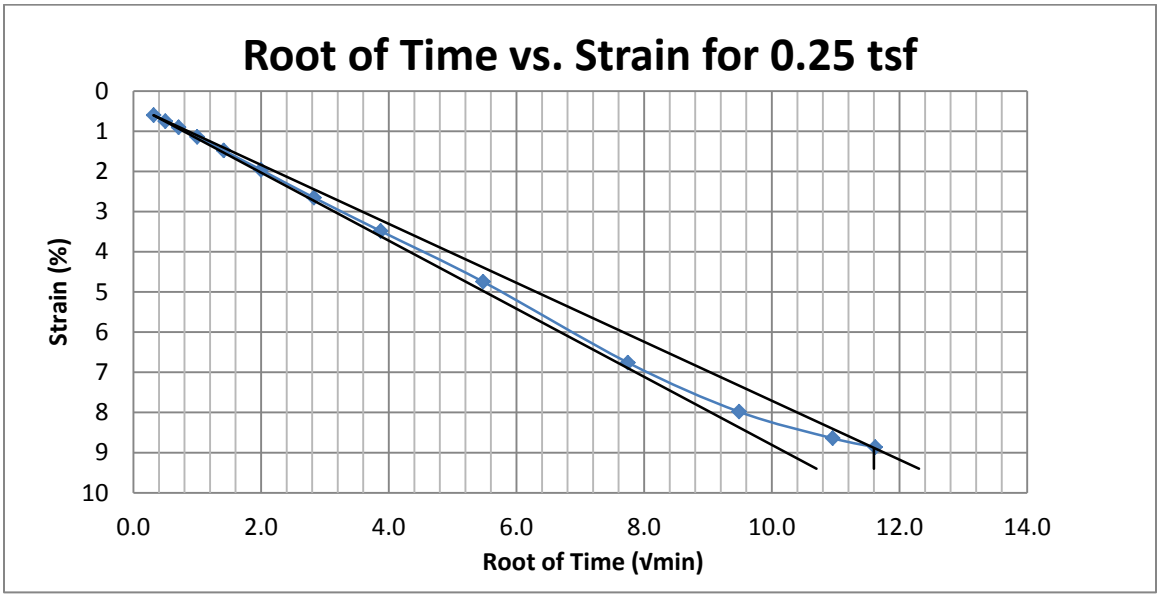

A210 Provo at 50-52 feet

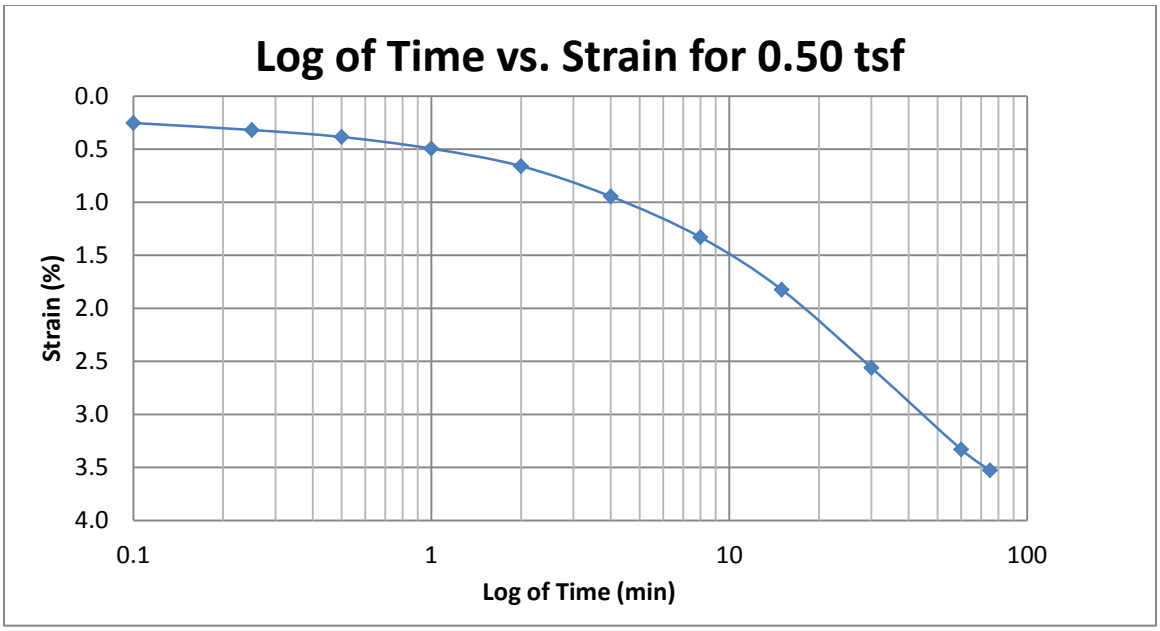

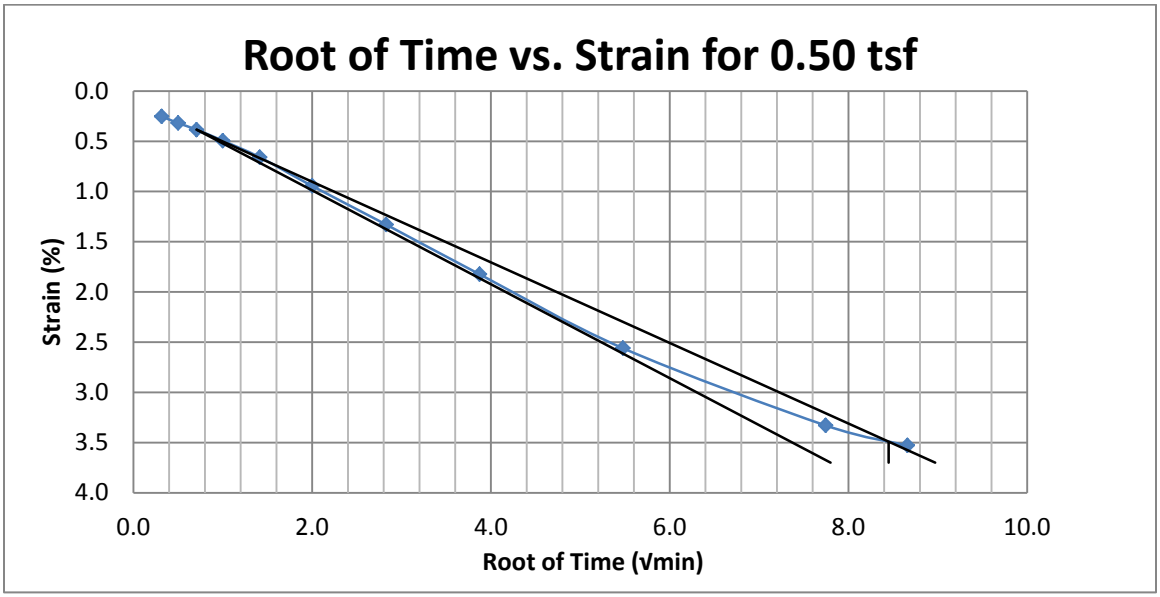

A211 Provo at 50-52 feet

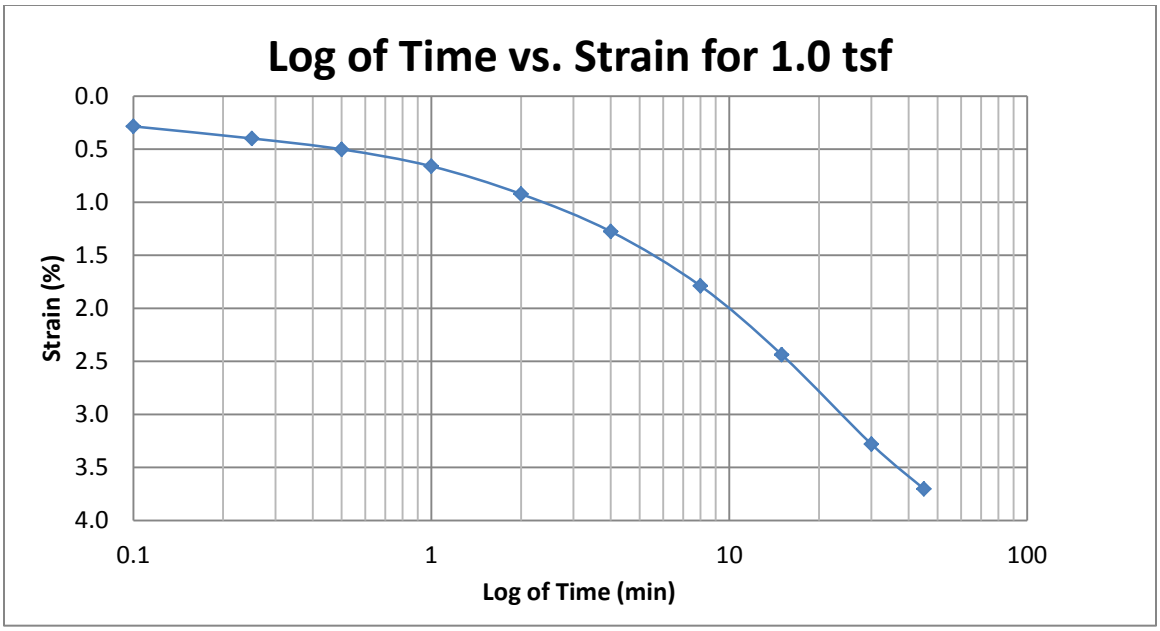

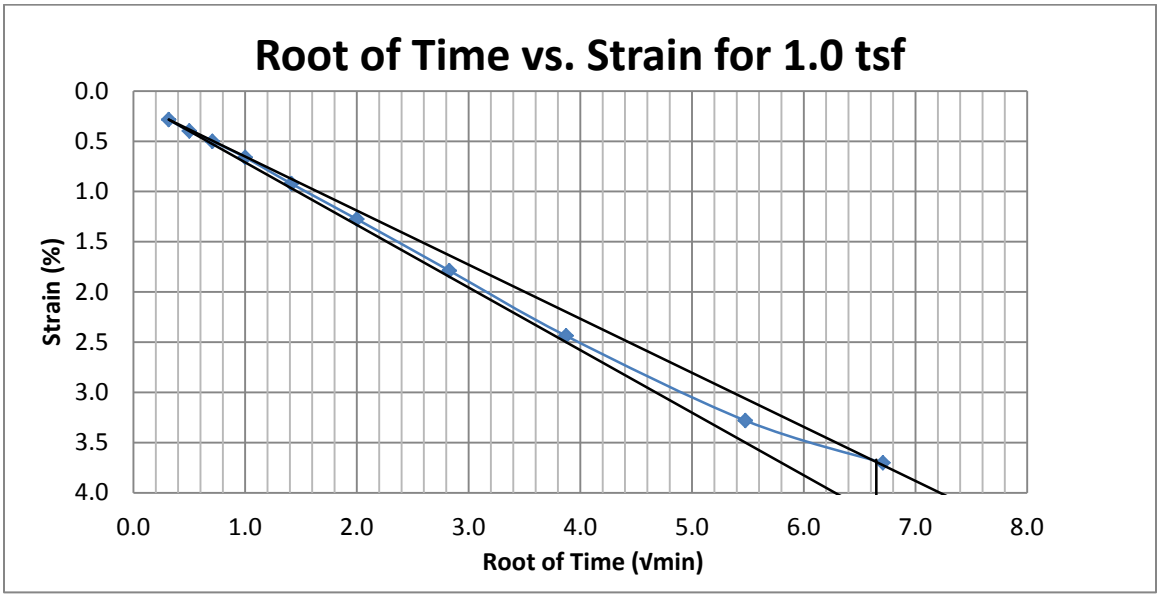

A212 Provo at 50-52 feet

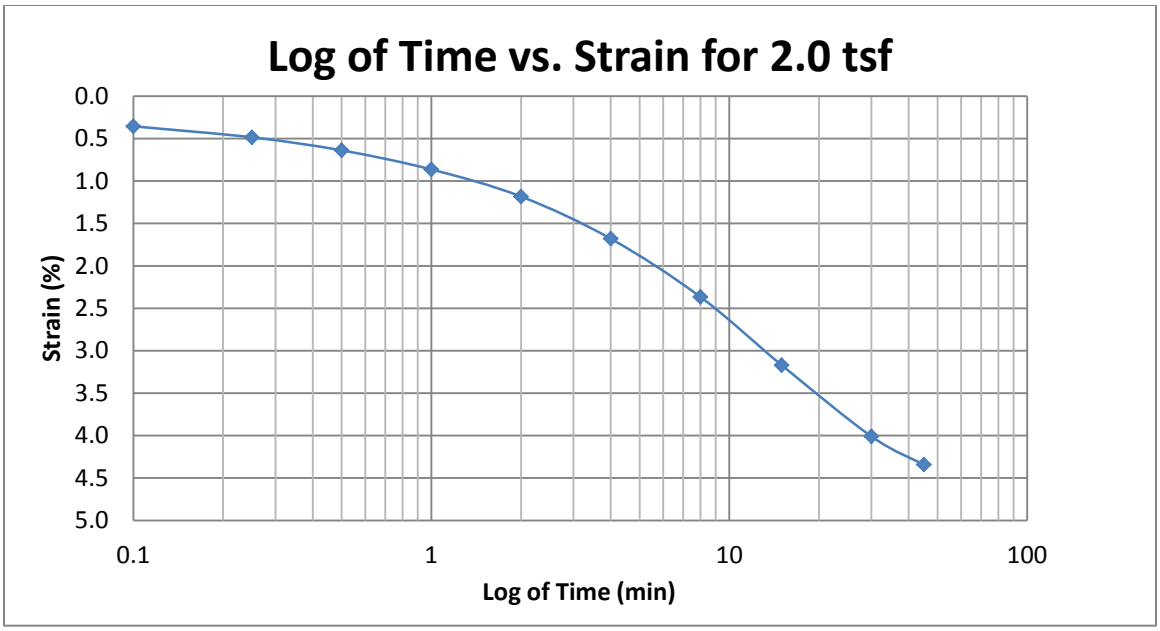

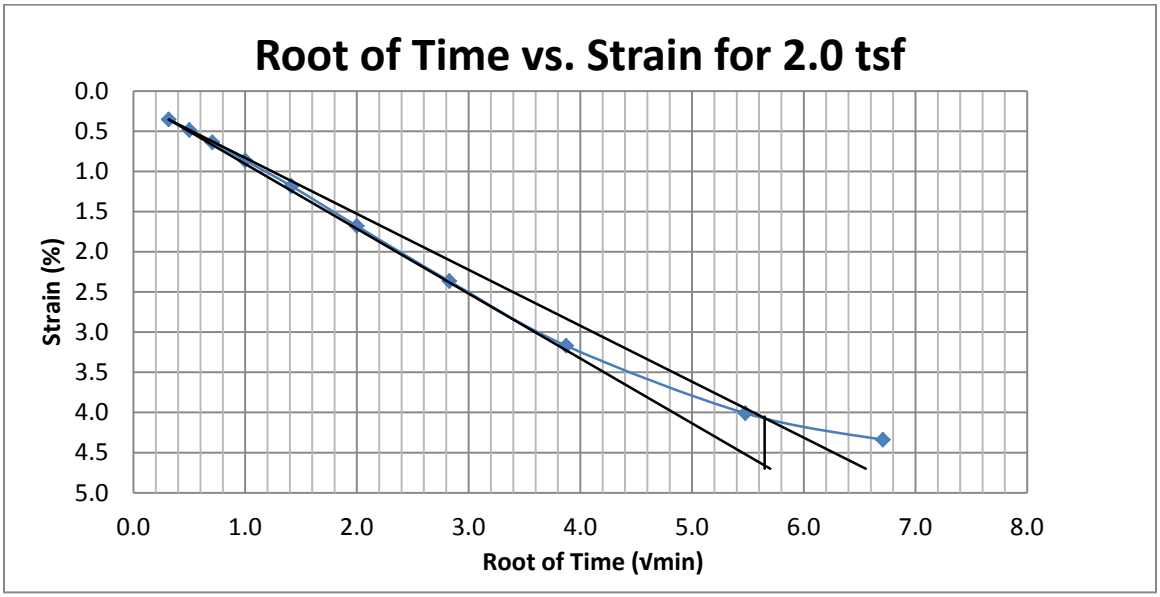

A213 Provo at 50-52 feet

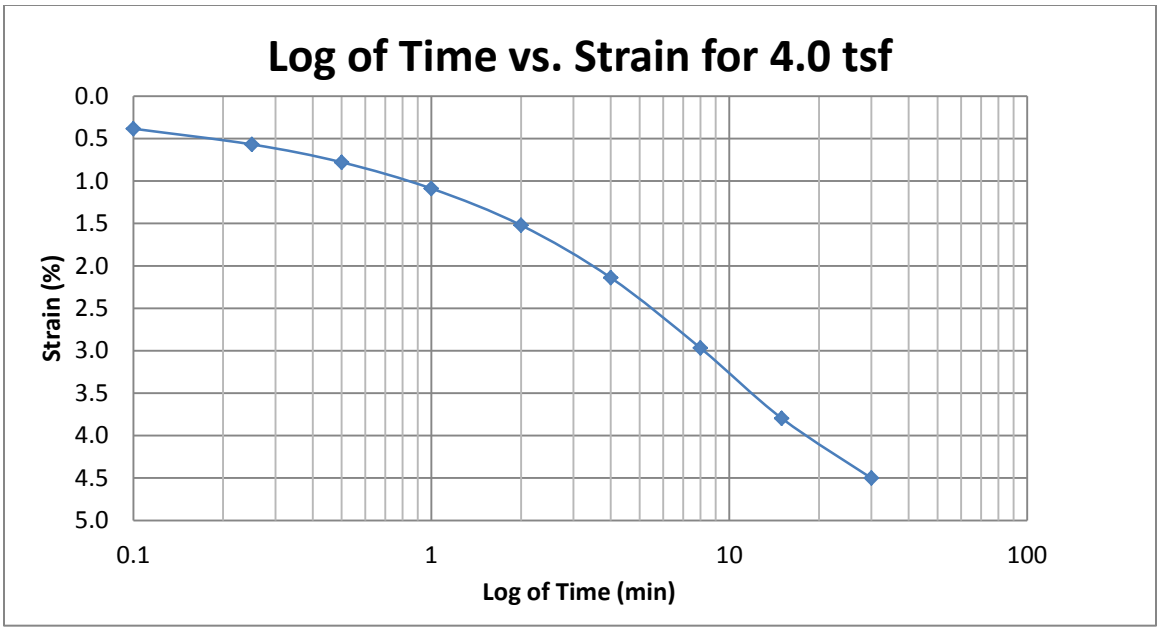

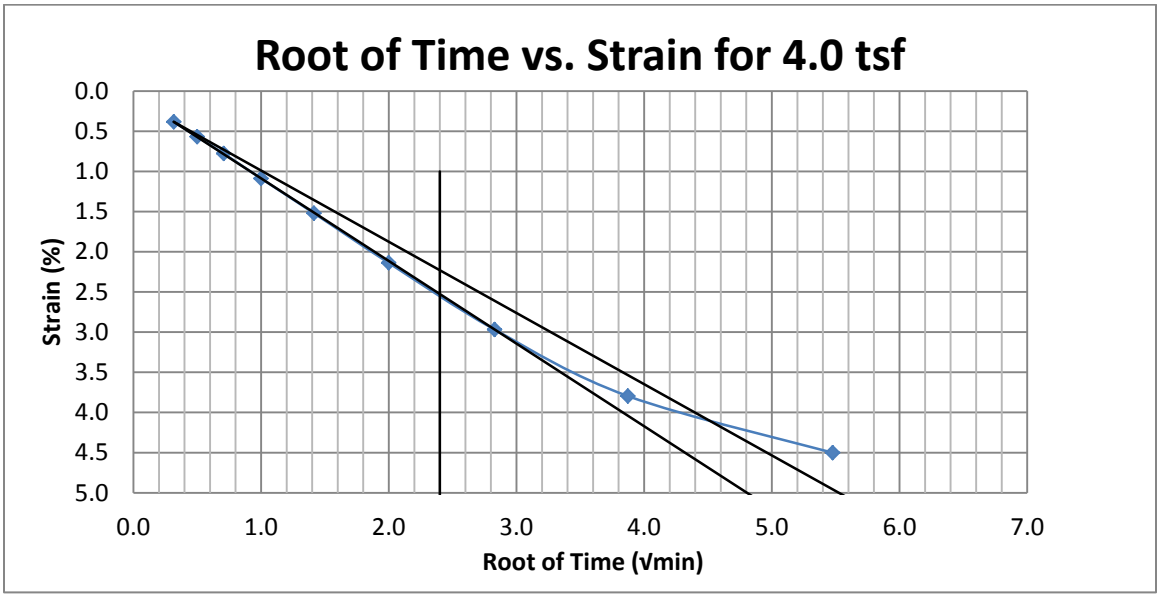

A214 Provo at 50-52 feet

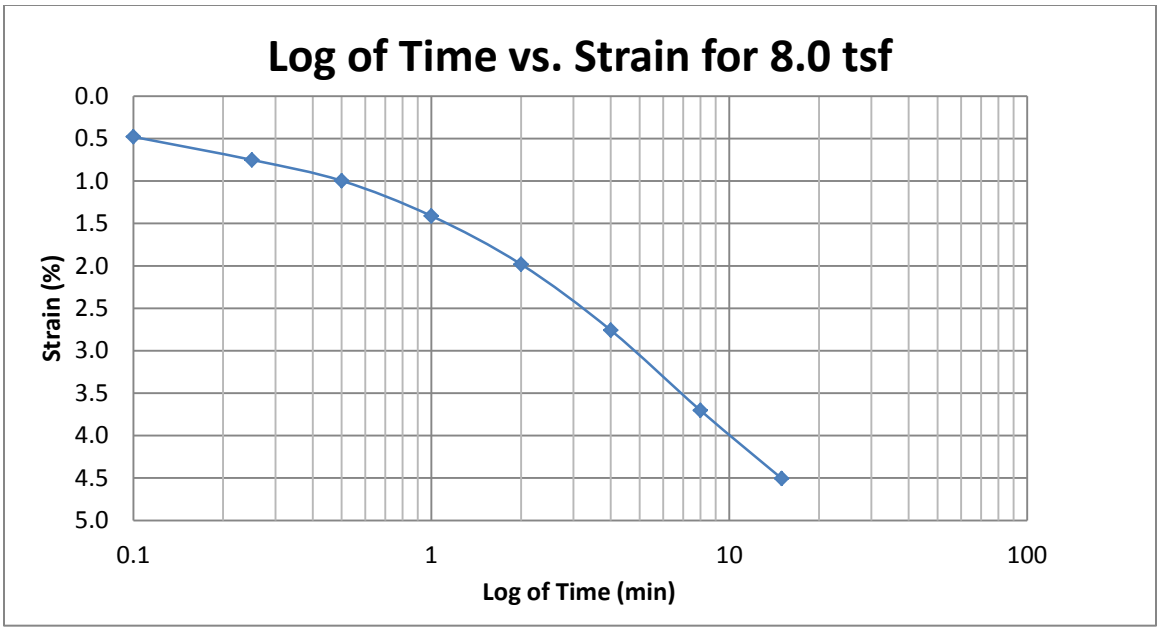

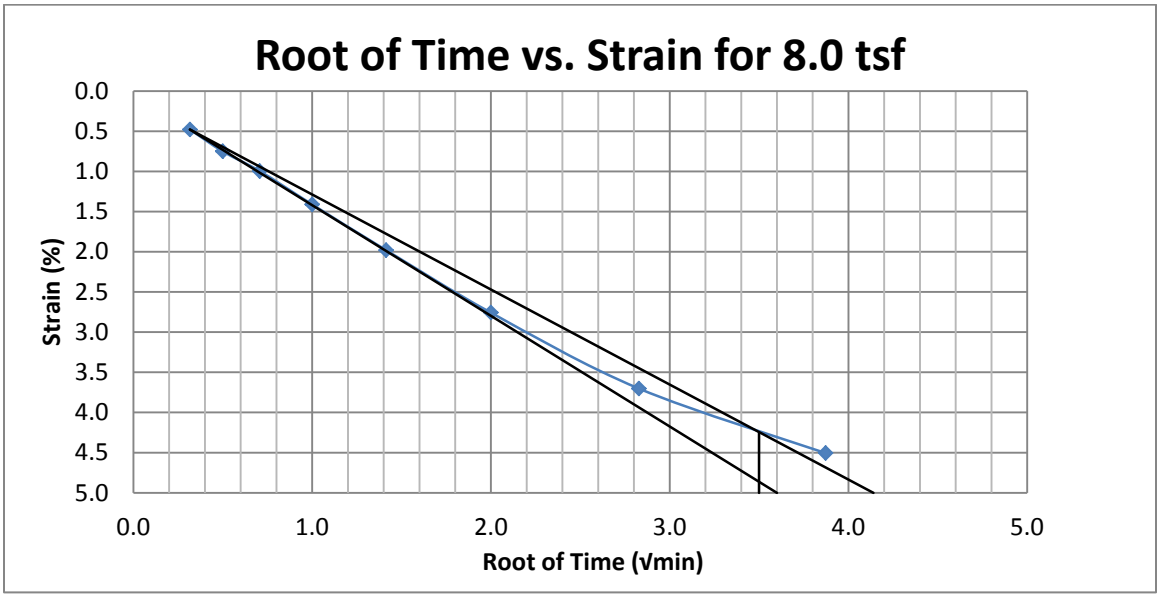

A215 Provo at 50-52 feet

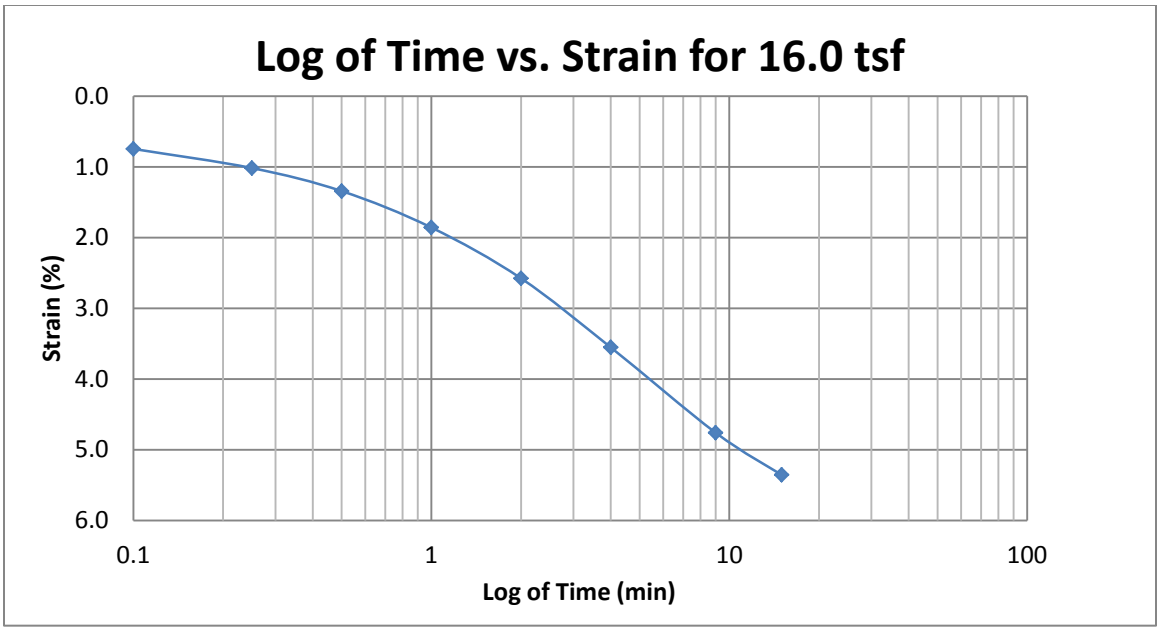

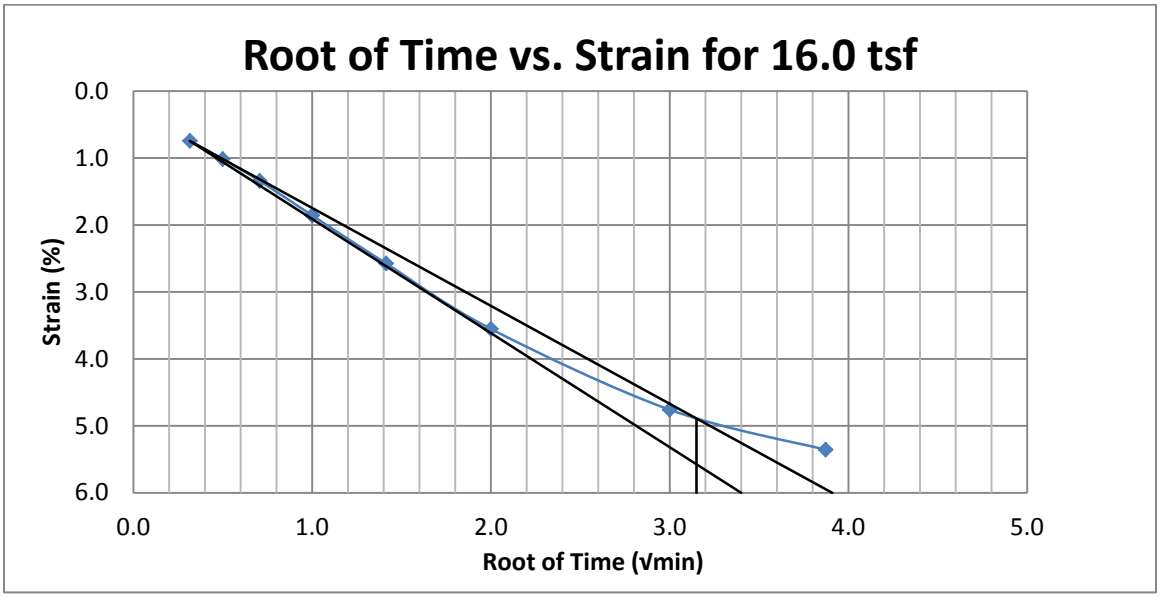

A216 Provo at 50-52 feet

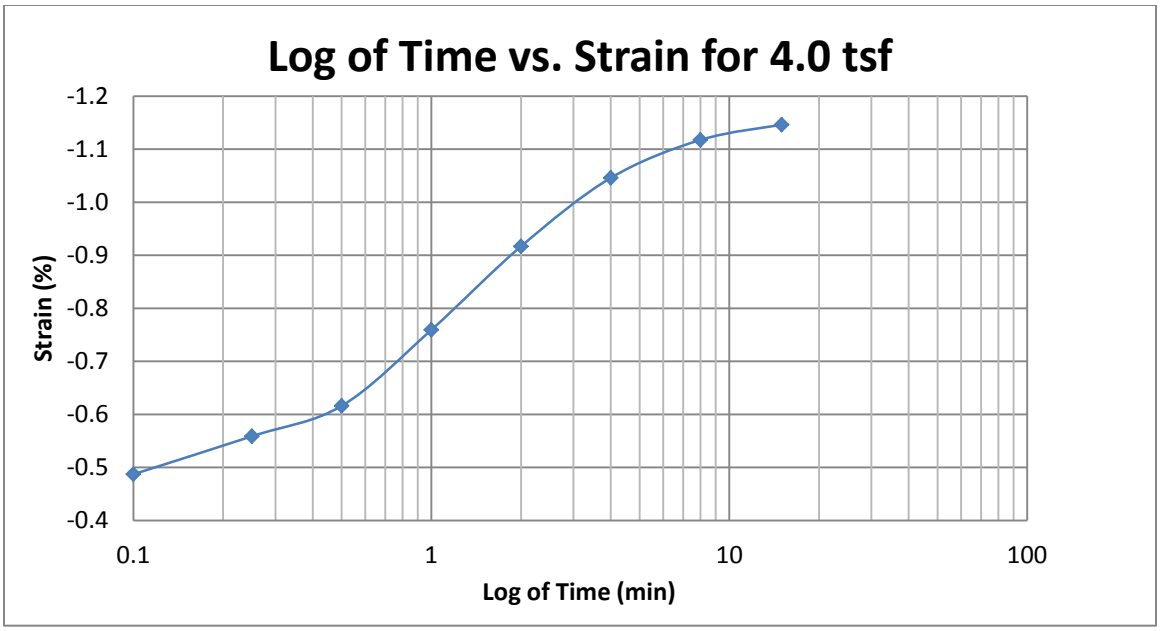

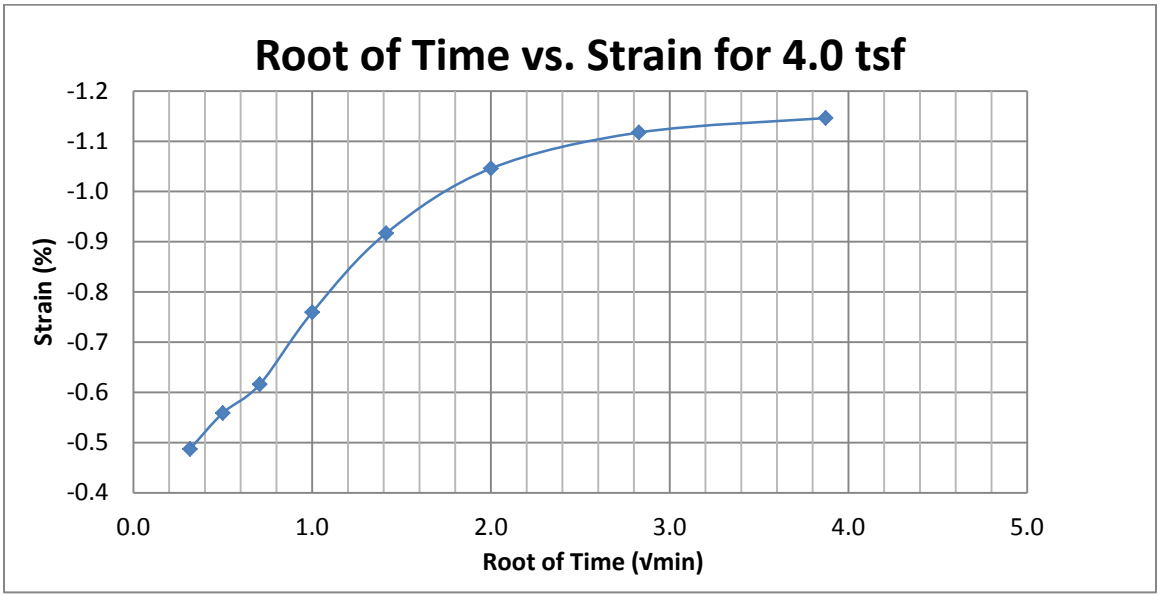

A217 Provo at 50-52 feet

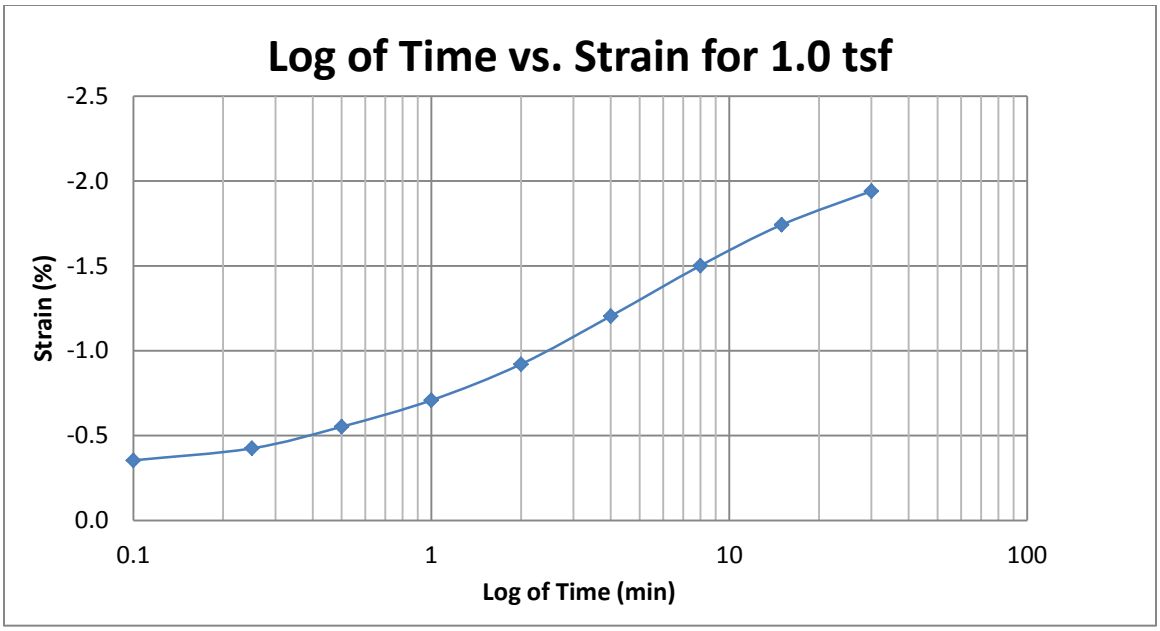

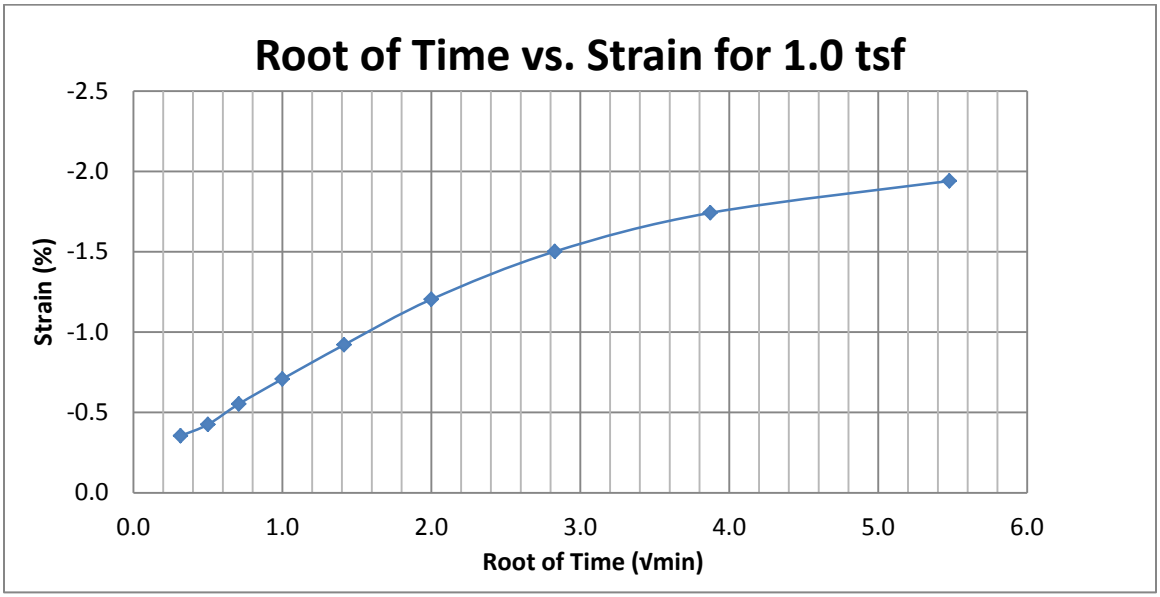

A218 Provo at 50-52 feet

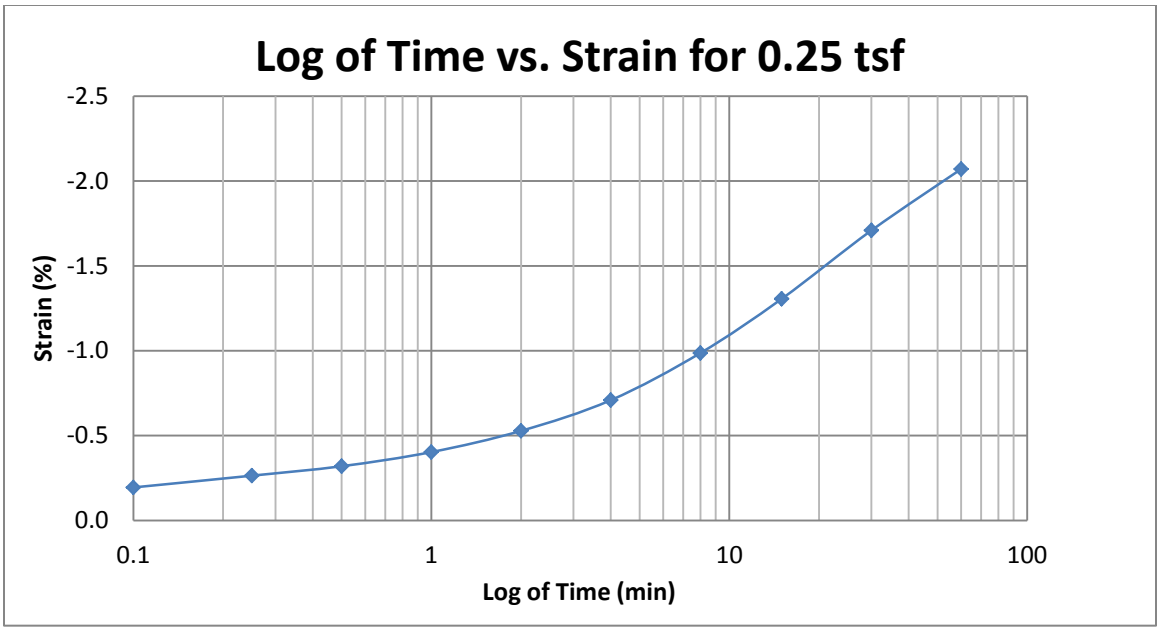

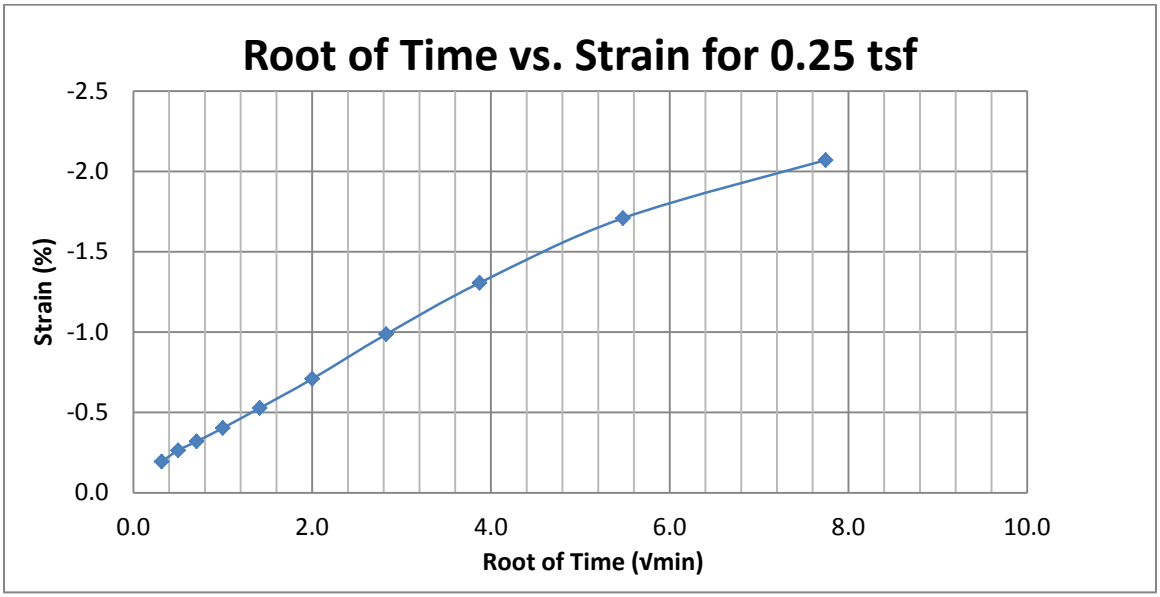

A219 Provo at 50-52 feet

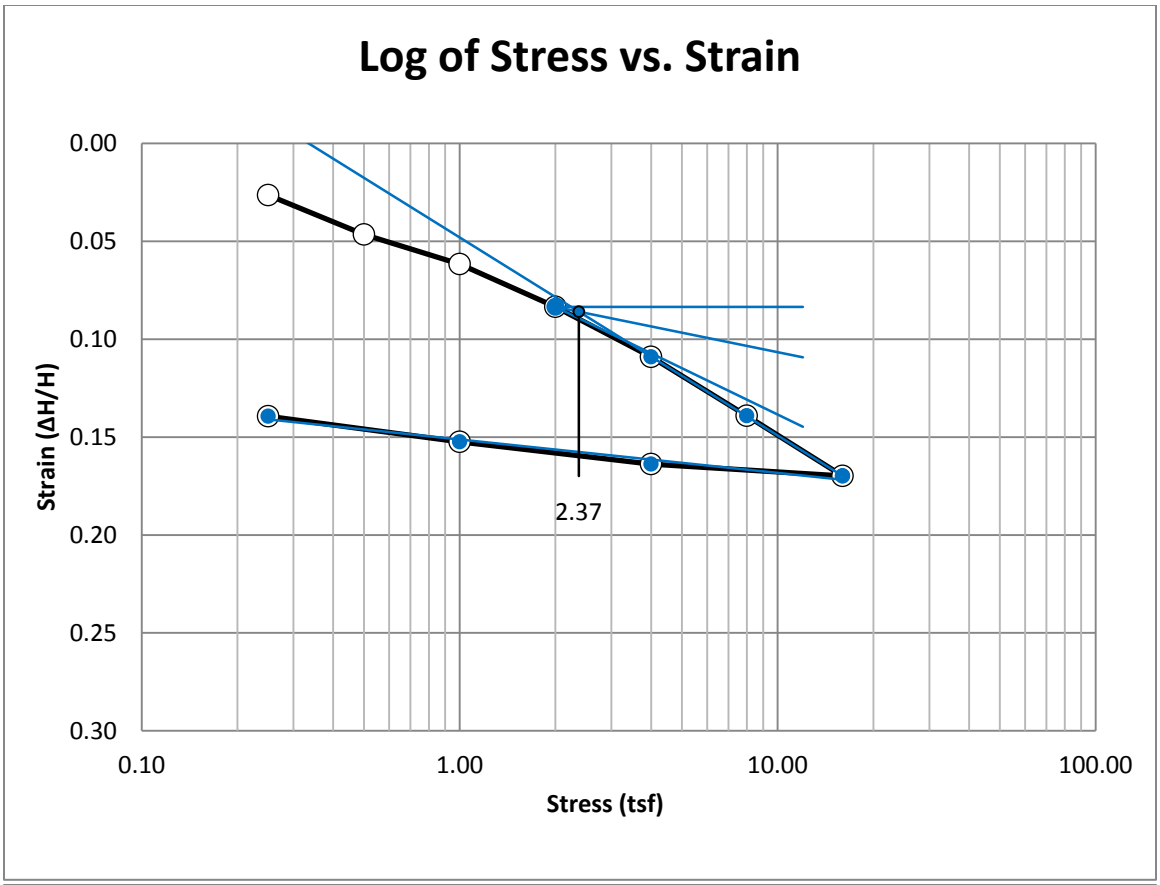

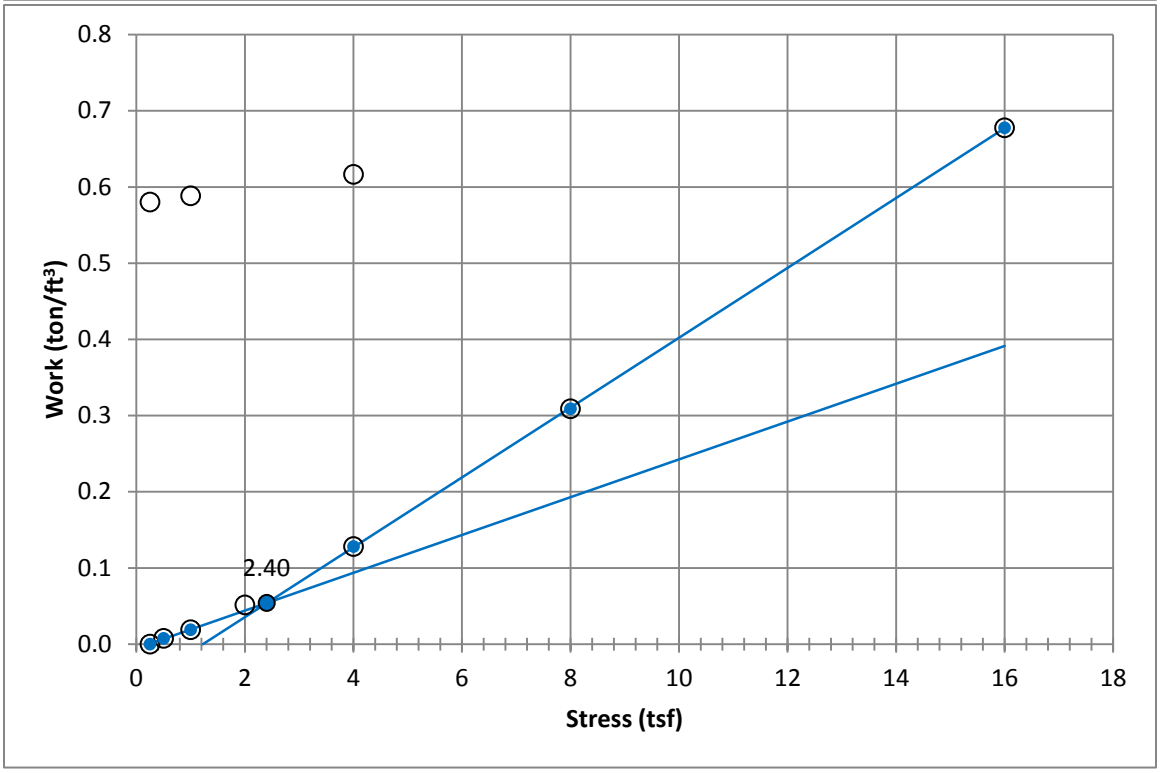

A220 Provo at 60-62 feet

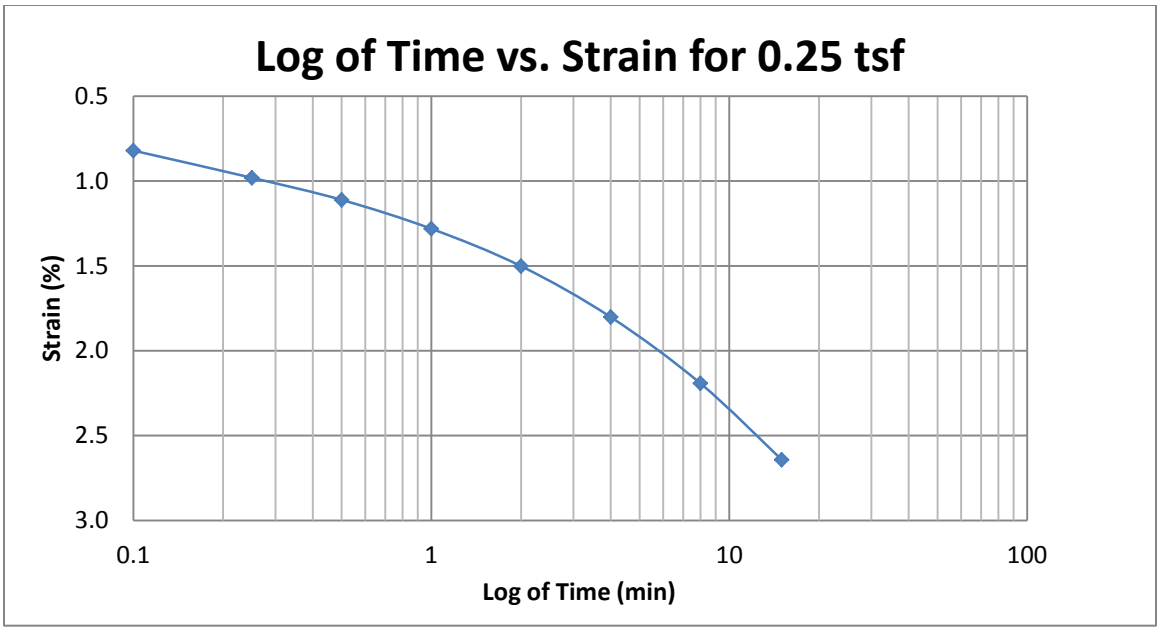

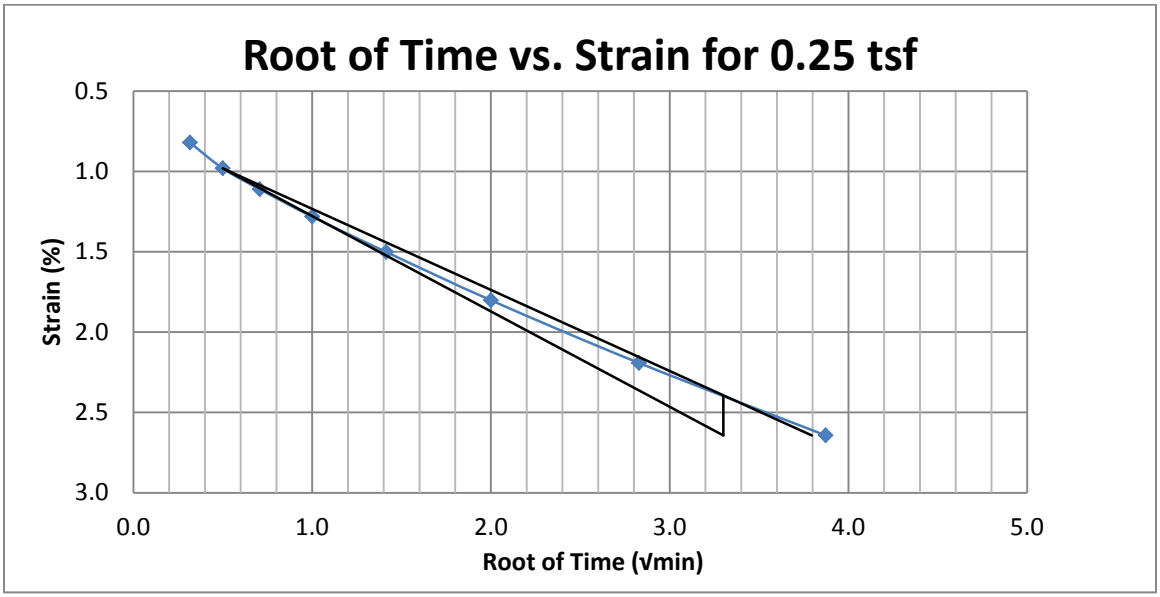

A221 Provo at 60-62 feet

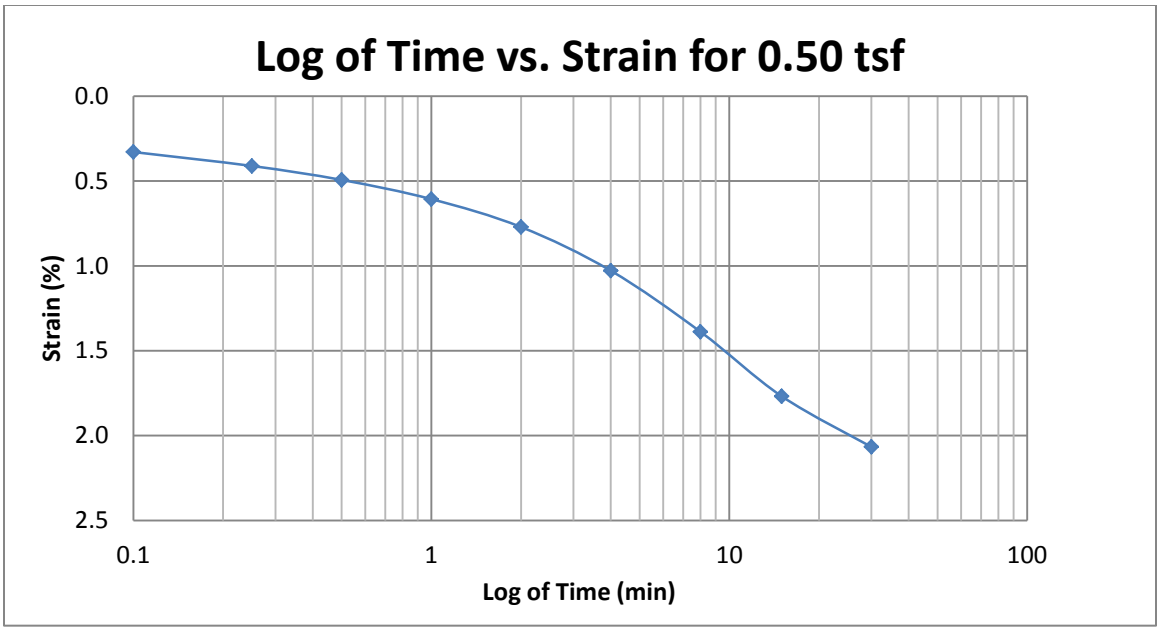

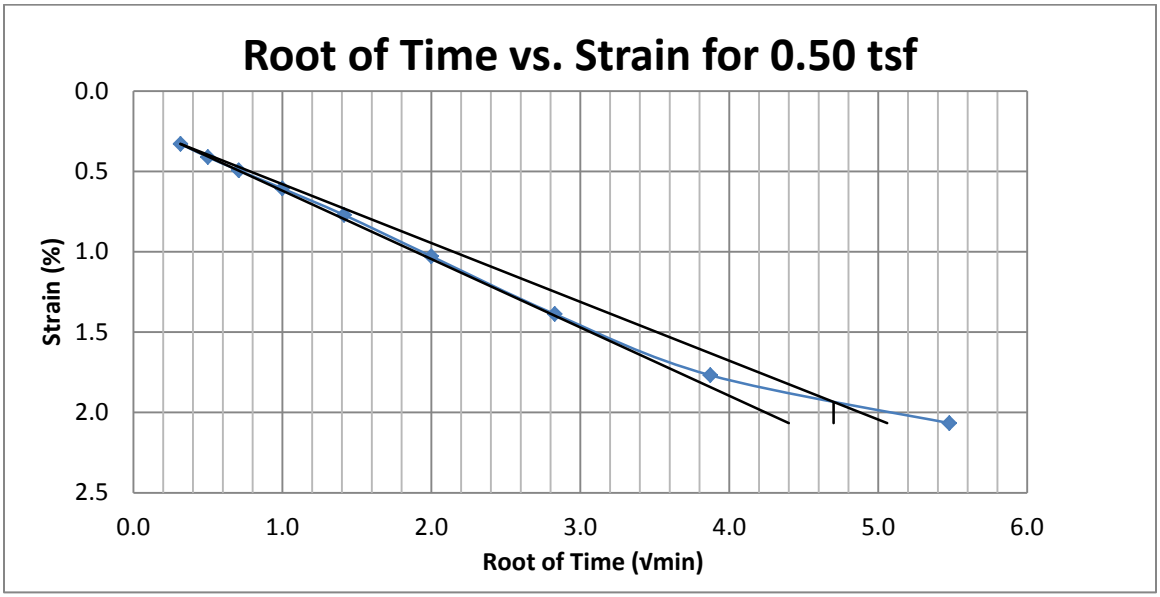

A222 Provo at 60-62 feet

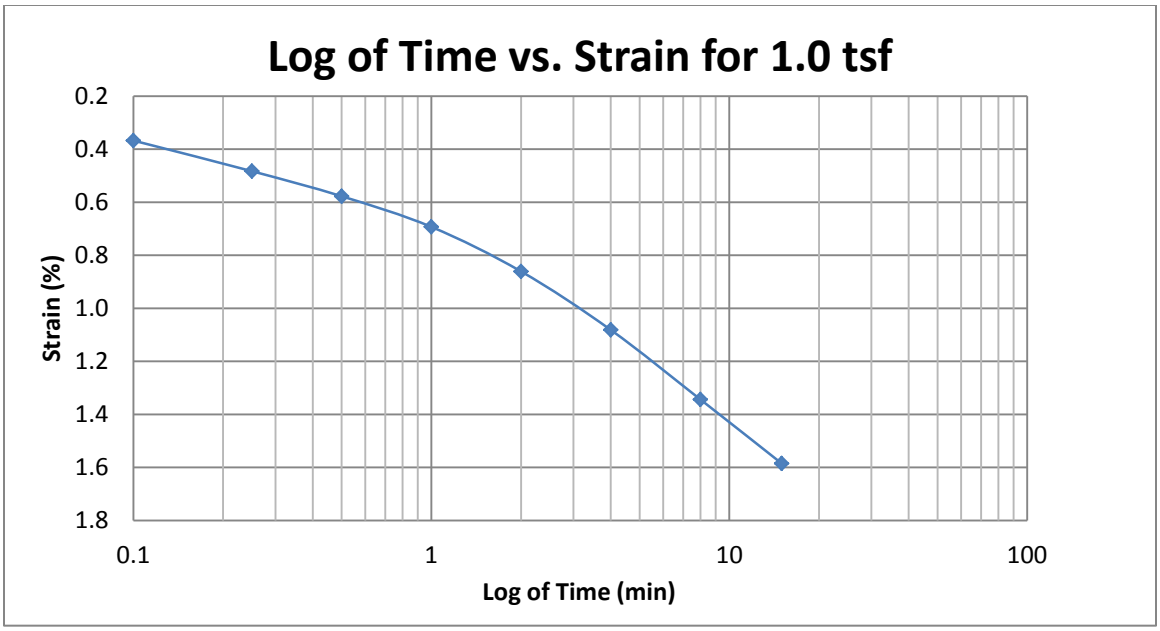

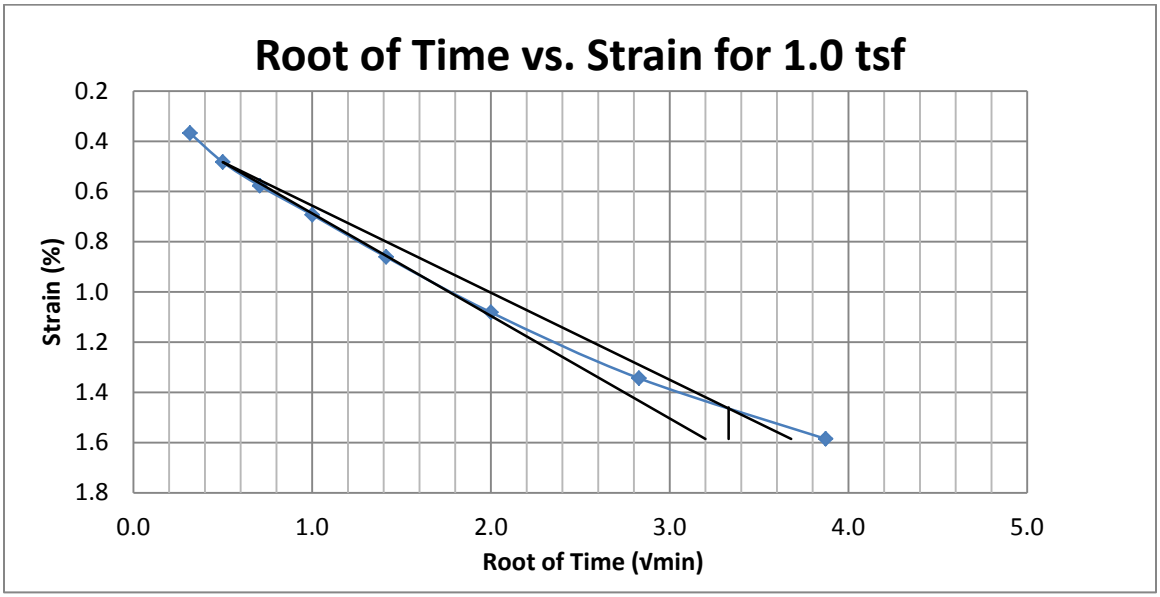

A223 Provo at 60-62 feet

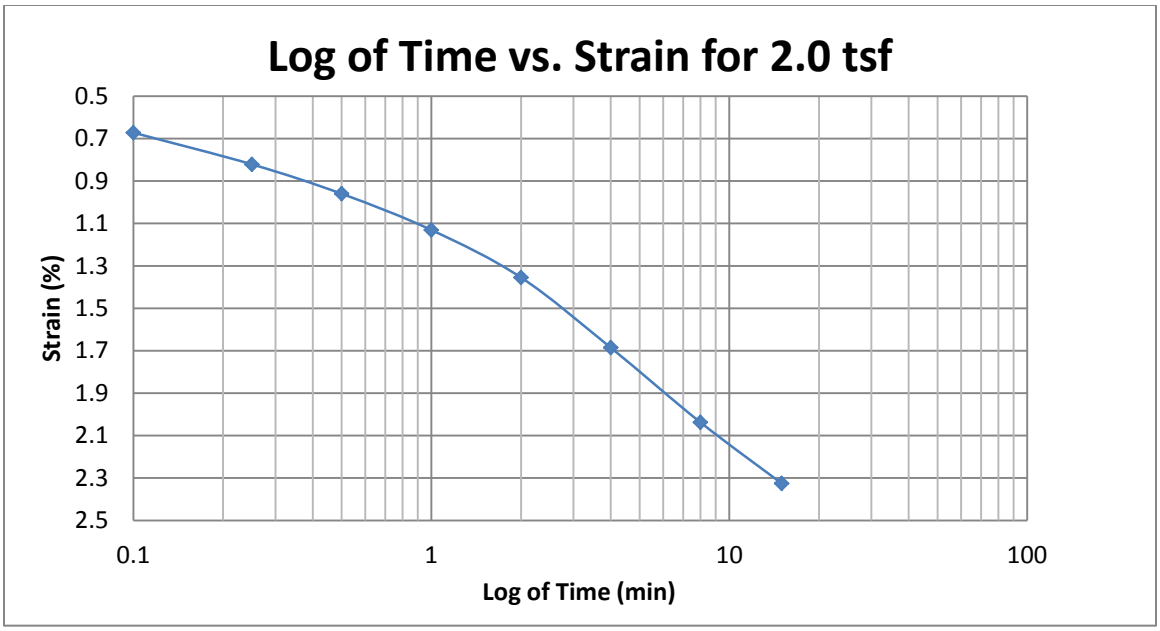

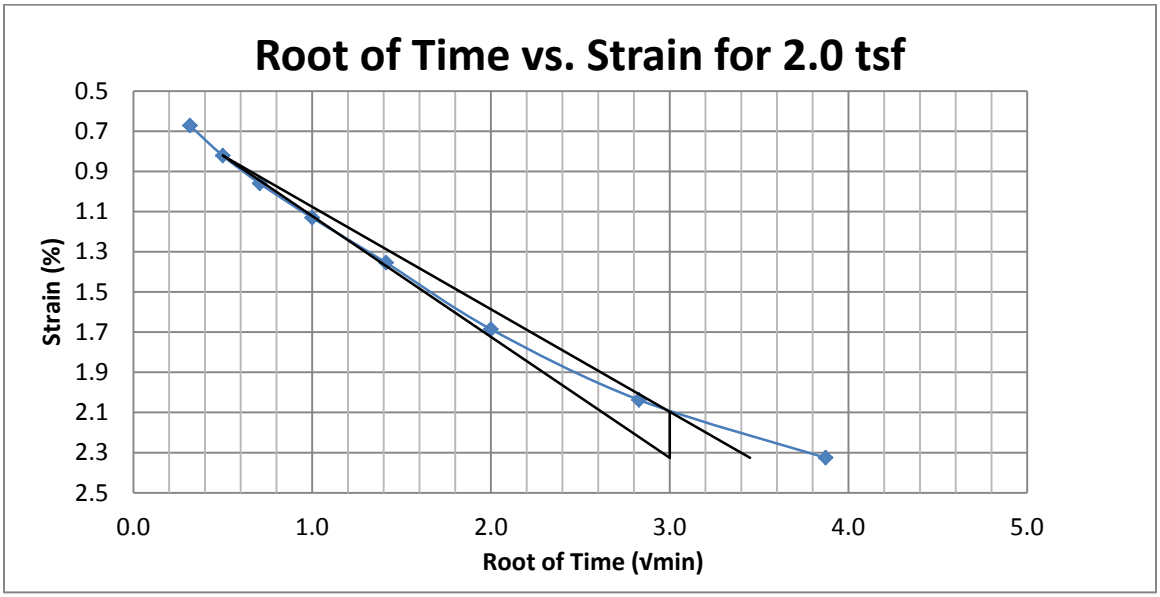

A224 Provo at 60-62 feet

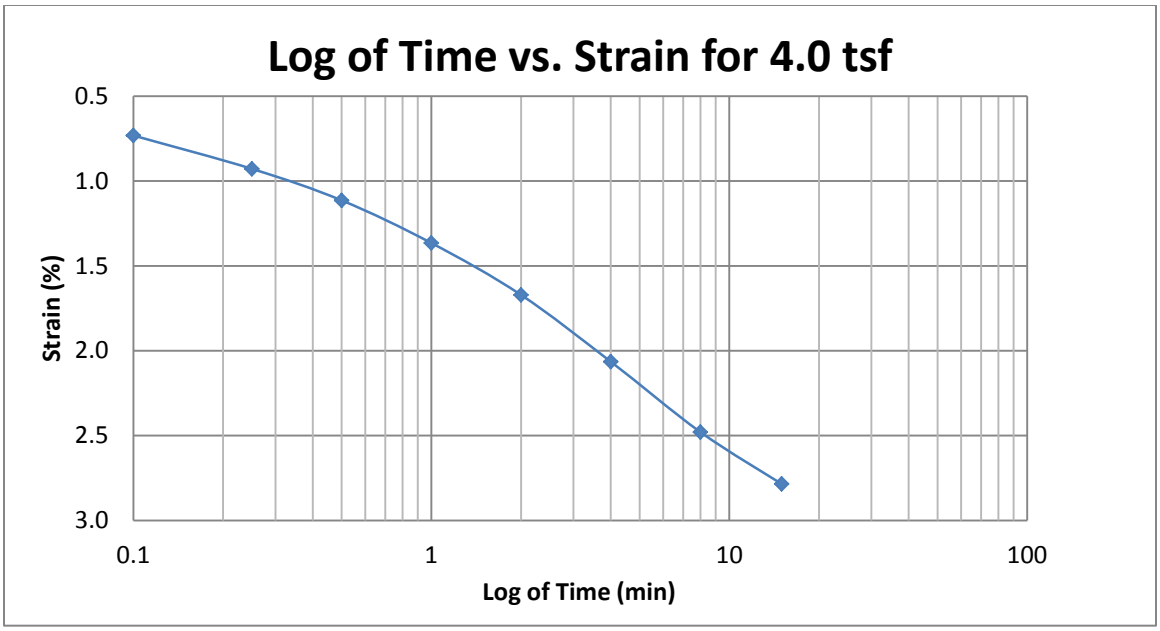

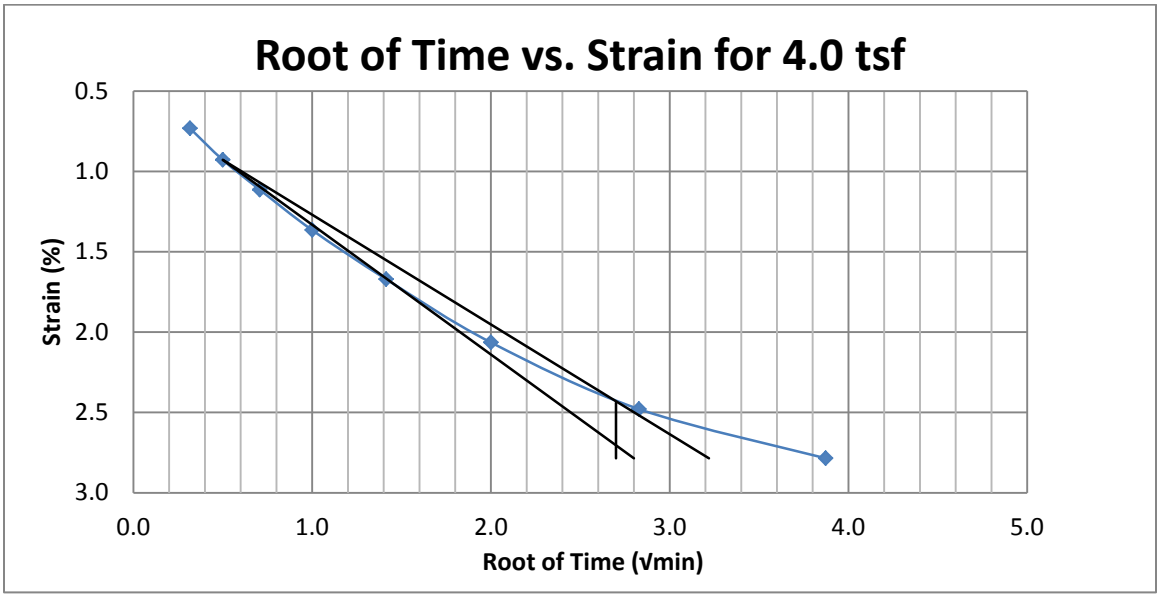

A225 Provo at 60-62 feet

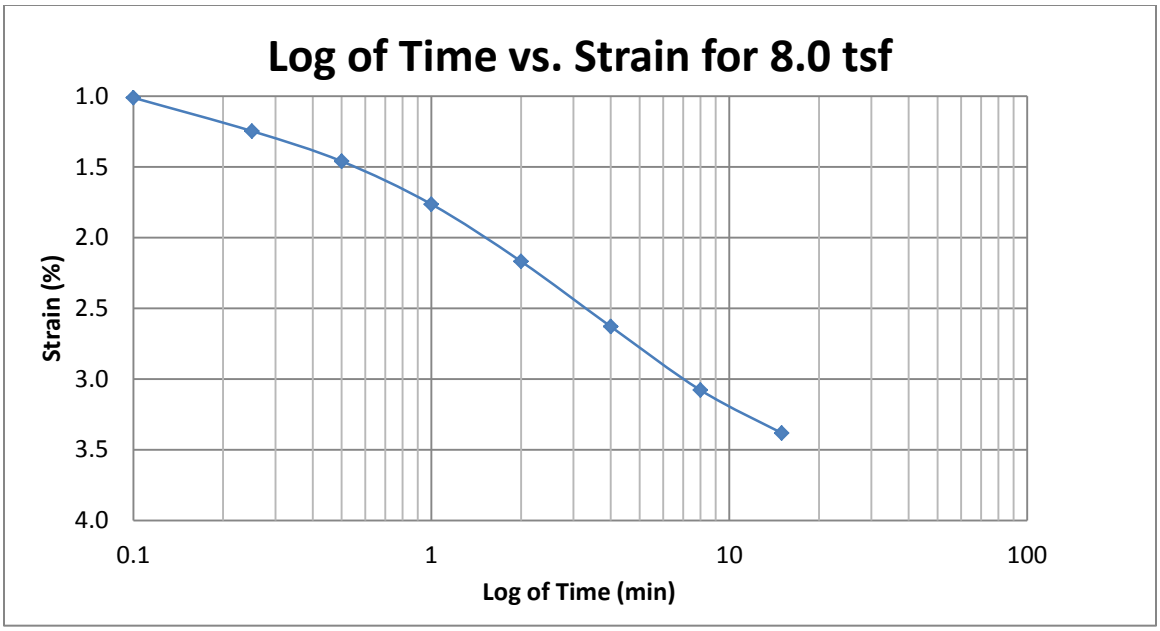

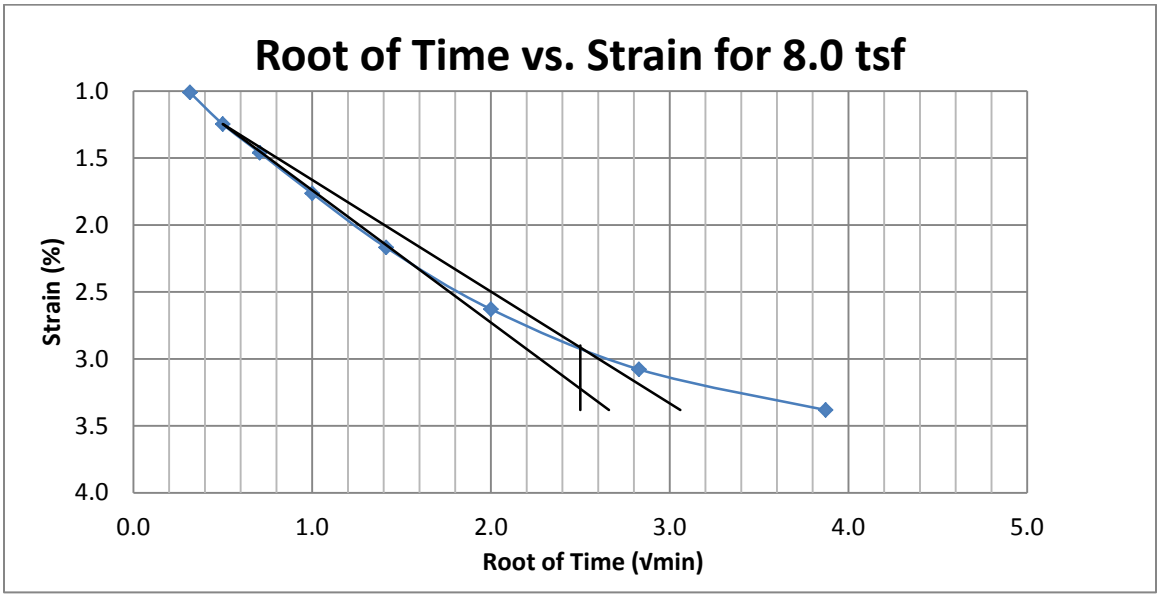

A226 Provo at 60-62 feet

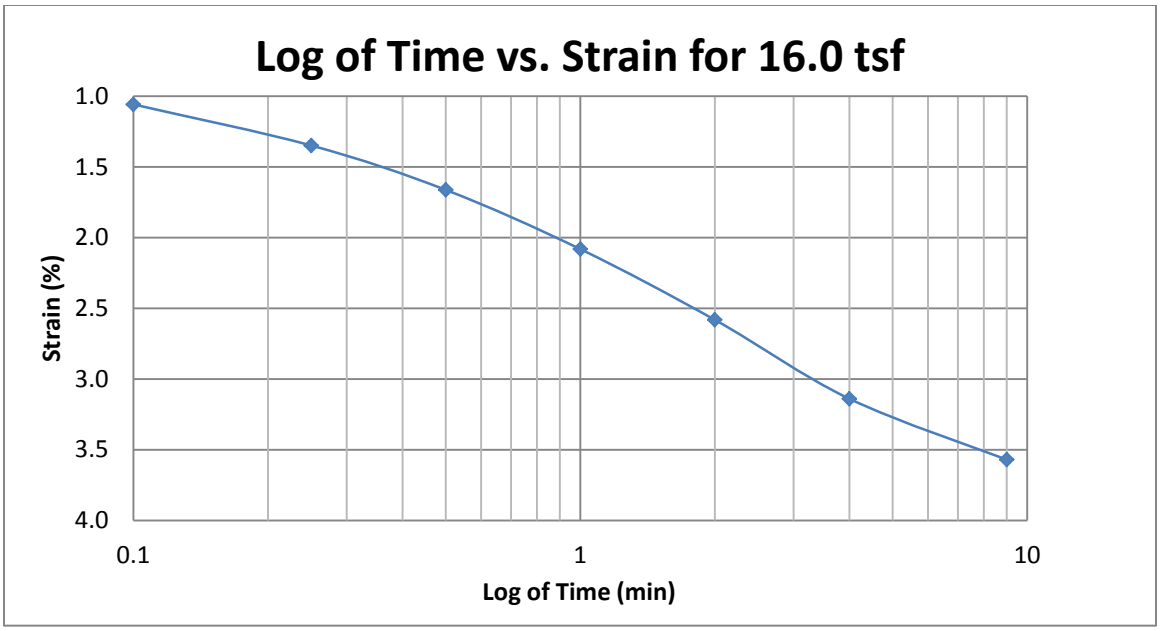

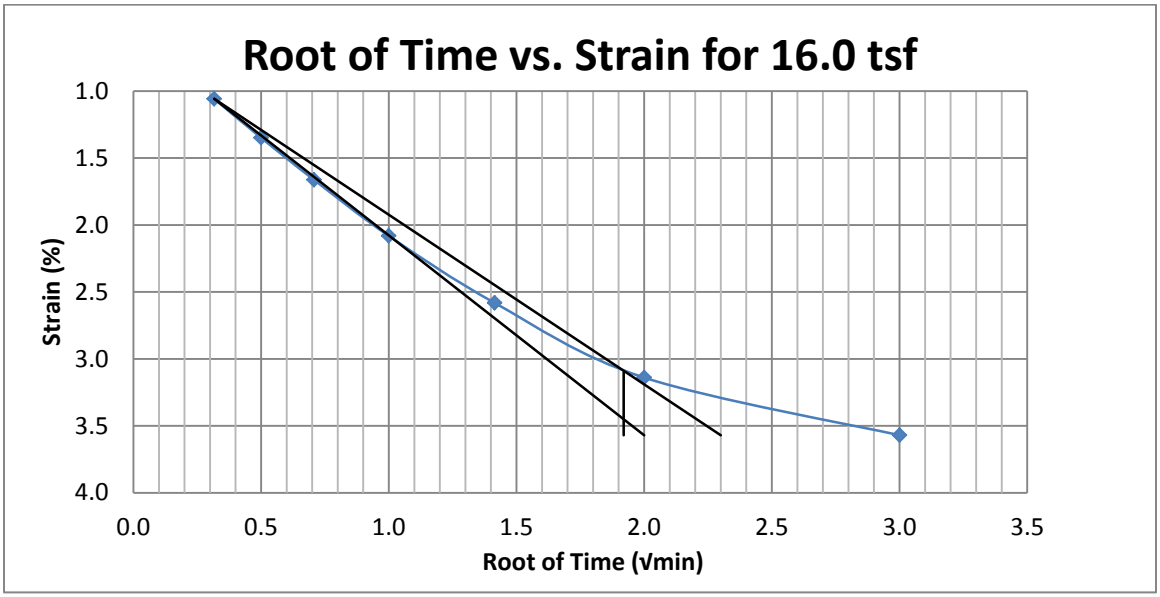

A227 Provo at 60-62 feet

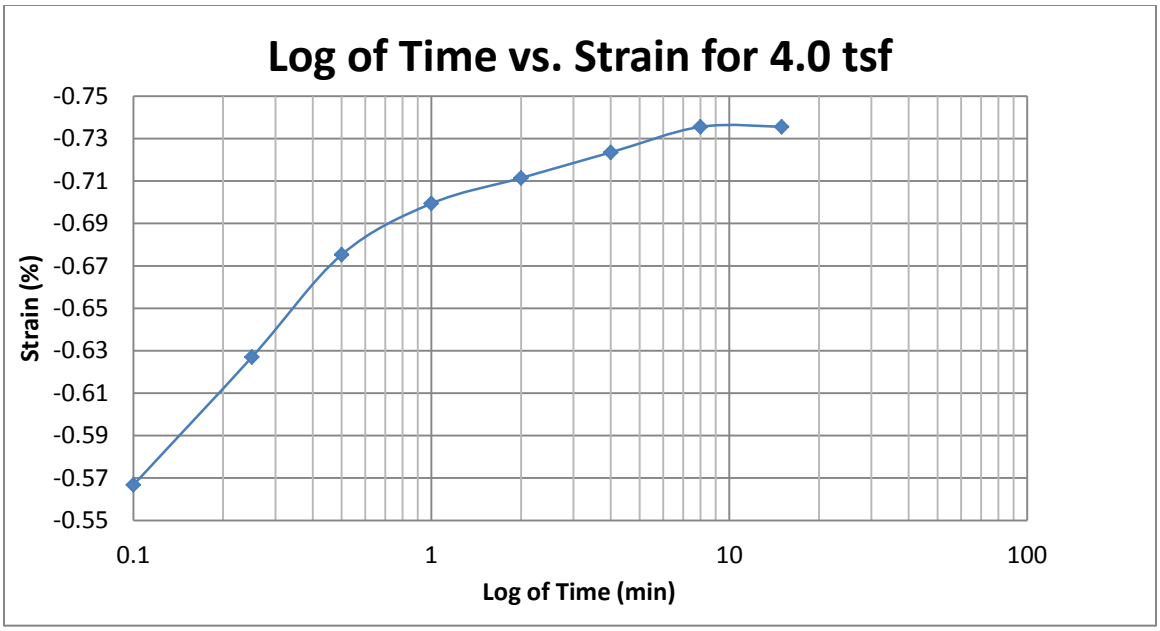

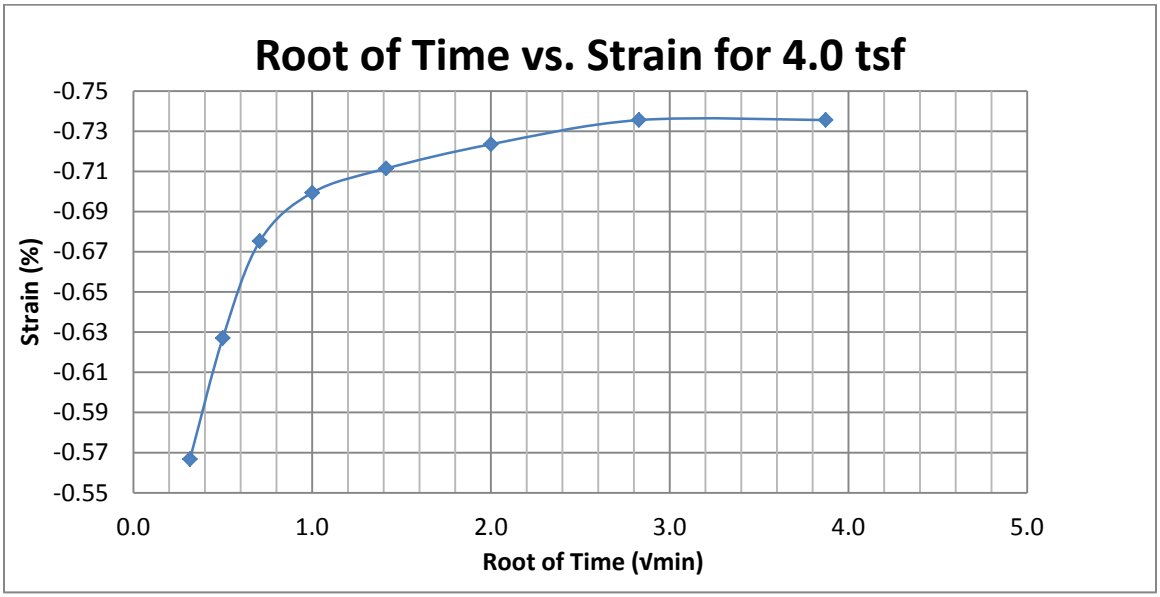

A228 Provo at 60-62 feet

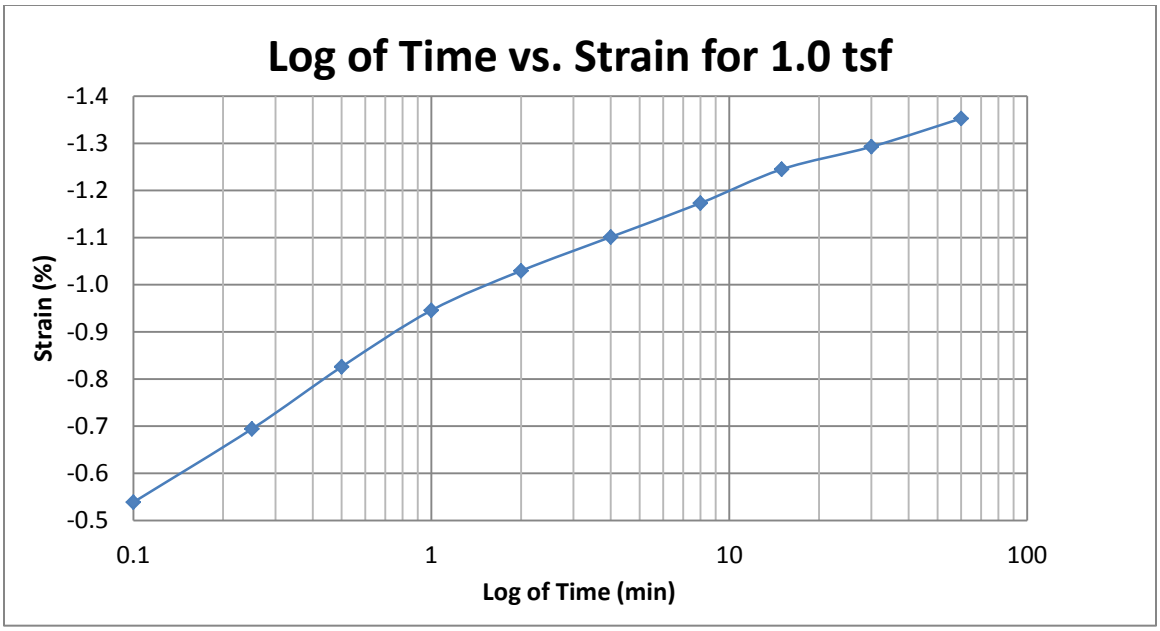

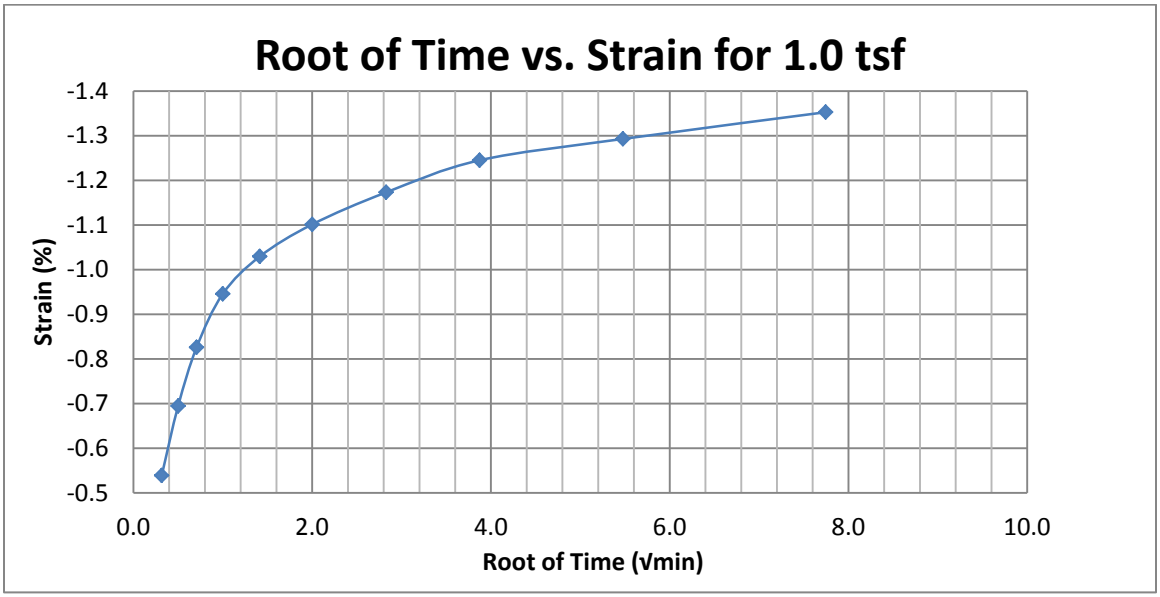

A229 Provo at 60-62 feet

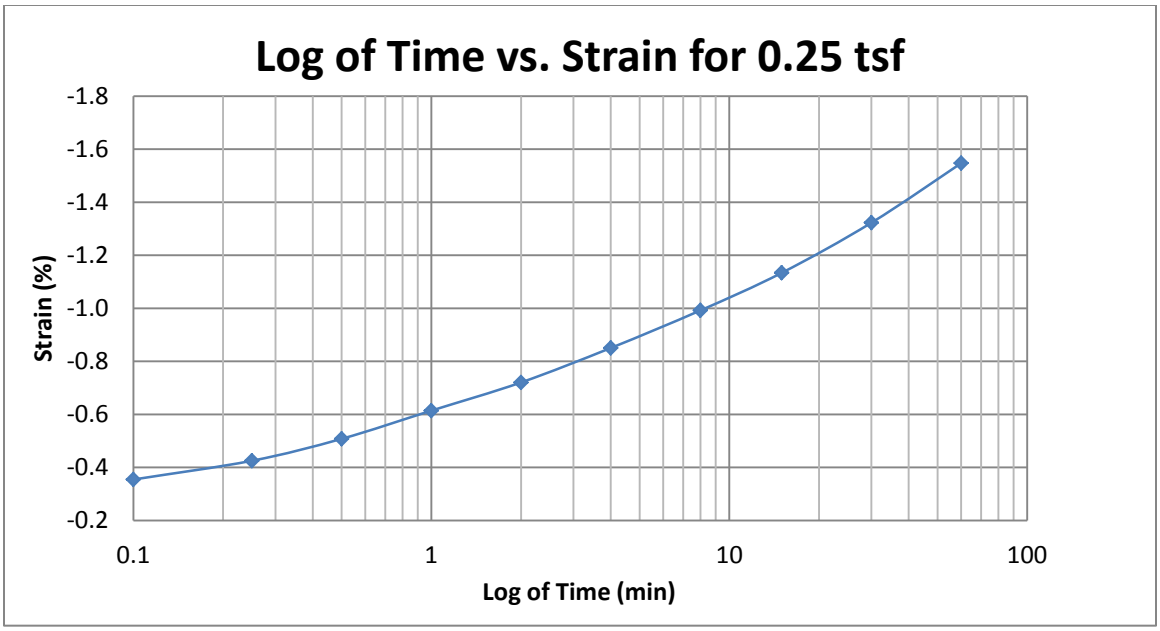

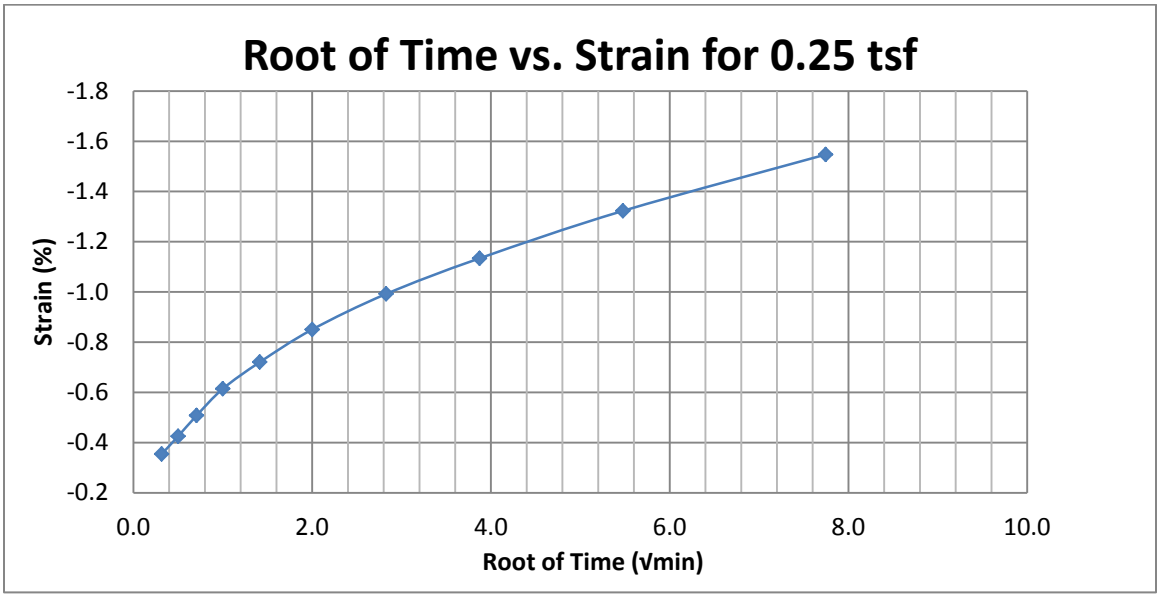

A230 Provo at 60-62 feet

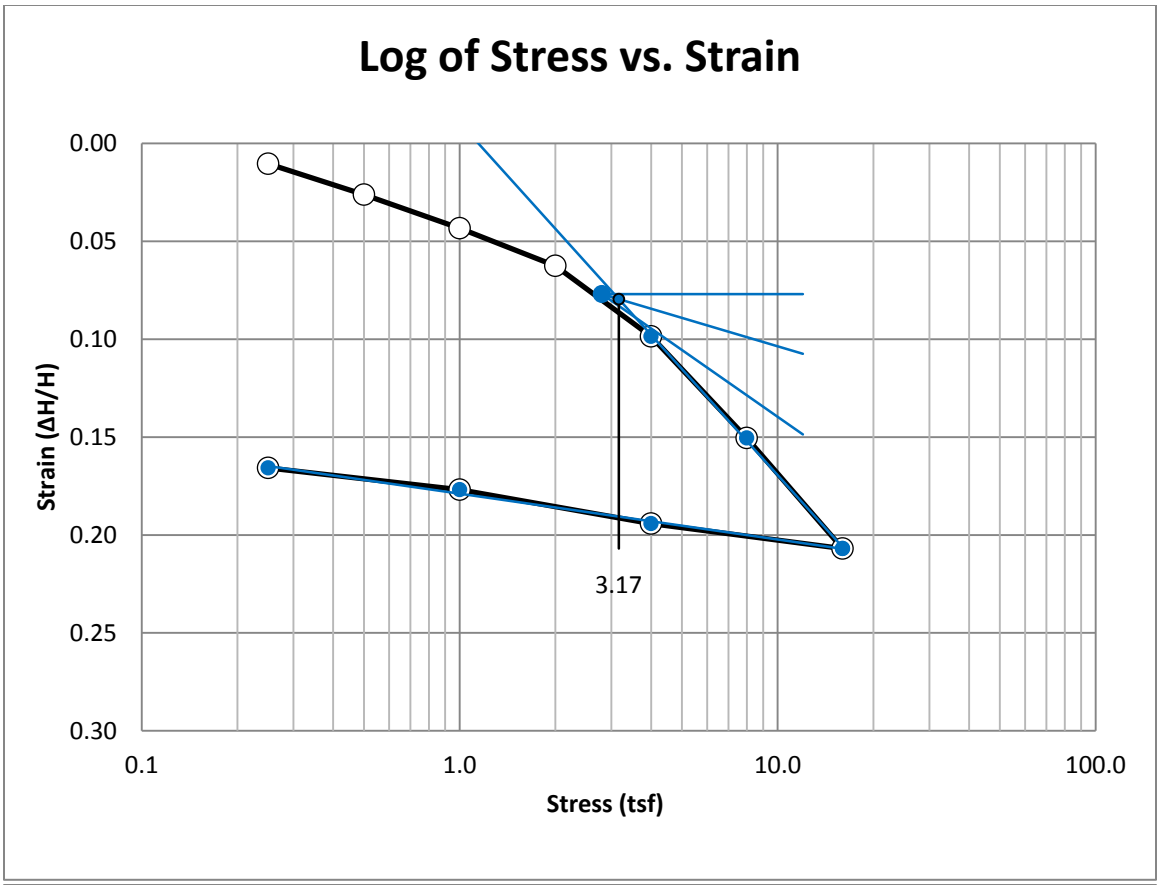

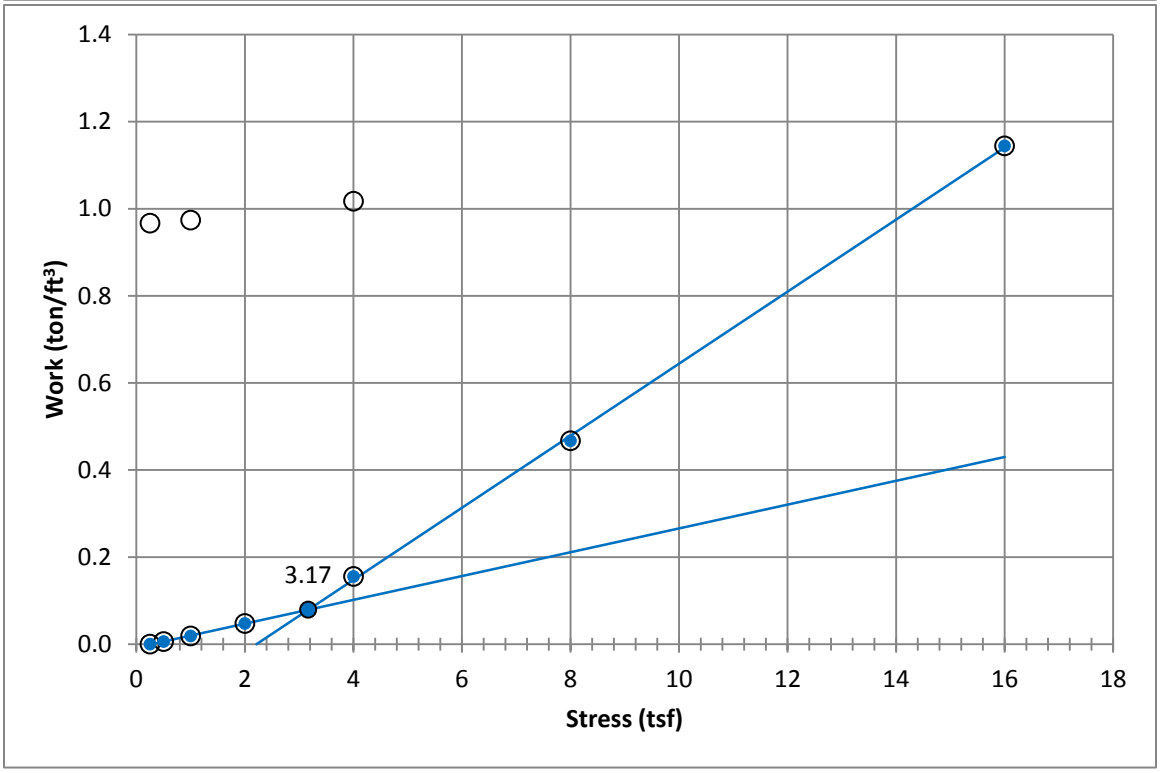

A231 Provo at 80-82 feet

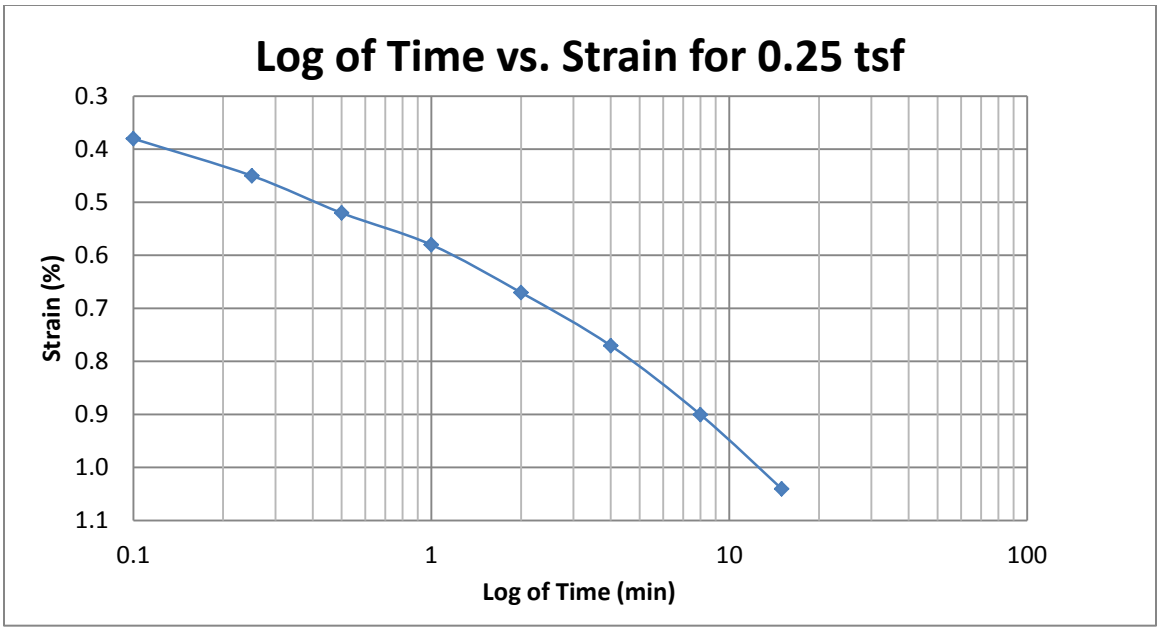

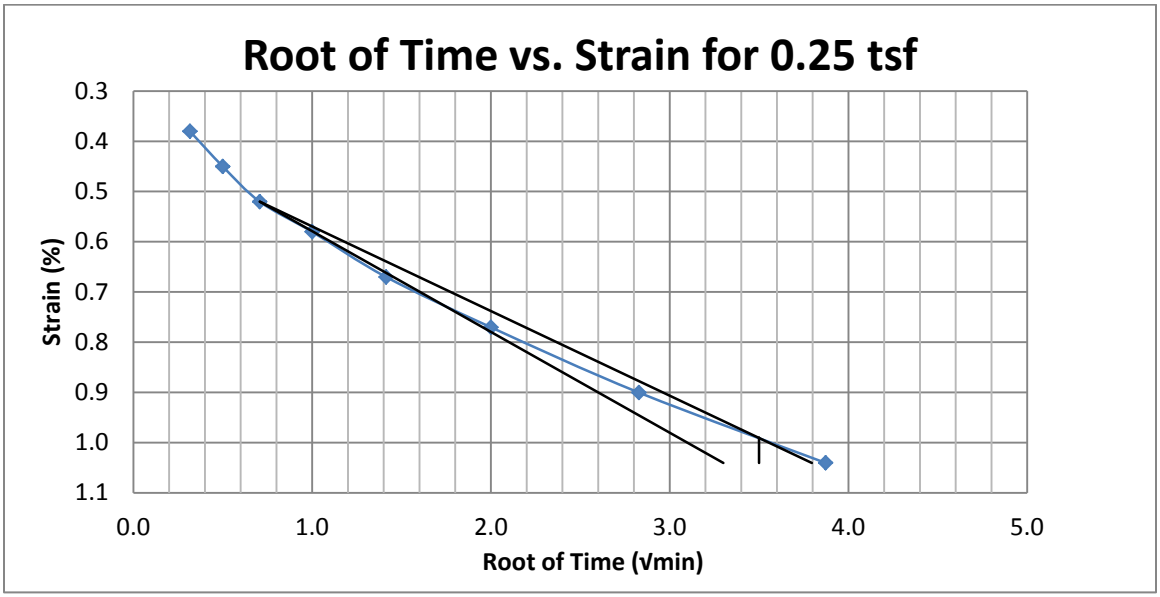

A232 Provo at 80-82 feet

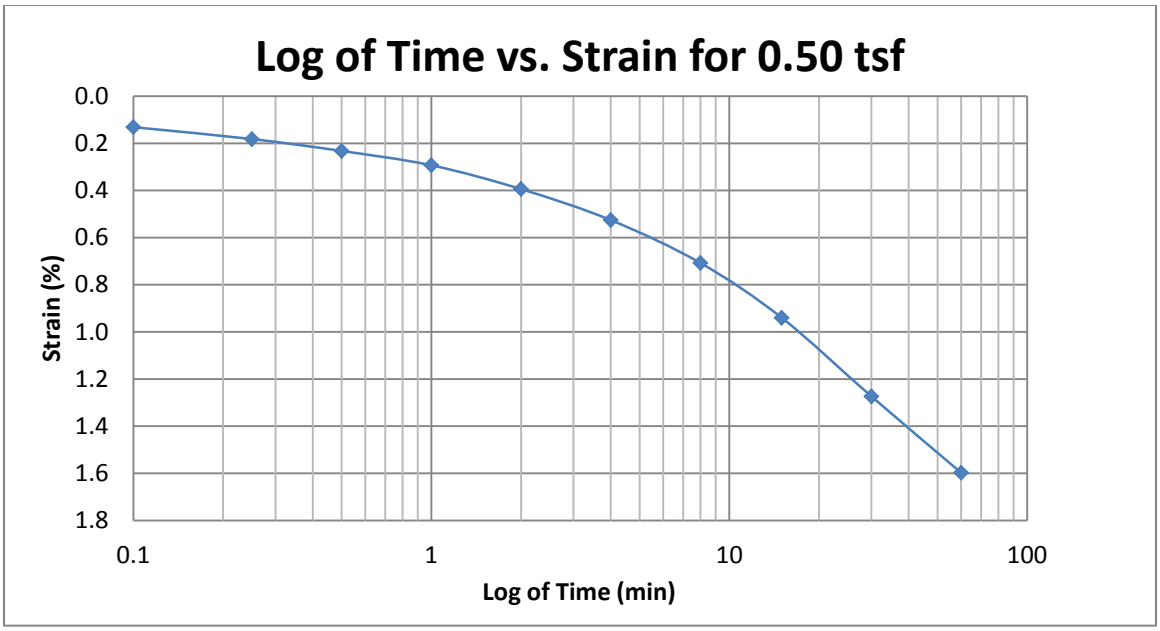

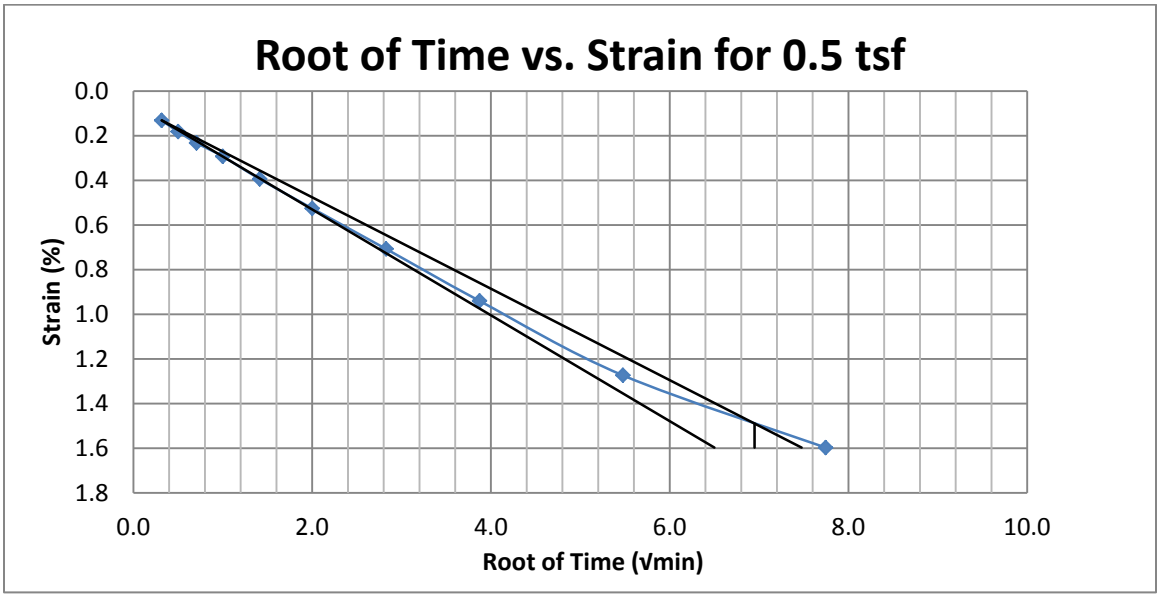

A233 Provo at 80-82 feet

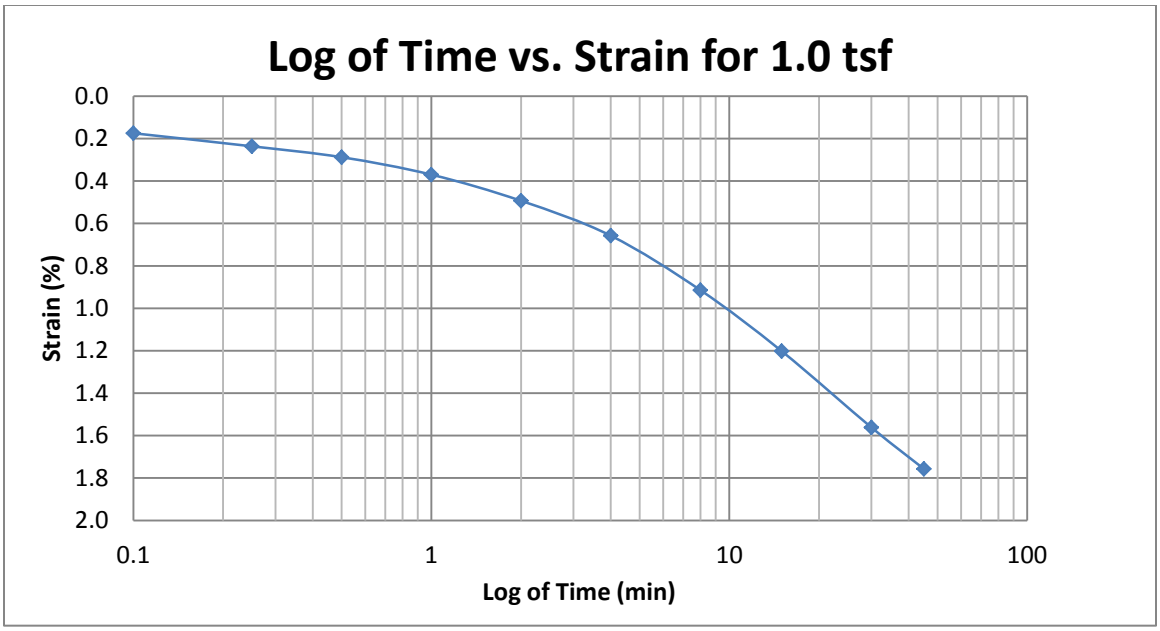

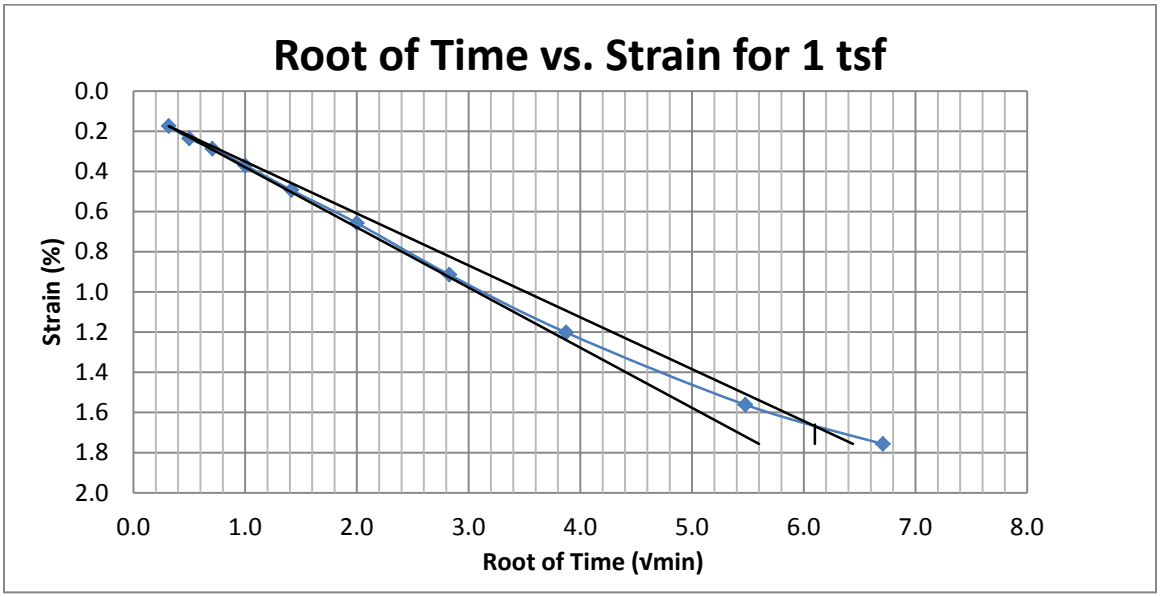

A234 Provo at 80-82 feet

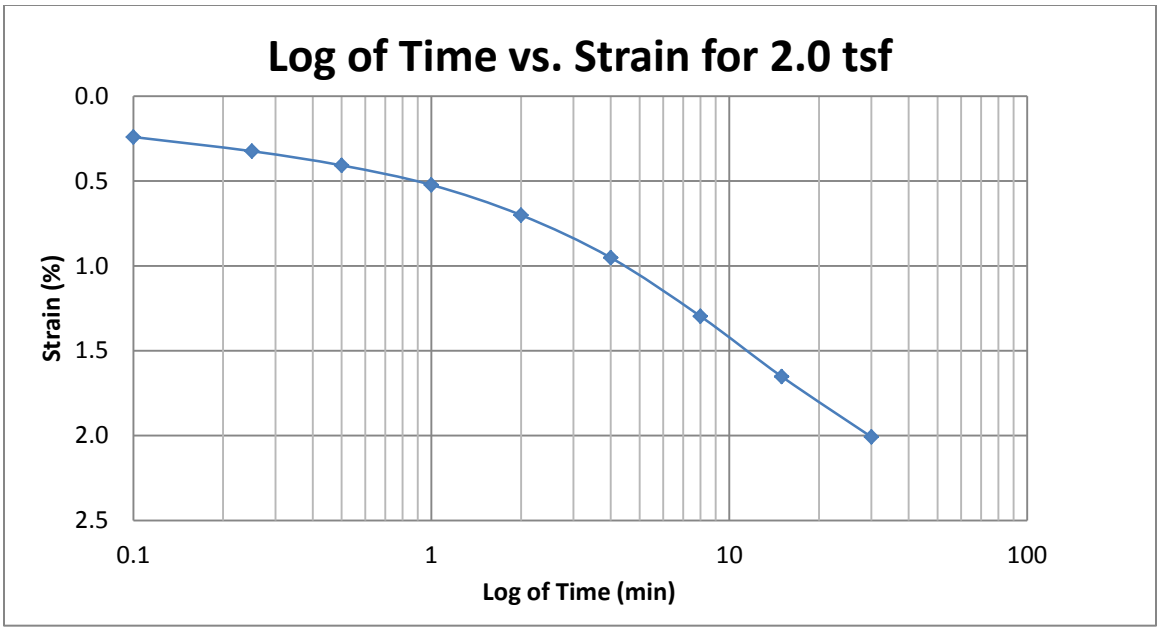

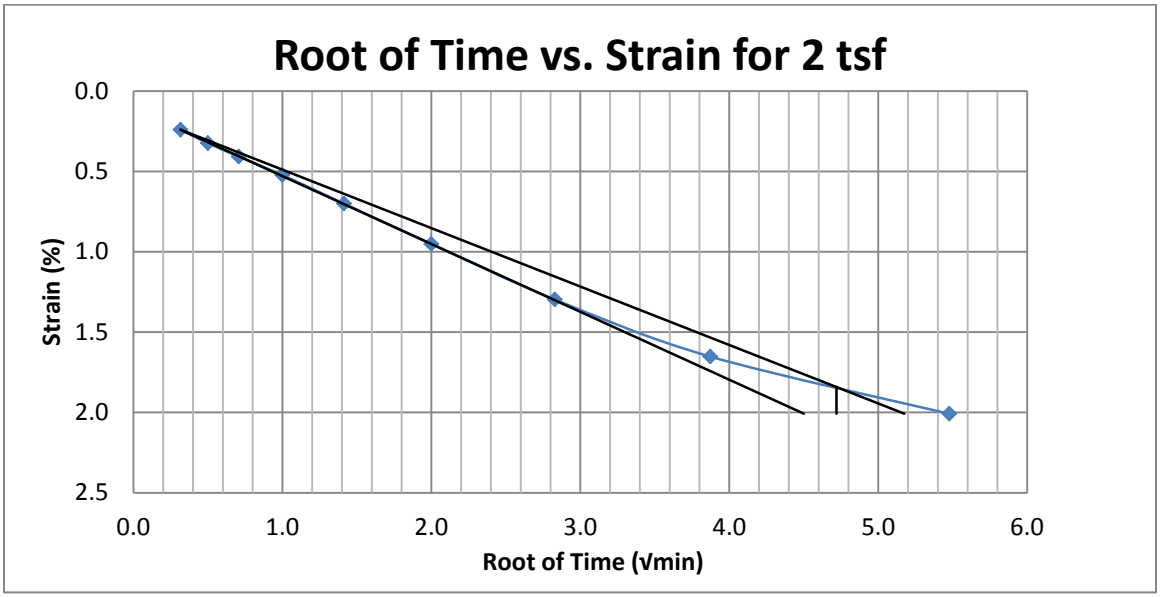

A235 Provo at 80-82 feet

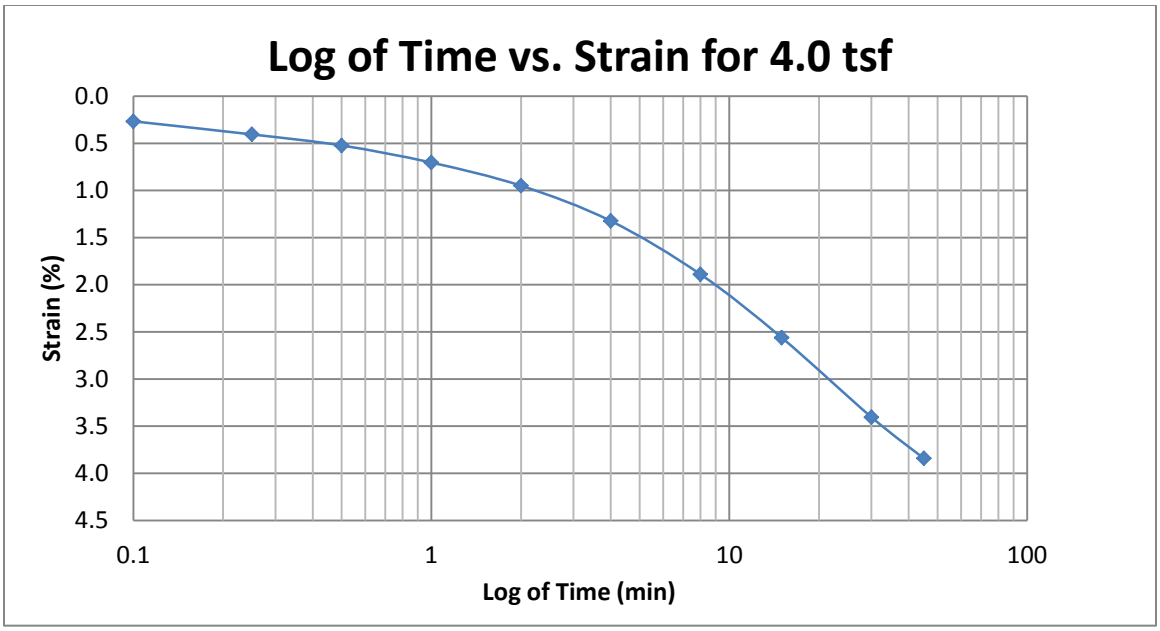

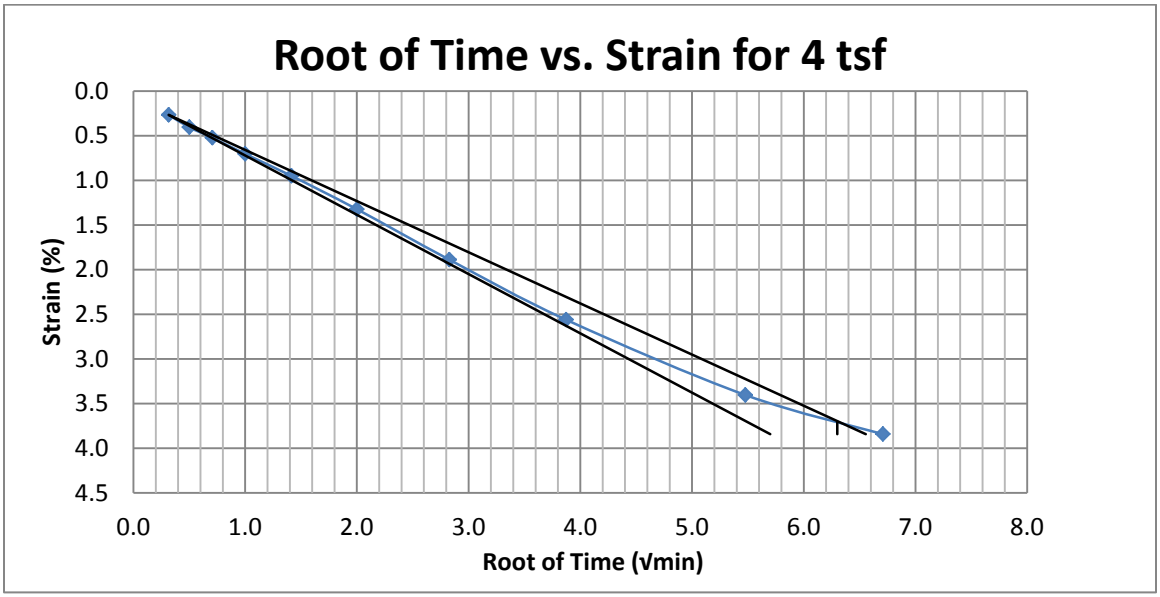

A236 Provo at 80-82 feet

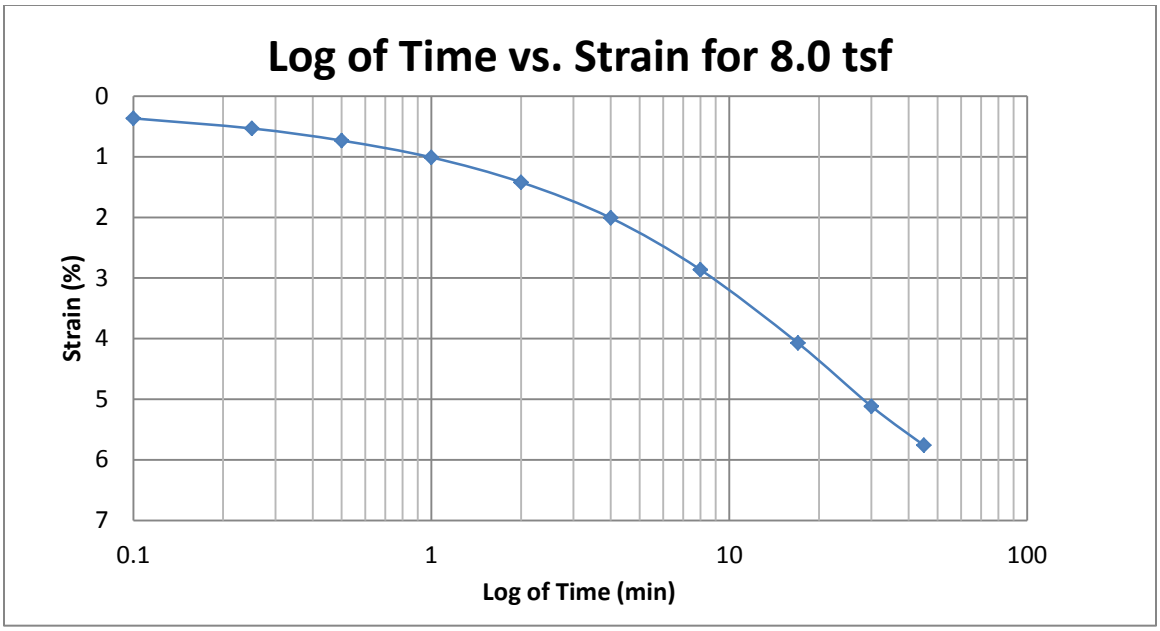

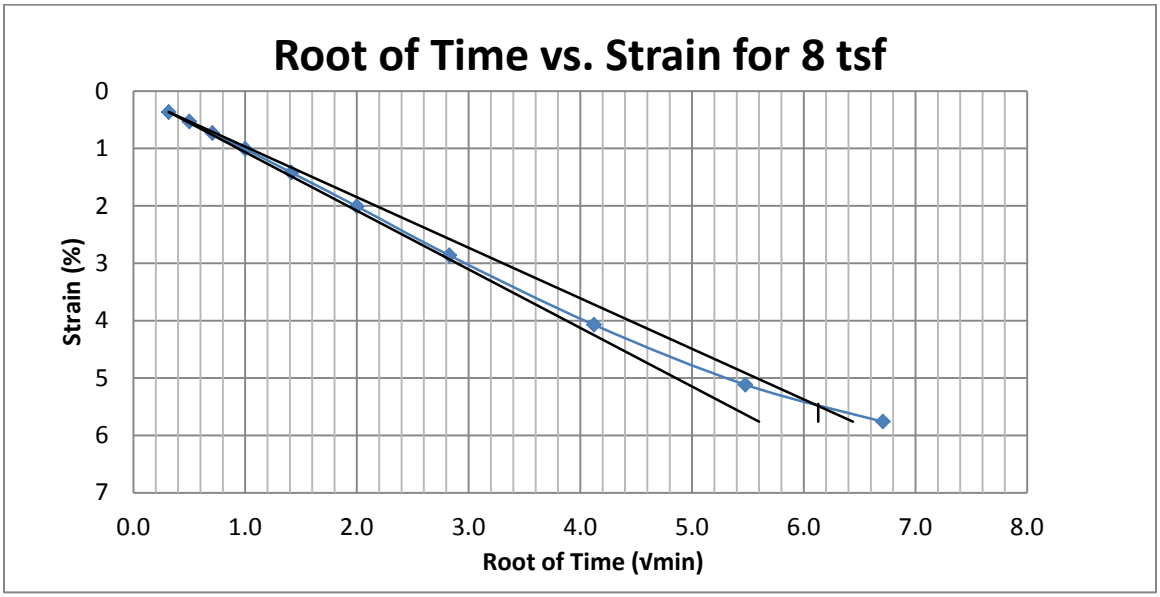

A237 Provo at 80-82 feet

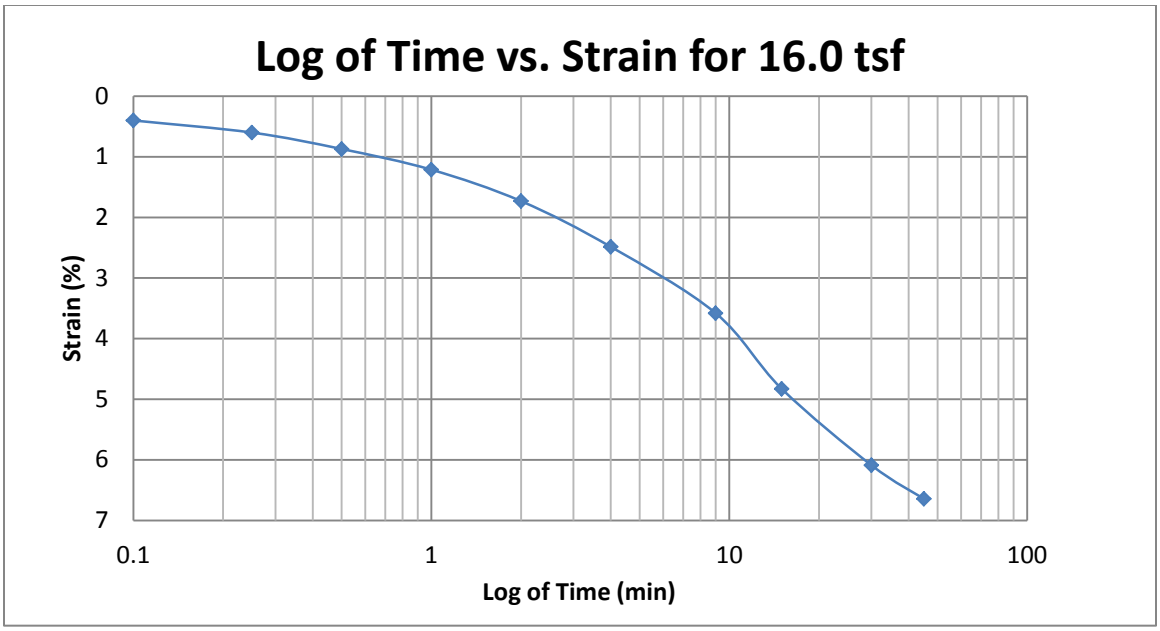

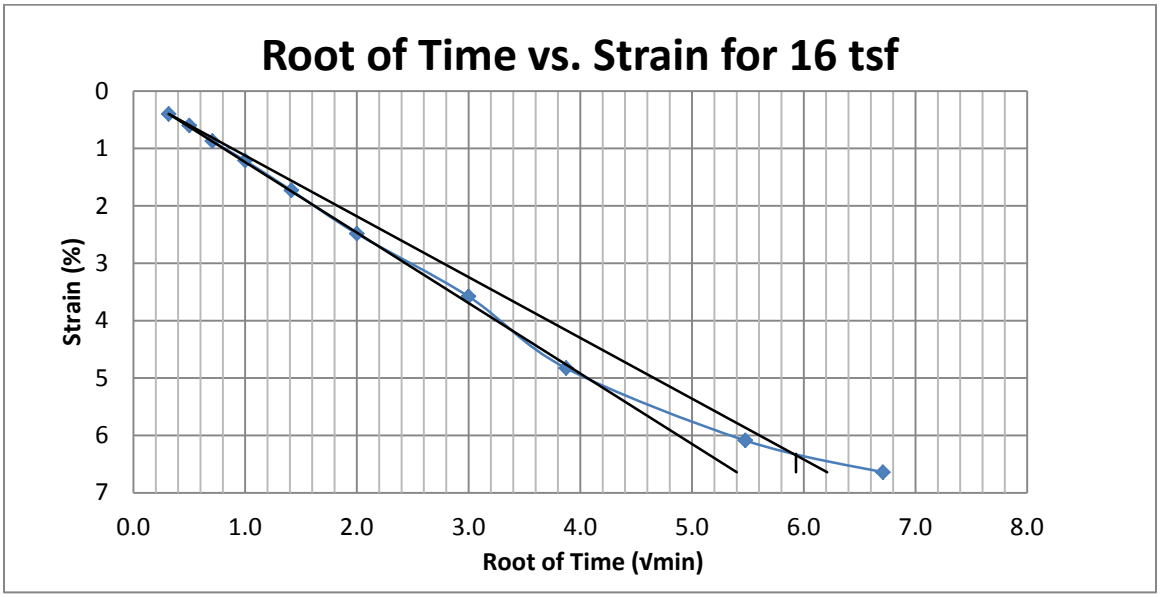

A238 Provo at 80-82 feet

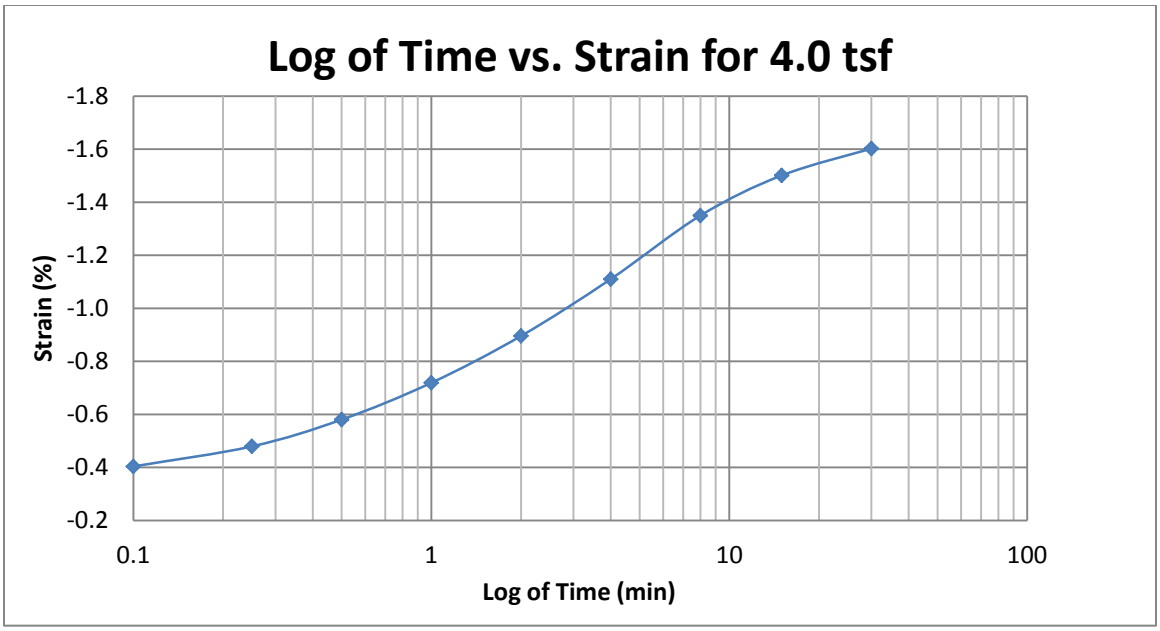

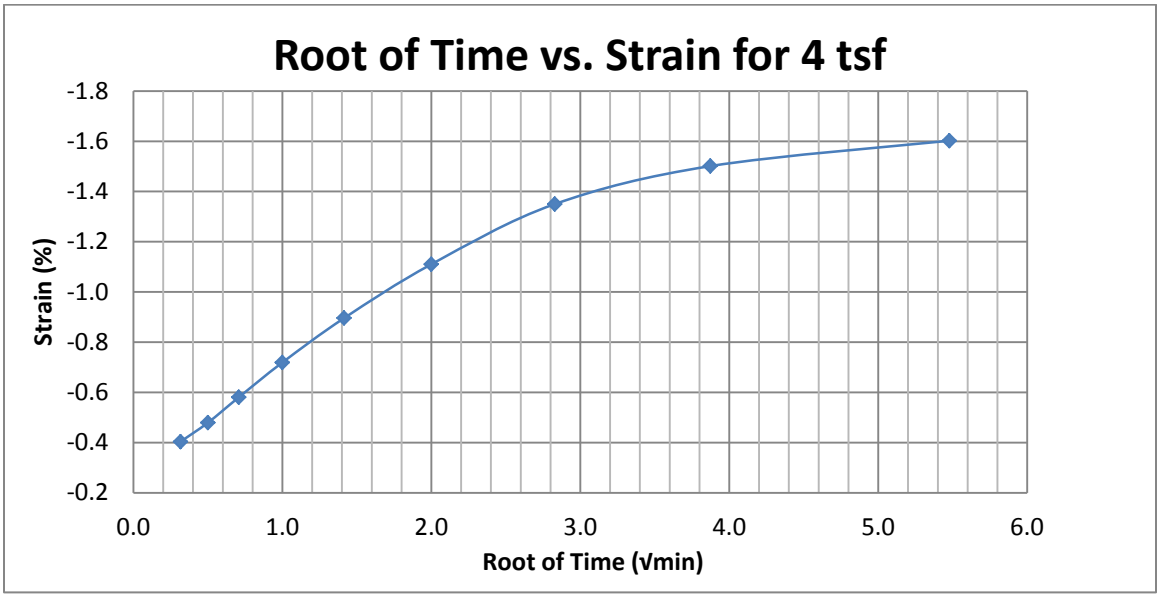

A239 Provo at 80-82 feet

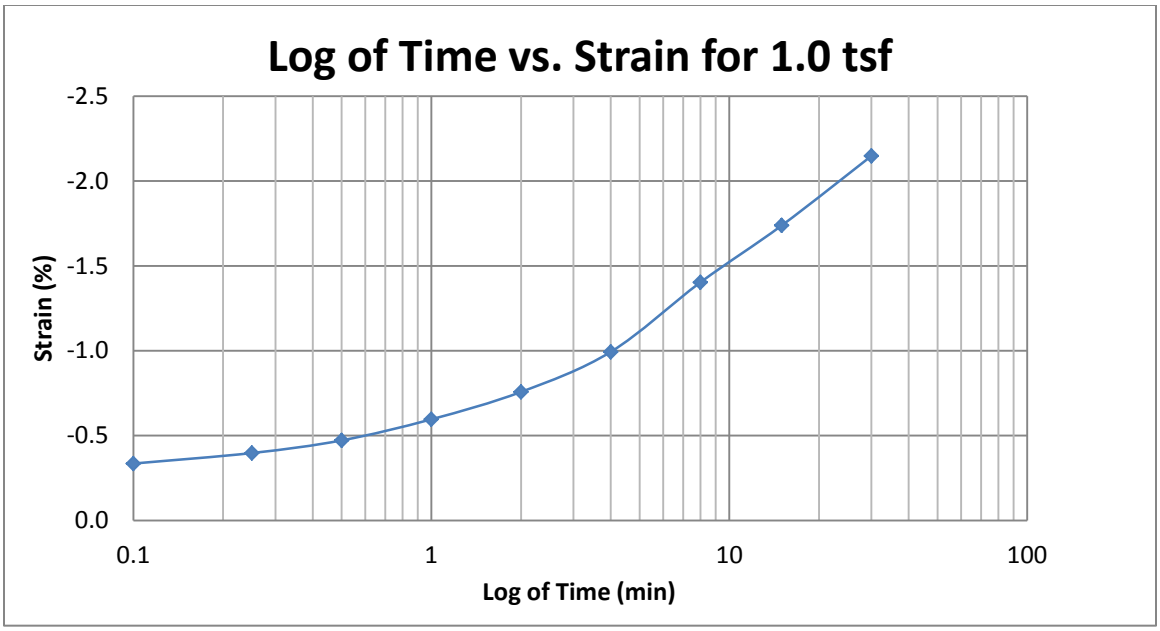

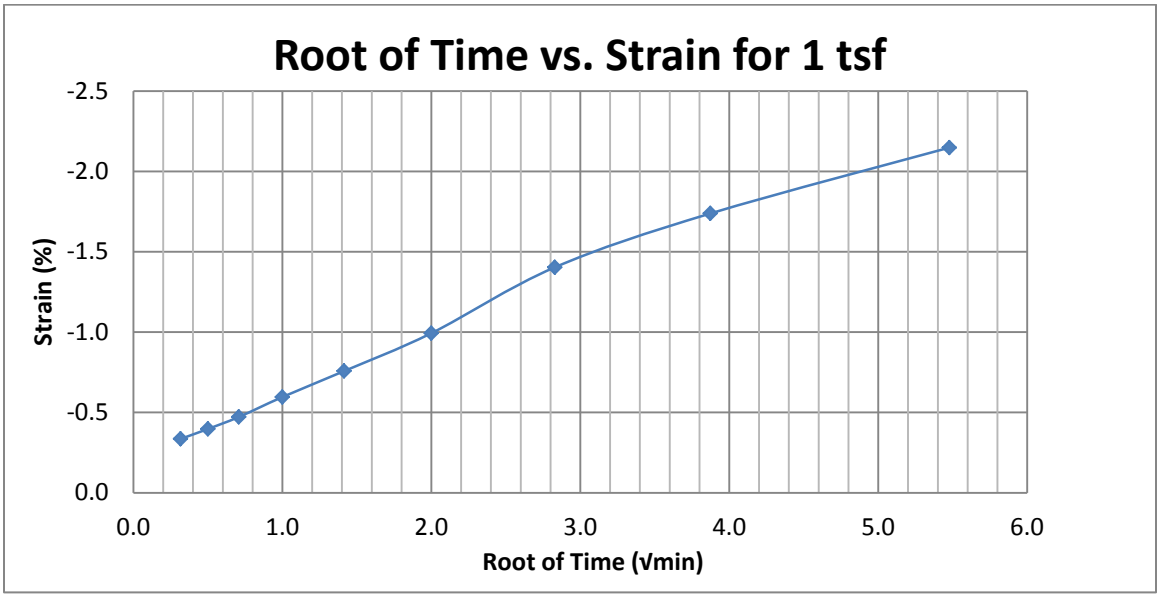

A240 Provo at 80-82 feet

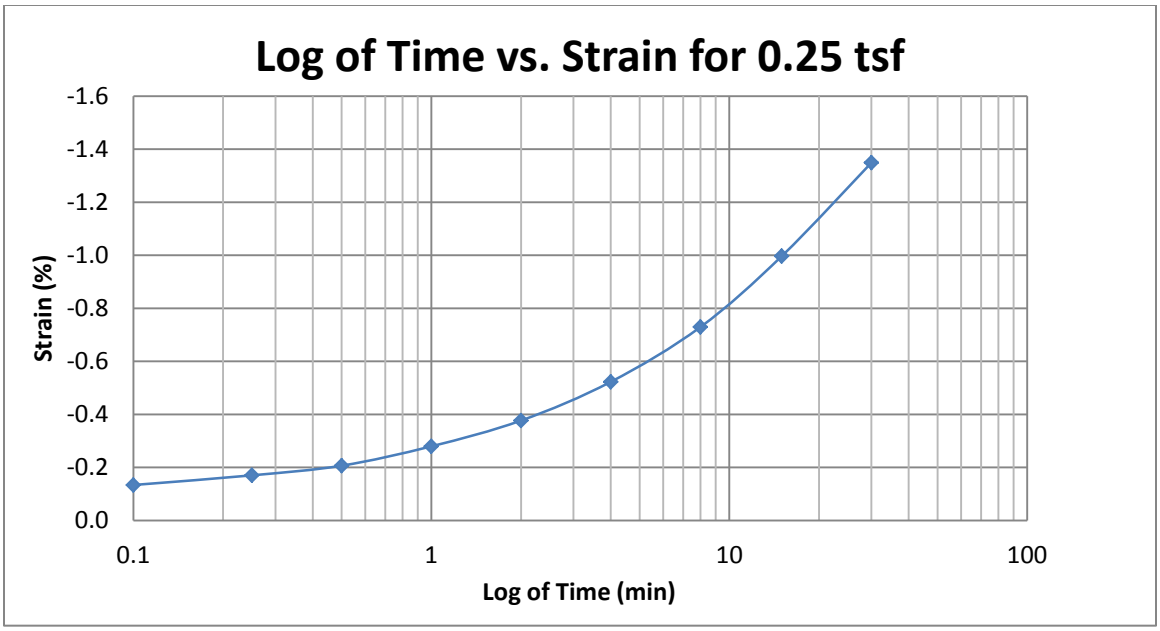

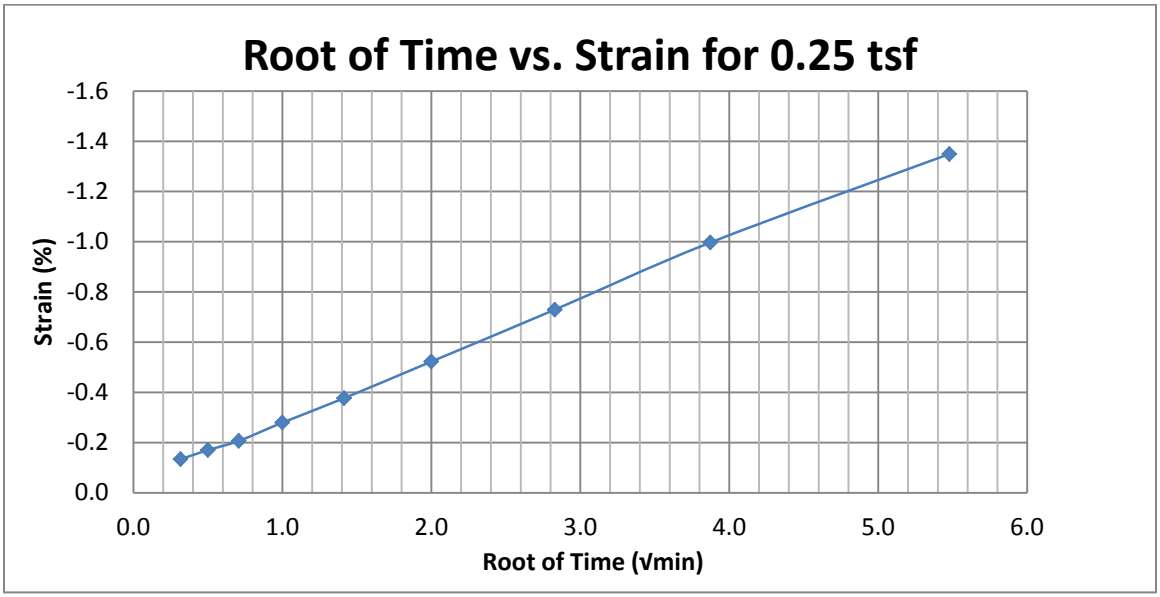

A241 Provo at 80-82 feet

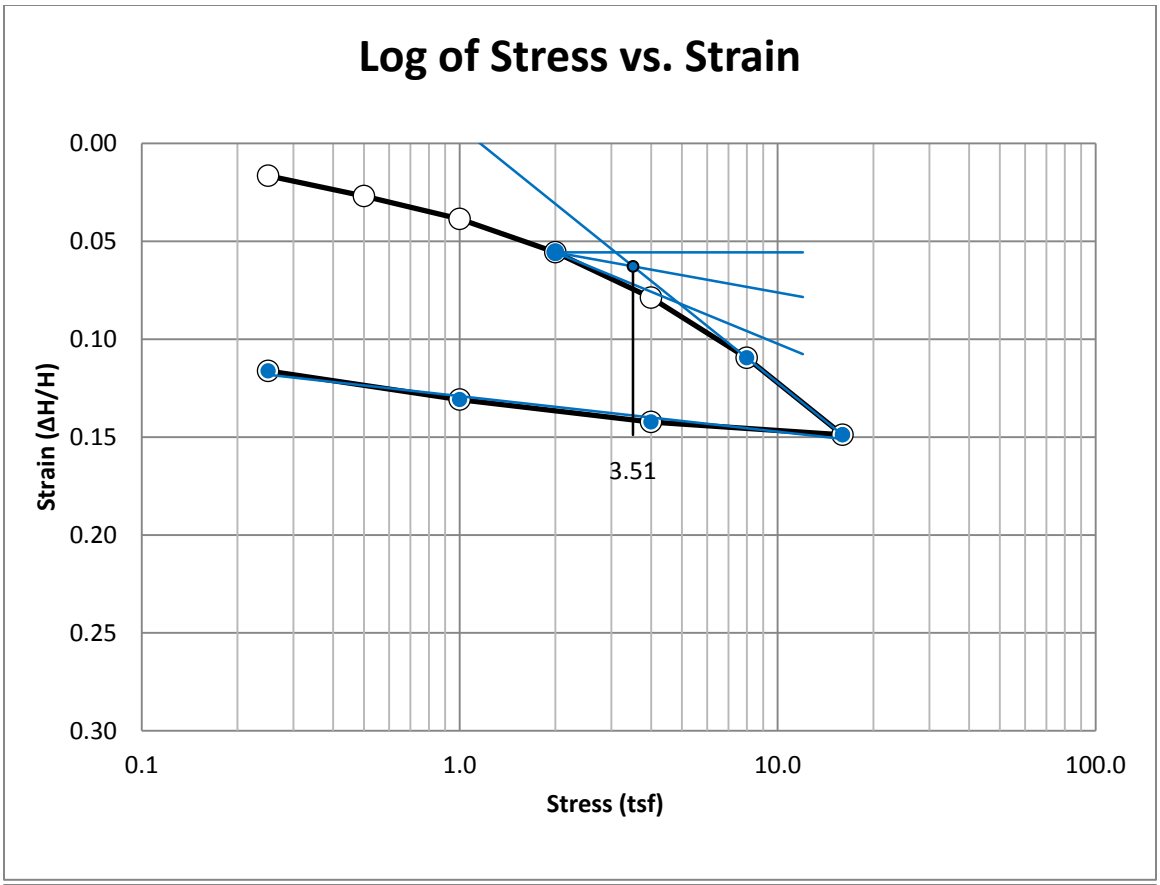

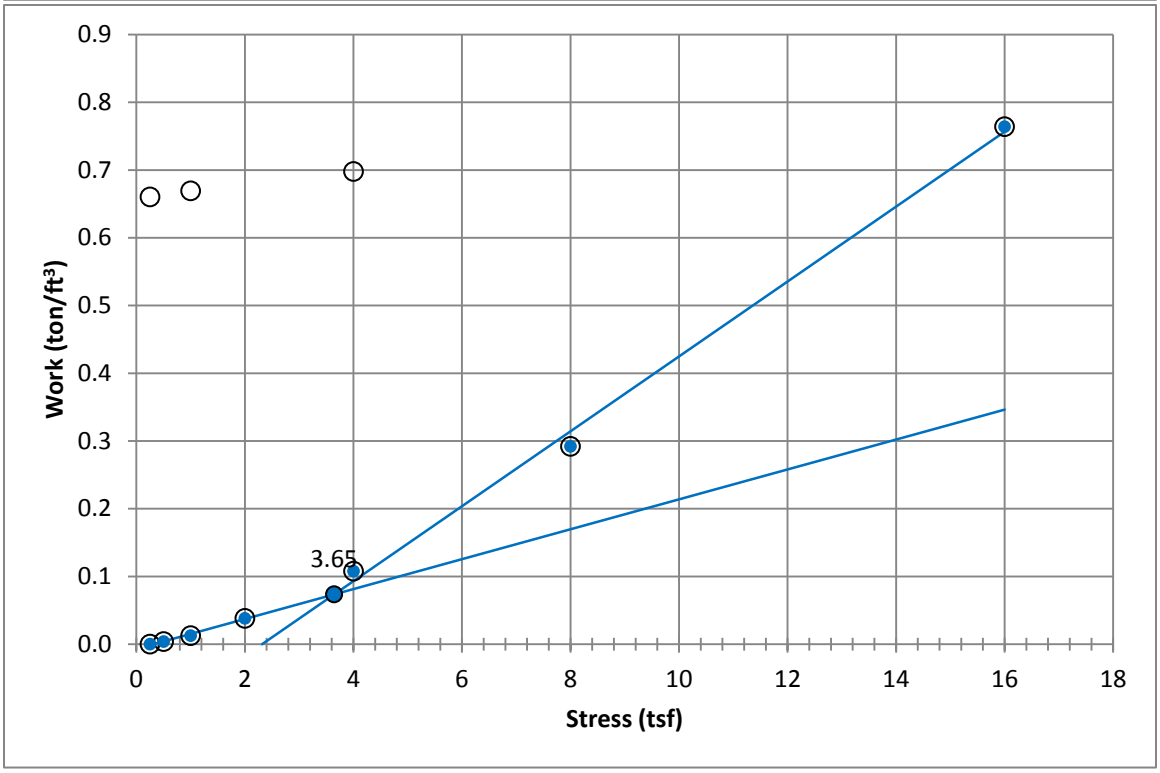

A242 Provo at 90-92 feet

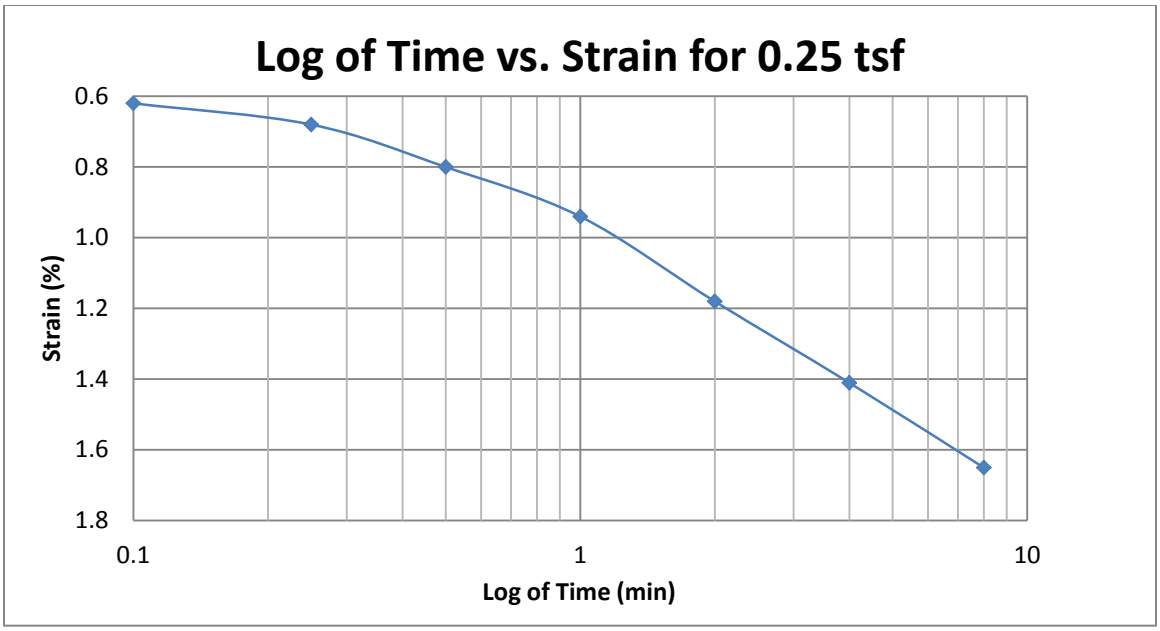

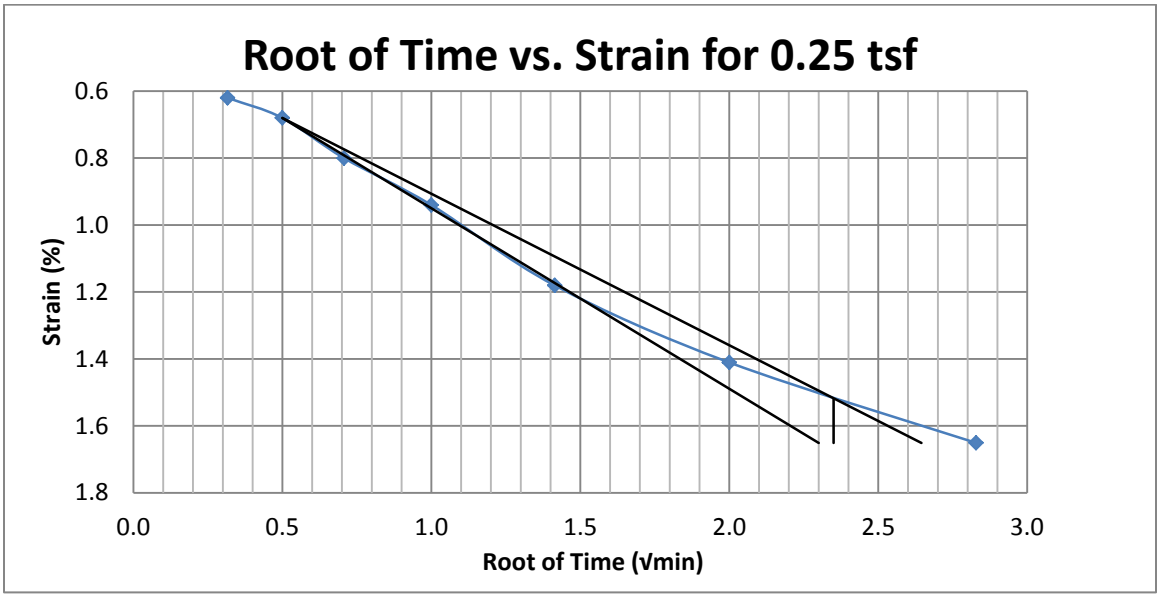

A243 Provo at 90-92 feet

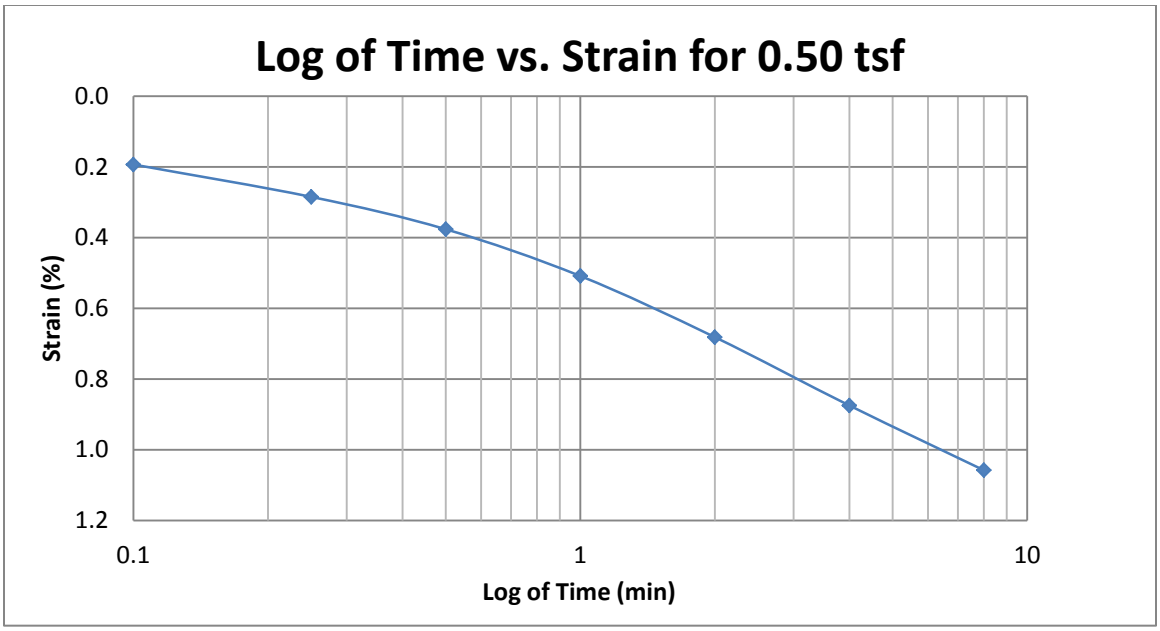

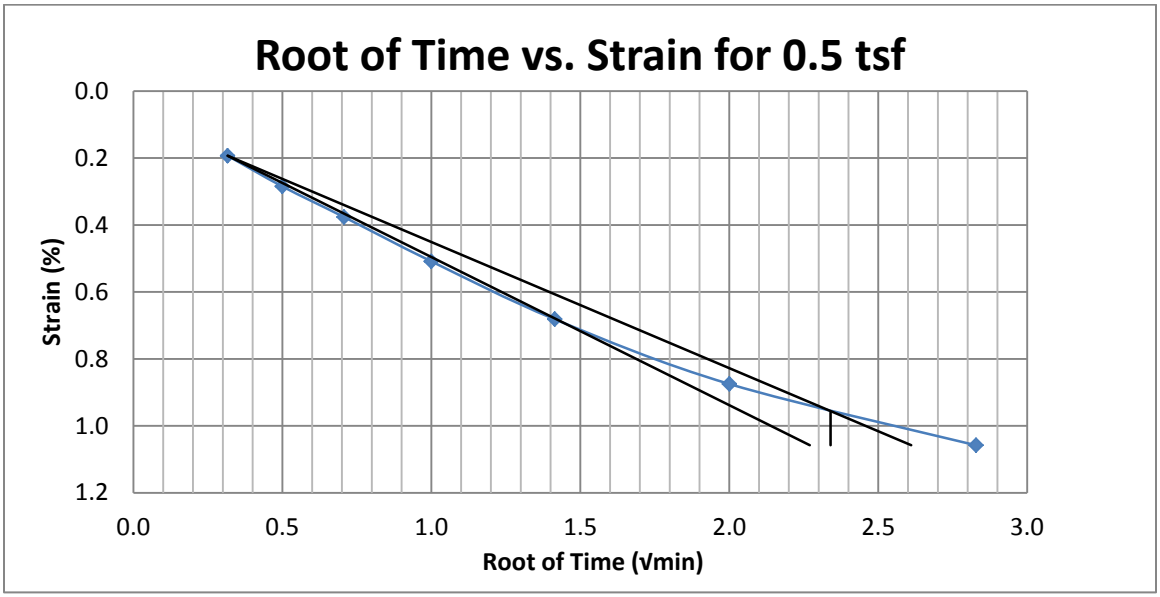

A244 Provo at 90-92 feet

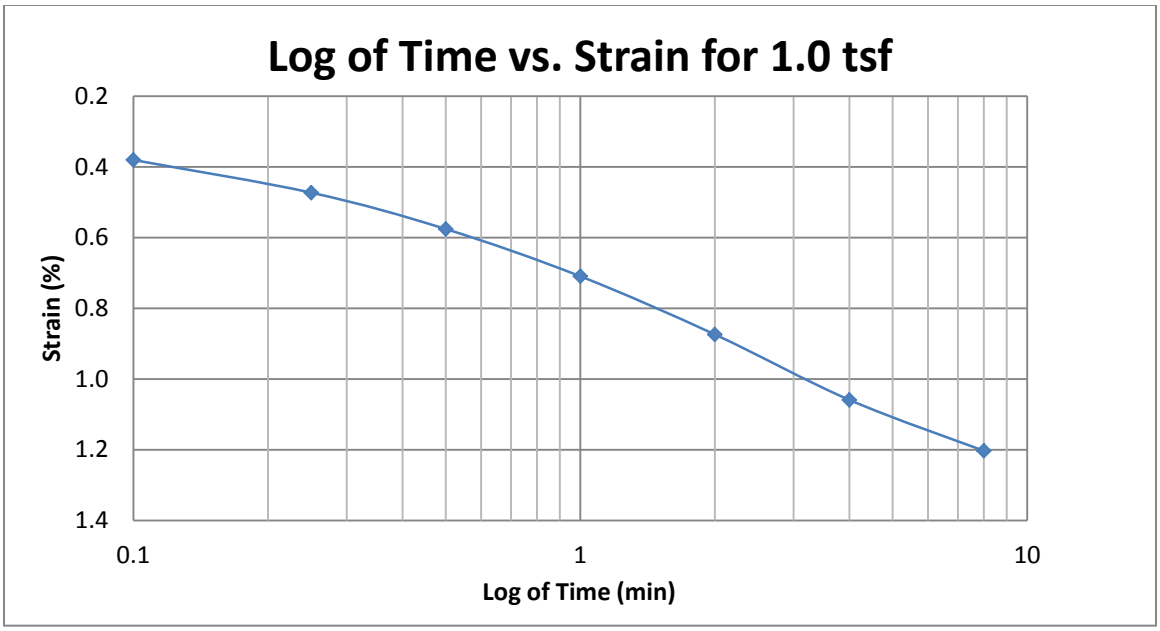

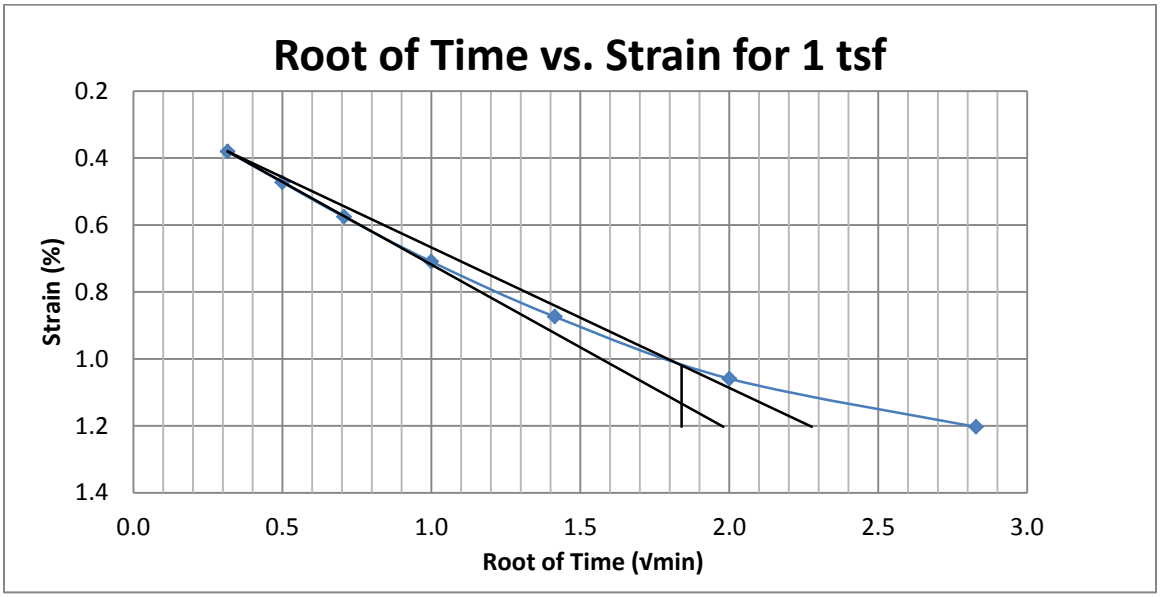

A245 Provo at 90-92 feet

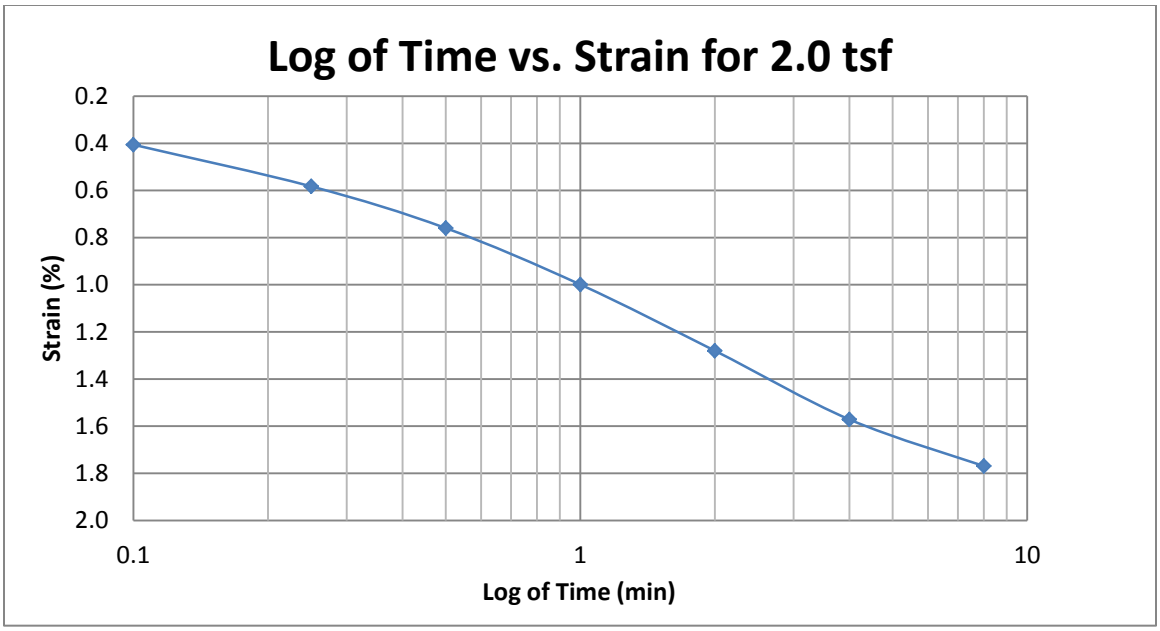

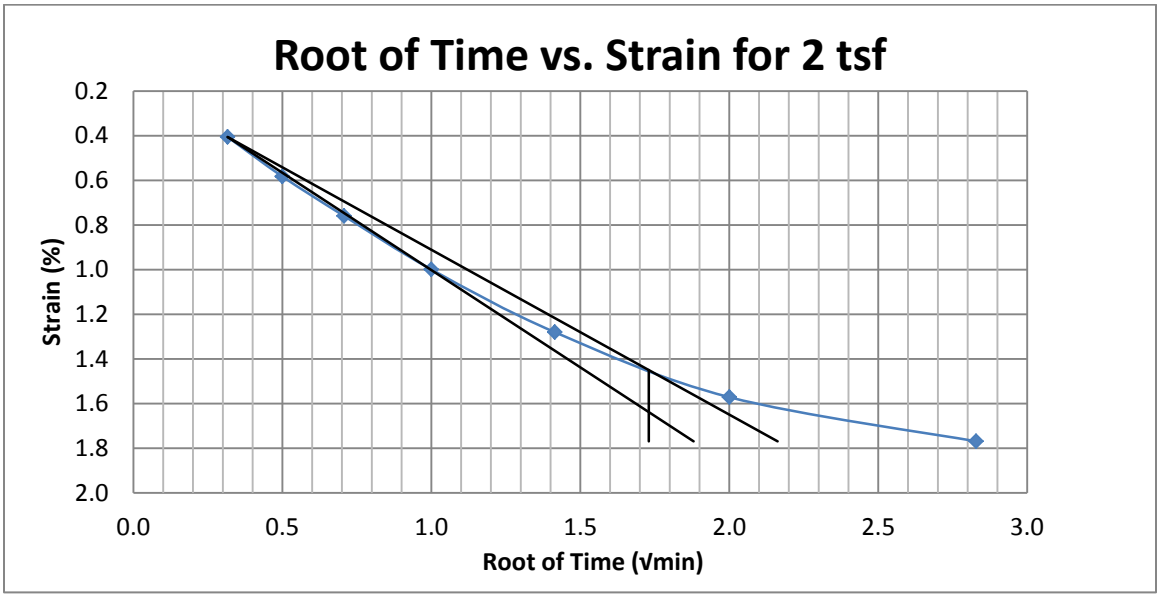

A246 Provo at 90-92 feet

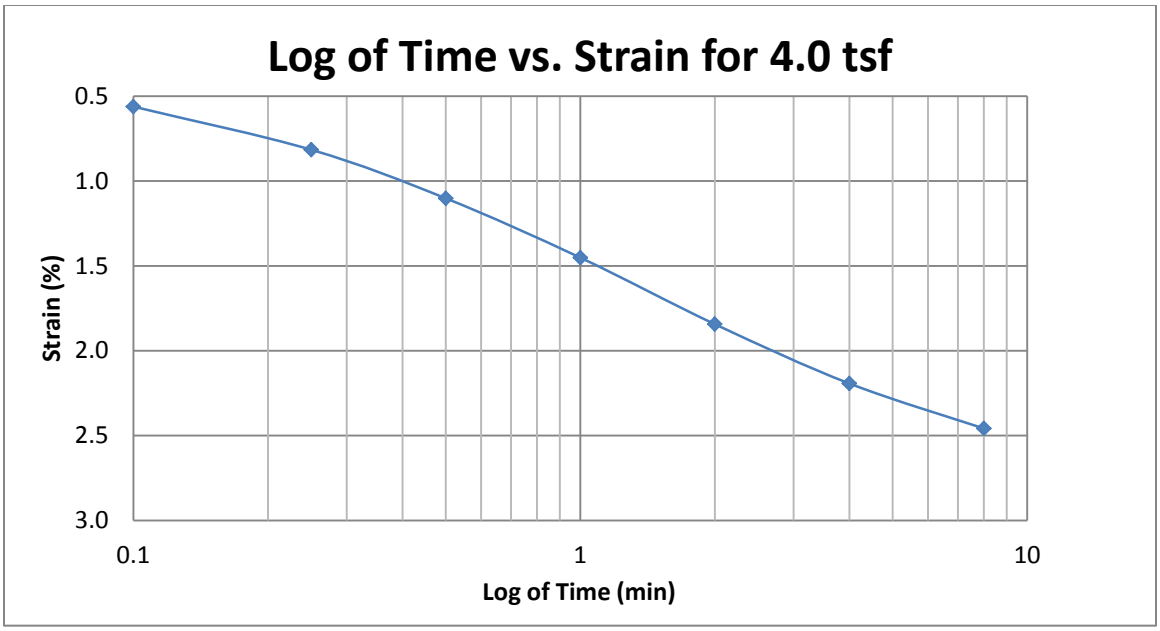

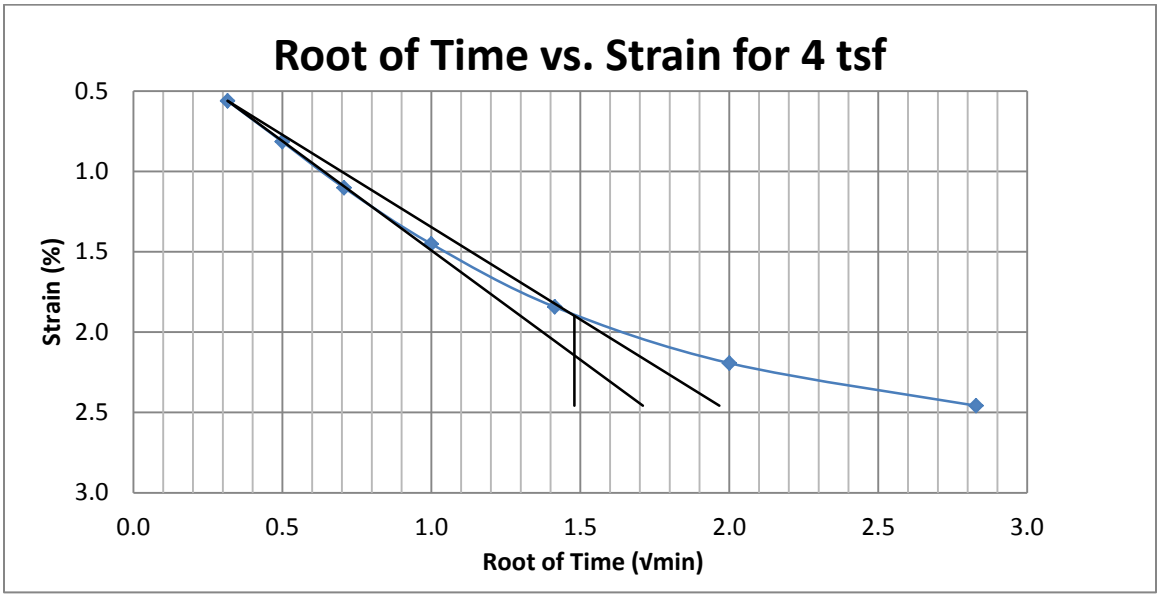

A247 Provo at 90-92 feet

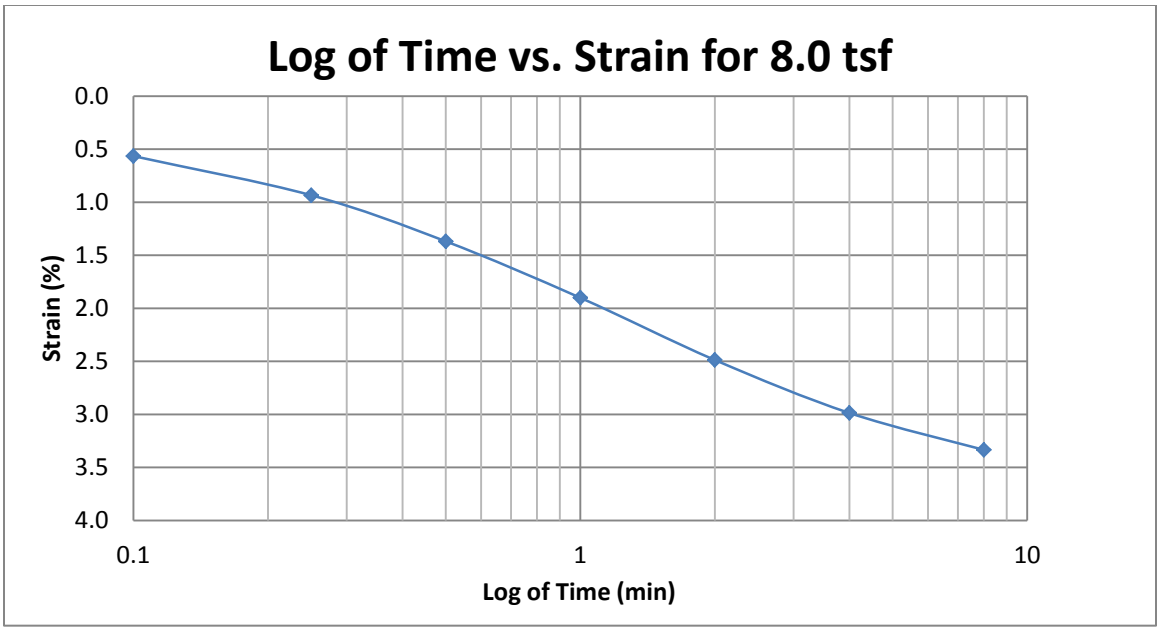

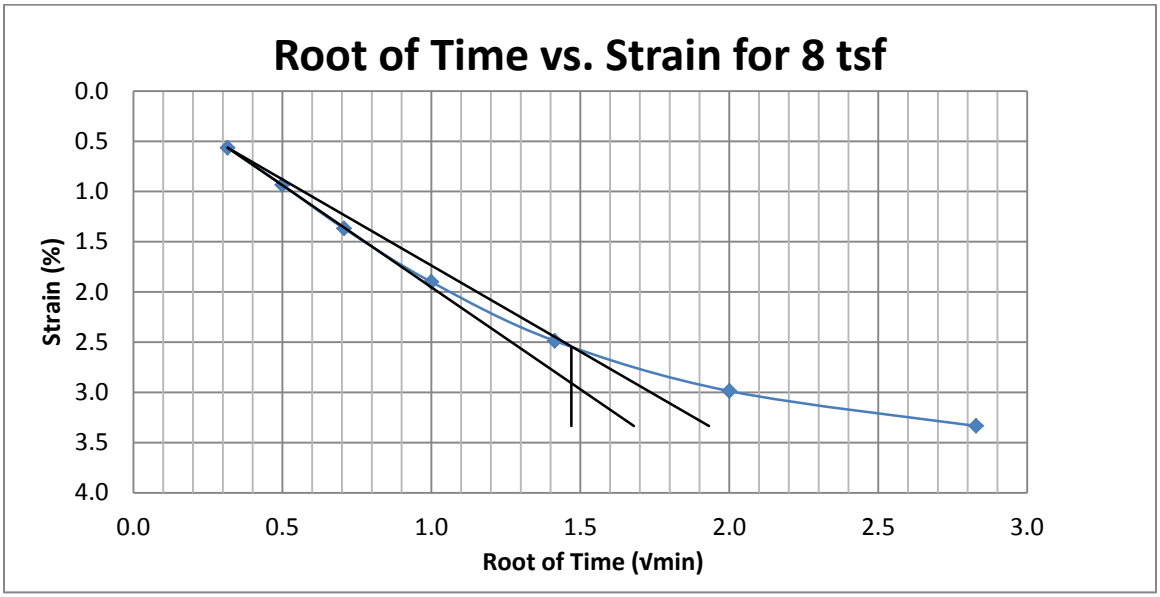

A248 Provo at 90-92 feet

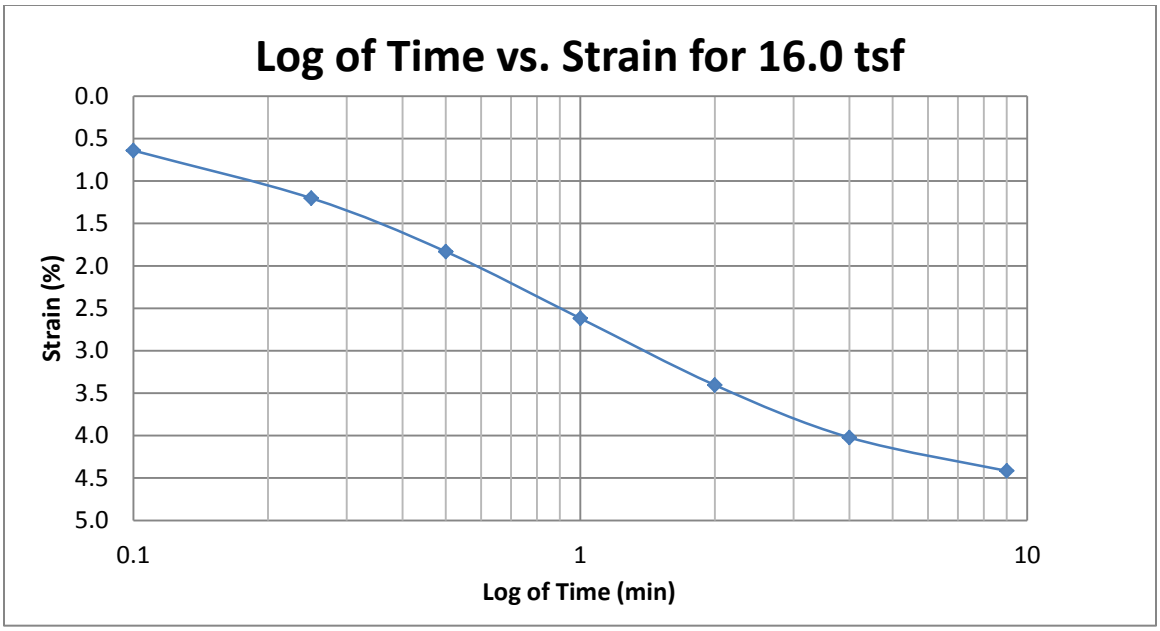

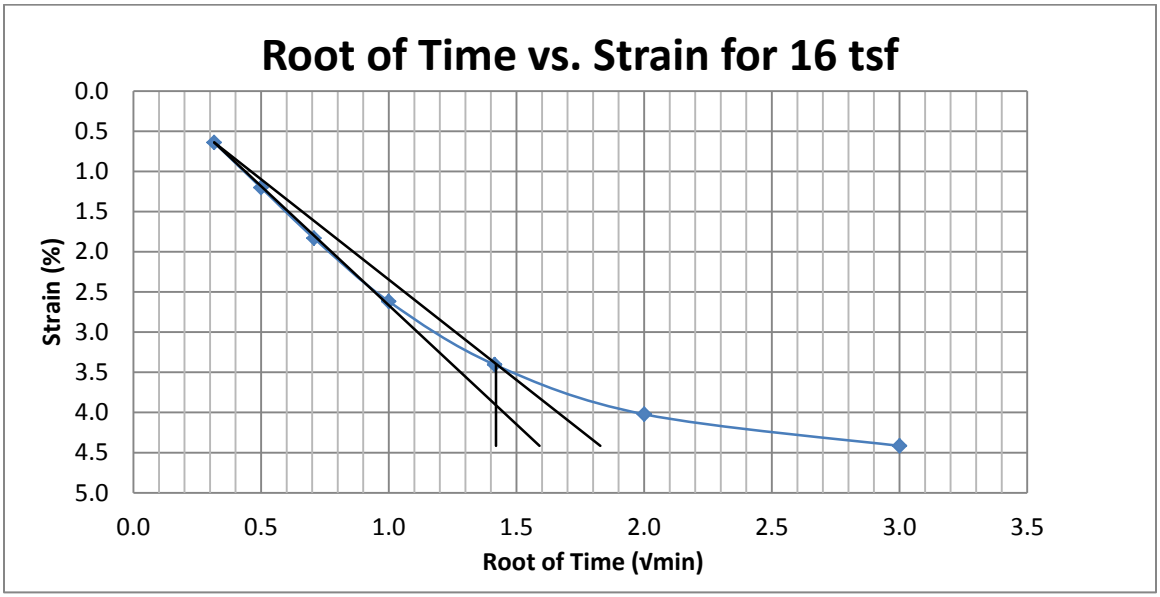

A249 Provo at 90-92 feet

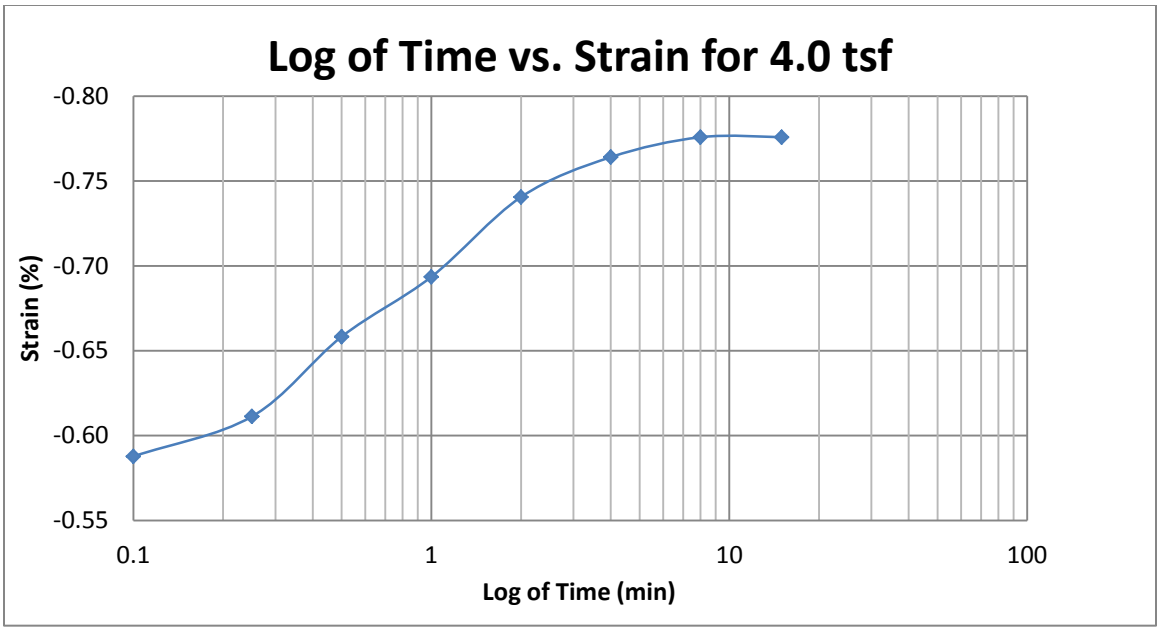

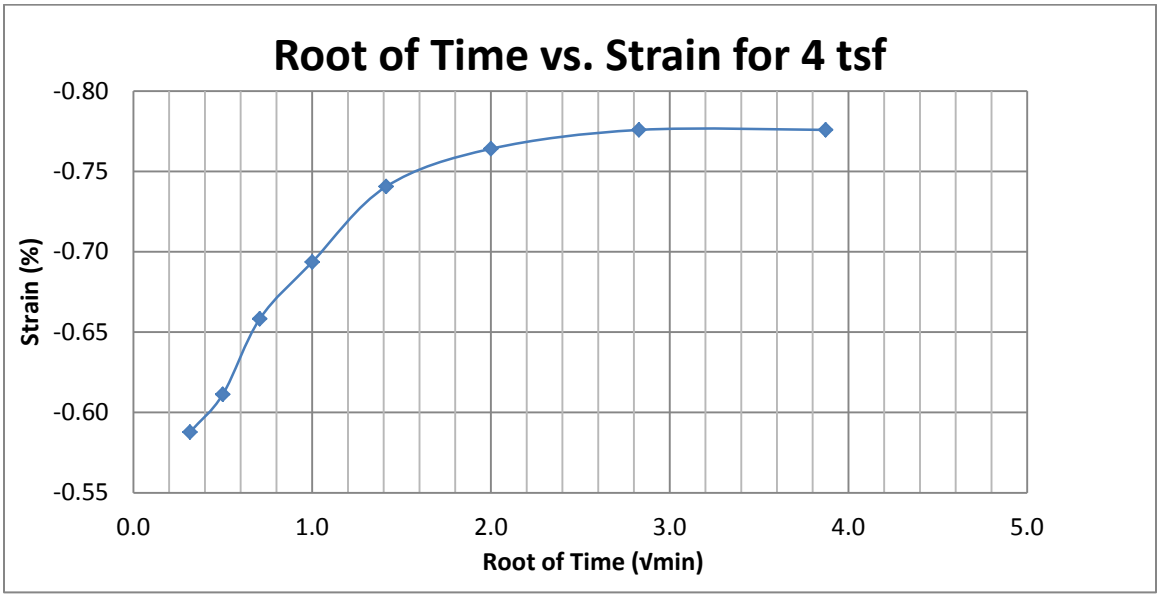

A250 Provo at 90-92 feet

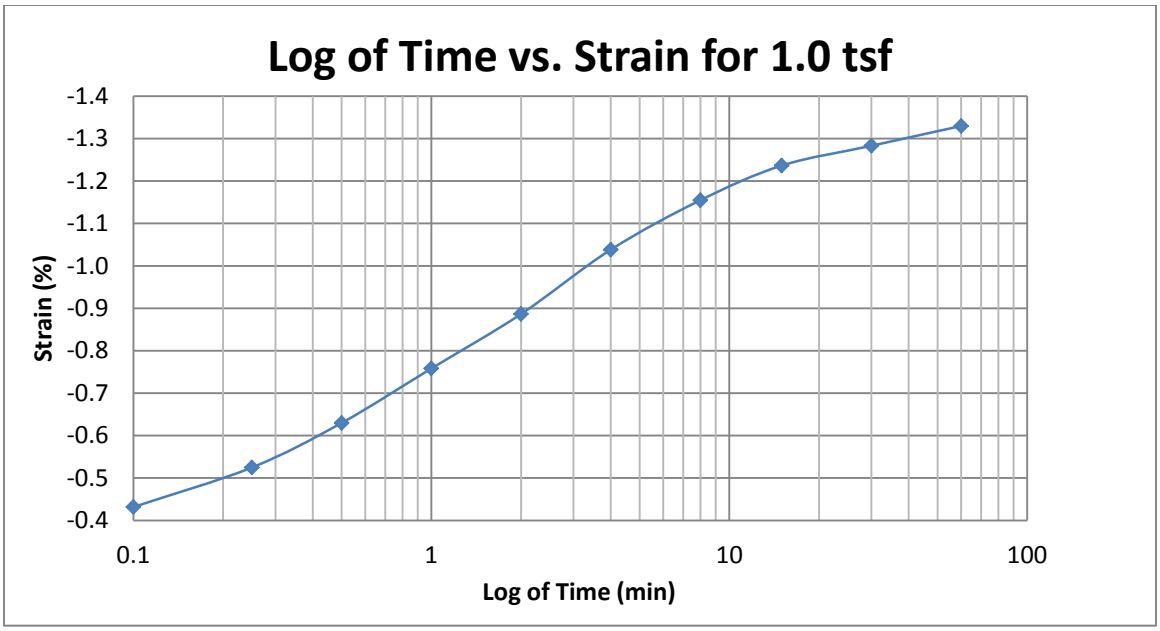

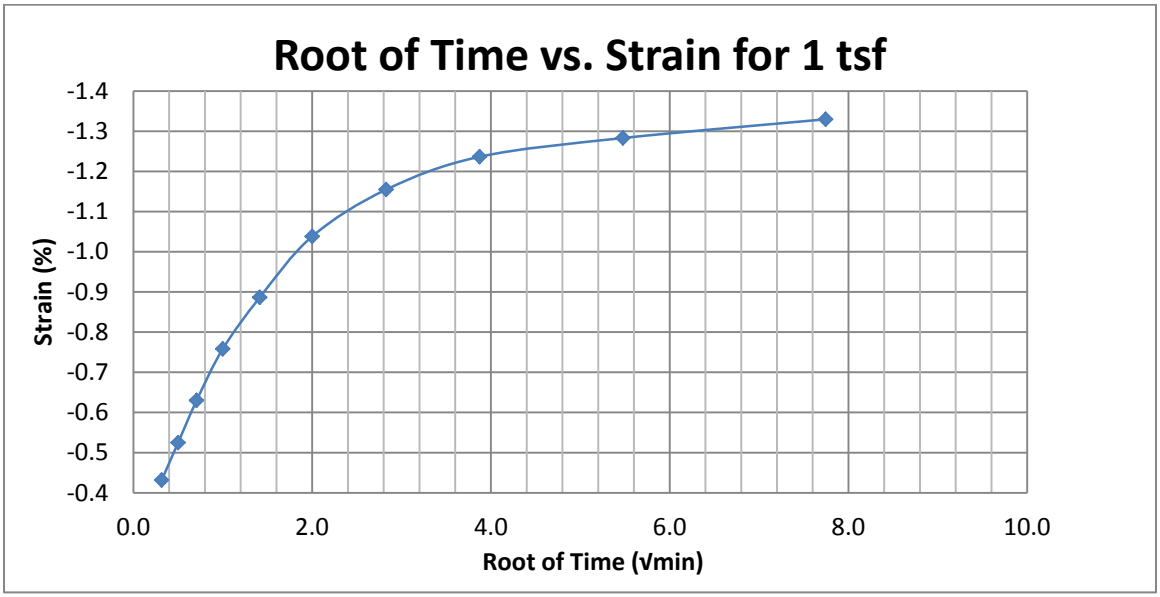

A251 Provo at 90-92 feet

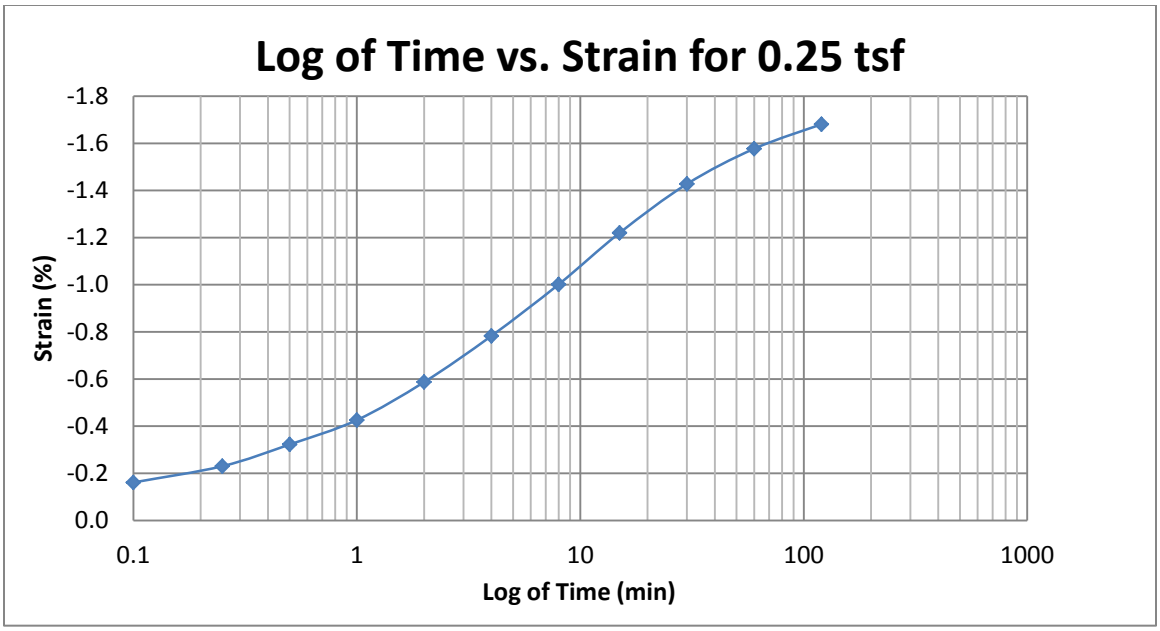

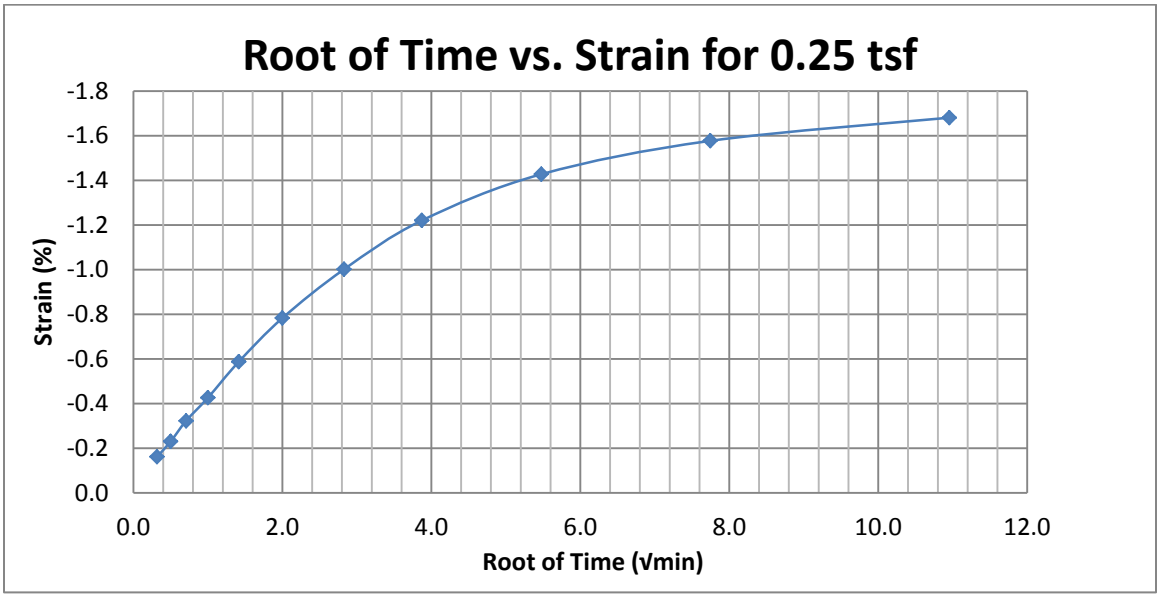

A252 Provo at 90-92 feet

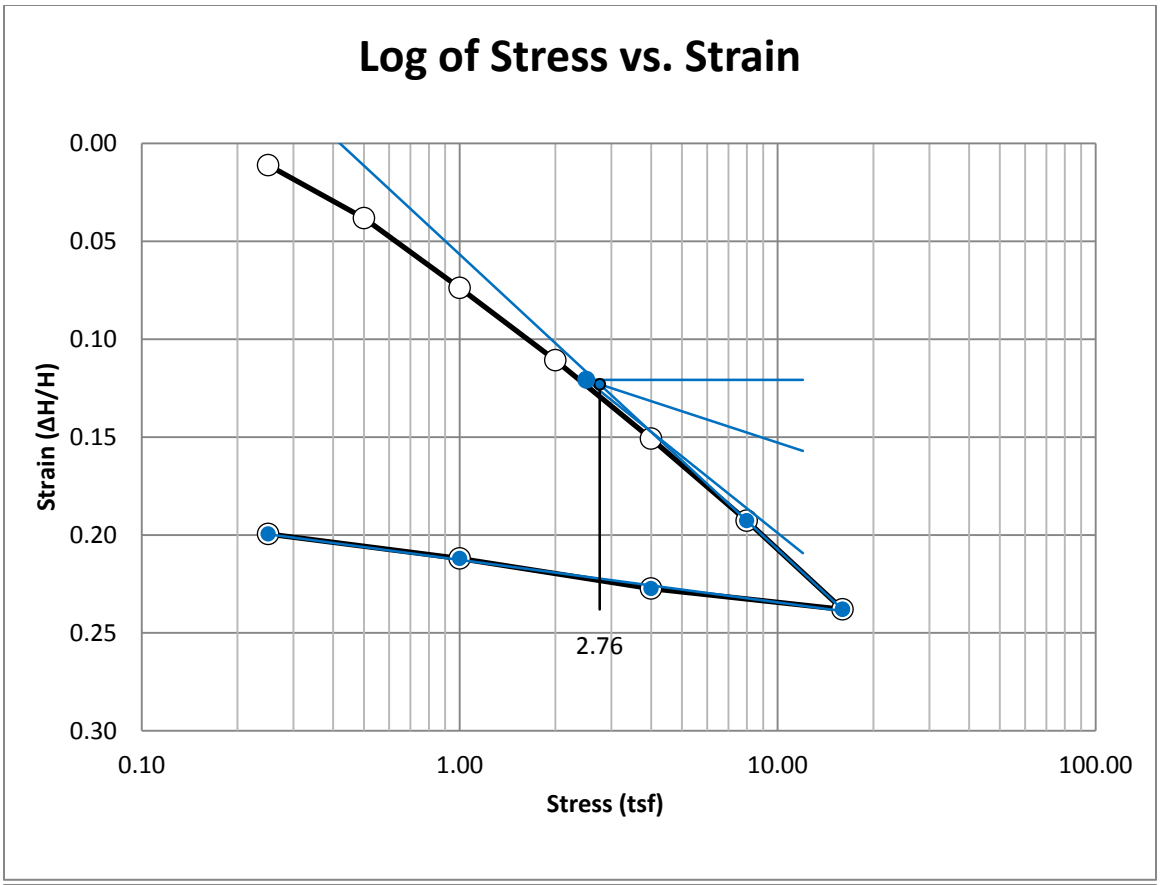

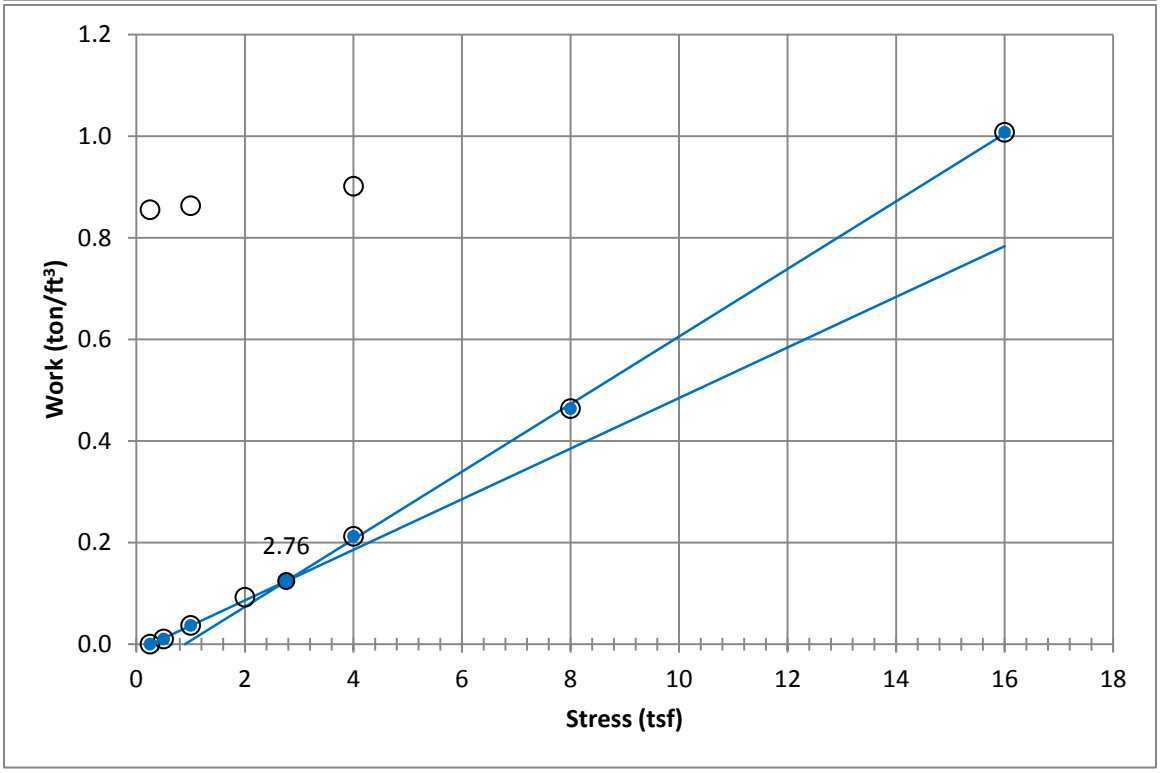

A253 Provo at 110-112 feet

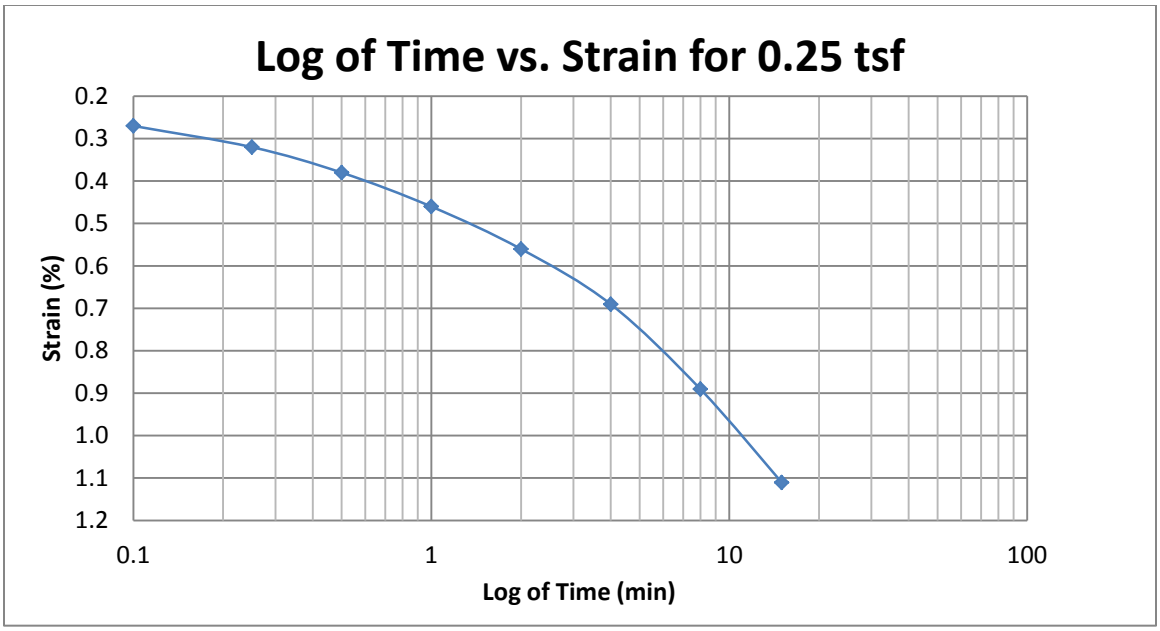

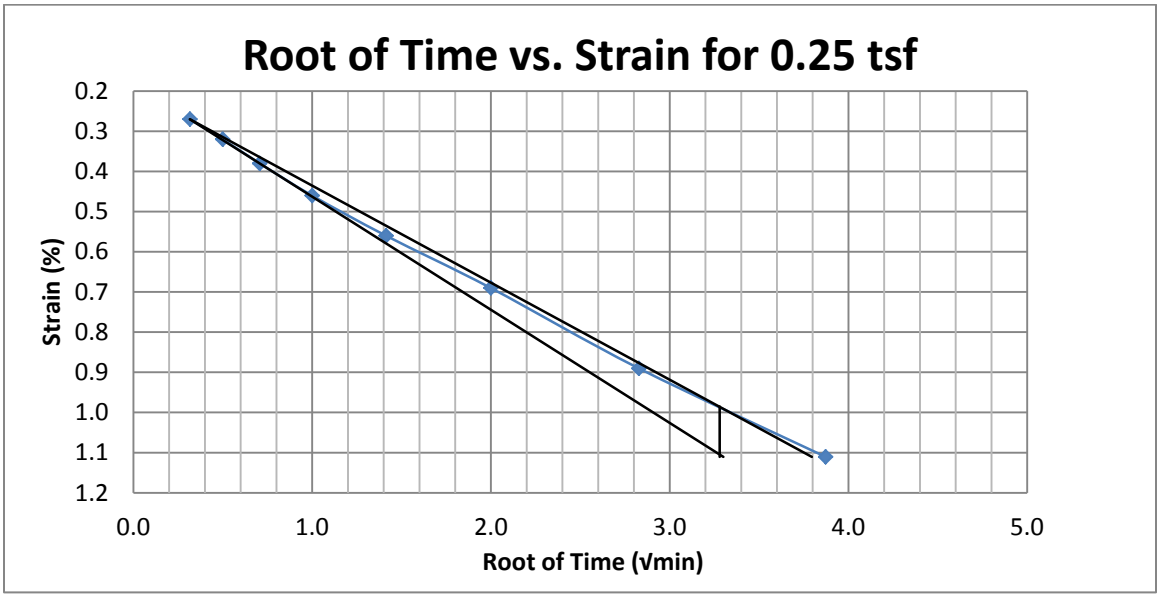

A254 Provo at 110-112 feet

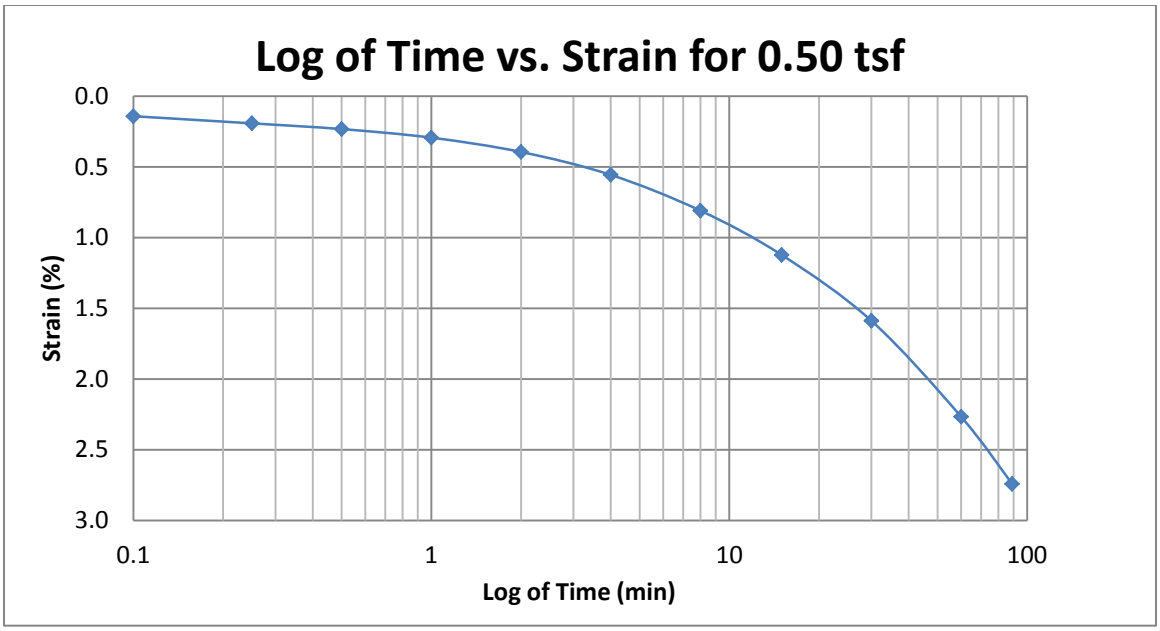

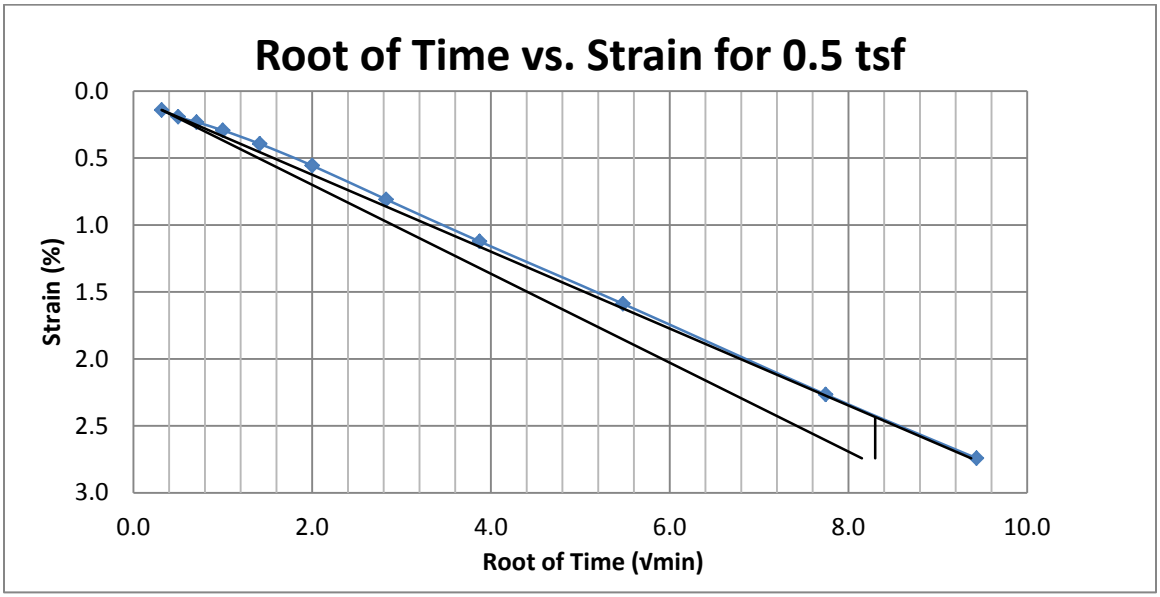

A255 Provo at 110-112 feet

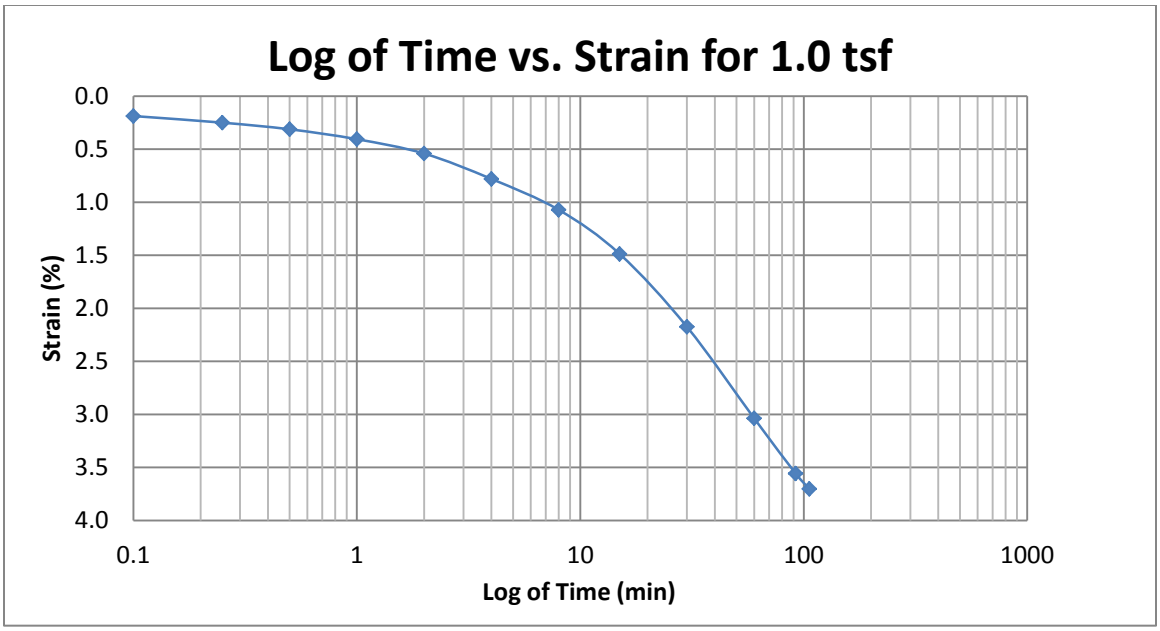

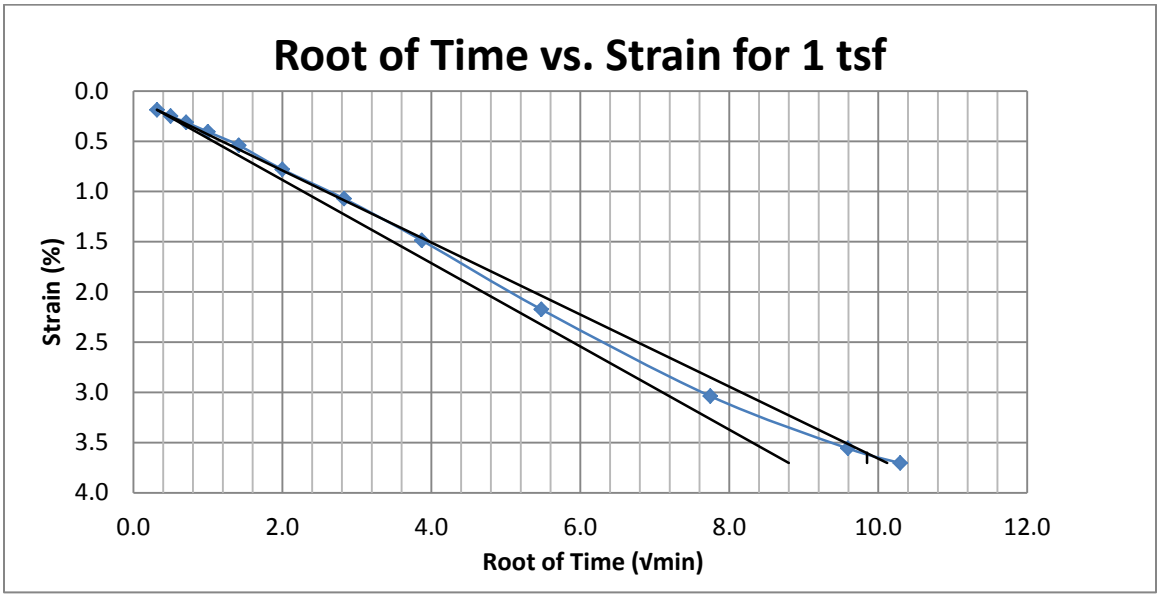

A256 Provo at 110-112 feet

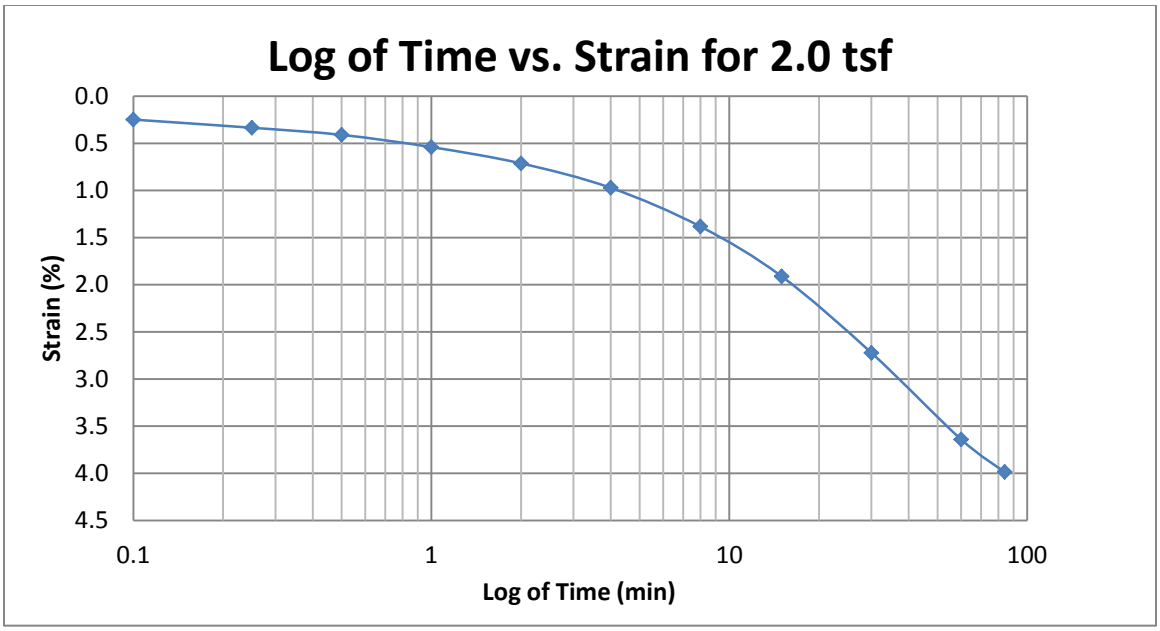

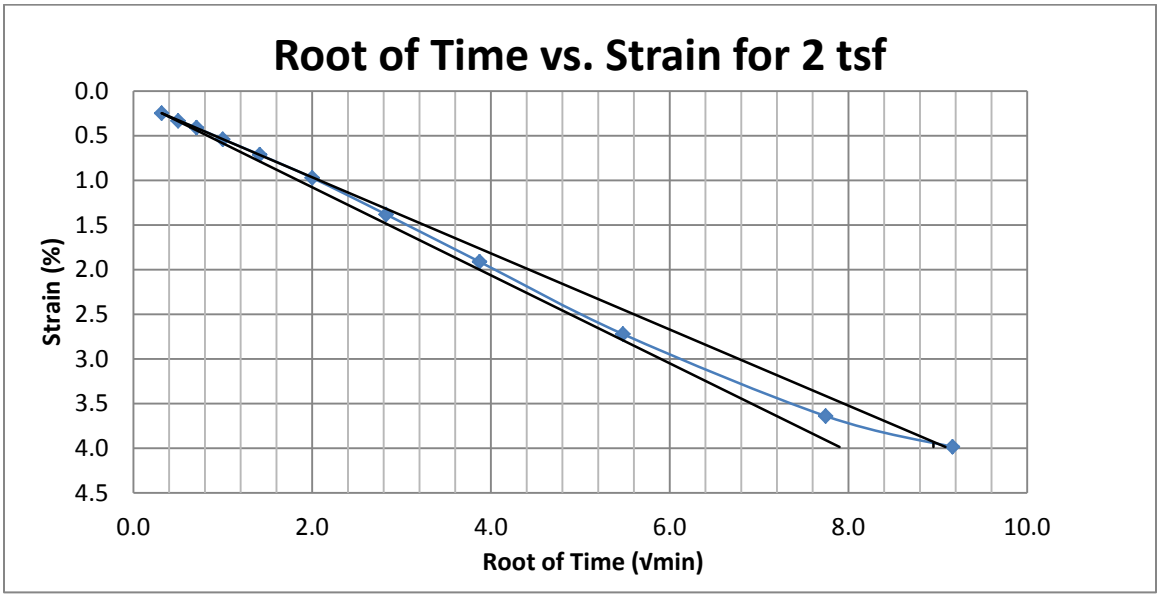

A257 Provo at 110-112 feet

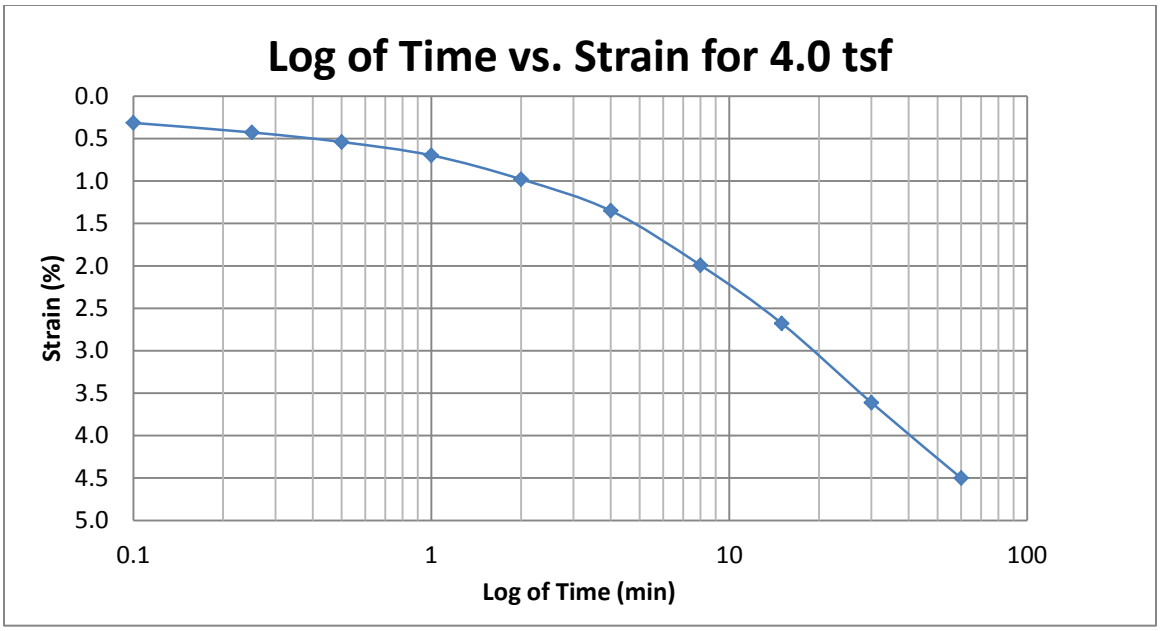

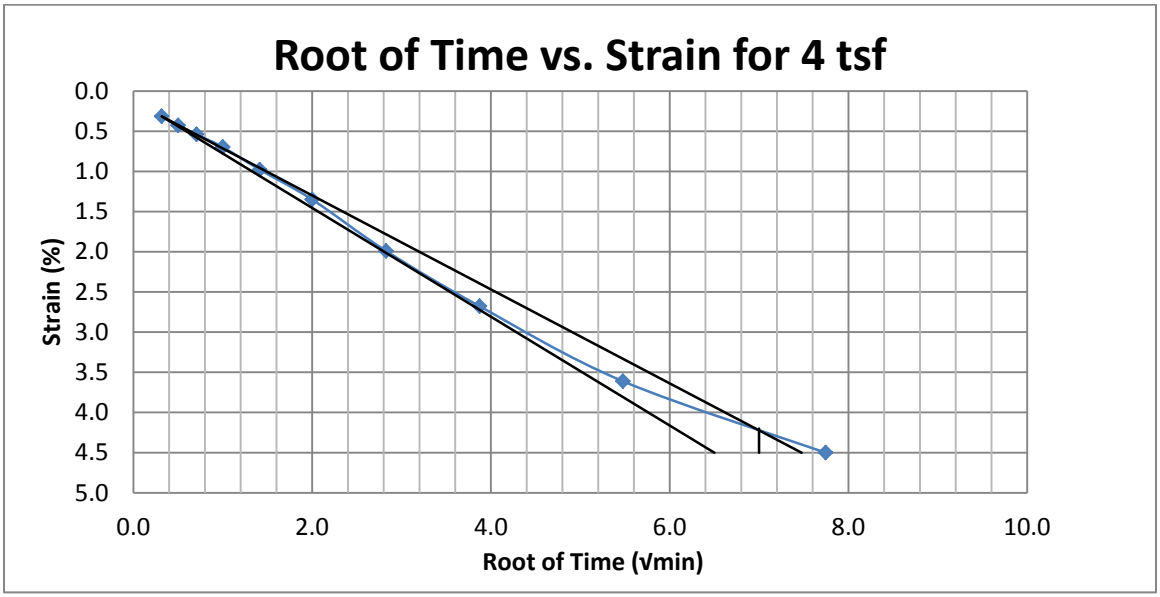

A258 Provo at 110-112 feet

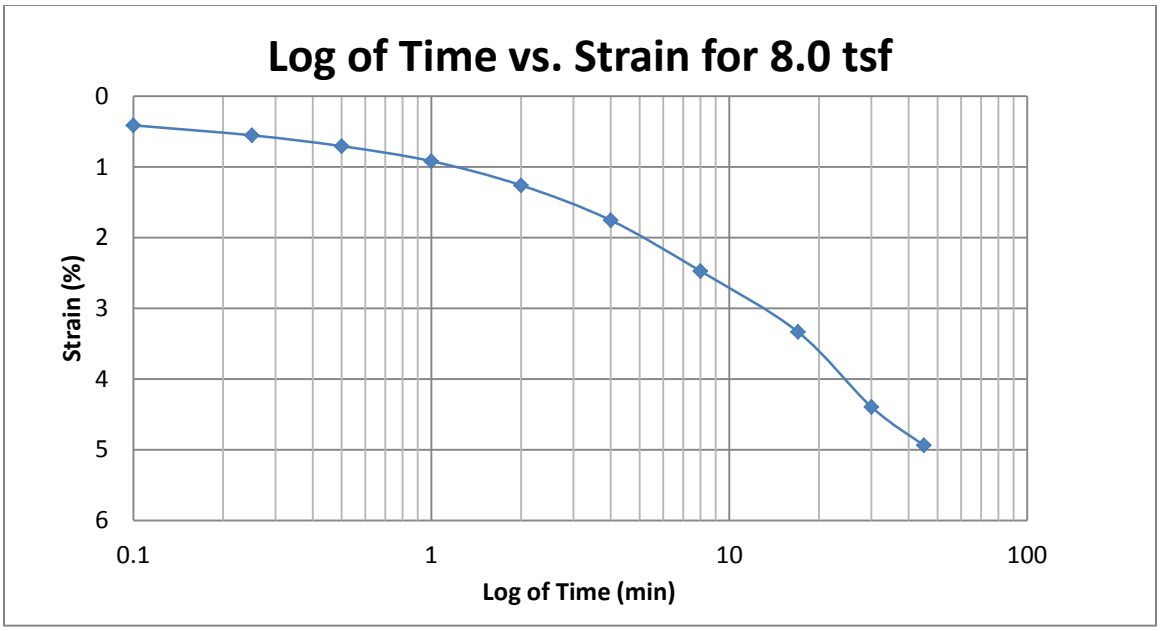

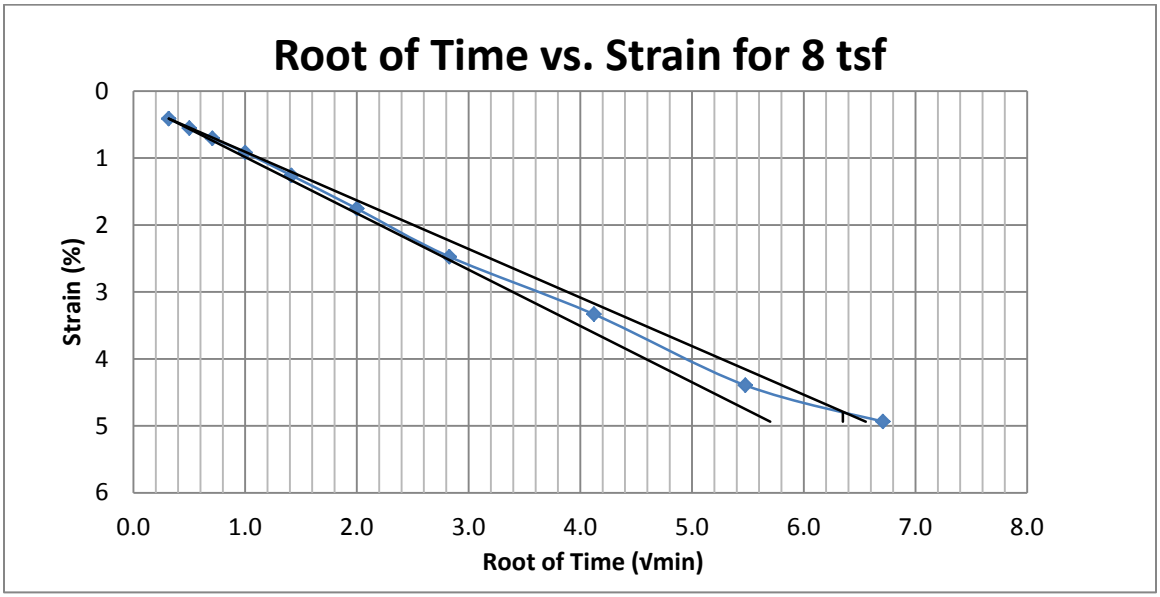

A259 Provo at 110-112 feet

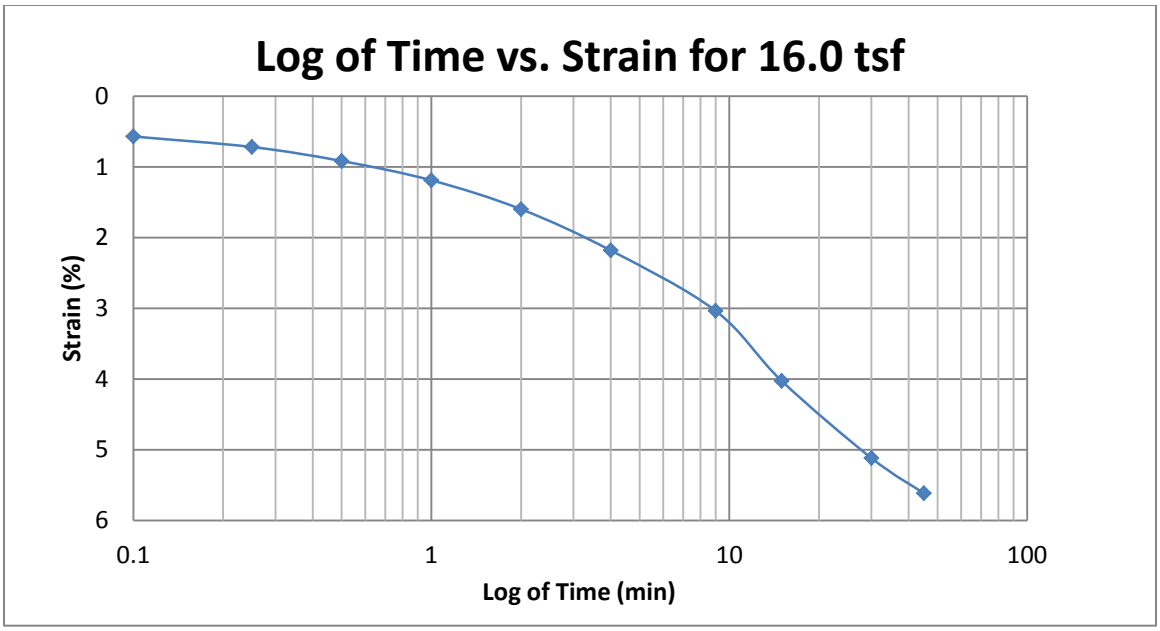

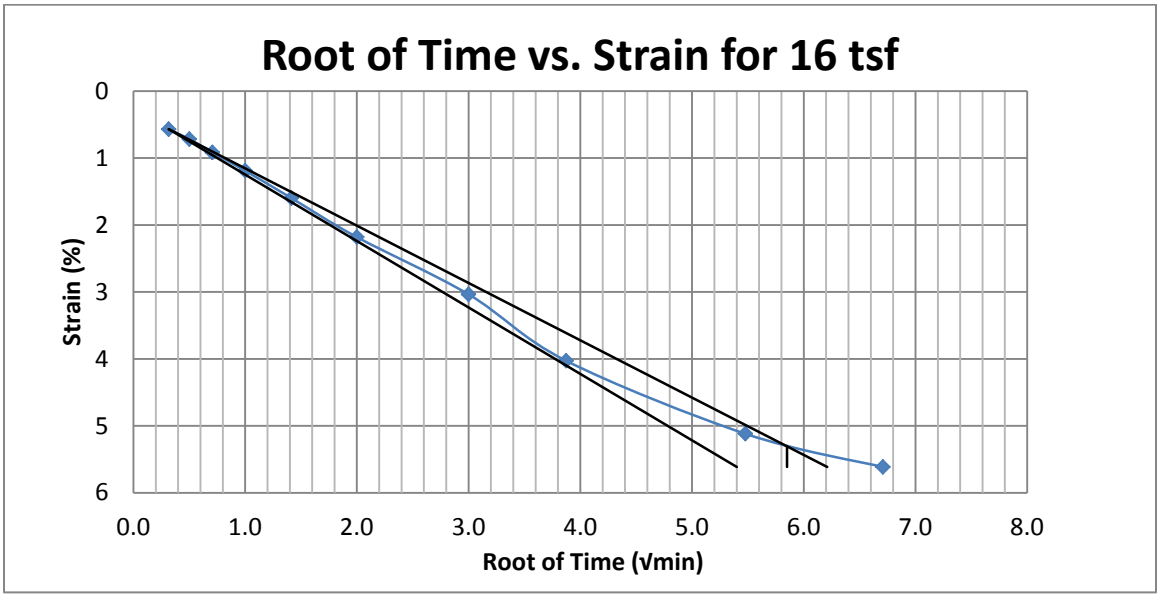

A260 Provo at 110-112 feet

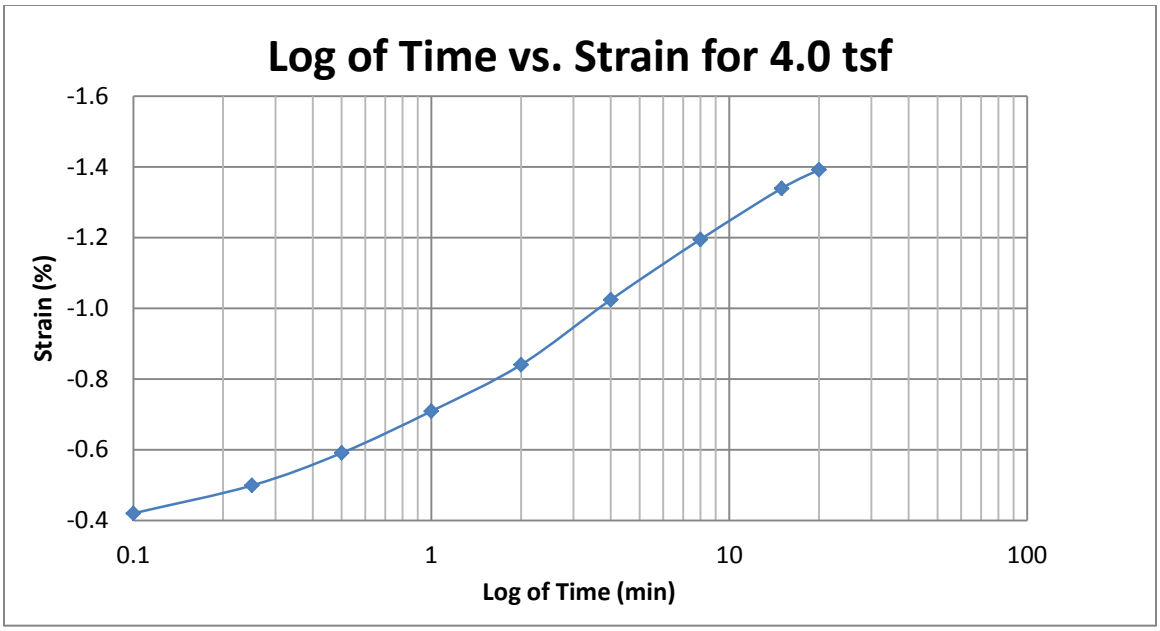

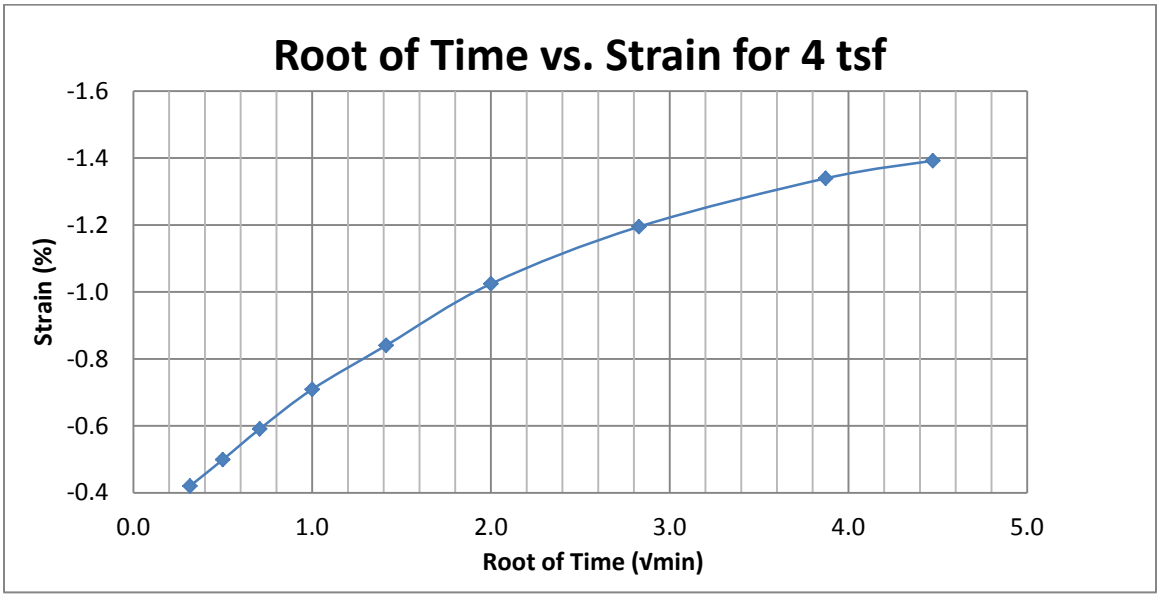

A261 Provo at 110-112 feet

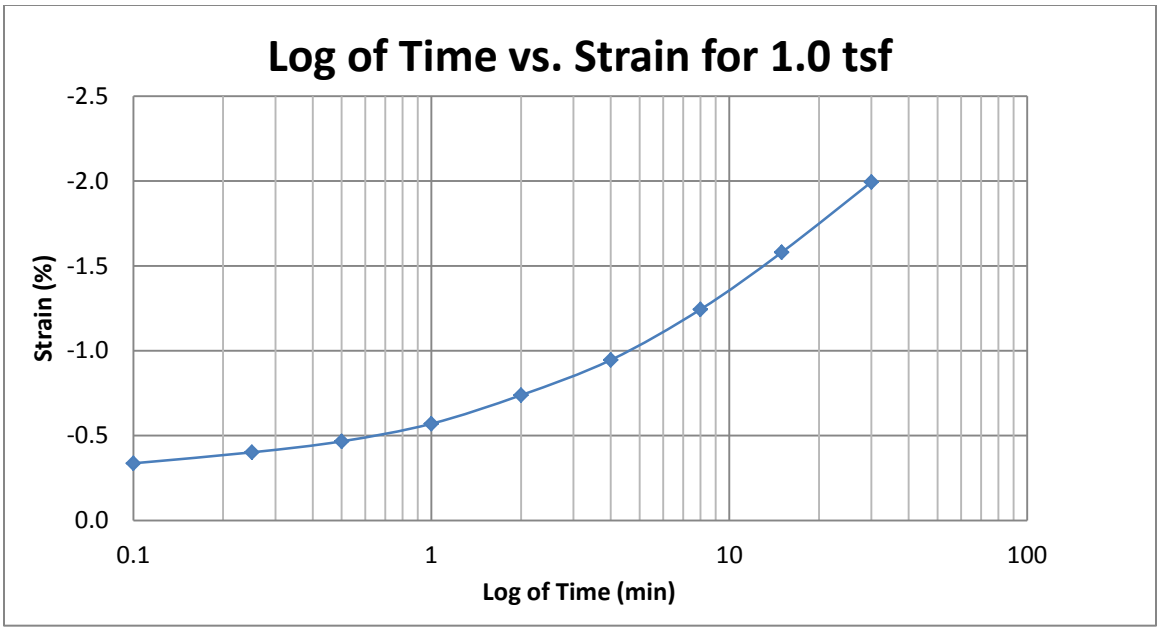

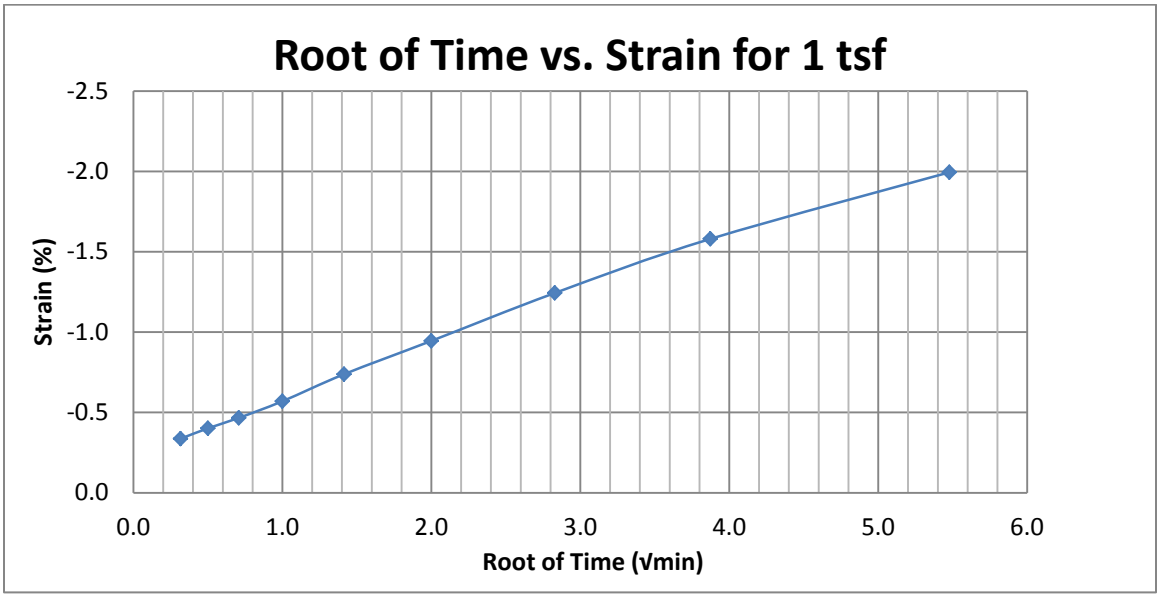

A262 Provo at 110-112 feet

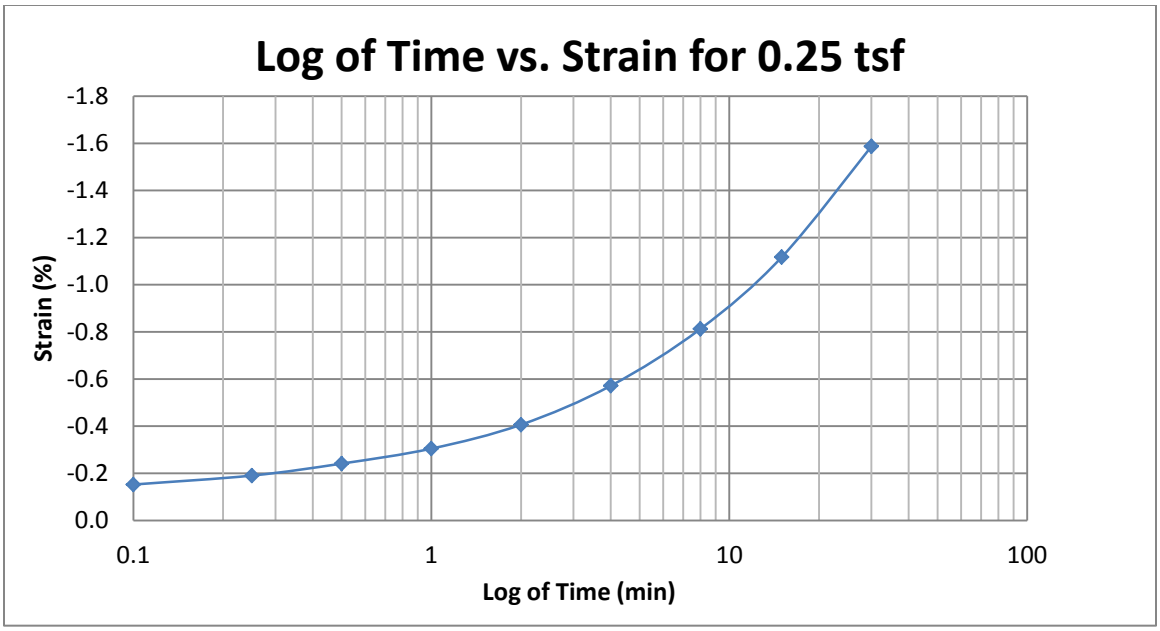

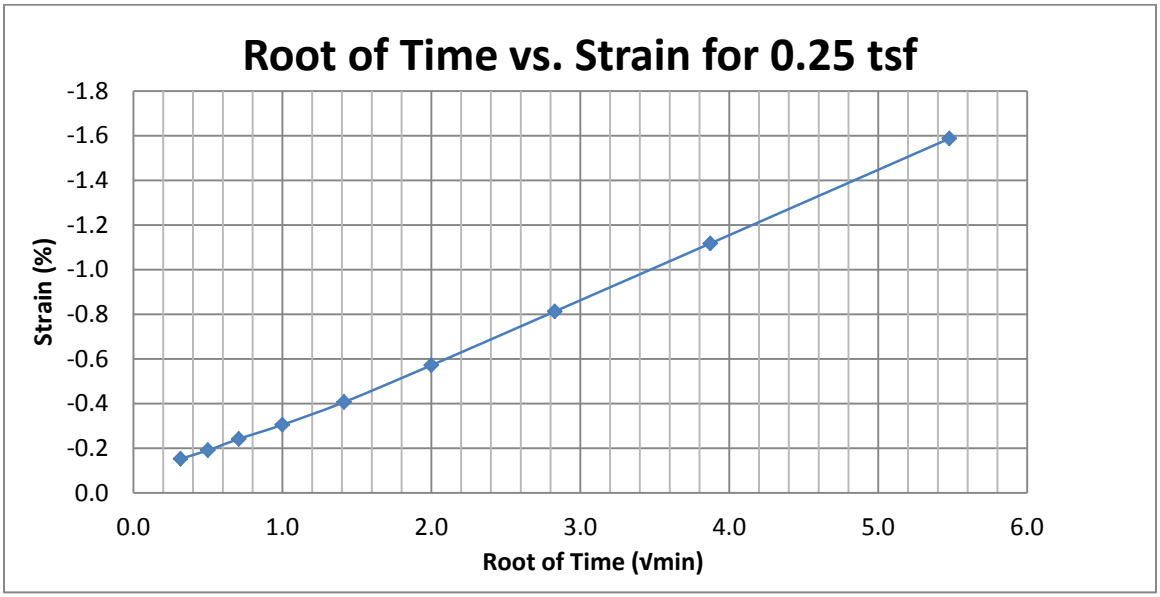

A263 Provo at 110-112 feet

APPENDIX B

PLOTS OF RATE OF SECONDARY SETTLEMENT

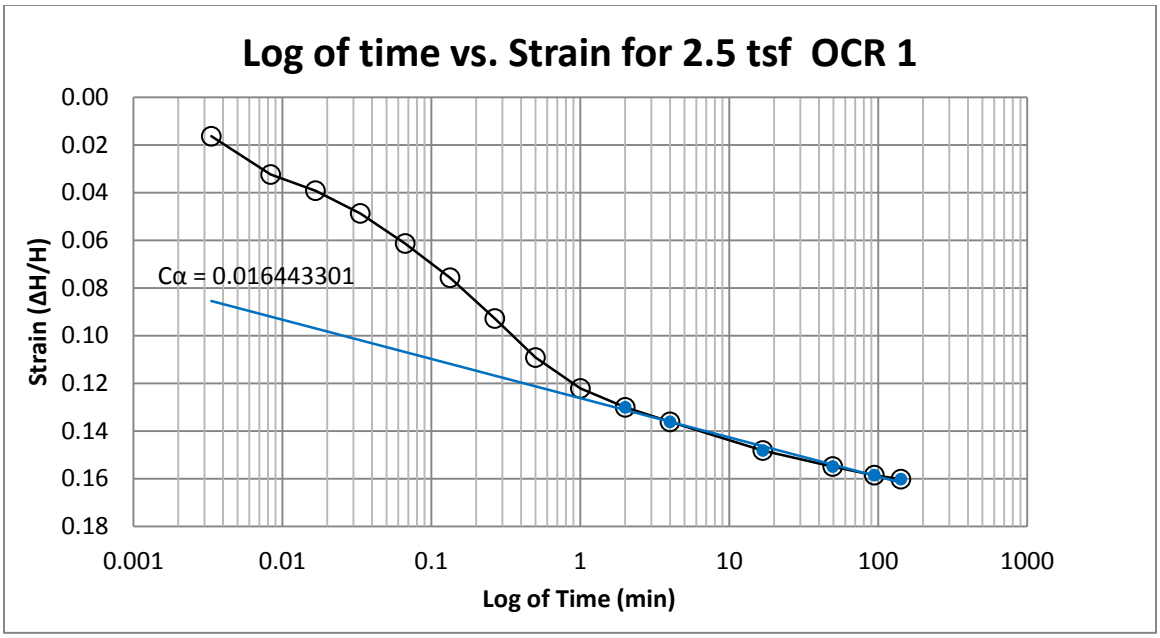

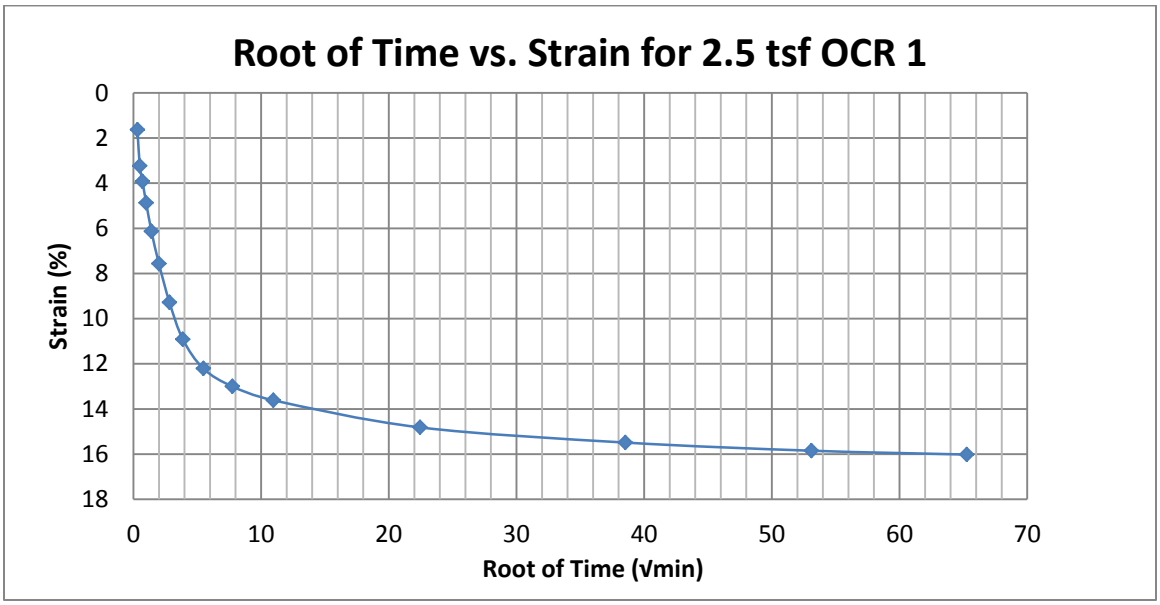

B1 400 South at 15-17 feet

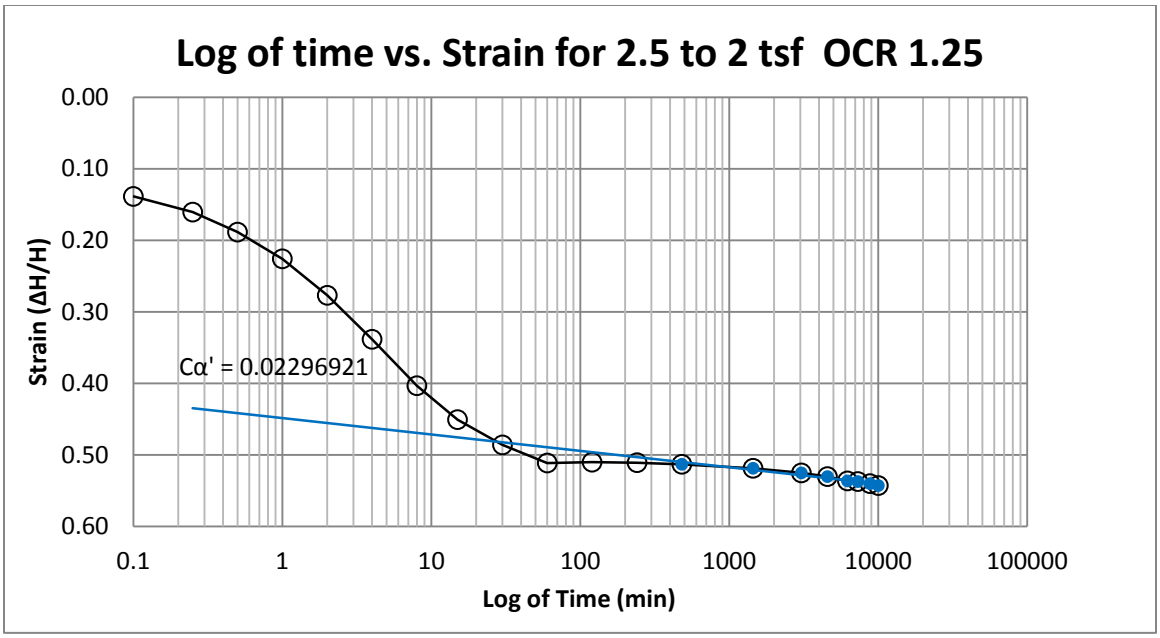

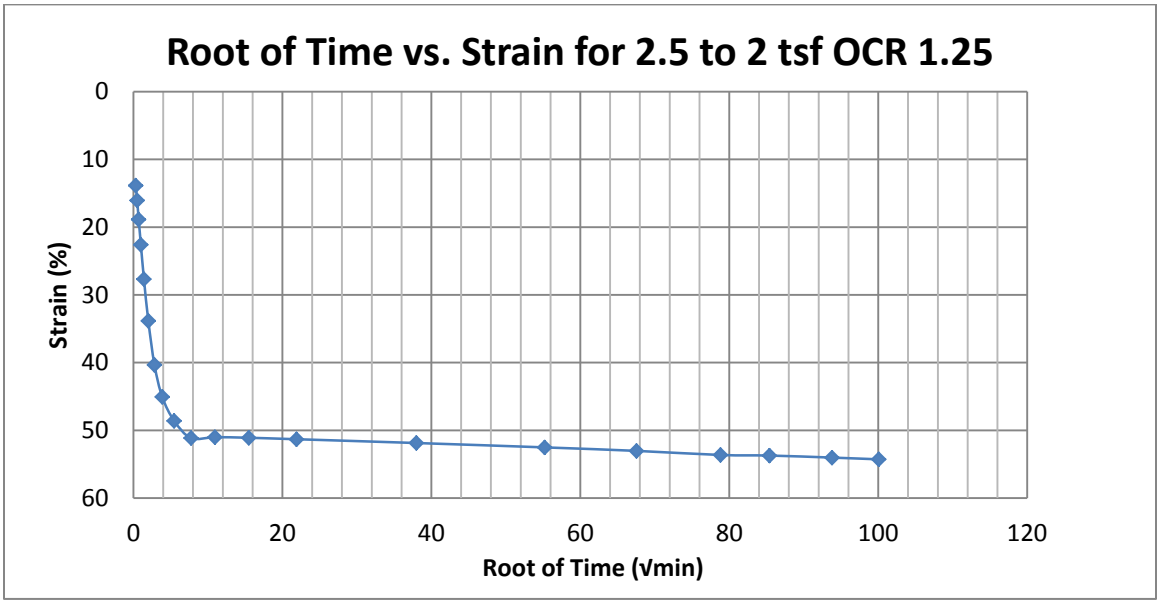

B2 400 South at 15-17 feet

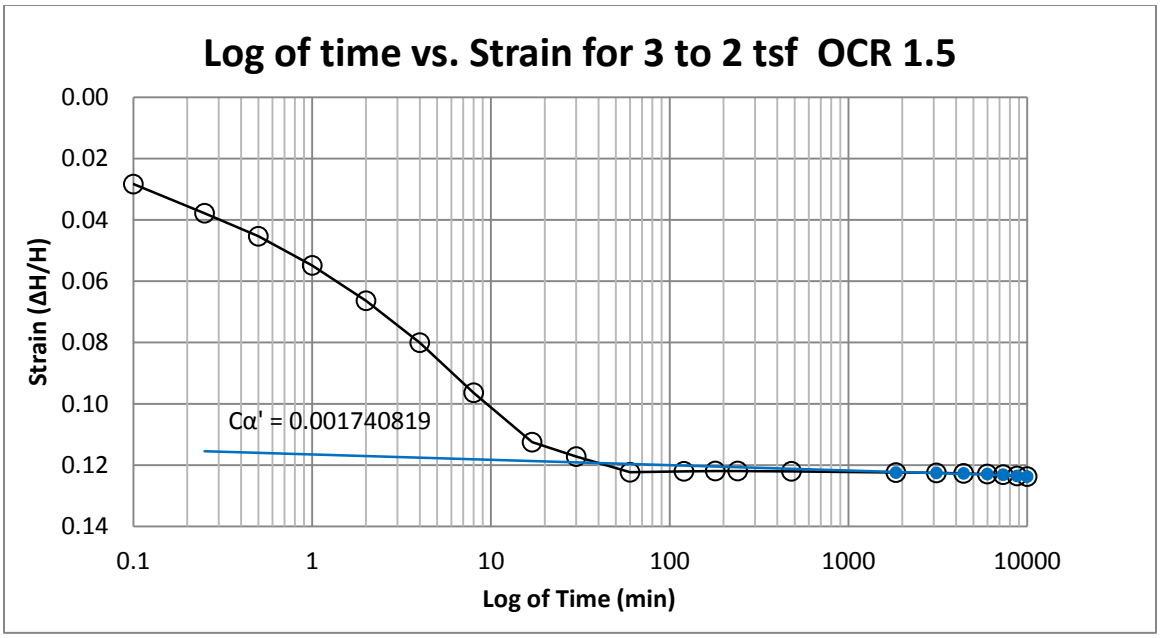

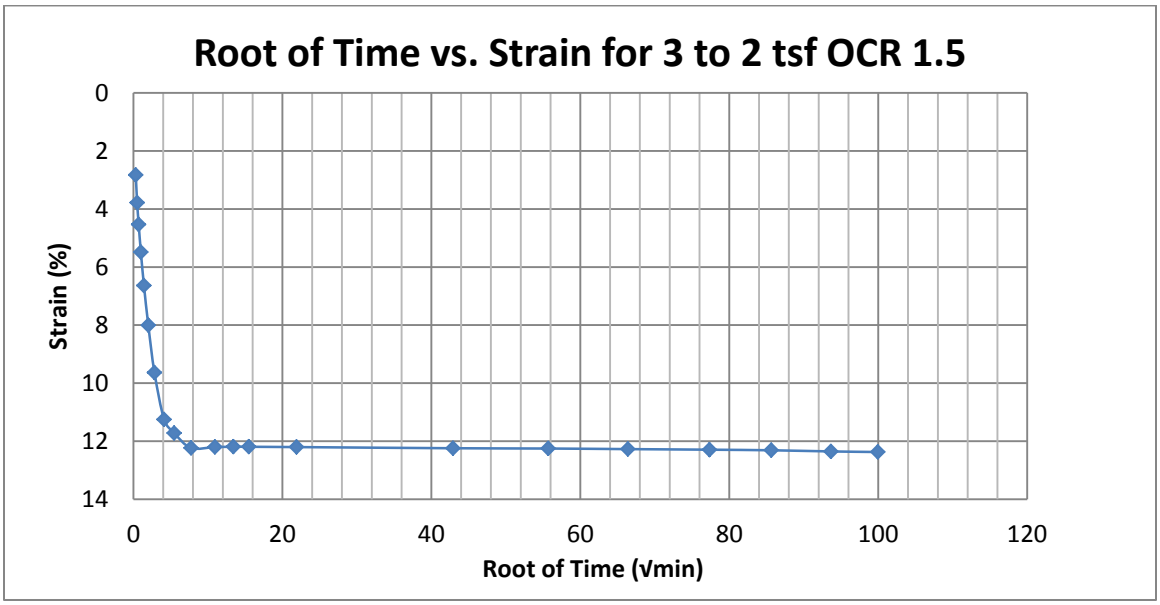

B3 400 South at 15-17 feet

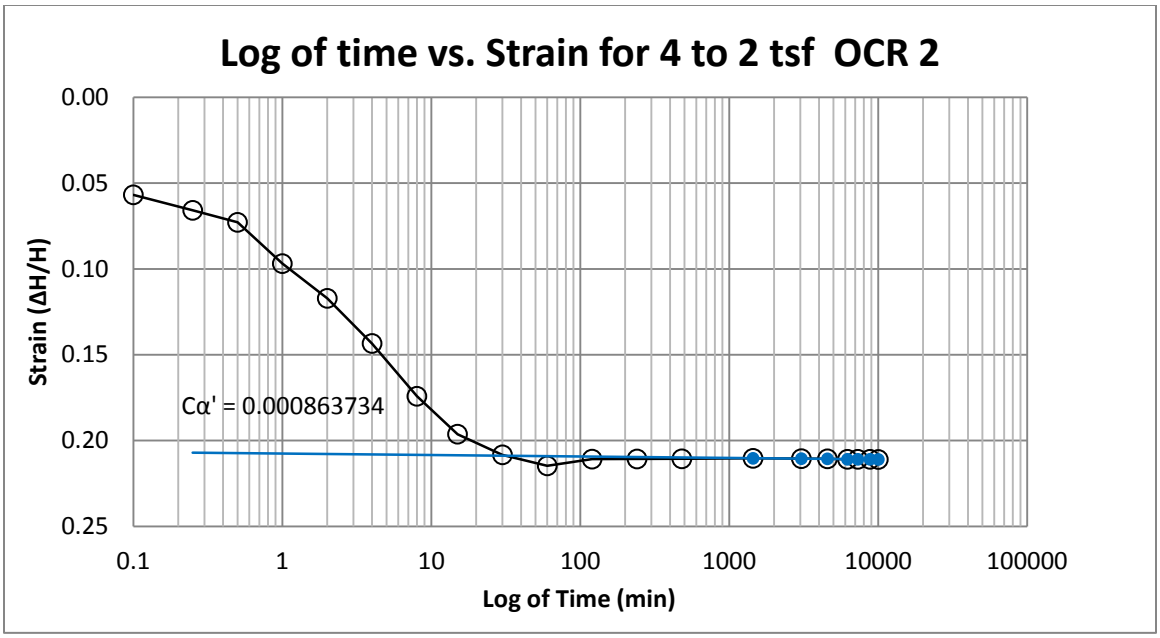

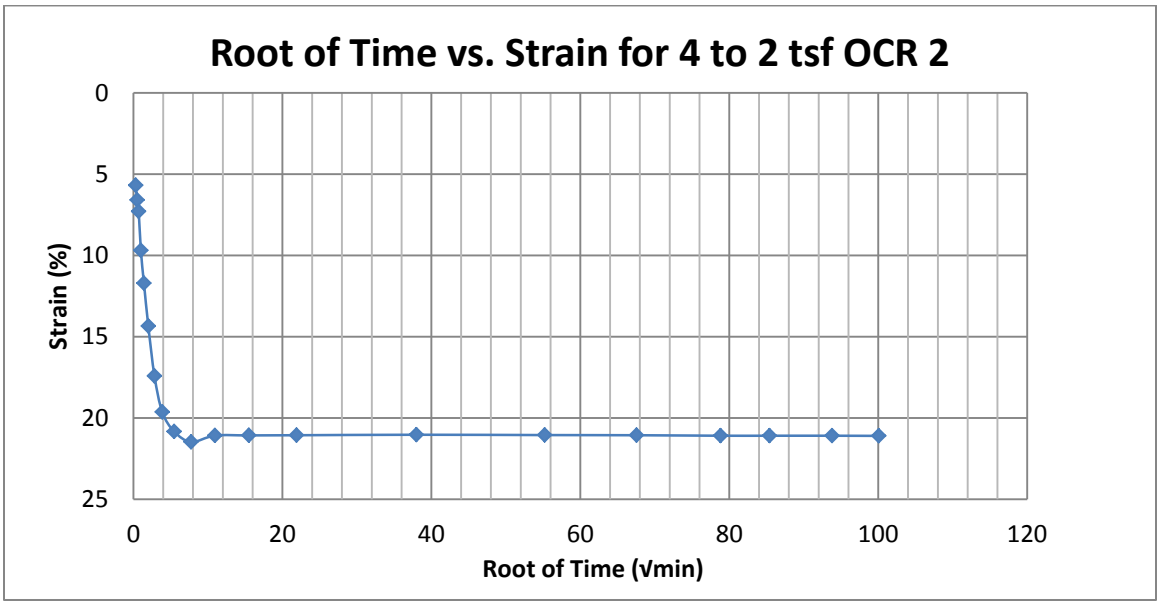

B4 400 South at 15-17 feet

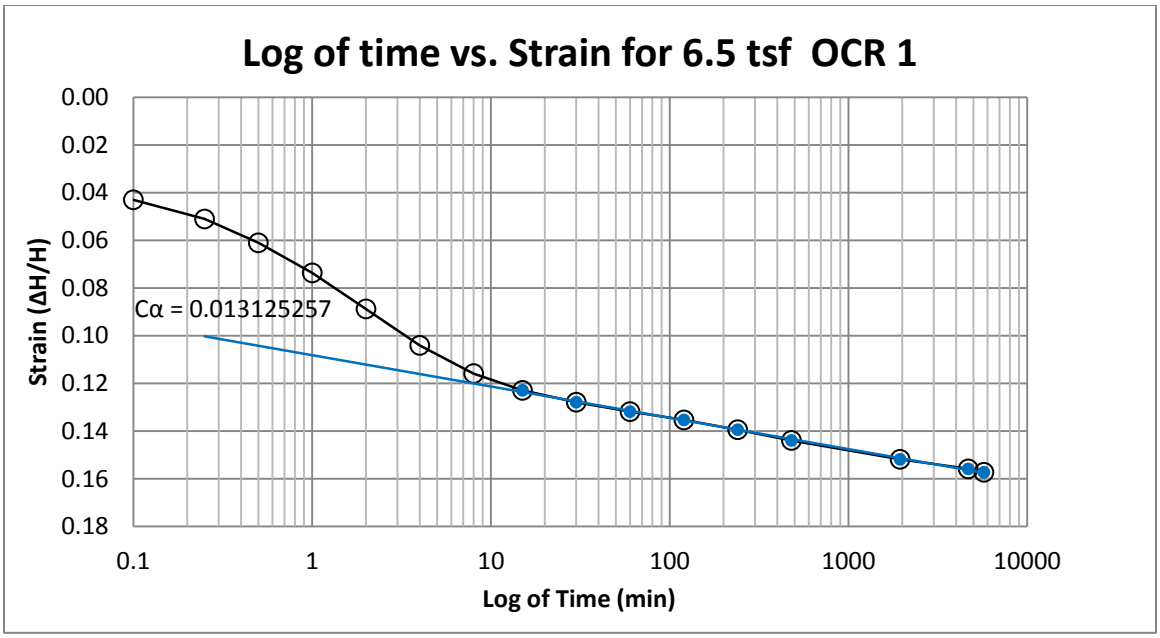

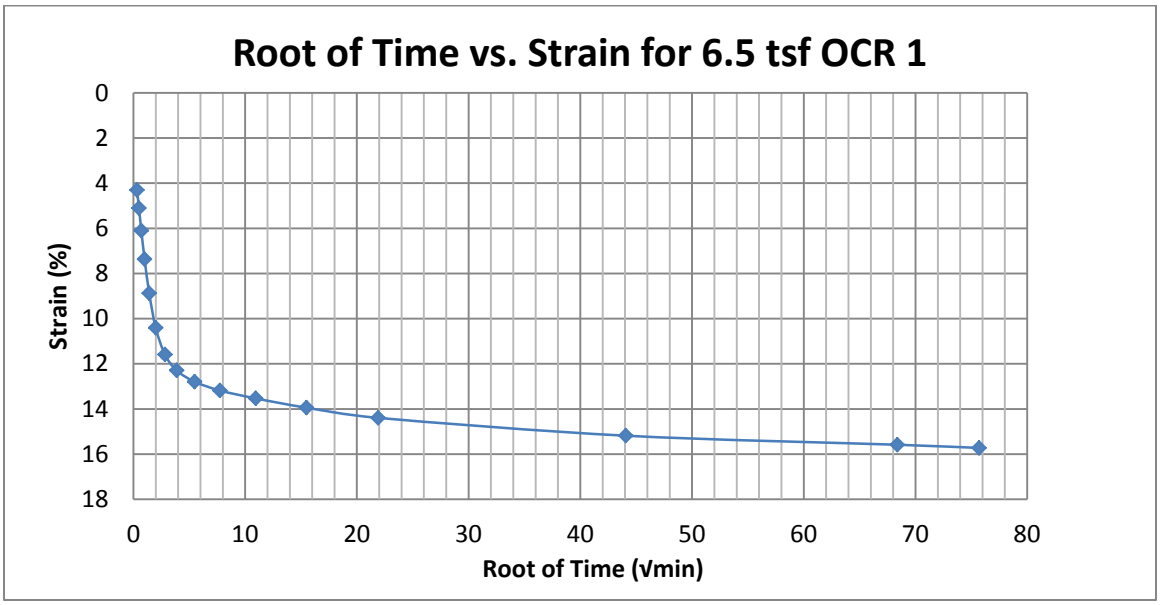

B5 400 South at 20-22 feet

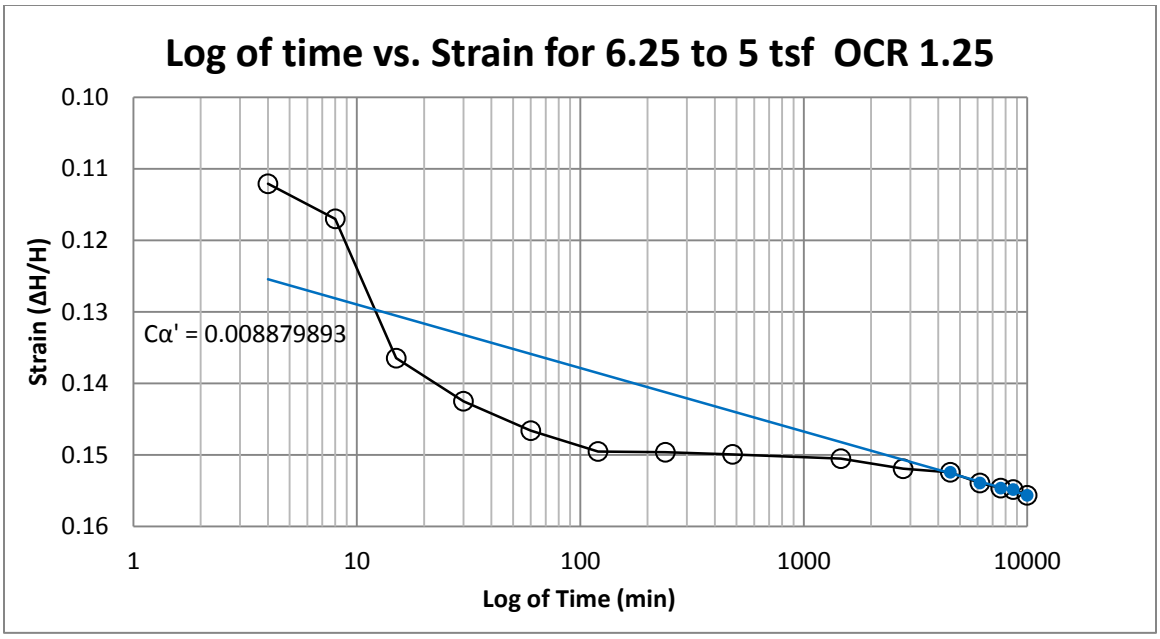

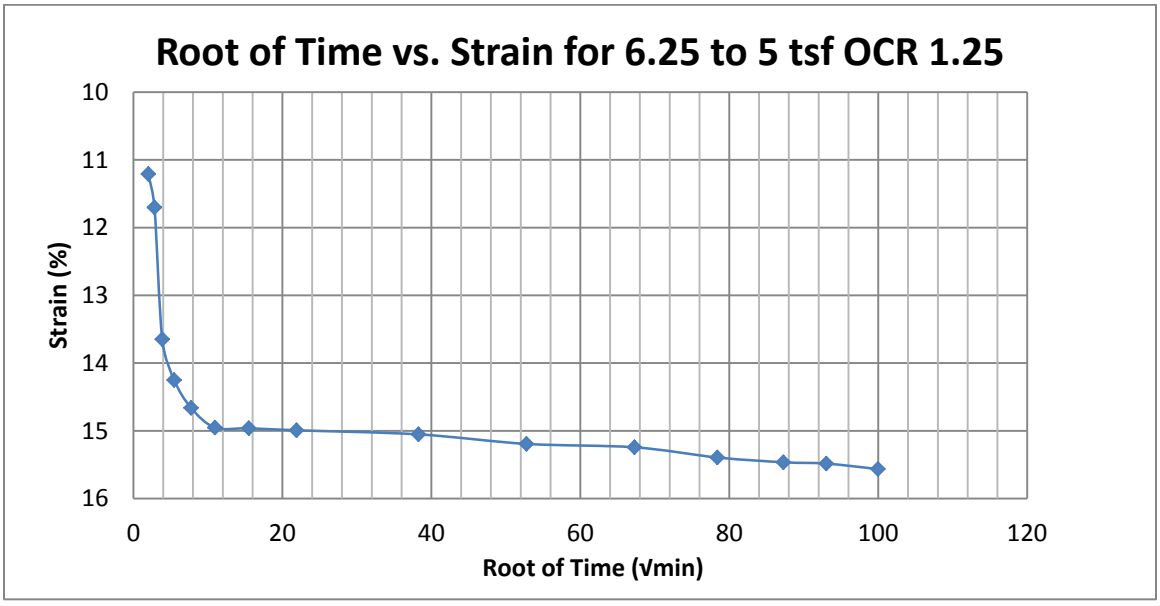

B6 400 South at 20-22 feet

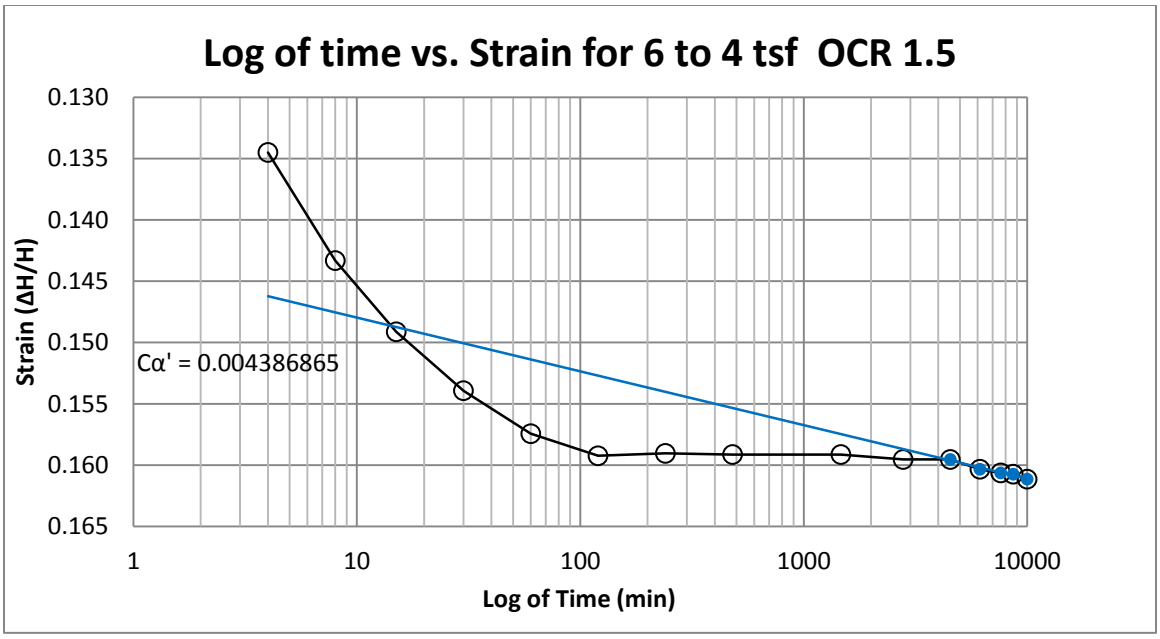

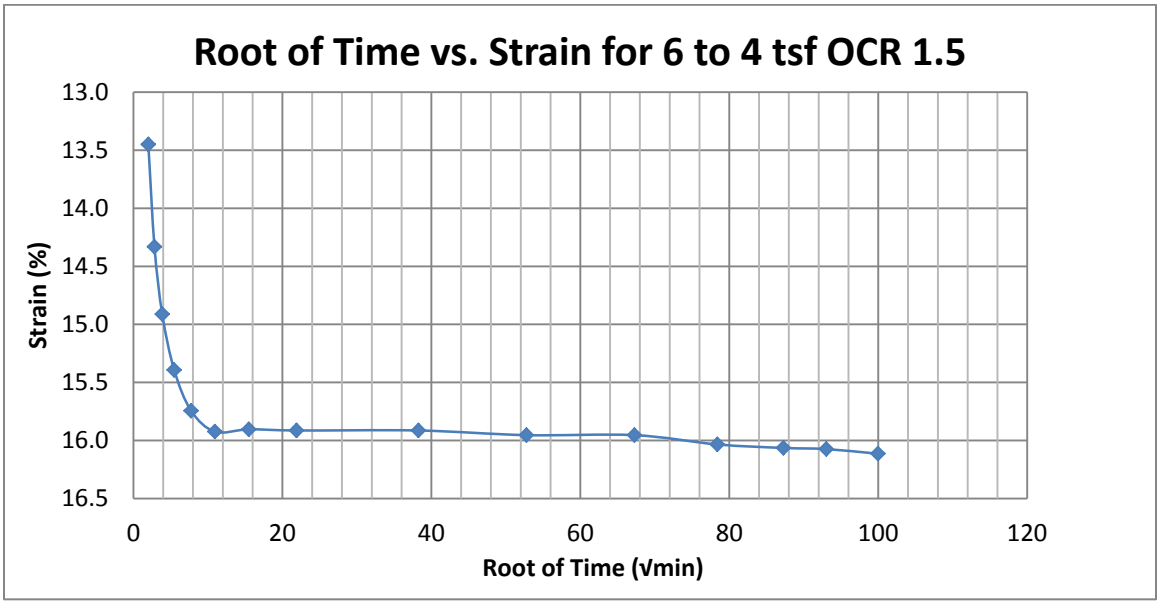

B7 400 South at 20-22 feet

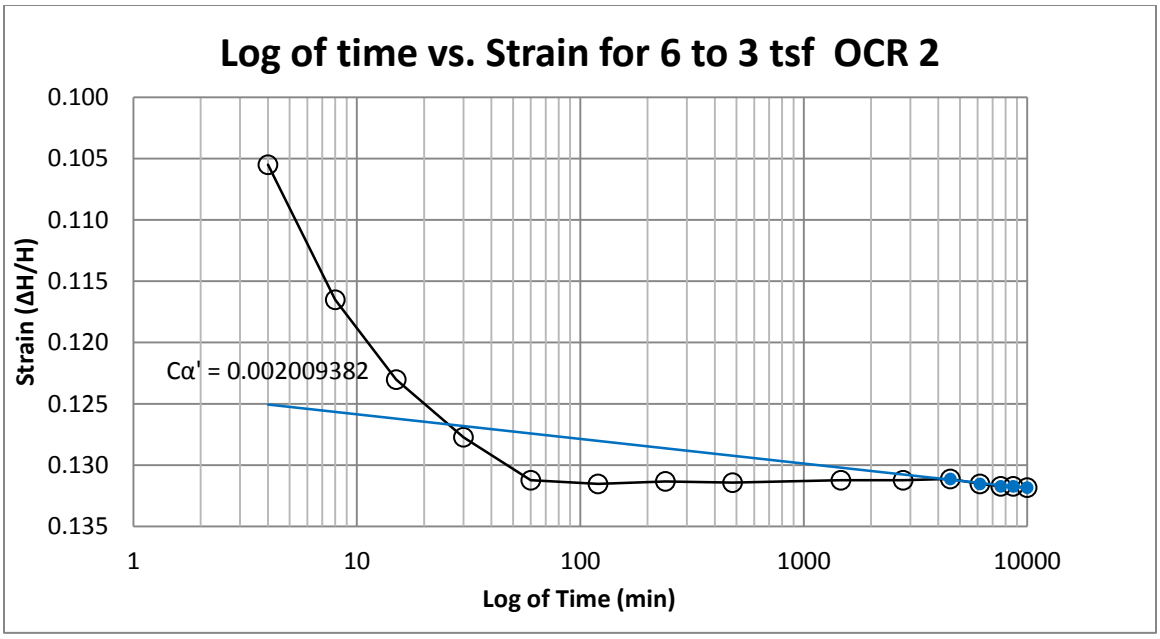

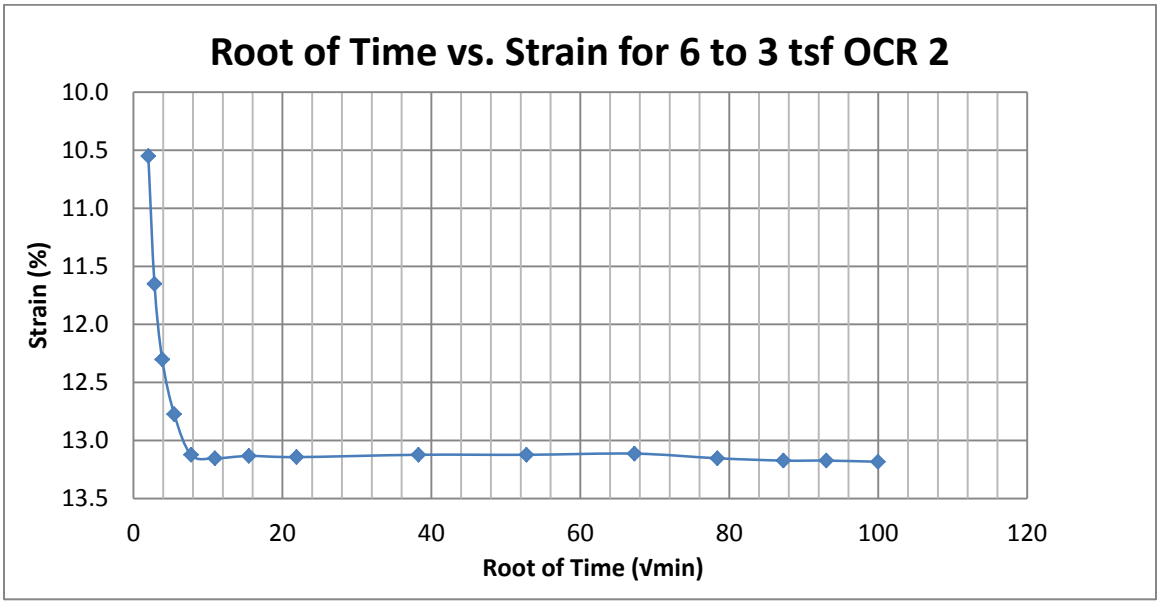

B8 400 South at 20-22 feet

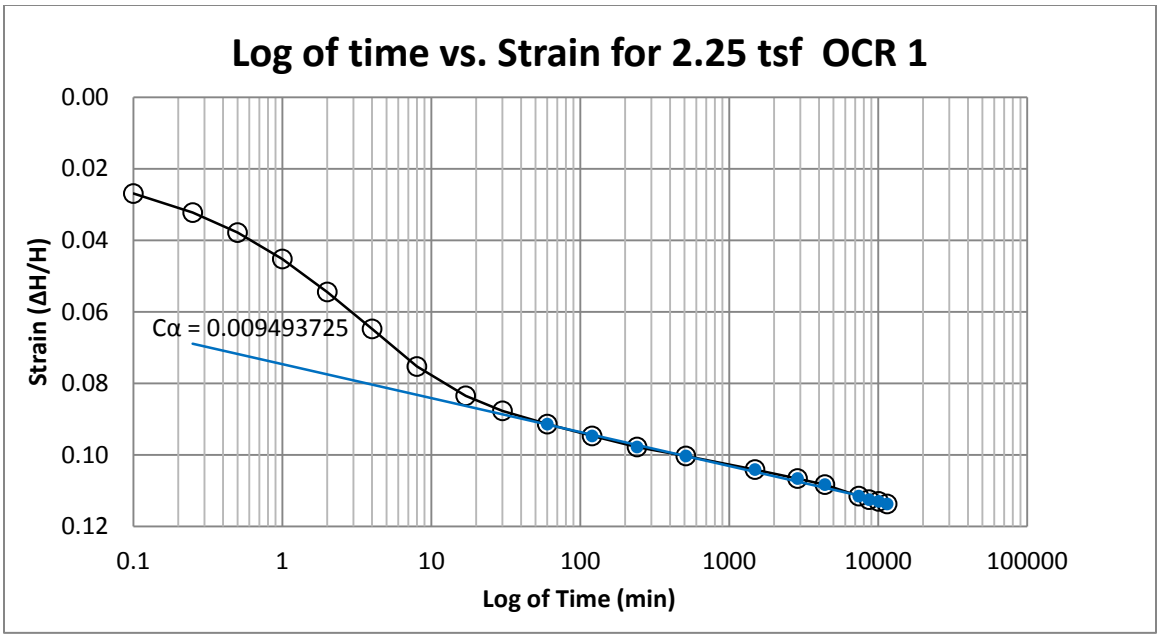

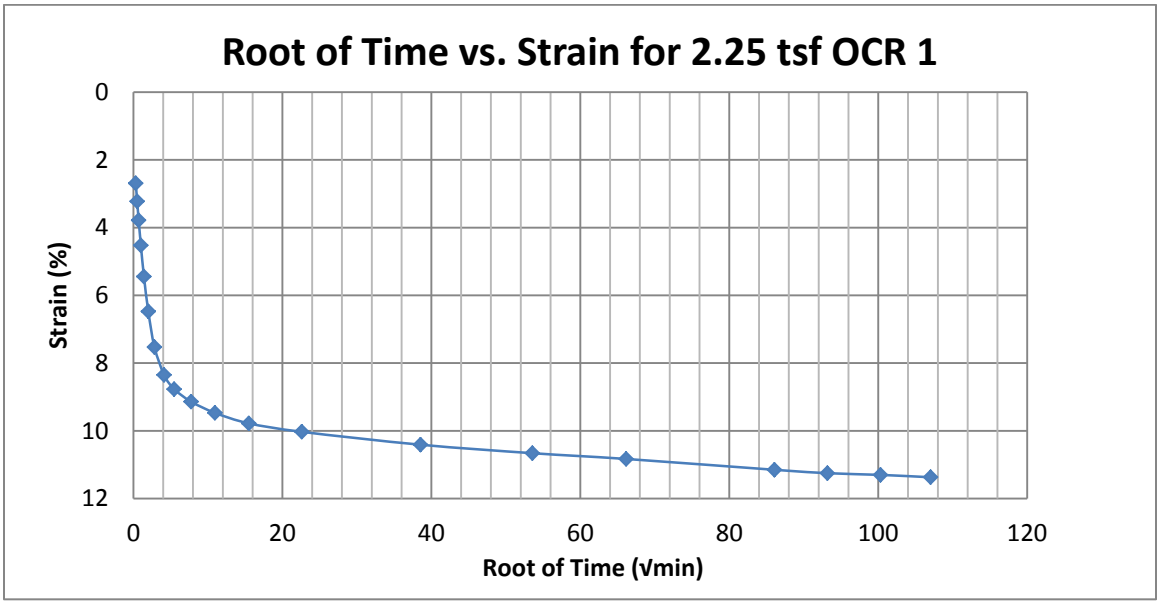

B9 400 South at 25-27 feet

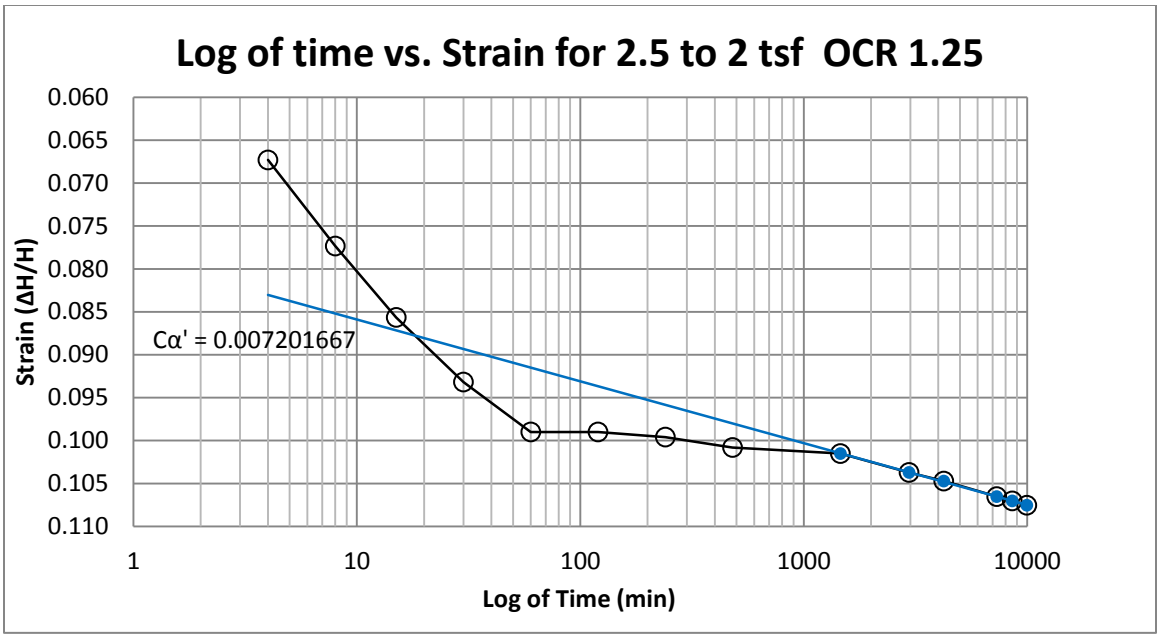

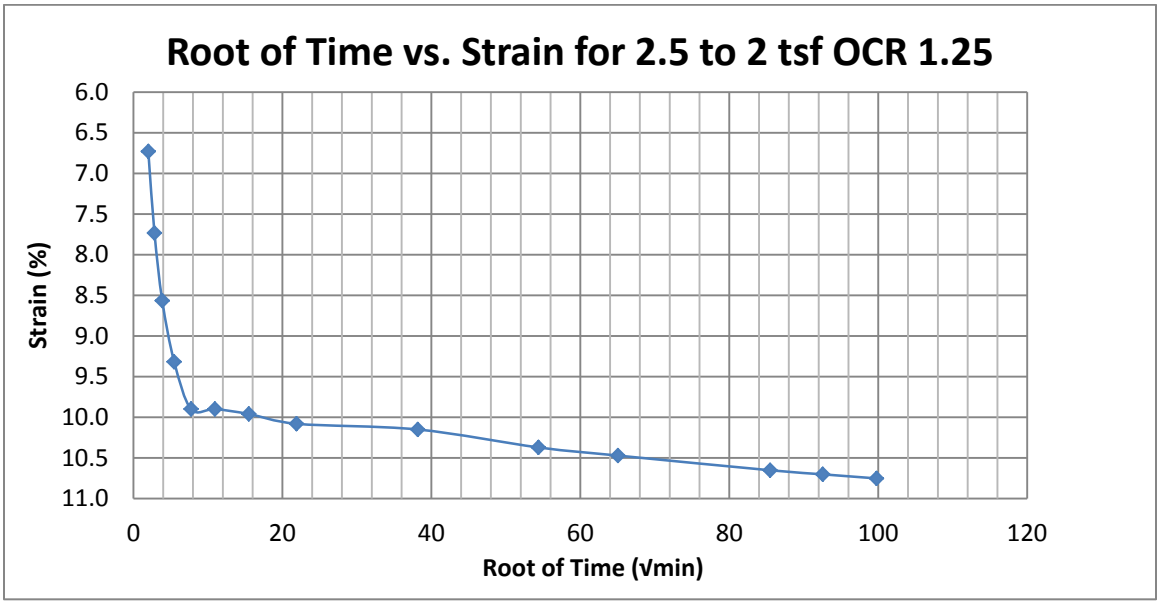

B10 400 South at 25-27 feet

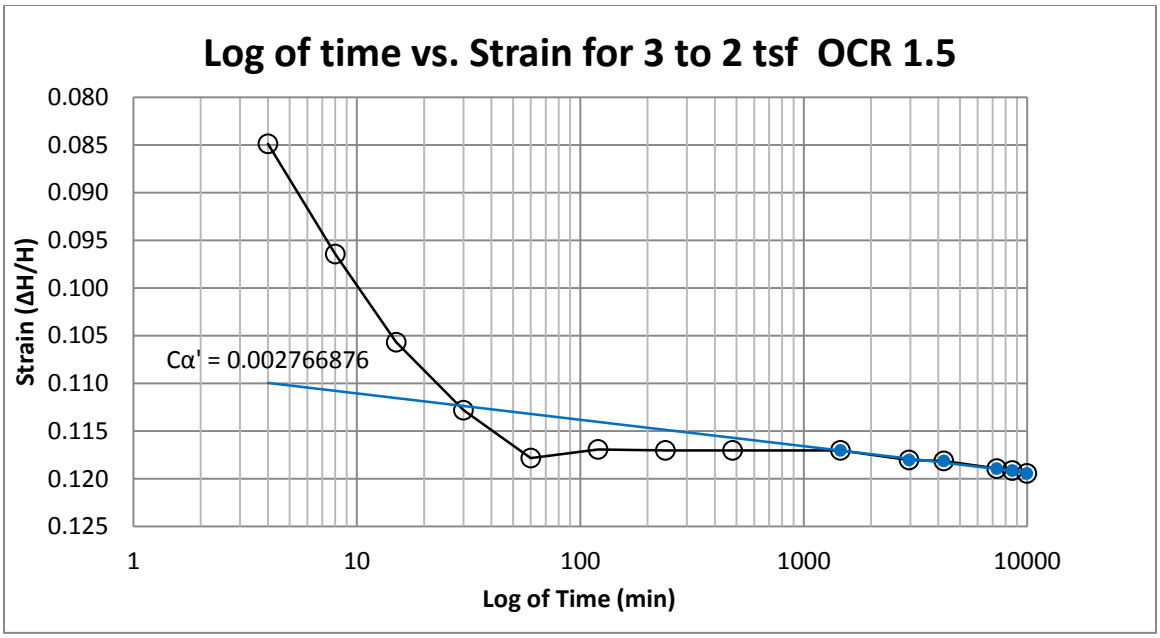

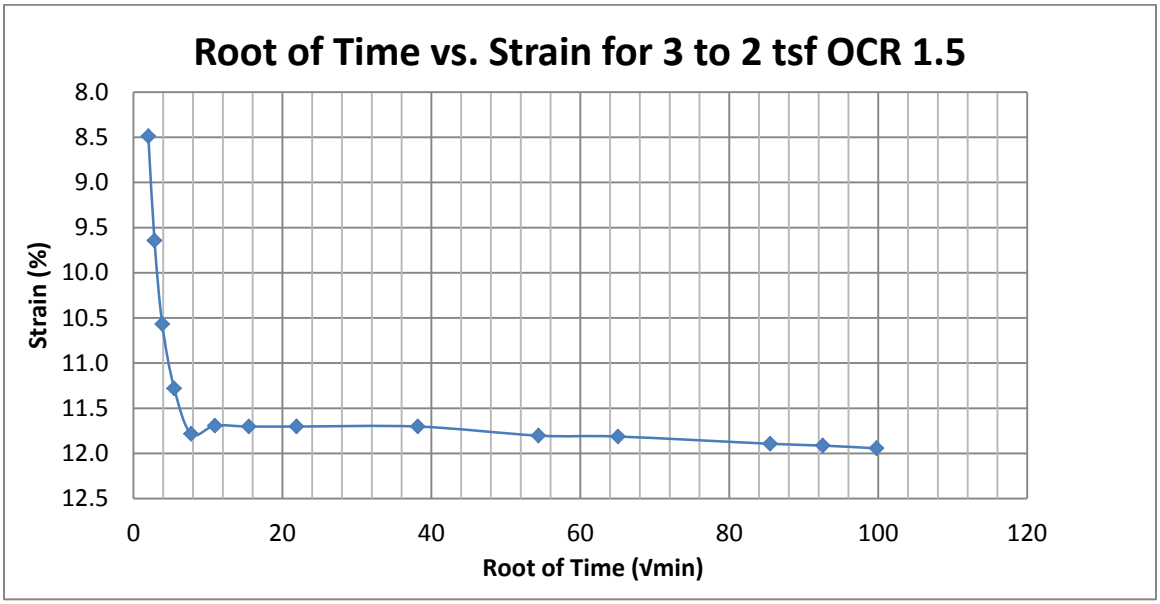

B11 400 South at 25-27 feet

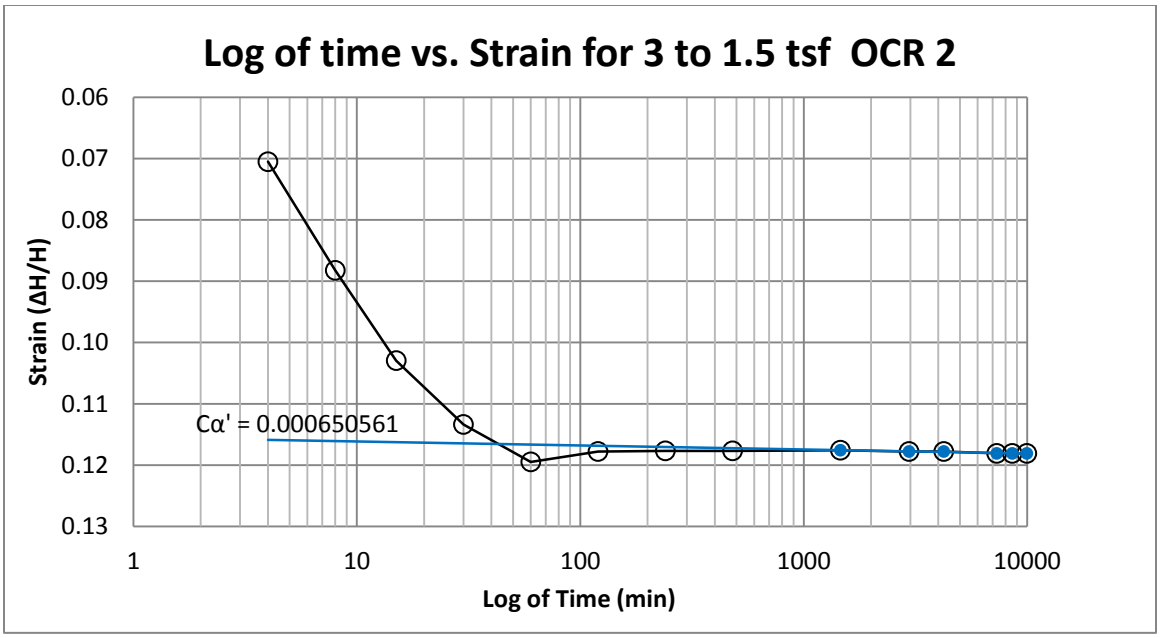

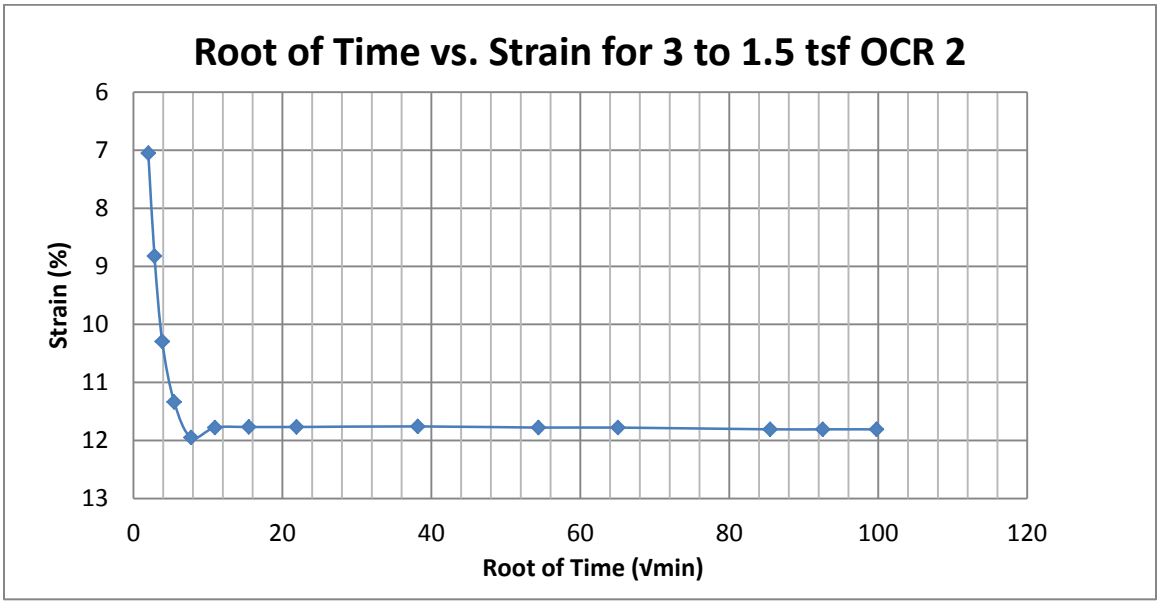

B12 400 South at 25-27 feet

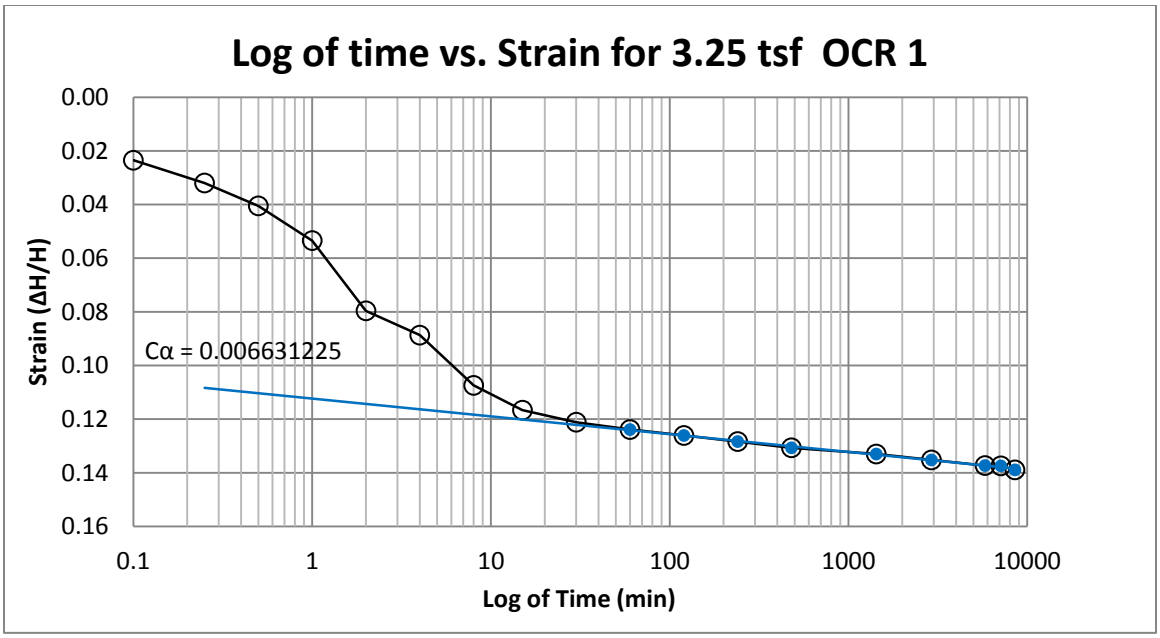

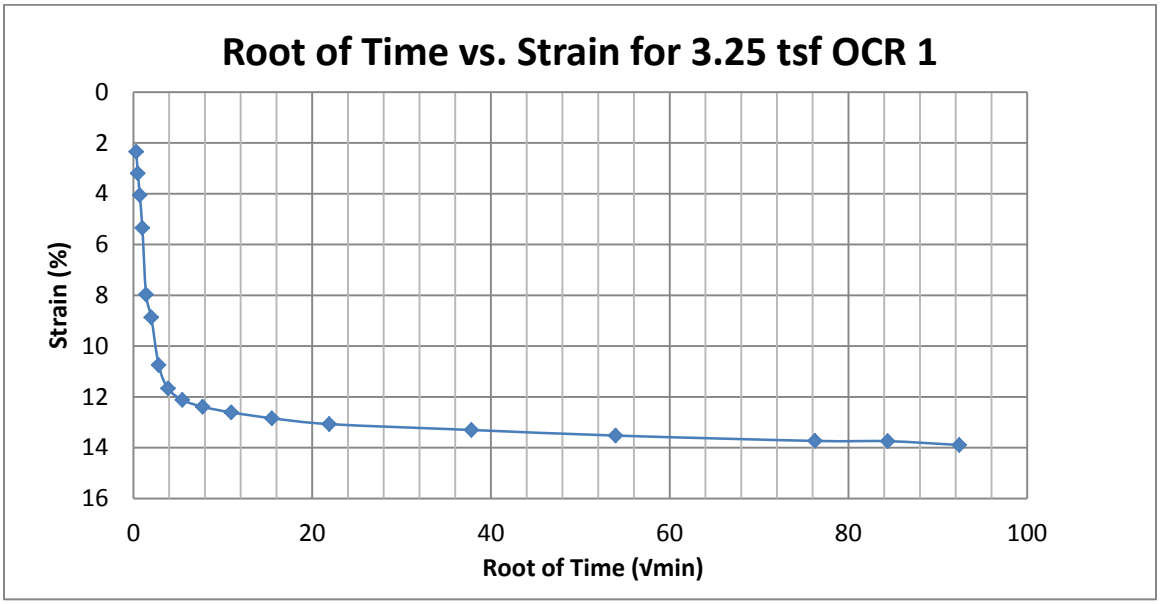

B13 400 South at 30-32 feet

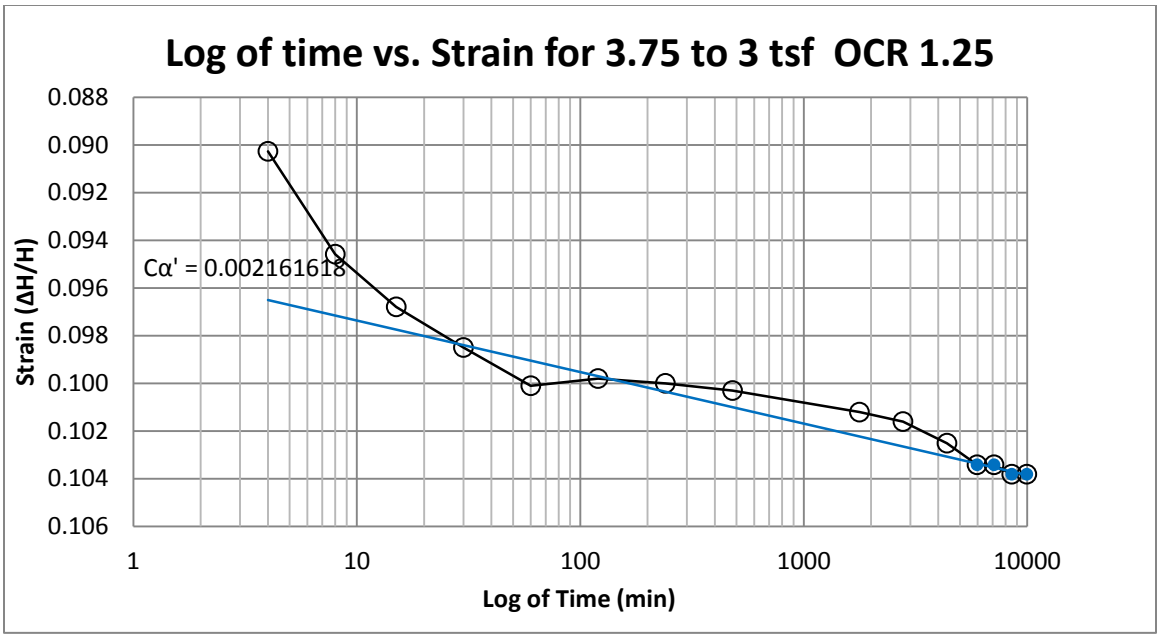

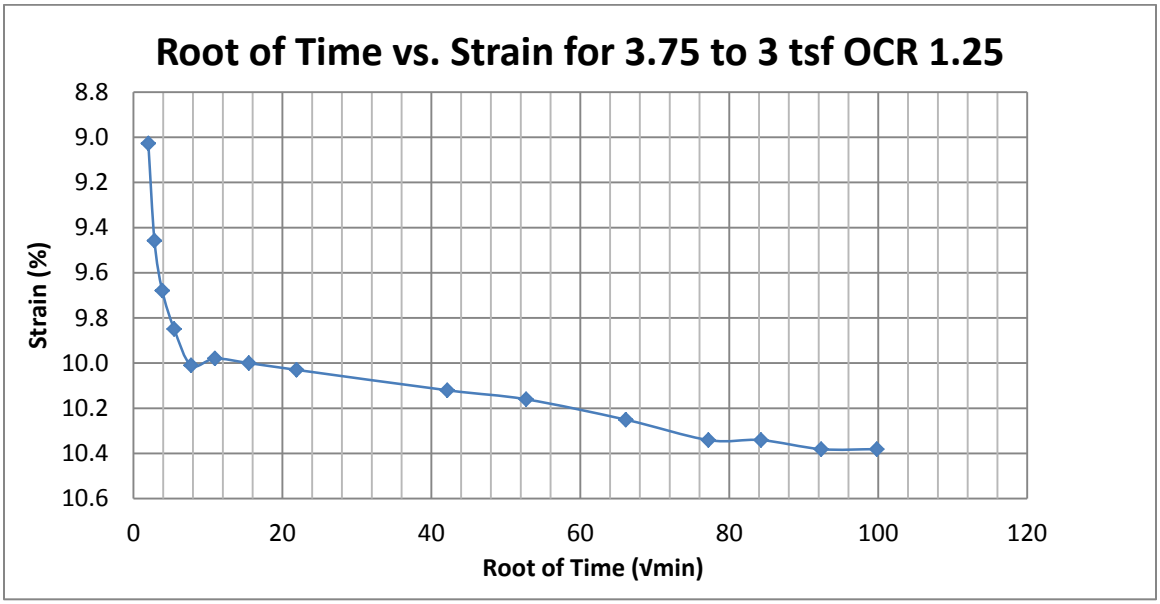

B14 400 South at 30-32 feet

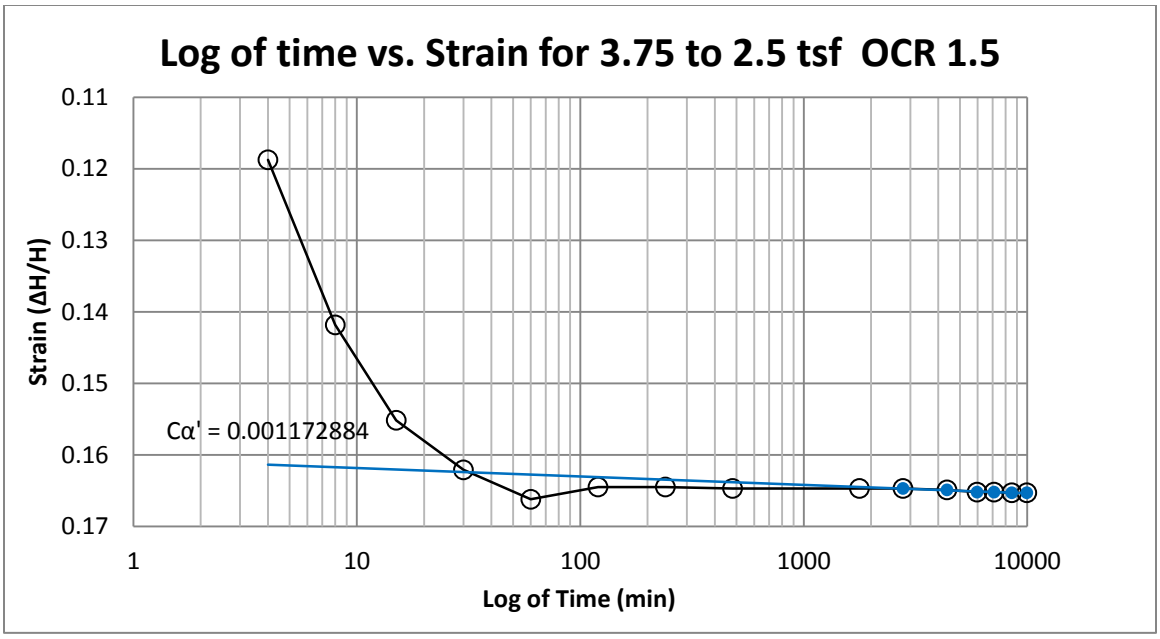

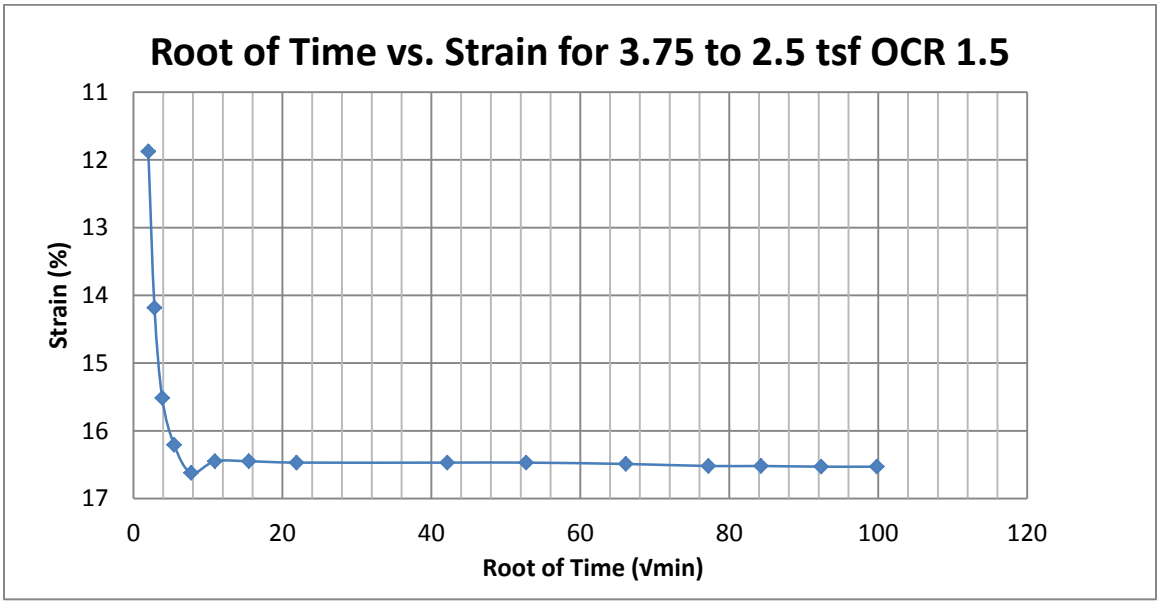

B15 400 South at 30-32 feet

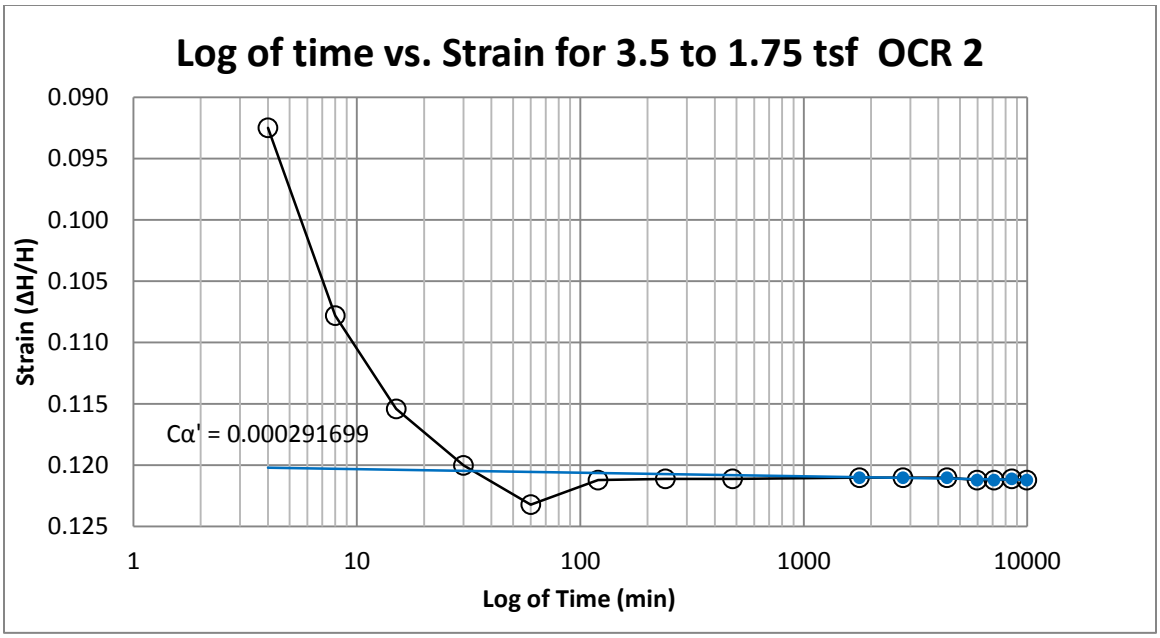

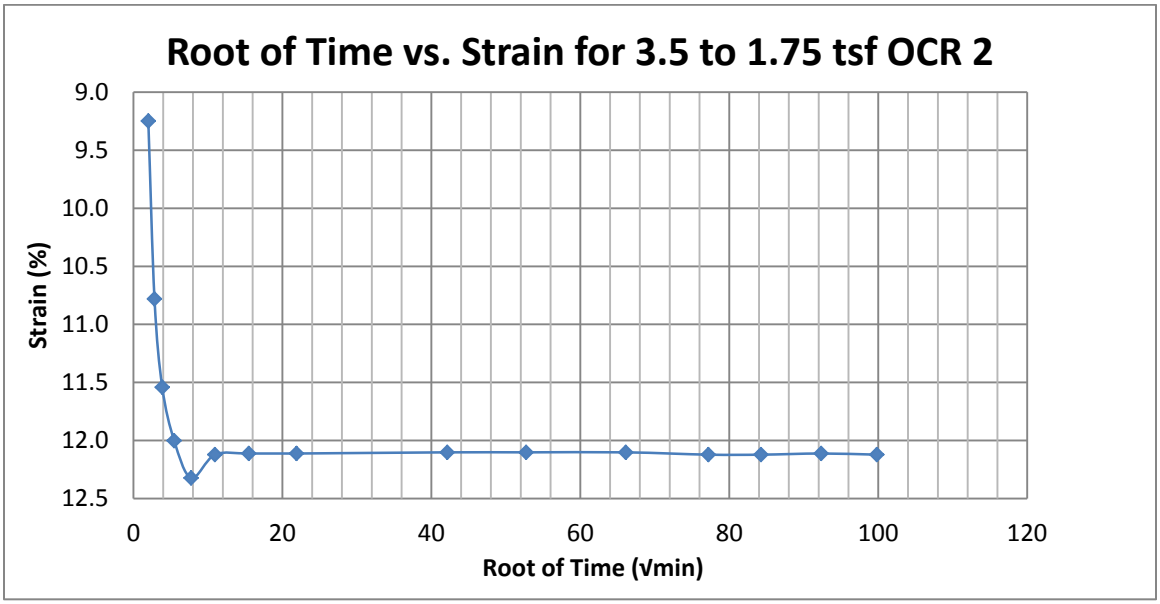

B16 400 South at 30-32 feet

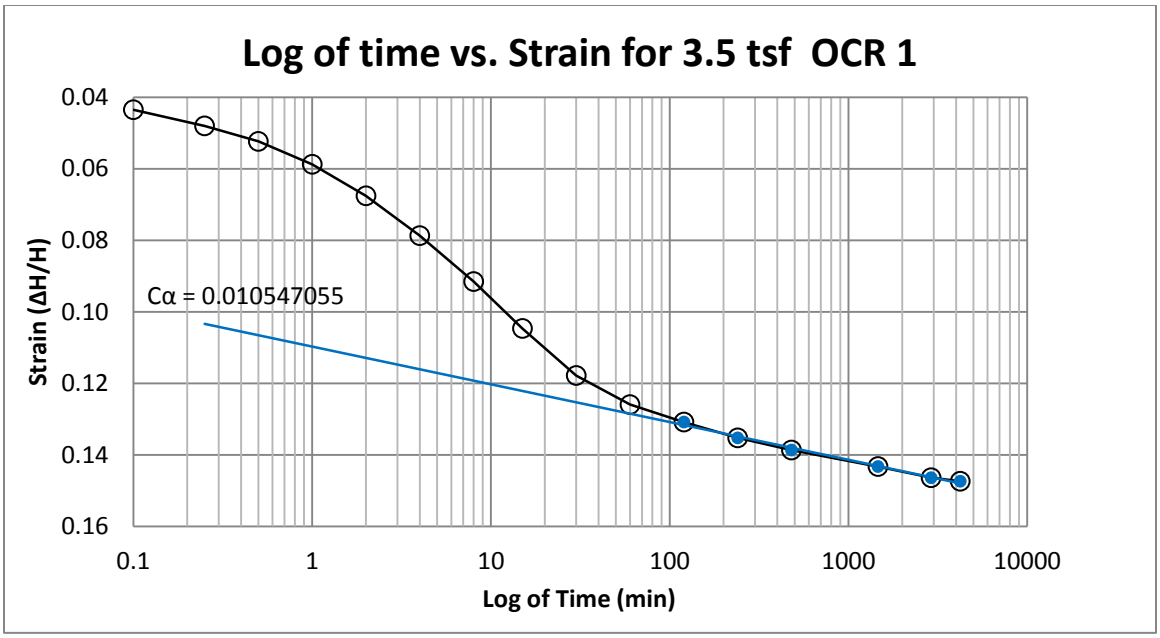

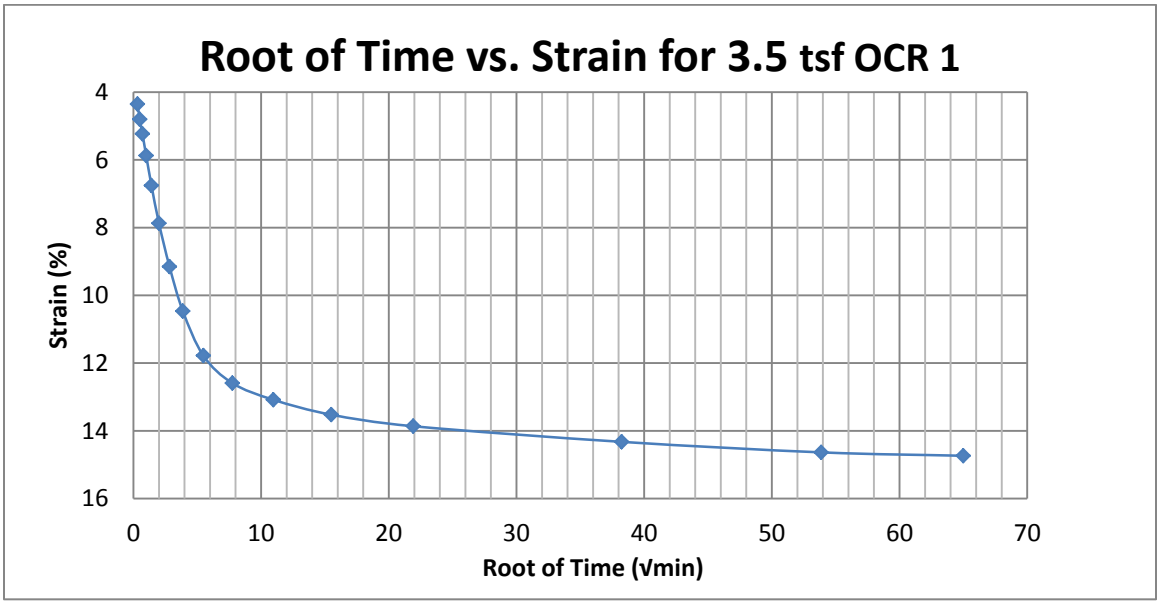

B17 400 South at 37.5-39.5 feet

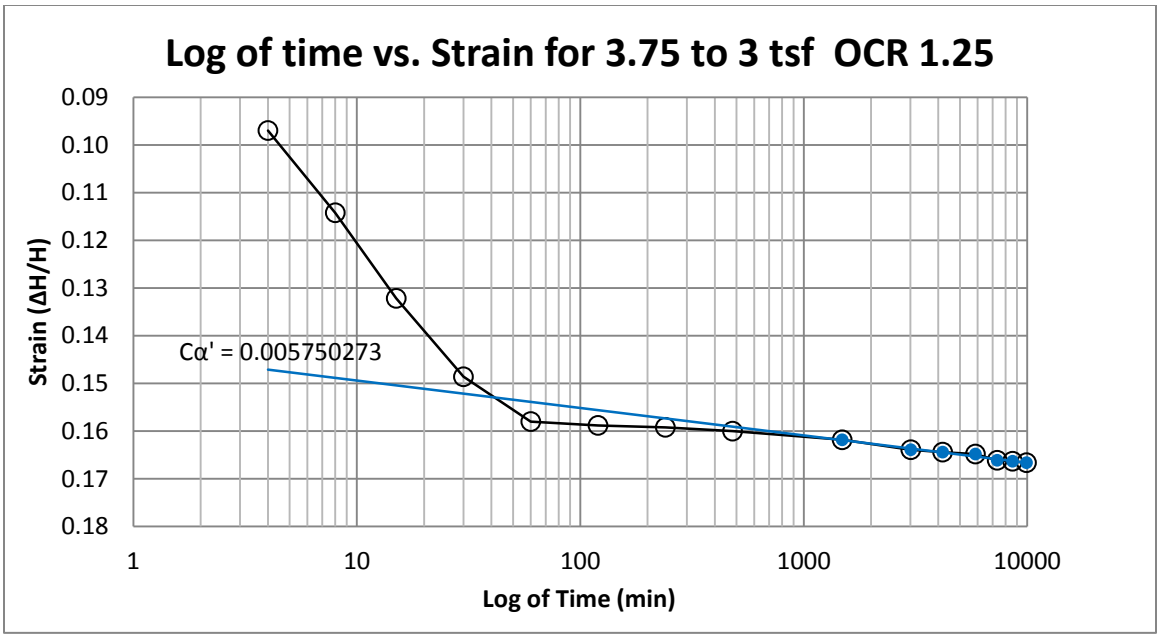

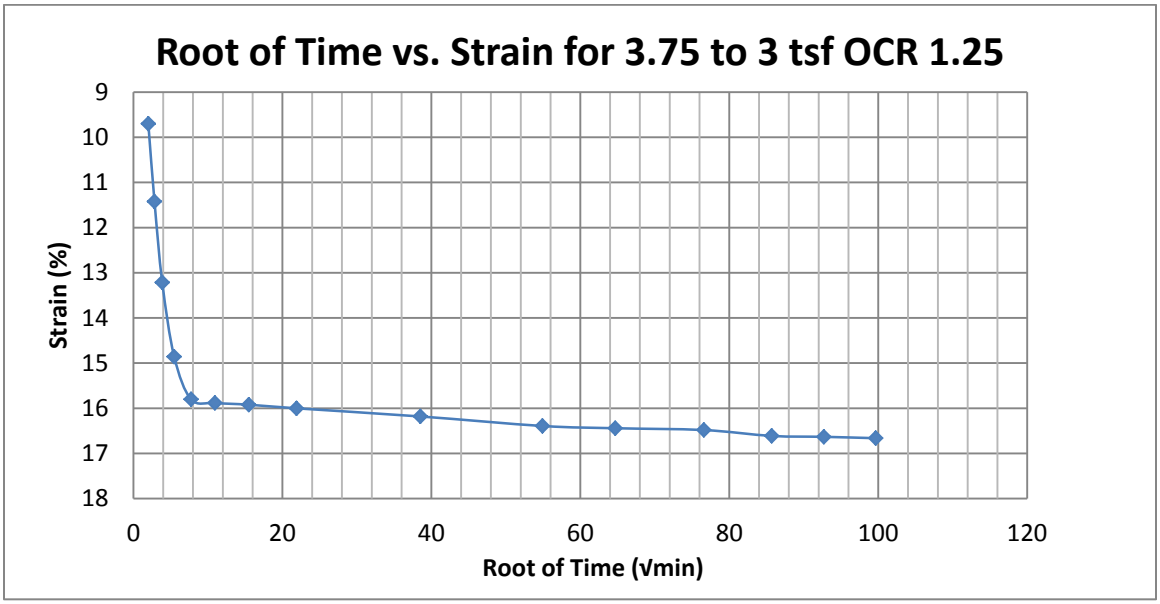

B18 400 South at 37.5-39.5 feet

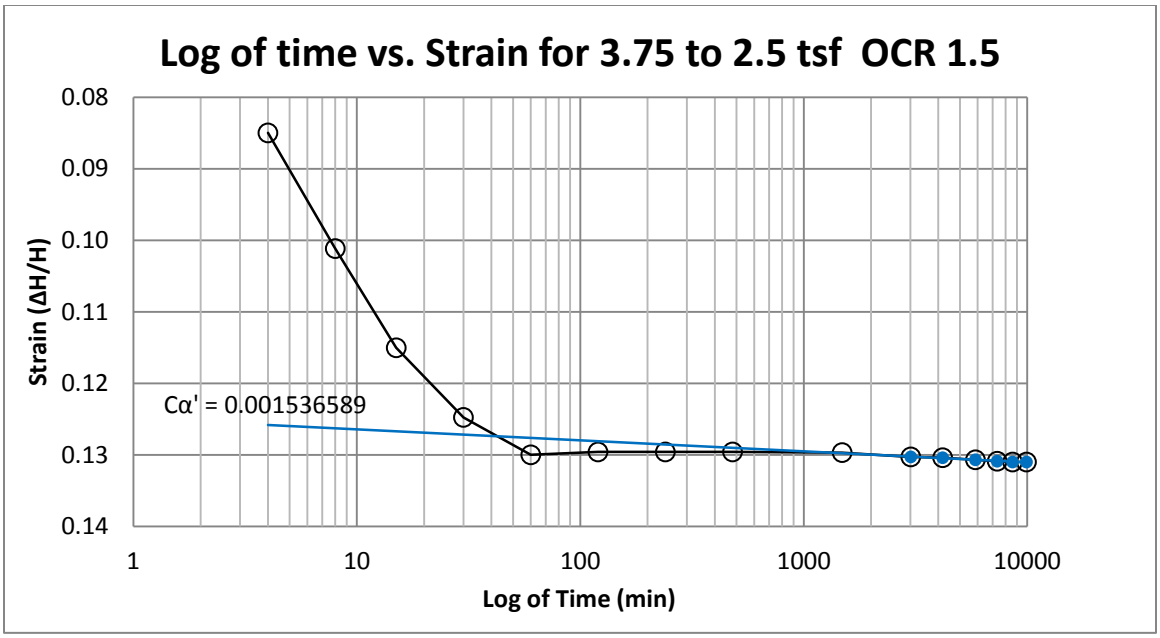

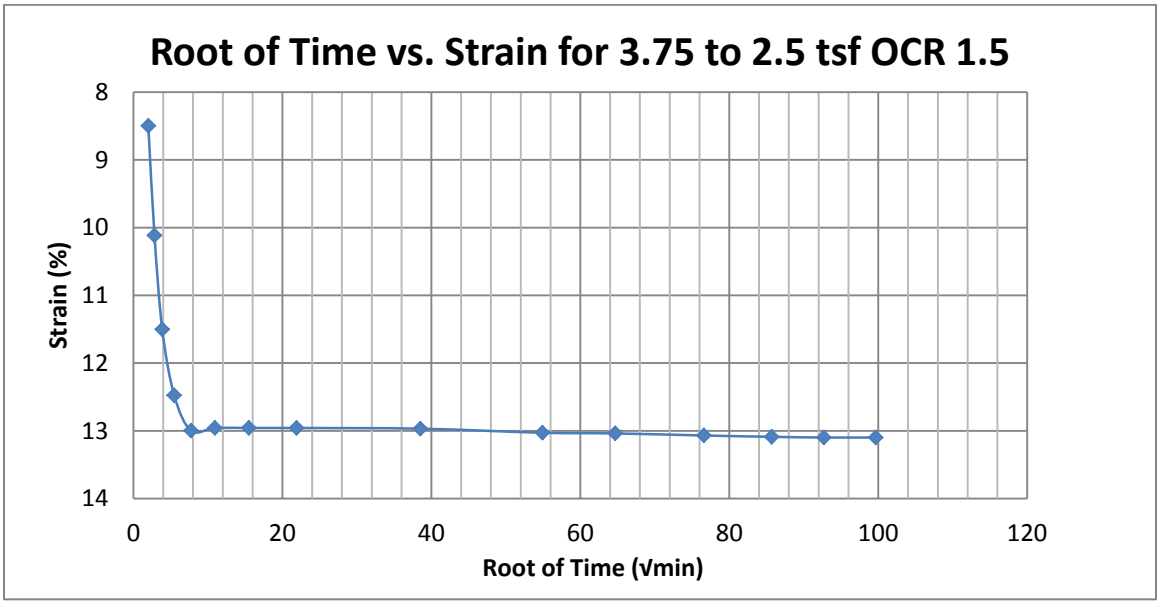

B19 400 South at 37.5-39.5 feet

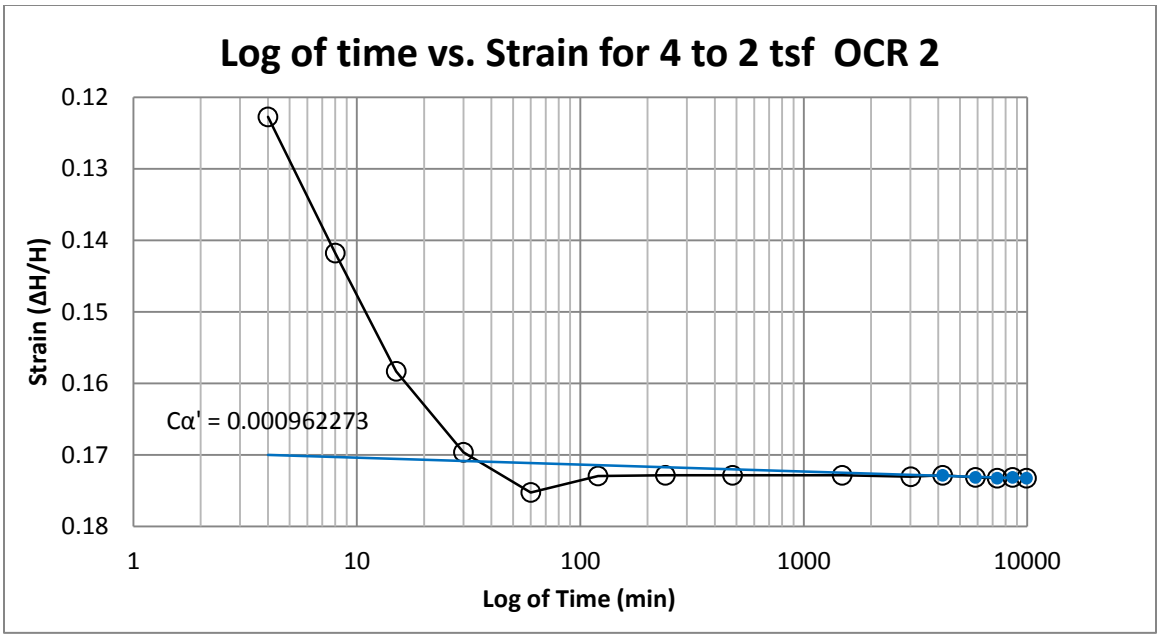

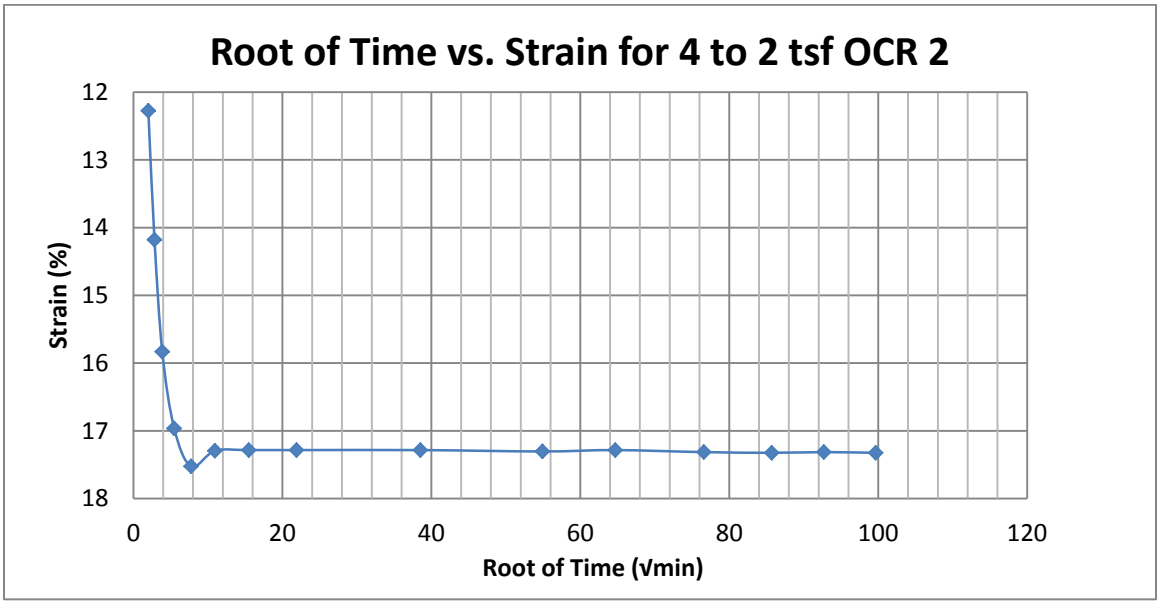

B20 400 South at 37.5-39.5 feet

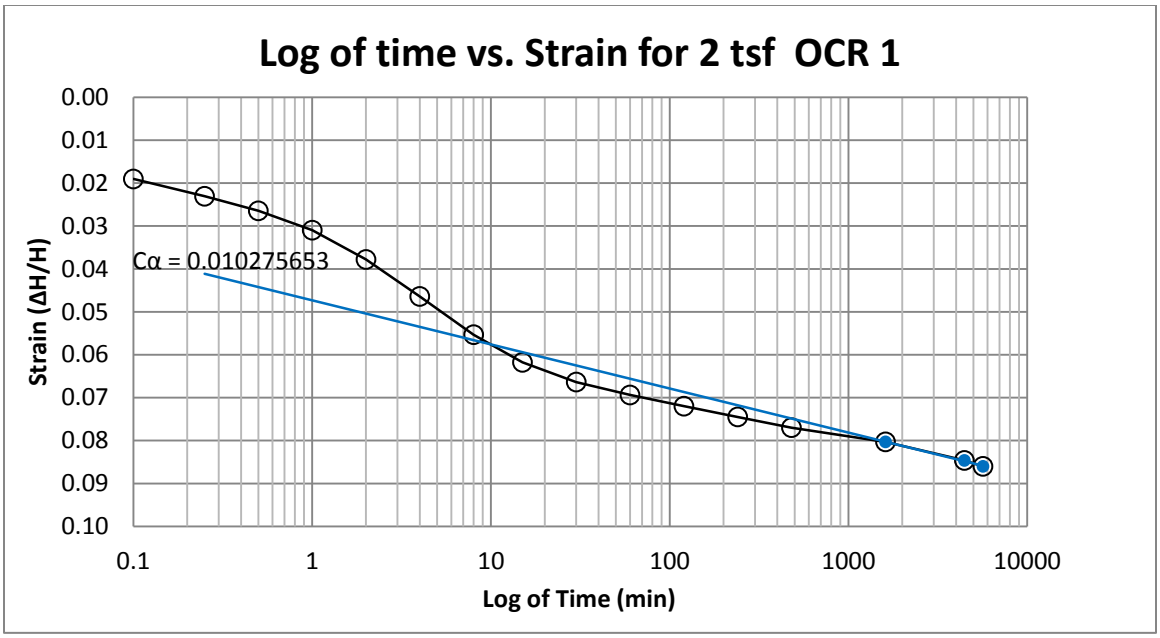

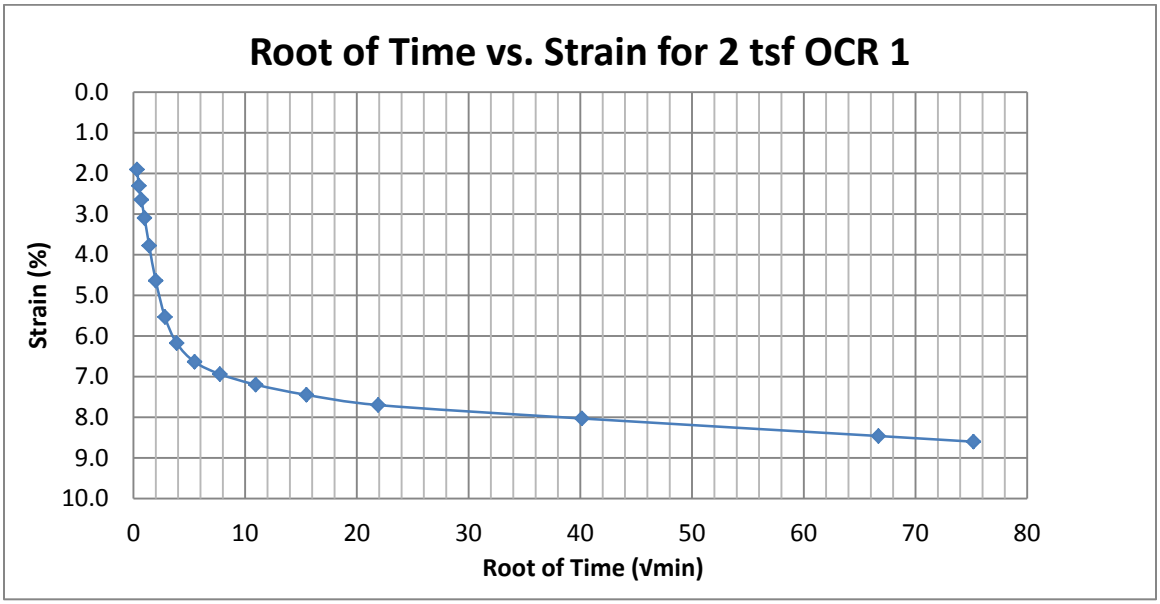

B21 400 South at 40-42 feet

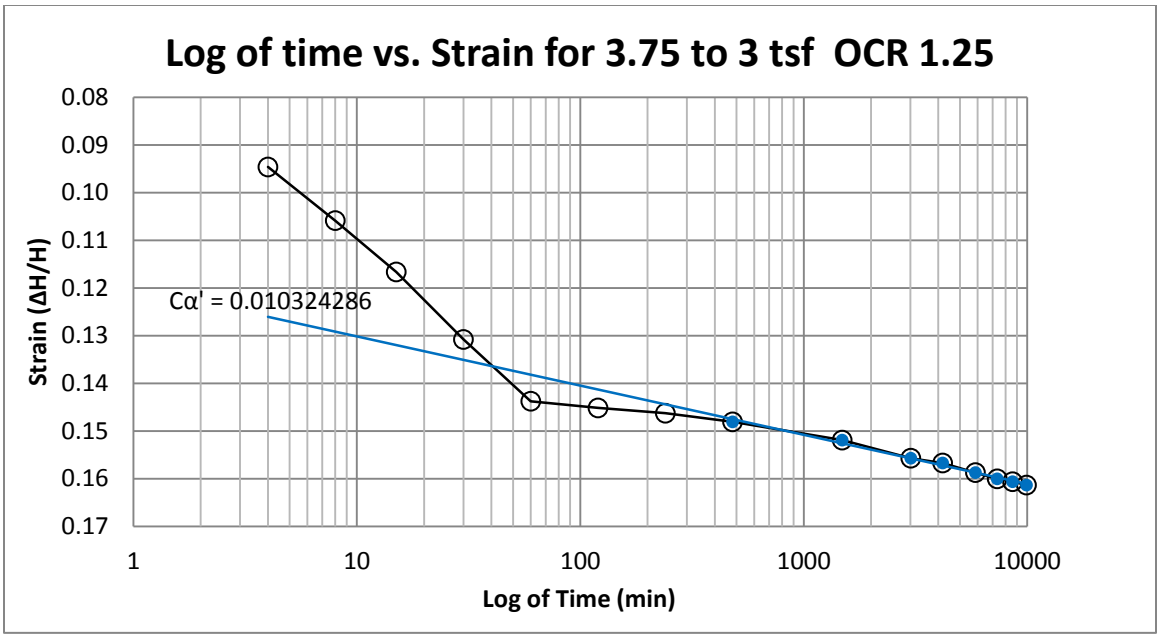

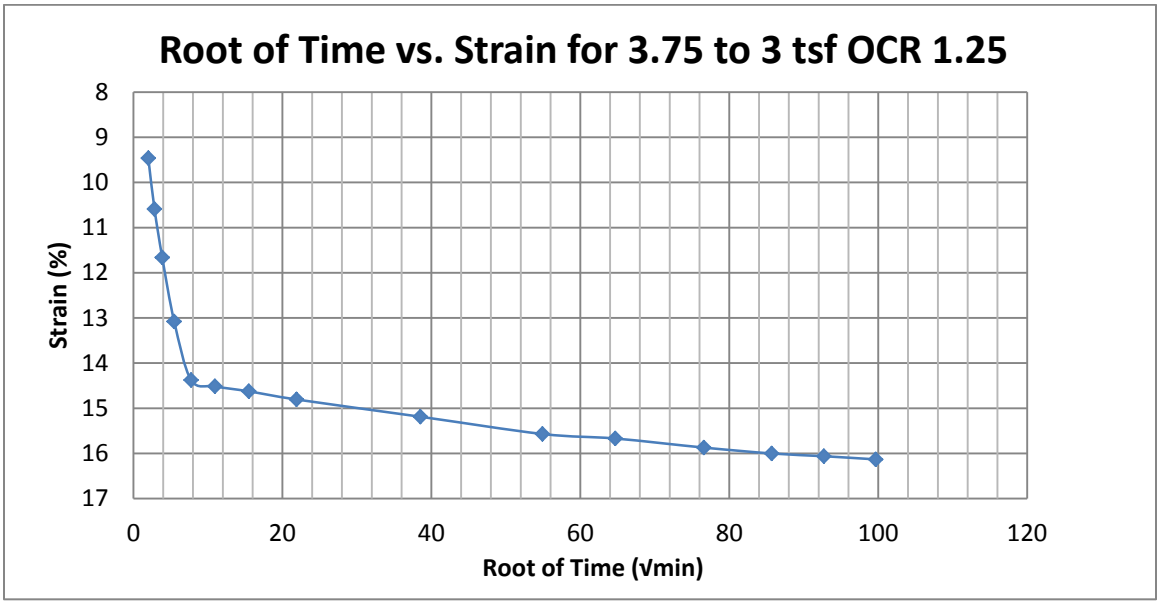

B22 400 South at 40-42 feet

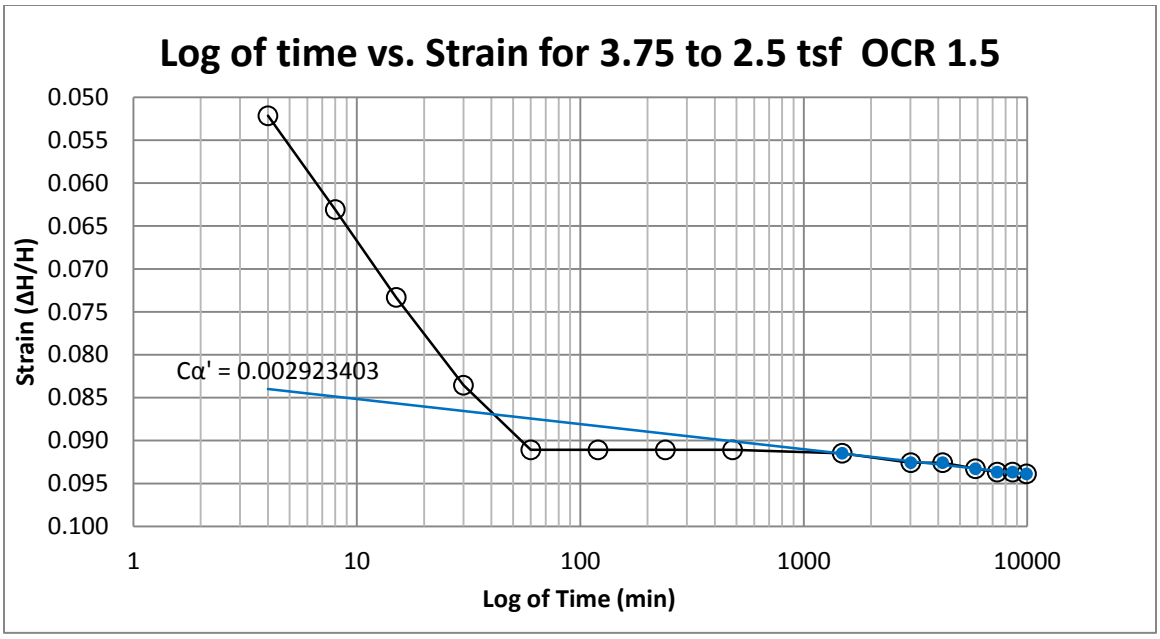

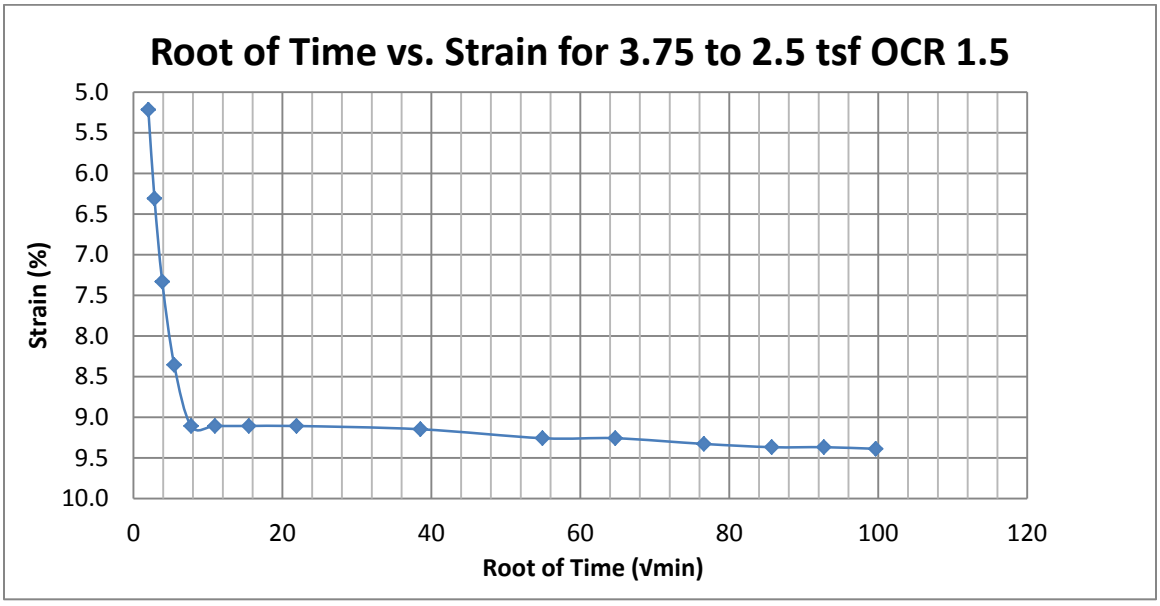

B23 400 South at 40-42 feet

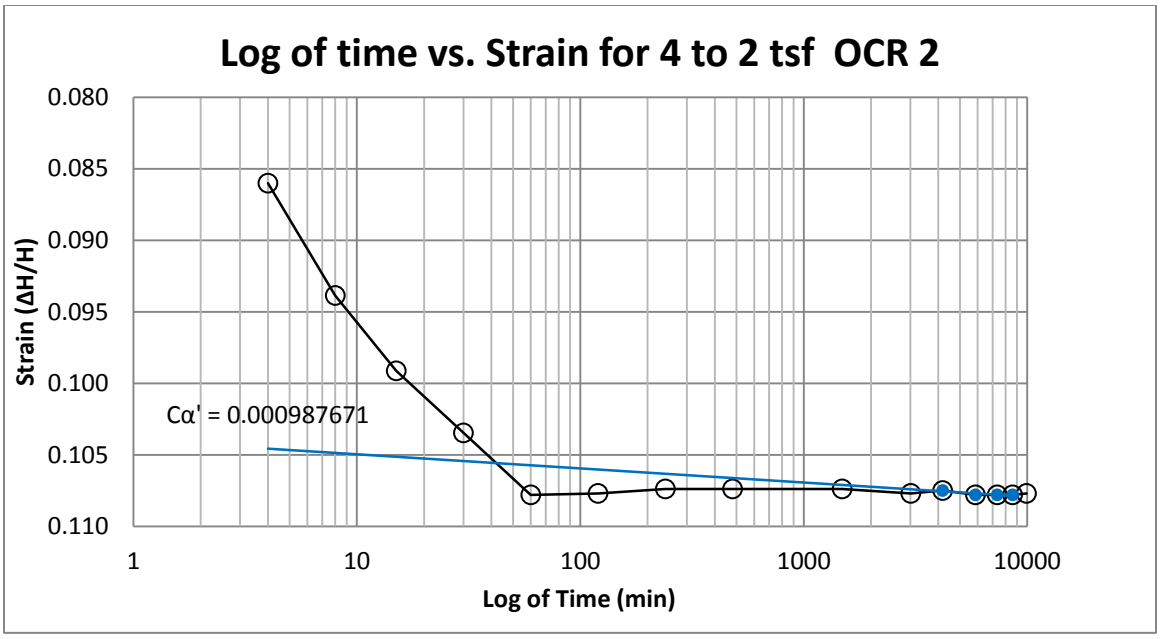

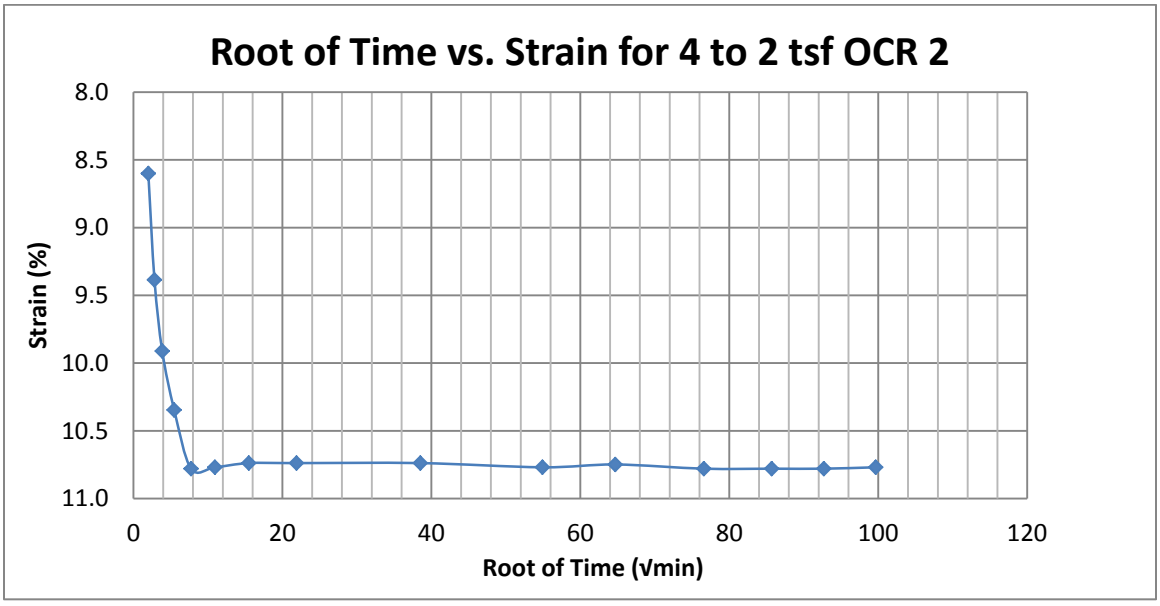

B24 400 South at 40-42 feet

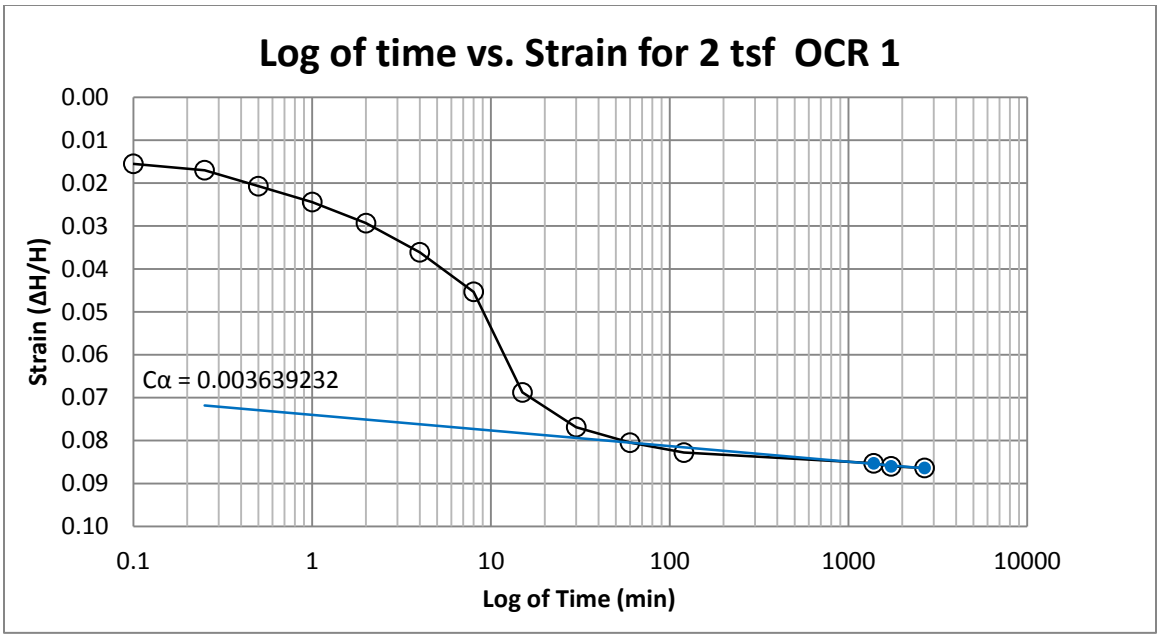

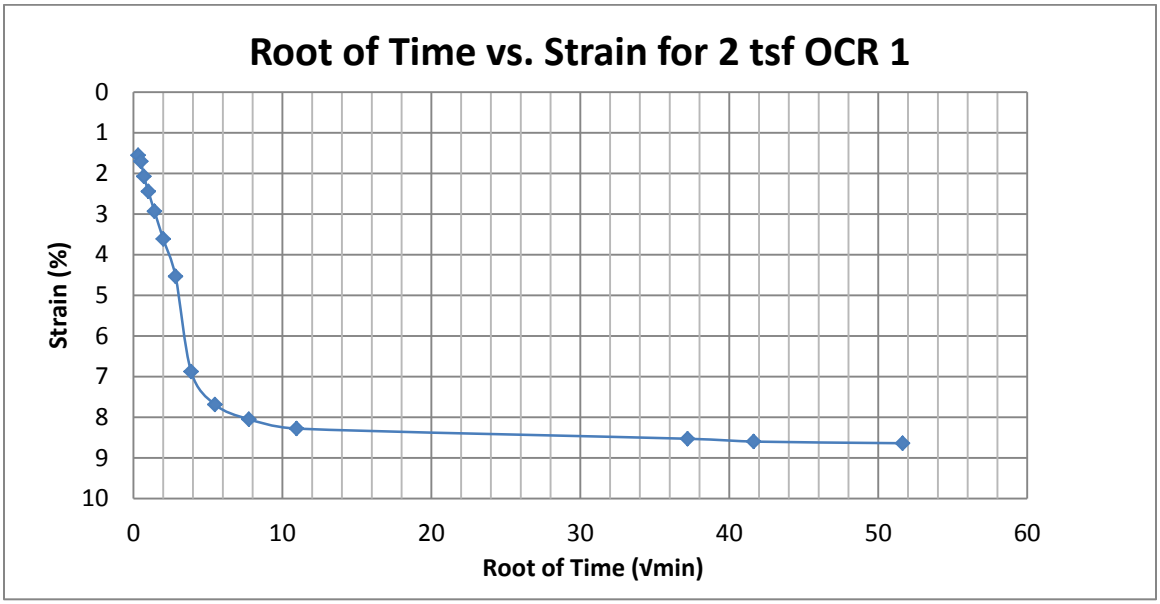

B25 400 South at 45-47 feet

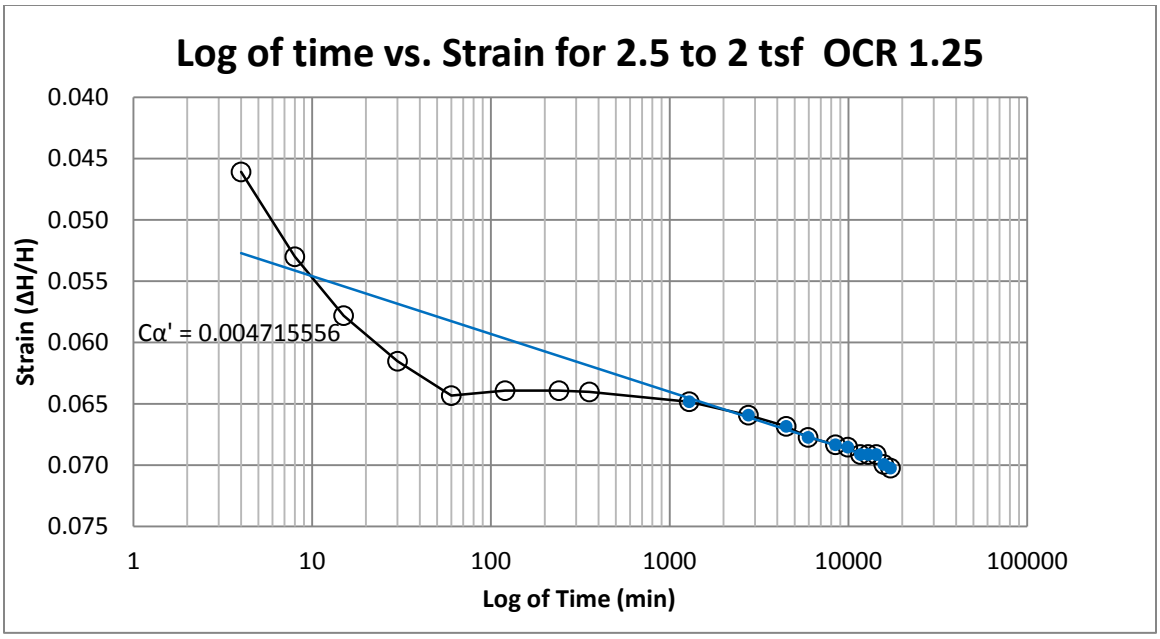

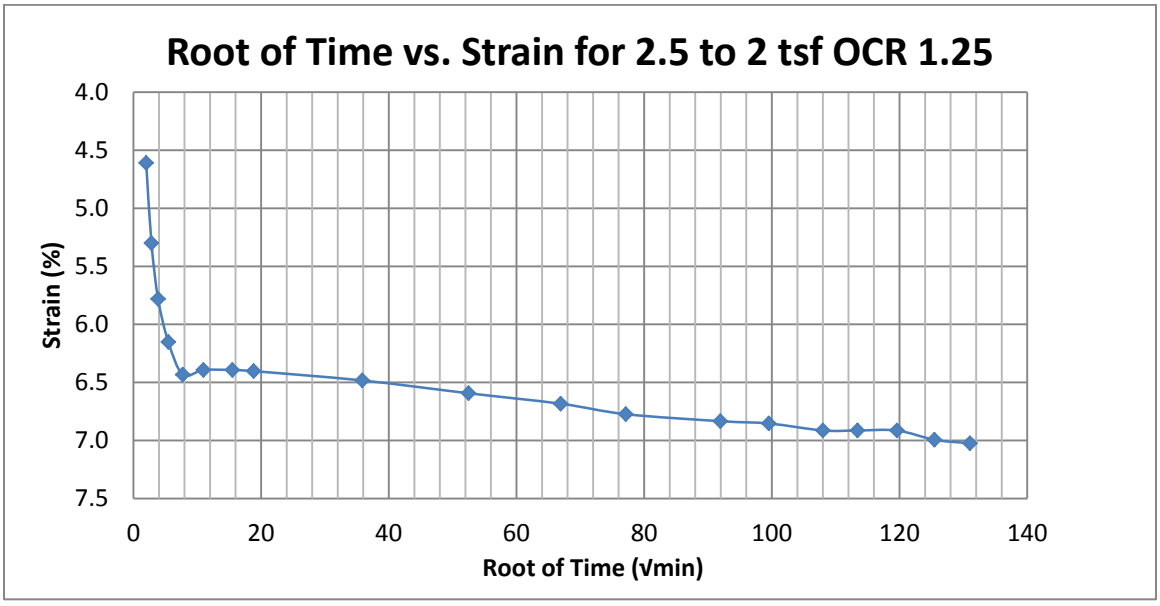

B26 400 South at 45-47 feet

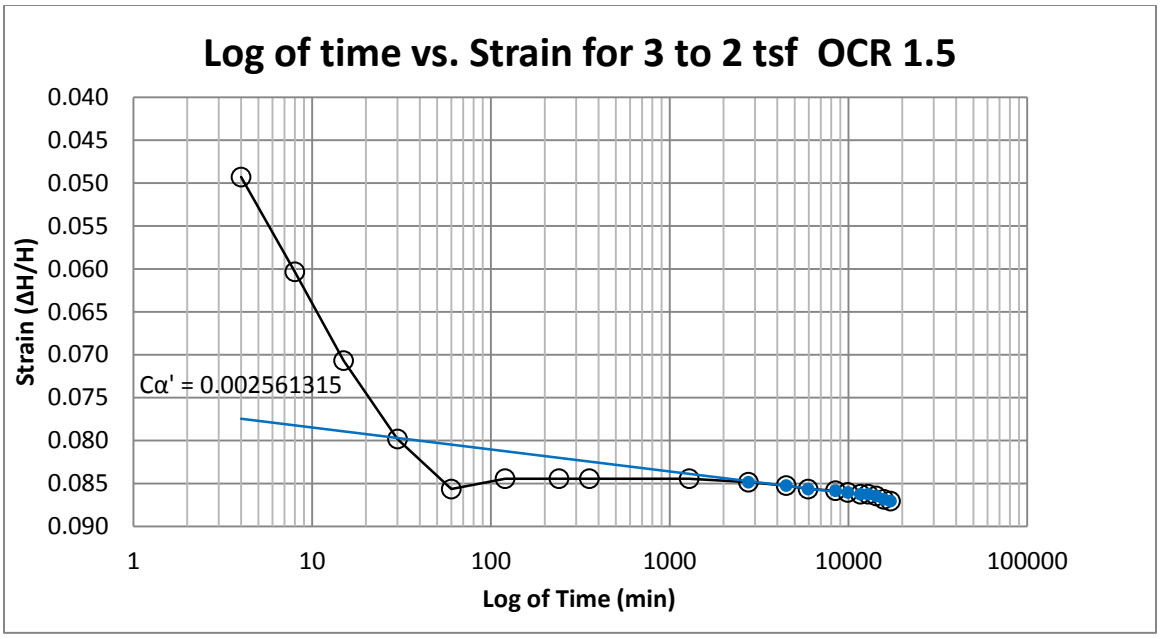

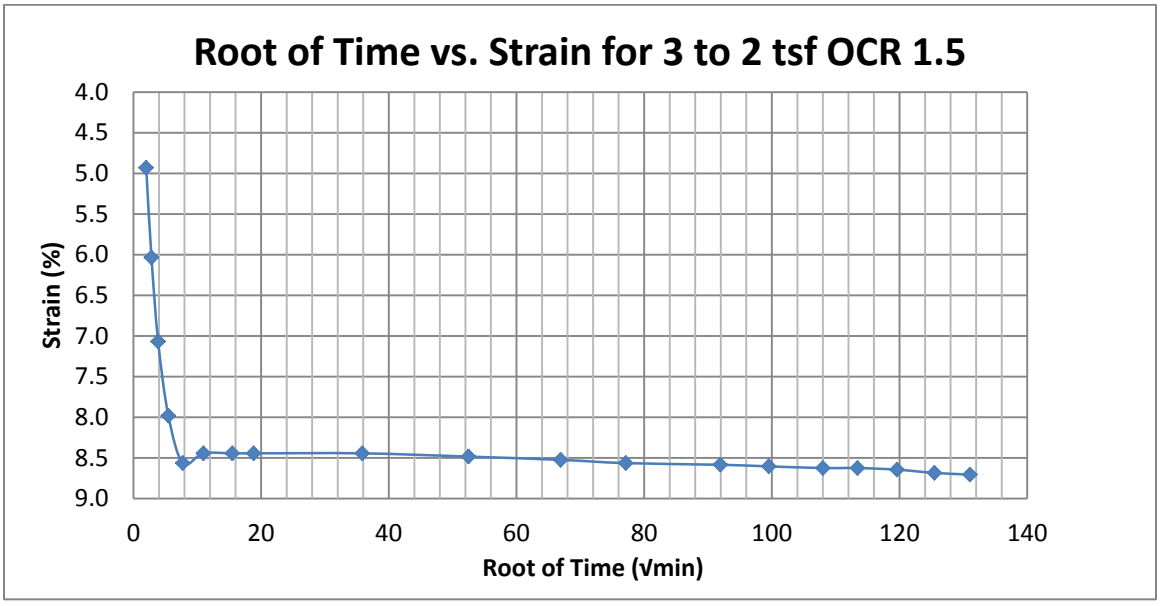

B27 400 South at 45-47 feet

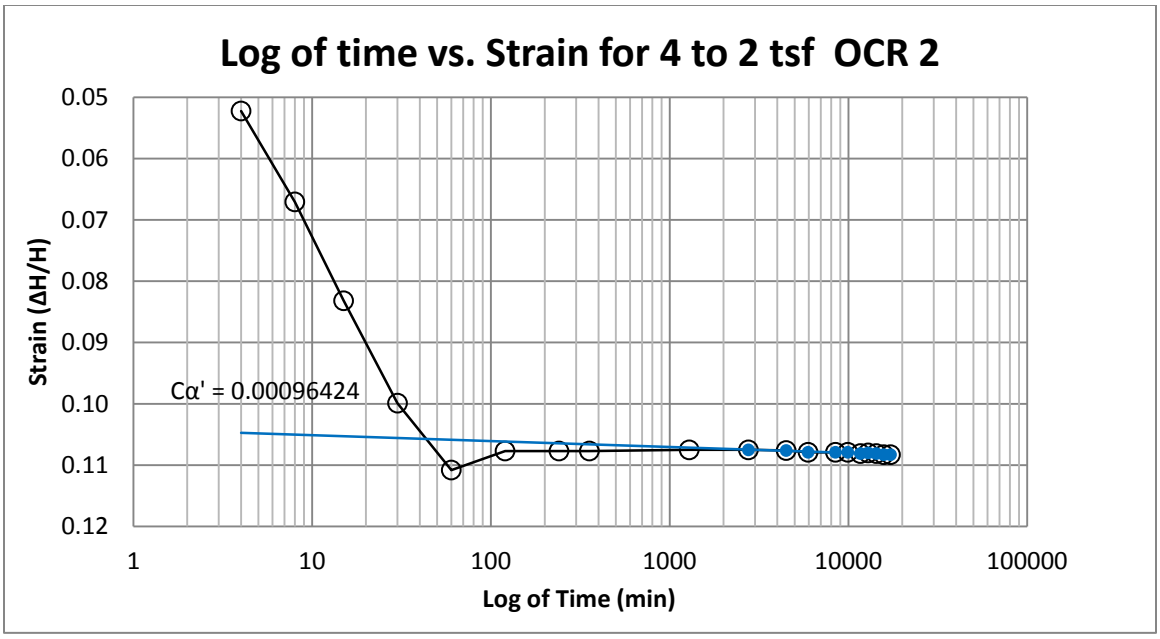

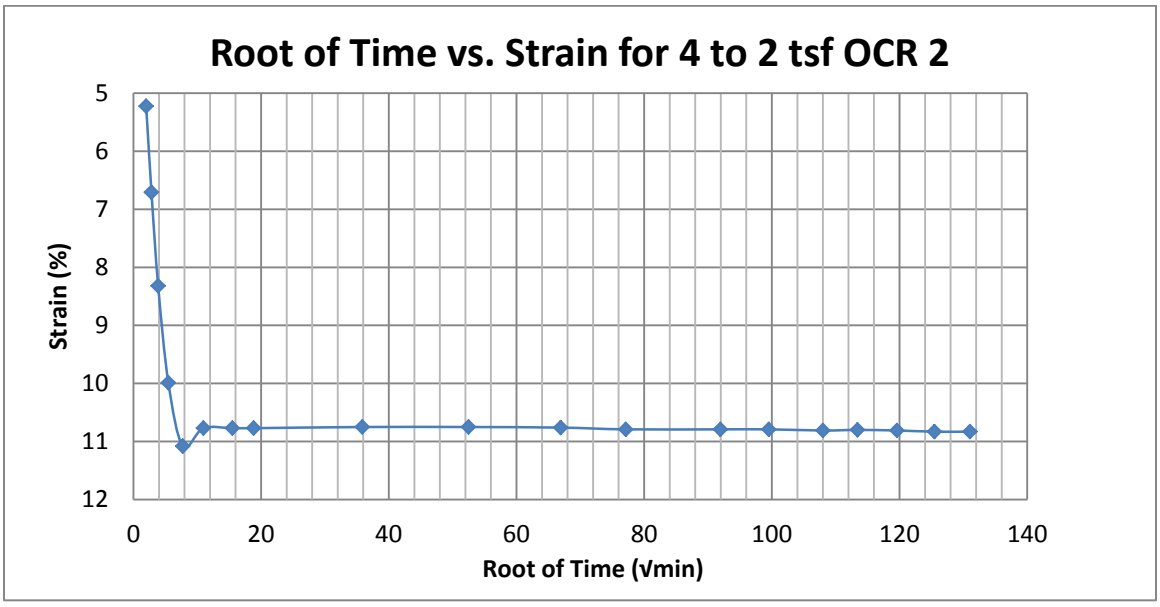

B28 400 South at 45-47 feet

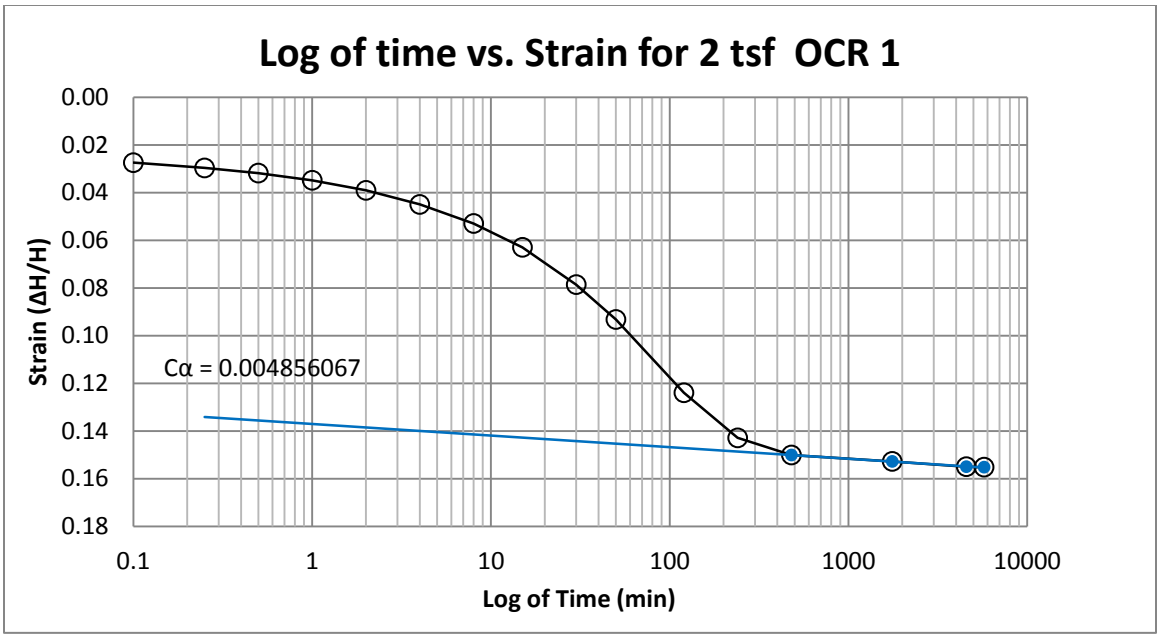

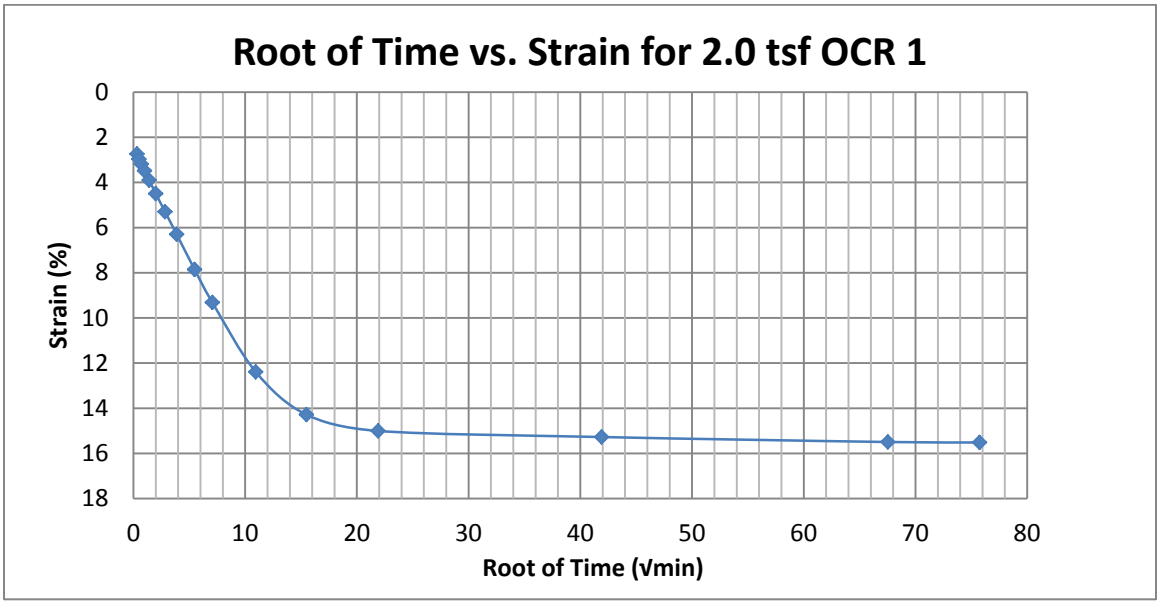

B29 400 South at 50-52 feet

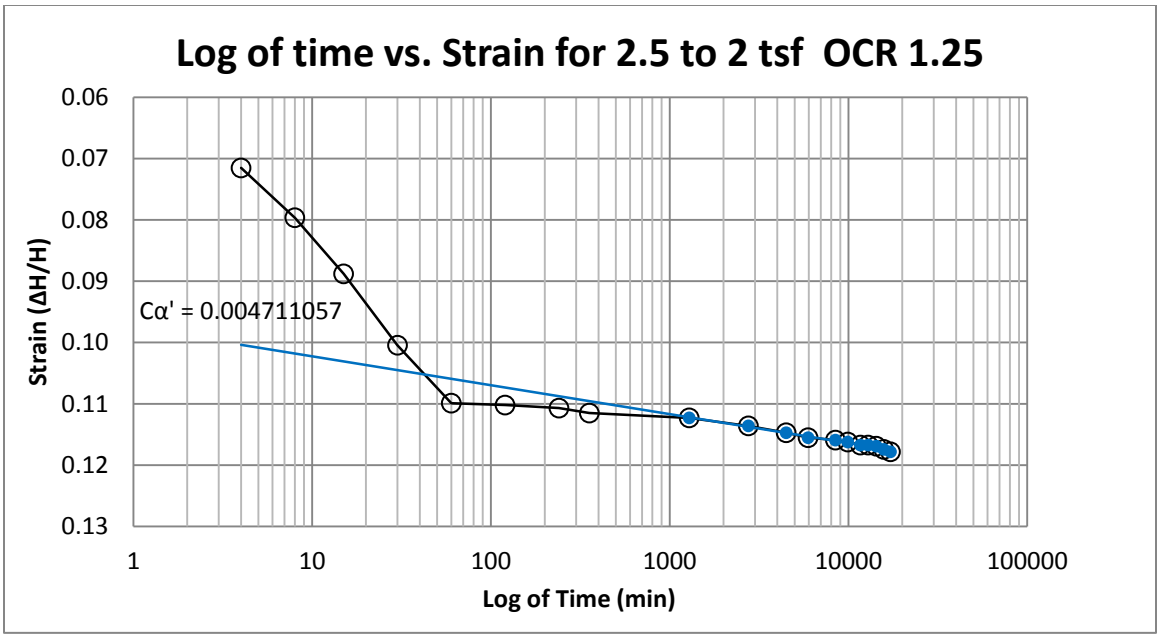

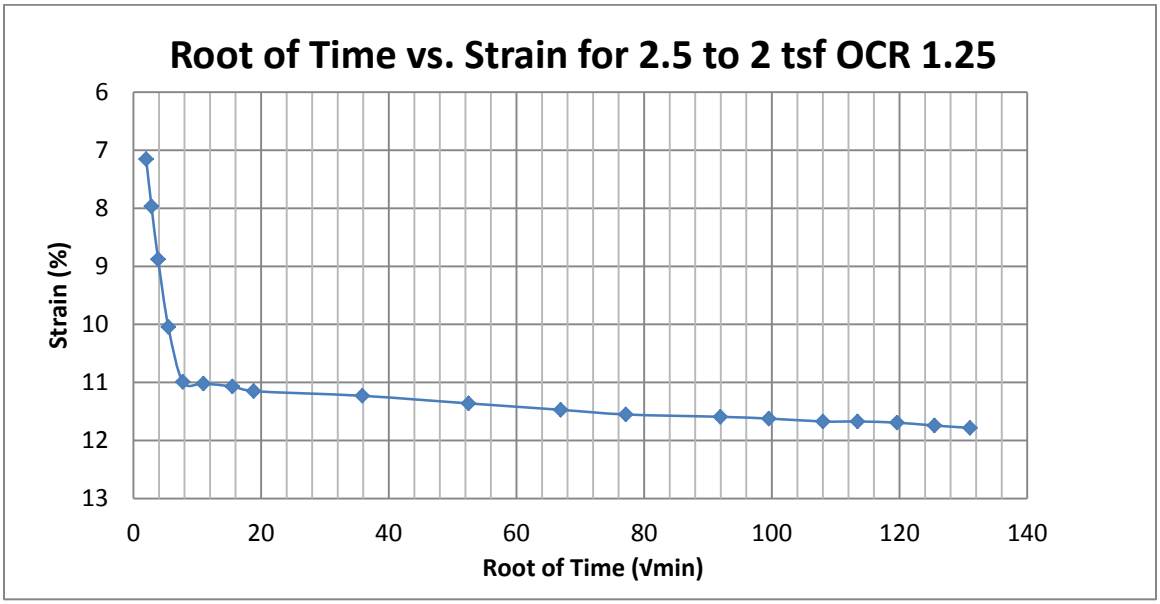

B30 400 South at 50-52 feet

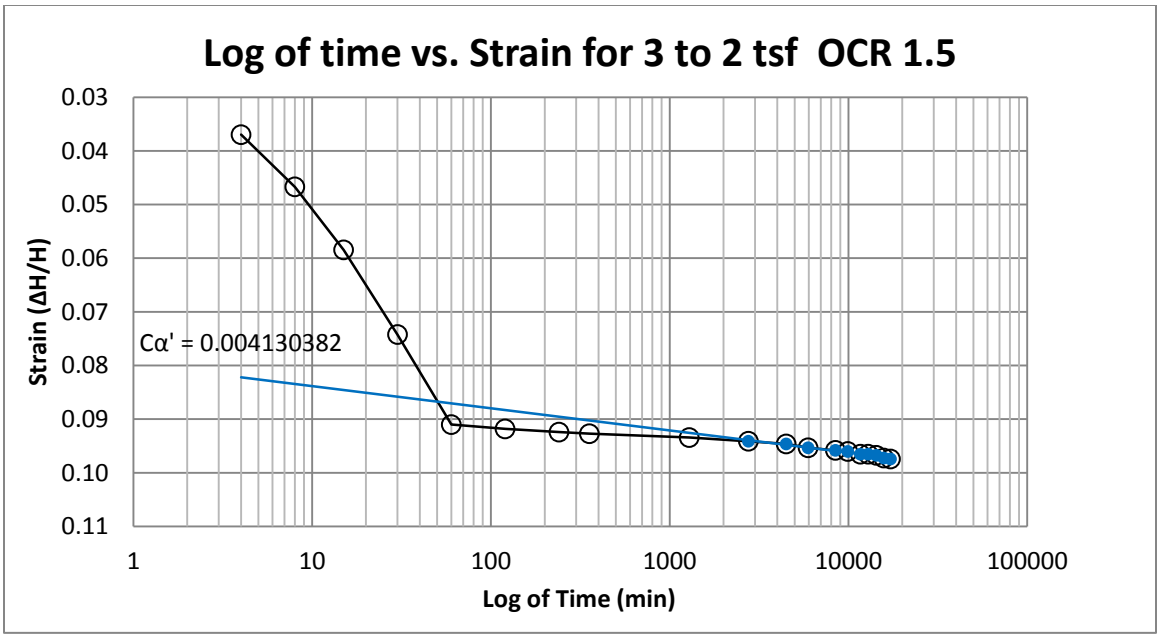

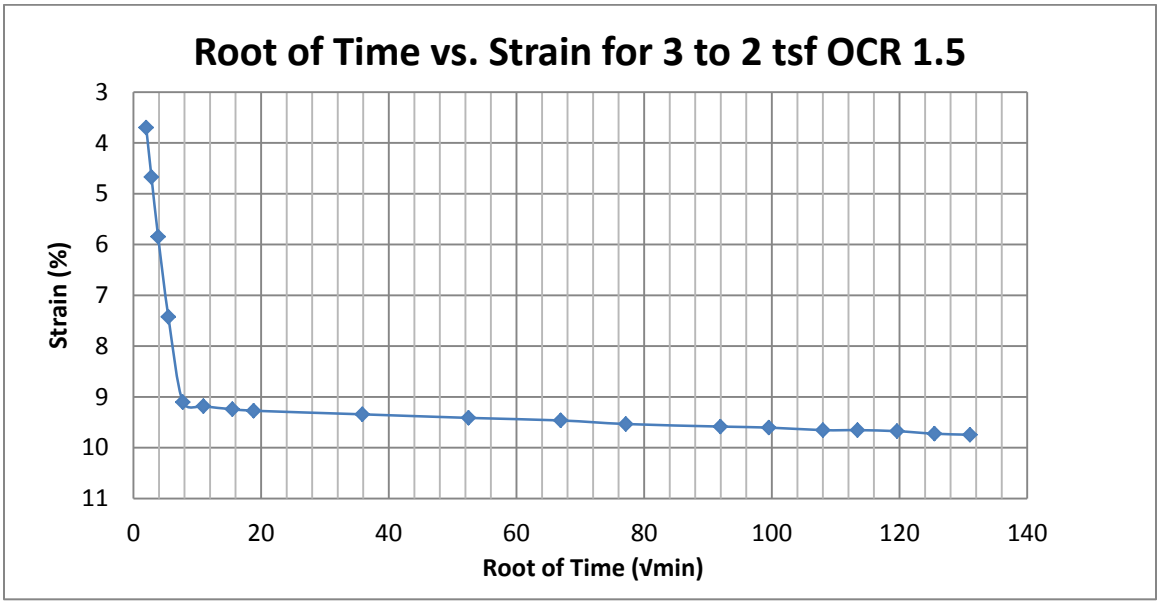

B31 400 South at 50-52 feet

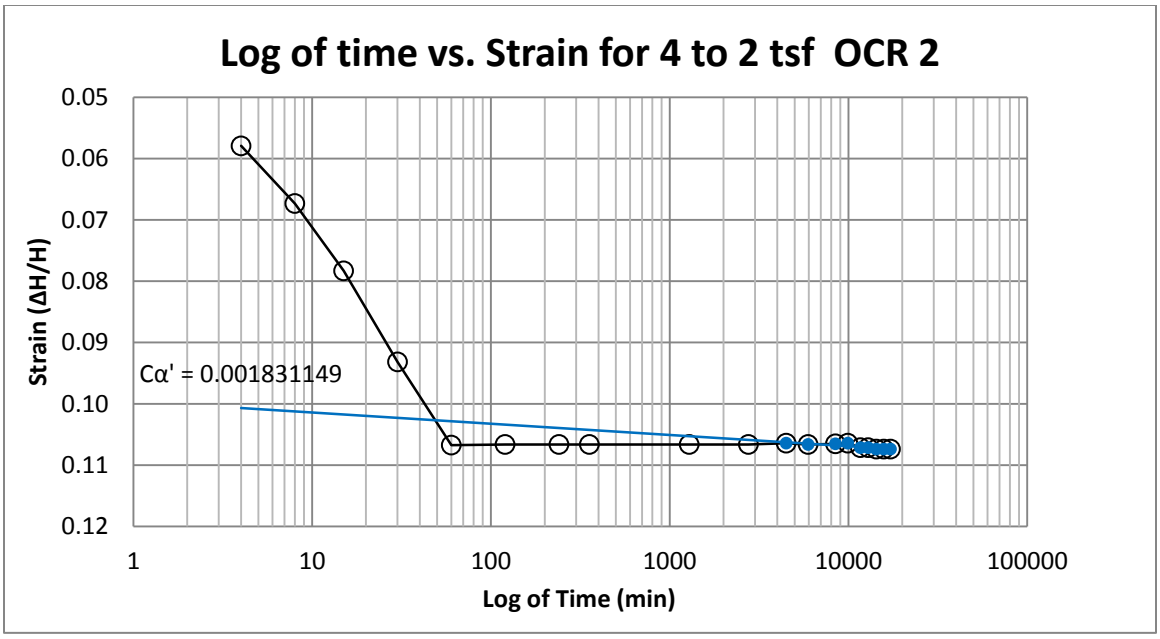

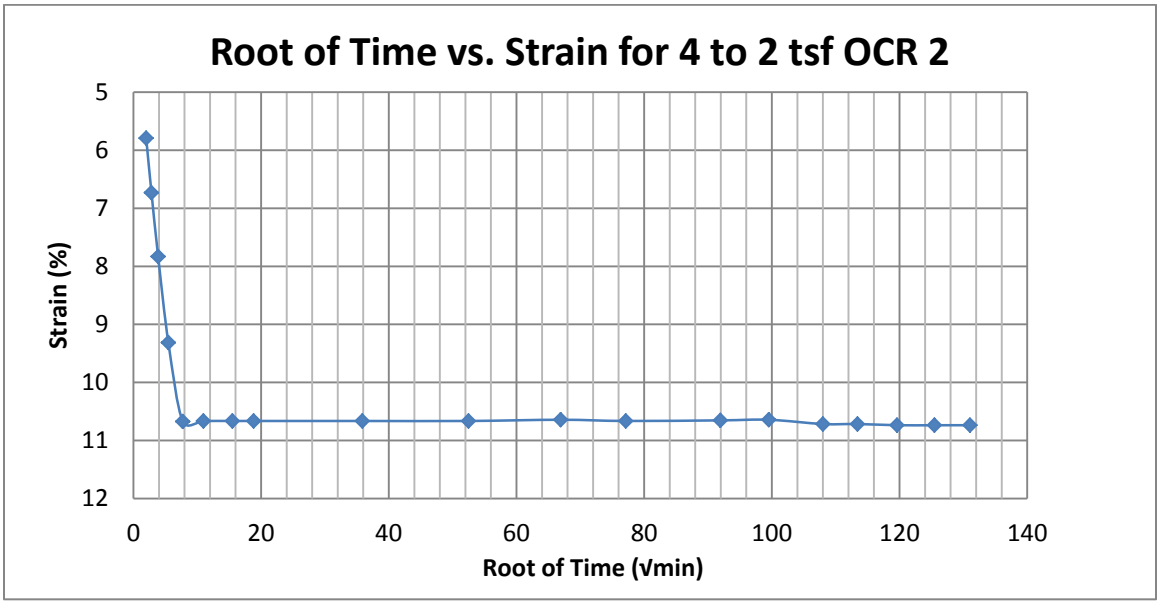

B32 400 South at 50-52 feet

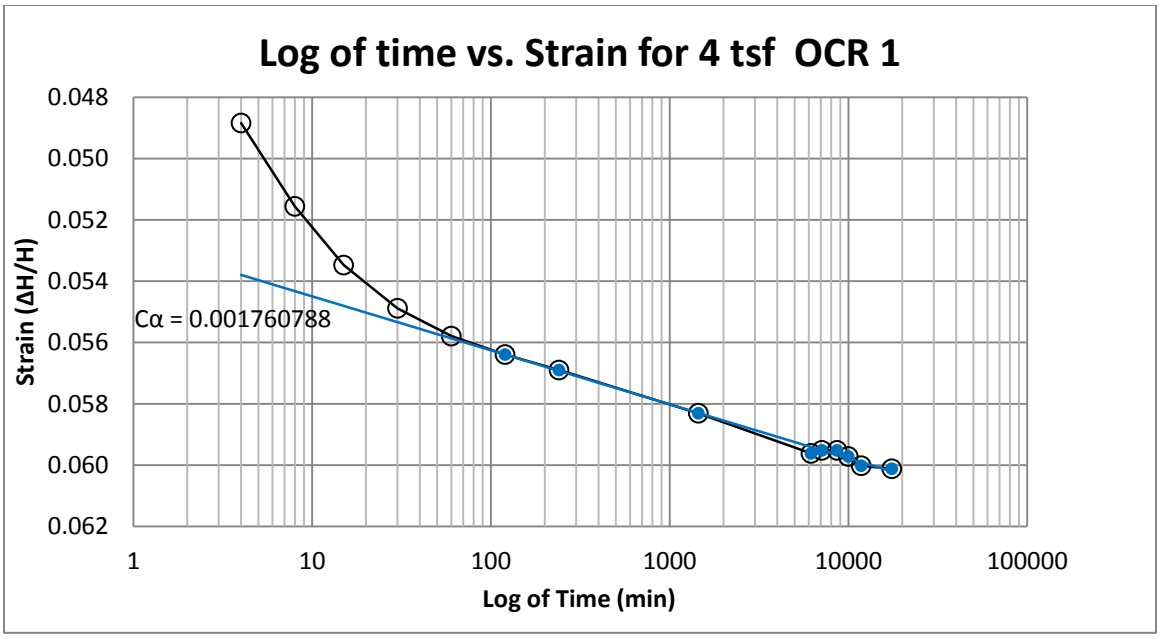

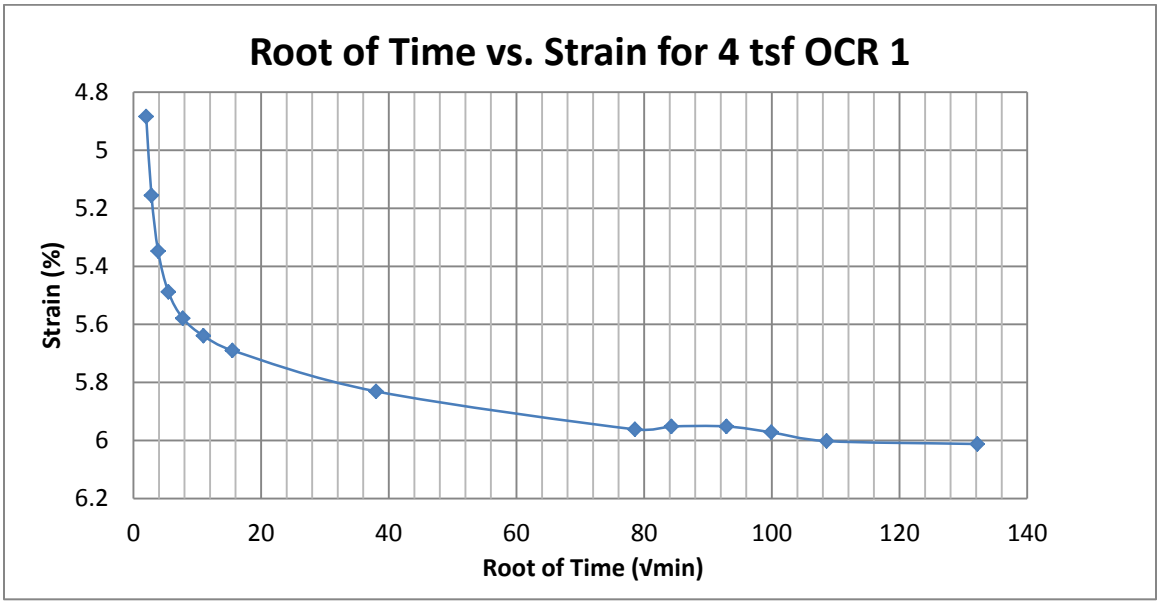

B33 Springville at 30-32 feet

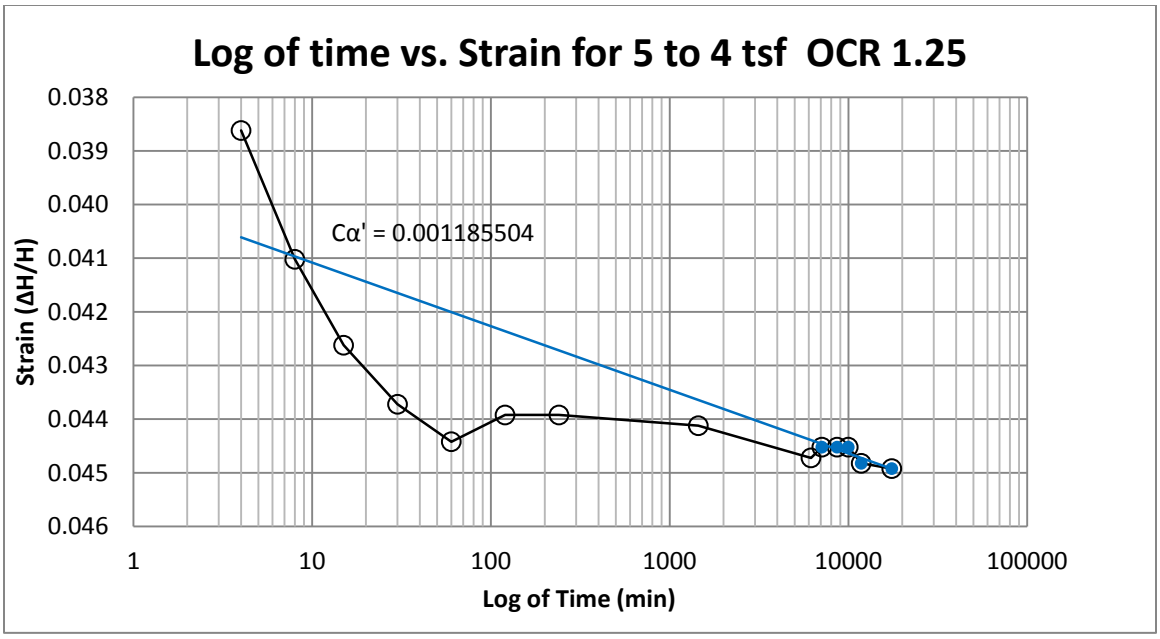

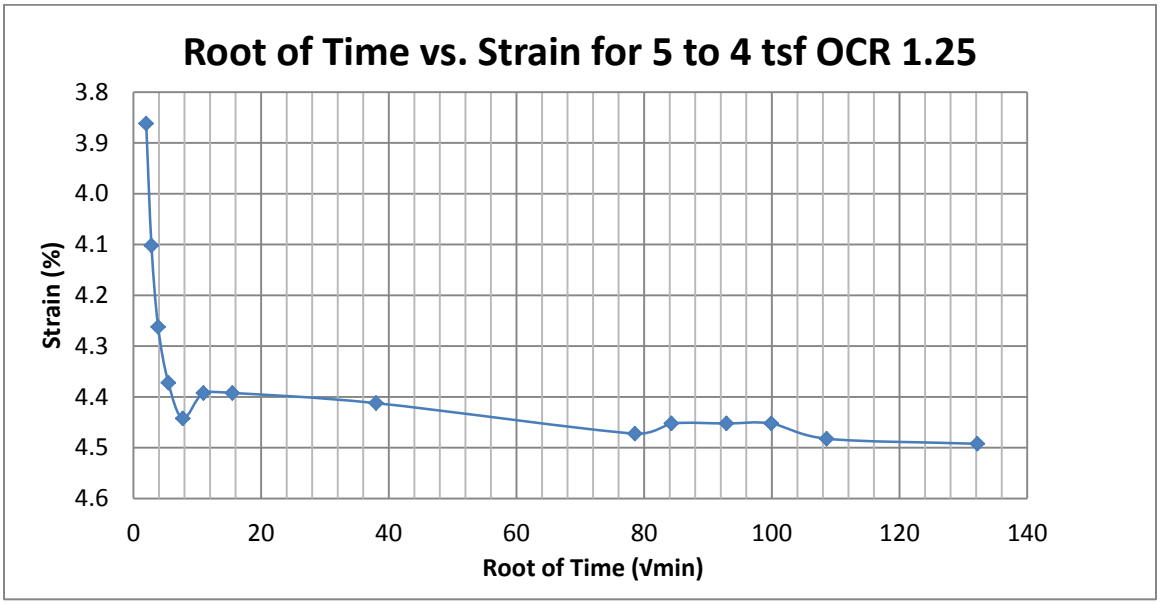

B34 Springville at 30-32 feet

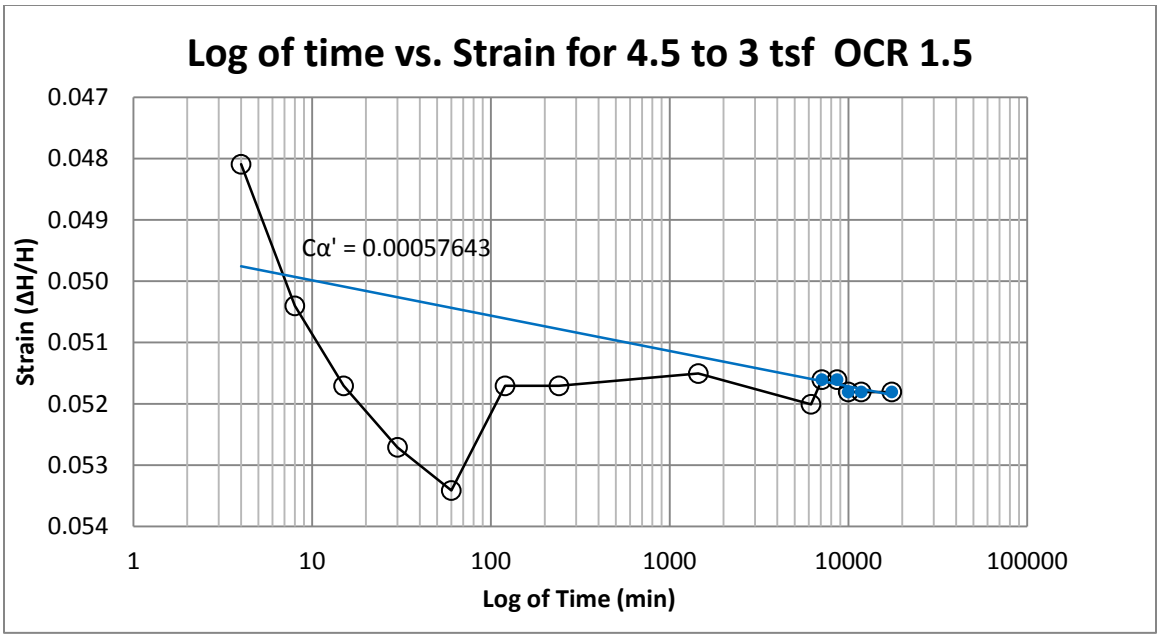

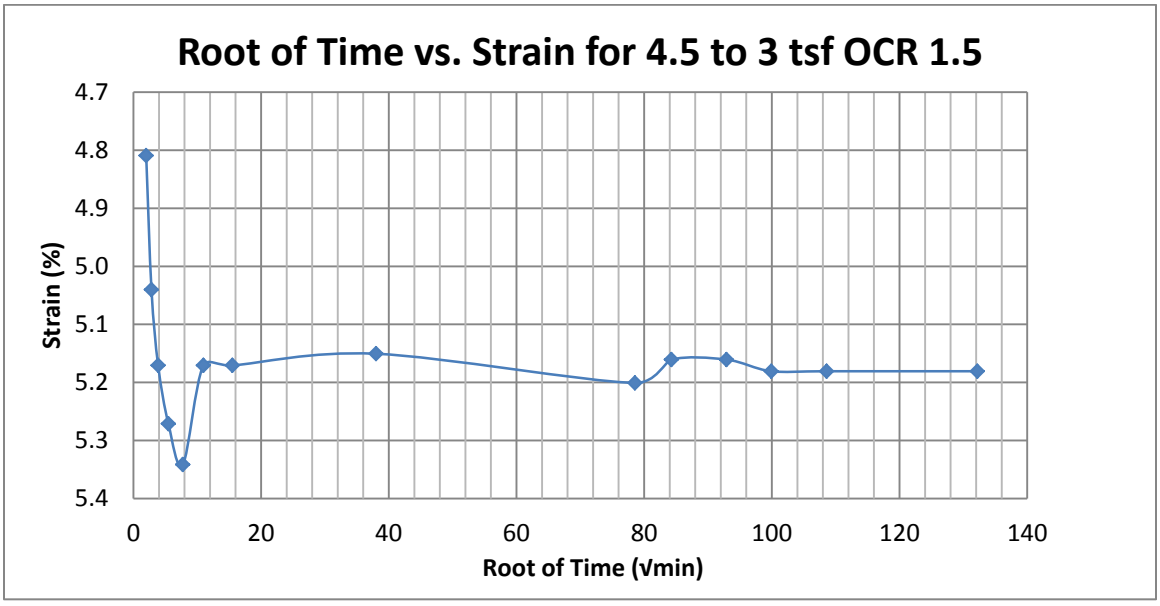

B 35 Springville at 30-32 feet

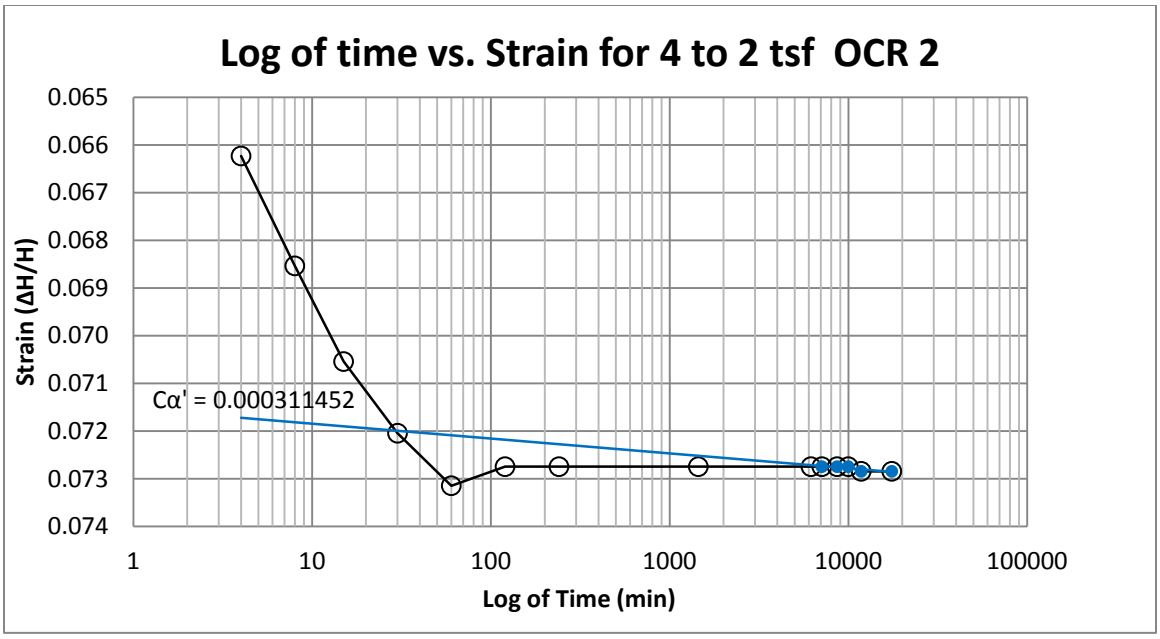

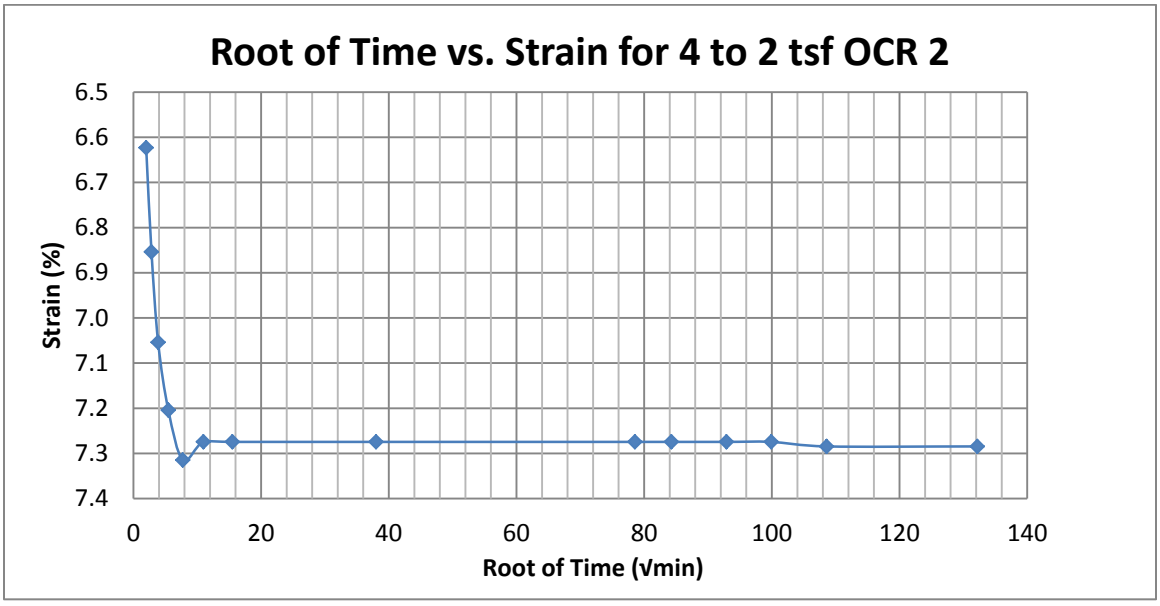

B36 Springville at 30-32 feet

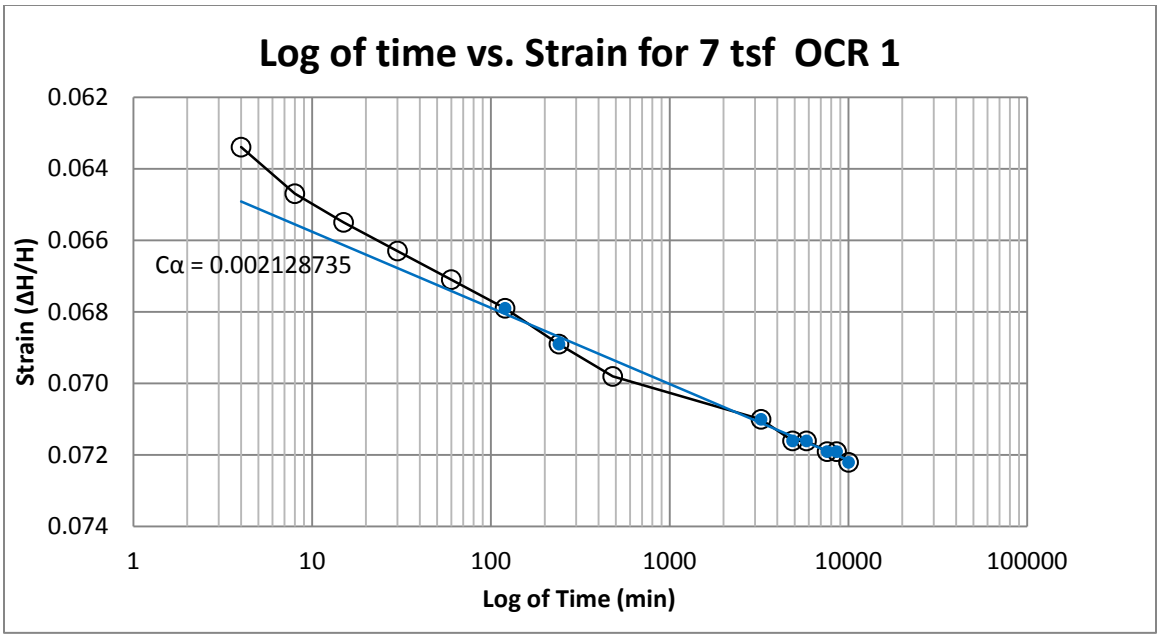

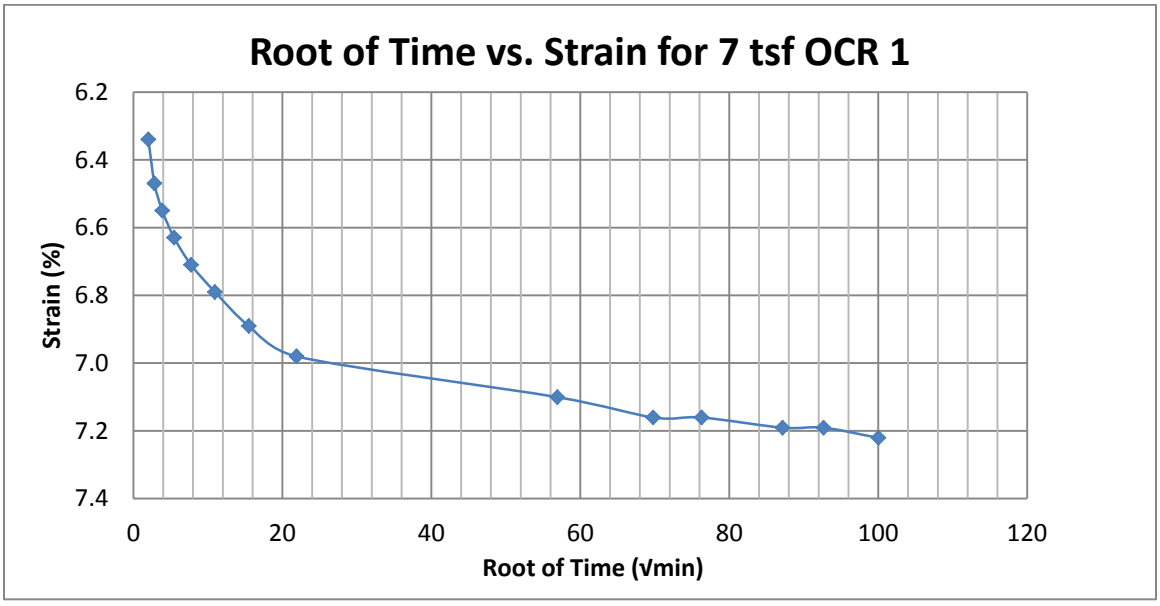

B 37 Springville at 40-42 feet

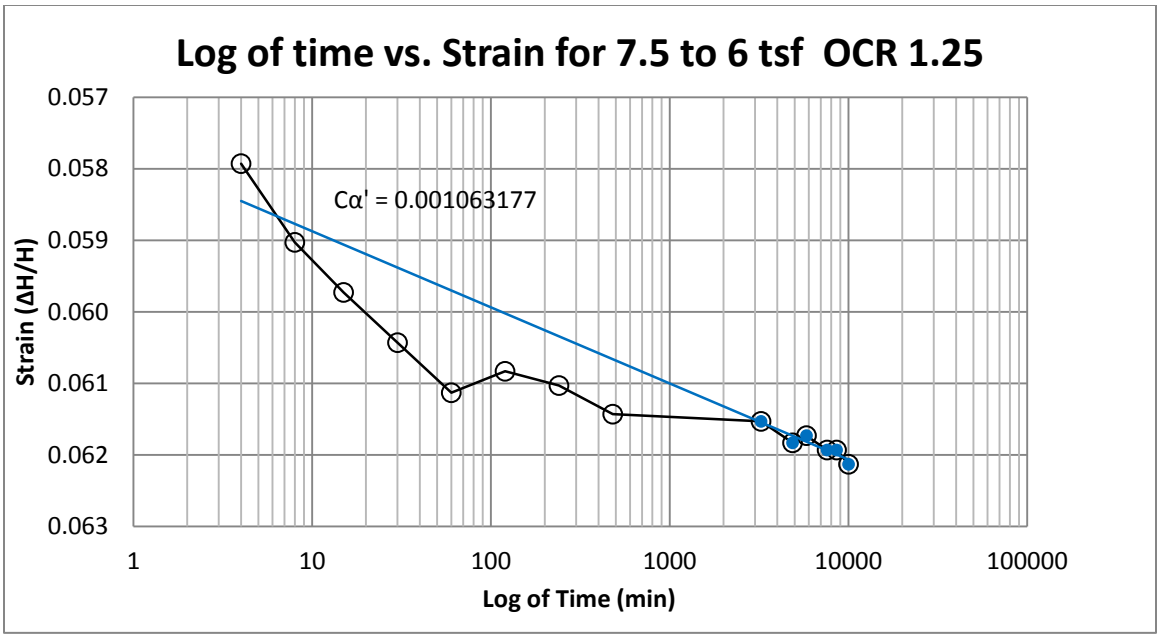

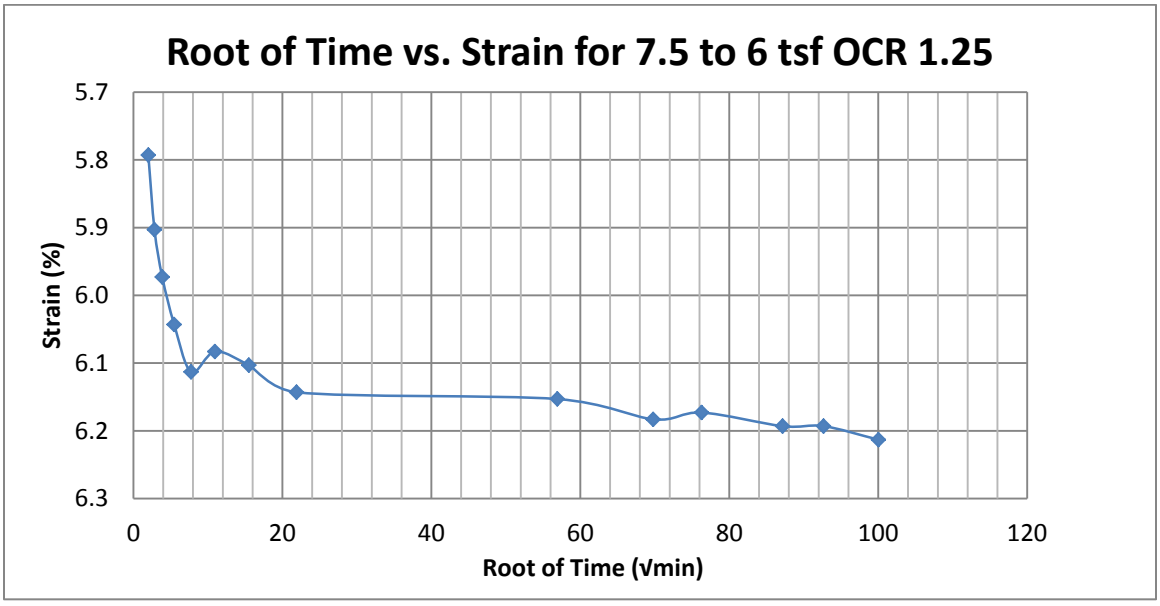

B38 Springville at 40-42 feet

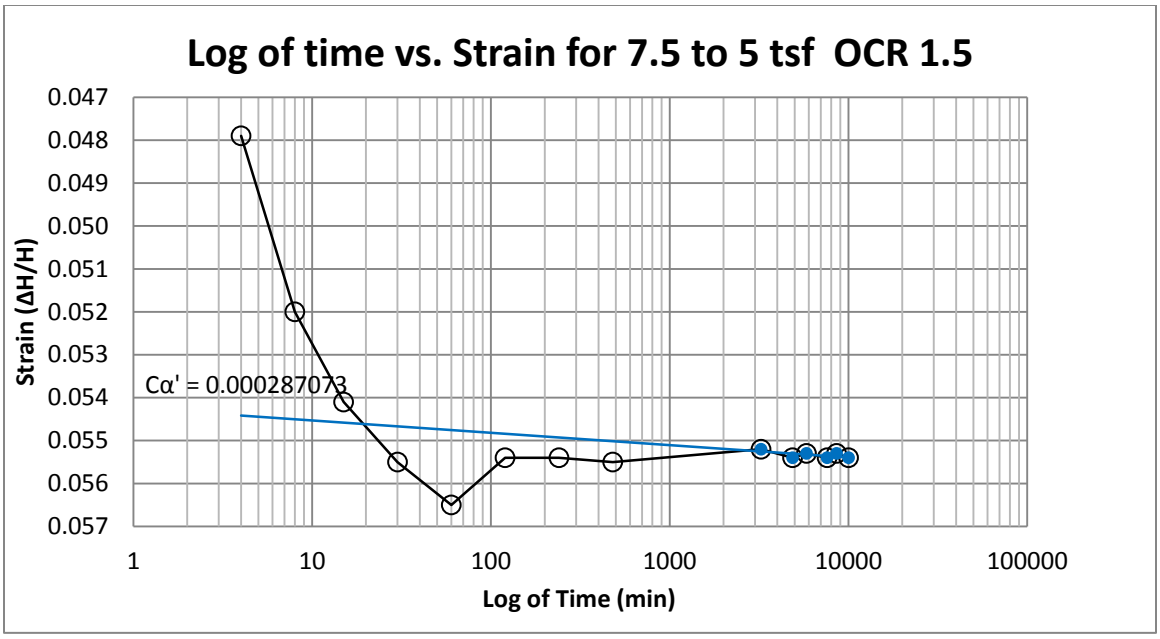

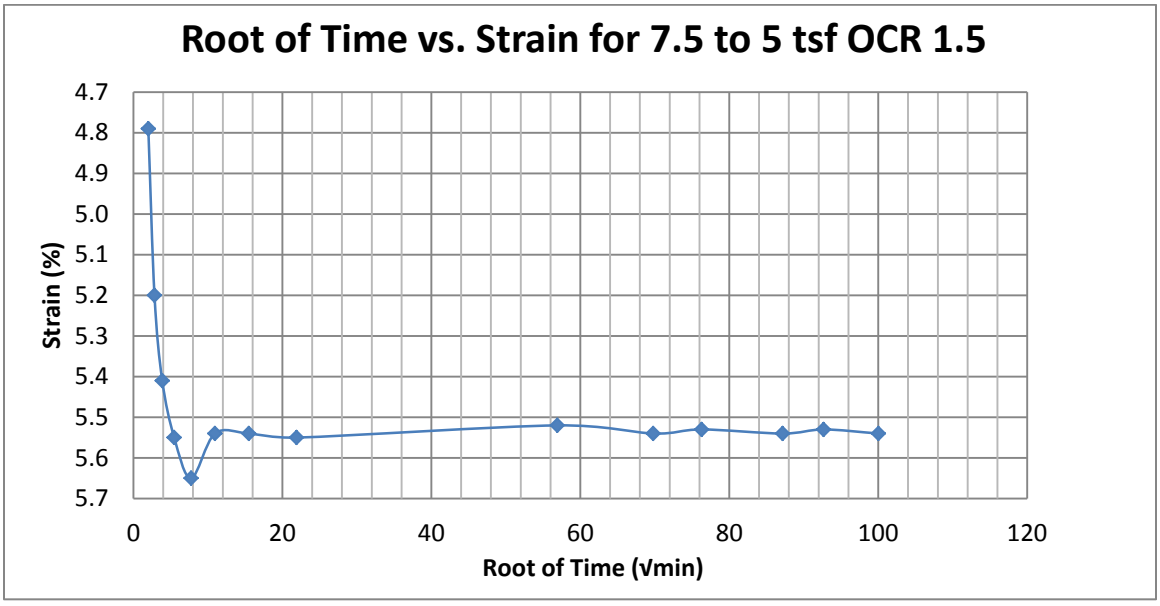

B39 Springville at 40-42 feet

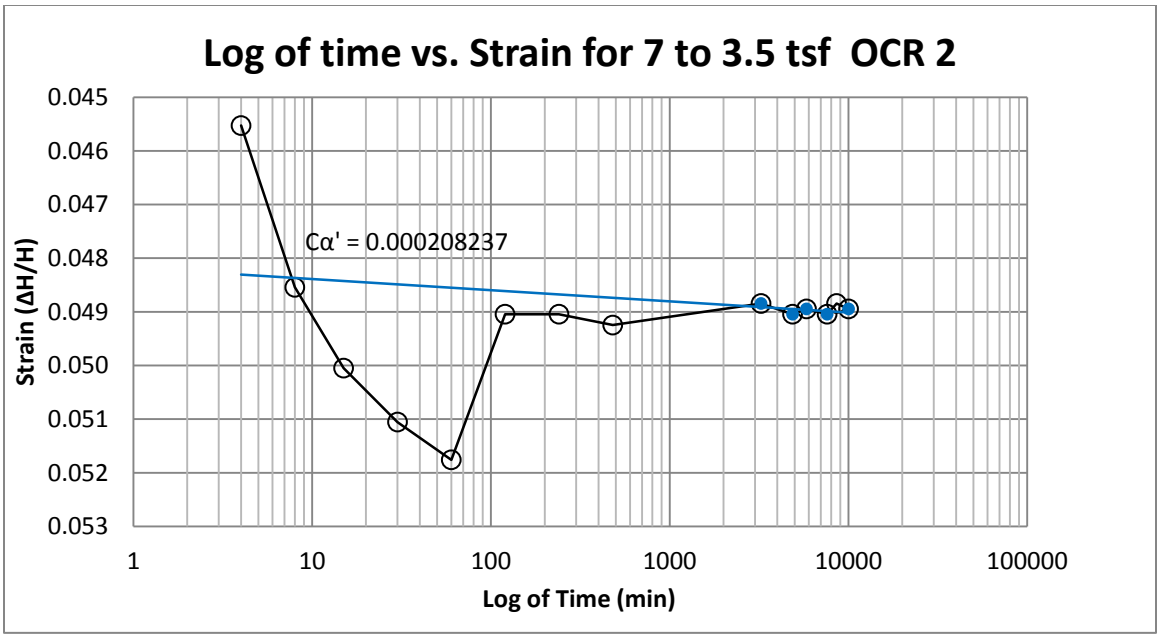

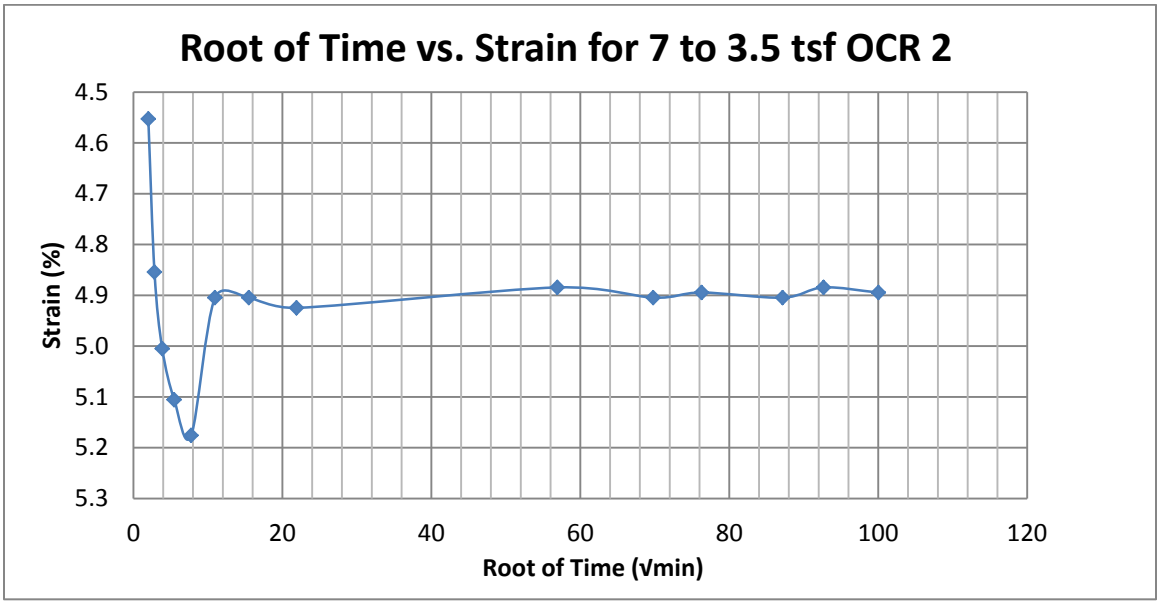

B40 Springville at 40-42 feet

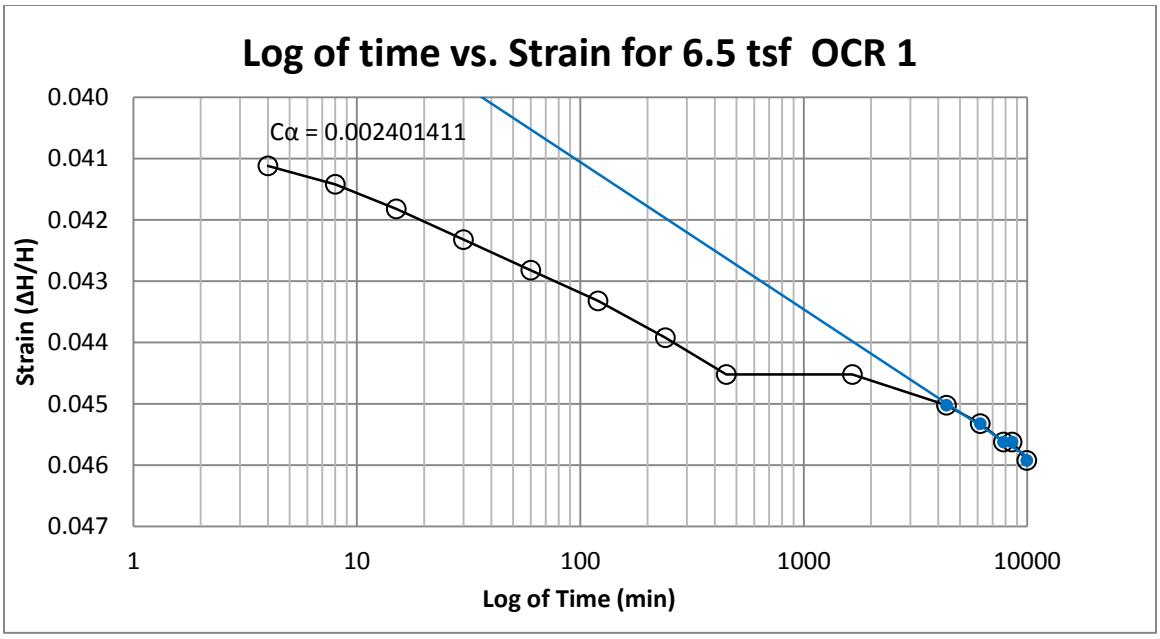

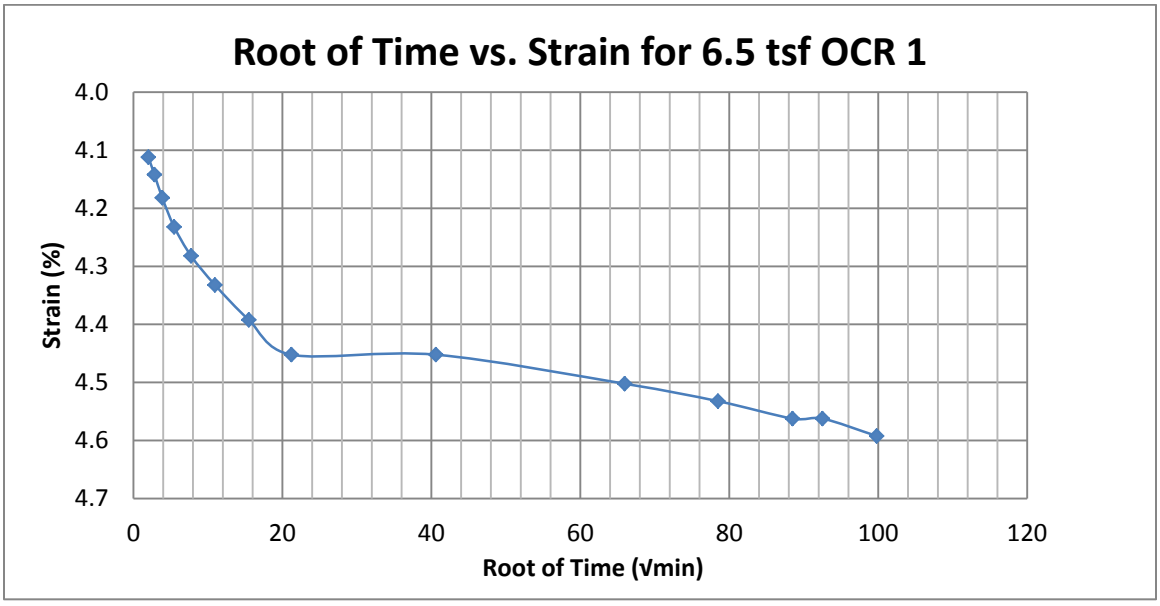

B41 Springville at 65-67 feet

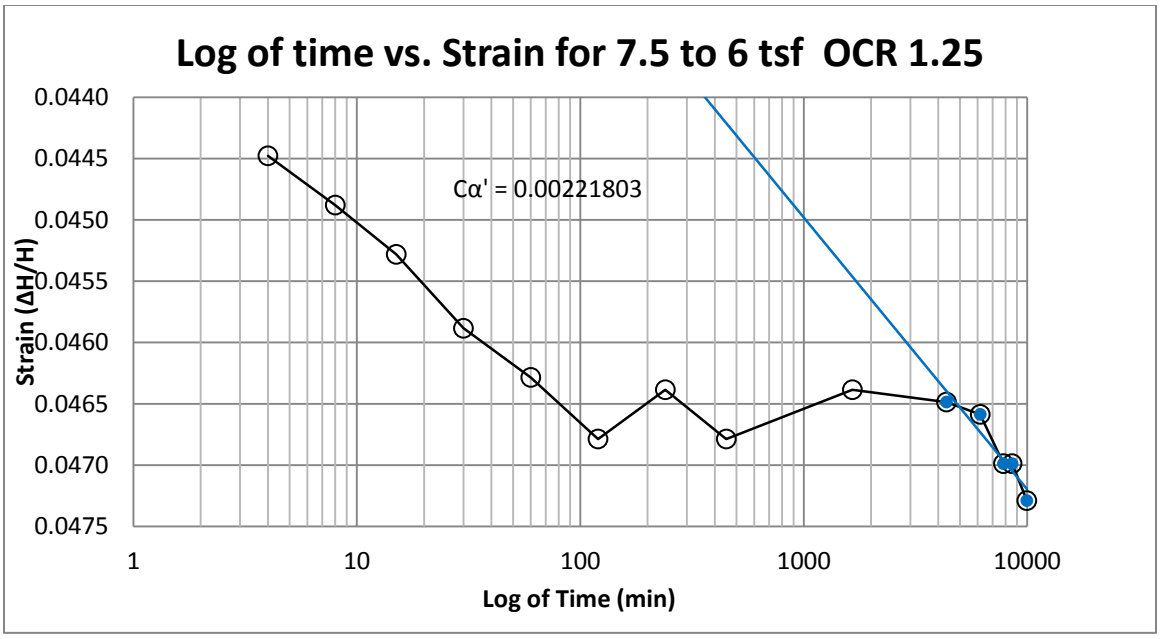

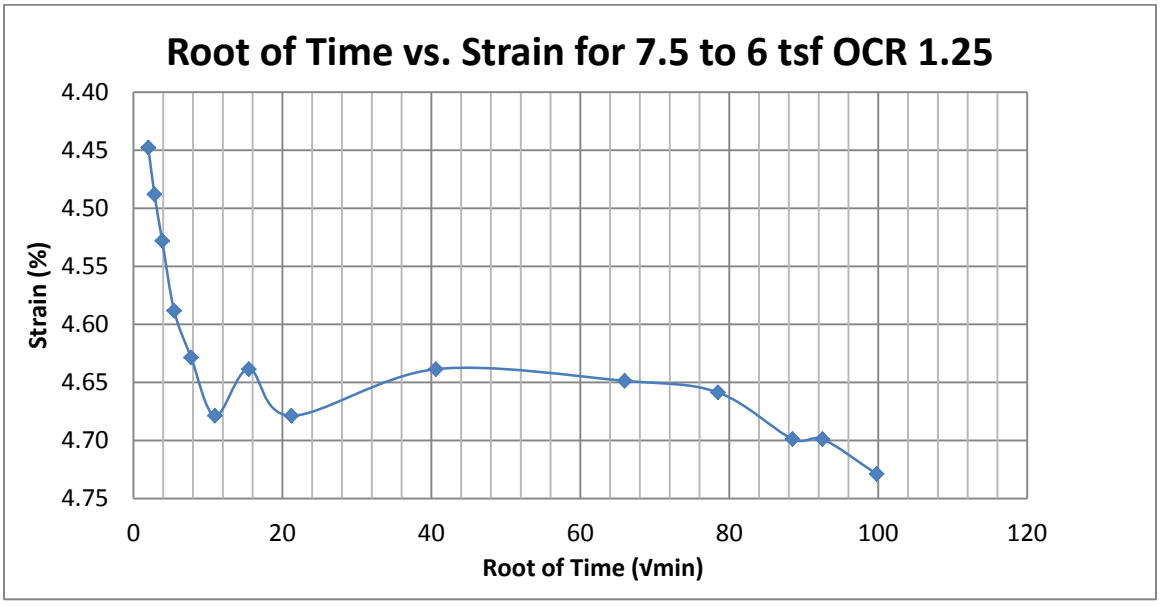

B42 Springville at 65-67 feet

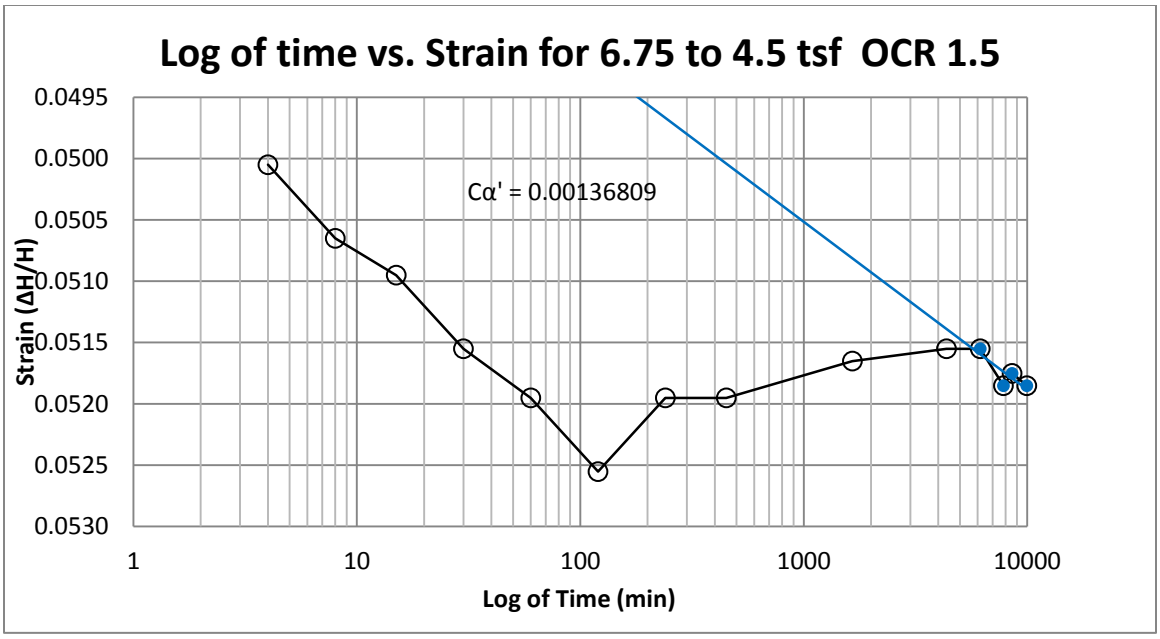

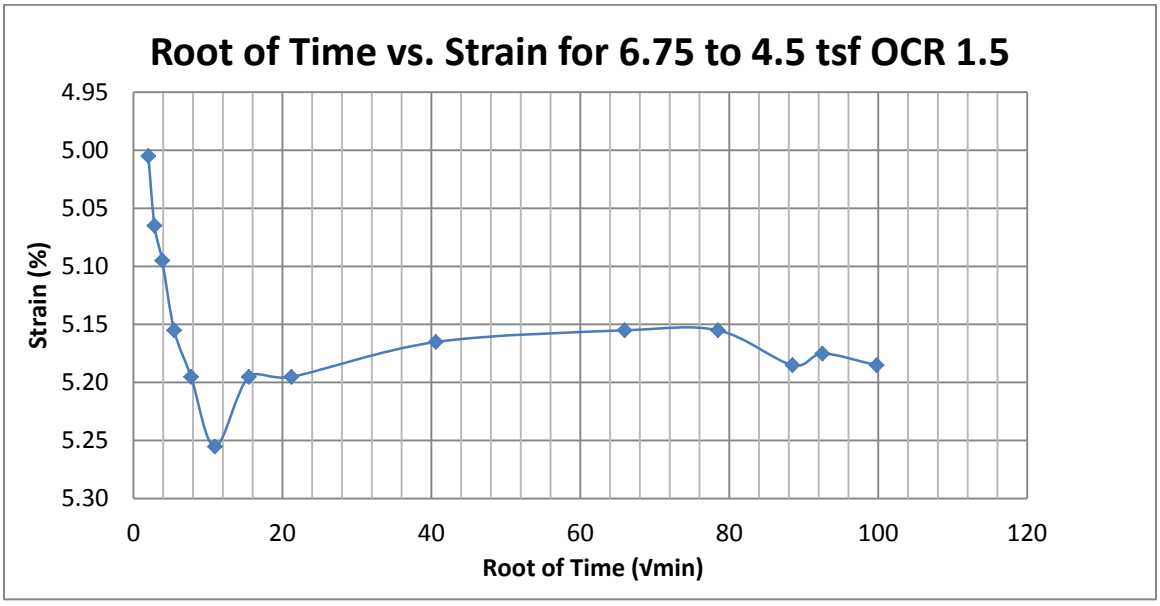

B43 Springville at 65-67 feet

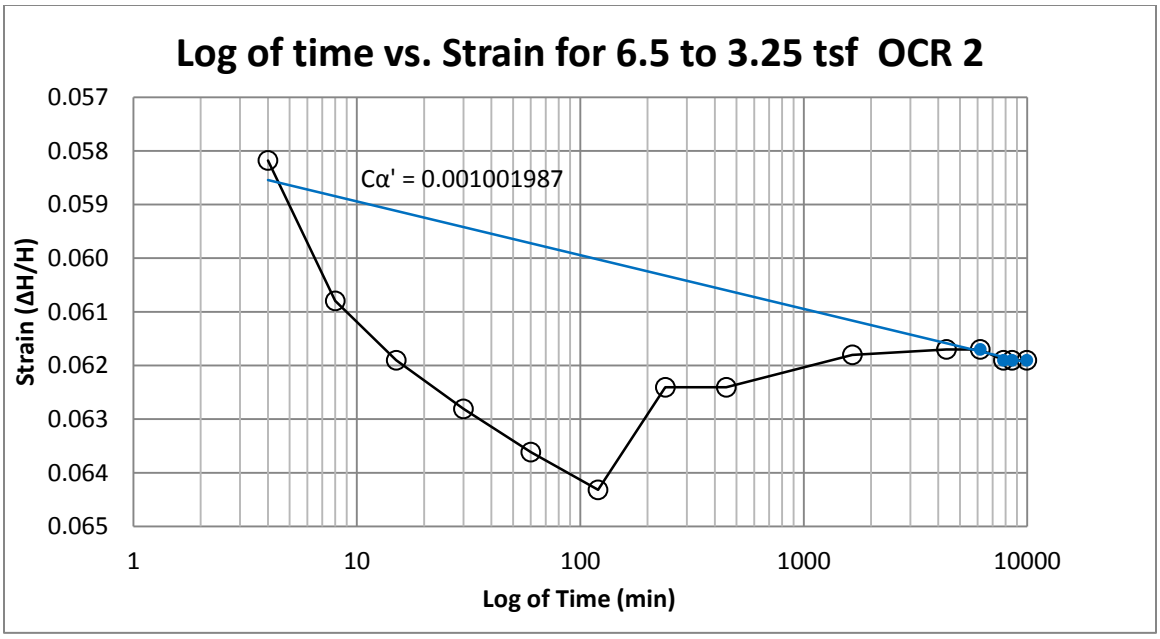

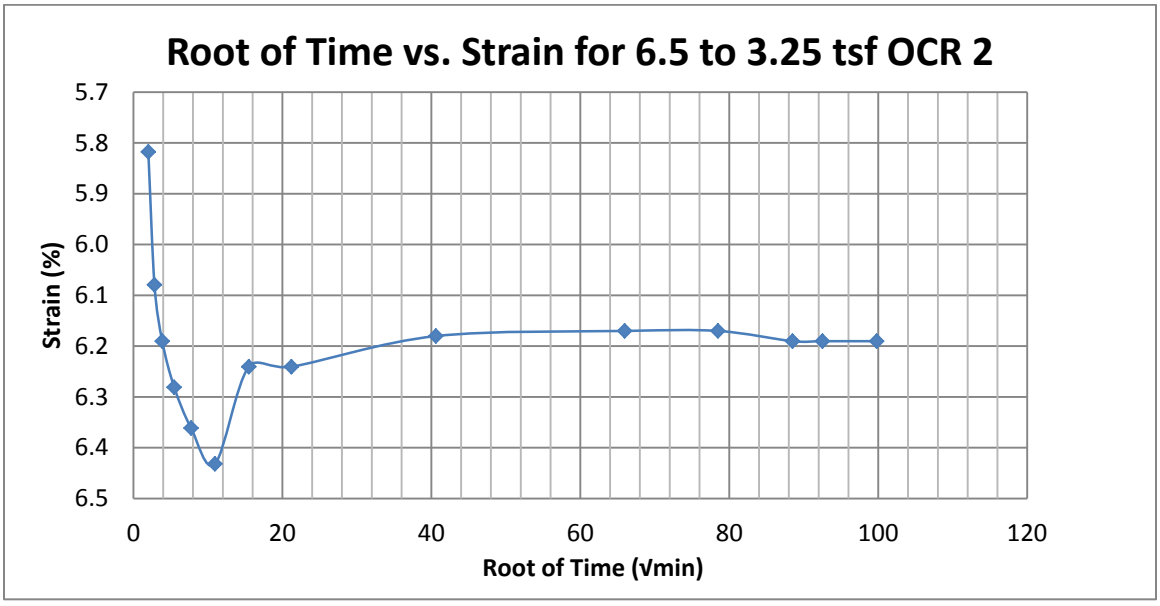

B44 Springville at 65-67 feet

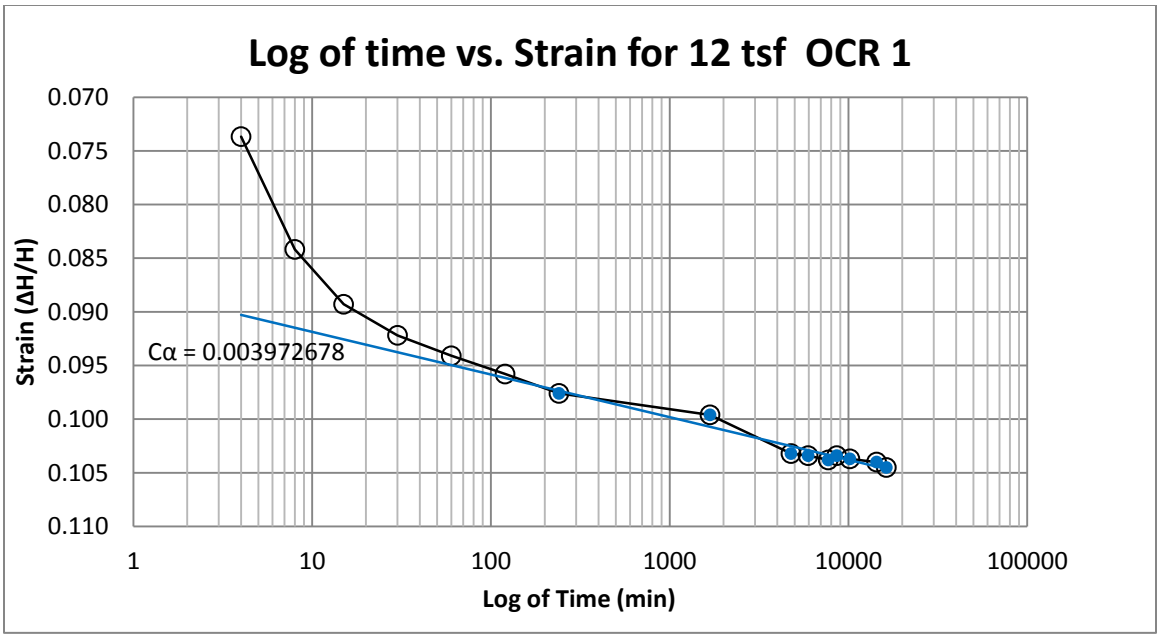

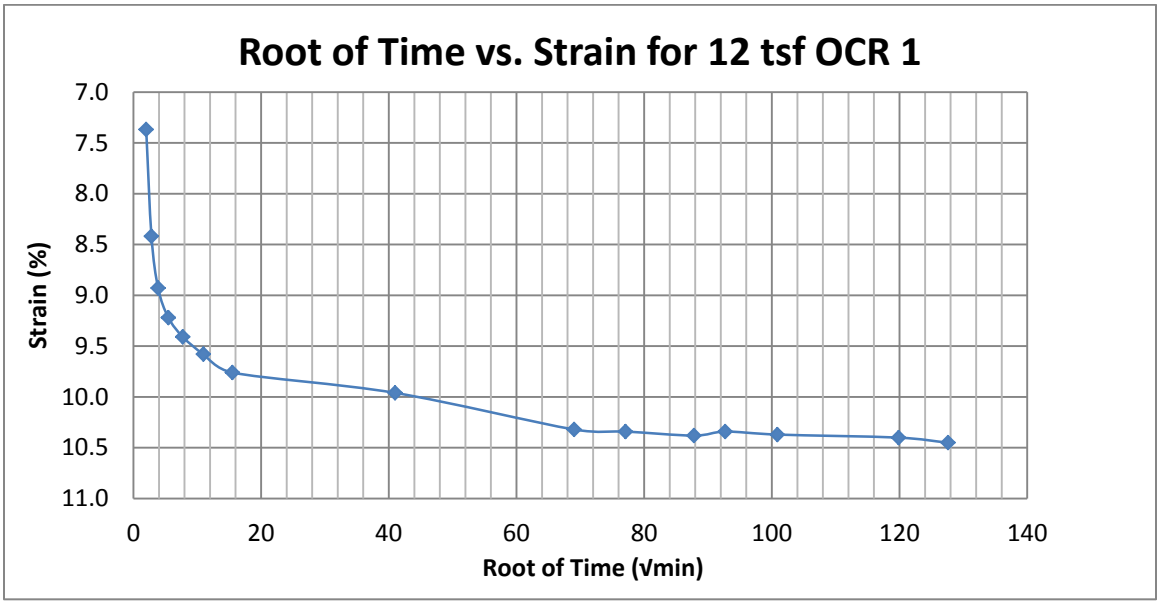

B 45 Springville at 70-72 feet

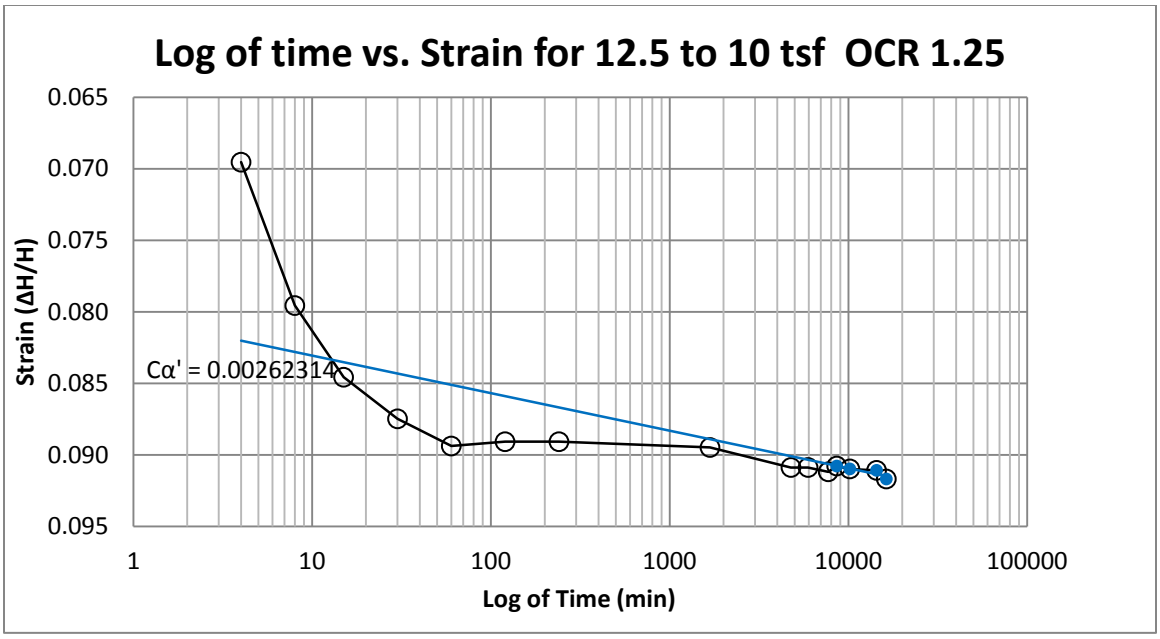

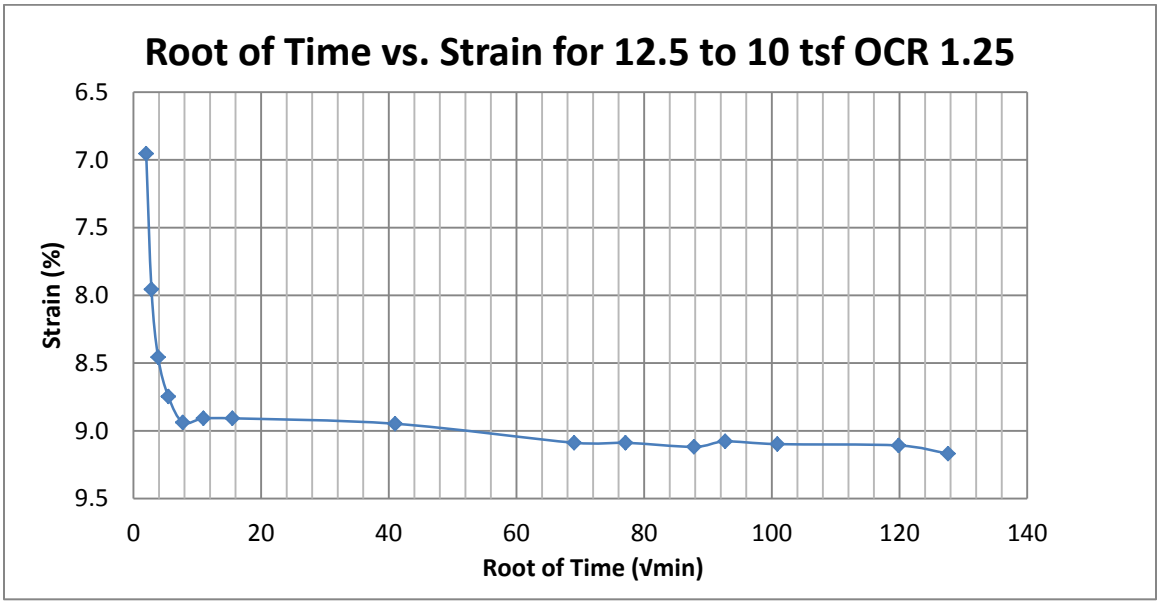

B46 Springville at 70-72 feet

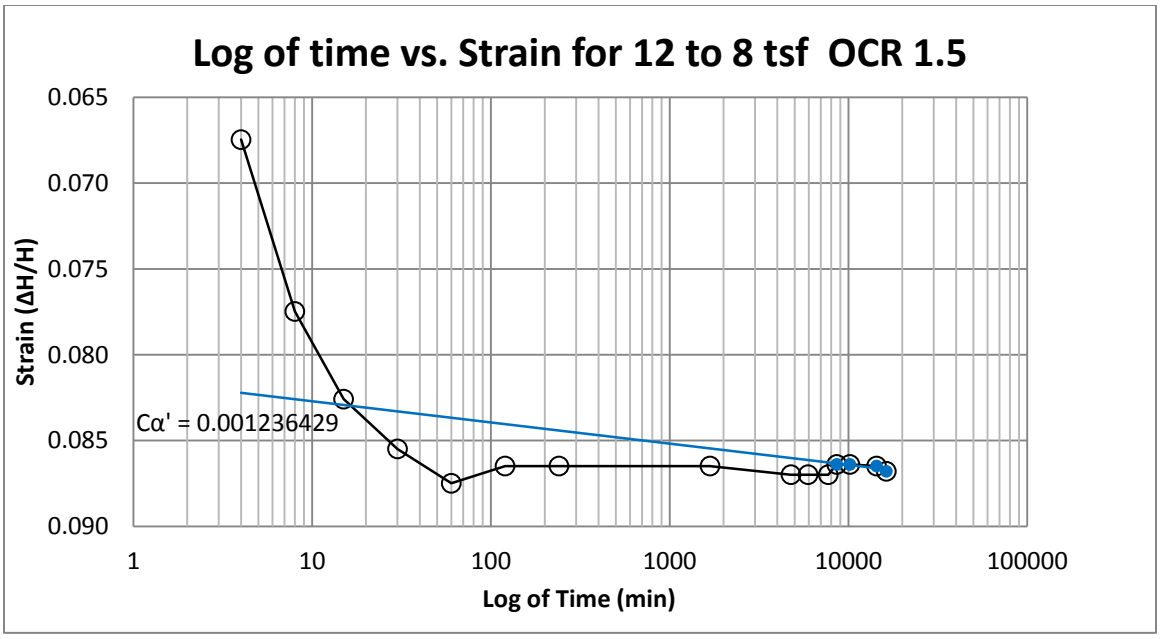

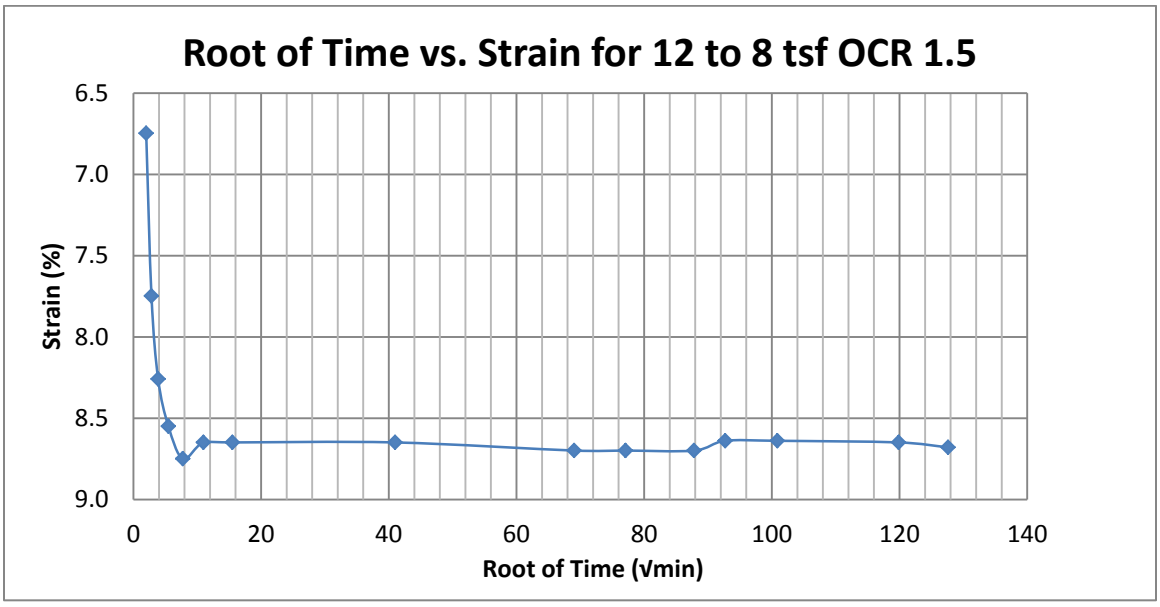

B47 Springville at 70-72 feet

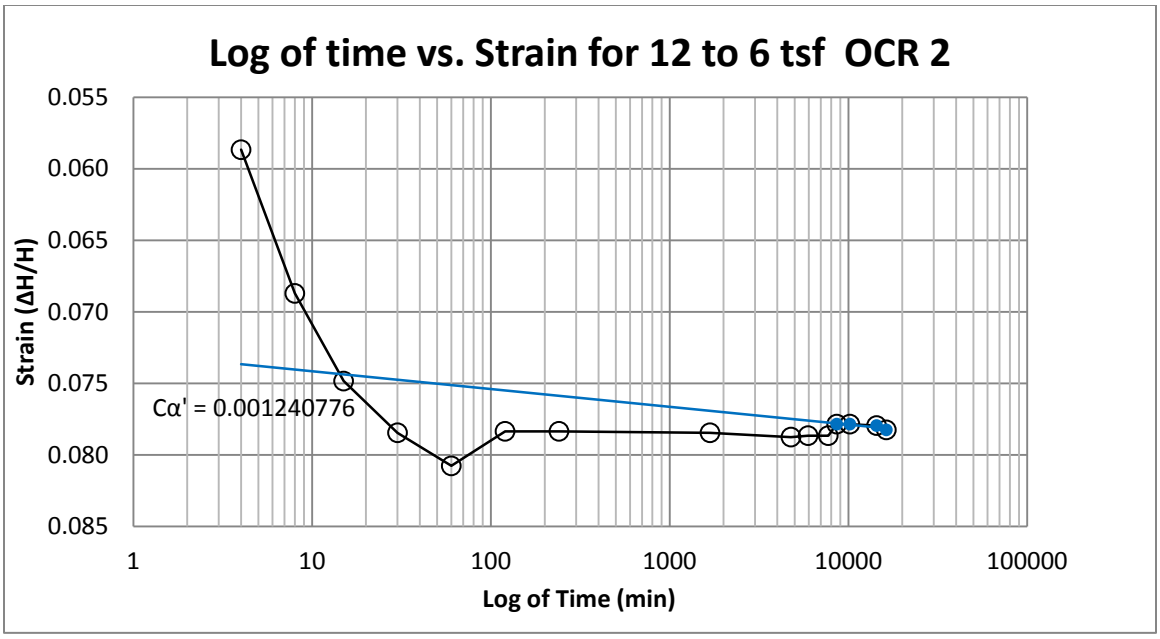

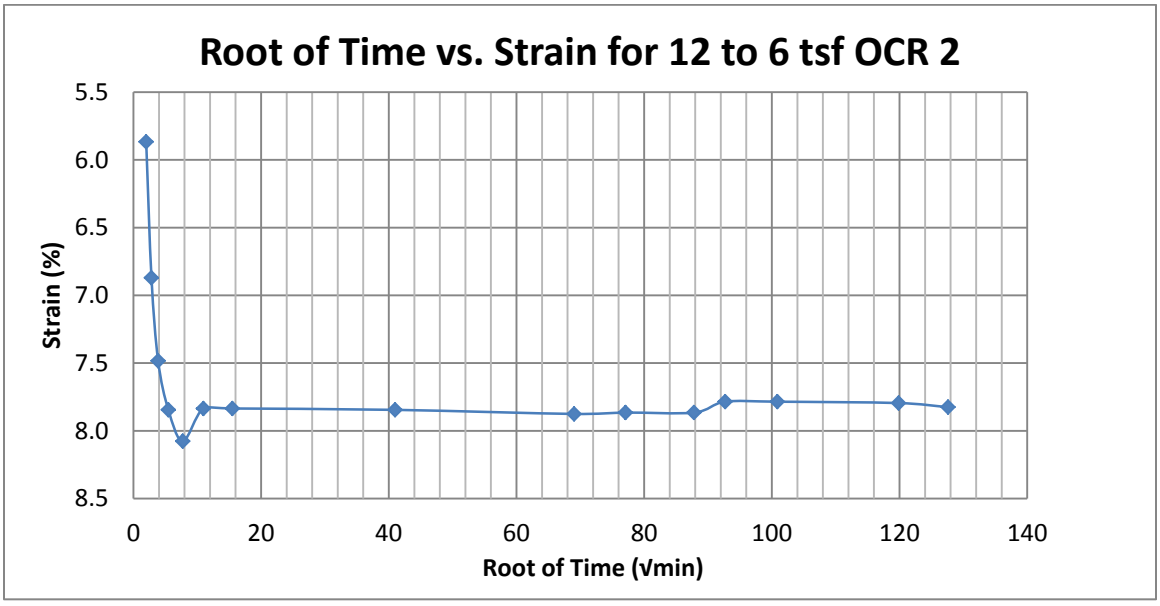

B48 Springville at 70-72 feet

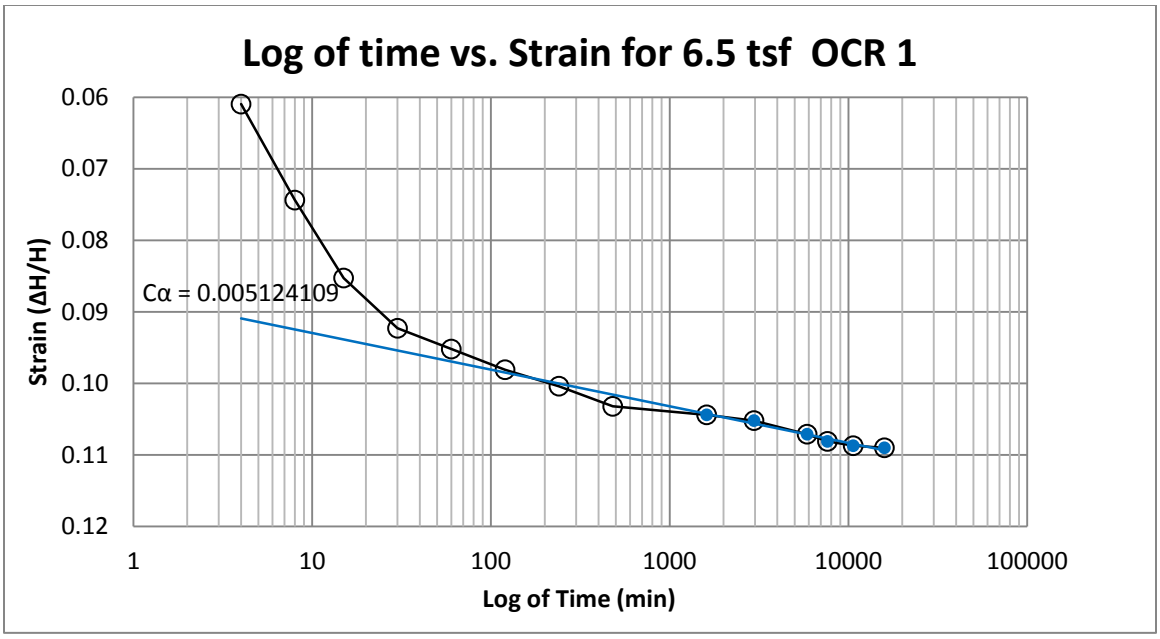

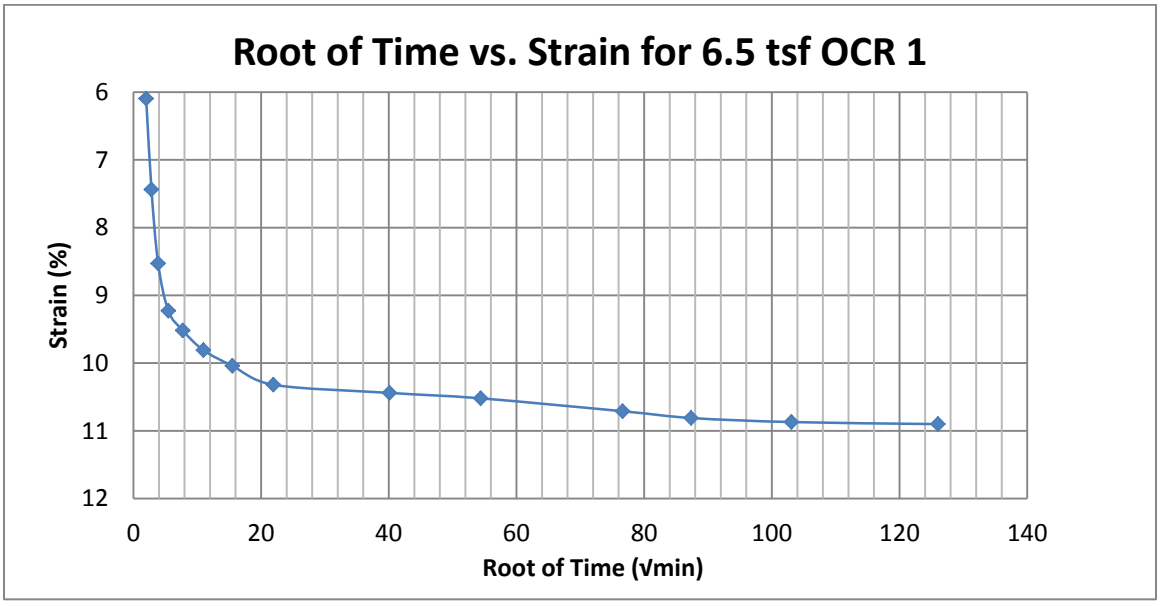

B49 Springville at 75-77 feet

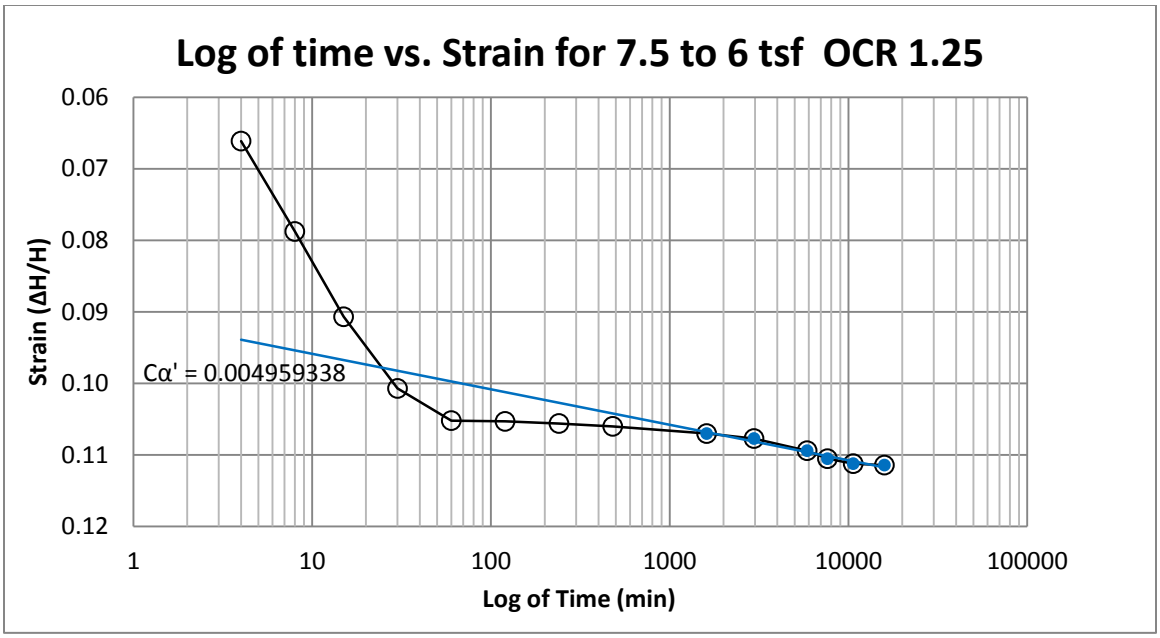

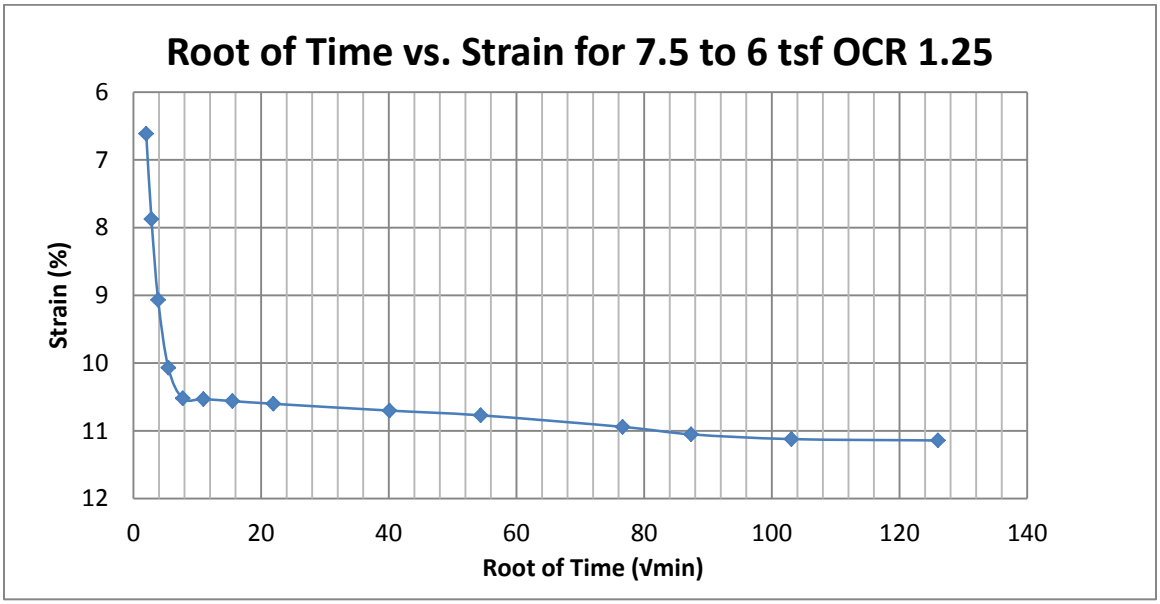

B50 Springville at 75-77 feet

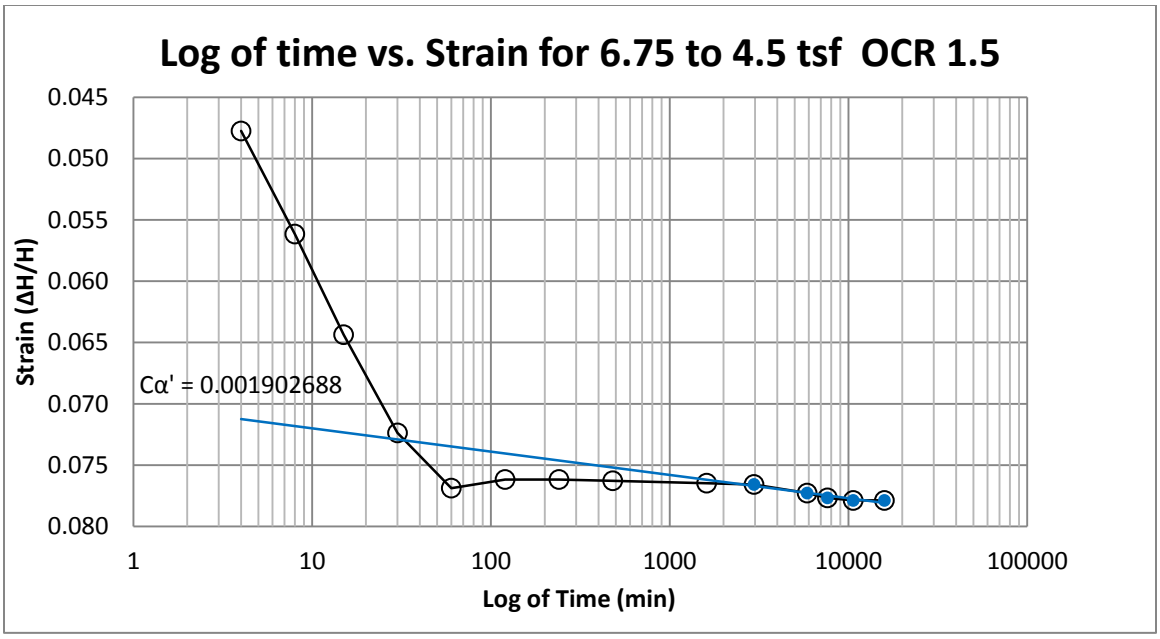

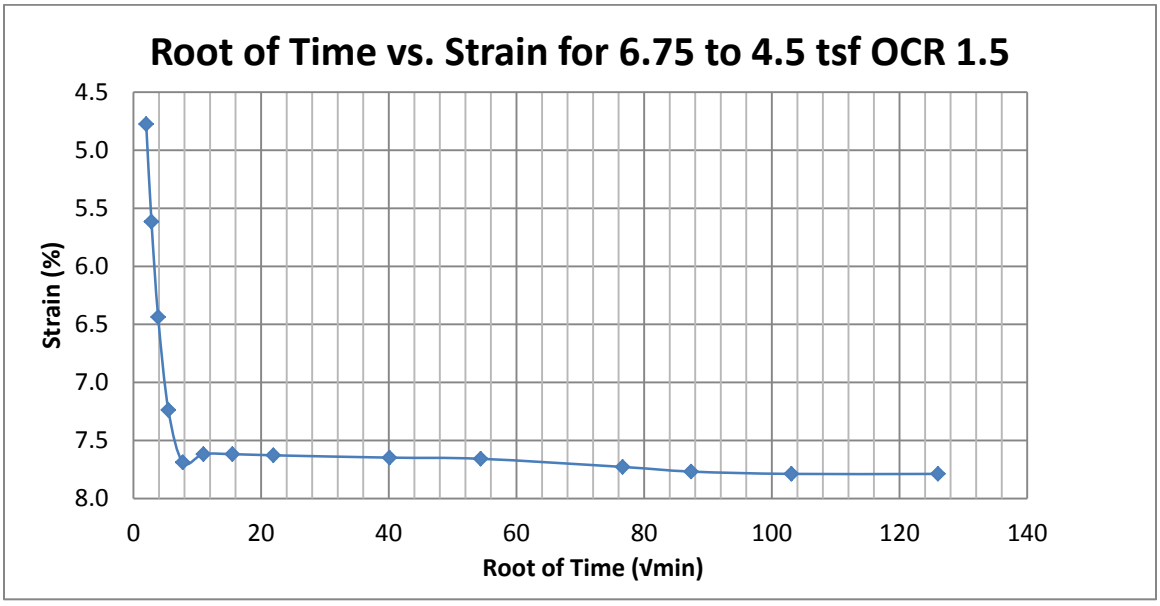

B51 Springville at 75-77 feet

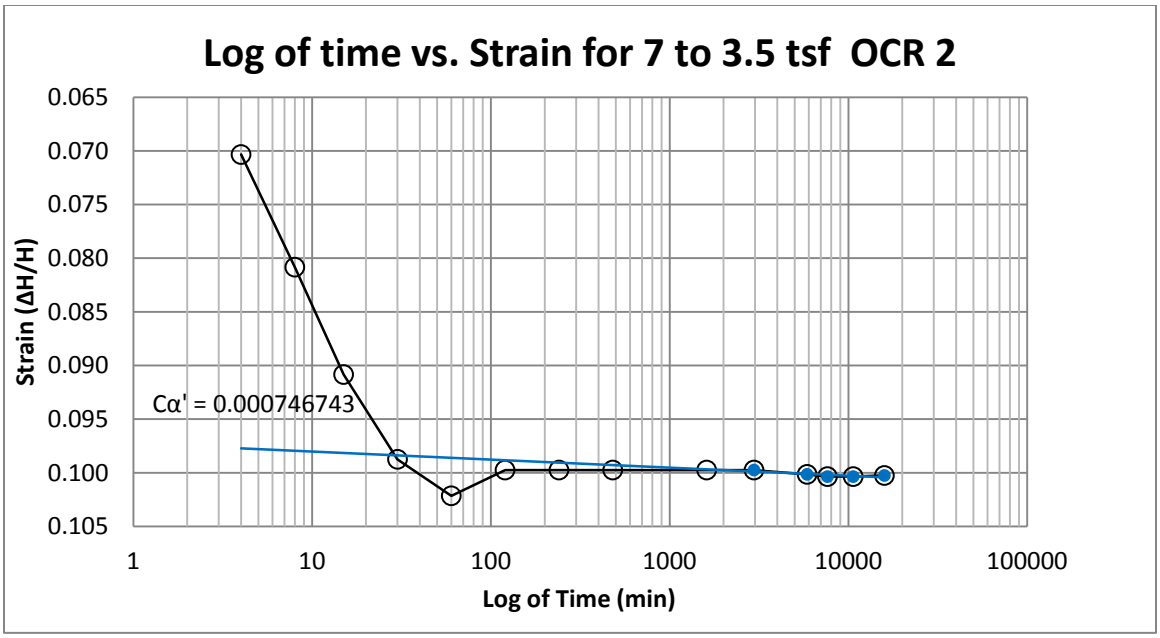

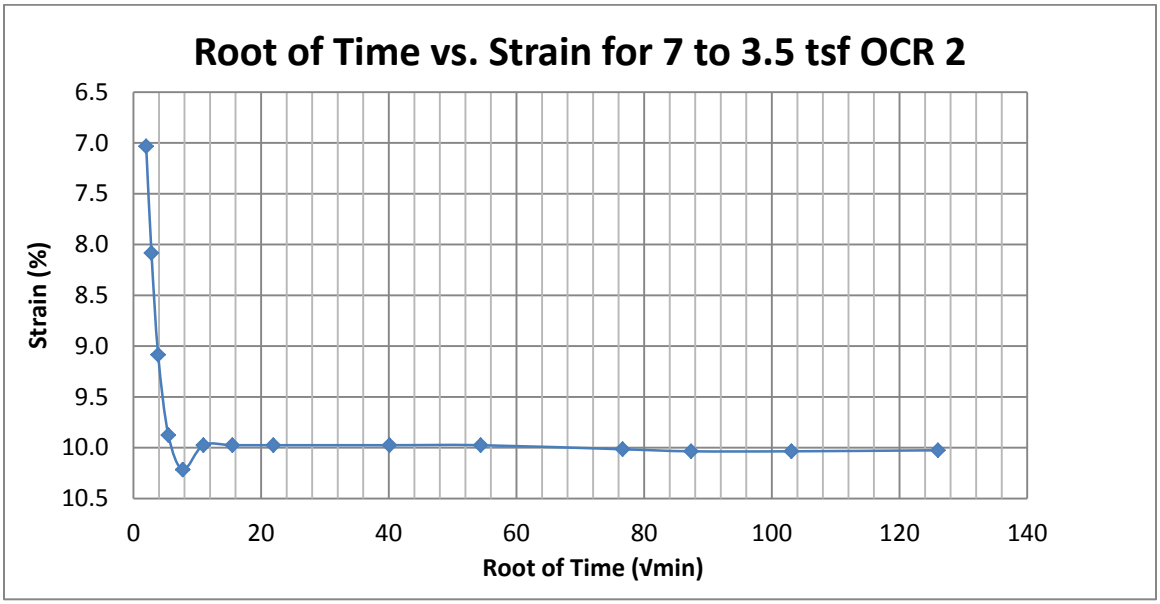

B52 Springville at 75-77 feet

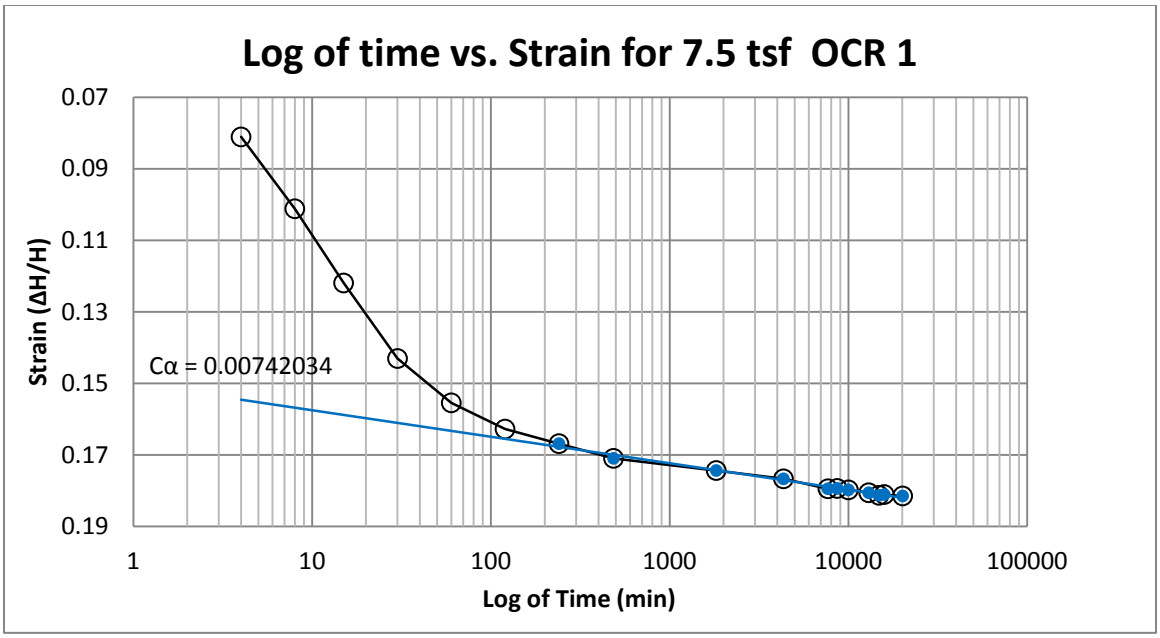

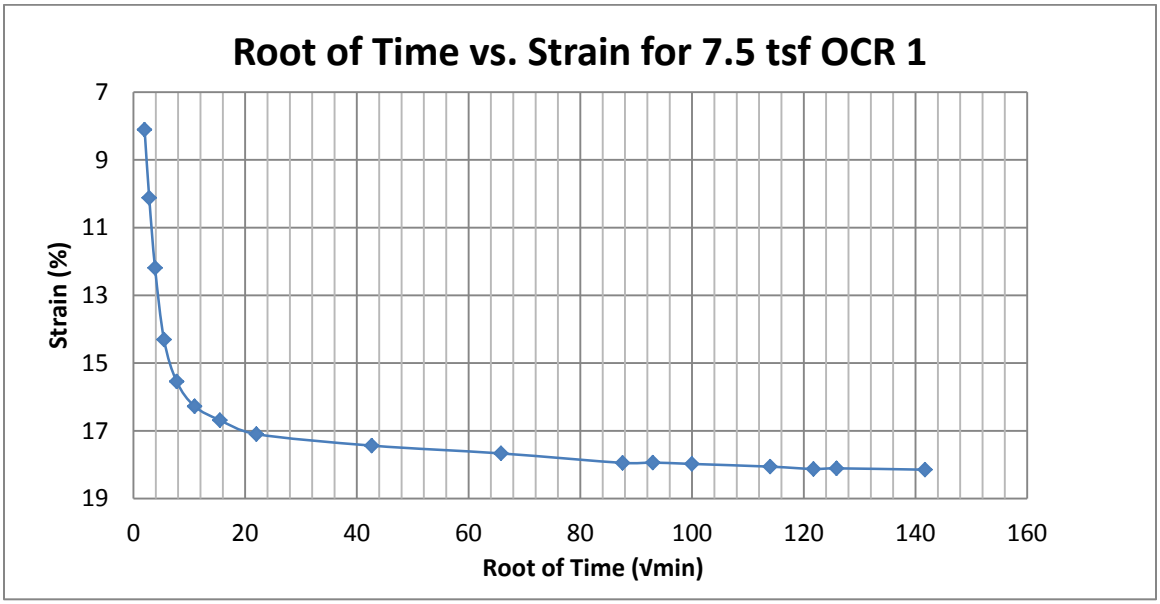

B53 Springville at 80-82 feet

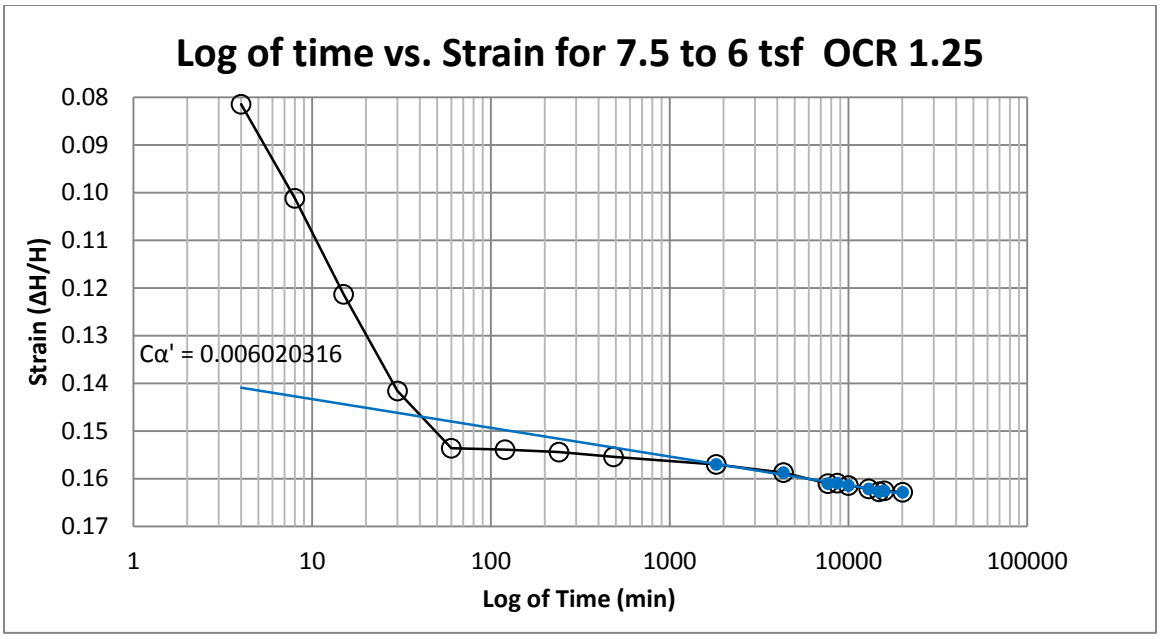

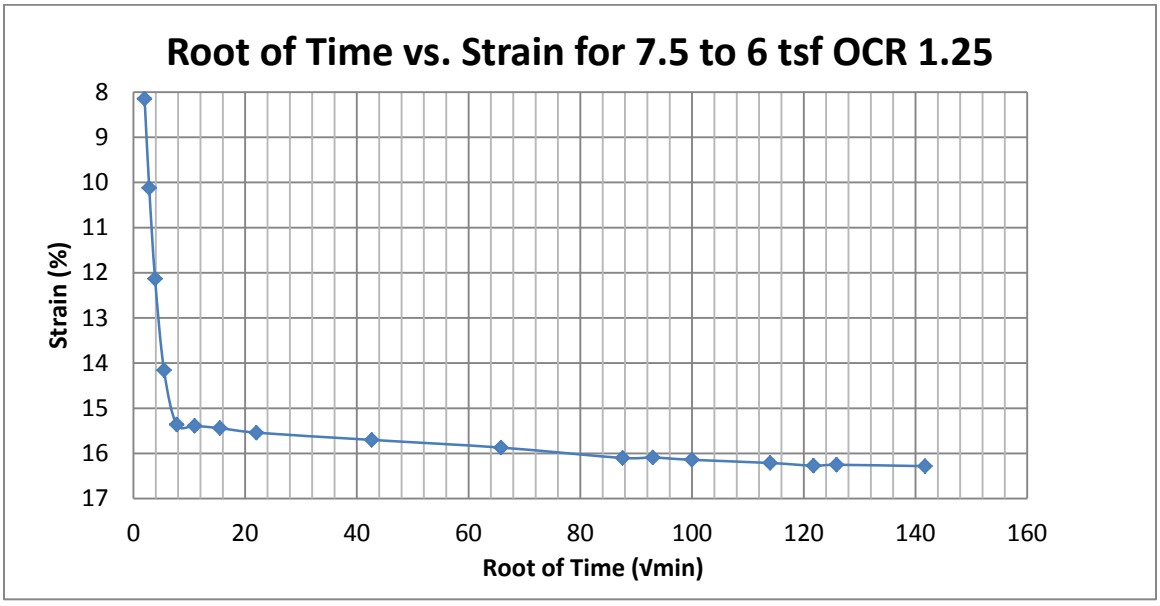

B54 Springville at 80-82 feet

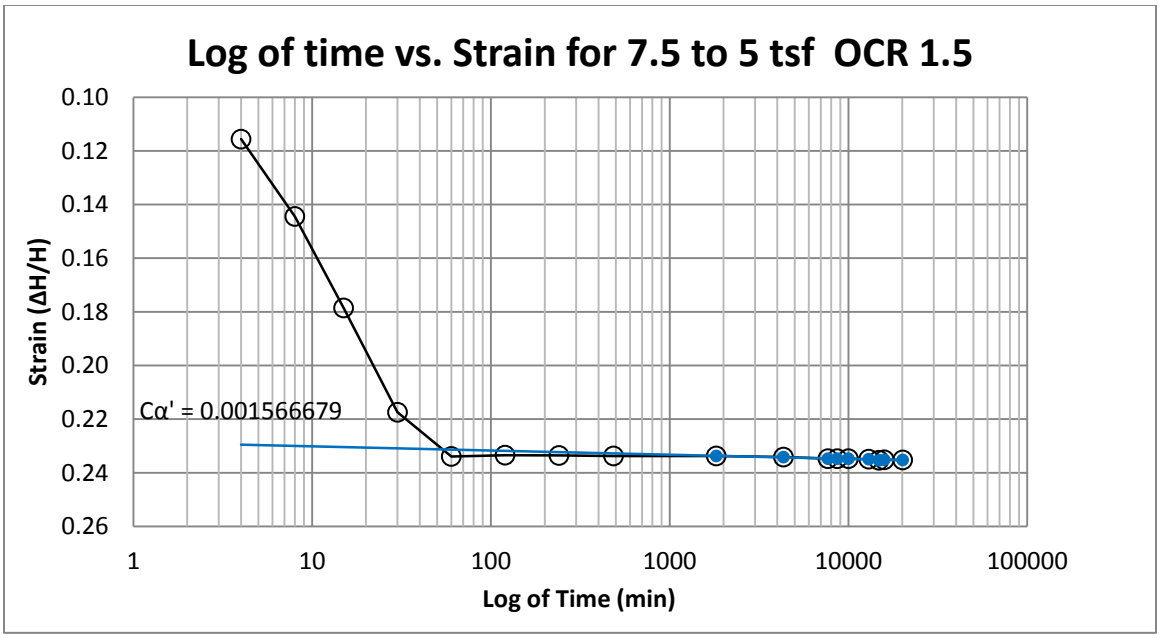

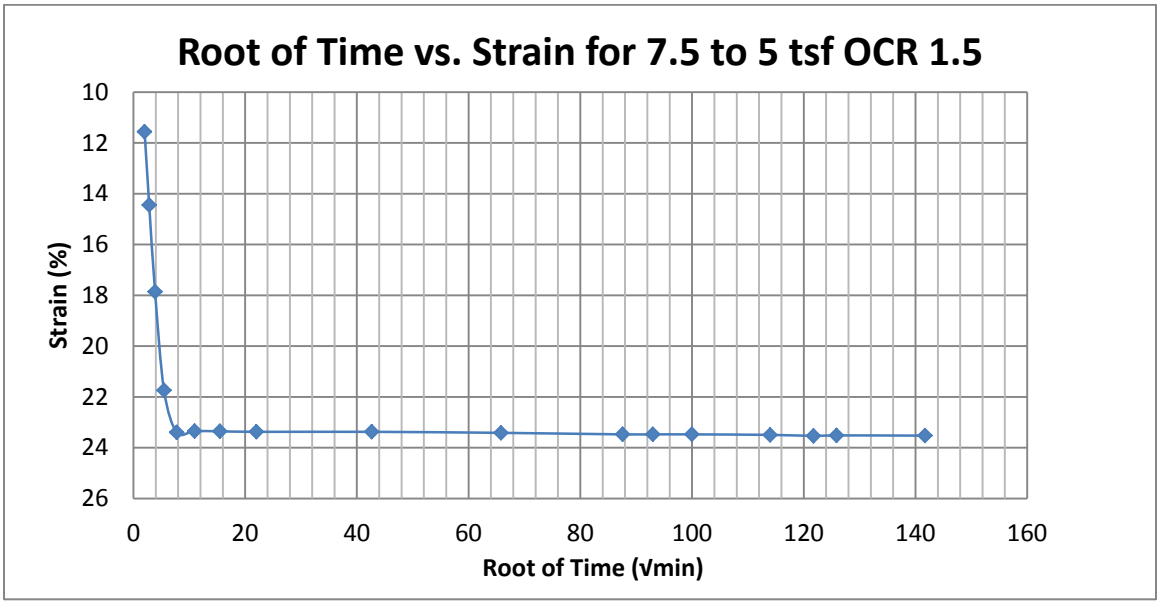

B55 Springville at 80-82 feet

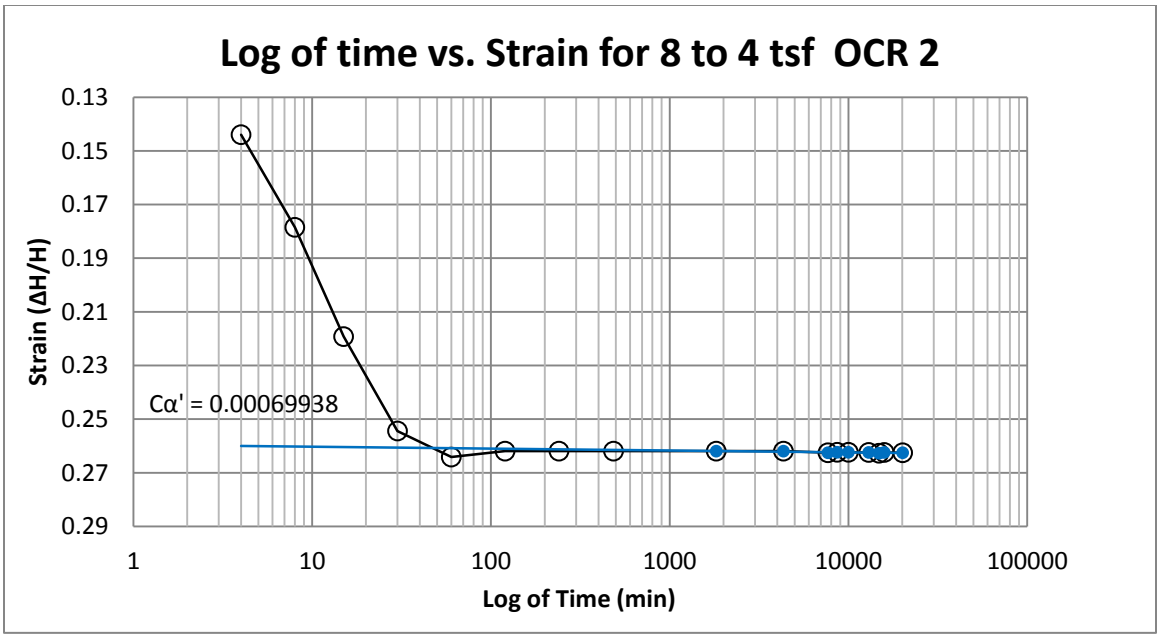

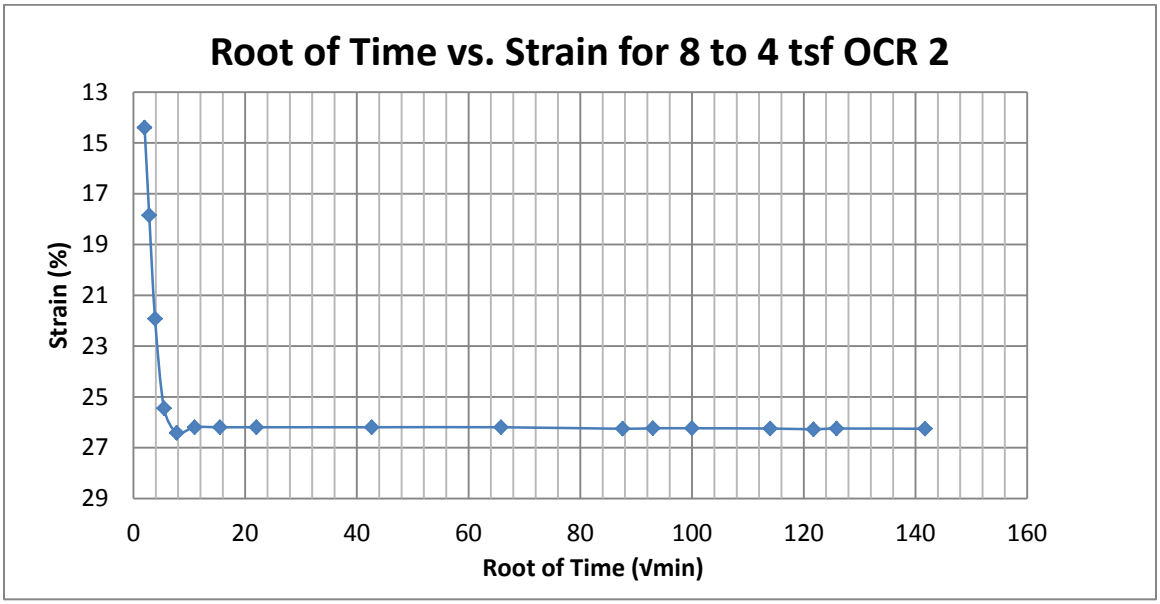

B 56 Springville at 80-82 feet

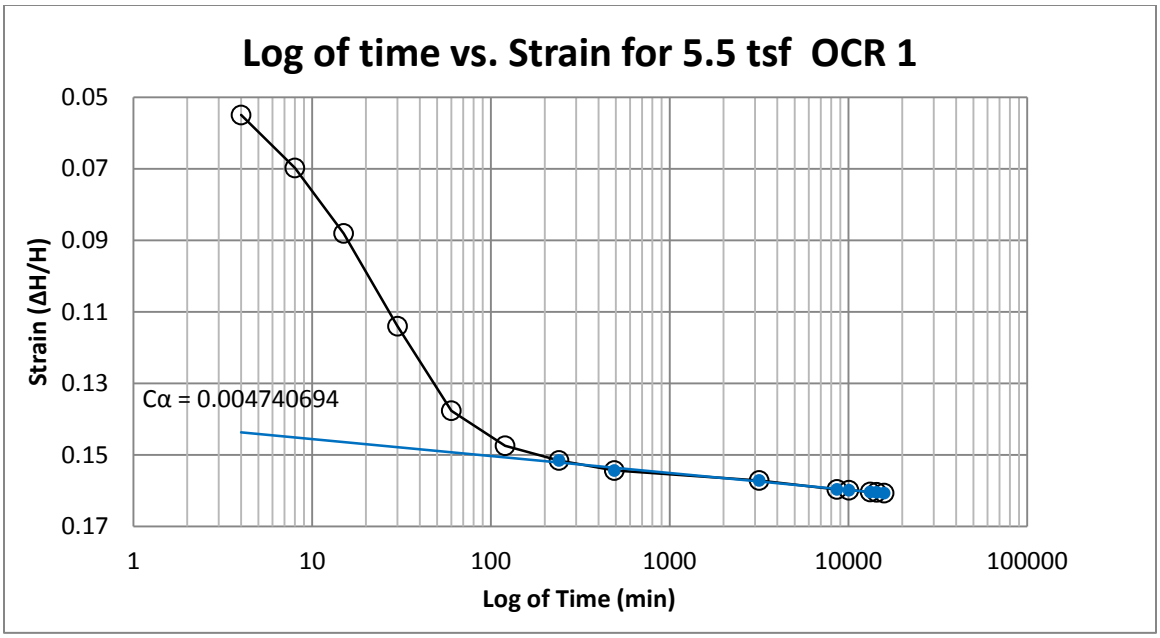

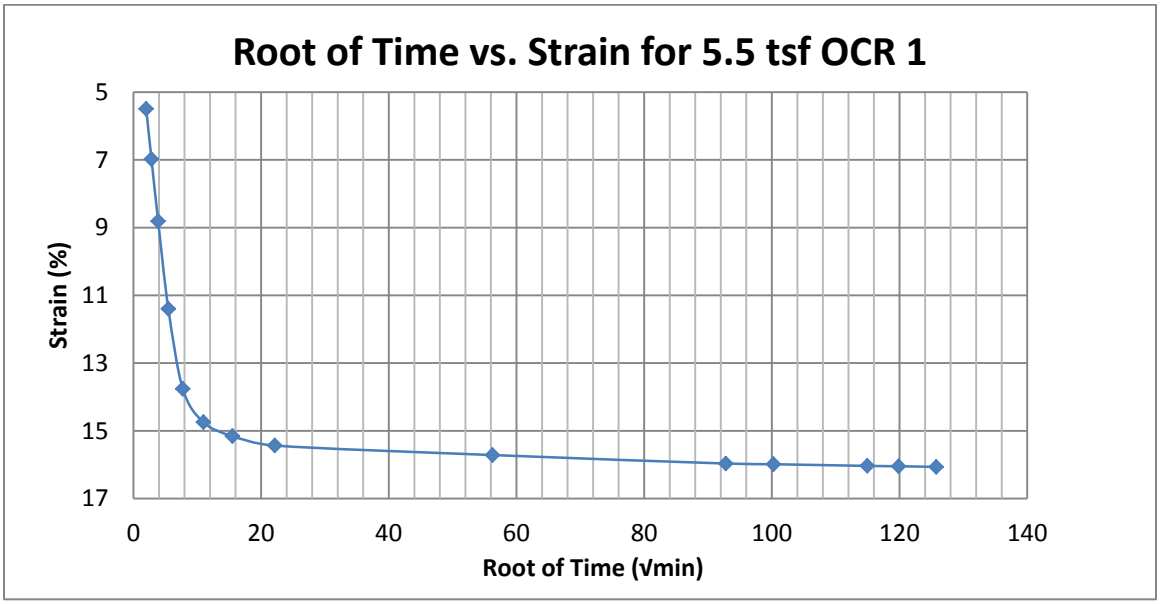

B 57 Springville at 84-86 feet

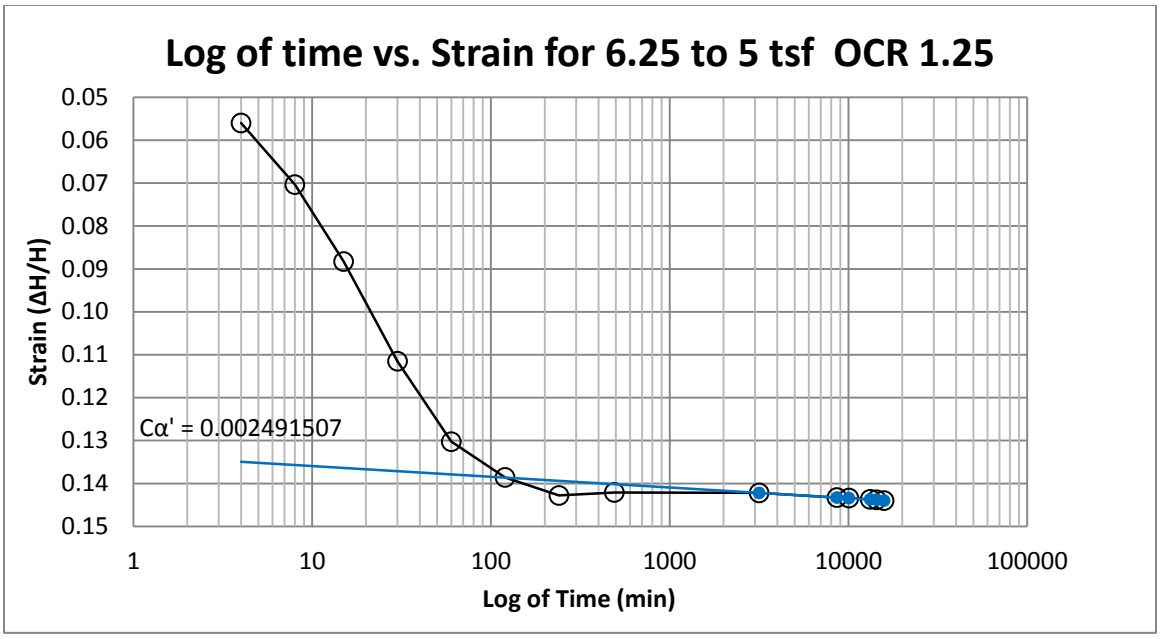

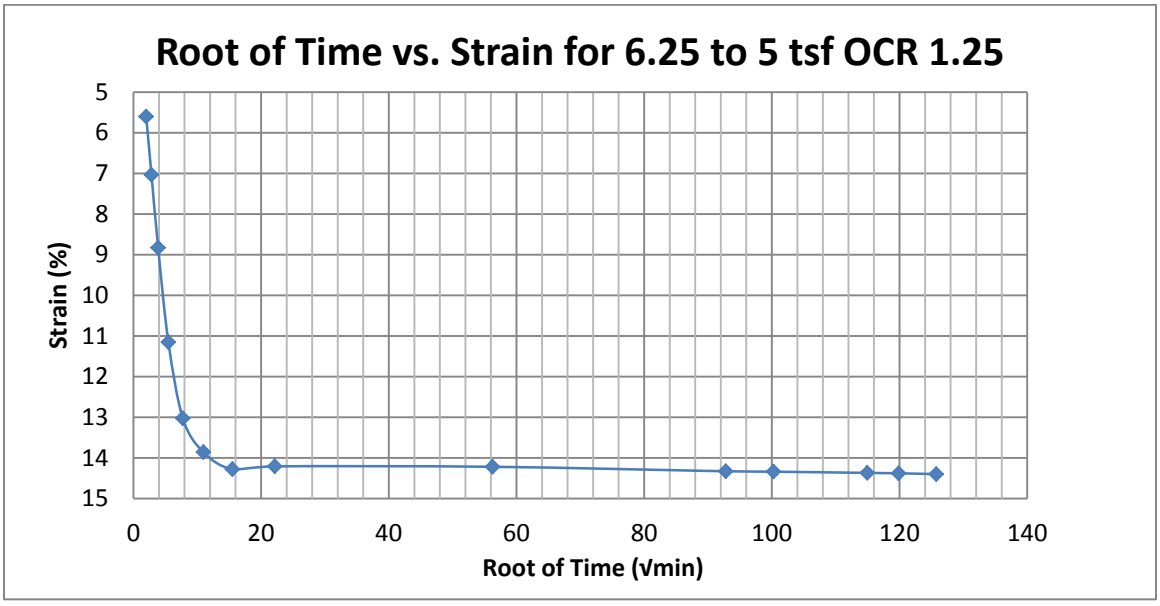

B 58 Springville at 84-86 feet

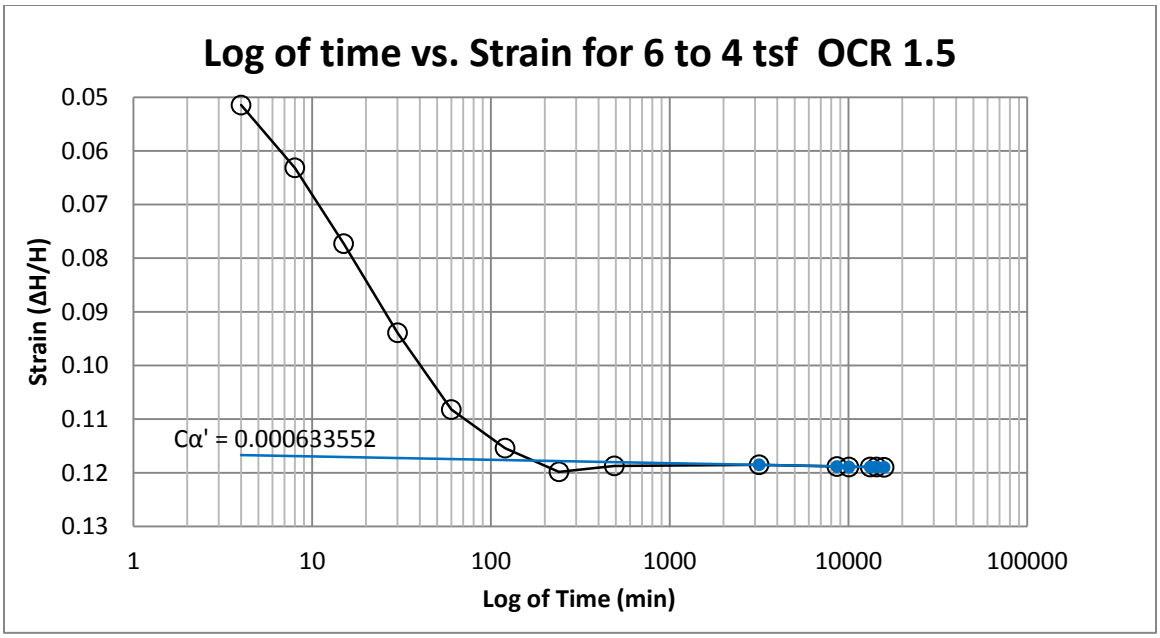

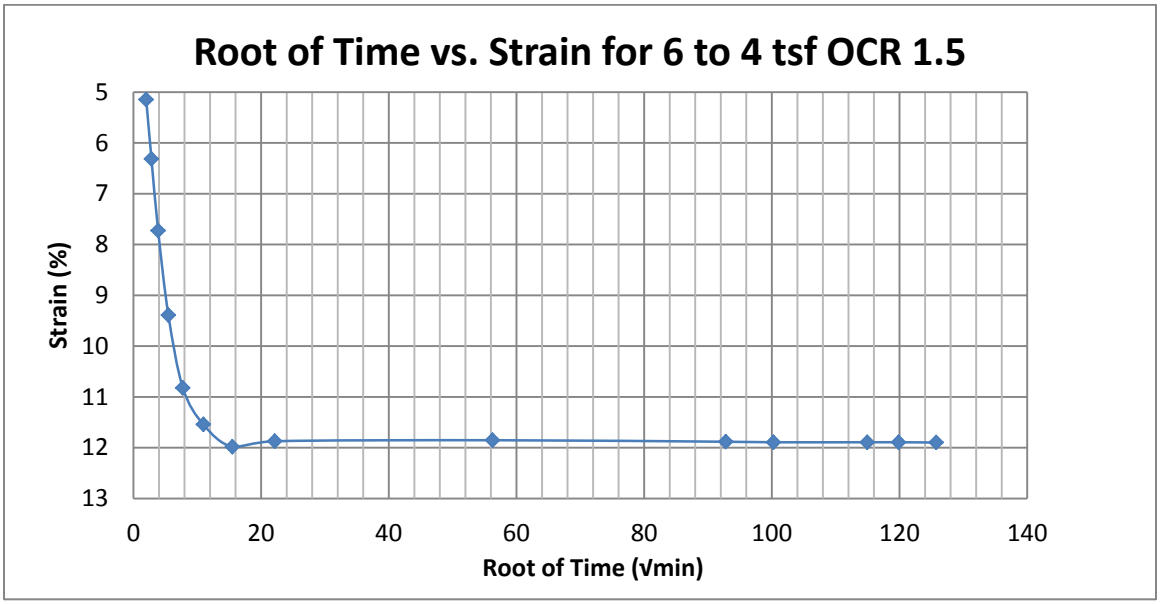

B 59 Springville at 84-86 feet

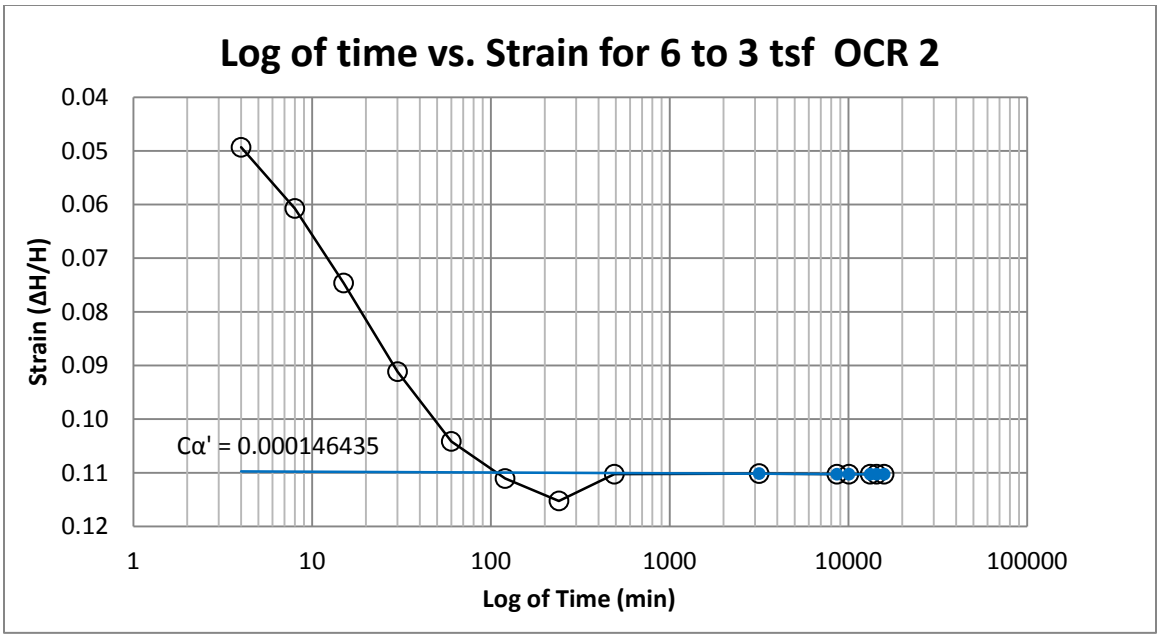

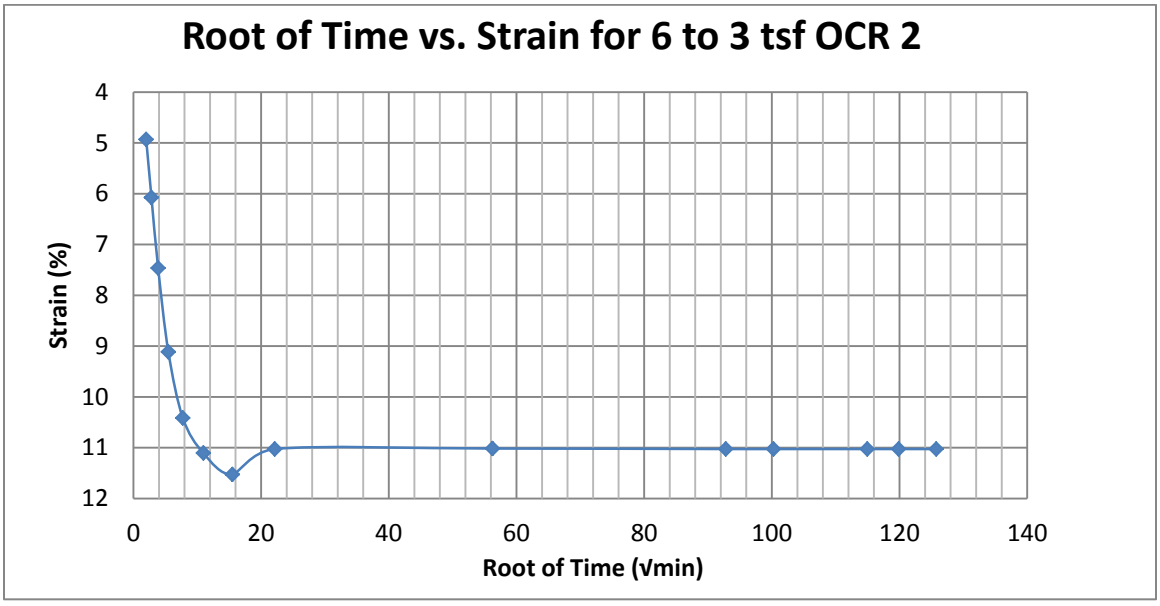

B 60 Springville at 84-86 feet

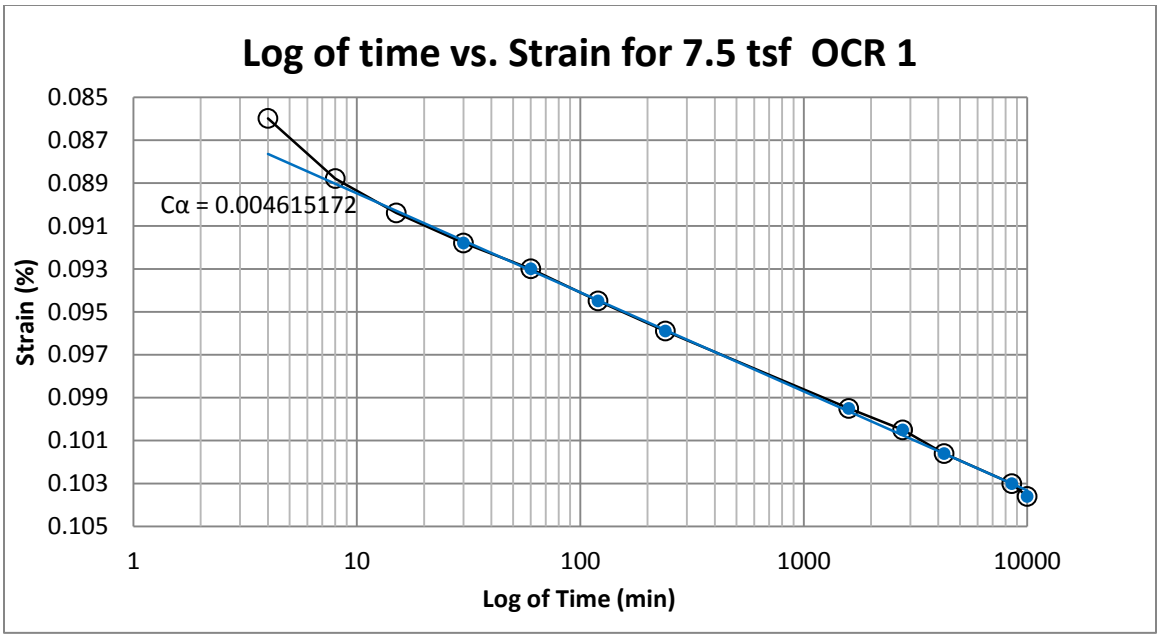

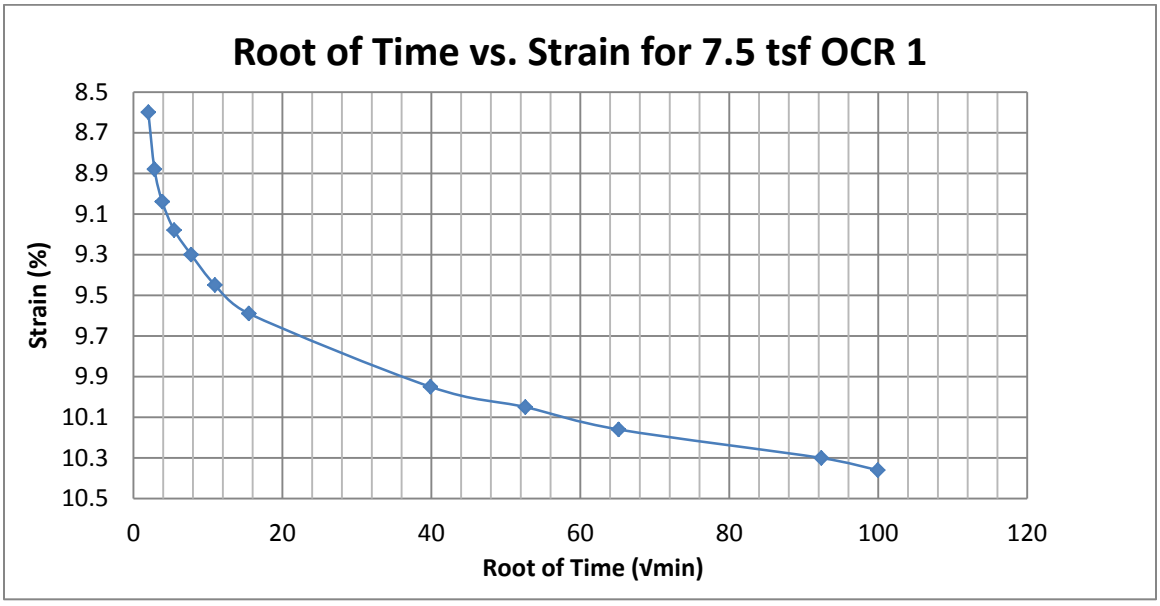

B61 Provo at 12-14 feet

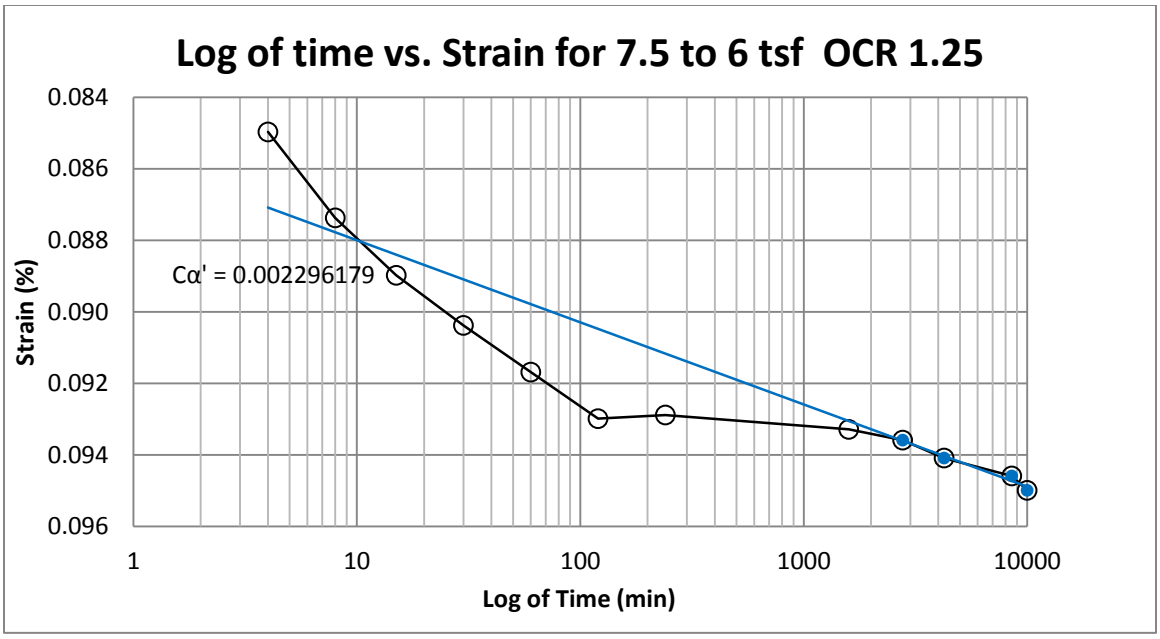

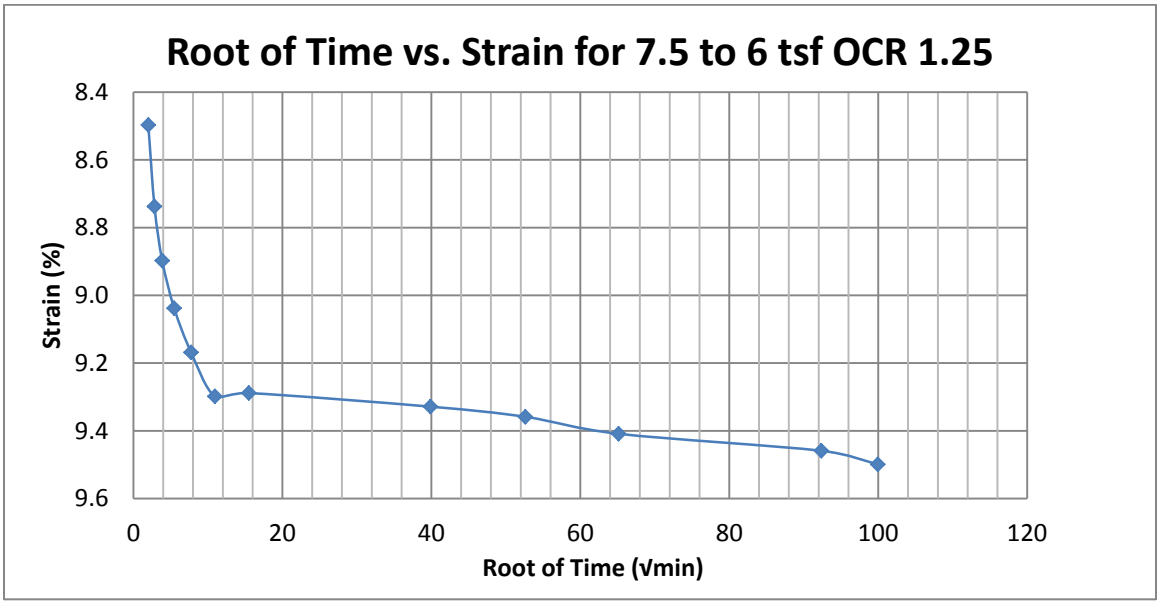

B62 Provo at 12-14 feet

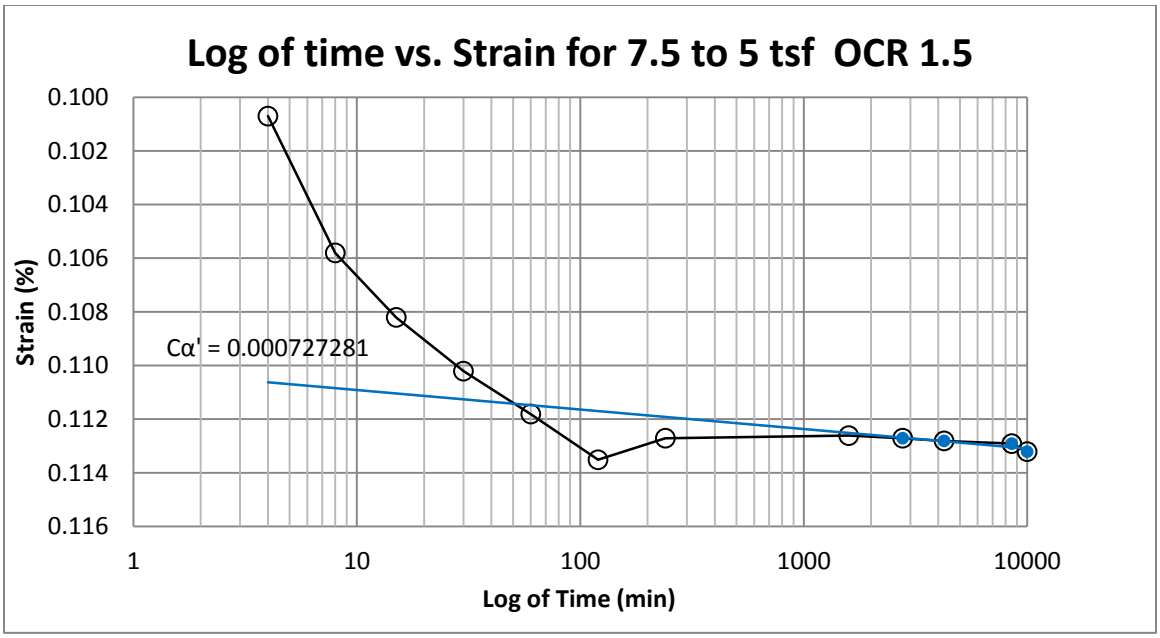

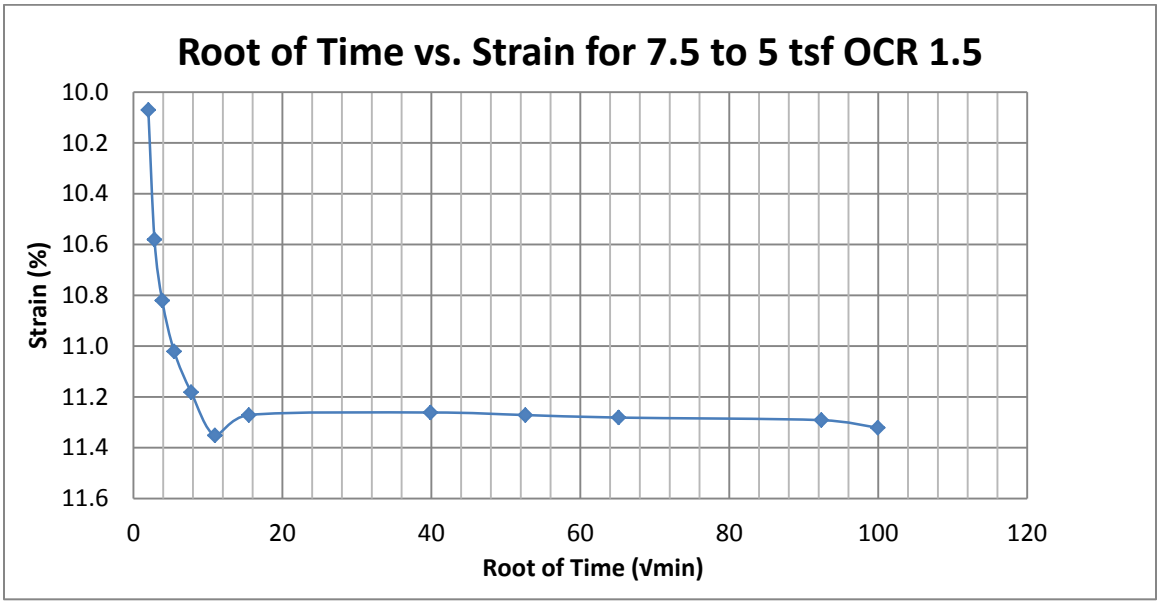

B63 Provo at 12-14 feet

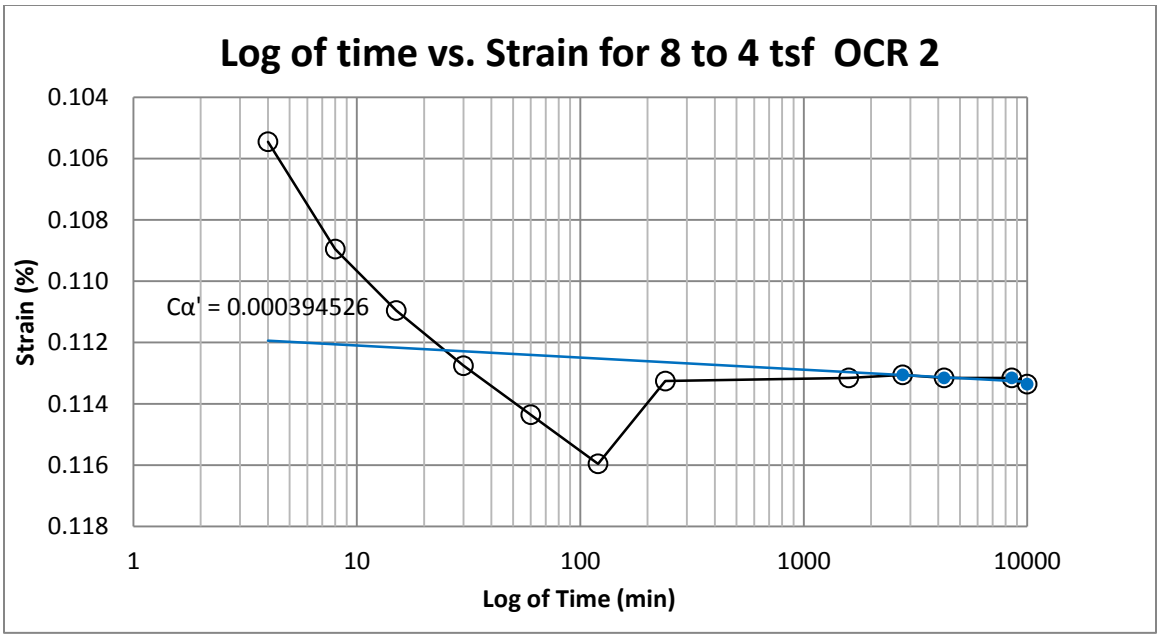

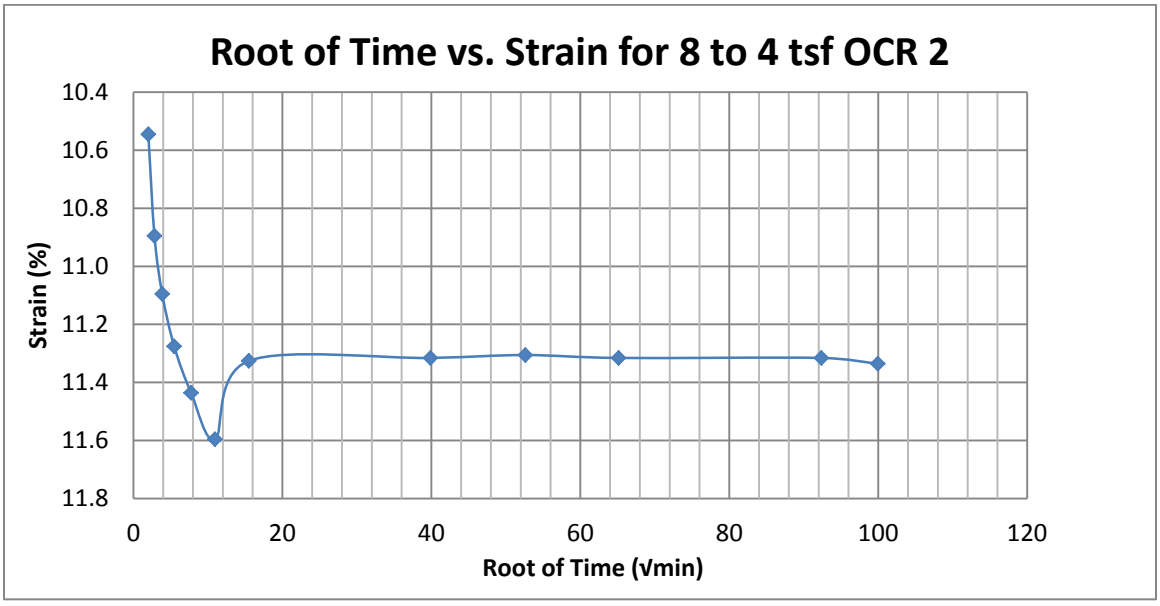

B64 Provo at 12-14 feet

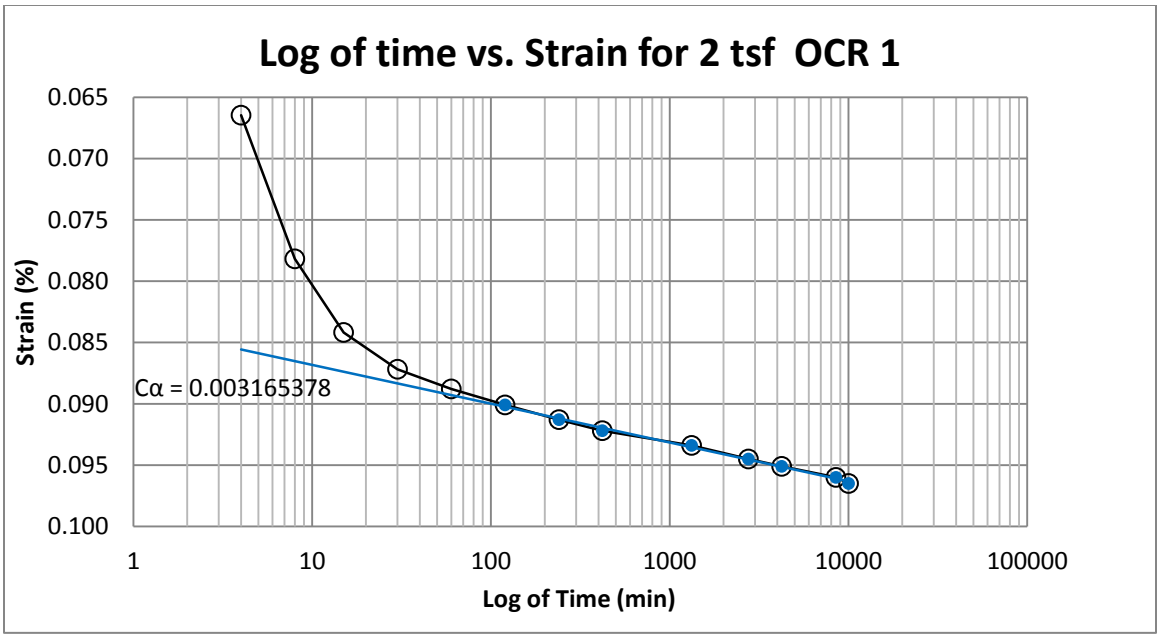

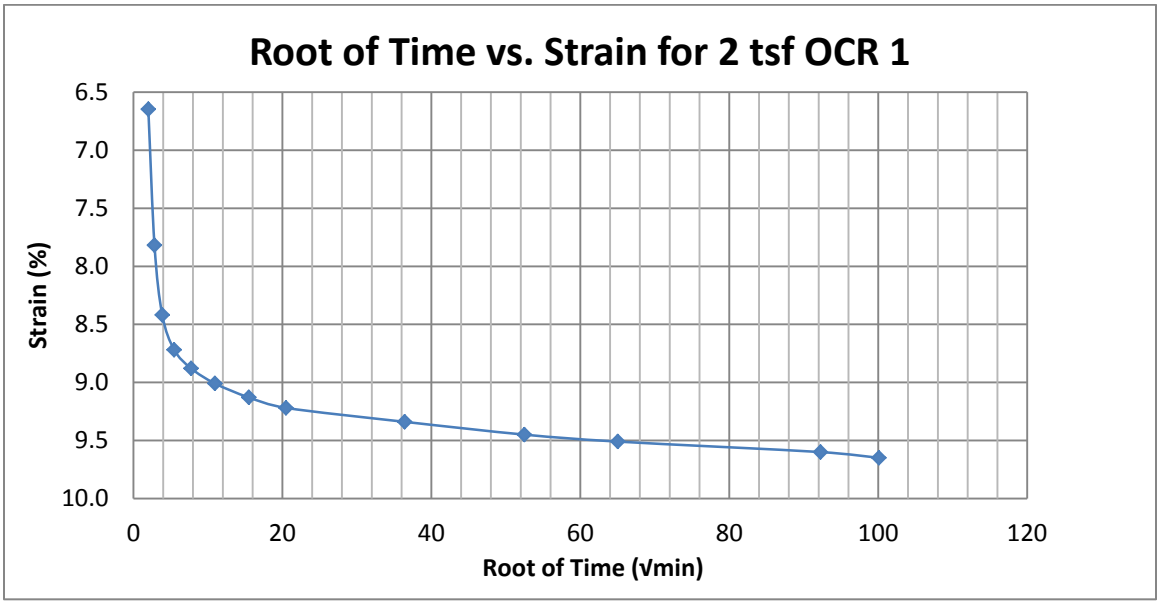

B65 Provo at 17-19 feet

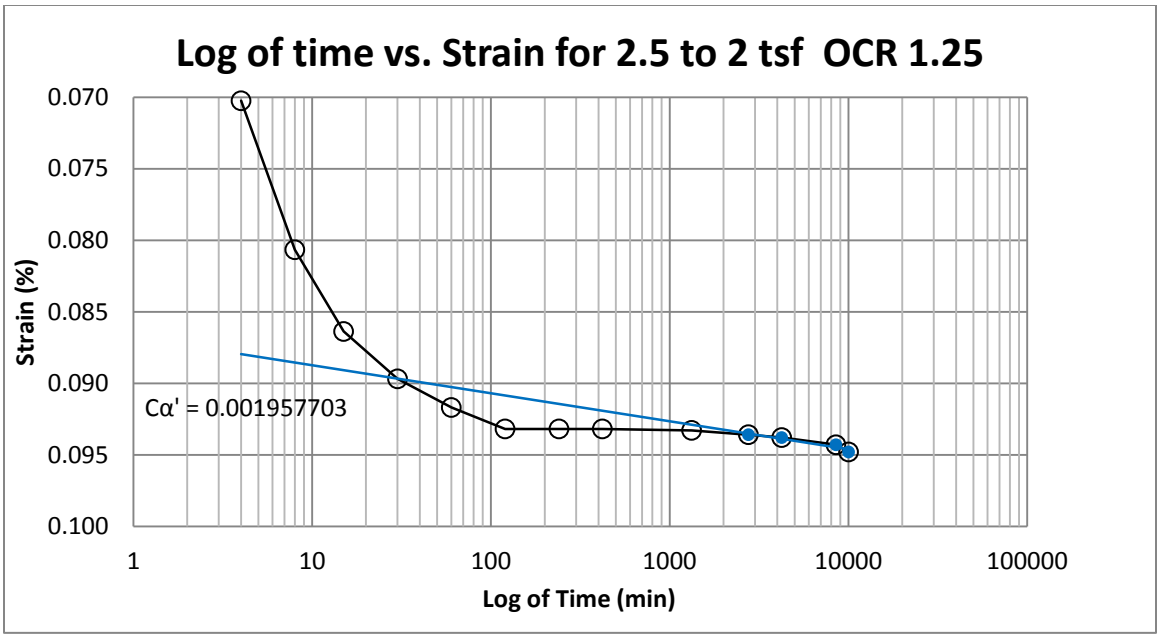

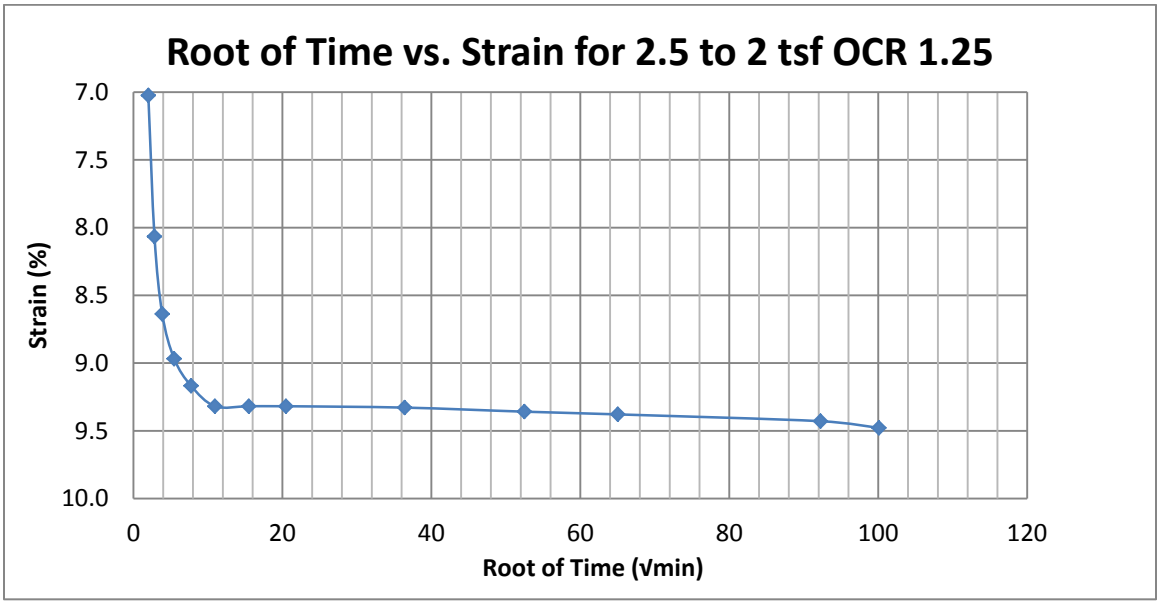

B66 Provo at 17-19 feet

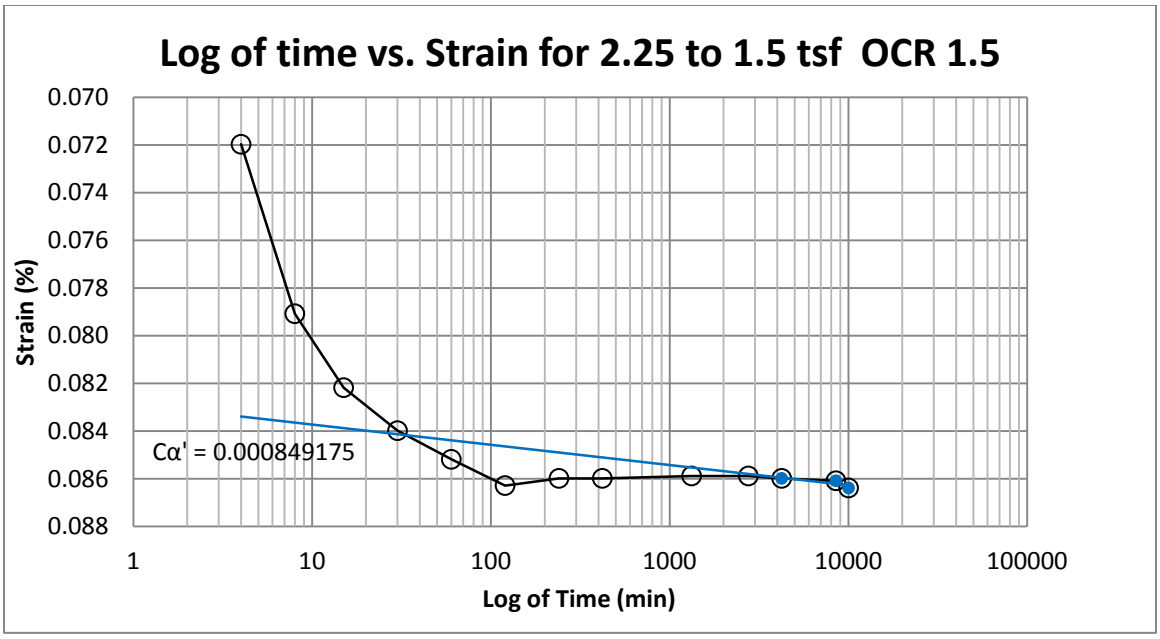

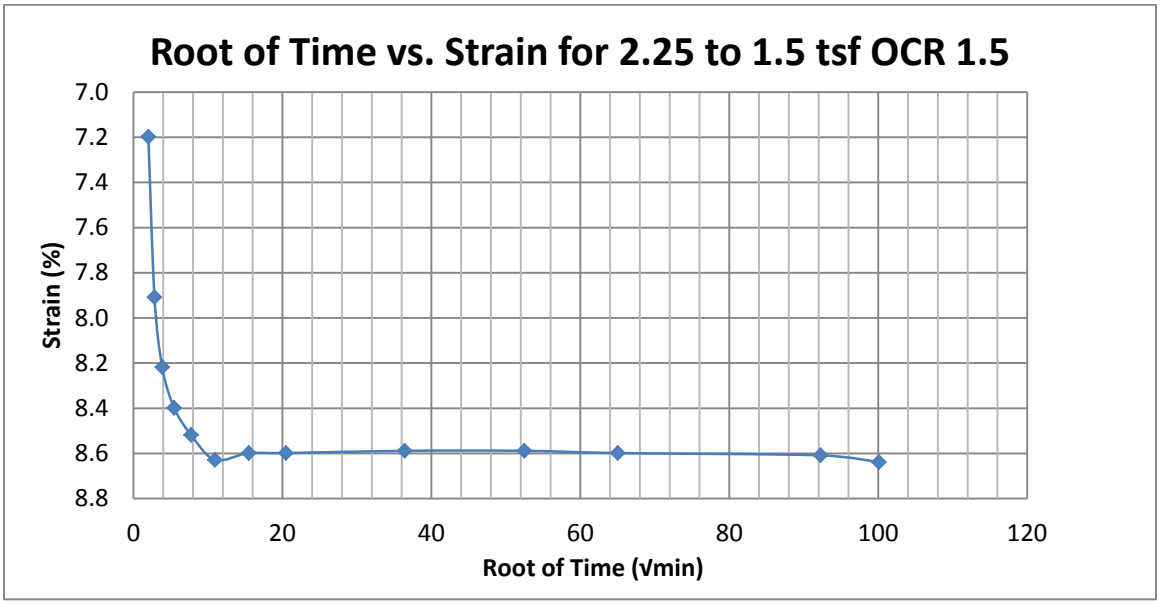

B67 Provo at 17-19 feet

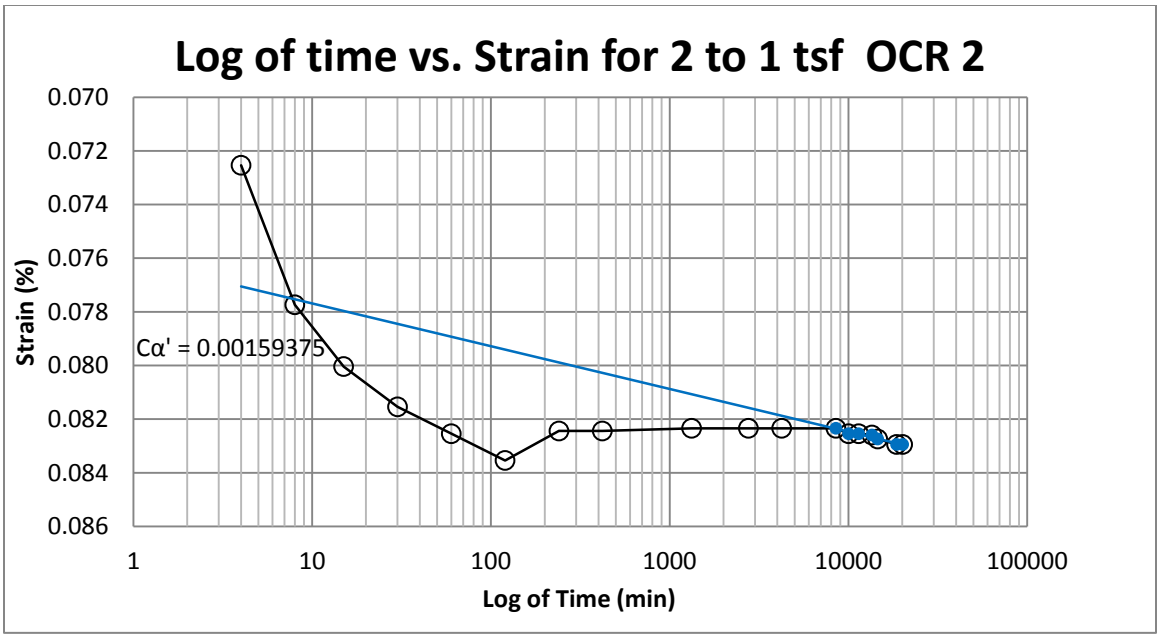

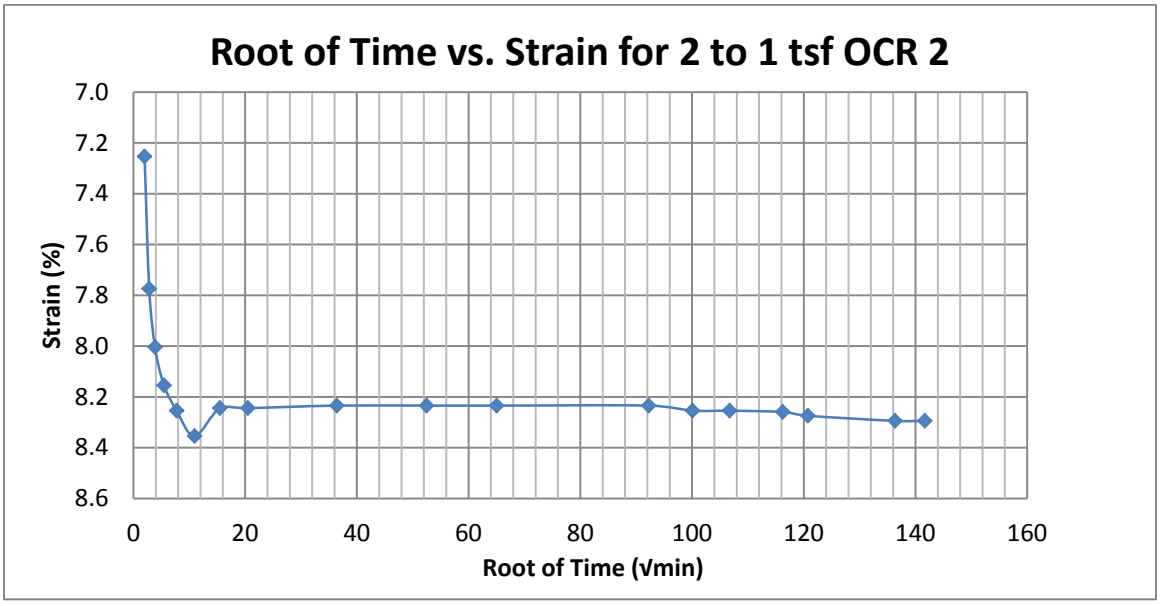

B68 Provo at 17-19 feet

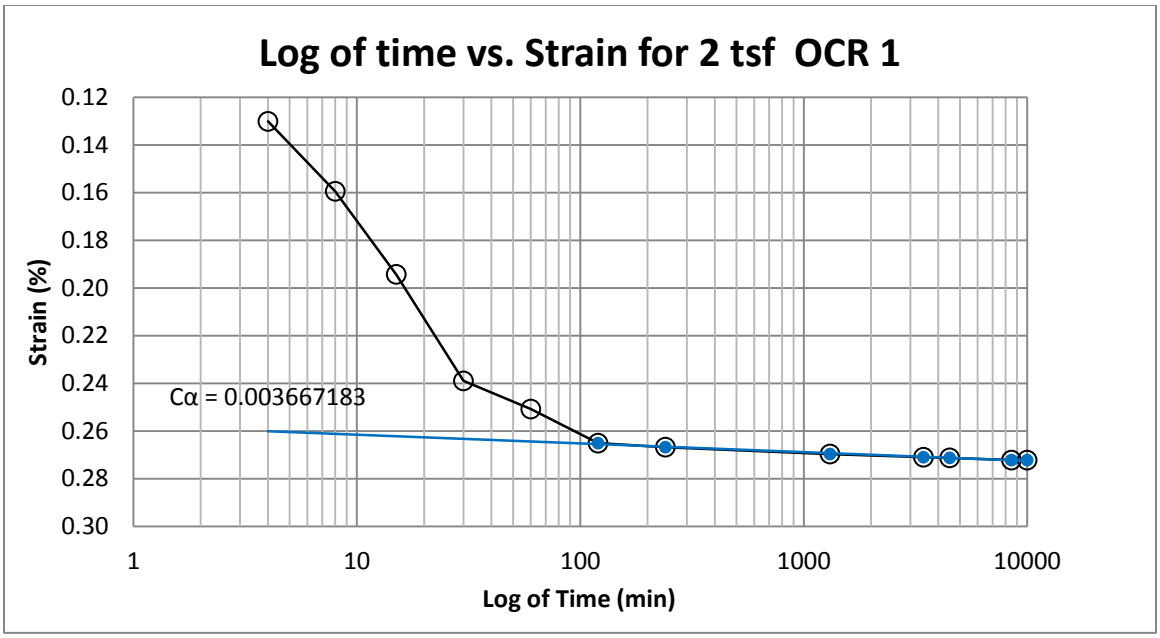

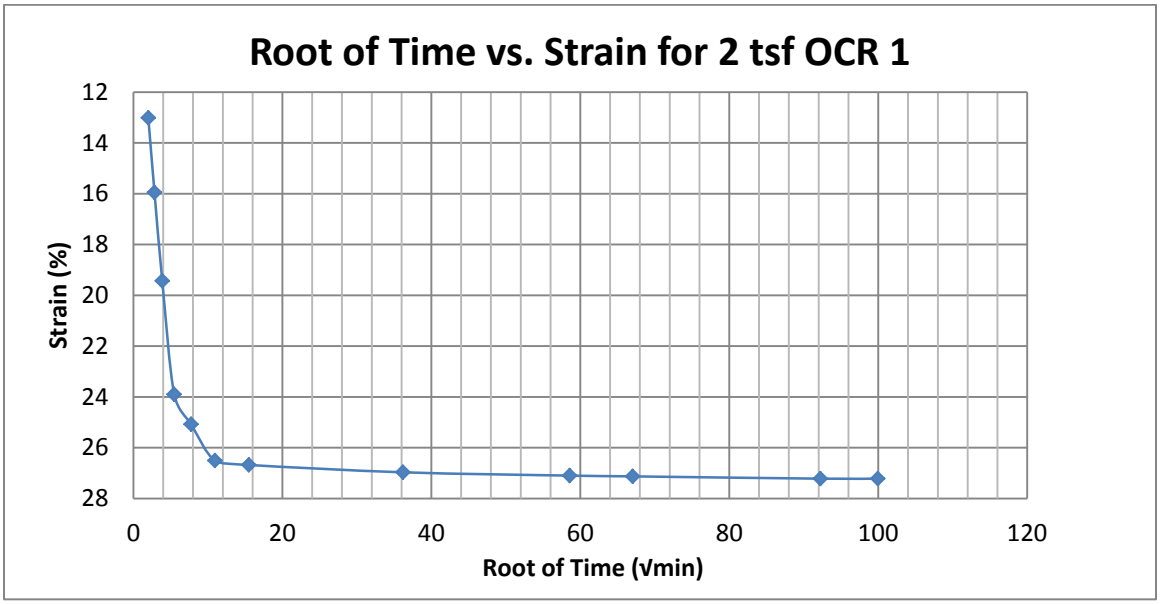

B69 Provo at 50-52 feet

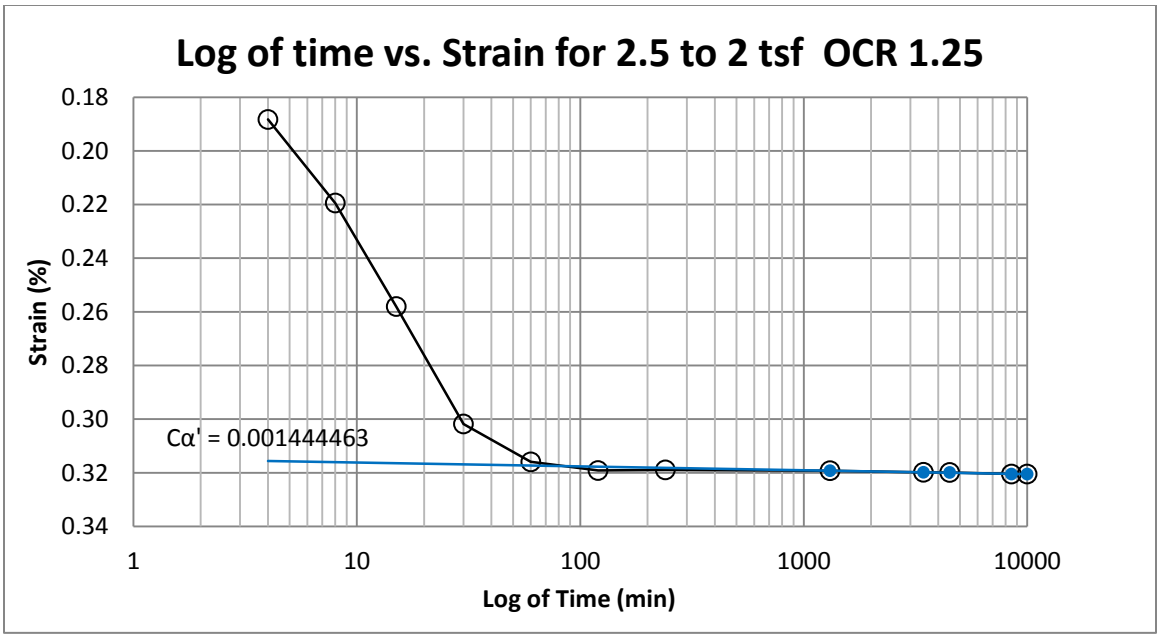

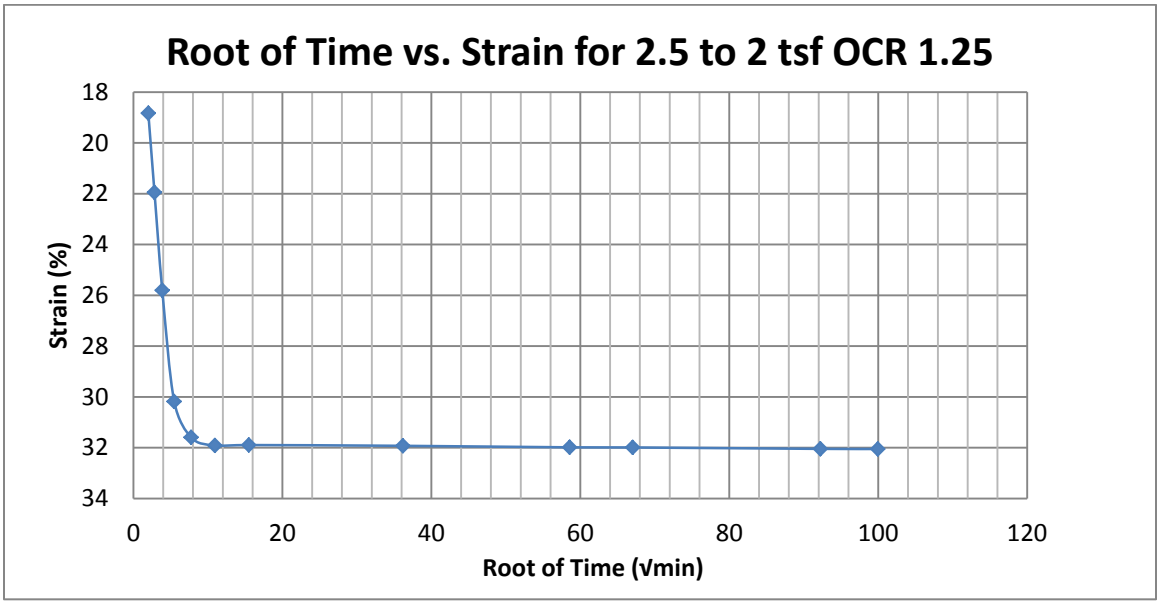

B70 Provo at 50-52 feet

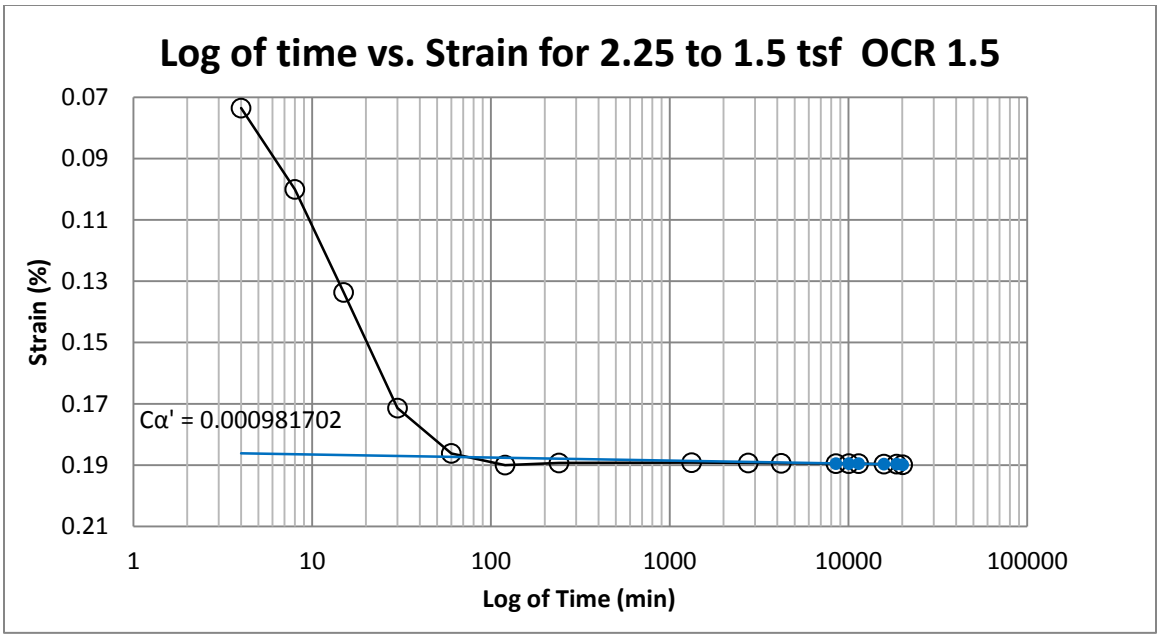

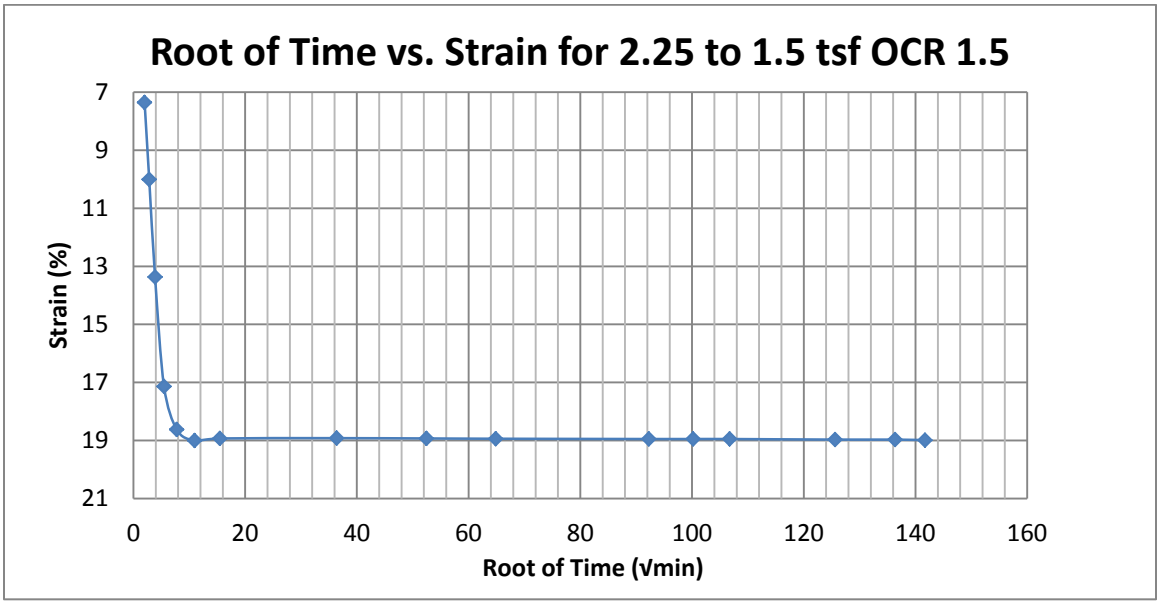

B71 Provo at 50-52 feet

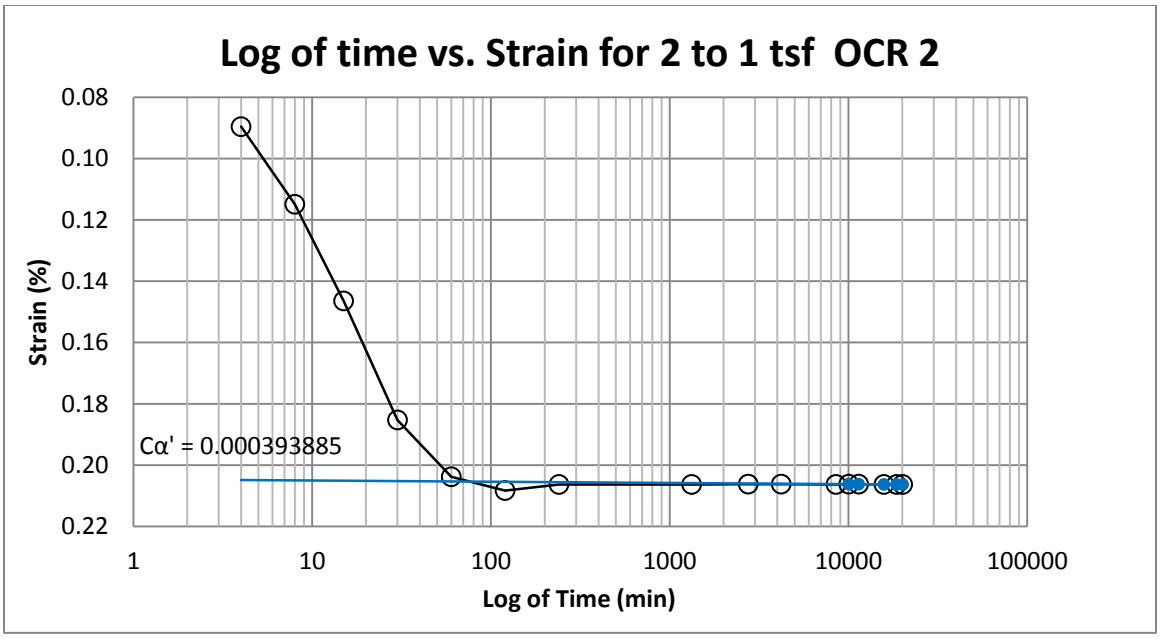

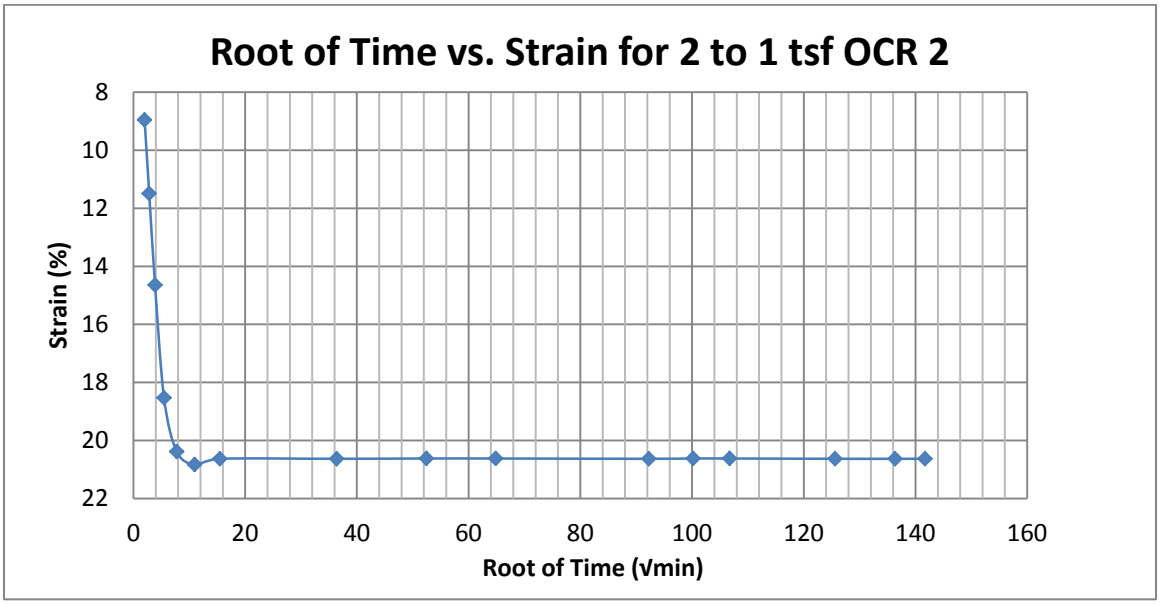

B72 Provo at 50-52 feet

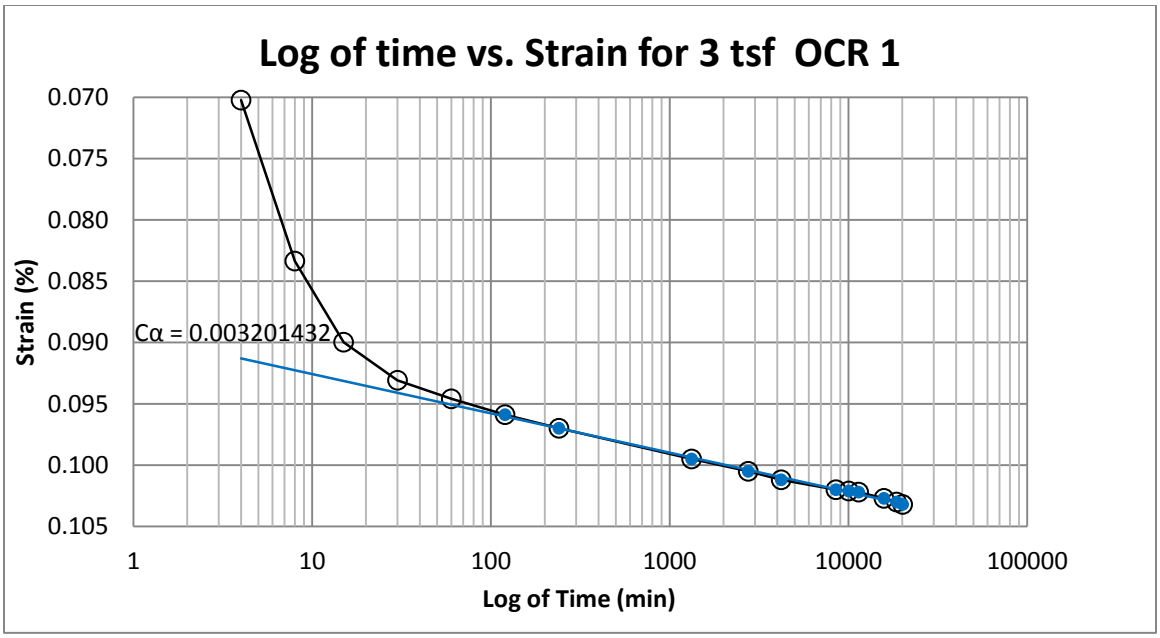

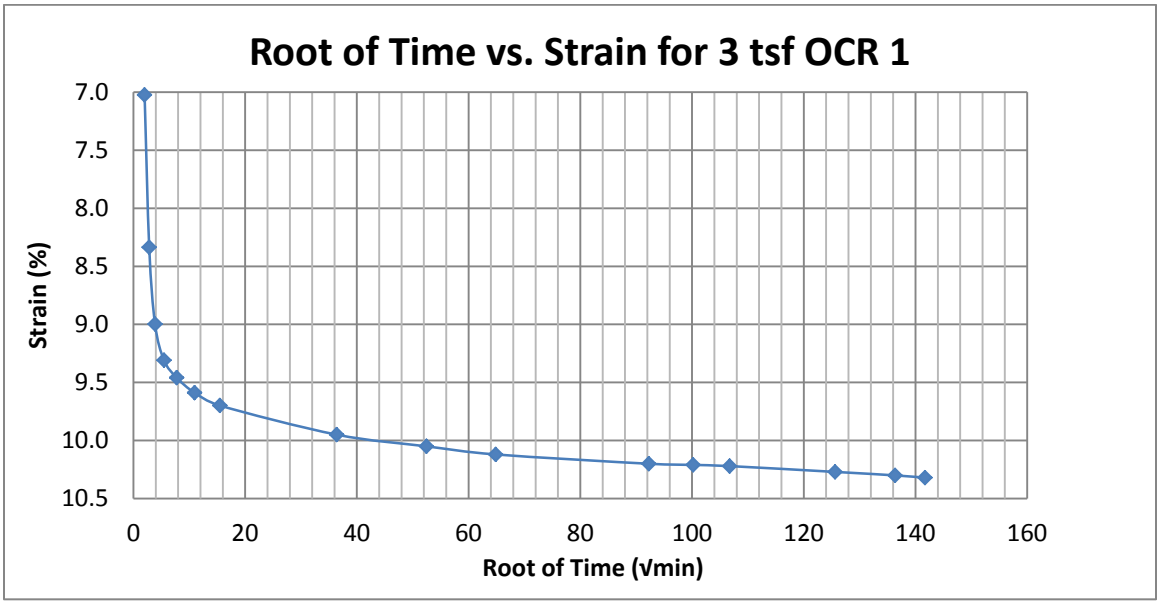

B73 Provo at 60-62 feet

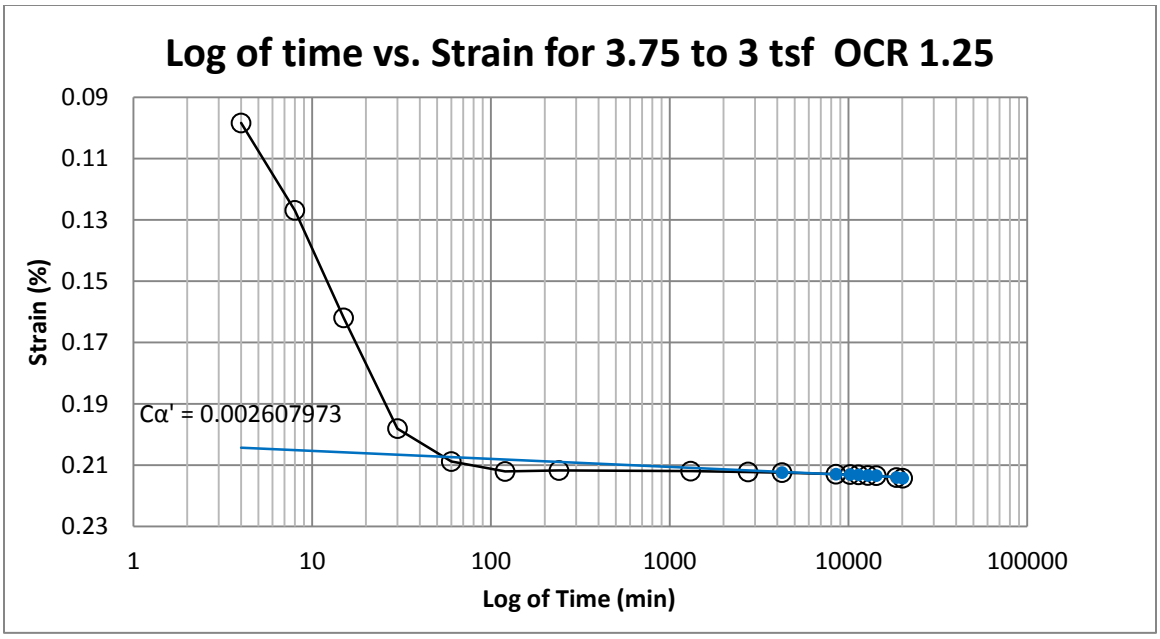

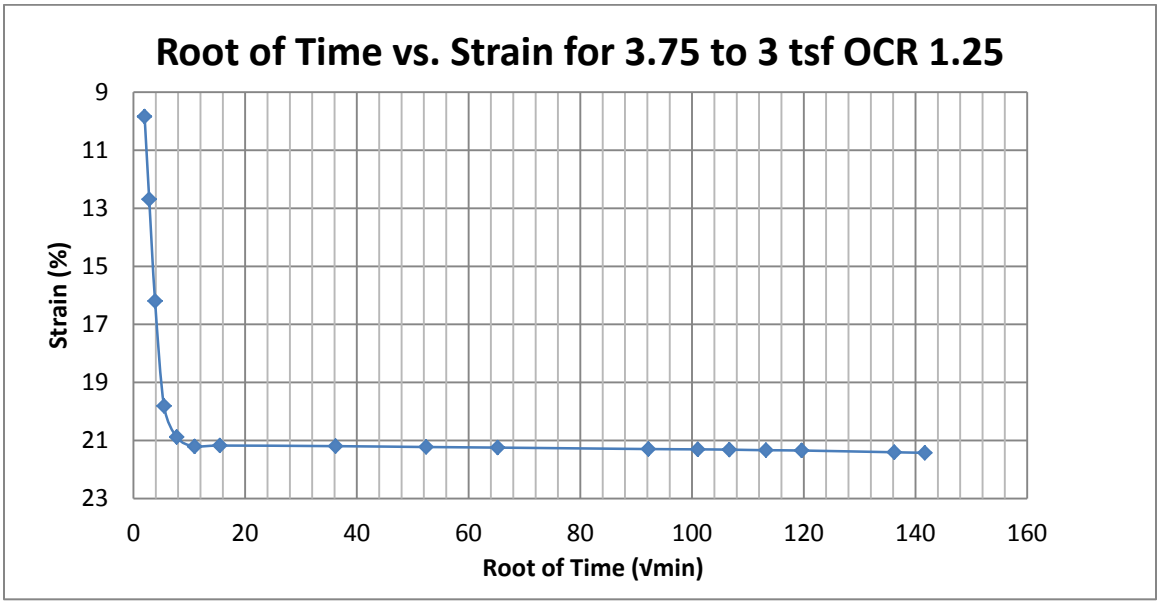

B74 Provo at 60-62 feet

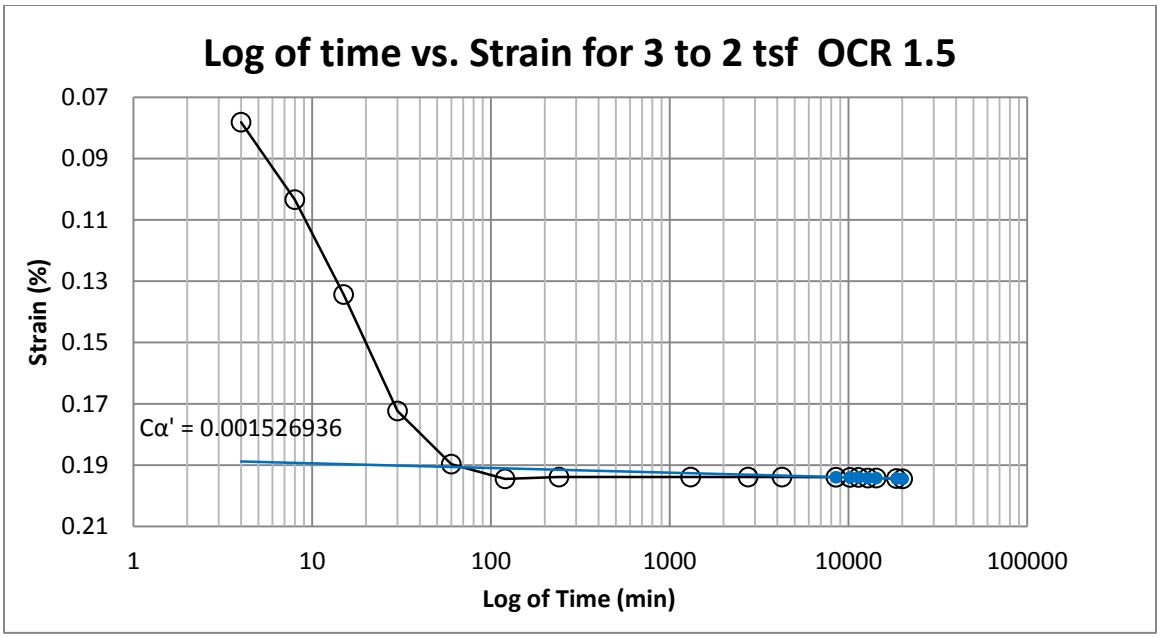

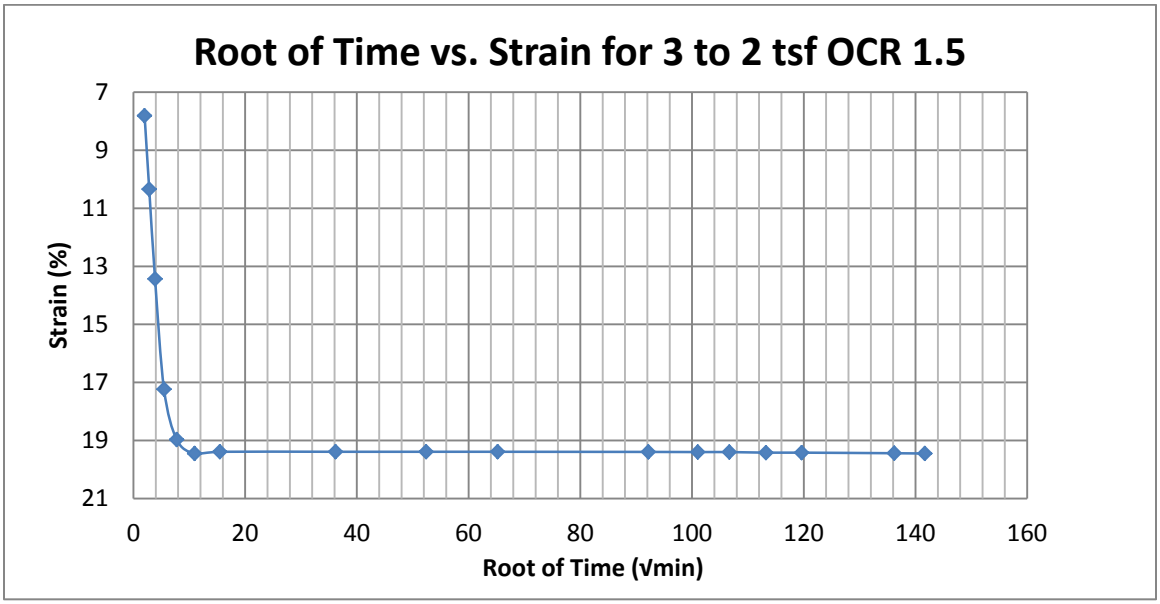

B75 Provo at 60-62 feet

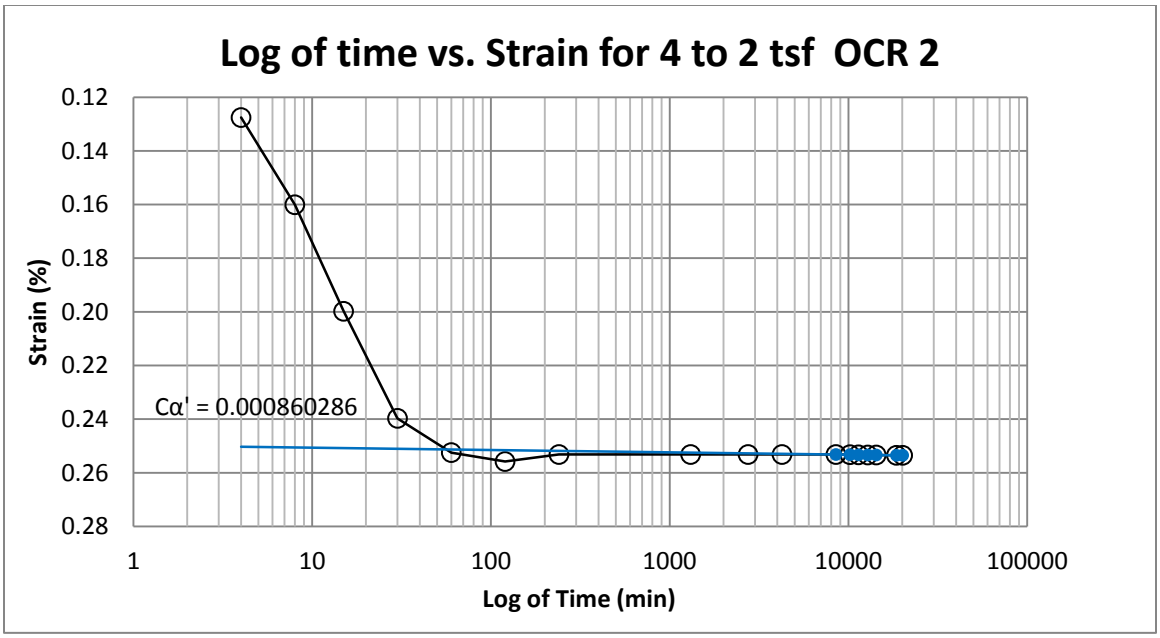

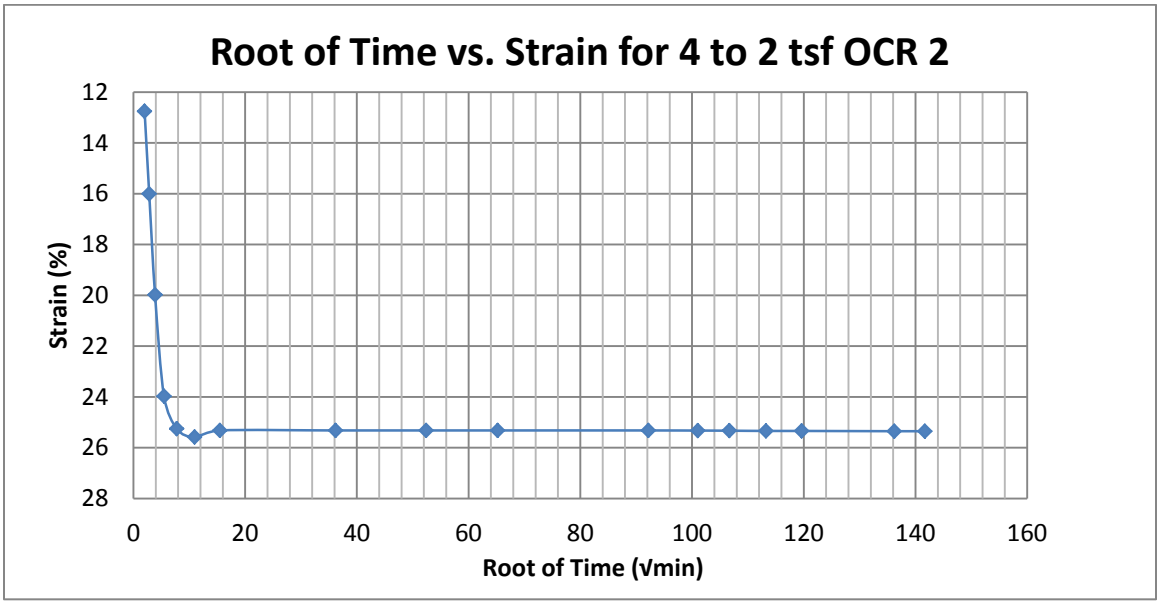

B76 Provo at 60-62 feet

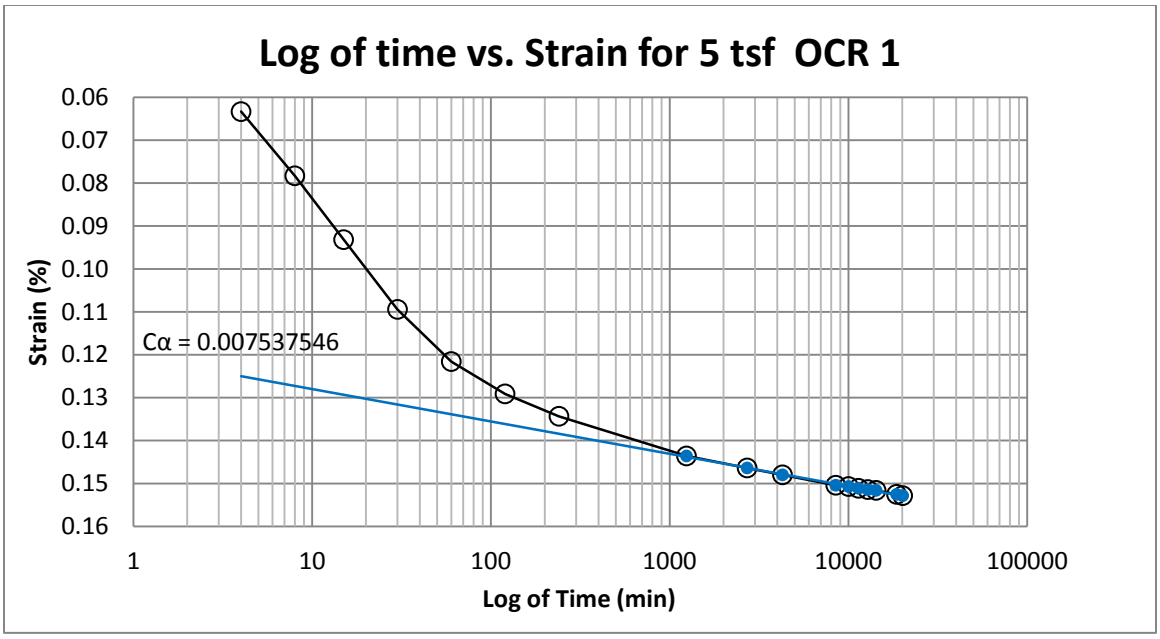

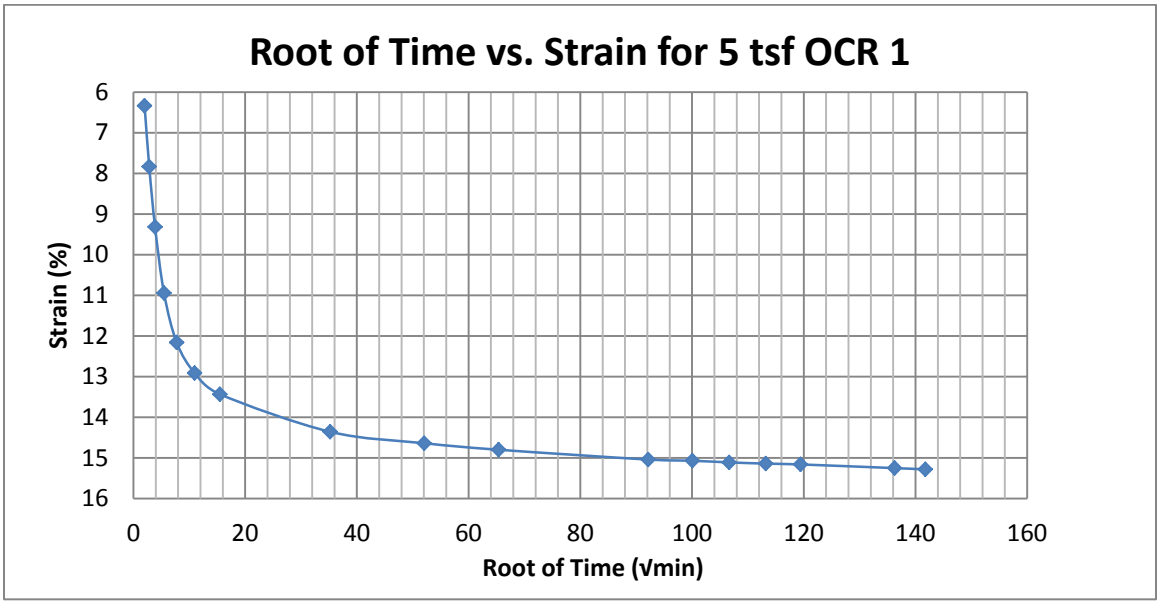

B77 Provo at 80-82 feet

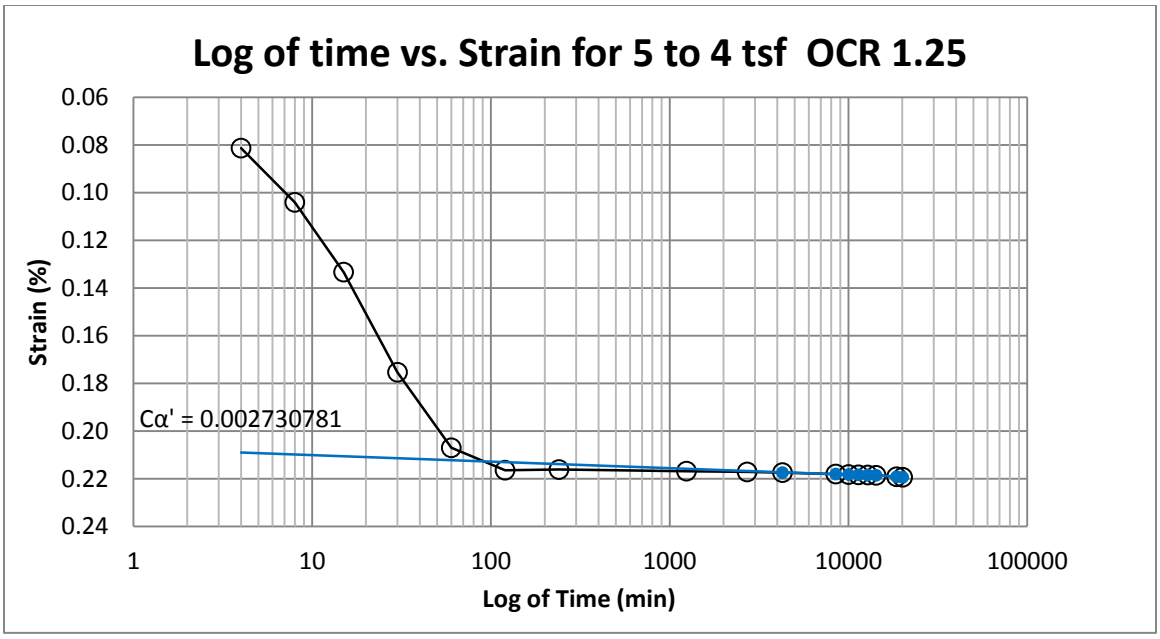

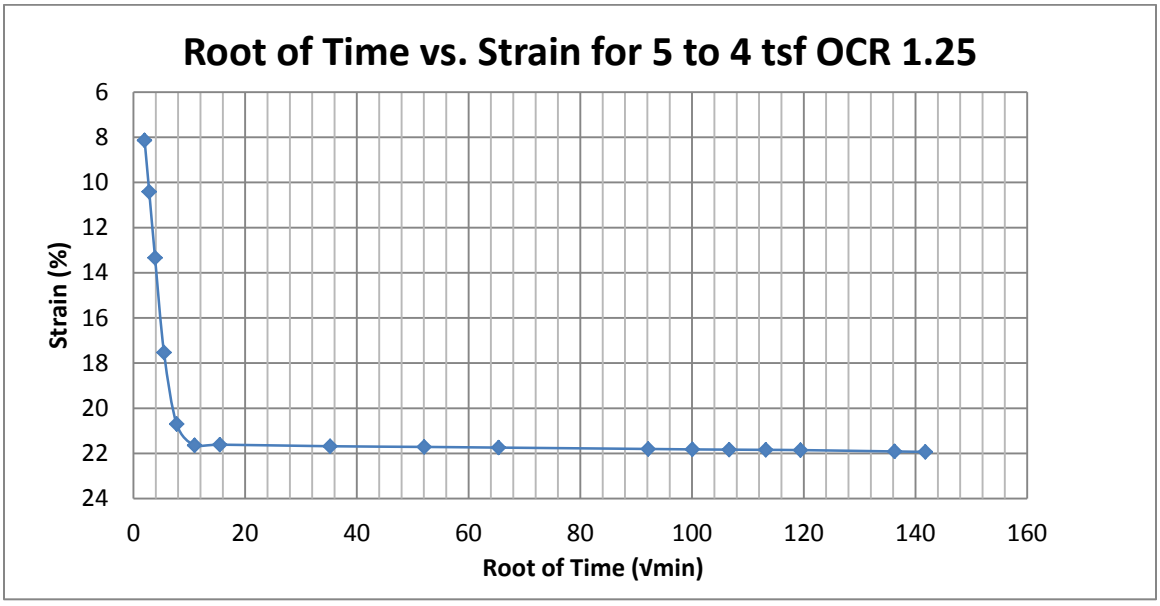

B78 Provo at 80-82 feet

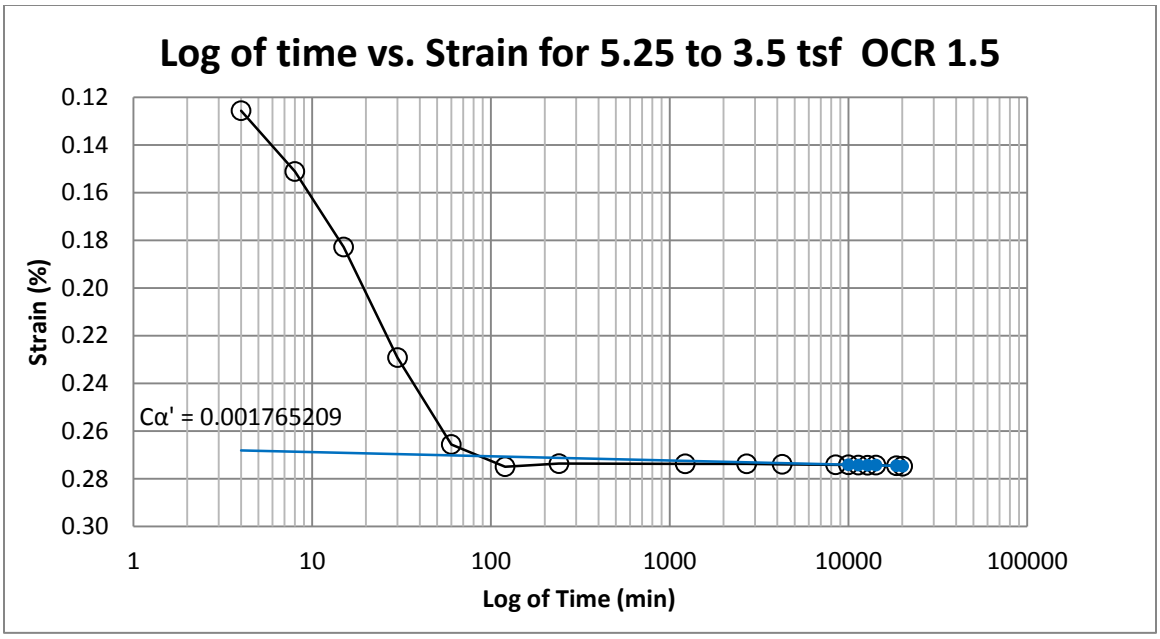

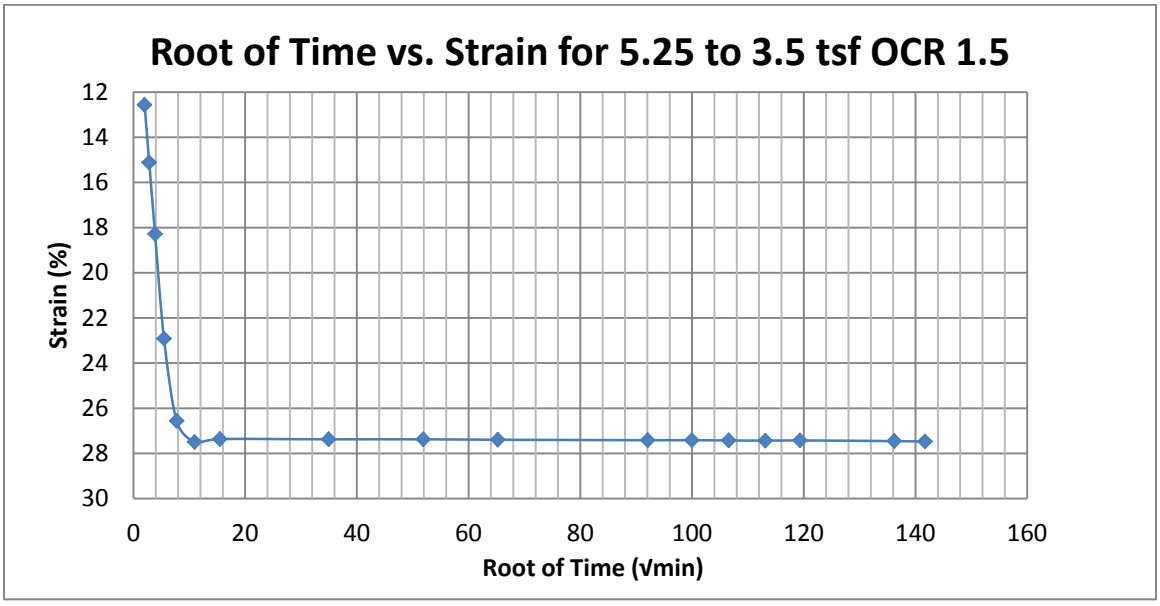

B79 Provo at 80-82 feet

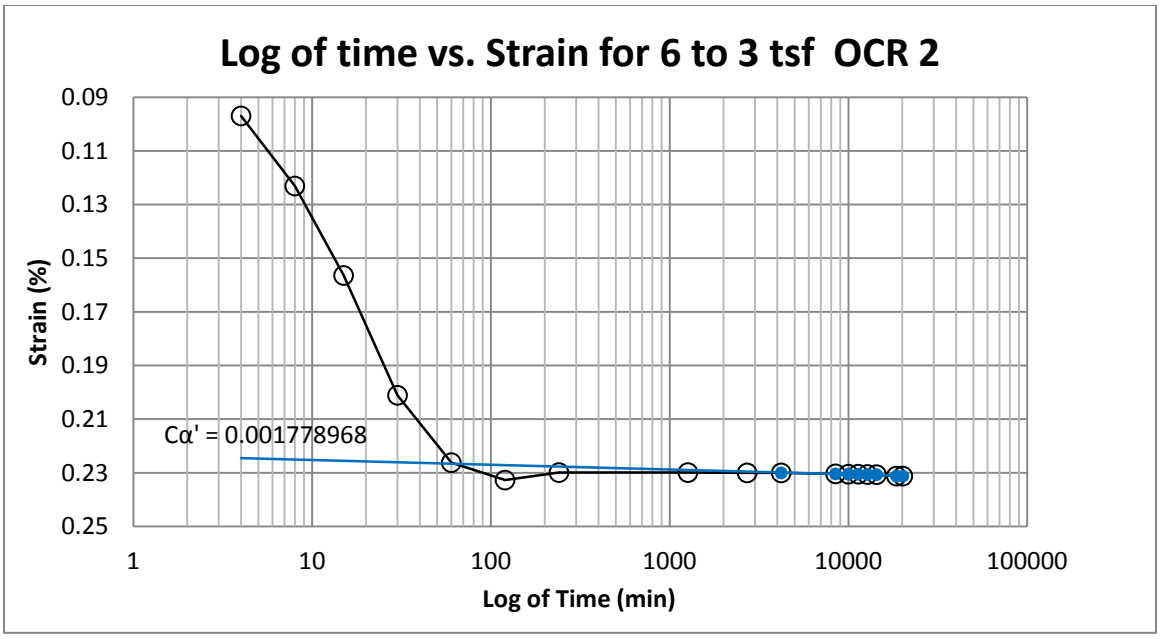

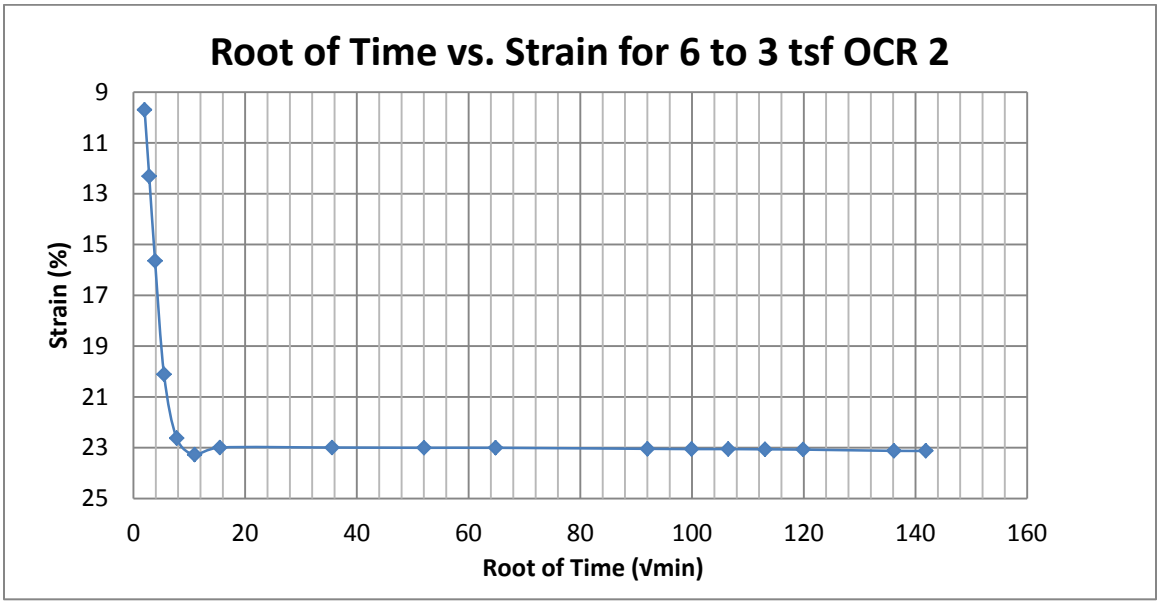

B80 Provo at 80-82 feet

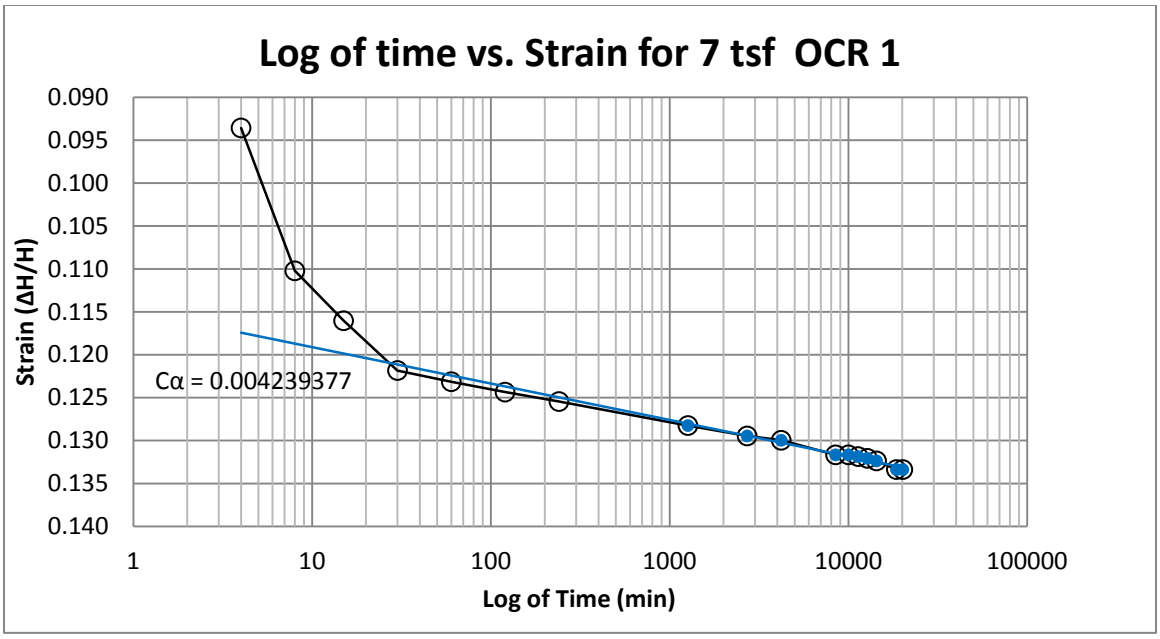

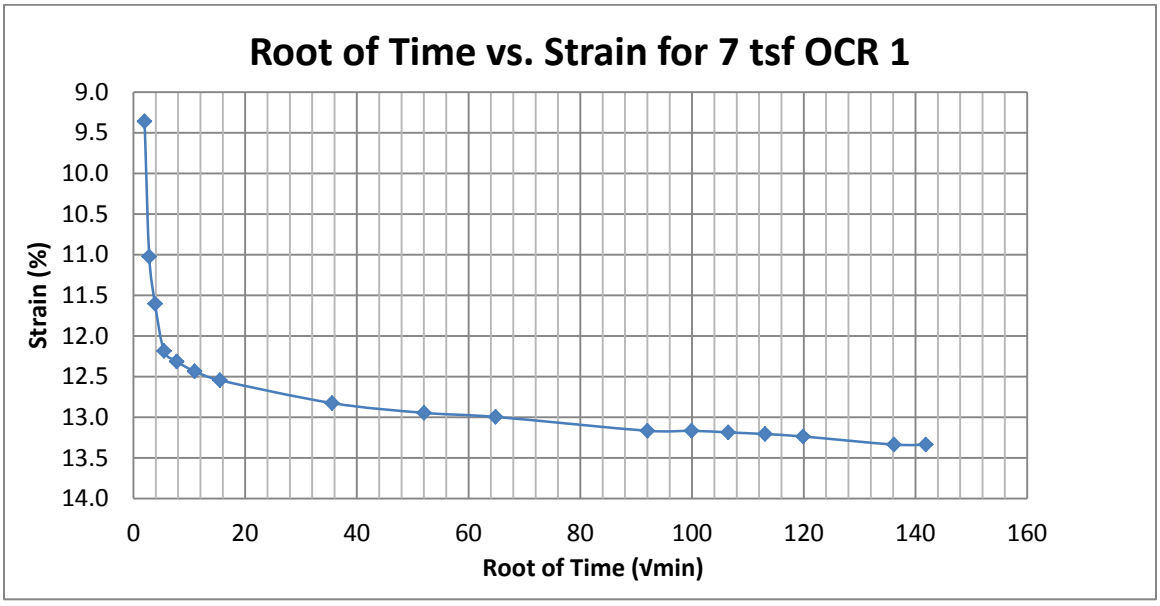

B81 Provo at 90-92 feet

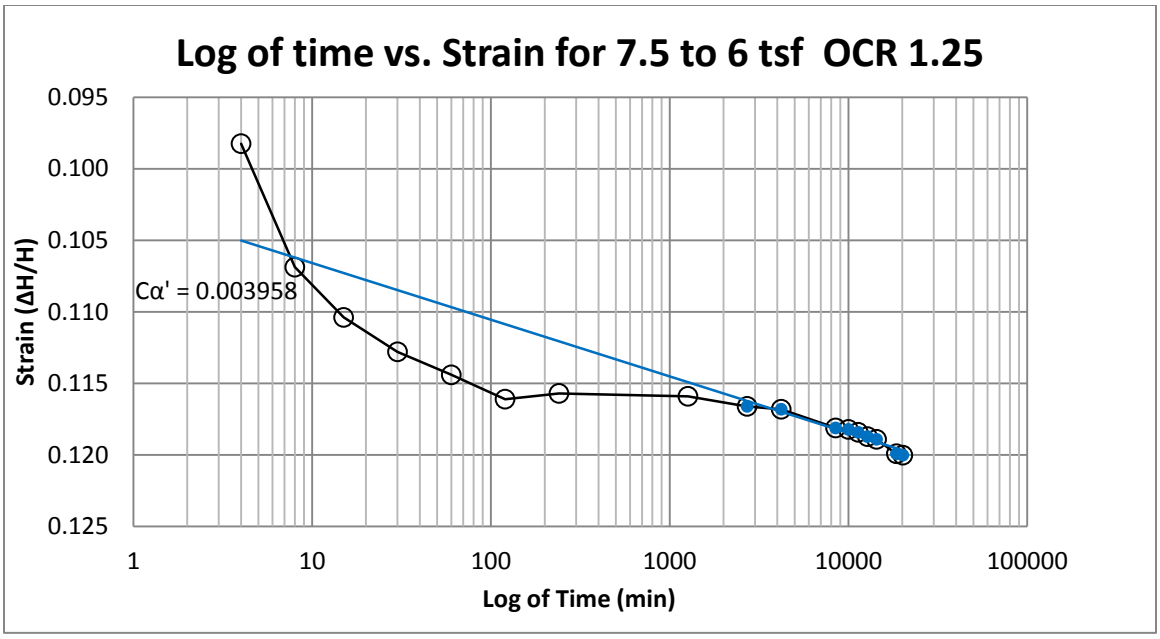

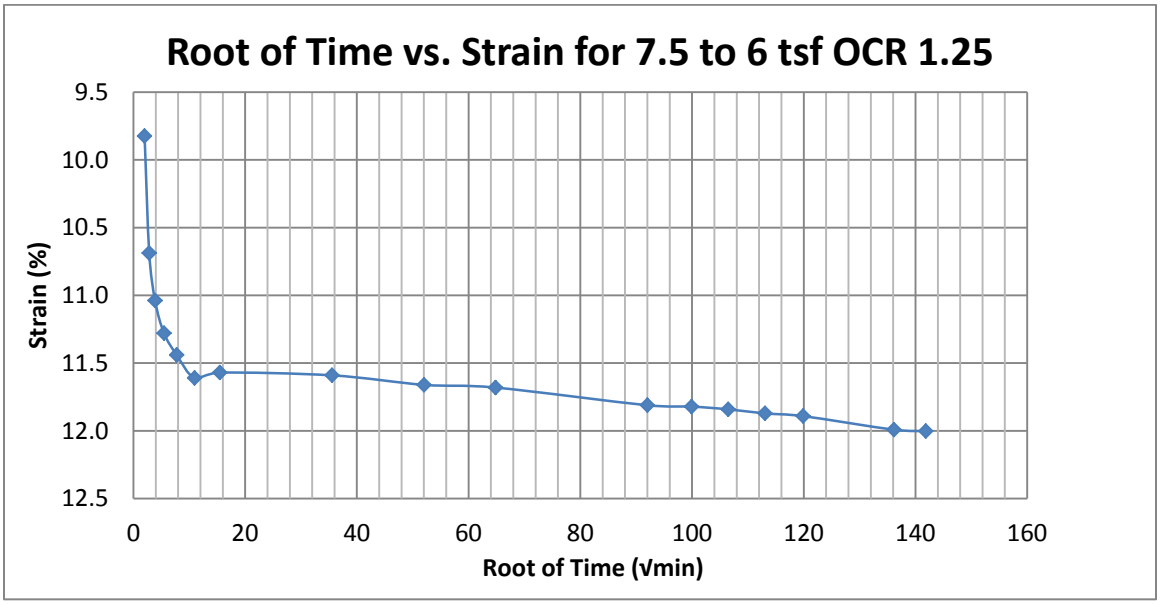

B82 Provo at 90-92 feet

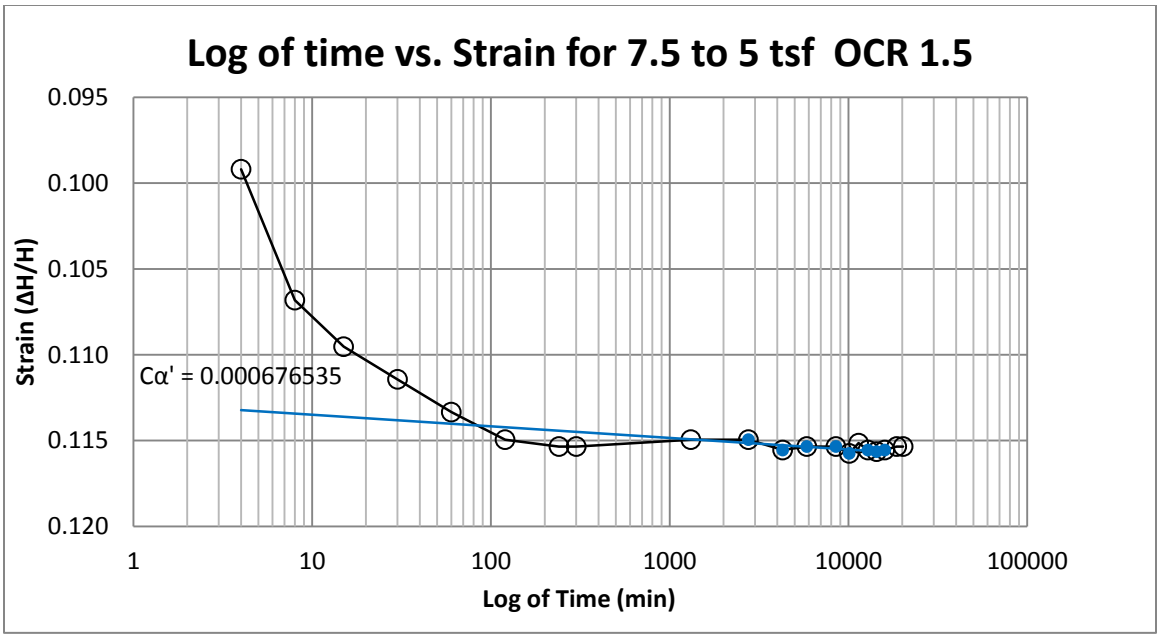

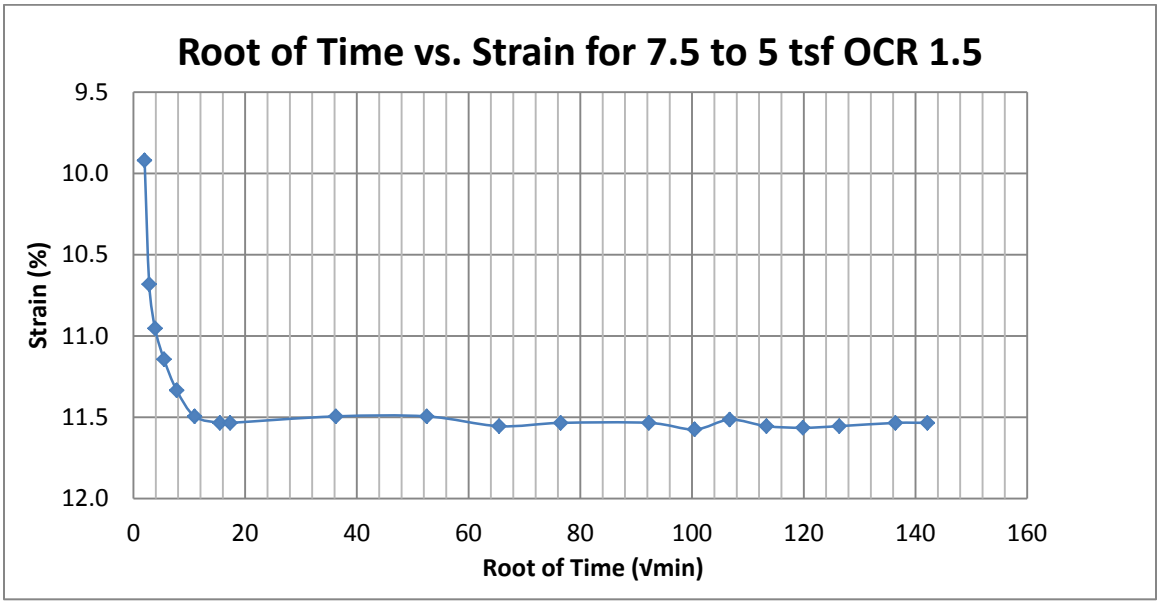

B83 Provo at 90-92 feet

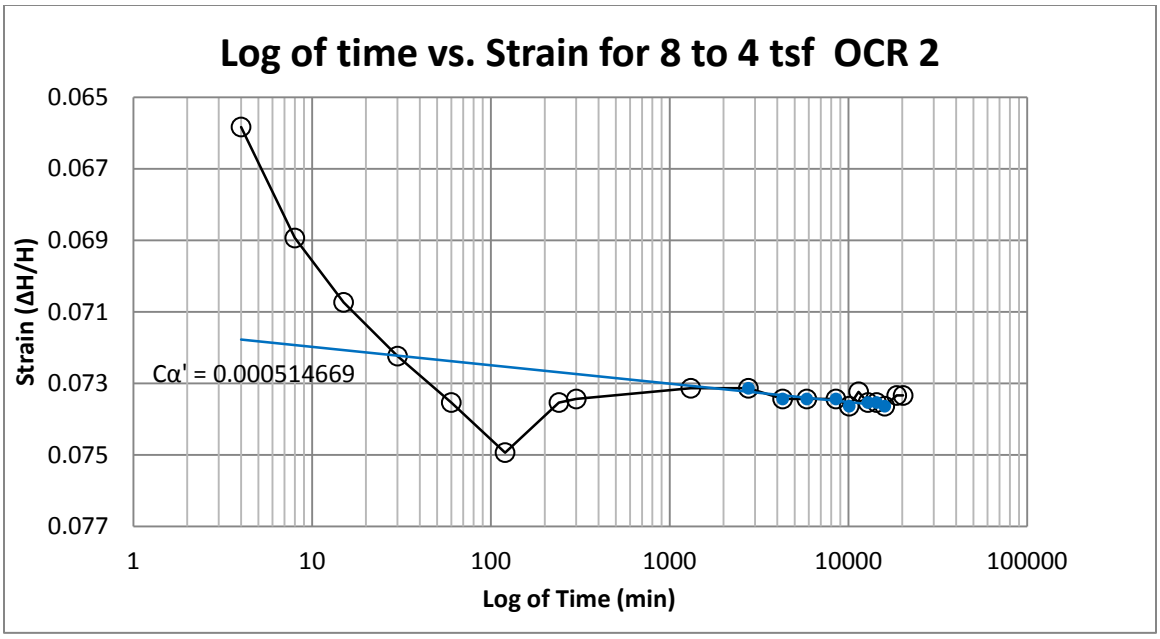

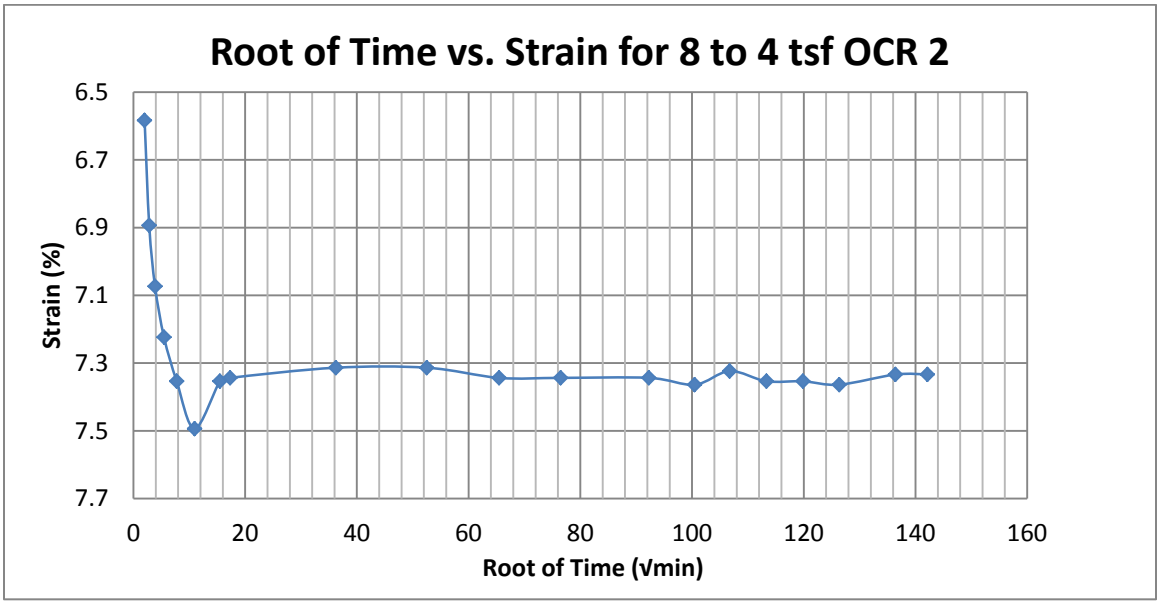

B84 Provo at 90-92 feet

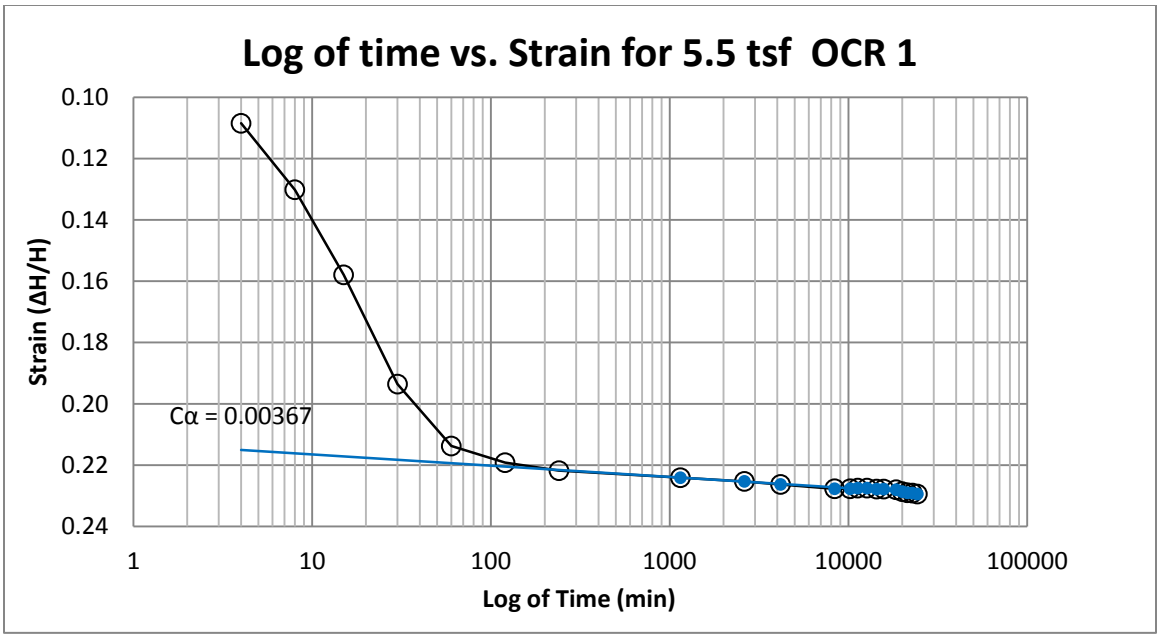

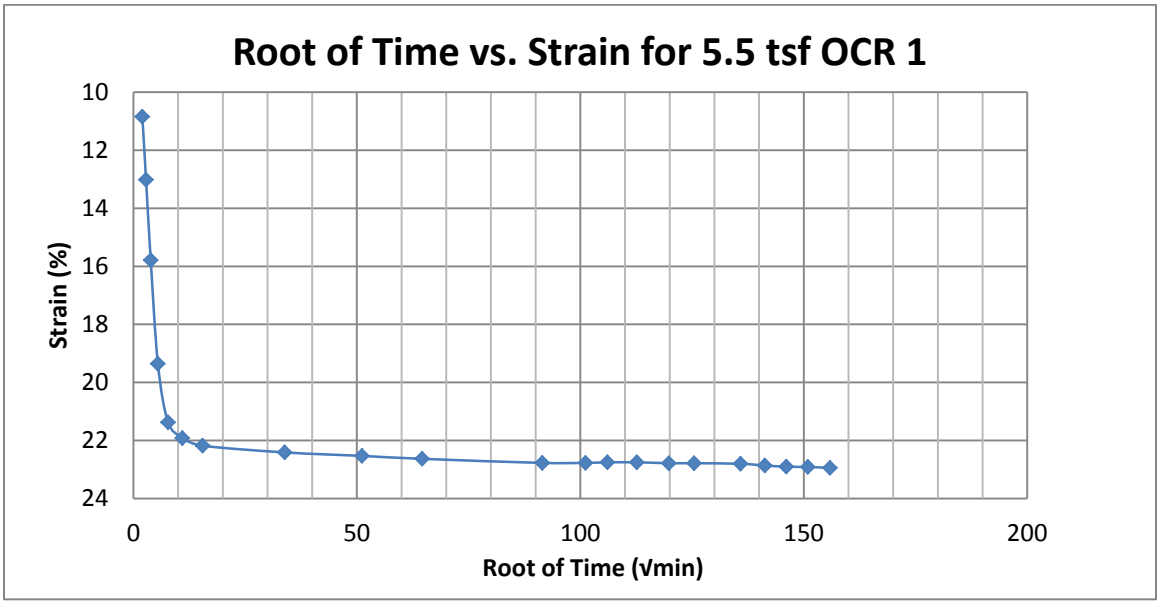

B85 Provo at 110-112 feet

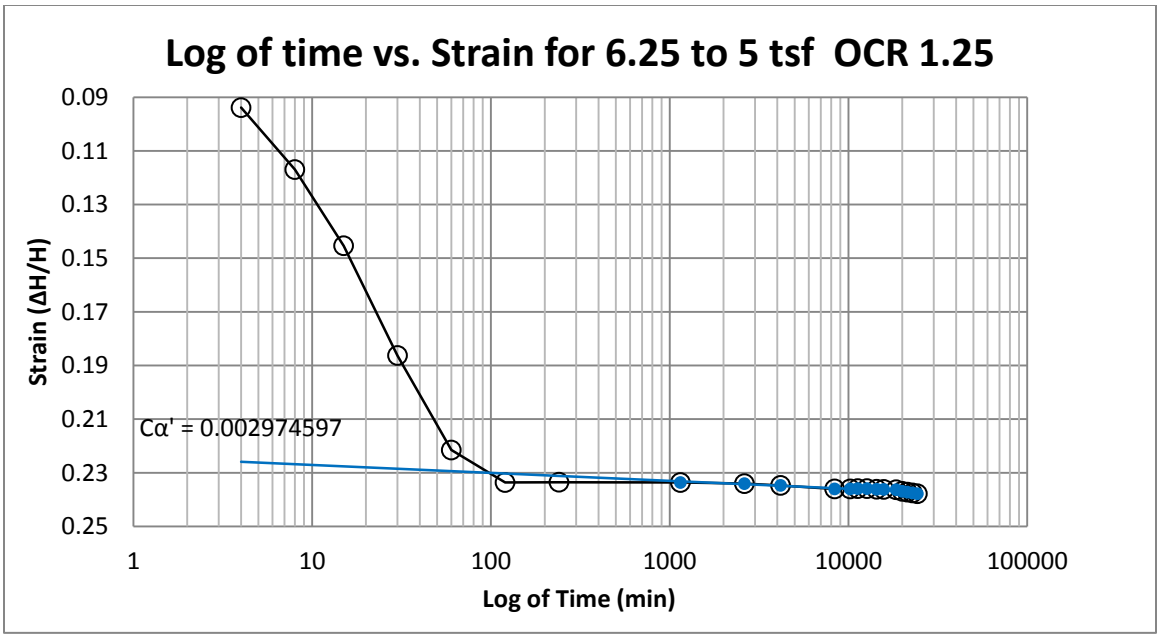

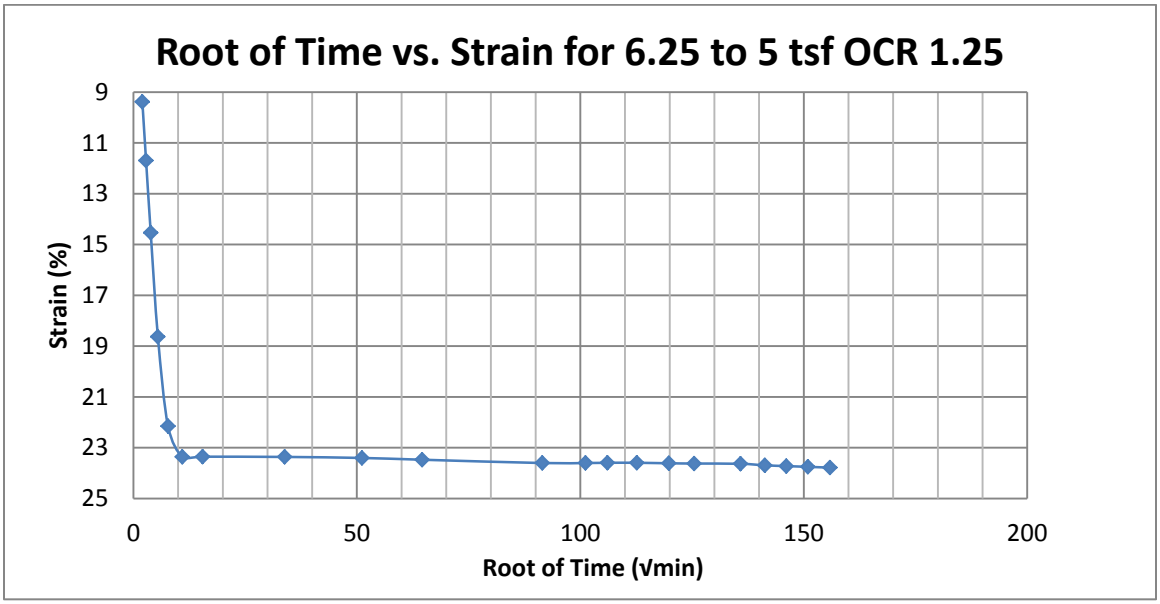

B86 Provo at 110-112 feet

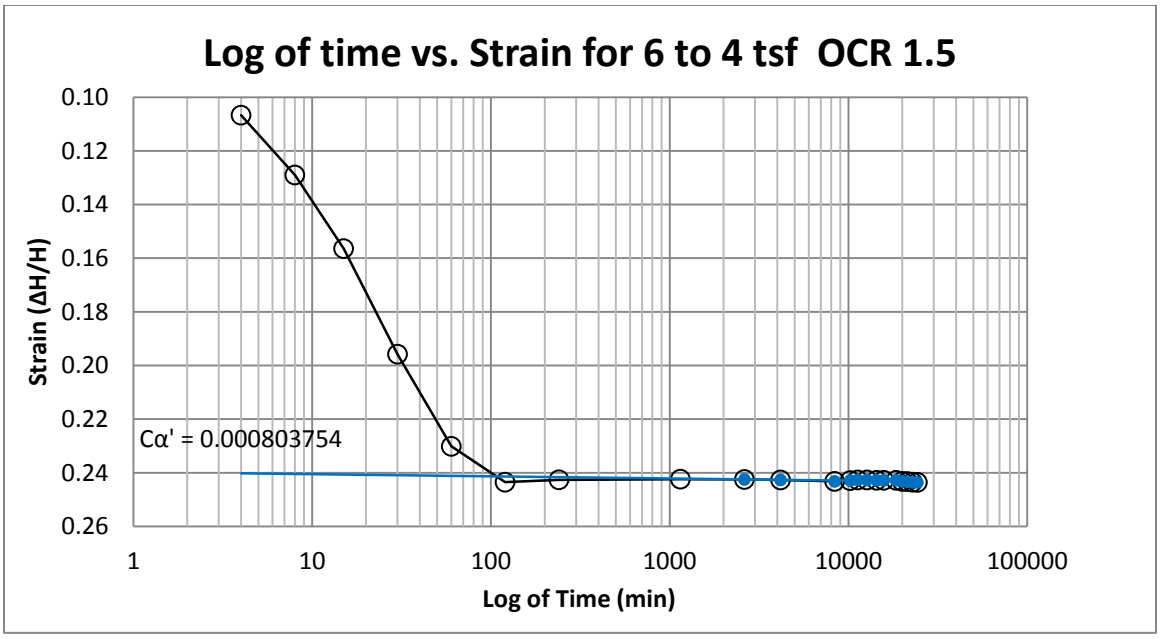

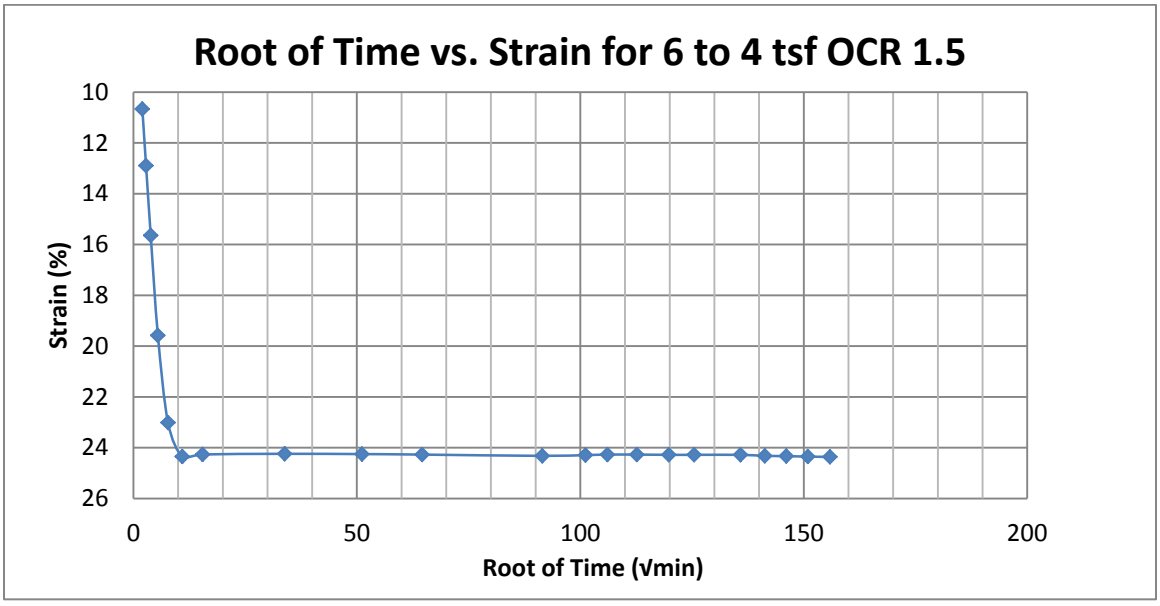

B87 Provo at 110-112 feet

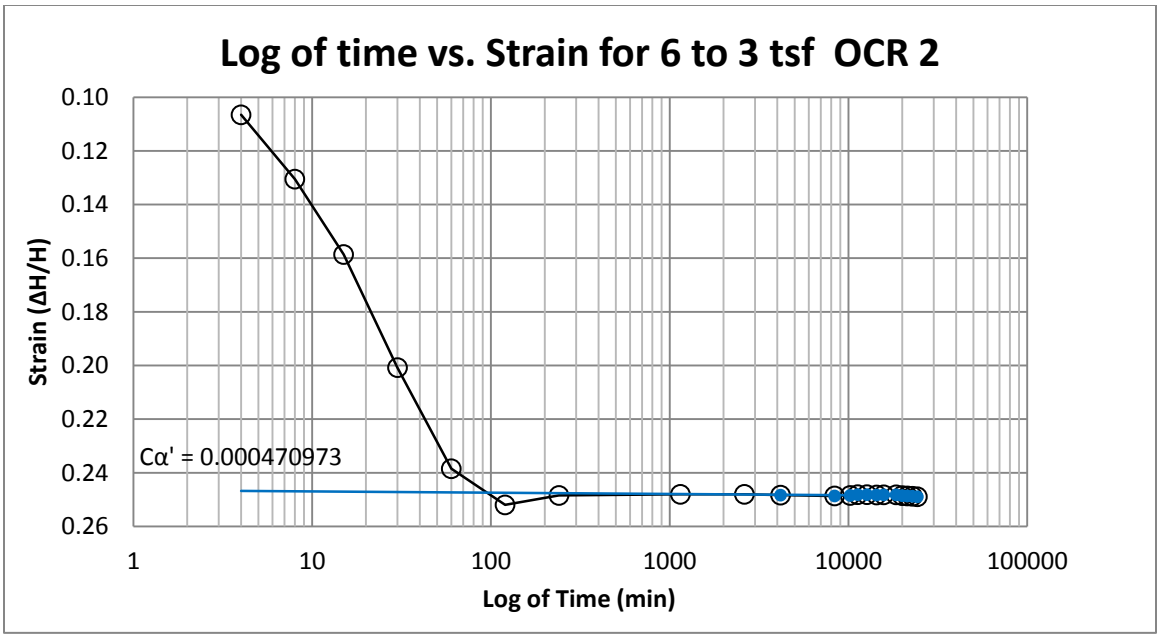

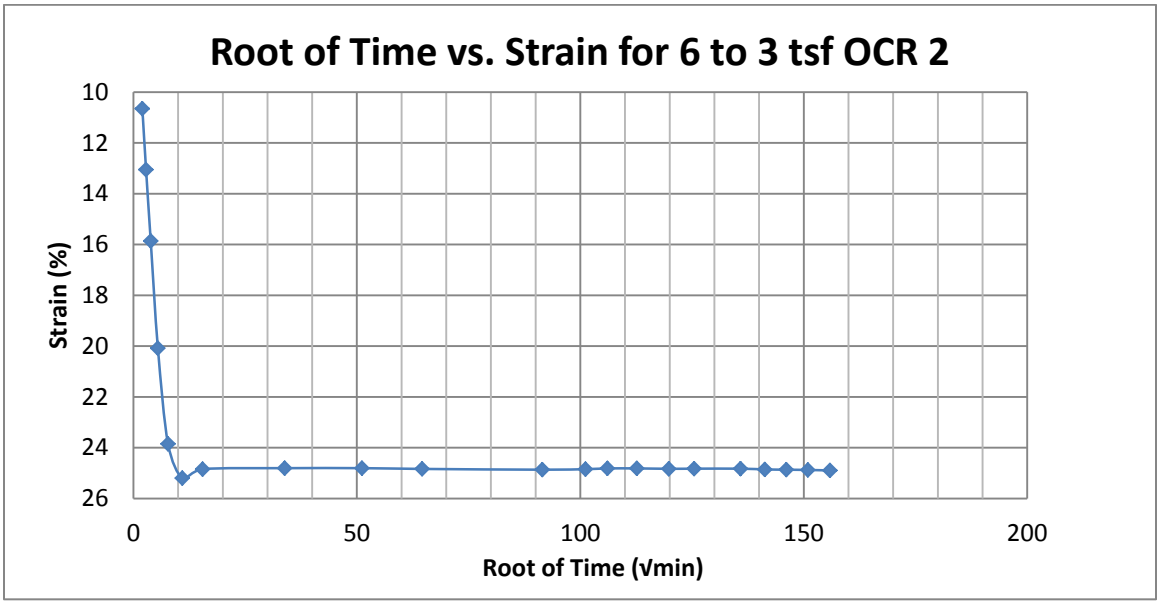

B88 Provo at 110-112 feet

APPENDIX C

LABORATORY TESTING PROCEDURE

C.1. Sample Preparation

C.1.1. Determine the mass, height and diameter of the consolidation ring.

C.1.2. Obtain an undisturbed sample from the selected test depth.

C.1.3. Trim the sample to size and insert it into the consolidation ring.

C.1.3.1. When trimming the sample to size, for soft to medium soils it is recommended to use a wire saw for the trimming to minimize the disturbance to the sample.

C.1.3.2. Coating the inside of the consolidation ring with a silicon lubricant will reduce the amount of disturbance when inserting the soil into the ring.

C.1.4. Trim the sample flush with the top and bottom of the consolidation ring.

C.1.4.1. For soft to medium soils use a wire saw to trim the sample flush with the top and bottom, and after the excess soil is removed a straight edge with a sharp cutting edge may be used for the final trim. For stiff soils use the straightedge to trim the soil flush on the top and bottom.

C.1.4.2. If there are any small voids on the sample, fill them with remolded trimming.

C.1.5. Determine the mass of the soil in the ring by getting the mass of the soil and ring and subtracting out the mass of the consolidation ring.

C.1.6. Use the trimmings to determine the moisture content.

C.1.7. Assemble the consolidometer and place in the loading device.

C.2. Determining The Preconsolidation Pressure

C.2.1. Apply the seating load and take the initial reading.

C.2.1.1. In ASTM D2435 it is recommended that the seating load to be used is 5 kPa (100 psf)

C.2.1.2. Inundate shortly after the application of the seating load.

C.2.2. When determining the preconsolidation stress use a 1-D incremental loading test with time rate of consolidation measurements taken for each loading increment.

C.2.3. The loading schedule will have a load increment ratio (LIR) of one which is obtained by doubling the pressure on the soil. LIR is defined as the added load divided by the previous total load on the specimen ($\Delta P/P$).

C.2.3.1. Recommended loading schedule from ASTM D2435 is 12, 25, 50, 100, 200, etc. kPa (250, 500, 1000, 2000, 4000, etc. psf)

C.2.3.2. Recommended unloading schedule from ASTM D2435 is to either half the loading or to one-fourth the loading. When unloading it is recommended to use the one-fourth schedule to shorten the test time.

C.2.4. Apply the first loading and begin taking time rate readings.

C.2.4.1. Aging of the soil can affect the test results; to avoid aging, the next loading will be applied with as little secondary settlement occurring. Use Taylor's square root of time method to determine when 90% of primary settlement has occurred then apply the next loading. For an explanation of the square root of time method (refer to Figure C1).

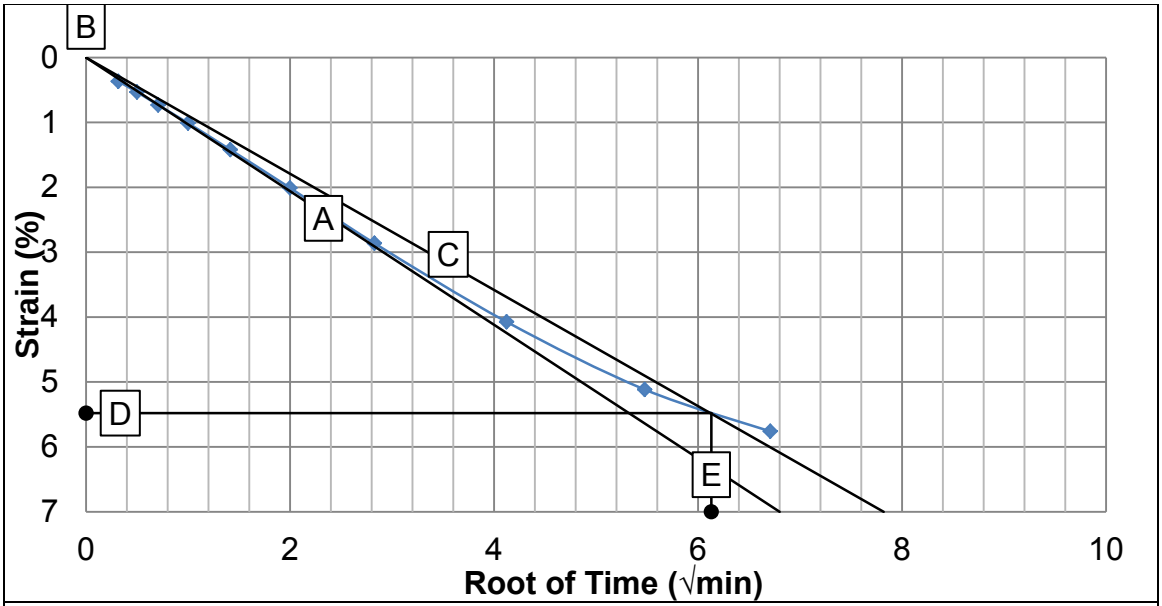

A - Time strain curve from data points.
B - Extention of initial linear portion of cure A to time = 0 minutes.
C - Constructon line with slope = 1.15 times inital linear portion of curve A.
D - ε_{90} strain at point where curve A crosses line C.
E - t_{90} time at point where curve A crosses line C.

Figure C1 Time-Deformation Curve from Square Root of Time Method

C.2.4.2. Procedure for the square root of time method:

C.2.4.2.1. Plot square root of time versus strain.

C.2.4.2.2. Draw a straight line through the points representing the initial readings that exhibit a straight line trend.

C.2.4.2.3. Draw a second straight line through the 0% ordinate so that the abscissa of this line is 1.15 times the abscissa of the first straight line through the data.

C.2.4.2.4. The point where the second line crosses the plotted data is the point that corresponds to 90% primary consolidation.

C.2.4.3. For each load increment the time rate readings are as follows; 0.1, 0.25, 0.5, 1, 2, 4, 8, 15, 30 minutes, and 1, 2, 4, 8, and 24 hours.

C.2.5. Keep applying loads until the preconsolidation stress can be determined by having a minimum of two points after the break in the curve. After a minimum of two points have been determined past the break in the curve and then start the unloading. Refer to Figure C2.

C.2.6. Use Casagrande's (1936) method and Becker et al. (1987) also known as the work method to determine the preconsolidation stress.

C.2.6.1. Procedure for Casagrande method (Figure C2):

C.2.6.1.1. Plot vertical effective stress versus strain.

C.2.6.1.2. Estimate the point of maximum curvature on the consolidation curve.

C.2.6.1.3. Draw a line tangent to the consolidation curve at the point of maximum curvature.

C.2.6.1.4. Draw a horizontal line through the point of maximum curvature.

C.2.6.1.5. Draw a line that bisects the angle between lines drawn in steps 3 and 4 through the point of maximum curvature.

C.2.6.1.6. Draw a line tangent to the steep, linear portion of the consolidation curve (virgin compression branch) upwards to intersect line drawn in step 5.

C.2.6.1.7. The point of intersection of the lines drawn in step 5 and 6 correspond to the estimated preconsolidation pressure.

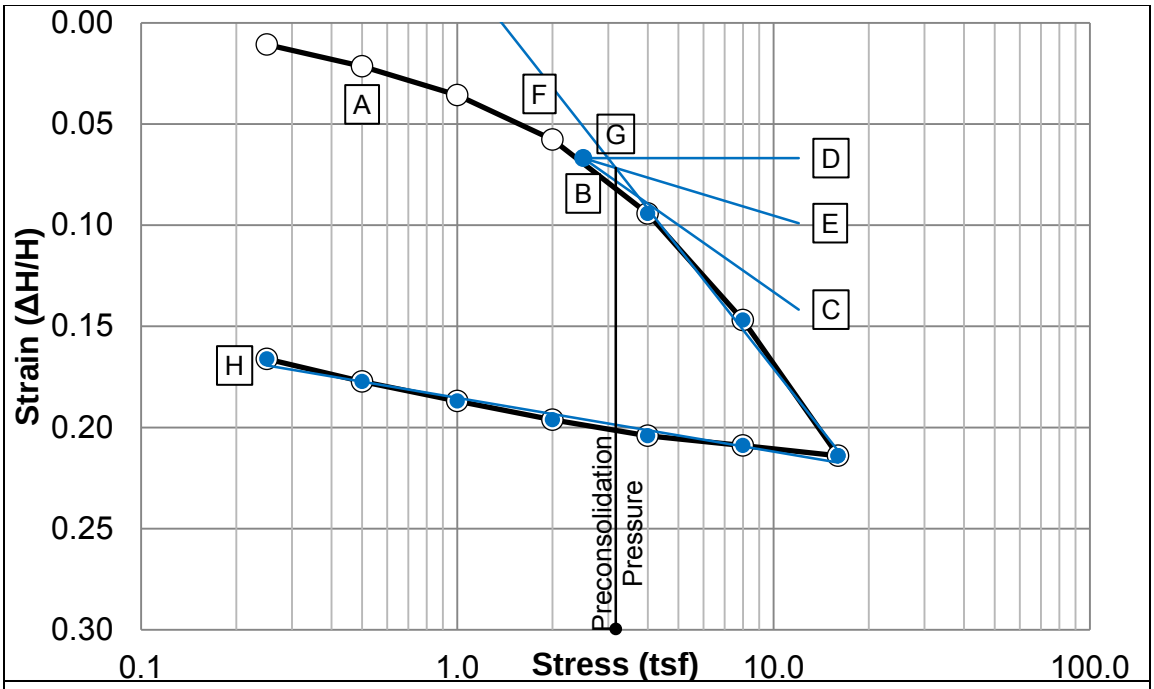

A - Stress strain curve from data points
B - Point of maximum curvature
C - Tangent line to curve at point B
D - Horizontal line through point B
E - Line bisecting angle between lines C and D
F - Tangent to linear portion of curve in vergin compression range
G - Intersection of lines E and F (vertical effetive stress at point G equals the preconsolidation pressure)

Figure C2 Evaluation for Preconsolidation Pressure Using Casagrande Method

C.2.7. Procedure for Becker et al. (1987)/Work method (Figure C3):

C.2.7.1. Calculate the incremental work for each loading step using the equation C.1 below

$$\Delta W = \left[\frac{(\sigma'_z)_{i+1} + (\sigma'_z)_i}{2}\right] \times \left[(\varepsilon_z)_{i+1} - (\varepsilon_z)_i\right] \quad \text{..... C.1}$$

Where $(\sigma'_z)_{i+1}$ and $(\varepsilon_z)_{i+1}$ are the vertical effective stresses and vertical strain at the end of the *i+1* increment and $(\sigma'_z)_i$ and $(\varepsilon_z)_i$ are the vertical effective stresses and vertical strain

at the end of the *i* increment.

C.2.7.2. Calculate the cumulative work by summing the incremental work determined in step 1.

C.2.7.3. Plot the cumulative work (ordinate, arithmetic scale) versus the vertical effective stress (abscissa, arithmetic scale). You would normally get two distinct averaged straight lines (see Figure C3).

C.2.7.4. Project the upper averaged straight line to intersect the projection of the lower averaged straight line.

C.2.7.5. The vertical effective stress at the intersection of the two lines in step 4 corresponds to the estimated preconsolidation pressure, σ'_p.

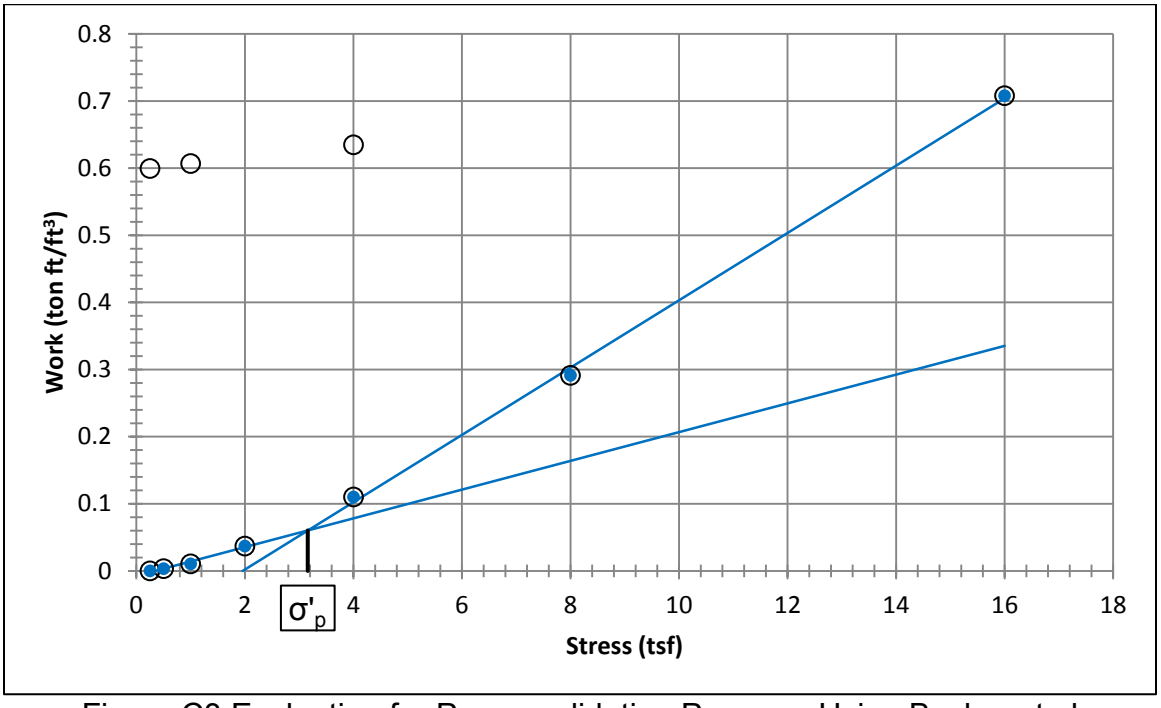

Figure C3 Evaluation for Preconsolidation Pressure Using Becker et al (1987)/Work Method

C.3. Determining the Rate of Secondary Settlement Normally Consolidated C_α

C.3.1. Using the preconsolidation stress determined from the incremental load test performed previously. Load the sample to 1.5 to 2 times that of the preconsolidation stress.

C.3.1.1. This ensured that the samples have reached a new normally consolidated state and any effects of aging or past preconsolidation had been removed.

C.3.2. The standard reading schedule for the time rate testing are as follows:

6, 15, 30 seconds, 1, 2, 4, 8, 15, 30 minutes, 1, 2, 4, 8, 24 hours.

C.3.2.1. Take readings about every 24 hours after the initial 24 hours

C.3.2.2. Run the test long enough to be sure that a good value of C_α is achieved; this test could run for 1 to 2 weeks.

C.3.3. Use Ladd's methodology to determine the value of C_α.

C.3.3.1. Ladd's procedure for determining the rate of secondary settlement normally consolidated, C_α (Figure C4):

C.3.3.1.1. Plot strain versus the log of time.

C.3.3.1.2. Determine the end of primary settlement, t_p.

C.3.3.1.2.1. This is done by extending forward the slope of the steep portion of the plotted data and extending backwards the shallow portion of the plotted data, after the steep portion, until they intersect.

C.3.3.1.2.2. Draw a line horizontal from this intersection point. Where this horizontal line crosses the plotted data is the time to end of primary settlement.

C.3.3.1.3. The rate of secondary settlement normally consolidated, C_α is determined by the slope of the linear most portion of the data after primary consolidation has occurred, also known as end of primary $t_{p,}$ on the strain vs. log of time plot (refer to Figure C4).

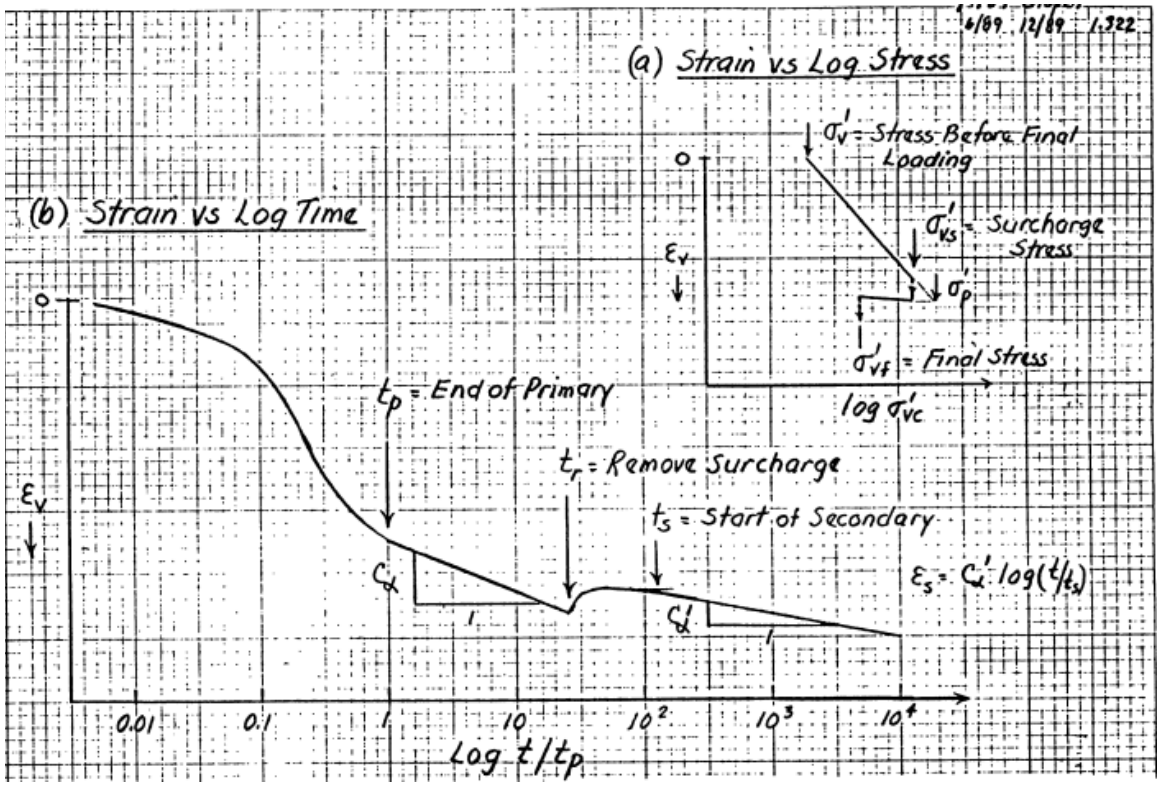

Figure C4 Ladds' method for determining the rate of secondary settlement (after Ladd, unpublished notes)

C.4. Determining the Rate of Secondary Settlement Over Consolidated C'_{α}

C.4.1. Using the preconsolidation stress determined from the incremental load test performed previously. Load the sample to 1.5 to 2 times that of the preconsolidation stress.

C.4.1.1. This ensured that the samples have reached a new normally consolidated state and any effects of aging or past preconsolidation had been removed.

C.4.2. Using the same reading schedule as stated in section C.3.2 and the square root of time method stated in section C.2.4.2, determine when 90% of primary consolidation has occurred; this usual took about 1 to 2 hours.

C.4.2.1. After 90% of primary consolidation has occurred decrease the stress on the sample to a known OCR of ether 1.25, 1.5, or 2.0.

C.4.2.1.1. It is important to keep the sample from undergoing a large amount of secondary settlement. If the sample undergoes secondary settlement, this will cause an aging effect to occur in the sample and the effect of aging can have an impact on the rate of secondary settlement.

C.4.2.1.2. After the stress has been reduced it is recommended to restart the reading schedule.

C.4.2.2. Run the test long enough to be sure that a good value of C'_{α} is achieved; this test could run for 1 to 2 weeks.

C.4.3. Use Ladd's methodology to determine the value of C'_{α} (refer to Figure C4).

C.4.3.1. Plot strain versus the log of time.

C.4.3.2. Determine the end of primary settlement, t_p using the same procedure as stated in section C.3.3.1.2.

C.4.3.3. Reduce the stress on the sample to a known OCR; this is the removal of surcharge, t_r.

C.4.3.3.1. After the surcharge has been removed there is a brief heaving event before the beginning of the reduced rate of secondary settlement. This heaving event is the time between the removal of surcharge, t_r and start of secondary settlement, t_s.

C.4.3.3.2. The value of t_s is the point in time when the soil has reached its maximum heave value.

C.4.3.4. The rate of secondary settlement over consolidated, C'_α is determined by the slope of the linear most portion of the data after t_s, (refer to Figure C4).

APPENDIX D

CPT PLOTS OF SOIL BEHAVIOR TYPES

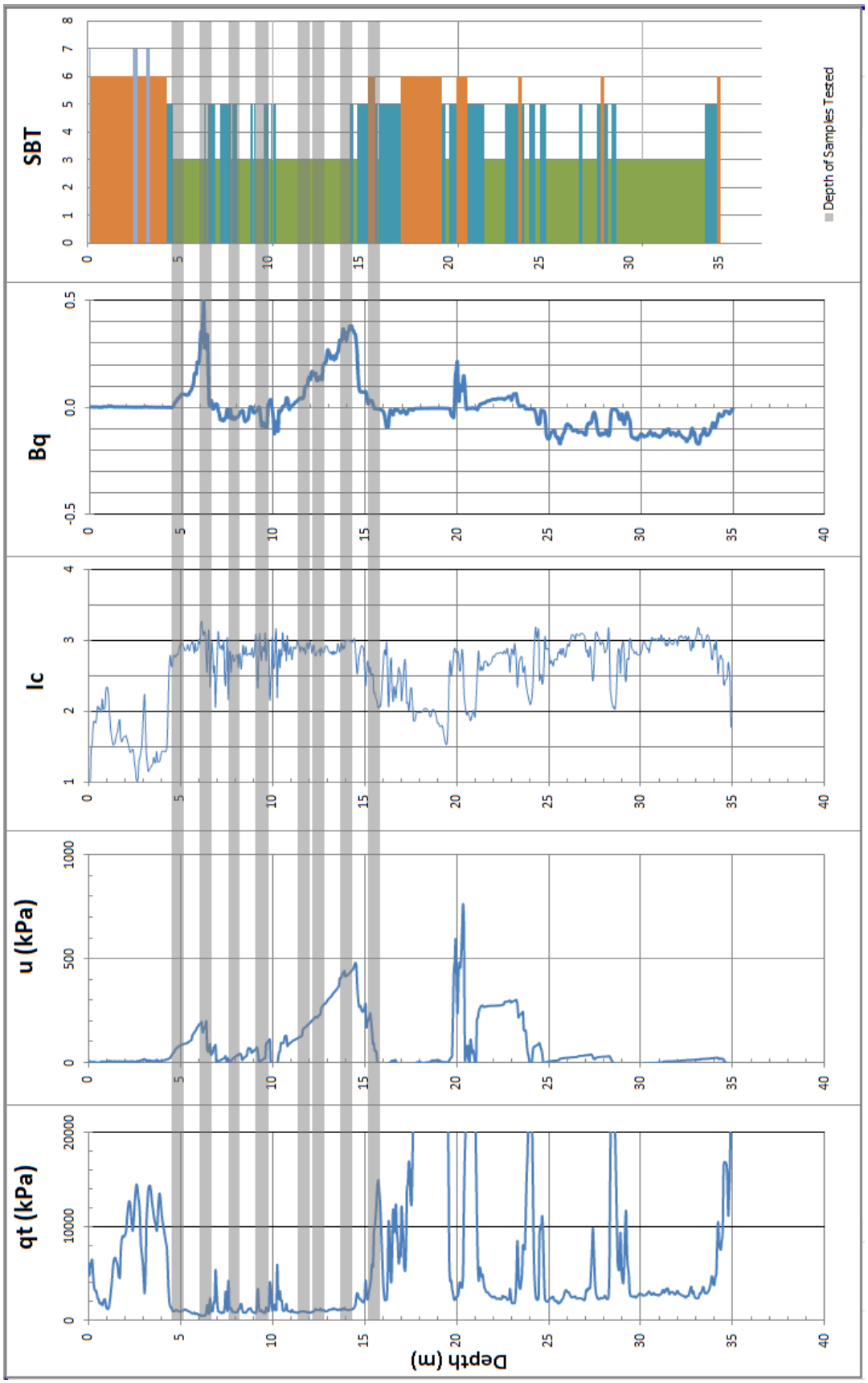

D1 400 South CPT plots with Ic, Bq, and SBT and depths where samples were tested

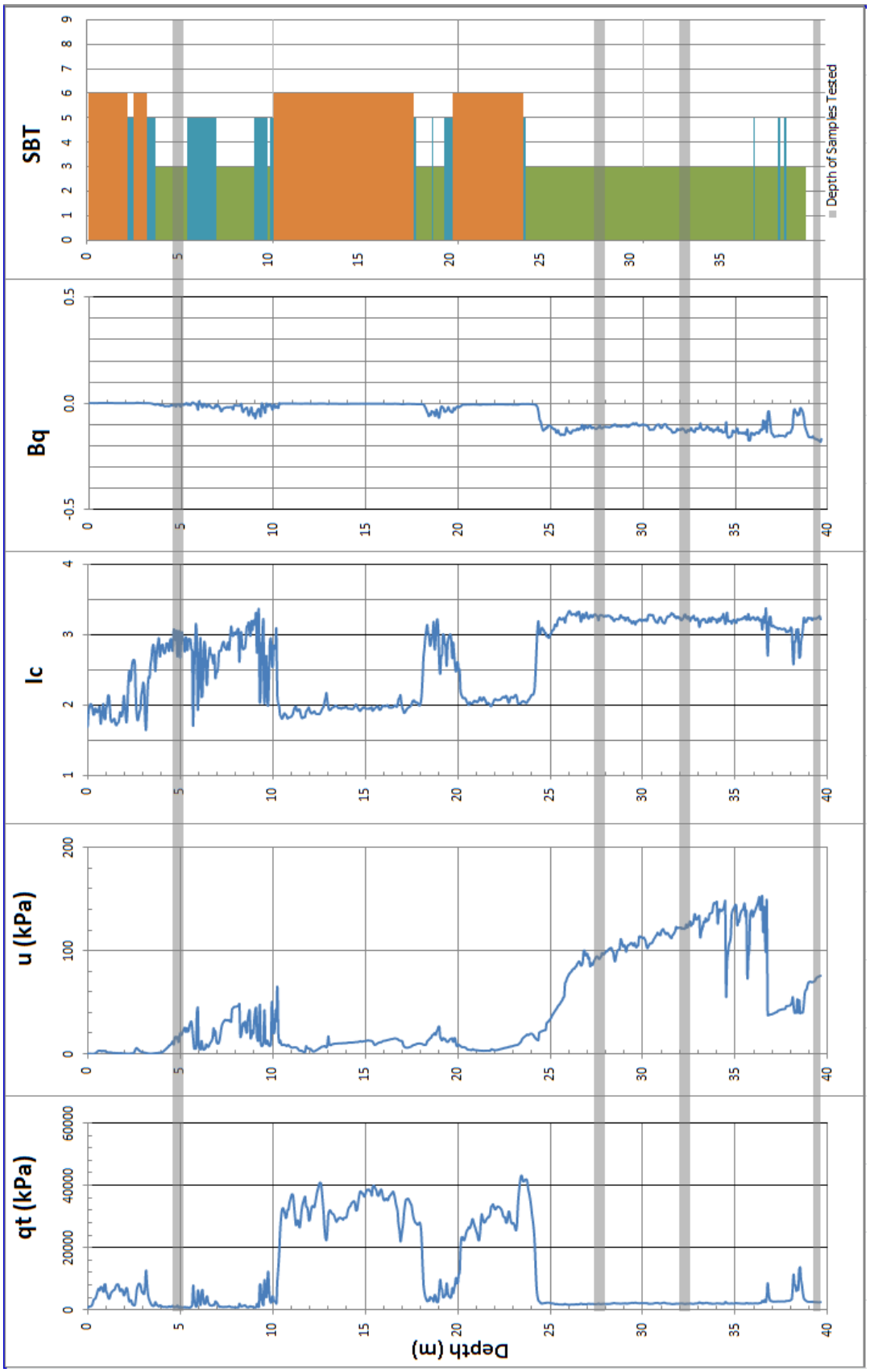

D2 South Layton CPT plots with Ic, Bq, and SBT and depths where samples were tested

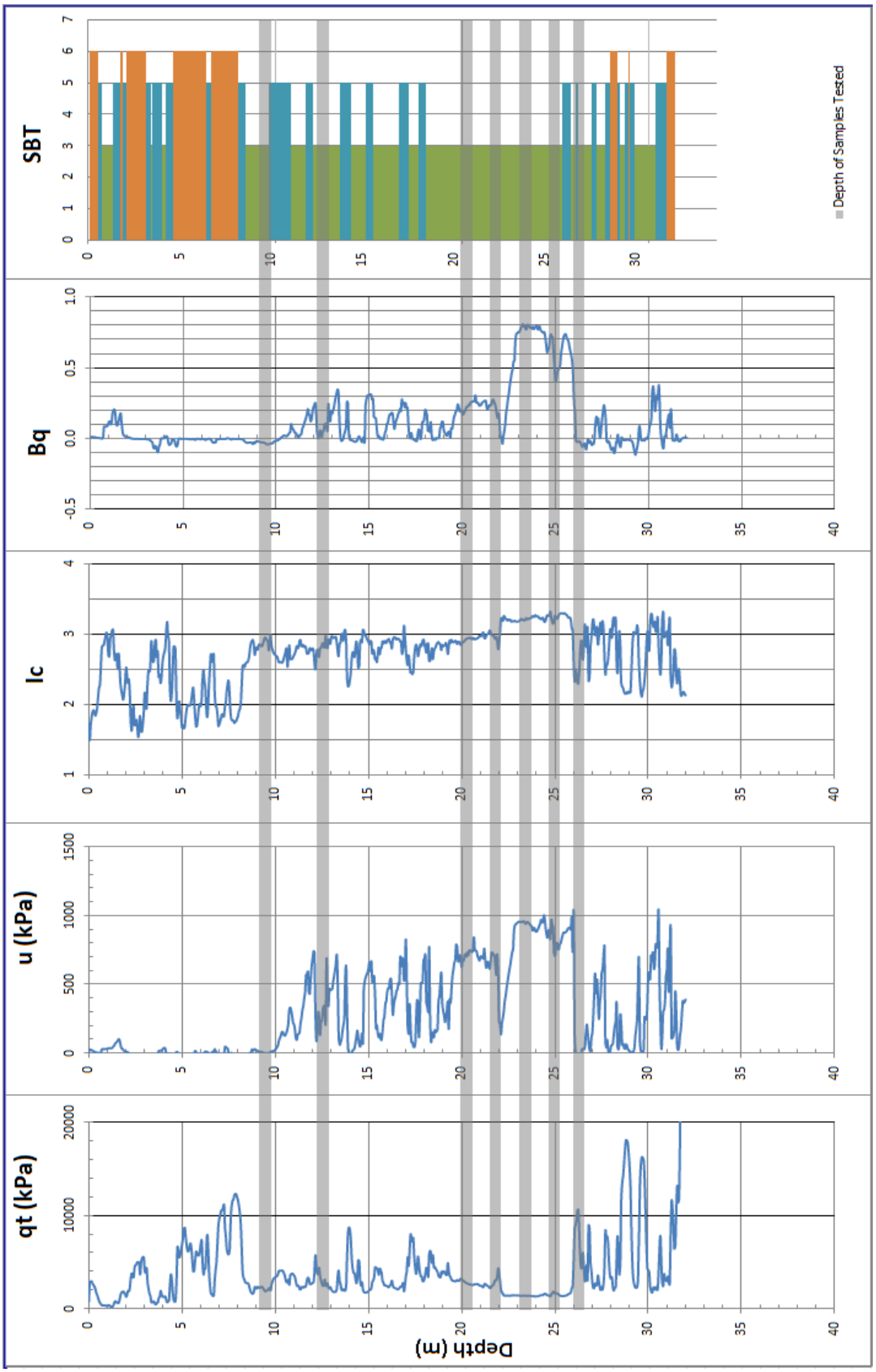

D3 Springville CPT plots with Ic, Bq, and SBT and depths where samples were tested

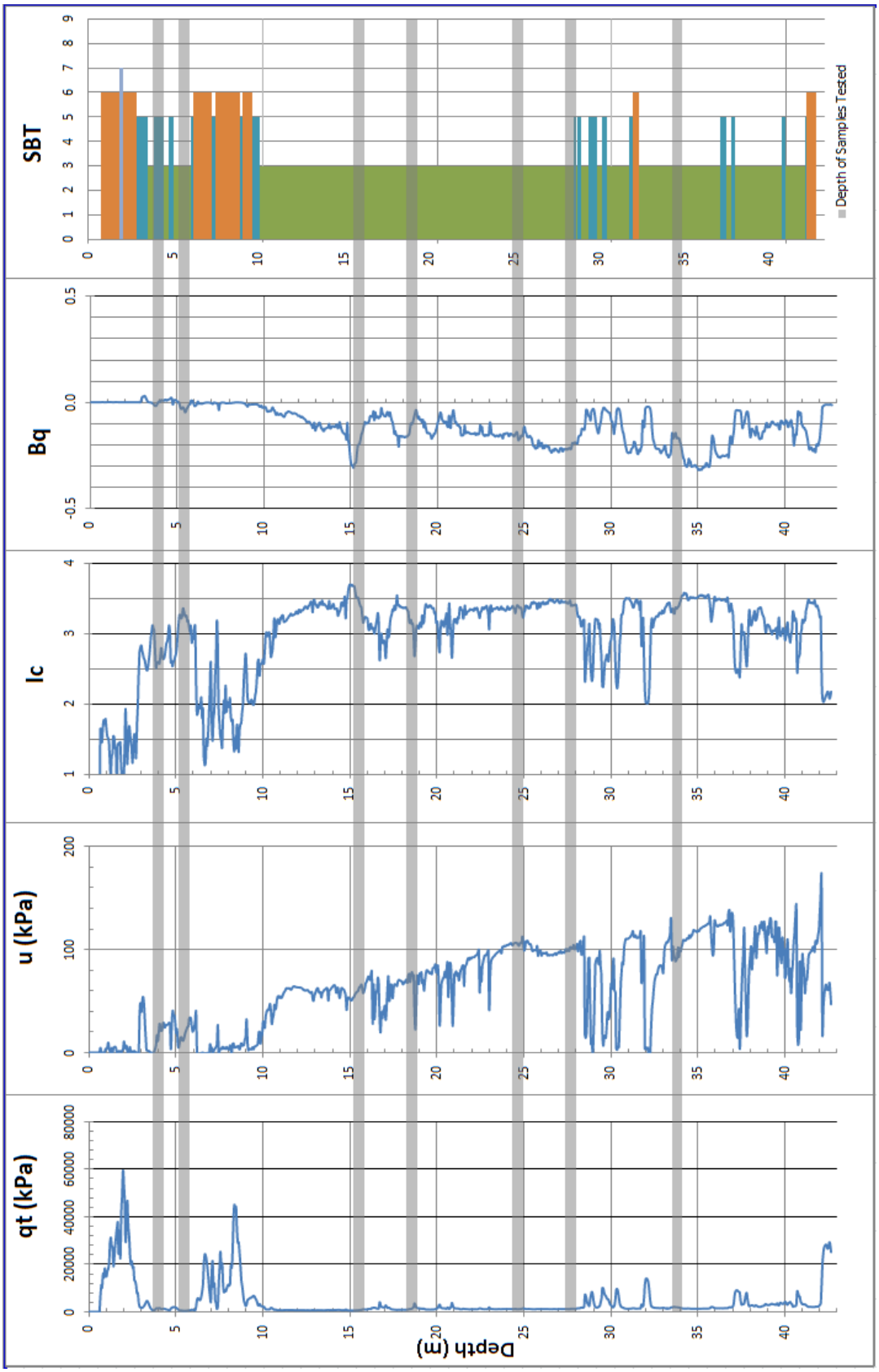

D4 Provo CPT plots with Ic, Bq, and SBT and depths where samples were tested

APPENDIX E

COMPARISON OF INCREMENTAL LOADING AND INSTANT LOADING

E.1 Comparison of Incremental Loading and Instant Loading

When performing the laboratory testing to determine the value of C_α and C'_α, the samples were loaded to the desired stress in one step. This is the equivalent to loading the sample with a large load increment ratio, LIR, whereas incremental loading was used when determining the preconsolidation of the soil. Does a large LIR have an effect on the value of C_α and C'_α? The literature seems to be mixed on the effect of what a large LIR will do to the test results.

Large LIRs will cause the soil to squeeze past the gap of the consolidation ring and the porous stone. This extrusion of soil is due to a large hydraulic gradient caused by the large step in stress. This will in turn cause an error in the measurement in the deformation due to the loss of soil (Germaine and Germaine (2009)). However, the value of C_α is independent of the load increment ratio (LIR), as long as some primary consolidation occurs (Raymond and Wahls (1976)). This concept that the value of C_α is not affected by LIR is what will be tested for this part of the report.

To determine if a large LIR has an effect on the value of C_α, parallel tests will be run. One sample will have an instant loading where the soil will be brought to the desired stress in one step. The other sample will have an incremental loading where the soil will have and LIR of 1 and time rate readings will be taken and the next loading will be added when more than 90% of primary consolidation has occurred. The samples were selected using data from nearby CPTs; these were soft soils with low tip resistance and high pore water pressures. A total of

four samples were tested, one from each site. The results of each of these tests are in Table E1.

The data were then plotted with the instantaneous loading on the x-axis and the incremental loading on the y-axis. A 45 degree line was then added to the plot for reference to see how the values of C_α instantaneous loading and C_α incremental loading deviate from each other. The value of C_α, determined using an incremental loading, did not change much when compared to the value of C_α that was determined using an instantaneous loading. This can be seen in Figure E1.

It should be noted that the samples that were subjected to the instantaneous loading tended to have a higher overall strain then the samples that underwent the incremental loading; this could be due to the squeezing effect stated earlier. However, this squeezing effect did not seem to affect the rate of secondary settlement. There may have been higher strains with the instantaneous loading, but once the pore water pressure dissipated and primary

Table E1 Test Results for Incremental Loading and Instantaneous Loading

Site	Depth	C_α Incremental load (OCR=1)	C_α Instantaneous load (OCR=1)
400 South	20-22	0.01163	0.01270
Provo	90-92	0.00496	0.00454
South Layton	105-107	0.00221	0.00227
Springville	75-77	0.00512	0.00512

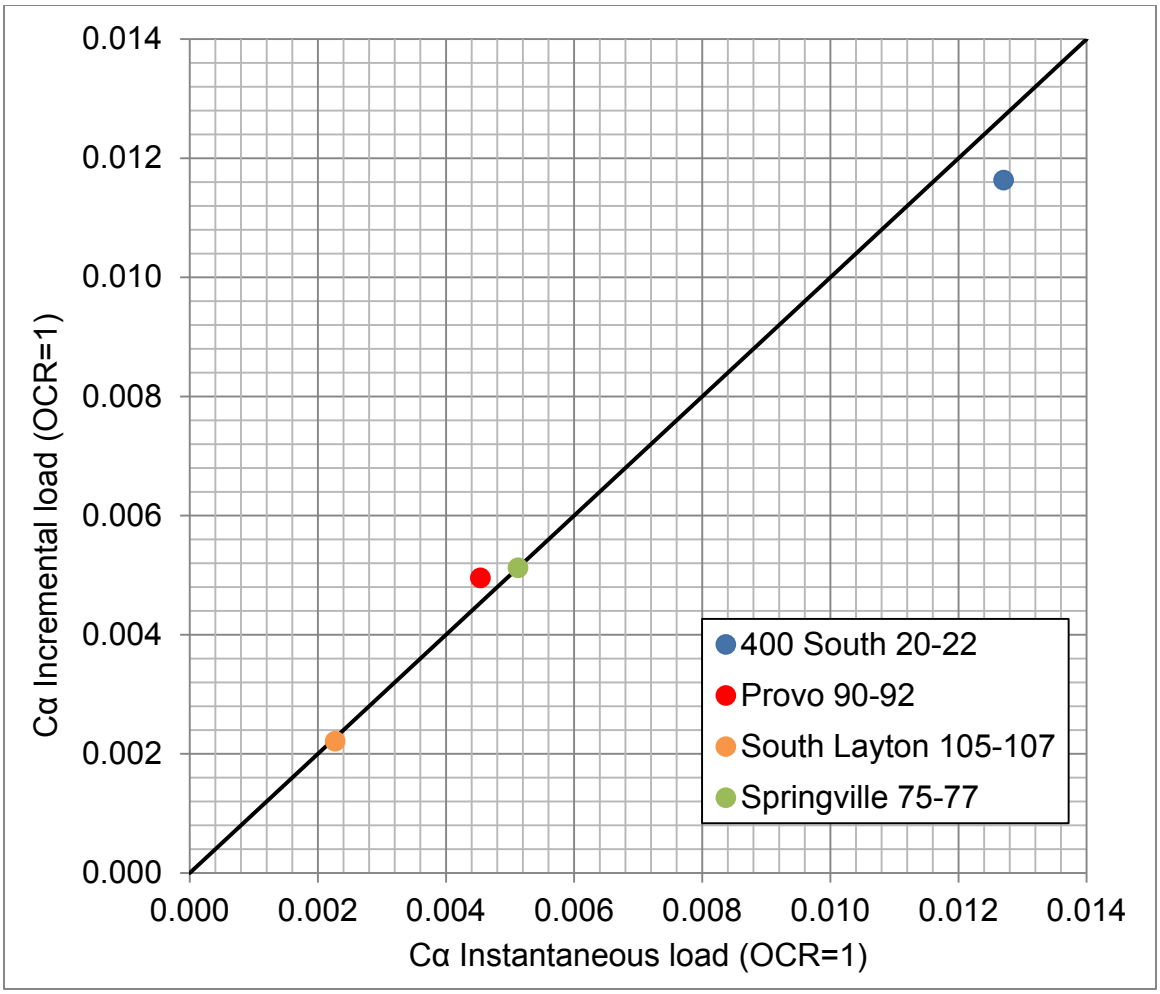

Figure E1 Plot of C_α Instantaneous Loading Versus C_α Incremental Loading

settlement had occurred, the value of C_α did not change much regardless of the use of a large LIR. This higher strain could have an effect on the value of the compression ratio, CR and the recompression ratio, RR but the value of C_α seems to be unaffected.

In conclusion, two things were observed: 1) the value of C_α is independent of the load increment ratio (LIR); when using large LIRs, C_α seems to be constant for the same material and 2) with large LIR's there seems to be larger overall strains on the sample, probably due to a loss of soil caused by high hydraulic gradient.

REFERENCES

Andresen, A.A., and Kolstad, P. (1979). “The NGI 54-mm samplers for undisturbed sampling of clays and resentative sampling of coarser material.” Proceedings of the International Symposium on Soil Sampling, Singapore. 13-21.

ASTM D2435 / D2435M-11, “Standard Test Methods for One-Dimensional Consolidation Properties for Soils Using Incremental Loading.”

ASTM D4186 / D4186M-12e1, “Standard Test Method for One-Dimensional Consolidation Properties of Saturated Cohesive Soils Using Controlled-Strain Loading.”

Bartlett, S. F., and Lee, H., (2004). “Estimation of Compression Properties of Clayey Soils, Salt Lake Valley, Utah,” Utah Department of Transportation Research Report No. UT-04.28, 44 p.

Bartlett, S.F., and Ozer, T. (2005). “Estimation of Consolidation Properties from In-Situ and Laboratory Testing,” Utah Department of Transportation Research, Research Division, Report, 206 p. (unpublished).

Farnsworth C. F., Bartlett S. F., Negussey., D. and Stuedlein A. (2008). “Construction and Post-Construction Settlement Performance of Innovative Embankment Systems, I-15 Reconstruction Project, Salt Lake City, Utah,” Journal of Geotechnical and Geoenvironmental Engineering, ASCE (Vol. 134 pp. 289-301, March 2008).

Germaine John T., Germaine Amy V., (2009). Geotechnical Laboratory Measurements for Engineers.

Holtz. R. D., Kovacs, W. D., and Sheahan, T. C. (2011). An Introduction to Geotechnical Engineering, Second Edition, Prentice Hall.

Jamiolkowski, M., Ladd, C. C., Germanie. J. T., and Lancellotta, R. (1985). “New developments in field and laboratory testing of soils,” Proceedings of the Eleventh International Conference on Soil Mechanics and Foundation Engineering, Vol. 1, San Francisco, 57-153

Ladd, C. C. (1971). “Settlement Analyses for Cohesive Soils,” Research Report R71-2, Soils Publication 272, Department of Civil Engineering, Massachusetts Institute of Technology, 107 p.

Ladd, C. C., and Foott, R. (1974). “A new design procedure for stability of soft clays.” Journal Geotechnical Engineering Division, ASCE, 100(7), 763-786.

Ladd, C. C., (1998). “Engineering Properties of Boston Blue Clay from Special Testing Program,” Proceedings of Special Geotechnical Testing Central Artery/Tunnel Project in Boston Massachusetts, ASCE Geotechnical Special Publication (GSP) No. 91, October 18-21, Boston Massachusetts.

Ladd, C. C., (1999). “Parameter Development For Estimating Settlements Due to Primary Consolidation and Secondary Compression,” Proceedings of the 34th Symposium on Engineering Geology and Geotechnical Engineering, Utah State University, Logan Utah, April 28-30, 1999.

Mesri, G., and Castro, A. (1987). “C_α/C_c concept and K_o during secondary compression,” Journal Geotechnical Engineering Division, ASCE, 113 (30), 230-249.

Mesri, G., and Feng, T. W. (1991). “Surcharging to Reduce Secondary Settlements,” Geo-Coast ’91, September 1991, Yokohama, Japan.

Mesri, G., Lo, D.O., and Feng, T. W. (1994). “Settlement of embankments on soft clay,” Proceedings *Vertical Deformations of Foundations and Embankments*, ASCE Geotechnical Special Publication No. 40, Vol. 1, pp. 8-56.

Ng, N. S. Y. (1998). “Characterization of consolidation and creep properties of Salt Lake City clays,” Msc. Thesis, Department of Civil and Environmental Engineering, Massachusetts Institute of Technology, Cambridge, Massachusetts.

Ozer, A. T., Lawton, E. C., and Bartlett, S. F., (2012). "New Method to Determine Proper Strain Rate for Constant Rate of Strain Consolidation Tests." Canadian Geotechnical Journal, Vol. 49, No. 1, January, pp. 18-26.

Raymond, G. P., and Wahls, H. E. (1976). “Estimating One-Dimensional Consolidation, Including Secondary Compression of Clay Loaded from Overconsolidated to Normally Consolidated State,” Special Report 163, Transportation Research Board, pp. 17-23.

Saye, S. R., and Ladd, C. C. (2000). “Design and Performance of the Foundation Stabilization Treatments for the Reconstruction of Interstate 15 in Salt Lake City, Utah,” Unpublished report presented to URS Consultants, June 24th, 2000, 92 p.

Takeda, T., Sugiyama, M., Akaishi, M. and Chang, H. (2013). “Initial Rate of Secondary Compression in One-Dimensional Consolidation Analysis,” Journal of GeoEngineering, Vol. 8, No. 2, pp. 55-60, August 2013